

18th International Conference on
Chemistry and Migration Behaviour of Actinides
and Fission Products in the Geosphere

Migration 2023



Nantes - France

September 24 – 29, 2023



Book of Abstracts

Conference Committees

International Steering Committee:

H. Geckeis (Chairman) (Germany)	P. Toulhoat (France)
D.L. Clark (USA)	V. Vallet (France)
S.B. Clark (USA)	L. Van Loon (Switzerland)
B. Grambow (France)	J.-I. Yun (Korea)

International Scientific Committee:

M.H. Baik (Korea)	T. Missana (Spain)
D. Bosbach (Germany)	G. Montavon (France)
S. Brassinnes (Belgium)	K. Morris (UK)
V. Brendler (Germany)	S. Nagasaki (Canada)
C. Bruggeman (Belgium)	T. Ohnuki (Japan)
J. Bruno (Spain)	T. Payne (Australia)
P. de Canniere (Belgium)	B. Powell (USA)
W. Cha (Korea)	D. Reed (USA)
L. Duro (Spain)	T. Sasaki (Japan)
N. Evans (UK)	S. Savoye (France)
V. Havlová (Czech Republic)	P. Sellin (Sweden)
A.-M. Jakobsson (Sweden)	M. Siitari-Kauppi (Finland)
G. Law (Finland)	B.S. Tomar (India)
Chunli Liu (China)	C. Tournassat (France)
M. Marques (Switzerland)	M. Zavarin (USA)

Scientific Secretary:

X. Gaona (Germany)	B. Grambow (France)
	G. Montavon (France)

Local Organizing Committee:

B. Grambow (Subatech)	I. Ollitrault (Subatech)
A. Abdelouas (Subatech)	M. Decatoire (Subatech)
C. Landesman (Subatech)	F. Plas (Andra)
G. Montavon (Subatech)	S. Savoye (CEA)
T. Suzuki-Muresan (Subatech)	F. Claret (BRGM)
T. Pierret (Subatech)	Ch. Wittebroodt (IRSN)

Contacts

Technical and programmatic content

Bernd Grambow (IMT Atlantique / SUBATECH)

Email: grambow@subatech.in2p3.fr

Gilles Montavon (CNRS / SUBATECH)

Phone: + 33 2 51 85 84 20

Email: montavon@subatech.in2p3.fr

Xavier Gaona (KIT-INE)

Phone: +49 721 608 26134

Email: xavier.gaona@kit.edu

Secretary and Logistics

Tanja Pierret (CNRS / SUBATECH)

Email: migration2023@scienceconf.org

Supported by

Migration 2023 is organised by IMT Atlantique - CNRS / SUBATECH and KIT



and is supported by:



Background

The MIGRATION conferences provide an international forum for the timely exchange of scientific information on chemical processes controlling the migration behaviour of actinides and fission products in natural aquifer systems. Experimental investigations and predictive modelling of these processes are the main topics of the conferences. The information generated from the MIGRATION conferences is the basis for the mechanistic understanding of the migration behaviour of long-lived radionuclides in the geosphere, which is essential for the long-term performance assessment of nuclear waste disposal.

The first MIGRATION conference was held in 1987 in Munich, Germany. It was followed by MIGRATION '89 in Monterey, California, USA; MIGRATION '91 in Jerez de la Frontera, Spain; MIGRATION '93 in Charleston, South Carolina, USA; MIGRATION '95 in Saint-Malo, France; MIGRATION '97 in Sendai, Japan, MIGRATION '99 at Lake Tahoe, Nevada, USA, MIGRATION '01 in Bregenz, Austria, MIGRATION '03 in Gyeongju, Korea, MIGRATION '05 in Avignon, France, MIGRATION '07 in Munich, MIGRATION '09 in Kennewick, Washington, USA, MIGRATION 2011 in Beijing, China, MIGRATION 2013 in Brighton, UK, MIGRATION 2015 in Santa Fe, New Mexico, USA, MIGRATION 2017 in Barcelona, Spain and MIGRATION 2019 in Kyoto, Japan.

Scope

The MIGRATION conferences focus on recent developments in the fundamental chemistry of actinides, fission and activation products in natural aquifer systems, their interactions and migration in the geosphere, and the processes involved in modelling their geochemical behaviour.

The sessions in MIGRATION'23 cover the following areas:

A Aquatic chemistry of actinides and fission products

- 1) Solubility and dissolution
- 2) Solid solution and secondary phase formation
- 3) Complexation with inorganic and organic ligands
- 4) Redox reactions and radiolysis effects
- 5) Solid-water interface reactions
- 6) Colloid formation
- 7) Experimental methods
- 8) Computational chemistry

B Migration behaviour of radionuclides

- 1) Sorption/desorption phenomena in dynamic systems
- 2) Diffusion and other migration processes
- 3) Colloid migration
- 4) Effects of biological and organic materials
- 5) Field and large-scale experiments
- 6) Natural analogues

C Geochemical and transport modelling

- 1) Data selection and evaluation
- 2) Coupling chemistry and transport
- 3) Development and application of models
- 4) Model validation
- 5) Safety assessment and repository concepts

D Application to Case Studies

E Special sessions:

CIGÉO and NORM

TABLE OF CONTENT

PROGRAMME8
ABSTRACTS41

PROGRAMME

SUNDAY (24. SEPTEMBER)

15:00 **REGISTRATION**

17:00 **WELCOME**

B. Grambow, G. Montavon (France)

H. Geckeis (Germany)

OPENING SESSION:

EVOLUTION OF WASTE PROGRAMS AND IMPACT ON RESEARCH

Chair: B. Grambow and G. Montavon (France)

	ID	PAGE
17:10 DEEP GEOLOGICAL DISPOSAL OF RADIOACTIVE WASTE: WHERE ARE WE AND WHERE ARE WE GOING TO? <i>F. Plas (INVITED) (France)</i>	E-1	
17:50 MIGRATION OF ACTINIDES AND FISSION PRODUCTS – AN OVERVIEW TO PUT THE DIFFERENT ISSUES OF IMPORTANCE FOR THE POST-CLOSURE SAFETY OF GEOLOGICAL REPOSITORIES IN CONTEXT <i>P. Zuidema (INVITED) (Switzerland)</i>	E-2	51
18:30 MIGRATION SCIENCE, A KEY ASSET FOR THE ENERGY TRANSITION <i>C. Poinssot (INVITED) (France)</i>	E-3	
19:10 RECEPTION		

MONDAY (25. SEPTEMBER)8:25 **CONFERENCE ANNOUNCEMENTS****SESSION 1 A8: COMPUTATIONAL CHEMISTRY**Chair: *V. Vallet (France) and D. Clark (USA)*

		ID	PAGE
8:30	COMPUTATIONAL CHEMISTRY APPROACHES TO PREDICTIVE MULTISCALE MODELLING OF MIGRATION PROCESSES: CURRENT CHALLENGES AND OPPORTUNITIES <i>A. G. Kalinichev (INVITED) (France)</i>	A8-1	52
9:15	ENABLING LONG TIME-SCALE QUANTUM MOLECULAR DYNAMICS SIMULATION FOR 5F-ELEMENTS <i>P. Yang, E. R. Batista, M. Cawkwell, C. Liu, R. Carlson, S. Wu, D. Perez (USA)</i>	A8-2	54
9:40	DENSITY FUNCTIONAL MODELING OF AM(III) HYDROXO COMPLEXES WITH Ca OR Mg COUNTER IONS. DO Mg STABILIZED SPECIES EXIST? <i>I. Chiorescu, S. Krüger (Germany)</i>	A8-3	55
10:05	COORDINATION AND THERMODYNAMIC PROPERTIES OF AQUEOUS PROTACTINIUM(V) BY COMPUTATIONAL CHEMISTRY TECHNIQUES <i>H. Oher, J. Delafoulhouze, E. Renault, V. Vallet, R. Maurice (France)</i>	A8-4	57
10:30	SORPTION OF Eu(III) ON C-S-H PHASES IN THE PRESENCE OF GLUCONATE: A MOLECULAR DYNAMICS STUDY <i>I. Androniuk, R. E. Guidone, M. Altmaier, X. Gaona (Germany)</i>	A8-5	58
10:55	BREAK		

SESSION 2 A5: SOLID-WATER INTERFACE REACTIONSChair: *M. Marques Fernandes (Switzerland) and B. Powell (USA)*

		ID	PAGE
11:15	IMPACT OF FORMATE, CITRATE AND GLUCONATE ON THE UPTAKE OF An(III)/Ln(III) AND An(IV) BY CEMENT <i>R. E. Guidone, A. Tasi, I. Androniuk, X. Gaona, B. Lothenbach, M. Altmaier, H. Geckeis (Germany, Switzerland)</i>	A5-1	60
11:40	INTERFACIAL CHEMISTRY OF GIBBSITE UNDER CONDITIONS RELEVANT TO NUCLEAR WASTE <i>Z. Wang, H. Zhang, Y. Zhao, W. Cui, X. Zhang, S. Wang, E. D. Walter, M. J. Sassi, C. I. Pearce, S. B. Clark, K M. Rosso (USA)</i>	A5-2	62
12:05	RETENTION OF ²²⁶ Ra BY ILLITE AND MONTMORILLONITE: AN ADSORPTION STUDY <i>F. Brandt, M. Klinkenberg, B. Baeyens, D. Bosbach, M. Marques Fernandes (Germany, Switzerland)</i>	A5-3	64
12:30	U(VI) RETENTION ON BENTONITE AND CEMENTITIOUS MATERIALS: EFFECT OF INCREASED IONIC STRENGTHS AND PRESENCE OF ORGANICS <i>K. Schmeide, T. Philipp, N. Huittinen, S. Shams, A. Azzam, J. Kretschmar (Germany)</i>	A5-4	66
12:55	BREAK		

SESSION 3 B4: EFFECTS OF BIOLOGICAL AND ORGANIC MATERIALSChair: *T. Ohnuki (Japan) and K. Morris (UK)*

		ID	PAGE
14:30	MECHANISM OF URANIUM REDUCTION: THE ROLE OF PENTAVALENT SPECIES <i>R. Bernier-Latmani, M. Molinas, Z. Pan, B. Bartova, T. LaGrange (INVITED) (Switzerland, China)</i>	B4-1	68
15:15	IN SITU BIOMINERALISATION FOR GROUNDWATER RADIONUCLIDE REMEDIATION <i>C. Robinson, S. Shaw, J. R. Lloyd, J. Graham, J. Rothe, K. Dardenne, K. Morris (UK, Germany) (Uni Manchester)</i>	B4-2	70
15:40	PHYTOREMEDIATION OF SOIL FROM GERMAN NUCLEAR FACILITIES <i>T. Blenke, S. Dubchak, K. Grossmann, C. Geisler, C. Walther (Germany)</i>	B4-3	72
16:05	DISSOLVED ORGANIC MATTER IN BOOM CLAY AND ITS ROLE ON RADIONUCLIDE MIGRATION: WE HAVE COME A LONG WAY <i>D. Durce, J. Govaerts, N. Maes, S. Salah, L. Van Laer, S. Brassinnes (Belgium)</i>	B4-4	74
16:30	POTENTIAL IMPACT OF BIOGENIC CHELATORS ON THE MIGRATION OF ACTINIDES <i>G. J.-P. Deblonde, N. Wasserman, A. B. Kersting, K. Morrison, M. Zavarin (USA)</i>	B4-5	76
16:55	BREAK		

SESSION 4 C3: DEVELOPMENT AND APPLICATION OF MODELS: MACHINE LEARNINGChair: *V. Brendler (Germany) and D. Kulik (Switzerland)*

		ID	PAGE
17:15	NEXT GENERATION ENVIRONMENTAL MONITORING FRAMEWORK FOR NUCLEAR WASTE AND RADIOLOGICALLY CONTAMINATED SITES <i>H. Wainwright, C. Eddy-Dilek (USA)</i>	C3-1	77
17:40	DETERMINING 3D POROSITY MAP OF BUKOV CALCITE WITH A MULTIMODAL DEEP LEARNING APPROACH <i>J. Kuva, M. Jooshaki, E. Jolis, J. Sammaljärvi, M. Siitari-Kauppi, F. Jankovský, L. Mareda, P. Sardini (Finland, Czech Republic, France)</i>	C3-2	79
18:05	A CHEMISTRY-INFORMED HYBRID MACHINE LEARNING APPROACH TO PREDICT RADIONUCLIDE SORPTION TO MINERAL SURFACES E. CHANG, M. ZAVARIN, L. BEVERLY, H. WAINWRIGHT (USA)	C3-3	81
18:30	END OF ORAL SESSIONS OF MONDAY		

SESSION 5 POSTER SESSION I (19:00 – 22:00)**PA1 SOLUBILITY AND DISSOLUTION**

	ID	PAGE
SEQUENTIAL EXTRACTION OF SIMULATED FUEL DEBRIS FOR EVALUATION OF THE CHEMICAL STABILITY <i>A. Kirishima, H. Nakazumi, D. Akiyama (Japan)</i>	PA1-1	83
SOLUBILITY BEHAVIOR AND CHARACTERIZATION OF NEODYMIUM(III) TRIHYDROXIDE SOLID PHASE <i>R. Choi, J.-Y. Lee (Korea)</i>	PA1-2	85
CHARACTERIZATION OF SYNTHETIC MAGNESIUM/CALCIUM URANYL SILICATE MINERALS AND THEIR SOLUBILITIES IN GROUNDWATER ENVIRONMENTS <i>W. Cha, J. Park, H. R. Noh, E. C. Jung, S. H. Lim, H.-R. Cho, H.-K. Kim (Korea)</i>	PA1-3	87
(U,Ce)O ₂ : A SUITABLE ANALOGUE TO STUDY THE ALTERATION OF (U,Pu)O ₂ MOX FUEL IN ENVIRONMENTAL CONDITIONS <i>T. Montaigne, S. Szenknect, V. Broudic, F. Miserque, F. Tocino, C. Martin, C. Jégou, N. Dacheux (France)</i>	PA1-4	89
SOLUBILITY BEHAVIOR OF NEPTUNIUM(V) IN EXPECTED WIPP CONDITIONS <i>U. Kaplan, C. Kutahyali Aslani, J. L. Knox, A. E. Navarrette, J. Beam, J.-F. Lucchini, D. T. Reed (USA)</i>	PA1-5	91

PA2 SOLID SOLUTION AND SECONDARY PHASE FORMATION

	ID	PAGE
DECIPHERING THE DYNAMIC PROCESSES OF MINERAL PRECIPITATION INDUCED POROSITY CLOGGING. COMBINING MICROFLUIDIC EXPERIMENTS AND SOLUTE TRANSPORT MODELLING <i>M. I. Lönartz, Y. Yang, G. Deissmann, D. Bosbach, J. Poonoosamy (Germany)</i>	PA2-1	93
KINETICS OF ²²⁶ RA INCORPORATION INTO (Ba,Ra)SO ₄ SOLID SOLUTIONS <i>S. Rudin, P. M. Kowalski, M. Klinkenberg, T. Bornhake, D. Bosbach, F. Brandt (Germany)</i>	PA2-2	95
FREEZING AND DEFROSTING OF IONIC AND MAGNETIC CONFIGURATIONS IN ZIRCONIUM MOLYBDATE FORMED IN NUCLEAR FUEL WASTE GLASSES <i>M. Morishita, T. Miyatake, H. Yamamoto (Japan)</i>	PA2-3	97

PA3 COMPLEXATION WITH INORGANIC AND ORGANIC LIGANDS

	ID	PAGE
NEW SPECIATION DIAGRAM OF THE PU(IV)-ACETATE SYSTEM TAKING INTO ACCOUNT POLYNUCLEAR SPECIES <i>G. Chupin, C. Tamain, T. Dumas, P. Lorenzo Solari, P. Moisy, D. Guillaumont (France)</i>	PA3-1	99
SOLUBILITY OF FERROUS IRON HYDROXIDE IN THE PRESENCE OF CITRATE: EFFECT OF IONIC STRENGTH <i>T. Platte, J. Je-Hun Jang (USA)</i>	PA3-2	101
THERMODYNAMIC AND STRUCTURAL STUDIES OF Am(III)-ISOSACCHARINATE COMPLEXATION UNDER ACIDIC TO ALKALINE CONDITIONS: AQUEOUS COMPLEXES TO COLLOIDAL PARTICLES <i>H.-K. Kim, H. Cho, K. Jeong, U. H. Yoon, H.-R. Cho (Korea)</i>	PA3-3	103
TRIBUTYL PHOSPHATE: COMPETITIVE ADSORPTION AND EFFECT ON RADIONUCLIDES RETENTION <i>M. Assaf, E. Thory, P. Henocq, R. V. H. Dagnelie (France)</i>	PA3-4	105
THERMODYNAMIC STUDY OF COMPLEXATION OF LANTHANIDE/ACTINIDE WITH CEMENT ADDITIVES BY ISOTHERMAL MICRO-TITRATION CALORIMETRY <i>M. Acker, A. Wollenberg, S. Taut, T. Stumpf (Germany)</i>	PA3-5	106

PA4 REDOX REACTIONS AND RADIOLYSIS EFFECTS

	ID	PAGE
PERRHENATE (ReO_4^-) REMOVAL FROM AQUEOUS SOLUTIONS BY MONO-, BI-, AND TRI-METALLIC IRON NANOPARTICLES: A COMPARATIVE STUDY <i>I. Maamoun, K. Tokunaga, O. Falyouna, O. Eljamal, K. Tanaka (Japan)</i>	PA4-1	108
REDOX-ACTIVE DONOR-ACCEPTOR CONJUGATED MICROPOROUS POLYMER FOR PHOTOCATALYTIC REDUCTION OF URANIUM(VI) <i>F. Yu, Z. Zhang, Y. Liu (China)</i>	PA4-2	110
CHLORIDE GREEN RUST AS SCAVENGER OF TECHNETIUM: IMMOBILIZATION AND SPECTROSCOPIC STUDIES <i>N. Mayordomo, A. Rossberg, D. M. Rodríguez, D. Schild, A. C. Scheinost, V. Brendler, K. Müller (Germany, France)</i>	PA4-3	112
Tc(VII) REDUCTIVE IMMOBILIZATION BY S(-II) PRE-SORBED ON ALUMINA <i>S. Garcia-Gomez, C. Börner, J. Gimenez, I. Casas, J. Llorca, J. de Pablo, K. Müller, N. Mayordomo (Spain, Germany)</i>	PA4-4	114
PORPHYRIN-BASED HYDROGEN-BONDED ORGANIC FRAMEWORK FOR VISIBLE LIGHT DRIVEN PHOTOCATALYTIC REMOVAL OF U(VI) FROM AQUEOUS SOLUTIONS <i>P. Wu, X. Yin, Y. Zhao, F. Li, J. Liao, Y. Yang, N. Liu, T. Lan (China)</i>	PA4-5	116

EXCITON DISSOCIATION AND TRANSFER BEHAVIOR AND SURFACE REACTION MECHANISM IN DONOR–ACCEPTOR ORGANIC SEMICONDUCTOR PHOTOCATALYTIC SEPARATION OF URANIUM <i>Z. Dong, Z. Li, C. Meng, Z. Zhang, Y. Liu (China)</i>	PA4-6	118
SELENIUM REACTIONS IN FERROUS AND SULFIDE-RICH ENVIRONMENTS: EFFECTS OF SULFIDE SPECIATION <i>P. Clarence Francisco, T. Ishidera, H. Shiwaku, R. Kikuchi, D. Matsumura, Y. Tachi (Japan)</i>	PA4-7	120
INSIGHTS INTO THE URANIUM ENRICHMENT MECHANISM ON MINERALS CONTAINING Fe(II) IN DEEP GEOLOGICAL REPOSITORIES <i>X. Zhao, D. Pan, W. Wu (China)</i>	PA4-8	122

PA5 SOLID-WATER INTERFACE REACTIONS

	ID	PAGE
SORPTION BEHAVIOR OF SELENITE ON CLAY MINERAL SURFACES IN THE PRESENCE OF AQUATIC FULVIC ACID <i>H. Eun, S. Choi, J.-I. Yun (Korea)</i>	PA5-1	124
APPLICATION OF METAL IONS DOPED HYDROXYAPATITE IN URANIUM ADSORPTION <i>Y. Wang, L. Chen, Y. Liu (China)</i>	PA5-2	126
SORPTION OF Eu(III) AND Cm(III) ON C-S-H PHASES IN PRESENCE OF EDTA AT INTERMEDIATE IONIC STRENGTH CONDITIONS <i>A. K. Thumm, A. Skerencak-Frech, X. Gaona, M. Altmaier, H. Geckeis (Germany)</i>	PA5-3	128
CONSTRUCTION AND APPLICATION OF AN ULTRAHIGHLY SELECTIVE PHOTOISOMERIC METAL-ORGANIC FRAMEWORKS MATERIAL FOR URANIUM EXTRACTION FROM SEAWATER <i>P. Zhang, D. Pan, W. Wu (China)</i>	PA5-4	130
TRIVALENT LANTHANIDES SORPTION ONTO ILLITE IN THE PRESENCE OF CARBONATE <i>Y. Sugiura, T. Ishidera, N. Aoyagi, H. Mei, T. Saito, Y. Tachi (Japan)</i>	PA5-5	132
URANIUM SORPTION ON OXYHYDROXIDE MINERALS BY SURFACE COMPLEXATION AND PRECIPITATION <i>J. Wang, C. Liu (China)</i>	PA5-6	135
Eu(III) AND Cm(III) COMPLEXATION BY NITRILOTRIACETIC ACID TO FURTHER EVALUATE ITS IMPACT ON THE RADIONUCLIDE RETENTION BY CEMENTITIOUS PHASES <i>C. Sieber, J. Kretzschmar, B. Drobot, S. Tsushima, K. Schmeide, T. Stumpf (Germany)</i>	PA5-7	136
MINERAL SPECIFIC SORPTION OF RADIUM ON CRYSTALLINE ROCK <i>O. Fabritius, T. Sorokina, R. Dehqanzada, J. Sammaljärvi, A.-M. Jakobsson, T. Sojakka, M. Siitari-Kauppi (Finland, Sweden)</i>	PA5-8	138
ANCHORING SELF-ASSEMBLY ANTIBACTERIAL AG NANOSHEETS ONTO THE MAGNETIC MICROSPHERES ENHANCED URANIUM IMMOBILIZATION <i>M. Zhao, D. Pan, W. Wu (China)</i>	PA5-9	140

FUNCTIONALIZED DIOXIN-LINKED COVALENT ORGANIC FRAMEWORKS FOR RAPID AND SELECTIVE EXTRACTION OF URANIUM <i>Y. Xu, D. Pan, W. Wu (China)</i>	PA5-10	142
Cs(I) AND Ba(II) SORPTION ON BIOTITE AT pH 5-9 AND 25, 40 AND 60°C <i>P. Kumar, S. Holgersson (Sweden)</i>	PA5-11	144
MICROMECHANISM OF ADSORPTION OF STRONTIUM AND CESIUM ON DIFFERENT EXPANSIVE CLAY MINERALS <i>J. Hou, D. Pan, W. Wu (China)</i>	PA5-12	145
ADSORPTION OF CESIUM ON MICACEOUS MINERALS WITH STRUCTURAL TRANSFORMATION AND THE IMPLICATION FOR DIFFUSION <i>H. Wu, W. Wang, M. Kang, Y. Takahashi, Q. Fan (China, Japan)</i>	PA5-13	147
ILLITIZATION UNDER HIGH TEMPERATURES AND ITS EFFECT ON CESIUM SORPTION <i>S. Chang, M. Kong, D.H. Lee, J.S. Kim (Korea)</i>	PA5-14	149
ANTI-BIOLOGICAL CONTAMINATION URANIUM ADSORBING CELLULOSE GEL <i>Y. Jiang, Y. Zhang, Z. Li, G. He, Z. Zhang, Y. Liu (China)</i>	PA5-15	151
RETENTION MECHANISMS OF SELENIUM IN DEEP SUBSURFACE SEDIMENTARY FORMATIONS IN HORONOBÉ AREA, HOKKAIDO, JAPAN <i>S. Dei, Y. Tachi, Y. Amano, P. C. M. Francisco, Y. Sugiura, Y. Takahashi (Japan)</i>	PA5-16	153

PA6 COLLOID FORMATION

	ID	PAGE
FORMATION OF STABLE U(VI) COLLOIDAL PARTICLES IN RELEVANT ENVIRONMENTAL CONDITIONS <i>H. Barbier, S. Szenknect, D. Rebiscoul (France)</i>	PA6-1	155
STABILITY OF EUROPIUM(III)/THORIUM(IV)-SILICATE COLLOIDS: EFFECT OF SI CONTENT, pH, ELECTROLYTE AND FULVIC ACID <i>D. Zhang, Q. Jin, Z. Chen, Z. Guo (China)</i>	PA6-2	157
THE STABILITY AND INTERACTION OF COLLOIDS AND THEIR EFFECTS ON RADIONUCLIDE TRANSPORT REGARDING TO HLW DISPOSAL IN GRANITIC FORMATION <i>Z. Guo, P. Gao, Z. Chen, Q. Jin, W. Wu (China)</i>	PA6-3	159

PA7 EXPERIMENTAL METHODS

	ID	PAGE
AN "ON-OFF" RATIO-METRIC FLUORESCENT SENSOR FOR UO_2^{2+} BASED ON Ag^+ -MODIFIED GOLD NANOCCLUSERS HYBRID <i>X. Cao, Z. Zhang, Y. Liu (China)</i>	PA7-1	161
TRACING AND QUANTIFICATION OF ^{226}Ra IN TAILINGS BY SPECTROSCOPIC AUTORADIOGRAPHY <i>H. Lefevre, S. Billon, M. Descostes, J. Donnard, S. Duval, P. Sardini (France)</i>	PA7-2	163

DEVELOPMENT OF ANALYTICAL PROTOCOL FOR DIFFICULT TO MEASURE RADIONUCLIDES IN METALLIC MATRIX; EXAMPLE OF ZR-93 IN STAINLESS STEEL AND INCONEL METALS **PA7-3** 165
T. Suzuki-Muresan, M. Mokili, A. Abdelouas, N. Bessaguet, P. Cassette, S. Happel, G. Montavon (France, Bulgaria)

A RAPID DETERMINATION OF SELENIUM IN TEA SAMPLES USING ANION CHROMATOGRAPHIC COLUMN COMBINED WITH AUTOMATIC SYSTEM SEPARATION AND HR-ICP-MS MEASUREMENT **PA7-4** 167
Y. Chen, N. Guo, K. Shi (China)

PA8 COMPUTATIONAL CHEMISTRY

	ID	PAGE
AN ATOMIC SCALE COMPUTATIONAL APPROACH TO UNDERSTANDING REDOX SPECIATION OF KEY ACTINIDES ON IRON BEARING MINERALS <i>C. Hatton, N. Kaltsoyannis, L. Natrajan, S. Shaw (UK)</i>	PA8-1	168
DENSITY FUNCTIONAL THEORY STUDY OF THE CRYSTAL STRUCTURE AND INFRARED SPECTRUM OF ETTRINGITE <i>F. Colmenero, O. Almendros, A. M. Fernández, T. Missana (France, Spain)</i>	PA8-2	170
ACTINIDE(IV) INTERACTIONS WITH CALCIUM SILICATE HYDRATE: SORBED SPECIES AND COMPARISON OF SORPTION MODES BY MEANS OF DENSITY FUNCTIONAL CALCULATIONS <i>I. Chiorescu, A. Kremleva, S. Krüge (Germany)</i>	PA8-3	172
EXPLORING THE COMPLEXATION OF CURIUM(III) AND EUROPIUM(III) WITH AQUEOUS PHOSPHATES: A COMBINED EXPERIMENTAL AND AB INITIO STUDY <i>F. Réal, N. Huittinen, I. Jessat, V. Vallet, N. Jordan (France, Germany)</i>	PA8-4	174

PB2 DIFFUSION AND OTHER MIGRATION PROCESSES

	ID	PAGE
IONIC DIFFUSIVE TRANSPORT THROUGH PARTIALLY-WATER SATURATED CEMENT-BASED MATERIALS <i>S. Savoye, S. Lefevre, N. Macé, J.-C. Robinet (France)</i>	PB2-1	176
EFFECTS OF BIOTITE ON DIFFUSION AND SORPTION OF CATIONS IN CRYSTALLINE ROCKS BY THROUGH-DIFFUSION AND LASER-ABLATION ICP-MS EXPERIMENTS <i>Y. Fukatsu, Q. Hu, Y. Tachi (Japan, USA)</i>	PB2-2	178
DIFFUSION AND RETENTION OF DIVALENT TRANSITION METAL TRACERS IN COMPACTED ILLITE CONVERTED TO DIFFERENT CATIONIC FORMS <i>D. Zerva, M. A. Glaus, S. Churakov (Switzerland)</i>	PB2-3	180
RELEVANCE OF UPWARDS MIGRATION OF RADIONUCLIDES IN SOIL IN THE CONTEXT OF NUCLEAR WASTE MANAGEMENT <i>A. Kogiomtzipidis, V. Hormann, C. Walther (Germany)</i>	PB2-4	182

ZINC(II) TRANSPORT IN COMPACT ILLITE IN THE PRESENCE OF ORGANIC LIGANDS <i>X. Wei, M. A. Glaus, L. R. Van Loon, M. Marques Fernandes, B. Ma (Switzerland, China)</i>	PB2-5	184
DIFFUSION AND SORPTION OF HTO AND Eu-152 IN CRYSTALLINE ROCK WITH AND WITHOUT BENTONITE COLLOIDS <i>N. Pakkanen, L. Biez, J. Arkko, E. Jolis, J. Kuva, P. Sardini, A. Mazurier, J. Sammaljärvi, M. Siitari-Kauppi (Finland, France)</i>	PB2-6	186
METAL ION DIFFUSION THROUGH METAKAOLIN-BASED GEOPOLYMER <i>A. C. Yildirim, K. Toda, T. Saito (Japan)</i>	PB2-7	188
A SENSITIVE METHOD TO MEASURE GEOMETRY FACTORS FOR DIFFUSION ON SMALL SAMPLES OF CLAY ROCK <i>M. A. Glaus, D. Zerva, L. R. Van Loon, R. A. J. Wüst (Switzerland)</i>	PB2-8	190
EFFECTS OF ALTERATION BY LEACHING ON MIGRATION OF CESIUM IN HARDENED CEMENT PASTE <i>N. Watanabe, K. Watanabe, K. Matsumoto, S. Uematsu, T. Kozaki, Y. Morinaga, D. Minato, T. Nagaoka (Japan)</i>	PB2-9	192

PB3 COLLOID MIGRATION

	ID	PAGE
BENTONITE COLLOIDS MEDIATED Eu(III) MIGRATION IN HOMOGENEOUS AND HETEROGENEOUS MEDIA OF BEISHAN GRANITE AND FRACTURE-FILLING MATERIALS <i>Y. Chen, C. Liu, N. Guo (China)</i>	PB3-1	194
COUPLING MECHANISM OF Eu(III) TRANSPORT IMPACTED BY COMPOSITE COLLOIDS OF BENTONITE AND ORGANIC MATTER <i>Z. Xu, D. Pan, W. Wu (China)</i>	PB3-2	195

PB4 EFFECTS OF BIOLOGICAL AND ORGANIC MATERIALS

	ID	PAGE
INTERACTION OF TECHNETIUM WITH METABOLITES, MICROORGANISMS AND AT THE MINERAL-WATER INTERFACE: RADIOECOLOGICAL CONSIDERATIONS <i>N. Mayordomo, I. Cardaio, A. Bureika, C. Börner, K. Müller (Germany)</i>	PB4-1	197
ACCUMULATION OF ACTINIDES(III, VI) IN THE FILAMENTOUS FUNGUS <i>PODOSPORA ANSERINA</i> <i>M. Maloubier, C. Le Naour, Y. Pei, G. Creff, A. Jeanson, C. Den Auwer, F. Chapeland-Leclerc, G. Ruprich-Robert, E. Cabet (France)</i>	PB4-2	199
RIGIDITY AND FLEXIBILITY: UNRAVELING THE ROLE OF FULVIC ACID IN URANYL SORPTION ON GRAPHENE OXIDE USING MOLECULAR DYNAMICS SIMULATIONS <i>T. Lan, P. Wu, X. Yin, Y. Zhao, J. Liao, D. Wang, N. Liu (China)</i>	PB4-3	201
THE MECHANISM OF URANIUM(VI) BIOMINERALIZATION IN THE GROWTH OF <i>BACILLUS</i> SP. DWC-2 <i>Y. Guo, H. Tu, F. Li, Y. Yang, J. Yang, T. Lan, N. Liu, J. Liao (China)</i>	PB4-4	203

THE BEHAVIOR AND MECHANISM OF URANIUM BIOREDUCTION INDUCED BY A NATURAL BACILLUS THURINGIENSIS <i>S. Chen, J. Gong, Y. Guo, H. Li, F. Li, T. Lan, Y. Yang, J. Liao, N. Liu (China)</i>	PB4-5	205
BIOMIMETIC PHOTOCATALYTIC SYSTEMS DESIGNED BY SPATIALLY SEPARATED COCATALYSTS ON Z-SCHEME HETEROJUNCTION WITH IDENTIFIED CHARGE-TRANSFER PROCESSES FOR BOOSTING REMOVAL OF U(VI) <i>Y. Liu, Z. Dong, Z. Li, X. Cao, Z. Zhang (China)</i>	PB4-6	206
ORGANICALLY BOUND TRITIUM SPECIATION IN ENVIRONMENTAL MATRICES BY ISOTOPIC EXCHANGE <i>A.-L. Nivresse, N. Baglan Nicolas, G. Montavon, O. Péron (France)</i>	PB4-7	208

PB5 FIELD AND LARGE-SCALE EXPERIMENTS

	ID	PAGE
MIGRATION OF ⁶⁰ Co, ¹³³ Ba, ¹³⁷ Cs, AND ¹⁵² Eu FROM CEMENTITIOUS WASTEFORMS IN FIELD LYSIMETER EXPERIMENTS <i>R. Williams, D. I. Kaplan, T. A. DeVol, B. J. Erdmann, B. A. Powell (USA)</i>	PB5-1	210
MODELING A RADIONUCLIDE TRANSPORT EXPERIMENT IN GRANITIC ROCK MATRIX AT GRIMSEL. THE ROLE OF ADVECTION <i>J. M. Soler, D. Jurado, M. W. Saaltink, L. Martínez, J. J. Hidalgo, G. W. Lanyon, A. J. Martin (Spain, UK, Switzerland)</i>	PB5-2	212
CHARACTERISTICS OF GRANITIC AQUIFER COLLOIDS IN THE KURT GROUNDWATER SYSTEM <i>J. Ha, J.-Y. Lee (Korea)</i>	PB5-3	214
THE HETEROGENEITY OF THE SANDY FACIES OF OPALINUS CLAY ACROSS SCALES, FROM SEISMIC SURVEYS TO RADIONUCLIDE DIFFUSION - AN IN-SITU TEST IN THE SWISS ROCK LABORATORY MONT TERRI <i>F. Heberling, H. Albers, T. Beilecke, G. Deissmann, C. Fischer, M. Furche, H. Geckeis, E.-M. Hoyer, C. Joseph, A. Liebscher, L. Van Loon, S. Lüth, B. Ma, V. Metz, K. Müller, U. Nowak, F. Quinto, D. Rebscher, W. Rühaak, F. Schulte, F. Steegborn, T. Tietz (Germany, Switzerland)</i>	PB5-4	216
STRONTIUM BEHAVIOUR IN RADIOACTIVELY CONTAMINATED LAND – UNDERPINNING OPTIONS FOR IN-SITU DISPOSAL <i>J. Blagden, S. Shaw, V. Coker, J. Graham, K. Morris (UK)</i>	PB5-5	217

PB6 NATURAL ANALOGUES

	ID	PAGE
IDENTIFICATION ON THE ORIGIN AND FATE OF DISSOLVED U IN BOEUN AQUIFER, BASED ON C, O, Fe, S, Sr AND U-SERIES ISOTOPIC SIGNATURES <i>Y. Ju, M. H. Baik, S. Y. Lee, D. Kaown, K.-K. Lee, D. Shin, J. H. Ryu (Korea)</i>	PB6-1	219
GEOCHEMICAL BEHAVIORS OF URANIUM IN A URANIUM DEPOSIT OF THE OGcheon METAMORPHIC BELT, KOREA <i>M. H. Baik, Y. Ju, J. H. Ryu, J. O. Jeong (Korea)</i>	PB6-2	220

PC1 DATA SELECTION AND EVALUATION

	ID	PAGE
THE NEA THERMOCHEMICAL DATABASE (TDB) PROJECT: HIGH QUALITY DATA, ACCESSIBILITY AND CAPACITY BUILDING <i>J. S. Martinez, A. Mercier (France)</i>	PC1-1	222
DEVELOPMENT OF A DATABASE FOR RADIONUCLIDE SORPTION ON CLAY AND CEMENT SYSTEMS IN SUPPORT TO RADIOACTIVE WASTE MANAGEMENT <i>D. García, M. López-García, D. Pérez, I. Canals, A. Nardi, L. Duro, S. Brassinnes (Spain, Belgium)</i>	PC1-2	224
THERMODYNAMIC MODELS DATABASE: A TOOL FOR UNDERSTANDING RADIONUCLIDE SORPTION MECHANISMS ON CLAY AND CEMENT SYSTEMS <i>I. Canals, M. López-García, D. Pérez, A. Nardi, L. Duro, D. García, S. Brassinnes (Spain, Belgium)</i>	PC1-3	226
A THERMODYNAMIC DATABASE FOR THE SOLUTION CHEMISTRY AND SOLUBILITY OF EUROPIUM(III) INORGANIC SPECIES: RECENT DEVELOPMENTS <i>N. Jordan, T. Thoenen, S. Starke, K. Spahiu, V. Brendler (Germany, Switzerland, Sweden)</i>	PC1-4	228
THERMOCHEMIE: A THERMODYNAMIC DATABASE USED IN RADIOACTIVE WASTE DISPOSAL EVALUATION <i>B. Madé, W. Bower, S. Brassinnes (France, UK, Belgium)</i>	PC1-5	230

PC2 COUPLING CHEMISTRY AND TRANSPORT

	ID	PAGE
INTERPRETATION OF DIFFUSION EXPERIMENTS WITH A NUMERICAL REACTIVE TRANSPORT APPROACH <i>C. Tournassat, C. I. Steefel, P. M. Fox, R. M. Tinnacher (USA, France)</i>	PC2-1	231
MODEL INTERPRETATION OF INTERACTION BETWEEN GLASS AND ORDINARY PORTLAND CEMENT IN AN INTEGRATED GLASS DISSOLUTION EXPERIMENT <i>S. Liu, K. Ferrand, J. Goethals, D. Jacques, K. Lemmens (Belgium, France)</i>	PC2-2	232
REACTIVE TRANSPORT MODELLING OF TCO ₄ ⁻ DIFFUSION IN OPALINUS CLAY WITH PFLOTTRAN <i>P. Chen, L. R. Van Loon, S. Koch, P. Alt-Epping, T. Reich, S. Churakov (Switzerland, Germany)</i>	PC2-3	234

PC3 DEVELOPMENT AND APPLICATION OF MODELS

	ID	PAGE
COMPARISON OF THE CAPACITY OF TWO ADSORPTION MODELS TO DESCRIBE Sr ²⁺ AND Cs ⁺ BEHAVIOR ON SOILS SURROUNDING NUCLEAR FACILITIES <i>S. Savoye, C. Latrille, M. Krimissa, M. Lorthioy (France)</i>	PC3-1	234

PORE-SCALE MODELLING OF SOLUTE TRANSPORT IN PARTIALLY AND FULLY SATURATED POROUS MEDIA **PC3-2** 236
Y. Yang, R. A. Patel, G. Deissmann, J. Poonoosamy, D. Bosbach (Germany)

PC4 MODEL VALIDATION

	ID	PAGE
GEOCHEMISTRY AND MACHINE LEARNING BENCHMARK WITHIN EURAD JOINT PROJECT <i>N.I. Prasianakis, E. Laloy, D. Jacques, J.C.L. Meeussen, C. Tournassat, G.D. Miron, D. A. Kulik, A. Idiart, E. Demirer, B. Cochevin, M. Leconte, M. Savino, M. Marques Fernandes, J. Samper II, M. De Lucia, C. Yang, S. V. Churakov, V. Montoya, J. Samper, O. Kolditz, F. Claret (Switzerland, Belgium, The Netherlands, France, Spain, Germany, USA)</i>	PC4-1	238

PD APPLICATION TO CASE STUDIES

	ID	PAGE
A CRITICAL ANALYSIS OF THE RADIOECOLOGICAL MODEL USED IN THE GERMAN CALCULATION BASIS FOR THE ESTIMATION OF RADIATION DOSES DUE TO THE STORAGE OF HIGHLY ACTIVE NUCLEAR WASTE <i>V. Hormann, C. Walther (Germany)</i>	PD-1	240
TRANSPORT OF RADIOACTIVE WASTE ALONG THE SELLAFIELD SHORELINE: CLIMATE CHANGE IMPACT AND MITIGATION STRATEGIES THROUGH NATURE-BASED SOLUTIONS <i>L. Bacon-Hall, N. Leonardi, A. Plater, L. Abrahamsen-Mills, S. Kwong (UK)</i>	PD-2	242
PRELIMINARY LONG-TERM HYDROGEOCHEMICAL EVOLUTION STUDY CASE IN TAIWAN <i>Y.-H. Huang, P.-H. Kuo, P.-Y. Chuang, C.-C. Ke, P. Trinchero (Taiwan, Spain)</i>	PD-3	244
MICROBIAL IMPACT ON MINERALOGICAL TRAPPING OF URANIUM IN DEEP ANOXIC AQUIFERS: CASE STUDIES FOR ÄSPÖ HARD ROCK LABORATORY AND FORSMARK SITE, SWEDEN <i>I. Pidchenko, J. Christensen, M. Kutzschbach, K. Ignatyev, I. Puigdomenech, L. Krall, T. Rasbury, H. Drake (Sweden, USA, Germany, UK) (245)</i>	PD-4	246

PE CIGÉO AND NORM

	ID	PAGE
EFFECT OF CITRIC ACID AND MALIC ACID ON THE URANIUM UPTAKE INTO <i>BRASSICA NAPUS</i> PLANTS IN HYDROPONIC CULTURE <i>W. A. John, J. Jessat, R. Steudtner, R. Hübner, S. Sachs (Germany)</i>	PE-1	248
GEOCHEMICAL BEHAVIOR OF RADIUM IN A URANIUM MILL TAILINGS POND OF THE NINGYO-TOGE MINE AREA <i>K. Tanaka, Y. Kurihara, J. Tomita, I. Maamoun, S. Yamasaki, K. Tokunaga, K. Fukuyama, N. Kozai (Japan)</i>	PE-2	250

CONFERENCE ANNOUNCEMENT

9TH CLAY CONFERENCE, HANNOVER, GERMANY, 25 – 28 NOVEMBER
2024, SAVE THE DATE
A. Göbel (BGE) and J. Lippmann-Pipke (BGR)

TUESDAY (26. SEPTEMBER)**8:25 CONFERENCE ANNOUNCEMENTS****SESSION 6 C2: COUPLING CHEMISTRY AND TRANSPORT**Chair: *P. De Cannière (Belgium) and J. Soler (Spain)*

		ID	PAGE
8:30	TOWARDS A PROCESS-BASED MODEL DESCRIBING TRANSPORT-INDUCED CO-PRECIPITATION AND RADIONUCLIDE RETENTION. LAB ON CHIP EXPERIMENTS AND REACTIVE TRANSPORT MODELLING DIAGNOSTICS <i>J. Poonoosamy, E. Curti, A. Obaid, N. I. Prasianakis, G. Deissmann, S. Churakov, D. Bosbach (INVITED) (Germany, Switzerland)</i>	C2-1	252
9:15	CLAYSORDIF: A NEW MODEL FOR RADIONUCLIDE SORPTION AND DIFFUSION IN ARGILLACEOUS MEDIA (GEMS IMPLEMENTATION AND VERIFICATION AGAINST PHREEQC RESULTS AND EXPERIMENTAL DATA) <i>D. A. Kulik, M. A. Glaus, T. Gimmi, L. R. Van Loon, R. Wüst (Switzerland)</i>	C2-2	254
9:50	GLASS ALTERATION MODELISATION USING GRAAL2 MODEL <i>M. Delcroix, P. Frugier, C. Noiriél (France)</i>	C2-3	258
10:10	REACTIVE TRANSPORT MODELS OF LABORATORY CORROSION TESTS AT THE IRON/BENTONITE INTERFACE: FB4, FB5 AND FEMO TESTS <i>J. Samper, A. Mon, L. Montenegro, E. Torres, M. J. Turrero, J. Cuevas (Spain)</i>	C2-4	260
10:35	BREAK		

SESSION 7 A7: EXPERIMENTAL METHODSChair: *J.-I. Yun (Korea) and M. Schmidt (Germany)*

		ID	PAGE
10:55	RADIONUCLIDE DISTRIBUTIONS IN (TIME-RESOLVED) NATURAL ARCHIVES DETERMINED BY AMS <i>K. Hain, S. Adler, A. Cundy, T. Faestermann, K. Fenclová, K. Fifield, F. Gülce, G. Korschinek, M. Martschini, S. Pavetich, J. Pitters, G. Rugel, P. Steier, S. Tims, S. Turner, J. Wolf, J. Zinke (Austria, UK, Germany, Czech Republic, Australia)</i>	A7-1	262
11:20	ON THE TRACE (LEVEL) OF A HIGH-LEVEL NUCLEAR WASTE DISPOSAL - METHOD DEVELOPMENT FOR MIGRATION EXPERIMENTS USING HPLC, ICP-MS AND LA-ICP-MS <i>A. Haben, K. Brix, R. Kautenburger (Germany)</i>	A7-2	264

11:45	MULTI-TECHNIQUE ANALYSIS OF THE BEHAVIOR OF URANIUM IN NATURAL SOIL <i>S. Bayle, P. Crancon, P.-L. Solari, C. Den Auwer (France)</i>	A7-3	266
12:10	INVESTIGATING GEOCHEMICAL INTERACTIONS OF PLUTONIUM WITH OPALINUS CLAY AND HARDENED CEMENT PASTE VIA TOF-SIMS AND RL-SNMS <i>F. Berg, M. Breckheimer, T. Reich (Germany)</i>	A7-4	268
12:35	BREAK		

SESSION 8 A1: SOLUBILITY AND DISSOLUTIONChair: *S. Szenknect (France) and D. García (Spain)*

		ID	PAGE
14:00	SAFETY AND SCIENCE: THE FRAGILE CONNECTION – PART II <i>R. C. Ewing, B. Grambow (INVITED) (USA, France)</i>	A1-1	270
14:45	SPENT NUCLEAR FUEL IN CLOSED GLASS AMPOULES: RADIOLYSIS AND RADIONUCLIDE RELEASE AFTER ONE AND FIVE YEARS <i>L. Z. Evins, C. Askeljung, K. Johnson, A. Puranen, A. Barreiro Fidalgo, O. Roth, K. Spahiu (Sweden)</i>	A1-2	272
15:10	EFFECT OF TEMPERATURE ON THE OXIDATIVE DISSOLUTION OF UO ₂ DOPED WITH A RADIOACTIVE ALPHA EMITTER IN SYNTHETIC CALLOVIAN-OXFORDIAN GROUNDWATER IN THE PRESENCE OF IRON <i>V. Broudic, C. Marques, G. Jouan, M. Autillo, S. Miro, S. Peugeot, F. Tocino, C. Martin, L. De Windt, C. Jegou (France)</i>	A1-3	274
15:35	SOLUBILITY AND STRUCTURAL CHARACTERIZATION OF Zr(IV) HYDROUS OXIDES <i>C. Kiefer, T. Suzuki-Muresan, X. Gaona, D. Schild, O. Dieste Blanco, T. Kobayashi, D. Grekov, M. Calatayud, B. Grambow, H. Geckeis (France, Germany, Japan)</i>	A1-4	276
16:00	GEOLOGICAL DISPOSAL OF CARBON-14: FROM SOURCE TO SINK <i>W. Bower, A. Yorkshire, D. Lever, A. Hoch, S. Swanton, B. Swift, L. Payne, A. Cooke, S. Vines, S. Norris (UK)</i>	A1-5	278
16:25	BREAK		

SESSION 9 D: APPLICATION TO CASE STUDIESChair: *B. Grambow (France) and T. Sasaki (Japan)*

		ID	PAGE
16:45	RADIOCAESIUM MIGRATION WITHIN A FUKUSHIMA FOREST ECOSYSTEM AND THE ROLE OF BIOMONITORING <i>T. Dohi, T. Niizato, Y. Sasaki, K. Iijima (Japan)</i>	D-1	280

17:10	APPLICATION OF ACCELERATOR MASS SPECTROMETRY TO MEASURE RATIOS OF PLUTONIUM ISOTOPES AND EVALUATE AMERICIUM DISTRIBUTIONS AT THE LITTLE FOREST LEGACY SITE, AUSTRALIA <i>T. E. Payne, D. P. Child, T. Cunynghame, J. J. Harrison, M. A.C. Hotchkis, M. P. Johansen, L. Mokhber Shahin, A Silitonga, S. Thiruvoth (Australia)</i>	D-2	282
17:35	RENEWED LEAKAGE FROM SELLAFIELD'S MAGNOX SWARF STORAGE SILOS: OBSERVATIONS & OPPORTUNITIES FOR IMPROVED UNDERSTANDING OF RADIONUCLIDE MIGRATION <i>J. Graham, J. Heneghan (UK)</i>	D-3	283
18:00	APPROACH OF HANDLING THE SORPTION AND DIFFUSION HETEROGENEITY ACROSS THE OPALINUS CLAY AND ADJACENT CONFINING UNITS IN THE SAFETY CASE FOR THE SWISS DEEP GEOLOGICAL REPOSITORY <i>R. A. J. Wüst, L. R. Van Loon, M. A. Glaus, D. A. Kulik, M. Marques Fernandes, X. Li (Switzerland)</i>	D-4	285
18:25	END OF ORAL SESSIONS OF TUESDAY		

SESSION 10 POSTER SESSION II (19:00 – 22:00)**PA1 SOLUBILITY AND DISSOLUTION**

	ID	PAGE
TECHNETIUM DIOXIDE SOLUBILITY AT ELEVATED TEMPERATURES <i>M. Riss, S. L. Estes, B. A. Powell (USA)</i>	PA1-6	287
EVALUATING THE CHEMICAL DURABILITY OF IODINE BEARING GLASS SYNTHESIZED AT HIGH PRESSURE: VAPOR HYDRATION AND AQUEOUS ALTERATION STUDY <i>K. Roy, T. Suzuki-Muresan, V. Bosse, L. Campayo, Y. Morizet, A. Abdelouas (France)</i>	PA1-7	289
SOLUTION AND SOLID-LIQUID-EQUILIBRIUM PROPERTIES OF RADIONUCLIDE-NITRATE AQUEOUS SYSTEMS: EXPERIMENTS AND SIT PARAMETERIZATION <i>A. Lassin, P. F. dos Santos, X. Gaona, M. Altmaier, B. Madé (France, Germany)</i>	PA1-8	291
DISSOLUTION AND AGING OF METAL MONOURANATES: SIMULATED DEBRIS OF FUKUSHIMA DAIICHI NUCLEAR POWER STATION <i>T. Sasaki, Y. Kato, R. Tonna, T. Kobayashi, Y. Okamoto (Japan)</i>	PA1-9	293
STABILITY & PHYSICO-CHEMICAL CHARACTERISATION OF A RECONDITIONED WASTE FORM RELECANANT TO RADIOACTIVE WASTES <i>G. F. Vettese, T. Vierinen, T. Oey, S. Lanninmaki, T. Vehmas, M. Nieminen, J. Laatikainen-Luntama, M. Leivo, E. Myllykylä, G. T. W. Law (Finland)</i>	PA1-10	295

PA2 SOLID SOLUTION AND SECONDARY PHASE FORMATION

	ID	PAGE
SOLUBILITY EVALUATION OF THE COPRECIPITATE URANIUM AND PLUTONIUM OXIDE UNDER HYPERALKALINE AND REDUCING CONDITIONS IN THE CONTEXT OF DEEP DISPOSAL OF ILW RADIOACTIVE WASTES <i>M. Le Meur, T. Suzuki-Muresan, S. Ribet, C. Landesman, T. Verron, A. Piscitelli, B. Grambow (France)</i>	PA2-4	296
SOLUBILITY AND SOLID PHASE FORMATION IN THE Nd ₂ O ₃ -EuCl ₃ -NdCl ₃ -NaCl-H ₂ O(L) SYSTEM <i>R. M. Rao Dumpala, F. Heberling, X. Gaona, K. Garbev, D. Schild, M. Altmaier, H. Geckeis (Germany)</i>	PA2-5	298
STRUCTURE AND PROPERTIES OF CRYSTALLINE CERAMIC PHASES CONTAINING ACTINIDES – FROM BULK TO THE MOLECULAR LEVEL <i>N. Huittinen, L. Braga Ferreira dos Santos, S. E. Gilson, G. L. Murphy, S. Richter, K. Popa, O. Valu, V. Svitlyk, C. Hennig (Germany)</i>	PA2-6	300

PA3 COMPLEXATION WITH INORGANIC AND ORGANIC LIGANDS

	ID	PAGE
INVESTIGATION OF ACTINIDE SPECIATION AND COMPLEXATION WITH SMALL ORGANIC LIGANDS USING CE-ICP-MS <i>T. Reich, T. Kutyma, J. Lohmann, J. Stietz (Germany)</i>	PA3-6	302
INVESTIGATION OF THE CARBONATE COMPLEXATION OF ACTINIDES AND THE INFLUENCE OF ALKALI CATIONS USING CE-ICP-MS <i>J. Lohmann, T. Reich (Germany)</i>	PA3-7	304
COMPLEXATION OF Ni(II) WITH CITRATE IN CEMENTITIOUS SYSTEMS: THERMODYNAMIC DESCRIPTION <i>O. Almendros-Ginestà, S. Duckworth, T. Missana, M. Altmaier, X. Gaona (Spain, Germany)</i>	PA3-8	306
COMPLEXATION OF NEPTUNIUM(V) WITH AQUEOUS PHOSPHATE USING A DUAL EXPERIMENTAL AND QUANTUM CHEMICAL APPROACH <i>E. Miladi, F. Real, V. Vallet, N. Jordan, N. Huittinen (France, Germany)</i>	PA3-9	308
LUMINESCENCE SPECTROSCOPIC INVESTIGATIONS OF U(VI) COMPLEXATION WITH AQUEOUS SILICATES AT (HYPER)ALKALINE CONDITIONS <i>C. Shang, H. Oher, S. Duckworth, R. Polly, A. Skerencak-Frech, M. Altmaier, X. Gaona (Germany, France)</i>	PA3-10	310
SOLUBILITY OF Tc(IV) IN THE PRESENCE OF ISOSACCHARINIC ACID: THERMODYNAMIC DESCRIPTION <i>K. Kim, S. Duckworth, W. Um, M. Altmaier, X. Gaona (Korea, Germany)</i>	PA3-11	312

PA4 REDOX REACTIONS AND RADIOLYSIS EFFECTS

	ID	PAGE
DESIGN AND SYNTHESIS OF NOVEL D/A BULK HETEROJUNCTION ORGANIC CONJUGATED FILM MATERIALS AND PHOTOCATALYTIC REDUCTION FOR REMOVAL OF IONS <i>Z. Li (China)</i>	PA4-9	314
ROLE OF Fe-PHASES ON SELENITE MIGRATION IN BENTONITE: UP-SCALING FROM DISPERSED TO COMPACTED SYSTEM <i>U. Alonso, M. García-Gutiérrez, T. Missana (Spain)</i>	PA4-10	316
INFLUENCE OF IRON OXIDE NANOPARTICLE CRYSTALLITE SIZE ON THE SORPTION AND REDUCTION OF PLUTONIUM <i>F. E. Zengotita, M. R. Vejar, A. E. Hixon (USA)</i>	PA4-11	318
PLUTONIUM REDOX CHEMISTRY IN THE PRESENCE OF CITRATE <i>M. B. Comins, A. E. Hixon, J. Beam, J.-F. Lucchini (USA)</i>	PA4-12	320
REDOX BEHAVIOUR AND SPECIATION OF PLUTONIUM IN THE PRESENCE OF ALUMINIUM-DOPED IRON OXIDE MINERAL SURFACES <i>M. R. Vejar, F. E. Zengotita, S. E. Bone, D. Sokaras, S. Weiß, S. Shams Aldin Azzam, N. M. Huittinen, E. F. Bazarkina, K. O. Kvashnina, A. E. Hixon (USA, Germany, France)</i>	PA4-13	322
THE REDOX BEHAVIOR OF URANIUM AND SELENIUM UNDER RADWASTE REPOSITORY CONDITION <i>M. Kang, Y. Kang, W. Jin, J. She, Q. Lin, J. Wang (China)</i>	PA4-14	324
SELENITE SORPTION STUDIES ONTO Fe(II) - AND Fe(III) - NONTRONITES <i>F. J. León Vicente, A. M. Fernández, T. Missana (Spain)</i>	PA4-15	326
IS THERE A ROLE FOR Pu(III) IN PREDICTING THE SUBSURFACE MIGRATION OF PLUTONIUM? <i>D. T. Reed (USA)</i>	PA4-16	328

PA5 SOLID-WATER INTERFACE REACTIONS

	ID	PAGE
DETERMINATION OF URANIUM(VI) SPECIATION DURING SORPTION TO GIBBSITE USING PARALLEL FACTOR ANALYSIS ON EXCITATION EMISSION MATRICES <i>L. Lopez-Odrizola, S. Shaw, L. Abrahamsen-Mills, L. Natrajan (UK)</i>	PA5-17	330
THE COMBINED EFFECT OF ISA- AND Ca-CONCENTRATION ON Pu-SORPTION TO A CEM III/C-BASED MORTAR FOR IMMOBILIZATION OF NUCLEAR WASTE <i>K. Wouters, E. Coppens, B. de Blohouse, D. Durce (Belgium)</i>	PA5-18	332
THE EFFECT OF CELLULOSE DEGRADATION PRODUCTS ON THE SORPTION AND DIFFUSION OF NICKEL IN DEGRADED HARDENED CEMENT PASTE <i>D. Durce, N. Bleyen, K. Wouters, N. Maes (Belgium)</i>	PA5-19	334

- RETENTION OF RADIONUCLIDES (CAESIUM, NICKEL) IN FRACTURE INFILLS UNDER DIFFERENT GEOCHEMICAL CONSTRAINTS **PA5-20** 336
F. Jankovský, K. Kočan, V. Havlová, M. Zuna, L. Mareda (Czech Republic)
- INFLUENCE OF THE COMPETITION OF AI ON THE RETENTION OF TRIVALENT ACTINIDES AND THEIR HOMOLOGUES IN FELDSPAR **PA5-21** 338
J. Lessing, J. Neumann, F. Bok, J. Lützenkirchen, V. Brendler, M. Schmidt, T. Stumpf (Germany, USA)
- CHEMICAL TOMOGRAPHY OF PYRITE COMPOSITES EXTRACTED FROM OPALINUS CLAY AND REACTED WITH NEPTUNIUM AND PLUTONIUM **PA5-22** 340
M. Breckheimer, S. Amayri, D. Ferreira Sanchez, D. Grolimund, T. Reich (Germany, Switzerland)
- INTERACTIONS BETWEEN RADIONUCLIDES AND CALCITE SURFACE **PA5-23** 342
X. Li, M. Matulova, A. Sticker, E. Puhakka, S. Guo, M. Delnero, F. Jankovsky, L. Mareda, M. Siitari-Kauppi (Finland, Czech Republic, Germany, France)
- THE STUDY OF MARINE SOLUTIONS INFLUENCES ON THE SORPTION OF ^{226}Ra TO MINERALS **PA5-24** 344
J. Wang, B. A. Powell (USA)
- MOLECULAR SCALE UNDERSTANDING OF Ni^{2+} ADSORPTION ON SWELLING CLAY MINERALS **PA5-25** 345
V. Stotskyi, F. Di Lorenzo, M. Marques Fernandes, M. Krack, A. Scheinost, M. Lanson, B. Lanson, S. V. Churakov (Switzerland, Germany, France)
- SORPTION PROPERTIES OF Eu ONTO GRANITE AND MX-80 BENTONITE IN Ca-Na-Cl SOLUTIONS **PA5-26** 347
J. Liu, S. Nagasaki, T. Yang (Canada)
- SORPTION OF SELECTED RADIONUCLIDES ON CANADIAN SEDIMENTARY AND CRYSTALLINE ROCKS UNDER SALINE CONDITIONS **PA5-27** 349
T. Yang, S. Nagasaki (Canada)
- UPTAKE OF NIOBIUM BY CEMENT AND C-S-H PHASES IN THE ABSENCE AND PRESENCE OF ISA AND CHLORIDE: QUANTITATIVE DESCRIPTION AND MECHANISTIC UNDERSTANDING **PA5-28** 350
Y. Jo, N. Cevirim-Papaioannou, M. Fuss, K. Franke, B. de Blohouse, M. Altmaier, X. Gaona (Germany, Korea)
- INFLUENCE OF Na-Ca-Cl AND Ca-Na-Cl PHYSICO-CHEMICAL SOLUTION PROPERTIES ON THE ADSORPTION OF $^{79}\text{Se}(\text{-II})$ AND $^{99}\text{Tc}(\text{IV})$ ONTO SEDIMENTARY AND CRYSTALLINE ROCKS **PA5-29** 352
J. Racette, S. Nagasaki, T. Yang (Canada)
- INFLUENCE OF TEMPERATURE ON CATION ION EXCHANGE AND SORPTION TO MONTMORILLONITE CLAY **PA5-30** 353
B. A. Powell, R. Williams, X. Tang, S. Kwong-Moses, M. Riss, S. L. Estes (USA)
- PLUTONIUM ADSORPTION TO HEMATITE AT VARIABLE pH, TEMPERATURE, AND CONCENTRATION **PA5-31** 355
S. Kwong-Moses, S. L. Estes, B. A. Powell (USA)
- METAL IONS ADSORPTION AND MODELING ON A PRE-NEOGENE SEDIMENTARY ROCK **PA5-32** 357
L. Hou, K. Toda, T. Saito (Japan)

PA6 COLLOID FORMATION

	ID	PAGE
STRENGTHENED EROSION RESISTANCE OF COMPACTED BENTONITE BY OPPOSITELY-CHARGED MATERIALS: FROM COLLOIDAL PARTICLES INTERACTION TO EROSION EXPERIMENTS <i>Z. Chen, G. Zu, H. Hou, Z. Zhang, P. Gao, Q. Jin, W. Wu, Z. Guo (China)</i>	PA6-4	359
PROBING THE NUCLEATION AND GROWTH OF PuO ₂ NANOPARTICLES IN AQUEOUS SOLUTION <i>S. Bayle, M. Virost, T. Dumas, X. Le Goff, D. Menut, S. Dourdain, S. I. Nikitenko (France)</i>	PA6-5	361

PA7 EXPERIMENTAL METHODS

	ID	PAGE
GEOCHEMICAL INFLUENCE ON THE RADIONUCLIDE MOBILITY IN GEOLOGICAL FORMATIONS ANALYSED BY ICP-MS AND ICP-QQQ COUPLING METHODS <i>R. Kautenburger, K. Brix, A. Haben (Germany)</i>	PA7-5	363
SIMULTANEOUS DETERMINATION OF TRANSURANIUM RADIONUCLIDES BY COMPACT ACCELERATOR MASS SPECTROMETRY <i>S. Xing, C. Peng, M. Christl, K. Shi, H.-A. Synal, X. Hou, N. Kuzmenkova (China, Switzerland, Russia)</i>	PA7-6	365
IMPROVED SOLID PHASE EXTRACTION MATERIALS FOR Sr-90 AND Cs-137 <i>J. He (China)</i>	PA7-7	367
MIXED FROM A WASTE COCKTAIL: CONSIDERATIONS ON BACKGROUND ELECTROLYTE'S COMPOSITION AND SALINITY, PBTC AND IRON INFLUENCING THE RETENTION OF REPOSITORY-RELEVANT ELEMENTS ON POTENTIAL BARRIER MATERIALS <i>K. Brix, A. Haben, R. Kautenburger (Germany)</i>	PA7-8	368
X-RAY ANALYSES ON RADIOACTIVE MATTER AT THE MARS BEAMLINER OF SYNCHROTRON SOLEIL <i>P. L. Solari, D. Menut, M. Hunault, W. Breton (France)</i>	PA7-9	370

PA8 COMPUTATIONAL CHEMISTRY

	ID	PAGE
MOLECULAR UNDERSTANDING OF HYDROGEN ADSORPTION AND TRANSPORT IN HYDRATED Na- AND Ca-MONTMORILLONITES IN THE CONTEXT OF GEOLOGICAL DISPOSAL OF RADIOACTIVE WASTE <i>P. Citli, A. Kalinichev (France)</i>	PA8-5	371
MOLECULAR LEVEL INSIGHTS ON THE PHYSISORPTION MECHANISMS OF HYDROGEN GAS ON MONTMORILLONITE CLAY SURFACES <i>S. M. Mutisya, A. G. Kalinichev (France)</i>	PA8-6	372

MOLECULAR DYNAMICS COMPUTER SIMULATIONS OF THE EFFECTS OF ORGANIC MOLECULES ON THE CLAY-RADIONUCLIDE INTERACTIONS IN THE CONTEXT OF GEOLOGICAL DISPOSAL OF RADIOACTIVE WASTE **PA8-7** 373
J. Licko, A. G. Kalinichev (France)

SITE-SPECIFIC STRUCTURE AND ENERGETICS OF URANYL ADSORPTION AT HYDRATED MUSCOVITE (001) SURFACE PROBED BY CLASSICAL MOLECULAR DYNAMICS SIMULATIONS **PA8-8** 375
N. Loganathan, A. G. Kalinichev (USA, France)

PB2 DIFFUSION AND OTHER MIGRATION PROCESSES

	ID	PAGE
IN SITU INVESTIGATIONS: RADIONUCLIDE MOBILITY AT CONCRETE-ROCK-INTERFACE <i>J. Sammaljärvi, X. Li, A. Martin, U. Mäder, M. Siitari-Kauppi (Finland, Switzerland)</i>	PB2-10	377
HOW STRONG DOES NICKEL AFFECT THE SORPTION AND DIFFUSION OF ZINC IN COMPACTED ILLITE? <i>L. Van Laer, D. Verhaegen, M. Aertsens, N. Maes (Belgium)</i>	PB2-11	379
INTERACTION OF RADIONUCLIDES WITH FRACTURE FILLINGS AND MIGRATION THROUGH A MATRIX OF CRYSTALLINE HOST ROCK <i>M. Zuna, F. Jankovský, K. Kočan, V. Znamínko, E. Bedrníková (Czech Republic)</i>	PB2-12	381
STUDY OF THE INFLUENCE OF FRACTURE FILLINGS ON RADIONUCLIDE TRANSPORT IN CRYSTALLINE ROCK SYSTEMS <i>M. Zuna, F. Jankovský, K. Kočan, J. Smutek, J. Kulenkampff (Czech Republic)</i>	PB2-13	383
HOW DO ALTERATION AND STRUCTURAL HETEROGENEITIES INFLUENCE DIFFUSIVITY WITHIN GRANODIORITES? <i>A. Kusturica, T. Schäfer (Germany)</i>	PB2-14	385
ASSESSMENT OF CESIUM MIGRATION IN THE SHALLOW GROUNDWATER-SOIL SYSTEM OF A PROPOSED NNP SITE <i>L. Sun, Q. Lin, D. Chen, W. Chen, Y. Chen, J. Yang, Y. Li, H. Wu, M. Kang (China)</i>	PB2-15	387
OUT-LEACHING EXPERIMENTS OF ROCK CORES AFTER IRRADIATION BY NEUTRONS; STUDY OF PORE WATER SALINITY IN CRYSTALLINE ROCK <i>M. Nyman, N. Pakkanen, X. Li, K. Helariutta, M. Siitari-Kauppi, L. Aioanei, T. Morales, A.-M. Jakobsson, J. Byegård (Finland, Romania, Sweden)</i>	PB2-16	389
THE MIGRATION BEHAVIOR OF RADIOACTIVE COBALT AT THE REGION FOR A PROPOSED NUCLEAR POWER PLANT: EXPERIMENTS AND SIMULATION STUDIES <i>Q. Lin, L. Sun, J. Zhou, D. Chen, W. Chen, Y. Chen, J. Yang, Y. Li, H. Wu, M. Kang (China)</i>	PB2-17	391

PB3 COLLOID MIGRATION

	ID	PAGE
INSIGHT INTO IMPACT OF PHOSPHATE ON THE COTRANSPORT AND CORELEASE OF Eu(III) WITH BENTONITE COLLOIDS IN SATURATED QUARTZ COLUMNS <i>Q. Tang, Z. Xu, D. Pan, W. Wu (China)</i>	PB3-3	393
CO-TRANSPORT OF U(VI) AND COLLOIDAL BIOCHAR IN QUARTZ SAND HETEROGENEOUS MEDIA <i>Q. Jin, Y. Sun, Z. Chen, Z. Guo (China)</i>	PB3-4	395
COLLOID-MEDIATED TRANSPORT AND MECHANISM OF U(VI/IV) IN REDUCTION CONDITIONS <i>D. Pan, X. Wei, X. Shi, W. Wu (China, Switzerland)</i>	PB3-5	397

PB4 EFFECTS OF BIOLOGICAL AND ORGANIC MATERIALS

	ID	PAGE
EXPLORATION OF THE BIO-REDUCTION BEHAVIOR AND MECHANISM OF ⁹⁹ Tc(VII) BY <i>KLEBSIELLA VARIICOLA</i> STRAIN X-21 <i>J. Gong, S. Chen, Y. Guo, F. Li, T. Lan, Y. Yang, J. Liao, N. Liu (China)</i>	PB4-8	399
OVERVIEW ON THE EURAD WORKPACKAGE CORI (CEMENT-ORGANIC-RADIONUCLIDE-INTERACTIONS) <i>M. Altmaier, D. Garcia, P. Henocq, N. Mace, T. Missana, D. Ricard, J. Vandenborre (Germany, Spain, France)</i>	PB4-9	401
IMPACT OF THE DEGRADATION PRODUCTS OF UP2W FILTER AID MATERIAL ON THE UPTAKE OF RADIONUCLIDES BY CEMENT <i>P. Szabó, A. Tasi, X. Gaona, A. C. Maier, S. Hedström, M. Altmaier, H. Geckeis (Germany, Sweden)</i>	PB4-10	403
INFLUENCE OF MICROORGANISMS ON THE MOBILITY OF +3 ACTINIDES FROM THE WASTE ISOLATION PILOT PLANT <i>J. Swanson, A. Navarrette, F. Stanley, H. Kim, J. Knox (USA)</i>	PB4-11	404
IMPACT OF THE EXTRACTION OF SOLUBLE ORGANIC MATTER (SOM) FROM SOILS ON THE QUALITY OF INSOLUBLE ORGANIC MATTER (IOM) IN VIEW OF PROTON BINDING SITES AND RADIONUCLIDE BINDING <i>M. Tesfa, J. Raya, R. Gougeons, P. Schmitt-Kopplin, G. Montavon (France, Germany)</i>	PB4-12	406
CHARACTERIZATION OF BOOM CLAY (BC) DISSOLVED ORGANIC MATTER (DOM) AND ITS INTERACTION WITH RADIONUCLIDES <i>M. Bouby, A. Thumm, A. Lunz, F. Geyer, C. Beiser, M. Altmaier, H. Geckeis, S. Brassinnes (Germany, Belgium)</i>	PB4-13	408

PB5 FIELD AND LARGE-SCALE EXPERIMENTS

	ID	PAGE
PLUTONIUM TRANSPORT IN VADOSE ZONE SEDIMENTS UNDER ACIDIC SOLUTION CONDITIONS AT THE HANFORD SITE, USA <i>T. Baumer, M. Zavarin, C. Pearce, H. P. Emerson, A. B. Kersting (USA)</i>	PB5-6	410

STUDY OF THE MIGRATION BEHAVIOUR OF ANTHROPOGENIC ACTINIDES IN LAKE SEDIMENTS AND PEAT BOG CORES <i>J. Wolf, S. Glatzel, R. Golser, A. Maier, M. Meszar, P. Steier, M. Strasser, M. Wagreich, A. Wiederin, K. Hain (Austria, Germany)</i>	PB5-7	411
FULL-SCALE PROTOTYPE, A LONG-TERM EXPERIMENT AT ÄSPÖ LABORATORY, SWEDEN <i>T. Morales Aguilera, J. Dahlström, S. Pontér, L. Alakangas, M. Kronberg (Sweden)</i>	PB5-8	413
URANIUM SPECIATION IN SOILS AND SEDIMENTS IMPACTED BY ACIDIC RUNOFF ORIGINATING FROM ALUM SHALE WASTE ROCK <i>M. K. Pelkonen, E. Reinoso-Maset (Norway)</i>	PB5-9	415
PLUTONIUM AND Cs-137 MOBILITY IN AN EPHEMERAL STREAM BED AT NEVADA NATIONAL SECURITY SITE (NNSS), USA <i>N. L. Wasserman, J. Stanberry, A. B. Kersting, M Zavarin (USA)</i>	PB5-10	416

PB6 NATURAL ANALOGUES

	ID	PAGE
HYDRO-GEOPHYSICAL APPROACH TO UNDERSTAND THE DEPOSITIONAL AND GEOCHEMICAL CHARACTERISTICS OF THE URANIUM DEPOSITS IN THE OKCHEON METAMORPHIC BELT, KOREA <i>S.-S. Lee, D. Shin, S.-W. Jeon, M. S. Sim, M.-H. Baik, J.-H. Ryu, Y. Yu, K.-K. Lee (Korea)</i>	PB6-3	418

PC1 DATA SELECTION AND EVALUATION

	ID	PAGE
THE PSI CHEMICAL THERMODYNAMIC DATABASE TDB 2020 TO SUPPORT NAGRA SAFETY ASSESSMENTS FOR DEEP GEOLOGICAL REPOSITORY <i>G. D. Miron, D. A. Kulik, R Wüst (Switzerland)</i>	PC1-6	420
SOLUBILITY ASSESSMENT IN CRYSTALLINE AND SEDIMENTARY ROCKS <i>E. Colàs, O. Riba, J. Rodríguez-Mestres, A. Valls, D. García, T. Yang, L. Duro (Spain, Canada)</i>	PC1-7	422
BENCHMARKING THE THERMOCHEMISTRY DATABASE FOR ITS APPLICATION TO CEMENTITIOUS AND ARGILLACEOUS ENVIRONMENTS <i>D. Jacques, S. Liu, V. Montoya, B. Madé, W. Bower, S. Brassinnes (Belgium, France, UK)</i>	PC1-8	424
THEREDA - THERMODYNAMIC REFERENCE DATABASE <i>X. Gaona, V. Brendler, D. Freyer, H. Moog, L. Wissmeier (Germany, Switzerland)</i>	PC1-9	425
DIGITIZATION OF LITERATURE DATA AND SURFACE COMPLEXATION MODEL PARAMETER ESTIMATION FOR TRIVALENT AMERICIUM, CURIUM, AND EUROPIUM SORPTION <i>E. Fix, F. M. Coutelot, M. Zavarin, B. A. Powell (USA)</i>	PC1-10	426

STATE OF THE ART REPORT IN REDOX AND KINETICS APPLIED TO NUCLEAR WASTE DISPOSAL FACILITIES **PC1-11** 428
O. Riba, X. Gaona, P. E. Reiller, E. Colàs, G. Román-Ross, J. Begg, D. García, L. Duro, S. Brassinnes, B. Madé, W. Bower (Spain, Germany, France, Belgium, UK)

PC2 COUPLING CHEMISTRY AND TRANSPORT

	ID	PAGE
REACTIVE TRANSPORT MODEL OF THE LONG-TERM GEOCHEMICAL EVOLUTION AT THE DISPOSAL CELL SCALE IN A HLW REPOSITORY IN GRANITE <i>J. Samper, L. Montenegro, A. Mon, L. De Windt, A.-C. Samper, E. García (Spain, France)</i>	PC2-4	430

DEVELOPMENT AND IMPROVEMENT OF NUMERICAL METHODS AND TOOLS FOR MODELLING COUPLED PROCESSES <i>F. Claret, G. Pepin, C. Cances, O. Kolditz, N. Prasianakis, A. Baksay, D. Lukin (France, Germany, Switzerland, Hungary, Czech Republic)</i>	PC2-5	432
--	--------------	-----

VARS GLOBAL SENSITIVITIES FOR REACTIVE TRANSPORT SIMULATIONS IN A HLW REPOSITORY IN GRANITE <i>J. Samper, C. López, A. Mon, B. Pisani, A.-C. Samper, J. Samper, F. Lentijo (Spain, Uruguay)</i>	PC2-6	433
--	--------------	-----

PC3 DEVELOPMENT AND APPLICATION OF MODELS

	ID	PAGE
SUPPORTING TOOLS IN THE DEVELOPMENT OF THE THERMOCHIMIE DATABASE: THE XCHECK TOOL <i>D. Pérez, J. Rodríguez-Mestres, E. Colàs, D. García, L. Duro, L. Harvey, W. Bower, S. Brassinnes, B. Madé (Spain, UK, Belgium, France)</i>	PC3-3	435

PC5 SAFETY ASSESSMENT AND REPOSITORY CONCEPTS

	ID	PAGE
APPROACH OF CONSEQUENCE ANALYSES SUPPORTING THE SAFETY-BASED COMPARISON OF THE CANDIDATE SITING REGIONS FOR THE SWISS DEEP GEOLOGICAL REPOSITORY <i>X. Li, O. X. Leupin, N. Diomidis, R. Wüst (Switzerland)</i>	PC5-1	437

PD APPLICATION TO CASE STUDIES

	ID	PAGE
THE UK'S RADIOACTIVE WASTE MANAGEMENT AND ENVIRONMENTAL REMEDIATION (RADER) NATIONAL NUCLEAR USER FACILITY <i>K. Morris, F. Livens, J. Lloyd, S. Shaw, A. Stockdale (UK)</i>	PD-5	439
EFFECT OF SEASONAL ANOXIA ON TRACE ELEMENT AND PLUTONIUM CYCLING IN A WARM MONOMICTIC LAKE <i>F. Coutelot, J. Wheeler, R. Williams, N. Edayilam, N. Merino, N. Wasserman, D. I. Kaplan, A. B. Kersting, B. A. Powell, M. Zavarin (USA)</i>	PD-6	440

PRELIMINARY APPROACH FOR SAFETY DISPOSAL OF RADIOACTIVE WASTES FROM FDNPS FOR OPTIMIZATION OF WASTE MANAGEMENT STREAM **PD-7** 442
K. Iikima (Japan)

OVERVIEW OF THE JAPANESE RADIOACTIVE WASTE DISPOSAL PROJECT **PD-8** 444
A. Koike, K. Ishida, K. Kaku (Japan)

PE CIGÉO AND NORM

ID **PAGE**
 MODELING OF HYDROGEOCHEMICAL PROCESSES INFLUENCING URANIUM MIGRATION IN ANTHROPIZED SUB-SAHARAN ENVIRONMENTS **PE-3** 446
L. De Windt, P. Grizard, C. Besançon, N. Seigneur, P. E. Reiller, M. Descostes (France)

HIGHLY SENSITIVE QUANTIFICATION OF AQUATIC NANOPARTICLES BY LIBD **PE-4** 447
T. Verron, M. Le Meur, M. Dia, P.-E. Peyneau, G. Montavon, B. Béchet, A. Piscitelli (France, Germany)

BACTERIAL DIVERSITY DOWNSTREAM FROM A FORMER URANIUM MINE AND IN WATERS FROM NATURALLY RADIOACTIVE MINERAL SOURCES: POTENTIAL ROLE ON URANIUM MIGRATION IN THE ENVIRONMENT **PE-5** 449
C. Sergeant, G. Holub, C. Mallet, M.-H. Vesvres, A. Beauger, P. Chardon, M. del Nero, O. Courson, G. Montavon, V. Breton (France)

WEDNESDAY (27. SEPTEMBER)8:25 **CONFERENCE ANNOUNCEMENTS****SESSION 11 A5: SOLID-WATER INTERFACE REACTIONS**Chair: *S. Brassinnes (Belgium) and M. Zavarin (USA)*

		ID	PAGE
8:30	ELECTROSTATIC INTERACTIONS AT CLAY MINERAL SURFACES: AT THE CROSSROADS BETWEEN MINERALOGY, GEOCHEMISTRY, AND GEOPHYSICS <i>C. Tournassat (INVITED) (France, USA)</i>	A5-5	451
9:15	U(VI) SORPTION ON ILLITE IN THE PRESENCE OF CARBONATE STUDIED BY CRYOGENIC TIME-RESOLVED LASER FLUORESCENCE SPECTROSCOPY AND PARALLEL FACTOR ANALYSIS: COMPARISON WITH TRIVALENT LANTHANIDES <i>H. Mei, N. Aoyagi, T. Saito, Y. Sugiura, T. Ishidera, K. Tanaka, Y. Tachi (Japan)</i>	A5-6	452
9:40	RETENTION OF SILVER IN CEMENTITIOUS MATERIALS <i>N. Macé, J. Page (France)</i>	A5-7	454
10:05	ANALYSIS OF COBALT RETENTION BY Na- AND Ca- SMECTITE AND THE EFFECT OF EDTA PRESENCE <i>T. Missana, U. Alonso, M. García-Gutiérrez (Spain)</i>	A5-8	456
10:30	ACTINIDE ADSORPTION TO HEMATITE AT ELEVATED TEMPERATURES <i>S. L. Estes, S. Kwong-Moses, F. M. Coutelot, B. A. Powell (USA)</i>	A5-9	458
10:55	BREAK		

SESSION 12 A4: REDOX REACTIONS AND RADIOLYSIS EFFECTSChair: *L. Duro (Spain) and D. Reed (USA)*

		ID	PAGE
11:15	EFFICIENT PHOTOREDUCTION STRATEGY FOR URANIUM IMMOBILIZATION BASED ON GRAPHITE CARBON NITRIDE HETEROJUNCTION NANOCOMPOSITES <i>S. Li, D. Pan, W. Wu (China)</i>	A4-1	460
11:40	URANIUM(VI) REDUCTION BY A DESULFITOBACTERIUM SPECIES IN PURE CULTURE AND IN ARTIFICIAL MULTISPECIES BIO-AGGREGATES <i>S. Hilpmann, I. Jeschke, D. Deev, M. Zupan, A. Lapanje, T. Rijavec, R. Hübner, F. Bok, S. Schymura, A. Cherkouk (Germany, Slovenia)</i>	A4-2	462
12:05	THE IMPACT OF SULFIDATION ON MAGNETITE-BOUND ⁹⁹ Tc <i>T. Neill, O. Stagg, S. Shaw, K. Morris (UK, USA)</i>	A4-3	464

- | | | | |
|-------|---|-------------|-----|
| 12:30 | RECENT EXPERIMENTAL DEVELOPMENTS ON PLUTONIUM OXIDATION STATE DISTRIBUTION UNDER WIPP RELEVANT CONDITIONS
<i>J.-F. Lucchini, U. Kaplan, A. E. Navarrette, J. L. Knox, C. Kutahyali Aslani, J. Beam (USA)</i> | A4-4 | 466 |
| 12:55 | REDUCTION OF PERTECHNETATE BY MAGNETITE – INFLUENCE OF pH AND TIME
<i>T. Zimmermann, A. F. Oliveira, N. Mayordomo, A. C. Scheinost (Germany, France)</i> | A4-5 | 468 |
| 13:20 | END OF ORAL SESSIONS OF WEDNESDAY | | |

THURSDAY (28. SEPTEMBER)**8:25 CONFERENCE ANNOUNCEMENTS****SESSION 13 B2: DIFFUSION AND OTHER MIGRATION PROCESSES**Chair: *M. Glaus (Switzerland) and M. Siitari-Kauppi (Finland)*

		ID	PAGE
8:30	MIGRATION OF REDOX-SENSITIVE PLUTONIUM AND NEPTUNIUM IN OPALINUS CLAY ROCK: DEEPER INSIGHTS FROM IN-SITU REACTIVE TRANSPORT PATTERNS <i>D. Grolimund, S. Amayri, U. Kaplan, M. Breckheimer, P. J. B. Börner, T. Reich (Switzerland, Germany)</i>	B2-1	470
8:55	DIFFUSIVE TRANSPORT OF U(VI) AND AM(III) THROUGH OPALINUS CLAY STUDIED DOWN TO ULTRA-TRACE LEVELS <i>D. Glückman, F. Quinto, C. Joseph, V. Metz, K. Hain, P. Steier, H. Geckeis (Germany, Austria)</i>	B2-2	472
9:20	EFFECT OF THE WATER SATURATION ON THE DIFFUSION OF WATER AND SOLUTES IN REFERENCE CLAY-RICH POROUS MEDIA <i>L. Desert, S. Savoye, E. Ferrage, P. Hénocq, C. Tournassat, E. Tertre (France)</i>	B2-3	474
9:45	IMPACT OF CRACKING ON THE TRANSFER OF RADIONUCLIDES IN CEMENTITIOUS MATERIALS <i>J. Marliot, P. Sardini, C. Landesman, P. Henocq, M. Siitari-Kauppi, S. Hedan, J. Bodin (France, Finland)</i>	B2-4	476
10:10	BREAK		

SESSION 14 E: CIGÉOChair: *J.-C. Robinet (France) and P. Toulhoat (France)*

		ID	PAGE
10:30	DEVELOPMENT OF R&D ON RADIONUCLIDE MIGRATION FOR CIGÉO <i>J.-C. Robinet, C. Martin (INVITED) (France)</i>	E-1	478
11:15	IN SITU DIFFUSION OF ORGANIC COMPOUNDS IN ANDRA'S UNDERGROUND LABORATORY: A 4-YEAR INSIGHT FROM THE "DRO" EXPERIMENT <i>R. V. H. Dagnelie, S. Wechner, M. Labat, S. Daumas, C. Le Milbeau, Y. Lettry, M. Lundy (France, Germany, Switzerland)</i>	E-2	479
11:40	EVALUATING RADIONUCLIDES MOBILITY <i>IN SITU</i> IN THE CALLOVIAN-OXFORDIAN ARGILLACEOUS ROCK <i>M. I. Agnel, R. V. H. Dagnelie, E. Thory, B. Hautefeuille, Y. Lettry, M. Parisi, A. Vinsot (France, Switzerland)</i>	E-3	481

12:05 QUANTITATIVE ANALYSIS OF RADIONUCLIDE CONTAINMENT AS PART OF THE SAFETY ASSESSMENTS IN THE GERMAN SITE SELECTION PROCEDURE
C. Behrens, M. Gelleszun, S. Miro, A. Renz, P. Kreye, W. Rühaak (Germany)

E-4 484

12:30 **BREAK****SESSION 15 E: NORM**Chair: *G. Montavon (France) and T. Schäfer (Germany)*

	ID	PAGE
14:00 WHAT RESEARCH CHALLENGES FOR NORM AND TE-NORM MANAGEMENT WORLDWIDE? <i>L. Fevrier (INVITED) (France)</i>	E-5	486
14:45 MODELLING OF RADIONUCLIDES MOBILITY AFTER LEGACY SITE RESTORATION: THE CASE OF FLUORITE SLUDGE NORM <i>M. Plachciak, F. Grandia (Spain)</i>	E-6	486
15:10 UNDERSTANDING URANIUM FATE IN WETLAND SOILS: A SPECIATION AND LABILE BEHAVIOR STUDY IN THE FORMER EXTRACTION MINE OF ROPHIN (FRANCE) <i>A.-L. Nivresse, C. Landesman, T. Arnold, S. Sachs, T. Stumpf, A. Scheinost, F. Coppin, L. Fevrier, C. Den Auwer, A. Gourgiotis, M. Del Nero, G. Montavon (France, Germany)</i>	E-7	489
15:35 MODELLING WATER CIRCULATION AND SOLUTE TRANSPORT AT A FORMER FRENCH URANIUM MINING SITE <i>A. Katz, E. Veilly, L. Février, D. Pérez-Sánchez, T. Arnold, F. Bok, G. Montavon, C. Bertin, P. Chardon, D. Sarramia, P. Vaudelet, C. Mallet, L. Urso (France, Germany)</i>	E-8	491
16:00 BREAK		

SESSION 16 A3: COMPLEXATION WITH INORGANIC AND ORGANIC LIGANDSChair: *M. Altmaier (Germany) and W. Cha (Korea)*

	ID	PAGE
16:20 THE AQUATIC CHEMISTRY OF PENTAVALENT ACTINIDES (Np, Pu): DETERMINATION OF THE FIRST TWO HYDROLYSIS CONSTANTS <i>J. Aupiais, C. Chistin, M. Levier (France)</i>	A3-1	493
16:45 SPECTROSCOPIC STUDY ON FORMATION OF AQUEOUS URANIUM(VI)-SILICATE COMPLEXES AT ALKALINE pH <i>T.-H. Kim, E. C. Jung, Y. Jo, H.-K. Kim, H.-R. Cho, W. Cha, J.-I. Yun (Korea)</i>	A3-2	495

- | | | | |
|-------|--|-------------|-----|
| 17:10 | STRUCTURAL IDENTIFICATION OF AQUATIC U(VI)-PBTC COMPLEXES BY SPECTROSCOPIC INVESTIGATIONS
<i>A. Wollenberg, J. Kretzschmar, S. Tsushima, R. Kraft, M. Kumke, M. Acker, S. Taut, T. Stumpf (Germany)</i> | A3-3 | 497 |
| 17:35 | CHEMICAL EQUILIBRIUM OF PLUTONIUM(VI) IN WEAKLY ALKALINE SYSTEMS CONTAINING ALKALINE EARTH METAL IONS AND CARBONATE
<i>Y. Jo, H.-R. Cho, X. Gaona, D. Fellhauer, K. Dardenne, J. Rothe, M. Altmaier, J.-I. Yun (Korea, Germany)</i> | A3-4 | 499 |
| 18:00 | END OF ORAL SESSIONS OF THURSDAY.
MOVE TO BANQUET | | |

FRIDAY (29. SEPTEMBER)**8:25 CONFERENCE ANNOUNCEMENTS**

- 8:30 EURAD, A EUROPEAN PROGRAMME ON RADIOACTIVE WASTE MANAGEMENT, SCIENTIFIC OUTCOMES AND CHALLENGES AS SEEN BY THE EXTERNAL ADVISORY BOARD **D-5** 501
P. Toulhoat, S. Engstroem Laarouchi, P. Lalieux, H. Wanner (INVITED)
(France, Sweden, Belgium, Switzerland)

SESSION 17 A6: COLLOIDS

Chair: *U. Alonso (Spain) and M. Bouby (Germany)*

- | | | ID | PAGE |
|-------|--|-------------|-------------|
| 9:05 | FORMATION, REACTIVITY AND COLLOIDAL BEHAVIORS OF TETRAVALENT URANIUM NANOPARTICLES UNDER GROUNDWATER CONDITIONS
<i>W. Cha, I. H. Yoon, H. Cho, H.-R. Cho, E. C. Jung (Korea)</i> | A6-1 | 503 |
| 9:30 | EVIDENCES ABOUT THE CONTRIBUTION OF PU(IV) OXOHYDROXO CLUSTER $[Pu_6(OH)_4O_4]^{12+}$ DURING THE FORMATION OF Pu(IV) INTRINSIC COLLOIDS
<i>M. Virost, M. Cot-Auriol, T. Dumas, D. Menut, O. Diat, S. Dourdain, P. Moisy, S. I. Nikitenko (France)</i> | A6-2 | 505 |
| 9:55 | ROLE OF NITRATE ON THE FORMATION AND RETENTION OF Th ^{IV} NANOPARTICLES AT THE MUSCOVITE (001)-WATER INTERFACE
<i>J. Neumann, J. Lessing, A. J. Carr, S. S. Lee, M. Patzschke, C. Taylor, P. J. Eng, J. E. Stubbs, P. Fenter, M. Schmidt (USA, Germany)</i> | A6-3 | 507 |
| 10:20 | NEW CFM RADIONUCLIDE TRACER TEST DEDICATED TO KINETIC PROCESSES UNDER IN-SITU CONDITIONS AT THE GRIMSEL TEST SITE
<i>F. Quinto, I. Blechschmidt, M. Bouby, Z. Chen, H. Geckeis, B. Lanyon, C. Marquardt, U. Noseck, M. Plaschke, R. Schneeberger, T. Schäfer (Germany, Switzerland, UK)</i> | A6-4 | 509 |
| 10:45 | REVEALING THE ORIGIN AND ION-BINDING PROPERTIES OF DISSOLVED ORGANIC MATTERS IN DEEP SEDIMENTARY GROUNDWATER
<i>T. Saito, S. Nishi, H. Sato, K. Toda, K. Miyakawa (Japan)</i> | A6-5 | 511 |
| 11:10 | BREAK | | |

SESSION 18 A5: SOLID-WATER INTERFACE REACTIONS: EXPERIMENTS AND MODELLINGChair: *B. Madé (France) and T. Missana (Spain)*

		ID	PAGE
11:30	RETENTION AND TRANSPORT BEHAVIOUR OF SELENIUM(IV) IN HARDENED CEMENT PASTE: EFFECT OF HIGH SULPHATE CONCENTRATIONS <i>C. Landesman, S. Ribet, K. David, N. Bessaguet, P. Henocq (France)</i>	A5-10	513
11:55	RETENTION OF STRONGLY HYDROLYZING METAL IONS IN CEMENT SYSTEMS: QUANTITATIVE DESCRIPTION AND MECHANISTIC UNDERSTANDING <i>X. Gaona, N. Cevirim-Papaioannou, Y. Jo, N. Huber, A. Tasi, R. E. Guidone, I. Androniuk, K. Dardenne, J. Rothe, M. Altmaier, H. Geckeis (Germany, Korea)</i>	A5-11	515
12:20	THE OPTIMIZED GEMS CLAYSOR MODEL AND DATA BASES TO SUPPORT NAGRA SAFETY ASSESSMENTS FOR DEEP GEOLOGICAL REPOSITORY <i>G. D. Miron, O. Marinich, M. Marques Fernandes, D. A. Kulik, B. Baeyens, Raphael Wüst (Switzerland)</i>	A5-12	517
12:45	BENCHMARKING THE THERMOCHIMIE DATABASE: SOLUBILITY AND SPECIATION CALCULATIONS <i>E. Colàs, J. Rodríguez-Mestres, R. Mas, D. García, L. Duro, W. Bower, S. Brassinnes, B. Madé (Spain, England, Belgium, France)</i>	A5-13	519
13:10	END OF THE CONFERENCE		

ABSTRACTS

E-2	MIGRATION OF ACTINIDES AND FISSION PRODUCTS – AN OVERVIEW TO PUT THE DIFFERENT ISSUES OF IMPORTANCE FOR THE POST-CLOSURE SAFETY OF GEOLOGICAL REPOSITORIES IN CONTEXT	51
A8-1	COMPUTATIONAL CHEMISTRY APPROACHES TO PREDICTIVE MULTISCALE MODELLING OF MIGRATION PROCESSES: CURRENT CHALLENGES AND OPPORTUNITIES	52
A8-2	ENABLING LONG TIME-SCALE QUANTUM MOLECULAR DYNAMICS SIMULATION FOR 5F-ELEMENTS.....	54
A8-3	DENSITY FUNCTIONAL MODELING OF AM(III) HYDROXO COMPLEXES WITH CA OR MG COUNTER IONS. DO MG STABILIZED SPECIES EXIST?	55
A8-4	COORDINATION AND THERMODYNAMIC PROPERTIES OF AQUEOUS PROTACTINIUM(V) BY COMPUTATIONAL CHEMISTRY TECHNIQUES.....	57
A8-5	SORPTION OF EU(III) ON C-S-H PHASES IN THE PRESENCE OF GLUCONATE: A MOLECULAR DYNAMICS STUDY.....	58
A5-1	IMPACT OF FORMATE, CITRATE AND GLUCONATE ON THE UPTAKE OF AN(III)/LN(III) AND AN(IV) BY CEMENT	60
A5-2	INTERFACIAL CHEMISTRY OF GIBBSITE UNDER CONDITIONS RELEVANT TO NUCLEAR WASTE.....	62
A5-3	RETENTION OF ²²⁶ RA BY ILLITE AND MONTMORILLONITE: AN ADSORPTION STUDY	64
A5-4	U(VI) RETENTION ON BENTONITE AND CEMENTITIOUS MATERIALS: EFFECT OF INCREASED IONIC STRENGTHS AND PRESENCE OF ORGANICS.....	66
B4-1	MECHANISM OF URANIUM REDUCTION: THE ROLE OF PENTAVALENT SPECIES.....	68
B4-2	IN SITU BIOMINERALISATION FOR GROUNDWATER RADIONUCLIDE REMEDIATION	70
B4-3	PHYTOREMEDIATION OF SOIL FROM GERMAN NUCLEAR FACILITIES.....	72
B4-4	DISSOLVED ORGANIC MATTER IN BOOM CLAY AND ITS ROLE ON RADIONUCLIDE MIGRATION: WE HAVE COME A LONG WAY	74
B4-5	POTENTIAL IMPACT OF BIOGENIC CHELATORS ON THE MIGRATION OF ACTINIDES.....	76
C3-1	NEXT GENERATION ENVIRONMENTAL MONITORING FRAMEWORK FOR NUCLEAR WASTE AND RADIOLOGICALLY CONTAMINATED SITES	77
C3-2	DETERMINING 3D POROSITY MAP OF BUKOV CALCITE WITH A MULTIMODAL DEEP LEARNING APPROACH.....	79
C3-3	A CHEMISTRY-INFORMED HYBRID MACHINE LEARNING APPROACH TO PREDICT RADIONUCLIDE SORPTION TO MINERAL SURFACES	81
PA-1	SEQUENTIAL EXTRACTION OF SIMULATED FUEL DEBRIS FOR EVALUATION OF THE CHEMICAL STABILITY.....	83
PA1-2	SOLUBILITY BEHAVIOR AND CHARACTERIZATION OF NEODYMIUM(III) TRIHYDROXIDE SOLID PHASE	85
PA1-3	CHARACTERIZATION OF SYNTHETIC MAGNESIUM/CALCIUM URANYL SILICATE MINERALS AND THEIR SOLUBILITIES IN GROUNDWATER ENVIRONMENTS	87
PA1-4	(U,CE)O ₂ : A SUITABLE ANALOGUE TO STUDY THE ALTERATION OF (U,PU)O ₂ MOX FUEL IN ENVIRONMENTAL CONDITIONS.....	89
PA1-5	SOLUBILITY BEHAVIOR OF NEPTUNIUM (V) IN EXPECTED WIPP CONDITIONS	91
PA2-1	DECIPHERING THE DYNAMIC PROCESSES OF MINERAL PRECIPITATION INDUCED POROSITY CLOGGING. COMBINING MICROFLUIDIC EXPERIMENTS AND SOLUTE TRANSPORT MODELLING.....	93
PA2-2	KINETICS OF ²²⁶ RA INCORPORATION INTO (BA,RA)SO ₄ SOLID SOLUTIONS	95
PA2-3	FREEZING AND DEFROSTING OF IONIC AND MAGNETIC CONFIGURATIONS IN ZIRCONIUM MOLYBDATE FORMED IN NUCLEAR FUEL WASTE GLASSES	97
PA3-1	NEW SPECIATION DIAGRAM OF THE PU(IV)-ACETATE SYSTEM TAKING INTO ACCOUNT POLYNUCLEAR SPECIES	99
PA3-2	SOLUBILITY OF FERROUS IRON HYDROXIDE IN THE PRESENCE OF CITRATE: EFFECT OF IONIC STRENGTH	101
PA3-3	THERMODYNAMIC AND STRUCTURAL STUDIES OF AM(III)-ISOSACCHARINATE COMPLEXATION UNDER ACIDIC TO ALKALINE CONDITIONS: AQUEOUS COMPLEXES TO COLLOIDAL PARTICLES.....	103
PA3-4	TRIBUTYL PHOSPHATE: COMPETITIVE ADSORPTION AND EFFECT ON RADIONUCLIDES RETENTION.....	105
PA3-5	THERMODYNAMIC STUDY OF COMPLEXATION OF LANTHANIDE/ACTINIDE WITH CEMENT ADDITIVES BY ISOTHERMAL MICRO-TITRATION CALORIMETRY.....	106

PA4-1 PERRHENATE (ReO_4^-) REMOVAL FROM AQUEOUS SOLUTIONS BY MONO-, BI-, AND TRI-METALLIC IRON NANOPARTICLES: A COMPARATIVE STUDY	108
PA4-2 REDOX-ACTIVE DONOR-ACCEPTOR CONJUGATED MICROPOROUS POLYMER FOR PHOTOCATALYTIC REDUCTION OF URANIUM(VI)	110
PA4-3 CHLORIDE GREEN RUST AS SCAVENGER OF TECHNETIUM: IMMOBILIZATION AND SPECTROSCOPIC STUDIES	112
PA4-4 TC(VII) REDUCTIVE IMMOBILIZATION BY S(-II) PRE-SORBED ON ALUMINA.....	114
PA4-5 PORPHYRIN-BASED HYDROGEN-BONDED ORGANIC FRAMEWORK FOR VISIBLE LIGHT DRIVEN PHOTOCATALYTIC REMOVAL OF U(VI) FROM AQUEOUS SOLUTIONS	116
PA4-6 EXCITON DISSOCIATION AND TRANSFER BEHAVIOR AND SURFACE REACTION MECHANISM IN DONOR-ACCEPTOR ORGANIC SEMICONDUCTOR PHOTOCATALYTIC SEPARATION OF URANIUM	118
PA4-7 SELENIUM REACTIONS IN FERROUS AND SULFIDE-RICH ENVIRONMENTS: EFFECTS OF SULFIDE SPECIATION	120
PA4-8 INSIGHTS INTO THE URANIUM ENRICHMENT MECHANISM ON MINERALS CONTAINING FE(II) IN DEEP GEOLOGICAL REPOSITORIES	122
PA5-1 SORPTION BEHAVIOR OF SELENITE ON CLAY MINERAL SURFACES IN THE PRESENCE OF AQUATIC FULVIC ACID.....	124
PA5-2 APPLICATION OF METAL IONS DOPED HYDROXYAPATITE IN URANIUM ADSORPTION	126
PA5-3 SORPTION OF EU(III) AND CM(III) ON C-S-H PHASES IN PRESENCE OF EDTA AT INTERMEDIATE IONIC STRENGTH CONDITIONS.....	128
PA5-4 CONSTRUCTION AND APPLICATION OF AN ULTRAHIGHLY SELECTIVE PHOTOISOMERIC METAL-ORGANIC FRAMEWORKS MATERIAL FOR URANIUM EXTRACTION FROM SEAWATER.....	130
PA5-5 TRIVALENT LANTHANIDES SORPTION ONTO ILLITE IN THE PRESENCE OF CARBONATE	132
PA5-6 URANIUM SORPTION ON OXYHYDROXIDE MINERALS BY SURFACE COMPLEXATION AND PRECIPITATION ^[1]	135
PA5-7 EU(III) AND CM(III) COMPLEXATION BY NITRILOTRIACETIC ACID TO FURTHER EVALUATE ITS IMPACT ON THE RADIONUCLIDE RETENTION BY CEMENTITIOUS PHASES.....	136
PA5-8 MINERAL SPECIFIC SORPTION OF RADIUM ON CRYSTALLINE ROCK	138
PA5-9 ANCHORING SELF-ASSEMBLY ANTIBACTERIAL AG NANOSHEETS ONTO THE MAGNETIC MICROSPHERES ENHANCED URANIUM IMMOBILIZATION.....	140
PA5-10 FUNCTIONALIZED DIOXIN-LINKED COVALENT ORGANIC FRAMEWORKS FOR RAPID AND SELECTIVE EXTRACTION OF URANIUM	142
PA5-11 CS(I) AND BA (II) SORPTION ON BIOTITE AT PH 5-9 AND 25, 40 AND 60°C.....	144
PA5-12 MICROMECHANISM OF ADSORPTION OF STRONTIUM AND CESIUM ON DIFFERENT EXPANSIVE CLAY MINERALS..	145
PA5-13 ADSORPTION OF CESIUM ON MICACEOUS MINERALS WITH STRUCTURAL TRANSFORMATION AND THE IMPLICATION FOR DIFFUSION	147
PA5-14 ILLITIZATION UNDER HIGH TEMPERATURES AND ITS EFFECT ON CESIUM SORPTION	149
PA5-15 ANTI-BIOLOGICAL CONTAMINATION URANIUM ADSORBING CELLULOSE GEL	151
PA5-16 RETENTION MECHANISMS OF SELENIUM IN DEEP SUBSURFACE SEDIMENTARY FORMATIONS IN HORONobe AREA, HOKKAIDO, JAPAN*.....	153
PA6-1 FORMATION OF STABLE U(VI) COLLOIDAL PARTICLES IN RELEVANT ENVIRONMENTAL CONDITIONS.....	155
PA6-2 STABILITY OF EUROPIUM(III)/THORIUM(IV)-SILICATE COLLOIDS: EFFECT OF SI CONTENT, PH, ELECTROLYTE AND FULVIC ACID	157
PA6-3 THE STABILITY AND INTERACTION OF COLLOIDS AND THEIR EFFECTS ON RADIONUCLIDE TRANSPORT REGARDING TO HLW DISPOSAL IN GRANITIC FORMATION	159
PA7-1 AN "ON-OFF" RATIO-METRIC FLUORESCENT SENSOR FOR UO_2^{2+} BASED ON Ag^+ -MODIFIED GOLD NANOCCLUSERS HYBRID	161
PA7-2 TRACING AND QUANTIFICATION OF ^{226}Ra IN TAILINGS BY SPECTROSCOPIC AUTORADIOGRAPHY	163
PA7-3 DEVELOPMENT OF ANALYTICAL PROTOCOL FOR DIFFICULT TO MEASURE RADIONUCLIDES IN METALLIC MATRIX; EXEMPLE OF ZR-93 IN STAINLESS STEEL AND INCONEL METALS.....	165

PA7-4 A RAPID DETERMINATION OF SELENIUM IN TEA SAMPLES USING ANION CHROMATOGRAPHIC COLUMN COMBINED WITH AUTOMATIC SYSTEM SEPARATION AND HR-ICP-MS MEASUREMENT ^[1]	167
PA8-1 AN ATOMIC SCALE COMPUTATIONAL APPROACH TO UNDERSTANDING REDOX SPECIATION OF KEY ACTINIDES ON IRON BEARING MINERALS.	168
PA8-2 DENSITY FUNCTIONAL THEORY STUDY OF THE CRYSTAL STRUCTURE AND INFRARED SPECTRUM OF ETTRINGITE..	170
PA8-3 ACTINIDE(IV) INTERACTIONS WITH CALCIUM SILICATE HYDRATE: SORBED SPECIES AND COMPARISON OF SORPTION MODES BY MEANS OF DENSITY FUNCTIONAL CALCULATIONS	172
PA8-4 EXPLORING THE COMPLEXATION OF CURIUM(III) AND EUROPIUM(III) WITH AQUEOUS PHOSPHATES: A COMBINED EXPERIMENTAL AND AB INITIO STUDY	174
PB2-1 IONIC DIFFUSIVE TRANSPORT THROUGH PARTIALLY-WATER SATURATED CEMENT-BASED MATERIALS.....	176
PB2-2 EFFECTS OF BIOTITE ON DIFFUSION AND SORPTION OF CATIONS IN CRYSTALLINE ROCKS BY THROUGH-DIFFUSION AND LASER-ABLATION ICP-MS EXPERIMENTS.....	178
PB2-3 DIFFUSION AND RETENTION OF DIVALENT TRANSITION METAL TRACERS IN COMPACTED ILLITE CONVERTED TO DIFFERENT CATIONIC FORMS.....	180
PB2-4 RELEVANCE OF UPWARDS MIGRATION OF RADIONUCLIDES IN SOIL IN THE CONTEXT OF NUCLEAR WASTE MANAGEMENT.....	182
PB2-5 ZINC(II) TRANSPORT IN COMPACT ILLITE IN THE PRESENCE OF ORGANIC LIGANDS	184
PB2-6 DIFFUSION AND SORPTION OF HTO AND EU-152 IN CRYSTALLINE ROCK WITH AND WITHOUT BENTONITE COLLOIDS.	186
PB2-7 METAL ION DIFFUSION THROUGH METAKAOLIN-BASED GEOPOLYMER.....	188
PB2-8 A SENSITIVE METHOD TO MEASURE GEOMETRY FACTORS FOR DIFFUSION ON SMALL SAMPLES OF CLAY ROCK ...	190
PB2-9 EFFECTS OF ALTERATION BY LEACHING ON MIGRATION OF CESIUM IN HARDENED CEMENT PASTE.....	192
PB3-1 BENTONITE COLLOIDS MEDIATED EU(III) MIGRATION IN HOMOGENEOUS AND HETEROGENEOUS MEDIA OF BEISHAN GRANITE AND FRACTURE-FILLING MATERIALS.....	194
PB3-2 COUPLING MECHANISM OF EU(III) TRANSPORT IMPACTED BY COMPOSITE COLLOIDS OF BENTONITE AND ORGANIC MATTER.....	195
PB4-1 INTERACTION OF TECHNETIUM WITH METABOLITES, MICROORGANISMS AND AT THE MINERAL-WATER INTERFACE: RADIOECOLOGICAL CONSIDERATIONS.....	197
PB4-2 ACCUMULATION OF ACTINIDES (III, VI) IN THE FILAMENTOUS FUNGUS <i>PODOSPORA ANSERINA</i>	199
PB4-3 RIGIDITY AND FLEXIBILITY: UNRAVELING THE ROLE OF FULVIC ACID IN URANYL SORPTION ON GRAPHENE OXIDE USING MOLECULAR DYNAMICS SIMULATIONS	201
PB4-4 THE MECHANISM OF URANIUM(VI) BIOMINERALIZATION IN THE GROWTH OF <i>BACILLUS SP. DWC-2</i>	203
PB4-5 THE BEHAVIOR AND MECHANISM OF URANIUM BIOREDUCTION INDUCED BY A NATURAL <i>BACILLUS THURINGIENSIS</i>	205
PB4-6 BIOMIMETIC PHOTOCATALYTIC SYSTEMS DESIGNED BY SPATIALLY SEPARATED COCATALYSTS ON Z-SCHEME HETEROJUNCTION WITH IDENTIFIED CHARGE-TRANSFER PROCESSES FOR BOOSTING REMOVAL OF U(VI)	206
PB4-7 ORGANICALLY BOUND TRITIUM SPECIATION IN ENVIRONMENTAL MATRICES BY ISOTOPIC EXCHANGE	208
PB5-1 MIGRATION OF ⁶⁰ CO, ¹³³ BA, ¹³⁷ CS, AND ¹⁵² EU FROM CEMENTITIOUS WASTEFORMS IN FIELD LYSIMETER EXPERIMENTS	210
PB5-2 MODELING A RADIONUCLIDE TRANSPORT EXPERIMENT IN GRANITIC ROCK MATRIX AT GRIMSEL. THE ROLE OF ADVECTION.	212
PB5-3 CHARACTERISTICS OF GRANITIC AQUIFER COLLOIDS IN THE KURT GROUNDWATER SYSTEM	214
PB5-4 THE HETEROGENEITY OF THE SANDY FACIES OF OPALINUS CLAY ACROSS SCALES, FROM SEISMIC SURVEYS TO RADIONUCLIDE DIFFUSION - AN <i>IN-SITU</i> TEST IN THE SWISS ROCK LABORATORY MONT TERRI.....	216
PB5-5 STRONTIUM BEHAVIOUR IN RADIOACTIVELY CONTAMINATED LAND – UNDERPINNING OPTIONS FOR IN-SITU DISPOSAL.....	217
PB6-1 IDENTIFICATION ON THE ORIGIN AND FATE OF DISSOLVED U IN BOEUN AQUIFER, BASED ON C, O, FE, S, SR AND U-SERIES ISOTOPIC SIGNATURES	219

PB6-2	GEOCHEMICAL BEHAVIORS OF URANIUM IN A URANIUM DEPOSIT OF THE OGcheon METAMORPHIC BELT, KOREA..	220
PC1-1	THE NEA THERMOCHEMICAL DATABASE (TDB) PROJECT: HIGH QUALITY DATA, ACCESSIBILITY AND CAPACITY BUILDING.....	222
PC1-2	DEVELOPMENT OF A DATABASE FOR RADIONUCLIDE SORPTION ON CLAY AND CEMENT SYSTEMS IN SUPPORT TO RADIOACTIVE WASTE MANAGEMENT.....	224
PC1-3	THERMODYNAMIC MODELS DATABASE: A TOOL FOR UNDERSTANDING RADIONUCLIDE SORPTION MECHANISMS ON CLAY AND CEMENT SYSTEMS	226
PC1-4	A THERMODYNAMIC DATABASE FOR THE SOLUTION CHEMISTRY AND SOLUBILITY OF EUROPIUM(III) INORGANIC SPECIES: RECENT DEVELOPMENTS.....	228
PC1-5	THERMOCHEMIE: A THERMODYNAMIC DATABASE USED IN RADIOACTIVE WASTE DISPOSAL EVALUATION.....	230
PC2-1	INTERPRETATION OF DIFFUSION EXPERIMENTS WITH A NUMERICAL REACTIVE TRANSPORT APPROACH.....	231
PC2-2	MODEL INTERPRETATION OF INTERACTION BETWEEN GLASS AND ORDINARY PORTLAND CEMENT IN AN INTEGRATED GLASS DISSOLUTION EXPERIMENT.....	232
PC2-3	REACTIVE TRANSPORT MODELLING OF TCO ₄ - DIFFUSION IN OPALINUS CLAY WITH PFLOTAN.....	234
PC3-1	COMPARISON OF THE CAPACITY OF TWO ADSORPTION MODELS TO DESCRIBE SR ²⁺ AND CS ⁺ BEHAVIOR ON SOILS SURROUNDING NUCLEAR FACILITIES	235
PC3-2	PORE-SCALE MODELLING OF SOLUTE TRANSPORT IN PARTIALLY AND FULLY SATURATED POROUS MEDIA	236
PC4-1	GEOCHEMISTRY AND MACHINE LEARNING BENCHMARK WITHIN EURAD JOINT PROJECT	238
PD-1	A CRITICAL ANALYSIS OF THE RADIOECOLOGICAL MODEL USED IN THE GERMAN CALCULATION BASIS FOR THE ESTIMATION OF RADIATION DOSES DUE TO THE STORAGE OF HIGHLY ACTIVE NUCLEAR WASTE.....	240
PD-2	TRANSPORT OF RADIOACTIVE WASTE ALONG THE SELLAFIELD SHORELINE: CLIMATE CHANGE IMPACT AND MITIGATION STRATEGIES THROUGH NATURE-BASED SOLUTIONS	242
PD-3	PRELIMINARY LONG-TERM HYDROGEOCHEMICAL EVOLUTION STUDY CASE IN TAIWAN	244
PD-4	MICROBIAL IMPACT ON MINERALOGICAL TRAPPING OF URANIUM IN DEEP ANOXIC AQUIFERS: CASE STUDIES FOR ÄSPÖ HARD ROCK LABORATORY AND FORSMARK SITE, SWEDEN	246
PE-1	EFFECT OF CITRIC ACID AND MALIC ACID ON THE URANIUM UPTAKE INTO <i>BRASSICA NAPUS</i> PLANTS IN HYDROPONIC CULTURE.....	248
PE-2	GEOCHEMICAL BEHAVIOR OF RADIUM IN A URANIUM MILL TAILINGS POND OF THE NINGYO-TOGE MINE AREA..	250
C2-1	TOWARDS A PROCESS-BASED MODEL DESCRIBING TRANSPORT-INDUCED CO-PRECIPITATION AND RADIONUCLIDE RETENTION.....	252
	LAB ON CHIP EXPERIMENTS AND REACTIVE TRANSPORT MODELLING DIAGNOSTICS.....	252
C2-2	VERIFICATION OF NEW CLAYSORDIF MODEL FOR SORPTION AND DIFFUSION IN ARGILLACEOUS MEDIA AGAINST PHREEQC RESULTS AND EXPERIMENTAL DATA.....	254
C2-2	GEMS IMPLEMENTATION OF AN INTEGRATED CLAYSORDIF MODEL FOR RADIONUCLIDE SORPTION AND DIFFUSION IN ARGILLACEOUS MEDIA.....	256
C2-3	GLASS ALTERATION MODELISATION USING GRAAL2 MODEL.....	258
C2-4	REACTIVE TRANSPORT MODELS OF LABORATORY CORROSION TESTS AT THE IRON/BENTONITE INTERFACE: FB4, FB5 AND FEMO TESTS	260
A7-1	RADIONUCLIDE DISTRIBUTIONS IN (TIME-RESOLVED) NATURAL ARCHIVES DETERMINED BY AMS.....	262
A7-2	ON THE TRACE (LEVEL) OF A HIGH LEVEL NUCLEAR WASTE DISPOSAL - METHOD DEVELOPMENT FOR MIGRATION EXPERIMENTS USING HPLC, ICP-MS AND LA-ICP-MS	264
A7-3	MULTI-TECHNIQUE ANALYSIS OF THE BEHAVIOR OF URANIUM IN NATURAL SOIL	266
A7-4	INVESTIGATING GEOCHEMICAL INTERACTIONS OF PLUTONIUM WITH OPALINUS CLAY AND HARDENED CEMENT PASTE VIA TOF-SIMS AND RL-SNMS	268
A1-1	SAFETY AND SCIENCE: THE FRAGILE CONNECTION – PART II.....	270

A1-2	SPENT NUCLEAR FUEL IN CLOSED GLASS AMPOULES: RADIOLYSIS AND RADIONUCLIDE RELEASE AFTER ONE AND FIVE YEARS	272
A1-3	EFFECT OF TEMPERATURE ON THE OXIDATIVE DISSOLUTION OF UO ₂ DOPED WITH A RADIOACTIVE ALPHA EMITTER IN SYNTHETIC CALLOVIAN-OXFORDIAN GROUNDWATER IN THE PRESENCE OF IRON	274
A1-4	SOLUBILITY AND STRUCTURAL CHARACTERIZATION OF ZR(IV) HYDROUS OXIDES	276
A1-5	GEOLOGICAL DISPOSAL OF CARBON-14: FROM SOURCE TO SINK.....	278
D-1	RADIOCAESIUM MIGRATION WITHIN A FUKUSHIMA FOREST ECOSYSTEM AND THE ROLE OF BIOMONITORING....	280
D-2	APPLICATION OF ACCELERATOR MASS SPECTROMETRY TO MEASURE RATIOS OF PLUTONIUM ISOTOPES AND EVALUATE AMERICIUM DISTRIBUTIONS AT THE LITTLE FOREST LEGACY SITE, AUSTRALIA	282
D-3	RENEWED LEAKAGE FROM SELLAFIELD'S MAGNOX SWARF STORAGE SILOS: OBSERVATIONS & OPPORTUNITIES FOR IMPROVED UNDERSTANDING OF RADIONUCLIDE MIGRATION	283
D-4	APPROACH OF HANDLING THE SORPTION AND DIFFUSION HETEROGENEITY ACROSS THE OPALINUS CLAY AND ADJACENT CONFINING UNITS IN THE SAFETY CASE FOR THE SWISS DEEP GEOLOGICAL REPOSITORY.....	285
PA1-6	TECHNETIUM DIOXIDE SOLUBILITY AT ELEVATED TEMPERATURES.....	287
PA1-7	EVALUATING THE CHEMICAL DURABILITY OF IODINE BEARING GLASS SYNTHESIZED AT HIGH PRESSURE: VAPOR HYDRATION AND AQUEOUS ALTERATION STUDY	289
PA1-8	SOLUTION AND SOLID-LIQUID-EQUILIBRIUM PROPERTIES OF RADIONUCLIDE-NITRATE AQUEOUS SYSTEMS: EXPERIMENTS AND SIT PARAMETERIZATION	291
PA1-9	DISSOLUTION AND AGING OF METAL MONOURANATES: SIMULATED DEBRIS OF FUKUSHIMA DAIICHI NUCLEAR POWER STATION	293
PA1-10	STABILITY & PHYSICO-CHEMICAL CHARACTERISATION OF A RECONDITIONED WASTE FORM RELEANT TO RADIOACTIVE WASTES	295
PA2-4	SOLUBILITY EVALUATION OF THE COPRECIPITATE URANIUM AND PLUTONIUM OXIDE UNDER HYPERALKALINE AND REDUCING CONDITIONS IN THE CONTEXT OF DEEP DISPOSAL OF ILW RADIOACTIVE WASTES.....	296
PA2-5	SOLUBILITY AND SOLID PHASE FORMATION IN THE ND ₂ O ₃ -EUCL ₃ -NDCL ₃ -NACL-H ₂ O(L) SYSTEM.....	298
PA2-6	STRUCTURE AND PROPERTIES OF CRYSTALLINE CERAMIC PHASES CONTAINING ACTINIDES – FROM BULK TO THE MOLECULAR LEVEL.....	300
PA3-6	INVESTIGATION OF ACTINIDE SPECIATION AND COMPLEXATION WITH SMALL ORGANIC LIGANDS USING CE-ICP-MS	302
PA3-7	INVESTIGATION OF THE CARBONATE COMPLEXATION OF ACTINIDES AND THE INFLUENCE OF ALKALI CATIONS USING CE-ICP-MS.....	304
PA3-8	COMPLEXATION OF NI(II) WITH CITRATE IN CEMENTITIOUS SYSTEMS: THERMODYNAMIC DESCRIPTION.....	306
PA3-9	COMPLEXATION OF NEPTUNIUM(V) WITH AQUEOUS PHOSPHATE USING A DUAL EXPERIMENTAL AND QUANTUM CHEMICAL APPROACH.....	308
PA3-10	LUMINESCENCE SPECTROSCOPIC INVESTIGATIONS OF U(VI) COMPLEXATION WITH AQUEOUS SILICATES AT (HYPER)ALKALINE CONDITIONS.....	310
PA3-11	SOLUBILITY OF TC(IV) IN THE PRESENCE OF ISOSACCHARINIC ACID: THERMODYNAMIC DESCRIPTION	312
PA4-9	DESIGN AND SYNTHESIS OF NOVEL D/A BULK HETEROJUNCTION ORGANIC CONJUGATED FILM MATERIALS AND PHOTOCATALYTIC REDUCTION FOR REMOVAL OF IONS.....	314
PA4-10	ROLE OF FE-PHASES ON SELENITE MIGRATION IN BENTONITE: UP-SCALING FROM DISPERSED TO COMPACTED SYSTEM	316
PA4-11	INFLUENCE OF IRON OXIDE NANOPARTICLE CRYSTALLITE SIZE ON THE SORPTION AND REDUCTION OF PLUTONIUM . 318	
PA4-12	PLUTONIUM REDOX CHEMISTRY IN THE PRESENCE OF CITRATE.....	320
PA4-13	REDOX BEHAVIOUR AND SPECIATION OF PLUTONIUM IN THE PRESENCE OF ALUMINIUM-DOPED IRON OXIDE MINERAL SURFACES	322
PA4-14	THE REDOX BEHAVIOR OF URANIUM AND SELENIUM UNDER RADWASTE REPOSITORY CONDITION	324
PA4-15	SELENITE SORPTION STUDIES ONTO FE(II) - AND FE(III) - NONTRONITES.....	326

PA4-16 IS THERE A ROLE FOR PU(III) IN PREDICTING THE SUBSURFACE MIGRATION OF PLUTONIUM?.....	328
PA5-17 DETERMINATION OF URANIUM(VI) SPECIATION DURING SORPTION TO GIBBSITE USING PARALLEL FACTOR ANALYSIS ON EXCITATION EMISSION MATRICES.....	330
PA5-18 THE COMBINED EFFECT OF ISA- AND CA-CONCENTRATION ON PU-SORPTION TO A CEM III/C-BASED MORTAR FOR IMMOBILIZATION OF NUCLEAR WASTE	332
PA5-19 THE EFFECT OF CELLULOSE DEGRADATION PRODUCTS ON THE SORPTION AND DIFFUSION OF NICKEL IN DEGRADED HARDENED CEMENT PASTE.....	334
PA5-20 RETENTION OF RADIONUCLIDES (CAESIUM, NICKEL) IN FRACTURE INFILLS UNDER DIFFERENT GEOCHEMICAL CONSTRAINS.....	336
PA5-21 INFLUENCE OF THE COMPETITION OF AL ON THE RETENTION OF TRIVALENT ACTINIDES AND THEIR HOMOLOGUES IN FELDSPAR	338
PA5-22 CHEMICAL TOMOGRAPHY OF PYRITE COMPOSITES EXTRACTED FROM OPALINUS CLAY AND REACTED WITH NEPTUNIUM AND PLUTONIUM.....	340
PA5-23 INTERACTIONS BETWEEN RADIONUCLIDES AND CALCITE SURFACE	342
PA5-24 THE STUDY OF MARINE SOLUTIONS INFLUENCES ON THE SORPTION OF ²²⁶ RA TO MINERALS.....	344
PA5-25 MOLECULAR SCALE UNDERSTANDING OF NI ²⁺ ADSORPTION ON SWELLING CLAY MINERALS.....	345
PA5-26 SORPTION PROPERTIES OF EU ONTO GRANITE AND MX-80 BENTONITE IN CA-NA-CL SOLUTIONS	347
PA5-27 SORPTION OF SELECTED RADIONUCLIDES ON CANADIAN SEDIMENTARY AND CRYSTALLINE ROCKS UNDER SALINE CONDITIONS.....	349
PA5-28 UPTAKE OF NIOBIUM BY CEMENT AND C-S-H PHASES IN THE ABSENCE AND PRESENCE OF ISA AND CHLORIDE: QUANTITATIVE DESCRIPTION AND MECHANISTIC UNDERSTANDING.....	350
PA5-29 INFLUENCE OF NA-CA-CL AND CA-NA-CL PHYSICOCHEMICAL SOLUTION PROPERTIES ON THE ADSORPTION OF ⁷⁹ SE(-II) AND ⁹⁹ TC(IV) ONTO SEDIMENTARY AND CRYSTALLINE ROCKS	352
PA5-30 INFLUENCE OF TEMPERATURE ON CATION ION EXCHANGE AND SORPTION TO MONTMORILLONITE CLAY.....	353
PA5-31 PLUTONIUM ADSORPTION TO HEMATITE AT VARIABLE PH, TEMPERATURE, AND CONCENTRATION	355
PA5-32 METAL IONS ADSORPTION AND MODELING ON A PRE-NEOGENE SEDIMENTARY ROCK	357
PA6-4 STRENGTHENED EROSION RESISTANCE OF COMPACTED BENTONITE BY OPPOSITELY-CHARGED MATERIALS: FROM COLLOIDAL PARTICLES INTERACTION TO EROSION EXPERIMENTS	359
PA6-5 PROBING THE NUCLEATION AND GROWTH OF PUO ₂ NANOPARTICLES IN AQUEOUS SOLUTION.....	361
PA7-5 GEOCHEMICAL INFLUENCE ON THE RADIONUCLIDE MOBILITY IN GEOLOGICAL FORMATIONS ANALYSED BY ICP-MS AND ICP-QQQ COUPLING METHODS.....	363
PA7-6 SIMULTANEOUS DETERMINATION OF TRANSURANIUM RADIONUCLIDES BY COMPACT ACCELERATOR MASS SPECTROMETRY.....	365
PA7-7 IMPROVED SOLID PHASE EXTRACTION MATERIALS FOR SR-90 AND CS-137	367
PA7-8 MIXED FROM A WASTE COCKTAIL: CONSIDERATIONS ON BACKGROUND ELECTROLYTE'S COMPOSITION AND SALINITY, PBTC AND IRON INFLUENCING THE RETENTION OF REPOSITORY-RELEVANT ELEMENTS ON POTENTIAL BARRIER MATERIALS	368
PA7-9 X-RAY ANALYSES ON RADIOACTIVE MATTER AT THE MARS BEAMLINE OF SYNCHROTRON SOLEIL.....	370
PA8-5 MOLECULAR UNDERSTANDING OF HYDROGEN ADSORPTION AND TRANSPORT IN HYDRATED NA- AND CA-MONTMORILLONITES IN THE CONTEXT OF GEOLOGICAL DISPOSAL OF RADIOACTIVE WASTE.....	371
PA8-6 MOLECULAR LEVEL INSIGHTS ON THE PHYSISORPTION MECHANISMS OF HYDROGEN GAS ON MONTMORILLONITE CLAY SURFACES	372
PA8-7 MOLECULAR DYNAMICS COMPUTER SIMULATIONS OF THE EFFECTS OF ORGANIC MOLECULES ON THE CLAY-RADIONUCLIDE INTERACTIONS IN THE CONTEXT OF GEOLOGICAL DISPOSAL OF RADIOACTIVE WASTE	373
PA8-8 SITE-SPECIFIC STRUCTURE AND ENERGETICS OF URANYL ADSORPTION AT HYDRATED MUSCOVITE (001) SURFACE PROBED BY CLASSICAL MOLECULAR DYNAMICS SIMULATIONS.....	375
PB2-10 IN SITU INVESTIGATIONS: RADIONUCLIDE MOBILITY AT CONCRETE-ROCK-INTERFACE.....	377

ABSTRACTS

PB2-11 HOW STRONG DOES NICKEL AFFECT THE SORPTION AND DIFFUSION OF ZINC IN COMPACTED ILLITE?	379
PB2-12 INTERACTION OF RADIONUCLIDES WITH FRACTURE FILLINGS AND MIGRATION THROUGH A MATRIX OF CRYSTALLINE HOST ROCK.....	381
PB2-13 STUDY OF THE INFLUENCE OF FRACTURE FILLINGS ON RADIONUCLIDE TRANSPORT IN CRYSTALLINE ROCK SYSTEMS	383
PB2-14 HOW DO ALTERATION AND STRUCTURAL HETEROGENEITIES INFLUENCE DIFFUSIVITY WITHIN GRANODIORITES? 385	
PB2-15 ASSESSMENT OF CESIUM MIGRATION IN THE SHALLOW GROUNDWATER-SOIL SYSTEM OF A PROPOSED NNP SITE	387
PB2-16 OUT-LEACHING EXPERIMENTS OF ROCK CORES AFTER IRRADIATION BY NEUTRONS; STUDY OF PORE WATER SALINITY IN CRYSTALLINE ROCK	389
PB2-17 THE MIGRATION BEHAVIOR OF RADIOACTIVE COBALT AT THE REGION FOR A PROPOSED NUCLEAR POWER PLANT: EXPERIMENTS AND SIMULATION STUDIES.....	391
PB3-3 INSIGHT INTO IMPACT OF PHOSPHATE ON THE COTRANSPORT AND CORELEASE OF EU(III) WITH BENTONITE COLLOIDS IN SATURATED QUARTZ COLUMNS	393
PB3-4 CO-TRANSPORT OF U(VI) AND COLLOIDAL BIOCHAR IN QUARTZ SAND HETEROGENEOUS MEDIA	395
PB3-5 COLLOID-MEDIATED TRANSPORT AND MECHANISM OF U(VI/IV) IN REDUCTION CONDITIONS	397
PB4-8 EXPLORATION OF THE BIO-REDUCTION BEHAVIOR AND MECHANISM OF ⁹⁹ Tc(VII) BY <i>KLEBSIELLA VARIICOLA</i> STRAIN X-21	399
PB4-9 OVERVIEW ON THE EURAD WORKPACKAGE CORI (CEMENT-ORGANIC-RADIONUCLIDE-INTERACTIONS)	401
PB4-10 IMPACT OF THE DEGRADATION PRODUCTS OF UP2W FILTER AID MATERIAL ON THE UPTAKE OF RADIONUCLIDES BY CEMENT.....	403
PB4-11 INFLUENCE OF MICROORGANISMS ON THE MOBILITY OF +3 ACTINIDES FROM THE WASTE ISOLATION PILOT PLANT	404
PB4-12 IMPACT OF THE EXTRACTION OF SOLUBLE ORGANIC MATTER (SOM) FROM SOILS ON THE QUALITY OF INSOLUBLE ORGANIC MATTER (IOM) IN VIEW OF PROTON BINDING SITES AND RADIONUCLIDE BINDING	406
PB4-13 CHARACTERIZATION OF BOOM CLAY (BC) DISSOLVED ORGANIC MATTER (DOM) AND ITS INTERACTION WITH RADIONUCLIDES	408
PB5-6 PLUTONIUM TRANSPORT IN VADOSE ZONE SEDIMENTS UNDER ACIDIC SOLUTION CONDITIONS AT THE HANFORD SITE, USA	410
PB5-7 STUDY OF THE MIGRATION BEHAVIOUR OF ANTHROPOGENIC ACTINIDES IN LAKE SEDIMENTS AND PEAT BOG CORES	411
PB5-8 FULL-SCALE PROTOTYPE, A LONG-TERM EXPERIMENT AT ÄSPÖ LABORATORY, SWEDEN.	413
PB5-9 URANIUM SPECIATION IN SOILS AND SEDIMENTS IMPACTED BY ACIDIC RUNOFF ORIGINATING FROM ALUM SHALE WASTE ROCK	415
PB5-10 PLUTONIUM AND CS-137 MOBILITY IN AN EPHEMERAL STREAM BED AT NEVADA NATIONAL SECURITY SITE (NNS), USA	416
PB6-3 HYDRO-GEOPHYSICAL APPROACH TO UNDERSTAND THE DEPOSITIONAL AND GEOCHEMICAL CHARACTERISTICS OF THE URANIUM DEPOSITS IN THE OKCHEON METAMORPHIC BELT, KOREA.....	418
PC1-6 THE PSI CHEMICAL THERMODYNAMIC DATABASE TDB 2020 TO SUPPORT NAGRA SAFETY ASSESSMENTS FOR DEEP GEOLOGICAL REPOSITORY.....	420
PC1-7 SOLUBILITY ASSESSMENT IN CRYSTALLINE AND SEDIMENTARY ROCKS	422
PC1-8 ENCHMARKING THE THERMOCHIMIE DATABASE FOR ITS APPLICATION TO CEMENTITIOUS AND ARGILLACEOUS ENVIRONMENTS.....	424
PC1-9 THEREDA - THERMODYNAMIC REFERENCE DATABASE	425
PC1-10 DIGITIZATION OF LITERATURE DATA AND SURFACE COMPLEXATION MODEL PARAMETER ESTIMATION FOR TRIVALENT AMERICIUM, CURIUM, AND EUROPIUM SORPTION.....	426
PC1-11 STATE OF THE ART REPORT IN REDOX AND KINETICS APPLIED TO NUCLEAR WASTE DISPOSAL FACILITIES.....	428

PC2-4	REACTIVE TRANSPORT MODEL OF THE LONG-TERM GEOCHEMICAL EVOLUTION AT THE DISPOSAL CELL SCALE IN A HLW REPOSITORY IN GRANITE	430
PC2-5	DEVELOPMENT AND IMPROVEMENT OF NUMERICAL METHODS AND TOOLS FOR MODELLING COUPLED PROCESSES	432
PC2-6	VARS GLOBAL SENSITIVITIES FOR REACTIVE TRANSPORT SIMULATIONS IN A HLW REPOSITORY IN GRANITE	433
PC3-3	SUPPORTING TOOLS IN THE DEVELOPMENT OF THE THERMOCHEMIE DATABASE: THE XCHECK TOOL	435
PC5-1	APPROACH OF CONSEQUENCE ANALYSES SUPPORTING THE SAFETY-BASED COMPARISON OF THE CANDIDATE SITING REGIONS FOR THE SWISS DEEP GEOLOGICAL REPOSITORY	437
PD-5	THE UK'S RADIOACTIVE WASTE MANAGEMENT AND ENVIRONMENTAL REMEDIATION (RADER) NATIONAL NUCLEAR USER FACILITY	439
PD-6	EFFECT OF SEASONAL ANOXIA ON TRACE ELEMENTS PLUTONIUM CYCLING IN A WARM MONOMICTIC LAKE..	440
PD-7	PRELIMINARY APPROACH FOR SAFETY DISPOSAL OF RADIOACTIVE WASTES FROM FDNPS FOR OPTIMIZATION OF WASTE MANAGEMENT STREAM	442
PD-8	OVERVIEW OF THE JAPANESE RADIOACTIVE WASTE DISPOSAL PROJECT	444
PE-3	MODELING OF HYDROGEOCHEMICAL PROCESSES INFLUENCING URANIUM MIGRATION IN ANTHROPIZED SUB-SAHARAN ENVIRONMENTS	446
PE-4	HIGHLY SENSITIVE QUANTIFICATION OF AQUATIC NANOPARTICLES BY LIBD	447
PE-5	BACTERIAL DIVERSITY DOWNSTREAM FROM A FORMER URANIUM MINE AND IN WATERS FROM NATURALLY RADIOACTIVE MINERAL SOURCES: POTENTIAL ROLE ON URANIUM MIGRATION IN THE ENVIRONMENT	449
A5-5	ELECTROSTATIC INTERACTIONS AT CLAY MINERAL SURFACES: AT THE CROSSROADS BETWEEN MINERALOGY, GEOCHEMISTRY, AND GEOPHYSICS.....	451
A5-6	U(VI) SORPTION ON ILLITE IN THE PRESENCE OF CARBONATE STUDIED BY CRYOGENIC TIME-RESOLVED LASER FLUORESCENCE SPECTROSCOPY AND PARALLEL FACTOR ANALYSIS: COMPARISON WITH TRIVALENT LANTHANIDES*	452
A5-7	RETENTION OF SILVER IN CEMENTITIOUS MATERIALS	454
A5-8	ANALYSIS OF COBALT RETENTION BY NA- AND CA- SMECTITE AND THE EFFECT OF EDTA PRESENCE	456
A5-9	ACTINIDE ADSORPTION TO HEMATITE AT ELEVATED TEMPERATURES	458
A4-1	EFFICIENT PHOTOREDUCTION STRATEGY FOR URANIUM IMMOBILIZATION BASED ON GRAPHITE CARBON NITRIDE HETEROJUNCTION NANOCOMPOSITES.....	460
A4-2	URANIUM(VI) REDUCTION BY A <i>DESULFITOBACTERIUM</i> SPECIES IN PURE CULTURE AND IN ARTIFICIAL MULTISPECIES BIO-AGGREGATES.....	462
A4-3	THE IMPACT OF SULFIDATION ON MAGNETITE-BOUND ⁹⁹ Tc.....	464
A4-4	RECENT EXPERIMENTAL DEVELOPMENTS ON PLUTONIUM OXIDATION STATE DISTRIBUTION UNDER WIPP RELEVANT CONDITIONS.....	466
A4-5	REDUCTION OF PERTECHNETATE BY MAGNETITE – INFLUENCE OF PH AND TIME	468
B2-1	MIGRATION OF REDOX-SENSITIVE PLUTONIUM AND NEPTUNIUM IN OPALINUS CLAY ROCK: DEEPER INSIGHTS FROM IN-SITU REACTIVE TRANSPORT PATTERNS	470
B2-2	DIFFUSIVE TRANSPORT OF U(VI) AND AM(III) THROUGH OPALINUS CLAY STUDIED DOWN TO ULTRA-TRACE LEVELS ..	472
B2-3	EFFECT OF THE WATER SATURATION ON THE DIFFUSION OF WATER AND SOLUTES IN REFERENCE CLAY-RICH POROUS MEDIA	474
B2-4	IMPACT OF CRACKING ON THE TRANSFER OF RADIONUCLIDES IN CEMENTITIOUS MATERIALS.....	476
E-1	DEVELOPMENT OF R&D ON RADIONUCLIDE MIGRATION FOR CIGÉO.....	478
E-2	<i>IN SITU</i> DIFFUSION OF ORGANIC COMPOUNDS IN ANDRA'S UNDERGROUND LABORATORY: A 4-YEAR INSIGHT FROM THE "DRO" EXPERIMENT	479
E-3	EVALUATING RADIONUCLIDES MOBILITY <i>IN SITU</i> IN THE CALLOVIAN-OXFORDIAN ARGILLACEOUS ROCK.....	481
E-4	QUANTITATIVE ANALYSIS OF RADIONUCLIDE CONTAINMENT AS PART OF THE SAFETY ASSESSMENTS IN THE GERMAN SITE SELECTION PROCEDURE.....	484

ABSTRACTS

E-5	WHAT RESEARCH CHALLENGES FOR NORM AND TE-NORM MANAGEMENT WORLDWIDE?	486
E-6	MODELLING OF RADIONUCLIDES MOBILITY AFTER LEGACY SITE RESTORATION: THE CASE OF FLUORITE SLUDGE NORM	487
E-7	UNDERSTANDING URANIUM FATE IN WETLAND SOILS: A SPECIATION AND LABILE BEHAVIOR STUDY IN THE FORMER EXTRACTION MINE OF ROPHIN (FRANCE)	489
E-8	MODELLING WATER CIRCULATION AND SOLUTE TRANSPORT AT A FORMER FRENCH URANIUM MINING SITE	491
A3-1	THE AQUATIC CHEMISTRY OF PENTAVALENT ACTINIDES (NP, PU): DETERMINATION OF THE FIRST TWO HYDROLYSIS CONSTANTS	493
A3-2	SPECTROSCOPIC STUDY ON FORMATION OF AQUEOUS URANIUM(VI)-SILICATE COMPLEXES AT ALKALINE PH	495
A3-3	STRUCTURAL IDENTIFICATION OF AQUATIC U(VI)-PBTC COMPLEXES BY SPECTROSCOPIC INVESTIGATIONS	497
A3-4	CHEMICAL EQUILIBRIUM OF PLUTONIUM(VI) IN WEAKLY ALKALINE SYSTEMS CONTAINING ALKALINE EARTH METAL IONS AND CARBONATE	499
D-5	EURAD, A EUROPEAN PROGRAMME ON RADIOACTIVE WASTE MANAGEMENT, SCIENTIFIC OUTCOMES AND CHALLENGES AS SEEN BY THE EXTERNAL ADVISORY BOARD	501
A6-1	FORMATION, REACTIVITY AND COLLOIDAL BEHAVIORS OF TETRAVALENT URANIUM NANOPARTICLES UNDER GROUNDWATER CONDITIONS	503
A6-2	EVIDENCES ABOUT THE CONTRIBUTION OF PU(IV) OXO-HYDROXO CLUSTER $[PU_6(OH)_4O_4]^{12+}$ DURING THE FORMATION OF PU(IV) INTRINSIC COLLOIDS	505
A6-3	ROLE OF NITRATE ON THE FORMATION AND RETENTION OF Th^{IV} NANOPARTICLES AT THE MUSCOVITE (001)-WATER INTERFACE	507
A6-4	NEW CFM RADIONUCLIDE TRACER TEST DEDICATED TO KINETIC PROCESSES UNDER IN-SITU CONDITIONS AT THE GRIMSEL TEST SITE	509
A6-5	REVEALING THE ORIGIN AND ION-BINDING PROPERTIES OF DISSOLVED ORGANIC MATTERS IN DEEP SEDIMENTARY GROUNDWATER	511
A5-10	RETENTION AND TRANSPORT BEHAVIOUR OF SELENIUM(IV) IN HARDENED CEMENT PASTE: EFFECT OF HIGH SULPHATE CONCENTRATIONS	513
A5-11	RETENTION OF STRONGLY HYDROLYZING METAL IONS IN CEMENT SYSTEMS: QUANTITATIVE DESCRIPTION AND MECHANISTIC UNDERSTANDING	515
A5-12	THE OPTIMIZED GEMS CLAYSOR MODEL AND DATA BASES TO SUPPORT NAGRA SAFETY ASSESSMENTS FOR DEEP GEOLOGICAL REPOSITORY	517
A5-13	BENCHMARKING THE THERMOCHEMIE DATABASE: SOLUBILITY AND SPECIATION CALCULATIONS	519

E-2 MIGRATION OF ACTINIDES AND FISSION PRODUCTS – AN OVERVIEW TO PUT THE DIFFERENT ISSUES OF IMPORTANCE FOR THE POST-CLOSURE SAFETY OF GEOLOGICAL REPOSITORIES IN CONTEXTPiet Zuidema ⁽¹⁾*(1) Chief Scientific Officer EURAD, Zuidema Consult GmbH, Switzerland*

The safety of deep geological repositories for spent fuel and high-level radioactive waste is investigated since many years. The numerous editions of the ‘*Conference on the Chemistry and Migration Behavior of Actinides and Fission Products in the Geosphere*’ have made significant contributions to our understanding of the processes of relevance to retention and retardation of radionuclides in the barriers of a disposal system.

In the presentation, in a first part a broad overview will be given on the importance of the different processes contributing to post-closure safety, looking at a spectrum of repository systems in different types of host rocks. When assessing the different safety-relevant processes, it becomes obvious, that the chemistry and migration of radioelements is very important; however, it is not the only process that plays an important role. Furthermore, the migration behavior of radioelements is also strongly influenced by the flow-related properties of the host rock where in the case of fractured rocks, the abundance, and properties of the so-called fast channels play an important role. Such fast channels cannot be excluded in fractured crystalline rocks whereas in argillaceous media with favorable self-sealing properties they do not occur. However, besides the geosphere, also the system of engineered barriers plays an important role for the post-closure safety of disposal systems. There exists a broad spectrum of options for the system of the engineered barriers – the detailed design of them depends upon the waste properties and is tailored to the needs of the local geological environment; this geological environment, however, has in all cases to fulfil certain minimum requirements.

In a second part of the presentation, an analysis of the current understanding and of the importance of the remaining uncertainties will be given. Taking the expected performance of the different barrier elements into account, one comes to the conclusion that current understanding on the chemistry and migration behavior of actinides and fission products is advanced. This is also confirmed by the status of development of disposal projects in the advanced programs. The work done today and in the near future is in my view not anymore related to the feasibility of safe disposal but much more on the refinement of the detailed scientific understanding. These conclusions are also compared with current findings in EURAD, the European Joint Programme on Radioactive Waste Management that has several work packages looking at the behavior of radioelements in disposal systems [1]. In EURAD, not only the chemistry and migration behavior of the radioelements but also the performance other barrier elements is investigated [1].

Reference

- [1] EURAD - European Joint Programme for research on radioactive waste management: homepage, <https://www.ejp-eurad.eu/>

A8-1 COMPUTATIONAL CHEMISTRY APPROACHES TO PREDICTIVE MULTISCALE MODELLING OF MIGRATION PROCESSES: CURRENT CHALLENGES AND OPPORTUNITIESAndrey G. Kalinichev ⁽¹⁾

(1) *SUBATECH (UMR 6457 – IMT-Atlantique, Nantes Université, CNRS-IN2P3) Nantes, France*

Over the last 15-20 years, there has been a significant and steady progress in the application of theoretical methods of computational chemistry to very diverse sets of fundamental and applied problems of environmental science, materials science, geoscience, including the complex practical problems of migration behavior of actinides and fission products in the geosphere. This progress continues to be strongly stimulated by the recent advances in high performance computing and the availability of more sophisticated software packages with user-friendly graphical-based interfaces, which make the theoretical tools of computational chemistry readily available as just another powerful instrument in any multidisciplinary research [1, 2].

The so-called classical methods of molecular simulations rely heavily on the accurate description of the interactions among all atoms of the system, which are usually represented by a set of interatomic potentials, often based on empirical fits to available experimental data for thermodynamic and structural properties of materials or on the results of corresponding quantum chemical calculations. The practical success of these empirical potential functions—referred to collectively as a *force field*—ultimately depends on the quality and accuracy with which they are capable of reproducing experimental chemical structures, physical properties, and spectroscopic observations. Quantum-based simulation methods, including the widely used density functional theory (DFT), avoid the need for an empirical force field. Potential energy here is iteratively calculated through approximate solutions of various representations of the Schrödinger equation describing the quantized energy states of electrons in a chemical system. However, the price to pay in these high-level quantum-based approaches, compared with the classical methods, is their high computational cost. Even with the recent great advances in high performance supercomputing, the quantum-based methods remain limited by the orders of magnitude smaller time and size scales of the systems and processes they can realistically handle [1-3].

This becomes especially important for the complex multiscale phenomena associated with the migration and environmental evolution of actinides and other radionuclides in the geosphere. The complexity here originates not only from the challenges of accurate quantum chemical treatment of the electron structure of actinide atoms themselves, but also from the need to realistically describe the environmental materials with which these elements are interacting, such as clay and other minerals [3], soil organic matter [4], multicomponent aqueous environment, etc. All these materials are typically not very well characterized in terms of their atomic composition and structure. Nevertheless, computational chemistry approaches involving classical potential energy force fields and first principle (i.e., *ab initio*) methods are already capable of providing important quantitative information about the behavior of such systems.

This talk will provide a brief overview of the quantum and classical computational chemistry approaches as applied to the complex problems of the actinides and other radionuclides in natural and engineered environments. A special emphasis will be given to the most recent results of the classical simulations and the capabilities to address the multiscale nature of the materials and processes involved.

References

- [1] Liu, X., Tournassat, C., Grangeon, S., Kalinichev, A. G., Takahashi, Y., Marques Fernandes, M. (2022). Molecular-level understanding of metal ion retention in clay-rich materials. *Nature Reviews Earth & Environment* 3, 461-476.
- [2] Cygan, R. T., Greathouse, J. A., Kalinichev, A. G. (2021). Advances in Clayff molecular simulation of layered and nanoporous materials and their aqueous interfaces. *Journal of Physical Chemistry C* 125, 17573-17589.
- [3] Kalinichev, A. G. (2021). Atomistic modeling of clays and related nanoporous materials with ClayFF force field. In: *Computational Modeling in Clay Mineralogy*, Sainz-Díaz, C. I., Ed. Association Internationale pour l'Etude des Argiles (AIPEA): Bari, Italy, 2021; Vol. 3, pp 17-52.
- [4] Kalinichev, A. G., Kirkpatrick, R. J. (2007). Molecular dynamics simulation of cationic complexation with natural organic matter. *European Journal of Soil Science* 58, 909-917.

A8-2 ENABLING LONG TIME-SCALE QUANTUM MOLECULAR DYNAMICS SIMULATION FOR 5F-ELEMENTS

Ping Yang, Enrique R. Batista, Marc Cawkwell, Chang Liu, Rebecca Carlson, Shanshan Wu, Danny Perez

*Theoretical Division, Los Alamos National Laboratory, Los Alamos, NM 87545, USA
pyang@lanl.gov*

5f-element chemistry in solution is very intricate in nature. There is a pressing need to develop molecular dynamics (MD) methods that can describe quantum mechanical behavior, such as bond breaking and forming, at long timescales. Current first-principle MD methods can only reach tens of picoseconds, while classical force fields cannot accurately describe bond breaking and forming. To achieve this goal, we developed semiempirical density functional theory tight-binding (DFTB) parameters for 5f-elements that enable MD simulations at long time scales. Such simulations will be instrumental in understanding the evolution of speciation and reaction mechanisms. In this talk, we will share our recent development on a hybrid model that combines modern machine learning approaches with physics-based methods. We will demonstrate the transferability of this hybrid model on prediction of molecular structural parameters of various molecular clusters and a variety of chemical reaction free energies. Using these parameters, we also demonstrate microsecond-long quantum-MD simulations of nanoparticle systems for complex f-elements, shedding light on their dynamics and kinetics.

References

- [1] RK Carlson, MJ Cawkwell, ER Batista, P Yang, J. Chem. Theory Comp. 2020, 16, 3073-3083
- [2] NF Aguirre, A Morgenstern, MJ Cawkwell, ER Batista, P Yang, Chem. Theory Comp. 2020, 16, 1469-1481
- [3] NF Aguirre, J Jung, P Yang, Phys Chem Chem Phys 2020, 22, 18614
- [4] G Wang, ER Batista, P Yang, Appl Sci 2020, 10, 4655
- [5] C Liu, ER Batista, NF Aguirre, P Yang, MJ Cawkwell, E Jakubikova, , J Phys Chem A 2020, 124, 9674-9682

A8-3 DENSITY FUNCTIONAL MODELING OF AM(III) HYDROXO COMPLEXES WITH CA OR MG COUNTER IONS. DO MG STABILIZED SPECIES EXIST?

I. Chiorescu⁽¹⁾, S. Krüger⁽¹⁾

(1)Theoretische Chemie, Technische Universität München, 85748 Garching, Germany

While binary actinide complexes in aqueous solution have been studied for long and in depth, ternary species are less well known and characterized [1]. In recent years the class of complexes (Ca, Mg)-An-(OH, CO₃) has attracted interest as these complexes might contribute to the solubility of actinides in saline solutions of CaCl₂ and MgCl₂ at basic pH conditions. These conditions exist in geological repositories for radioactive waste in salt or clay rocks with saline pore waters and due to their interaction with cement of constructions or waste containments [1].

Solubility and TRLFS experiments on Nd(III) [2] and Cm(III) [3], respectively, in highly alkaline solutions of NaCl, CaCl₂ and MgCl₂ have been used together with earlier data to suggest a comprehensive thermodynamic model for Am(III), Cm(III) and Nd(III) in such solutions for the entire pH range. In order to explain the increasing solubility of Cm(III) in very basic CaCl₂ solutions, the formation of the ternary complexes Ca[M(III)(OH)₃]²⁺, Ca₂[M(III)(OH)₄]³⁺, and Ca₃[M(III)(OH)₆]³⁺ (Fig. 1) was suggested and their complexation constants have been determined for Cm(III) [2]. Experiments at the pertinent pH > 9 for MgCl₂ solutions were not possible due to precipitation. The thermodynamic model including these complexes consistently describes the solubility and hydrolysis of M(III) in various saline solutions [3].

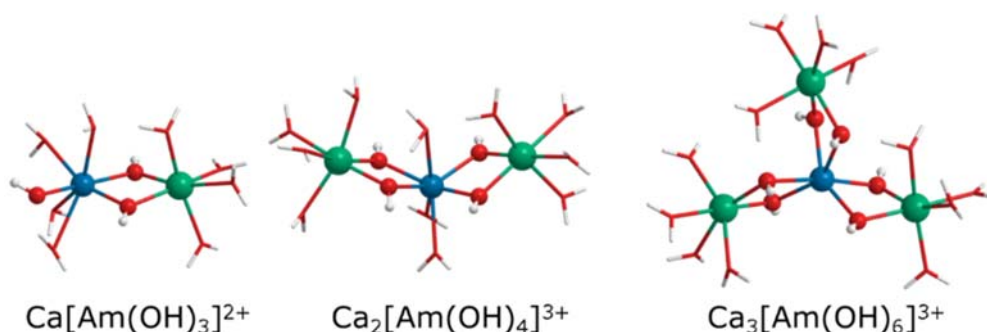


Figure 1: Structures of ternary Ca-Am(III) hydroxo complexes as suggested in saline CaCl₂ solutions.

To verify the existence of Ca-M(III) hydroxo complexes, their composition, structure, and thermochemistry, we have undertaken a computational study for the example of Am(III). Besides the complexes suggested, Ca_n[Am(OH)_m]^{3-2n-m} for (n,m) = (1,3), (2,4), and (3,6) (Fig. 1), we also inspected Ca[Am(III)(OH)₂]³⁺, with (n,m) = (1,2). In addition we modelled the corresponding Mg species. Electronic structures have been determined with all-electron spin-polarized scalar-relativistic density functional calculations with the PBE exchange-correlation functional of generalized gradient approximation type, employing the code ParaGauss. The complexes have been modeled including possible aqua ligands of Am(III). Alkaline earth counter ions have been added without and with aqua ligands to the Am hydroxo complex core.

The coordination number (CN) of Am(III) in the ternary complexes varies between 8 and 5 for the Ca complexes due to a varying number of aqua ligands. Small energy differences below 15 kJ/mol for aqua ligand addition show that variants of these complexes with different CNs might coexist. Similar results have been obtained for the Mg complexes, but for all of them Am prefers a CN of 6. Average Am-O bond lengths between 237 pm (CN = 5) and 250 pm (CN = 8) are essentially the same in the complexes

with Ca and Mg ions and their variation follows the CN. When aqua ligands at Ca and Mg ions are considered (Fig. 1), Ca shows a preferred CN of 6 and Mg of 5. Am-OH bond lengths tend to increase with the increasing number of OH ligands due to bonding competition. Consequently Ca-OH and Mg-OH bond lengths slightly decrease with increasing complex size. Deviations from these trends appear due to varying coordination numbers and charges of the complexes. Am-Ca and Am-Mg distances amount to 370 pm for Ca and to 362 pm for Mg on average for complexes with counter ion hydration. They are nearly constant for Ca and slightly increasing for Mg with increasing complex size. Overall, all complexes show a surprisingly similar geometry, independent of their size and the type of counter ion.

Endothermic complex formation Gibbs free energies with aqua complexes as reactants show an increasing trend for all complexes, in agreement with experiment [3]. Formation of the ternary complexes from Am hydroxide species yield small endothermic energies for the smaller Ca complexes, which are also in agreement with experimental values. An exothermic energy is computed only for $\text{Ca}_3[\text{Am}(\text{OH})_6]^{3+}$. These energies confirm that such complexes can be formed at basic pH conditions. For the Mg complexes, on the other hand, with the exception of the smallest one, increasingly larger exothermic formation energies from Am hydroxides are calculated. As Gibbs free reaction energies are overestimated in our calculations, comparison to experiment is best done for relative energies of formation from aqua ions $\Delta G(n,m)/\Delta G(1,3)$. These relative energies amount to 1, 1.4 and 2.3 in experiment [3] and to 1, 1.4 and 2.4 in the calculations for the Ca complexes with and without counter ion hydration. Smaller values have been obtained for the Mg complexes without counter ion hydration, suggesting a higher stability of these species. Addition of aqua ligands to the Mg ions leads to comparable relative energies as for Ca. Comparison of absolute energies confirms that Mg species without counter ion solvation are considerably more stable than Ca complexes. This finding would imply that such complexes increase the solubility of Am(III) considerably, most probably already in the pH range covered by experiment [3]. Inclusion of aqua ligands for Ca and Mg yields the Mg species to be slightly less stable than Ca ones. Thus, explicit solvation of the Mg counter ions is shown to be essential to gain reliable absolute complexation energies. These results suggest that the Mg analogs of $\text{Ca}_n[\text{Am}(\text{OH})_m]^{3-2n-m}$ complexes exist, but due to their slightly lower stability they should not have a sizeable effect on An(III) or Ln(III) solubility in MgCl_2 solutions at $\text{pH} \leq 9$. In summary, our computational findings are in agreement with current experimental evidence [3] and support the formation of the complexes $\text{Ca}_n[\text{Am}(\text{OH})_m]^{3-2n-m}$ as suggested from experiment [3].

References

- [1] Altmaier, M.; Gaona, X. and Fanghänel, T. (2013) Recent Advances in Aqueous Actinide Chemistry and Thermodynamics. *Chemical Reviews* 113: 901-943.
- [2] Rabung, T.; Altmaier, M.; Neck, V. and Fanghänel, T. (2008) A TRLFS study of Cm (III) hydroxide complexes in alkaline CaCl_2 solutions. *Radiochimica Acta* 96: 551-560.
- [3] Neck, V.; Altmaier, M.; Rabung, T.; Lützenkirchen, J. and Fanghänel, T. (2009) Thermodynamics of trivalent actinides and neodymium in NaCl , MgCl_2 , and CaCl_2 solutions: Solubility, hydrolysis, and ternary Ca-M(III)-OH complexes. (2009) *Pure & Applied Chemistry* 81: 1555-1568.

A8-4 COORDINATION AND THERMODYNAMIC PROPERTIES OF AQUEOUS PROTACTINIUM(V) BY COMPUTATIONAL CHEMISTRY TECHNIQUES

Hanna Oher^(1,2), Jeremy Delafoulhouze⁽³⁾, Eric Renault⁽³⁾, Valérie Vallet⁽⁴⁾ and Rémi Maurice^(1,2)

(1) *Subatech, CNRS-IN2P3/IMT Atlantique/Université de Nantes, Nantes, France*

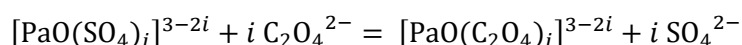
(2) *Univ Rennes, CNRS, ISCR (Institut des Sciences Chimiques de Rennes), Rennes, France*

(3) *Nantes Université, CNRS, CEISAM, Nantes, France*

(4) *Univ. Lille, CNRS, PhLAM-Physique des Lasers, Atomes et Molécules, Lille, France*

Protactinium ($Z = 91$) is a very rare actinide with peculiar physico-chemical properties. In fact, although one may naively think that it behaves similarly to either thorium or uranium (its immediate neighbors in the periodic table), it may follow its own rules. Because of the quite small energy gap between its valence shells (in particular the $5f$ and $6d$ ones) and also the strong influence of relativistic effects on its properties, it is actually a challenging element for computational chemists.

In this work [1], we combine experimental information, chemical arguments and quantum chemistry techniques to revisit the stepwise complexation of aqueous protactinium(V) with sulfate and oxalate dianionic ligands (SO_4^{2-} and $\text{C}_2\text{O}_4^{2-}$, respectively), whose resulting complexes have previously been characterized by spectroscopy and/or liquid-liquid extraction [2,3]. For this, we rely density functional theory, thermodynamic cycles and implicit and explicit solvation models to derive the 1:1, 2:2 and 3:3 ligand-exchange reaction constants, the generic reactions being defined as follows ($i = 1-3$):



From a methodological viewpoint, we conclude that it is necessary to at least saturate the coordination sphere of protactinium(V) to reach converged equilibrium constant values. Furthermore, in the case of single complexations, we show that it is necessary to maintain the coordination of one hydroxyl group, thought of in the $[\text{PaO}(\text{OH})]^{3+}$ precursor, to obtain coherent complexation constants.

Therefore, we predict that this hydroxyl group is maintained in the formation of the 1:1 complexes while we confirm that it is withdrawn when coordinating three sulfate or oxalate ligands. This proof-of-concept concerning the added value of computational chemistry outcomes is a first step toward the use of theoretical predictions to elucidate the enigmatic chemistry of protactinium in solution.

This work was supported by grants funded by the “Région Pays de la Loire” (RCT-PaPAn project) and the French National Agency for Research (ANR-21-CE29-0027 contract).

References

- [1] H. Oher, J. Delafoulhouze, E. Renault, V. Vallet and R. Maurice (2023). Coordination and thermodynamic properties of aqueous protactinium(V) by first-principle calculations. ArXiv: 2301.08515.
- [2] M. Di Giandomenico and C. Le Naour (2009). Complex formation between protactinium(V) and sulfate ions at 10 and 60°C. *Inorg. Chim. Acta* 362: 3253–3258.
- [3] M. Mendes, S. Hamadi, C. Le Naour, J. Roques, A. Jeanson, C. Den Auwer, P. Moisy, S. Topin, J. Aupiais, C. Hennig and M.-V. De Giandomenico (2010). Thermodynamical and structural study of protactinium(V) oxalate complexes in solution. *Inorg. Chem.* 49: 9962–9971.

A8-5 SORPTION OF EU(III) ON C-S-H PHASES IN THE PRESENCE OF GLUCONATE: A MOLECULAR DYNAMICS STUDY

Iuliia Androniuk⁽¹⁾, Rosa Ester Guidone⁽¹⁾, Marcus Altmaier⁽¹⁾, Xavier Gaona⁽¹⁾

(1)Institute for Nuclear Waste Disposal (INE), Karlsruhe Institute of Technology (KIT), Karlsruhe, Germany

Cement is an important material used in the design and construction of waste storage facilities, especially for low- and intermediate-level waste (L/ILW). The calcium silicate hydrate phases (C-S-H) are the major binding phases of cement, have high specific surface area, and have been described to sorb cationic and (to lesser extent) anionic species. A variety of organic ligands is expected in repositories for L/ILW as a component of the waste (e.g. EDTA, citrate, etc.), degradation products of complex organic materials (e.g. ISA), additives of cement (e.g. gluconate), among others. The presence of organic complexants in the cement pore water may affect the radionuclide mobility: organic molecules can form water-soluble complexes and compete with the radionuclides for sorption sites. This modelling work was designed to obtain a detailed understanding of the mechanisms of such interactions on the molecular level. Based on their similar charge-to-size (z/d) ratios, Eu(III) was considered as representative of key trivalent actinides expected in nuclear waste, *i.e.* Pu(III) and Am(III).

We used classical molecular dynamics (MD) simulations and the potential of mean force (PMF) calculations to obtain a mechanistic understanding of the surface sorption process for Eu(III) species on the surface of C-S-H in the presence of gluconate. For this, several representative models have been developed. Calculations were carried out using the ClayFF force field parameters for C-S-H [1], the SPC/E water model, the Eu(III) potentials from [2], and the GAFF/OPLS parameters [3] for gluconate.

The (001) surface of C-S-H is the most common and stable surface and therefore it is in the focus of this computational study. The surface model was developed to fit the available experimental data and recent theoretical descriptions of the molecular structure of C-S-H. Three of the most probable sorption sites on the (001) surface were considered: the bridging site (deprotonated silanol group of the bridging Si), the defect site (deprotonated silanol groups of pairing Si) and the silicate chain site (as shown in Figure 1). First, the binary systems were studied in detail to provide the reference data for understanding processes in the ternary system (Eu(III)/gluconate/C-S-H). A series of classical MD simulations of Eu(III)/Ca/gluconate model solutions revealed that both 1:1 and 1:2 complexes of Eu(III) and organics are possible, and Ca ions are an important component of their stability. This is in line with recent solubility and TRLFS data reported for Nd(III) and Cm(III) systems [4]. The results from the Eu(III)/C-S-H binary system confirmed strong sorption and showed that the most common sorption sites are the deprotonated silanol groups of the bridging and defect sites.

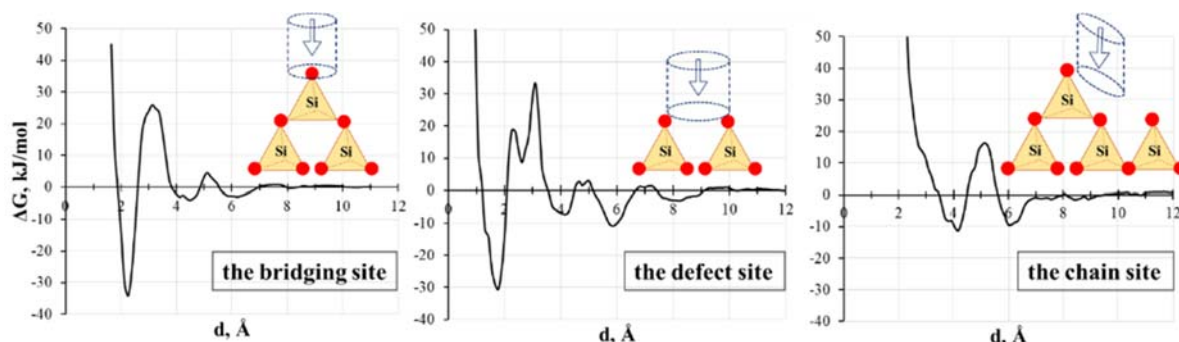


Figure 1. Potential of mean force of Eu(III) sorption on three sorption sites on the C-S-H surface with schematic representations of the sites.

We have also shown that the presence of Ca^{2+} ions in the C-S-H interface stabilizes Eu(III) as $\text{Eu}(\text{OH})_4^-$ species in cementitious environment. This is also in line with the reported stability of the aqueous complexes $\text{Ca}_2[\text{M}(\text{OH})_4]^{3+}$, and $\text{Ca}_3[\text{M}(\text{OH})_6]^{3+}$ (with $\text{M} = \text{Nd}, \text{Cm}$) in hyperalkaline CaCl_2 solutions with Ca concentrations above 0.05 M [4, 6]. The strength of Eu(III) binding, calculated with PMF, is similar to those of Ca^{2+} at the same sorption sites [5] and validates the experimental findings. The molecular dynamics study was carried out in close collaboration with experimental work that was performed for this ternary system, and it supports, validates, and further explains the results [7]. The calculations on the ternary system are ongoing.

References

- [1] Cygan, R.T., Liang, J.J., Kalinichev, A.G. (2004). Molecular models of hydroxide, oxyhydroxide, and clay phases and the development of a general force field. *J. Phys. Chem. B* 108: 1255–1266.
- [2] Van Veggel, F. C. J. M. and Reinhoudt, D.N. (1999). New, Accurate Lennard-Jones Parameters for Trivalent Lanthanide Ions, Tested on [18]Crown-6. *Chem. Eur. J.* 5 (1): 90–95.
- [3] Wang, J., Wolf, R. M., Caldwell, J. W., Kollman, P. A., Case, D. A. (2004) Development and testing of a general AMBER force field. *J. of Comp. Chem.* 25: 1157–1174.
- [4] Rojo, H., Gaona, X., Rabung, T., Polly, R., García-Gutiérrez, M., Missana, T., Altmaier, M. (2021). Complexation of Nd(III)/Cm(III) with gluconate in alkaline NaCl and CaCl_2 solutions: Solubility, TRLFS and DFT studies. *Appl. Geochem.* 126: 104864.
- [5] Androniuk, I. and Kalinichev, A.G. (2020). Molecular dynamics simulation of the interaction of uranium (VI) with the C-S-H phase of cement in the presence of gluconate. *Appl. Geochem.* 113: 104496.
- [6] Neck, V., Altmaier, M., Rabung, T., Lützenkirchen, J., Fanghänel, T. (2009). Thermodynamics of trivalent actinides and neodymium in NaCl, MgCl_2 , and CaCl_2 solutions: Solubility, hydrolysis, and ternary Ca–M(III)–OH complexes. *Pure Appl. Chem.* 81: 1555–1568.
- [7] Guidone, R.E., Lothenbach, B., Tasi, A., Androniuk, I., Gaona, X., Altmaier, M., Geckeis, H. (2023). Impact of formate, citrate and gluconate ligands (L) on the uptake of radionuclides (RN) by cement, this conference.

A5-1 IMPACT OF FORMATE, CITRATE AND GLUCONATE ON THE UPTAKE OF AN(III)/LN(III) AND AN(IV) BY CEMENT

R. E. Guidone^(1,2), A. Tasi⁽¹⁾, I. Androniuk⁽¹⁾, X. Gaona⁽¹⁾, B. Lothenbach⁽²⁾, M. Altmaier⁽¹⁾, H. Geckeis⁽¹⁾

(1) Karlsruhe Institute of Technology, Institute for Nuclear Waste Disposal, Karlsruhe, Germany

(2) Swiss Federal Laboratories for Materials Science and Technology (Empa), Laboratory for Concrete & Asphalt, Dübendorf, Switzerland

In the context of low and intermediate level nuclear waste (L/ILW), cementitious materials are widely used for the conditioning and storage of the waste, as well as for the construction of engineered barrier systems (backfill, container and liner materials). The main solid phases in hydrated cements (calcium silicates hydrates (C-S-H), ettringite, monosulfoaluminate, monocarboaluminate, and hemicarboaluminate (AFm phases)) can retain radionuclides present in the waste, thus preventing or slowing down their release from the disposal site. Soluble small organic molecules are expected in the repository as a component of the emplaced waste, as degradation products of organic components disposed of, but also as additives in different cement formulations. The potential interaction of these organic ligands with actinides may importantly alter both their solubility and sorption properties. Although expected to be weak, the interaction of organic ligands with cement hydrates can also alter the surface properties of the latter. This study aims at a quantitative description of the interaction of low molecular weight organics (formate, citrate and gluconate) with selected cement phases, *i.e.* AFm, ettringite and C-S-H phases. The impact of these organic ligands on the uptake of Eu(III), Cm(III) and Pu(III/IV) by cement and individual cement phases is investigated with a combination of sorption experiments and advanced spectroscopic techniques.

The cement phases AFm, ettringite and C-S-H (with Ca/Si ratio C/S = 0.8-1.4) were prepared and stored under N₂ atmosphere with a solid to liquid ratio (S:L) of $\approx 50 \text{ g} \cdot \text{dm}^{-3}$, and equilibrated for 2 months before further use. Sorption experiments were performed with the synthesized cement phases in the presence of formate, citrate or gluconate at $10^{-4} \text{ M} \leq [\text{L}] \leq 0.1 \text{ M}$ and at $\text{pH} \approx 13.3$. The samples were filtered with $0.45 \mu\text{m}$ nylon filters, and dried in a desiccator (37% relative humidity) for 14 days. The separated solid phases were characterized by X-ray diffraction (XRD), thermogravimetric analysis and FT-IR analysis. Supernatant solutions were characterized after filtration by ICP-OES (Ca, Al, Si, Na, sulfate) and NPOC (total organic content). Sorption experiments with ¹⁵²Eu + ^{nat}Eu and ²⁴²Pu were carried out in the absence and presence of organic ligands and varying the S:L ratio, order of addition and organic concentration. In the sorption experiments with plutonium, redox conditions were buffered with hydroquinone (HQ, pe + pH ≈ 9) or Sn(II)Cl₂ (pe + pH ≈ 1.5). Phase separation was achieved by ultrafiltration via 10 kD filters. The measurement of ²⁴²Pu and ¹⁵²Eu was carried out by ICP-MS and

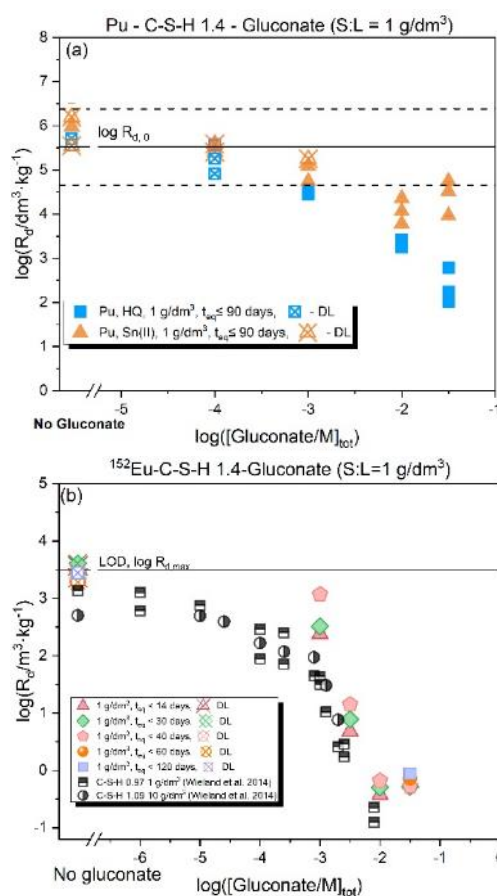


Figure 1. R_d values determined for the uptake of (a) Pu(III/IV) and (b) Eu(III) by C-S-H 1.4 in the absence and presence of GLU at $\text{pH}=13.3$. Solid line indicates the $R_{d,0}$ values in the absence of gluconate. Symbols crossed with X correspond to samples at / below the detection limit (DL).

gamma counter analysis respectively. TRLFS investigation was conducted exclusively on the Cm(III)-C-S-H-GLU system. Both solution and solid phase speciation were investigated at the same pH and ligand concentrations considered in the sorption experiments. TRLFS spectra were collected for equilibration times $7 \leq t_{\text{eq}} \text{ (days)} \leq 56$.

Formate sorption was found to be very weak ($R_d \approx 10^{-3} \text{ m}^3 \cdot \text{kg}^{-1}$) for all investigated cement phases (AFm, ettringite and C-S-H), in agreement with previous observations reported in the literature [1]. Significantly higher R_d values were quantified for the uptake of citrate and gluconate. The uptake of citrate and gluconate by C-S-H phases with Ca/Si = 0.8-1.4 was found to be relatively high with $R_d \approx 10^{-3} - 10^{-2} \text{ m}^3 \cdot \text{kg}^{-1}$. Furthermore, both gluconate and citrate show a systematic increase in log R_d values with increasing Ca/Si ratio. This observation hints towards a Ca complexation mediated process at the surface of C-S-H phases. This mechanism has been recently validated by molecular dynamics calculations for the C-S-H-gluconate system [2]. Formate and citrate have a negligible impact on the uptake of Pu(III/IV) by C-S-H phases for both redox-buffer systems. Figure 1 shows the log R_d values for the uptake of Pu (a) and Eu (b) by C-S-H phases with C/S ratios of 1.4 as a function of gluconate total concentrations ($10^{-4} \text{ M} \leq [\text{GLU}]_{\text{tot}} \leq 10^{-1.5} \text{ M}$). In line with previous studies with Th(IV) and Eu(III) [3], gluconate significantly decreases the uptake of Pu(III/IV) and Eu(III) by C-S-H phases. These observations are explained by the possible formation of stable ternary / quaternary complexes in the aqueous phase, *i.e.* Ca-An(IV)-OH-GLU and Ca-An(III)/Ln(III)-OH-GLU [4, 5]. Figure 1(a) shows also that log R_d values determined at the two highest ligand concentrations in the Sn(II)-buffered system follow a rather increasing trend, opposite of that observed in the HQ-buffered system. This finding hints towards (i) a different chemical behavior induced by the redox buffer, expectedly involving the predominance of Pu(IV) and Pu(III) for HQ and Sn(II) systems, respectively, and (ii) the possibility of a co-adsorption process of Pu(III)_{aq} with GLU and the subsequent surface complexation of Pu onto these GLU-complexed surface sites, as also observed in [6]. TRLFS confirmed the key role of Ca in the formation of quaternary aqueous complexes Ca-An(III)/Ln(III)-OH-GLU, whereas at low ligand concentrations the incorporation of Cm(III) in the C-S-H structure was observed. This experimental study was complemented with molecular dynamics calculations on the binary and ternary systems defined by C-S-H / Eu(III) / GLU, which provide key insights for the mechanistic understanding of the retention processes in cementitious systems [7].

Acknowledgments: *The EURAD-CORI project leading to this application has received funding from the European Union's Horizon 2020 research and innovation programme under grant agreement No 847593.*

References

- [1] E. Wieland, A. Jakob, J. Tits, B. Lothenbach, D. Kunz, *Applied Geochemistry*, 67 (2016) 101-117.
- [2] I. Androniuk, C. Landesman, P. Henocq, A.G. Kalinichev, *Physics and Chemistry of the Earth, Parts A/B/C*, 99 (2017) 194-203.
- [3] E. Wieland, Paul Scherrer Institute (PSI), 2014.
- [4] X. Gaona, V. Montoya, E. Colàs, M. Grivé, L. Duro, *Journal of Contaminant Hydrology*, 102 (2008) 217-227.
- [5] J. Tits, E. Wieland, M. Bradbury, *Applied Geochemistry*, 20 (2005) 2082-2096.
- [6] A. Tasi, X. Gaona, T. Rabung, D. Fellhauer, J. Rothe, K. Dardenne, J. Lützenkirchen, M. Grivé, E. Colàs, J. Bruno, *Applied Geochemistry*, 126 (2021) 104862.
- [7] I. Androniuk, R. Guidone, M. Altmaier, X. Gaona, (2023), this conference.

A5-2 INTERFACIAL CHEMISTRY OF GIBBSITE UNDER CONDITIONS RELEVANT TO NUCLEAR WASTE

Zheming Wang¹, Hailin Zhang,¹ Yatong Zhao,¹ Wenwen Cui,¹ Xin Zhang,¹ Suyun Wang,¹ Eric D. Walter² Michel J. Sassi,¹ Carolyn I. Pearce,¹ Sue B. Clark,² and Kevin M. Rosso¹

(1) Pacific Northwest National Laboratory, Richland, WA 99352, United States

(2) Savannah River National Laboratory, Aiken, SC 29808, United States

Aluminum (oxy)hydroxides, such as gibbsite ($\text{Al}(\text{OH})_3$) and boehmite (AlOOH), are major mineral components of Al ores, such as bauxite, and are common mineral weathering products in soils and sediments.¹ They are also of particular importance in the nuclear industry. For example, in early nuclear fuel fabrication, such as at the Hanford site, aluminum was used as the fuel rod casing material, and a large amount was co-disposed with the nuclear waste and ended up as the major mineral phases in highly radioactive tank waste sludge.² The unpredictable solubility of some of the associated aluminum mineral phases is a risk driver for waste extraction and processing into stable long-term waste forms. Al-(oxy)hydroxide minerals are also expected to be important reactive minerals in host rock and engineered clay buffer layers in designs for below-ground nuclear waste repositories. Finally, in industrial applications, hydrated surfaces of alumina have structural and chemical similarities with Al-(oxy)hydroxide surfaces.³⁻⁴ Hence there is an ongoing need to improve our fundamental understanding of the structure and reactivity at surfaces of Al-(oxy)hydroxide minerals.

In this work, platelet gibbsite nanoparticles were synthesized via hydrothermal treatment of solids from hydrolysis of aluminum nitrate and are subjected to i) hydration at different relative humidity levels; ii) ⁶⁰Co-irradiation at selected dose levels with and without subsequent re-hydration treatment; iii) adsorption of Cr^{3+} , Eu^{3+} and UO_2^{2+} ions as representatives of the transition metal, lanthanide and actinide ions, respectively; and iv) doping of Cr^{3+} ion. The pristine and treated gibbsite samples are then investigated using surface-/interface-specific vibrational sum frequency generation (VSFG) spectroscopy in combination with laser-induced time-resolved luminescence spectroscopy (TRLFS), Raman spectroscopy, thermogravimetric analysis, and electron microscopy methods. VSFG is a second-order nonlinear optical spectroscopy technique for which there is no sum frequency signal in centrosymmetric media.⁵ Thus, bulk solutions and most bulk solids do not produce a signal. It's only at surface and interfaces where the centrosymmetry is broken, molecules display a sum frequency signal. Our results show that gibbsite displays strong, well-resolved VSFG bands of the surface hydroxyl stretch vibrational bands for all samples at frequencies $\sim 3623, 3525, 3425, \text{ and } 3355 \text{ cm}^{-1}$. The peak positions were nearly identical to those in the IR and Raman spectra of the bulk nanoparticles. However, the absolute spectral intensity as well as the relative intensity of the four bands varied depending on sample treatment. There is little change on the VSFG spectra when exposed the samples to various humidity levels, implying only weak H-bonding between the surface hydroxyls and hydration waters. ⁶⁰Co irradiation at 17.4 Mrem/h for 17 h leads to significant reduction of the VSFG spectral intensity. Based on the integrated areas of the VSFG spectra before and after irradiation, 83% of the surface hydroxyls were removed after irradiation, while the center positions of the SFG bands only show subtle shifts. In addition to the overall intensity drop, the relative intensities of the bands varied as manifested by a larger drop of the 3623 cm^{-1} band compared to those at lower frequencies. VSFG analysis of a series of gibbsite samples irradiated at different dose levels by varying the distances of the samples from the ⁶⁰Co source showed that the VSFG spectral intensity decreased exponentially in the dose range from 0.60 to 29.3 Mrads. At doses of 29.3 Mrads and 6.9 Mrads, which corresponded to 17 h and 4 h irradiations at a dose rate of 1.72Mrads/h, the VSFG spectral changes were small, implying that the de-hydrogenation reactions were approaching steady state in both cases. The 17 h irradiated samples were also re-analyzed by VSFG after being kept in capped vials under ambient conditions for 60 days and after exposure to saturated water vapor overnight. Spectral changes were minimal after the 60-day storage period, and subsequent exposure to water vapor did not lead to complete recovery of the VSFG signal intensity.

Batch sorption data show that sorption of metal ions on gibbsite occurs in broad pH range. VSFG spectra (Figure 1) reveals that metal ion sorption leads to reduction of the spectral intensity of gibbsite surface O-H groups, indicating participation of the surface OH in metal ion bonding. The spectral profiles upon Cr^{3+} sorption is similar to that of pristine gibbsite and reduction of the VSFG bands inversely correlates to Cr^{3+} concentration, suggesting equal involvement among the six distinct surface hydroxyls. But sorption of Eu^{3+} and UO_2^{2+} alters its spectral profile where the reduction of the intra-layer OH bands are more pronounced and the correlation between the spectral reduction and metal ion concentration is weaker, indicating differed sorption mechanism. The latter was confirmed by the results of TRLFS analysis of both Eu^{3+} and UO_2^{2+} adsorbed on gibbsite.

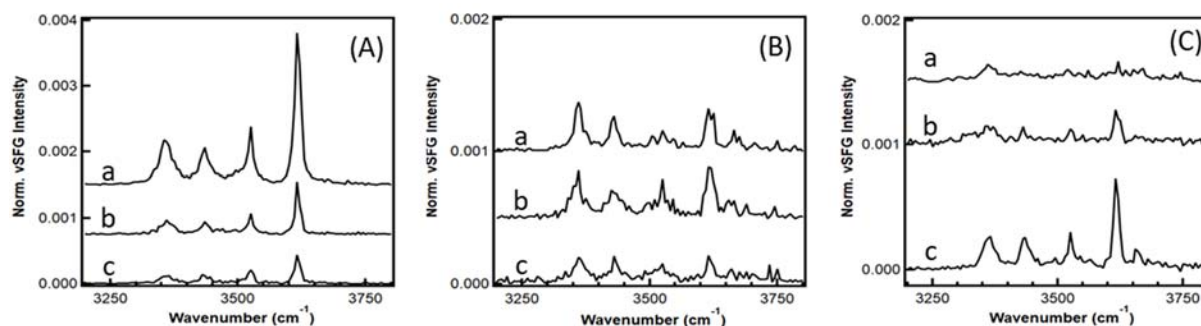


Figure 1. VSFG spectra of the synthesized gibbsite with adsorbed metal ions in 0.1 M NaOH (Cr^{3+} , panel A; UO_2^{2+} , panel B; Eu^{3+} , panel C). In (A): a – gibbsite only; b – $[\text{Cr}] = 50 \text{ ppm}$; c – $[\text{Cr}] = 200 \text{ ppm}$. In (B): a – $[\text{U}] = 0.01\%$, b – $[\text{U}] = 0.1\%$, c – $[\text{U}] = 1\%$. In (C): a – $[\text{Eu}] = 0.01\%$, b – $[\text{Eu}] = 0.1\%$, c – $[\text{Eu}] = 1\%$. All metal ion concentrations are relative to $[\text{Al}]$. Spectral traces are off-set in the Y-axis for clarity.

References

- [1] McKeague, J. A.; Grant, D. R.; Kodama, H.; Beke, G. J.; Wang, C., Properties and Genesis of a Soil and the Underlying Gibbsite-Bearing Saprolite, Cape Breton Island, Canada. *Canadian Journal of Earth Sciences* 1983, 20, 37-48.
- [2] Peterson, R. A.; Lumetta, G. J.; Rapko, B. M.; Poloski, A. P., Modeling of Boehmite Leaching from Actual Hanford High-Level Waste Samples. *Separation Science and Technology* 2007, 42, 1719-1730.
- [3] Eng, P. J.; Trainor, T. P.; Brown, G. E.; Waychunas, G. A.; Newville, M.; Sutton, S. R.; Rivers, M. L., Structure of the Hydrated Alpha- Al_2O_3 (0001) Surface. *Science* 2000, 288, 1029-1033.
- [4] Kupcik, T.; Rabung, T.; Lutzenkirchen, J.; Finck, N.; Geckeis, H.; Fanghanel, T., Macroscopic and Spectroscopic Investigations on $\text{Eu}(\text{III})$ and $\text{Cm}(\text{III})$ Sorption onto Bayerite ($\text{Beta-Al}(\text{OH})_3$) and Corundum ($\text{Alpha-Al}_2\text{O}_3$). *Journal of Colloid and Interface Science* 2016, 461, 215-224.
- [5] Wang, H.; Borguet, E.; Yan, E. C. Y.; Zhang, D.; Gutow, J.; Eisenthal, K. B., Molecules at Liquid and Solid Surfaces. *Langmuir* 1998, 14, 1472-1477.

A5-3 RETENTION OF ²²⁶RA BY ILLITE AND MONTMORILLONITE: AN ADSORPTION STUDY

F. Brandt⁽¹⁾, M. Klinkenberg⁽¹⁾, B. Baeyens⁽²⁾, D. Bosbach⁽¹⁾, M. Marques Fernandes⁽²⁾

(1) *Forschungszentrum Jülich GmbH, Institute of Energy and Climate Research, IEK-6: Nuclear Waste Management, 52425 Jülich, Germany*

(2) *Paul Scherrer Institut, Laboratory for Waste Management, 5232 Villigen PSI, Switzerland*

The fate of important radionuclides must be assessed in geochemical scenarios to ensure the long-term safety of deep nuclear waste geological repositories. Depending on the host-rock, some of these scenarios have examined the consequences of contact with the interstitial “in situ” porewaters with spent nuclear fuel, indicating that ²²⁶Ra can become a main contributor to the total dose after 10⁴ - 10⁵ years of waste disposal [1]. The fate of ²²⁶Ra is also relevant from the environmental perspective as it is also a main contributor to naturally occurring radioactive materials (NORM) and the environmental hazards associated with NORM e.g. in the surroundings of mining operations or geothermal operations [2].

Argillaceous rocks are considered suitable for the construction of deep geological waste repositories for high-level nuclear waste in several waste management programs e.g. in Switzerland [3], Belgium [4], or France [5]. Clay minerals are major constituents of these formations and due to their low permeability and high adsorption properties they considerably retard the migration of potentially released positively charged radionuclides in the biosphere. To account for these retardation properties in safety studies, thermodynamic models capable of predicting the retention of radionuclides over a wide range of physico-chemical conditions are crucial. Illite and illite/smectite mixed layers are relevant constituents of many argillaceous host rocks. In addition, bentonites are envisaged as engineered barriers in underground waste disposal concepts (e.g. [1], [2]). For example, in the Swiss concept, bentonite is foreseen as a buffer material to seal waste canisters, while bentonite-sand mixtures are foreseen as backfill material for access tunnels [7]. Montmorillonite, the major constituent of bentonite (up to 90 wt.-%) is an important sink for potentially released radionuclides and a common mineral in soils and sediments.

Adsorption data for ²²⁶Ra onto illite and montmorillonite are sparse in the open literature. Because of this knowledge gap, the adsorption and diffusion of ²²⁶Ra in clay minerals are assumed to be like that for Ba, based on chemical analogy. In order to verify this assumption and improve the quantitative understanding of the retention of ²²⁶Ra by 2:1 clay minerals relevant for radioactive waste disposal, a combined adsorption and modelling study was carried out. Parallel adsorption experiments were carried out onto the homo-ionic Na form of Wyoming montmorillonite (SWy-2) and illite (Na-illite, IdP-2; Illite de Puy, Le Puy-en-Velay, France) in diluted systems and compared to the adsorption of Ba under the same conditions. ²²⁶Ra and Ba adsorption edges in the pH range 5 to 10 at different ionic strengths (0.01 - 0.3 M NaCl) and an isotherm (pH 7, 10⁻⁹ M < [Ra,Ba] > 10⁻² M) were carried out on Na-SWy and IdP.

For montmorillonite, the 2-site Protolysis Non Electrostatic Surface Complexation and Cation Exchange adsorption model (2SPNE SC/CE, [8]) reproduces the experimental data for both elements quite well [9]. The K_c values for Ba²⁺-Na⁺ and ²²⁶Ra²⁺-Na⁺ exchange equilibria are in good agreement at low ionic strength (log K_c = 0.70 - 0.84), whereas at high ionic strength, the K_c (Ba-Na) is slightly higher (log K_c of 0.90 (0.3 M) vs 0.70 (≤ 0.02 M)). In contrast, the K_c (Ra-Na) exhibits a clear dependency on ionic strength, with log K_c values of 0.7, 1.14 and 1.34 at NaCl background concentrations of 0.01/0.02 M, 0.14 M and 0.3 M, respectively. For illite, the 2SPNE SC/CE model derived in earlier studies (?) reproduces the experimental Ba adsorption data quite well. In comparison to Ba, pH edges at varying ionic strengths consistently reveal a higher selectivity of illite for ²²⁶Ra. The ²²⁶Ra pH edges are well

described by an adjusted 2SPNE SC/CE model for illite. Additional ^{226}Ra -Ba adsorption experiments with Ba intended as a carrier for ^{226}Ra again showed a higher affinity of ^{226}Ra . The distinct differences in the behavior of ^{226}Ra compared to Ba can only be described by a more complex model, which includes two additional high affinity sites for ^{226}Ra . These sites are characterized by a low capacity and high selectivity for ^{226}Ra . These may be sub-sites of the Ba high affinity sites, leading to a partial competition between Ba and ^{226}Ra .

The results presented here indicate that Ba can be used as a good analogue for ^{226}Ra regarding the adsorption on montmorillonite at ionic strengths $< 0.1\text{ M}$ and $\text{pH} < 8$ but deviates in its behaviour at higher ionic strength. Different from the adsorption on montmorillonite, for the adsorption on illite Ba cannot be considered a very good analogue for ^{226}Ra but needs to be described by a more complex adsorption model.

References

- [1] SKB (2011). Long-term Safety for the Final Repository of Spent Nuclear Fuel at Forsmark. Main Report of the Sr-Site Project I-III. Stockholm, Sweden.
- [2] Fisher, R.S. (1998). Geologic and geochemical controls on naturally occurring radioactive materials (NORM) in produced water from oil, gas, and geothermal operations. *Environ. Geosci.* 5, 139–150.
- [3] Nagra (2002). Project Opalinus Clay: Safety Report. Demonstration of Disposal Feasibility (Entsorgungsnachweis) for Spent Fuel, Vitrified High-Level Waste and Long-Lived Intermediate-Level Waste. Technical Report NTB 02-05. Wettingen, Switzerland.
- [4] ONDRAF/NIRAS (2001). SAFIR 2: Safety assessment and feasibility report 2. Technical report NIROND 2001-05 E. ONDRAF/NIRAS, Brussels, Belgium.
- [5] Andra (2001). Référentiel géologique du site de Meuse/Haute Marne. Rapp. A RP ADS 99-005 de l'Agence nationale pour la gestion des déchets radioactifs, Châtenay-Malabry, France
- [6] Nagra (2014). Modellhaftes Inventar für radioaktive Materialien MIRAM 14. Wettingen, Switzerland
- [7] Jenni, A., Wersin, P., Thoenen, T., Baeyens, B., Ferrari, A., Gimmi, T., Mäder, U., Marschall, P., Hummel, W., Leupin, O. (2019). Bentonite Backfill Performance in a High-Level Waste Repository: a Geochemical Perspective (Nagra: Technical Report, Report No.: NTB 19-03).
- [8] Bradbury, M.H., Baeyens, B. (1997). A mechanistic description of Ni and Zn sorption on Na-montmorillonite Part II: modelling. *J. Contam. Hydrol.* 27, 223–248.
- [9] Klinkenberg, M., Brandt, F., Baeyens, B., Bosbach, D., Fernandes, M.M., 2021. Adsorption of barium and radium on montmorillonite: A comparative experimental and modelling study. *Applied Geochemistry* 135, 105117.

A5-4 U(VI) RETENTION ON BENTONITE AND CEMENTITIOUS MATERIALS: EFFECT OF INCREASED IONIC STRENGTHS AND PRESENCE OF ORGANICS

Katja Schmeide, Thimo Philipp ⁽¹⁾, Nina Huittinen, Salim Shams Aldin Azzam, Jérôme Kretzschmar

Helmholtz-Zentrum Dresden – Rossendorf e.V., Institute of Resource Ecology, Bautzner Landstraße 400, 01328 Dresden, Germany

The safe disposal of radioactive waste from operation and decommissioning of nuclear power plants in geological repositories requires the application of multiple barriers to isolate the waste from the biosphere. Most disposal concepts consider the extensive use of bentonite and cementitious materials in the geoenvironmental barrier as buffer and borehole sealing material as well as to enforce mechanical stability of disposal facilities. To evaluate the radionuclide retention potential of these barrier materials, it is necessary to examine the effects of various repository-relevant conditions that are expected to develop over time, such as altered pH, increased ionic strengths or temperatures, or the release of organic constituents.

Pore waters of the North German clay deposits are characterized by high ionic strengths up to 4 M [1,2]. The contact of such saline formation waters with concrete will result in an enhanced corrosion of concrete and to the evolution of highly alkaline cement pore waters ($10 < \text{pH} < 13$), which in turn, can react with the bentonite buffer as well as with the clay host rock, changing their retention potential towards radionuclides. Moreover, the role of organics (as admixtures in cement-based materials or waste constituents [3]) on actinide retention has to be studied.

The U(VI) retention on Ca-bentonite in mixed electrolyte solutions ('diluted Gipshut solution', $I = 2.6$ M) was found to be very effective at $\text{pH} > 10$, even in the presence of carbonate and despite the prevalence of anionic aqueous uranyl species [4]. By means of luminescence and X-ray absorption spectroscopy, two dominating U(VI) surface species at hyperalkaline conditions were identified: (i) a ternary U(VI) complex, where U(VI) is bound to the surface via bridging Ca cations with the configuration surface $\equiv \text{Ca}-\text{OH}-\text{U}(\text{VI})$ and, (ii) U(VI) sorption into the interlayer space of calcium (aluminum) silicate hydrates (C-(A)-S-H), which form as secondary phases in the presence of Ca due to partial dissolution of aluminosilicates at hyperalkaline conditions (Figs. 1 and 2) [5]. Citrate and 2-phosphonobutane-1,2,4,-tricarboxylate (PBTC) were found to reduce U(VI) retention only when present at high concentrations.

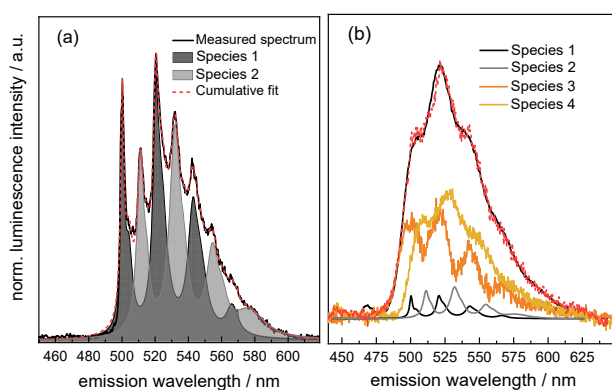


Figure 1. Extracted pure component signals from the decomposition of the measured U(VI) emission spectra in the Ca-bentonite suspension at pH 11 (a) and at pH 12.5 (b).

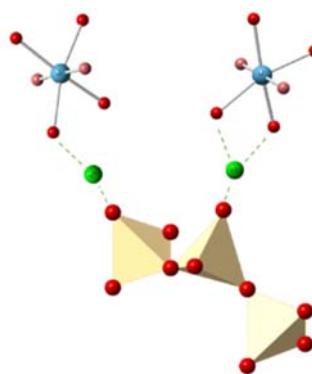


Figure 2. Proposed structures for ternary surface complexes showing a Ca-bridge between silanol surface sites of the minerals and uranyl hydroxide species predominant in the hyperalkaline pH range.

The U(VI) retention by C-A-S-H, formed due to Al-rich additives in cement formulations, was studied applying samples with Ca/Si molar ratios of 0.8, 1.2 and 1.6, representing different alteration stages of concrete, and with increasing Al/Si molar ratios of 0, 0.06 and 0.18 in each series. Furthermore, the impact of temperature (25°C, 100°C, 200°C) on both the C-A-S-H structure and the U(VI) retention mechanism was studied. Solid-state ^{27}Al and ^{29}Si NMR spectroscopy along with XRD revealed that enhanced temperatures increase the crystallinity of the material with the appearance of neoformed crystalline phases. Surface-sorbed and interlayer-sorbed U(VI) species were detected by luminescence spectroscopy. U(VI) mobilization due to high ionic strengths or presence of organics (gluconate or PBTC) was very low [6,7].

The results show that both bentonite and cementitious material constitute an important geoengineered retention barrier for U(VI) under hyperalkaline conditions at increased ionic strengths and in presence of organics. Thus, both bentonite and cementitious material strongly contribute to the safe confinement of radionuclides in a repository to isolate radiotoxic contaminants from the hydrosphere and biosphere.

Acknowledgements: This work was supported by the German Federal Ministry for Economic Affairs and Energy (BMWi) within the GRaZ II project (no. 02E11860B) and by the European Union's Horizon 2020 Research and Innovation Programme (CORI project, no. 847593).

⁽¹⁾ Present address: Federal Office for the Safety of Nuclear Waste Management (BASE), Berlin, Germany.

References

- [1] Lommerzheim, A. and Jobmann, M. (2014). Endlagerkonzept sowie Verfüll- und Verschlusskonzept für das Standortmodell NORD, TEC-08-2014-Z. DBE Technology, Germany.
- [2] Brewitz, W. (1982) Eignungsprüfung der Schachanlage Konrad für die Endlagerung radioaktiver Abfälle. GSF-T 136.
- [3] Altmaier, M. et al. (2022). Long-term radionuclide retention in the near field: collaborative R&D studies within EURAD focusing on container optimisation, mobility, mechanisms and monitoring. EPJ Nuclear Sci. Technol. 8: 27.
- [4] Philipp, T. et al. (2019). U(VI) sorption on Ca-bentonite at (hyper)alkaline conditions – Spectroscopic investigations of retention mechanisms. Sci. Tot. Environ. 676: 469-481.
- [5] Philipp, T. et al. (2022). Effect of Ca(II) on U(VI) and Np(VI) retention on Ca-bentonite and clay minerals at hyperalkaline conditions – New insights from batch sorption experiments and luminescence spectroscopy. Sci. Total Environ. 842: 156837.
- [6] Wolter, J.-M. et al. (2019). Cm(III) retention by calcium silicate hydrate (C-S-H) gel and secondary alteration phases in carbonate solutions with high ionic strength: A site-selective TRLFS study. Sci. Rep. 9: 14255.
- [7] Dettmann, S. et al. (accepted, 2023). Influence of gluconate on the retention of Eu(III), Am(III), Th(IV), Pu(IV), and U(VI) by C-S-H (C/S = 0.8). Front. Nucl. Eng.

B4-1 MECHANISM OF URANIUM REDUCTION: THE ROLE OF PENTAVALENT SPECIES

Rizlan Bernier-Latmani⁽¹⁾, Margaux Molinas⁽¹⁾ Zezhen Pan^(1,2), Barbora Bartova⁽¹⁾, Thomas La Grange⁽¹⁾

(1) *Ecole Polytechnique Federale de Lausanne, Lausanne, Switzerland*

(2) *Fudan University, Shanghai, China*

Uranium is the heaviest natural element and is of economic importance for its role as a fuel in nuclear power generation. However, due to historical lapses in proper disposal of mining and processing waste, and the use of uranium as anti-tank ammunition in war theaters, it is also a contaminant in the subsurface in various sites around the world. The isotopic signature of naturally-occurring uranium in geological strata also serves as a proxy for past oxygenation levels and is used to reconstruct the redox state of Earth in the geological past.

Uranium reduction entails the transformation of hexavalent uranium (U(VI)), typically in the uranyl cation form (UO_2^{2+}) to a tetravalent (U(IV)) chemical form, typically either uranium oxides such as UO_2 or non-crystalline forms in which uranium is coordinated to carbon, phosphorus or silicon via oxygen atoms (e.g., [1]). Thus, it results in the net immobilization of uranium from a soluble and mobile complexed hexavalent form to a solid phase tetravalent form.

In the first decade of this century, much of the work investigating uranium reduction, microbial or abiotic, focused on the product of the reduction. This is because uranium reduction is proposed as a strategy for remediation of the uranium-contaminated subsurface, and the chemical form of the reduced phase has implications for its long-term stability as an *in-situ* waste form.

More recently, the focus has been on the mechanism of uranium reduction. It has long been established that the biological reduction of uranium is catalyzed by, among others, metal-reducing bacteria via the same mechanism as iron reduction. Therefore, electrons from central metabolism are shuttled to the cell surface by a series of *c*-type cytochromes, culminating with the delivery of electrons to U(VI) by the outer-membrane decaheme *c*-type cytochrome, MtrC [2]. This protein delivers one electron to U(VI), forming pentavalent uranium (U(V)), an intermediate in the reduction. In turn, U(V) can either undergo further reduction by the delivery of a second electron [3] or it can undergo disproportionation with two U(V) molecules forming one U(VI) and one U(IV) molecule [4]. There is evidence for both mechanisms and the prevalence of one vs. the other likely depends on U(VI) speciation. When coordinated to carbonate, likely as the dinuclear U(VI)-carbonate complex, the reduction proceeds via disproportionation of U(V). In contrast, when U(VI) is coordinated to ligands such as dpaea, that stabilize U(V), two one-electron transfers occur. The ligand-dependent reduction mechanism is also reflected in the kinetics of the transformation. U(VI)-carbonate is reduced considerably more slowly than U(VI) coordinated to EDTA or citrate. The current hypothesis is that U(VI)-carbonate complexes covalently bind to the protein while other U(VI) complexes (with EDTA, DPAEA, citrate, NTA) are reduced by electron hopping from the hemes to U(VI).

Biological U(VI) reduction can also take place indirectly, via the biological production of reduced iron or sulfur compounds that, in turn, reduce U(VI). One such reduction pathway involves magnetite, Fe_3O_4 . The reaction of U(VI) with magnetite results in the formation of uraninite, UO_2 , as clusters of nanoparticles bearing the same orientation rather than a layer of UO_2 at the magnetite surface [5].

However, the formation of the UO_2 nanoclusters is the final step of a multi-step process involving the formation of single U oxide nanocrystals (1-5 nm) followed by the formation of nanowires that extend from the magnetite surface outward (Figure 1) [5]. Over time, the nanowires collapse into UO_2 nanoclusters. Based on recent microscopic evidence for a range of crystallinity and order in the nanoparticles, we acquired the O K-edge EELS spectra from individual nanoparticles within the nanowires and compared the edge feature to that of U oxide reference standards in order to characterize the valence state of individual nanocrystals within the nanowires.

The mechanism that emerges at the scale of individual nanoparticles (1-5 nm) is the initial reduction of U(VI) to U(V) at the magnetite surface, producing mixed valence oxides (UO_{2+x}) that self-assemble into nanowires. These nanowires are stable as long as no further reduction occurs. However, if sufficient electrons are available from magnetite, they are delivered to the mixed valence U oxides, resulting in the formation of fully reduced UO_2 . The nanowires are no longer thermodynamically stable at the stage and collapse into nanoclusters.

Overall, both the biological and abiotic reduction involve intermediate U(V) species whose persistence depends on the chemical conditions. A more complete understanding of the reduction process is key in constraining the fate and transport of uranium in the subsurface.

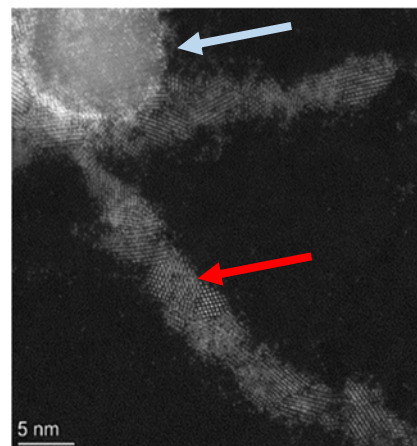


Figure 1: Magnetite particle (blue arrow) with UO_{2+x} nanoparticles self-assembled into nanowires (red arrow).

References

- [1] Bernier-Latmani, R., Veeramani, H., Dalla Vecchia, E., Junier, P., Lezama-Pachoco, J., Suvorova Buffat, E., Sharp, J. O., Wigginton, N. S., Bargar, J. R. (2010) Non-uraninite products of microbial U(VI) reduction. *Environ. Sci. Technol.* 44 (24): 9456-9462.
- [2] Marshall, M.J., Beliaev, A.S., Dohnalkova, A.C., Kennedy, D.W., Shi, L., Wang, Z., Boyanov, M.I., Lai, B., Kemner, K.M., McLean, J.S., Reed, S.B., Culley, D.E., Bailey, V.L., Cody J Simonson, C.J., Saffarini, D.A., Romine, M.F., Zachara, J.M., Fredrickson, J.M. (2006) c-Type cytochrome-dependent formation of U(IV) nanoparticles by *Shewanella oneidensis*. *PLOS Biol* 4(9): e268.
- [3] Molinas, M., Meibom, K.L., Faizova, R., Mazzanti, M. and R. Bernier-Latmani (2023) Mechanism of reduction of aqueous U(V)-dpaea and solid-phase U(VI)-dpaea complexes: the role of multiheme c-Type cytochromes. *Env. Sci. & Technol.* Vol. 57 (19): 7537-7546.
- [4] Vettese, G.F., Morris, K., Natrajan, L.S., Shaw, S., Vitova, T., Galanzew, J., Jones, D.L., and J. R. Lloyd. (2020) Multiple Lines of evidence identify U(V) as a key intermediate during U(VI) reduction by *Shewanella oneidensis* MR1. *Environ. Sci. Technol.* 2020, 54, 4, 2268–2276
- [5] Pan, Z., Bartova, B., LaGrange, T., Butorin, S. M., Hyatt, N. C., Stennett, M. C., Kvashnina, K. O. and Bernier-Latmani, R. (2020). Nanoscale mechanism of UO_2 formation through uranium reduction by magnetite. *Nat. Comm.* 11(1): 4001.

B4-2 IN SITU BIOMINERALISATION FOR GROUNDWATER RADIONUCLIDE REMEDIATION

Callum Robinson¹, Sam Shaw¹, Jonathan R. Lloyd¹, James Graham², Jörg Rothe³, Kathy Dardenne³ and Katherine Morris¹

(1) *Research Centre for Radwaste Disposal, Department of Earth and Environmental Sciences, University of Manchester, Manchester, M13 9PL, UK*

(2) *National Nuclear Laboratory, Chadwick House, Birchwood Park, Warrington, Cheshire, WA3 6AE*

(3) *Institute for Nuclear Waste Disposal (INE), Karlsruhe Institute of Technology, Karlsruhe 76131, Germany*

Globally, nuclear fuel cycle activities over the last 70+ years have led to unanticipated discharges of radionuclides to the sub-surface at key sites such as Hanford, USA and Sellafield UK. This has led to a significant legacy of radioactively contaminated land, for example, estimated to be in millions cubic meters at Sellafield. Typically, uranium and strontium-90 contamination plumes are present at these sites. Here, ⁹⁰Sr is one of the more challenging radionuclides due to its relatively high mobility in the sub-surface and U is often the most significant radionuclide contaminant by mass. Developing (co-)remediation strategies for ⁹⁰Sr and U is therefore important in maintaining the stewardship of these complex sites in the medium to long term. Calcium phosphate minerals such as hydroxyapatite (HAp) have been suggested as promising radionuclide (including ⁹⁰Sr and U) sinks, as they can incorporate a range of radionuclides within their structure. The formation of phosphate minerals can be achieved *in situ* through both biotic and abiotic approaches. In previous studies conducted at the Hanford nuclear site, USA, aqueous injection of phosphate-generating solutions have reduced the amount of mobile ⁹⁰Sr and U within contaminated groundwater at both laboratory and field scale [1].

In this study, biotic (calcium citrate / sodium phosphate, glycerol phosphate) and abiotic (polyphosphate) phosphate *in-situ* amendments were tested using sediment microcosm and flowing column experiments. The aim was to extend the envelope of application of these techniques to the Sellafield, UK using relevant sediment and groundwater systems [2],[3]. For both U(VI) and stable Sr challenged microcosms, aqueous geochemical results suggest the addition of phosphate generating amendments enhanced Sr and U removal from solution when compared to the sediment only sorption controls. After treatment with Ca- citrate / Na-phosphate and glycerol phosphate amendments microcosm sediment endpoints were taken for x-ray absorption near edge structure (XANES) extended x-ray absorption fine structure (EXAFS) analysis. XANES identified the U was present as U(VI), with analysis of the EXAFS region showing evidence for a P shell at ~3Å, suggesting the U was present as a non-crystalline U(VI) phosphate. For the Sr microcosm endpoints scanning electron microscopy (SEM) in conjunction with energy dispersive x-ray spectroscopy (EDX) was conducted on sediments after treatment with Ca- citrate / Na-phosphate and glycerol phosphate amendments. This showed the clear presence of Sr containing calcium phosphate phases deposited on the surface of larger sediment grains. 16S rRNA analysis of the microbial community present in these sediment endpoints showed ingrowth of likely citrate and glycerol phosphate degrading bacteria after treatment with Ca-citrate/Na-phosphate and glycerol phosphate respectively. Finally, Sr K-edge EXAFS analysis was conducted on sediment end point samples and an untreated sediment sorption control. For the sorption control, fitting of the EXAFS data was achieved with a single shell of nine oxygen backscatters, consistent with outer sphere sorption of Sr to the sediment. By contrast, shell-by-shell fitting of the treated sediments was best achieved using fitting parameters consistent with partial Sr incorporation into hydroxyapatite [4][5]. Here, informed by the relevant literature, P and Ca shells were statistically significant in the fitting, confirming some Sr incorporation into Ca-phosphate precipitates. The precipitation of these calcium phosphate phases and formation of U phosphates and Sr incorporated Ca-phosphates confirmed by XAS, demonstrates the potential for these techniques to provide a toolkit for remediation at nuclear sites.

Further investigation was conducted using flowing column studies with non-active Sr and ^{90}Sr . Here, columns were designed to represent typical groundwater flow regimes, enabling critical assessment of the phosphate generating treatments under dynamic flowing conditions. The addition of both glycerol phosphate and Ca-Citrate/Na-phosphate for a 3-week period prior to challenge with Sr-containing groundwaters decreased the rate of Sr breakthrough when compared to a sediment only sorption control column. This suggested that Sr mobility was reduced due to its sorption to newly precipitated Ca-phosphate phases within columns with the citrate treatment offering highest Sr-retardation. Post treatment, columns were sectioned (bulk EXAFS) and resin embed (μXRF ; INE-beamline, KIT, Germany) to enable solid phase characterisation of Sr speciation down the length of the column. Here, bulk EXAFS analysis showed some evidence for Sr incorporated Ca-phosphate phases in the Ca-citrate / Na-phosphate phases treated column although the incorporation signature was less clear than the batch experiments. Initial analysis of μXRF data showed hot spots of Sr at the bases of treated columns. Ca-phosphate phases were identified in the treated columns using SEM, consistent with the distribution of Sr from μXRF . However, SEM imaging found these ‘hot spots’ were caused by naturally occurring Sr containing minerals within the sediment. Future work includes the ambition to work with ^{90}Sr flowing columns to enable field relevant ^{90}Sr concentrations in experiments and autoradiography. This work shows for the first time a comparative assessment of these mineralisation techniques and their end-points and widens the envelope for their application at nuclear facilities.

References

- [1] Vermeul, V. R.; Szecsody, J. E.; Fritz, B. G.; Williams, M. D.; Moore, R. C.; Fruchter, J. S. (2014) An Injectable Apatite Permeable Reactive Barrier for In Situ ^{90}Sr Immobilization. *Groundw. Monit. Remediat.* 34 (2), 28–41.
- [2] Newsome, L.; Morris, K.; Trivedi, D.; Bewsher, A.; Lloyd, J. R. (2015) Biostimulation by Glycerol Phosphate to Precipitate Recalcitrant Uranium(IV) Phosphate. *Environ. Sci. Technol.*, 49 (18), 11070–11078.
- [3] Szecsody, J. E.; Zhong, L.; Oostrom, M.; Vermeul, V. R.; Fruchter, J. S.; Williams, M. D. (2012) Use of Polyphosphate to Decrease Uranium Leaching in Hanford 300 Area Smear Zone Sediment.
- [4] Handley-Sidhu, S.; Renshaw, J. C.; Yong, P.; Kerley, R.; Macaskie, L. E. (2011) Nano-Crystalline Hydroxyapatite Bio-Mineral for the Treatment of Strontium from Aqueous Solutions. *Biotechnol. Lett.*, 33 (1), 79–87.
- [5] Cleary, A.; Lloyd, J. R.; Newsome, L.; Shaw, S.; Boothman, C.; Boshoff, G.; Atherton, N.; Morris, K. (2019) Bioremediation of Strontium and Technetium Contaminated Groundwater Using Glycerol Phosphate. *Chem. Geol.*, 509, 213–222.

B4-3 PHYTOREMEDIATION OF SOIL FROM GERMAN NUCLEAR FACILITIES

Tobias Blenke⁽¹⁾, Sergiy Dubchak⁽¹⁾, Kai Grossmann⁽²⁾, Carsten Geisler⁽³⁾, Clemens Walther⁽¹⁾

(1) *Institute of Radioecology and Radiation Protection, Leibniz University Hannover, Germany*

(2) *VKTA – Radation Protection, Analytics & Disposal Rossendorf Inc., Germany*

(2) *Entsorgungswerk für Nuklearanlagen GmbH (EWN), Germany*

Germany decided on a shutdown of nuclear power plants until April 14, 2023, and hence the need for research on the decommissioning of nuclear facilities has never been greater in Germany. This work is part of the RENA (biological radionuclide removal by using natural association processes) project. The goal is to reduce the volume of medium and low-level radioactive waste - precisely soil - for a final repository. Excavated soil from the decommissioning of German nuclear facilities is the basis for this work. In contrast to previous remediation projects, only natural association processes are used. Therefore, we focus on plants, fungi and their symbiosis. Based on the results, a process for the ex-situ treatment of radionuclide-contaminated soils in a dismantling area in Germany will be developed.

The soil investigated originates from sites of the first and the second nuclear reactors build in former Eastern Germany. The research reactor in Dresden, Saxony, operated from 1957 until 1991 and the nuclear power plant in Rheinsberg, Brandenburg, followed 1966 until 1990. Hence, the soil was contaminated over decades and all equilibria have settled to date which would not be possible through subsequent spiking of inactive material. In the delivered soil, pieces of concrete were found as expected to be in a deconstruction process. Consequently, all the soil, with the exception of a control group, was sieved to a corn size of 2 mm and homogenized pot wise. In the control group, the plants grew in untreated soil to observe the influence of the concrete.

The setup for the plant and plant-fungi cultivation consists of plant pots (Ø x H: 18 cm x 17 cm) in a climate chamber with optimized growth parameters such as daylight, temperature and humidity. Small-growing sunflower and lucerne are the chosen plants because they displayed promising results in inactive pretests. To ensure sufficient growth Hoagland solution was used to water the plants. Figure 1 shows the complete setup.



Figure 1: The setup for the plant cultivation inside the climate chamber. The lucerne is on the left and the sunflower on the right. A hose connects each pot to the Hoagland solution supply in the center.

The fungus of choice is a strain of *schizophyllum commune* because it has a good uptake of strontium and therefore also for ^{90}Sr . A commercially available mix of fungi serves as an additional reference point based on the theory that different sprouts support different uptake.

For the general monitoring of radionuclides, the plants were divided into roots and shoots and afterwards dried, ashed and digested. The γ -emitters (^{241}Am , ^{152}Eu , ^{137}Cs and ^{60}Co) were monitored by HPGE-detectors. Additionally, ^{90}Sr was chemical separated and measured via liquid scintillation counting. The stable isotopes of each radionuclide were measured by ICP-AES for comparison.

Starting with a precise analysis of the soil, the main radionuclide contaminants were ^{137}Cs and ^{90}Sr . A grain size analysis of the soil showed a high percentage of 90 % sand. The share of silt and clay was combined 10 %. However, the proportion of activity of this fraction exceeds its mass share, as presented in Figure 2.

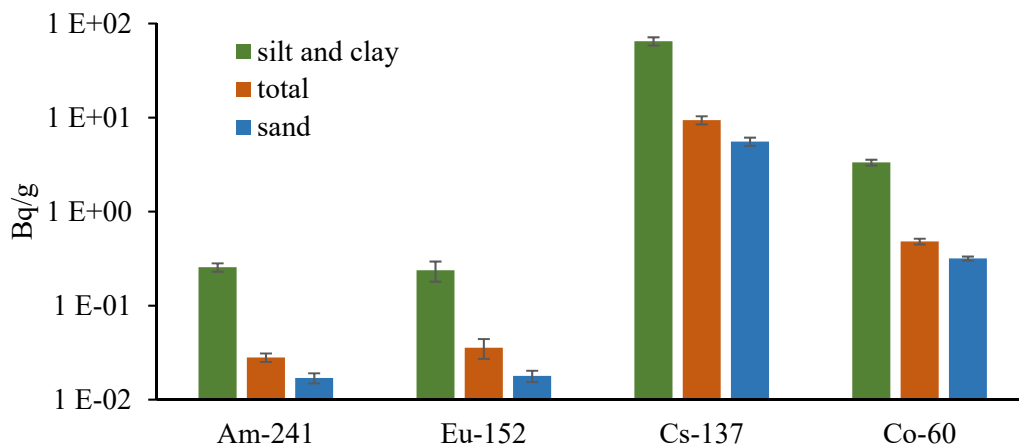


Figure 2: Activity concentration of γ -emitters in different corn sizes in soil from the site of the research reactor in Dresden.

The activity concentration in silt and clay exceeds the one in the sand fraction by an order of magnitude. However, the mechanical procedure to separate by corn size is only possible once and therefore limited. Nevertheless, it will serve as a benchmark for the determined transfer factor and the uptake of radionuclides into the plants with and without fungi.

In summary, this work gives new transfer factors, might give a deeper insight into the migration of radionuclides into plants and shows problems of soil from the dismantling of nuclear power plants.

B4-4 DISSOLVED ORGANIC MATTER IN BOOM CLAY AND ITS ROLE ON RADIONUCLIDE MIGRATION: WE HAVE COME A LONG WAY

Delphine Durce⁽¹⁾, Joan Govaerts⁽¹⁾, Norbert Maes⁽¹⁾, Sonia Salah⁽¹⁾, Liesbeth Van Laer⁽¹⁾, Stephane Brassinnes⁽²⁾

(1) SCK CEN, Belgium

(2) ONDRAF/NIRAS, Belgium

In 2021 we celebrated the 40th anniversary of the HADES underground research laboratory (Mol, Belgium), a pioneering facility for clay host rocks. Since the first ring was put in place at 200 m below the surface in the Boom Clay (BC) Formation, a tremendous amount of knowledge was acquired for the development of deep geological repository of nuclear waste in clays.

However, only one drop of the caramel Boom Clay pore water was enough to understand that a killjoy had invited itself: Dissolved Organic Matter (DOM). With its ill-defined structure, its high complexing capabilities towards several relevant radionuclides (RN) and its low retention on clay surfaces and corresponding relatively high mobility, it was clear that DOM would keep researchers busy for the next decades.

Over the years, we have looked at DOM from many different angles: in the frame of European projects (TRANCOM, TRANCOM-Clay, Funmig) and national programs, in lab-scale as well in in-situ experiments focusing on its physico-chemical properties, on its complexation with RNs, on its mobility in Boom Clay or on its direct effect on RN retention and migration in clay. It had been scrutinized by experimentalists in a variety of experiments from solution chemistry to percolation experiments passing by a various range of characterization approaches. Complexation, sorption and transport models have been optimized and applied to describe its behavior and its effect on RN behavior. And though DOM did not yet reveal all its secrets, we have come a long way and have definitively a better insight on its role with respect to RNs mobility in BC.

In this presentation, we do not intend to detail 40 years of research on DOM in Boom Clay, but we will present the biggest achievements with a special focus on the most recent experimental and modelling results obtained on DOM physico-chemical properties (reactivity, size distribution [1]), DOM transport (in-situ [2] and lab-scale experiments [3]), DOM-RN complexation (U(VI), Sn(IV) [4], Th(IV)) and the effect of DOM on the RN sorption (U(VI), Sn(IV)[5], Am(III) and on RN transport [6]). These results supported by the previous researches ([7] and references therein) reveal that there is not one DOM, but a distribution of DOM that can be gathered in different pools according to their transport properties (mobile vs immobile, fast vs slow) or their reactivity (Humic acid vs Fulvic acid, low molecular weight vs high molecular weight). They also confirmed the high affinity of several relevant radionuclides towards BC DOM and how the latter can affect the sorption of these RNs. The applied models, 1D [3] or 2D [2] reactive transport models, Tipping Model VII [8] and the 2-site protolysis non-electrostatic surface complexation and cation exchange model [9] allowed to extract transport and (surface) complexation parameters to better apprehend and predict RN transport in undisturbed conditions satisfactorily.

References

- [1] Durce, D., et al.,(2015). Partitioning of organic matter in Boom Clay: Leachable vs mobile organic matter. Applied Geochemistry. 63: p. 169-181.

- [2] Govaerts, J., et al.,(2023). Coupled flow and transport modelling of a large-scale in-situ migration experiment with ¹⁴C-labelled natural organic matter colloids in Boom Clay. Geological Society, London, Special Publications. 536(1): p. SP536-2022-22.
- [3] Durce, D., et al.,(2018). Transport of dissolved organic matter in Boom Clay: Size effects. Journal of Contaminant Hydrology. 208: p. 27-34.
- [4] Durce, D., et al.,(2020). Complexation of Sn with Boom Clay natural organic matter under nuclear waste repository conditions. Applied Geochemistry. 123: p. 104775.
- [5] Durce, D., et al.,(2022). Sn(IV) Sorption onto Illite and Boom Clay: Effect of Carbonate and Dissolved Organic Matter. Minerals. 12(9).
- [6] Maes, N., et al.,(2011). A consistent phenomenological model for natural organic matter linked migration of Tc(IV), Cm(III), Np(IV), Pu(III/IV) and Pa(V) in the Boom Clay. Physics and Chemistry of the Earth, Parts A/B/C. 36(17-18): p. 1590-1599.
- [7] Bruggeman, C. and M. De Craen,(2012). Boom Clay natural organic matter. External report SCK•CEN-ER-206 (Mol, Belgium).
- [8] Tipping, E., S. Lofts, and J.E. Sonke,(2011). Humic Ion-Binding Model VII: A revised parameterisation of cation-binding by humic substances. Environmental Chemistry. 8(3): p. 225-235.
- [9] Bradbury, M.H. and B. Baeyens,(1997). A mechanistic description of Ni and Zn sorption on Na-montmorillonite Part II: modelling. Journal of Contaminant Hydrology. 27(3-4): p. 223-248.

B4-5 POTENTIAL IMPACT OF BIOGENIC CHELATORS ON THE MIGRATION OF ACTINIDESG. J.-P. Deblonde*,^[1] Kersting,^[1] K. Morrison,^[1] M. Zavarin^[1]*[1] Lawrence Livermore National Laboratory, Livermore, California 94550, USA.***Deblonde1@LLNL.gov*

Anthropogenic radionuclides have been released in significant quantities in the environment due to civilian and military activities and will be present in various ecosystems for thousands of years [1]. Understanding the biogeochemistry of radionuclides is essential for developing effective means of isolation for future nuclear waste repositories and managing contaminated sites. In particular, actinide elements are major contributors to the long-term radiotoxicity of nuclear waste. In this context, it is important to decipher the interplay between actinide ions, soluble inorganic ligands, minerals, and also the wide variety of water-soluble organic molecules that can be present in the environment (Figure 1). Our studies focus the solution complexation and sorption behavior of actinides (i.e., Np, Pu, Am, Cm) in the presence of organic chelators. While the vast majority of the literature on actinide chemistry is focused on small compounds (i.e., metals, oxides, small inorganic or organometallic complexes), our studies put the emphasis of macromolecules such as proteins or complex organic matter. The results presented will show that under certain environmentally-relevant conditions, specific biogenic ligands can significantly increase the overall mobility of actinides, and even reverse solubility trends traditionally observed amongst actinide ions. The results will be put in context of the selection of future nuclear waste repository sites and the survey of potential biogenic chelators.

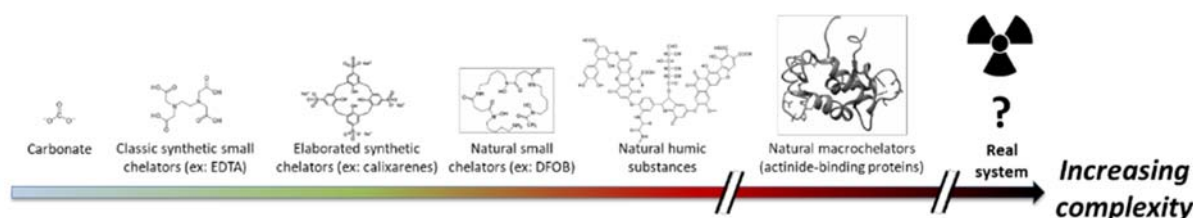


Figure 1: Radionuclides, such as actinides, can interact with a wide variety of natural organic matter, going from small inorganic ions to water-soluble macromolecules [2]. Determining which family of chelators drives the geochemistry of actinides is key to understand and model their migration behavior.

References

- [1] G.J.-P. Deblonde, A.B. Kersting, M. Zavarin, Open questions on the environmental chemistry of radionuclides, *Commun Chem.* 3 (2020) 1–5. <https://doi.org/10.1038/s42004-020-00418-6>.
- [2] G.J.-P. Deblonde, J.A. Mattocks, H. Wang, E.M. Gale, A.B. Kersting, M. Zavarin, J.A. Cotruvo, Characterization of Americium and Curium Complexes with the Protein Lanmodulin: A Potential Macromolecular Mechanism for Actinide Mobility in the Environment, *J. Am. Chem. Soc.* 143 (2021) 15769–15783. <https://doi.org/10.1021/jacs.1c07103>.

C3-1 NEXT GENERATION ENVIRONMENTAL MONITORING FRAMEWORK FOR NUCLEAR WASTE AND RADIOLOGICALLY CONTAMINATED SITES

Haruko Wainwright⁽¹⁾ and Carol Eddy-Dilek⁽²⁾

(1) *Massachusetts Institute of Technology, USA*

(2) *Savannah River National Laboratory, USA*

Environmental monitoring – including radiation sensors and soil/water sampling – plays a critical role in managing nuclear waste disposal sites and soil and groundwater contaminated sites. It confirms the performance of engineering systems as well as provides assurance to surrounding communities [1, 2]. In addition, monitoring data is important to develop conceptual models for radionuclide transport prediction and confirm the model performance over time. Groundwater assessments done in the 1990s were reviewed at the ten uranium contaminated sites in the US. Except for one site, all the predictions were failed within 20 years, having the concentration time series beyond the predicted confidence intervals. One successful model at the Naturita site was based on the careful analysis of long-term monitoring datasets.

The Advanced Long-term Environmental Monitoring Systems (ALTEMIS) project – funded by the US Department of Energy Office of Environmental Management– aims to establish the new paradigm of long-term monitoring based on state-of-art technologies – in situ groundwater sensors, geophysics, drone/satellite-based remote sensing, reactive transport modeling, and AI – that will improve effectiveness and robustness, while reducing the overall cost. In this presentation, we present our recent progress and updates from the past two years in this project. Specifically, we have developed (1) open-source machine learning framework, PyLEnM (Python for Long-term Environmental Monitoring) for spatiotemporal interpolations and monitoring design optimization [3], (2) geophysical 3D in situ real-time monitoring of the surface cap systems, (3) geophysical-based characterization and monitoring of groundwater/surface water interfaces, and (4) 3D gamma-ray and LiDAR integrated surface imaging, and (5) hybrid machine learning models for contaminant transport modeling to evaluate climate vulnerability/resilience [4 - 6]. We aim to transform the monitoring paradigm from reactive monitoring – respond after plume anomalies are detected – to proactive monitoring – detect the changes associated with the plume mobility before concentration anomalies occur. In addition, through the open-source package, we aim to improve the transparency of data analytics at contaminated sites, empowering concerned citizens as well as improving public relationship.

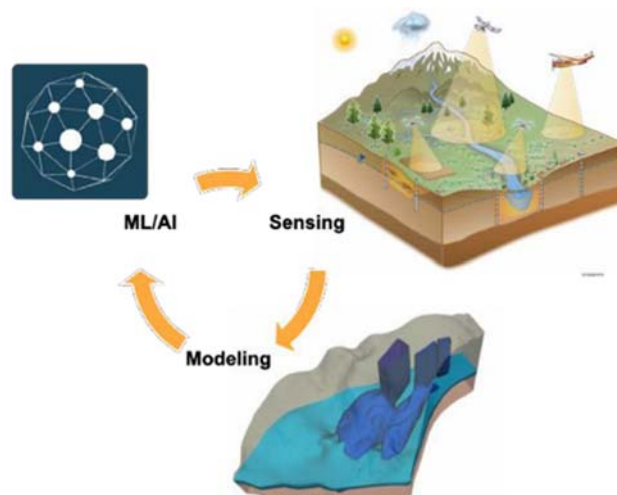


Figure 1: ALTEMIS Conceptual Diagram; the integration of new sensing technologies, modeling capabilities and ML/AI

References

- [1] Denham, M. E., Amidon, M. B., Wainwright, H. M., Dafflon, B., Ajo-Franklin, J., & Eddy-Dilek, C. A. (2020). Improving Long-term Monitoring of Contaminated Groundwater at Sites where Attenuation-based Remedies are Deployed. *Environmental Management*, 1-20.
- [2] Conca, J. (2017). Environmental monitoring programs and public engagement for siting and operation of geological repository systems: Experience at the waste isolation pilot plant. In *Geological Repository Systems for Safe Disposal of Spent Nuclear Fuels and Radioactive Waste* (pp. 667-709). Woodhead Publishing.
- [3] Meray, A. O., Sturla, S., Siddiquee, M. R., Serata, R., Uhlemann, S., Gonzalez-Raymat, H., ..& Wainwright, H. M. (2022). PyLEnM: A Machine Learning Framework for Long-Term Groundwater Contamination Monitoring Strategies. *Environmental science & technology*, 56(9), 5973-5983.
- [4] Libera, A.; de Barros, F. P. J.; Faybishenko, B.; Eddy-Dilek, C.; Denham, M.; Lipnikov, K.; Moulton, D.; Maco, B.; Wainwright, H. Climate Change Impact on Residual Contaminants under Sustainable Remediation. *Journal of Contaminant Hydrology* 2019, 226. <https://doi.org/10.1016/j.jconhyd.2019.103518>.
- [5] Xu, Z., Serata, R., Wainwright, H., Denham, M., Molins, S., Gonzalez-Raymat, H., ... & Eddy-Dilek, C. (2022). Reactive transport modeling for supporting climate resilience at groundwater contamination sites. *Hydrology and Earth System Sciences*, 26(3), 755-773.
- [6] Wang, L., Kurihana, T., Meray, A., Mastilovic, I., Praveen, S., Xu, Z., ... & Wainwright, H. (2022). Multi-scale Digital Twin: Developing a fast and physics-informed surrogate model for groundwater contamination with uncertain climate models. arXiv preprint arXiv:2211.10884.

C3-2 DETERMINING 3D POROSITY MAP OF BUKOV CALCITE WITH A MULTIMODAL DEEP LEARNING APPROACH

J. Kuva⁽¹⁾, M. Jooshaki⁽¹⁾, E. Jolis⁽¹⁾, J. Sammaljärvi⁽²⁾, M. Siitari-Kauppi⁽²⁾, F. Jankovský⁽³⁾, L. Mareda⁽⁴⁾, P. Sardini⁽⁵⁾

(1) Geological Survey of Finland, Finland

(2) Department of Chemistry, University of Helsinki, Finland

(3) ÚJV Řež, a.s., Hlavní 130, 250 68 Husinec, Czech Republic

(4) SÚRAO, Czech Republic

(5) IC2MP, Equipe HydrASA, University of Poitiers, France

To accurately model radionuclide migration in bedrock, e.g., when assessing the performance and safety of a spent nuclear fuel repository, it is vital to determine the transport properties of the bedrock. Previous studies [1,2] have shown that a simple homogeneous approach is not sufficient to model the results of in-situ measurements. X-ray computed microtomography (XCT) has been previously combined with carbon-14 labeled polymethylmethacrylate (C-14-PMMA) autoradiography, mineral staining and scanning electron microscopy (SEM) to provide a three-dimensional porosity map [3] and to model transport including also sorption [4].

Here we present a more robust and advanced method, where XCT is used to obtain the three-dimensional structure of a sample (Fig. 1), C-14-PMMA autoradiography is used to obtain the porosity (Fig. 2) and scanning micro-X-ray fluorescence (μ XRF) is used to obtain elemental maps from the same surface (Fig. 3), which are then converted into mineral maps using the Bruker AMICS automated mineralogy software. The mineral maps and XCT data are then combined using an in-house modified version of the deep learning method presented in [5] to obtain 3D mineral maps. Unlike segmentation methods based on k-means clustering that have been applied in [3,4], the deep learning segmentation technique adopted in this work does not solely rely on individual gray-scale pixel values and can extract and take advantage of textural information, thereby providing more robust outcomes. When the porosity map and mineral map are combined to calculate mineral-specific porosities a 3D porosity map suitable for simulations and modeling of radionuclides diffusion and sorption is obtained. This undisturbed rock sample with calcite infill was extracted from the borehole located in the Bukov Underground Research Facility (Bukov URF) 550 m below the surface [6], which acts as a test site for nuclear waste repository sites in the Czech Republic and is thus an interesting site regarding radionuclide migration.

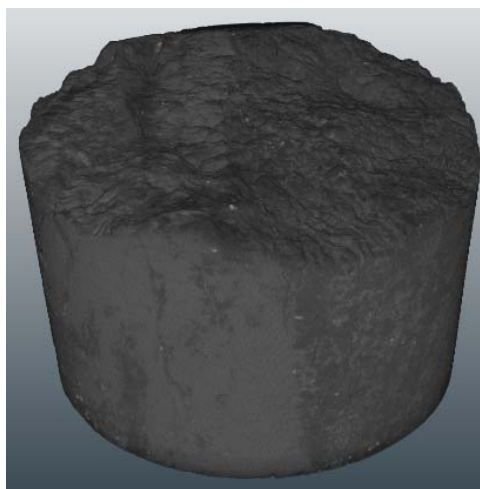


Figure 1. 3D XCT image of a Bukov calcite sample.

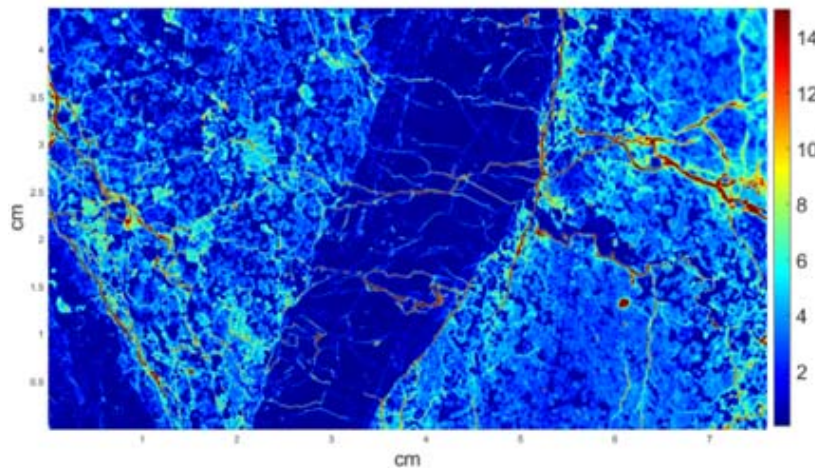


Figure 2. Porosity map of a Bukov calcite sample obtained by C-14-PMMA autoradiography.

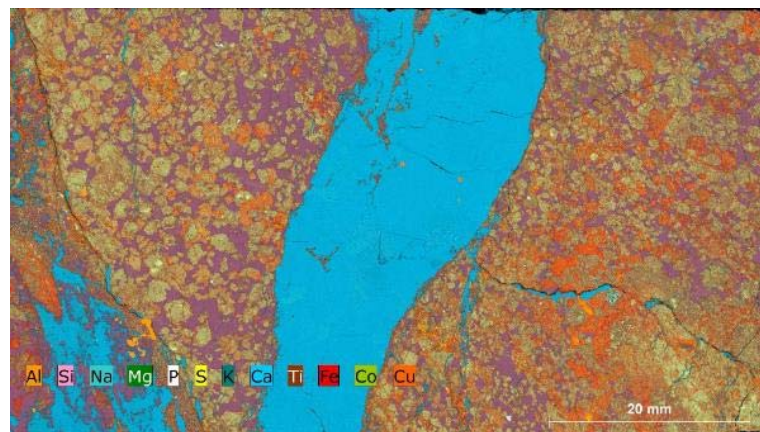


Figure 3. Elemental map from a Bukov calcite sample obtained by μ XRF.

Acknowledgement: The project leading to this work has received funding from the European Union's Horizon 2020 research and innovation program under grant agreement No. 847593.

References

- [1] Widestrand, H., Byegård, J., Nilsson, K., Höglund, S., Gustafsson, E., and Kronberg, M. (2010). "Long Term Sorption Diffusion Experiment (LTDE-SD) - Performance of main in situ experiment and results from water phase measurements" SKB report R-10-67, SKB AB, Stockholm, Sweden.
- [2] Poteri, A., Nilsson, K., Andersson, P., Siitari-Kauppi, M., Helariutta, K., Voutilainen, M., Kekäläinen, P., Ikonen, J., Sammaljärvi, J., Lindberg, A., Byegård, J., Skålberg, M., and Kuva, J. (2017) "The first matrix diffusion experiment in the water phase of the REPRO project" Posiva working report 2017-23, Posiva Oy, Eurajoki, Finland
- [3] Voutilainen, M., Siitari-Kauppi, M., Sardini, P., Lindberg, A., and Timonen, J. (2012). "Pore-space characterization of an altered tonalite by X-ray computed microtomography and the ^{14}C -labeled-polymethylmethacrylate method" J. Geophys. Res. 117: B01201
- [4] Voutilainen, M., Siitari-Kauppi, M., Sardini, P., Kekäläinen, P., Muuri, E., Timonen, J., and Martin, A. (2017) "Modeling transport of cesium in Grimsel granodiorite with heterogeneous structure and dynamic update of K_d ." Water Resour. Res. 53 (11): 9245-9265
- [5] Da Wang, Y., Blunt, M.J., Armstrong, R.T., and Mostaghimi, P. (2021) "Deep learning in pore scale imaging and modeling." Earth-Sci. Rev. 215: 103555
- [6] Souček, K., Vavro, M., Staš, L., Vavro, L., Waclawik, P., Konicek, P., Ptáček, J., Vondrovic, L. (2017) "Geotechnical Characterization of Bukov Underground Research Facility" Procedia Engineer. 191: 711-718

C3-3 A CHEMISTRY-INFORMED HYBRID MACHINE LEARNING APPROACH TO PREDICT RADIONUCLIDE SORPTION TO MINERAL SURFACES

Elliot Chang⁽¹⁾, Mavrik Zavarin⁽¹⁾, Linda Beverly⁽²⁾, and Haruko Wainwright^(2,3)

(1)Seaborg Institute, Lawrence Livermore National Laboratory, USA

(2) Lawrence Berkeley National Laboratory, USA

(3) University of California, Berkeley, USA

The Lawrence Livermore National Laboratory-Surface Complexation/Ion Exchange (L-SCIE) database is a recent effort to unify community adsorption experiments and metadata in a findable, accessible, interoperable, and reusable (FAIR) format[1]. To date, it has mined over 27,000 raw adsorption data from the literature and provides a platform to test novel approaches to surface complexation modeling and surface complexation database development. Briefly, L-SCIE mines sorption data (K_d , % sorbed, surface excess) and dataset experimental conditions (background electrolyte, mineral surface area, gas composition, etc.) from journal manuscripts and loads them into a database. The sorption data undergo a series of unit conversions to yield a unified database which includes propagated conversion errors from the original extracted data. The database can then be filtered for a mineral-metal pair of interest in order to display a corresponding experimental dataset. The application of the L-SCIE database to traditional surface complexation modeling was illustrated in a recent publication [2].

Here, we present an alternative hybrid machine learning (ML) approach that shows promise in achieving equivalent high-quality predictions compared to traditional surface complexation models (Figure 1). At its core, the hybrid random forest (RF) ML approach is motivated by the proliferation of incongruent SCMs in the literature that limit their applicability in reactive transport models. Our hybrid ML approach implements PHREEQC-based aqueous speciation calculations; values from these simulations are automatically used as input features for a random forest (RF) algorithm to quantify adsorption and avoid SCM modeling constraints entirely. Named the LLNL Speciation Updated Random Forest (L-SURF) model, this hybrid approach is shown to have applicability to U(VI) sorption cases driven by both ion-exchange and surface complexation, as is shown for quartz and montmorillonite cases. The approach can be applied to reactive transport modeling and may provide an alternative to the costly development of self-consistent SCM reaction databases.

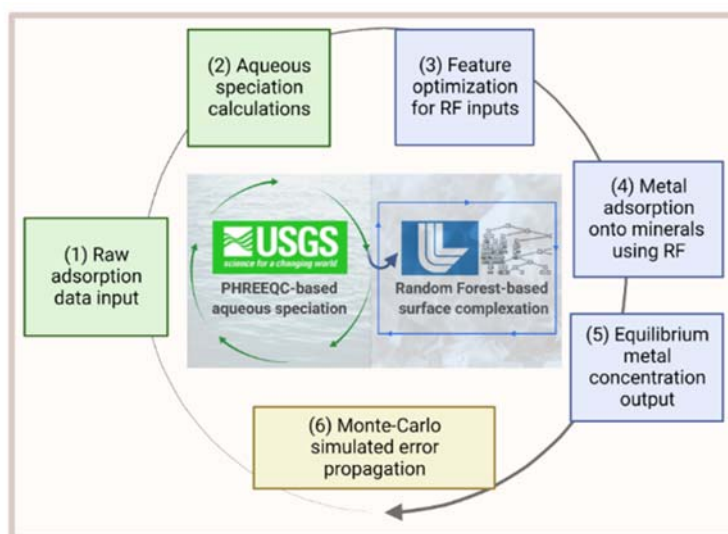


Figure 1. L-SURF workflow chart with chronological steps: (1) Adsorption data and selected thermodynamic database are imported into L-SURF module, (2) Aqueous speciation calculations are conducted and all geochemical features are output, (3) Choice of most impactful geochemical features and hyperparameters are optimized, (4) Optimal features are used to train and test a random forest adsorption model, (5) Equilibrium aqueous metal sorbate concentrations are output, and (6) Steps 1-5 are repeated using Monte-Carlo simulations with randomly sampled input data +/- experimentally-determined measurement uncertainty.

The database and codes are freely available, following the principles of FAIR data. The L-SCIE data can be accessed by contacting the authors. The associated software used to perform traditional surface complexation modeling and hybrid ML modeling of sorption data can be accessed through the following portals:

<https://ipo.llnl.gov/technologies/software/llnl-surface-complexation-database-converter-scdc>
<https://ipo.llnl.gov/technologies/software/l-surf>

References

- [1] Wilkinson, M., Dumontier, M., Aalbersberg, I. *et al.* 2016. The FAIR Guiding Principles for scientific data management and stewardship. *Sci Data* **3**, 160018.
- [2] Zavarin, M., Chang, E., Wainwright, H., Parham, N., Kaukuntla, R., Zouabe, J., Deinhart, A., Genetti, V., Shipman, S., Bok, F., Brendler, V., 2022. Community Data Mining Approach for Surface Complexation Database Development. *Environmental Science & Technology* **56**, 2827-2838.

PA-1 SEQUENTIAL EXTRACTION OF SIMULATED FUEL DEBRIS FOR EVALUATION OF THE CHEMICAL STABILITY

Akira Kirishima(1), Hiroki Nakazumi(1), Daisuke Akiyama(1)

(1) Institute of Multidisciplinary Research for Advanced Materials (IMRAM), Tohoku University, Sendai, Japan

I. Introduction

In the accident at Fukushima Daiichi Nuclear Power Station (FDNPS) in 2011, the loss of coolant accident occurred, where the reactor cores reached high temperatures and then melted. During this process, various materials, including uranium dioxide, zirconium alloy cladding, and structural materials melted and formed “Fuel Debris”. In the retrieval plan for the fuel debris, a small amount of fuel debris will be retrieved first, and then it will be scaled up based on the information obtained by the analysis of the retrieved small debris to perform this task safely. For this purpose, extracting as many chemical properties as possible from a minimal amount of fuel debris is critically essential. In this study, therefore, a Sequential Extraction Technique for the fuel debris was developed and demonstrated. “Sequential Extraction” is generally used to evaluate the chemical properties of natural soils and rocks in the earth science field. In this procedure, the chemical stability of a sample is evaluated by immersing a sample into a variety of reagent solutions sequentially, from chemically soft reagent solutions to hard (or active) ones. The fuel debris version of sequential extraction in this study was intended to propose a standard evaluation procedure for the FDNPS fuel debris. Thus, the procedure was demonstrated using several simulated fuel debris synthesized from fuel material (=U) and cladding material (=Zr) by heat treatment.

II. Materials and methods

a) Synthesis of the simulated fuel debris

The appropriate amount of UO_2 and ZrO_2 were weighed to prepare the designated $\text{UO}_2:\text{ZrO}_2$ composition, then well mixed and ground in an agate mortar. The mixtures were heated by an electric furnace at $1600\text{ }^\circ\text{C}$ for the designated time under a 20 mL/min ultrapure Ar (grade 1), 90 vol.% Ar + 10 vol.% H_2 , or 98 vol.% Ar + 2 vol.% O_2 gas flow. The detail of the heat treatment is described in our previous studies [1, 2]. The sample compositions and the heating conditions were selected as shown in Table 1 to synthesize four types of simulated fuel debris, that is, solid solutions of cubic $(\text{U,Zr})\text{O}_2$, monoclinic $(\text{Zr,U})\text{O}_2$, orthorhombic $(\text{Zr,U})\text{O}_2$, and tetragonal $(\text{Zr,U})\text{O}_2$, respectively.

Table 1. The sample compositions and the heating conditions of the simulated fuel debris ($T = 1600^\circ\text{C}$)

Target crystal structure	Molar ratio		Heating condition	Purification
	UO_2	ZrO_2		
Cubic	90	10	4h in 10 % H_2	
Monoclinic	5	95	4h in 10 % H_2	Washed by HNO_3
Orthorhombic	15	85	4h in 10 % H_2 + quenching in air	Washed by HNO_3
Tetragonal	10	90	1h in 2 % O_2	

b) Sequential extraction

A small centrifugal filter unit having $0.1\text{ }\mu\text{m}$ filter pore size was used in the sequential extraction. 0.2 g of the simulated debris sample was sequentially immersed in 0.4 ml of deionized water (DI water), seawater, sodium bicarbonate, hydrogen peroxide, acetic acid, hydrochloric acid, and nitric acid for one hour each. After each immersion step, the amount of leached uranium was measured by ICP-MS to calculate the uranium leaching ratio at each extraction step.

III. Results and discussion

The crystal structures of the synthesized fuel debris samples were analyzed by XRD to confirm the formation of the desired solid solution phases. The XRD pattern of a sample having a composition of U: Zr=1:1 (molar ratio) and heated under the reducing condition (10 % H₂) showed it consisted of cubic-(U,Zr)O₂ phase and monoclinic-(Zr,U)O₂ phase. This sample was treated as the simulated fuel debris containing two phases. The other samples of simulated fuel debris after the heat treatment and the purification treatment were confirmed to be single-phase debris consisting of cubic-(U,Zr)O₂, monoclinic-(Zr,U)O₂, orthorhombic-(Zr,U)O₂, and tetragonal-(Zr,U)O₂, respectively.

The uranium leaching ratios from the five types of simulated fuel debris and UO₂ at each step of the sequential extraction are shown in Fig. 1. The U leaching ratio from the cubic (U,Zr)O₂ sample was smaller than that from UO₂ for all the extractants. The solid solution formation of Zr(IV) in the cubic UO₂ phase suppressed the leaching of U in all of the extracts, which corresponds with the observed trend in the previous studies [1, 3, 4]. It was also found that the U leaching ratios in nitric acid from the Zr-rich (Zr,U)O₂ samples, i.e. Monoclinic, Orthorhombic, and Tetragonal phases, were much smaller than that from pure UO₂ and U-rich cubic (U, Zr)O₂ samples. Generally, U in UO₂ crystal leaches to the solution phase as uranyl(VI) ion by an oxidation dissolution when immersed in nitric acid, while Zr in ZrO₂ crystal is hardly leached by nitric acid since Zr(IV) in ZrO₂ cannot be further oxidized. Thus, the U leaching from the Zr-rich samples was remarkably suppressed in nitric acid. It was also found that tetragonal (Zr,U) O₂ was the most stable uranium-zirconium solid solution in this study. A comparison of a calculated solubility curve of U(VI) with the leached U concentration in the extraction tests of different leaching times showed that U leaching progressed toward the equilibrium solubility of U(VI) in each extraction stage. Additionally, Sr(II) and Eu(III) tracers doped cubic (U,Zr)O₂ solid solution was also synthesized and was devoted to the leaching test, for observation of the leaching behavior of fission products from the simulated debris. The comparison of the leaching behaviors of Sr(II) and Eu(III) with that of U will be discussed in the presentation.

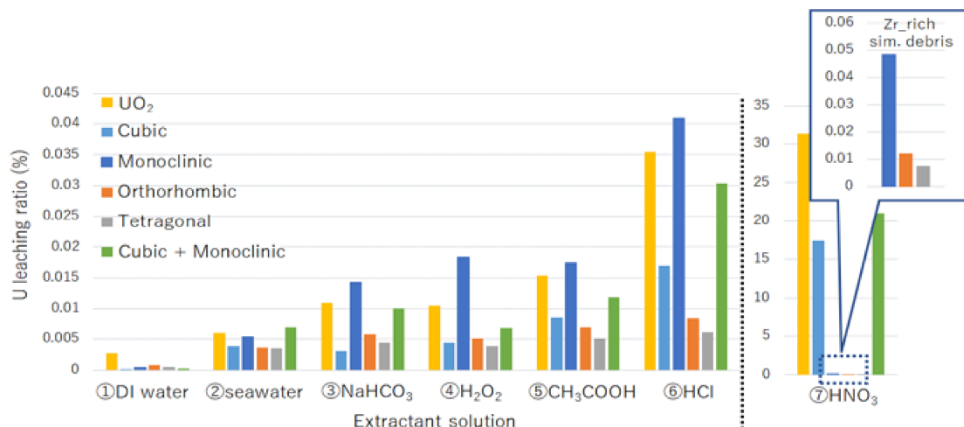


Fig. 1. Uranium leaching ratio at each extraction step

References

- [1] A. Kirishima, et al., "Study on the leaching behavior of actinides from nuclear fuel debris," *Journal of Nuclear Materials*, 502, 169-176 (2018).
- [2] A. Kirishima, et al., "Structure, Stability, and Actinide Leaching of Simulated Nuclear Fuel Debris Synthesized from UO₂, Zr, and Stainless-Steel," *Journal of Nuclear Materials*, 567, 153842 (2022).
- [3] A. Kirishima, et al., "Leaching of actinide elements from simulated fuel debris into seawater," *Journal of Nuclear Science and Technology*, 52, 1240-1246 (2015).
- [4] Bernd Grambow, et al., "Ten years after the NPP accident at Fukushima : review on fuel debris behavior in contact with water," *Journal of Nuclear Science and Technology*, 59, 1-24 (2022).

PA1-2 SOLUBILITY BEHAVIOR AND CHARACTERIZATION OF NEODYMIUM(III) TRIHYDROXIDE SOLID PHASE

Ranyeong Choi and Jun-Yeop Lee

*School of Mechanical Engineering, Pusan National University
2, Busandaehak-ro 63beon-gil, Geumjeong-gu, Busan 46241, Republic of Korea*

Regarding the long-term safety of geological disposal, it is important to predict the migration/retardation behavior of radionuclides in the natural groundwater system. Hence, improving knowledge about geochemical reactions in the natural environment is of great significance for the safety assessment of the geologic repository. In this respect, one of the key chemical parameters influencing the migration behavior of radionuclides is solubility. Under neutral to alkaline pH conditions, the solubility of An(III)/Ln(III) is significantly controlled by the hydrolysis reaction that forms a sparingly soluble solid phase, which affects their mobility. The aim of the present work is to investigate the solubility behavior of hydrolyzed Nd(III) solid phase as a chemical analogue of trivalent actinides.

All experimental samples were treated and prepared under the inert atmospheric condition ($O_2 < 5$ ppm) with a CO_2 -free glovebox. The initial Nd(III) solid phase was precipitated by the dropwise addition of 4 M NaOH in the aqueous solution of $NdCl_3 \cdot 6H_2O$. Successively, the purplish Nd(III) solid phase was washed with 10^{-3} M NaOH three times. For the solubility experiment, an under-saturation approach was employed in the pH_c range of 6.5 to 10.5 at 0.1 M NaCl condition. The pH_c values of the aqueous solution were continuously monitored with ROSS type combination electrode over the entire period of the solubility experiment. After reaching the equilibrium, the concentration of Nd(III) was quantitated with ICP-OES/MS and UV-Vis absorption spectroscopy. For ICP-OES/MS analysis, the aliquot of the solution was acidified with 2 % HNO_3 after the phase separation with a 10 kDa membrane filter. In addition, the UV-Vis absorption spectroscopy equipped with the liquid waveguide capillary cell (LWCC) was employed to analyze the concentration of Nd(III) in the aqueous solution.

According to the solid phase characterization by using XRD, TA-DTG, and SEM/TEM-EDS, the initial Nd(III) solid phase employed in the present work was assessed to be polycrystalline $Nd(OH)_3 \cdot 1.4H_2O(s)$ nanorod. As represented in Fig. 1, the aqueous Nd(III) concentrations determined after the filtration with two different pore sizes were almost identical to each other indicating almost no presence of colloidal substances in the aqueous solution, and no significant change in the UV-Vis spectrum was found with respect to pH changes. For the calculation of the solubility product constant, the approach based on the nonlinear least squares was used with the hydrolysis constants of Nd(III) taken from the literature [1]. In the present work, the solubility product constant of the Nd(III) solid phase was calculated by assuming the presence of $Nd(OH)_3 \cdot 1.4H_2O(s)$ as a solubility limiting phase. The authors note that due to the remarkable uncertainty of the Nd(III) solubility at the pH value higher than 8.5, where the solubility of Nd(III) reached the detection limit of the instrument, the experimental solubility data obtained at the pH value lower than 8.5 were selectively employed to be used in the chemical thermodynamic calculation. According to the result, the solubility product constant of $Nd(OH)_3 \cdot 1.4H_2O(s)$ was determined to be $\log^* K_{s,0}^\circ = 17.3 \pm 0.1$ based on the specific ion-interaction theory (SIT) [2]. The solubility product constant determined in this work was relatively well associated with $\log^* K_{s,0}^\circ = 17.2 \pm 0.4$ reported in the literature [1]. The chemical thermodynamic data obtained in the present work is expected to be used in the geochemical modeling of trivalent actinides for the safety assessment of deep-geologic repositories. In addition, complementary experiments considering the solubility behavior of crystalline $Nd(OH)_3(cr)$ solid phase at elevated temperature conditions are planned to be performed in the future.

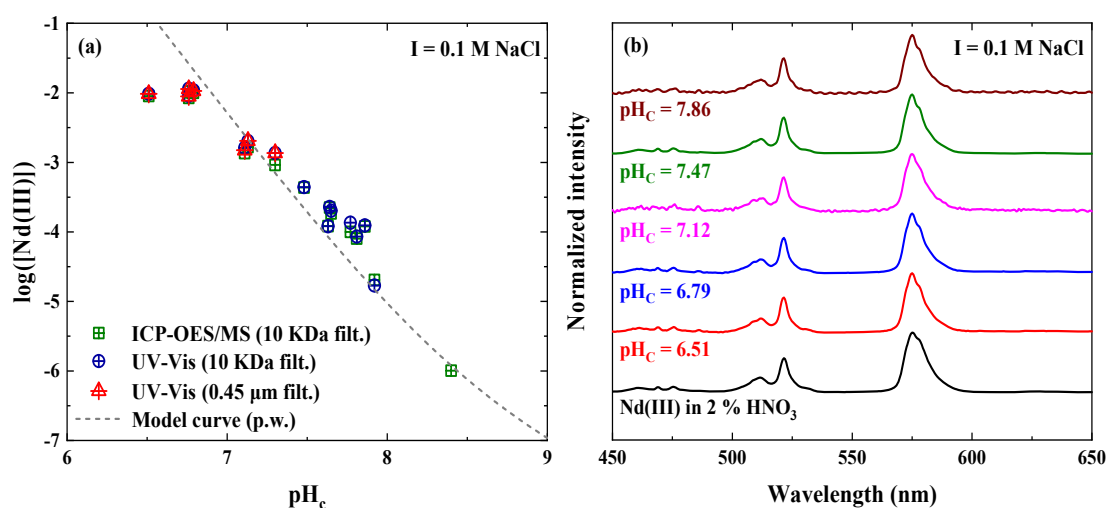


Fig. 1. (a) The experimental $Nd(III)$ concentration determined in the present work equilibrated at 0.1 M NaCl medium and (b) the normalized UV-Vis absorptions spectra of aqueous $Nd(III)$ solution observed at various pH_c conditions.

Acknowledgement: This work was supported by the National Research Foundation of Korea grant funded by the Korean government [No. NRF-2021M2E1A1085204].

References

- [1] Neck, V., Altmaier, M., Rabung, T., Lützenkirchen, J., Fanghänel, T. (2009). Thermodynamics of trivalent actinides and neodymium in NaCl, MgCl₂, and CaCl₂ solutions: Solubility, hydrolysis, and ternary Ca-M(III)-OH complexes. *Pure Appl. Chem.* 81: 1555-1568
- [2] Ciavatta, L. (1980). The Specific Interaction Theory in Evaluating Ionic Equilibria. *Ann. Chim-Rome* 70: 551-567

PA1-3 CHARACTERIZATION OF SYNTHETIC MAGNESIUM/CALCIUM URANYL SILICATE MINERALS AND THEIR SOLUBILITIES IN GROUNDWATER ENVIRONMENTS

Wansik Cha^{1,*}, Junghwan Park¹, Hye Ran Noh^{1,2}, Euo Chang Jung¹, Sang Ho Lim^{1,2}, Hye-Ryun Cho^{1,2}, Hee-Kyung Kim¹

1 Korea Atomic Energy Research Institute

2 University of Science and Technology

Daejeon, Republic of Korea

Disposal of spent nuclear fuel (SNF) in deep geological repositories (DGR) is accepted as one of options for the long-term and safe sequestration of radiotoxic SNF. The chemical behaviors of various radionuclides that originated from SNF should be well understood to properly evaluate the long-term safety of DGR using geochemical modeling of the reactions and interactions of radionuclides with various geochemical components. Formation of secondary minerals, colloids, and other insoluble precipitates is of interest since the concentrations of radionuclides in groundwater can be limited by the solubility of those solid phases. Particularly when evaluating their solubility, the use of well-defined solid materials in terms of chemical composition and molecular structure is crucial to obtain reliable measurement results. Our preliminary studies showed that uranophane (Ca-U(VI)-silicate) was identified as the solubility limiting mineral phase under the representative condition of oxic granitic groundwater in Korea [1]. In this study, two uranyl silicates, i.e., uranophane and sklodowskite (Mg-U(VI)-silicate), were synthesized and characterized using various analytical methods, including powder X-ray diffraction (pXRD), scanning electron microscopy/energy dispersive X-ray spectrometry (SEM/EDX), and vibrational (FTIR and Raman) spectroscopies. We also used these synthetic minerals to evaluate their solubilities in the model groundwater solutions.

Uranophane and sklodowskite are naturally occurring uranyl silicate minerals with a U:Si ratio of 1:1 ($X[\text{UO}_2\text{SiO}_3\text{OH}]_2 \cdot 5\text{H}_2\text{O}$, X= Ca or Mg) and a layered crystal structure. For the laboratory synthesis of these minerals, we applied a two-step hydrothermal synthetic procedure for uranophane as reported in the literature [2,3] with modification. For Ca-U(VI)-silicate, we concluded that the obtained mineral phase is the ' α -uranophane'; our characterization results showed that the structural and spectroscopic properties of the synthetic Ca-U(VI)-silicate agreed well with those of α -uranophane (see Figs. 1 (a)-(c)). For instance, the pXRD patterns obtained from the solid showed diffraction peak positions nearly identical to those from the reference XRD pattern of α -phase. The IR and Raman spectra demonstrated that the stretching modes of UO_2^{2+} and SiO_4^{4-} ions resulted in strong absorption bands in a region of 790 – 860 cm^{-1} and 940 – 1020 cm^{-1} , respectively. Elemental compositions of the synthetic solids were also estimated using EDX analysis, which resulted in a Ca:U:Si ratio close to 1:2:2 on average. However, we found that it is difficult to obtain good crystallinity of uranophane, which can be observed using SEM and its image analysis. We think that most of uranophane exists in forms of nano-crystallites. Similar results were obtained for Mg-U(VI)-silicate; spectroscopic characterizations confirmed that the obtained mineral phase was identified as the sklodowskite mineral. We also found that an excess amount of calcium or magnesium ions and low pH conditions during the initial step of mineral synthesis resulted in the production of a mixed phase with soddyite ($(\text{UO}_2)_2\text{SiO}_4 \cdot 2\text{H}_2\text{O}$).

To measure the solubility of the synthetic minerals, we prepared a stock of laboratory-formulated groundwater (LFGW), with a composition similar to that of representative oxic granitic groundwater in Korea [4]. For example, the concentrations of Ca, SiO_2 , and HCO_3^- of the LFGW were approximately 0.14, 0.13, and 1.3 mM, respectively, and the solution pH was ~ 9 (see Fig. 1 (d)). As a result of long-term monitoring of dissolved [U] after the supernatant filtration (0.1- μm pore) of each sample, the equilibrium solubility of uranophane measured at room temperature was approximately $\log [\text{U}](\text{M}) = -$

5.4. A period of at least two months of equilibrium was required. The filtration effects and the properties of ‘dissolved’ species existing in the filtrate were also examined using the nanoparticle tracking analysis and time-resolved laser-induced luminescence spectroscopy. We believe that this work serves as a model study to examine synthetic routes of mineral phases related to DGR/natural barriers and applicable solid phase characterization methods.

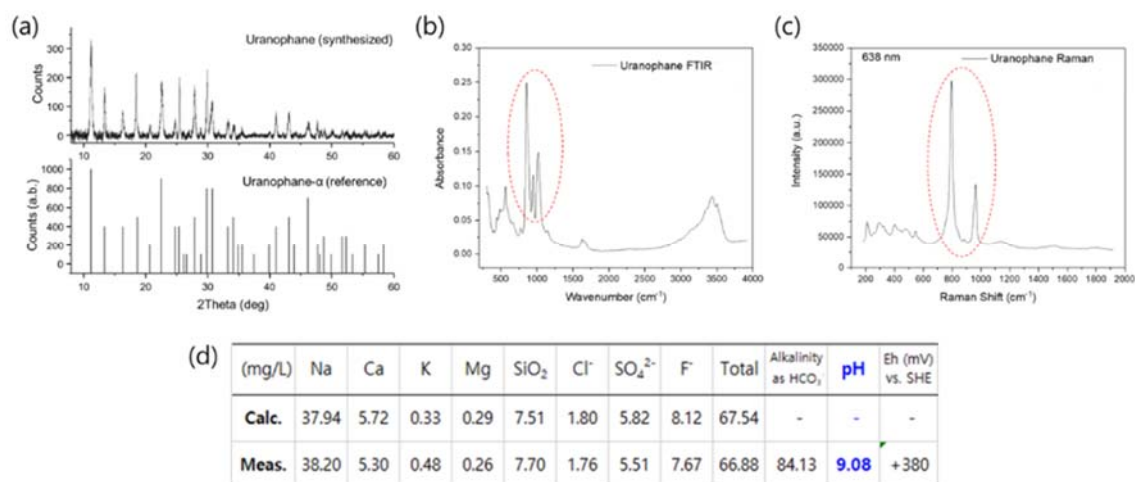


Figure 1. (a) pXRD pattern; (b) FTIR spectrum; (c) Raman spectrum obtained from synthetic uranophane and (d) the concentrations of each component of oxalic LFGW, pH and Eh.

Acknowledgments: This study was supported by the Nuclear Research and Development program of the National Research Foundation of Korea and the Institute for Korea Spent Nuclear Fuel (Grant Nos. 2021M2E3A3040092 and 2021M2E1A1085202).

References

- [1] Kim, H.-K., W. Cha, H.-R. Cho, T.-H. Kim. (2022) Thermodynamic evaluation of chemical reactions of radionuclides under domestic groundwater conditions: Actinides, lanthanides and transition metals. iKSNF-SD2/3-22-SCR-1, RWD-NCD-ST-SR-22-01, KAERI, Daejeon.
- [2] Cesbron, F. (1993) New mineralogical data on uranophane and β -uranophane; synthesis of uranophane, Mineral. Mag. 57: 301-308
- [3] Nguyen, S. N., R. J. Silva, H. C. Weed and J. E. Andrews Jr. (1992) Standard Gibbs free energies of formation at the temperature 303.15K of four uranyl silicates: soddyite, uranophane, sodium boltwoodite, and sodium weeksite, J. Chem. Thermodyn. 24: 359-376
- [4] Cho, H.-R., H.-K. Kim, W. Cha, H. Ju, J. Kim, K. Kim and W. Um (2022) Analysis of the solubilities of radioactive materials in oxidative groundwater conditions – geochemical modeling, KAERI/TR-9156/2022, KAERI, Daejeon

PA1-4 (U,Ce)O₂: A SUITABLE ANALOGUE TO STUDY THE ALTERATION OF (U,Pu)O₂ MOX FUEL IN ENVIRONMENTAL CONDITIONS

Montaigne Théo ⁽¹⁾, Szenknect Stéphanie ⁽¹⁾, Broudic Véronique ⁽²⁾, Miserque Frédéric ⁽³⁾, Tocino Florent ⁽⁴⁾, Martin Christelle ⁽⁵⁾, Jégou Christophe ⁽²⁾, Dacheux Nicolas ⁽¹⁾

(1) ICSM, Univ Montpellier, CNRS, CEA, ENSCM, France

(2) CEA/DES/ISEC/DPME, Univ Montpellier, France

(3) CEA/DES/ISAS/DRMP, Univ Paris-Saclay, France

(4) EDF R & D, France

(5) ANDRA, R & D Division, France

Although the reprocessing of spent fuel remains the reference scenario in France, direct disposal in deep geological repository is also studied as an option within the framework of the French national plan for the radioactive waste management. Especially the case of Mimas® MOX spent fuel. This kind of fuel, industrially produced after reprocessing of UO₂-based spent fuel, is characterized by a heterogeneous microstructure and variable plutonium contents [1]. Although UO₂ spent fuel have been intensively studied, the alteration mechanisms of U_{1-x}Pu_xO₂ fuels and especially, Mimas® MOX fuels deserve investigation to establish long-term evolution models and projections. Regarding UO₂ spent fuel, the key mechanism controlling the uranium dioxide dissolution and the radionuclides associated release is an oxidizing dissolution induced by hydrogen peroxide produced by water radiolysis [2]. Such mechanism can be affected by the MOX microstructure and plutonium content, for plutonium is reported to stabilize the fluorite structure with respect to oxidation [3-6]. Moreover, the radionuclides release from MOX spent fuel is affected by the groundwater chemistry, especially the presence of cementitious backfill material (in the current spent fuel disposal design) should create alkaline chemical environment likely to affect the water radiolysis yield [7] and the nature of secondary phases formed at the interface [8]. It is thus of primary importance to study the kinetics and the mechanisms of Mimas® MOX fuels alteration in various environmental chemistry. Furthermore, the use of a non-radioactive surrogate material with comparable properties to MOX fuel has relevant practical advantages. As such, finding a suitable surrogate material allowing multi-parametric studies is a major challenge to improve our knowledge of the alteration of Mimas® MOX fuels. This work aims to investigate the analogy between U_{1-x}Ce_xO₂ surrogate materials and fresh Mimas® MOX fuel in hydrogen peroxide presence. Once this analogy is verified, the behavior of Mimas® MOX fuel and heterogeneous U_{1-x}Ce_xO₂ surrogate in alkaline solution is compared to evaluate alpha radiation influence on the alteration mechanisms.

Firstly, both homogeneous and heterogeneous U_{1-x}Ce_xO₂ dense pellets with x ranging from 0 to 0.25 were prepared through wet and dry chemistry routes, respectively. Surrogate materials were then submitted to dynamic leaching experiments at room temperature and pH = 7.2. The feeding solution containing 0.20 mmol.L⁻¹ H₂O₂, was kept under air ([HCO₃⁻] = 0.16 mmol.L⁻¹; [O₂] = 0.26 mmol.L⁻¹) and renewed every 48 to 72 h to guarantee the H₂O₂ stability during the whole experiment. Normalized alteration rates were determined from uranium concentration measured in the leachates using ICP-MS after reaching the steady state. Post-alteration characterizations by Raman spectroscopy, environmental SEM and XPS were achieved. The secondary phase precipitation did not occur at the homogeneous (U,Ce)O₂ materials surface and the dissolution rate was divided by a factor 3 when increasing the Ce molar content from 0.08 to 0.25. However, studtite precipitation was observed all over UO₂ surface, leading to a continuous uranium concentration decreases in the outflow. The same results were obtained with heterogeneous U_{0.92}Ce_{0.08}O₂. However, studtite was found to precipitate on UO₂ grains only. This result was consistent with that observed for heterogeneous (U,Pu)O₂ in the same conditions [9], which confirm the reliability of cerium as a valuable plutonium analogue (Figure 1).

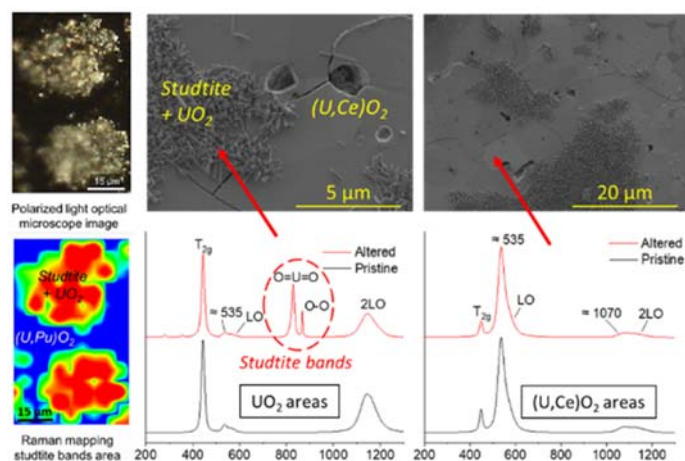


Figure 1: Surface of Mimas® MOX fuel [9] and of heterogeneous $(U,Ce)O_2$ surrogate material after alteration in $[H_2O_2] = 0.2 \text{ mmol.L}^{-1}$ at $\text{pH} = 7.2$ and 25°C .

Secondly, heterogeneous Mimas® MOX fuel and surrogate material with an average composition of $U_{0.93}Pu_{0.07}O_2$ and $U_{0.92}Ce_{0.08}O_2$, respectively were altered over several months under static conditions in alkaline solutions containing $[Na^+] = 24 \text{ mmol.L}^{-1}$, $[Si] = 2 \text{ mmol.L}^{-1}$ at $\text{pH} 12$ and room temperature and under anoxic conditions. The α -activity of the MOX pellet was $1.34 \text{ GBq.g}_{\text{MOX}}^{-1}$. No matter the presence of alpha-radiation, the uranium concentration in solution reached the same stable value of $(5.5 \pm 0.6) \times 10^{-6} \text{ mmol.L}^{-1}$ after 120 days of alteration. Geochemical calculations using the Thermochemie V10d database showed that the uranium concentration measured at equilibrium was compatible with the solubility of the U(VI)-phase, clarkeite ($Na(UO_2)O(OH)$), or U(IV)-phases coffinite ($USiO_4$) and $UO_2 \cdot 2H_2O$. However, altered surfaces characterizations by SEM and Raman spectroscopy did not reveal the presence of secondary phases. The Raman spectra of the altered MIMAS MOX fuel were characteristic of non-oxidised UO_2 and PuO_2 surfaces. These results rather indicated an oxidative dissolution limitation caused by silicate ions adsorption at the solid/solution interface, as already observed for UO_2 SIMFUEL by Santos et al. [10].

References

- [1] Oudinet, G. et al. (2008). Characterization of plutonium distribution in MIMAS MOX by image analysis. *J. Nucl. Mater.* 375: 86-94
- [2] Eriksen, T. E., D. W. Shoesmith and M. Jonsson (2012). Radiation induced dissolution of UO_2 based nuclear fuel – A critical review of predictive modelling approaches. *J. Nucl. Mater.* 420: 409-423
- [3] Carbol, P., P. Fors, S. Van Winkel, and K. Spahiu (2009). Corrosion of irradiated MOX fuel in presence of dissolved H_2 . *J. Nucl. Mater.* 392: 45-54
- [4] Odorowski, M. et al. (2016). Oxidative dissolution of unirradiated Mimas MOX fuel (U/Pu oxides) in carbonated water under oxic and anoxic conditions. *J. Nucl. Mater.* 468: 17-25
- [5] Jegou, C. et al. (2022). MOX Fuel corrosion processes under waste disposal conditions. *Corr. Sci.* 195: 109964
- [6] Kerleguer, V. et al. (2020). The mechanisms of alteration of a homogeneous $U_{0.73}Pu_{0.27}O_2$ MOx fuel under alpha radiolysis of water. *J. Nucl. Mater.* 529: 151920
- [7] Ferradini, C. and J. P. Jay-Gerin (2000). The effect of pH on water radiolysis: A still open question — A minireview. *Res. Chem. Interm.* 26: 549-565
- [8] Mennecart, T., C. Cachoir and K. Lemmens (2015). Influence of the alpha radiation on the UO_2 dissolution in high pH cementitious waters. *J. Radioanal. Nucl. Chem.* 304: 61-66
- [9] Sarrasin, L. et al. (2021). Studtite Formation Assessed by Raman Spectroscopy and O-18 Isotopic Labeling during the Oxidative Dissolution of a MOX Fuel. *J. Phys. Chem. C* 125: 19209-19218
- [10] Santos, B. G., J. J. Noel and D. W. Shoesmith (2006). The influence of silicate on the development of acidity in corrosion product deposits on SIMFUEL (UO_2). *Corr. Sci.* 48: 3852-3868

PA1-5 SOLUBILITY BEHAVIOR OF NEPTUNIUM (V) IN EXPECTED WIPP CONDITIONS

Ugras Kaplan, Ceren Kutahyali Aslani, Jandi L. Knox, Adrienne E. Navarrette, Jeremiah Beam, Jean-Francois Lucchini, Donald T. Reed

Actinide Chemistry and Repository Science Program (ACRSP) / Los Alamos National Laboratory (LANL) / NM-USA

The Waste Isolation Pilot Plant (WIPP) is the nation's only deep geologic radioactive waste repository and also the first operated salt-based deep geologic Transuranic (TRU) radioactive waste repository in the world. The Compliance Recertification Application (CRA)-2024 will update the oxidation state- specific model used to calculate actinide solubility in the WIPP. The only An(V) actinide that is important in the WIPP is the pentavalent neptunyl (Np(V)O^+) ion. This ion also has high oxidation- state stability and high solubility in oxic and suboxic aqueous systems. In the²predicted WIPP scenario, neptunium is the only TRU component that increases in the inventory with time as it is the main daughter product of ^{241}Am decay (alpha, n), so its relative importance increases throughout WIPP's 10,000-year performance period [1].

The aqueous chemistry of Np(V) in 5 M NaCl and synthetic WIPP brines as a function of pCH+ in the presence or the absence of borate, WIPP-relevant ligands (EDTA, oxalate, citrate, acetate), and carbonate at $T = 23 \pm 2$ °C was thoroughly studied by long-term batch solubility experiments (approximately 150 days) from an undersaturation approach [2]. Applying a comprehensive set of experimental and spectroscopic techniques including UV-VIS-NIR, Np-LIII-edge X-ray Absorption Near Edge Spectroscopy (XANES) and SEM (Scanning Electron Microscopy), the solubility controlling Np(V) solid phases and the predominant aqueous Np(V) species were identified.

Figure 1 shows the Np-LIII-edge XANES spectra of the solid phases from undersaturated experiments. For comparison, Figure 1 also shows the $\text{Np(IV)(OH)}_4(\text{s})$ and $\text{Np(V)O}_2\text{OH}(\text{s})$ reference spectra. The observed spectral features were used to distinguish between the two different Np oxidation states by focusing on the Np-LIII- edge XANES part of the spectra. The oxidation state of Np-LIII-edge XANES based on the shape and energy position of the white line agrees with solid Np(V) reference samples in Figure 1. The oxidation state of Np in the samples was determined by fitting the XANES region between 17605 and 17725 eV by a linear combination of reference spectra for Np(IV) and Np(V). A more detailed analysis employing linear combination fitting analysis (LCFA) based on reference spectra show that all measured sample consist of 100% Np(V) maximum with ± 8 % error.

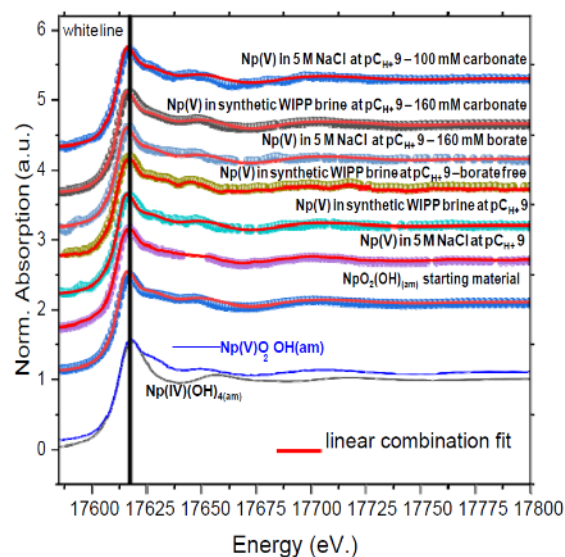


Figure 1: Experimental Np-LIII-edge XANES spectra. Each experimental data are compared to corresponding linear combination fits of Np(IV) and Np(V) standards.

Variable kinetic effects were noted in the interactions of organic ligands with Np(V). It was observed that acetate increased the neptunium solubility within the 150-days experimental period, and this result confirms WIPP model predictions. The effect of carbonate on Np(V) solubility was mostly seen at $pCH+ \approx 9$ and $pCH+ 11$. Also, the impact of borate on the aqueous speciation and especially on the solubility of Np(V) in 5 M NaCl and synthetic WIPP brines at $pCH+ \approx 9$ was confirmed.

Altogether, these experimental WIPP-specific results confirm the WIPP conceptual model and, correspondingly, the predicted neptunium (V) solubility [3].

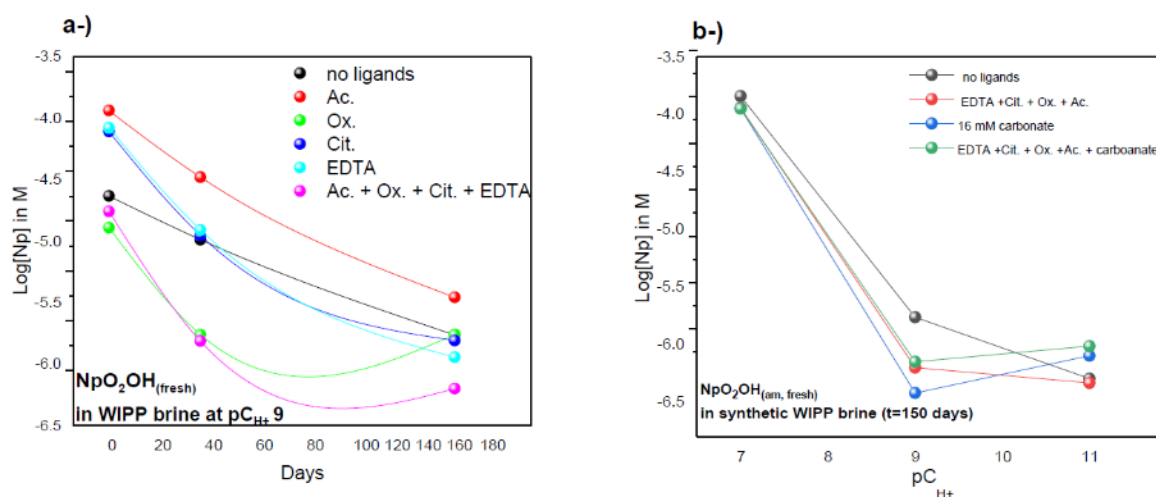


Figure 2. Solubility of $NpO_2(OH)(am, fresh)$ in the absence and presence of (in)organic ligands citrate: $2.30 \times 10^{-3} M$, acetate: $2.83 \times 10^{-2} M$, oxalate: $1.13 \times 10^{-2} M$, EDTA: $7.92 \times 10^{-5} M$, and carbonate: $1.6 \times 10^{-2} M$ in synthetic WIPP brine solutions as a function of time (a) and $pCH+$ (b). The results obtained with a maximum error rate of $\pm 15\%$.

This important result supports the accuracy of the WIPP conceptual model. The thermodynamic database for the An(V) actinides currently used in the Fracture-Matrix Transport (FMT) database is described by [4]. Np(V) speciation and solubility were parameterized in the Pitzer activity-coefficient model for the $[Na^+] - [K^+] - [Mg^{2+}] - [Cl^-] - [SO_4^{2-}] - [CO_3^{2-}] - [HCO_3^-] - [OH^-] - [H_2O]$ system. The model contains the solid species $NpO_2OH(am)$, $NpO_2OH(aged)$, $Na_3NpO_2(CO_3)_2(s)$, $KNpO_2CO_3 \cdot 2H_2O(s)$, $K_3NpO_2(CO_3)_2 \cdot 0.5H_2O(s)$ and $NaNpO_2CO_2 \cdot 3.5H_2O(s)$ to explain the available data.

The data obtained from this work quantify the effects of WIPP-relevant concentrations of organics/borate/carbonate on the solubility of Np(V) to challenge the predictions of the WIPP actinide model and inform decisions and recommendations made in the upcoming recertification of the WIPP (CRA-2024).

References:

- [1] U.S. Department of Energy (DOE) (2019). Title 40 CFR Part 191 Subparts B and C Compliance Recertification Application 2019, Appendix SOTERM. Carlsbad Field Office, Carlsbad, NM.
- [2] Kaplan, U (2022). Neptunium (V) Solubility in the Presence and Absence of WIPP Relevant Ligands. Los Alamos Report LCO-ACP-30. Los Alamos National Laboratory, Carlsbad NM, 88220
- [3] Domski, P. and C. Sisk-Scott (2019). Prediction of Baseline Actinide Solubilities for CRA 2019 with and Updated EQ3/6 Pitzer Thermodynamic Database, DATA0.FM4. Carlsbad, NM: Sandia National Laboratories. ERMS 571178.
- [4] Giambalvo, E. R. (2002). Memorandum to L.H. Brush (Subject: Recommended Parameter Values for Modeling An(V) Solubility in WIPP Brines). 26 July 2002. ERMS 522990. Carlsbad, NM: Sandia National Laboratories

PA2-1 DECIPHERING THE DYNAMIC PROCESSES OF MINERAL PRECIPITATION INDUCED POROSITY CLOGGING. COMBINING MICROFLUIDIC EXPERIMENTS AND SOLUTE TRANSPORT MODELLING

Mara I. Lönartz⁽¹⁾, Yuankai Yang⁽¹⁾, Guido Deissmann⁽¹⁾, Dirk Bosbach⁽¹⁾, Jenna Poonoosamy⁽¹⁾

(1) Institute of Energy and Climate Research, Nuclear Waste Management (IEK-6), Forschungszentrum Jülich GmbH, Germany

A mechanistic understanding of mineral precipitation induced clogging and its non-linear feedback on macroscopic transport properties of porous media is essential for predicting the long-term evolution of nuclear waste repositories. Most disposal concepts rely on a multibarrier system, combining engineered and geological barriers to provide a safe containment of the radioactive waste. At the interfaces between different barriers, chemical and thermal gradients promote mineral precipitation reactions, resulting in a reduction of porosity and potentially localized clogging [1-3]. Clogging of transport pathways may appear desirable to inhibit radionuclide migration, but can also be detrimental, particularly in the case of a hindered removal gases generated, for example, due to anoxic corrosion of metallic waste canisters or degradation of organic waste components [4]. Commonly applied porosity-diffusivity relations in continuum-scale reactive transport modelling based on Archie's law and extended versions thereof predict the case of clogging as a final state [5]. However, recent experiments and pore scale modelling investigations suggest that dissolution – recrystallization processes cause a non-negligible inherent diffusivity of newly formed precipitates [2-3,6]. To verify this hypothesis, we present a microfluidic reactor design that combines time-lapse optical microscopy and confocal Raman spectroscopy, providing real-time insights into mineral precipitation induced porosity clogging under purely diffusive transport conditions, using the precipitation of celestine (SrSO_4) as a model system. Based on 2D optical images of the reaction progress (Figure 1a), the effective diffusivity of the evolving porous medium was determined as a function of time using pore scale modelling. At the clogged state, isotopic tracer experiments were conducted and monitored by *in situ* Raman spectroscopy to visualize the transport of deuterium through the evolving microporosity of the precipitates, demonstrating the non-final state of clogging (Figure 1b). The evolution of the porosity – diffusivity relation in response to precipitation reactions shows a contradictory behavior to Archie's law.

The application of an extended power law improved the description of the evolving porosity – diffusivity relation, but still neglected post-clogging features. Currently, we continue to develop a microfluidic setup to answer the question how clogging-related processes depend on initial pore geometries. The innovative combination of microfluidic experiments and pore-scale modelling opens new possibilities to validate and identify relevant pore-scale processes, providing data for upscaling approaches to derive key relationships for continuum-scale reactive transport simulations.

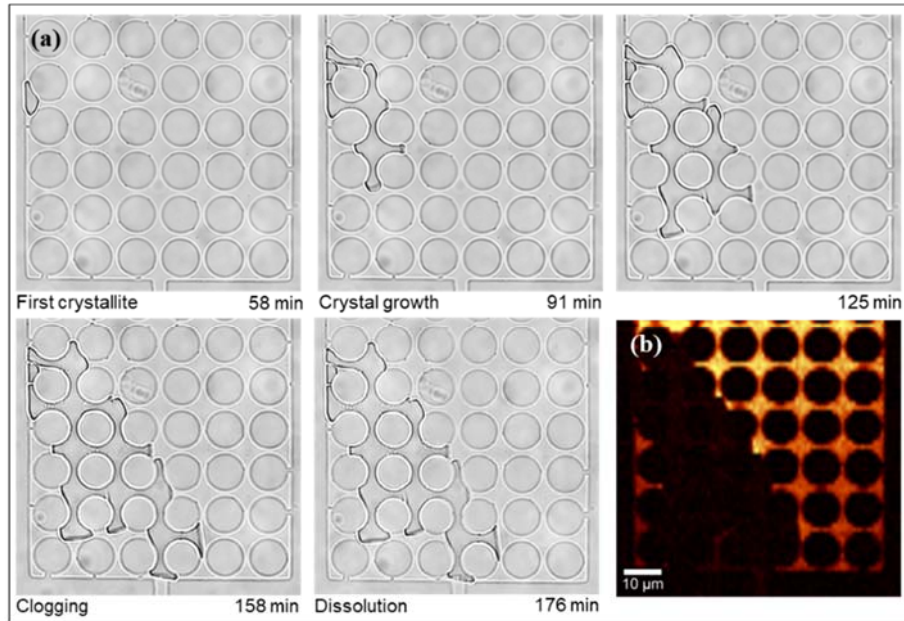


Figure 1. (a) Time-lapse bright field images of celestine growing in the reaction chamber of the microfluidic chip until porosity clogging. (b) Raman image of D_2O distribution during porosity clogging.

References

- [1] Seigneur et al. (2019). Reactive transport in evolving porous media. *Rev. Mineral Geochem.* 85: 197-238.
- [2] Chagneau et al. (2015). Mineral precipitation-induced porosity reduction and its effect on transport parameters in diffusion-controlled porous media. *Geochem. Trans.* 35: 13.
- [3] Deng et al. (2021). A pore-scale investigation of mineral precipitation driven diffusivity change at the column-scale. *Water Resour. Res.* 57(5): 1-16.
- [4] Xu et al. (2008). Corrosion-induced gas generation in a nuclear waste repository: Reactive geochemistry and multiphase flow effects. *Appl. Geochem.* 23: 3423 – 3433.
- [5] Xie et al. (2022). Reactive transport investigations of the long-term geochemical evolution of a multibarrier system including bentonite, low-alkali concrete and host rock. *Appl. Geochem.* 143: 105385.
- [6] Deng et al. (2022). A reactive transport modeling perspective on the dynamics of interface-coupled dissolution-precipitation. *Appl. Geochem.* 137: 105207.

PA2-2 KINETICS OF ^{226}Ra INCORPORATION INTO $(\text{Ba,Ra})\text{SO}_4$ SOLID SOLUTIONS

Stefan Rudin (1), Piotr M. Kowalski (2), Martina Klinkenberg (1), Thomas Bornhake (2), Dirk Bosbach

(1) Forschungszentrum Jülich GmbH, Institute of Energy and Climate Research, IEK-6: Nuclear Waste Management, 52425 Jülich, Germany

(2) Forschungszentrum Jülich GmbH, Institute of Energy and Climate Research, IEK-13: Theory and Computation of Energy Materials, 52425 Jülich, Germany

In some scenarios for the direct disposal of spent nuclear fuel, ^{226}Ra dominates the dose after 100,000 years. The formation of $(\text{Ba,Ra})\text{SO}_4$ solid solutions is relevant as a retention mechanism for the safety assessment of deep geological nuclear waste repositories. Several studies have shown that upon contact with ^{226}Ra , pure barite is replaced by the $(\text{Ba,Ra})\text{SO}_4$ solid solution during recrystallization, lowering the ^{226}Ra aqueous solubility by several orders of magnitude compared to pure RaSO_4 [1, 2]. Although thermodynamic models were successfully developed [3], and microscopic observations down to the nanoscale are available [4, 5], a fundamental theoretical understanding of the kinetics of Ra-uptake into barite is still missing. Since (re)crystallization is a surface process, a simulation of this process needs to take into account the barite-water interface. The main challenge is the proper representation of water (explicit and implicit) at the mineral-water interface, delivering an accurate simulation of bulk water, ion hydration shells and the water structure at the mineral surface.

The rate limiting step for the growth of the most relevant barite (001) surface is the kink-site nucleation at [120] steps [6, 7]. The first aim of this study was to determine the role of the structurally different kink sites at these steps for the crystal growth kinetics by computing the activation energies of the Ba^{2+} , Ra^{2+} and SO_4^{2-} ion attachment processes. Here, we have combined several advanced methods of computational quantum mechanics to optimize accuracy and efficiency of the simulations: a hybrid Density Functional Theory (DFT) and Soft-sphere Continuum Solvation (SSCS) approach for computation of barite-aqueous phase interface, and a Nudged Elastic Band (NEB) approach for calculation of activation energies.

A barite (001) surface structure was constructed, including steps and all relevant attachment positions for kink-site nucleation, and verified by comparison with experimental data. Our simulations show that Ba^{2+} attachment to the [120] steps of the (001) surface is a complicated multistep process, involving several water detachment-steps and the formation of outer, inner sphere and bidentate complexes with the barite surface (Fig.1). Two mechanisms mainly determine the shape of the energy path, the creation of bonds and the dehydration of the attaching ion. Energy differences between ion attachment processes at different sites are predominantly caused by the influence of the different [120] steps.

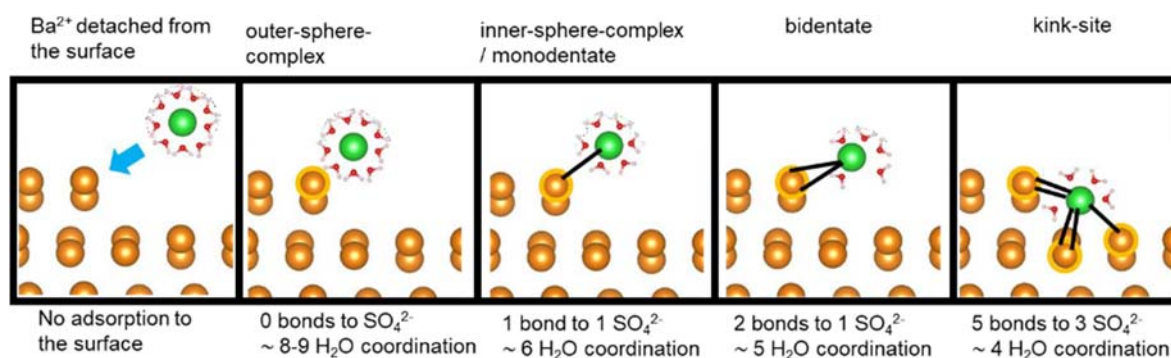


Figure 1: Minimum energy configurations occurring at Ba^{2+} -attachment to the barite stepped (001) surface.

The rate-limiting steps for Ba^{2+} attachment were the formation of the first bond to the barite surface and complete uptake. The Ba^{2+} ion completely attached to the barite surface is the configuration with the lowest energy, and the Ba^{2+} ion completely dissolved is the minimum energy configuration with the highest energy. The energy pathway derived from this study can explain the barite growth exclusively by

the driving forces of surface processes, which are also postulated to be responsible for the anisotropic barite (001) surface growth [8]. This is not the case with the classical force-field-based approach of Stack et al. 2012, which shows the same basic minimum energy structures but with different relative energies and the inner sphere complex as the configuration with the lowest energy [7].

The DFT-NEB-SSCS approach also provides more detailed energy paths that allow for an in-depth comparison of the different ion attachment processes at a certain site. On-going simulations for the uptake of ^{226}Ra into the (001) barite surface indicate distinct differences between Ra^{2+} and Ba^{2+} , related to the different water coordination numbers, and slight variations within the attachment path. Ra^{2+} could therefore be kinetically favored during recrystallization due to an easier dehydration compared to Ba^{2+} at the barite (001) surface.

References

- [1] Brandt, F., M. Klinkenberg, J. Poonoosamy and D. Bosbach (2020). Recrystallization and Uptake of ^{226}Ra into Ba-Rich (Ba, Sr) SO_4 Solid Solutions. *Minerals* 10(9): 812.
- [2] Klinkenberg, M., J. Weber, J. Barthel, V. Vinograd, J. Poonoosamy, M. Kruth, D. Bosbach and
- [3] F. Brandt (2018). The solid solution–aqueous solution system (Sr, Ba, Ra) SO_4 + H_2O : A combined experimental and theoretical study of phase equilibria at Sr-rich compositions. *Chemical geology* 497: 1-17.
- [4] Vinograd, V., F. Brandt, K. Rozov, M. Klinkenberg, K. Refson, B. Winkler and D. Bosbach (2013). Solid–aqueous equilibrium in the BaSO_4 – RaSO_4 – H_2O system: first-principles calculations and a thermodynamic assessment. *Geochimica et Cosmochimica Acta* 122: 398-417.
- [5] Weber, J., J. Barthel, F. Brandt, M. Klinkenberg, U. Breuer, M. Kruth and D. Bosbach (2016). Nano-structural features of barite crystals observed by electron microscopy and atom probe tomography. *Chemical geology* 424: 51-59.
- [6] Weber, J., J. Barthel, M. Klinkenberg, D. Bosbach, M. Kruth and F. Brandt (2017). Retention of ^{226}Ra by barite: The role of internal porosity. *Chemical geology* 466: 722-732.
- [7] Stack, A. G. (2009). Molecular dynamics simulations of solvation and Kink Site formation at the {001} Barite– Water interface. *The Journal of Physical Chemistry C* 113(6): 2104-2110.
- [8] Stack, A. G., P. Raiteri and J. D. Gale (2012). Accurate rates of the complex mechanisms for growth and dissolution of minerals using a combination of rare-event theories. *Journal of the American Chemical Society* 134(1): 11-14.
- [9] de Antonio Gomez, S., C. M. Pina and I. Martin-Bragado (2013). Lattice kinetic modeling of the anisotropic growth of two-dimensional islands on barite (001) surface. *Crystal growth & design* 13(7): 2840-2845.

PA2-3 FREEZING AND DEFROSTING OF IONIC AND MAGNETIC CONFIGURATIONS IN ZIRCONIUM MOLYBDATE FORMED IN NUCLEAR FUEL WASTE GLASSES

Masao Morishita, Tatsuya Miyatake, Hiroaki Yamamoto

Department of Chemical Engineering and Materials Science, University of Hyogo, Japan

This study was done as one of OECD NEA Mo TDB project [1,2]. $ZrMo_2O_8$ composed of Mo as fission product of U and Zr as nuclear-fuel cladding tube is one of harmful yellow phases having water solubility. Therefore, phase stability of $ZrMo_2O_8$ should be investigated for nuclear waste management. It has various polymorphs, that is, cubic [3, 4], trigonal [5, 6], and monoclinic [7] structures appear as functions of temperature, T , and pressure, p . In cubic polymorphs, inverse temperature dependence of thermal expansion (negative thermal expansion) [3, 4] is caused. Recently, we found a freezing and defrosting of ionic and magnetic configurations in the trigonal structure for the first time. These singular freezing and defrosting phenomena is presented in the present report.

P31c trigonal $ZrMo_2O_8$ [5, 6] was synthesized from hydrothermal method. Its magnetization, σ , electric resistivity, ρ , and heat capacity, $C_{p,m}^o$, during cooling at 320 – 2 K and warming 2 – 320 K were measured. Change in structure as a function of T during cooling and warming were investigated using the synchrotron radiation XRD (Spring 8) [8].

Figure 1 shows change in σ as a function of temperature, T , during colling and warming for P31c trigonal crystal. In both of cooling at 320 – 2 K and warming at 2 – 320 K, the magnetic phase transitions were caused to form the dia-, para-, and ferri-magnetic phases.

Figure 2 (a) and (b) show change in the diffraction degree, 2θ , of the (330) plane as a function of T during cooling and warming, respectively. In cooling (a), 2θ was found to be shifted to the lower with decreasing T , that is, negative thermal expansion was found. However, at forming the ferri-magnetic phase, the negative thermal expansion was come to halt and 2θ was observed to be constant. In warming (b), although 2θ shift was similar to cooling, these critical temperatures of the phase transitions, T_c , were found to be high.

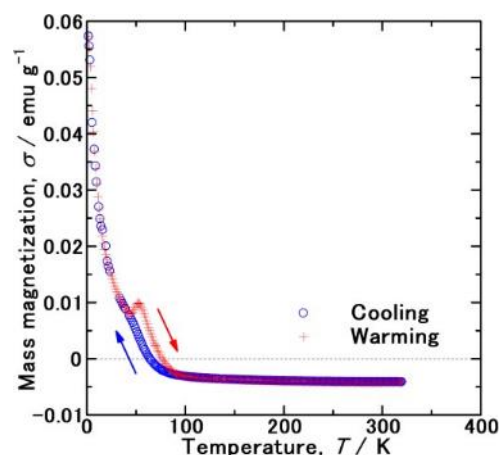


Figure 1 Magnetizations as a function of T during colling and warming for P31c- $ZrMo_2O_8$.

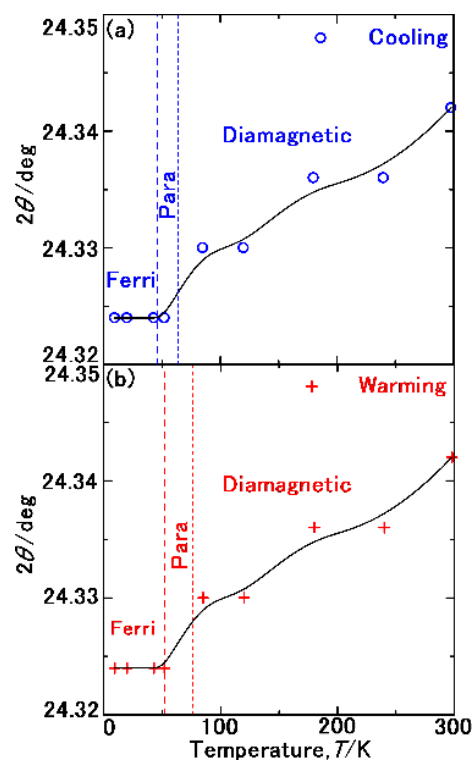


Figure 2 Change in magnetic properties with negative thermal expansion of P31c- $ZrMo_2O_8$.

In the four oxygen ions in tetrahedral cluster of MoO_4 in this P31c structure, three of them is bridging oxygen ion (O_B) vibrating librational and one of them is non-bridging oxygen ion (O_NB) vibrating with high motion freedom. Mo^{6+} ion vibrates with none unpaired-electron. At low temperatures, the bonding length between O_NB and Mo^{6+} appears to decrease from Coulomb interaction. As a result, Mo^{6+} is likely to accept unpaired-electron from O_NB , resulting in the para- and ferri-magnetism happen. On the other hand, the bond length between O_B and Mo^{6+} is increased from the negative thermal expansion resulting from librational motion of O_B [4]. Such counter balancing decrease and increase of the bond length appears to result in the constant lattice structure.

The reason for that warming is higher in the T_c data than cooling is discussed. The site occupancy of O_NB is likely to be freeze by cooling to 2 K at once, and defrosting the site occupancy is not likely to be easy. As a result, the T_c data of warming are concluded to be higher than ones of cooling. The ρ and C^p_m data also support expression of the freezing and defrosting phenomena. The present results contribute understanding the phase stability of trigonal ZrMo_2O_8 .

References

- [1] Ragoussi, M.E. and Brassinnes, S. (2015). The NEA Thermochemical Database Project: 30 Years of Accomplishments, *Radiochim. Acta.* 103: 679-685.
- [2] Morishita, M. Kinoshita, Y. Houshiyama, H. Nozaki, A. Yamamoto, H. Thermodynamic Properties for Calcium Molybdate, Molybdenum Tri-Oxide and Aqueous Molybdate Ion. (2017). *J. Chem. Thermodyn.* 114: 30-43.
- [3] Lind, C. Wilkinson, P. Hu, Z. Short, S. Jorgensen, J. D. Synthesis and Properties of the Negative Thermal Expansion Material Cubic ZrMo_2O_8 . (1998). *Chem. Mater.* 10: 2335-2337.
- [4] Evans, J. S. O. Hanson, P. A. Ibberson, R. M. Dean, N. Kameswari, U. Sleight, A. W. (2000). Low-Temperature Oxygen Migration and Negative Thermal Expansion in $\text{ZrW}_2\text{-XMoXO}_8$. *J. Am. Chem. Soc.* 122: 8694-8699.
- [5] Allen, S. Ward, R. J. Hampson, M. R. Gover, R. K. B. Evans, J. S. O. (2004). Structures and Phase Transitions of Trigonal ZrMo_2O_8 and HfMo_2O_8 . *Acta Crystallogr. B*60: 32-40.
- [6] XRD reference data: JCPDS [04-009-0701].
- [7] Sahoo., P. R. Sumithra, S. Madras, G. and Row, T. n. G. Synthesis, Structure and Photocatalytic Properties of β - ZrMo_2O_8 . *Bull. Mater. Sci.* (2009). 32: 337-342.
- [8] Kawaguchi, S. Takemoto, M. Osaka, K. Nishibori, E. Moriyoshi, C. Kubota, Y. Kuriwa, Y. and Sugimoto, K. High-throughput Powder Diffraction Measurement System Consisting of Multiple Mythen Detectors at Beamline BL02B2 of Spring-8. (2017). *Rev. Sci. Instrumens.*88: 085111.

PA3-1 NEW SPECIATION DIAGRAM OF THE PU(IV)-ACETATE SYSTEM TAKING INTO ACCOUNT POLYNUCLEAR SPECIES

Geoffroy Chupin (1), Christelle Tamain (1), Thomas Dumas (1), Pier Lorenzo Solari (2), Philippe Moisy (1), Dominique Guillaumont (1)

(1) CEA, DES, ISEC, DMRC, Univ Montpellier, Marcoule, France

(2) Synchrotron SOLEIL, L'Orme des Merisiers, BP 48, St Aubin, 91192 Gif sur Yvette, France

The speciation of actinides is fundamental to better understand the behavior of these radioelements in condensed phases. Recently, it has been admitted that the competition between hydrolysis and complexation can lead to the formation of polynuclear species (or clusters) with actinide cations connected through oxo (O), hydroxo (OH) or aquo (H₂O) bridges [1]. These species, stabilized at the surface by organic or inorganic ligands, can appear for low acidities and therefore be formed during geological storage. Different stoichiometries are possible depending on the conditions ranging from compounds with 2 metal centers to extreme cases involving 38 actinide cations [2], but most of the clusters observed in the solid state are hexameric clusters with octahedral geometry and are complexed at the surface with carboxylate functional ligands [3, 4]. If the structures of the clusters are often described in the solid state, they are much less so in solution they are not always correctly identified in solution. Therefore, they are not taken into account in the main thermodynamic/speciation models. While few data exist for the hexameric clusters of Th(IV), U(IV) and Np(IV) in solution with formate and acetate [5], no information is reported for Pu(IV). The objective of this study is the analysis of Pu(IV) clusters in solution in the presence of carboxylate ligand: acetate is used as a surrogate of this family. Moreover, available data on speciation in solution of "classical" monomeric complexes of plutonium (IV) acetate are rare, incomplete and sometimes contradictory.

To detect all potentially formed plutonium-acetate species, solutions were first characterized by Vis-NIR absorption spectroscopy. Large variations of pH and acetate concentrations were used and six different species were identified: the Pu(IV) aquo cation (Pu⁴⁺), and five plutonium complexes with acetate. Those five acetate complexes were characterized by coupling experimental (Vis-NIR and EXAFS spectroscopies and ESI-MS spectrometry) and quantum chemistry. As a result, Pu₆O₄(OH)₄(AcO)₁₂(H₂O)₆ hexameric cluster has been identified [6]: the missing block in the An(IV) series with formate and acetate ligands. The four other complexes are attributed to Pu(IV) acetate monomeric complexes. Species of Pu(IV) with acetate being described, their fractions in solution were evaluated and reported on a speciation diagram. The hexanuclear complex was not mentioned in the literature (despite chemical conditions equivalent to ours), this study allowed to define the new and more reliable Pu(IV)-acetate speciation diagram given in figure 1.

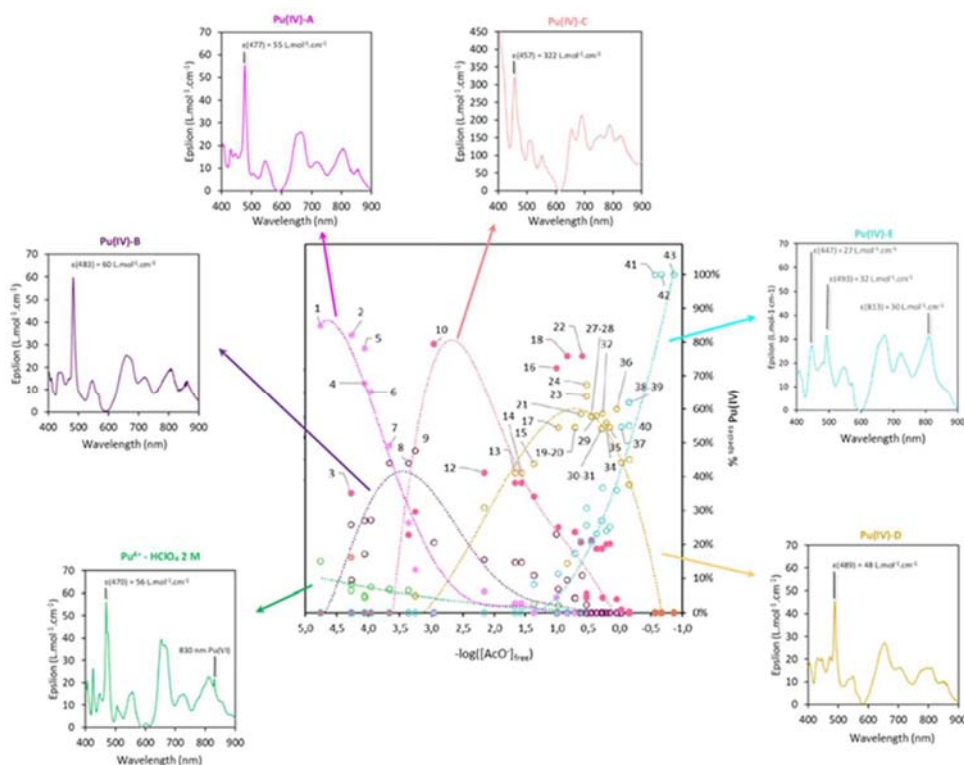


Figure 1: Speciation diagram of the Pu(IV)-acetate system and the isolated UV-vis absorption spectra of the different species.

References

- [1] Knope, K. E. and Soderholm, L. (2013). Solution and Solid-State Structural Chemistry of Actinide Hydrates and Their Hydrolysis and Condensation Products. *Chem. Rev.* 113: 944-994.
- [2] Qiu, J. and Burns, P. C. (2013). Clusters of Actinides with Oxide, Peroxide, or Hydroxide Bridges. *Chem. Rev.* 113: 1097-1120.
- [3] Knope, K. E. and Soderholm, L. (2013). Plutonium(IV) Cluster with a Hexanuclear $[\text{Pu}_6(\text{OH})_4\text{O}_4]^{12+}$ Core. *Inorg. Chem.* 52: 6770-6772.
- [4] Tamain, C., Dumas, T., Guillaumont, D., Hennig, C. and Guilbaud, P. (2016). First Evidence of a Water-Soluble Plutonium(IV) Hexanuclear Cluster. *Eur. J. Inorg. Chem.*: 3536–3540.
- [5] Takao, K., Takao, S., Scheinost, A. C., Bernhard, G. and Hennig, C. (2012). Formation of Soluble Hexanuclear Neptunium(IV) Nanoclusters in Aqueous Solution: Growth Termination of Actinide(IV) Hydrated Oxides by Carboxylates. *Inorg. Chem.* 51: 1336-1344.
- [6] Chupin, G., Tamain, C., Dumas, T., Lorenzo Solari, P., Moisy, P., Guillaumont, D. (2022). Characterization of a Hexanuclear Plutonium(IV) Nanostructure in an Acetate Solution via Visible-Near Infrared Absorption Spectroscopy, Extended X-ray Absorption Fine Structure Spectroscopy, and Density Functional Theory. *Inorg. Chem.* 61(12): 4806-4817.

PA3-2 SOLUBILITY OF FERROUS IRON HYDROXIDE IN THE PRESENCE OF CITRATE: EFFECT OF IONIC STRENGTH

Tim Platte (1), Jay Je-Hun Jang (1)

(1) Sandia National Laboratories¹, United States

The Waste Isolation Pilot Plant (WIPP) in New Mexico, U.S.A., is the only repository for the disposal of defense-related transuranic waste, and it is located in the Permian Salado Formation, a bedded salt deposit. To ensure long-term repository safety, the chemical behavior of the aqueous species formed by the contact of infiltrating groundwater with the waste needs to be investigated according to the WIPP chemical conceptual model. A geochemical thermodynamic database (GTD) built on the Pitzer activity coefficient model [1] is used to calculate the concentration of the formed chemical species to provide solubility of WIPP-relevant metals for the WIPP Performance Assessment. Anionic ligands like citrate have the potential to increase the dissolved concentration of actinides [2], but these interactions compete with other complexing metal ions like $\text{Fe}^{2+/3+}$ or Pb^{2+} . Iron and lead are major canister constituents for contact- and remote-handled waste. Therefore, competitive complexation of metals with these ligands within specific solutions need to be investigated in order to develop the GTD.

The solubility of $\text{Fe}(\text{OH})_2(\text{s})$ in the presence of citrate was analyzed by ICP-OES, IC, and TOC in low to high ionic strength solutions containing NaCl and Citrate or MgCitrate. The solid phase at the end of experiments was characterized by XRD, confirming no formation of secondary crystal phases. [3] Citrate stayed in solution over the duration of experiments. Results at higher pH (10 – 12) show no influence of the ionic strength (0.7 – 5.4 M) on the species formed or the solubility of $\text{Fe}(\text{OH})_2(\text{s})$ after 34 days. Only 3 – 4 % of the dissolved citrate forms Fe^{2+} - Citrate³⁻ complexes (Figure 1A). A second experiment at lower pH (7 – 8) shows an increase of the citrate fraction forming the Fe^{2+} - Citrate³⁻ complex(es) up to 100 % of the available Citrate (Figure 1B). No influence of the Na^+ -concentration (0.08 – 4.1 m) on the concentration of the species formed was determined in this study. IC/TOC results show no change of total Citrate, suggesting no microbial interaction for 900 days.

Since these measurements do not agree with a model prediction using just the complexation constant of Fe-Citrate^- from the literature [4] (dashed line Figure 1A and B), the formation of a second species is postulated. By including the formation of FeOHCitrate^{2-} into the calculation [5], an improved delineation of the experimental to the modeled data could be observed (Figure 1C and D). FeOHCitrate^{2-} is presumed to be stable at the investigated pH ranges and is a chemical analogue to the $\text{Cu}(\text{II})\text{Citrate}$ complex of the literature [4]. Best fit results could be achieved with a log K value of 2.24 for FeOHCitrate^{2-} .

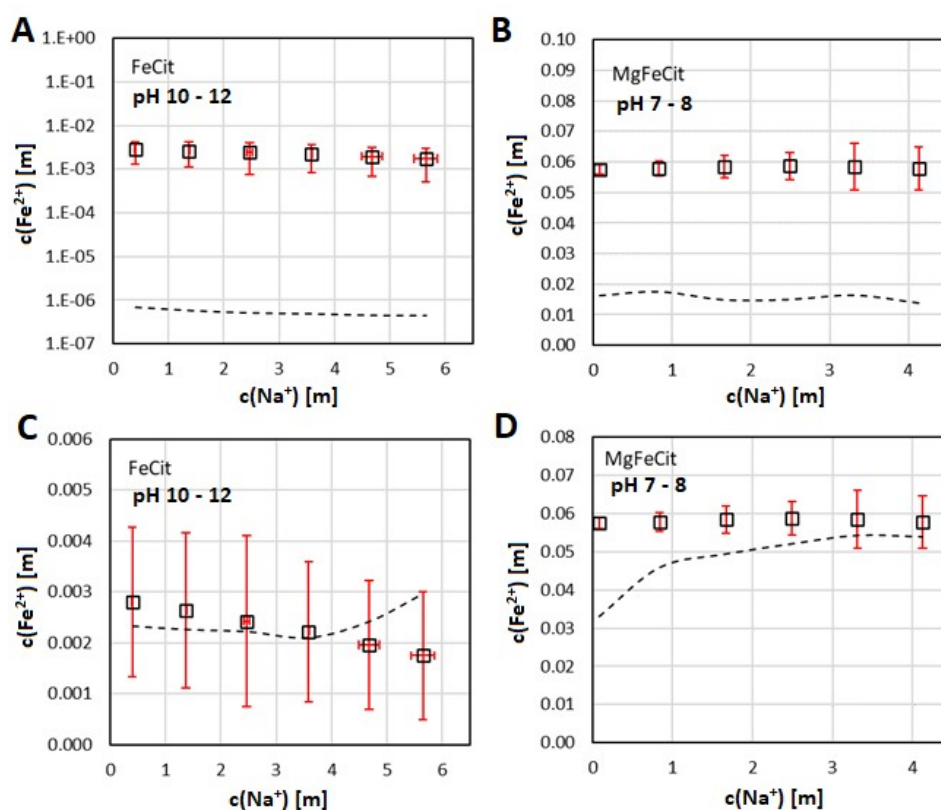


Figure 1. Comparison between dissolved Fe at pH 10 – 12 and pH 7 – 8 in NaCl solutions of different ionic strength. Dashed lines show model predictions. **A and B:** Experimental data before ^[4] and after (**C & D**) including the FeOHCitrate^{2-} species.

Acknowledgement: Sandia National Laboratories is a multimission laboratory managed and operated by National Technology and Engineering Solutions of Sandia, LLC., a wholly owned subsidiary of Honeywell International, Inc., for the U.S. Department of Energy's National Nuclear Security Administration under contract DE-NA-0003525. This research is funded by WIPP programs administered by the Office of Environmental Management (EM) of the U.S. Department of Energy.

References

- [1] Harvie, C. E., N. Møller and J. H. Weare (1984). The prediction of mineral solubilities in natural waters: The Na-K-Mg-Ca-H-Cl-SO₄-OH-HCO₃-CO₃-CO₂-H₂O system to high ionic strengths at 25°C. *Geochim. Cosmochim. Acta* 48: 723-751.
- [2] Choppin, G. R., A. H. Bond, M. Borkowski, M. G. Bronikowski, J. F. Chen, S. Lis, J. Mizera, O. Pokrovsky, N. A. Wall, Y.-X. Xia, and R. C. Moore (2001). Waste Isolation Pilot Plant Actinide Source Term Test Program: Solubility Studies and Development of Modeling Parameters. Sandia Report, SAND99-0943. Sandia National Laboratories. ERMS 518556.
- [3] Jang, J., P. Hora, L. Kirkes, C. Miller, and L. Zhang (2021). Analysis Report documenting Solubility and Complexation of Iron, Lead, Magnesium, Neodymium, and Boron in the WIPP-Relevant Brines under TPs 06-03, 08-02, 12-02, 14-03, 14-05, 16-02, 19-01, and 20-01. Revision 0. GEOC-21-11. Sandia National Laboratories, Carlsbad, New Mexico, U.S.A. ERMS 576381. SAND2022-13723R.
- [4] Morel, F. M. M. and Hering, J. G. (1993) Principles and Applications of Aqueous Chemistry. John Wiley & Sons, New York.
- [5] Hamm, R. E. et al. (1954) Citrate Complexes with Iron(II) and Iron(III). *J. Am. Chem. Soc.* 76, 8: 2111-2114

PA3-3 THERMODYNAMIC AND STRUCTURAL STUDIES OF AM(III)-ISOSACCHARINATE COMPLEXATION UNDER ACIDIC TO ALKALINE CONDITIONS: AQUEOUS COMPLEXES TO COLLOIDAL PARTICLES

Hee-Kyung Kim⁽¹⁾, Hyejin Cho⁽¹⁾, Keunhong Jeong⁽²⁾, Ung Hwi Yoon⁽²⁾, Hye-Ryun Cho⁽¹⁾

(1) Korea Atomic Energy Research Institute, Republic of Korea

(2) Korea Military Academy, Republic of Korea

Physicochemical behaviors of actinides in natural environments should be understood for the long-term performance assessment of radioactive waste repository. Isosaccharinic acid (ISA) is a concerned small organic ligand that can increase the mobility of radionuclides by reducing mineral uptakes and increasing solubility [1-3]. ISA is a major cellulose degradation product in highly alkaline Ca^{2+} rich environment of cementitious materials [4], which are used for the fixation of low to intermediate level radioactive wastes and for constructions of repositories. In this study, the formation of Am(III) complexes with α -D-ISA was studied by combined use of spectrophotometry, time-resolved laser fluorescence spectroscopy (TRLFS), and density functional theory (DFT) calculations. First, aqueous Am(III)-ISA complexes were studied using absorption and TRLFS of Am(III) in weakly acidic condition of pH~5.5 [5]. The reaction enthalpy and entropy changes were measured from the formation constants determined at various temperatures in the range of 15–70 °C. Formation of 1:1 Am(III)-ISA complex is driven by entropy increase, while 1:2 complex formation is exothermic with much less increase in entropy. DFT calculations predicted that C2 and C4-hydroxyl groups, along with the carboxyl group, participate in the tridentate chelate binding of the primary ISA. The thermodynamic, TRLFS, and DFT results collectively suggest tridentate binding of the primary ISA to Am(III) via a carboxylate and C2 and C4-hydroxyl groups in the protonated state and reduced dentate binding of the secondary ISA, such as a bidentate binding, forming a four-membered ring structure via the carboxylate group. Next, we examined the complexation of Am(III)-ISA under alkaline conditions. We will discuss about the effects of deprotonated hydroxyl groups of ISA on the binding structures and the stability. Formation of colloidal particles as well as aqueous ternary complexes of Am(III)-OH-ISA will also be discussed.

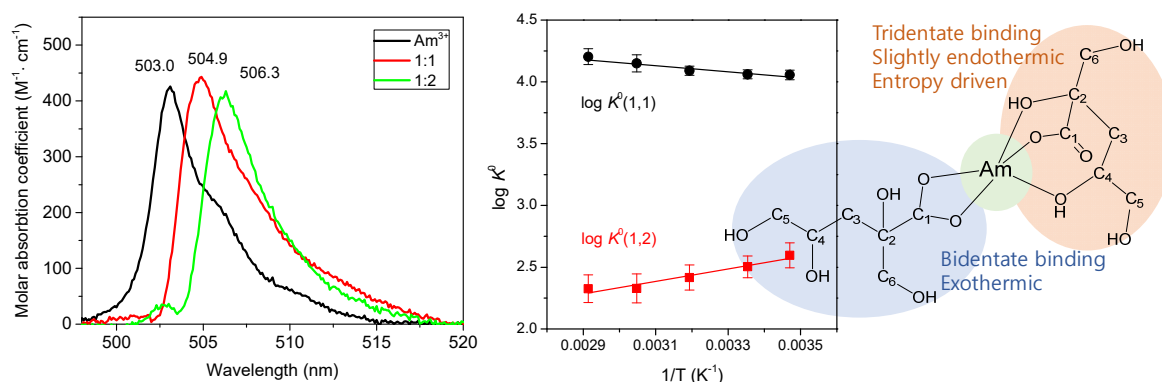


Figure 1: (Left) Deconvoluted absorption spectra of Am(III)-ISA complexes. (Right) Temperature-dependent equilibrium constants of Am(III)-ISA complexes and proposed binding structures [5].

References

- [1] Van Loon, L. R. and Glaus, M. A. (1998) Experimental and Theoretical Studies on Alkaline Degradation of Cellulose and its Impact on the Sorption of Radionuclides; Paul Scherrer Institut & Nagra: Switzerland.
- [2] Tits, J.; Wieland, E.; Bradbury, M. (2005) The Effect of Isosaccharinic Acid and Gluconic Acid on the Retention of Eu(III), Am(III) and Th(IV) by Calcite. *Appl. Geochem.* 20: 2082–2096.

- [3] Tasi, A., Gaona, X., Fellhauer, D., Böttle, M., Rothe, J., Dardenne, K., Polly, R., Grivé, M., Colàs, E., Bruno, J., Källström, K., Altmaier, M., Geckeis, H. (2018) Thermodynamic Description of the Plutonium- α -D-Isosaccharinic Acid System I: Solubility, Complexation and Redox Behavior. *Appl. Geochem.* 98: 247–264.
- [4] Glaus, M. A., van Loon, L. R., Achatz, S., Chodura, A. and Fischer, K. (1999) Degradation of Cellulosic Materials under the Alkaline Conditions of a Cementitious Repository for Low and Intermediate Level Radioactive Waste: Part I: Identification of Degradation Products. *Anal. Chim. Acta* 398: 111–122
- [5] Kim, H.-K., Cho, H., Jeong, K., Yoon, Y. H. and Cho, H.-R. (2022) Thermodynamic Study of Am(III)-Isosaccharinate Complexation at Various Temperatures Implicating a Stepwise Reduction in Binding Denticity. *Inorg. Chem.* 61: 19369-19378.

PA3-4 TRIBUTYL PHOSPHATE: COMPETITIVE ADSORPTION AND EFFECT ON RADIONUCLIDES RETENTION

Assaf Marwa(1), Thory, Emilie(1), Henocq, Pierre(2), Dagnelie, Romain V.H.(1)

(1) *Université Paris-Saclay, CEA, Service de Physico-Chimie, 91191, Gif-sur-Yvette, France*

(2) *Andra, R&D Division, parc de la Croix Blanche, 92298, Châtenay-Malabry, France*

In addition to actinides and fission products, the degradation of radioactive waste and engineered barriers may release simultaneously non-radioactive compounds such as organic or saline plumes. For that reason, the effect and confinement of inorganic salts and organic compounds is widely investigated for disposal concepts. The effects of organic complexing species on radionuclides (RNs) retention have been described in a previous work, as well as the various underlying mechanisms [1]. In the case of the geological disposals, studies are currently ongoing on tributyl-phosphate (TBP) in terms of speciation and migration properties. In this context, this study focuses on the retention of TBP, its degradation products in Callovo-Oxfordian clay-rock (COx) and their effects on radionuclides retention.

A first part deals with binary systems {TBP / COx}, with a focus on the retention of TBP, as well as competitive or synergistic effects in presence of other complexing compounds. The migration of usual complexing species (e.g. EDTA) has been well investigated on COx clay rock [2]. Still, the retention properties strongly vary with the adsorbates; indeed, ionisable compounds preferentially sorb on clay surfaces, while strongly lipophilic compounds, such as TBP, may be absorbed by natural organic matter [3]. Hence, the competition observed during co-adsorption of ionizable complexing species (EDTA, Isa) and TBP may be limited, while their potential perturbation of the media may add up.

The second part deals with complexing properties in ternary systems: {RNs / TBP / COx}. Various cationic species are investigated, e.g. Ni(II), Eu(III), Th(IV). At first, available thermodynamic databases were used in order to estimate the effect of TBP on cationic radionuclides retention. The direct effect due to the complexation of RNs with TBP is assessed as well as the indirect effect induced by the perturbation of the material properties. Then, a modelling exercise is proposed with early experimental data in the context of the French deep geological disposal facility (CIGEO).

References

- [1] Fralova et al. (2021). Effect of organic compounds on the retention of radionuclides in clay rocks: Mechanisms and specificities of Eu(III), Th(IV), and U(VI). *Applied Geochem.* 127, 104859.
- [2] Dagnelie R.V.H., et al. (2018). Perturbation induced by EDTA on HDO, Br- and Eu(III) diffusion in a large-scale clay rock sample. *Applied Clay Science*; 105–106, 142–149.
- [3] Guo et al. (2021). Mobility of organic compounds in a soft clay-rich rock (Tégulines clay, France). *Chemosphere*, 275, 130048.

PA3-5 THERMODYNAMIC STUDY OF COMPLEXATION OF LANTHANIDE/ACTINIDE WITH CEMENT ADDITIVES BY ISOTHERMAL MICRO-TITRATION CALORIMETRY

M. Acker⁽¹⁾, A. Wollenberg^(1,2), S. Taut⁽¹⁾, T. Stumpf^(2,3)

(1) Technische Universität Dresden, Radiation Protection, Central Radionuclide Laboratory, 01062 Dresden, Germany

(2) Technische Universität Dresden, Professorship for Radioecology and Radiochemistry, Germany, 01062 Dresden, Germany

(3) Helmholtz-Zentrum Dresden-Rossendorf, Institute of Resource Ecology, 01328 Dresden, Germany

There is a worldwide consensus that safety assessments of a nuclear waste repository have to consider water ingress as the worst-case scenario. For such assessments, reliable thermodynamic data on complexation reactions between actinides and common dissolved inorganic and organic ligands are required. Both the repository construction and the conditioning of the radioactive waste will introduce a large number of organic ligands into the repository. These organic ligands can have a significant influence on the chemical behavior and thus on the retention of the disposed radionuclides. A group of ligands that could act as potential complex partners for radionuclides are part of various cement-based materials that contain cement additives. Water may induce the aging and degradation of such cement-based constructions in the repository, resulting in the release of organic cement admixtures and their degradation products. Cement additives are, for example, polycarboxylate-ether macromolecules, (poly)hydroxycarboxylates (like gluconate, citrat, malate) or various phosphonocarboxylates. Phosphonate carboxylates whose most prominent representative is 2-phosphonobutane-1,2,4-tricarboxylic acid (PBTC) have barely been considered in the context of complexation with radionuclides. PBTC is known in industrial applications as strong complexation agent for various metal ions.[1,2] In very recent investigations in our group, structural investigations on the speciation and complexation of U(VI) with PBTC have been carried out. In these studies, highly soluble U(VI)-PBTC complex species were found and characterized up to the alkaline pH range. [3]

Besides the equilibrium constants corresponding to the free energy, the reaction enthalpies and entropies are also important thermodynamic quantities for modeling of the influence of organics on the mobility of radionuclides, especially at higher temperatures and ionic strength as are expected in the repository. There are hardly any enthalpy values for complexation reactions of actinides/lanthanides with cement additives. Isothermal micro-titration calorimetry (ITC) is the method of choice for the direct determination of the reaction enthalpies of An/Ln complexation reactions, especially as a function of ionic strength, as nicely demonstrated by us on the example of An(III)-malate [4] and Eu(III)-lactate [5] complexation.

For the first time, we carried out ITC studies of the interaction of U(VI) and Nd/Eu(III) (as inactive models for trivalent actinides) with 2-phosphonobutane-1,2,4-tricarboxylic acid (PBTC). The calorimetric complexation experiments were performed as a function of ionic strength using NaCl as the background electrolyte and were limited to a pH of up to 4 for U(VI) and 6 for Eu/Nd(III) to avoid hydrolysis of the metal ion. A mandatory prerequisite for the analysis of the calorimetric curves of the complexation reactions are the protonation enthalpies of the PBTC. In the present investigation, these enthalpies were determined in separate ITC experiments using the protonation constants recently determined by NMR spectroscopy [6].

In a first approximation, for the Nd/Eu(III)-PBTC complexation the calorimetric heat curves can be described with a simple 1:1 complexation (s-shaped curve, example Fig. 1). The situation is more complex for the calorimetric titration of U(VI) with PBTC: Here, the pH of the sample solutions do not remain constant during the titration. The complexation leads to a forced deprotonation of the carboxyl group involved in the complexation [3]. The heat contribution of the pH changes must be considered in the

analysis of the calorimetric titration curves (ongoing work). The results of the ITC studies and data analysis will be presented.

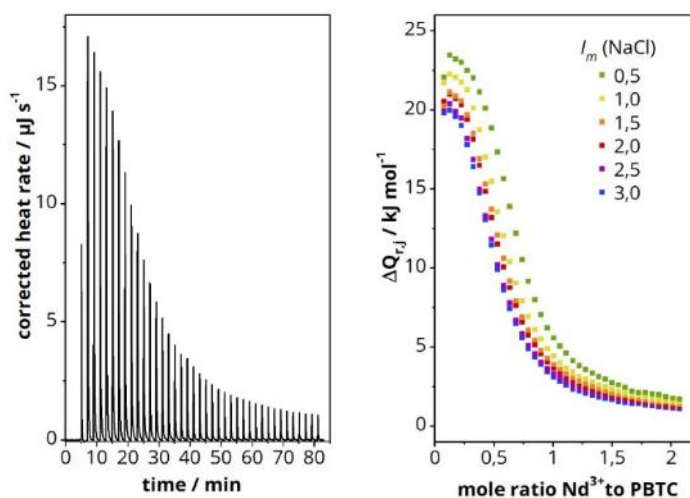


Figure 1. Example of ITC thermogram (left) and integrate heat curves (right) of the Nd(III)-PBTC complexation in NaCl, ($[Nd(III)] = 10 \text{ mM}$, $[PBTC] = 1 \text{ mM}$, $pH_C = 5.7$)

Acknowledgement: The German Federal Ministry for Economic Affairs and Energy (BMWi) is thanked for financial support within the GRaZ II project, no. 02E11860G

References

- [1] Demadis, K. D. et al. (2006). Phosphonopolycarboxylates as chemical additives for calcite scale dissolution and metallic corrosion inhibition based on a calcium-phosphonotricarboxylate organic-inorganic hybrid. *Cryst. Growth Des.* 6.5: 1064-1067.
- [2] Solvadó, V. et al. (1999). A study of the complex formation between trivalent ions (Al^{3+} , Fe^{3+}) and 2-phosphonobutane-1, 2, 4-tricarboxylic acid and their industrial applications. *Polyhedron.* 18.25: 3275-3280.
- [3] Wollenberg, A. et. al. (2023). Structural Identification of aquativ U(VI)-PBTC complexes by spectroscopic investigations, conference contribution, 18th International Conference on the Chemistry and Migration Behaviour of Actinides and Fission Products in the Geosphere, 24-29 September 2023, Nantes, France
- [4] Taube, F. et. al (2019). Thermodynamic and Structural Studies on the Ln(III)/An(III) Malate Complexation, *Inorg. Chem.* 58(1), 368-381
- [5] Skerencak-Frech, A. and Taube, F. et. al. (2019). A potentiometric and microcalorimetric study of the complexation of trivalent europium with lactate: The ionic strength dependency of $\log \beta_n$, $\Delta_r H_{m,n}$ and $\Delta_r S_{m,n}$, *Thermochim. Acta*, 678, 178316
- [6] Kretzschmar, J. and Wollenberg, A. et al. (2022). 2-Phosphonobutane-1, 2, 4,-Tricarboxylic Acid (PBTC): pH-Dependent Behavior Studied by Means of Multinuclear NMR Spectroscopy. *Molecules.* 27.13: 4067

PA4-1 PERRHENATE (ReO₄⁻) REMOVAL FROM AQUEOUS SOLUTIONS BY MONO-, BI-, AND TRI-METALLIC IRON NANOPARTICLES: A COMPARATIVE STUDY

Ibrahim Maamoun⁽¹⁾, Kohei Tokunaga⁽²⁾, Omar Falyouna⁽³⁾, Osama Eljamal⁽³⁾, Kazuya Tanaka⁽¹⁾

(1) *Advanced Science Research Center, Japan Atomic Energy Agency, 2-4 Shirakata, Tokai, Ibaraki 319-1195, Japan*

(2) *Ningyo-toge Environmental Engineering Center, Japan Atomic Energy Agency, Tomata, Okayama 708-0698, Japan*

(3) *Interdisciplinary Graduate School of Engineering Sciences, Kyushu University, 6-1 Kasuga-koen, Fukuoka 816-8580, Japan*

Recently, the rapid development of nuclear power technologies and the continuous energy demand around the world exhibited massive amounts of contaminated water with radionuclides. Pertechnetate (TcO₄⁻) is the highly mobile and soluble anionic form of the long-lived technetium-99 (⁹⁹Tc) (i.e., around 2.13 × 10⁵ years half-life) [1]. The exposure to Tc^{VII}-contaminated water can be harmful to human health, causing toxic effects and organs damage when ingested [2]. Therefore, TcO₄⁻ removal from aqueous solutions can be challenging, in terms of fast and efficient immobilization. Correspondingly, perrhenate (ReO₄⁻) was considered as TcO₄⁻ surrogate to ease the radioactivity-related complications, owing to the physiochemical similarities between Tc and rhenium (Re); as they share the stable oxidation state (VII) in aqueous solutions and both ReO₄⁻ and TcO₄⁻ can be reduced to IV oxidation state by electron-donor materials (E⁰: -0.548 V (ReO₄⁻), and -0.361 V (TcO₄⁻)) [3]. Meanwhile, metallic iron nanoparticles (Fe⁰) have been intensively reported as an efficient reactive material for reducible contaminants (e.g., Cr^{VI}, U^{VI}, As^V, etc.), due to the unique core-shell structure and the suitable redox potential (E⁰: -0.44 V). Doping Fe⁰ surface with other metals has been introduced in the literature to exhibit bi- and tri-metallic particles with higher catalytic properties and improved contaminants removal capabilities. Hence, the aim of this work is providing a comparative study on ReO₄⁻ removal efficiency using mono-, bi-, and tri-metallic Fe⁰. In this study, nickel (Ni) and zirconium (Zr) were considered in the preparation of bi- and tri-metallic Fe⁰ nanoparticles, as they both showed the highest ReO₄⁻ removal performance comparing with other metals (e.g., copper (Cu), palladium (Pd), silver (Ag), and cobalt (Co)). Unlike the aforementioned metals, the reduction potential of Ni (E⁰: -0.25 V) and Zr (E⁰: -1.44 V) enables those metals to act as reducing agents, contributing to ReO₄⁻ reduction. Fe⁰ was experimentally synthesized using chemical reduction approach. Bi-metallic Fe⁰ was prepared using liquid-phase deposition considering either addition of bi-metal salt to Fe^{III} precursor solution (annotated as pre) or saturation of synthesized Fe⁰ in bi-metal solution (annotated as post). Tri-metallic Fe⁰ preparation involved the consecutive deposition of bi- and tri-metals. Different characterization techniques were considered, including scanning electron microscopy coupled with energy dispersive X-ray spectroscopy (SEM-EDS), X-ray diffraction (XRD), and X-ray absorption near edge structure (XANES). The effect of reaction conditions on ReO₄⁻ removal was investigated, including mass ratio of iron to the doped metal (Fe⁰/Me: 20, 10, 5, and 2.5), material dosage (0.25 – 2.0 g/L), and initial pH (3.0 – 12.0). Results showed enhanced ReO₄⁻ removal rate when using bi-metallic Ni/Fe⁰ (mass ratio 2.5) and Zr/Fe⁰ (mass ratio 20) comparing with Fe⁰. The difference in ReO₄⁻ removal using mono-, bi-, and tri-metallic was not clear at high material dosage, such as 2.0 and 1.0 g/L. Nevertheless, comparing lower dosage (0.5 g/L) of bi- and tri-metallic to 1.0 g/L mono-metallic Fe⁰ dosage exhibited a clear superiority of tri-metallic Zr-Ni/Fe⁰ to other materials; where 0.5 g/L of the material could efficiently achieve around 98.0% ReO₄⁻ removal within just 10 min reaction time (1.8 times higher than 1.0 g/L Fe⁰). As shown in Fig. 1, SEM imaging indicated that particles aggregation phenomenon was maintained in mono-, bi-, and tri-metallic Fe⁰ with, suggesting stabilization using polymeric or non-magnetic materials as anti-aggregation techniques. However, particles aggregation may not greatly influence the goal of this work, as reduction is the main involved mechanism in ReO₄⁻ removal. Still, aggregation can diminish the available sportive sites influencing secondary removal mechanisms (i.e., electrostatic attraction). The significant enhancement in ReO₄⁻ removal rate by tri-metallic Fe⁰ nanoparticles can be attributed to the induced rate of electron transfer from iron core through the mixed Zr/Ni deposits on Fe⁰ surface. The promising potential

of tri-metallic Zr-Ni/Fe⁰ in ReO₄⁻ removal with a rapid rate and efficient performance may suggest its utilization in pilot-scale applications of Tc^{VII} removal from nuclear wastewater.

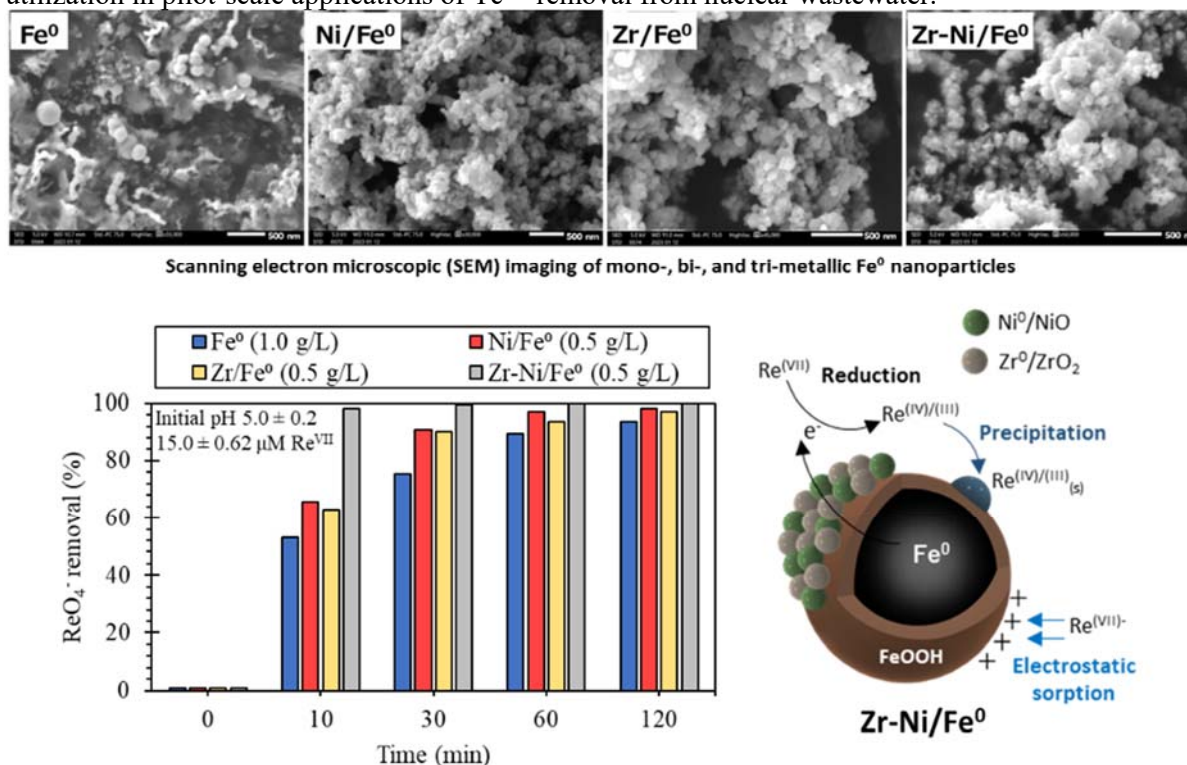


Fig. 1. ReO₄⁻ removal by mono-, bi-, and tri-metallic Fe⁰ nanoparticles.

Acknowledgement: This research was funded by Environmental Radioactivity Research Network Center (ERAN) FY2022 Collaborative Researcher Grants (Y-22-03, and F-22-21)

References

- [1] D. Fan, R.P. Anitori, et al. (2013). Reductive Sequestration of Pertechnetate (⁹⁹TcO₄⁻) by Nano Zerovalent Iron (nZVI) Transformed by Abiotic Sulfide. Environ. Sci. Technol. 47: 5302–5310.
- [2] C.R. Cothorn, W.L. Lappenbusch (1985). Radioactivity in drinking water. Heal. Phys. 48.
- [3] T. Wu, H. Wang, et al. (2014). Effect of EDTA on the diffusion behavior of ⁹⁹TcO₄⁻ and ReO₄⁻ in GMZ bentonite. J. Radioanal. Nucl. Chem. 299: 2037–2041.

PA4-2 REDOX-ACTIVE DONOR-ACCEPTOR CONJUGATED MICROPOROUS POLYMER FOR PHOTOCATALYTIC REDUCTION OF URANIUM(VI)

Fengtao Yu , Zhibin Zhang, and Yunhai Liu

State Key Laboratory of Nuclear Resources and Environment, School of Chemistry, Biology and Materials Science, East China University of Technology, Nanchang 330013, PR China

Achieving photoreduction uranium with D-A type conjugated microporous polymers in strongly acidic radioactive wastewater holds great promise but is extremely challenging, as it requires proper electron transport channels. Herein, a redox-active perylene-anthraquinone D-A conjugated microporous polymer photocatalyst (ECUT-AQ) which electron-rich perylene unit as donor and electron-deficient anthraquinone (AQ) as acceptor is innovatively reported. The results clearly demonstrates that AQ with dual characteristics of electron deficiency and redox activity plays a key role in photocatalytic reduction of UO_2^{2+} to UO_2 . On one hand, the constructed D-A structure induces the formation of a huge built-in electric field, which enhances the intramolecular charge transfer, thus significantly broadening visible light absorption range and improving electron-hole pairs separation efficiency. On the other hand, and very significantly, the redox-active AQ acts as a matched electron transfer channel, which further accelerates the photogenerated electrons transfer from the photocatalyst to the UO_2^{2+} . Consequently, the ECUT-AQ achieves 86% photoreduction UO_2^{2+} removal within two hours irradiation and obtains an impressive reduction rate constant ($k = 0.015 \text{ min}^{-1}$, $\text{pH}=1$ and $T = 293.15 \text{ K}$).

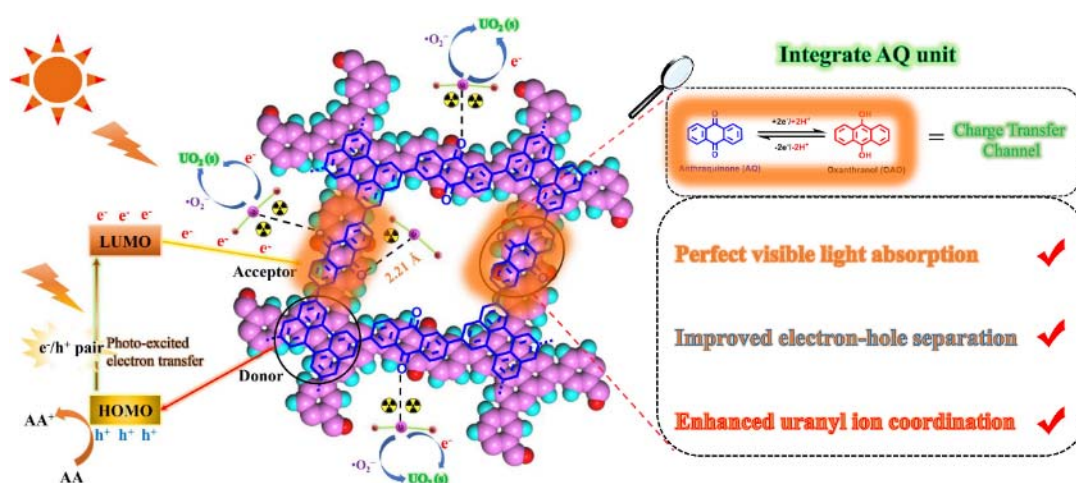


Fig.1. Photocatalytic U(VI) reduction mechanism of the ECUT-AQ

Realizing an efficient photochemical uranium reduction process using metal-free conjugated polymers is highly desirable, but is extremely challenging, as it requires a broad photo-response range and efficient electron transmission channels. Herein, three novel full-spectrum ($200 \leq \lambda \leq 800 \text{ nm}$) responsive biomimetic donor-acceptor conjugated microporous polymers (CMPs) were successfully constructed to photoreduce uranium through a molecular engineering strategy. The optical band gap and built-in electric field of the CMPs were conveniently optimized via various quinone-containing acceptors. Furthermore, the quinone-containing block exhibited outstanding redox activity, which could serve as a unique electron shuttle to rapidly transfer electrons. Consequently, ECUT-TQ with 2,6-dibromobenzo[1,2-b:4,5-b'] dithiophene-4,8-dione block exhibited a narrow band gap as low as 1.70 eV and stronger built-in electric field, achieving an impressive photoreaction rate constant of 0.057 min^{-1} (at 293.15 K), which was considerably higher than those of most reported metal-free polymer photocatalysts. Briefly, this work provides a novel approach for designing high-performance green biomimetic photocatalysts for removing radioactive pollution.

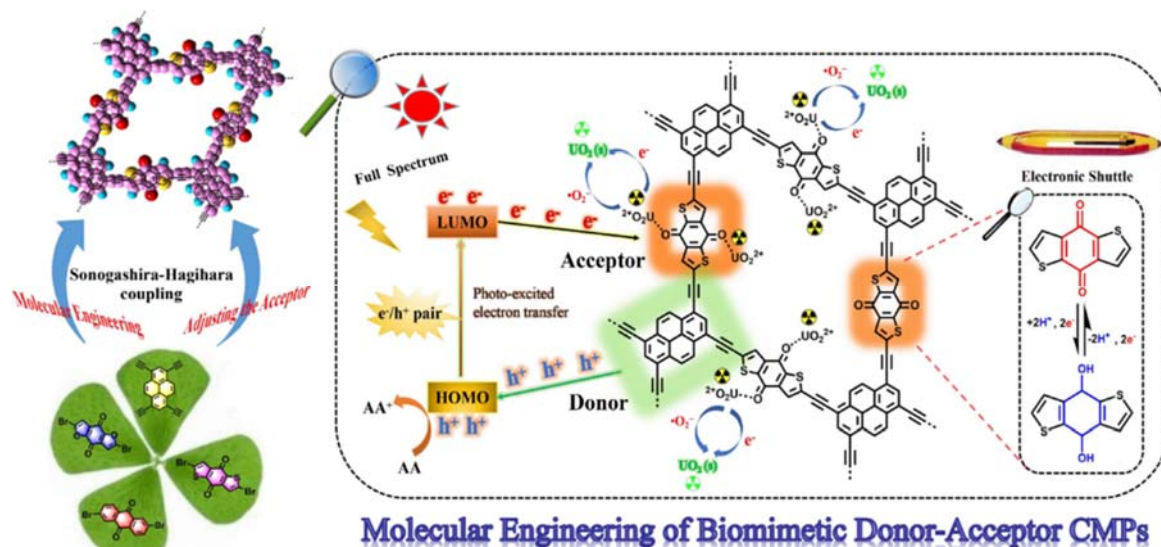


Fig.2. Schematic mechanism of biomimetic D-A CMPs photocatalyst.

References

- [1] Yu, FT, et al. (2018). Molecular engineering of donor-acceptor conjugated polymer/g-C₃N₄ heterostructures for significantly enhanced hydrogen evolution under visible-light irradiation. *Adv. Funct. Mater.*, 28: 1804512.
- [2] Yu, FT, et al. (2022). Novel donor-acceptor-acceptor ternary conjugated microporous polymers with boosting forward charge separation and suppressing backward charge recombination for photocatalytic reduction of uranium (VI). *Appl. Catal. B Environ.*, 301: 120819.
- [3] Yu, FT, et al. (2022). A redox-active perylene-anthraquinone donor-acceptor conjugated microporous polymer with an unusual electron delocalization channel for photocatalytic reduction of uranium (VI) in strongly acidic solution. *Appl. Catal. B Environ.*, 314: 121467.
- [4] Yu, FT, et al. (2021). Tunable perylene-based donor-acceptor conjugated microporous polymer to significantly enhance photocatalytic uranium extraction from seawater. *Chem. Eng. J.*, 412: 12758.

PA4-3 CHLORIDE GREEN RUST AS SCAVENGER OF TECHNETIUM: IMMOBILIZATION AND SPECTROSCOPIC STUDIES

Natalia Mayordomo ⁽¹⁾, André Rossberg ^(1,2), Diana M. Rodríguez ⁽¹⁾, Dieter Schild ⁽³⁾, Andreas C. Scheinost ^(1,2), Vinzenz Brendler ⁽¹⁾, Katharina Müller ⁽¹⁾

(1) Helmholtz-Zentrum Dresden-Rossendorf e.V (HZDR). Institute of Resource Ecology, 01328 Dresden (Germany).

(2) The Rossendorf Beamline at ESRF (ROBL), 38043 Grenoble (France).

(3) Karlsruhe Institute of Technology (KIT). Institute for Nuclear Waste Disposal, 76344 Eggenstein-Leopoldshafen (Germany).

Technetium-99 (⁹⁹Tc) is one of the most concerning fission products due to its long half-life ($2.13 \cdot 10^5$ years) and the high mobility of the anion pertechnetate (TcO_4^-) [1]. Tc migration decreases significantly when Tc(VII) is reduced to Tc(IV). This scavenging step can be induced by Fe(II) minerals, which have been widely studied due to their versatility, low cost, and ubiquity [2]. In addition, Fe(II) minerals will play an important role in the near-field of the nuclear waste repository, in case that corrosion of the waste canisters will occur and radioactive material be leaked in the environment.

Green rust is formed when Fe^{2+} interacts with Fe(III) minerals [3]. Thus, its presence is expected in both the near- and far-field of a repository. It is a Fe(II)-Fe(III) hydroxide that can immobilize radionuclides by adsorption, anion exchange, and reduction mechanisms. A previous work reports the interaction of green rust with Tc, but the results are limited to very narrow experimental conditions [4]. Thus, further studies are needed to both identify the optimal Tc scavenging conditions by green rust and the mechanism responsible of Tc retention.

Our studies consisted of a combination of batch contact studies, microscopic and spectroscopic analysis. Batch contact studies were performed under a wide range of conditions, i.e. pH (3.5 - 11.0), Tc concentration (nM - mM), and ionic strength (0.0 - 0.1 M). X-ray powder diffraction, Raman microscopy, X-ray photoelectron spectroscopy (XPS), and X-ray absorption spectroscopy provided information on Tc oxidation state and speciation as well as on secondary redox products related to the Tc interaction with chloride green rust (GR(Cl)). In addition, re-oxidation experiments have been performed for one year to analyze the Tc retention reversibility.

The results show that GR(Cl) removes Tc from solution with efficiencies between 80% ($K_d = 8.0 \cdot 10^3$ mL/g) and $\approx 100\%$ ($K_d = 9.9 \cdot 10^5$ mL/g) for pH > 6.0 (Figure 1). In contrast, Tc removal for pH < 6.0 drops with decreasing pH, and ranges from 80% to 50% ($K_d = 2.0 \cdot 10^3$ mL/g), reaching a minimum at pH 3.5.

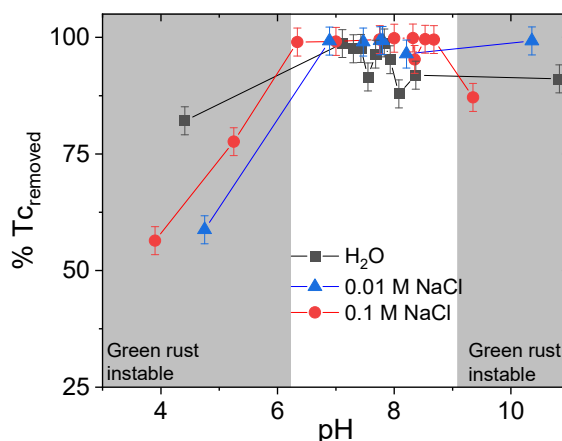


Fig. 1: Tc removal (%) by GR(Cl) as a function of pH for different ionic strengths H₂O (square), 0.01 M NaCl (triangle) and 0.1 M NaCl (circle).

XPS analysis reveals the predominance of Tc(IV) at all evaluated pH values (3.5 to 11.5), supporting that Tc reductive immobilization is the main retention mechanism. Re-oxidation experiments show that Tc is slowly solubilized when time increases.

The analysis of the extended X-ray absorption fine structure indicates a change of the Tc(IV) atomic environment depending on pH and Tc loading. The most probable structural rearrangements are represented by Tc(IV) sorption on Fe(III) minerals formed as secondary phases with Tc polynuclear species contribution.

Acknowledgement: The authors acknowledge the German Federal Ministry of Education and Research (BMBF) for the financial support of the NukSiFutur TecRad young investigator group (02NUK072) [4].

References

- [1] Meena, A. H. and Arai, Y (2017). Environmental geochemistry of technetium. *Env. Chem. Lett.* 15: 241-263.
- [2] Pearce, C. I. et al. (2020). Technetium immobilization by materials through sorption and redox-driven processes: A literature review. *Sci. Total Environ.* 716: 132849.
- [3] Usman, M. et al (2018). Magnetite and green rust: Synthesis, Properties, and Environmental Applications of Mixed-Valent Iron Minerals. *Chem. Rev.* 118: 3251-3304.
- [4] Pepper, S. et al. (2003). Treatment of radioactive wastes: An X-ray absorption spectroscopy study of the reaction of technetium with green rust. *J. Colloid Interface Sci.* 268: 408-412.
- [5] TecRad webpage: <https://www.hzdr.de/db/Cms?pNid=1375>, vis. Feb 9th 2023.

PA4-4 TC(VII) REDUCTIVE IMMOBILIZATION BY S(-II) PRE-SORBED ON ALUMINA

Sonia Garcia-Gomez⁽¹⁾, Caroline Börner⁽²⁾, Javier Gimenez⁽¹⁾, Ignasi Casas⁽¹⁾, Jordi Llorca⁽¹⁾, Joan de Pablo⁽¹⁾, Katharina Müller⁽²⁾, Natalia Mayordomo⁽²⁾

(1) UNIVERSITAT POLITÈCNICA DE CATALUNYA (UPC), SPAIN

(2) HELMHOLTZ ZENTRUM DRESDEN ROSSENDORF (HZDR), GERMANY

Tc is a fission product of ²³⁵U and ²³⁹Pu with a long half-life ($\tau_{1/2} \sim 2.14 \cdot 10^5$ years). Under oxidizing conditions, Tc main species (Tc(VII)O₄[□]) exhibits a high solubility and hardly interacts with minerals. In contrast, under reducing conditions, Tc(IV) presents a more limited mobility, either because Tc(IV) interacts with minerals or Tc(IV)O₂ is formed^[1]. However, the formation of Tc(IV)O₂ is not sufficient to ensure the immobilization of Tc, since when it is in contact with O₂, the reoxidation of Tc(IV) to Tc(VII) would be thermodynamically favorable. In contrast, the formation of Tc(IV) polysulfide species (such as TcS_x or Tc₂S₇) could inhibit Tc oxidation under oxidizing conditions^[2]. Therefore, S(-II) seems a promising candidate to immobilize Tc.

Sulfide would be present in the nuclear waste repository due to the addition of fly ash in the concrete, as well as the presence of minerals such as pyrite (FeS₂). It has been proven for Fe(II) that Tc(VII) reduction is more favorable when Fe(II) takes part in the mineral structure or it is sorbed on a surface than when Tc(VII) reduction is carried by dissolved Fe(II) (homoreduction)^[3]. We have recently showed that Tc(VII) heteroreduction (reduction occurring at the mineral-water interface) by Fe(II) pre-sorbed on alumina nanoparticles is highly efficient^[4]. Thus, in this work, we have studied kinetically as a function of pH: i) S(□II) sorption on alumina, and ii) subsequent Tc uptake promoted by S(-II) pre-sorbed on alumina. We have also focused on the effect of different sulfide sources on Tc(VII) reduction.

All the experiments were performed in a N₂ glove box free of CO₂ and O₂ (< 2 ppm). The alumina nanoparticles used in the experiments has been previously characterized with 127 m²/g N₂ BET and pH 9 as isoelectric point pH^[5]. For the batch sorption experiments, suspensions of alumina (0.5 g/L) containing 50 μM of NaHS at pH 5.3, 6.7 and 7.7 were prepared and shaken for two days. Then, KTcO₄ was added to the suspensions to obtain 5 μM of TcO₄[□]. Subsequently, the suspensions were placed in a horizontal shaker. The suspension pH was monitored frequently and readjusted when needed. Samples were taken periodically and centrifuged at 14,000 rpm for 45 min. The Tc concentration in the supernatant solution was measured by liquid scintillation counter to determine the percentage of Tc removed using the following equation.

$$\% Tc_{removed} = \frac{([Tc]_0 - [Tc]_t)}{[Tc]_0} \cdot 100 \quad (1)$$

where $[Tc]_0$ represents the initial concentration of Tc in solution (5 μM) and $[Tc]_t$ is the concentration of Tc in solution at a given time.

Figure 1 shows the uptake of Tc in % as a function of time and pH. Tc removal increases with decreasing pH. This is in agreement with the highest anion sorption on alumina nanoparticles at lower pH, when alumina surface is positive charged^[5]. The maximum Tc retention is 70% at pH 5.3, being complete after one day of contact. Whereas at higher pH values, Tc removal is significantly lower, i.e., 10% at pH 6.7 and 5% at pH 7.7. It is noteworthy to mention that the NaHS reactant used for the experiments in Figure 1. was partially oxidized. Despite of its oxidation, reduction of Tc(VII) yield at pH 5.3 was above 70% after one day of contact.

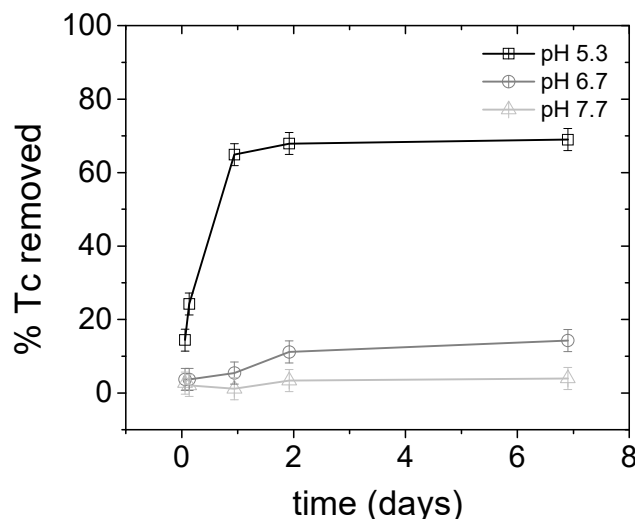


Figure 1: Tc removal (% $Tc_{removed}$) by S(-II) pre-sorbed on alumina at several pH values. NaHS partially oxidized was used in the experiments.

Further contact experiments have been performed to isolate the contribution of S(-II) in Tc(VII) heteroreduction, and the effect of the sulfide source on Tc removal. Raman microscopy and X-ray absorption spectroscopy have been used to determine the changes occurring at a molecular level when Tc(VII) is heteroreduced by S(-II).

Acknowledgements: The authors acknowledge the Spanish Ministry of Research and Universities for the abroad internship fellowship (PRE2018-085618) and the project (ENE2017-83048-R). Part of this work was financially supported by the German Federal Ministry of Education and Research (BMBF) NukSiFutur TecRad young investigator group (02NUK072).

References

- [1] Meena, A. et al. (2017) Environmental geochemistry of technetium. *Environ. Chem. Letters*. 15, 241–263.
- [2] Lukens, W. W. et al. (2005) Evolution of Technetium Speciation in Reducing Grout. *Environ. Sci. Technol.* 39, 8064–8070.
- [3] Zachara, J.M. et al. (2007) Reduction of pertechnetate [Tc(VII)] by aqueous Fe(II) and the nature of solid phase redox products. *Geochim. Cosmochim. Acta* 71, 2137–2157
- [4] Mayordomo, N. et al. (2020). Technetium retention by gamma alumina nanoparticles and the effect of sorbed Fe²⁺. *J. Hazard. Mater.* 388, 122066.
- [5] Mayordomo, N. et al. (2018). Selenium(IV) sorption onto γ -Al₂O₃: a consistent description of the surface speciation by spectroscopy and thermodynamic modeling. *Environ. Sci. Technol.* 52, 581–588.

PA4-5 PORPHYRIN-BASED HYDROGEN-BONDED ORGANIC FRAMEWORK FOR VISIBLE LIGHT DRIVEN PHOTOCATALYTIC REMOVAL OF U(VI) FROM AQUEOUS SOLUTIONS

Peng Wu⁽¹⁾, Xiaoyu Yin⁽¹⁾, Yufan Zhao⁽¹⁾, Feize Li⁽¹⁾, Jiali Liao^{(1)*}, Yuanyou Yang⁽¹⁾,
Ning Liu⁽¹⁾, Tu Lan^{(1)*}

(1) Key Laboratory of Radiation Physics and Technology of the Ministry of Education, Institute of Nuclear Science and Technology, Sichuan University, Chengdu, P. R. China

In the context of carbon neutrality and the worsening international energy crisis, nuclear power will become an important part of basic energy in the future with its advantages of high efficiency, low pollution, and environmental friendliness [1]. Uranium is the primary nuclear fuel used in nuclear power plants today, but radioactive wastewater is unavoidably produced in the process of uranium mining [2]. As a result, enrichment and recovery of uranium from uranium-containing radioactive wastewater is critical for the long-term development of nuclear energy and environmental protection. Many methods have been used to remove U(VI) from aqueous solutions, such as adsorption, ion exchange, membrane separation, photocatalysis. Among them, photocatalysis is considered to be one of the most promising separation methods using visible light to generate electrons on the catalyst surface to reduce the soluble U(VI) to the insoluble U(IV) deposits.

Hydrogen-bonded organic frameworks (HOFs) are a kind of frame materials formed by the intermolecular hydrogen bonds of organic building units [3]. Compared with other organic framework materials including covalent organic frameworks (COFs) and metal organic frameworks (MOFs), HOFs have mild synthesis condition, high crystallinity, good chemical and thermal stability, and ease of repair and regeneration [4]. Porphyrin is an 18 π electron conjugated system with excellent charge transfer and photostability [5]. Using porphyrin as organic framework units for hydrogen bonding not only retains its excellent photochemical properties but also has the advantages of HOFs such as rich pore structure, chemical stability, and ease of regeneration and reuse. Unfortunately, to our knowledge, the studies on porphyrin-based HOFs mainly are focused on the photocatalytic CO₂ reduction and antimicrobial applications [6], and there is so far no report on the field of radioactive wastewater treatment.

Motivated by this, three porphyrins with different functional groups (COOH-porphyrin, CN-porphyrin, and DAT-porphyrin) were prepared and their photoelectric properties were studied. The UV-Vis diffuse reflectance spectroscopy (DRS) shows that DAT-porphyrin has a broad absorption boundary and more visible light can be utilized. The electrochemical impedance spectroscopy (EIS) shows that DAT-porphyrins has a lower resistance and a higher internal electron transmission efficiency, which is beneficial to the separation and transfer of $e^- - h^+$ pairs. Mott-Schottky results show that DAT-porphyrins has a higher conductivity and a greater charge carrier density, which will be favorable to the reduction of U(VI). The transient photocurrent response shows that DAT-porphyrin has better electron transfer ability and photogenerated charge utilization. Furthermore, DAT-porphyrin can self-assemble into a structurally stable crystalline porous HOF material (UPC-H4a), and its surface morphology is shown in Figure 1a. Clearly, UPC-H4a presents an uneven stick-like structure, and some apertures are distributed on the surface. The effects of pH, catalyst dosage, sacrificial agents, initial U(VI) concentration, and coexisting ions on the photocatalytic reduction of U(VI) by UPC-H4a were further investigated. The experimental results show that after illumination for 120 min, the removal rate of U(IV) by UPC-H4a can reach 98.55%, and its kinetic rate constant is 0.0323 min⁻¹. UPC-H4a has a high selectivity for the removal of U(VI) in the presence of the coexisting non-oxidizing competing cations. After 5 repeated utilization experiments, the photocatalytic removal rate of U(VI) by UPC-H4a can still reach 83.29%, suggesting an excellent reusability of UPC-H4a for photocatalysis. XPS analysis indicates that the most soluble U(VI) were photocatalytically reduced to the insoluble U(IV) by UPC-H4a (Figure 1b). In order to explore deeply the photocatalytic reduction mechanism, electron paramagnetic resonance (EPR) test was performed to determine the generated radicals during photoreduction process. As shown in Figure 1c, no EPR signals of $\cdot\text{O}_2^-$ and $\cdot\text{OH}$ radicals were detected under dark condition. When illuminated with visible light for 20 min,

both $\cdot\text{OH}^-$ and $\cdot\text{O}_2^-$ radicals were produced by UPC-H4a. After adding the radical scavenger P-BQ, the photoreduction of U(VI) was significantly affected (Figure 1d), indicating that the radical of $\cdot\text{O}_2^-$ is a critical participant in U(VI) photoreduction by UPC-H4a.

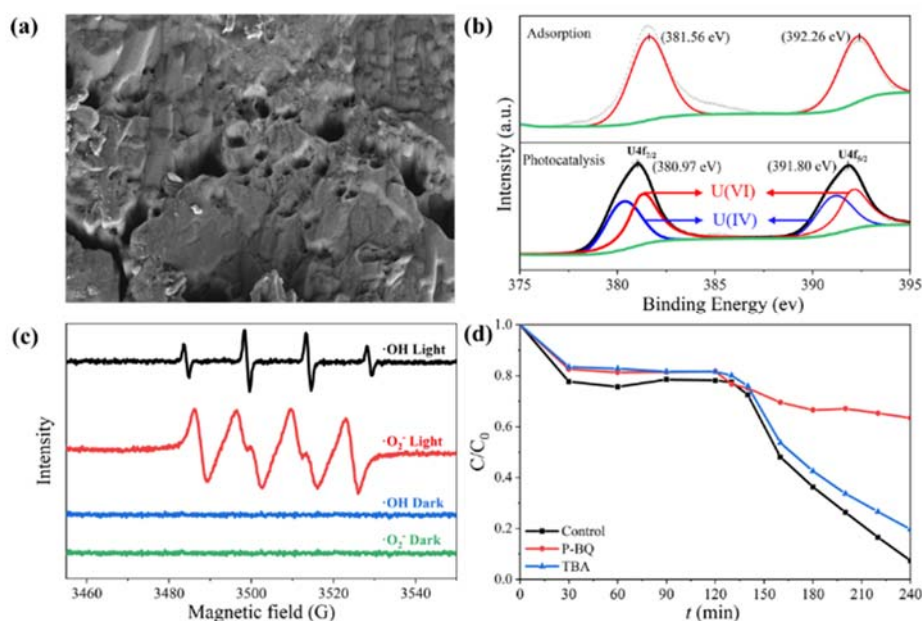


Figure 1. (a) SEM image of UPC-H4a, (b) XPS spectra of U4f before and after photocatalysis, (c) EPR spectra of radical adducts trapped by DMPO ($\cdot\text{O}_2^-$ and $\cdot\text{OH}^-$) in UPC-H4a, and (d) effect of radical scavengers on the photocatalytic removal of U(VI) by UPC-H4a.

Acknowledgments: Financial support from the National Natural Science Foundation of China (22106111) and the Natural Science Foundation of Sichuan Province (2022NSFSC0239) is gratefully acknowledged.

References

- [1] Wang, J. and Li, P. (2022) New strategy for the persistent photocatalytic reduction of U(VI): Utilization and storage of solar energy in K^+ and cyano Co-decorated poly(heptazine imide). *Adv. Sci.* 10: 2205542.
- [2] Chen, L. and Gao, Y. (2023) Efficient photoreduction removal of uranium(VI) by O, K co-doped $\text{g-C}_3\text{N}_4$ under air atmosphere without sacrificial agents. *Sep. Purif. Technol.* 307: 122873.
- [3] Nandi, S. and Chakraborty, D. (2016) A permanently porous single molecule H-bonded organic framework for selective CO_2 capture. *Chem. Commun.* 52: 7249-7252.
- [4] Han, Y. and Zhang, T. (2021) Guest-regulated luminescence and force-stimuli response of a hydrogen-bonded organic framework. *ACS Appl. Mater. Interfaces* 13: 32270-32277.
- [5] Chen, L. and Chen, B. (2022) The synthesis of a novel conjugated microporous polymer and application on photocatalytic removal of uranium(VI) from wastewater under visible light. *Chem. Eng. J.* 431: 133222.
- [6] Yin, Q. and Alexandrov, E. V. (2022) Metallization-prompted robust porphyrin-based hydrogen-bonded organic frameworks for photocatalytic CO_2 reduction. *Angew. Chem. Int. Ed.* 61: e202115854.

PA4-6 EXCITON DISSOCIATION AND TRANSFER BEHAVIOR AND SURFACE REACTION MECHANISM IN DONOR-ACCEPTOR ORGANIC SEMICONDUCTOR PHOTOCATALYTIC SEPARATION OF URANIUM

Zhimin Dong, Zifan Li, Cheng Meng⁽¹⁾, Zhibin Zhang*, Yunhai Liu⁽¹⁾

(1) State Key Laboratory of Nuclear Resources and Environment, East China University of Technology, Nanchang, Jiangxi 330013, P.R. China

Utilizing photocatalysis technology to convert U(VI) into insoluble uranium precipitation has become an effective method for separating U(VI) from radioactive uranium-containing wastewater. g-C₃N₄ has been gaining increasing attention due to its advantages of easy preparation, non-pollution, and responsiveness to light. However, g-C₃N₄ commonly suffer from the major constraints of carriers recombination and low utilization of visible light, which is mainly ascribed to its low specific surface area.

To address these issues, the hollow tubular g-C₃N₄ (TCN) composed of with enlarged specific surface area, better hydrophilicity and visible light response were developed. Moreover, a donor-acceptor (D-A) system was successfully constructed by molecular modification to further improve the electronic separation rate of TCN, which enhanced photocatalytic separation activity of U(VI). This work mainly focusses on the preparation of D-A photocatalyst based on hollow TCN and its application in photocatalytic separation of U(VI). Furthermore, the photocatalysis reaction mechanism was discussed in detail, which will provide insights and guidance for further understanding the effect of excitation and dissociation process of electrons on photocatalytic separation of uranium. The specific research contents of this work are as follows:

(1) Hollow TCN was successfully constructed by molecular self-assembly strategy, then 2,7-dibromocarbamole (Dbc) was introduced into the framework of TCN through post-grafting to construct D-A system. This unique hollow structure endowed TCN greatly advantages of abundant active sites for the reaction and enhanced visible light absorption capability. In D-A system, Dbc and TCN separately acted as the electron donor and electron acceptor to improve the separation rate of electrons. Therefore, the removal rate of U(VI) by 0.03Dbc/TCN in 120 min reached up to 96.4% that was 1.85 times than that of TCN. The results of mechanism research demonstrated that U(VI) precipitated from the solution in the form of (UO₂)O₂•2H₂O under air atmosphere, and H₂O₂ and photogenerated electrons played a crucial role in the photocatalytic process.

(2) Sodium alginate and melamine were used as raw materials, and the carbon ring was successfully introduced into the skeleton structure of TCN by hydrothermal and high-temperature calcination. The intramolecular D-A system was constructed and used to separate U(VI) from solution. The introduction of carbon ring endowed g-C₃N₄ with unique hollow hexagonal tubular shape, which would adjust the electronic excitation model of g-C₃N₄ and reduce the energy of exciton dissociation to promote the adsorption and activation of O₂. In addition, D-A photocatalyst exhibited high photocatalytic separation efficiency of U(VI) under the interference of LED light and various anions and cations. The influence of H₂O₂ in the reaction process and the mechanism of interaction with uranyl ions were deeply explored. Notably, we put forward a new theory namely photocatalytic induced uranyl coordination reaction, which can well explain many extraordinary experimental phenomena. The formation rate and pathway of crystal nucleus are the most critical steps of photocatalytic uranium separation surface reaction.

To sum up, this study explored the preparation of D-A photocatalyst based on hollow tubular g-C₃N₄ in the application of photocatalytic separation of U(VI). The clear structure-activity relationship provides valuable input for efficient treatment and recovery uranium by well-designed photocatalysts to simultaneously address environmental contamination and uranium resource crisis, which is conducive to the development of clean and renewable nuclear energy.

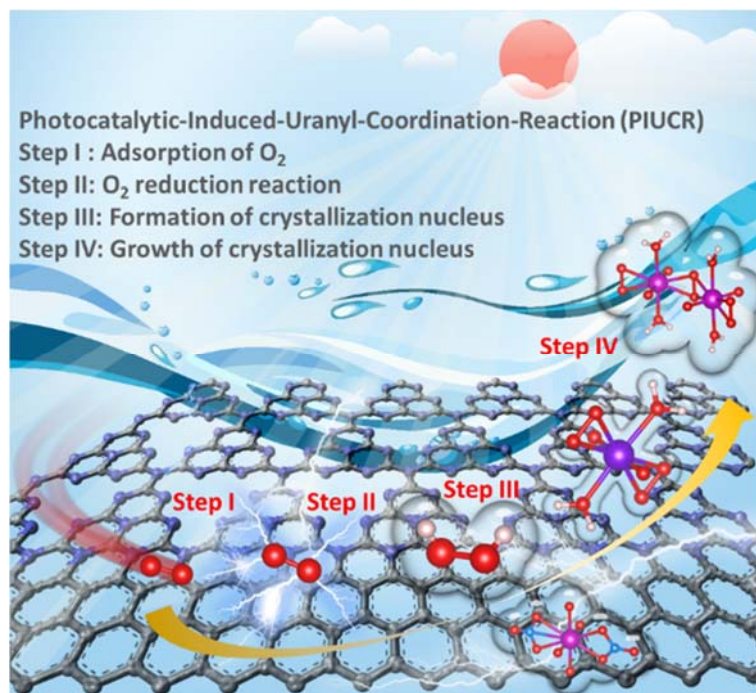


Figure 1: Schematic of possible mechanistic pathway for the photoinduced reduction of U(VI) by g-C₃N₄ based D-A photocatalysts.

PA4-7 SELENIUM REACTIONS IN FERROUS AND SULFIDE-RICH ENVIRONMENTS: EFFECTS OF SULFIDE SPECIATION

Paul Clarence Francisco ⁽¹⁾, Takamitsu Ishidera ⁽¹⁾, Hideaki Shiwaku ⁽²⁾, Ryosuke Kikuchi ⁽³⁾, Daiju Matsumura ⁽²⁾, Yukio Tachi ⁽¹⁾

(1) Nuclear Fuel Cycle Engineering Laboratories, Japan Atomic Energy Agency, Japan

(2) Materials Sciences Research Center, Japan Atomic Energy Agency, Japan

(3) Faculty of Engineering, Hokkaido University, Japan

As a long-lived fission product, Se-79 is predicted to account for a significant proportion of radioactivity long after the closure of a geological repository for high-level wastes. Predicting its behavior for long-term safety assessment of repositories thus requires a detailed understanding of its reactions with various geological repository components. Interaction with ferrous and sulfide aqueous species and solid phases could help attenuate Se concentrations under anoxic and reducing conditions in repositories. Many previous experimental studies of Se sequestration by iron sulfides involved coprecipitation with HS⁻, resulting in the incorporation of Se within the lattice of the iron monosulfide mackinawite (FeS), a fast-forming but metastable phase [e.g. 1]. However, it is possible that in deep sedimentary formations that are likely to host geological repositories, a broader array of sulfide species may be present; processes like the reaction of monosulfides with elemental sulfur, or the partial reoxidation (chemical/microbial) of monosulfides may generate intermediate sulfide species like polysulfides [2]. Thus far, the role of polysulfides in Se immobilization and retention has not been clarified. Polysulfides may play a potentially important role in the long-term retention of Se in pyrite, which has been identified as a thermodynamically stable sink for Se in both experiments and studies of natural samples [3, 4]. Because pyrite contains a disulfide anion chain in its structure, polysulfides are likely involved in their formation [5].

In this work, we investigate the role of sulfide speciation in the immobilization of Se. We performed four sets of coprecipitation experiments where Se(-II) was reacted with aqueous Fe(II) and with either monosulfides or polysulfides, at Fe/S ratios of 1 and 0.5. The precipitates were aged under anoxic conditions at ~25°C for up to 5 months. The solid phase was characterized with XRD, Se K-edge XANES and EXAFS, and (S)TEM to examine bulk solid phase composition, Se speciation and local environment, and particle morphology, respectively. Se concentrations in the aqueous phase were determined using ICP-MS. Our goal is to clarify the behavior and speciation of Se resulting from interaction with different sulfide species and how they change over time.

The monosulfide coprecipitation experiments efficiently sequestered Se(-II) from solutions and produced mackinawite (Fig. 1). XANES analyses showed that it retained its -II oxidation state throughout the 5 month aging period, and EXAFS fitting results were consistent with Se being incorporated in the mackinawite lattice. The absence of meaningful changes over 5 months suggests that Se retention in mackinawite was stable. Uptake was similarly efficient in the polysulfide experiments, though lesser Se was sequestered than in the monosulfide experiments (Fig. 1A). The reaction products were predominantly amorphous; but in the experiment at Fe/S 1, pyrite formed after aging for 5 months (Fig. 1B). Unlike in the monosulfide experiments, Se was initially oxidized and precipitated as elemental Se(0). Aging did not alter the speciation of Se in the experiment at Fe/S 0.5. On the other hand, aging drastically altered Se local environment in the experiment at Fe/S 1, with EXAFS indicating that Se became incorporated into the structure of pyrite (Fig. 2). Despite the very low abundance of pyrite, it was clear that it hosted most of the Se.

In summary, monosulfide coprecipitation sequesters and retains Se in mackinawite, while reaction with polysulfides sequesters Se first as Se(0), then incorporates it in pyrite. Because sulfide speciation is tied to redox conditions, the results provide fundamental insights into the processes governing Se retention across

a broad range of redox environments, which may aid in predicting Se migration behavior in geological repositories.

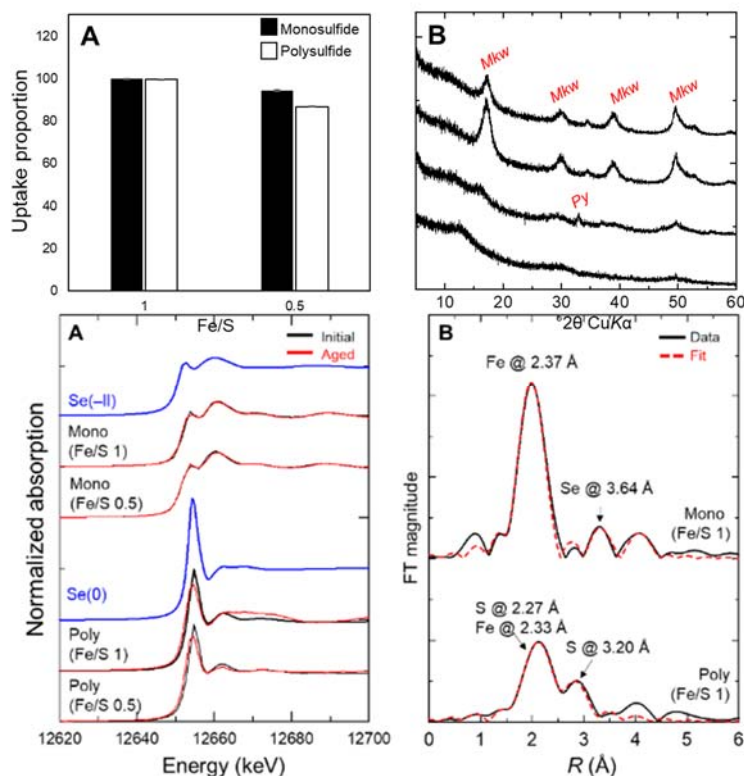


Figure 1. (A) Se uptake proportion after aging for 5 months. (B) XRD patterns of coprecipitates aged for 5 months.

Figure 2. (A) Se K-edge XANES of initial and aged samples. (B) EXAFS FTs of aged monosulfide and polysulfide coprecipitation solids at Fe/S 1.

Acknowledgements: This work was part of “The project for validating near-field assessment methodology in geological disposal (FY2022, JPJ007597)” supported by the Ministry of Economy, Trade and Industry of Japan. Synchrotron experiments were performed at BL22XU (2021B3719, 2022B3719) and BL14B1 of SPring-8, Japan.

References

- [1] Finck, N. and Dardenne, K. (2016). Interaction of selenite with reduced Fe and/or S species: An XRD and XAS study. *J. Contaminant Hydrol.* 188: 44-51.
- [2] Diener, A., Neumann, T., Kramar, U. and Schild D. (2012) Structure of selenium incorporated in pyrite and mackinawite as determined by XAFS analyses. *J. Contaminant Hydrol.* 133: 30-39.
- [3] Matamoros-Veloza, A., Peacock, C.L. and Benning, L.G. (2014) Selenium speciation in framboidal and euhedral pyrites in shales. *Environ. Sci. Technol.* 48: 8972-8979.
- [4] Vairavamurthy M.A., Orr, W.L. and Manowitz, B. (1995) *Geochemical Transformations of Sedimentary Sulfur*. American Chemical Society.
- [5] Rickard, D. and Luther, G.W. III. (2007) Chemistry of iron sulfides. *Chem. Rev.* 107, 514-562.

PA4-8 INSIGHTS INTO THE URANIUM ENRICHMENT MECHANISM ON MINERALS CONTAINING FE(II) IN DEEP GEOLOGICAL REPOSITORIES

Xiaolan Zhao⁽¹⁾, Duoqiang Pan⁽¹⁾, Wangsuo Wu⁽¹⁾

(1) School of Nuclear Science and Technology (Lanzhou University), No. 222 South Tianshui Road, Lanzhou 730000, Gansu Province, P. R. China

Deep geological repositories are an option for the disposal of radioactive waste, and granite is considered one of the best options for the geological disposal of the reservoir envelope due to its characteristics of being hard, dense, impermeable, and stable. Previous researches have shown that radionuclides such as Cs, U, Eu, and Se are not evenly distributed on granite, with higher concentrations typically found on biotite [1]. Biotite, a Fe(II)-rich phyllosilicate (ideally $K(Mg, Fe)_3(AlSi_3O_{10})(OH, F)_2$), has been identified as a dominant sorbent for radionuclides in granitic terrains and has been proposed as a potential material for radionuclide waste disposal [2]. Pyrite (FeS_2) is indeed widespread and abundant mineral and occurs in a variety of geological settings including granite and claystone. In geological repositories, pyrite can play an important role in controlling the redox potential of the system. The presence of even small amounts of pyrite (~1 wt %) can help to maintain a reducing environment, which can help to prevent the migration of certain contaminants such as uranium or technetium [3].

Uranium is a redox-sensitive element that can exist in different oxidation states, and its mobility is largely controlled by these states [2-3]. The migration of uranium in the geosphere is a complex process. Therefore, it is necessary to investigate the adsorption behavior and mechanisms of U(VI) on biotite and pyrite to better understand the performance of uranium repositories or to develop remediation strategies for contaminated sites.

The adsorption mechanisms of U(VI) on biotite interface were investigated with batch experiments, X-ray photoelectron spectroscopy (XPS), and transmission electron microscopy (TEM). The batch experiments revealed that the adsorption of U(VI) on biotite was obviously affected by the various environmental factors including pH, initial concentration, ion strength, alkali cations, anions, and nature organism material. Under the lower pH, the adsorption was increased with increasing pH. While under the higher pH, the adsorption was inhibited. This is mainly due to the hydrolysis of U(VI). Within the pH range of 4-7, U(VI) gradually undergoes hydrolysis, primarily existing in the forms of $UO_2(OH)^+$ and $UO_2(OH)_2$. At $pH > 7$, $UO_2(OH_3)^-$ is the main form. At low pH, ion strength revealed no significant effect on the adsorption, indicating that the adsorption of U(VI) on the surface of biotite was mainly controlled by inner-sphere complexation. Adsorption was inhibited at high pH with the effect of ion strength. Different cations showed no significant effect on the adsorption of U(VI). Among different anions, the effect of PO_4^{3-} on the adsorption of U(VI) was significant because PO_4^{3-} had a strong complexation with U(VI). On the one hand, the phosphate group attached to the biotite surface further interacts with U(VI) to form a ternary complex, promoting adsorption. On the other hand, the interaction of phosphate with U(VI) led to surface precipitation and promoted adsorption. The effects of other anions such as SO_4^{2-} , Cl^- , and NO_3^- were relatively negligible. Humic acid (HA) had a significant effect on the adsorption of U(VI). It promoted adsorption at low pH and inhibited adsorption at high pH. In addition, the greater the concentration of HA, the more pronounced the promoting and inhibiting effects. The results of XPS and TEM confirmed that, due to the relatively high iron content in biotite, some U(VI) can be reduced by Fe(II) in the biotite structure, forming U(V)/U(IV) mineral products or nanoclusters on the surface of biotite.

The enrichment mechanism of U(VI) on the pyrite facet as a function of pH, coexisting anion, and contact time were studied with or without oxygen. In addition, the dissolution of pyrite was also explored. The results indicated that the enrichment of U(VI) was significantly affected by pH. Under the acidic conditions, U(VI) was reduced to UO_2 and enriched on the pyrite facet. Above pH 5.5, inner-sphere complexation and precipitates were the primary enrichment mechanisms. Cl^- and HCO_3^- ions are easy to form complex ions

with U(VI) as ligands. These complex ions have stronger solubility and require more and stronger reducing agents to react with them. The effect of contact time on U(VI) enrichment mainly occurred under acidic conditions. With the increase of contact time, the enrichment of U(VI) on the surface of pyrite under acidic conditions decreased, mainly because of the hydroxyl radicals which were generated on the surface of pyrite. Under the ambient condition, the reduction of U(VI) was reduced due to the pyrite was oxidized by the oxygen. The dissolution of pyrite is mainly controlled by pH, which mainly occurred in acidic conditions. The existence of oxygen and U(VI) also affected its dissolution.

The above findings are expected to define U(VI) reactivity and fate with reduced mineral phases and explore the potential for transformation of the oxic mobile U(VI) to reduced, less soluble forms in deep geological repositories. It could also be significant to benefit the assessment of the migration and transform behaviors of U(VI) in deep geological repositories.

References

- [1] Yang, X., Ge, X., He, J., et al. (2017). Effects of Mineral Compositions on Matrix Diffusion and Sorption of ⁷⁵Se(IV) in Granite. *Environ. Sci. Technol.* 52(3): 1320-1329.
- [2] Brookshaw, D.R., Patrick, R.A.D., Bots, P., et al. (2015) Redox Interaction of Tc(VII), U(VI), and Np(V) with Microbially Reduced Biotite and Chlorite. *Environ. Sci. Technol.* 49: 13139-13148.
- [3] Yang, Z.W., Kang, M.L., Ma, B., et al. (2014) Inhibition of U(VI) Reduction by Synthetic and Natural Pyrite. *Environ. Sci. Technol.* 48: 10716-10724.

PA5-1 SORPTION BEHAVIOR OF SELENITE ON CLAY MINERAL SURFACES IN THE PRESENCE OF AQUATIC FULVIC ACID

Hyeonjin Eun⁽¹⁾, Seonggyu Choi⁽²⁾, Jong-Il Yun⁽¹⁾

(1) Department of Nuclear and Quantum Engineering, Korea Advanced Institute of Science and Technology (KAIST), Daejeon 34141, Republic of Korea

(2) Disposal Performance Demonstration Research Division, Korea Atomic Energy Research Institute (KAERI), Daejeon 34057, Republic of Korea

The sorption behavior of Se(IV) on kaolinite (KGa-2b) and montmorillonite (STx-1b) was investigated in the presence of aquatic fulvic acid. The clay minerals are generally considered to be the major components of both the engineered and natural barriers in radioactive waste disposal facilities. Besides, since natural organic matters being ubiquitous in natural waters tend to strongly bind to the clay minerals, it is essential to examine and understand their geochemical impacts on the radionuclide retention capacity of mineral adsorbents, particularly for anionic Se(IV) species [1,2]. However, since the natural organic matters have highly intricate and heterogeneous structures, elucidating the molecular mechanisms regarding the chemical effects of the organic compounds on the migration of Se(IV) in natural waters is a challenge and has been studied as a longstanding goal in the field of environmental science [3,4].

The Suwannee River fulvic acid (standard batch III) and reference clay minerals were obtained from the International Humic Substances Society (IHSS) and the Clay Minerals Society, respectively. All suspension analytes were pre-equilibrated for 4 days under ambient atmosphere, and the batch sorption experiments were then performed for 7 days using a horizontal mixer at room temperature ($23.8 \pm 0.5^\circ\text{C}$) and at a solid/liquid ratio (S/L) = 5 g/L in I = 0.1 M NaCl. The remaining amounts of Se(IV) and fulvic acid in the supernatants after the sorption experiments were measured by inductively coupled plasma–mass spectrometry (ICP-MS) and total organic carbon (TOC) analysis, respectively. Attenuated total reflectance–Fourier transform infrared spectroscopy (ATR-FTIR) was also utilized to identify the formation of chemical bonds between selenite and fulvic acid species in the present aqueous system.

As a result, it was verified that fulvic acid strongly binds to kaolinite and montmorillonite in both acidic and alkaline conditions. Its distribution coefficients were found to be 7.4×10^4 L/kg at pH 3.2 and 3.6×10^4 L/kg at pH 7.5 for kaolinite and 4.9×10^4 L/kg at pH 3.2 and 2.0×10^4 L/kg at pH 7.5 for montmorillonite. Since fulvic acid extensively covers the surface of clay minerals, selenite anions can chemically interact with not only the bare mineral surficial functionalities but also the carboxyl groups of sorbed fulvic acid species. Fig. 1 shows the ATR-FTIR spectra of aqueous phases separated from fulvic acid-Se(IV)-kaolinite suspensions at pH 4.5 and pH 10. At pH 4.5, no clear bond between fulvic acid and selenite anion was observed, whereas a new absorption peak at 721 cm^{-1} was observed at pH 10, indicating the formation of a hydrogen bond between the organic compound's carboxylic group and selenite [3]. The chemical sorption of Se(IV) onto clay minerals can be enhanced in the presence of fulvic acid species under alkaline conditions.

In general, humic substances are thought to reduce the sorption of anionic radionuclides in the geosphere because they compete with anionic species on the surface of natural minerals. However, it was first scrutinized in this study that the retention of Se(IV) onto the clay minerals can be noticeably enhanced by fulvic acid under alkaline conditions as they form a stable selenite-fulvic acid-mineral surface species, while such a tendency was not observed under acidic conditions.

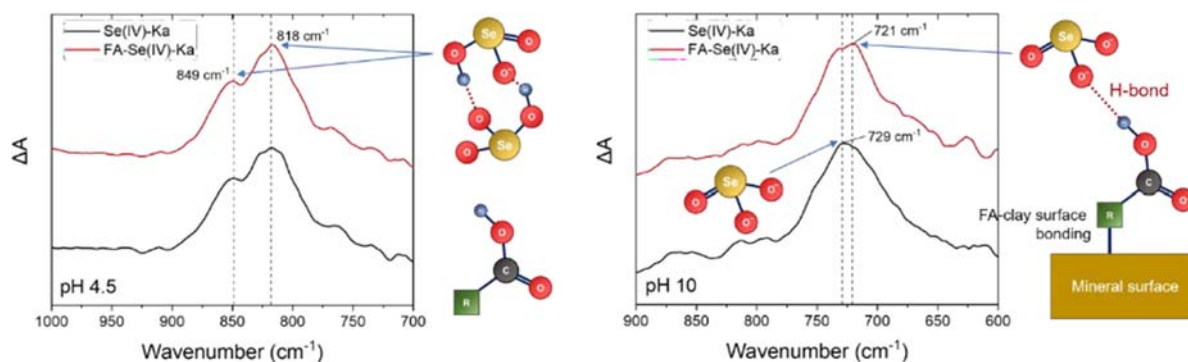


Figure 1: ATR-FTIR spectra of supernatants separated from the fulvic acid-Se(IV)-kaolinite suspensions at pH 4.5 (left) and pH 10 (right) (0.1 M Na₂SeO₃, 0.01 wt% fulvic acid).

References

- [1] Yamada, H., Kang, Y., Aso, T., Uesugi, H., Fujimura, T., Yonebayashi, K. (1998). Chemical forms and stability of selenium in soil. *Soil Sci. Plant Nutr.* 44: 385-391
- [2] Mayer, L. M., Xing, B. (2001). Organic matter – Surface area relationships in acid soils. *Soil Sci. Soc. Am. J.* 65: 250-258
- [3] Geng, R., Wang, W., Din, Z., Luo, D., He, B., Zhang, W., Liang, J., Li, P., and Fan, Q. (2020). Exploring sorption behaviors of Se(IV) and Se(VI) on Beishan granite: Batch, ATR-FTIR, and XPS investigations. *J. Mol. Liq.* 309: 113029
- [4] Masset, S., Monteil-Rivera, F., Dupont, L., Dumonceau, J., Aplincourt, M. (2000). Influence of humic acid on sorption of Co(II), Sr(II), and Se(IV) on goethite. *Agronomie*: 525-535

PA5-2 APPLICATION OF METAL IONS DOPED HYDROXYAPATITE IN URANIUM ADSORPTION

Youqun Wang⁽¹⁾, Lei Chen⁽²⁾, Yunhai Liu^{(1),(2)}

(1) Engineering Research Center of Nuclear Technology Application (East China University of Technology), Jiangxi, 330013, China

(2) State Key Laboratory of Nuclear Resources and Environment, East China University of Technology, Nanchang, Jiangxi, 330013, China

In the 21st century, the demand for energy has increased dramatically and nuclear energy has developed and utilized, but the process of mining, conversion and processing of nuclear energy inevitably produces large quantities of radioactive uranium-containing waste liquids[1]. This not only leads to a waste of uranium resources, but also causes irreparable damage to the natural environment. The efficient removal, separation and enrichment of uranium from waste streams is therefore a major focus of current research in the field of environmental radiochemistry[2]. Hydroxyapatite (HAP) was considered as an environmentally friendly and efficient adsorbent for the removal of heavy metal ions from aqueous solutions due to its wide range of sources, low solubility, lack of secondary hazards and its good ion exchange properties and its ability to adsorb heavy metal ions. However, HAP has a unique ionic crystal structure with a hexagonal crystal system, and the calcium ions (Ca^{2+}) in its structure can be easily replaced by other cations (Ag^+ , Zn^{2+} , Se^{2+} , etc.) through a surface ion exchange mechanism. In this way, HAP materials are endowed with new functions, expanding their applications in various fields such as biomedical, dental and purification systems. Szenknect et al [3] synthesized Cu-Hap by replacing Ca^{2+} in hydroxyapatite with Cu^{2+} , which reduced the crystallinity of HAP, increased the specific surface area and improved its efficiency in the removal of uranium. Meanwhile, Zhou et al [4] doped Sr into HAP and experimentally showed that it could enhance its adsorption capacity for Cr(VI). These studies suggest that cation-doped HAP positively affects its adsorption function by increasing the specific surface area and decreasing the crystallinity of HAP. Moreover, HAP can be uniformly loaded on suitable carrier materials such as graphene, carbon nanotubes, MXene and polymeric materials, which will effectively prevent its agglomeration behaviour and improve its adsorption performance. Therefore, the use of an inexpensive carrier material with a simple preparation process and a large specific surface area is important to prevent the agglomeration behaviour of HAP and to increase the specific surface area. In this paper, hydroxyapatite (HAP-M, M=Cu, Sr, Al, Ce and Ti) doped with metal cations of different ionic radii was prepared by co-precipitation method and its adsorption performance on U(VI) was investigated by batch experiments. The results of the batch experiments showed that HAP-Sr exhibited good adsorption performance at pH=4 (Fig. 1), with faster adsorption rate (<30 min) and larger adsorption capacity ($865.80 \text{ mg}\cdot\text{g}^{-1}$) listed in Table 1, and its adsorption process of U(VI) was consistent with the quasi-secondary kinetic model, the intraparticle diffusion model and the Langmuir adsorption isotherm model, which is a spontaneous process of entropy-increasing heat absorption. Combining the experimental results with XRD, FT-IR and XPS characterisation, it could be seen that the effective removal of U(VI) by HAP-Sr is mainly due to the complexation of P-O and P=O in the phosphate group of the material and the ion exchange effect of HAP.

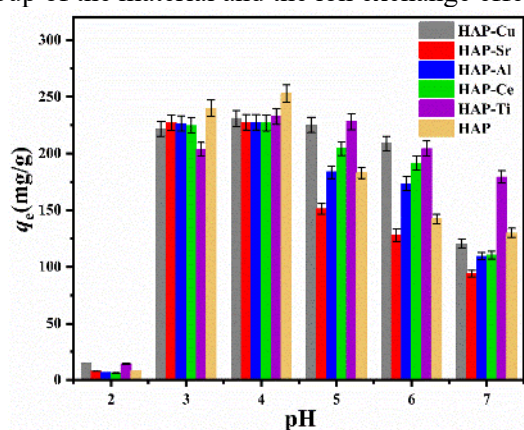


Figure 1: Effect of pH on U(VI) adsorption by HAP-M and HAP (m : 0.0100 g, V : 50 mL, C_0 : 50 $\text{mg}\cdot\text{L}^{-1}$, T : 298 K, t : 360 min)

Table 1 Parameters of Langmuir and Freundlich models for the adsorption of HAP-M and HAP

Adsorbents	Langmuir model			Freundlich model			Sips model		
	K_L	$q_m(\text{mg}\cdot\text{g}^{-1})$	R^2	K_F	n	R^2	K_S	$q_m(\text{mg}\cdot\text{g}^{-1})$	R^2
HAP-Cu	1.40	845.21	0.82	502.18	8.06	0.94	0.82	1089.24	0.97
HAP-Sr	3.83	646.57	0.81	362.34	7.41	0.97	0.55	865.80	0.99
HAP-Al	0.43	560.67	0.25	359.09	10.99	0.99	0.22	783.57	0.99
HAP-Ce	1.02	754.61	0.73	434.77	8.00	0.99	0.27	896.41	0.99
HAP-Ti	4.66	794.64	0.84	486.13	8.20	0.96	0.90	1086.51	0.98
HAP	2.51	613.23	0.82	325.06	6.99	0.97	0.36	850.36	0.98

References

- [1] Chen, L., Y. Wang, X. Cao, Z. Zhang, and Y. Liu, (2023). Effect of doping cation on the adsorption properties of hydroxyapatite to uranium, *J. Solid State Chem.* 317: 123687.
- [2] Zeng, D., Y. Dai, Z. Zhang, Y. Wang, X. Cao, and Y. Liu (2020) Magnetic solid-phase extraction of U(VI) in aqueous solution by Fe_3O_4 @hydroxyapatite, *J. Radioanal. Nucl. Chem.* 324(3): 1329-1337.
- [3] Szenknect, S., A. Mesbah, M. Descostes, A. Maihatchi-Ahamed, L. Bonato, M. Massonnet, Y. Ziouane, E. Vors, T. Vercoeur, and N. Clavier (2020). Uranium removal from mining water using Cu substituted hydroxyapatite, *J. Hazard. Mater.* 392: 122501.
- [4] Zhou, Y., W. Li, X. Jiang, Y. Sun, H. Yang, Q. Liu, Y. Cao, Y. Zhang, and H. Cheng (2021). Synthesis of strontium (Sr) doped hydroxyapatite (HAp) nanorods for enhanced adsorption of Cr (VI) ions from wastewater, *Ceram. Int.* 47(12): 16730-16736.

PA5-3 SORPTION OF EU(III) AND CM(III) ON C-S-H PHASES IN PRESENCE OF EDTA AT INTERMEDIATE IONIC STRENGTH CONDITIONS

A. K. Thumm⁽¹⁾, A. Skerencak-Frech⁽¹⁾, X. Gaona⁽¹⁾, M. Altmaier⁽¹⁾, H. Geckeis⁽¹⁾

⁽¹⁾ Institute for Nuclear Waste Disposal, Karlsruhe Institute of Technology, Karlsruhe, Germany

Storage in deep geological formations, within a multibarrier system, represents the preferred option for the final disposal of radioactive waste. In context of the Safety Case, long-term prediction of the migration of radionuclides is required.^[1] Intermediate ionic strength conditions ($I = 2 - 3$ M) are found in Cretaceous argillites in Northern Germany, with pore waters mostly dominated by NaCl and CaCl₂. Cementitious materials are ubiquitous in many disposal concepts for nuclear wastes, mainly for construction purposes and for the sealing of the excavated tunnels. In repositories for low and intermediate level (L/ILW), cementitious materials may be extensively used as waste packages, overpacks, backfill, as well as for the solidification and stabilization of the waste.^[2] Calcium-silicate-hydrate (C-S-H) phases are the main component in most cement-based materials, and provide strong sorption capacities for tri- and tetravalent actinides and lanthanides.^[3] EDTA is a chelating ligand present in L/ILW, which shows a very strong affinity for the complexation of metal ions.^[4] The impact of EDTA on the retention of An(III) by C-S-H phases is not yet fully understood. This work provides new experimental data for the uptake of Eu(III) and Cm(III) on C-S-H phases in the presence of EDTA in NaCl and CaCl₂ solutions with intermediate ionic strength. Eu(III) and Cm(III) are used as chemical analogues for trivalent actinides, e.g. Am(III) and Pu(III).

The study was performed by batch sorption experiments and Time Resolved Laser Fluorescence Spectroscopy (TRLFS) under argon atmosphere ($O_2 \sim 2$ ppm) at constant solid-to-liquid ratio of S:L = 1 g/L. The C-S-H phases were prepared according to L'Hôpital *et al.* NaCl and CaCl₂ were used as electrolyte solutions with $I_m = 1.02$ m. The calcium-to-silicon (C/S) ratio in the C-S-H phases was varied from 0.6 to 1.4 ($pH_m \sim 9.5 - 12.5$, with $pH_m = -\log [H^+]$). Batch sorption experiments and TRLFS measurements were performed with $[^{152}Eu]_{tot} = 2 \cdot 10^{-8}$ M and $[Cm]_{tot} = 1 \cdot 10^{-7}$ M, respectively. Different sorption times (7 – 90 d) were investigated at varying $[EDTA] = 10^{-6} - 10^{-2}$ m.

Log R_d values for the Eu(III) uptake on C-S-H phases in the absence and presence of [EDTA] in NaCl and CaCl₂ solutions are displayed in Figure 1 for C/S 1.1 at different contact times.

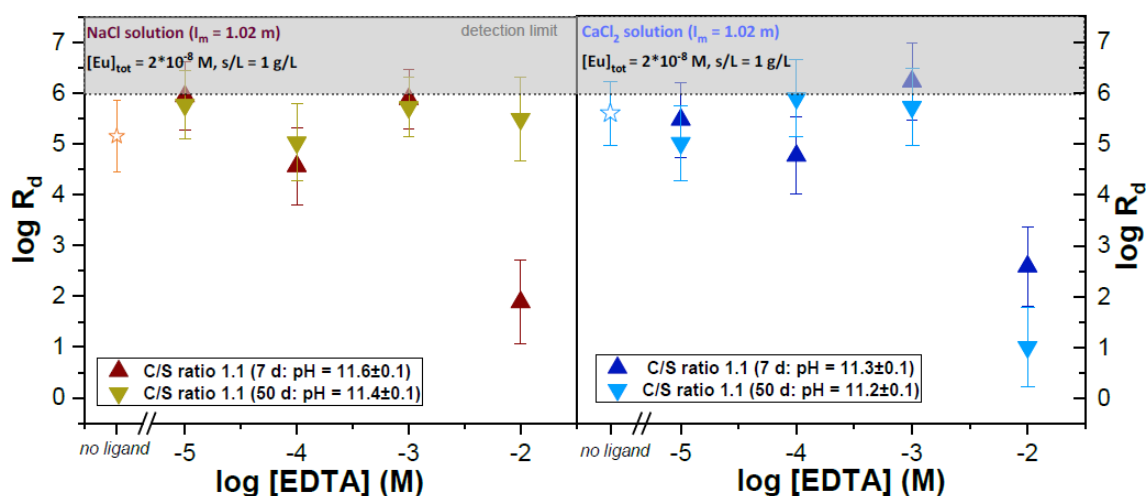


Figure 1: Distribution coefficients for the adsorption of Eu(III) on C-S-H phases (C/S = 1.1) in presence of $10^{-6} - 10^{-2}$ m EDTA in NaCl (left) and CaCl₂ (right) solutions at an ionic strength of 1.02 m after 7 and 50 d of sorption time. R_d values are reported in $[L \cdot kg^{-1}]$.

In both electrolyte solutions, at $[\text{EDTA}] \leq 10^{-3}$ M, very high $\log R_d$ values are detected in presence and absence of EDTA, indicating no significant effect of EDTA on the Eu(III) sorption at these low concentrations. In NaCl and CaCl₂ solutions, at $[\text{EDTA}] = 10^{-2}$ M, significantly decreased $\log R_d$ values are detected after 7 d of sorption time, which indicates a significant decrease in the sorption of Eu(III). After 50 d of sorption time, $\log R_d$ values rise significantly in NaCl solution, indicating again a very strong retention. Contrary, in CaCl₂ solution, the $\log R_d$ values remain low, which indicates a stabilization of Eu(III) in the aqueous phase. These observations suggest the possible stabilization of ternary Ca-Eu(III)-EDTA or quaternary Ca-Eu(III)-OH-EDTA complexes in CaCl₂ systems.

In both electrolyte solutions, at $[\text{EDTA}] \leq 10^{-3}$ M, TRLFS results showed that Cm(III) is completely incorporated into the C-S-H phase after all sorption times. Hence, at $[\text{EDTA}] \leq 10^{-3}$ M no significant effect of the organic ligand on the Eu(III) sorption is visible. In contrast to this, at $[\text{EDTA}] = 10^{-2}$ M and in NaCl solution, two ternary hydrolysis species, $\text{Cm}(\text{OH})(\text{EDTA})^{2-}$ and $\text{Cm}(\text{OH})_x(\text{EDTA})^{-(x+1)}$ are formed in solution after 7 d of sorption time. After longer contact times, again the incorporation species of Cm(III) into the C-S-H phase forms, resulting in the observed strong increase of the retention. TRLFS shows the possible formation of ternary Ca-Cm-EDTA or quaternary Ca-Cm-OH-EDTA complexes in CaCl₂ solution even after 50 d, thus resulting in the stabilization of Cm(III) in the aqueous phase. The formation of analogous complexes was recently reported by DiBlasi and co-workers in dilute NaCl systems containing Ca.^[5]

This work provides new insights for the quantitative and mechanistic description of An(III)/Ln(III) uptake by cementitious materials in the presence of EDTA at intermediate ionic strength conditions. Future studies will include the elucidation of the structure of Ca-Cm-EDTA. Moreover, longer contact times for TRLFS studies are planned.

Acknowledgements: *This work was funded by the German Federal Ministry for Economic Affairs and Energy (BMWi) under the contract number 02E11860C (GRaZ II).*

References:

- [1] H. Geckeis, K. J. Röhlig, K. Mengel, *Chemie in unserer Zeit* 2012, 5, 282-293.
- [2] M. L. Schlegel, I. Pointeau, N. Coreau, P. Reiller, *Environmental science & technology* 2004, 38, 4423-4431.
- [3] M. Ochs, D. Mallants, L. Wang, *Radionuclide and metal sorption on cement and concrete*, Vol. 2, Springer, 2016.
- [4] W. Hummel, F. J. Mompean, M. Illemassène, J. Perrone, *Chemical thermodynamics of compounds and complexes of U, Np, Pu, Am, Tc, Se, Ni and Zr with selected organic ligands*, Vol. 9, Elsevier Amsterdam, 2005.
- [5] N. A. DiBlasi, A. G. Tasi, M. Trumm, A. Schnurr, X. Gaona, D. Fellhauer, K. Dardenne, J. Rothe, D. T. Reed, A. E. Hixon, *RSC advances* 2022, 12, 9478-9493.

PA5-4 CONSTRUCTION AND APPLICATION OF AN ULTRAHIGHLY SELECTIVE PHOTOISOMERIC METAL-ORGANIC FRAMEWORKS MATERIAL FOR URANIUM EXTRACTION FROM SEAWATER

Pengcheng Zhang⁽¹⁾, Duoqiang Pan⁽¹⁾⁽²⁾, Wangsuo Wu⁽¹⁾⁽²⁾

(1) School of Nuclear Science and Technology, Lanzhou University, Lanzhou 730000, China

(2) Frontiers Science Center for Rare Isotopes, Lanzhou University, Lanzhou 730000, China

Nuclear power is viewed as playing a significant part in replacing coal-fired power generation under the notion of green chemistry because of its advantages for the environment, low fuel consumption, and high energy density. In addition, nuclear energy can offer a more consistent base load compared to renewable energy sources like wind and solar. Resources for uranium are essential to the nuclear industry, and it is obvious that the global distribution of uranium ores is characterized by low quality and an erratic geographic and temporal distribution. Despite the fact that numerous studies have shown that the total reserves of uranium in the ocean are nearly a thousand times larger than those in terrestrial deposits, however, due to the extremely low concentration of uranium per liter of seawater and the presence of a large number of interfering ions, which makes it challenging to implement this uranium extraction process in large-scale engineering applications. Solid phase extraction (SPE), a method for extracting uranium from seawater that was created using functionalized sorbent materials, is seen to be the most promising in this area, which has verified its engineering viability in several kinds of research. To further explore the commercial value of unconventional means of obtaining uranium resources represented by seawater extraction, the construction of new adsorbent materials that meet the technical specifications of high adsorption capacity, excellent acid and alkali resistance, stable material regeneration and remarkable ion selectivity will be an important research direction in this field in the future due to economic cost considerations.

Inspired by the phenomenon that fluorescent corals themselves modulate their internal proteins to achieve selective light absorption for survival, here we introduce a novel photoheterogeneous composite adsorbent material and discuss how it can be used for the study of uranium extraction from seawater. We inserted diarylethylene derivatives into the material substrate as photoswitch units to accomplish the composite material's ability to function photoheterogeneously. By manually switching the external irradiation light source, we can study the adsorption behavior of the photoisomeric material under the "open" and "close" behavior modes by utilizing the excellent photochemical stability and fatigue resistance before and after the isomerization of the thiophene ring inside the photoswitch monomer. In the selection of material substrate, MOFs are widely utilized in gas separation, photocatalysis, and drug delivery due to their high specific surface area, excellent porosity, and superior design ability. In addition to the benefits shared by all MOFs listed above, zeolite imidazolium ester skeletons (ZIFs), a significant member of the MOFs material family, have a heterogeneous linkage structure and are more diverse and selective in their pore distribution than other materials. ZIF-70 has the highest specific surface area of the series among the ZIFs that have been reported so far, which means that the adsorbent material employing it as the substrate would have an exceptional adsorption capability. Because ZIF-82 has cyano at the end of the imidazole structural unit, which can enhance uranium coordination through the process of approximation, it was chosen as a secondary substrate rather than ZIF-70 because it partially makes up for its lower specific surface area. By choosing the material matrix in this approach, we may better comprehend the crucial elements that influence how well adsorbent materials express their performance in the ternary system of "specific surface area - chelating coordination - photoisomerization regulation." In our investigation of adsorption behavior, we explained how the material's adsorption capacity changed before and after the grafting of the DAE photoswitch.

The experimental results demonstrated that the addition of the photoswitch unit significantly increased the material's affinity towards uranium, and the increment in the two materials' adsorption capacity reached 150 mg/g, which phenomenon can be attributed to the coordination process between the increased electron-rich structure inside the molecule and the emptier orbitals of metal ions in the solution system. In order to analyze the combination of gated ion rectification and adsorption experiments for mutual validation, we used a multi-physics field theoretical model. Based on this, we were able to obtain experimental data on the thermodynamic behavior of adsorption of photoheterostructured composites, the kinetic parameters of photoswitching based on the change of adsorption capacity, and the percentage of metal ion adsorption selectivity in the simulated seawater system. Based on the advantages of the material performance demonstrated in the above experiment, we applied the composite photoisomeric material to a natural seawater environment with high salinity and high background electrolyte, and investigated the adsorption capacity of the two materials in the "fully open" and "fully closed" states under a certain concentration gradient of spiked uranium. The data results have successfully confirmed that the material has the potential to precisely capture the uranium components in the practical application environment. This work also offers a significant concept for the development of functional adsorbent materials for the photoisomerization-based extraction of uranium from seawater.

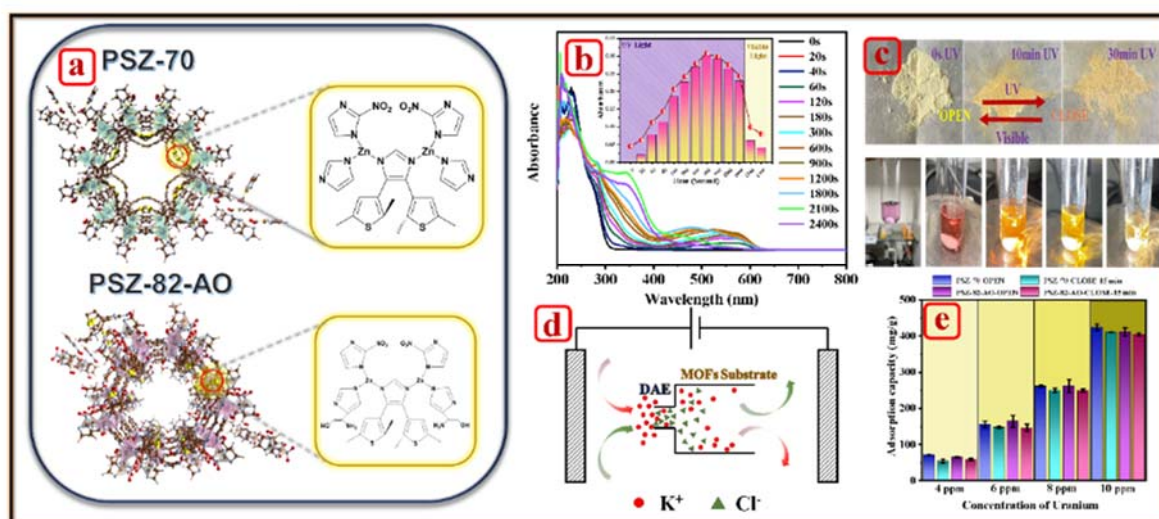


Figure a) Schematic diagram of the structure of composite photoisomeric materials **b)** DAE photoswitch monomer UV-Vis spectroscopy **c)** Variation of the apparent color of photoisomeric materials with time driven by different external irradiation sources **d)** Schematic diagram of simulated gated rectification model for composite photoheterostructured materials **e)** Study of U-spiked natural seawater system's adsorption behavior.

References

- [1] B.J. Furlong, M.J. Katz (2017). Bistable Dithienylethene-Based Metal–Organic Framework Illustrating Optically Induced Changes in Chemical. *J. Am. Chem. Soc.* 139: 13280-13283.
- [2] G. Cheng, A. Zhang, Z. Zhao, Z. Chai, X. Wang (2021). Extremely stable amidoxime functionalized covalent organic frameworks for uranium extraction from seawater with high efficiency and selectivity. *Science Bulletin.* 66: 1994-2001.
- [3] J. Wang, M. Zhang, J. Zhai, L. Jiang (2014). Theoretical simulation of the ion current rectification (ICR) in nano-pores based on the Poisson-Nernst-Planck (PNP) model. *Phys. Chem. Chem. Phys.* 16: 23-32.

PA5-5 TRIVALENT LANTHANIDES SORPTION ONTO ILLITE IN THE PRESENCE OF CARBONATE

Yuki Sugiura⁽¹⁾, Takamitsu Ishidera⁽¹⁾, Noboru Aoyagi⁽²⁾, Huiyang Mei⁽²⁾, Takumi Saito⁽³⁾, Yukio Tachi⁽¹⁾

(1) Nuclear Fuel Cycle Engineering Laboratories, Japan Atomic Energy Agency, Japan

(2) Advanced Science Research Center, Japan Atomic Energy Agency, Japan

(3) Nuclear Professional School, School of Engineering, The University of Tokyo, Japan

The sorption of radionuclides onto the components of engineered barriers and host rocks is one of the key phenomena in the safety assessment of geological disposal of radioactive waste. Dissolved inorganic carbon (DIC) in groundwater is considered to form carbonate complexes with actinide elements (An) and inhibit their sorption onto clay minerals [1]. Therefore, it is important to quantitatively evaluate the effect of DIC on its sorption behaviors. In this study, sorption experiments of trivalent lanthanide elements (Ln)—chemical analogs of trivalent An—onto illite in the presence of DIC were performed. The obtained sorption distribution coefficients (K_d) as a function of pH and DIC concentrations were interpreted using a thermodynamic sorption model. Additionally, time-resolved laser fluorescence spectroscopy (TRLFS) was performed to investigate the chemical form of Eu sorbed on illite. The TRLFS data were subjected to parallel factor analysis (PARAFAC) and compared with the predictions of the thermodynamic sorption model.

The experiments, except for instrumental analyses, were performed in a N₂-filled glove box. The illite was pretreated to remove impurities and replace exchangeable cations with Na⁺ [2]. Batch sorption experiments were performed as follows: the illite suspension, NaCl, and NaHCO₃/Na₂CO₃ solutions were mixed to a given concentration, then aliquots of a Eu or Sm stock solution were added to the suspension and allowed to react until sorption equilibrium was reached. After the reaction period, solid-liquid separation was performed by centrifugation, and the concentration of Eu or Sm in the supernatant was measured by inductively coupled plasma-mass spectrometry to calculate the K_d values. The obtained K_d values were modeled with the 2-site protolysis non-electrostatic surface complexation and cation exchange (2SPNE SC/CE) model [3]. Samples for TRLFS measurements were prepared in a similar way, but with higher initial Eu concentration than the batch experiments to obtain sufficient signal intensity; the solid phase was collected by centrifugation and dried. TRLFS measurements were performed by irradiating the samples with a 394-nm laser at room temperature. Fluorescence spectra were collected by a time-gated charge-coupled device camera. The data were smoothed and background subtracted, then arranged in a three-dimensional array (solution conditions × wavelength × time) and processed by PARAFAC using the *N*-way Toolbox for MATLAB [4].

Figure 1(A) shows the pH and DIC concentration dependence of K_d values of Eu/Sm onto illite. The K_d values decreased with increasing DIC concentration. In the presence of DIC, the K_d values decreased at pH 8–10 and increased at pH 10–11. Figure 1(B) shows the fitting results of the obtained K_d values with the 2SPNE SC/CE model. The K_d values at pH 10.5–11 are reproduced by the sorption of hydrolyzed Eu (hydroxide ternary complex). To reproduce the K_d values at pH 8–10.5, it was necessary to assume the sorption of carbonate-coordinated Eu (carbonate ternary complex). Figure 2 shows the fluorescence spectra, pH, and DIC concentration dependence of the relative intensities, and fluorescence decay profiles of the components derived from PARAFAC of the TRLFS data. Two components were found, and the ratio of the intensities of the peaks at 616 nm and 592 nm suggested that these components formed inner-sphere complexes with illite [5]. Component 2 was dominant at pH 8.5–11 in the absence of DIC, and its relative intensity increased from pH 10 to 11 in the presence of DIC. On the other hand, component 1 was dominant at pH 8–10 in the presence of DIC, and its relative intensity decreased with pH at pH >10. The pH and DIC concentration dependence of the relative intensities of components 1

and 2 were consistent with the trends of the carbonate ternary complexes and hydroxide ternary complexes predicted by the 2SPNE SC/CE model, respectively. The fluorescence lifetime ($T_{1/2}$) of component 1 was longer than that of component 2, which was attributed to the coordination of carbonate ions [6]. These results confirm that Eu sorbs onto illite, forming carbonate ternary complexes in the presence of DIC at pH 8–10.

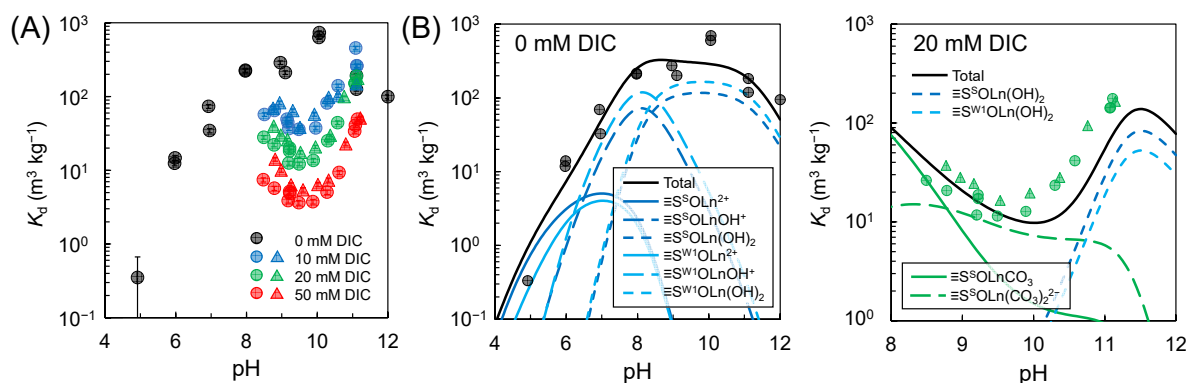


Fig. 1. (A) pH and DIC concentration dependence of K_d values of Eu(circle)/Sm(triangle) onto illite and (B) results of fitting the K_d values with the 2SPNE SC/CE model.

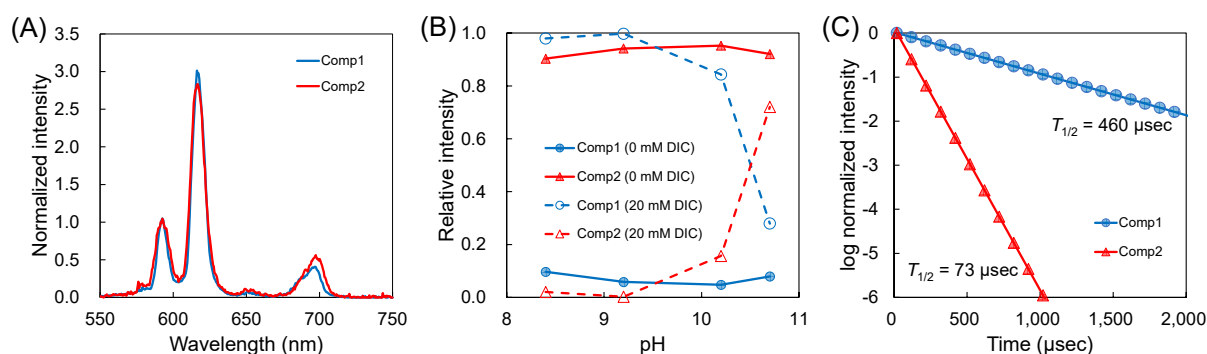


Fig. 2. (A) Fluorescence spectra, (B) pH and DIC concentration dependence of relative intensities, and (C) fluorescence decay profiles of components derived from PARAFAC analysis.

Acknowledgement: This work was part of “The project for validating near-field assessment methodology in geological disposal (FY2020-2022, JPY007597)” supported by the Ministry of Economy, Trade and Industry of Japan.

References

- [1] Marques Fernandes, M. et al. (2008). The influence of carbonate complexation on lanthanide/actinide sorption on montmorillonite. *Radiochim. Acta.* 96: 691–697.
- [2] Bradbury, M. H. and Baeyens, B. (2009). Sorption modeling on illite. Part I: Titration measurements and the sorption of Ni, Co, Eu and Sn. *Geochim. Cosmochim. Acta.* 73: 990–1003.
- [3] Bradbury, M. H. and Baeyens, B. (2009). Sorption modeling on illite. Part II: Actinide sorption and linear free energy relationships. *Geochim. Cosmochim. Acta.* 73: 1004–1013.
- [4] Andersson, C. A. and Bro, R. (2000). The *N*-way Toolbox for MATLAB. *Chem. Intell. Lab. Syst.* 52: 1–4.
- [5] Takahashi, Y. et al. (1998). Characterization of Eu(III) species sorbed on silica and montmorillonite by laser-induced fluorescence spectroscopy. *Radiochim. Acta.* 82: 227–232.

- [6] Stumpf, Th. et al. (2002). Inner-sphere, outer-sphere and ternary surface complexes: A TRLFS study of the sorption process of Eu(III) onto smectite and kaolinite. *Radiochim. Acta.* 90: 345–349.

PA5-6 URANIUM SORPTION ON OXYHYDROXIDE MINERALS BY SURFACE COMPLEXATION AND PRECIPITATION ^[1]Jingyi Wang, Chunli Liu,*Beijing National Laboratory for Molecular Sciences, Fundamental Science Laboratory on Radiochemistry & Radiation Chemistry, College of Chemistry and Molecular Engineering, Peking University, Beijing 100871, China*

Uranium could be released during the chemical weathering of the uranium mill tailings, and immobilized by the newly formed secondary minerals such as oxyhydroxides. This investigation aimed to elucidate the interaction between uranium and common oxyhydroxide minerals, such as Al-, Mn-, and Fe-oxyhydroxides (i.e., boehmite, manganite, goethite, and lepidocrocite), under relevant environmental conditions. Through batch experiments, we observed that the sorption behavior of uranium on these minerals exhibits significant disparities, with Al-oxyhydroxide demonstrating a distinct mechanism from the other minerals. Specifically, the sorption of uranium on boehmite primarily occurs via the precipitation of uranium-bearing carbonates and hydroxides, while the other minerals conform to the Langmuir model. The uranium sorption behavior is strongly influenced by the presence of carbonate and phosphate. Boehmite exhibits high uranium removal efficiency, exceeding 98% after three sorption-desorption cycles, highlighting its potential as a material for uranium recovery and removal.

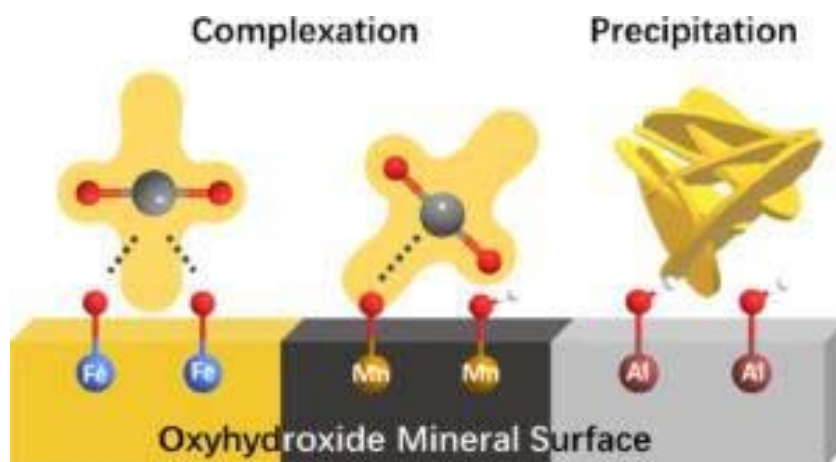


Figure 1: Interaction between uranium and oxyhydroxide mineral surface [1]

Reference

- [1] Wang, J., Zhou, W., Shi, Y., Li, Y., Xian, D., Guo, N., & Liu, C. (2022). Uranium sorption on oxyhydroxide minerals by surface complexation and precipitation. *Chinese Chemical Letters*, 33(7): 3461–3467.

PA5-7 EU(III) AND CM(III) COMPLEXATION BY NITRILOTRIACETIC ACID TO FURTHER EVALUATE ITS IMPACT ON THE RADIONUCLIDE RETENTION BY CEMENTITIOUS PHASES

Claudia Sieber⁽¹⁾, Jerome Kretzschmar⁽¹⁾, Björn Drobot⁽¹⁾, Satoru Tsushima⁽¹⁾, Katja Schmeide⁽¹⁾, Thorsten Stumpf⁽¹⁾

(1) Helmholtz-Zentrum Dresden – Rossendorf e.V., Institute of Resource Ecology, Germany

Aminopolycarboxylates (APCs) show great complexation potential towards (lanthanide and actinide) metal ions. As such they are often used as decontamination or decorporation agents. Especially trivalent actinides are of great interest, due to their prevalence in spent nuclear fuel. Accurate thermodynamic data on this complexation behavior is key for safety assessments of nuclear waste repositories. In a worst-case scenario – a groundwater intrusion into the repository a (re-)mobilization of radionuclides (RNs) is to be avoided. Low molecular weight organic ligands may however alter the retention potential of the repository relevant solid phases towards the RNs. A ligand of interest is nitrilotriacetic acid (NTA), which is a typical representative of the APCs. It has been previously shown that it forms complexes with trivalent RNs such as Eu(III)^[1] and Am(III)^[2] and is used as a decontaminating agent. This work focuses on Eu(III) as a nonradioactive analog to some trivalent actinides with outstanding luminescence properties which make it a great probe for time-resolved laser-induced fluorescence spectroscopy (TRLFS) study.

This work utilizes a multi-method approach with nuclear magnetic resonance (NMR) spectroscopy, TRLFS and isothermal titration calorimetry (ITC) to gain accurate and reliable thermodynamic and spectroscopic data on the Eu(III)-NTA system. NMR spectroscopic experiments showed three distinct complexes, which could be attributed to a 1:1, a 1:2 and a 2:2 Eu(III)-NTA complex, the latter of which existing only at increased concentrations. This observation could be confirmed by TRLFS^[3]. Complex formation constants were determined from pH and concentration series applying TRLFS. TRLFS data were evaluated using parallel factor analysis as described elsewhere^[4]. Verification of those $\log \beta$ values as well as information about the reaction enthalpy ΔH , the reaction entropy ΔS and the Gibbs free energy ΔG were obtained via ITC measurements.

To confirm the proposed similarities in thermodynamic data for complex formation, similar experiments have been conducted with Cm(III). The formation of the 1:1 and the 1:2 complex could be confirmed with $\log \beta$ values similar to Eu(III).

The retention of Eu(III) on calcium aluminum silicate hydrate (C-A-S-H) phases was observed using batch experiments. Preliminary results have shown little to no impact of NTA on the Eu(III) retention. This may be explained by the high concentration of Al(III) and Ca(II) ions in the supernatants of the samples, as NTA readily complexes these ions as well.

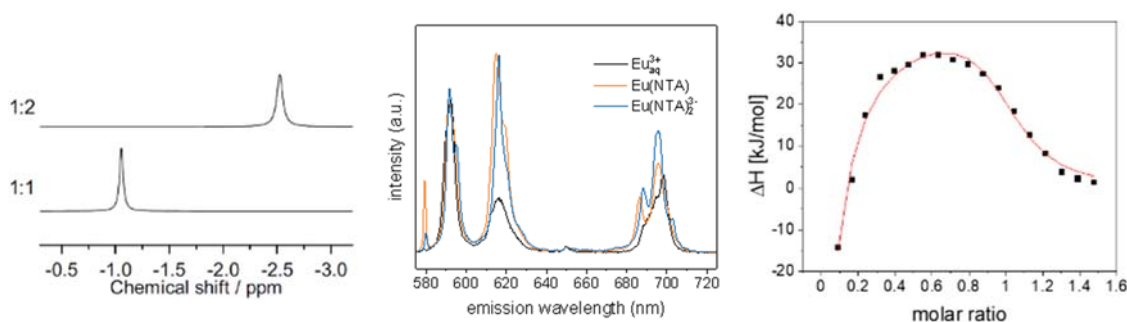


Figure 1: NMR, TRLFS and ITC measurements of the Eu(III)-NTA 1:1 and 1:2 complexes.

Acknowledgement: The German Federal Ministry for Economic Affairs and Energy (BMWi) is thanked for financial support within the GRaZ II project, no. 02E11860B.

References

- [1] Choppin, G. R. et al. (1977). The complexation of lanthanides by aminopolycarboxylate ligands - II. *J. Inorg. Nucl. Chem.* 39: 2025-2030
- [2] Akram, N. and Bourbon, X. (1995). Analyse critique de donnees thermodynamiques: pouvoir complexant de l'EDTA, du NTA, du citrate et de l'oxalate vis a vis de cations metalliques. *Etudes Experimentations Calculs.* Andra.
- [3] Sieber, C. et al. (2023). Eu(III) and Cm(III) complexation of NTA, EDTA, and EGTA studied by means of NMR, TRLFS, and ITC – an improved approach to more robust thermodynamics. *in preparation*
- [4] Drobot, B. et al. (2015). Combining luminescence spectroscopy, parallel factor analysis and quantum chemistry to reveal metal speciation—a case study of uranyl (VI) hydrolysis. *Chem. Sci.* 6: 964-972

PA5-8 MINERAL SPECIFIC SORPTION OF RADIUM ON CRYSTALLINE ROCK

Otto Fabritius⁽¹⁾, Tatiana Sorokina⁽¹⁾, Rohafza Dehqanzada, Juuso Sammaljärvi⁽¹⁾, Anna-Maria Jakobsson⁽²⁾, Tiina Sojakka⁽³⁾ and Marja Siitari-Kauppi⁽¹⁾

(1) Department of Chemistry, University of Helsinki, A.I. Virtasen aukio 1, 00560 Helsinki, Finland

(2) SKB, Evenemangsgatan 13, 16903 Solna, Sweden

(3) Posiva, Olkiluoto, 27160 Eurajoki, Finland

The spent nuclear fuel of Finnish and Swedish power plants will be permanently disposed of in deep geological facilities at the depth of 400-500 m¹. As a part of the KBS-3 disposal principle, the spent nuclear fuel waste will be disposed of in specially engineered canisters with carefully considered containment procedures. In the case of a containment failure, however, the final, and perhaps most important, barrier against the spread of harmful nuclear waste-borne compounds into the biosphere is the stable crystalline bedrock surrounding the facilities. As ²³⁸U is the dominant species in spent nuclear fuel, ²³⁸U and its radioactive progeny are of special interest when assessing the behavior of radionuclides in the lithosphere¹. As a part of ²³⁸U decay chain, ²²⁶Ra has been recognized as one the most safety-relevant radionuclides and dose contributors in the safety case calculations of the Finnish and Swedish disposal programs². In this study, the sorption properties of ²²⁶Ra were examined in the form of geological thin section sorption studies and spatial distribution of specific activity via digital autoradiography. Mineral specific sorption of Ra was determined.

For the thin section distribution coefficient study of ²²⁶Ra sorption on crystalline rock, the activity of ²²⁶Ra was measured through its gamma emission (186.2 keV, I = 3.64%) with High Purity Germanium (HPGe) gamma detector (Canberra Semiconductor Detector GX8021). Due to the low intensity of the ²²⁶Ra gamma emission, result accuracy control was done by measuring selected gamma detection samples with Liquid Scintillation Counting (LSC) (PerkinElmer Quantulus 1220) and alpha-particle spectroscopy (ALPHA-KINGTM) with multi-channel analyzer software (MAESTRO by ORTEC). The control measurement results were found to agree very well with the initial gamma detection activity results.

Site and mineral specific sorption of Ra on crystalline rock was studied with digital autoradiography using both Storage Phosphor Autoradiography (SPA) (Fujifilm FLA5100) and Micro Pattern Gas Detector autoradiography (MPGD) BeaQuantTM (Ai4r)^{3,4}. Comparing the ²²⁶Ra spatial distribution map of the autoradiography imaging with the mineral map of the sorption surface (from FE-SEM EDS, JEOL JSM-7100F Schottky with Oxford Instruments EDX-spectrometer X-Max), Ra sorption relevant minerals were identified and with the quantitative analysis of the BeaQuantTM autoradiography, sorption ratios between different minerals was established (Fig. 1). Mineral-specific Ra sorption data is vital information for the safety case calculations and radionuclide migration modeling of the deep geological disposal facilities. Sorption site-specific data of this study is used in the sorption modeling of Ra with the geochemical modeling tool PHREEQC².

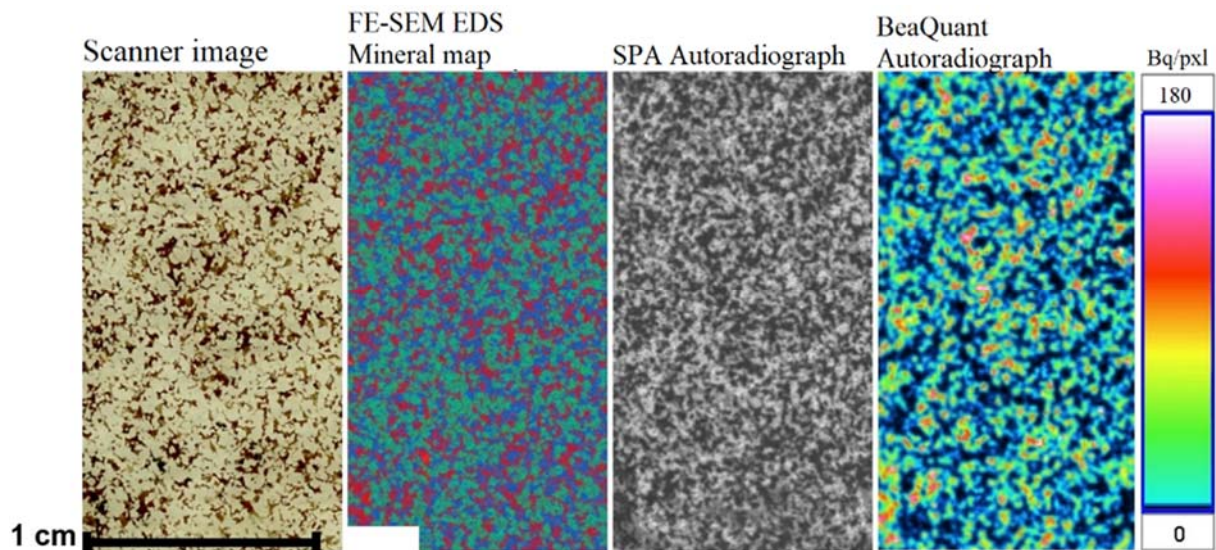


Figure 1: Spatial distribution of ^{226}Ra sorption on crystalline rock (mica gneiss). Left – regular tabletop scanner image of the studied mica gneiss thin section surface; middle-left – FE-SEM EDS mineral map of the same surface (red – biotite, cyan – plagioclases/feldspar, blue – quartz); middle-right – phosphor imaging plate autoradiograph of the surface (darker spots indicate higher activity of ^{226}Ra); right – BeaQuantTM autoradiograph of the surface with legend on the right, showing scale of the specific activity of ^{226}Ra in the mica gneiss minerals (Bq/pxl), pixel size 100x100 μm .

Acknowledgements: This work was supported by the Finnish and Swedish nuclear waste disposal expert companies Posiva Oy and SKB, respectively. The project leading to this work has received funding from the European Union's Horizon 2020 research and innovation program under grant agreement No. 847593 via the EURAD initiative.

References

- [1] Posiva SKB (2017). Posiva SKB Report 01
- [2] Fabritius, O., Puhakka, E., Li, X., Nurminen, A. and Siitari-Kauppi, M. (2022). Radium sorption on biotite; surface complexation modeling study. *Appl. Geochem.* 140: 105289
- [3] Angileri, A., Sardini, P., Donnard, J., Duval, S., Lefeuvre, H., Oger, T., Patrier, P., Rivid, N., Siitari-Kauppi, M., Toubon, H. and Descostes, M. (2018) Mapping ^{238}U decay chain equilibrium state in thin sections of geo-materials by digital autoradiography and microprobe analysis. *Appl. Radiat. Isot.* 140: 228-237
- [4] Delavre, C., Sammaljärvi, J., Billon, S., Muuri, E., Sardini, P. and Siitari-Kauppi, M. (2020) Comparison of phosphor screen autoradiography and micro-pattern gas detector based autoradiography for the porosity of altered rocks. *Sci. Rep.* 10: 9455

PA5-9 ANCHORING SELF-ASSEMBLY ANTIBACTERIAL AG NANOSHEETS ONTO THE MAGNETIC MICROSPHERES ENHANCED URANIUM IMMOBILIZATION

Min Zhao (2), Duoqiang Pan (1)(2), Wangsuo Wu (1)(2)

*(1) Frontiers Science Center for Rare Isotopes, Lanzhou University, Lanzhou, China**(2) School of Nuclear Science and Technology, Lanzhou University, Lanzhou, China*

Uranium(U), a long-lived radioactive element, is the indispensable part in nuclear energy as nuclear fuel. The recovery and separation of U from U(VI)-containing wastewater are related to the sustainable development of nuclear energy and environmental protection. Among all the separation methods for U(VI)-containing wastewater treatment in recent years, adsorption gets attention for its simple and effective characteristic [1]. However, a variety of microorganisms in the environmental U(VI)-containing wastewater (such as seawater) erode the structure of the adsorbent and affect its adsorption performance. The hindering by microorganisms (such as bacteria) cannot be ignored in environmental uranium-containing wastewater and seawater, which poses a great challenge for U(VI) immobilization [2][3]. Therefore, it is necessary to confer antibacterial activity onto adsorbents, as well as high adsorption capacity, excellent adsorption selectivity and stable structure. As far as we know, some metal nanoparticles (Au, Ag, Cu and Zn et al.) exhibit rapid and efficient antibacterial performance. Particularly, nano-silver (Ag)[4], as a spectrum antibacterial agent, can destroy nearly 650 kinds of microorganisms. The introduction of nano-Ag into the inner and outer surfaces of the material can theoretically endow the material with antibacterial activity. The flower-like Fe₃O₄@TiO₂-AO previously synthesized by our group introduced TiO₂ nanosheets onto Fe₃O₄ followed with the amidoxime functionalization[5], which showed great adsorption performance. Considering the complexity of true wastewater, an ideal water treatment material should possess not only high adsorption capacity and recycling capability, but also catalysis or antibacterial property to overcome different obstacles.

Herein, the intelligent and facile strategy was selected that the Ag nanosheets was created as the shell to endow magnetic adsorbent with antibacterial properties. A novel functional magnetic core-shell adsorbent with antibacterial property had been designed and fabricated. It is worth mentioning that anchoring self-assembly silver (Ag) nanosheets into the bulk of magnetic Fe₃O₄@SiO₂ (Fe₃O₄@SiO₂@Ag nanosheets) not only endowed it obvious antibacterial activity but also provided it the excellent platform for the incorporation of functional amidoxime (AO) groups to fabricate high-efficiency U(VI) adsorbent (denoted as Fe₃O₄@SiO₂@Ag nanosheets-AO). The structure was tested by XRD, FTIR, TEM, SEM, XPS and other characterization methods to evaluate the physical and chemical properties of Fe₃O₄@SiO₂@Ag nanosheets-AO. The adsorption performance of the material was tested by batch adsorption experiments as the function of pH, contact time, electrolyte, temperature, coexisting ions, selectivity and regeneration. At the same time, the disk diffusion test was used to preliminarily verify the antibacterial performance against Gram-negative (*E. coli*) and Gram-positive (*S. aureus*) of Fe₃O₄@SiO₂@Ag nanosheets-AO. Moreover, the corresponding adsorption and antibacterial mechanisms were deeply discussed.

Specifically, the TEM images revealed that Ag nanosheets were assembled in orientation along (111) crystal plane by 2D nanoplates of approximately 23 nm in size, which can be confirmed from the SEM images. After the anchoring of Ag nanosheets, the specific surface area was obviously facilitated to graft more AO groups. Consequently, comparing with amidoxime functional Fe₃O₄ (Fe₃O₄-AO) without Ag nanosheets, the adsorption efficiency of Fe₃O₄@SiO₂@Ag nanosheets-AO increased by 70%, reaching up to 343.8 mg·g⁻¹. The kinetic experiment suggested that the adsorption kinetics of the material was relatively fast, and it can adsorb more than 90% within 1 hour, and the adsorption equilibrium was reached within 5 hours. The second-order kinetic model fitted the experimental data better than the first-order kinetic model with higher correlation coefficient (0.9999), which indicating that the UO₂²⁺ adsorption process onto active sites of Fe₃O₄@SiO₂@Ag nanosheets-AO dominated by adsorption kinetics (i.e., predominantly chemisorption or surface complexation mechanism). Moreover,

$\text{Fe}_3\text{O}_4@\text{SiO}_2@\text{Ag}$ nanosheets-AO presented high affinity for U(VI) with a considerable adsorption capacity as well as great adsorption selectivity (Exactly, adsorption efficiency of U(VI) by $\text{Fe}_3\text{O}_4@\text{SiO}_2@\text{Ag}$ nanosheets-AO was up to 80%, far more than the other metal ions, including K^+ , Ba^{2+} , Sr^{2+} , Ca^{2+} , Mg^{2+} , Cu^{2+} , Ni^{2+} , Zn^{2+} and Eu^{3+}) for U(VI), both of which resulted from strong binding interactions between AO groups and U(VI). Since the ease of magnetic separation attenuated the loss of adsorbents, the U(VI) removal efficiency of as high as 90% could still maintained even after 10 cycles of adsorption-desorption. In addition, owing to the excellent antibacterial property of Ag nanosheets, $\text{Fe}_3\text{O}_4@\text{SiO}_2@\text{Ag}$ nanosheets-AO could effectively resist the bacteria, which exhibits significant inhibition against the growth of Gram-negative (*E. coli*) and Gram-positive (*S. aureus*) bacteria. Overall, the combinatorial multifunctionality of antibacterial activity and enough adsorption sites in $\text{Fe}_3\text{O}_4@\text{SiO}_2@\text{Ag}$ nanosheets-AO promise it great prospect in the remediation and purification of the environmental U(VI)-containing wastewater.

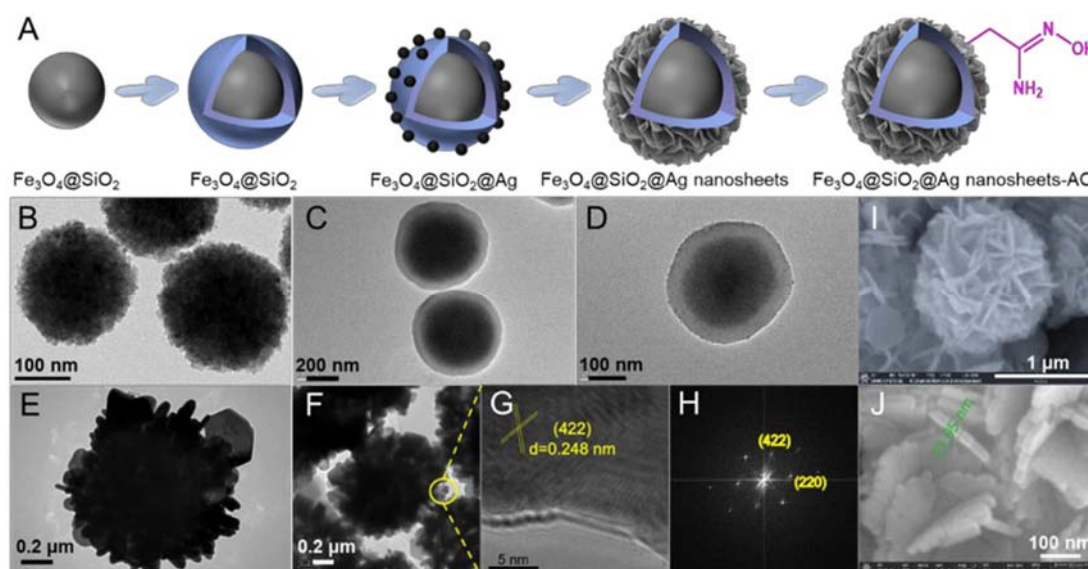


Figure 1. The structural characterization of samples.

References

- [1] Abdel Maksoud, M. I. A.; Elgarahy, A. M.; Farrell, C.; Al-Muhtaseb, A. a. H. and Rooney, D. W. (2020). Insight on water remediation application using magnetic nanomaterials and biosorbents. *Coord. Chem. Rev.* 403: 213096
- [2] Gao, J.; Yuan, Y.; Yu, Q.; Yan, B. and Qian, Y. (2020). Bio-inspired antibacterial cellulose paper-poly(amidoxime) composite hydrogel for highly efficient uranium(VI) capture from seawater. *Chem. Commun.* 56: 3935-3938
- [3] Guo, X.; Chen, R.; Liu, Q.; Liu, J. and Zhang, H. (2018). Superhydrophilic phosphate and amide functionalized magnetic adsorbent: a new combination of anti-biofouling and uranium extraction from seawater. *Environ. Sci.: Nano.* 5: 2346-2356
- [4] Wang, Y.; Wang, K.; Zou, B.; Gao, T. and Zhang, X. (2013). Magnetic-based silver composite microspheres with nanosheet-assembled shell for effective SERS substrate. *J. Mater. Chem. C.* 1: 2441-2447
- [5] Zhao, M.; Cui, Z.; Pan, D.; Fan, F.; Tang, J. (2021). An Efficient Uranium Adsorption Magnetic Platform Based on Amidoxime-Functionalized Flower-like $\text{Fe}_3\text{O}_4@\text{TiO}_2$ Core-Shell Microspheres. *ACS Appl. Mater. Interfaces.* 13: 17931-17939

PA5-10 FUNCTIONALIZED DIOXIN-LINKED COVALENT ORGANIC FRAMEWORKS FOR RAPID AND SELECTIVE EXTRACTION OF URANIUM

Yang Xu (1), Duoqiang Pan (1), Wangsuo Wu (1)

(1) School of Nuclear Science and Technology (Lanzhou University), P. R. China

The adsorption method is simple, efficient, easy to operate, and requires less equipment, which is an attractive method for purifying uranium(U(VI))-containing wastewater. However, there are varieties of interfering cations in the wastewater, which will consume effective uranium adsorption sites and reduce the adsorption efficiency of the sorbents. Although previously reported uranyl proteins have solved the problem of selectively adsorbing uranium by properly designing adsorption sites in confined environments, the weak stability of the protein limits the practical application. Combining protein design strategies with stable organic porous polymers is a promising solution [1], but the precise design of organic porous materials, especially the proper arrangement of adsorption sites, remains a huge challenge.

Therefore, covalent organic framework (COF) materials with large specific surface area, easy functionalization and adjustable structure were reasonably selected as uranium sorbents. Herein, carboxyl (COOH), amino (NH₂) and amidoxime (AO) group materials were obtained from cyano-functionalized dioxin-linked covalent organic framework through post-modification strategy, being used to adsorb U(VI) in uranium solution. According to the design strategy, the unique AB-stacking structure of two-dimensional COF material can construct subnanometer channel range from 0.5 to 1.0 nm, which is favorable for the synergistic coordination of adjacent groups with U(VI). It is noted that the oxygen atoms of dioxin-linkage caused the material surface negatively charged, which is conducive to the capture of uranyl cation in the acidic environment [2]. The batch adsorption experiments showed that COOH and AO group materials possessed excellent adsorption property with the adsorption capacity of 515 mg/g and 450 mg/g, respectively. More importantly, more than 90% of uranium could be moved within 15 minutes. In addition, they can selectively adsorb uranium from ten kinds of coexisted cations. Zeta potential analysis showed that the zeta potential of COOH group and AO group materials ranged from -20 mV to 0 mV in an acidic environment of pH 4.0 - 6.0, which was consistent with the design conjecture and facilitated U(VI) adsorption. In order to further explore the application potential of functionalized subnanopore COFs, EXAFS characterization and theoretical calculation of COOH and AO group materials were carried out to further clarify the U(VI) adsorption mechanism by microporous COFs.

Herein, the samples are composed of one standard crystal (UO₂(NO₃)₂·6H₂O) containing six oxygen atoms in equatorial plane and one COF-316s (COF-316-COOH or COF-316-AO with common uranyl coordination groups). Taking into account of a higher affinity for U(VI) by functional groups relative to water oxygen, the second coordination shell is divided into two subshells (U-O/Neq₁ and U-Oeq₂) [3]. As Fourier transform spectra was unable to distinguish the overlapping contribution of different atoms around, wavelet transform was performed on the K₃-weight EXAFS spectra to pick out the possible paths. Results of wavelet transform showed that the second shell field of U-loaded sorbents are lower than that of UO₂(NO₃)₂·6H₂O, implying that the U-O/Neq paths in U-loaded samples may be shorter than those in UO₂(NO₃)₂·6H₂O. Combined with the above results, the second shell are fitted by two paths respectively. In the case of COF-316-AO+U, fitting results of the second shell is composed of 2.0 equatorial Oxygen or Nitrogen atoms (O/Neq₁) at 2.16 Å and 4.0 equatorial Oxygen atoms (Oeq₂) at 2.35 Å, which belong to one AO group and four water molecules, respectively. Furthermore, concerning the carbon atom of AO group, the last shell was fitted by a single scattering U-C path with 1.0 carbon atom. In general, the average distance of the second shell in U-loaded sorbents (2.1-2.3 Å) are obviously shorter than UO₂(NO₃)₂·6H₂O (2.3-2.4 Å), which confirmed the strong coordination between U(VI) and COOH or AO group. In addition to the decrease of U-Oeq distance, the increase of U-Oax distance is also observed, which is common in uranyl complex. In summary, EXAFS analysis strongly supported the 6-

coordinate model in U-loaded samples and elucidate that functionalized groups (carboxyl and amidoxime) of COF-316s prefer to bind with U(VI) by forming inner-sphere surface complexes. The theoretical calculation results showed that the limited environment created by AB stacking makes the distance between adjacent groups close enough, thus increasing the affinity of the adsorption site for uranyl ions. Therefore, the COOH group, which is generally hardly selective for U, can also selectively adsorb uranium very well in this particular pore. In conclusion, stable, designable and regulated subnanometer-channel COFs provided a promising strategy for the efficient purification of uranium-containing wastewater.

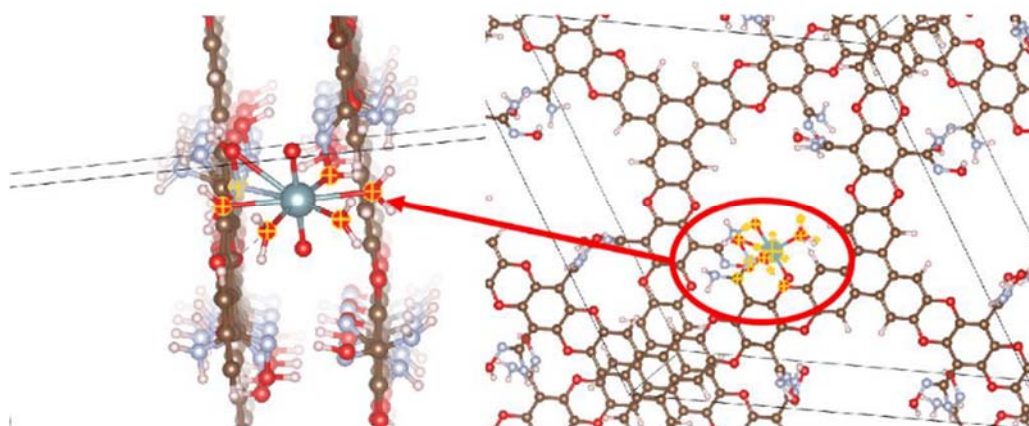


Figure 1. Schematic of the synergistic coordination of U(VI) by AB-stacking subnanometer COF.

References

- [1] Y. Li, and L. Ma (2020). Redox-Active Two-Dimensional Covalent Organic Frameworks (COFs) for Selective Reductive Separation of Valence-Variable, Redox-Sensitive and Long-Lived Radionuclides. *Angew. Chem. Int. Ed. Engl.* 59: 4168-4175
- [2] D. Pan, and W. Wu (2022). Insights into sorption speciation of uranium on phlogopite: Evidence from TRLFS and DFT calculation. *J. Hazard. Mater.* 427: 128164
- (3) L. Thierry, and V. Christophe (2014). The crystal chemistry of uranium carboxylates. *Coordin. Chem. Rev.* 266: 69-109

PA5-11 CS(I) AND BA (II) SORPTION ON BIOTITE AT PH 5-9 AND 25, 40 AND 60°C

Pawan Kumar and Stellan Holgersson

*Department of Chemical Engineering, Division of Nuclear Chemistry
Chalmers University of Technology, Kemivägen 4,
SE41296 Göteborg, Sweden*

In Sweden 31% of the electricity is obtained from nuclear energy. The use of nuclear fuel produces a highly radioactive waste that has to be placed far from the human reach and environment for a long time, about 100.000 years, until it reaches radioactivity levels of natural ores. To accomplishing the goal for the waste disposal, the Swedish nuclear fuel and waste management company, SKB, has developed a so-called KBS-3 concept for a final repository for spent nuclear fuel. The concept includes corrosion-resistant copper canister with spent nuclear fuel to be further protected by a placement in bentonite clay 400-500 m below in the geological formation. Based on extensive geological surveys, the Forsmark area located in the municipality of Östhammar has been selected as the most promising site for such a repository.

According to the site survey, the granitic rock consists of 3-12% biotite, which is considered to play a major part in providing sorption capacity for radionuclides. To predict radionuclide migration in a scenario with a broken canister, this mineral has been selected for our study. The aim of this work is to obtain experimental data and model it with existing Thermodynamic Sorption Models for determining the sorption capacity of the biotite.

A biotite size fraction of 0.07-0.125 mm was selected, The specific surface area was determined with Kr-BET to 0.4742 m²/g and cation exchange capacity was measured with NH₄Ac method to 1.01 meq/100g and the acidic site density was determined with tritium exchange method [1] to 6.7μmol/m².

Surface acidity constants of biotite were determined with potentiometric titration to pK_{a1}= 4.6 and pK_{a2}=6.9, assuming just one amphoteric surface site. For the fitting to data the acidity constants was optimized using PHREEQC geochemical modelling software coupled with optimization routine written in PYTHON programming language.

Cs [10⁻⁶M] and Ba [10⁻⁷M] sorption onto biotite minerals at fixed metal concentration [10⁻⁶M] was studied using the batch method with S:L = 1:50 at three different ionic strengths (0.001, 0.01 and 0.1M NaClO₄), five different pH (5,6,7,8,9) and at three different temperatures (25, 40 and 60°C) for two months in an inert atmosphere glovebox. The sorption was observed to be the pH dependent, with *R_d* values for Cs of varying between 0.6-1.6, 0.7-2.5 and 0.7-8.5 m³/kg for 25, 40 and 60°C, respectively. For Ba the corresponding *R_d* values were 0.2-4.5, 0.2-3.8 and 0.3-4.4 m³/kg. Cs sorption increased with temperature while both Cs and Ba sorption decreased with increased ionic strength.

Sorption was successfully modelled with a one-site acidic, two pK_a model, both constant and variable capacitance models were evaluated [2]. In future work, the data is to be used together with corresponding data for K-feldspar to model Cs and Ba sorption onto Forsmark granite by the component additivity (CA) approach.

References

- [1] Berubé et al., Surface Science 8 (1967) 448-461.
- [2] Dzombak and Morel. Surface Complexation Modeling – Hydrous Ferric Oxide. Wiley, (1990).

PA5-12 MICROMECHANISM OF ADSORPTION OF STRONTIUM AND CESIUM ON DIFFERENT EXPANSIVE CLAY MINERALS

Junjun Hou⁽¹⁾, Duoqiang Pan⁽¹⁾, Wangsuo Wu⁽¹⁾

(1) School of Nuclear Science and Technology, Lanzhou University, China

With the development of the nuclear industry over several decades, geological disposal is considered as one of the most effective methods of dealing with radioactive waste. Inevitably, in order to ensure the long-term stable operation of repository, sufficient attention should be paid to the environmental chemical behavior of some typical radionuclides during geological disposal, such as strontium (Sr) and cesium (Cs).

Generally, the presence of Sr^{2+} and Cs^+ in the environment is mainly controlled by adsorption on environmental media. Former studies have shown that the widespread occurrence of layered aluminosilicate clay minerals in soil has a significant capacity for adsorbing Sr^{2+} and Cs^+ . These layered aluminosilicate minerals are mainly composed of Si-O tetrahedron and Al-O octahedron combination. According to the different combination ratios, layered aluminosilicate minerals have 1:1 and 1:2 types, respectively. There are four main adsorption sites on clay minerals that can strongly capture Sr^{2+} and Cs^+ in the soil environment, namely FES site (formed by weathering), type II site (formed by fracture of mineral crystals), planar site and interlayer site (ion exchange site). As a rule, clay minerals with different expansive properties have various interlayer distances, and the differences in interlayer distances result in multiple numbers of adsorption sites for clay minerals. For example, the interlayer site of non-expanding clay minerals (illite) is not available, so that the different adsorption sites of the layered clay minerals contribute differently to the adsorption of radionuclides, which is also one of the main reasons for exhibiting different environmental chemical behaviors in different environmental media. Given that, three clay minerals (illite, vermiculite and smectite) with different swelling properties were selected to explore the contribution of different sites to the adsorption of strontium and cesium in this study.

In addition to environmental factors, the differences between Sr^{2+} and Cs^+ also make their migration behaviors different. A series of studies on the migration of Sr^{2+} and Cs^+ under the same soil conditions pointed out that the migration ability of Sr^{2+} is much stronger than that of Cs^+ , and clay minerals tend to adsorb Cs^+ . From the solvent chemical properties of Sr^{2+} and Cs^+ , Sr^{2+} has a higher number of charges (two units of positive charge), so the binding of Sr^{2+} to the negative potential site should be more stable (stronger electrostatic interaction), and Sr^{2+} can bind more ligands and generate stable complex well. Therefore, Sr^{2+} should be able to be more easily fixed on clay minerals. However, on the contrary, the adsorption amount of Cs^+ on clay minerals is much larger than that of Sr^{2+} , and the adsorption of Sr^{2+} on clay minerals is not stable enough.

In summary, the main purpose of this study is to: (1) Exploring whether the diversity of site concentration caused by the difference in mineral structure can affect the adsorption behavior of strontium and cesium on clay minerals; (2) Differences in microscopic mechanisms of combination between Sr^{2+} and Cs^+ with clay minerals.

The results revealed a clear distinction in the binding mechanisms of Sr and Cs on clay minerals under the effect of pH, ionic strength, temperature, and HA. Sorption capacity of Sr^{2+} was observed to increase as pH increased, and it was evidently influenced by the ionic strength. Increasing temperature led no significant change. Further analysis using EXAFS revealed that Sr was surrounded by ~ 8.0 atoms at $R_{\text{Sr-O}} \approx 2.6$ Å. All the above results indicated that the main mechanisms of Sr adsorption on clay minerals

were outer-sphere complexation (OS) and ion exchange. The diversity of clay minerals does not affect Sr adsorption; however, it does have impact on Cs adsorption. The batch adsorption results showed that Cs adsorption on clay minerals was inhibited in the presence of HA, which were consistent with the sequential extraction and XRD results. The IS complexation of Cs was the dominant mechanism, which was mainly formed at the frayed edge sites (FES) on illite, the surface sites and interlayer sites on vermiculite and montmorillonite. In addition, the adsorption of Cs on vermiculite caused interlayer collapse of vermiculite, leading to more stable adsorption. Discrepancy of the adsorption mechanisms come into being the entirely different environmental behavior between Sr and Cs. These findings provided a theory for constructing the migration model of Sr and Cs on clay minerals and in-depth description of the environmental behavior of Sr and Cs support.

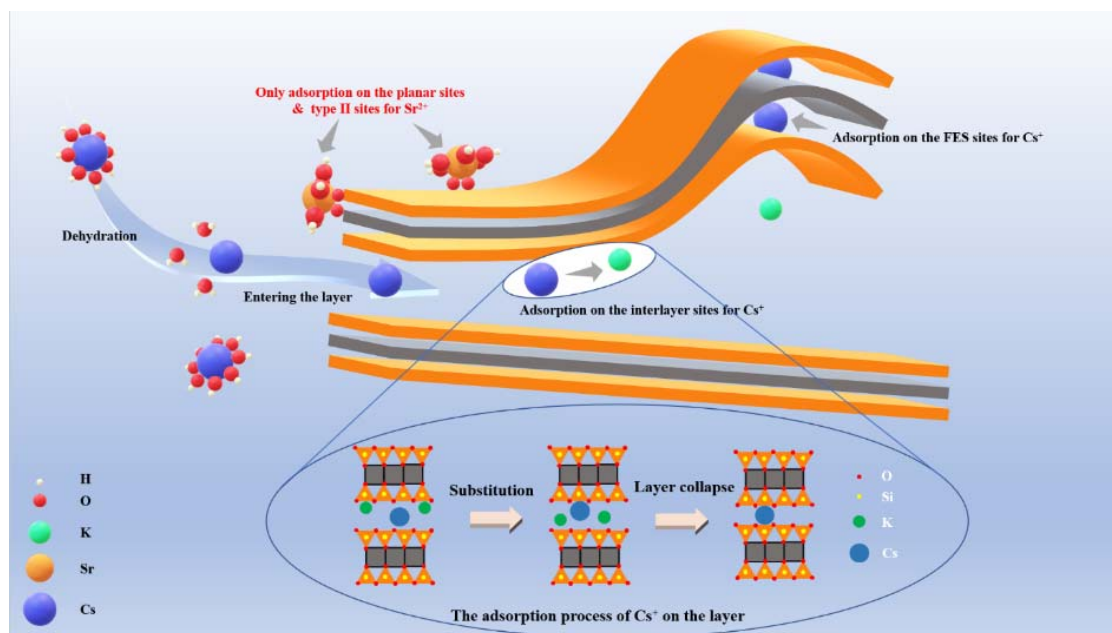


Figure 1: Adsorption mechanism diagram of strontium and cesium on clay minerals

References

- [1] Fan, Q.H. and M, Tanaka (2014). An EXAFS study on the effects of natural organic matter and the expandability of clay minerals on cesium adsorption and mobility. *Geochim. Cosmochim. Acta* 135: 49-65.
- [2] Yuki S, Takamitsu I, and T Yukio (2021). Surface complexation of Ca and competitive sorption of divalent cations on montmorillonite under alkaline conditions. *Appl. Clay Sci.* 200.
- [3] Montoya V, and B Baeyens (2018). Sorption of Sr, Co and Zn on illite: Batch experiments and modelling including Co in-diffusion measurements on compacted samples. *Geochim. Cosmochim. Acta* 223: 1-20.
- [4] Fuller A J, and S Shaw (2016). EXAFS Study of Sr sorption to Illite, Goethite, Chlorite, and mixed sediment under hyperalkaline conditions. *Langmuir* 32: 2937-2946.
- [5] I. Smičiklas, M. Jović, M. Šljivić-Ivanović, V. Mrvić, D. Čakmak, and Dimović S (2015). Correlation of Sr²⁺ retention and distribution with properties of different soil types. *Geoderma* 253: 21-29.
- [6] Kenji Tamura, Toshihiro Kogure, Yujiro Watanabe, Chiemi Nagai, and Yamada Hirohisa (2014). Uptake of Cesium and Strontium ions by artificially altered phlogopite. *Environ. Sci. Technol.* 48: 5808-5815.

PA5-13 ADSORPTION OF CESIUM ON MICACEOUS MINERALS WITH STRUCTURAL TRANSFORMATION AND THE IMPLICATION FOR DIFFUSIONHanyu Wu^{(1),*}, Wei Wang⁽²⁾, Mingliang Kang⁽¹⁾, Yoshio Takahashi⁽³⁾, Qiaohui Fan^{(2),*}*(1) Sino-French Institute of Nuclear Engineering and Technology, Sun Yat-sen University, Zhuhai, 519082, China**(2) Key Laboratory of Petroleum Resources Research, Gansu Province, Northwest Institute of Eco-Environment and Resources, Chinese Academy of Sciences, Lanzhou 730000, China**(3) Department of Earth and Planetary Science, The University of Tokyo, Hongo 7-3-1, Bunkyo-ku, Tokyo 113- 8654, Japan*

Green remediation of radioactive cesium (RCs) remains a concern since the adsorption mechanism would be affected by weathering, which has not been adequately considered. The geochemically close minerals in the mica group, including the secondary clay minerals, presented distinct-different behaviors of immobilization and release for RCs. The nuclear contamination remediation and emergency response plan should take into account the impact of the structural transformation of constituents in the soil on the migration of cesium. In light of the aforementioned complexities, the goals of this study were to determine (i) a uniform description of composition/structure versus structural transformation relation for geochemically close micaceous minerals, (ii) the availability and capacities of adsorption sites affected by structural transformation and their contribution to RCs adsorption, and (iii) how the occurrence and migration of RCs controlled by structural transformation of micaceous minerals. Muscovite, biotite and phlogopite were treated by different methods and then characterized. The adsorption behaviors of RCs on treated micaceous minerals were explored through batch experiments and the four-site generalized adsorption model (GAM). The desorption and chemical environments of RCs on treated micaceous minerals were investigated by sequential extraction and extended X-ray absorption fine structure (EXAFS). The results of structural transformation affecting the adsorption mechanism of RCs were further applied to explain the diffusion of Cs in soils containing micaceous minerals.

Here three micaceous minerals were investigated comparatively in the different stages of structural transformation. The more di-octahedral characteristics in the octahedron of micaceous minerals, the more difficult the structures are to be changed^[1]. The effects on micaceous minerals can come down to the changes in permanent charges and site capacities, which are directly related to the RCs adsorption^[2]. The adsorption capacity of muscovite was more difficult to improve than phlogopite under the same conditions. Adsorption isotherms of ultratrace to trace level RCs further magnified the differences among geochemically close micaceous minerals. The capacities and availability analysis of adsorption sites by the four-site GAM shows that the excellent RCs retardation on treated micas with more trioctahedral (or structural transformation) properties benefited from a high percent of interlayer sites (ITSs). At RCs concentration $< 10^{-7}$ mol/L, frayed edge sites (FESs), as wedged zones at the interlayer entrance generated from the weathering with the limited capacity ($< 10^{-6}$ mol/g), mainly contributed to all the treated micaceous minerals through incredibly selective adsorption^[3]. Notably, since ITSs are almost unavailable in non-expandable muscovite but available in the expandable micaceous minerals, ITSs were not considered in the fit of muscovite series and nearly fresh biotite, which has also been supported by XRD patterns (Figures 1A and 1B). At RCs concentration $> 10^{-5}$ mol/L, planar sites (PSs) and ITSs were the dominating sites for the micaceous minerals did not consider ITSs (non-expandable muscovite and nearly fresh biotite) and for the others respectively. RCs adsorption on treated micaceous minerals can be summed up as three sites control pathways: (i) FES→TIIS→PS, (ii) FES→TIIS→ITS, and (iii) FES→ITS. PSs accounted for more than 90% of CEC for muscovite and nearly fresh biotite, which were similar to non-expansion or fresh minerals, such as illite (80%) and fresh Beishan granite (99%). While limitations gradually displayed on Na^+ promoting RCs desorption from biotite/phlogopite with different structural transformations. And sequential extraction by NH_4^+ could desorb more than 60% RCs from biotite/phlogopite of light structural transformation, which showed that rising the extents of structural transformation led to mobility reduction of RCs. Further reduction of RCs mobility appeared

in heavily structural transformation micaceous minerals, where 85%-90% RCs could not be desorbed. The second shells in R -space confirmed that structural transformation generally enhanced inner-sphere complexes (ISCs) contents of RCs on micaceous minerals. And the oscillatory frequency at 4.2 \AA^{-1} in k -pace distinguished the RCs occurrence among lightly and heavily structural transformation. Therefore, it could be expected that the stable ISCs were mainly responsible for the less mobility and bioavailability of RCs in the contaminated soil or sediment, which weakened the vertical migration^[4]. The important indicators for evaluating vertical migration of RCs were not only the contents of micaceous minerals in the topsoil but also their extents of structural transformation. It was the microscopic diversities in structures and properties that led to the time-scale differences in polluted ranges observed in RCs contamination incidents. Three soil samples with different contents of clay minerals were used to verify the results, which are 5 m below the surface from the same area. The diffusion trend of RCs in the soils is basically the same, which is illustrated by the relationship between the cumulative concentration and time. The orders of retardation by three soils changed in the first 50 days and the period of 100-140 days, which is mainly attributed to the diversities of site capacities caused by the structural difference of micaceous minerals in the soils.

This work provides heretofore missing information on the comparisons of RCs adsorbed by characteristically similar micaceous minerals with regards to structural transformation and thereby advances a more holistic understanding of timescale RCs remediation in the environment.

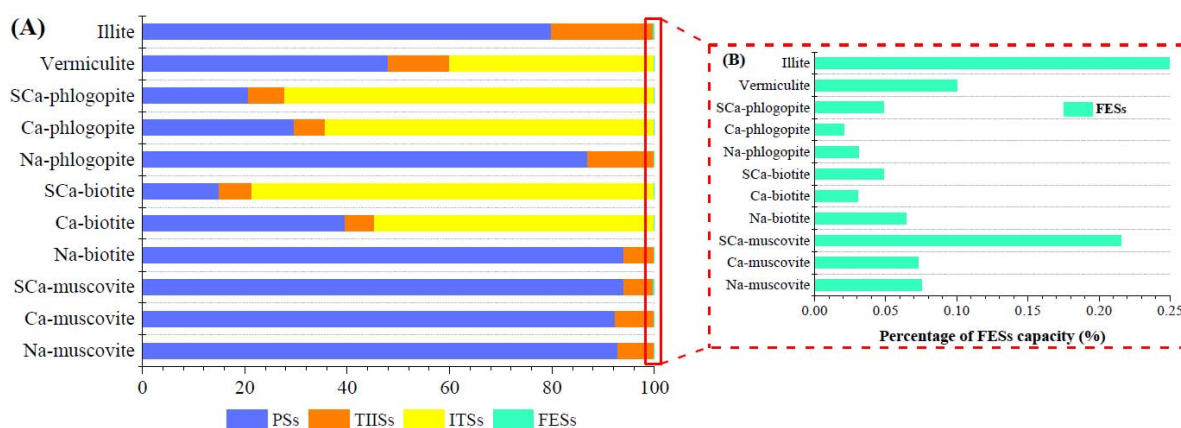


Fig.1. The sites proportions of (A) treated micaceous minerals and (B) FESs. The data of illite and vermiculite came from our previous work^[3].

References

- [1] Taylor, A. S., Blum, J. D., Lasaga, A. C. and MacInnis, I. N. (2000). Kinetics of dissolution and Sr release during biotite and phlogopite weathering. *Geochim. Cosmochim. Ac.* 64(7), 1191-1208.
- [2] Siroux, B., Wissocq, A., Beaucaire, C., Latrille, C., Petcut, C., Calvaire, J. and et al. (2018). Adsorption of strontium and caesium onto an Na-illite and Na-illite/Na-smectite mixtures: implementation and application of a multi-site ion-exchange model. *Appl. Geochem.* 99, 65-74.
- [3] Fan, Q. H., Tanaka, M., Tanaka, K., Sakaguchi, A. and Takahashi, Y. (2014). An EXAFS study on the effects of natural organic matter and the expandability of clay minerals on cesium adsorption and mobility. *Geochim. Cosmochim. Ac.* 135, 49-65.
- [4] Zaunbrecher, L. K., Cygan, R. T., & Elliott, W. C. (2015). Molecular models of cesium and rubidium adsorption on weathered micaceous minerals. *J. Phys. Chem. A.* 119(22), 5691-5700.
- [5] Tameta, Y., Tamura, R., Kimura, M., Sasamoto, M., Kamei-Ishikawa, N. and Ito, A. (2021). Effect of dissolved soil organic matter on cesium adsorption by zeolite and illite. *J. Environ. Manage.* 289, 112477.

PA5-14 ILLITIZATION UNDER HIGH TEMPERATURES AND ITS EFFECT ON CESIUM SORPTION

Seeun Chang, Mihye Kong, DeukHwan Lee, and JinSeok Kim

Korea Atomic Energy Research Institutes, KAERI, South Korea

In this study, the mineral transformation of bentonite, Bentonil WRK, one of the smectites, was investigated under different conditions of temperature and K ions concentration. Smectites are swellable clays in which the interlayer cation can be easily exchanged. Bentonill WRK has Ca ions in its interlayer as Ca-smectite, and the intercalation of K ions in exchange for Ca ions within Bentonil WRK is relevant to radionuclides migration as it is a step in the transformation of smectite to illite.

We prepared the transformed bentonite sample with different temperatures (125 – 175 °C) and K ion concentrations of 0.01 M and 1.0 M, respectively. One gram of Bentonil WRK was reacted with 20 times the volume of fluids containing K ions for 10 days while maintaining the desired temperature. As the reactions were conducted for only 10 days, there were no differences observed between the reactions carried out at 125 to 175 °C. The reaction with 0.01 M of K was also did not show any critical points of mineral transformation. However, when the material reacted with 1M of K ions, the interlayer Ca ions were fully exchanged with K ions. Therefore, the main XRD peak of smectites at low 2θ ($\sim 10^\circ$) was completely replaced by K types of smectite with their corresponding d(001) spacing (Fig. 1). Although the smectite transformation reactions occurred at high temperature there was no evidence to suggest illitization. Mineral transformation reactions require the availability of K ions, which means that the permeability of the clay to K-rich fluids is an important factor in the process.

The sorption distribution coefficient of Cesium ($K_d\text{-Cs}$) of Bentonil WRK was found to be 1,438 mL/g, while the exchanged sample showed a value of 1,552 mL/g. The changed interlayer cation reactions did not affect the sorption ability of cesium. The intercalation of K in Bentonil WRK was also confirmed by XRF results (Table 1). The Ca content was reduced while K content was increased. No new product such as SiO₂ was found, which indicates that illite formation from smectite via a dissolution and precipitation reaction (silica crystallize phase) was also not observed.

In the case of deep disposal of high-level radioactive waste, there is a possibility that bentonite in the buffer may transform into illite due to high temperature. However, even if the bentonite is transformed, the effect on the sorption and migration of radionuclides (such as cesium) is considered to be minimal. Nevertheless, this study only provides results over a short period of time, and it is necessary to evaluate the migration of radionuclides in response to high-temperature mineral transformation of the buffer material, bentonite, over a longer period. Currently, Korea Atomic Energy Research Institutes, KAERI, is conducting bentonite high-temperature mineral transformation experiments for up to 20 years to evaluate the extent to which the buffer is degraded by high temperatures.

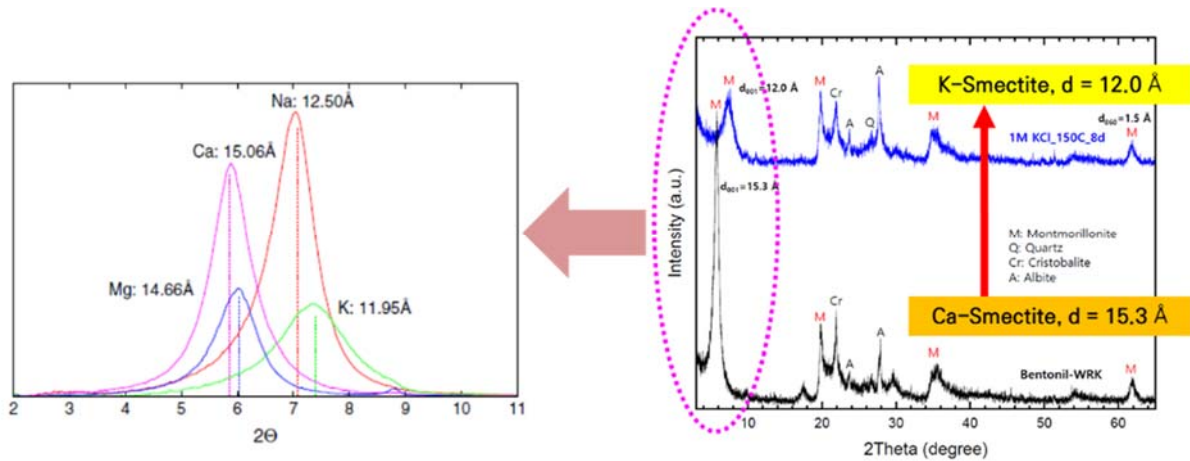


Figure 1. The XRD patterns of the reference and empirical samples. The left pattern is from J. Behnsen and D. R. Faulkner (2013), and the right pattern shows the results of Bentonil WRK (black line) and the transformed sample (blue line) under 150 °C, 1 M KCl reaction for 8 days.

Table 1. The XRF results for both the before and after transformation reactions.

XRF [%]	Samples	SiO ₂	Al ₂ O ₃	Fe ₂ O ₃	CaO	MgO	K ₂ O	Na ₂ O	TiO ₂	MnO	P ₂ O ₅	Ig.loss
	Bentonil WRK	64.69	16.36	3.55	2.79	2.88	0.83	1.02	0.47	0.09	0.09	6.95
Rxn 1M KCl @150°C, 10 d	64.99	15.96	3.93	0.93	2.47	4.93	0.95	0.45	0.05	0.10	4.94	

Table 2. The sorption distribution coefficients (Kd) results for before and after transformation reactions.

SD	Kd-Cs [mL/g]		Stastics		
	1	2	Mean	SD	RSD
Bentonil WRD (drying @ 105 °C)	1438	1411	1424	18.9	1%
1M KCl @ 150 °C for 8d	1552	1563	1558	8.1	1%

Reference

[1] J. Behnsen and D. R. Faulkner (2013). Permeability and frictional strength of cation-exchanged montmorillonite. J. Geophysical Res: Solid Earth. 118: 2788-2798.

PA5-15 ANTI-BIOLOGICAL CONTAMINATION URANIUM ADSORBING CELLULOSE GEL

Yuanping Jiang, Yunxiu Zhang, Zuoja Li, Guohang He, Zhibin Zhang*, Yunhai Liu*

School of Chemistry, Biology and Materials Science, East China University of Technology, China

The use of biomass adsorbent materials for uranium enrichment in seawater is to develop clean energy by using renewable resources, and is a sustainable development strategy that organically combines the utilization of renewable resources with the development of energy. In this study, biomass cellulose and chitosan were used as matrix, and anti-fouling hydrogels were prepared by additive modification and solution-gel method. Biodopamine was introduced into pore-inducing agent to construct multistage pore structure to make full use of internal and surface active sites, and biophytic acid was chemically modified to introduce phosphate base group to further improve uranium adsorption capacity: Anti-fouling design, structural design and chemical modification of the three pipeline preparation of anti-biological fouling, high adsorption capacity, can be recycled whole biomass seawater uranium extraction gel adsorption material, explore the organic combination of resource utilization and environmental protection, to provide a new guarantee for the development of clean energy nuclear energy.

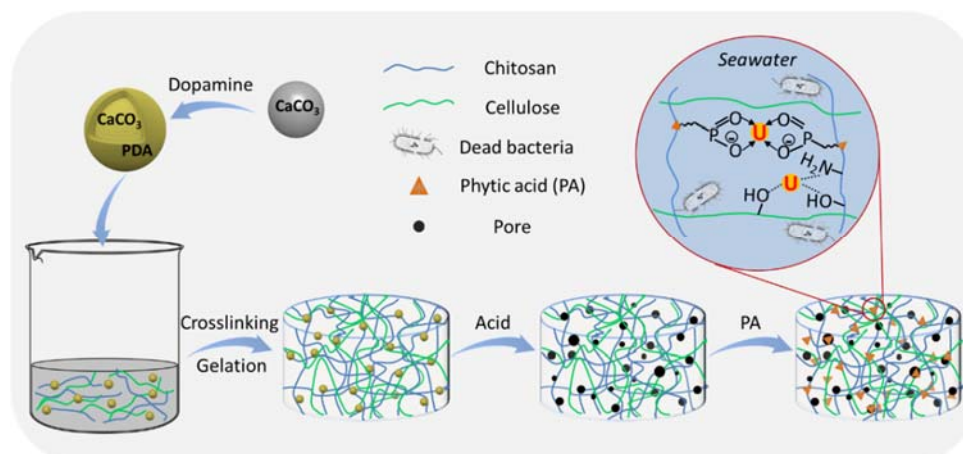


Figure 1: Schematic diagram of the preparation of porous whole biomass uranium adsorption gel material resistant to biological fouling.

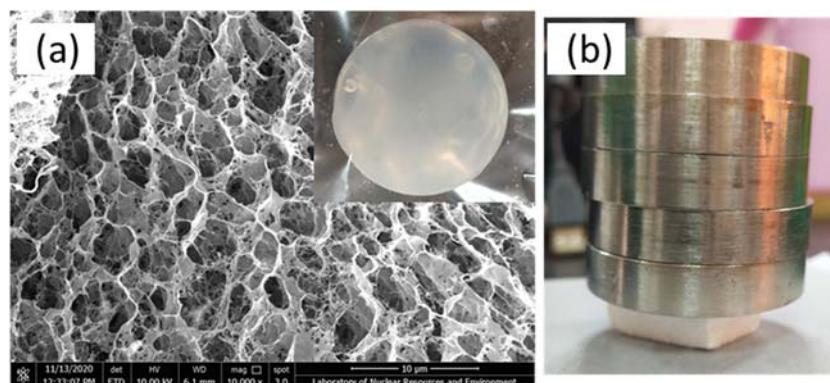


Figure 2: (a) Chitosan-cellulose composite hydrogel and its microscope image; (b) Load-bearing diagram of aerogel.

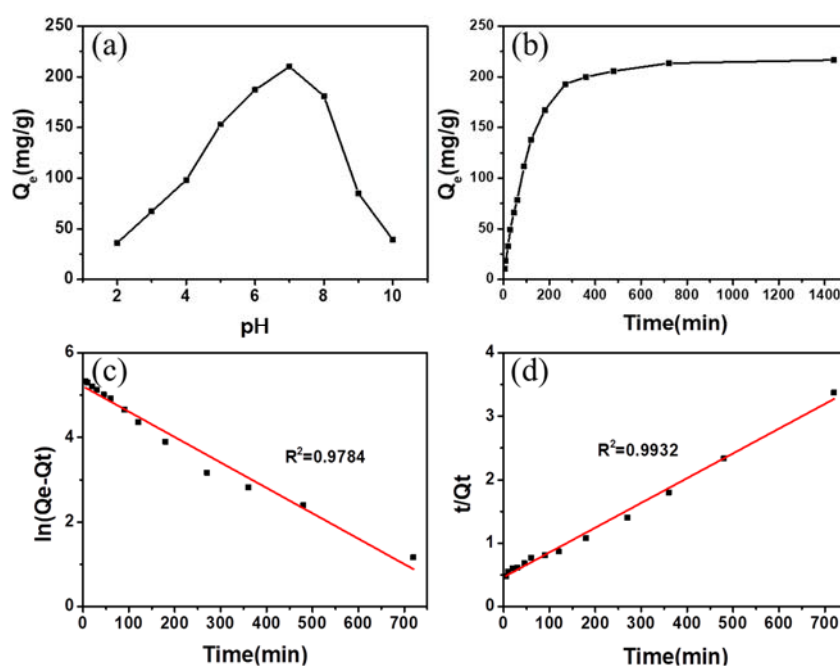


Figure 3: (a) Effect of initial pH of solution on uranium adsorption by porous chitosan-cellulose composite gel (p-CS/Ce); (b) The effect of adsorption time on p-CS/Ce adsorption of uranium; (c) quasi-first-order kinetic fitting curve of p-CS/Ce adsorption of uranium; (d) Quasi-second-order kinetic fitting curve of p-CS/Ce adsorption of uranium.

References

- [1] Sholl D S, Lively R P. Seven chemical separations: to change the world: purifying mixtures without using heat would lower global energy use, emissions and pollution--and open up new routes to resources .Nature, 2016, 532: 435-437.
- [2] Kim J, Tsouris C, Oyola Y, et al. Uptake of uranium from seawater by amidoxime-based polymeric adsorbent: field experiments, modeling, and updated economic assessment .Industrial & Engineering Chemistry Research, 2014, 53(14): 6076-6083.
- [3] Abney C W , Mayes R T , Saito T , et al. Materials for the recovery of uranium from seawater [J].Chemical Reviews, 2017, 117(23): 13935-14013.
- [4] Park J, Gill G A, Strivens J E, et al. Effect of biofouling on the performance of amidoxime-based polymeric uranium adsorbents [J].Industrial & Engineering Chemistry Research, 2016, 55(15): 4328-4338.
- [5] Huang Z, Dong H, Yang N, et al. Bifunctional phosphorylcholine-modified adsorbent with enhanced selectivity and antibacterial property for recovering uranium from seawater [J].ACS Applied Materials and Interfaces, 2020, 12(14): 16959-16968.

PA5-16 RETENTION MECHANISMS OF SELENIUM IN DEEP SUBSURFACE SEDIMENTARY FORMATIONS IN HORONOBE AREA, HOKKAIDO, JAPAN*

Shuntaro Dei^{(1),(2)}, Yukio Tachi⁽²⁾, Yuki Amano^{(1),(2)}, Paul C. M. Francisco⁽²⁾, Yuki Sugiura⁽²⁾ and Yoshio Takahashi⁽³⁾

(1) Horonobe Underground Research Center, Japan Atomic Energy Agency, Hokkaido, Japan

(2) Nuclear Fuel Engineering Laboratories, Japan Atomic Energy Agency, Ibaraki, Japan

(3) Department of Earth and Planetary Science, Graduate School of Science, The University of Tokyo, Tokyo, Japan

⁷⁹Se is one of the key radionuclides for safety assessment of geological disposal of the high-level radioactive waste (HLW) due to its long half-life and complex speciation depending on the redox condition. Since selenium is considered to easily migrate as anion chemical species, it is important to understand the retention mechanism of Se in the subsurface environment. The aim of this study is to elucidate the retention mechanisms of Se in the deep subsurface by clarifying the speciation of Se.

We focused on sedimentary rocks in the Horonobe area (Hokkaido, Japan), where detailed studies of the geological environment have been conducted at the Horonobe Underground Research Laboratory (URL). The rocks consist of the Neogene to Quaternary Wakkanai (siliceous mudstone) and Koetoi (diatomaceous mudstone) Formations. Several core samples drilled in and around the URL were used for analyses. Sequential extraction experiments [1] were performed using powdered rock samples to investigate the macroscopic speciation of Se in the rocks. Since pyrite is considered to play an important role in Se retention, sulfur isotope analysis was performed using powdered rock samples to determine the formation mechanism of pyrite. Micro-X-ray analyses (μ -XRF and μ -XAFS) were also performed at BL-4A and/or BL-15A of the Photon Factory (Tsukuba, Japan) to examine the microscopic distribution and speciation of Se in the rocks. The rock samples were processed into thin sections and Se, Fe and S distribution was mapped by μ -XRF. Micro-XAFS measurements were performed in Se-enriched areas identified by μ -XRF mapping to determine the speciation of Se and Fe. After the micro-X-ray analyses, Se-enriched areas were further examined by SEM.

The sequential extraction experiments showed that sulfide/selenide was the dominant (37 to 59%) speciation of Se in both the Wakkanai and Koetoi Formations. The total Se concentration, calculated from the sum of the Se concentrations extracted in each extraction process, was 1 to 2%, with no significant differences between the Wakkanai and Koetoi Formations. μ -XRF mapping showed the presence of Fe and S in the Se-enriched areas (Fig. 1). Fe *K*-edge XANES spectra of Se-, Fe- and S-enriched spots matched the pyrite standard, while their Se *K*-edge XANES spectra resembled FeSe₂ and Se(0) in terms of white line position and intensity (data not shown). However, further examination by Se *K*-edge EXAFS showed that their oscillations differed from those of FeSe₂ and Se(0) (Fig. 2). Quantitative EXAFS fitting suggested that Se substituted for S in the crystal structure of pyrite. These results were identified in pyrites from both the Wakkanai and Koetoi Formations. SEM observations of Se-enriched areas revealed that pyrite was framboidal (Fig. 1), which is known to form by microbial activity [2]. Sulfur isotope ratios is low ($\delta^{34}\text{S} = -34.3$ to -24.7%) with low variability.

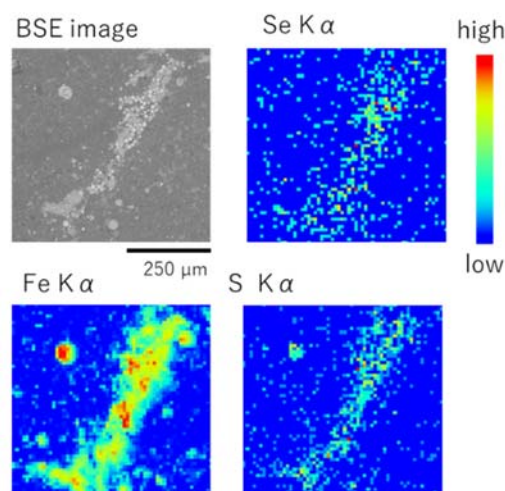


Fig. 1 SEM-BSE image and μ -XRF map of Se concentrated pyrite

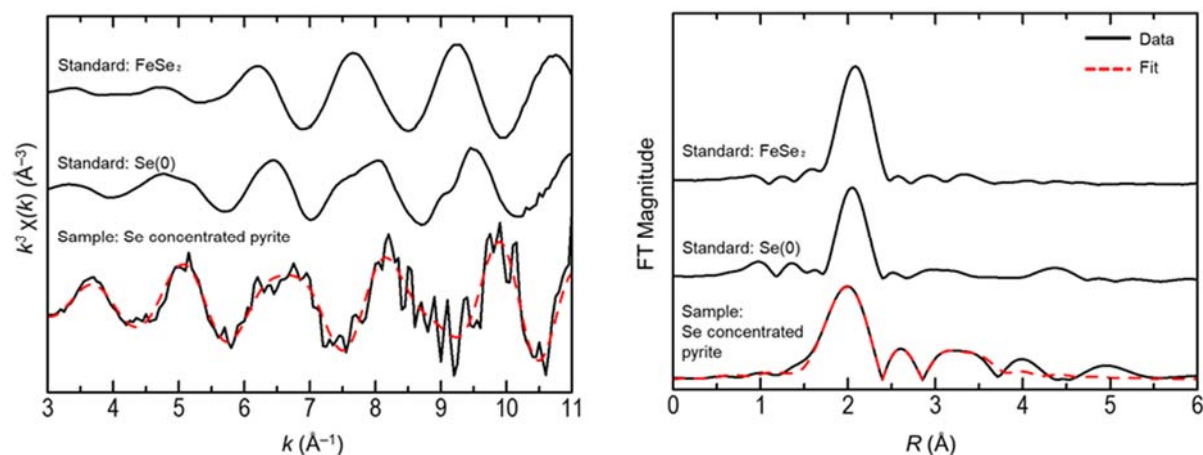


Fig. 2. k^3 -weighted Se K-edge EXAFS spectra (left) and corresponding phase-shift uncorrected Fourier transforms of Se concentrated pyrite (right), compared with standard phases.

Previous study [3] examining Se incorporation in natural pyrite reported that Se was structurally incorporated into euhedral pyrite, whereas it was associated with framboidal pyrite as a discrete FeSe_x phase. The different retention mechanism of Se in framboidal pyrites between our study and previous study may be explained by how Se initially reacted with pyrite: adsorption or coprecipitation. In laboratory experiments [4], selenide ($\text{Se}(-\text{II})$) ion adsorbed on pyrite was oxidized on the pyrite surface to phases like $\text{Se}(0)$ and FeSe_2 . On the other hand, coprecipitation experiments of Se with pyrite showed that selenide was incorporated into the pyrite structure [5]. Based on these results, in the Horonobe area, it is likely that Se was coprecipitated with framboidal pyrite under the strongly reducing condition which selenide ion could exist as a dissolved species.

This study is the first to show that Se was incorporated into the crystal structure of framboidal pyrite in natural environment. Since pyrite is contained within bedrock, it could be a potential sink for Se in the safety assessment of geological disposal. In addition, pyrite is expected to precipitate as a secondary mineral continuously, as the active cycling of sulfur between solid and dissolved forms would occur by organisms capable of oxidizing and reducing sulfur species in the sedimentary rock [6]. Our results suggest that Se released from HLW would be incorporated into the crystal structure of framboidal pyrite.

References

- [1] Kulp, T. R. and Pratt, L. M. (2004): Speciation and weathering of selenium in upper cretaceous chalk and shale from South Dakota and Wyoming, USA, *Geochim. Cosmochim. Acta*, 68, 3687–3701.
- [2] Wilkin, R. T. and Barnes, H. L. (1997): Formation process of framboidal pyrite, *Geochim. Cosmochim. Acta*, 61, 323–339.
- [3] Matamoros-Veloza, A., et al. (2014): Selenium speciation in framboidal and euhedral pyrites in shales, *Environ. Sci. Technol.*, 48, 8972–89794.
- [4] Naveau, A. et al. (2007): Interactions of aqueous selenium ($-\text{II}$) and (IV) with metallic sulfide surfaces. *Environ. Sci. Technol.*, 41, 5376–5382.
- [5] Diener, A. et al. (2012): Structure of selenium incorporated in pyrite and mackinawite as determined by XAFS analyses. *J. Contam. Hydrol.*, 133, 30–39.
- [6] Hermsdorf, A. W. et al. (2017): Potential for microbial H_2 and metal transformations associated with novel bacteria and archaea in deep terrestrial subsurface sediments, *ISME J.*, 11, 1915–1929.

*This work was part of “The project for validating near-field assessment methodology in geological disposal (FY2020-2022, JPJ007597)” supported by the Ministry of Economy, Trade and Industry of Japan.

PA6-1 FORMATION OF STABLE U(VI) COLLOIDAL PARTICLES IN RELEVANT ENVIRONMENTAL CONDITIONSBarbier H el ene ⁽¹⁾, Szenknect St ephanie ⁽¹⁾, Rebiscoul Diane ⁽¹⁾*(1) ICSM, Univ Montpellier, CNRS, CEA, ENSCM, France*

Contamination of the environment by actinides results from military activities and activities related to the nuclear fuel life cycle from uranium mining to radioactive waste materials disposal. Potential dissemination of these elements in the geosphere occurs mainly by transport in surface water and groundwater. However, the mobility of actinides is strongly limited by their solubility and by the sorption capacity of geological materials. The behavior of these elements in environmental conditions is evaluated by geochemical transport modeling that rely on the accurate prediction of their speciation in various situations. Nevertheless, most of these models do not take into account the existence of actinides intrinsic colloids or polynuclear species due to lack of knowledge regarding their nature and their stability domains. In this context, this work is dedicated to the identification of U(VI) colloids or polynuclear species, which form under geochemical conditions relevant for radioactive waste disposal, uranium mining sites, or unsaturated zone of sites contaminated by former military activities or nuclear accidents.

To reach this goal, we propose a simple, reliable and systematic method based on geochemical simulations, elemental analyses by ICP-AES and *in situ* Small Angle X-ray Scattering (SAXS) characterization of aerated solutions having simplified composition. This method ultimately allows the identification of unknown U(VI) species and their predominance domain.

Several synthetic solutions were prepared under air by dissolving NaCl, Na₂SO₄, Na₂SiO₃ or CaCl₂ salts in 200 mL of deionized water. The concentrations in Si and Ca were limited by the solubility of silica and calcite, respectively at room temperature and under air (pCO₂ = 400 ppm). A 0.2 mol.L⁻¹ UO₂(NO₃)₂ stock solution (pH ~ 1) was used to prepare simplified solutions at 1 mmol.L⁻¹. The pH of these solutions was then adjusted to 7, 8, 9, 10 with 1 mol.L⁻¹ NaOH solution. The solutions were introduced in a Teflon reactor and placed on an orbital shaker for the total duration of the experiment. At regular time interval, 2.5 mL of solution were sampled and centrifuged at 4500 rpm during 5 min. 0.5 mL of the supernatant were added to 4.5 mL of 0.2 mol.L⁻¹ HNO₃ solution and 1.5 mL were filtered using 10 KDa membrane in Vivaspin® tubes. These membranes retained particles smaller than 2 nm in diameter. The distribution of U between soluble and colloidal forms was deduced from the analysis of the two samples by ICP-AES. SAXS was used to characterize the colloidal particles in solutions as soon as the elemental concentration in U in the centrifuged and 10 KDa filtered fractions were stabilized. The solution was introduced in glass capillary, then SAXS analyses were carried out in transmission geometry with a Xenocs setup equipped with a Mo anode ($\lambda = 0.71 \text{ \AA}$). The scattered intensity at an absolute scale (cm⁻¹) was expressed versus the magnitude of the scattering vector $q = (4\pi \sin \theta)/\lambda$, where θ was the scattering angle. The experimental set-up allows covering a scattering vector range of 0.2 to 10 nm⁻¹. From the SAXS patterns, the density of objects in solution, their gyration radius their volume and their density were calculated from the Guinier approximation and the Kratky plot using the invariant value [1].

The results obtained showed the presence of colloidal particles in all the solutions. The fraction of uranium in colloids was found to increase from 50 % to 90 % with the pH of the NaCl and Na₂SO₄ solutions, whereas it was higher than 95 % and independent of the pH for Na₂SiO₃ and CaCl₂ solutions. These results indicated a strong impact of Ca and Si in the formation of U(VI) colloids. Shi et al. [2] also concluded that Ca, Na and Si were responsible for the formation of U(VI) intrinsic colloids under near neutral and alkaline conditions. Geochemical simulations with Phreeqc software and the

Thermochimie V10 database [3] indicated that U speciation was dominated by uranyl carbonates species $(\text{UO}_2)(\text{CO}_3)_2^{2-}$ and $(\text{UO}_2)_2(\text{CO}_3)(\text{OH})_3^-$. In presence of Ca, ternary complexes of $\text{Ca}_x\text{UO}_2(\text{CO}_3)_3^{-4+2x}(\text{aq})$ ($x = 1 ; 2$) were predominant at pH 9 and 10. By considering their size, these complexes should not be retained by the 10 KDa membrane [4, 5]. The solutions were all oversaturated with respect with uranyl phases, however the precipitation of uranium was not observed at the timescale of the experiments and the colloidal suspensions formed within hours remained stable (Figure 1a). Similar results were obtained by Bots et al. [1] in hyperalkaline solutions.

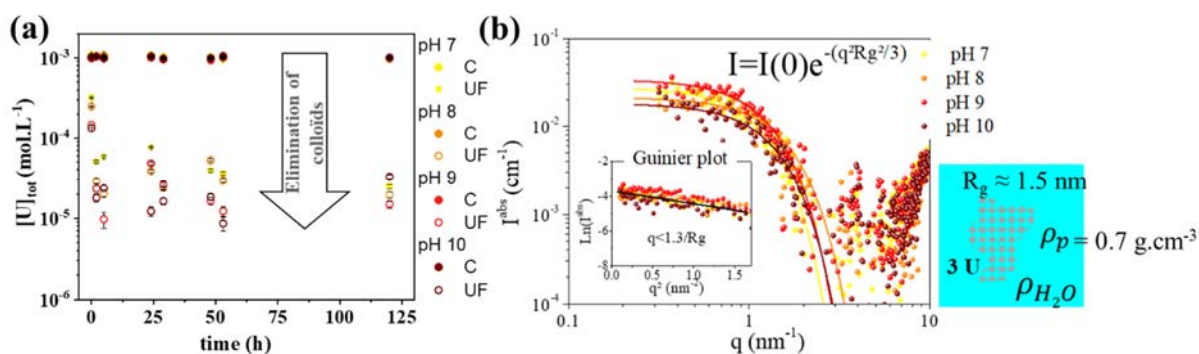


Figure 1: (a) Evolution of the elemental concentration in uranium in solution containing 2 mmol.L^{-1} of Si at pH 7 to 10 after centrifugation (C) and after filtration at 10 KDa (UF). (b) Scattering patterns of the solutions containing 1 mmol.L^{-1} of U and 2 mmol.L^{-1} of Si at pH 7 to 10 after 120 h (dots) and corresponding models (lines).

Using SAXS we were able to determine the concentration and the size of the colloids in suspension in the different solutions. As an example, Figure 1 b shows the experimental data obtained in the Na_2SiO_3 solution with the calculated characteristics of the colloids existing in solution. In addition, knowing the concentration of dissolved U(VI) in solution and the one in colloids we were able to estimate the energetics of the underlying process of integration of U(VI) in the colloids. This method opens new perspectives to understand the actinide behavior in solution.

References

- [1] Bots, P. et al. (2014). Formation of Stable Uranium(VI) Colloidal Nanoparticles in Conditions Relevant to Radioactive Waste Disposal. *Langmuir* 30: 14396-14405
- [2] Shi, Y. L. et al. (2021). Effect of pH on the formation of U(VI) colloidal particles in a natural groundwater. *Journal of Radioanalytical and Nuclear Chemistry* 328: 785-794
- [3] Grivé, M., L. Duro, E. Colàs and E. Giffaut (2015). Thermodynamic data selection applied to radionuclides and chemotoxic elements: An overview of the ThermoChimie-TDB. *Applied Geochemistry* 55: 85-94
- [4] Gückel, K., S. Tsushima and H. Foerstendorf (2013). Structural characterization of the aqueous dimeric uranium(VI) species: $(\text{UO}_2)_2\text{CO}_3(\text{OH})_3^-$. *Dalton Transactions* 42: 10172-10178
- [5] Bernhard, G. et al. (2001). Uranyl(VI) carbonate complex formation: Validation of the $\text{Ca}_2\text{UO}_2(\text{CO}_3)_3(\text{aq})$ species. *Radiochimica Acta* 89: 511-518

PA6-2 STABILITY OF EUROPIUM(III)/THORIUM(IV)-SILICATE COLLOIDS: EFFECT OF SI CONTENT, PH, ELECTROLYTE AND FULVIC ACID

Daming Zhang ^(1,2), Qiang Jin ^(1,2), Zongyuan Chen ^(1,2), Zhijun Guo ^(1,2) □

(1) *Frontiers Science Center for Rare Isotopes, Lanzhou University, 730000 Lanzhou, China*

(2) *Radiochemistry Laboratory, School of Nuclear Science and Technology, Lanzhou University, 730000 Lanzhou, China*

Actinides (An) are of most concern among the radionuclides in terms of nuclear waste disposal because their major isotopes have very long half-lives and are extremely toxic. In recent years, it is recognized that the contribution of An-containing colloids is non-negligible and must be considered for precise prediction of the migration of An in the environment ^[1,2]. In this context, the tendency of An to form colloids has been a topic in actinide research for more than a decade. Silicon is ubiquitous in the environment as a result of weathering dispersion of amorphous silica and silicate minerals. It has long been known that there is a strong affinity between An of different valences and dissolved silicic acid. Considering the high concentration of silicon in the aqueous phase (10^{-5} – 10^{-3} M) and sparing solubility of An silicates, the generation of An bearing silicate colloids cannot be neglected when investigating the chemical behavior of An in natural aquatic systems. Although the structure and formation of An-silicate colloids have been fundamentally understood ^[3,4], further research is still needed to elucidate the environmental behavior of this type of colloids.

The stability of An-silicate colloids may be essential to reveal the role of An-bearing colloids in the environment but few investigations have been dedicated to this issue. In the present work, Eu(III) and Th(IV) were chosen as representative of hexavalent and tetravalent actinides. Eu(III)/Th(IV)-silicate colloids of different compositions were prepared, and the stability of the colloids was characterized by investigating the aggregation kinetics as a function of Si/An molar ratio, pH, background electrolyte, ionic strength and fulvic acid (FA). In addition, the Derjaguin-Landau-Verwey-Overbeek (DLVO) theory was employed to better illustrate the experimental results.

Results indicated that stable colloids could form in aqueous phase by the reaction of An (0.1–0.2 mM) with silicic acid (2–5 mM) at alkaline conditions (pH 7.9–9.4). As the increase of Si concentration in the reaction system, the final Si/An molar ratio of both colloids increased. The stability of Eu(III)/Th(IV)-silicate colloids increased with the Si/An molar ratio. More negative charges were developed on the surfaces of the colloids with higher Si/An molar ratio, which resulted in stronger electrostatic repulsion between the colloidal particles. The inhibition effect of monovalent ions on the stability of Eu(III)/Th(IV)-silicate colloids followed the order of $\text{Na}^+ < \text{K}^+ < \text{Cs}^+$ and $\text{Cl}^- < \text{NO}_3^- < \text{ClO}_4^-$, which was consistent with the Hofmeister effects, i.e., ions with larger ionic radii have smaller hydrated radii and thus show stronger charge screen effect. The presence of FA significantly increased the colloid stability due to the increase in surface electrostatic potential and the steric effect of FA as well. The stability of the colloids decreased somewhat with decreasing pH due to the decrease in the absolute value of the zeta potential. The influences of pH, electrolytes, the presence of FA, and the Si/An molar ratio of the colloids could be well illustrated by the DLVO theory. Finally, it was found that the aggregation process of Eu(III)-silicate colloids was not fully reversible. There was a time-related size memory effect in the disaggregation process. The mean size of the disaggregated colloids was larger than that before aggregation.

This study revealed that An(III)/An(IV)-silicate colloids have a high stability under environmentally relevant conditions. Thus, the transport of An(III)/An(IV) could be expected in the silicon-rich environments. The further studies on transport and fate information of An(III)/An(IV)-silicate colloids should be performed under the alkaline conditions relevant to geological disposal of radioactive waste.

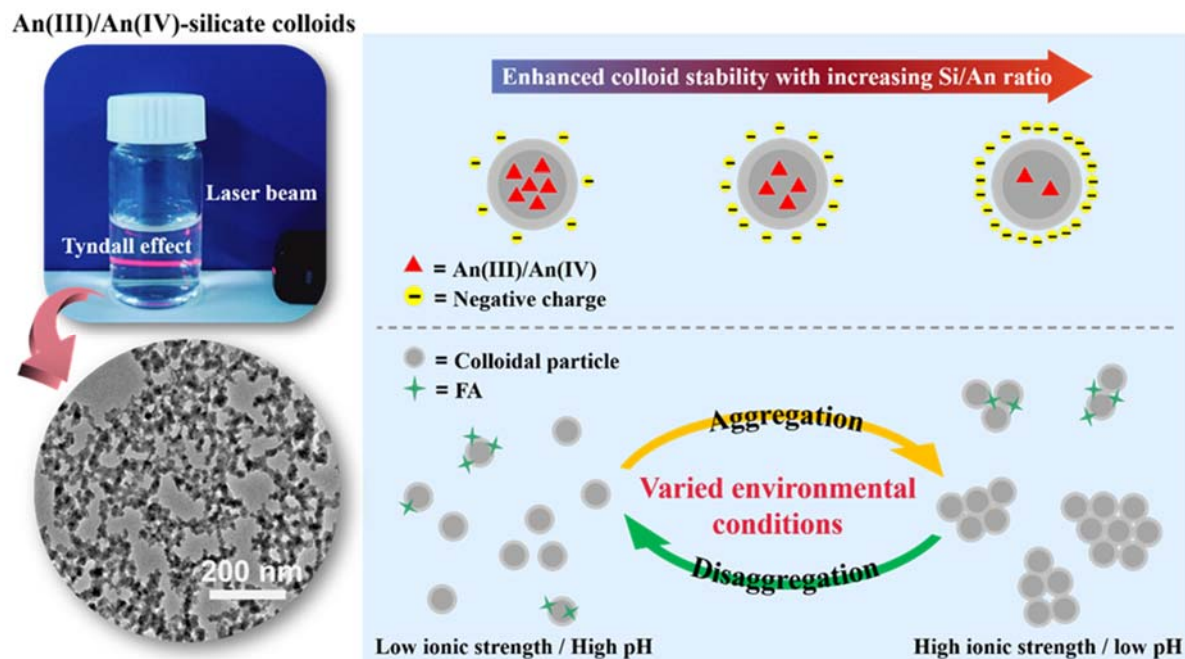


Figure 1. Schematic diagram of the effect of environmental factors on An(III)/An(IV)-silicate colloid stability.

References

- [1] Kersting, A.B., Efurud, D.W., Finnegan, D.L., Rokop, D.J., Smith, D.K., Thompson, J.L. (1999). Migration of plutonium in ground water at the Nevada Test Site. *Nature* 397: 56-59.
- [2] Novikov, A.P., Kalmykov, S.N., Utsunomiya, S., Ewing, R.C., Horreard, F., Merkulov, A., Clark, S.B., Tkachev, V.V., Myasoedov, B.F. (2006). Colloid transport of plutonium in the far-field of the Mayak Production Association, Russia. *Science* 314: 638–641.
- [3] Hennig, C., Weiss, S., Banerjee, D., Brendler, E., Honkimäki, V., Cuello, G., Ikeda-Ohno, A., Scheinost, A.C., Zänker, H. (2013). Solid-state properties and colloidal stability of thorium(IV)-silica nanoparticles. *Geochim. Cosmochim. Acta* 103: 197-212.
- [4] Husar, R., Weiss, S., Hennig, C., Hübner, R., Ikeda-Ohno, A., Zänker, H. (2015). Formation of neptunium (IV)-silica colloids at near-neutral and slightly alkaline pH. *Environ. Sci. Technol.* 49: 665-671.

PA6-3 THE STABILITY AND INTERACTION OF COLLOIDS AND THEIR EFFECTS ON RADIONUCLIDE TRANSPORT REGARDING TO HLW DISPOSAL IN GRANITIC FORMATION

Zhijun Guo ^(1,2), Pengyuan Gao ⁽²⁾, Zongyuan Chen ^(1,2), Qiang Jin ^(1,2), Wangsuo Wu ^(1,2)

(1) *Frontiers Science Center for Rare Isotopes, Lanzhou University, P. R. China*

(2) *Radiochemistry Laboratory, School of Nuclear Science and Technology, P. R. China*

The disposal of high-level radioactive waste (HLW) is one of bottleneck problems restricting sustainable development of nuclear industry, especially the nuclear power plant. Since 1980s, a "three-step" development strategy has been adopted for China's HLW geological disposal, i.e., from sitting to research in underground research laboratory (URL), and then to the construction of HLW repository. At present, an URL in granitic formation located in Beishan region is under construction. Before in-situ radionuclide (RN) migration research in URL, it is necessary to carry out adsorption and transport studies of key RNs under ambient conditions.

The stability of colloids from engineering barriers. Besides the interactions of the autochthonal colloids in the groundwater, factious colloids from engineering barriers play an important role regarding the alteration of radionuclide transport behaviors, especially for highly charged actinides which were considered to be immobile. The formation and stability of intrinsic colloids of trivalent and tetravalent lanthanides /actinides (Ln/An) silicate/borate have been studied to evaluate their speciation and potential transport (as colloids or ions) when released from the corrosion of vitrification glass.

Adsorption of RNs on Beishan granite and related minerals. Adsorption of Eu(III)/Am(III), Co(II)/Ni(II), U(VI), Se(IV) and Se(VI) on crushed Beishan granite has been studied as a function of important in-situ factors, such as pH, ionic strength, temperature, background electrolyte, atmosphere and the presence of fulvic/humic acid. Granite is an igneous rock consisting of a number of minerals, which makes adsorption modeling still a challenge. A generalized composite (GC) approach, in which granite is integrally considered and surface reactions are assumed to take place on a type of "general" surface sites, was applied for modeling. Surface complexation models (SCMs) based on GC approach can quantitatively describe the adsorption on crushed Beishan granite, and we also found that: 1) different site capacities have to be considered for different elements; 2) the model for Eu(III) could be extended to describe Am(III) adsorption [1]; and 3) the model for U(VI) could describe the literature data for granite from different regions [2].

Theoretical calculation has been considered as a useful tool to elucidate adsorption reaction mechanism at solid-liquid interface. We carried out the DFT simulations for Am(III) adsorption on montmorillonite. By comparing the DFT calculation results and a surface complexation model based on batch experiments, we found that "monodentate surface complex" in the context of SCM means only stoichiometric coefficient of 1, other than structurally monodentate binding. Besides, we calculated the pKa values of 2:1-type cis-vacant clay edge surfaces and then apply the atomic-level acidity constants to construct an SCM and predict surface properties as a function of pH and ionic strength [3]. By comparing obtained results with the previous pKa values and SCM models of trans-vacant layer edge surfaces, we elucidated that the cis and trans-vacant clay edge surfaces possess different acid-base properties.

The effect of colloids on RN transport in granite/quartz media. Colloids composed of inorganic minerals and organic matter in the environment can act as carriers for RNs, and significantly alter RN transport behaviors. Thus, a systematic co-transport study was performed with RN and colloidal oxygen/hydroxide, clay minerals and humic/fulvic acid (HA/FA) in the saturated quartz sand and

Beishan granite media. In general, colloidal clay minerals (kaolin, bentonite and illite) promoted RN transport. The presence of akaganeite colloid (AKC) facilitated U(VI) transport at relatively low U(VI) concentration, but impeded U(VI) transport at relatively high U(VI) concentration [4]. HA strongly affected the transport of colloidal aluminum and ferric hydroxide/oxide by forming composite colloids with them. The effect of HA on the co-transport of U(VI) and gibbsite colloids is dependent to HA amount. Gibbsite colloids impeded U(VI) transport at relatively low HA concentration, and facilitated U(VI) transport at relatively high HA concentration.

References

- [1] Jin Q. et al., (2014). The adsorption of Eu(III) and Am(III) on Beishan granite: XPS, EPMA, batch and modeling study. *Appl. Geochem.* 47: 17-24.
- [2] Jin Q. et al., (2016). Surface complexation modeling of U(VI) adsorption on granite at ambient/elevated temperature: Experimental and XPS study. *Chem. Geol.* 433: 81-91.
- [3] Gao P. et al., (2023). Acid–Base Properties of Cis-Vacant Montmorillonite Edge Surfaces: A Combined First-Principles Molecular Dynamics and Surface Complexation Modeling Approach. *Environ. Sci. Technol.* 2023, 57: 1342–1352.
- [4] Ge Z. et al., (2018). Co-transport of U(VI) and akaganéite colloids in water-saturated porous medium: Role of U(VI) concentration, pH and ionic strength, *Water Res.* 147: 350-261.

PA7-1 AN “ON-OFF” RATIOMETRIC FLUORESCENT SENSOR FOR UO_2^{2+} BASED ON Ag^+ -MODIFIED GOLD NANOCCLUSERS HYBRID

Xiaohong Cao, Zhibin Zhang, and Yunhai Liu

State Key Laboratory of Nuclear Resources and Environment, East China University of Technology, Nanchang, Jiangxi 330013, P.R. China

Since its discovery in 1789, uranium has been widely used in military and civilian applications. In an aqueous environment, uranium with high ionic mobility can enter the human body through inhalation, wounds and other pollution channels, causing irreversible harm to the human body. The World Health Organization (WHO) defines the guideline value of uranium in water as 15 ppb. Therefore, there is an urgent need to develop a sensitive and selective method for detecting uranyl ions (UO_2^{2+}). Fluorescence analysis of heavy metal ions and radioactive ions has attracted increasing attention in recent years owing to its affordability, high sensitivity, facile operation, and portability.

Herein, we successfully designed an "on-off", shell-protected novel ratiometric fluorescent probe ($\text{B-CDs@SiO}_2\text{@GSH-AuNCs/Ag}^+$) by first encapsulating blue-fluorescent carbon dots (B-CDs) with SiO_2 , coupling gold nanoclusters (GSH-AuNCs) to the surface, and finally anchoring a layer of Ag^+ . The prepared $\text{B-CDs@SiO}_2\text{@GSH-AuNCs/Ag}^+$ probes showed two fluorescence emission peaks corresponding to the emission peaks of B-CDs@SiO_2 ($\lambda_{\text{em}} = 440 \text{ nm}$) and GSH-AuNCs ($\lambda_{\text{em}} = 627 \text{ nm}$), respectively, indicating the successful synthesis of the ratiometric fluorescent sensor (Fig. 1).

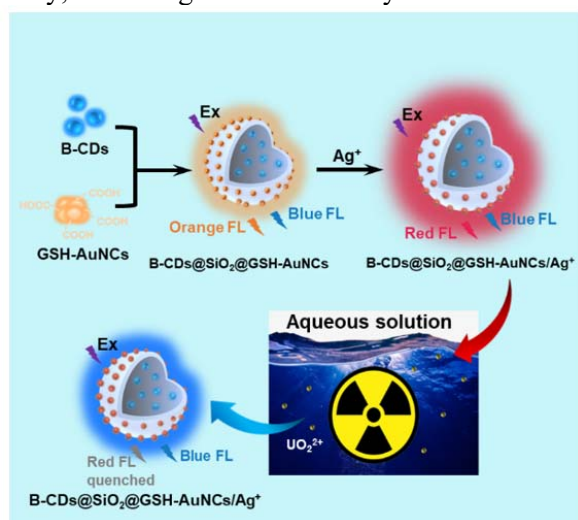


Figure 1. The preparation process of $\text{B-CDs@SiO}_2\text{@GSH-AuNCs/Ag}^+$ and the schematic diagram of the detection of UO_2^{2+}

In chloroacetate-sodium acetate buffer solution at pH 3.0, the fluorescence emission peak at 627 nm was gradually quenched with increasing UO_2^{2+} concentration. A linear relationship was observed over the concentration range of 0.5–1 $\mu\text{mol/L}$, and the limit of detection (LOD) was calculated as 37 nmol/L ($S/N = 3$). It is worth mentioning that the ratiometric fluorescent sensor underwent a color change from red to purple to blue with the increasing UO_2^{2+} concentration, making it particularly suitable for on-site visual detection. The ratiometric fluorescent probes also exhibited excellent selectivity, especially for Hg^{2+} , indicating good potential for rapid monitoring in practical applications (Fig. 2).

In addition, we demonstrated the quenching mechanism between $\text{B-CDs@SiO}_2\text{@GSH-AuNCs/Ag}^+$ and UO_2^{2+} using HOMO–LUMO orbital theory. From the UV-Vis and Tauc plots, the optical band gaps (E_g) of both can be calculated to be located at 3.80 eV and 2.71 eV, respectively, while the valence band X-ray photoelectron spectroscopy (VB-XPS) revealed the HOMO energies (E_{HOMO}) of both to be -2.90 eV and -3.14 eV, respectively. According to the equation ($E_{\text{LUMO}} = E_{\text{HOMO}} + E_g$), the corresponding LUMO energies (E_{LUMO}) of both can be calculated as 0.90 eV and -0.43 eV, respectively. Therefore, the

quenching mechanism between B-CDs@SiO₂@GSH-AuNCs/Ag⁺ and UO₂²⁺ can be attributed to photoinduced electron transfer (PET), as shown in Fig. 3.

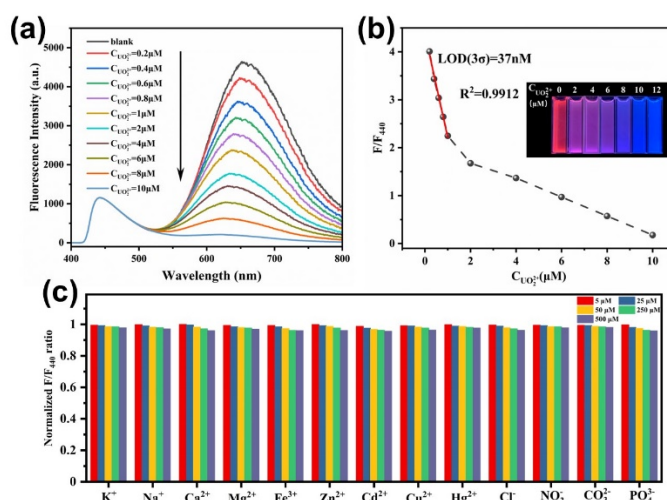


Figure 2. The performance and mechanism of B-CDs@SiO₂@GSH-AuNCs/Ag⁺ for UO₂²⁺ detection.

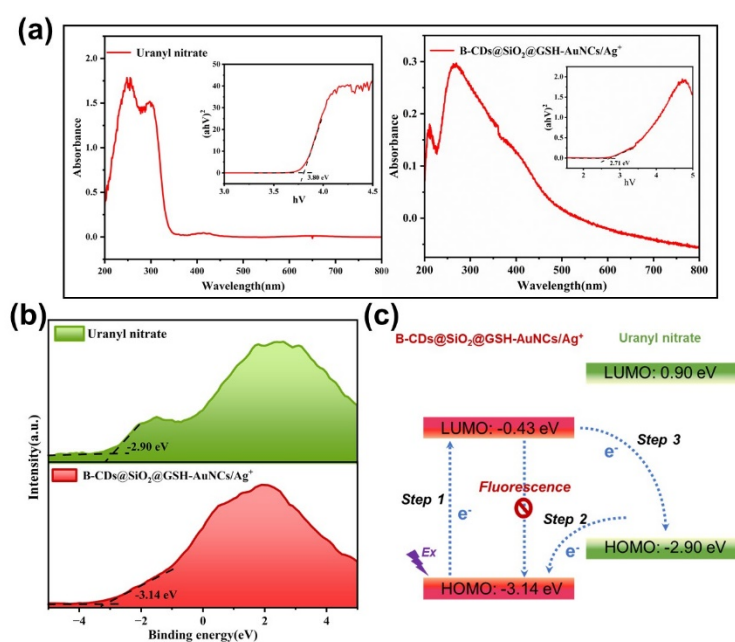


Figure 3. (a) UV-Vis absorption spectra and Tauc plot (inset). (b) XPS-VB spectra. (c) PET process between B-CDs@SiO₂@GSH-AuNCs/Ag⁺ and uranyl nitrate.

References

- [1] Hua-Rui Nan, and Xiao-Hong Cao et al. (2022), An inner-filter-effect based ratiometric fluorescent sensor for the detection of uranyl ions in real samples, *Anal. Methods*. 14:532-540.
- [2] Sang-Hyun and Injae Shin et al. (2020) Synthetic ratiometric fluorescent probes for detection of ions, *Chem. Soc. Rev.* 49:143-179.
- [3] Yu-Syuan Lin, and Huan-Tsung Chang, et al. (2021) Polymer/glutathione Au nanoclusters for detection of sulfides, *Sens. Actuators B Chem.* 333:129356.
- [4] Yi-Fan Wang, and Li Xu, et al. (2022) One-pot synthesis of boron and nitrogen co-doped silicon-carbon dots for fluorescence enhancement and on-site colorimetric detection of dopamine with high selectivity, *Appl. Surf. Sci.* 573 : 151457.

PA7-2 TRACING AND QUANTIFICATION OF ²²⁶Ra IN TAILINGS BY SPECTROSCOPIC AUTORADIOGRAPHY

Hugo Lefevre ^(1,2), Sophie Billon ⁽¹⁾, Michael Descostes ⁽³⁾, Jérôme Donnard ⁽⁴⁾, Samuel Duval ⁽⁴⁾, Paul Sardini ⁽¹⁾

(1) IC2MP – HydrASA, Poitiers University, France, (2) ERM, France (3) ORANO Mining, Env. R&D Dpt, France, (4) AI4R (SAS), France

Geoscience is a field of study where nuclear instruments find their place for conducting specific measurements of radioactivity, usually to monitor natural occurring radioactivity, such as for uranium mining activities. Among the radiometric techniques that measure the bulk radioactivity of a sample, there are gamma and alpha spectrometers. Then, to have an idea of the chemical elements distribution inside the sample, a commonly used instrument is scanning electron microscope (SEM) associated with Energy-dispersive X-ray spectroscopy (EDS) or wavelength-dispersive X-ray spectroscopy (WDS).

In uranium mine site, tailings that are stored at surface, still contain 85% of the initial radioactivity of the uranium ore, mainly due to the ²³⁸U decay products. In these uranium mine tailings, the location and identification of the minerals bearing this remaining radioactivity is important for relating radionuclide (RN) concentrations to mineralogy. Indeed, it is crucial to understand the trapping mechanisms of these RN in the solid, in order to predict their long-term stability into the tailings or their possible migration into the surrounding environment. However, locate these RN (such as ²²⁶Ra) remains a challenge since they occur at ultra-trace level, far lower than the detection limit [1] of conventional techniques such as EDS.

Autoradiography technique [2] can locate, at the thin-section scale (4.5 × 3.0 cm²), these radionuclides, using their radioactive emissions. BeaQuant, a parallel ionization multiplier gaseous detector, can discriminate beta emissions from alpha emissions. But this gaseous device is limited to perform discrimination among different beta emitters or among different alpha emitters: identifying ²²⁶Ra (alpha emitter) when other alpha emitting RN such as ²³⁸U, ²³⁴U, ²³⁰Th... are present, is not possible.

The present study aims to provide spectroscopic autoradiography (SA) [3] analysis method for measuring the initial energy of alpha particles with the BeaQuant gaseous detector. This method, that has been developed thanks to Geant4 [4] modelling of the detector, focuses on alpha particles because 1- the RN of interest are alpha emitters, 2- the detection efficiency is better for alpha than for beta, 3- alpha particles have a discrete energy of emission compared to beta that have a continuous emission spectrum. This spectroscopic autoradiography method was successfully used to reproduce the alpha spectra from a uranium ore at secular equilibrium (the whole ²³⁸U decay chain) with a spatial resolution of at least 50 μm and an energy spectrum resolution of 17.2% (FWHM) at 4647 keV. Even if the efficiency of SA is low (4.4%) compared to the simple detection efficiency of autoradiography (50%), this measurement approach offers the opportunity to select areas of interest on an autoradiography to perform an energy spectrum analysis within that area.

The alpha emitters from ²³⁸U decay chain present initial emission energy ranging from 4.2 MeV for ²³⁸U to 7.7 MeV for ²¹⁴Po. By studying more precisely the alpha energy spectrum and the half-life of each RN, it appears possible to apply a thresholding on the energy spectrum to discriminate the ²²⁶Ra from the first alpha emitters of the ²³⁸U decay chain (i.e. ²³⁸U, ²³⁴U and ²³⁰Th, all below 5 MeV).

The developed method is applied to mine tailings prepared in the form of thin sections, and the resulting maps (Figure 1c) highlight different signals area: signal “1” with areas close to the secular equilibrium, signal “2” with areas presenting a deficit of the 3 first alpha emitters of the ²³⁸U decay chain (i.e. ²³⁸U, ²³⁴U and ²³⁰Th) (in green in Figure 1c) and signal “3” for areas with a deficit of the 5 last alpha emitters (from ²²⁶Ra to the end of the decay chain) (in dark blue in Figure 1c). Some of these regions of interest have been observed/analyzed with SEM-EDS, allowing to highlight:

-radium-rich barite (BaSO_4 with 5 ppm of ^{226}Ra) in the signal “2” area. ^{226}Ra is incorporated into the mineral structure through solid solution mechanism.

-siderite (FeCO_3) containing uranium (up to 1% detected in EDS) in the signal “3” (Figure 1a). Uranium in the siderite is not at secular equilibrium, that means this uranium has been remobilized during the ore treatment (for uranium recovery), and later trapped by surface mechanisms on siderite.

If areas showing a secular equilibrium have been highlighted (that is not the case in the studied tailings), they should correspond to uranium bearing minerals inherited from ore and thus not impacted by ore treatment.

Spectroscopic autoradiography opens up possibilities for the detailed analysis of heterogeneous geological samples containing natural alpha emitters such as uranium-238 and radium-226: The ^{226}Ra can be localized and quantify at ultra-trace content; and the method devolved also can help to identify newformed young uranium phases by measuring $^{238}\text{U}/^{226}\text{Ra}$ ratio equilibrium state. These analyses will then be used to implement the reactive transport models build to study the mobility of ^{238}U and ^{226}Ra in the mine tailings and the surrounding.

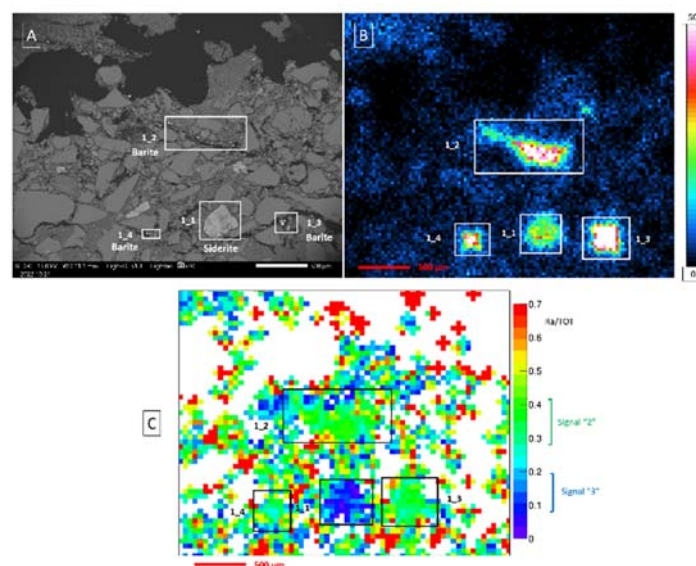


Figure 1: Analyse in a region of mine tailing: A) SEM mapping, B) autoradiography mapping of alpha particle, C) Ra/U ratio analyse with SA method.

References:

- [1] H.E. Çubukçu, O. Ersoy, E. Aydar, U. Çakir (2008). WDS versus silicon drift detector EDS: A case report for the comparison of quantitative chemical analyses of natural silicate minerals. *Micron*. 39: 88–94.
- [2] P. Sardini, A. Angileri, M. Descostes, S. Duval, T. Oger, P. Patrier, N. Rividi, M. Siitari-Kauppi, H. Toubon, J. Donnard (2016). Quantitative autoradiography of alpha particle emission in geo-materials using the BeaverTM system, *Nuclear Instruments and Methods in Physics Research Section A*. 833: 15–22
- [3] H. Lefeuvre, J. Donnard, M. Descostes, S. Billon, S. Duval, T. Oger, H. Toubon, P. Sardini (2022). Spectroscopic autoradiography of alpha particles using a parallel ionization multiplier gaseous detector. *Nuclear Instruments and Methods in Physics Research Section A*. 1035: 166807
- [4] S. Agostinelli et al., (2003). Geant4—a simulation toolkit. *Nuclear Instruments and Methods in Physics Research Section A*. 506: 250–303.

PA7-3 DEVELOPMENT OF ANALYTICAL PROTOCOL FOR DIFFICULT TO MEASURE RADIONUCLIDES IN METALLIC MATRIX; EXEMPLE OF ZR-93 IN STAINLESS STEEL AND INCONEL METALS

Suzuki-Muresan Tomo ⁽¹⁾, Mokili Marcel ⁽¹⁾, Abdelouas Abdesselam ⁽¹⁾, Bessaguet Nicolas ⁽¹⁾, Cassette Philippe ⁽³⁾, Happel Steffen ⁽²⁾, Montavon Gilles ⁽¹⁾

(1) *SUBATECH UMR6457 (IMT Atlantique-CNRS IN2P3-Nantes Université), France*

(2) *TRISKEM International, France*

(3) *Sofia University, "St. Kliment Ohridski", Bulgaria*

The environmental monitoring of the radioactivity of difficult to measure radionuclides (DTM) released during and after deconstruction and dismantling operations or the evaluation of DTM radioactivity from nuclear wastes for disposal to minimize uncertainties for safety assessment require methods for their accurate detections and measurements.

These radionuclides (e.g. Cl-36, Fe-55, C-14, Ca-41, Mo-93, Ni-59, Se-79, Zr-93) are mainly characterized by their beta- emissions, X-ray or very low gamma-intensity emissions ($I < 0.003\%$). They are usually estimated by scaling factors when the characterization and the inventory are not available or accessible. The evaluation is based on the correlation between the activity of the sample and a key radionuclide (eg. Co-60, Cs-137). Unlike this correlation may work for activated samples with a knowledge of the characteristics of the sample, it becomes more complex and difficult for contaminated samples (for example: liquid effluents, metallic surfaces in nuclear facilities, environmental solids (eg. soil), ion exchange resins...). Origins may be found in the various physico-chemistry (pH/Eh) properties of radionuclides, in precipitation/volatilization reactions... This study is motivated by the development of a robust analytical method dedicated to the measurement of DTM. Therefore, in this context we intend to develop and optimize radiochemical protocols for the detection of DTM in order to quantify precisely their activity.

For this purpose, we have selected Zr-93 formed by the neutron activation of Zr-92 in the zircaloy cladding (a few ppm) and also resulting from the fission of U-235 (20% of the zirconium fission products inventory). Zr-93 is a long-lived radionuclide ($T_{1/2} 1.61 \times 10^6$ years) decaying via two beta minus transitions, with maximum beta energies of 59.5 keV (73%) to Nb-93m and 90.3 keV (27%) to the Nb-93 ground state. As the half-life of Nb-93m is 16 years, there is no coincident gamma emission with the beta transition. In the repository, Zr-93 contributes significantly to the long-term nuclear waste activity: it is the second largest contributor to the fission product activity after 1000 years [1]. It is therefore important to develop measurement and quantification methods to refine the quantity of Zr-93 and thus its activity in the waste packages. For the experiments, we used oxidized and non-oxidized metallic solids (nickel based alloy – inconel) on which surface contamination may be found in steam generator. Steam generator metallic wastes are planned to be stored in repository site, and the knowledge of a precise radioactivity will also allow to reduce uncertainties on the performance assessment of the site. The figure 1 shows the general strategy deployed for the measurement of Zr-93 from solid metal. It is based on three main optimizations: 1/Optimization of the detection and measurement of Zr in acidic media by ICP-MS; 2/ Optimization of the separation of Zr from other chemical elements present in the metallic material on chromatographic resins; 3/ Optimization of the detection and measurement of Zr-93 by Liquid Scintillation Counting (LSC). Stable Zr-90 is used as a tracer for separation efficiency, but it is also used as a reference element for protocol optimization because of the difficulties in obtaining Zr-93 as a radioactive source and standard. The separation yield (Zr-90) is measured by ICP-MS and the activity of Zr-93 by LSC. The optimization of the separation on resins and of the detection sensitivity by ICP-MS give an efficiency of Zr recovery of 80%, and a retention of 100% of Fe, Ni, Cr, Mn, Sb, Ce, Y, Nb and Mo.

To overcome the supply of Zr-93 as a standard in the event of its unavailability, an efficiency tracing method using a Ni-63 standard is currently studied to calculate the Zr-93 detection efficiency in LSC. For this purpose, liquid scintillation counting of Ni-63 is carried out under similar conditions as Zr-93, i.e. from Zr elution solution of the last separation condition by UTEVA. Subsequently, Ni-63 standard measurement results are exploited to determine the theoretical counting efficiency of Zr-93 by theoretical calculation using the free parameter model in LSC [4]. The first results show that, even if the maximum beta energies of Ni-63 and Zr-93 are close, the counting efficiencies of Zr-93 are significantly different from those of Ni-63 and the direct use of Ni-63 as a standard [2, 3] leads to a systematic underestimation of the counting efficiency of Zr-93 by about 20%. This can be explained by the different shapes of the beta spectra of these two radionuclides.

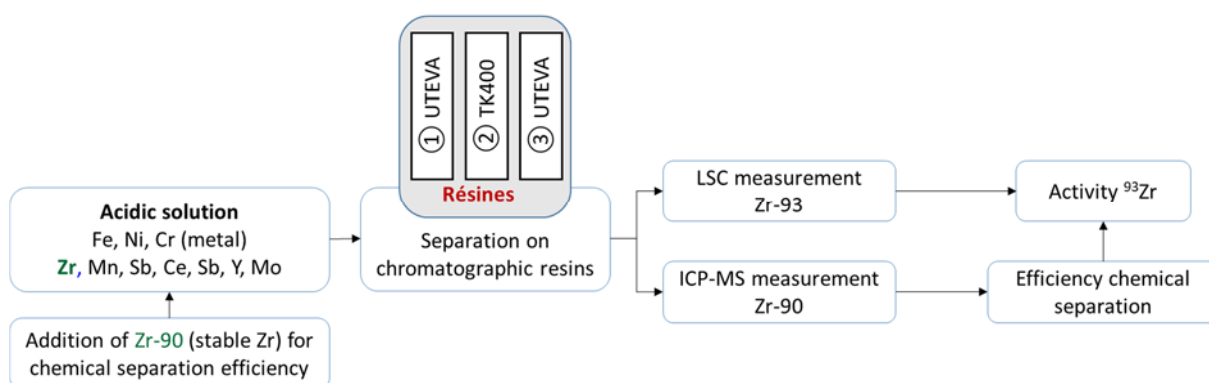


Figure 1: Strategy and methodology of Zr-93 activity evaluation from a metal sample

Acknowledgements: This work has received funding from the European Union's Horizon 2020 research and innovation programme (PREDIS) under agreement No 945098, and from the Labcom TESMARAC project.

References:

- [1] Cassette P, Chartier F, Isnard H, Fréchu C, Laszak I, Degros JP, Bé MM, Lépy MC, Tartes I (2010) Determination of ^{93}Zr decay scheme and half-life. *Appl Radiat Isot* 68:122–130
- [2] Monteiro RPG, Oliveira TC, Amaral AM, Mingote RM (2009) Radiochemical determination of ^{93}Zr in low and intermediate nuclear wastes. In: *International Nuclear Atlantic Conference*. Rio de Janeiro Brazil
- [3] Oliveira TC, Monteiro RPG, Oliveira AH (2011) A selective separation method for ^{93}Zr in radiochemical analysis of low and intermediate level wastes from nuclear power plants. *J Radioanal Nucl Chem* 289:497–501
- [4] Broda R, Cassette P, Kossert K. (2007). Radionuclide Metrology using Liquid Scintillation Counting. *Metrologia*. 44. S36. 10.1088/0026-1394/44/4/S06.

PA7-4 A RAPID DETERMINATION OF SELENIUM IN TEA SAMPLES USING ANION CHROMATOGRAPHIC COLUMN COMBINED WITH AUTOMATIC SYSTEM SEPARATION AND HR-ICP-MS MEASUREMENT ^[1]

Yawen Chen ^{(1) (2)}, Ning Guo ^{(2)*}, Keliang Shi ^{(1) (3)*}

(1) School of Nuclear Science and Technology, Lanzhou University, Lanzhou 730000, China

(2) Beijing National Laboratory for Molecular Sciences, Fundamental Science Laboratory on Radiochemistry & Radiation Chemistry, College of Chemistry and Molecular Engineering, Peking University, Beijing 100871, China

(3) Frontier Science Center for Rare Isotopes, Lanzhou University, Lanzhou 730000, China

The accurate determination of selenium (Se) concentration in tea is of utmost importance for ensuring quality control and safety as a Se supplement. Here, we present a rapid and automated method for determining Se in tea samples, involving mixed acid ($V_{\text{HNO}_3}:V_{\text{HClO}_4} = 4:1$) digestion followed by ion exchange chromatographic separation, coupled with high-resolution inductively coupled plasma mass spectrometry (HR-ICP-MS) measurement. The automated separation system applied in this work shortened the analytical time to less than 3 hours. Elution of Se from the column was achieved using 20 mL of HNO_3 ($> 5 \text{ mol L}^{-1}$), and more than 95% of Se was eluted using 20 mL of $6 \text{ mol L}^{-1} \text{ HNO}_3$. Interfering elements (Ca, Zn, and Cu) were effectively removed with decontamination factors of more than 1×10^6 . Additionally, most of the bromine (Br) was removed, thus the key interference of $^{81}\text{Br}^1\text{H}^+$ was significantly suppressed in the HR-ICP-MS measurement of ^{82}Se . The radionuclide ^{75}Se was used as a tracer to monitor Se loss during the entire separation procedure with an average chemical yield of $93.2 \pm 0.5\%$, which was within the 95% confidence interval. The developed method was validated using certified reference materials, and the measured values were in good agreement with the certified values, confirming the reliability and accuracy of the analytical method. This method was successfully applied to analyze Se content in commercially available tea samples, and could be further used for the investigation on Se migration in biological systems.

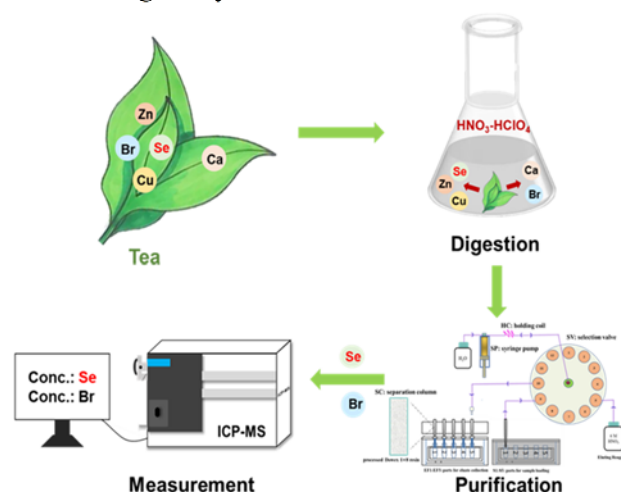


Figure 1. Scheme of Se determination in tea sample.

Acknowledgement: The financial support from National Natural Science Foundation of China (Nos. 22061132004, U21A20442, 21771093) are gratefully appreciated.

Reference

- [1] Chen, Y., Guo, N., Zhang, L., Hu, K., Yang, J., Shi, K. (2023). A rapid determination of selenium in tea samples using anion chromatographic column combined with automatic system separation and HR-ICP-MS measurement. *J Radioanal Nucl Chem.* <https://doi.org/10.1007/s10967-022-08707-1>

PA8-1 AN ATOMIC SCALE COMPUTATIONAL APPROACH TO UNDERSTANDING REDOX SPECIATION OF KEY ACTINIDES ON IRON BEARING MINERALS.

Corinne Hatton (1), Professor Nik Kaltsoyannis (1), Dr Louise Natrajan (1), and Professor Sam Shaw (1)

(1) University of Manchester, UK

The UK has been utilising nuclear power since 1956 and this has led to a build-up of nuclear waste, particularly high-level waste, which requires a cost effective, long-term storage solution in order to ensure important radionuclides and contaminated materials are not released into the environment. Currently, the UK and other nations around the globe have identified that a Geological Disposal Facility (*GDF*) may be the best long-term disposal route. Within a *GDF*, corrosion of steel leads to the formation of iron (oxyhydr)oxide minerals, and they are also being considered as a favourable mineral to use as the final *GDF* barrier. Uranium is the main component of spent nuclear fuel, although other actinides such as Np and Pu are also present. It is important to understand the interactions that occur between these elements and materials used within a *GDF* and how this might affect their long-term fate within a *GDF*. Ubiquitous natural minerals, such as those containing iron, can bind to uranium, inducing chemical changes that have important implications for its mobility in the geosphere. The focus of this research is to look at how key actinides (U, Pu and Np) interact with iron (oxyhydr)oxides of interest through adsorption and absorption. There is limited information on the REDOX (electron transfer) reactions that occur between iron minerals and key actinides but it has recently been shown that Fe(II) minerals (green rust and magnetite) can reduce U(VI) to its less mobile (V) state.^{1, 2} One method of doing this is by incorporating U(VI) into goethite (α -FeOOH) through its transformation from ferrihydrite.³ During this study, it was hypothesised that uranium may remain incorporated within goethite as U(V) even under iron-reducing conditions, showing the potential for using goethite as a secondary barrier to prevent radionuclide migration. From EXAFS spectroscopy, uranium is hypothesised to replace an iron atom adjacent to an iron vacancy in the near-surface, allowing for U-O bonds at 2.18Å and 2.03Å, which are associated with U(VI) and were shown to be reduced to U(V) during the experiment.³ Reducing U(VI) to U(V) for an extended amount of time would be very useful for preventing the release of uranium into the geosphere, and the generation of reactive and mobile species which could react with other chemical entities, leading to an entire cycle of products.

This project uses state of the art atomic-level calculations with accompanying experiments to accurately describe the interaction, chemical bonding and REDOX transformations of aqueous uranium species with iron minerals, both to improve current models and to develop a holistic description of uranium transport and retardation behavior. Further work will look into establishing thermodynamic parameters for sorption, desorption, and incorporation, of various key actinides in a variety of oxidation states onto a given crystallographic plane.

Density functional theory (DFT) is used with the Periodic Electrostatic Embedded Cluster Method (*PEECM*) in order to model the interaction of actinides with mineral surfaces and bulk. This method uses quantum mechanics to treat a small subsection of the mineral whilst also using point charges in an infinite array to incorporate the long-range effects of the mineral on the actinide-mineral interaction sites. The main focus of the calculations is to determine the effect of actinide incorporation into the mineral and to predict various spectroscopic markers to compare to experimental results, such as IR, Raman and EXAFS. Figure 1 is an example of the embedded section of goethite that is quantum mechanically treated, presenting the 010 surface of the goethite where absorption and adsorption of actinides may occur.

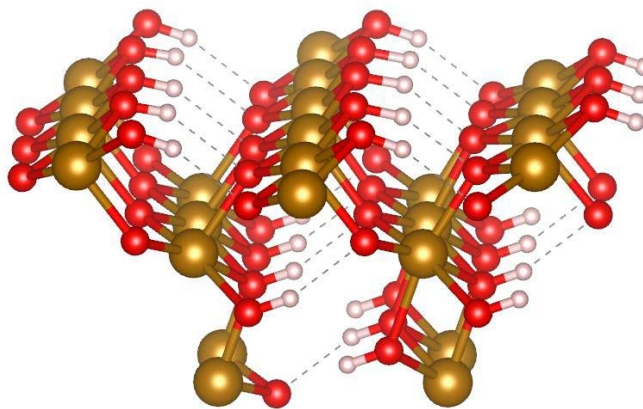


Figure 1: Model of goethite (α -FeOOH) at the 010 surface used for PEECM calculations.

The PEECM will be used to simulate the interaction of key actinides with goethite in a variety of different conditions, including potential incorporation into the bulk and solvation effects. These models will provide accurate descriptions of the chemical behaviour occurring at these sites in order to lead to more informed decisions about how to build a *GDF*.

References

- [1] Roberts, H. E., Morris, K., Law, G. T., Mosselmans, J. F. W., Bots, P., Kvashnina, K., & Shaw, S. (2017). Uranium (V) incorporation mechanisms and stability in Fe (II)/Fe (III)(oxyhydr) oxides. *Environmental Science & Technology Letters*, 4(10), 421-426.
- [2] Pidchenko, I., Kvashnina, K. O., Yokosawa, T., Finck, N., Bahl, S., Schild, D., ... & Vitova, T. (2017). Uranium redox transformations after U (VI) coprecipitation with magnetite nanoparticles. *Environmental science & technology*, 51(4), 2217-2225.
- [3] Stagg, O., Morris, K., Lam, A., Navrotsky, A., Velázquez, J. M., Schacherl, B., ... & Shaw, S. (2021). Fe (II) induced reduction of incorporated U (VI) to U (V) in goethite. *Environmental Science & Technology*, 55(24), 16445-16454.

PA8-2 DENSITY FUNCTIONAL THEORY STUDY OF THE CRYSTAL STRUCTURE AND INFRARED SPECTRUM OF ETTRINGITE

Francisco Colmenero¹, Oscar Almendros², Ana María Fernández², Tiziana Missana²

(1) *Géosciences Environnement Toulouse (GET) - Centre National de la Recherche Scientifique (CNRS), France*

(2) *Centro de Investigaciones Energéticas, Medioambientales y Tecnológicas (CIEMAT), Spain*

Introduction. Cement paste is intended to be used for containing radioactive waste in future nuclear repositories. Contact of cement with water is a hazard due to the dissolution/precipitation processes leading to transport of chemical species by diffusion and chemical reactions leading to material degradation. Understanding hydration and adsorption mechanisms in cement is crucial in materials science. However, cement is a complex multi-component assemblage, and its description requires the knowledge of the properties of the individual phases. Among the individual components ettringite, $(\text{Ca}_6[(\text{OH})_6]_2(\text{SO}_4)_4 \cdot 26 \text{H}_2\text{O}$ [1], is important because its structure includes abundant structural water and hydroxyl groups and, therefore, ettringite has the capacity to incorporate anionic species in the structure via substitution for sulfate (SO_4^{2-}), such as pertechnetate (TcO_4^-), chromate (CrO_4^{2-}), selenate (SeO_4^{2-}) and arsenate (AsO_4^{2-}), and adsorb cationic elements via substitution for Ca^{2+} , such as Sr^{2+} , Zr^{+} , Pb^{2+} and Co^{2+} . The purpose of this work is the theoretical description of ettringite towards its use for modelling its surface properties and reactivity. The first step in this study is the computation of the structure of ettringite and the associated X-ray diffraction pattern and infrared spectrum to assess the accuracy of the model. From the computed structure, the analysis of the mineral surfaces should allow correlating the structural properties of surface hydroxyls with their reactivity. Furthermore, surface adsorption calculations for different ionic species could be performed.

Methods.

Experimental. The experiments were performed using a crystalline powder sample synthesized in our laboratory (CIEMAT). The synthesis was performed by mixing $\text{Al}_2(\text{SO}_4)_3 \cdot 18\text{H}_2\text{O}$ and $\text{Ca}(\text{OH})_2$ solutions inside an anoxic glove box. The final solution was diluted to 500 mL with deionized water and 0.5 mL of 1N NaOH, sealed in a high-density polyethylene bottle, heated and stirred at 400 rpm. After 48h, the precipitate was filtered, dried and stored in a desiccator. The powder X-ray diffraction pattern of ettringite was collected by using a Philips X'Pert –PRO MPD diffractometer, from 2° to 80° (2θ) in steps of 0.017° . The infrared spectrum was recorded using a Nicolet iS50 spectrometer with a DTGS KBr detector on KBr-pressed discs in transmission technique. The spectral manipulations were performed using Omnic 9 software. The identity of the material was confirmed by XRD analysis using the Power Diffraction File database (ICDD).

Theoretical. The structure and infrared spectrum of ettringite were modeled employing CASTEP program [2]. The theoretical treatment employed is based on Periodic DFT using plane waves and pseudopotentials [2]. The computations were performed using the PBE density functional [3] complemented with Grimme's dispersion correction. The pseudopotentials utilized were norm-conserving. The lattice parameters and atomic positions were fully optimized by means of BFGS technique. A plane wave cut-off of $\epsilon = 900$ eV and a k -mesh of $2 \times 2 \times 2$ were employed. The software REFLEX was used to derive the X-ray diffraction patterns from the experimental and computed structures. The computation of the infrared spectrum was performed by means of density functional perturbation theory using the harmonic approximation.

Results. The computed structure of ettringite is shown in Figure 1. The structure of ettringite [1] contains columns with formula $[\text{Ca}_3\text{Al}(\text{OH})_6 \cdot 12\text{H}_2\text{O}]^{3+}$ composed of $\text{Al}(\text{OH})_6$ octahedra alternating with triangular groups of edge-sharing CaO_8 polyhedra. Four oxygen atoms coordinating Ca atom are from

H₂O molecules forming the cylindrical surface of the column (Figure 1). The columns delimitate channels containing sulfate ions and zeolitic water. The different columns are linked through sulfate ions via hydrogen bonds.

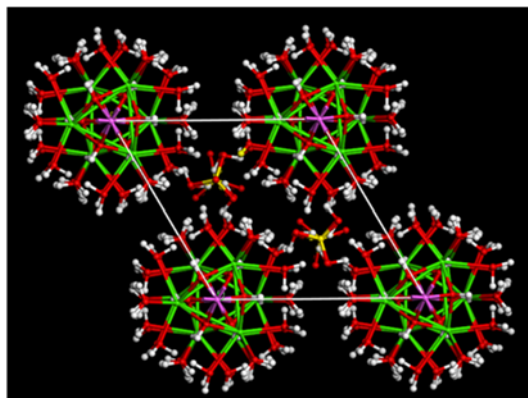


Fig 1. Computed structure of ettringite from [100]. Colors: Ca-green; Al -violet; O-Oxygen; S-Yellow; H-White.

The computed lattice parameters, $a=b=11.21$ Å and $c=21.14$ Å (P31c space group), are in excellent agreement with the experimental ones $a=b=11.17$ Å and $c=21.35$ Å [1]. From the calculated structure, the X-ray powder pattern was derived and is compared with the experimental one in Figure 2(A). Both patterns are highly consistent. The computed infrared spectrum is compared with the experimental infrared spectrum in Fig.2(B). Again, both spectra are in excellent agreement.

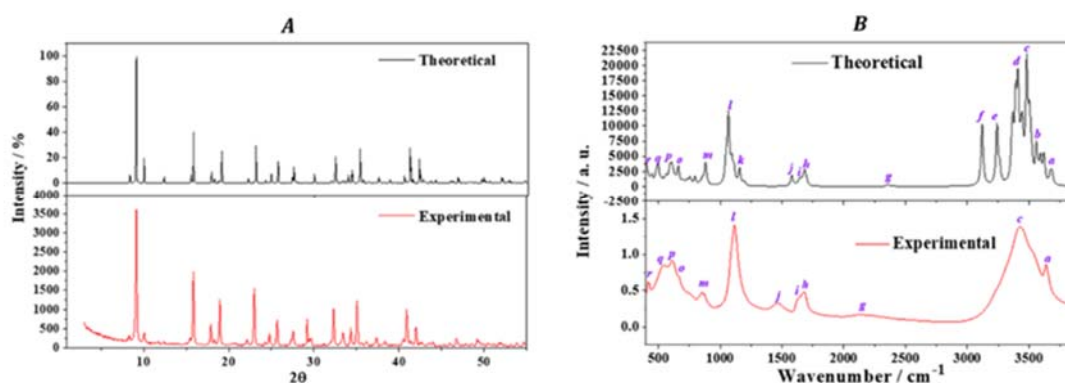


Fig 2. Computed and experimental X-ray diffraction patterns (A) and infrared spectra (B) of ettringite.

Conclusion

The good agreement in the computed X-ray diffraction pattern and infrared spectrum with those obtained from the experimental sample give strong support to the computed structure and the methods employed for its determination. Therefore, they may be used for accurately studying the surface properties and reactivity of ettringite. These studies are currently being carried out.

References

- [1] Hartman, M. R and Berliner, R. (2006). Investigation of the structure of ettringite by time-of-flight neutron powder diffraction techniques. *Cement Concrete Res.* 36: 364-370.
- [2] Clark, S. J., Segall, M. D., Pickard, C. J.; Hasnip P. J.; Probert, M. I. J.; Refson, K.; Payne, M. C. (2005). First Principles Methods Using CASTEP. *Z. Kristallogr.* 220, 567–570.
- [3] Perdew, J. P.; Burke, K.; Ernzerhof, M. (1996) Generalized Gradient Approximation Made Simple. *Phys. Rev. Lett.* 77, 3865–3868.

PA8-3 ACTINIDE(IV) INTERACTIONS WITH CALCIUM SILICATE HYDRATE: SORBED SPECIES AND COMPARISON OF SORPTION MODES BY MEANS OF DENSITY FUNCTIONAL CALCULATIONS

I. Chiorescu⁽¹⁾, A. Kremleva⁽¹⁾, S. Krüger⁽¹⁾

(1)Theoretische Chemie, Technische Universität München, 85748 Garching, Germany

Cement and concrete are foreseen as construction materials to be used in geological repositories for radioactive waste and also for the solidification of liquid waste. For these reasons the interaction of uranium and other actinide elements, appearing as fission and decay products, with the mineral phases of cementitious materials is of interest with respect to safety considerations. The main products of cement hydration are calcium silicate hydrate phases (C-S-H). These minerals, resembling structurally tobermorite, exhibit a rather low level of crystallinity and a decreasing Ca/Si ratio with age. Tobermorite is a layered mineral and the layers consist of a central CaO sheet covered on both sides by silicate chains (Fig. 1)..

We inspected computationally the sorption of U(IV) on C-S-H with a Ca/Si ratio of 1 [1], corresponding to aged cement. As a model mineral we used 14 Å-tobermorite. This study aims to identify favorable sorption sites and sorption complexes also by comparison to EXAFS experiments for Np(IV) [2] and Pu(IV) [3]. Also the sorption mechanism is investigated. For that purpose sorption at the (001) surface, absorption in the interlayer, and incorporation into the CaO layer of tobermorite have been considered [1]. The results of this study are further compared with the sorption of the larger ion Th(IV) and with Fe(II) as a possible competitor.

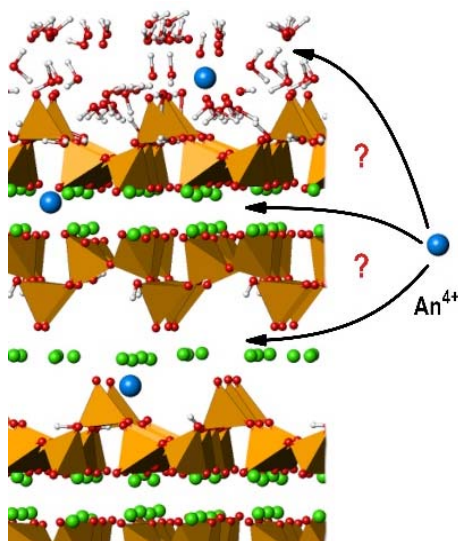


Figure 1: Schematic representation of the sorption of An(IV) at the tobermorite (001) surface, by incorporation into CaO layer, or by absorption in the interlayer. Ca ions in green, oxygens in red, silica tetrahedra in orange. Blue balls indicate exemplary sorption sites for An(IV) ions.

For the electronic structure calculations the density functional approach with a generalized gradient approximation form of the exchange-correlation interaction (PBE) is used. Core electrons are treated with the projector augmented wave method [4]. The large unit cell of tobermorite as well as its water content, leading to soft degrees of freedom, prevent a straight-forward geometry optimization for finding stable sorption species. To achieve a representative set of stable sorption complexes in this complex substrate, repeated steps of geometry optimization and dynamic equilibration at room temperature have been applied. This approach has been shown earlier as successful in a study on U(VI) sorption in C-S-H phases [5].

For U(IV) sorption at the surface and in the interlayer of tobermorite we find hydroxo species with two to five hydroxide ligands as adsorbate. The appearance of hydroxo complexes is in line with the basic conditions expected for C-S-H and in cement. Most of these sorption complexes are stabilized by Ca²⁺

in a second-sphere position and thus resemble corresponding ternary complexes in solution. The coordination number of the sorbed complexes of 6-7 is lower than experimental determinations for Np(IV) [2] and Pu(IV) [3] of 8. The average U-O bond lengths of 228-237 pm of various sorption complexes agree favorably with the measured values of 231 pm for Np(IV) [2] and 227 pm for Pu(IV) [3]. For U(IV) surface adsorption and absorption in the interlayer lower numbers of close U-Si and U-Ca distances have been obtained than for the incorporation of U(IV) into the CaO layer. This finding as well as the good agreement of the U-Si and U-Ca distances with EXAFS measurements [2,3] suggest U(IV) incorporation into the CaO layer as the favorable sorption mode. Also the comparison of sorption energies for various sorption sites yields U(IV) incorporation into the CaO layer as favorable, together with a tridentate binding species between silicate rows in the interlayer, which is by about 30 kJ/mol less stable. Thus, the calculated sorption energies support the interpretation of incorporation into the CaO layer as the preferred but not exclusive sorption mode, in contrast to earlier interpretations for Np(IV) [2]. A similar good agreement of calculated structures with experiment has earlier been obtained of U(VI) in C-S-H [5], which supports the present findings. In contrast to U(IV), U(VI) favorably absorbs in the interlayer.

It is commonly assumed that actinides in the same oxidation state exhibit the same sorption behavior. To verify this assumption we compare the sorption of Th(IV) with U(IV). As Th(IV) ions are by about 10 pm larger in diameter than U(IV), this comparison also yields insight into the variation of sorption along the actinide series for a specific oxidation state. Preliminary results from structure optimizations, which will be refined by dynamical equilibration, yield the same sorbed species for Th(IV) than for U(IV). Rare exceptions tend to weaker hydrolysis for Th(IV). Also the energy spectrum of the complexes is comparable with that for U(IV), suggesting again incorporation into the CaO layer as the favorable sorption mode.

We also inspected the sorption of Fe(II) in tobermorite, which may compete with actinides for sorption sites and is present in sizeable amounts under reducing conditions as a result of steel corrosion. Similar sorption sites as for U(IV) with a tendency to lower coordination to the substrate have been obtained, but incorporation into the CaO layer is unfavorable. In contrast to uranium no good agreement with a recent EXAFS measurement [6] has been obtained. This result demands further experimental and computational investigations.

References

- [1] Chiorescu, I.; Kremleva, A. and Krüger, S. (2022) On the Sorption Mode of U(IV) at Calcium Silicate Hydrate: A Comparison of Adsorption, Absorption in the Interlayer, and Incorporation by Means of Density Functional Calculations. *Minerals* 12: 1541.
- [2] Gaona, X.; Dähn, R.; Tits, J.; Scheinost, A. C. and Wieland, E. (2011) Uptake of Np (IV) by C-S-H phases and cement paste: An EXAFS study. *Environmental Science & Technology* 45: 8765-8771.
- [3] Dettmann, S.; Huittinen, N. M.; Jahn, N.; Kretzschmar, J.; Kumke, M. U.; Kutyma, T.; Lohmann, J.; Reich, T.; Schmeide, K.; Shams Aldin Azzam, S.; Spittler, L. and Stietz, J. (2023) Influence of gluconate on the retention of Eu(III), Am(III), Th(IV), Pu(IV), and U(VI) by C-S-H (C/S = 0.8). *Frontiers in Nuclear Engineering* 2: 1124856.
- [4] Kresse, G. and Joubert, D. (1999) From ultrasoft pseudopotentials to the projector augmented-wave method. *Physical Review B* 59:1758-1775.
- [5] Kremleva, A.; Krüger, S. and Rösch, N. (2020) Uranyl(VI) sorption in calcium silicate hydrate phases. A quantum chemical study of tobermorite models. *Applied Geochemistry* 113: 104463.
- [6] Mancini, A.; Wieland, E.; Geng, G.; Lothenbach, B.; Wehrli, B. and Dähn, R. (2021) Fe(II) interaction with cement phases: Method development, wet chemical studies and X-ray absorption spectroscopy. *Journal of Colloid and Interface Science* 588: 692-704.

PA8-4 EXPLORING THE COMPLEXATION OF CURIUM(III) AND EUROPIUM(III) WITH AQUEOUS PHOSPHATES: A COMBINED EXPERIMENTAL AND AB INITIO STUDY

Florent Réal⁽¹⁾, Nina Huittinen⁽²⁾, Isabelle Jessat⁽²⁾, Valérie Vallet⁽¹⁾, Norbert Jordan⁽²⁾

(1) Université de Lille, CNRS, UMR 8523 – PhLAM – Physique des Lasers Atomes et Molécules, F-59000 Lille, France

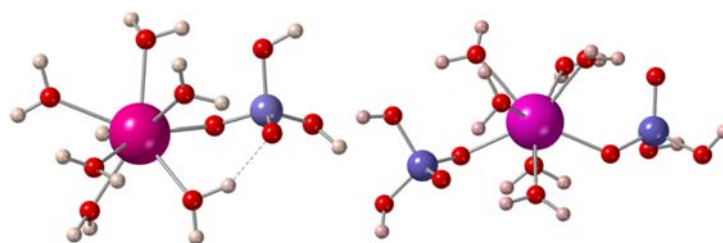
(2) Helmholtz-Zentrum Dresden-Rossendorf, Institute of Resource Ecology, Bautzner Landstraße 400, 01328 Dresden, Germany

The environmental fate of radionuclides (RNs) such as actinides and fission products disposed in underground nuclear waste repositories is of major concern. Long-term safety assessments of these disposal sites rely on the ability of geochemical models and thermodynamic databases (TDB) to forecast the mobility of RNs over very long time periods. One example where large data gaps in TDB still exist is related to the complexation of trivalent actinides and lanthanides with aqueous phosphates. Indeed, solid phosphate monazites are one of the candidates for the immobilization of specific high-level waste streams for safe storage in deep underground repositories in the future, which could locally increase the occurrence of phosphate in the repository.

Recent works [1-3] have been carried out to partially close these gaps in order to provide reliable complexation constants at 298K and at elevated temperature. However, obtaining this information is challenging and requires the identification of the formed complexes by means of spectroscopic techniques, such as UV-Vis or TRLFS (Time-Resolved Laser Fluorescence Spectroscopy). Depending on the phosphate concentration, mono or bi-dendate phosphate complexes can be formed with various coordination numbers (8, 9). However, it is often a challenge to obtain further information about the complex structures from the spectroscopic data alone.

In this context, relativistic quantum chemical (QC) methods can be seen as an additional tool to complement the experimental observations. In this study, structural properties, electronic structures and thermodynamics of the 1:1 and 1:2 phosphate complexes of Cm(III) and Eu(III) (see below) have been extracted by state-of-the-art QC calculations. In particular, QC methods allowed i) studying the complexation strengths of Cm(III) and Eu(III) with aqueous phosphates, ii) suggesting a potential change of the coordination number with increasing temperature and iii) probing the character (ionic/covalent) of the Cm/Eu-water and Cm/Eu-phosphate bonds.

Combining the information obtained from the quantum chemical calculations with the observed spectral changes, facilitates a conclusive assignment of the phosphate complex structures and their overall coordination [2,3].

**References**

- [1] Jordan, N., Demnitz, M., Löscher, H., Starke, S., Brendler, V., and Huittinen, N. (2018). Complexation of trivalent lanthanides (Eu) and actinides (Cm) with aqueous phosphates at elevated temperatures. *Inorg. Chem.* 57:7015–7024.

ABSTRACTS

- [2] Huittinen, N., Jessat, I., Réal, F., Vallet, V., Starke, S., Eibl, M., and Jordan, N. (2021). Revisiting the complexation of Cm(III) with aqueous phosphates: new insights from luminescence spectroscopy and ab initio simulations. *Inorg. Chem.* 60:10656–10673.
- [3] Jessat, I., Jordan, N., Kretzschmar, J., Réal, F., Vallet, V., Stumpf, T., and Huittinen, N. (2023). Impact of temperature on the complexation of Eu(III) with phosphate ions: a spectroscopic and ab initio study. *Inorg. Chem.* (in preparation).

PB2-1 IONIC DIFFUSIVE TRANSPORT THROUGH PARTIALLY-WATER SATURATED CEMENT-BASED MATERIALS

Savoye Sébastien ⁽¹⁾, Serge Lefevre ⁽¹⁾, Nathalie Macé ⁽¹⁾, Jean-Charles Robinet ⁽²⁾

(1) Université Paris-Saclay, CEA, Service de Physico-Chimie, France

(2) Andra, France

Cement-based materials are widely used in radioactive waste disposal facilities owing to their mechanical performances and their very low permeability so that transport of chemical species is mainly driven by the slow mechanism of diffusion. Moreover, in the French deep geological repository planned by Andra in the framework of the Cigéo project, recent calculations indicate that the generation of hydrogen due to the corrosion of canisters may partially dehydrate clayey host rocks and engineered barriers (including cement-based materials) for more than 100,000 years [1], and thus change the diffusive properties of these porous materials.

While the ionic diffusive transport in unsaturated conditions is relatively well described in literature for clay-based materials, with indications of (i) increase of anionic exclusion effect and (ii) decrease of cationic enhanced diffusion when dehydrated [see e.g. 2], knowledge is more incomplete for cement-based materials [3]. Therefore, the aim of this work is to investigate the effect of water saturation on the ion diffusive transport in an hardened cement paste (HCP) (expected to be used as a grouting material in Cigéo). For that purpose, through-diffusion experiments were performed in HCP samples submitted to suction value at 0, 1.9 MPa or 9 MPa by means of the osmotic technique and with water (HDO), anionic (¹²⁵I) and cationic (²²Na⁺) tracers that are known at full water saturation to behave as very weakly sorbing tracers.

Results obtained at full saturation show similar diffusive rates for water and ionic tracers when taking into account their distinct diffusion coefficient in bulk water (Figure 1). However, when the water saturation degree of HCP samples decreases down to 0.4, each type of tracer exhibits very distinct diffusive evolution. A relatively low decrease of the extent of the effective diffusion coefficient (D_e) values is observed for HDO (water tracer) compared to ions. This could be related to a phenomenon already evidenced in partially-saturated clayey materials [2] where, the diffusion of HDO in gaseous phase limits the decrease of the effective diffusion coefficient induced by desaturation.

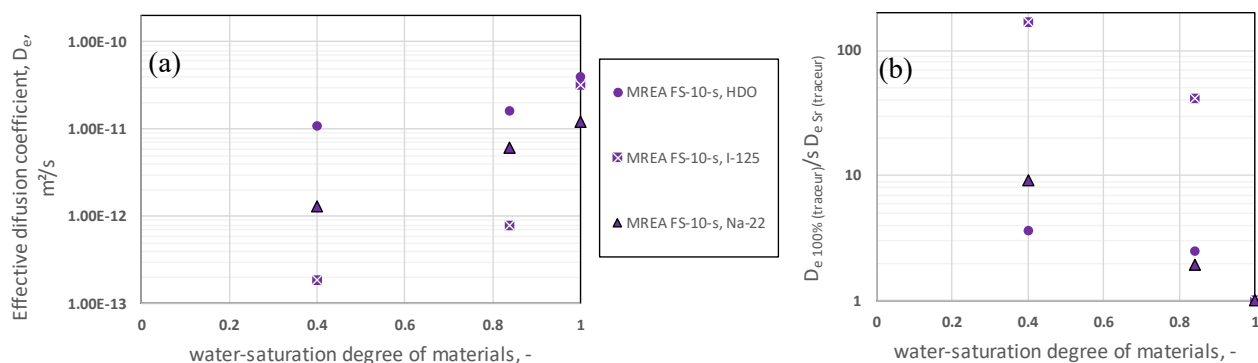


Figure 1. Evolution of effective diffusion coefficients, D_e , values (a) and of the $D_{e,100\%}$ over $D_{e,Sr}$ ratio (b) with water saturation degree of HCP samples for the water, anionic and cationic tracers.

Conversely, the anionic diffusive rate shows a sharp drop by a factor of more than 150 from 1 to 0.4 of saturation degree, while cationic diffusive rate decreases by a factor of about 10 only (Figure 1b). Such a distinct evolution between anion and cation suggests that dehydration would enhance the effect of

anionic exclusion. Indeed, the emptying of the largest pores that would control diffusion at full saturation would restrict anion tracer diffusion to take place in the smallest pores associated to CSH phases, and where anionic exclusion would be more pronounced, especially at the pH prevailing in the HCP samples (about 12.6-12.8).

Based on a comparison with previous data obtained on cement- and clay-based materials under partially-water saturated conditions, we lastly discuss the role played by several parameters such as surface charges, pore size distribution, tracer types, etc. on the evolution of the ionic diffusion with water saturation.

References

- [1] Andra (2016) Dossier d'options de sûreté, partie après fermeture (DOS-AF) https://www.andra.fr/sites/default/files/2018-04/dossier-options-surete-apres-fermeture_0.pdf
- [2] Wang, J. Savoye, S. Ferrage, E. Hubert, F. Lefevre, S. Radwan, J. Robinet, J.C. Tertre, E. Gouze, P. (2022) Water and ion diffusion in partially-water saturated compacted kaolinite: Role played by vapor-phase diffusion in water mobility, *Journal of Contaminant Hydrology*, 248.
- [3] Savoye, S., Macé, N., Lefèvre, S., Spir, G., Robinet, J.-C. (2018) Mobility of chloride through cement-based materials under partially saturated conditions. *Applied Geochemistry* 96, 78–86.

PB2-2 EFFECTS OF BIOTITE ON DIFFUSION AND SORPTION OF CATIONS IN CRYSTALLINE ROCKS BY THROUGH-DIFFUSION AND LASER-ABLATION ICP-MS EXPERIMENTS

Yuta Fukatsu⁽¹⁾, Qinhong Hu⁽²⁾, Yukio Tachi⁽¹⁾

(1) Japan Atomic Energy Agency, 4-33, Muramatsu, Tokai-mura, 319-1194 Ibaraki, Japan

(2) Department of Earth and Environmental Sciences, the University of Texas at Arlington, TX 76019, USA

Matrix diffusion and sorption are key processes to predict the transport of radionuclides in crystalline rocks for geological repository. A through-diffusion technique using tracers is a typical experimental method to evaluate the diffusion and sorption behaviors for rocks. The depletion and breakthrough curves, and depth profiles obtained from the diffusion tests show that Na^+ and Cs^+ have higher diffusivity than Γ^- in granodiorite samples from the Grimsel Test Site in Switzerland [1]. This trend could be explained by the negatively-charged surface on biotite which is one of the main minerals in crystalline rocks, because cations are intensively sorbed near the surface while anions are expelled. In addition, it is shown that disturbed biotite of the rock caused by cutting has a higher affinity for Cs^+ sorption than Na^+ after the diffusion tests. The difference could be explained by their different sorption mechanism with the frayed edge sites (FES) of biotite for dominant Cs^+ sorption [1]. Based on these findings, cationic sorption onto biotite would play an important role to evaluate the sorption and diffusivity of radionuclides in crystalline rock. In order to investigate the impact of sorption of cations in biotite on the diffusivity, in this study, we conducted through-diffusion tests of Cs^+ , Co^{2+} and Sr^{2+} for several types of crystalline rocks, and compared the results in different concentrations of K^+ that is one of the major cations of groundwater and also strong competitor for Cs^+ sorption onto biotite. Moreover, the elemental maps of multiple tracers sorbed onto biotite of these rocks were directly obtained by using a laser ablation (LA)-ICP-MS, which provides microscale distribution of tracer elements within the rocks [2]. Several types of crystalline rocks such as gneiss granodiorite (Japan) and granodiorite (Grimsel, Switzerland) were used, and cut into a cylinder shape (ϕ :20 mm, L:5 mm) for through-diffusion tests. The rock samples were fixed in the diffusion cells with epoxy, and saturated with electrolyte solution (NaCl : 1×10^{-2} M, CaCl_2 : 1×10^{-4} M, KCl : 0, 1×10^{-5} , 1×10^{-4} , 1×10^{-3} M) during two weeks. One side of the diffusion cell was connected to an inlet reservoir with the electrolyte containing tracers (Cs^+ , Co^{2+} and Sr^{2+} : 1×10^{-5} M), and the other side with an outlet reservoir with the electrolyte without the tracers. The concentrations of the tracers in both reservoirs were monitored by sampling the solution for ICP-MS analysis. At the end of the diffusion test of durations around 200 days, the rock samples were freeze-dried under vacuum for two days and then cut in half to the diffusion direction. The cross-section of the cut sample was measured by LA-ICP-MS under the sampling conditions of 100 μm spot size at 100 μm intervals.

In Figure 1, the breakthroughs of Cs^+ for Japanese gneiss granodiorite showed its increasing concentration at high KCl concentrations of above 1×10^{-4} M. The similar trend was observed for the breakthroughs of Co^{2+} and Sr^{2+} , but the effect was smaller than Cs^+ . These results suggest that an existence of K^+ in the solution enhances the diffusivity of cations and reduce the sorption, especially for Cs^+ sorption at the FES of biotite where it is in competition with K^+ [3]. In order to selectively investigate the diffusion and sorption in biotite of the rocks, elemental maps of Cs^+ , Co^{2+} and Sr^{2+} on the cross-section of the cut rock samples were evaluated by LA-ICP-MS. The biotite area was determined based on the black region in the image as shown in Figure 2 a and ^{57}Fe , ^{39}K , and ^{24}Mg signals obtained from LA-ICP-MS. Figure 2 b shows the elemental maps of the tracers for Japanese gneiss granodiorite at the condition of 1×10^{-5} M KCl. The maps were normalized by ^{28}Si as the intrinsic element of the rocks. In the Co^{2+} map, the concentration gradually decreases toward the deep matrix. The Cs^+ map is high on the surface within a few μm from the contact surface with tracer solution. In contrast, Sr^{2+} concentration near the surface is relatively lower than the deeper matrix where exhibits almost similar distribution with the map of Cs^+ . The difference in these effects among Cs^+ , Co^{2+} and Sr^{2+} can be interpreted by

taking account into the difference in sorption mechanism, i.e., the affinities of the cations for sorption sites including FES in biotite. That could explain the higher diffusivity of Sr^{2+} than Cs^+ and Co^{2+} at 1×10^{-5} M KCl as shown in the breakthroughs (Figure 1). This study could provide key insights to evaluate reliable diffusivity of cations in crystalline rocks with biotite rich.

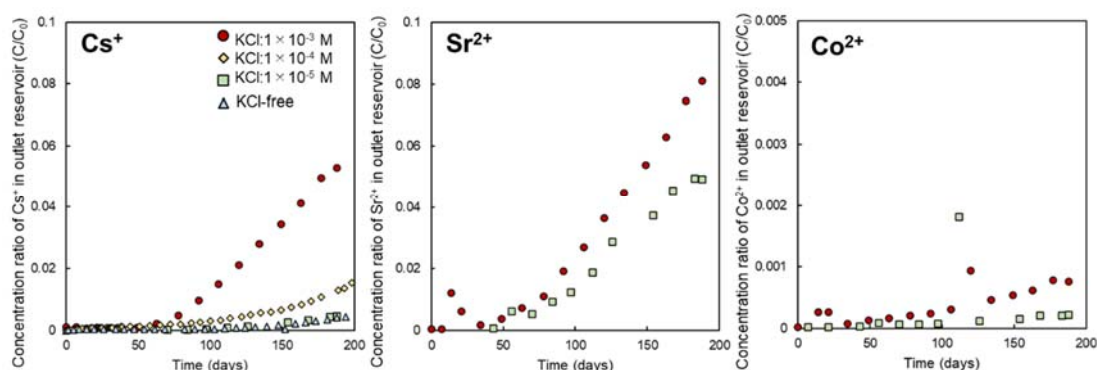


Figure 1 Breakthrough curves of tracers for Japanese gneiss granodiorite at different KCl concentrations.

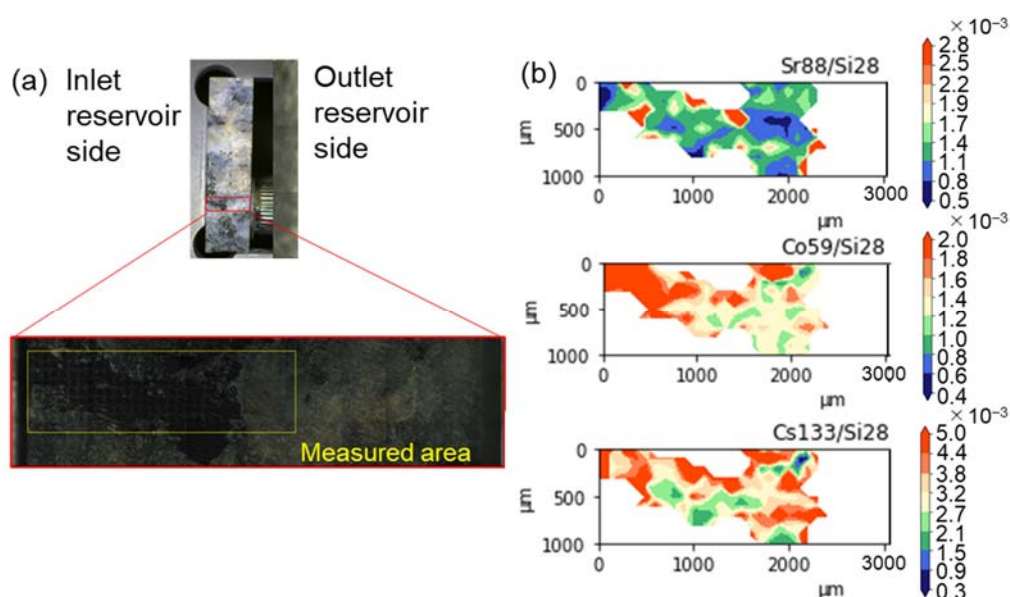


Figure 2 (a) Pictures of analysis area for Japanese gneiss granodiorite in 1×10^{-5} M KCl with LA-ICP-MS, (b) elemental maps of Cs^+ , Co^{2+} , and Sr^{2+} .

Acknowledgements: This study was performed as part of ‘The project for validating near-field assessment methodology in geological disposal (FY2020-2022, JPJ007597)’ supported by the Ministry of Economy, Trade and Industry of Japan. This work was also supported by JSPS KAKENHI Grant Number JP21K14569.

References

- [1] Tachi et al., Journal of Contaminant Hydrology 179, 10–24 (2015).
- [2] Hu et al., Geochemical Journal 46, 459–475 (2012).
- [3] Fuller et al., Applied Geochemistry 40, 32–42 (2014).

PB2-3 DIFFUSION AND RETENTION OF DIVALENT TRANSITION METAL TRACERS IN COMPACTED ILLITE CONVERTED TO DIFFERENT CATIONIC FORMS

Dimitra Zerva ^(1,2), Martin A. Glaus ⁽¹⁾ Sergey Churakov ^(1,2)

(1) *Laboratory for Waste Management, Paul Scherrer Institut, CH-5232 Villigen PSI, Switzerland*

(2) *Institute of Geological Sciences, University of Bern, CH-3012 Bern, Switzerland*

Clay rocks and clay minerals are considered as natural and engineered barriers for the safe disposal of radioactive waste in deep geological repositories. Due to the very low permeability of argillaceous rocks (among other beneficial properties, such as strong retention of radionuclides), diffusion is the dominant mass transport mechanism in such systems.

Despite decades of intensive research in this area, there are still open questions related to the distinct diffusive behavior of solvated ions in charged clay minerals. This behavior can be influenced by differences in the microstructure and/or the electrical potential at the clay surfaces (triggered by changes in the chemical composition of the pore water) and consequently affect the diffusion and retardation of the charged radioactive pollutants [1, 2]. The permanent negative charge of the TOT layer of clay minerals is responsible for an enrichment of cationic species and a concurrent depletion of anionic species in the solution phase immediately adjacent to the basal surfaces of clay particles relative to their respective concentrations in the bulk aqueous phase. This is widely recognized as the principal cause of surface diffusion and anion exclusion phenomena in these systems.

According to our assumptions regarding a surface diffusion model involving an electrical double layer (EDL), the observed overall diffusive flux is the sum of fluxes in the free pore water and the flux in the diffuse layer, whereas the Stern layer species are considered as immobile. Increasing the fraction of mobile species in the EDL's diffuse layer may reduce the retardation of some radioisotopes and increase the risk of enhanced radiation doses. The effect of surface diffusion is expected to depend on the concentration ratio between species in free water, Stern layer and diffuse layer. The affinity of a given cation to be present as a surface complex in the Stern layer depends on its hydration energy (Δ_H) [3]. Experiments in which the type of the index cation exhibit different hydration energy may be used to test such a concept [4].

Here we report the results of in-diffusion experiments with $^{57}\text{Co}^{2+}$ and $^{65}\text{Zn}^{2+}$ tracer using compacted homoionic forms of Na^+ -, Li^+ -, K^+ and Cs^+ -illite in which the electrolyte concentration was varied from 0.03 M to 0.5 M at pH <5.5 to partly suppress the contribution of surface complexes at the edge sites [5].

The results of these experiments illustrate the role of the index cation on the surface diffusion for ϕ ($\phi = \frac{D_e(\text{cation})}{D_e(\text{HTO})} * \frac{D_w(\text{HTO})}{D_w(\text{cation})}$) values greater than 1 [1] and the impact on the apparent diffusion coefficient (D_a) estimation (Fig. 1). The effective diffusion coefficients (D_e) and sorption distribution values (R_d) were derived from numerical transport models implemented in Comsol Multiphysics® using the experimentally measured concentration depletion in the source reservoir and the in-diffusion profiles as the basic input data. The distribution of mobile and immobile surface tracer species near the basal surfaces of the illite depends clearly on the type of index cation. Along the series of the different alkali cations, the shielding of the clay lattice charges – and the concomitant effect on the mean Donnan potential – is expected to differ according to their different tendency to form Stern layer complexes (according to their different hydration enthalpies). At the lowest ionic strength, this trend may be overshadowed partly by the relatively large fitting uncertainties caused by the uncertainties of the diffusion properties of the membrane separating the solution and the clay phase. The retardation of the

$^{65}\text{Zn}^{2+}$ follows the expected affinity trend for the dependence on ionic strength (the increase of ionic strength leads to a decrease of the R_d values) for each type of homoionic illite (Fig. 2).

These studies are complemented by measurements of the geometrical factors using through-diffusion experiments with $^3\text{H}_2\text{O}$, by the measurement of the specific surface area and by measurements of the anion accessibility and cation exchange properties in compacted forms of these clays. These auxiliary experiments help to reduce the degrees of freedom of the parameter choices for the geochemical speciation calculations carried out with Phreeqc. The outcome of this study provides deeper insight into the validity of the 2 Site Protolysis Non-Electrostatic Surface Complexation /EDL diffusion and sorption model. It demonstrates for the first time that surface diffusion and anion exclusion effects are not only affected by the overall net charge of the clays, but more specifically by the hydration properties of the cation exchange cations.

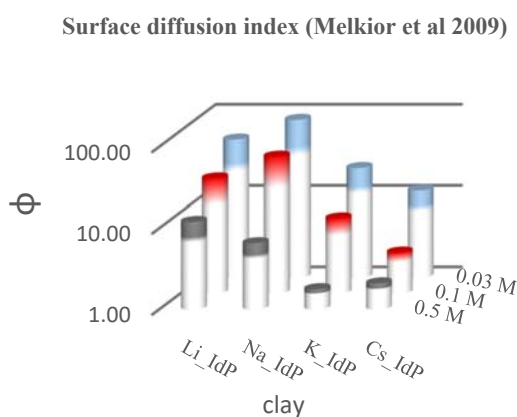


Fig.1: evidence of surface diffusion)

$$\left(\phi = \frac{D_e(\text{cation})}{D_e(\text{HTO})} * \frac{D_w(\text{HTO})}{D_w(\text{cation})}\right)$$

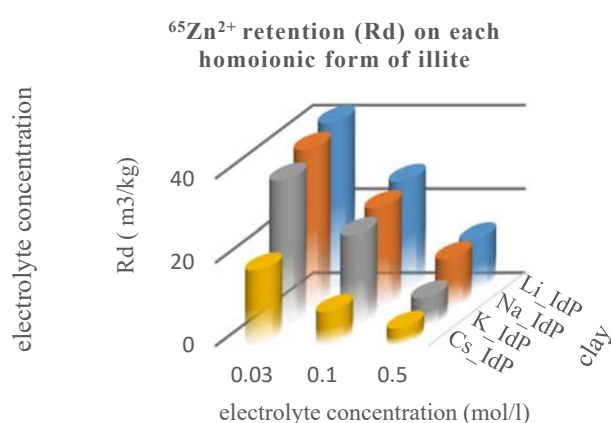


Fig.2: the higher competition between Zn and Cs leads to lower R_d values comparing to the other forms of illite

References

- [1] Melkior T., et al (2009). Na^+ and HTO diffusion in compacted bentonite: Effect of surface chemistry and related texture. J. Hydrol. 370, 9–20.
- [2] Glaus M.A. et al. (2015). Cation diffusion in the electrical double layer enhances the mass transfer rates for Sr^{2+} , Co^{2+} and Zn^{2+} in compacted illite. Geochim. Cosmochim. Acta 165, 376–388.
- [3] Van Loon, L.R., Glaus, M.A., 2008. Mechanical compaction of smectite clays increases ion exchange selectivity for cesium. Environ. Sci. Technol. 42, 1600–1604.
- [4] Bourg I.C. et al. (2017). Stern Layer structure and energetics at mica-water interface. Phys. Chem. C2 2017, 121, 9402-9412.
- [5] Montoya V., et al. (2018). Sorption of Sr, Co and Zn on illite: Batch experiments and modelling including Co in-diffusion measurements on compacted samples Geochim. Cosmochim. Acta 223, 1-20.

PB2-4 RELEVANCE OF UPWARDS MIGRATION OF RADIONUCLIDES IN SOIL IN THE CONTEXT OF NUCLEAR WASTE MANAGEMENT

Anna Kogiomtzidis⁽¹⁾, Volker Hormann⁽¹⁾, Clemens Walther⁽¹⁾

(1) Leibniz University Hannover, Institute of Radioecology and Radiation Protection

Radioecologic modelling is an important part of the safety assessment of deep geological repositories for nuclear waste. By predicting the migration and dispersion of radionuclides in the biosphere, the potential effective dose to future residents shall be estimated and thus a link between potential release rates and associated health risk for future human beings can be established.

Among the radionuclides considered dose-relevant in the context of nuclear waste are many long-lived fission and activation products such as Cs-135, I-129, Se-79, Tc-99 and Cl-36. For these nuclides, in most scenarios contaminated plants contribute to the major exposure pathways either by direct ingestion or indirectly as feed for livestock [1,2]. Since the activity concentration in plants is directly related to the contamination of the soil, radionuclide transport to and from the root zone plays a key role in dose assessment.

Regarding deep geological disposal of nuclear waste, two main transport pathways could lead to a radioactive contamination of soil. On one side, radionuclides can be introduced to the topsoil by irrigation water, e.g. from a contaminated well. On the other side, nuclides from a contaminated aquifer might migrate upwards through layers of deep soil to the root zone. Except for the dependence on many unknown parameters (e.g. future agricultural practices and climate conditions), for the first pathway entry rates to the topsoil are comparatively easy to model. The transfer velocity of the upwards migration on the other hand is the result of a complex interaction between soil characteristics, hydrological conditions and chemical behavior of the considered nuclides.

Although both experimental and modelling studies suggest that upwards migration through soil might be a relevant transport mechanism for at least some radionuclides [3,4,5,6], literature on this topic is sparse. So far, little is known about the potential relevance this pathway might develop over the course of the assessment period of a nuclear waste repository.

Therefore, this work aims to investigate the relative contribution of upwards transport to the radionuclide concentration in the root zone compared to the contamination through the irrigation pathway. For some selected scenarios, long-term behavior of radionuclides from a contaminated aquifer is modelled with respect to soil properties and hydrologic situation. Since radionuclide migration in soil is assumed to be dominated by advective transport, water fluxes throughout the soil profile are of great importance and can be simulated by the transport code HYDRUS [7] based on soil hydrologic characteristics and climatic conditions. Considering the long-time scales of interest, also dispersive effects can play a significant role and have to be taken into account accordingly.

Aside from the water movement, radionuclide transport is mainly governed by physical and chemical interactions with soil, particularly in the form of sorption behavior described by the solid-liquid distribution coefficients, the so-called K_d values. Many existing models rely on fixed K_d values often based for example on the IAEA best estimates [8]. In reality, radionuclide sorption is strongly influenced by soil properties and can vary by several orders of magnitude between different soil types. In addition, the hydrologic situation can be a highly relevant factor as it affects the redox conditions and consequently the speciation of radionuclides in soil. As a result, sorption behavior can be subject to significant seasonal variations. In fact, previous studies have shown that periods of maximum radionuclide concentration in the root zone often coincide with the growth cycle of plants, which is why the radioactive contamination during the growth period can strongly exceed the annual average [9]. Consequently, taking into account both spatial and temporal variations of sorption behavior is essential for realistic transport simulations.

For this purpose, the extended UNiSeCs model by Hormann et al. [10] is deployed to predict the K_d values depending on soil properties and redox conditions. The model is based on the geochemical speciation and transport code PHREEQC [11] and implements interaction of radionuclides with the major soil components. Here, first results will be presented on the long-term migration behavior of selected radionuclides in soils as modelled by coupling the UNiSeCs model with the transport code HYDRUS. For initial investigations Cs, U and Se have been chosen as elements of interest since they are both relevant for nuclear waste management and included in the UNiSeCs model and show a range of different migration behavior. Due to the high sensitivity to various soil parameters, for an accurate estimation of sorption coefficients the soil under consideration must be well characterized. For this reason the so-called RefeSols have been chosen, a set of reference soils established for chemical soil testing in Germany [12]. During the TRANS-LARA project [13] they have been used in several column and lysimeter experiments. These previous experiments provide a possible foundation for model validation. Additionally, further batch and column experiments with selenium are planned in the future for this purpose.

References

- [1] Chen, Q. et al. (2006). Application of a generic biosphere model for dose assessments to five European sites. *Journal of Radiological Protection*, Vol. 26: 161–187
- [2] Agüero, A. et al. (2008). Application of the Spanish methodological approach for biosphere assessment to a generic high-level waste disposal site. *Science of The Total Environment*, Vol. 403: 34–58
- [3] Ashworth, D. J. and Shaw, G. (2006). A comparison of the soil migration and plant uptake of radioactive chlorine and iodine from contaminated groundwater. *Journal of Environmental Radioactivity*, Vol. 89: 61–80
- [4] Pérez-Sánchez, D. and Thorne, M. C. (2014). Modelling the behaviour of uranium-series radionuclides in soils and plants taking into account seasonal variations in soil hydrology. *Journal of Environmental Radioactivity*, Vol. 131: 19–30
- [5] Wheater, H. et al. (2007). *Biosphere Implications of Deep Disposal of Nuclear Waste*. World Scientific Publishing Company, London
- [6] Demirkanli, Deniz I. , Molz, Fred J. , Kaplan, Daniel I. , and Fjeld, Robert A. (2009). Soil–Root Interactions Controlling Upward Plutonium Transport in Variably Saturated Soils. *Vadose Zone Journal*, Vol. 8: 574–585
- [7] Šimůnek, J. , Šejna, M. , Saito, H. , Sakai, M. , and th. van Genuchten, M. (2013). *The HYDRUS-1D Software Package for Simulating the One-Dimensional Movement of Water, Heat, and Multiple Solutes in Variably-Saturated Media*. Department of Environmental Science, University of California Riverside, California
- [8] IAEA, (2010). *Handbook of Parameter Values for the Prediction of Radionuclide Transfer in Terrestrial and Freshwater Environments*. International Atomic Energy Agency, Vienna
- [9] Elert, M. and Lindgren, M. (1993). The influence of the unsaturated zone on the upward transport of radionuclides in soils. *KEMAKTA*, Stockholm
- [10] Hormann, V. and Fischer, H. W. (2013). Estimating the distribution of radionuclides in agricultural soils – Dependence on soil parameters. *Journal of Environmental Radioactivity*, Vol. 124: 278–286
- [11] Parkhurst, D. L. and Appelo, C. A. J. (2013). *Description of input and examples for PHREEQC version 3—A computer program for speciation, batch-reaction, one-dimensional transport, and inverse geochemical calculations*. U.S. Geological Survey Techniques and Methods, Denver
- [12] Kordel, W. et al. (2009). The reference-matrix concept applied to chemical testing of soils. *Trends in Analytical Chemistry*, Vol. 28: 51–63
- [13] Böhm, M. , Heredia, D. J. , and Schäfer, T. (2021). *Trans-LARA Abschlussbericht Teilprojekt FSU-AnGeo*. Friedrich-Schiller-Universität Jena, Jena

PB2-5 ZINC(II) TRANSPORT IN COMPACT ILLITE IN THE PRESENCE OF ORGANIC LIGANDS

Xiaoyan Wei (1, 2), Martin A. Glaus (1), Luc R. Van Loon (1), Maria Marques Fernandes (1), Bin Ma (1)

(1) Laboratory for Waste Management, Paul Scherrer Institut, CH-5232 Villigen PSI, Switzerland

(2) School of Nuclear Science and Technology, Lanzhou University, Lanzhou 730000, China

Illite, as one of the most common argillaceous minerals, plays an important role in the environmental behavior of hazardous species. In compacted illite, the transport processes of radionuclides or other cations are largely controlled by diffusion and characterized by strong retardation [1]. In contrast to the conventional understanding, recent studies showed that the cation species enriched in the electrical double layer (EDL) at the negatively charged illite surface are mobile and can provide a substantial contribution to the diffusive flux [2]. Organic ligands (OLs) widely exist in natural and engineered systems and have strong complexation capabilities, affecting the charge, size and geometry of metal cations and their speciation. The presence of OLs result in a re-distribution of the cations in the EDL and between the solid/liquid, which is decisive for the diffusive flux. For this reason, OLs are assumed not only to have the well-known negative effect on the retardation of radionuclides by lowering their sorption on clay surfaces. In view of the more recent studies on the role of the EDL in the overall diffusion of cations [2], this is not *a priori* the only effect given. Depending on the speciation in the EDL, organic ligands can even decrease diffusion. In this study, we systematically investigate the transport (including both diffusion and sorption) behavior and mechanism of cations (Zn) in the presence of organic ligands (oxalate and 1,10-Phenanthroline) in an illite system. These ligands were chosen for their model character in terms of differently charged chelates.

Due to chemical similarity, Zn(II) is a good analogue of divalent transition metal cations for sorption/diffusion studies in soils and clays. As a post-transition element, Zn gives cleaner K-edge EXAFS spectra without the influence of the lower-Z neighbor transition metals (e.g., Fe), which are also common in soils and clays. In this study, transport of Zn(II) (representative of the transition metal cations) in Na⁺-conditioned illite du Puy (Na-IdP) was investigated by in-diffusion and batch sorption experiments in the presence of either negatively charged OL [oxalate (Ox²⁻)] or uncharged OL [1,10-Phenanthroline (Phen)], in order to clarify the role of positively charged (Phen) and/or negatively (or uncharged) charged (Ox) complexes of Zn(II) and to validate the diffusion/sorption models in terms of thermodynamic modelling. The coordination environments of the sorbed Zn(II) will be characterized by Zn K-edge X-ray absorption spectroscopy.

Preliminary results of Zn(II) sorption as a function of pH are shown in Fig. 1. It clearly shows that Zn(II) species are strongly sorbed at pH 3.5 – 7 and that the sorption behavior is different in presence and absence of OL complexation. Compared to the system without OLs, the weaker sorption of Zn(II) with Ox is probably caused by the formation of neutral Zn(II)-Ox(-II) complexes (Table 1), which prohibits the cation exchange in the EDL of illite surface and/or the surface complexation of Zn by silanol and aluminol groups. In contrast, the presence of Phen enhances the sorption of Zn(II). This might be explained by the formation of ternary surface complexes between illite–Phen–Zn induced by the formation of ion- π bonding between Phen and Na-IdP [3]. In contrast to the Ox and the bare Zn(II) system, sorption in the Phen system was independent of the ionic strength, indicating that the predominant sorption mechanism was not cation exchange in the EDL. The accurate coordination environment of sorbed Zn will be investigated by XAS. The sorption study is providing critical information for the subsequent in-diffusion experiments. We expect to obtain effective diffusion coefficients and sorption distribution coefficients under relevant geochemical conditions, and to improve our understanding of the migration mechanism of cations in the EDL on a molecular scale, both in presence and absence of different OLs. The outcome of the study will advance our knowledge on the

coordination chemistry of Zn with OLs and illite and provide valuable insights for reliably predicting the migration of cations in the geochemical system of nuclear waste repositories.

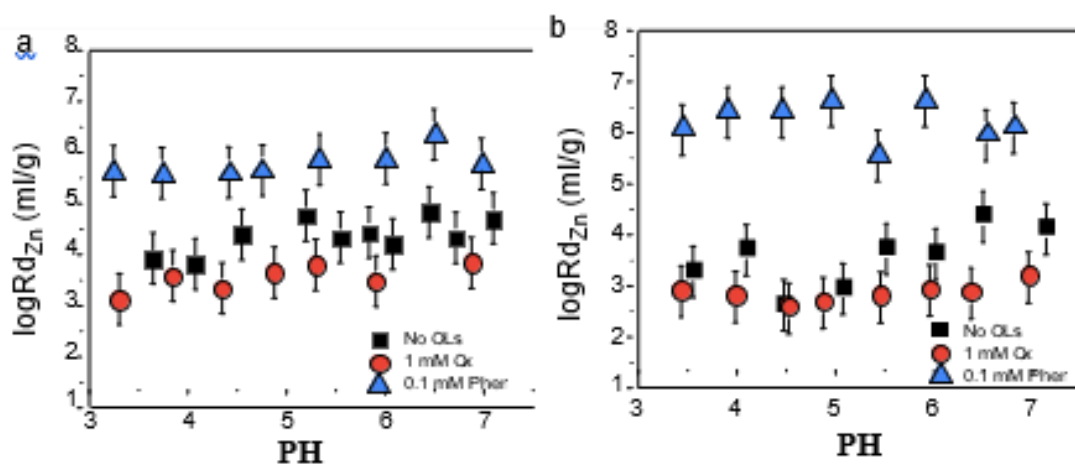


Fig. 1. pH dependence of Zn(II) sorption onto Na-conditioned illite at trace Zn(II) levels (1.84×10^{-7} M) in the presence of OLs. (a) 0.01 M NaCl; (b) 0.1 M NaCl.

Table 1. Theoretical distribution (in percentage) of Zn(II) species in the presence of oxalate, calculated by PHREEQC code

C_{ox} (mM)	pH = 4			pH = 5			pH = 6			pH = 7		
	Zn ²⁺	ZnOx	Zn(Ox) ₂ ²⁺	Zn ²⁺	ZnOx	Zn(Ox) ₂ ²⁺	Zn ²⁺	ZnOx	Zn(Ox) ₂ ²⁺	Zn ²⁺	ZnOx	Zn(Ox) ₂ ²⁺
1	5	75	20	2	64	34	2	61	37	2	61	37
0.7	8	78	14	4	70	26	3	68	29	3	68	29
0.5	12	78	10	5	75	20	5	73	22	5	73	22
0.1	41	57	2	4	71	25	23	73	4	23	73	4
0.05	58	40	0.5	40	57	2	38	60	2	37	60	2

References

- [1] Dahn R., Baeyens B., Fernandes M.M. (2021) Zn uptake by illite and argillaceous rocks. *Geochim. Cosmochim. Ac.* 312: 180–193
- [2] Glaus M.A., Frick S., and Van Loon, L.R. (2020) A coherent approach for cation surface diffusion in clay minerals and cation sorption models: Diffusion of Cs⁺ and Eu³⁺ in compacted illite as case examples. *Geochim. Cosmochim. Ac.* 274: 79-96
- [3] Lan Y.Q., Li C., Mao J.D., Sun J. (2008) Influence of clay minerals on the reduction of Cr⁶⁺ by citric acid. *Chemosphere* 71: 781-787

PB2-6 DIFFUSION AND SORPTION OF HTO AND EU-152 IN CRYSTALLINE ROCK WITH AND WITHOUT BENTONITE COLLOIDS

N. Pakkanen⁽¹⁾, L. Biez⁽¹⁾, J. Arkko⁽¹⁾, E. Jolis⁽²⁾, J. Kuva⁽²⁾, P. Sardini⁽³⁾, A. Mazurier⁽³⁾, J. Sammaljärvi⁽¹⁾, M. Siitari-Kauppi⁽¹⁾

(1) Department of Chemistry, FI-00014 University of Helsinki, Finland

(2) Geological Survey of Finland, Espoo, Finland

(3) Université de Poitiers, UMR 7285, IC2MP, rue Michel Brunet, Bat. 35, 86073 Poitiers cedex 9, France

In Finland, the spent nuclear fuel (SNF) will be disposed of 400 - 450 meters underground into crystalline bedrock at Olkiluoto Island for 100,000 years at least. Disposal of SNF follows the Swedish KBS-3 principle of multiple barriers, where SNF will be protected with engineered and natural barriers [1-3]. Nonetheless, even with the multiple-barrier system the possibility of SNF leakage still exists. If several of the multiple engineered barriers were to fail, radionuclides (RN) of the SNF could migrate into the surrounding biosphere. In a futuristic scenario, oxic glacial melting waters might penetrate the repository level into the bedrock of Olkiluoto Island and change the chemical conditions towards oxic. As a result, the redox-sensitive RNs may become more mobile and migrate through the bentonite buffer with colloids [4]. Therefore the role of colloids in RN transport needs to be assessed. In the previously described scenario, RN of most concern would be the long-living and toxic actinides, which may pose serious harm to the environment and public health alike.

For safety assessments to be more reliable, deeper knowledge of actinides' environmental behavior and migration in crystalline rock is required. This project aims to study and compare the effect of detached bentonite colloids on the sorption and migration behavior of an oxidation state +3 actinide analogue, Eu-152, in two different rocks from the Olkiluoto site. The project strives to deepen our knowledge of actinide behavior under the changing conditions of the nuclear waste repository of multiple barriers. Additionally, our goal is to take into account the mineralogical and structural heterogeneities in interpreting the experimental results of the through-diffusion and batch sorption experiments. A new way to model radionuclide transport in a heterogeneous rock would help estimate the migration of RN, with or without colloids and pseudo colloids.

Diffusion and retention properties of europium were studied in metatextitic gneiss (MTG) and granite pegmatoid (GP) rock cores. Two solutions, low saline groundwater simulant and MX-80 bentonite colloid solution, were used in both sorption and diffusion experiments. Besides europium's sorption on crushed rocks, sorption on pure minerals (quartz, biotite, K-feldspar, plagioclase) was also studied by batch sorption method. In through-diffusion experiments parallel to europium, conservative tracer HTO was used. Two different autoradiography methods were used to determine the spatial distribution of Eu-152 from the through-diffusion samples. Experimental results were further complemented with rock characterization methods; μ XRF for mineral mapping, C-14-PMMA autoradiography for porosity mapping and X-Ray Computed Tomography for 3D structure characterization to gain a deeper knowledge of the structure and mineralogy of the studied granitic rocks.

Depending on the used tracer, granitic rock and the presence of colloids, different diffusion breakthrough results were gained. Both diffusion and sorption experiment results imply that europium's sorption on dark minerals, e.g. biotite, is very strong. In comparison, europium's sorption on montmorillonite colloid particles was found to be even stronger and thus increasing colloid concentration was found to have a linear weakening effect on europium's sorption on biotite. Due to this high sorption on both biotite and colloids, europium did not migrate through neither of the used granitic rocks during the 140 days of experimental time, whereas conservative tracer HTO's breakthrough from them both was fast and successful. Through-diffusion of HTO was found to be faster in GP than in MTG; effective diffusion D_e

– values of $3.1 \cdot 10^{-12} \text{ m}^2/\text{s}$ and $2.1 \cdot 10^{-12} \text{ m}^2/\text{s}$ were determined for MTG and GP, respectively. Europium's autoradiography on diffusion rock samples further proved that the presence of colloids weakened europium's sorption on biotite and on both used granitic rocks (Eu-152 autoradiograph example in Fig.1). Based on preliminary results, colloids were not found to increase europium's breakthrough from neither of the granitic rocks. This result may indicate that the pore apertures of the rocks were below the size of the colloids in this study. Next, experimental results and those gained through rock characterization analyses will be combined to be used in modeling exercises to inspect and predict europium's diffusion behavior in different granitic rocks.

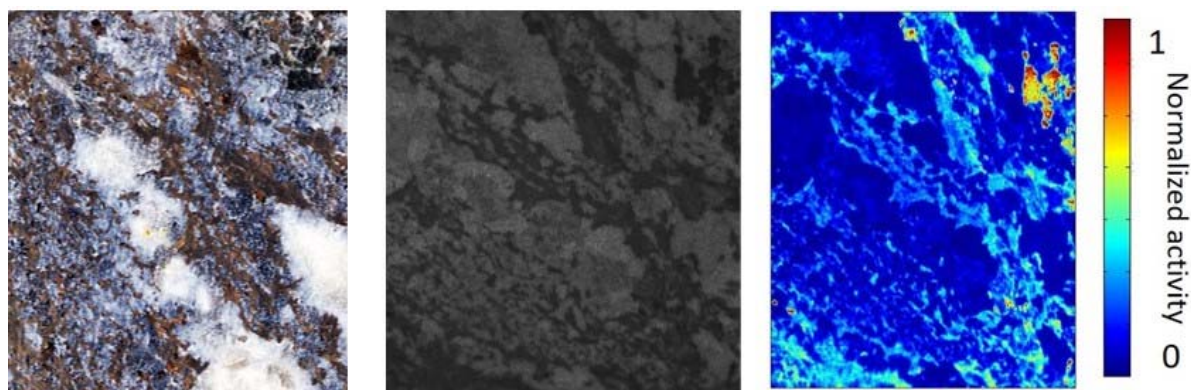


Fig.1. The photograph image of metatextitic gneiss through-diffusion sample (left), the corresponding autoradiograph (center), and the corresponding normalized activity map (right) showing activity distribution of Eu-152 in rock's minerals after 140 days diffusion time. The darker the shade, the more europium has sorbed on the rock minerals.

Acknowledgements: Funding for this research has been received from Fortum and Neste foundation under grant agreements No 20210117 and 20220097.

References

- [1] Hellä, P., Pitkänen, P., Löfman, J., Partamies, S., Vuorinen, U. and Wersin, P. (2014). Safety case for the disposal of spent nuclear fuel at Olkiluoto: Definition of reference and bounding groundwaters, buffer and backfill porewaters. POSIVA report 2014-04.
- [2] Posiva Oy (2012). Safety case for the Disposal of Spent Nuclear Fuel at Olkiluoto – Description of the Disposal System 2012. POSIVA report 2012-05.
- [3] Karvonen, T.H. and Sacklén, N. (2020). Material of the disposal facility – update of estimated quantities. POSIVA Working report 2020-030.
- [4] Novikov, A.P., Kalmykov, S.N., Utsunomiya, S., Ewing, R.C., Horreard, F., Merkulov, A., Clark, S.B., Tkachev, V.V. and Myasoedov, B.F. (2006). Colloid transport of plutonium in the far-field of the Mayak production association, Russia. *Science*. 314: 638-641

PB2-7 METAL ION DIFFUSION THROUGH METAKAOLIN-BASED GEOPOLYMERAnil Can YILDIRIM⁽¹⁾, Kanako TODA⁽¹⁾, Takumi SAITO⁽¹⁾*(1) The University of Tokyo, Japan***Introduction**

Geopolymers (GPs) are defined as chains or networks of inorganic molecules linked with covalent bonds. Their physical and chemical properties like thermal resistance, sorption properties, and structural strength have received great attention [1]. Accordingly, it has been pointed out that GPs have equal or even better structural properties than cement in terms of settling time and structural strength [1]. Moreover, GPs showed high thermal resistance up to 1000 °C, where conventional cement loses its integrity [1]. Japan Atomic Energy Agency (JAEA) [2] reviewed many companies' and universities' GP laboratory studies to discuss the potential use of GPs for nuclear fields and concluded that metakaolin-based geopolymer (MKGPs) is a good candidate. Although the structural features and ion sorption characteristics of GPs have been studied, the ion diffusion characteristics of GPs have not been detailed. Furthermore, the leaching mechanism of the immobilized metal ions still hasn't been detailed for the sodium-activated MKGP (Na-MKGP). Therefore, in this study diffusion of metal ions, namely, cesium (Cs^+), strontium (Sr^{2+}), and iodine (I^-), is studied by a through-diffusion technique with the Na-MKGP. The leaching studies with GP specimens containing these ions are also conducted by referring to the IAEA leaching method [3]. The outcomes of these studies are evaluated by a simple diffusion model and compared with those of cement and clays.

Experimental

About 50 grams of Na-MKGP were produced with the Si: Al ratio of 2:1 in PFA molds with a 2 cm diameter and cured at humidified environment for a week. Geopolymerized samples were cut to specimens with 0.5-cm thickness by wet cutting. Later, the specimens were dried at 105 °C for 6 hours to remove water, and the dry masses were recorded. Before conducting the through diffusion experiments, the specimens were conditioned with Milli-Q water for 2 weeks to remove excess alkali ions. Then, the same specimens were weighted again for the wet weight that was utilized for the porosity determination. Finally, they were further conditioned with a solution with the same composition as that of the test solutions for the subsequent diffusion experiments which have ionic strength of 0.1 or 0.01 M NaNO_3 .

To conduct the through-diffusion experiments, the specimens were mounted to sample holders with epoxy resin, which were sandwiched by two compartments: one with a high concentration of a target ion and the other without it. The high-concentration compartment contained one of the target ions, cesium nitrate ($\text{Cs}(\text{NO}_3)$), strontium nitrate ($\text{Sr}(\text{NO}_3)_2$), or sodium iodate (NaI), with sufficient concentrations. The solutions in both compartments also contain 0.01 M NaNO_3 as a background electrolyte.

For the leaching studies, Na-MKGP have been manufactured through the same formula as above except for adding 1 mL of the 10 mM stock solutions of the target ions to 10 g Na-MKGP before pouring to PFA molds with a 0.6-cm diameter and a 1-cm height. The specimens were initially checked for proper geopolymerization without the target ion by a boiling water test. Then, the specimens were placed into Milli-Q water (W), a synthetic groundwater (GW), and a synthetic seawater (SW) for a month with the water-to-solid ratio of 100.

For both the diffusion and leaching studies, the pH of the systems was measured before each sampling. The concentrations of the target ions in the sampled solutions were measured with an inductively coupled plasma mass spectrometer (ICP-MS, Agilent 7500cx) for Cs^+ and Sr^{2+} and with ion chromatography (930 IC Flex, Metrohm) for I^- .

Results and discussion

Preliminary results showed that the diffusion of D₂O, a tracer of H₂O, occurred through a 0.5-cm Na-MKGP specimen within 3 months. Diffusion of Cs⁺, Sr²⁺, and I⁻ are being examined, which will be reported in the conference. Meanwhile, the leaching studies showed that metal ion nature and speciation are directly affecting the leaching where Cs⁺ leached out by cation exchange reaction but Sr²⁺ did not leach out.

Coupling the diffusion and leaching studies, we will report the immobilization and diffusivities of the target ions, considering the porosity and tortuosity of the medium, and compare them with those of other barrier materials such as clays and cement.

References

- [1] Davidovits, J. (2015), *Geopolymer: Chemistry & Applications*, Saint-Quentin: Institut Géopolymère. France
- [2] Cantarel, V.; Morooka, T; Yamagishi, I., *Geopolymers and their potential applications in the nuclear waste management field; A Bibliographical study*, JAEA-Review 2017-014 (2017).
- [3] E.D. Hesse, *Leach testing of immobilized radioactive waste solids*, At. Energy Rev. 9 (1971) 195–207.

PB2-8 A SENSITIVE METHOD TO MEASURE GEOMETRY FACTORS FOR DIFFUSION ON SMALL SAMPLES OF CLAY ROCK

Martin A. Glaus⁽¹⁾, Dimitra Zerva⁽¹⁾, Luc R. Van Loon⁽¹⁾, Raphael A.J. Wüst⁽²⁾

(1) Laboratory for Waste Management, Paul Scherrer Institut, CH-5232 Villigen PSI, Switzerland,

(2) National Cooperative for the Disposal of Radioactive Waste (Nagra), CH-5430 Wettingen, Switzerland

In-diffusion experiments combined with profile analysis is a common method to measure diffusion and sorption characteristics of strongly sorbing radiotracers. An unambiguous interpretation of such experiments is only possible if the geometry factors for diffusion and electrostatic effects of the charged solutes can be properly discriminated. Knowledge of the effective diffusion coefficients of a non-reactive tracer such as tritiated water (HTO) is therefore necessary and may be taken from the literature. However, in-situ measurements using the same rock samples as for the subsequent in-diffusion measurements, would be preferable. Such a claim cannot be easily met using the through-diffusion method because the samples used for in-diffusion are rather small and may provide only a single cross-sectional area for solution contact.

Here we introduce a method derived from classical diffusion techniques to fulfill these requirements. It is named *DSOD* (*d*iffusive *s*aturation *o*ut-*d*iffusion) according to the two-steps comprising (i) homogeneous diffusive saturation (*DS*) of the clay plug with tracer after a sufficiently long contact time with the tracers electrolyte solution and (ii) replacing the contacting solution by a tracer-free electrolyte solution. In the second step, out-diffusion (*OD*) of HTO is monitored almost until equilibration of the pore solution in the clay sample with the electrolyte solution. Provided that the solution exchange occurs without carry-over, this method allows for a very accurate measurement of the HTO-accessible porosity. Moreover, the effective diffusion coefficient can be derived according to the dynamical evolution of tracer concentration during *OD*. Because this method is non-destructive and the clay sample is devoid of tracer after *OD*, it can be readily followed by any type of in-diffusion experiment.

Fig. 1 shows the evolution of HTO concentration in the *OD* phase measured on a sample of Opalinus Clay. The clay sample has a diameter of ~2.6 mm and a length of ~10 mm and has been embedded in epoxy resin after mechanical preparation with a single frontal cylindrical sample area open for solution contact. Such samples are used for the 'filter-free' in-diffusion method [1] which has the advantage that no porous interface between the clay and the solution phase is required reducing thus uncertainties introduced by poorly known properties of these interfaces [2]. Unexpectedly, the evolution of the tracer concentration in the *OD* phase could not be appropriately modelled by the assumed inventory of tracer in the clay pore solution. The process was overlaid by a second slow diffusion process. Obviously, the epoxy resin has a measurable capacity for tracer uptake which diffuses slower than the tracer inventory in the clay. *DSOD* measurements on epoxy resin dummy samples confirmed this expectation. According to these measurements, the epoxy resin has a capacity of ~2% (per volume) for uptake of HTO which is in good agreement with reported values of water uptake of hardened epoxy resin [3]. After correction of the native *OD* data for the uptake and release of HTO from the resin, valuable diffusion results could be obtained for the rock samples. However, the accuracy of the results is impaired compared to a situation in which no uptake in the resin had occurred.

Similar observations were also made on experimental setups made from polyether-ether-ketone (PEEK). In those cases, the uptake capacity of PEEK was found to be ~1% (per volume). All these results shed important light on the general importance of the materials used to encase rock samples for diffusion measurements. It was shown that almost all plastic materials, in contrast to stainless steel, exhibit a given volume capacity for water uptake, and thus for the uptake of HTO. Note that such effects can only be

detected in out-diffusion experiments. The classical through-diffusion method is not sensitive enough for such purposes. It could also be demonstrated that a certain volume expansion of samples of Opalinus Clay in epoxy resin occurred during the saturation phase, depending on the thickness of the coating and on the orientation of the stratification relative to the cylindrical axis.

Model calculations involving appropriate diffusion parameters for the epoxy resin demonstrated that the uptake of HTO tracer in the epoxy encasement had no significant impact on the results of through-diffusion measurements on the sedimentary rock samples from the potential siting areas for a deep geological radioactive waste repository in Northern Switzerland [4]. This is mainly due to a favorable choice of cross-sectional area of the clay sample respective to the dimensions of the epoxy encasement.

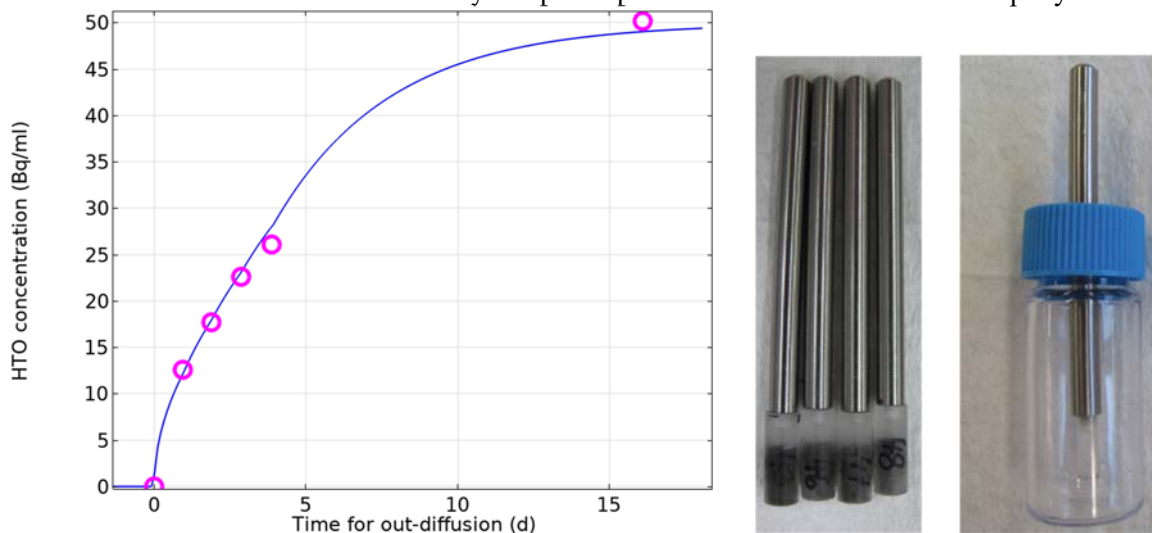


Fig. 1: Evolution during OD of HTO concentration in the contact solution of a sample of Opalinus Clay from the deep drilling campaign of Nagra at the Bözberg 1-1 site (left). Picture of Opalinus Clay test plugs embedded in hardened epoxy resin attached to steel rods used for suspension of the samples in the electrolyte solution (right).

Acknowledgment: We thank the National Cooperative for the Disposal of Radioactive Waste (Nagra) for the financial support. The help from Andreas Spahr (Department Hot Laboratory of PSI) for the mechanical preparation of the Opalinus Clay samples is greatly acknowledged.

References

- [1] Van Loon, L. R. and W. Mueller (2014). A modified version of the combined in-diffusion/abrasive peeling technique for measuring diffusion of strongly sorbing radionuclides in argillaceous rocks: A test study on the diffusion of caesium in Opalinus Clay. *Appl. Radiat. Isot.* 90: 197-202.
- [2] Glaus, M. A., Rossé, R., Van Loon, L. R. and A.E. Yaroshchuk (2008). Tracer diffusion in sintered stainless steel filters: Measurement of effective diffusion coefficients and implications for diffusion studies with compacted clays. *Clays Clay Miner.* 56: 677-685.
- [3] Adamow, K. (2014). Influence of water on the carbon fibre/epoxy polymer interaction, Dissertation Universität Bremen FB2 Biologie/Chemie.
- [4] Van Loon, L. R., Glaus, M. A. and R. Wüst (2023). Diffusion of HTO, ^{36}Cl and ^{22}Na in the Mesozoic cover of Northern Switzerland I: Measurement of diffusion coefficients and capacity factors. *Appl. Geochem.* **2023**, to be submitted to *Appl. Geochem.*

PB2-9 EFFECTS OF ALTERATION BY LEACHING ON MIGRATION OF CESIUM IN HARDENED CEMENT PASTE

Naoko Watanabe ⁽¹⁾, Kyoya Watanabe ⁽¹⁾, Keisuke Matsumoto ⁽¹⁾, Shinichiro Uematsu ⁽¹⁾, Tamotsu Kozaki ⁽¹⁾, Yuka Morinaga ⁽²⁾, Daisuke Minato ⁽²⁾ and Toru Nagaoka ⁽²⁾

(1) Hokkaido University, Japan

(2) Central Research Institute of Electric Power Industry, Japan

Introduction Decommissioning of the Fukushima Daiichi Nuclear Power Station (FDNPS) is expected to generate a significant amount of radioactive concrete waste, making effective waste management essential. For a reliable estimation and assessment of the amount of the radioactive concrete waste in each waste class, understanding of the migration behaviors of radionuclides in concrete is important. It is especially the case for concrete materials which have been submerged in contaminated water and subject to alteration due to leaching. In this study, sorption and diffusion coefficients of ¹³⁷Cs were experimentally determined for hardened cement paste (HCP) altered by leaching with different solutions. The migration behaviors of ¹³⁷Cs are discussed from the viewpoints of the activation energy for diffusion and the microstructure of altered HCP.

Experimental Hardened cement paste was prepared by mixing ordinary portland cement with deionized water at the water-to-cement (w/c) ratio of 0.36, followed by curing in a cement-equilibrated water for 28 d at 323 K. The HCP specimen were leached in different solutions simulating different leaching conditions at FDNPS in de-ionized water, synthesized sea-water, and 6 mol L⁻¹ ammonium nitrate solution. Surface morphology and microstructure of altered HCP samples were analyzed with ²⁹Si-MAS NMR, XRD, MIP, and SEM-EDX.

The batch-type sorption experiment was conducted for ground HCP samples under different temperature conditions (288–323 K). The mixture of ground HCP and the cement-equilibrated water spiked with ¹³⁷CsCl (solid/liquid ratio of 1/100) was periodically shaken for 28 d. Sorption coefficients (K_d) of ¹³⁷Cs were determined using the initial and final ¹³⁷Cs concentrations in liquid phase measured with NaI(Tl) scintillation counter.

The one-dimensional non-steady diffusion experiment was performed under constant temperature conditions (288–323 K) using ¹³⁷Cs tracer for blocks of the HCP samples altered with the ammonium nitrate solution. The concentration profiles of ¹³⁷Cs in the HCP samples after diffusion were obtained with an imaging plate (BAS IP SR2025E, Fujifilm).

Results and discussion The HCP samples were altered to different degrees of leaching. The EDX analysis confirmed the decreases in Ca/Si ratio, while NMR and XRD analyses showed the decline in portlandite and C-S-H in the altered HCP. The increase in porosity and a shift in pore size distribution towards larger pore sizes were also observed after leaching alteration.

The K_d values of ¹³⁷Cs are shown in Table 1. The ¹³⁷Cs sorption to unaltered HCP was negligibly small, whereas sorption of ¹³⁷Cs was observed to the altered HCP samples. The sorption enthalpy (ΔH) of ¹³⁷Cs was approximately -21 ± 1.9 kJ mol⁻¹ and -34 ± 3.5 kJ mol⁻¹ for the HCP samples altered in synthesized sea-water and in ammonium nitrate solution, respectively.

Fig. 1 shows the temperature dependence of the apparent diffusion coefficient (D_a) of ¹³⁷Cs in the HCP samples altered with the ammonium nitrate solution, together with the D_a for the unaltered HCP samples. The D_a values for the altered HCP samples were slightly lower than those for unaltered HCP samples. Although it can be speculated that the changes in pore structure due to leaching may have increased the

diffusion coefficients of ^{137}Cs , the leaching treatment decreased the D_a value, suggesting a significant retardation of Cs by sorption in the altered HCP.

The activation energy for diffusion (E_a) of ^{137}Cs was determined to be $52 \pm 4.3 \text{ kJ mol}^{-1}$ for the altered HCP from the slope of the regression line in Fig. 1 (solid line). It was larger than the E_a value reported for unaltered HCP ($36 \pm 2.2 \text{ kJ mol}^{-1}$) [1]. Since the value of E_a was determined from the temperature dependence of D_a , the E_a value includes the effects of the temperature dependence of K_d (i.e. the effect of ΔH). Thus, the activation energy without the effects of sorption was determined from E_a and ΔH to be approximately 18 kJ mol^{-1} , which is almost the same as the activation energy for diffusion of Cs^+ ions in free water (16.2 kJ mol^{-1}) [2]. These findings suggest that Cs in the altered HCP predominantly diffuse in relatively large pores filled with free water, simultaneously being affected by the retardation by sorption to the altered solid phases.

Conclusions The HCP samples with different degrees of alteration were obtained by leaching in different solutions. Diffusion and sorption coefficients as well as activation energy for diffusion and enthalpy of sorption were determined to suggest that Cs in the altered HCP predominantly diffuses in relatively large pores filled with free water, simultaneously being affected by the retardation by sorption to the altered solid phases.

Table 1 Sorption coefficients (K_d) in various HCP samples

HCP type	K_d (L kg^{-1}) (at 298 K)
Unaltered	≈ 0
Altered -deionized water	≈ 0
-sea water	23~69
-ammonium nitrate sol.	48~400

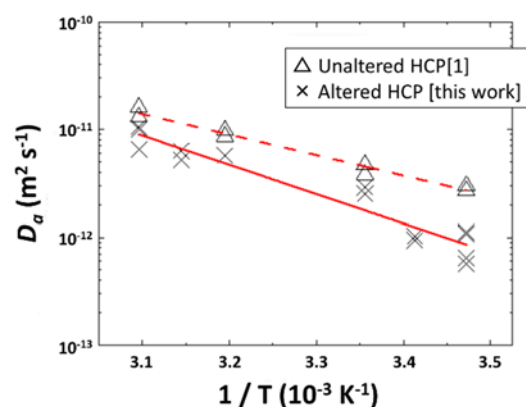


Figure 1 Temperature dependence of the apparent diffusion coefficient (D_a) of ^{137}Cs in the HCP samples

Acknowledgements This study was a part of the outcomes of the “Nuclear science and technology and human resource development program”, “Study on rational treatment/disposal of contaminated concrete waste considering leaching alteration” (2020–2022) funded by the MEXT, Japan. A part of this work has been performed in the Central Institute of Isotope Science, Hokkaido University.

References

- [1] Morishita *et al.*, ICONE26-82570, London (2018);
 [2] Parsons, Handbook of Electrochemical Constants, Butterworths Sci. Publ. (1959).

PB3-1 BENTONITE COLLOIDS MEDIATED EU(III) MIGRATION IN HOMOGENEOUS AND HETEROGENEOUS MEDIA OF BEISHAN GRANITE AND FRACTURE-FILLING MATERIALS

Yawen Chen, Chunli Liu, Ning Guo*

(1) Beijing National Laboratory for Molecular Sciences, Fundamental Science Laboratory on Radiochemistry & Radiation Chemistry, College of Chemistry and Molecular Engineering, Peking University, Beijing 100871, China

The study of the interactions between radionuclides and minerals/colloids is critical to evaluate the safety of high-level radioactive waste geological disposal repository. For now, the transport and release process of radionuclides with colloids in homogeneous and heterogeneous media of granite and fracture-filling materials have not been well documented. In this work, both individual migration and co-migration of Eu(III) and bentonite colloids at weak alkaline conditions were investigated in homogeneous and heterogeneous media of granite and fracture-filling materials. The migration experiments of Eu(III) and colloids were carried out at various environmentally relevant conditions, including colloids concentration and ionic strength with laboratory-scale column experiments. Four phases were set up to describe the effect of BCs on Eu(III) migration. The content of BCs was determined by UV spectrophotometer and the activity of $^{152}\text{Eu(III)}$ was measured with a γ detector. The results showed that the role of colloids in facilitating or retarding the Eu(III) transport in porous media varies with ion strength, heterogeneity and/or homogeneity configurations. The studied media show a retardation ability on bentonite colloids in the order of fracture-filling materials > heterogeneous media > granites. Almost all Eu(III) can be retarded in the fracture filling materials and granite. However, part of the retarded Eu(III) can be carried out by bentonite colloids, and the amount of Eu(III) release was affected by the characterization of colloids (aggregated or not). Meanwhile, it is worth noticing that the type of media can play an important role in the release of Eu(III). Fig.1. showed the Scheme of migration and release of Eu(III) and bentonite colloids in homogeneous and heterogeneous media of granite and fracture filling materials. These findings are important for predicting the migration of radionuclides in geological repositories.

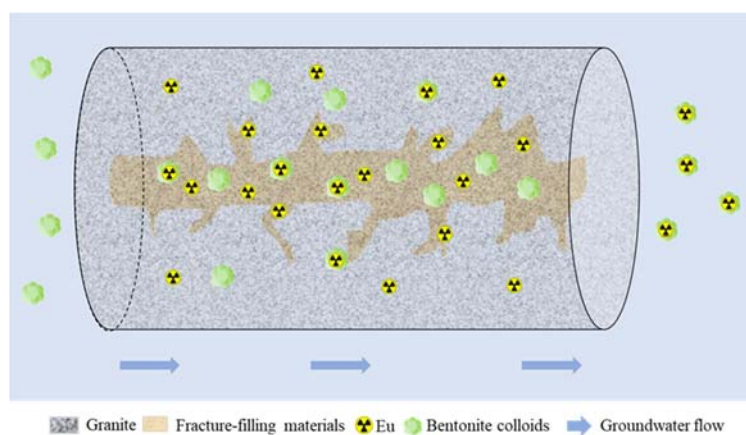


Fig.1. Scheme of migration and release of Eu(III) and bentonite colloids in homogeneous and heterogeneous media of granite and fracture filling materials.

PB3-2 COUPLING MECHANISM OF EU(III) TRANSPORT IMPACTED BY COMPOSITE COLLOIDS OF BENTONITE AND ORGANIC MATTER

Zhen Xu*, Duoqiang Pan, Wangsuo Wu

*E-mail: xuz@lzu.edu.cn

(1) School of Nuclear Science and Technology, Lanzhou University, China

(2) Frontiers Science Center for Rare Isotopes, Lanzhou University, China

The ecological and environmental safety of high-level radioactive waste has always been a worldwide problem, which is as important as nuclear safety. It is also a major issue related to the sustainable development of China's nuclear industry and environmental protection. The existence of environmental colloids can facilitate the transport of environmental contaminants including radionuclides as well as hydrophobic organic compounds. How to effectively control and block the transport of radionuclides in engineering barriers and predict their potential hazards has become an urgent problem. Meanwhile, it is also one of the key scientific problems in the performance and safety evaluation of high-level radioactive waste geological repository. The premise and foundation to solve this problem is to deeply understand and scientifically evaluate the mechanism of environmental colloids on radionuclide transport. Although it has been recognized that bentonite colloids play an important role in the transport of radionuclides¹⁻³, there are still some limitations in the understanding of the binding properties of composite colloids and radionuclides.

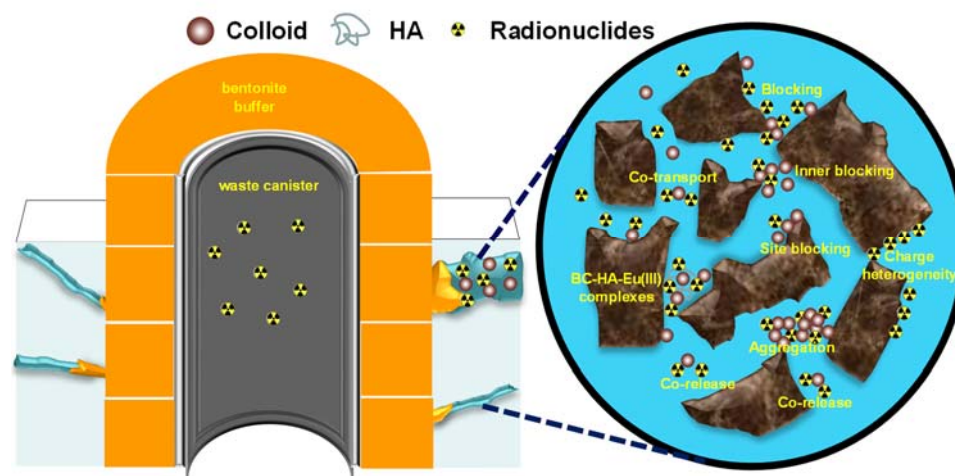


Fig. 1. schematic diagram of co-transport mechanism in HA-BC-Eu(III) system.

In present work, the impact of humic acid (HA) and bovine serum albumin (BSA) on co-transport behavior of bentonite colloids and Eu(III) in saturate porous media were investigated by static batch and dynamic column experiments. Results showed that the bentonite colloids facilitated the transport of Eu(III) at low ionic strength or high pH, but this promotion was related to the concentration of the colloid and the optimal colloid concentration was 150 mg/L. The effect of HA and BC on Eu(III) transport was a synergistic effect rather than a simple cumulative effect. The decrease of NaCl concentration in the solution system and the change of ion type can redisperse the deposited colloidal agglomerates. However, colloidal agglomeration caused by the decrease of CaCl₂ concentration was an irreversible process. Once HA was introduced into the suspension containing Ca²⁺, the deposited colloids released again. Eu(III) blocked by the adsorption of the medium will be loaded by the BC and re-transport again, but supposing Eu(III) adhered to the surface of the colloidal aggregate, the change of transient chemical conditions will not affect its release behavior.

For the ternary BSA-BC-Eu(III) system, the coupling effect of BSA and BC at low pH or high ionic strength significantly inhibited the transport of Eu(III) in quartz sand column, whereas it was beneficial to the transport of Eu(III). This is due to the fact that BSA coated on the surface of BC provided more attachment sites for Eu(III) deposition and thus enhanced the adsorption of Eu(III). In addition, protein corona covering the surface of BC enhanced the steric hindrance between colloidal particles, which improved the stability and dispersibility of the bentonite colloids, thereby promoting the co-transport of the BC-Eu(III) in saturated porous media. It is expected that through further understanding of the environmental behavior of bentonite colloid and organic matter (HA, BSA et al), we can accurately grasp the transport and fate of radionuclides carried by colloid in groundwater environment, and provide an important reference for the safety evaluation of the repository as well as nuclear emergency.

References

- [1] Xu, Z.; Pan, D.; Tang, Q.; Wei, X.; Liu, C.; Li, X.; Chen, X. and W. Wu (2022). Co-transport and co-release of Eu(III) with bentonite colloids in saturated porous sand columns : Controlling factors and governing mechanisms. *Environ. Pollut.* 118842.
- [2] Xu, Z.; Niu, Z.; Pan, D.; Zhao, X.; Wei, X.; Li, X.; Tan, Z.; Chen, X.; Liu, C. and W. Wu (2021). Mechanisms of bentonite colloid aggregation, retention, and release in saturated porous media: Role of counter ions and humic acid. *Sci. Total Environ.* 2021, 793: 148545
- [3] Wei, X.; Pan, D.; Xu, Z.; Xian, D.; Li, X.; Tan, Z.; Liu, C. and W. Wu (2021). Colloidal stability and correlated migration of illite in the aquatic environment: The roles of pH, temperature, multiple cations and humic acid. *Sci. Total Environ.* 768: 144174

PB4-1 INTERACTION OF TECHNETIUM WITH METABOLITES, MICROORGANISMS AND AT THE MINERAL-WATER INTERFACE: RADIOECOLOGICAL CONSIDERATIONS.

Natalia Mayordomo ⁽¹⁾, Irene Cardaio ⁽¹⁾, Arkadz Bureika ⁽¹⁾, Caroline Börner ⁽¹⁾, Katharina Müller ⁽¹⁾

(1)Helmholtz-Zentrum Dresden-Rossendorf e.V. Institute of Resource Ecology, 01328 Dresden (Germany).

Technetium-99 (⁹⁹Tc) is a long-lived fission product ($2.13 \cdot 10^5$ years) of uranium-235 (²³⁵U) and plutonium-239 (²³⁹Pu) and therefore, of great concern for the long-term safe management of nuclear waste. The migration of Tc in the environment is highly influenced by the redox conditions, since Tc may be present in various oxidation states. Under environmental conditions, Tc is expected to mainly occur as Tc(VII) under oxidizing conditions and as Tc(IV) under reducing conditions. The anion pertechnetate (Tc(VII)O_4^-) is known to barely interact with mineral surfaces; this, in turn, enhances its migration in groundwater and favors its entry in the biosphere. On the contrary, the formation of Tc(IV) limits the migration of Tc since it forms a low soluble solid (TcO_2) and/or species whose interaction with minerals is more favorable. In the last decades Tc migration has been focused on the reduction of Tc(VII) to Tc(IV) by various reductants, such as Fe(II), Sn(II) or S(-II) either present in solution, taking part in mineral structures, [1] or metabolically induced by microbial cascades [2].

Most of the published studies have been focused on binary systems i.e., studies of the interaction of Tc with a given reductant. However, the environment is a complex system where different components often depend on and modify each other. Thus, Tc migration is susceptible and varies upon environmental conditions and should not be studied in an isolated manner. The young investigator group TecRad [3], funded by the German Federal Ministry of Education and Research, aims at analyzing Tc chemistry from a wider perspective. Our goal is to study the biogeochemical behavior of Tc when it interacts with: i) microorganisms, ii) metabolites, iii) Fe(II) minerals, and iv) Fe(II) minerals in presence of metabolites (Figure 1).

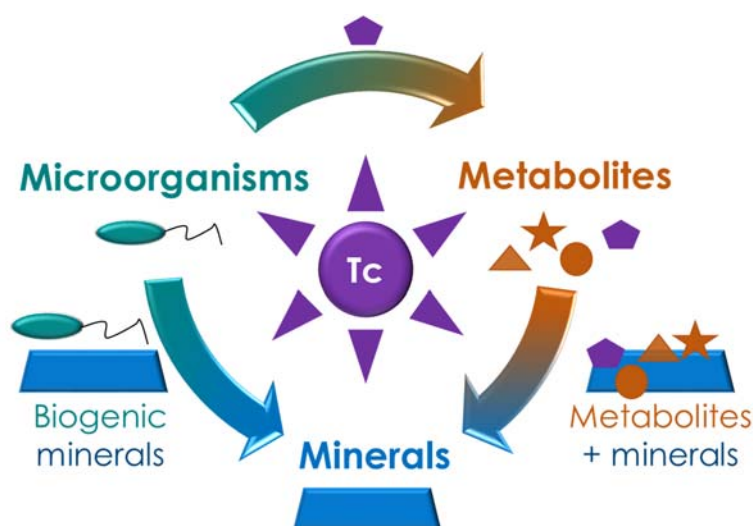


Figure 1. Research focus on Tc interactions with metabolites, microorganisms, and minerals within TecRad project.

An important part of this project deals with implementing new spectro-electrochemical methods to monitor in situ the behavior of Tc in solution and at interfaces as a function of the redox potential. With

these tools we aspire at characterizing the molecular structures of Tc species under a variable range of redox conditions, to broaden the understanding of the chemical behavior of the pollutant.

Our goal is to generate valuable thermodynamic data (complex formation constants, solubility constants of minerals, redox potentials and Tc distribution coefficients) that we will use to implement a geochemical modeling able to explain Tc environmental fate even under different redox conditions.

Acknowledgement: *The authors acknowledge the German Federal Ministry of Education and Research (BMBF) for the financial support of NukSiFutur TecRad young investigator group (02NUK072).*

References

- [1] Pearce, C. et al. (2020). Technetium immobilization by materials through sorption and redox-driven processes: A literature review. *Sci. Total Env.* 716: 132849.
- [2] Newsome, L. et al. (2014). The biogeochemistry and bioremediation of uranium and other priority radionuclides. *Chem. Geol.* 363: 164-184.
- [3] TecRad webpage: <https://www.hzdr.de/db/Cms?pNid=1375> vis on February 9th 2023.

PB4-2 ACCUMULATION OF ACTINIDES (III, VI) IN THE FILAMENTOUS FUNGUS *PODOSPORA ANSERINA*

Maloubier Melody (1), Le Naour Claire (1), Pei Yang(1), Creff Gaëlle(2), Jeanson Aurélie(2), Den Auwer Christophe(2), Chapeland-Leclerc Florence (3), Ruprich-Robert Gwenaël(3), Cabet Eva(3)

(1) IJCLab, UMR 9012, CNRS-IN2P3, Université Paris-Saclay, 91406 Orsay Cedex, France

(2) ICN, UMR7272, Université Côte d'Azur/CNRS, 06108 Nice, France

(3) LIED, UMR CNRS 8236, Université Paris Cité, 75205 Paris Cedex 13, France

Natural and anthropogenic actinides are present in the different compartments of the environment (lithosphere, hydrosphere, atmosphere, and biosphere) and remain a major concern of modern nuclear societies. They feature a significant toxicological impact (chemical toxicity and radiological toxicity) and can therefore impact the development of the biosphere. The complexity of their chemistry, especially of the lightest An (from U to Am), leads still to a non-well understanding of their behavior in the environment. Their ability to be found under different oxidation states from (+III to +VI) influences their reactivity and interactions. Within the biosphere, fungi play a key role in decomposition and nutrient recycling. Numerous studies have demonstrated their ability to accumulate metals such as arsenic and cadmium, lead and mercury^[1]. Because of their wide geographical dispersion, their abundance, their great variety and their ability to grow even in extreme conditions, they can be good bio-indicators of pollution. Until now, most studies have focused on the determination of An concentrations in different fungi species without explaining the molecular mechanisms involved in their accumulation, their impact on the fungus development, and on their transfer in the trophic chain^[2]. Thus, we focused first on americium(III) and uranium(VI), that can have a simpler redox chemistry, as compared to plutonium, in the conditions of fungi culture. The high specific activity of americium limits its manipulation, which is why europium(III) was used as a chemical analogue. The accumulation of the actinides was followed in a filamentous model fungus, *Podospira anserina*^[3]. This fungus is easily cultivated under laboratory conditions and grows rapidly with a complete life cycle of 7 days in standard conditions. The culture medium used is a synthetic one whose composition is perfectly known. The medium has been adapted (absence of phosphates) in order to work with actinides without leading directly to the precipitation of the latter.

First, the influence of actinide concentration on the fungus development was evaluated to identify the concentration range that the fungi can cope with. In order to better understand the mechanisms involved, the actinide accumulation was studied during the different development stages of the fungus (mycelium growth and sexual reproduction). Once actinides have been accumulated in fungi, they were localized in the different fungus parts (mycelia and perithecia, the site of the sexual reproduction) using ICP-MS and confocal fluorescence microscopy. The fungi part responsible of the actinides accumulation was then pinpointed by comparing the initial speciation of actinide in the culture medium with the one in fungi, thanks to speciation modelling combined to spectroscopic techniques like x-ray absorption spectroscopy.

For instance, the presence of europium in the culture medium, at concentrations higher than 10^{-4} M, has a strong impact on both mycelial growth and sexual reproduction, inhibiting the growth and leading to the formation of non-mature perithecia. Moreover, the accumulation mechanisms at europium concentrations 10^{-5} M and 5×10^{-4} M seems to be different. These distinct behaviors could be explained by a difference in speciation of europium in the culture medium. At 10^{-5} M, europium is mainly present as citrate complexes, whereas at higher europium concentration, sulfate species and non-complexed species prevailed. However, in each case, europium(III) accumulation was observed, reaching concentrations from 180 to 4500 ppm in the mycelia and from 36 and 1900 ppm in the perithecia after 14 days of doping at 10^{-5} M and 5×10^{-4} M respectively. The accumulated europium could be localized as homogeneously distributed in the mycelium. The use of concanavalin A, a fluorescent lectin displaying high affinity for glycoproteins present at the cellular membranes, could pinpoint the absence

of europium on the membranes of the mycelia. Within the perithecia, the accumulation of europium occurs mainly during the differentiation of the asci and then is concentrated in the ascospores during the meiotic division (Figure 1). Europium fluorescence is not observed in nonmature asci and therefore does not appear to be accumulated at this time of development. First results on uranium accumulation in *P. anserina* will be also presented.

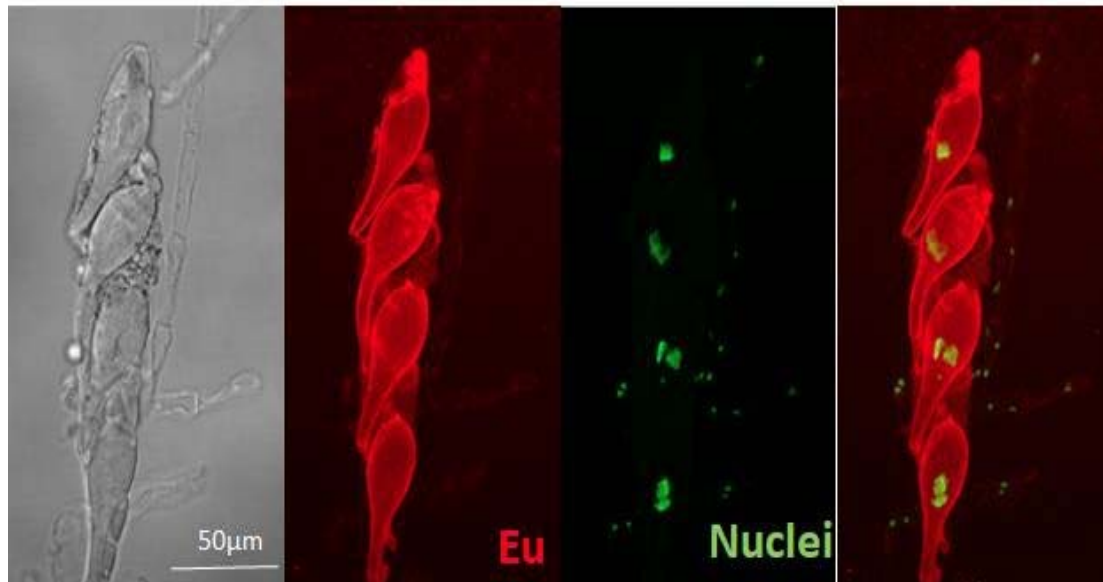


Figure 1: Interior of perithecia in presence of 10^{-5} M europium observed by confocal fluorescence microscopy. Nuclei are labeled with the green fluorescent protein (MCM1-GFP) and europium fluoresces in red.

References

- [1] Wuilloud, R.G., Kannamkumarath, S.S. and Caruso, J.A. (2004). Multielemental speciation analysis of fungi porcini (*Boletus edulis*) mushroom by size exclusion liquid chromatography with sequential on-line UV-ICP-MS detection. *Journal of Agricultural and Food Chemistry*. 52: 1315-1322.
- [2] Baeza, A., Guillén, J. and Mietelski, J.W. (2004). Uptake of alpha and beta emitters by mushrooms collected and cultured in Spain. *Journal of radioanalytical and nuclear chemistry*. 261: 375- 380.
- [3] Xie, N., Ruprich-Robert, G., Silar, P., Herbert, E., Ferrari, R. and Chapeland-Leclerc, F. (2018). Characterization of three multicopper oxidases in the filamentous fungus *Podospora anserina*: A new role of an ABR1-like protein in fungal development? *Fungal Genetics and Biology*. 116: 1-13.

PB4-3 RIGIDITY AND FLEXIBILITY: UNRAVELING THE ROLE OF FULVIC ACID IN URANYL SORPTION ON GRAPHENE OXIDE USING MOLECULAR DYNAMICS SIMULATIONS

Tu Lan⁽¹⁾, Peng Wu⁽¹⁾, Xiaoyu Yin⁽¹⁾, Yufan Zhao⁽¹⁾, Jiali Liao⁽¹⁾, Dongqi Wang^{(2),*}, Ning Liu^{(1),*}

(1) Key Laboratory of Radiation Physics and Technology of the Ministry of Education, Institute of Nuclear Science and Technology, Sichuan University, Chengdu, P. R. China

(2) School of Chemical Engineering, Dalian University of Technology, Dalian, P. R. China

Fulvic acids (FAs), a class of natural organic compounds, are widespread in natural environment and soluble in acid and alkali [1]. FAs retain a variety of functional groups such as carboxyl, hydroxyl, carbonyl, and aromatic rings, which enables it strong chelating ability to interact with metal ions in groundwater and soils [2]. This raises growing interest in understanding the role of FA in the transformation, migration, and removal of toxic heavy metal ions including actinides in the contaminated sites. Although some previous experiments have shown that FA can promote the sorption of metal ions on sorbents [3,4], whereas no studies have focused specifically on the sorption dynamics of such a sorbent/metal/FA ternary system, as well as the coordination structures, the types of surface ternary complexes, and the sorption mechanism. Additionally, FAs are a complex class of organic compounds with different rigidity and flexibility, which can dominate their sorption properties. However, the effect of molecular rigidity and flexibility on the sorption of metal ions on sorbents has not been reported yet so far. These are hard to investigate experimentally, and molecular dynamics (MD) simulations can address this issue to improve our understanding of such ternary systems.

This work targets a molecular understanding on the rigidity and flexibility of FA in uranyl sorption on graphene oxide (GO) using MD simulations. Molecular structures of GO and two FA models are shown in Figure 1. The simulations demonstrated that both rigid Wang's FA (WFA) and flexible Suwannee River FA (SRFA) can provide multiple sites to cooperate with GO for uranyl sorption and act as "bridges" to connect uranyl and GO to form GO-FA-U (Type B) ternary surface complexes (Figure 2). The presence of flexible SRFA was more beneficial to uranyl sorption on GO. The interactions of WFA and SRFA with uranyl were primarily driven by electrostatics, and the electrostatic interaction of SRFA-uranyl was significantly stronger owing to the formation of more complexes. The flexible SRFA could markedly enhance the bonding strength of uranyl with GO by folding itself to provide more sites to coordinate with uranyl. The rigid WFAs tended to be adsorbed on GO surface in parallel due to π - π interactions, whereas the flexible SRFAs took more slant configurations resulting from intermolecular hydrogen bonds (Figure 2). This work provides new insights into the sorption dynamics, structure, and mechanism, and addresses the effect of molecular rigidity and flexibility, with great significance for FA-based remediation strategies of uranium-contaminated sites.

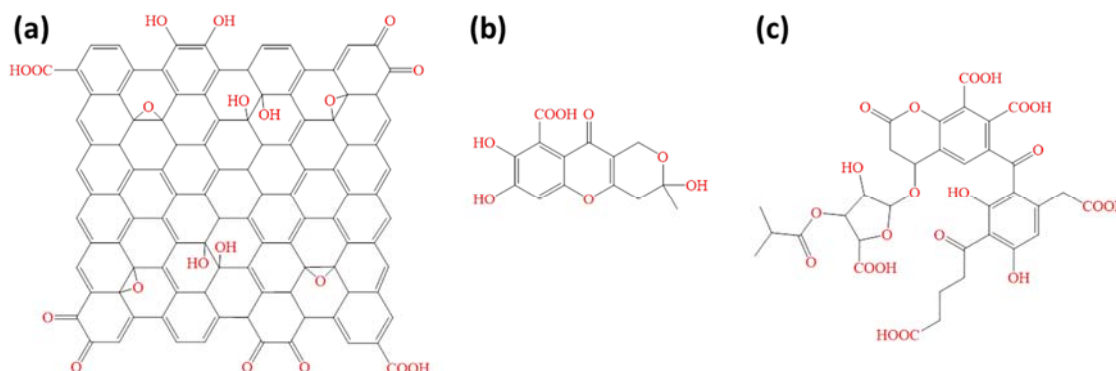


Figure 1. Molecular structures of GO and two FA models: (a) GO, (b) the rigid Wang's FA (WFA), and (c) the flexible Suwannee River FA (SRFA).

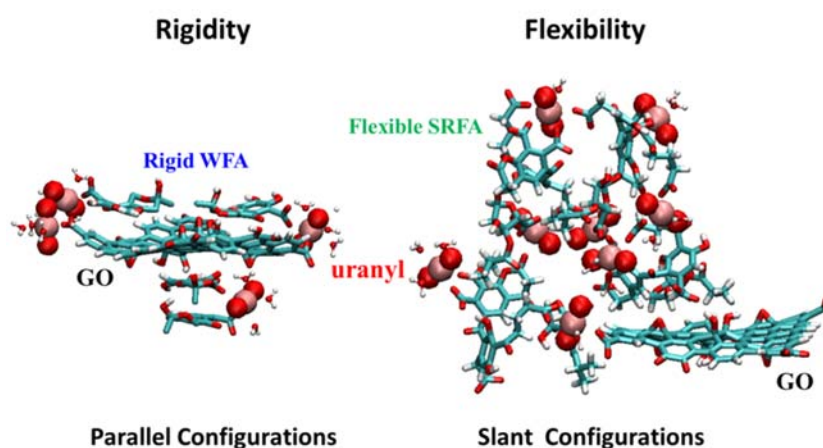


Figure 2. The configurations formed by GO with the rigid WFAs (left) and the flexible SRFAs (right).

Acknowledgments: Financial support from the National Natural Science Foundation of China (22106111), the Natural Science Foundation of Sichuan Province (2022NSFSC0239), and the LiaoNing Revitalization Talents Program (XLYC2002015) is gratefully acknowledged.

References

- [1] Yang, F. Tang, C. Antonietti, M. (2021) Natural and artificial humic substances to manage minerals, ions, water, and soil microorganisms. *Chem. Soc. Rev.* 50: 6221-6239.
- [2] Tang, W.-W. Zeng, G.-M. Gong, J.-L. Liang, J. Xu, P. Zhang, C. Huang, B.-B. (2014) Impact of humic/fulvic acid on the removal of heavy metals from aqueous solutions using nanomaterials: A review. *Sci. Total Environ.* 468-469: 1014-1027.
- [3] Chang, K. Li, X. Liao, Q. Hu, B. Hu, J. Sheng, G. Linghu, W. Huang, Y. Asiri, A. M. Alamry, K. A. (2017) Molecular insights into the role of fulvic acid in cobalt sorption onto graphene oxide and reduced graphene oxide. *Chem. Eng. J.* 327: 320-327.
- [4] Zong, P. Shao, M. Cao, D. Xu, X. Wang, S. Zhang, H. (2021) Synthesis of potential Ca–Mg–Al layered double hydroxides coated graphene oxide composites for simultaneous uptake of europium and fulvic acid from wastewater systems. *Environ. Res.* 196: 110375.

PB4-4 THE MECHANISM OF URANIUM(VI) BIOMINERALIZATION IN THE GROWTH OF *BACILLUS* SP. DWC-2

Yuqi Guo¹, Hong Tu¹, Feize Li¹, Yuanyou Yang¹, Jijun Yang¹, Tu Lan¹, Ning Liu¹, Jiali Liao^{1,*}

(1) Key Laboratory of Radiation Physics and Technology, Ministry of Education, Institute of Nuclear Science and Technology, Sichuan University, Chengdu 610064, PR China

The U(VI) biomineralization on microorganisms will affect the chemical form and migration behavior of uranium in the environment. However, there are few studies on the kinetic behavior and the relevant mechanism of U(VI) biomineralization in the growth of microorganisms. In this work, the effects of pH values, sodium glycerophosphate (SGP) and U(VI) concentration on the biomineralization behavior of U(VI) in the growth of *Bacillus* sp. dwc-2, a bacterial strain isolated from a low-uranium radioactive waste disposal site, and the possible mechanism were investigated. The results showed that the deposition/mineralization of U(VI) on *Bacillus* sp. dwc-2 was an enzymatic reaction, which was significantly affected by pH value, sodium glycerophosphate (SGP) concentration and U(VI) concentration. The initial U(VI) concentration affected the kinetics process of U(VI) biomineralization^[1]. The increase of U(VI) concentration (50 ppm-150 ppm) stimulated the expression of phosphatase activity and phosphate metabolism at the initial stage of biomineralization (0-12 hours), leading to a shift of biomineralization time from 48 hours to 12 hours (Fig 1a).^[2] While in the decay period of the cell, the toxicity of U(VI) would further reduce the cell activity, thereby reducing the activity of phosphatase and U(VI) biomineralization; The increase of the SGP concentration could promote the catalytic reaction rate of phosphatase, and then promote the U(VI) biomineralization. When the SGP concentration increased from 5 mM to 25 mM, the time of biomineralization advanced from 24 hours to 12 hours; The phosphatase activity increased rapidly at the initial stage of biomineralization (0-12 hours) under neutral and alkaline conditions (Fig 1b), thus promoting the consumption of phosphate and the U(VI) biomineralization. Especially under alkaline conditions, the sediment was transformed into obvious crystal minerals at the 8th hour. The results of EXAFS analysis showed that the sediment of biomineralization under neutral and alkaline conditions were uranium-bearing mica. However, due to the low activity of enzyme under acidic condition (pH 5.5), U(VI) that failed to form phosphate precipitation may be hydrolyzed with the increase of pH value^[3]. In addition to uranium-bearing mica, the final sediment also contained a small amount of hydroxide precipitation (7%). The above research results are helpful to better understand uranium biomineralization induced by microorganisms, and provide certain reference value for the subsequent bioremediation of uranium.

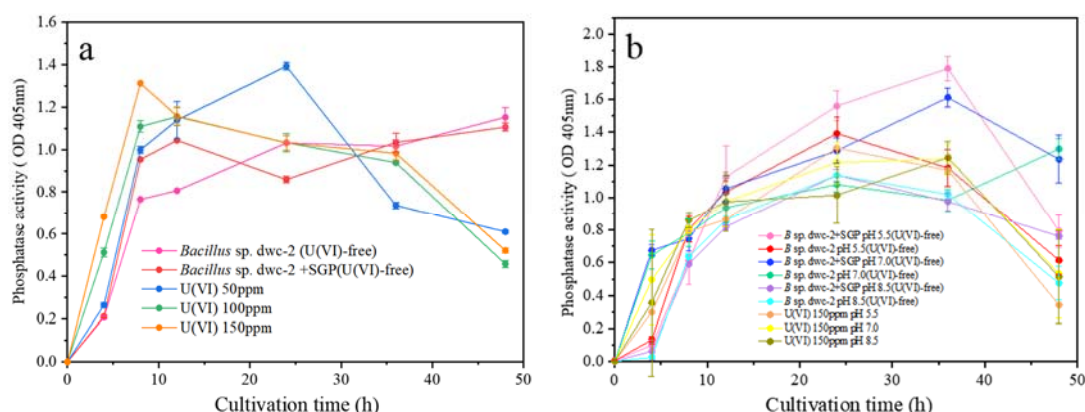


Fig 1. The phosphatase activity of U(VI) biomineralization under different conditions: (a) Initial U(VI) concentration; (b) Initial pH value

* Corresponding author.

E-mail address: liaojiali@scu.edu.cn (J. Liao)

Acknowledgments: *This work is financially supported by the National Natural Science Foundation of China (No.21876123) and the Fundamental Research Funds for the Central Universities. We acknowledge the technical support of Prof. Linjuan Zhang of the Shanghai Institute of Applied Physics for extend X-ray absorption fine structure (EXAFS) analysis.*

References

- [1] Wei, YaliChen, ZhiSong, HanZhang, JianLin, ZhangDang, ZhiDeng, Hong. (2019). The immobilization mechanism of u(vi) induced by bacillus thuringiensis 016 and the effects of coexisting ions. *Biochemical Engineering Journal*, 144.
- [2] Beazley, M. J. , Martinez, R. J. , Webb, S. M. , Sobecky, P. A. , & Taillefert, M. . (2011). The effect of ph and natural microbial phosphatase activity on the speciation of uranium in subsurface soils. *Geochimica Et Cosmochimica Acta*, 75(19), 5648-5663.
- [3] Beazley, M. J. , Martinez, R. J. , Sobecky, P. A. , Webb, S. M. , & Taillefert, M. . (2007). Uranium biomineralization as a result of bacterial phosphatase activity: insights from bacterial isolates from a contaminated subsurface. *Environmental Science & Technology*, 41(16), 5701-5707.

PB4-5 THE BEHAVIOR AND MECHANISM OF URANIUM BIOREDUCTION INDUCED BY A NATURAL BACILLUS THURINGIENSIS

Shunzhang Chen, Junyuan Gong, Yuqi Guo, Hui Li, Feize Li, Tu Lan, Yuanyou Yang, Jiali Liao*, Ning Liu

Key Laboratory of Radiation Physics and Technology of the Ministry of Education, Institute of Nuclear Science and Technology, Sichuan University, Chengdu 610064, China

Uranium is one of the widely concerned pollution element in radioactive contaminated environment as its long-term radioactivity and biochemical toxicity. Under natural conditions, soluble hexavalent uranium (U(VI)) is the universal form with migrated ability in environment. As an important environmental media with abundant chemical component and prominent biological activity, microorganism can induce the changes in the chemical behavior of migrated U(VI) in the environment through various pathways. Especially in anaerobic condition, bioreduction of U(VI) induced by microorganisms is extensively concerned due to the changes of uranium species, in which U(VI) can be reduced to U(IV), leading to uranium deposition. In this study, a *Bacillus thuringiensis* strain (identified as *B. thuringiensis* x-27 by 16SRNA) with natural uranium tolerance was isolated from uranium contaminated soil for the investigation of U(VI) bioreduction. In anaerobic atmosphere, Reduced U(IV) from bioreduction induced by *B. thuringiensis* x-27 could reached to 1.63 mg/g when bacteria were cultured in a medium with U(VI) concentration of 60 mg/L, initial pH of 6.0 and biomass content of 10 g/L at 30°C, and sodium lactate of 0.02 mol/L was used as electron donor. The reduction product of uranium was amorphous U(IV) sediment. Bioreduction of U(VI) induced by *B. thuringiensis* x-27 mainly depended on the electron transmission through the intracellular nicotinamide adenine dinucleotide dehydrogenase-ubiquinone system. Electrons for the bioreduction was originated from the metabolism of sodium lactate via lactate dehydrogenase, pyruvate dehydrogenase and citric acid cycle. Moreover, operation of U(VI) bioreduction could further keep the biological activity of bacteria. Through the investigation of U(VI) bioreduction in widely distributed atypical U(VI) reducing microorganisms, it can provide basis for the change in the uranium migration behavior affected by the bioreduction in broader natural anaerobic environment.

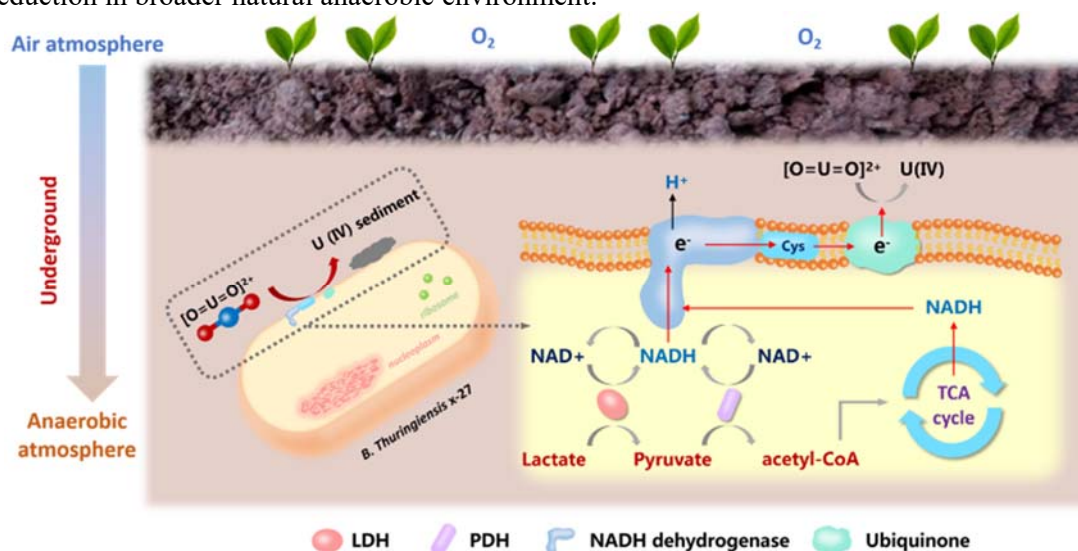


Figure 1 Schematic of uranium bioreduction induced by *B. thuringiensis* x-27

Acknowledgments: This work was financially supported by National Natural Science Foundation of China (Grant No. 21876123) and the National Fund of China for Fostering Talents in Basic Science (J1210004).

* E-mail: liaojiali@scu.edu.cn

PB4-6 BIOMIMETIC PHOTOCATALYTIC SYSTEMS DESIGNED BY SPATIALLY SEPARATED COCATALYSTS ON Z-SCHEME HETEROJUNCTION WITH IDENTIFIED CHARGE-TRANSFER PROCESSES FOR BOOSTING REMOVAL OF U(VI)

Yunhai Liu, Zhimin Dong, Zifan Li, Xiaohong Cao, Zhibin Zhang*

State Key Laboratory of Nuclear Resources and Environment, East China University of Technology, Nanchang, Jiangxi 330013, P.R. China

Nuclear energy has becoming a relatively clean energy source because it does not produce greenhouse gases. Radionuclide uranium is a key element for the long-term sustainable development of nuclear power that will generate huge uranium demands in the future. However, a large amount of radioactive waste will be produced in the process of mining and mineral processing of uranium minerals, in which the uranium concentration is much higher than $5 \text{ mg}\cdot\text{L}^{-1}$ set by the World Health Organization. The discharge of uranium-containing wastewater inevitably poses potential threats to the environment and humans.

Photocatalytic reduction technology has proven to be one of the most promising methods for transforming soluble U(VI) into a uranium precipitate from uranium mining wastewater, which is conducive to the development of clean and renewable nuclear energy and the resolution of environmental crises. Even though various photocatalysts demonstrated excellent photocatalytic reduction capability for U(VI), the photocatalytic process usually requires additional scavengers or protective gases. Moreover, practical applications of photocatalysts in treating natural uranium mine wastewater have rarely been reported. On the one hand, the photogenerated charges cannot efficiently flow to the surface reaction sites before bulk recombination in natural uranium mine wastewater with high salinity (such as $\text{Cl}^- 40 \text{ g}\cdot\text{L}^{-1}$) and organic pollutants under natural light. The high salinity concentration will compress the electric double layer at the photocatalytic interface, making uranium more difficult to contact with excited electrons. On the other hand, uranium precipitated after photoreduction would easily block the active sites of the photocatalyst or reoxidize to U(VI) due to the closed active sites of redox. Therefore, designing a unique photocatalytic system to remove U(VI) from natural uranium mine wastewater could break through these obstacles by completely inhibiting reverse electron transfer. Based on the above analysis, we proposed our research contents.

Inspired by natural photosynthesis, we assemble a biomimetic photocatalytic system $\text{MnO}_x@\text{TiO}_2@\text{CdS}@\text{Au}$ (MCTA) by designing a novel biomimetic photocatalysts with loading oxidative cocatalysts (MnO_x) and reduction cocatalysts (Au NP) on the inner and outer surfaces of the $\text{TiO}_2@\text{CdS}$. Z-scheme heterojunction in $\text{TiO}_2@\text{CdS}$ would efficiently suppress the charge recombination in bulk. Meanwhile, the spatially separated cocatalysts could further drive electrons and holes near the surface to migrate in opposite directions without reverse charge transfer. Theoretical calculation identifies multiple consecutive forward charge transfers without charge recombination within biomimetic photocatalysts. Thus, MCTA could efficiently remove 99.61% of U(VI) after 15 min of simulated sunlight irradiation within $3 \text{ mmol}\cdot\text{L}^{-1} \text{ NaHCO}_3$ with 0.231 min^{-1} of the reduction rate constant, outperforming most previously reported photocatalysts. The biomimetic photocatalytic platform achieved unassisted solar treatment of radioactive contaminants (degradation of organic pollutants and anionic reoxidation of uranium precipitates), and the U(VI) removal ratio reached 91.83% from natural uranium mine wastewater under sunlight irradiation.

In view of the feasibility of the synergistic strategy between Z-scheme heterojunction and spatially separated co-catalyst, a bifunctional $\text{Co}_3\text{O}_4@\text{TiO}_2@\text{CdS}@\text{Au}$ double-shelled nanocages (CTCA) was synthesized through Co_3O_4 and Au NP cocatalysts loaded on the inner and outer surfaces of the Z-scheme heterojunction ($\text{TiO}_2@\text{CdS}$). Under simulated sunlight irradiation, the reduction rate constant

of U(VI) by CTCA reached 0.218 min^{-1} , which was 6.6, 3.2 and 36.3 times than that of monolayer CTCA (0.033 min^{-1}), CTC (0.068 min^{-1}) and CT (0.006 min^{-1}). The removal rates of U(VI) and phenol were both over 90%, and photothermal degradation of various organic pollutants were 92.5% for bisphenol A, 98.2% for Rodamine B, 98.4% for methylene blue, and 98.3% for tannic acid, respectively. The full-spectrum light-assisted photothermal catalytic performance can rival the performance of the current excellent photocatalytic system. Detailed characterizations and theory calculations revealed that the photogenerated holes and electrons in CTCA flow inward and outward, accumulating on the corresponding cocatalysts. More importantly, Co_3O_4 as a “nanoheater” generated the photothermal effect for further enhancing the charge transfer to underpin its superior activity and accelerate the surface reduction–oxidation kinetics. Meanwhile, the photogenerated electrons and superoxide radicals play an dominant role in reducing the adsorbed U(VI) to insoluble $(\text{UO}_2)\text{O}_2 \cdot 2\text{H}_2\text{O}(\text{s})$.

According to natural photosynthetic structures, the synergistic effect of nature-inspired Z-scheme and spatially separated cocatalysts was used to construct two novel biomimetic photocatalytic platform ($\text{MnO}_x@\text{TiO}_2@\text{CdS}@\text{Au}$ and $\text{Co}_3\text{O}_4@\text{TiO}_2@\text{CdS}@\text{Au}$). This unique double-shelled hollow structure significantly increases the utilization of photoinduced charges for high-efficiency removal of U(VI). This study provides valuable insights into a biomimetic photocatalytic system for treating natural uranium mine wastewater to address environmental contamination issue.

PB4-7 ORGANICALLY BOUND TRITIUM SPECIATION IN ENVIRONMENTAL MATRICES BY ISOTOPIC EXCHANGE

Nivesse Anne-Laure ⁽¹⁾, Baglan Nicolas ⁽²⁾, Montavon Gilles ⁽¹⁾, Péron Olivier ⁽¹⁾

(1) SUBATECH, UMR 6457, IMT Atlantique/IN2P3-CNRS/Nantes Université, 4, Rue Alfred Kastler,

BP 20722, Nantes Cedex 3, 44307, France

(2) Autorité de Sûreté Nucléaire (ASN), 15, Rue Louis Lejeune, Montrouge, 92120, France

Tritium (³H or T), the radioactive isotope of the hydrogen element, is one of the main radionuclides released by nuclear installations during normal operation and the only one for which release forecasts in future years are on the rise. Once released into the environment, tritium enters the hydrogen cycle and incorporates into living organisms in which it integrates organic matter in the form of organically bound tritium (OBT). In 2017, the IRSN published a report on the update of knowledge on tritium [1], taking up some of the questions that have been waiting to be answered since the publication of the Livre Blanc du Tritium by ASN in 2010 [2]. Among these, those concerning the behavior, the fate and the speciation of this radionuclide in the environment are still relevant.

The existence of two forms of OBT is commonly accepted: an "exchangeable" fraction (E-OBT) in permanent equilibrium with the surrounding environment and a "non-exchangeable" fraction (NE-OBT) which persists in the carrier molecule until its degradation. However, there is currently no consensus to describe the exact distribution of these two forms in an organic molecule and several variations are found in the literature depending on the considered application [3]. According to a widespread point of view, the nature of the exchangeable and non-exchangeable forms of OBT could be established in an organic molecule depending on the type of chemical bond in which the tritium is involved. However, this description has been questioned several times since the highlighting of major limitations of the exchange capacities of this supposedly exchangeable fraction of the OBT within environmental matrices. The molecular conformations adopted by certain macromolecules carrying OBT would then be responsible for bonding phenomena and obstructions of hydrogen positions in their structure, significantly reducing the exchange capacities of the atoms involved. To take into consideration these so-called buried form, several studies have suggested including the structural properties of carrier organic molecules to describe the distribution of exchangeable and non-exchangeable forms of OBT. Furthermore, a validated method is currently lacking for the analysis of OBT forms in an environmental matrix. The intrusiveness of current procedures has been assumed to be responsible for a potential analytical bias, which does not make it possible to benefit from certainty as to the nature of the fractions of OBT analyzed.

An original ³H/¹H isotopic exchange process in a controlled atmosphere was developed in order to access the parameter (α_{iso}), a representation of the global exchange capacity of the hydrogen atoms of a studied matrix (see Eq. 1). This parameter is then compared to a theoretical exchangeability parameter (α_{model}) deduced from the molecular models of the constituents of the matrix in order to assess the occurrence of burial phenomena.

$$\left(\frac{T}{H}\right)_{OBT} = \alpha_{iso} \times \left(\frac{T}{H}\right)_{E-OBT} + (1 - \alpha_{iso}) \times \left(\frac{T}{H}\right)_{NE-OBT} \quad (\text{Eq. 1})$$

From this procedure, it was thus possible to study the nature of OBT found in matrices of the human food chain (wheat grain and apple), as well as in a bio-indicator (aquatic milfoil). Certain specific molecular structures (in particular the semi-crystalline structure of cellulose) have been clearly identified as responsible for the phenomena of reduced accessibility of theoretically exchangeable hydrogen positions with a quantifiable impact on the nature of the OBT found in the carrier matrix. These results then led to the development of a method for reliably determining the speciation of OBT found in environmental matrices based solely on the knowledge of the molecular characteristics of their major constituent

(starch, fructose, etc.) [4]. A specific study of the major constituent of all terrestrial biomass, cellulose, then made it possible to establish a direct link between the crystalline structure of this molecule and the accessibility of its OH groups [4]. The experimental model thus established must then make it possible on the one hand to estimate the potential NE-OBT contents contained in any environmental matrix consisting mainly of cellulose. On the other hand, the model may contribute to the evaluation of the complexation-retention capacities of this cellulose with respect to certain heavy metals found in the environment. In this same context, the isotopic exchange method has been adapted to the determination of the potential for soil complexation with certain pollutants - radioactive or not - based on a study of several types of humic substances [6].

Finally, a robust statistical comparative study made it possible to evaluate and quantify the analytical biases of the conventional method of analyzing the forms of OBT in the environment. By combining a set of analytical techniques and metrological optimization processes, this latest work has been able to highlight the relevance of the different methods for analyzing known forms of TOL, depending on the application considered, from environmental monitoring to fundamental research [7].

References

- [1] IRSN. (2017). Rapport Actualisation des connaissances Tritium Environnement. Editor : Institut de Radioprotection et de Sûreté Nucléaire (IRSN).
- [2] ASN. (2010). Le livre blanc du tritium, groupes de réflexion menés de mai 2008 à avril 2010 sous l'égide de l'ASN. published by ASN.
- [3] Kim, S. B., Baglan, N. et Davis, P. A. (2013). Current understanding of organically bound tritium (OBT) in the environment. *Journal of Environmental Radioactivity*, Vol. 126(1), 83-91.
- [4] Nivesse, A-L., Baglan, N., Montavon, G., Granger, G. et Péron, O. (2021). Cellulose, proteins, starch and simple carbohydrates molecules control the hydrogen exchange capacity of bioindicators and foodstuffs. *Chemosphere*.
- [5] Nivesse, A-L., Baglan, N., Montavon, G. et Péron, O. (2021). New insights into the accessibility of native cellulose to environmental contaminants through an efficient analytical process. *Journal of Hazardous Materials*.
- [6] Nivesse, A-L., Thibault de Chanvalon, A., ...Péron, O. (2020). An overlooked pool of hydrogen stored in humic matter revealed by isotopic exchange: implication for radioactive ^3H contamination. *Environmental Chemistry Letters*, Vol. 18(2), 475-481.
- [7] Nivesse, A-L., Baglan, N., Montavon, G., Granger, G. et Péron, O. (2021). Non-intrusive and reliable speciation of organically bound tritium in environmental matrices. *Talanta*.

PB5-1 MIGRATION OF ^{60}Co , ^{133}Ba , ^{137}Cs , AND ^{152}Eu FROM CEMENTITIOUS WASTEFORMS IN FIELD LYSIMETER EXPERIMENTS

Reid Williams⁽¹⁾ Daniel I. Kaplan⁽²⁾, Timothy A. DeVol^(1,4), Bryan J. Erdmann⁽³⁾, and Brian A. Powell^(1,4)

(1) Department of Environmental Engineering and Earth Sciences, Clemson University, Anderson, SC, 29625, USA.

(2) Savannah River Ecology Laboratory, University of Georgia, Aiken, SC 29802, USA

(3) Environmental Restoration Group, Albuquerque, NM, 87113, USA

(4) Center for Nuclear Environmental Engineering Sciences and Radioactive Waste Management Center (NEESRWM), Clemson University, Clemson, SC, 29634, USA

The need to develop effective and reliable systems for the storage of radioactive wastes has become increasingly apparent. To reach this objective, it is essential to understand and predict the transport of radionuclides through the vadose zone. Field-scale lysimeter studies are an advantageous method to evaluate the long-term transport of radionuclides under conditions representative of the vadose zone. Additionally, this method allows for the quantification of radionuclide transport and provides insight into the geochemistry of the vadose zone. Furthermore, studies of this nature will reduce the uncertainty and improve geochemical models, yielding better waste storage designs.

The present work describes a 10-year-long, ongoing experiment at the Radionuclide Field Lysimeter Experiment (RadFLEX) facility at the United States Department of Energy Savannah River Site (SRS). The field lysimeters deployed in this work contained a sandy clay loam soil and the gamma-ray emitting isotopes ^{137}Cs , ^{60}Co , ^{133}Ba , and ^{152}Eu incorporated into cementitious wasteform (Portland cement or reducing grout) or a filter paper. This work serves as a follow-up to a study conducted in 2017 which non-destructively measured the concentration of each radionuclide in the soil column as a function of depth after 4 years of deployment in the field [1]. Following the measurement, the lysimeter were redeployed in 2017, recovered in late 2021, and similarly analyzed in 2022 to determine the extent of transport after another 4 years of deployment. The filter paper containing lysimeters were intended to function as a control, with the filter paper serving as a proxy for direct exposure of the radionuclides to the soil. The initial radionuclide activities varied by waste form type; cementitious pucks contained 4.0 to 9.0 MBq total activity and the filter papers contained 0.25 to 0.47 MBq.

The non-destructive analytical technique used to measure the lysimeters in this study was initially developed for the 2017 work [1]. Essential components of the detection system include a high-purity germanium (HPGe) detector, a high-voltage power supply, an amplifier, a multi-channel analyzer, collimated lead shielding, and a stepping motor. Slight alterations of the detector system geometry and the measurement procedure were made for the present work. In practice, the two detection systems were nearly identical.

Comparison of the radionuclide soil profiles measured in 2017 with those measured in 2022 detected increased relative activity concentrations for the radionuclides further from the wasteforms in all four lysimeters, indicating that transport increased during the period following redeployment. Both upward and downward transport were observed indicating diffusion from the source is a significant transport pathway. The analyses of the ^{152}Eu distributions from the 2017 and 2022 studies produced nearly identical symmetric spatial distributions. The similarity of the spatial distribution in both years demonstrates that there was little to no change in the ^{152}Eu distribution, indicating that the radionuclide is predominantly still contained within the wasteforms. The 2017 analyses of the ^{60}Co and ^{133}Ba concentrations when the radionuclides were introduced directly to the soil (via the filter paper wasteform) demonstrated extensive downward movement and, to a lesser extent, upward movement from the location of the wasteform. However, the analyses of the concentrations in the cementitious

wasteform lysimeters demonstrated little to no movement of ^{60}Co and ^{133}Ba away from the source. Interestingly, the ^{60}Co activity concentration shifted in 2022 compared to 2017 with a greater increase in concentrations further above the source, relative to those below it. Consistent with the other radionuclides, the redeployment period increased the extent of ^{137}Cs transport away from the lysimeter sources and greater spreading of the ^{137}Cs was observed in the cementitious waste forms compared with the filter paper sources.

Since ^{137}Cs exhibited the greatest migration, our focus is on determining the specific chemical mechanisms controlling ^{137}Cs mobility. The observed spatial distributions suggest that advective transport does not play a large role in the mobility of ^{137}Cs away from the solid wasteforms [1]. Calculated average Darcy velocities of the four lysimeters yielded Peclet numbers that verified the systems are heavily diffusion-controlled [1]. However, the analyses demonstrated variability between the Cs distributions in the four lysimeters, indicating the presence of other mechanisms. Other factors that are thought to impact ^{137}Cs distribution are the concentration of ^{137}Cs present in the column, the material of the source, and the composition of the soil.

Differences were observed when comparing the ^{137}Cs spatial distributions. Of the ^{137}Cs leached from the source, ^{137}Cs traveled further from the cementitious wasteforms relative to the filter paper control. Soils used in the lysimeters and other SRS soils have been observed to contain a small fraction of frayed edge clay minerals which exhibit a high affinity for Cs^+ sorption [2,3]. Additionally, the cations present (Na^+ and Ca^+) in the Portland-cement and grout wasteforms have been shown to compete for ion exchange sites, thereby increasing Cs^+ mobility [4]. This competition could reduce the number of sites available for ^{137}Cs sorption in the non-control lysimeters leading to increased diffusion in these systems and explaining the lack of diffusion observed in the control lysimeters.

References

- [1] Erdmann, B., Powell, B.A., Kaplan, D.I., DeVol, T., (2018) One-dimensional spatial distributions of gamma-ray emitting contaminants in field lysimeters using a collimated gamma-ray spectroscopy system, *Health Physics*, 114 (5) 532-536.
- [2] Barber, K., (2017) Evaluation of Aging Processes Controlling Cesium Transport Through Savannah River Site Soils. MS Clemson University.
- [3] Goto, M., Rosson, R., Wampler, J. M., Elliott, W. C., Serkiz, S., & Kahn, B. (2008). Freundlich and Dual Langmuir Isotherm Models for Predicting ^{137}Cs Binding on Savannah River Site Soils. *Health Physics*, 94(1), 18–32.
- [4] Kaplan, D. I., (2016) Geochemical Data Package for Performance Assessment Calculations Related to the Savannah River Site. Geochemical Data Package for Performance Assessment Calculations Related to the Savannah River Site, Rep. No. SRNLSTI-2009-00473. Rev. 1.

PB5-2 MODELING A RADIONUCLIDE TRANSPORT EXPERIMENT IN GRANITIC ROCK MATRIX AT GRIMSEL. THE ROLE OF ADVECTION.

Josep M. Soler⁽¹⁾, Deby Jurado⁽¹⁾, Maarten W. Saaltink⁽²⁾, Lurdes Martínez⁽²⁾, Juan J. Hidalgo⁽¹⁾, G. William Lanyon⁽³⁾, Andrew J. Martin⁽⁴⁾

(1) IDAEA-CSIC, Catalonia, Spain

(2) UPC, Catalonia, Spain

(3) Fracture Systems Ltd, UK

(4) NAGRA, Switzerland

Within the framework of the GTS-LTD project (Grimsel Test Site – Long-Term Diffusion), funded by NAGRA (Switzerland), NUMO (Japan), SURAO (Czech Republic) and BASE (Germany), a radionuclide transport experiment in unfractured granitic rock matrix was performed. Grimsel groundwater containing several tracers (^3H as HTO, $^{36}\text{Cl}^-$, $^{22}\text{Na}^+$, $^{134}\text{Cs}^+$, $^{133}\text{Ba}^{2+}$) was continuously circulated through a packed-off borehole interval. The decrease in tracer concentrations in the solution was monitored for a period of 1266 days (05/03/2014 – 22/08/2017). Additionally, tracer breakthrough was monitored in an observation borehole a few cm away.

Initial modeling of the experiment (1D radial), considering transport only by diffusion, showed that the evolution of tracer concentrations departed from the expected trend after some time, with concentrations in the injection borehole decreasing faster than expected. Additional 2D calculations (section normal to the boreholes) were performed to check the possible effect of advection through the rock matrix. Advection could explain the evolution of concentrations in the injection borehole, but concentrations in the observation borehole were overestimated.

Core samples from new boreholes were collected immediately after the end of the experiment, allowing the measurement of tracer distributions in the rock. The observed patterns for the non-sorbing tracers (HTO, $^{36}\text{Cl}^-$) showed clear preferential transport directions, consistent with advective flow towards the gallery from which the boreholes were drilled. Final 3D modeling of the experiment can explain the measured concentrations in the boreholes and in the rock. Tracer transport for the conservative tracers (HTO, $^{36}\text{Cl}^-$; Fig. 1) is affected by both diffusion and advection through the granitic rock matrix. Also, in situ accessible porosities (about 0.0014) are smaller than those measured in rock samples (about 0.009), pointing to unloading of the rock samples after drilling. The effect of advection for weakly sorbing tracers ($^{22}\text{Na}^+$; Fig. 2) is only minor, and it is practically negligible for the strongly sorbing tracers ($^{134}\text{Cs}^+$, $^{133}\text{Ba}^{2+}$).

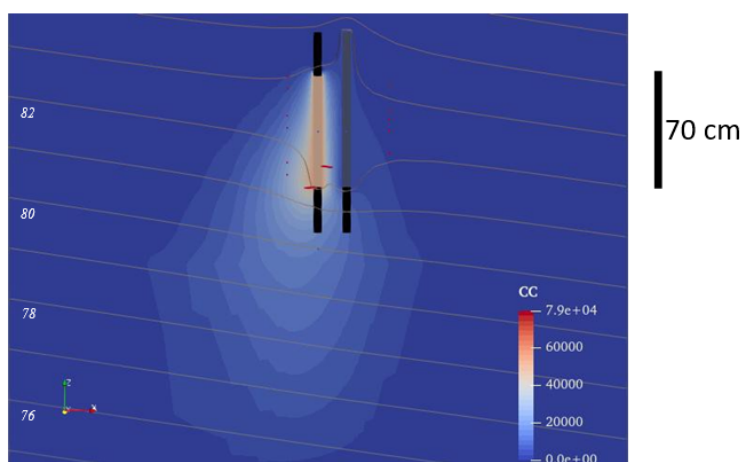


Figure 1. Model extension of the HTO tracer plume at the end of the experiment ($t = 3.5$ years). The distance between boreholes is 0.186 m. The length of the injection interval is 0.72 m. Concentrations in Bq/g_{water}.

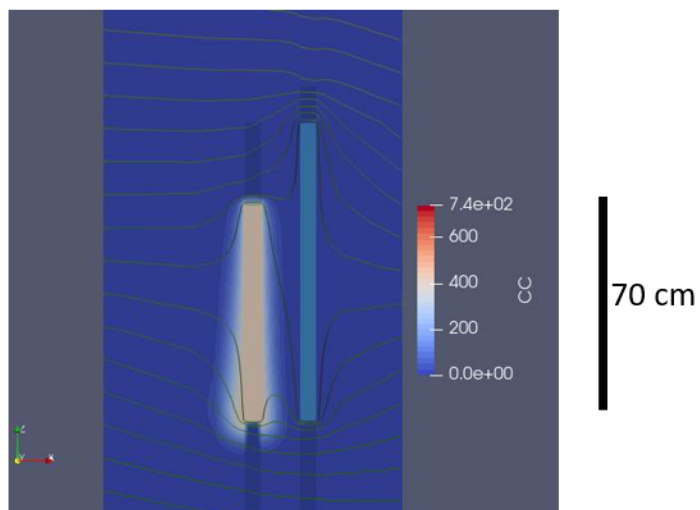


Figure 2. Model extension of the $^{22}\text{Na}^+$ tracer plume at the end of the experiment (3.5 years). The distance between boreholes is 0.186 m. The length of the injection interval is 0.72 m. Concentrations in Bq/g_{water}.

PB5-3 CHARACTERISTICS OF GRANITIC AQUIFER COLLOIDS IN THE KURT GROUNDWATER SYSTEM

Junhyuk Ha and Jun-Yeop Lee

*School of Mechanical Engineering, Pusan National University
2, Busandaehak-ro 63beon-gil, Geumjeong-gu, Busan 46241, Republic of Korea*

The colloidal particles formed in the deep aquifer consist of inorganic particles, natural organic matter, and microorganisms originating from the weathering of rocks, degradation of plants, soil organic substances, *etc.* [1]. Due to high mobility and large surface area, colloidal substances are known to facilitate the migration of radionuclides in the groundwater system. Thus, understanding of characteristics of groundwater colloids is essential for the reliable safety assessment of geologic repository. In this respect, the objective of this work is to characterize the colloidal substances in the natural groundwater taken from the KAERI Underground Research Tunnel (KURT) located in Daejeon, Republic of Korea

The groundwater sample was collected from the DB-3 borehole in the KURT. All sample preparation and experiments were conducted in the glovebox filled with Ar gas ($O_2 < 5$ ppm). For the analysis of colloidal substances, the groundwater sample was treated by using a tangential flow ultra-filtration (TFUF) system equipped with a 3 kDa membrane filter after the pre-filtration (0.45 μm). The physicochemical properties of the DB-3 groundwater colloids were determined by using various analysis methods. The chemical analyses of aqueous ions and colloidal substances in DB-3 groundwater were conducted with ICP-MS/OES, IC, and TOC. Furthermore, the particle size, morphology, and stability of groundwater colloids were analyzed by using DLS/ELS and SEM/TEM-EDS. For the speciation of organic carbon contents, TOC, ATR-FTIR, and LC-OCD (liquid chromatography-organic carbon detection) were employed.

After reaching the equilibrium, the pH and E_h of the DB-3 groundwater sample were determined to be pH = 8.9 and $E_h = -242$ mV, respectively. The chemical analysis results showed the predominant presence of Na, Si, and Ca ions as the colloidal substances in the DB-3 sample. The size distribution of DB-3 groundwater colloids was determined to be 5 – 400 nm with SEM/TEM methods, and the hydraulic diameter of colloidal substances of 182 ± 53 nm was obtained by using DLS/ELS with a zeta potential of -23.7 ± 1.3 mV. Relatively neutral values of the zeta potential indicated presumable coagulation of the colloidal substances, which agrees well with the results obtained from the SEM [2]. Furthermore, the TEM-EDX result showed two different types of colloids: the first with the size of ca. 50 nm composed mostly of Si and Al, and the second with less than 10 nm in size containing Mo (see Fig. 1). The Si and Al observed in the colloids were expected to be originated from the weathering of host rocks in the granitic groundwater system. On the other hand, the presence of Mo in the colloidal substances was presumably due to the metallic substances employed during the drilling work of the DB-3 borehole, such as metal casing, packing system, *etc.* According to the TOC analysis, the colloidal organic carbon (COC) of the groundwater sample was determined to be 0.2 ppm, which corresponds to approximately 11 % of the total organic carbon in the DB-3 groundwater. Moreover, the FTIR spectrum showed the organic carbon was composed of alkane compounds with the structure of single bonds between the C and H [3]. Additionally, the quantitative analysis of natural organic matter (NOM) conducted using the LC-OCD revealed the predominant presence of low molecular weight (LMW) neutral groups. In general, the LMW-neutrals are known to exist in the compounds composed of the degradation of humic substances such as hydrocarbons, alcohols, ketones, aldehydes, and amides with a molecular weight of less than 350 g/mol. The results obtained with the LC-OCD were in accordance with those observed with ATR-FTIR, indicating the predominant presence of alkane compounds in the colloidal substances in the KURT DB-3 groundwater sample.

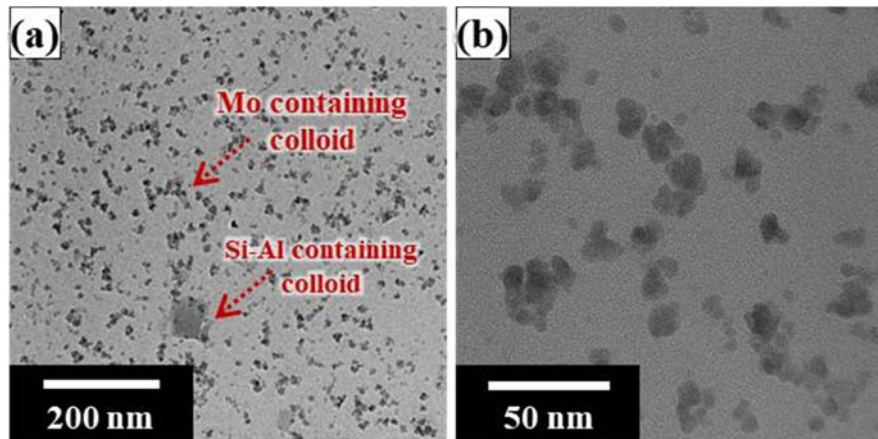


Fig. 1 TEM images of colloidal substances contained in KURT DB-3 groundwater sample with two different magnification ratios of (a) 1:50 K and (b) 1:300 K.

Acknowledgement: This work was supported by the National Research Foundation of Korea grant funded by the Korean government [No. NRF-2021M2E1A1085204].

References

- [1] Kamaraj, P., Sabarathinam, C., Seshadri, H., Panda, B., Karthikeyan, B., Viswanathan, P. M., Govindaraj, R., Nagappan, G. (2022). A study on geochemistry and sources of colloidal fractions in coastal groundwater from different lithologies. *J. Earth. Syst. Sci.* 131: 62
- [2] Hosseini, M. S., Khazaei, M., Misaghi, M., Koosheshi, M. H. (2022). Improving the stability of nanofluids via surface-modified titanium dioxide nanoparticles for wettability alteration of oil-wet carbonate reservoirs. *Mater. Res. Express* 9: 035005
- [3] Pavia, D. L., Lampman, G. M., Kriz, G. S., Vyvyan, J. R. (2015). *Introduction to Spectroscopy*. Cengage Learning, Boston.

PB5-4 THE HETEROGENEITY OF THE SANDY FACIES OF OPALINUS CLAY ACROSS SCALES, FROM SEISMIC SURVEYS TO RADIONUCLIDE DIFFUSION - AN *IN-SITU* TEST IN THE SWISS ROCK LABORATORY MONT TERRI

Frank Heberling¹, Hendrik Albers⁵, Thies Beilecke⁵, Guido Deissmann², Cornelius Fischer³, Markus Furche⁵, Horst Geckeis¹, Eva-Maria Hoyer⁶, Claudia Joseph¹, Axel Liebscher⁶, Luc Van Loon⁷, Stefan Lüth⁴, Bin Ma⁷, Volker Metz¹, Katharina Müller³, Ulf Nowak⁵, Francesca Quinto¹, Dorothee Rebscher⁵, Wolfram Rühaak⁶, Friedhelm Schulte⁵, Florian Steegborn¹, Torsten Tietz⁵

(1) Institute for Nuclear Waste Disposal, Karlsruhe Institute of Technology (KIT), Germany

(2) Institute of Energy and Climate Research – Nuclear Waste Management (IEK-6), Forschungszentrum Jülich (FZJ), Germany

(3) Institute of Resource Ecology, Helmholtz-Zentrum Dresden-Rossendorf (HZDR), Germany

(4) Helmholtz Centre Potsdam - German Research Centre for Geosciences (GFZ), Potsdam, Germany

(5) Federal Institute for Geosciences and Natural Resources (BGR), Hannover, Germany

(6) Federal Company for Radioactive Waste Disposal (BGE), Peine, Germany

(7) Laboratory for Waste Management, Paul Scherrer Institute (PSI-LES), Villigen PSI, Switzerland

Many countries consider clay rock formations as potential host rocks for high-level nuclear waste disposal. Clay rocks may exhibit heterogeneity on various scales, from the micro- to the facies-scale. In the Mont Terri rock laboratory, Switzerland, various experiments study properties and characteristics of the Jurassic Opalinus Clay, which is the target host rock for the Swiss nuclear waste repository but may also provide proxies for other considered clay rock formations. At Mont Terri, the Opalinus Clay mainly appears in a shaly and two sandy facies. So far, diffusion experiments at Mont Terri focussed on the relatively homogeneous shaly facies. The upper sandy facies (SF-OPA) exhibits a more pronounced internal – mineralogical and textural – heterogeneity. Clay rocks with comparable heterogeneity to SF-OPA may be present among the lower Cretaceous clay rocks of northern Germany, which are among the potential host rock candidates for a future German nuclear waste repository. Since 2020, seven institutions develop an *in-situ* diffusion experiment in SF-OPA, the so-called DR-D experiment, to explore the impact of rock heterogeneity on radionuclide diffusion in low permeability clay rocks.

So far, the DR-D experiment combined high-resolution seismic tomography, borehole logging, and detailed drill core analyses to characterize the heterogeneity of the selected SF-OPA area. The targeted rock zone exhibits a layer starting ca. 10 m below the gallery surface, which is characterized by relatively high seismic velocities. This layer is as well evident in the natural gamma- and the neutron backscattering logs. In the drill cores it stands out as whitish rock characterized by large concretions and traces of bioturbation in contrast to the dark layered clay-rock above and below with smaller concretions. Detailed analysis of seismic signals and drill-cores is still ongoing. In future, an *in-situ* diffusion test using various radioactive and non-radioactive tracers (HTO, ¹²⁹I, ²²Na, ¹³⁷Cs, ⁶⁰Co, potentially Se) will be conducted targeting the evidently heterogeneous rock section 10 m below the gallery surface. The evolution of tracer concentrations in a synthetic porewater circulating in the diffusion interval will be monitored. A second seismic tomography survey is planned after the termination of the diffusion experiment. Finally, overcoring and post-mortem analysis of the rock affected by tracer diffusion will be used to determine the local variability of diffusion parameters.

In this contribution, we present the general concept, technical layout, and expected scientific impact of the DR-D experiment, as well as first results from field and related laboratory studies.

PB5-5 STRONTIUM BEHAVIOUR IN RADIOACTIVELY CONTAMINATED LAND – UNDERPINNING OPTIONS FOR IN-SITU DISPOSAL

Jonathan Blagden ⁽¹⁾, Samuel Shaw ⁽¹⁾, Victoria Coker ⁽¹⁾, James Graham ⁽²⁾, Katherine Morris ⁽¹⁾

(1) *The University of Manchester, United Kingdom*

(2) *National Nuclear Laboratory, United Kingdom*

Decommissioning and site clearance activities at nuclear licensed sites in the UK are expected to produce significant volumes of concrete rubble from building demolition. This waste is expected to include on the order of 100,000s of cubic meters of crushed concrete waste contaminated to a low level with radionuclides (e.g. ⁹⁰Sr, ¹³⁷Cs) [1], efficient management and disposal of this material poses a significant liability to nuclear site operators. The potential for disposal of these waste materials on site is an emerging approach in the UK. This in-situ disposal approach has the potential to reduce waste inventories sent for disposal at specialist low level radioactive waste disposal facilities, minimise transport costs and the associated environmental burden, and offers a pathway for beneficial reuse of the already generated low level wastes at the originating site where this is compatible with achieving the desired site end-state [2]. In-situ disposal of radioactively contaminated materials require an understanding of radionuclide behaviour at the complex interfaces between the crushed concrete wastes and the sediment to develop an environmental safety case, and this is the focus of current work.

Strontium-90 is a high-yield fission product and a problematic contaminant as it is present in contaminant plumes at a number of nuclear sites around the world [3][4]. Strontium exists in the environment as the mobile Sr²⁺ cation and under ambient conditions typically interacts by reversible, outer-sphere sorption with sediments. This means subsurface mobility is controlled by available surface sites, pH, and the presence of competing cations [5]. Longer term retention of strontium has previously been achieved by in-situ mineralisation techniques, typically as strontium-substituted calcium carbonate (e.g. calcite, CaCO₃) or calcium phosphate (hydroxyapatite, Ca₁₀(PO₄)₆(OH)₂) phases due to their low solubility and capacity to incorporate strontium into their structure [6][7].

Here, aged concrete from a Nuclear Decommissioning Authority site (from the Low Level Waste Repository in West Cumbria), and sediment representative of the Sellafield nuclear licenced site have been characterised for experiments. In addition, the interaction of strontium with these materials has been investigated in batch systems with simulant groundwaters representative of the shallow sub-surface at Sellafield. Strontium was found to bind weakly to the sandy sediment by reversible outer sphere sorption with a K_d of 0.0019m³kg⁻¹ and well characterised by a Langmuir isotherm, consistent with the elevated ⁹⁰Sr mobility observed at Sellafield [4]. This Strontium K_d value is lower than values found in other sediments and indicates a coarse sandy sediment containing a small fraction of high surface area minerals such as clays, iron oxides and organic materials [8]. The composition, and therefore sorption capacity, of sediments is likely to vary both within and between nuclear licensed sites due to variations in local geology at each location [9], and the characterised material represents a poorly sorptive end-member sediment.

The behaviour of strontium in a crushed concrete/simulant groundwater system was investigated under air equilibrated (i.e. with CO₂) and air free (i.e. no CO₂) conditions as well as with and without additional phosphate amendments. Analyses of aqueous samples from experiments indicated that in air-free systems strontium uptake to the solid is poor (approximately 3.5% removal under experimental conditions after 1 day, not increasing significantly over the subsequent 1 week). Phosphate amendment of this system improved removal to 24% after 1 day with a continued increase to 34% at 1 week. The air equilibrated system showed 23% removal from solution after 24 hours increasing to greater than 64% after 1 week. This coincided with a drop in solution pH from the starting pH of 12.5 to a final pH of 8.4

presumably due to carbon dioxide dissolution. Indeed, XRD analysis of the reacted solid confirmed calcite (CaCO_3) formation was occurring in this experiment. Subsequent X-ray absorption spectroscopy on the solid phase confirmed strontium was incorporated into the newly formed calcium carbonate phase precipitated in the high pH environment from the cement leachate. The phosphate amended air-equilibrated system initially achieved >70% removal over 1 day followed by a slow re-release over 1 week. The pH conditions altered in this time, and Sr removal will be discussed in terms of likely controls on this system.

Overall, these data provide insight into the likely speciation of strontium in the complex interface environment between made ground and the natural environment and suggest both air (i.e. CO_2) and phosphate exposure may enhance strontium uptake into newly formed carbonate- and phosphate-mineral phases in the presence of crushed concrete wastes.

References

- [1] NDA and BEIS (2019). 2019 UK Radioactive Material Inventory
- [2] NDA (2021). Strategy Effective from March 2021
- [3] U.S. Department of Energy (2022). Hanford Annual Site Environmental Report for Calendar Year 2021 DOE/RL-2022-08 Rev. 0
- [4] Sellafield Ltd. (2016). Groundwater Monitoring at Sellafield: Annual Data Review 2016 LQTD000758
- [5] Wallace, S. H., Shaw, S., Morris, K., Small, J. S., Fuller, A. J., & Burke, I. T. (2012). Effect of groundwater pH and ionic strength on strontium sorption in aquifer sediments: Implications for ^{90}Sr mobility at contaminated nuclear sites. *Applied Geochemistry*, 27(8), 1482–1491.
- [6] Thorpe, C. L., Lloyd, J. R., Law, G. T. W., Burke, I. T., Shaw, S., Bryan, N. D., & Morris, K. (2012). Strontium sorption and precipitation behaviour during bioreduction in nitrate impacted sediments. *Chemical Geology*, 306–307, 114–122.
- [7] Cleary, A., Lloyd, J. R., Newsome, L., Shaw, S., Boothman, C., Boshoff, G., Atherton, N., & Morris, K. (2019). Bioremediation of strontium and technetium contaminated groundwater using glycerol phosphate. *Chemical Geology*, 509, 213–222.
- [8] Sohlenius, G., Saetre, P., Nordén, S., Grolander, S., & Sheppard, S. (2013). Inferences about radionuclide mobility in soils based on the solid/liquid partition coefficients and soil properties. *Ambio*, 42(4), 414–424.
- [9] Smith, N. T., Shreeve, J., & Kuras, O. (2020). Multi-sensor core logging (MSCL) and X-ray computed tomography imaging of borehole core to aid 3D geological modelling of poorly exposed unconsolidated superficial sediments underlying complex industrial sites: An example from Sellafield nuclear site, UK. *Journal of Applied Geophysics*, 178.

PB6-1 IDENTIFICATION ON THE ORIGIN AND FATE OF DISSOLVED U IN BOEUN AQUIFER, BASED ON C, O, FE, S, SR AND U-SERIES ISOTOPIC SIGNATURES

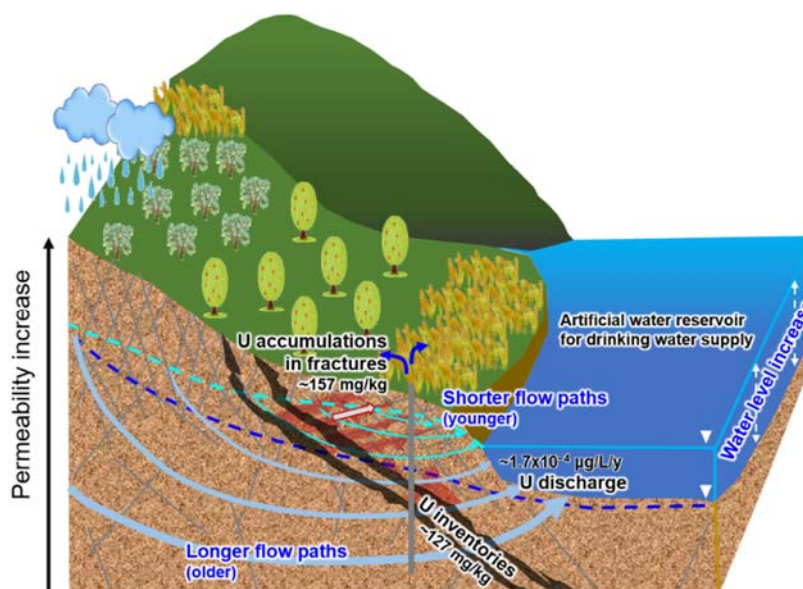
Y. Ju ⁽¹⁾, M. H. Baik ⁽¹⁾, S. Y. Lee ⁽¹⁾, D. Kaown ^{(2)*}, K.-K. Lee ⁽²⁾, D. Shin ⁽³⁾, J. H. Ryu ^{(1)*}

(1) Disposal Safety Evaluation Research Division, Korea Atomic Energy Research Institute, Daejeon 34057, Republic of Korea.

(2) School of Earth and Environmental Sciences, Seoul National University, 1 Gwanak-ro, Gwanak-gu, Seoul 08826, Republic of Korea

(3) Department of Geoenvironmental Sciences, Kongju National University, Gongju 32588, Republic of Korea

Uranium (U) inventory in Boeun aquifer is facing the artificial water reservoir that intended for water supply to nearby cities (40–70 m apart). In the site, major U ore is located in a shallow depth of aquifer (54–56 m bgl) where the toxic radionuclides might be arising from the U inventory and discharging into the nearby surface water. In order to understand the origin and fate of dissolved U in the Boeun aquifer, we analyzed the groundwater and fracture filling materials (FFMs) samples for multiple environmental tracers such as C, O, Fe, S, Sr and U-series isotopes. In the aquifer, the U discharge rate from solids to mobile zone (groundwater) ranged from 9.59×10^{-7} $\mu\text{g/L/y}$ to 1.70×10^{-4} $\mu\text{g/L/y}$ only. In FFMs, the $^{234}\text{U}/^{238}\text{U}$ activity ratio (AR) and $^{230}\text{Th}/^{234}\text{U}$ AR values ranged from 0.93 to 1.67 (1.05 ± 0.15) and from 0.22 to 1.97 (0.75 ± 0.39), respectively, and which apparently indicated that water-rock interactions have occurred significantly along the fractures. The U accumulations (~ 157 mg U/kg) in FFMs occurred with the Fe accumulations (~ 226798 mg Fe/kg) and the $\delta^{56}\text{Fe}$ and $\delta^{57}\text{Fe}$ anomalies, implied the U accumulations are associated with the enrichment of Fe in the fractured zones. The highest U and Fe accumulations were found at the shallow fracture (4.9 m below ground level), did occur in late Pleistocene. Meanwhile, the $\delta^{34}\text{S}$ - and $\delta^{18}\text{O}$ - SO_4 distribution in groundwater indicated the Fe-rich environment in the aquifer will continue, attributed to continuous Fe supplies from mineral dissolutions. In the Boeun aquifer, the $\delta^{18}\text{O}$ - H_2O , $^{87}\text{Sr}/^{86}\text{Sr}$ and ^{14}C signatures suggested the groundwater was originated from upland recharges (likely from nearby mountains) enabling the aquifer to maintain the reducing environments for the U inventory. In addition to that, the enrichment of Fe in shallow zone is capable of immobilizing the dissolved U inside the fractures, without significant U discharge into the nearby surface water.



PB6-2 GEOCHEMICAL BEHAVIORS OF URANIUM IN A URANIUM DEPOSIT OF THE OGCHON METAMORPHIC BELT, KOREA

M. H. Baik⁽¹⁾, Y. Ju⁽¹⁾, J. H. Ryu⁽¹⁾, J. O. Jeong⁽²⁾

(1) Korea Atomic Energy Research Institute, 989-111 Daedeok-daero, Yuseong-gu, Daejeon 34057, Republic of Korea

(2) Center for Research Facilities, Gyeongsang National University, 501 Jinju-daero, Jinju, Gyeongnam 52828, Republic of Korea

Various uranium deposits have been used as natural analogues for studying the long-term behavior of radionuclides in geological repositories for the disposal of radioactive wastes. In particular, complex geochemical behaviors of natural uranium (U) in groundwater and rock of a uranium deposit provide valuable data and information for understanding and evaluating the long-term behaviors of radionuclides and their interaction with geological media under various geochemical conditions. The Ogcheon metamorphic belt (OMB) is a NE trending fold-and-thrust belt located in the middle of South Korea. Metalliferous black slates in the OMB have drawn attention for their potential mineralization of U as well as other metallic elements. It has been shown that the metalliferous black slates are characterized by a high content of trace elements such as Ba, V, Mo, and U [1, 2]. Recently, it has been recognized that the metalliferous black slates in the OMB are interbedded with coaly slates, which are more enriched with U and other metallic elements than the surrounding black slates [2]. In this study, 5 groundwater samples were taken from 4 drilled boreholes using a packer system and 8 rock samples were taken from both the drilled rock cores and outcrops.

The concentrations of major and trace elements in the groundwater samples were analyzed using various analytical techniques. All the groundwater samples except one sample (Ca-HCO₃ type for OB3-80) were Ca-SO₄ type groundwaters. The concentration of U in the groundwater was relatively low ranged from 0.025 to 0.690 µg/L although the study site is a uranium deposit in the OMB. The uranium speciation and saturation index (SI) of the groundwater samples were calculated using the geochemical program, Geochemist's Workbench (Ver. 9.01) [3], using the recently published NEA thermochemical database [4]. As shown in the Figure 1, the dominant uranium species in the groundwater samples were Ca-UO₂-CO₃ complexes (mainly Ca₂UO₂(CO₃)₃(aq)) except BH1-15 sample (mainly UO₂CO₃(aq)). From the calculation, uranophane was predicted to be a dominant solid phase for all groundwater samples which can be precipitated in the given geochemical condition. Uranium isotopes and their activity ratios (AR) were also analyzed and their AR (²³⁴U/²³⁸U) ranged from 1.26 to 3.75, which means a retained reducing environment.

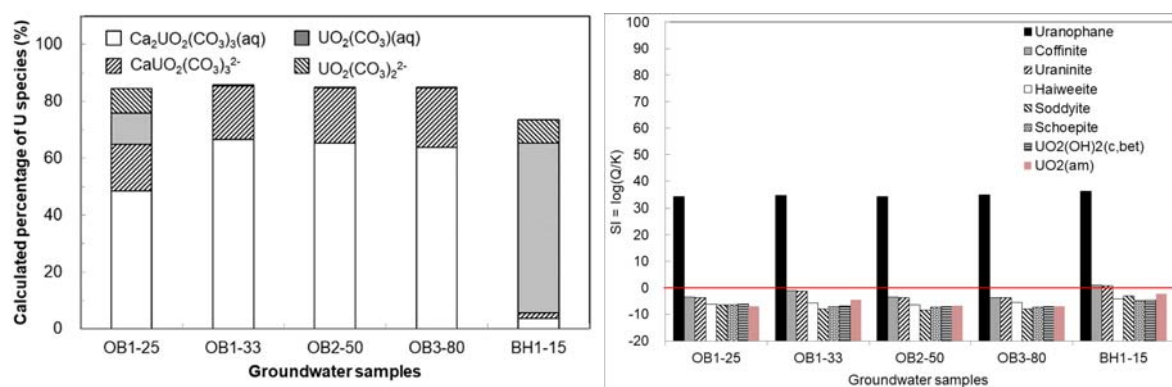


Figure 1. Calculated uranium speciation (left) and saturation index (SI) (right) for the groundwater samples from the study site in OMB, Korea.

Various mineralogical and geochemical analyses were performed for the 8 rock samples using various analytical methods such as ICP-MS, XRF, XRD, SEM/EDS, and EPMA. Primary constituent minerals of rock samples were quartz and mica, including small amounts of feldspar and chlorite. Secondary minerals observed were pyrite, chalcopyrite, arsenopyrite, apatite, barite, jarosite, rutile, monazite, xenotime, zircon, thorite, uraninite, and thorutite, mainly identified in the veinlets. U and Th contents in the rock samples from the study site were 1.3 ~ 71 ppm (average 17.4 ppm) and 1.3 ~ 11.4 ppm (average 5.9 ppm), respectively. Th/U ratio was 0.1 ~ 9.1 (average 1.7) which is smaller than average value of the crust (4.0). The contents of REEs (rare earth elements) such as La (169.9 ppm), Ce (294.8 ppm), and Nd (168.4 ppm) showed relatively higher values, which is considered to be originated from monazite. Contents of redox-sensitive elements such as V, Mo, Cr, Mn, and U and their ratios (V/(V+Ni), V/Cr, U/Th, etc) showed relatively higher values. This reveals that the reductive metals including U were mineralized by a reduction and concentration by reducing environments, rich in organic materials. Minerals containing U were identified to be uraninite, thorite, zircon, xenotime, and monazite. Major uranium minerals observed were uraninite (UO_{2+x}) (Figure 1a) and thorite ($(\text{U,Th})\text{SiO}_4$) (Figure 2b). Thorutite ($(\text{Th,U,Ca})\text{Ti}_2(\text{O,OH})_6$) mineral was also identified in a rock sample as a minor uranium mineral (Figure 2c). Alteration minerals from uraninite such as uranophane calculated to exist in the given groundwater condition (see Figure 1 right) have not been found from the rock samples used in this study although further investigations are necessary, particularly for the rock samples from water-conducting zones in the study site.

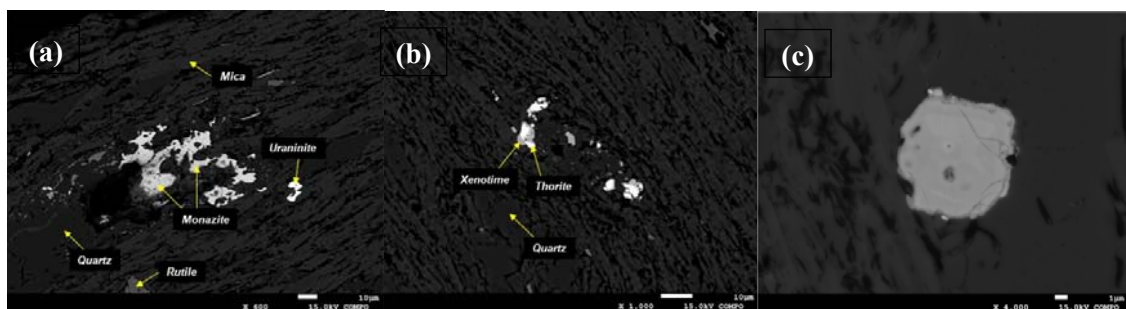


Figure 2. Back scattering electron (BSE) images of uranium minerals such as (a) uraninite, (b) thorite, and (c) thorutite for the rock samples from the study site in OMB, Korea.

The results of this study will provide basic data and information necessary for performing natural analogue studies for radionuclide behavior in uranium deposits and investigating evolution environments of uranium deposits in the OMB, Korea.

Acknowledgement: This work was supported by the Institute for Korea Spent Nuclear Fuel (iKSNF) and National Research Foundation of Korea (NRF) grant funded by the Korea government (Ministry of Science and ICT, MSIT) (No. 2021M2E1A1085186)

References

- [1] Kim, Y. J., Seo, J., Kang, S. A., Choi, S. G. and Lee, Y. J. (2015) Geochemistry and uranium mineralogy of the black slate in the Okcheon Metamorphic Belt, South Korea. *Geochem. J.* 49: 443-452.
- [2] Jeon, J., Shin, D. and Im, H. (2020). Depositional environments of redox-sensitive trace elements in the metalliferous black slates of the Okcheon Metamorphic Belt, South Korea. *Geosci. J.* 24: 177-193. [3] Bethke, C. M. and Yeakel, S. (2013) The Geochemist's Workbench Release 9.0: *GWB Essentials Guide*. Aqueous Solutions LLC.
- [4] Grenthe, I., Plyssunov, A. V., Runde W. H., Kinings, J. M., Moore, E. E., Gaona, X., Rao, L. and Grambow, B. (2020) Second Update on the Chemical Thermodynamics of Uranium, Neptunium, Plutonium, Americium and Technetium, OECD Nuclear Energy Agency.

PC1-1 THE NEA THERMOCHEMICAL DATABASE (TDB) PROJECT: HIGH QUALITY DATA, ACCESSIBILITY AND CAPACITY BUILDINGJesus S. Martinez ⁽¹⁾, Alexia Mercier ⁽¹⁾*(1) Nuclear Energy Agency (OECD/NEA), France**46, quai Alphonse Le Gallo, 92100 Boulogne-Billancourt, France**Corresponding author: Jesus.MARTINEZGONZALEZ@oecd-nea.org*

The NEA Thermochemical Database (TDB) Project [1] publishes high quality, internally consistent thermochemical data for compounds of relevance to the performance assessment of radioactive waste management systems [2]. This joint undertaking between the NEA Data Bank and the NEA Division of Radioactive Waste Management and Decommissioning was established in the mid-1980s and has become the internationally recognized reference in the field.

The NEA TDB Project publishes selected thermochemical values that result from a thorough critical review and analysis of experimental data sources available in the public scientific literature [3]. Designated teams of world-class experts conduct this work following a set of sound, long-established technical guidelines that are publicly available [4]. In addition, the critical reviews are peer-reviewed prior to publication in the volumes of the NEA Chemical Thermodynamics Series (CTS) [5]. Fifteen volumes have been published to date: fourteen critical reviews addressing the selection of thermochemical values for specific key elements and a State of the Art Report on the Thermodynamics of Solid Solutions of Interest in Nuclear Waste Management. Five more volumes (three new critical reviews and two state of the art reports) are expected for publication in 2023-2025.

Table 1. Past and forthcoming publications of the TDB Project

<i>Chemical Thermodynamic Series Publications</i>	
<i>Publications 1992-2020</i>	<i>Uranium; Americium; Technetium; Neptunium and Plutonium; Update of the Actinides and Technetium Volumes, Nickel, Selenium, Zirconium; Organic Ligands; Solid Solutions (State-of-the-Art Report); Thorium; Tin; Iron (Part 1); Iron (Part 2); Second Update of the Actinides and Technetium Volumes</i>
<i>Forthcoming Publications</i>	<i>Ancillary Data; Molybdenum; Cement Minerals (State-of-the-Art Report); High-Ionic Strength Systems (State-of-the-Art Report)</i>
<i>Projects recently launched</i>	<i>Rare Earth Elements</i>

To improve data accessibility and usability, the NEA TDB Project introduced a new and improved version of its electronic database in 2018 [6]. This state-of-the-art database features an intuitive, user-friendly interface that enables users to easily search for relevant thermochemical values [7]. Additionally, the data can be downloaded in a file format compatible with the widely utilized geochemical modeling software PHREEQC [8]. The new electronic database also serves as a quality control tool, ensuring the internal consistency of the data through the implementation of structural constraints and consistency checks that are based on fundamental thermochemical principles and conservation laws. The NEA TDB electronic database represents a major milestone in the project's ongoing commitment to providing the scientific community with accurate, reliable, and easily accessible thermochemical data.

The NEA TDB Project also provides a highly successful annual training course on Thermodynamic Data Collection and Assessment, aimed at early career scientists and professionals interested in the application of nuclear chemistry to radioactive waste management and other environmental fields. The

course, which is taught by renowned international experts, provides participants with a comprehensive overview of the NEA TDB activities, and offers a well-balanced blend of theoretical concepts and practical applications.

The NEA Thermochemical Database (TDB) Project has become an international reference for the radioactive waste management community. With over three decades of experience and achievements, the project continues to provide high-quality, selected thermochemical data that meets the highest standards of traceability, transparency, accessibility, and usability. Additionally, the project remains steadfast in its commitment to knowledge transfer and capacity building, ensuring that the latest advancements and best practices are shared with the wider scientific community. The project's commitment to excellence and its unwavering focus on meeting the needs of the scientific community will ensure its continued impact and success in the years to come.

References

- [1] Mompeán, F., et al. (2003). The OECD Nuclear Energy Agency Thermochemical Database Project, *Radiochim. Acta*, 91: 617-622.
- [2] Ragoussi, M. E. et al. (2019). Fundamentals of the NEA Thermochemical Database and its influence over national nuclear programs on the performance assessment of deep geological repositories, *J. Environ. Radioact.*, 196: 225-231
- [3] Ragoussi, M. E. et al. (2015). The NEA Thermochemical Database Project: 30 years of accomplishments *Radiochim. Acta*, 103: 679-685
- [4] TDB Project Guidelines are available at <http://www.oecd-nea.org/dbtdb/guidelines/>
- [5] TDB publications are available at <http://www.oecd-nea.org/dbtdb/info/publications/>
- [6] Martinez, Jesus S., et al. (2019). The new electronic database of the NEA Thermochemical Database Project, *Applied Geochemistry*, 107: 159-170
- [7] The new electronic TDB is accessible at <http://www.oecd-nea.org/dbtdb/tbdbdata/>
- [8] Parkhurst, D. L. et al. (1999). User's guide to PHREEQC (Version 2): A computer program for speciation, batch reaction, one-dimensional transport, and inverse geochemical calculations

PC1-2 DEVELOPMENT OF A DATABASE FOR RADIONUCLIDE SORPTION ON CLAY AND CEMENT SYSTEMS IN SUPPORT TO RADIOACTIVE WASTE MANAGEMENT

D. García¹⁾, M. López-García¹⁾, D. Pérez¹⁾, I. Canals¹⁾, A. Nardi¹⁾, L. Duro¹⁾, S. Brassinnes²⁾

1) *Amphos21, Carrer Veneçuela 103, 08019, Barcelona, Spain*

2) *Belgian Agency for Radioactive Waste and Enriched Fissile materials (ONDRAF/NIRAS), Belgium.*

Sorption is one of the most relevant processes retarding the migration of radionuclides through engineering and natural barriers of geological repositories of radioactive waste [1]. There is a complete body of scientific literature on the subject, accompanied by a large set of data of the sorption of different radionuclides onto different solid substrates of interest. To date, although there are some sorption databases available in the literature [2-5], a comprehensive database containing raw sorption data in a rationale manner as well as experimental conditions / parameters for the experiments is lacking. This contribution presents a Sorption DataBase (SDB) for radionuclides sorption developed for ONDRAF/NIRAS, with a first focus on clays and cementitious systems. The overarching objective of this work pursued by ONDRAF/NIRAS is to build a database with relevant sorption data in support to safety analysis and safety case preparations (i.e. for the selection of relevant sorption values in an easy and consistent way, for traceability purposes of selected parameters, for data gaps analysis, etc.). The added value of the SDB relies not only on the experimental raw data contained, but on how the SDB is structured and the associated software tools developed to help in feeding, analysing and extracting the sorption data.

The SDB has been developed over a non-relational database (MongoDB, www.mongodb.com). The SDB contains information on the solid phases (mineralogy, solid physical properties like CEC or surface area, etc.), the experimental details (aqueous solution composition, pH, Eh, ligand concentration, temperature, equilibrium time, etc.) and the raw results of the sorption experiments (i.e. sorption percentage, adsorbed concentration or K_d value). So far the SDB is populated with approximately 30,000 data points from about 300 literature references; being the content update up to 2021. The radionuclides included within the SDB range from alkaline and alkaline-earth elements (i.e. Cs and/or Sr), metallic elements (i.e. Ni and/or Fe), lanthanides (i.e. Eu), actinides (i.e. Th and/or U), oxoanions (i.e. Se and/or Mo) and halogens (i.e. Cl and/or I).

Besides the database itself, different IT tools have been developed and are integrated in the software package: Template Tool for sorption data a Sorption DataBase (SDB) Tool. The Template tool is used to generate the datasets. All the data within a publication (chemical conditions, sorption results) is introduced in the Template Tool generating a JSON file that will be later uploaded in the SDB Tool. The SDB Tool is designed to handle and manage the information included in the SDB, allowing the user to filter the data as a function of different parameters (solid phase, radionuclide of interest, range of pH, temperature, etc.). Additionally, several functionalities have been implemented within the tool as the possibility of extracting the data in a spreadsheet format, the possibility of plotting the data directly within the tool and the possibility of recalculating parameters as a function of the desired units (i.e. mg/L instead of Kg/L, Celsius degrees instead of Kelvin, etc.).

References

- [1] RETROCK, 2005, Treatment of radionuclide transport in geosphere within safety assessments. EC Project RETROCK (C.No.: FIKW-CT-2001-20201).
- [2] Baeyens, B., Thoenen, T., Bradbury, M. H., & Marques Fernandes, M. (2014). Sorption data bases for argillaceous rocks and bentonite for the provisional safety analyses for SGT-E2 (No. NTB--12-04). Paul Scherrer Institute (PSI).

ABSTRACTS

- [3] McKinley, I. G., and Scholtis, A. (1991) Proc. NEA Workshop, Interlaken, Switzerland (pp. 16-18).
- [4] Ochs, M., & Talerico, C. (2004). SR-Can. Data and uncertainty assessment. Migration parameters for the bentonite buffer in the KBS-3 concept (No. SKB-TR--04-18). Swedish Nuclear Fuel and Waste Management Co.
- [5] Wersin, P., Kiczka, M. & Rosch, D. (2012) Safety Case for a Spent Nuclear Fuel Repository at Olkiluoto: Radionuclide Solubility Limits and Migration Parameters for the Canister and Buffer. Posiva 2012-39.

PC1-3 THERMODYNAMIC MODELS DATABASE: A TOOL FOR UNDERSTANDING RADIONUCLIDE SORPTION MECHANISMS ON CLAY AND CEMENT SYSTEMS

I. Canals¹⁾, M. López-García¹⁾, D. Pérez¹⁾, A. Nardi¹⁾, L. Duro¹⁾, D. García¹⁾, S. Brassinnes²⁾

1) *Amphos21, Carrer Veneçuela 103, 08019, Barcelona, Spain*

2) *Belgian Agency for Radioactive Waste and Enriched Fissile materials (ONDRAF/NIRAS), Belgium.*

Sorption is a very broad term used to describe the process of retention of dissolved species onto mineral surfaces. Sorption mainly refers to retention by chemical bonding, although physical Van der Waals interactions are also possible. Ionic Exchange processes common in clays are also included within the broad “Sorption” term, although the mechanisms involved are different from the interactions occurring at the surface of a solid oxide, for example [1]. Thermodynamic Sorption Models (TSM) are based on the mechanistic understanding of the sorption process. As an example, the surfaces of metallic oxides and hydroxides are covered by oxo and hydroxy groups with amphoteric properties, this means that they can protonate and deprotonate depending on the environmental conditions. According to the TSM the description of the reactions between the surface and the solution are described in terms of mass action laws. In the same way as these surfaces can gain or lose protons, they can also act as ligands for aqueous species in solution, thus resembling the hydrolysis equilibrium established in water. On the contrary to the hydrolysis equilibrium where all species involved are aqueous, in the surface equilibrium the result is that the metal, initially in the aqueous phase, is now retained on the solid surface. Another consequence of this surface equilibrium is that the surface has acquired a positive charge. These surface equilibria type of reactions are known as surface complexation, given that the metal is complexed by the surface of the solid, which acts as an electron donor in this case [2]. This contribution presents a TSM DataBase (TSM-DB) for radionuclides sorption developed for ONDRAF/NIRAS, focused on clays systems. The main objective of this work pursued by ONDRAF/NIRAS is to build a database on TSM to improve system understanding, test current knowledge (i.e. available TSM vs available data [3]), improve the confidence on future safety case assessments and collect relevant sorption models in support to safety analysis and safety case preparations (i.e. for the selection of relevant sorption models in an easy and consistent way, for traceability purposes of selected parameters, for data gaps analysis, etc.).

The TSM-DB has been developed based on literature models and contains information on the solid phases (mineralogy, CEC, surface area, number of site, etc.), the experimental details (aqueous solution composition, pH, Eh, ligand concentration, temperature, etc.), model details if any (type of electrostatic model and their characteristics, ionic exchange definition, etc.) and surface/ionic exchange reactions definition (including stoichiometry and equilibrium constants). So far, the TSM-DB is populated with approximately 100 models from about the same amount of literature references; being the content updated up to 2021. The radionuclides included within the TSM-DB range from alkaline and alkaline-earth elements (i.e. Cs and/or Sr), metallic elements (i.e. Ni and/or Fe), lanthanides (i.e. Eu) and actinides (i.e. Th and/or U). Clay minerals included in the database are montmorillonite, illite, kaolinite and smectite.

Besides the database itself, a Template Tool for the definition of the models included in the TSM-DB have been developed. All the data within a publication (chemical conditions, sorption models) is compiled by using the Template Tool generating a JSON file that will be later uploaded in the database. The TSM Tool is designed to handle and manage the information included in the TSM-DB, allowing the user to filter the models as a function of different parameters (solid phase, radionuclide of interest, type of model, etc.). Additionally, the tool has the possibility of extracting the models in a script format that could be implemented in PhreeqC models [3].

References

- [1] RETROCK, 2005, Treatment of radionuclide transport in geosphere within safety assessments. EC Project RETROCK (C.No.: FIKW-CT-2001-20201).
- [2] Dzombak, D.A & Morel, F.M.M. (1990). Surface Complexation Modelling: Hydrous Ferric Oxide, Wiley-Interscience, New York, 393 pp
- [3] García, D., López-García, M., Pérez, D., Canals, I., Nardi, A., Duro, L., Brassinnes, S. (2023). Development of a database for radionuclide sorption on clay and cement systems in support to radioactive waste management. Contribution in “18th International conference on the chemistry and migration behaviour of actinides and fission products in the geosphere”, Nantes, France.
- [4] Parkhurst, D., Appelo, C. (2013) Description of input and examples for PHReeQC version 3 — A computer program for speciation, batch-reaction, one-dimensional transport, and inverse geochemical calculations. U.S. Geological Survey Techniques and Methods, book 6, chap. A43.

PC1-4 A THERMODYNAMIC DATABASE FOR THE SOLUTION CHEMISTRY AND SOLUBILITY OF EUROPIUM(III) INORGANIC SPECIES: RECENT DEVELOPMENTS

Norbert Jordan ⁽¹⁾, Tres Thoenen ^(2,3), Sebastian Starke ⁽⁴⁾, Kastriot Spahiu ⁽⁵⁾, Vinzenz Brendler ⁽¹⁾

(1) *Helmholtz-Zentrum Dresden - Rossendorf, Institute of Resource Ecology, Bautzner Landstraße 400, 01328 Dresden, Germany*

(2) *Paul Scherrer Institut, Waste Management Laboratory, Forschungsstrasse 111, 5232 Villigen PSI, Switzerland*

(3) *Present address: Am Rain 14, 4105 Biel-Benken, Switzerland*

(4) *Helmholtz-Zentrum Dresden - Rossendorf, Computational Science Group, Bautzner Landstraße 400, 01328 Dresden, Germany*

(5) *Swedish Nuclear Fuel and Waste Management Co, Box 250, SE-101 24 Stockholm, Sweden*

Performance assessments of geological repositories for the underground disposal of high-level radioactive waste require a deep understanding of the phenomena influencing the mobility of radionuclides, e.g. sorption, redox immobilization, surface precipitation, incorporation, etc. Reliable thermodynamic databases (TDB) are essential in order to generate speciation calculations, surface complexation and reactive transport models to predict the aforementioned mechanisms. In this work, the focus was set on europium (Eu), a lanthanide used for decades as a chemical analogue of trivalent actinides (Pu, Am). However, a consolidated and internationally recognized Eu TDB does currently not exist.

Several reviews and reports [1-4] on the aqueous chemistry/geochemistry of europium were published, but had various drawbacks, for example:

- Insufficient transparency about the selection procedure,
- Lack of systematic screening to gather primary literature sources,
- No original data but rather analogue values from other REE or compilations from secondary references,
- Postulation of species not independently evidenced by means of advanced spectroscopic techniques,
- Too high reliance on the analogy with trivalent actinides,
- For weak complexes such as chloride and nitrate, changes in the activity coefficients due to the replacement of up to 100 % of the background electrolyte anion by Cl^- or NO_3^- was either completely overlooked or, if recognized, not handled properly,
- Too high reliance on the charge analogy for the estimation of missing ion interaction coefficients when the Specific Ion Interaction theory was applied.

This study aims at significantly improving the situation by carefully addressing all aforementioned issues in order to provide a reliable, robust, and internally consistent TDB for europium. For this, an extensive data survey of more than 350 peer-reviewed publications from around 1900 until June 2021 was performed. Furthermore, technical reports, scientific books, collected editions as well as various thermodynamic databases (Nagra/PSI [2], Thermochemie [5], etc.) were surveyed to identify their original Eu(III) data sources and references used therein. Data up to 90 °C and 5 M ionic strength were selected for screening, but all data dealing with hydrothermal conditions were out of the scope of this review. Thermodynamic data determined in non-aqueous solvents were explicitly not considered either. For the three ligands (SO_4^{2-} , Cl^- , PO_4^{3-}) to which our attention was focused on in a first step, the result of the screening together with the number of selected data for aqueous complexation constants is shown in Table 1.

Table 1. Summary of the aqueous inorganic Eu complexation data records

System	#total	#selected
Eu – sulphate	244	34
Eu – chloride	186	0
Eu – phosphate	40	8

The complexation of Eu(III) with sulphate was investigated by ion exchange, solvent extraction, spectrophotometry, electrophoresis, and time resolved laser-induced fluorescence spectroscopy [6]. Despite the broad variety of methods used for the determination of the conditional complexation constants of the Eu(III) sulphate species in the literature, a consistent set of data was obtained for both EuSO_4^+ and $\text{Eu}(\text{SO}_4)_2^-$ aqueous complexes at 25 °C.

Chloride complexes with Eu(III) are very weak, and high chloride concentrations are required to form them. Related experiments (up to 4 mol·L⁻¹ Cl⁻ at 25 °C) need to be considered with extra care because the perchlorate ion was systematically substituted by the chloride ion by more than 10 %, and in some cases even completely. However, the resulting changes in the activity coefficients due to such large compositional modifications of the background electrolyte were simply ignored. All our recalculations [7] based on the exclusive consideration of changes in activity coefficients without considering the formation of Eu-chloro complexes as proposed in the original studies, are able to describe the experimental data of the literature [6]. This means that the formation of Eu(III)-chloro complexes postulated in the literature was an artefact [6].

Unfortunately, very little is known concerning the complexation of Eu(III) with phosphate ions. The only experimental study was performed recently [8], by means of laser-induced luminescence spectroscopy at 25 °C and at different ionic strengths (0.6 – 3.1 mol·L⁻¹) imposed by NaClO₄. The impact of temperature up to 80 °C on the formation of the $\text{EuH}_2\text{PO}_4^{2+}$ complex was also investigated [8].

Recently, results of our critical evaluation for the chloride, sulphate, and phosphate ligands were published [6]. The recommended complexation constants and solubility products for further inorganic ligands, e.g. hydroxide and carbonate, will also be presented [9].

References

- [1] Brown, P.L. and Ekberg, C. (2016) Hydrolysis of Metal Ions. Vol. 1, Wiley-VCH, Weinheim.
- [2] Hummel, W. et al. (2002) Nagra/PSI Chemical Thermodynamic Data Base 01/01, Technical Report 02-16.
- [3] Rard, J.A. (1985). Chemistry and thermodynamics of europium and some of its simpler inorganic compounds and aqueous species. *Chem. Rev.* 85(6): 555-582.
- [4] Spahiu, K. and Bruno, J. (1995) A selected thermodynamic database for REE to be used in HLNW performance assessment exercises, SKB Technical Report.
- [5] Giffaut, E, et al. (2014). Andra thermodynamic database for performance assessment: *ThermoChimie. Appl. Geochem.* 49: 225–236.
- [6] Jordan, N. et al. (2022). A critical review of the solution chemistry, solubility, and thermodynamics of europium: recent advances on the Eu^{3+} aqua ion and the Eu(III) aqueous complexes and solid phases with the sulphate, chloride, and phosphate inorganic ligands. *Coord. Chem. Rev.* 473, 214608.
- [7] Spahiu, K. and Puigdomènech, I. (1998). On weak complex formation: re-interpretation of literature data on the Np and Pu nitrate complexation. *Radiochim. Acta* 82: 413-419.
- [8] Jordan, N. et al. (2018). Complexation of trivalent lanthanides (Eu) and actinides (Cm) with aqueous phosphates at elevated temperatures. *Inorg. Chem.* 57(12): 7015-7024.
- [9] Jordan, N. et al. (2023). *Coord. Chem. Rev.* (in preparation).

PC1-5 THERMOCHIMIE: A THERMODYNAMIC DATABASE USED IN RADIOACTIVE WASTE DISPOSAL EVALUATION

Benoît Madé (1), Will Bower (2), Stéphane Brassinnes (3)

(1) Andra, France

(2) Nuclear Waste Services, Harwell, UK

(3) ONDRAF/NIRAS, Belgium

ThermoChimie (<http://www.thermochimie-tdb.com/>) is a thermodynamic database developed as part of a consortium of three radioactive waste management organizations (Andra, Nuclear Waste Services, and ONDRAF/NIRAS). The database is designed to be applied over the pH range of 6 to 14 at temperatures below 80°C within the water stability domain, with particular prioritisation towards cementitious and clay-based systems. ThermoChimie builds upon the Chemical Thermodynamics Series of the NEA Thermochemical Database Project (TDB) and extends the data selection by the NEA to allow for a complete (yet still consistent) representation of the processes of interest. It is primarily intended to be used in the geochemical calculations supporting radioactive waste management and Safety Analysis. As such, it contains thermochemical datasets on a large range of waste-relevant compounds including lanthanides, actinides, and toxic elements but also relevant ligands and stability constants of key disposal system components.

ThermoChimie database is under constant revision and development, being updated whenever new relevant scientific literature can be used to improve its content and also to broaden its applicability for the consortium members.

ThermoChimie version 11 was released in July 2022 and contains significant updates to the thermodynamic data selection for uranium, neptunium, plutonium, americium, and technetium, following the Second Update on the Chemical Thermodynamics of those elements published by the NEA-TDB. Furthermore, a comprehensive and accurate review of iron thermodynamic properties has been carried out, building on the NEA-TDB review, and supplemented with additional recent literature publications to allow an accurate modelling of steel corrosion and major element behaviour in repositories. Finally, two new elements, beryllium, and copper, were included as part of Version 11. The inclusion of these elements improves the usability of ThermoChimie due to their importance in high-level nuclear waste disposal. The newest version of the ThermoChimie database is currently undergoing a benchmarking study with the aim of evaluating its performance in systems relevant to geological disposal of high-level radioactive waste (benchmarking tests include speciation, solubility, and sorption calculations in argillaceous and cementitious systems).

ThermoChimie database is available for a list of geochemical codes including PhreeqC, Crunch, ToughReact, CHESS, Geochemist's Workbench, Spana and PFlotran.

The next release of ThermoChimie (version 12) is planned for mid-2023 and constitutes a major update regarding the radionuclide-organic interactions. Beyond that, forthcoming ThermoChimie versions will be focused on significant updates for cementitious phases and zeolites as well as key gaps on less-studied systems. A state-of-the-art review on handling redox processes in geochemical modelling is also being prepared.

Phase III of the ThermoChimie Consortium is scheduled to be completed in 2025, aligned with the release of the new versions described above, and up to date with the Chemical Thermodynamics Series of the NEA TDB project (i.e., "blue books").

PC2-1 INTERPRETATION OF DIFFUSION EXPERIMENTS WITH A NUMERICAL REACTIVE TRANSPORT APPROACH

Tournassat Christophe^{1,2}, Steefel Carl. I.¹, Fox Patricia M.¹, Tinnacher Ruth M.³

(1) *Earth and Environmental Sciences Area, Lawrence Berkeley National Laboratory, Berkeley, CA, USA*

(2) *Institut des Sciences de la Terre d'Orléans, Université d'Orléans–CNRS–BRGM, Orléans, France*

(3) *Department of Chemistry and Biochemistry, California State University East Bay, Hayward, CA, USA*

CrunchClay reactive transport code was used to interpret through-diffusion data with a set of parameters, including the effective diffusion coefficient, clay porosity, and the radionuclide adsorption distribution coefficient ($D_e - \varepsilon - K_D$). We demonstrate that our modeling approach can accurately include and characterize the influence of unavoidable experimental biases on the estimation of diffusion parameters in the quantitative interpretation of diffusion experiment results. These biases include the effects of filters holding the solid sample in place, the variations in the constant concentration gradient across the diffusion cell due to sampling events, the impact of tubing/dead volumes on the estimation of diffusive fluxes and sample porosity, and the effects of O-ring-filter setups on the delivery of solutions to the clay packing. A freely available graphical user interface, CrunchEase, was created for the reactive transport code CrunchClay. CrunchEase supports the user by automating the creation of input files, the running of simulations, and the extraction and comparison of data and simulation results. Furthermore, the CrunchEase/CrunchClay package allows the user to simulate raw through-diffusion data, *i.e.* (radio)tracer concentrations and volumes in reservoirs directly without the need to convert experimental concentration data into diffusive flux values. This direct modeling of raw data is more accurate if tubing volumes and the time of reservoir sampling events are specifically included. CrunchEase makes it also possible to transition more easily from a $D_e - \varepsilon - K_D$ modeling approach to a process-based understanding modeling approach. This is achieved by using the full capabilities of CrunchClay, which include surface complexation modeling and a multi-porosity description of the clay packing with charged diffuse layers. Overall, we believe that the development of the CrunchEase user interface will further facilitate the dialog between experimentalists and modelers on the most recent concepts applied to diffusion problems in clayey materials. This may ultimately lead to an improved decision-making process by radioactive waste agencies.

PC2-2 MODEL INTERPRETATION OF INTERACTION BETWEEN GLASS AND ORDINARY PORTLAND CEMENT IN AN INTEGRATED GLASS DISSOLUTION EXPERIMENT

Sanheng Liu⁽¹⁾, Karine Ferrand⁽¹⁾, Jules Goethals⁽²⁾, Diederik Jacques⁽¹⁾ and Karel Lemmens⁽¹⁾

(1) SCKCEN, Belgium

(2) SUBATECH, France

In many countries, the high-level reprocessing waste is immobilized in a borosilicate glass. In the vitrification process the molten glass is poured into a steel canister. These waste packages will be emplaced in a multiple-barrier system consisting of engineered and natural barriers (host rocks). Cementitious materials are foreseen in the engineered barriers and have both structural and buffer functions in a geological disposal of high-level waste (HLW). To reduce the corrosion of the steel components, cement types with a high pH are used. After the failure/perforation of the steel components, there will be an ingress of water from the host rock. The incoming pore water will be conditioned by the percolation through the cementitious materials. With high pH cement they can potentially become very alkaline. Understanding the dissolution behavior of the glass under cementitious conditions is therefore of great importance to assess the long-term geochemical evolution of waste disposal systems. To study the dissolution behavior of reference waste glasses in the proximity of a high pH cement, integrated experiments were performed at SCK CEN. Lab scale mock-ups of the waste package and near field barriers were developed, including a layer of glass powder, a stainless-steel filter and a hardened (ordinary Portland) cement paste (HCP) layer. As a result of the interaction between the glass and the HCP, processes take place both on the glass surface and in the neighboring HCP.

Glass and cement are, respectively, rich in silica and calcium. An important reaction between silica and cement is the pozzolanic reaction with C-S-H (calcium-silicate-hydrates) as reaction products. Additionally, the presence of alkalis from cement can further complicate the reaction by forming amorphous alkali-silica gel. On the one hand, the pozzolanic reaction is expected to speed up the dissolution of both glass and cement. On the other hand, the newly formed C-S-H or alkali-silica gel can adsorb elements such as alkalis from the glass and retard the migration of those elements through the cement. Therefore, glass dissolution in the proximity of cement and migration of dissolved elements through cement are coupled processes. The objectives of this research are to reproduce the measured glass dissolution data in the glass layer and elemental profiles in the cement using appropriate models and derive reaction and transport parameters controlling glass dissolution and elemental migration through cement in this system.

The results show that a diffusion-rate-limited kinetic glass dissolution model as the boundary condition together with a 1D diffusion-reaction model in the cement successfully captures most of the observed features of the experiments. The diffusion-rate-limited glass dissolution describes well the evolution of boron (glass dissolution indicator) concentrations in the glass layers for the duration of the experiments (about 900 days). It is not surprising that the interaction between glass and cement is driven by concentration gradients. For example, even though the pozzolanic reaction is expected to speed up the release of calcium from the cement, the results show that there is no significant dissolution of calcium in the cement close to the glass after 900 days due to a very low calcium solubility in the cement and thus a small concentration gradient. In the model the steel filter neither acts as a diffusion barrier due to its relatively large porosity nor reacts due to the high pH (above 13.3), even though precipitation of secondary phases may potentially decrease the porosity. It is found that the fitted effective diffusion coefficient of lithium in the cement is much larger than that of boron. Including sorption of lithium and boron in the model is required to increase the description of the measured boron and lithium profiles in the cement. However, sorption of lithium seems to occur only near the surface of the cement where there

is an abundance of secondary phase precipitation. The secondary phases are mostly amorphous and have a relatively low Ca/Si ratio with enrichment in alkalis and aluminum (the latter in the case of experiment with an aluminum-rich glass). A lack of thermodynamic data for those phases in the ThermoChimie database (Blanc et al., 2015) used for this research poses a challenge to the modelling. For simplicity, C-S-H with low Ca/Si ratios and/or C-A-S-H phases from the ThermoChimie database are used to represent those amorphous phases since C-S-H with low Ca/Si ratios and C-A-S-H phases tend to become supersaturated near the cement surface. The results highlight the complexity of the migration of elements from glass through cement.

References

- [1] Blanc, P.; Vieillard, P.; Gailhanou, H.; Gaboreau, S.; Marty, N.; Claret, F.; Madé, B.; Giffaut, E (2015). ThermoChimie database developments in the framework of cement/clay interactions. *Appl. Geochem.* 55: 95-107

PC2-3 REACTIVE TRANSPORT MODELLING OF TcO₄⁻ DIFFUSION IN OPALINUS CLAY WITH PFLOTRAN

Ping Chen¹, Luc R. Van Loon², Steffen Koch³, Peter Alt-Epping¹, Tobias Reich³, Sergey Churakov^{1,2},

¹ *Institute for Geological Sciences, University of Bern, CH-3012 Bern, Switzerland*

² *Laboratory for Waste Management, Paul Scherrer Institut, CH-5232 Villigen PSI, Switzerland*

³ *Department of Chemistry, Johannes Gutenberg-Universität Mainz, DE-55099 Mainz, Germany*

Because of its high mobility in the environment, its long half-life ($T_{1/2} = 2.1 \times 10^5$ years) and its high fission yield in nuclear reactors, ⁹⁹Tc is one of the important radionuclides in the field of safety assessment of a repository for radioactive waste and for the remediation of subsurface contamination at reprocessing sites. TcO₄⁻ through-diffusion experiments in Opalinus clay (OPA) were performed under air and argon conditions with a diffusion technique developed by Van Loon et al. (2003). No noticeable Tc-breakthrough was observed for over one year while the total Tc concentration in the source reservoir was steadily decreasing under both air and argon conditions. The total Tc activity distribution in the clay sample along the diffusion direction was obtained by slicing the OPA clay samples retrieved from the diffusion cells, using the abrasive peeling technique (Van Loon et al., 2005). In the case of diffusion under air conditions, almost no Tc was measured in that part of the sample close to the source reservoir, while much more Tc was retained under argon conditions. A reasonable explanation for this observation is that redox reactions of Tc(VII) with Fe(II) phases in OPA play a significant role during diffusion (Huang et al., 2021). A reactive transport model was implemented in PFLOTRAN (Lichtner et al., 2015) to simulate the diffusion process whereby the diffusion of Tc was coupled with redox reactions. Even though reduction of TcO₄⁻ by aqueous Fe²⁺ is thermodynamically feasible, it is not observed in the experiments. Furthermore, Fe²⁺ associated with solid phases was demonstrated to be more active than aqueous Fe²⁺ (Peretyazhko et al., 2009). Therefore, a surface complexation redox reaction was proposed. The dissolution rate of pyrite, equilibrium constants and the diffusion coefficient of TcO₄⁻ were considered as fitting parameters. Model results show that TcO₄⁻ diffuses into the clay column and is partially reduced into surface complexed Tc(IV) by pyrite. In contrast, under air condition, O₂ competitively consumes Fe²⁺ and pyrite, resulting in no Tc immobilized in the related zone.

References

- Huang, J., Jones, A., Waite, D., Chen, Y., Huang, X., Rosso, K.M., Kapler, A., Mansor, M., Tratnyek, P.G. Zhang, H. (2021). Fe(II) redox chemistry in the environment. *Chem. Rev.* 121, 8161-8233.
- Lichtner, P. C., Hammond, G. E., Lu, C., Karra, S., Bisht, G., Andre, B., Mills, R., Kumar, J. (2015). PFLOTRAN user manual: A massively parallel reactive flow and transport model for describing surface and subsurface processes. Technical Report LA-UR-15-20403, Los Alamos National Laboratories (LANL), Los Alamos, New Mexico, United States.
- Peretyazhko, T., Zachara, J.M., Heald, S.M., Jeon, B.-H., Kukkadapu, R.K., Liu, Moore, C. D., Resch, C.T. (2009). Heterogeneous reduction of Tc(VII) by Fe(II) at the solid–water interface. *Geochim. Cosmochim. Acta* 72, 1521–1539.
- Van Loon, L.R., Soler, J.M, Bradbury, M.H. (2003). Diffusion of HTO, ³⁶Cl⁻ and ¹²⁵I⁻ in Opalinus Clay samples from Mont Terri: Effect of confining pressure. *J. Contam. Hydrol.* 61, 73-83.
- Van Loon, L.R, Eikenberg, J. (2005). A high-resolution abrasive method for determining diffusion profiles of sorbing radionuclides in dense argillaceous rocks. *Appl. Radiat. Isotopes* 63, 11-21.

PC3-1 COMPARISON OF THE CAPACITY OF TWO ADSORPTION MODELS TO DESCRIBE Sr^{2+} AND Cs^+ BEHAVIOR ON SOILS SURROUNDING NUCLEAR FACILITIES

Savoye Sébastien⁽¹⁾, Latrille Christelle⁽¹⁾, Krimissa Mohamed⁽²⁾, Mélanie Lorthioy⁽²⁾

(1) *Université Paris-Saclay, CEA, Service de Physico-Chimie, France*

(2) *EDF R&D, France*

To contribute to the assessment of the environmental impact of industrial facilities such as in nuclear, a reliable prediction of radionuclides migration into the surrounding soils in case of incidents is required. ^{90}Sr and $^{134,137}\text{Cs}$ are the major radionuclides to account in such situations. They are known to display a low mobility in soils owing to their strong interactions with clay minerals. However, the physicochemical complexity of such environments makes challenging the description of the adsorption behavior of these radionuclides using empirical approaches like linear sorption isotherm or K_d model where the extent of the adsorption is constant independently of the prevailing physicochemical conditions [1]. Therefore, more complex approaches have been developed to better describe adsorption process. In the current study, among these approaches, two have been used in order to compare their predictive capacity. The first one is the multi-site equilibrium and/or kinetic (EK) model that mitigates K_d hypotheses by assuming that adsorption can occur on 2–3 different types of solid sites, governed by equilibrium and/or kinetic rates [2]. In this case, sorbed concentrations are distributed between ‘fast’ sites that are instantaneously in equilibrium with the aqueous phase and ‘slow’ sites that are controlled by kinetic first order mass transfer [2]. The second approach is the multi-site ion-exchange (MSIE) model. This model describes soil as an assemblage of pure reactive mineral phases like clay minerals, in accordance with the soil mineralogy. Then, using (i) database previously acquired on the adsorption properties of these pure phases towards Sr^{2+} , Cs^+ and also their competitors and (ii) the pore water chemistry, this model can simulate the adsorption behavior of Sr^{2+} and Cs^+ on the studied soils [3, 4]. For a benchmarking purpose, mineralogy and pore water chemistry of several soils in the vicinity of nuclear facilities were then used as input data for simulating the strontium and caesium isotherms by means of the two adsorption models. The results are therefore analyzed and discussed with respect to several key parameters like the proportion of clay minerals in soils, the concentration in pore water of major competitors.

References

- [1] IAEA (2010) Handbook of Parameter Values for the Prediction of Radionuclide Transfer in Terrestrial and Freshwater Environments. Vienna.
- [2] Chaif, H., Martin-Garin, A., Pierrisnard, S., Orjollet, D., Tormos, V., Garcia, Sanchez, L. (2023) Influence of non-equilibrium and nonlinear sorption of ^{137}Cs in soils. Study with stirred flow-through reactor experiments and quantification with a nonlinear equilibrium-kinetic model. *Journal of Environmental Radioactivity*: 257, 107067.
- [3] Savoye, S, Beaucaire, S., Grenut, B., Fayette, A. (2015) Impact of the solution ionic strength on strontium diffusion through the Callovo-Oxfordian clayrocks: an experimental and modeling study. *Appl. Geochem.* 61:41-52.
- [4] Latrille, C., and Bildstein, O. (2022) Cs selectivity and adsorption reversibility on Ca-illite and Ca-vermiculite. *Chemosphere*, 288:132582.

PC3-2 PORE-SCALE MODELLING OF SOLUTE TRANSPORT IN PARTIALLY AND FULLY SATURATED POROUS MEDIA

Yuankai Yang (1), Ravi A. Patel (2), Guido Deissmann (1), Jenna Poonoosamy (1), Dirk Bosbach (1)

(1) *Institute of Energy and Climate Research, Nuclear Waste Management (IEK-6), Forschungszentrum Jülich GmbH, Germany*

(2) *Institute of Building Materials and Concrete Structures (IMB), Karlsruhe Institute of Technology (KIT), Germany*

The prediction of radionuclide migration in partially and fully water saturated porous media such as compacted clays, clay rocks or tight rocks is relevant for safety assessments of deep geological repositories for radioactive wastes. Specifically, gases (such as H₂ or CH₄) generated due to corrosion of metallic waste canisters or degradation of organic waste components could reduce the saturation levels in surrounding barrier materials and the host rock formation, which alters the migration behaviour of radionuclides in these porous media. In order to improve the mechanistic understanding of solute transport processes in variably saturated porous media, in this work a three-dimensional pore-scale numerical framework to simulate solute transport in variably saturated microporous media (e.g., soils or sandstones) and nanoporous media (e.g., compacted clays or clay rocks) was established.

For partially saturated microporous media, we improved the Shen-Chen Lattice Boltzmann method (LBM) model to account for thin water films on the surface of soil/rock particles. The presence of a water film on the surfaces of minerals is resolved by defining numerical grids at the water-gas interface with a reduced diffusion coefficient. Figure 1-A shows an example of the phase distribution in a synthetically generated microstructure with a volumetric water content of 0.4. Figure 1-B compares the simulated diffusivity without a water film present and with a water film with a thickness of 1 μm, respectively. When the volumetric water content is larger than 0.25, the water film has little influence on ion transport. However, at low volumetric water content (0.05-0.15), transport pathways in absence of water films depercolate, indicating that the water film on the surface of the minerals controls solute diffusion at such low water contents. Thus, our model considering water films shows a better performance than previously existing pore-scale models.

Considering nanoporous media such as compacted clays, electrical double layer (EDL) effects caused by the charged surfaces of clay minerals can significantly enhance cation diffusion but reduce anion diffusion. On the other hand, since the polarizability of anions is normally larger than that of cations, anions are closer to the air/water interface than cations in partially saturated porous media [1, 2]. As the thickness of the water layer reaches the nanoscale, the air-water and water-solid interfaces may both have a significant influence on ion distribution and further affect ion transport in partially saturated porous media. We have developed a novel numerical framework that directly solves coupled Poisson-Nernst-Planck equations by LBM on GPUs, which can automatically capture the structure of the EDL in nanopores. In fully saturated conditions, the present study quantitatively characterises the influence of the EDL on ion diffusion in compacted clays in different situations. It is indicated that the normalized volume charge density has a significant impact on ionic tracer diffusion. In clays with a large normalized volume charge density, the EDL has a major impact on ion diffusion. When the ionic strength of the pore solution and temperature are constant, the flux from the electromigration term can be negligible. However, once a gradient in ionic strength or temperature is added, the electromigration process should be considered carefully due to its non-negligible role to balance the alteration of total flux. Our preliminary modelling results of sodium (Na⁺) and chloride (Cl⁻) diffusion in partially saturated nanoscale porous media are shown in Figure 2, which qualitatively replicates the trends of experiments in similar settings. The present study will help to improve the understanding of the mechanisms of ion transport in partially and fully saturated nanoporous media.

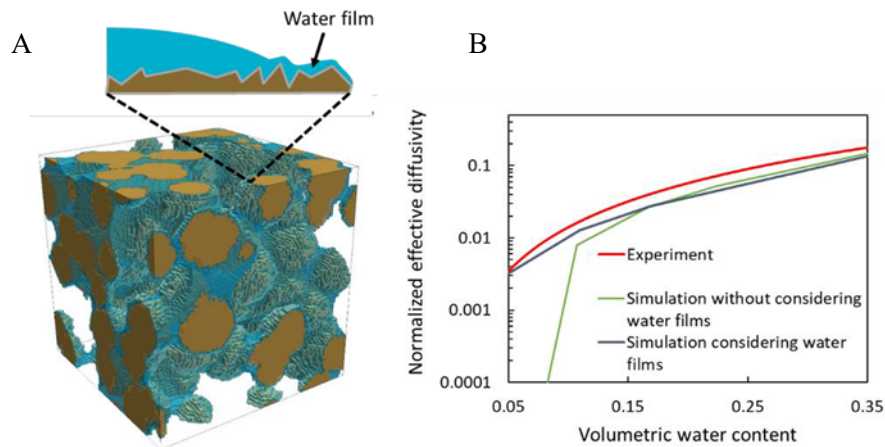


Figure 1. (A) Gas-liquid-solid distribution (yellow: solid phase; blue: liquid phase) and (B) comparison of simulated relative effective diffusivities of sandy soils with experimental results. Green line: simulation results without consideration of water films; dark blue line: simulation results with consideration of $1 \mu\text{m}$ water films; the red line is the fitting line of the experimental datasets [3].

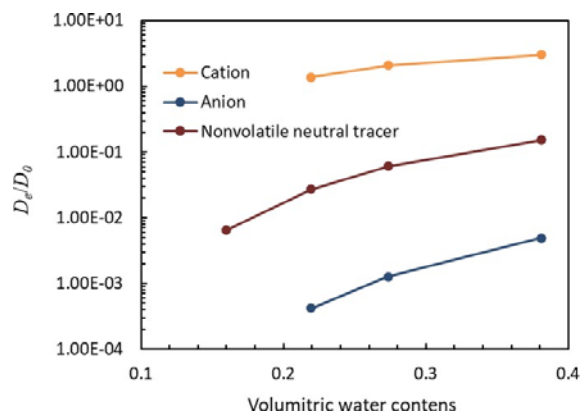


Figure 2. Normalized effective diffusivity as a function of the volumetric water content in compacted clays derived by our novel pore-scale simulations.

References

- [1] Jungwirth, P. and D. J. Tobias (2002). Ions at the air/water interface. *J. Phys. Chem. B.* 106: 6361-6373
- [2] Olivieri, G., K. M. Parry, R. D'Auria, D. J. Tobias and M. A. Brown (2018). Specific anion effects on Na^+ adsorption at the aqueous solution-air interface: MD simulations, SESSA calculations, and photoelectron spectroscopy experiments. *J. Phys. Chem. B.* 122: 910-918
- [3] Hu, Q. and J. Y. Wang (2003). Aqueous-phase diffusion in unsaturated geologic media: a review. *Crit. Rev. Env. Sci. Tec.* 33: 275-297

PC4-1 GEOCHEMISTRY AND MACHINE LEARNING BENCHMARK WITHIN EURAD JOINT PROJECT

N.I. Prasianakis ⁽¹⁾, E. Laloy ⁽²⁾, D. Jacques ⁽²⁾, J.C.L. Meeussen ⁽³⁾, C. Tournassat ⁽⁴⁾, G.D. Miron ⁽¹⁾, D. A. Kulik ⁽¹⁾, A. Idiart ⁽⁵⁾, E. Demirer ⁽⁵⁾, B. Cochevin ⁽⁶⁾, M. Leconte ⁽⁶⁾, M. Savino ⁽⁶⁾⁽⁷⁾, M. Marques Fernandes ⁽¹⁾, J. Samper II ⁽⁸⁾, M. De Lucia ⁽⁹⁾, C. Yang ⁽¹⁰⁾, S. V. Churakov ⁽¹⁾⁽¹¹⁾, V. Montoya ⁽²⁾, J. Samper ⁽⁸⁾, O. Kolditz ⁽¹²⁾, F. Claret ⁽¹³⁾

(1) *Laboratory for Waste Management, Paul Scherrer Institute, CH, 5232, Villigen PSI, Switzerland*

(2) *Engineered and Geosystems Analysis, Belgian Nuclear Research Centre, Belgium*

(3) *Nuclear Research and Consultancy Group (NRG), Petten, The Netherlands.*

(4) *Institut des Sciences de la Terre d'Orléans, Université d'Orléans—CNRS/INSU—BRGM, Orléans, France*

(5) *AMPHOS 21 Consulting, S.L., Calle Venezuela, 103, 08019, Barcelona, Spain*

(6) *ANDRA Andra, 1/7 Rue Jean Monnet, 92290, Chatenay-Malabry, France*

(7) *Université Paris-Saclay, AgroParisTech, INRAE, UMR MIA-Paris, 75005, Paris, France*

(8) *Centro de Investigaciones Científicas, ETS Ingenieros de Caminos, Universidad de Coruña, A Coruña, Spain*

(9) *Helmholtz Centre Potsdam - GFZ German Research Centre for Geosciences, Telegrafenberg, 14473 Potsdam, Germany*

(10) *Environmental Data Techniques, Inc, 4515 Gardendale, BLDG 902, San Antonio, TX 78240, USA*

(11) *Institute for Geological Sciences, Bern University, CH, 3012, Bern, Switzerland*

(12) *Department of Environmental Informatics, Helmholtz Centre for Environmental Research, UFZ, Leipzig, Germany*

(13) *BRGM, 3 Avenue Claude Guillemin, 45060 Orléans, France*

Thanks to the recent progress in numerical methods, the application fields of artificial intelligence (AI) and machine learning methods (ML) are growing at a very fast pace. The EURAD (European Joint Programme on Radioactive Waste Management) community has recently started using ML for a) acceleration of numerical simulations, b) improvement of multiscale and multiphysics couplings efficiency, and c) uncertainty quantification and sensitivity analysis. A number of case studies indicate that use of ML based approaches leads to overall acceleration of geochemical and reactive transport simulations between one to four orders of magnitude [1-4]. The observed speed-up depends on the chemical system, simulation code, application and problem formulation. Within EURAD-DONUT (Development and Improvement Of Numerical methods and Tools for modelling coupled processes), a benchmark is on-going to coordinate the relevant activities and to test a variety of ML techniques for geochemistry and reactive transport simulations in the framework of radioactive waste disposal. It aims at benchmarking some of the most widespread geochemical codes, at generating high-quality geochemical data for training/validation of existing/new methodologies, and at providing basic guidelines about the benefits, drawbacks, and current limitations of using ML techniques.

More specifically, the benchmark provides a point of reference for testing codes and models and for addressing the challenges relevant to:

- Streamline the production of high-quality consistent training datasets, using the most widespread geochemical solvers (PHREEQC, ORCHESTRA and GEMS). Setting the specifications such that the datasets may be directly used by all available and future ML techniques.
- Use Deep Neural Networks, Polynomial Chaos Expansion, Gaussian Processes, Active Learning, and other techniques to learn from the generated data.
- Setup appropriate metrics for the critical evaluation of the accuracy of ML models.

- Testing the accuracy of predictions for geochemical calculations, reactive transport and uncertainty analysis.

A joint effort has resulted in the definition of two reference benchmarks. The first system is relevant to cement hydration and degradation. The chemical system includes Ca-Si and simple C-S-H models while the CEMDATA-18 thermodynamic database is used. With increasing complexity, a more complete system is addressed, including Al-Mg-S-C-(Na-K) species. The second system is relevant to the sorption of U in claystone formations (e.g. Callovo-Oxfordian, Opalinus or Boom clay). Regarding the chemical complexity, a system containing Na-Cl-U-H-O is considered as the base case, and a more complex system with the addition of calcium and carbonate (CO₂) to change aqueous speciation of U. Parameters of interest, among others, are the resulting concentrations of U sorbed on edges (surface complexes), of U on ion exchange sites, and the amount of metaSchoepite, with the resulting K_d's.

The work performed so far leads to the following main conclusions: 1) Representative training datasets for the two benchmarks have been produced effectively with several geochemical codes at increasing levels of model complexity; 2) The groups participating in the benchmark succeeded in applying a wide range of ML techniques such as DNN, Polynomial Chaos, Gaussian Processes, Active Learning, Random Forest, and Classification Trees; 3) A complete set of metrics has been proposed to evaluate the accuracy of ML model predictions; 4) The cement hydration/degradation and uranium sorption systems exhibit complex nonlinear patterns which are represented by some teams by combining random forests for sample classification and Gaussian processes for interpolation. The workflows and preliminary results will be presented.

Acknowledgements: *The research leading to these results was performed within the Work Package DONUT of EURAD (European Joint Programme on Radioactive Waste Management of the European Union). EURAD has received funding from the European Union's Horizon 2020 research and innovation programme under Grant Agreement No 847593*

References

- [1] Jatnieks, J., De Lucia, M., Dransch, D., & Sips, M. (2016). Data-driven surrogate model approach for improving the performance of reactive transport simulations. *Energy Procedia*, 97, 447-453.
- [2] Laloy, E., & Jacques, D. (2019). Emulation of CPU-demanding reactive transport models: a comparison of Gaussian processes, polynomial chaos expansion, and deep neural networks. *Computational Geosciences*, 23(5), 1193-1215.
- [3] Prasianakis, N. I., Haller, R., Mahrous, M., Poonosamy, J., Pfingsten, W., & Churakov, S. V. (2020). Neural network based process coupling and parameter upscaling in reactive transport simulations. *Geochimica et Cosmochimica Acta*, 291, 126-143.
- [4] Laloy, E., & Jacques, D. (2022). Speeding up reactive transport simulations in cement systems by surrogate geochemical modeling: deep neural networks and k-nearest neighbors. *Transport in Porous Media*, 143(2), 433-462.

PD-1 A CRITICAL ANALYSIS OF THE RADIOECOLOGICAL MODEL USED IN THE GERMAN CALCULATION BASIS FOR THE ESTIMATION OF RADIATION DOSES DUE TO THE STORAGE OF HIGHLY ACTIVE NUCLEAR WASTE

Volker Hormann⁽¹⁾ and Clemens Walther⁽¹⁾

(1) Institute of Radioecology and Radiation Protection, Leibniz University Hannover, Germany

In late 2022, the German Federal Office for the Safety of Nuclear Waste Management issued the first edition of a calculation basis for the estimation of radiation doses due to the storage of highly active nuclear waste [1]. This document has been largely derived from the administrative regulation for the calculation of doses to members of the public due to operation of nuclear facilities [2] and is part of the regulatory framework that is intended to ensure the safety of long-term nuclear waste disposal. While the calculation of nuclide migration from the repository into the ecosphere is not explicitly given, there is a mathematical description of dose estimation based on a detailed radioecological model (Figure).

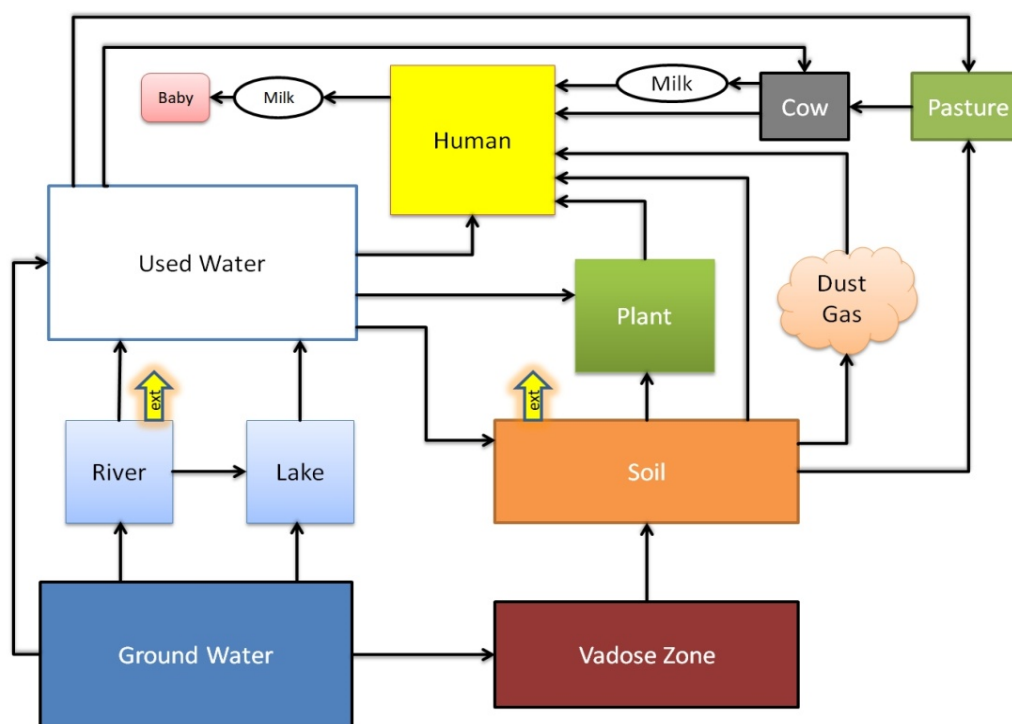


Figure 1 Nuclide paths of the radioecological model used in [1]; the yellow arrows denote external gamma irradiation

In our work, carried out in the context of the German-Swiss joint project TRANSENS [3], we compare this model and especially its parameters with radioecological studies and data from the literature and critically evaluate the choice of the parameter values. For several elements (e.g. Se, Nb, Tc and Pu), we estimate the relative importance of the individual paths, because this largely depends on the biological and physicochemical characteristics of the respective element. For some parameters, we suggest revision of the chosen values resp. their estimation.

Here we give an example that may illustrate how the estimated dose contributions of an individual path may change for particular elements if the respective parameters are updated.

In a scenario where well water is used for drinking water, but also for irrigating agricultural fields and pastures that produce local food, the ingestion path accounts for the predominant fraction of estimated dose for most radionuclides. The calculation basis [1] conservatively assumes that 100% of the consumed water originates from local wells and 50 % of the consumed food is produced locally. Figure 2 (left) shows the relative dose contributions using the transfer factors from [1] for meat and dairy products. Especially for Tc and Nb, an element that is known to be relevant for its role in external gamma exposition, the dose contribution due to meat consumption is remarkably high.

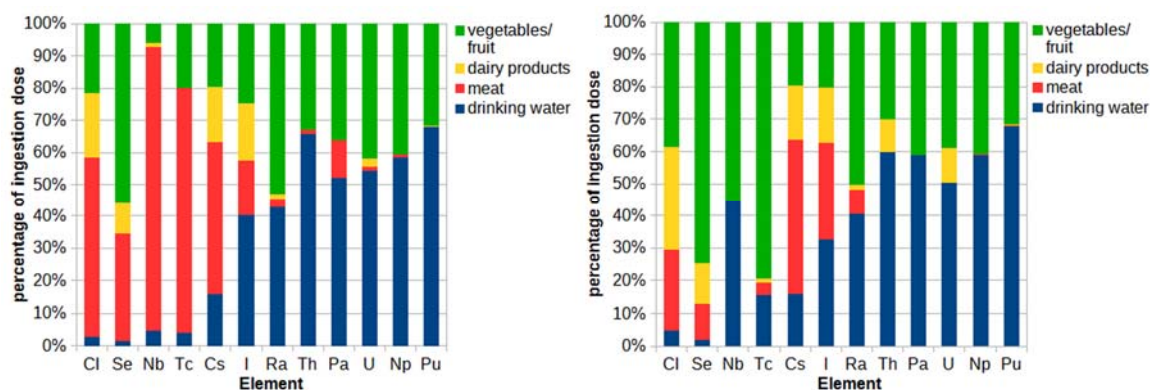


Figure 2 Relative dose contributions of drinking water and food in the ingestion path; left: calculations with transfer factors used in [1], right: calculations with transfer factors from [4,5].

In the calculations for Figure 2 (right), the transfer factors for meat and dairy products from the IAEA TecDocs 1799 [4] and 1950 [5] have been used. The contributions due to meat consumption are strongly reduced for Cl, Se, Tc and Ra. For Nb, the contribution is now even negligible, because the correspondent transfer factor from [4] is orders of magnitude lower than assumed in [1].

This example shows the importance of keeping the parameter values used in radioecological models up to date. Especially the current transfer factors given by the IAEA are based on more studies than in older sources and are thus more reliable.

References

- [1] Bundesamt für die Sicherheit der nuklearen Entsorgung (BASE) (2022). Berechnungsgrundlage für die Dosisabschätzung bei der Endlagerung von hochradioaktiven Abfällen. Berlin, December 2022.
- [2] Bundesministerium für Umwelt, Naturschutz und nukleare Sicherheit (2020). Allgemeine Verwaltungsvorschrift zur Ermittlung der Exposition von Einzelpersonen der Bevölkerung durch genehmigungs- oder anzeigebedürftige Tätigkeiten (AVV Tätigkeiten). BAnz AT 16.06.2020 B3.
- [3] <https://www.transens.de/en/>
- [4] IAEA TecDoc 1799. Environmental change in post-closure safety assessment of solid radioactive waste repositories. International Atomic Energy Agency, Vienna
- [5] IAEA TecDoc 1950. Approaches for Modelling of Radioecological Data to Identify Key Radionuclides and Associated Parameter Values for Human and Wildlife Exposure Assessments. International Atomic Energy Agency, Vienna.

PD-2 TRANSPORT OF RADIOACTIVE WASTE ALONG THE SELLAFIELD SHORELINE: CLIMATE CHANGE IMPACT AND MITIGATION STRATEGIES THROUGH NATURE-BASED SOLUTIONS

Louisa Bacon-Hall ⁽¹⁾, Prof Nicoletta Leonardi ⁽¹⁾, Prof Andy Plater ⁽¹⁾, Liam Abrahamsen-Mills ⁽²⁾, Simon Kwong ⁽²⁾

(1) *University of Liverpool, UK*

(2) *NNL, UK*

The abstract presented below is for research that will be presented in poster format at the Migration conference. This research aims to predict coastal change due to sedimentation and erosion, as a proxy to understanding physical remobilisation and transport of sediments contaminated by historic radioactive discharges. In addition to studying how hydrological processes influence the movement of radionuclides discharged to the Irish Sea in the present day. Liquid radioactive liquors have been discharged to the Irish Sea from Sellafield, NW England, since 1952, with discharge levels peaking in the mid-1970's (Kershaw, 1992). Some of these radionuclides have become associated with the Irish Sea sediment, while others exist as solutes in the sea water. Areas of sea bed sediments known as the Mud Patch and Mud Belt are of particular interest as they are known to be contaminated with radionuclides such as Cs-137 (Ray et al, 2020). By simulating sediment movement from the Mud Patch and Mud Belt, the movement of key Sellafield-derived radionuclides are also simulated.

Sedimentation and hydrodynamic processes of the Sellafield coastline are investigated by numerical modelling. Delft3D is an open-source coastal modelling software. The Delft3D flow (FLOW) module is a hydrodynamic and transport simulation program that can calculate non-steady flow and transport processes which result from tidal and meteorological forcing on a boundary fitted grid. The sediment transport and morphology modules simulate bed and suspended load transport of cohesive and non-cohesive sediments (oss.deltares.nl, 2011). The effect of the tide on sediment mobilization in the Irish Sea has been studied. The proxy study relating sediment transport to radionuclide transport will follow. Distribution coefficients of radionuclides can be included in Delft3D models to account for different interaction mechanisms of different elements with sediments. The radionuclides associated with clay and mud sediments bind to the crystal lattice structures (Fuller et el, 2015). Radionuclides such as Cs-137 can become permanently associated with clay sediments, however, some radionuclides can re-dissolve back into the liquid phase of the sea water. Distribution coefficients of radionuclides influence this re-dissolution behavior (Kershaw, 1992).

From the simulation results, a volumetric estimate of how much sediment is moving will be calculated. Once the moving sediment volume is calculated, the K_d values of a suitable radionuclide will be used to calculate the flux in the Irish Sea as a result of sediment migration within the study area. Further radionuclides will be added once the method has been established and validated. Volumetric budgets of additions radionuclides will need to be considered. Discharge point sources will be added around the Sellafield area of the model domain to represent the pipelines that discharge radioactive liquor to the Irish Sea. Discharge values from Sellafield Ltd will be used as input values. A comparison of radionuclide movement from sediment migration and direct discharge will be undertaken.

To gain a full understanding of the radionuclide contamination of the Irish Sea coastline and coastal sediments. The Delft3D model described above will simulate the last 70 years of the discharge history from Sellafield. The composition of the radioactive discharges to the Irish Sea changed from 1952 to today, with some considerable year to year differences in volume and chemical composition (Kershaw, 1992). To computationally predict how sea level rise and climate change will influence the movement of these Sellafield radionuclides, an accurate historical forecast will need to be created. An increase in storm frequency and intensity due to climate change will also be considered.

Results

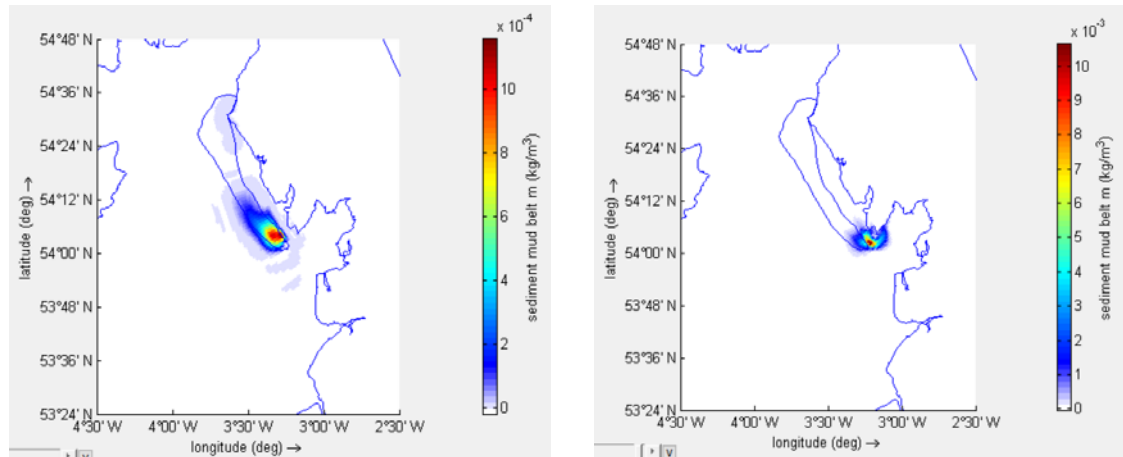


Figure 1: Sediment mass concentration per unit area of the Mud Belt sediment on 02/10/2014 (left) and 30/10/2014 (right) simulated in Delft3D

Figure 1 demonstrates how the Mud Belt sediment mass concentration moves over Oct 2014. The sediment increases in concentration at the south end of the Mud Belt, with a fraction entering the north of Morecambe bay, by the end of the simulation run time of the month of October 2014. This would suggest that any radionuclides associated with the Mud Belt sediment would move with the sediment as well, resulting in Sellafield radionuclides entering into Morecambe bay. Analysis of the data will be performed subsequently.

References

- [1] Kershaw(1992) Pentreath, Woodhead, Hunt. A review of radioactivity in the Irish Sea. Aquatic Environment Monitoring Report, 32, 1992.
- [2] Oss.deltares.nl.(2011). Home - Delft3D - oss.deltares.nl. [online] Available at: <<https://oss.deltares.nl/web/delft3d/home>>
- [3] Ray(2020) Leary, Livens, Gray, Morris, Law, Fuller, Abrahamsen-Mills, Howe, Tierney. Controls on anthropogenic radionuclide distribution in the Sellafield-impacted eastern Irish Sea. Science of the Total Environment, 743:140765, 2020.

PD-3 PRELIMINARY LONG-TERM HYDROGEOCHEMICAL EVOLUTION STUDY CASE IN TAIWAN

Yu-Hsiang Huang⁽¹⁾, Pin-Hsiu Kuo⁽¹⁾, Po-Yu Chuang⁽¹⁾, Chien-Chung Ke⁽¹⁾, Paolo Trincherò⁽²⁾

(1) *Advanced Geological Research Task Force, Sinotech Engineering Consultants, Inc., Taiwan*

(2) *AMPHOS 21 Consulting S.L., RSK Group, Spain*

Like other countries with nuclear power plants and use nuclear power to generate electricity, the disposal of spent nuclear fuel is an issue that must be dealt with in Taiwan. Taiwan's current disposal programme is scheduled to start operation of the final disposal facility in 2055. Currently Taiwan is in the stage of candidate site selection and approval. The research team conducts field investigations on potential research areas and obtains geochemical in situ data of potential investigation areas.

The hydrogeochemical changes and evolution at repository depth will be strongly conditioned by the hydrogeological conditions of the site. The main objective of this study was the construction of a geochemical model capable of reproducing the chemical composition measured for surface water and groundwater. To this end, two types of models were constructed: the first model without a rock matrix to evaluate the chemical processes in the fracture and the second model that allows to evaluate the interactions between fracture and rock matrix domains. A constant flux ($v_{flux}=0.5 \text{ m/day}$) is applied to the top boundary of the fracture and a Dirichlet boundary condition (i.e. prescribed pressure) is set at the top boundary.

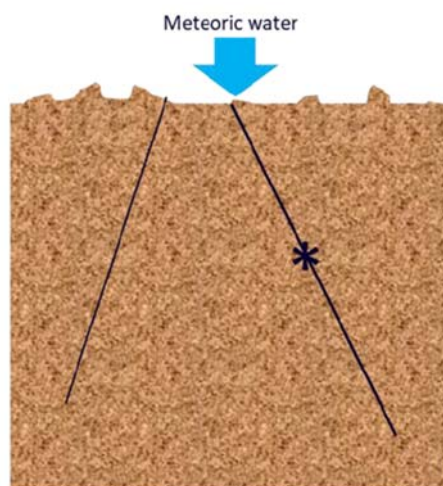


Figure 1. Model sketch of the 1D model. (*) Observation point at repository depth.

Figure 1 provides an idealized sketch of the conceptual model: meteoric water infiltrates at the surface and moves preferentially along one (or multiple) fracture(s). The flow and transport boundary conditions remain unchanged over time. The chemical calculations implemented in the 1D models are based on the preliminary results. A Base Case was defined assuming groundwater interaction with the fracture filling minerals is defined by imposing equilibrium conditions with calcite/ siderite (Reactions 1 and 2 in Table 1, respectively) in the fracture domain. In addition, kinetic dissolution of albite, biotite and K-feldspar and quartz is assumed to occur in the fracture domain following Reactions 3, 4, 5, 6 and 7. The rate kinetic laws were taken from Palandri and Kharaka (2004). Meteoric water is initially assumed to be in equilibrium with calcite and ferrihydrite (Reaction 7).

Table 1. Chemical reaction formula used in calculation

$\text{CaCO}_3 \rightarrow \text{Ca}^{2+} + \text{CO}_3^{2-}$	Reaction 1
$\text{FeCO}_3 \rightarrow \text{Fe}^{2+} + \text{CO}_3^{2-}$	Reaction 2
$\text{NaAlSi}_3\text{O}_8 + 4\text{H}_2\text{O} + 4\text{H}^+ \rightarrow \text{Na}^+ + 1 \text{Al}^{3+} + 3\text{H}_4(\text{SiO}_4)$	Reaction 3
$\text{KAlSi}_3\text{O}_8 + 4\text{H}^+ + 4\text{H}_2\text{O} \rightarrow \text{K}^+ + \text{Al}^{3+} + 3\text{H}_4(\text{SiO}_4)$	Reaction 4
$\text{Mg}_5\text{Al}_2\text{Si}_3\text{O}_{10}(\text{OH})_8 + 16\text{H}^+ \rightarrow 5\text{Mg}^{2+} + 2\text{Al}^{3+} + 3\text{H}_4(\text{SiO}_4) + 6\text{H}_2\text{O}$	Reaction 5
$\text{SiO}_2 + 2 \text{H}_2\text{O} \rightarrow \text{H}_4(\text{SiO}_4)$	Reaction 6
$\text{Fe}(\text{OH})_3 + 3\text{H}^+ \rightarrow \text{Fe}^{3+} + 3\text{H}_2\text{O}$	Reaction 7

A Variant Case was defined in order to test the impact of diffusion in the rock matrix by defined a case with a lower diffusion coefficient ($1 \cdot 10^{-12} \text{ m}^2/\text{s}$) with respect to the Base Case. The evolution of the system is monitored for a period of one thousand year by computing breakthrough curves at repository depth (500 m) and vertical profiles of temporal evolution groundwater composition along the fracture. The main objective of this exercise is to assess both numerical approaches by comparing the results with data measured on site.

In order to assess the safety of the future repository, a series of safety functions have been defined by the waste management organizations. The most complete description of safety functions and parameters throughout of the international literature is adopted in Sweden and Finland (Posiva, S. K. B., 2017).

In this research, the key focus is placed on the safety functions with respect to the geochemical conditions of the geosphere, which, in turn, depend on the hydrogeological conditions.

Four safety functions were evaluated from the calculated results (salinity, pH, pe and sum of cations). In all cases the calculated values fulfill the safety criteria established for these four parameters. However, in the case of the sum of cations, the SC (Single Continuum) model presents values very close to the minimum safety limits. The evolution of groundwater at the repository depth fulfils the safety functions assessed in this report (salinity, pH, pe, sum of cations).

From the results obtained with these models, it is possible to conclude that models accounting for a reactive rock matrix are able to reproduce the experimental data, and the proposed geochemical model has been validated by comparison with the data measured in the field.

More studies are needed for a complete validation of the hydrogeochemical model. The comparison between SC (Single Continuum) and DC (Dual Continuum) models allows to conclude, as for the other cations, that the rock matrix has an important impact on the control of Mg concentrations in the fracture groundwater. As mentioned for Na concentrations, the Variant Case displays the same effects observed for the SC model but attenuated in time because of the buffer effect of the rock matrix

References

- [1] Palandri, J. L., & Kharaka, Y. K. (2004). A compilation of rate parameters of water-mineral interaction kinetics for application to geochemical modeling. Geological Survey Menlo Park CA.
- [2] Posiva, S. K. B. (2017). Safety functions, performance targets and technical design requirements for a KBS-3V repository. Conclusions and recommendations from a joint SKB and Posiva working group. Posiva SKB Report, 1.

PD-4 MICROBIAL IMPACT ON MINERALOGICAL TRAPPING OF URANIUM IN DEEP ANOXIC AQUIFERS: CASE STUDIES FOR ÄSPÖ HARD ROCK LABORATORY AND FORSMARK SITE, SWEDEN

Ivan Pidchenko⁽¹⁾, John Christensen⁽²⁾, Martin Kutzschbach⁽³⁾, Konstantin Ignatyev⁽⁴⁾, Ignasi Puigdomenech⁽⁵⁾, Lindsay Krall⁽⁵⁾, Troy Rasbury⁽⁶⁾, Henrik Drake⁽¹⁾

(1) *Linnaeus University, Kalmar, Sweden*

(2) *Lawrence Berkeley National Laboratory, Berkeley, USA*

(3) *Technische Universität Berlin, Berlin, Germany*

(4) *Diamond Light Source, Didcot, UK*

(5) *Swedish Nuclear Fuel and Waste Management Co., Solna, Sweden*

(6) *Stony Brook University, Stony Brook, USA*

Natural uranium (U) in deep groundwater has been extensively studied in connection to the search for suitable locations for final disposal of spent nuclear fuel (SNF) [1]. The U removal process depends on environmental and biogeochemical conditions and is often associated with fractionation of the primordial U isotopes, ²³⁸U and ²³⁵U (as $\delta^{238}\text{U}$), during the reduction of geochemically mobile hexavalent uranium, U(VI), to relatively insoluble tetravalent, U(IV), species. Thus, $\delta^{238}\text{U}$ serves as an emerging isotope signature for redox specific scenarios, in local to global temporal and spatial scales [2]. In this contribution, two packed-off borehole sections at 415 and 500 m depths, isolating water-conductive fractures in Paleoproterozoic granitoid rock are investigated after in situ experiments of varying time, from 1.5 month to 17 years [3]. The first site is Äspö HRL, constructed and operated by the Swedish Nuclear Fuel and Waste Management Co. and serves as a full-scale tunnel as a test-facility for the actual SNF repository to be built at Forsmark, the second site of this project. Herein we show how various analytical techniques, modelling, and isotope methods can be utilized to reveal U speciation, mineralogical removal pathways, associated redox changes and related U isotope fractionations in the deep aquifers. Synchrotron and laser ablation mass spectrometric techniques reveal that calcite, amorphous Fe(II)-sulfides and Al-oxyhydroxides formed on the severely corroded borehole equipment contain intermittent elevated U, occurring as U(IV), and hence serves as a mineralogical sink for U. Thermodynamic modelling shows that dissolved sulfides formed after bacterial sulfate reduction is the main driving force for the reduction of U(VI) in the borehole water as well as observed corrosion of technical Al rods that connect packers. The bacterial-assisted degradation of technical polymer constituents present in the borehole equipment contribute to forming the carbonates and sulfides that facilitate reduction of U(VI) and subsequent immobilisation of U(IV) into secondary minerals. Measured $\delta^{238}\text{U}$ in water and precipitated calcites shows that U(VI) undergoes redox transformations in granitic rock aquifers, involving mineralogical and microbial pathways presumably taking place along redox fronts in the fracture network. The isotopic signatures recorded for Ca (as $\delta^{44/40}\text{Ca}$) in fracture water and calcite samples provide additional insights on calcite growth rate. The removal efficiency of U from groundwater, reaching up to 75% in the 415 m deep borehole section, and nearly quantitative U removal at 500 m depth, with subsequent selective U accumulation in secondary minerals of up to several hundred ppm in exceedingly U-deficient groundwater shows the potential of these widespread mineralogical sinks for U retention in deep anoxic environments [4]. The obtained data on removal of U by secondary minerals provide important insights for assessment of the geochemical behaviour of U and other redox-sensitive species in deep anoxic aquifers that is relevant for trace metal mobility and long-term storage of SNF.

References

- [1] Suksi, J., E-L. Tullborg, I. Pidchenko, L. Krall, B. Sandström, K. Kaksonen, T. Vitova, K. Kvashnina and J. Göttlicher (2021). Uranium remobilisation in anoxic deep rock-groundwater system in response to late Quaternary climate change – Results from Forsmark, Sweden. *Chem. Geol.* 584, 120551

ABSTRACTS

- [2] Brown, S., A. Basu, J. Christensen, P. Reimus, J. Heikoop, A. Simmons, G. Woldegabriel, K. Maher, K. Weaver, J. Clay, and D. DePaolo (2016). Isotopic Evidence for Reductive Immobilization of Uranium Across a Roll-Front Mineral Deposit. *Environ. Sci. Technol.* 50(12): 6189-6198
- [3] Drake, H., F. A. Mathurin, T. Zack, T. Schäfer, N. Roberts, M. Whitehouse, A. Karlsson, C. Broman and M. Åström (2018). Incorporation of Metals into Calcite in a Deep Anoxic Granite Aquifer. *Environ. Sci. Technol.* 52(2): 493-502
- [4] Pidchenko, I., J. Christensen, M. Kutzschbach, K. Ignatyev, I. Puigdomenech, E.-L. Tullborg, N. Roberts, T. Rasbury, P. Northrup, R. Tappero, K. Kvashnina, T. Schäfer, Y. Suzuki and H. Drake. (2023). Deep anoxic aquifers could act as sinks for uranium through microbial-assisted mineral trapping. *Commun. Earth Environ.* doi.org/10.1038/s43247-023-00767-9

PE-1 EFFECT OF CITRIC ACID AND MALIC ACID ON THE URANIUM UPTAKE INTO *BRASSICA NAPUS* PLANTS IN HYDROPONIC CULTUREWarren A. John ⁽¹⁾, Jenny Jessat ⁽¹⁾, Robin Steudtner ⁽¹⁾, René Hübner ⁽²⁾, Susanne Sachs ⁽¹⁾*(1) Helmholtz-Zentrum Dresden-Rossendorf, Institute of Resource Ecology, Germany**(2) Helmholtz-Zentrum Dresden-Rossendorf, Institute of Ion Beam Physics and Materials Research, Germany*

The transport and transfer of radionuclides in the environment is an important aspect with regard to the health risk assessment of sites contaminated with naturally occurring radionuclides. In addition, this knowledge is highly relevant for the long-term safety assessment of future nuclear waste repositories. Radionuclides such as uranium are non-essential elements for plants. However, when present in contaminated soil, they can be taken up by plants and thus enter the food chain, posing a health risk to humans. Plants exude organic acids such as citric acid, malic acid, and/or oxalic acid into the rhizosphere. Under deficiency conditions, this can induce the dissolution of previously unavailable insoluble compounds, e.g., iron and phosphate minerals [1]. However, these processes can lead to the acquisition not only of essential nutrients, but also of non-essential ones, such as uranium. Therefore, plants may influence the mobility and bioavailability of radionuclides in the environment.

In the present work, we investigated the effect of citric acid and malic acid, both characteristic plant exudates, on the solubility of uranium in hydroponic plant culture medium as well as on the uranium uptake by *Brassica napus* (canola) plants in hydroponic culture. Prior to plant exposure, the solubility and speciation of 20 μM uranium(VI) in a phosphate-reduced hydroponic solution (HR_{red}, [2]) in the absence and presence of citric acid or malic acid was studied. After 24 h equilibration of uranium(VI) in HR_{red} solution in the absence of citric acid or malic acid, a part of the uranium (~50%) precipitated, most probably in form of a uranyl(VI) phosphate. The control samples without organic acids stayed at the minimum concentration of dissolved uranium for 72 h, whereas those with citric acid or malic acid showed a re-solubilisation to the maximum uranium concentration of 20 μM within the first 24 h after addition of the respective organic acid. Following the uranium speciation in the hydroponic solutions during the exposure period by time-resolved laser-induced fluorescence spectroscopy (TRLFS) indicated the formation of uranium(VI) citrate and malate complexes, whereas in the organic-acid-free solution, the $\text{UO}_2(\text{CO}_3)_3^{4-}$ complex predominated.

B. napus plants were cultivated according to Jessat et al. [2]. To study the influence of the two organic acids on uranium exposure to *B. napus*, 20 μM U(VI) were added to HR_{red} solution and allowed to equilibrate for 24 h in a plant growth chamber. After pre-equilibration, citric acid or malic acid (100 and 1000 μM) were added to the solutions. Immediately after that, the plants were inserted for exposure to uranium. For comparison, control samples were studied under the same conditions, however, without addition of citric acid or malic acid. The uranium concentration of the solutions was regularly determined by inductively coupled mass spectrometry (ICP-MS) within 72 h. After 72 h, the uranium content in the roots, stems, and leaves was analyzed by ICP-MS after drying and incineration. Furthermore, scanning transmission electron microscopy (STEM) coupled with energy-dispersive X-ray spectroscopy (EDX) was used to qualitatively confirm the presence of uranium in the roots.

The time-dependent bioassociation experiments showed a strong immobilization of uranium by the *B. napus* plants either in the absence or in the presence of organic acids. However, in the presence of citric acid and malic acid, this process seems to be retarded due to the re-dissolution of the uranium precipitate by the organic acids. Using TRLFS, uranium(VI) citrate and malate complexes were identified in the hydroponic solutions in the presence of the plants at the beginning of exposure. After longer exposure times, however, their contribution decreased and the $\text{UO}_2(\text{CO}_3)_3^{4-}$ complex dominated the speciation. For all conditions, STEM/EDX results verified the uptake of uranium into the whole root tissue. After

72 h of uranium exposure in the presence of citric acid or malic acid, more uranium was found in the leaves of *B. napus* compared to the control samples, indicating a stronger translocation of uranium in the plants. Despite that, in the presence of 1000 μM malic acid, a significantly lower amount of uranium was observed in the roots. These results demonstrate the ability of plant metabolites to dissolve hardly soluble uranium precipitates and shed more light on the speciation-dependent uranium uptake into and translocation in canola plants.

The results of this study may contribute to a more pronounced process understanding on the uranium uptake into plants and their impact on the uranium mobility in the environment. This knowledge is required for the improvement of radioecological models to assess the migration and transfer of radionuclides in the environment, to develop efficient and cost-effective remediation technologies for contaminated sites, and to perform reliable dose predictions for humans and environment.

Acknowledgement: *This work was performed within the RadoNorm project. This project has received funding from the Euratom research and training programme 2019-2020 under grant agreement No. 900009.*

References

- [1] Jones, D. L. (1998). Organic acids in the rhizosphere - a critical review. *Plant and Soil* 205: 25-44.
- [2] Jessat, J., John, W.A., Moll, H., Vogel, M., Steudtner, R., Drobot, B., Hübner, R., Stumpf, T., Sachs, S. (2023), *Ecotox. Environ. Saf.*, under review.

PE-2 GEOCHEMICAL BEHAVIOR OF RADIUM IN A URANIUM MILL TAILINGS POND OF THE NINGYO-TOGE MINE AREA

Kazuya Tanaka ⁽¹⁾, Yuichi Kurihara ⁽²⁾, Jumpei Tomita ⁽³⁾, Ibrahim Maamoun ⁽¹⁾, Shinya Yamasaki ⁽⁴⁾, Kohei Tokunaga ⁽⁵⁾, Kenjin Fukuyama ⁽⁵⁾, Naofumi Kozai ⁽⁵⁾

(1) *Advanced Science Research Center, Japan Atomic Energy Agency, 2-4 Shirakata, Tokai, Ibaraki 319-1195, Japan*

(2) *Department of Nuclear Technology, Nagaoka University of Technology, 1603-1 Kamitomioka-cho, Nagaoka, Niigata 940-2188, Japan*

(3) *Department of Radiation Protection, Japan Atomic Energy Agency, 2-4 Shirakata, Tokai, Ibaraki 319-1195, Japan*

(4) *Center for Research in Isotopes and Environmental Dynamics, University of Tsukuba, 1-1-1 Tennodai, Tsukuba, Ibaraki 305-8577, Japan*

(5) *Ningyo-toge Environmental Engineering Center, Japan Atomic Energy Agency, 1550 Kamisaibara, Kagamino, Okayama 708-0698, Japan*

The Ningyo-toge U mine area is located at the boundary between Okayama and Tottori Prefectures, southwestern Japan. Since the termination of mining operation at Ningyo-toge, maintenance management of a U mill tailings pond has been carried out by Ningyo-toge Environmental Engineering Center of Japan Atomic Energy Agency (hereafter Ningyo-toge center). In the Ningyo-toge center, groundwater containing ²²⁶Ra (half-life: 1600 yr), a descendant nuclide of ²³⁸U, is being continuously produced in contact with U ores at a former open-pit mine site and closed mining tunnels. Such groundwater contains Fe(II) and is flowing into a mill tailings pond. Finally, Fe(III) oxyhydroxide is deposited over the tailings pond after exposure of groundwater to the air. Thus, Fe(III) oxyhydroxide can be the main host to control the behavior of Ra in the tailings pond. The tailings pond can be regarded as a semi-natural environment that is suitable for research on geochemical behavior of Ra. In this study, we investigated the geochemical behavior of Ra focusing on its distribution between sediment and water.

We collected surface sediment and water samples at a U mill tailings pond in the Ningyo-toge center in November, 2019 and 2020. Water samples were filtered with a 0.45 μm pore-size filter, followed by acidification with HNO₃ to pH2. Water temperature and pH were measured on site at each sampling point. Wet sediment samples were centrifuged to be separated from water, and then freeze-dried without washing before analysis. Ra-226 activities of sediment and water samples were measured by γ-ray spectrometry using Ge detectors. Sediment samples were observed with a scanning electron microscope (SEM). X-ray diffraction (XRD) and Fe K-edge X-ray absorption fine structure (XAFS) of sediment samples were analyzed for identification of Fe(III) precipitates. Also, Mn K-edge XAFS spectra were measured to determine oxidation state of Mn.

SEM images showed aggregates of Fe(III) precipitates together with various diatoms (Fig. 1). XRD and XAFS analyses indicated that Fe(III) precipitates were composed of ferrihydrite and goethite. Water temperature ranged between 9.5 and 14.8°C while pH values of water were from 6.0 to 7.1. Radioactivity concentrations of ²²⁶Ra in sediments were 12,000 – 29,000 Bq/kg while those in water ranged from 60 to 580 mBq/L. As a result, apparent distribution coefficients of Ra between ferric sediment and water were estimated to be 3.1×10^4 – 3.8×10^5 mL/g, which were higher than reported ones for ferrihydrite and goethite. Sajih et al. reported that experimentally determined distribution coefficients of Ra for ferrihydrite and goethite were ~1000 and ~300 mL/g, respectively, in 0.1 M NaClO₄ solution at pH7 [1]. This suggests that another host on which Ra is strongly fixed would be present in sediment if we assume equilibrium between sediment and water. Many fragments of diatom frustules, which are amorphous silica (SiO₂·nH₂O), were observed under SEM observation in sediments (Fig. 1). However, it is unlikely that Ra is adsorbed on silica and/or incorporated into its structure. Mn K-edge XAFS analysis indicated the presence of Mn(IV) in sediment samples. It is empirically known that Ra is strongly adsorbed on

Mn(IV) oxide although distribution coefficient of Ra has not been well determined. Thus, it is possible that Mn(IV) oxide as a minor component contributed to an increase in the apparent distribution coefficients. Another possibility is upward flow of pore water containing ^{226}Ra or diffusion of ^{226}Ra released from lower sediment layers. Either scenario provides additional input of ^{226}Ra to surface sediment. In this case, surface sediment and water did not reach equilibrium with each other, but ^{226}Ra concentrations in surface sediments were governed by dynamics through input of ^{226}Ra from porewater as well as groundwater in sediment-water interaction.

In addition to the discussion above, we will show the distribution of Sr and Ba along with Ra from the viewpoint of comparison of alkali earth elements in their chemical property.

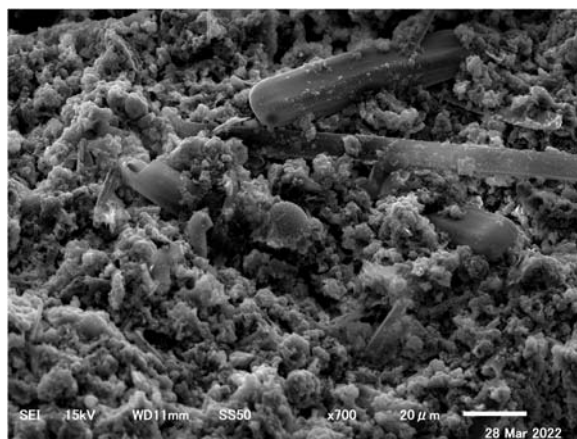


Figure 1. SEM image of surface sediment collected at a U mill tailings pond in the Ningyo-toge center.

Reference

- [1] Sajih, M., Bryan, N.D., Livens, F.R., Vaughan, D.J., Descostes, M., Phrommavanh, V., Nos, J. and Morris, K. (2014). Adsorption of radium and barium on goethite and ferrihydrite: A kinetic and surface complexation modelling study. *Geochim. Cosmochim. Acta* 146: 150-163

C2-1 TOWARDS A PROCESS-BASED MODEL DESCRIBING TRANSPORT-INDUCED CO-PRECIPIATION AND RADIONUCLIDE RETENTION LAB ON CHIP EXPERIMENTS AND REACTIVE TRANSPORT MODELLING DIAGNOSTICS

Jenna Poonoosamy⁽¹⁾, Enzo Curti⁽²⁾, Abdulmonem Obaeid⁽¹⁾, Nikolaos I. Prasianakis⁽²⁾, Guido Deissmann⁽¹⁾, Sergey Churakov⁽²⁾, Dirk Bosbach⁽¹⁾

(1) Institute of Energy and Climate Research, Nuclear Waste Management (IEK-6), Forschungszentrum Juelich, Germany

(2) Laboratory for Waste Management (LES), Paul Scherrer Institute, Switzerland

Co-precipitation of radionuclides in host phases is considered a relevant retention mechanism in some scenarios of safety cases for deep geological repositories for radioactive wastes. Ba and Ra released from the radioactive waste will react with porewater containing sulphate, triggering the formation of (Ba,Ra)SO₄ or even (Ba,Sr,Ra)SO₄ solid solutions. In the specific case of ²²⁶Ra, the solid solution with BaSO₄ irreversibly binds the contaminant in a stable phase, of which the mixing behaviour and thermodynamic properties are well described in the literature. However, for a rigorous assessment of the fate of ²²⁶Ra with reactive transport modelling a conceptual approach describing transport-induced crystallization of solid solutions in tightly confined porous media considering the effects of kinetics is needed¹. Indeed, the kinetics of crystallization of (Ba,Ra)SO₄ has to our knowledge not been determined so far. In addition, crystallization processes in tightly confined porous media are not properly understood with a postulated inhibition in small pores. Moreover, for the case of a solid solution, its crystallization in nature is often characterized by oscillatory zonation phenomena.

With the main objective of providing an integrated experimental and theoretical approach to predict transport-induced precipitation of solid solutions in tightly confined porous media or fractured crystalline rocks, we devised a series of investigations to (i) determine whether nucleation is inhibited in confinement, (ii) decipher crystallization processes of solid solutions leading to oscillatory zoning, and (iii) rationalize the crystallization kinetics of (Ba,Ra)SO₄. The methodology used in this work combines Lab on a chip experiments and reactive transport modelling^{2,3}.

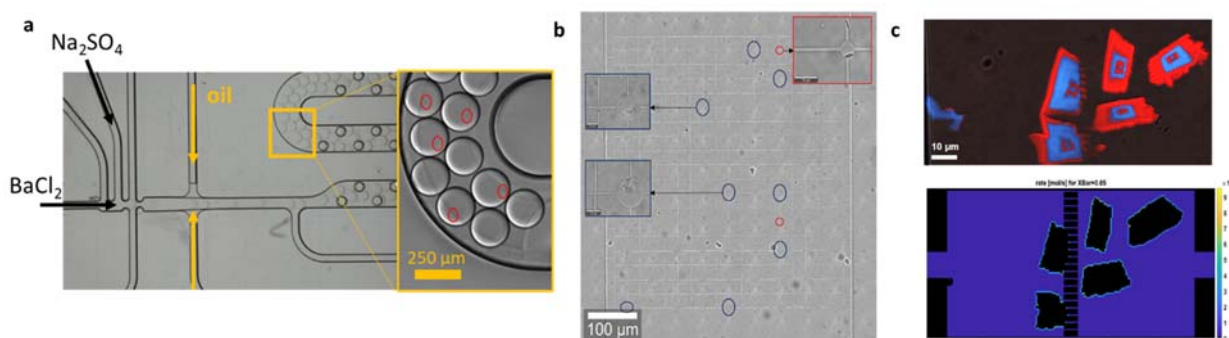


Fig. 1 *a* droplet generator chip, producing 100 (hundreds) of nL sized solution-filled droplets in an oil carrier phase to investigate nucleation processes in confinement with barite crystallites encircled; *b* crystallization of barite in a pore network model consisting of larger and smaller pores interconnected by capillaries indicating preferential mineralization in larger pores (blue circles) in contrast to smaller pores (red circles); *c* oscillatory zoned crystals of (Ba,Sr)SO₄ in a microfluidic device and results of complementary reactive transport modelling.

(i) Pore size dependency on nucleation:

For the sake of simplicity, we focused in our study on the crystallization of barite. Massive microfluidic experiments conducted in nano-confined volumes of solution, i.e., in droplets (Fig. 1a) ranging in volume between 0.3 and 3 nL, showed that nucleation is a probabilistic event that scales with the volume of fluid.

While our statistical analysis showed that inhibition of barite nucleation will start at pore sizes $< 1 \mu\text{m}$, theoretical calculations show that the pore size-controlled solubility effect⁴ (a thermodynamic effect) becomes effective only in pores of sizes less than $< 0.1 \mu\text{m}$. In a second step, the influence of diffusive transport was investigated by fostering the crystallization of barite in a pore network consisting of large and small micrometer-sized pores interconnected by fine squared capillaries of $1 \mu\text{m}^2$ cross-sectional area (Fig. 1b). Although preferential mineralization was observed in larger pores, at low supersaturation crystallization was observed only in the fine capillaries. In nano-porous media, the crystallization process is mainly controlled by the thermodynamic pore size effect, while in micro-porous media geometry effects and nucleation kinetics driven by the surface energy of the substrate play a major role. Consequently, it can be expected that mineralization occurs preferentially in larger pores in rock matrices, but other parameters might obscure or reverse this trend.

(ii) Deciphering the formation of oscillatory-zoned (Ba,Sr)SO₄ solid solutions

Our micromodel consisted of two parallel supply channels interconnected by microfluidic reaction chambers. A Na₂SO₄ solution and a mixed solution of BaCl₂ and SrCl₂ were injected into the supply channels. The co-precipitation of (Ba,Sr)SO₄ was fostered by the counter diffusion of solutes in the microfluidic reaction chambers. The compositions of the solid solutions were determined by in-situ Raman spectroscopy (Fig. 1c). We used reactive transport modelling with newly implemented theoretical approaches such as the supersaturation function and classical nucleation theory (CNT) extended to solid solutions to predict the composition of the nucleating phases, and to determine the driving forces for the oscillatory zoning. Our investigations showed that the composition of the nucleating phases can be approximated by using CNT and that the oscillatory zoning results from a combination of limited diffusional transport of solutes and kinetically controlled precipitation reactions⁵.

(iii) Rationalizing crystallization kinetics of (Ba,Ra)SO₄

Currently, we are developing a micromodel experimental framework to investigate the crystallization of (Ba,Ra)SO₄ both in an advective mixing regime and a diffusive regime. The advantage of using microfluidics compared to bulk experiments using flow crystallizers is that microfluidics offers the opportunity to work with a high concentration of ²²⁶Ra in solution while the radionuclide inventory in the experimental setup is low, keeping the radiation doses at levels similar to classical batch experiments or below. The experiments are monitored by time-lapse microscopy and in-situ Raman spectroscopy is used to determine the composition of solid solutions, while solute transport modelling enables the determination of the evolving fluid flow velocities and aqueous solution composition, which can be used to rationalize crystallization kinetics.

In future work, we will integrate these concepts in a reactive transport model to conduct large-scale simulations of solid solution formation in fractured crystalline rocks for a more realistic description of the fate of ²²⁶Ra in the repository environment.

References

- [1] Curti, E. et al. (2019) Modelling Ra-bearing baryte nucleation/precipitation kinetics at the pore scale: application to radioactive waste disposal. *European Journal of Mineralogy* 31, 247-262
- [2] Poonoosamy, J. et al. (2019). A microfluidic experiment and pore-scale modelling diagnostics for assessing mineral precipitation and dissolution in confined spaces. *Chem. Geol.* 528: 119264
- [3] Prasianakis, N. I. et al. (2020). Neural network based process coupling and parameter upscaling in reactive transport simulations. *Geochim. Cosmochim. Acta* 291: 126-143
- [4] Emmanuel, S. and Berkowitz, B. (2007). Effects of pore-size controlled solubility on reactive transport in heterogeneous rock. *Geophys. Res. Lett.* 34: L06404
- [5] Poonoosamy, J. et al. (2021). A lab-on-a-chip approach integrating in-situ characterization and reactive transport modelling diagnostics to unravel (Ba,Sr)SO₄ oscillatory zoning. *Sci. Rep.* 11: 23678

C2-2 VERIFICATION OF NEW CLAYSORDIF MODEL FOR SORPTION AND DIFFUSION IN ARGILLACEOUS MEDIA AGAINST PHREEQC RESULTS AND EXPERIMENTAL DATA

Martin A. Glaus ⁽¹⁾, Dmitrii A. Kulik ⁽¹⁾, Luc R. Van Loon ⁽¹⁾, Raphael A.J. Wüst ⁽²⁾

(1) Laboratory for Waste Management, Paul Scherrer Institut, CH-5232 Villigen PSI, Switzerland

(2) National Cooperative for the Disposal of Radioactive Waste (Nagra), CH-5430 Wettingen, Switzerland

The prediction of adequate diffusion parameters of radionuclides in the context of deep geological disposal of radioactive waste in clay-rich host rocks, like the Opalinus Clay and its confining units in Switzerland, requires a comprehensive understanding of the transport properties of charged solution species in charged (un)saturated porous media and the impact of related parameters (or their best estimates). The presence of permanent lattice charges near the basal (planar) clay surfaces results in a concentration enrichment of cationic species and a concurrent depletion of anionic species in the solution phase immediately adjacent to the surfaces relative to the bulk aqueous phase. This is widely recognized as the principal cause of surface diffusion and anion exclusion phenomena in argillaceous systems. To describe these phenomena, several modelling techniques have been developed and integrated in various geochemical speciation and transport codes to simulate the diffusive and/or advective transport of radionuclides in argillaceous porous media. In a companion contribution by Kulik et al. [this conf.], we present the GEMS implementation of *ClaySorDif*, a new integrated sorption and diffusion model that computes effective diffusion coefficients D_e and distribution ratios R_d of elements and ions using the existing sorption model *ClaySor* for cation exchange on basal and surface complexation on edge surfaces of illite and montmorillonite ([1], Miron et al. [this conf.]). *ClaySorDif* is simpler than previous mean potential in Donnan layer (MPDL) model implementations e.g. in Phreeqc code in two aspects: (i) it does not require any modification of the *ClaySor* ion exchange model by adding a negatively charged site as a chemical species, with respective changes of equilibrium constants for exchange ions; (ii) it introduces a “free charge capacity” (FCC) parameter of MPDL model, treated separately from the traditional cation exchange capacity (CEC) parameter, now used only in the *ClaySor* model. The aim of this contribution is to present our *ClaySorDif* verification results in order to demonstrate that the new integrated model, though simpler than previous ones, yields equally good description of experimental data [2] and an exact match with the Phreeqc model curves for mono- and divalent cations and anions.

The *ClaySorDif* model was tested and verified against Phreeqc calculations for the mean potential (Donnan) approach using the experimental data gained from more than hundred diffusion measurements on rock samples from deep borehole drillings performed by Nagra in the Mesozoic sedimentary layers of Northern Switzerland [3]. The boreholes covered a wide range of lithostratigraphic layers, resulting in rock compositions of variable contents of clays, quartz, feldspars or carbonates. The diffusion measurements were conducted using tritiated water (HTO), $^{36}\text{Cl}^-$ and $^{22}\text{Na}^+$ as radiotracers. The results of the HTO measurements were used to determine the total accessible porosity and the geometry (or tortuosity) factors for diffusion. An empirical model was developed as a basis to describe the diffusion behavior of charged species (total accessible porosity, geometry factor, average pore width) as a function of the total clay content and the composition of the artificial pore water applied in the diffusion experiment. Figure 1 shows a comparison of the model predictions from Phreeqc and by the *ClaySorDif* model for the tested tracers. Note that the rock capacity factor (α) is defined as $\alpha = \varepsilon + R_d \cdot \rho_{bd}$ where ε is the total porosity, and ρ_{bd} is the bulk-dry density.

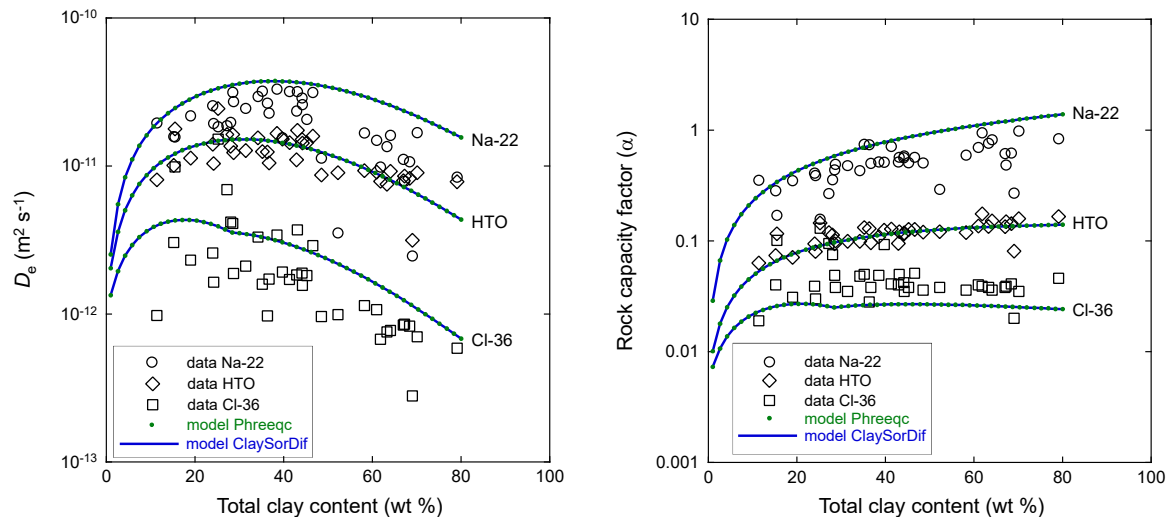


Fig. 1: Comparison of the predictions of D_e and α from *ClaySorDif* and *Phreeqc* MPDL models for the diffusion data measured for the deep borehole samples from Bözberg1-1.

The predictions from both models are virtually identical, despite the fact that they are just blind predictions using basic default assumptions, such as the Donnan layer thickness represented by twice the Debye length. For this reason, systematic deviations between the model curve and the experimental data are acceptable. Furthermore, it should be noted that using the total clay content as a primary input variable is a gross simplification of reality and may not be accurate for all rock sequences. Despite model simplifications, the agreement between the experimental data and the model description is remarkable. One value for the CEC and one value for FCC were sufficient for modeling of the experimental data for all four locations in Northern Switzerland [2,3] using *ClaySorDif*. An excellent match was also obtained between *ClaySorDif* and *Phreeqc* predictions of D_e and α for divalent species, for which no experimental data were measured. The case of sulfate is interesting because the model predictions compared to those for Cl^- are rather similar despite the difference in charges of the two anions. The reason for this behavior is found in the significant speciation fraction of neutral sulfate complexes with Ca^{2+} and Mg^{2+} in pore waters, which reduces the effect of higher charge of sulfate.

Verification results show that the integration of *ClaySorDif* surface diffusion and anion exclusion MPDL model into GEMS codes provides a comprehensive toolkit for building the databases for radionuclide solubility, sorption and diffusion in porous media such as clays or cement, based on the common foundation of consistent thermodynamic datasets combined with the process understanding. In turn, this constitutes an important optimistic step towards a robust and more reliable prediction of radionuclide transport in diffusion-dominated rocks through modeling future radiation doses at the surface or in the biosphere that may arise from deep geological disposal of radioactive waste.

References

- [1] Kulik, D.A., Marques Fernandes, M. and B. Baeyens (2018). The 2SPNE SC/CE sorption model in GEM-Selektor v.3.4 code package (*ClaySor*). Nagra Arbeitsbericht NAB 18-27, 152 pp.
- [2] Glaus, M.A., Van Loon, L.R. and R. Wüst (2023). Diffusion of HTO, $^{36}\text{Cl}^-$ and $^{22}\text{Na}^+$ in the Mesozoic cover of Northern Switzerland. II: Interpretation in terms of an electrical double layer model. *Appl. Geochem.*: to be submitted.
- [3] Van Loon, L.R., Glaus, M.A. and R. Wüst (2023). Diffusion of HTO, ^{36}Cl and ^{22}Na in the Mesozoic cover of Northern Switzerland: I: Measurement of diffusion coefficients and capacity factors. *Appl. Geochem.*: to be submitted.

C2-2 GEMS IMPLEMENTATION OF AN INTEGRATED CLAYSORDIF MODEL FOR RADIONUCLIDE SORPTION AND DIFFUSION IN ARGILLACEOUS MEDIA

Dmitrii A. Kulik ⁽¹⁾, Martin A. Glaus ⁽¹⁾, Thomas Gimmi ^(1,2), Luc R. Van Loon ⁽¹⁾, Raphael Wüst ⁽³⁾

(1) Laboratory for Waste Management, Paul Scherrer Institut, CH-5232 Villigen PSI, Switzerland

(2) Institute for Geological Sciences, University of Bern, CH-3012 Bern, Switzerland

(3) National Cooperative for the Disposal of Radioactive Waste (Nagra), CH-5430 Wettingen, Switzerland

The prediction of realistic diffusion parameters of radionuclides in clay-rich host rocks is relevant in the context of deep geological disposal of radioactive waste. The negative permanent charge of clay minerals (illite and smectite) enhances concentration of aqueous cationic species and depletes that of anionic species in porewater in the vicinity of clay surfaces relative to the “free” (bulk) porewater. This leads to greater diffusion rates of cations due to surface excess, and to anion exclusion in compacted clay rock systems. Modelling approaches such as the modified Gouy-Chapman (MGC) and the mean potential in Donnan layer (MPDL) [1] have been proposed to assess the Coulomb term and the relative electrostatic potential affecting concentrations of ions near clay-water interfaces. These models have been integrated in geochemical speciation and reactive transport codes to simulate the speciation and transport of radionuclides in porous argillaceous media, and have been used in the interpretation of diffusion and sorption experimental data obtained for real clay rocks [2,3].

In this contribution, we present the implementation of *ClaySorDif*, a new integrated sorption and diffusion model, in the Gibbs Energy Minimization Software (GEMS). The model accounts for effective diffusion coefficients D_e and distribution ratios R_d of elements and their aqueous species in argillaceous porous media. It extends the existing sorption model *ClaySor* [4], which is a GEMS re-implementation of the widely known 2SPNE SC/CE multi-site sorption model by Bradbury and Baeyens [5] for cation exchange on basal and surface complexation on edge surfaces of illite and montmorillonite. The *ClaySor* thermodynamic dataset has been re-parameterized at ambient conditions by Miron et al. [this conf.] for a full consistency with the latest PSI TDB 2020 chemical thermodynamic database [6]. The aim of creating the *Dif* model extension of the *ClaySor* model in GEMS was to assure a full consistency within the whole pipeline as shown in Figure 1, with further use of D_e and R_d estimates in compiling sorption- and diffusion databases, and in reactive transport simulations. Verification of the new model against recent experimental data for Swiss argillaceous rocks [7] and curves from Phreeqc Donnan model calculations will be given in a companion presentation by Glaus et al. [this conf.].

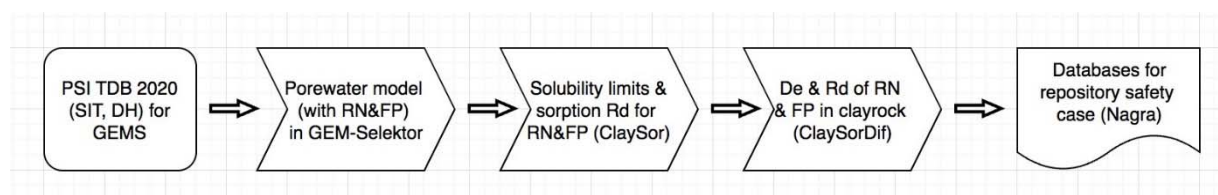


Figure 1. Place of *ClaySorDif* in the data pipeline. SIT: specific ion interaction, DH: Debye-Hückel activity models; RN: radionuclides; FP: fission products; R_d : distribution ratio (of an element between solid and aqueous phases); D_e : effective diffusion coefficient (of an element in argillaceous rock).

ClaySorDif extensions are implemented as Python scripts and Jupyter notebooks on the GeoML.io JupyterLab server (LES PSI) using the pre-installed GEMS3K and xGEMS/pyGEMS code packages. On the “geochemical system” side, the input consists of the GEMS3K I/O files exported from the GEM-

Selektor (<https://gems.web.psi.ch/GEMS3>) for model systems prepared using TDB2020 and ClaySor thermodynamic databases with the normative Opalinus Clay or synthetic porewater models. On the “diffusion” side, the .csv table input files with clay rock data for various clay contents are provided, along with JSON files containing diffusion coefficients of elements and ions in water, etc., as well as the setup of modelling task and settings for plotting the results. With automated selections for plotting and reporting defined in a dedicated Jupyter notebook, the model output is saved in .csv table files.

To estimate D_e , R_d values and anion accessible porosity, the MPDL model was implemented following [1,3]. Briefly, for each clay content fraction in argillaceous rock and dry density to estimate the porosity, first the aqueous phase speciation is computed in pyGEMS from the chosen normative Opalinus Clay pore water composition and the ClaySor model for illite. Next, the pore thickness and (volume) fractions of “free” and Donnan layer (DL) porewater are estimated as given in [7], followed by iterative charge balance calculations of the mean Donnan potential, ion concentration ratios C_{DL}/C_{free} , and D_e values of ions in the MPDL model. The D_e value of a chemical element is evaluated as a weighted sum of D_e values for its relevant aqueous species (taking $C_{DL}/C_{free} = 1$ for neutral species). Finally, the element R_d value in clay rock and the accessible porosity fraction (anions only) are calculated.

In other (e.g. Phreeqc) MPDL implementations, traditionally a negatively charged ion-exchange site on clay is introduced as a chemical species, and the equilibrium constants for exchange ions are corrected accordingly [1-3]. Our trial calculations showed that this only causes a rather high net charge on illite and on the whole system (problematic at high clay/water ratios), but gives no advantage relative to using the unmodified ClaySor ion exchange part. Without compromising the accuracy, the model becomes much simpler if the “Free charge capacity” (FCC) is treated as a separate MPDL parameter, independent of the cation exchange capacity (CEC) used only in the ClaySor model. In this case, CEC has no effect on the MPDL output, but only influences the calculated R_d values. FCC and CEC parameter values were optimized during the model verification against the available clay rock experimental data and Phreeqc modelling results (Glaus et al., this conf.). As exchange cations with selectivity constants are treated in ClaySor model as specifically adsorbed on planar surfaces, no amounts of cations in the DL volume need to be counted in R_d values calculated relative to ‘free’ porewater concentrations; the virtual composition and ionic strength in DL remain parts of MPDL output only. The MGP model as an option was implemented following Tournassat et al. [1] in order to assess the feasibility of MPDL results. Indeed, MGP potential and concentration ratio curves integrated over two Debye lengths can be reconciled well with those obtained from MPDL, though somewhat better at lower ionic strengths.

References

- [1] Tournassat, C. and I.C. Bourg, C.I. Steefel, F. Bergaya (2015). Surface properties of clay minerals. In: Developments in Clay Science, Vol. 6C, 5-31.
- [2] Glaus, M.A., and S. Frick, L.R. Van Loon (2020). A coherent approach for cation surface diffusion in clay minerals and cation sorption models. *Geochim. Cosmochim. Acta* 274, 79–96.
- [3] Gimmi, T., and P. Alt-Epping (2018). Simulating Donnan equilibria based on the Nernst-Planck equation. *Geochim. Cosmochim. Acta* 232, 1–13.
- [4] Kulik, D.A. and M. Marques Fernandes, B. Baeyens (2018). Nagra Arbeitsbericht NAB 18-27.
- [5] Bradbury, M.H. and Baeyens, B. (1997). A mechanistic description of Ni and Zn sorption on Namontmorillonite. 2. Modelling. *J. Contam. Hydrol.* 27, 223-248.
- [6] Hummel, W., and T. Thoenen (2022). The PSI Chemical Thermodynamic Database 2020. Nagra Technical Report NTB 21-03.
- [7] Glaus, M.A. and L.R. Van Loon, R. Wüst (2023), Diffusion of HTO, $^{36}\text{Cl}^-$ and $^{22}\text{Na}^+$ in the Mesozoic cover of Northern Switzerland. *Appl. Geochem.*: to be submitted.

C2-3 GLASS ALTERATION MODELISATION USING GRAAL2 MODEL

DELCROIX Maxime (1)(2), FRUGIER Pierre (1), NOIRIEL Catherine (2)

*(1) CEA, DES, ISEC, DPME, SEME, LEMC – Marcoule, France**(2) Géosciences Environnement Toulouse, UMR 5533 Université Paul Sabatier, Toulouse, France*

As part of the deep geological disposal of high-level nuclear waste in glass matrices, many studies are focusing on the ability of this material to resist alteration over time. Under these conditions, the glass will end up in contact with interstitial water and will be exposed to hydrolysis mechanisms followed by reactive diffusion through the passivating gel formed.

Long-term performance assessment of nuclear waste glasses in a geological repository relies on multiscale modeling, from atom scale models (Monte Carlo, Molecular Dynamics) up to geochemical models and reactive transport codes. The simpler the model is, the more it requires hypotheses whose demonstrations come from smaller scales models.

Implemented in the CHESS/HYTEC reactive transport code, the glass alteration model GRAAL 2 has been designed to interpret and then predict the alteration experiences of glasses in the complex chemical environment of their geological disposal [1]. Successfully applied in 2020 through the modelling of the alteration of AVM glasses in pure water and in magnesium-enriched solutions, it allows the various phenomena involved in the degradation of the glass (hydrolysis, interdiffusion, formation of passivating gel and possible secondary phases) to be taken into account. Based on the GRAAL 1 model [2], this new version allows, among other things, to take into account the chemical environment and its influence on the weathering layer and to define the minimum density threshold for passivation.

The model uses two main equations: the dissolution/precipitation equation at the external interface and a reactive diffusion equation. It is therefore important to provide the model with key parameters such as the apparent diffusion through the passivating gel and a kinetic constant for the formation of the gel.

In 2020, experiments were conducted on the alteration at 90°C of a glass with a composition of 64.9% SiO₂, -13.6% Na₂O-17.3% B₂O₃-4.1% Al₂O₃ (Figure 1) with the aim of studying the capacity of the model to reproduce the phenomena observed when the chemical composition of the environment in contact with the glass changes. The variable parameters were the composition of the altering solution (sodium and silicon loaded solution) and the ratio of glass surface to solution volume. The granulometry of the glass powders and the effect of the atmosphere (carbonation) were also studied. Finally, glasses that had been altered at the core were put back into solution in order to study specifically the solubility of the gels, independently of the presence of the underlying glass. An identical set of experiments was designed to test the reproducibility of the model. The gels formed during this study were composed of Si-Na-Al. The concentrations in solution were analysed by ICP-AES.

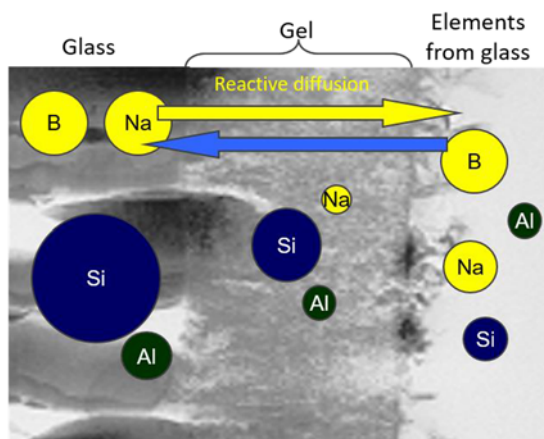
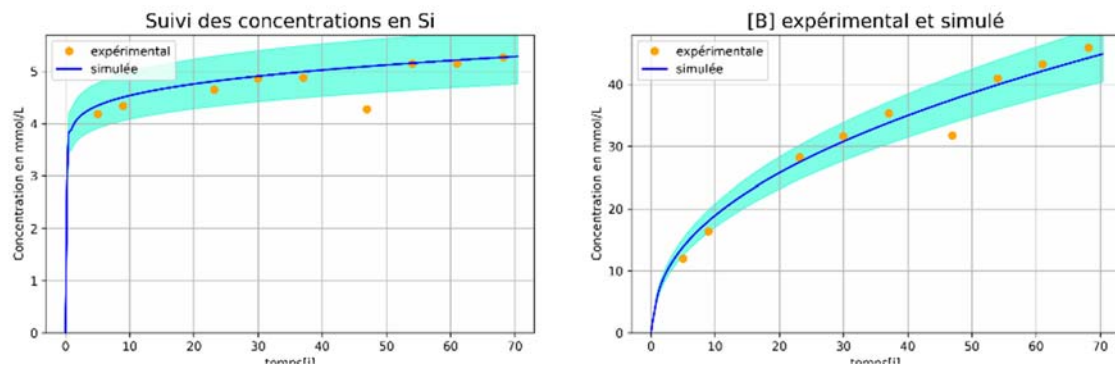


Figure 1 : Presentation of the working environment

The development of a modeling method makes it possible to determine the optimal parameters set for the modelling. The application of these parameters allows the prediction of altered glass, formed gel and precipitated secondary phase quantities. The model also provides information on the evolution of the solution composition over time. The results show that the model is able to reproduce rather accurately the experimental results, both in pure water and in ionic environments. The incorporation of this method in an automatic numerical tool allow the study of uncertainties through the multiplication of available modelling result. It is therefore possible to determine the parametric uncertainties based on the experimental uncertainties and consequently estimate the uncertainties on the results. Once the model has been optimally parameterised and the uncertainties quantified, it is possible to qualify the model in order to discuss its capacity to reflect the experiments as well as its limitations.



References

- [1] Frugier, P., Minet, Y., Rajmohan, N. et al (2018). Modeling glass corrosion with GRAAL. *npj Mater Degrad* 2, 35
- [2] Frugier, P., Gin, S., Minet, Y., Chave, T., Bonin, B. et al (2008). SON68 nuclear glass dissolution kinetics: Current state of knowledge and basis of the new GRAAL model. *Journal of Nuclear Materials*, Elsevier, 380 (1-3), pp.8-21.

C2-4 REACTIVE TRANSPORT MODELS OF LABORATORY CORROSION TESTS AT THE IRON/BENTONITE INTERFACE: FB4, FB5 AND FEMO TESTS

Javier Samper⁽¹⁾, Alba Mon⁽¹⁾, Luis Montenegro⁽¹⁾, Elena Torres⁽²⁾, María Jesús Turrero⁽²⁾, Jaime Cuevas⁽³⁾

(1) *Centro de Investigaciones Científicas Avanzadas (CICA). E.T.S.I. Caminos, Canales y Puertos. Universidad de A Coruña. Campus de Elviña, University of A Coruña, 15071 A Coruña.*

(2) *Centro de Investigaciones Energéticas, Medio Ambientales y Tecnológicas, Av. Complutense 40 - 28040 Madrid, Spain.*

(3) *Facultad de Ciencias, Universidad Autónoma de Madrid*

Carbon steel and compacted bentonite have been proposed as candidate materials for the overpack and buffer, respectively, in the multi-barrier system of deep geological repositories for high-level radioactive waste (HLW). The corrosion of the carbon steel may induce buffer alterations which could result in changes in bentonite parameters such as porosity, permeability, sorption and swelling. Here we present the numerical models of laboratory experiments performed by Ciemat on compacted FEBEX bentonite to study the interactions of iron-bentonite under repository conditions and analyze how such interactions affect the bentonite properties. The corrosion experiments include the FB4, FB5 and FeMo tests. The FB4 and FB5 column tests contain iron powder in contact with bentonite and simulates repository conditions through hydration from the bentonite and heating from the iron. It is focused on analysing corrosion products and to evaluate the potential alteration of bentonite at the contact. These experiments are the latest (7 and 13 years for the FB4 and FB5, respectively) in a series of 6 cells assembled in 2006 that have been dismantled sequentially to see the sequence of corrosion and how it affects bentonite properties [1,2,3]. The FeMo test contains steel sinters surrounded by iron powder emplaced in holes in contact with saturated bentonite at room temperature. It is focused on analyzing corrosion products and its mobility through the bentonite after 15 years of operation.

FB4 and FB5 tests have been modeled with a 1D coupled thermo-hydro-chemical-mechanical model which has been solved with INVERSE-FADES-CORE V2 [4,5]. A uniform liquid pressure of 600 kPa is adopted at the injection boundary. Hydrodynamic, thermal, and solute transport parameters were taken from those calibrated previously from a heating and hydration experiment [4]. The temperature at the bottom of the cell is fixed at 100°C. The FeMo test model has been performed with a 1D axisymmetric mesh by considering the sinter, the iron powder and the bentonite with the code CORE [4] under saturated conditions and at ambient temperature. The model used for FB4, FB5 and FeMo tests assumes a constant steel corrosion rate under anaerobic conditions. The corrosion products include magnetite, siderite, and goethite.

The model results for the FB4 and FB5 tests (Figure 1) indicate that: 1) Magnetite precipitates in the whole Fe powder, but only in a small amount in the first 2 mm into the bentonite near the bentonite-Fe powder interface which is consistent with some magnetite precipitation observed at the interface; 3) There is no precipitation of other iron corrosion products; and 4) Model results do not reproduce the precipitation of hematite and maghemite observed in the Fe powder near the bentonite-Fe interface. The model results of the FeMo tests (Figure 1) show that: 1) Magnetite precipitates in the whole Fe powder and sinter, but only in a small amount of magnetite precipitates (0.1 mm) into the bentonite-Fe powder interface; 2) calcite precipitates at bentonite-Fe interface; and 3) greenalite precipitates just at the interface.

The reactive transport model of the FB4, FB5 and FeMo tests could be improved by considering: 1) The early-stage aerobic corrosion stage in addition to anaerobic corrosion and considering and additional corrosion products such as hematite, maghemite, lepidocrocite, akageneite and Fe-phyllsilicates

(greenalite and cronstedtite); 2) A kinetically-controlled magnetite precipitation rate; 3) Kinetically-controlled dissolution of smectite; 4) The changes in porosity, permeability and diffusion coefficients caused by mineral dissolution/precipitation reactions; and 5) A more detailed geometry with a 2D axisymmetric vertical model in the case of the FeMo test.

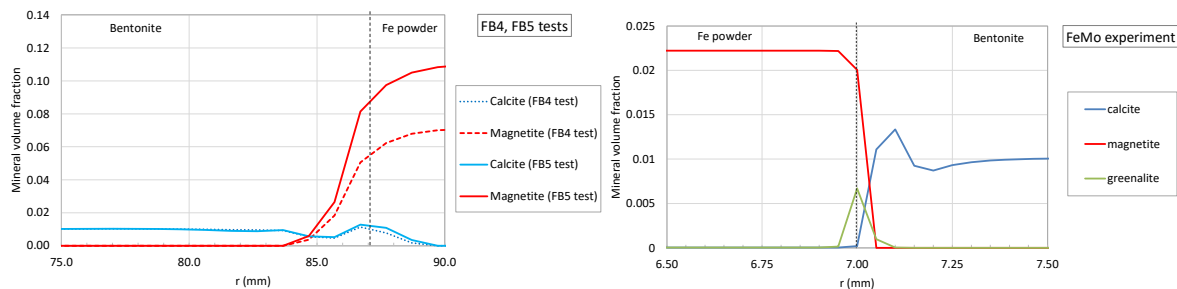


Figure 1. Spatial distribution of the mineral volume fractions at the end of FB4 and FB5 tests (left) and FeMo test (right).

Acknowledgments: The research leading to these results was funded by ENRESA through a Research Contract within the Work Package ACED of EURAD (European Joint Programme on Radioactive Waste Management of the European Union). The work was partly funded also by the Spanish Ministry of Science and Innovation (Project PID2019-109544RB100) and the Galician Regional Government (Grant number ED431C2021/54 from “Consolidación e estruturación de unidades de investigación competitivas”).

References

- [1] Torres, E., 2011. Geochemical processes at the C-steel / bentonite interface in a deep geological repository: experimental approach and modeling. Ph.D. thesis, Universidad Complutense de Madrid.
- [2] Torres, E., Turrero, M.J. and Escribano, A., 2013. Synthesis of corrosion phenomena at the iron/bentonite interface under unsaturated conditions. Technical Note CIEMAT/DMA/2G210/02/2013. PEBS Project.
- [3] Mon, A, J. Samper & L Montenegro, E Torres, MJ Turrero, E Torres, J Cuevas, R Fernández & L De Windt. 2023, Reactive transport models of geochemical interactions at the iron/bentonite interface in laboratory corrosion tests, Applied Clay Science (submitted).
- [4] Mon, A. (2017). Coupled thermo-hydro-chemical-mechanical models for the bentonite barrier in a radioactive waste repository. Ph. D. Dissertation. University of A Coruña, Spain.
- [5] Zheng, L., Samper, J., Montenegro, L. and Fernández, A.M. (2010). A coupled model of heating and hydration laboratory experiment in unsaturated compacted FEBEX bentonite. Journal of Hydrology 386, 80-94.

A7-1 RADIONUCLIDE DISTRIBUTIONS IN (TIME-RESOLVED) NATURAL ARCHIVES DETERMINED BY AMS

K Hain(1), S. Adler(1), A. Cundy(2), T. Faestermann(3), K. Fenclová(4), K. Fifield(5), F. Gülce(1), G. Korschinek(3), M. Martschini(1), S. Pavetich(5), J. Pitters(1), G. Rugel(6), P. Steier(1), S. Tims(5), S. Turner(7), J. Wolf(1,6), J. Zinke(8)

(1) *University of Vienna, Faculty of Physics, Austria*

(2) *University of Southampton, School of Ocean and Earth Science, United Kingdom*

(3) *Technical University of Munich, Physics Department, Germany*

(4) *Czech Technical University in Prague, Department of Nuclear Chemistry, Czech Republic*

(5) *Australian National University, Department of Nuclear Physics and Accelerator Applications, Australia*

(6) *Helmholtz-Zentrum Dresden-Rossendorf, Germany*

(7) *University College London, Department of Geography, United Kingdom*

(8) *University of Leicester, School of Geography Geology and The Environment, United Kingdom*

Accelerator Mass Spectrometry (AMS) has proven to be a powerful technique for the detection of long-lived anthropogenic radionuclides with highest sensitivity, in particular for several nuclides of the actinide series, e.g., ^{236}U , ^{237}Np , $^{239,240}\text{Pu}$, ^{241}Am . Analyzing the environmental distribution of radionuclides deposited on the global surface by nuclear weapons testing using AMS allows for the study of their migration behavior under real environmental physico-chemical conditions. Time resolved archives such as coral or sediment cores are particularly interesting as a shift of the so-called bomb peak with respect to the original bomb peak in 1963 indicates post-depositional radionuclide migration [1]. As absolute dating of the cores can be rather challenging, information on the differences in migration behavior can be most easily obtained by analyzing several radionuclides and comparing the resulting profiles. Isotope ratios help to identify contributions from emission sources other than nuclear weapons fallout, like for example the recently proposed $^{233}\text{U}/^{236}\text{U}$ signature for emissions from nuclear industry [2].

The AMS setup at the Vienna Environmental Research Accelerator (VERA) laboratory offers the opportunity to analyze long-lived actinides at high detection efficiency while achieving an outstanding suppression of neighboring masses [3]. This instrumentation enabled us to study the actinides mentioned above in parallel in a variety of natural archives with different chemical conditions including urban and lake sediments, peat bog and coral cores as well as water columns. In the case of the coral samples, where the macroscopic matrix can be fully dissolved, a chemical separation of the elements was not even required [4,5]. In that way, a quantitative ^{237}Np profile in a coral core could be obtained for the first time. When comparing this profile with those of ^{239}Pu and $^{236}\text{U}/^{238}\text{U}$, the conservative behavior of ^{237}Np in ocean water becomes clearly visible. The data indicate that Np is present as a carbonate complex in seawater since Np seems to be similarly well incorporated into the coral skeleton as U. This presentation will focus on the results obtained from a coral core collected at Flinders reef (Coral Sea, Australia) spanning the time range from 1900 to 2015, which will be compared to the corresponding distributions in a lake sediment (lake Hallstatt, Austria) and a peat bog core (Pürgschachen Mire, Austria).

Also, the migration behavior of the long-lived fission product ^{99}Tc under environmental conditions is still poorly studied. This is because quantitative analysis by mass spectrometry remains challenging due to the interfering background induced by stable isobars, i.e. ^{99}Ru in the case of ^{99}Tc detection.

Sufficiently high sensitivities for ^{99}Tc detection in environmental samples, i.e. $< 10^7$ atoms per sample, have so far only been achieved by few facilities providing high beam energies such as the tandem laboratory of the Maier-Leibnitz-Laboratory in Munich [6]. With this setup, the sample volume required to analyze ^{99}Tc concentration in water samples from the Northeast Pacific Ocean was reduced to 10 liters. The activity concentrations at a sampling station located about 250 km off the Japanese coast

varied between 0.5 and 1.0 uBq/L. For a second water column collected east of the southern tip of Kamchatka, however, only upper limits could be obtained for most of the samples during the limited beam time available at the Munich tandem accelerator before its decommissioning. The approach of high-energy AMS is being developed further in collaboration with our colleagues of the Australian National University (ANU). In addition to the discussion of the first results on the ocean water and peat bog samples obtained with high energy AMS, the current status of ^{99}Tc analysis using the new technique of Ion-Laser-Interaction Mass Spectrometry (ILIAMS) at VERA will be reported. A ^{99}Ru suppression factor of 10^5 was achieved with this method allowing a first application to ^{99}Tc detection in a peat bog sample (see Figure 1). Issues with normalization and detection efficiency remain to be solved.

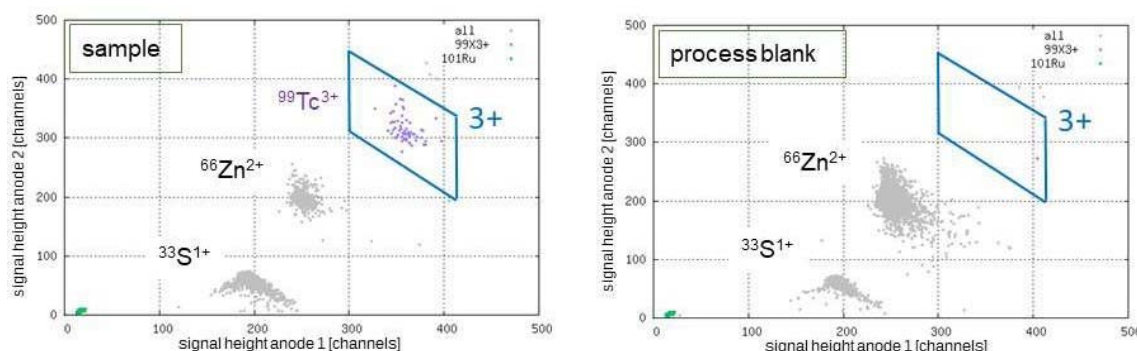


Figure 1: Spectra for an environmental sample (Rotmoos, surface water) and its corresponding process blank obtained with ILIAMS.

Acknowledgement: The work on ^{99}Tc received funding from the Austrian Science Fund (FWF): P 31614-N28. The authors thank M. Yamada (Marine Ecology Research Institute, Japan) for providing the Pacific Ocean water samples.

References

- [1] Quinto, F., Hrnccek, E., Krachler, M., et al. (2013). Determination of ^{239}Pu , ^{240}Pu , ^{241}Pu and ^{242}Pu at femtogram and attogram levels - evidence for the migration of fallout plutonium in an ombrotrophic peat bog profile. *Environ. Sci.: Process. Impacts* 15, 839–847.
- [2] Hain, K., Steier, P., Froehlich, M. B., et al. (2020). $^{233}\text{U}/^{236}\text{U}$ signature allows to distinguish environmental emissions of civil nuclear industry from weapons fallout. *Nat. Commun.* 11:1275.
- [3] Steier, P., Hain, K., Klötzli, U., et al. (2019). The actinide beamline at VERA. *Nucl. Instrum. Meth. in Phys. Res. B* 458, 82–89.
- [4] Quinto, F., Golser, R., Lagos, M. et al. (2015). Accelerator Mass Spectrometry of Actinides in Ground- and Seawater: An Innovative Method Allowing for the Simultaneous Analysis of U, Np, Pu, Am, and Cm Isotopes below ppq Levels. *Anal. Chem.* 87:5766-5773.
- [5] Nomura, T., Sakaguchi, A., Steier, P. et al. (2017). Reconstruction of the temporal distribution of $^{236}\text{U}/^{238}\text{U}$ in the northwest Pacific Ocean using a coral core sample from the Kuroshio Current area. *Mar. Chem.* 190, 28–34.
- [6] Quinto, F., Busser, C., Faestermann, T., et al. (2019). Ultratrace determination of ^{99}Tc in small natural water samples by accelerator mass spectrometry with the gas-filled analyzing magnet system. *Anal. Chem.* 91, 4585–4591

A7-2 ON THE TRACE (LEVEL) OF A HIGH LEVEL NUCLEAR WASTE DISPOSAL - METHOD DEVELOPMENT FOR MIGRATION EXPERIMENTS USING HPLC, ICP-MS AND LA-ICP-MS

Aaron Haben⁽¹⁾, Kristina Brix⁽¹⁾, Ralf Kautenburger⁽¹⁾

(1) WASTE group, Inorganic Solid-State Chemistry, Saarland University, Germany

The development of a repository for high level nuclear waste (HLW) in deep geological formations is a very important task for the future. The long-term safety assessment for more than hundred thousand years needs a full knowledge of all processes of interaction between the radioactive waste and the surrounding host rock formations as natural barrier but also the interaction with the engineered barriers. A wide set of geochemical parameters can influence the migration of radionuclides. For example, natural organic matter (NOM) as complexing agents or the chemical composition, pH-milieu and temperature of the deep geological aquifer. In addition, an intrusion of pore water into the repository leads to a release of competing ions from, for example, C-S-H (calcium silicate hydrate) phases, a main component of hydrated cement, or clay materials [1, 2].

To investigate the retention behaviour of radionuclides on the natural and technical barriers, batch experiments with subsequent measurements by mass spectrometry with inductively coupled plasma (ICP-MS) are predominantly used. In order to realise the geochemical conditions naturally occurring in a repository (such as those prevailing in northern Germany), the batch experiments must also be carried out with highly saline (>1 M ionic strength) and hyperalkaline (pH 12-13) electrolytes (caused by the dissolution of clay and cement concrete in the presence of water). To prevent possible damage to the ICP-MS system, environmental samples with a total dissolved salt content of >1% are usually diluted several times, but this can reduce the analyte concentration below the respective limits of detection (LOD). By the application of the developed transient ICP-MS measurement method a quantification of all elements in samples with high salinity (up to 5 M NaCl) without any complex sample preparation is realized using only 3- or 10-fold dilution. This transient method enables the determination of the classical static distribution coefficients (K_D or R_D values) even in highly saline and hyperalkaline background electrolytes [3].

Batch experiments are high-throughput methods but are not realistic because of stationary equilibrium and very low solid-liquid ratios. Therefore, a newly developed high performance/throughput liquid chromatography (HPLC) method with mini columns has emerged as a promising alternative. Those mini-column experiments (MCE) are less time consuming, need less material and enable the visualization of dynamic sorption and desorption processes of the waste cocktail elements used (such as U(VI), Mo(VI), Eu(III), Pd(II), Cs(I)) on clay or C-S-H phases, which is therefore closer to nature [4].

In the MCE, HPLC guard columns are filled with the adsorption material and the analyte is injected several times into the eluent using an autosampler. In all experiments, the retention behavior of the waste-cocktail elements is quantified using ICP-MS, whereby a possible LC-ICP-MS coupling holds great potential for optimising the sorption experiments. In the method currently used, the eluate is either collected with a fraction collector or fed directly into the ICP-MS (LC-ICP-MS-coupling). The experimental setup for both quantification methods is shown schematically in Figure 1. By using the MCE, maximum loading capacities can be determined, from which dynamic distribution coefficients can then be derived which can be used for geochemical modelling. This can provide a more realistic prediction for the retention of the metals on clay or other repository-relevant materials.

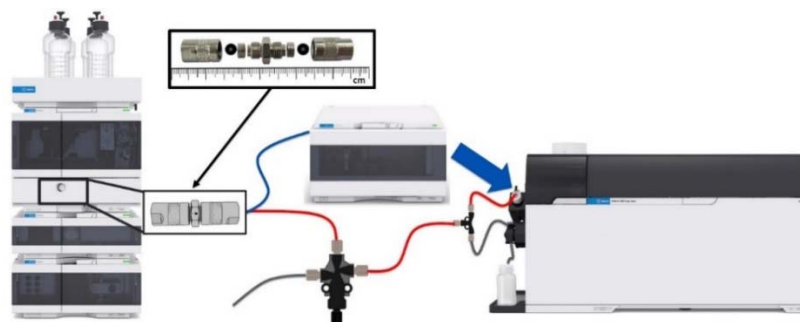


Figure 1: Schematic experimental set-up of the mini-column sorption experiments (MCE) with quantification by fraction collector and later ICP-MS measurement (blue) or quantification by LC-ICP-QQQ-coupling (red).

Figure 2 shows the breakthrough curves (BTC), the corresponding Thomas fits, the maximal loading capacities (q_{\max}) and the Thomas constants (K_{TH}) for two different MCE. One was performed with Cs(I) on C-S-H phases in 10 mM NaCl using the quantification via fraction collector (Figure 2 (a)) and the other one with Eu(III) on 10/90 w% kaolinite/sand-mixture in 10 mM NaCl using quantification via LC-ICP-QQQ-coupling (Figure 2 (b)).

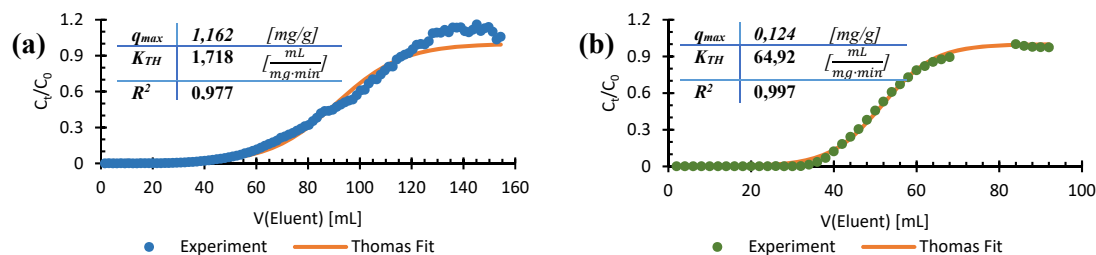


Figure 2: (a) BTC and Thomas fit resulting from MCE using fraction collector with Cs(I) on C-S-H phases. (b) BTC and Thomas fit resulting from MCE using LC-ICP-QQQ-coupling with Eu(III) on 30/70 w% kaolinite/sand mixture.

In both, batch experiments and MCEs, the analytes are determined in solution. In addition to this, further investigations of the adsorption material used are also of great interest. For this purpose, a method for solid analysis by means of LA-ICP-MS (laser ablation-ICP-MS) is in progress, whereby the analyte content on the adsorbent is to be determined subsequently to the respective sorption experiments.

Acknowledgements: We would like to thank the Federal Ministry for the Environment, Nature Conservation, Nuclear Safety and Consumer Protection (BMUV), represented by the Project Management Agency Karlsruhe (PTKA-WTE) for funding (projects 02E11415D and 02E11860D).

References

- [1] Baur, S., Brix, K., Feuerstein, A., Janka, O. and R. Kautenburger (2022). Retention of waste cocktail elements onto characterised calcium silicate hydrate (C-S-H) phases: A kinetic study under highly saline and hyperalkaline conditions, *Appl. Geochem.* 143: 105319
- [2] Brix, K., Baur, S., Haben, A. and R. Kautenburger (2021). Building the bridge between U(VI) and Ca-bentonite - Influence of concentration, ionic strength, pH, clay composition and competing ions. *Chemosphere* 285: 131445.
- [3] Hein, C., Sander, J.M. and R. Kautenburger (2017). New Approach of a transient ICP-MS measurement method for samples with high salinity. *Talanta* 164: 477-482.
- [4] Kautenburger, R., Brix, K., Baur, S. and J. M. Sander (2022). Development of mini column experiments (MCE) by coupling microliter flow HPLC with ICP-MS for the analysis of metal retention under conditions close to nature. *Talanta Open* 5: 100111.

A7-3 MULTI-TECHNIQUE ANALYSIS OF THE BEHAVIOR OF URANIUM IN NATURAL SOIL

BAYLE Simon (1,2,3) *, CRANCON Pierre (1), SOLARI Pier-Lorenzo (2), DEN AUWER Christophe (3),

(1) CEA, DAM, DIF, F-92297 Arpajon, France

(2) Université Côte d'Azur, CNRS, Institut de Chimie de Nice, 06100 Nice, France

(3) Synchrotron SOLEIL, Saint-Aubin, F-91192 Gif-sur-Yvette, France

* now at ICSM, CEA, Univ Montpellier, CNRS, ENSCM, Bagnols sur Cèze, France

The context of this work is to investigate the speciation and behavior of anthropogenic metallic uranium dispersed on a natural chalky soil. A multitechnique approach combining X ray spectroscopic techniques performed at the SOLEIL synchrotron, such as EXAFS (Extended X-ray Absorption Fine Structure), XANES (X-ray Absorption Near Edge Structure), micro-XRF mapping (X-ray Fluorescence), and more conventional techniques such as TRLFS (Time-Resolved Laser induced Spectrofluorimetry), was implemented. The evolution of the chemical form of originally metallic uranium could be investigated using field samples, as a function of depth below the subsurface of the studied site. The linear combination of EXAFS spectra obtained from samples collected at different depths proved to be a powerful tool for data analysis. The speciation of uranium at present time (an uranyl oxo-hydroxo) was observed in the first tens of centimeters below the surface. It is gradually replaced by an organic matter- uranium complex in the top soil section of the site. This form, in turn, decreases to a tri-carbonate form in the substrate section, which is composed of approximately 98% calcite. Ultimately, a strong correlation was established between the evolution of uranium speciation, its concentration profile, and the chemical and mineralogical composition of the soil and substrate of the site, suggesting the relevance of the selected analytical approach (see Figure 1).

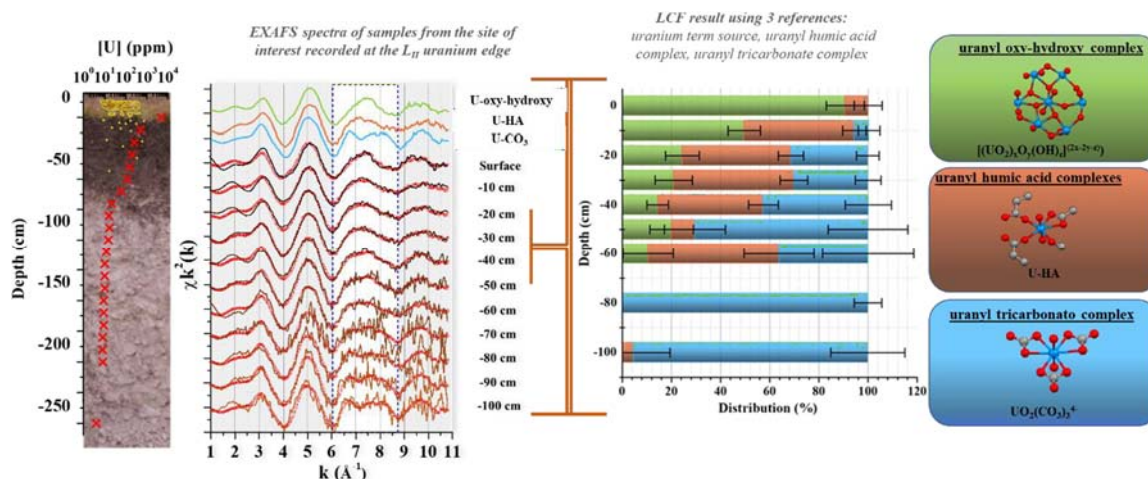


Figure 1: *On the left:* photograph of the soil and substrate profile with total uranium concentration (red cross) as a function of depth. *Second graph:* EXAFS spectra of references (green, brown, and blue for respectively uranyl oxo-hydroxo, U-HA complex, and uranyl tricarbonate). Experimental data from samples collected at different depths are plotted in black, and the results from the linear combination fitting of the three references are shown in red. *The third graph* shows the respective content evolution of the three references used, and on the far right, the chemical environment of uranium in each of these compounds is represented.

In addition to field studies, laboratory experiments were conducted to improve our understanding of the migration behavior of uranium. To do this, model columns consisting of an uranium source term and a stationary phase were leached for several months. Our results show the impact of humic acids on the behavior of uranium. In the presence of organic matter in the leaching water, it was shown to strongly interact with the uranium source term. When present in the column matrix, significant diffusion

phenomena were observed, correlated with a reduction in uranium. Taken together, these isotropic migration phenomena coupled with uranium reduction in the form of uraninite-like phase open up new hypothesis for the understanding of anthropogenic uranium behavior in natural soils (see Figure 2).

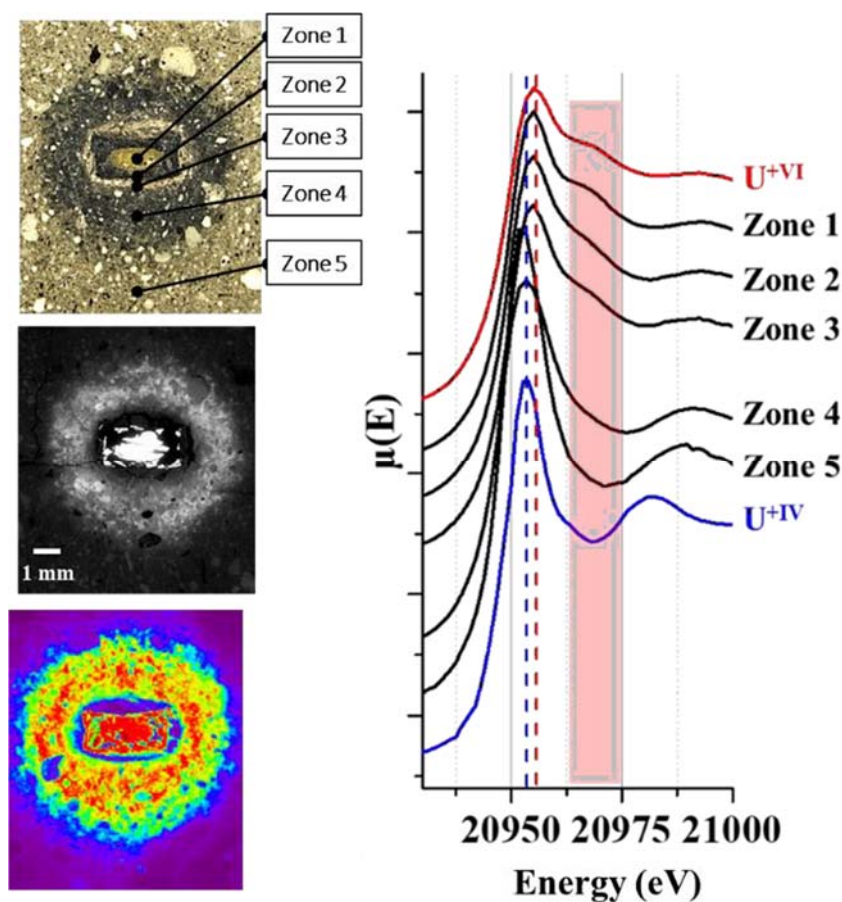


Figure 2: *On the top left:* Photograph of the longitudinal section of a metaschoepite pellet (a uranyl oxo-hydroxo) positioned in a soil column that was leached for 6 months.

In the middle: SEM imaging of the same sample using backscattered electron mode (bright areas are electron-dense).

At the bottom: X-ray fluorescence imaging performed at the LII threshold (20,948 eV) of uranium.

On the right: XANES spectra performed at the LII threshold of uranium from the 5 regions of interest (in black) located on the photograph. In comparison, two uranium references at the oxidation state of +IV and +VI were added to the graph (in blue and red, respectively).

This work also necessitated the development of X-ray fluorescence mapping on the MARS beamline at the SOLEIL synchrotron. Furthermore, approaches such as XANES mapping, open up numerous possibilities for field samples, particularly on systems with spatial variations.

A7-4 INVESTIGATING GEOCHEMICAL INTERACTIONS OF PLUTONIUM WITH OPALINUS CLAY AND HARDENED CEMENT PASTE VIA TOF-SIMS AND RL-SNMS

Felix Berg, Markus Breckheimer, Tobias Reich

Johannes Gutenberg-Universität Mainz, Department of Chemistry, Nuclear Chemistry, 55099 Mainz, Germany

The safety case for a deep geological long-term nuclear waste repository requires extensive knowledge about the interactions of the radioactive inventory with the (geo-)technical and geological barriers. The plutonium isotope ^{239}Pu with its long half-life, high radiotoxicity and complex aqueous chemistry is thereby of major concern when planning the safekeeping of high-level radioactive waste (HLW) for 1 million years according to current plans in Germany [1]. Therefore, it is vital to study the geochemical interactions of plutonium with materials considered for a long-term nuclear waste repository and assess their capability to retain possibly mobilized Pu species.

Next to crystalline and salt rock, argillaceous rock is considered as a potential host rock system for a deep geological repository. Here, Opalinus Clay (OPA) from the Mont Terri rock laboratory (St-Ursanne, Switzerland) with its extensive compositional and structural heterogeneities has already been studied as a reference material in batch sorption and bulk diffusion studies with plutonium [2,3]. Similarly, hardened cement paste (HCP), a heterogenous material as well, has been under investigation for its chemical interactions with plutonium in analogous experiments [4,5]. Unfortunately, due to the nature of batch sorption experiments or the abrasive peeling necessary to gain access to the diffusion profile in diffusion studies, any information about the microstructure of the host system and its role in the transport of the radionuclide is lost and only averaged parameters for transport and retention are retrieved. In addition, the samples are usually destroyed in the process and can no longer be investigated via different methods. Therefore, in order to gain further insights into the interactions between radionuclides and the microstructure of OPA and HCP, a spatially resolved approach would be favorable.

Time-of-flight secondary ion mass spectrometry (TOF-SIMS) allows for spatially resolved studies of surfaces at the micrometer or even nanometer scale by scanning a primary ion beam over a sample and retrieving a full mass spectrum for every pixel. Through comparison of the relative intensities for various masses detected, the composition of the surface is accessible and the distribution of an element or a chemical species on the surface can be analyzed. One intrinsic challenge of TOF-SIMS, especially regarding the low concentrations of plutonium expected under the conditions in the far field of a deep geological repository, is the possibility of isobaric interferences. A method addressing this issue is resonance ionization mass spectrometry (RIMS) [6]. In RIMS atoms are ionized utilizing multi-step photoionization via laser which is element selective and results in excellent background suppression. By combining TOF-SIMS with RIMS to resonant laser secondary neutral mass spectrometry (rL-SNMS), isobaric interferences can be suppressed, and the analyte signal isolated [7-9].

In our presentation we will demonstrate the current development state of the combined approach of TOF-SIMS and rL-SNMS for the study of sorption and diffusion samples of OPA and HCP with plutonium on the micrometer scale and assess the capabilities and limitations of both methods. The rL-SNMS setup consists of a TOF-SIMS III (IONTOF, Germany) and three Ti:Sa lasers jointly pumped by a Nd:YAG laser [8]. Experiments were conducted using samples of HCP and OPA under aerobic and anaerobic conditions with $^{239}\text{Pu(IV/V)}$ concentrations from 10^{-5} to 10^{-9} M in either artificial cement pore water or OPA pore water, respectively. In addition, the influence of the pore water composition on the surface was investigated by scanning electron microscopy. We will address a more tailored approach to sample preparation as well as present improvements over previous experiments [8].

Acknowledgements: Funding from the German Federal Ministry of Education and Research (BMBF) under contract number 02NUK044B and 02NUK075B, as well as from the European Union's Horizon 2020 project EURAD (WP FUTuRE), EC Grant agreement no. 847593, is acknowledged.

References

- [1] Gesetz zur Suche und Auswahl eines Standortes für ein Endlager für hochradioaktive Abfälle (Standortauswahlgesetz - StandAG) (2017)
- [2] Amayri, S., Fröhlich, D.R., Kaplan, U., Trautmann, N. and Reich, T. (2016). Distribution coefficients for the sorption of Th, U, Np, Pu, and Am on Opalinus Clay. *Radiochim. Acta* 104(1): 33- 40
- [3] Kaplan, U., Amayri, S., Drebert, J., Rossberg, A., Grolimund, D. and Reich, T. (2017). Geochemical Interactions of Plutonium with Opalinus Clay Studied by Spatially Resolved Synchrotron Radiation Techniques. *Environ. Sci. Technol.* 51: 7892-7902
- [4] Wieland, E. and Van Loon, L. R. Cementitious Near-Field Sorption Data Base for Performance Assessment of an ILW Repository in Opalinus Clay. PSI Bericht Nr. 03-06, Nagra NTB 02-20
- [5] Tasi, A., Gaona, X., Rabung, Th., Fellhauer, D., Rothe, J., Dardenne, K., Lützenkirchen, J., Grivé, M., Colàs, E., Bruno, J., Källstrom, K., Altmaier, M. and Geckeis, H. (2021) Plutonium retention in the isosaccharinate – cement system. *Appl. Geochem.* 126: 104862
- [6] Grüning, C. Huber, G. Klopp, P., Kratz, J.V., Kunz, P., Passler, G., Trautmann, N., Waldek, A. and Wendt, K. (2004). Resonance ionization mass spectrometry for ultratrace analysis of plutonium with a new solid state laser system. *Int. J. Mass Spectrom.* 235: 171-778
- [7] Franzmann, M., Bosco, H., Hamann, L., Walther, C. and Wendt, K. (2018). Resonant laser-SNMS for spatially resolved and element selective ultra-trace analysis of radionuclides. *J. Anal. At. Spectrom.* 33: 730-737
- [8] Schönenbach, D., Berg, F., Breckheimer, M., Hagenlocher, D., Schönberg, P., Haas, R., Amayri, S. and Reich, T. (2021). Development, characterization, and first application of a resonant laser secondary neutral mass spectrometry setup for the research of plutonium in the context of long-term nuclear waste storage. *Anal. Bioanal. Chem.* 413: 3987-3997
- [9] Raiwa, M., Kneip, N., Walther, C. and Wendt, K. (2023). Dem Kernbrennstoff auf der Spur. *Phys. unserer Zeit.* 54: 24-29

A1-1 SAFETY AND SCIENCE: THE FRAGILE CONNECTION – PART II

Rodney C. Ewing ⁽¹⁾, Bernd Grambow ⁽²⁾

(1) *Center for International Security & Cooperation, Stanford University, USA*

(2) *SUBATECH, IMT Atlantique, CNRS, Nantes, University, France*

“ . . . to shake all cares and business from our age/Conferring them on younger strengths, while
we/Unburdened crawl toward death.”

King Lear

This presentation is the second of a series of reflections of the relation of science to safety in geologic disposal of radioactive waste. The first was presented at *Key Topics of Deep Geological Disposal*, held in 2022 [1]. The basic thesis of these presentations is that, despite decades of research at a huge cost, the field of radioactive waste management and disposal has not, by and large, capitalized on this research in the development of a basic understanding of the key issues that dominate the safety case. In fact, as described in the first presentation, there is a tension between the science of near-field processes and performance assessments. Here, we review spent nuclear fuel and HLW-glass, as these two waste forms have received considerable attention during the past decades. Still, quantitative safety analyses have led some to posit that the performance of these waste forms is of little consequence.

The first issue is to answer the question: Has progress been made in the understanding of the performance of SNF and HLW-glass in a geologic repository? The answer is emphatically: Yes! This is evident in the comparison of the present state-of-knowledge with the review chapters on HLW-glass and spent nuclear fuel in *Nuclear Waste Forms for the Future* published in 1988 [2].

Thirty-five years later, key advances in the understanding of spent fuel corrosion include:

- Quantification of the instant release fraction for safety relevant nuclides as a function of burnup and fuel type [3].
- Recognition of the importance of reducing geochemical conditions.
- Understanding the role of hydrogen for assuring very low solubility of the fuel matrix in water; thus, supporting long-term stability of spent fuel in a repository [4].
- Recognition of the limited importance of temperature and hyperalkaline conditions on spent fuel performance. [5]

Key advances in the understanding of HLW-glass performance include:

- Identification of saturation effects in water of dissolved glass constituents and understanding of glass performance as a function of the geometry and water exchange rates in the disposal setting [6].
- Ability to predict the formation of secondary phases formed upon glass corrosion, fixing a large quantity of initially released and dissolved radionuclides.
- Appreciation of the large differences in glass behavior for different glass compositions.

There was also considerable progress in the use of natural systems of geologic age to provide both quantitative data for long term extrapolations of the behavior of waste forms in a geologic repository and qualitative data for the long-term safety case.

- Experimental results and observations from natural systems, such as the Oklo natural reactors, have been used to assess the long-term performance of SNF and fission product release over billions of years.
- Confirmation, using basaltic glasses formed in the ocean, of the low glass dissolution rates in confined spaces as has also been observed in laboratory experiments.

Despite this progress, waste forms still play a limited role in safety analyses and the arguments for long-term performance are mainly used for public relations rather than their scientific value. The research results on these two important waste forms, when being used in safety analyses typically show that the waste forms are not the key barrier to protecting the future environment, having only a limited impact on the calculated final dose from a repository in the long-term (100,000s to millions of years).

There is also the issue of the multi-barrier concept, closely tied to the use of multiple lines of evidence in support of safety. Even if the waste form is not the key barrier, its stability can provide important redundant evidence in support of safety claims and thus confidence in the disposal system. Confidence in safety analysis cannot be increased by increasing the calculated safety margins (relative to the legal dose threshold) of the repository system from a factor 100 to a factor 10,000 in the long-term, but redundancy does increase confidence. Specifically, "safety" as seen through the eyes of safety analysts, has become a numbers-game, for which calculated results (*e.g.*, dose to future populations), as they get lower and lower, are taken as evidence for "improving" safety. However, the physical meaning and societal significance of the resulting numbers are probably not even understood by those who do the calculations. As "safety" is a term that involves "feeling safe" we need to provide additional lines of evidence of safety. The goal should be to develop waste form research as "another line of evidence" as a complementary safety argument. When considering the role of the waste form, the question should not be: How much does it contribute to overall safety? Rather, we should be able to use safety analyses as a tool for identifying key factors in glass performance (like IRF of mobile radionuclides) and other factors of only little importance (*e.g.*, initial glass dissolution rate in large volumes of water). Unless we can reinvigorate the role of waste forms in containing radionuclides in the near-field, then waste disposal will rely mainly on dilution and sorption processes in the far-field to meet regulatory requirements, and major variations in waste form properties will be considered as of little significance for repository safety.

References

- [1] Bernd Grambow and Rodney C. Ewing (2022). Safety and Science: The Fragile Connection. abstract volume of 3rd Conference on Key Topics of Deep Geological Disposal, Cologne, Germany, July 5th, 2022.
- [2] W. Lutze and Rodney C. Ewing [Editors] (1988) Radioactive Waste Forms for the Future. North-Holland Physics Publishing, Amsterdam, Netherlands.
- [3] K. Lemmens *et al.* Instant release of fission products in leaching experiments with high burnup nuclear fuels in the framework of the Euratom project FIRST- Nuclides, K. Lemmens *et al.* (2017) Journal of Nuclear Materials 484, 307-323
- [4] P. Carbol, P. Fors, T. Gouder and K. Spahiu (2009) Hydrogen suppresses UO₂ corrosion. Geochimica et Cosmochimica Acta 73, 4366–4375.
- [5] Karel Lemmens, Christelle Cachoir and Thierry Mennecart (2019) Dissolution behaviour of spent nuclear fuel at highly alkaline conditions - Phenomenological Synthesis Report SCK•CEN/27622175.
- [6] B. Grambow (2006) Nuclear waste glasses – How durable? Elements, 2, 357-364.

A1-2 SPENT NUCLEAR FUEL IN CLOSED GLASS AMPOULES: RADIOLYSIS AND RADIONUCLIDE RELEASE AFTER ONE AND FIVE YEARS

Lena Z Evins⁽¹⁾, Charlotta Askeljung^(2,3), Kyle Johnson⁽²⁾, Anders Puranen⁽³⁾, Alexandre Barreiro Fidalgo⁽²⁾, Olivia Roth⁽¹⁾, Kastriot Spahiu⁽¹⁾

(1) SKB, Sweden

(2) Studsvik Nuclear AB, Sweden

(3) AB SVAFO, Sweden

Radiation from spent nuclear fuel affects the redox chemistry of water in the proximity of the fuel surface. Leaching experiments performed in open vessels, in contact with air, show that the overall effect of the radiolysis is oxidizing so that U(IV) in the spent nuclear fuel is oxidized to U(VI). Since dissolution of U(VI) is relatively fast in bicarbonate-containing solutions, radiolytic oxidation is considered the main driving force for spent fuel dissolution and radionuclide release in a spent fuel repository environment. Many studies over the years have aimed to further our understanding of this process and how it is influenced by available redox active components in open and closed systems. In an experimental program that was carried out ca 20 years ago [1], spent fuel fragments were leached in sealed glass ampoules for ca 900 days. The gas and water compositions were measured at various intervals and it was observed that between ca 400 and 900 days, the oxygen and hydrogen concentrations were constant. Radionuclides including U, Pu and Cs also display stable concentrations indicating that steady state was achieved after ca 400 days in these closed systems. A first attempt to model the kinetics of fuel dissolution using the experimental data did not reach satisfactory results (see Appendix in [1]), however, later the data could be modelled by taking surface mediated processes into account [2].

In 2016 a second, similar, experimental program, was initiated, results of which are presented here. Spent nuclear fuel fragments were placed in sealed glass ampoules in a low oxygen Ar atmosphere and leached in bicarbonate solutions. In some ampoules Fe-containing materials were included. The experimental plan included sampling after ca one year, five years and ten years of leaching. The current contribution concerns results from the one- and five-year long experiments. The results from the fuel ampoules with no Fe-materials are comparable to the results from the previous experiments: a steady state with regards to oxygen (Fig 1) and hydrogen composition is observed, with similar concentrations reached. Measured radionuclide concentrations are on similar levels or lower. The results support the hypothesis of catalytic recombination of radiolytically produced oxygen and hydrogen on the surface of the fuel after ca one year. In ampoules with Fe-materials the chemistry is significantly changed. The presence of Fe lowers the oxygen more than one order of magnitude, while hydrogen concentration is higher. The radionuclide concentrations are difficult to interpret due to some experimental complications, however, presence of Fe-materials lowers the concentration of some redox sensitive radionuclides such as U, Np and Tc, over time.

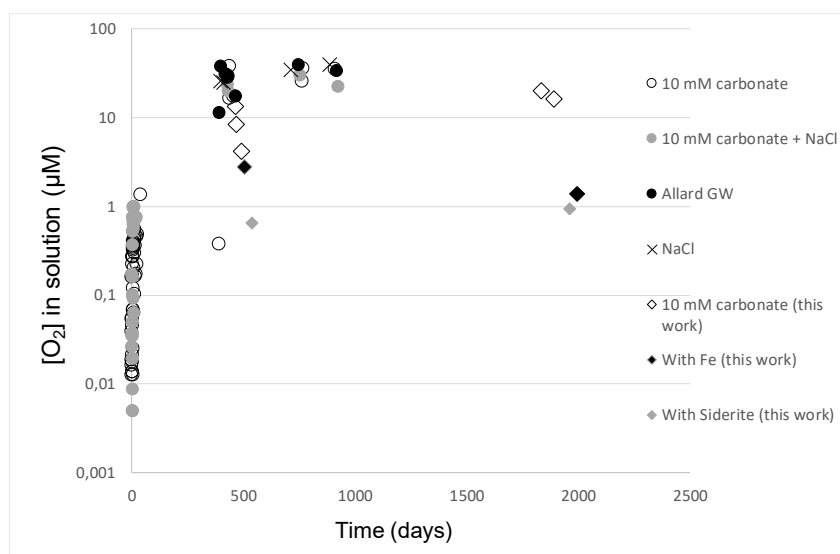


Figure 1. Oxygen concentrations in solution in glass ampoules. Previously published data [1] and data from the current contribution. Allard GW = synthetic groundwater.

The Fe powder and siderite were analysed using XRD. The results show that siderite, which originally contained ca 8% Fe(III)oxide, after leaching contained ca 8% Fe(III)hydroxide carbonate hydrate ($[\text{Fe}^{\text{II}}_4\text{Fe}^{\text{III}}_2(\text{OH})_{12}]^{2+}[\text{CO}_3, 3\text{H}_2\text{O}]^{2-}$). The Fe powder showed higher degree of alteration, containing ca 30% Chukanovite ($\text{Fe}^{\text{II}}_2(\text{CO}_3)(\text{OH})_2$). The phases are identified with high confidence, but note that the relative amounts are quite uncertain. Chukanovite has been observed as a corrosion product also in experiments involving aqueous solutions mimicking Callovo-Oxfordian groundwater [3].

Using the calculated radionuclide inventory in the fuel samples, the fraction of radionuclides released during leaching can be assessed. This fraction will be found in the water and sorbed on glass and Fe-materials. A significant result which remains unexplained is the thus calculated fraction of radionuclides that are found in the Fe-powder. The results need further analysis before any conclusion can be drawn.

This experimental program has provided important insights into the behavior of spent fuel in closed simplified systems. It has confirmed that steady state can be achieved for and maintained for ca 5 years, during which ~0.0035 % of the U has been released to the solution. Increasing the complexity of the chemical system, in this case via Fe materials with high surface area, has been seen to significantly change the chemistry. However, also in this case the radiolytic gases appear to stabilize and remain at concentrations established after ca one year.

References

- [1] Cera, E., Bruno, J., Duro, L., and Eriksen, T. (2006). Experimental determination and chemical modelling of radiolytic processes at the spent fuel/water interface. Long contact time experiments SKB-TR-06-07. Swedish Nuclear Fuel and Waste Management Co.
- [2] Eriksen, T.E., Jonsson, M., Merino, J. (2008) Modelling of time resolved and long contact time dissolution studies in 10 mM bicarbonate solutions-a comparison between two different models and experimental data, *J. Nucl. Mater.* 375 (2008) pp.331-339.
- [3] Odorowski, M., Jegou, C., De Windt, L., Broudic, V., Jouan, G., Peugeot, S., & Martin, C. (2017). Effect of metallic iron on the oxidative dissolution of UO_2 doped with a radioactive alpha emitter in synthetic Callovian-Oxfordian groundwater. *Geochimica et Cosmochimica acta*, 219, 1-21.

A1-3 EFFECT OF TEMPERATURE ON THE OXIDATIVE DISSOLUTION OF UO₂ DOPED WITH A RADIOACTIVE ALPHA EMITTER IN SYNTHETIC CALLOVIAN-OXFORDIAN GROUNDWATER IN THE PRESENCE OF IRON

Broudic Véronique⁽¹⁾, Marques Caroline⁽¹⁾, Jouan Gauthier⁽¹⁾, Autillo Matthieu⁽¹⁾, Miro Sandrine⁽¹⁾, Peugot Sylvain⁽¹⁾, Tocino Florent⁽²⁾, Martin Christelle⁽³⁾, De Windt Laurent⁽⁴⁾ and Jegou Christophe⁽¹⁾

(1) CEA, DES, ISEC, DPME, Univ Montpellier, Marcoule, (France)

(2) EDF R&D, Dept MMC, Site Renardières, Moret Sur Loing, (France)

(3) Agence Nationale pour la gestion des Déchets Radioactifs, 1/7 rue Jean Monnet, 92298 Châtenay-Malabry Cedex (France)

(4) MINES Paris, PSL University, Centre for geosciences and geoengineering, Fontainebleau (France)

The present study brought insights into the dissolution mechanisms of UO₂ spent fuel matrix under reducing repository environments in the presence of corroded iron with a focus on the effect of temperature. The approach combines leaching experiments to reactive transport modeling. Experimental data are based on two long-term leaching experiments of UO₂ pellets performed in synthetic COx claystone groundwater representative of the French disposal site in the presence of a corroded iron foil simulating the steel container. Plutonium-doped UO₂ pellets were used to reproduce the alpha activity of an aged spent fuel after 50 years of alpha radioactive decay. The first experiment was performed at ambient temperature 25°C [1] and the second one at 70°C, which is representative of the long-term temperature induced by spent nuclear fuels in underground disposal cells. The full set of experiments was simulated with the reactive transport code HYTEC [2] using the ThermoChimie thermodynamic database [3]. Kinetic control was implemented on H₂O₂ radiolytic production and disproportionation, oxidative and reducing dissolution of the UO₂ matrix, and anoxic corrosion of the iron foil. Sensitivity analysis was performed on temperature and Fe(II)-phases precipitation.

Despite a strong α irradiation field compared to those expected in a disposal situation, little uranium is released at 70°C (1 μ g after 2.3 years of alteration), most of which (80%) is adsorbed on the walls of the reactor and about 5% is dissolved in solution or in a colloidal form. The presence of U on the iron foil is low (15%), a massive precipitation of chukanovite (Fe₂(OH)₂CO₃) is observed while siderite (FeCO₃) is also identified. The doped UO₂ pellets are partially covered with a layer of magnetite (Fe₃O₄). No trace of uranium is detected in these precipitates. These observations reinforce the hypothesis that there is no oxidative dissolution of the fuel. The fast consumption of H₂O₂ by Fe(II) and the simultaneous precipitation of magnetite on the surface of the pellet prevent the oxidative dissolution of the fuel. These results and the associated mechanisms (Fig. 1) are similar to those obtained for the same system studied at 25°C, only the nature of the iron-based phase precipitating on the surface of the fuel is different. At 25°C akaganeite (β -FeOOH) precipitates whereas it is magnetite at 70°C. The modeling reproduces well the experimental data, in particular the change of corrosion products and Fe(II) concentration with temperature and the location of the redox front.

To sum up the increase of temperature did not globally change the release of uranium into the solution characterized by a low release of U(IV) controlled by amorphous UO₂:nH₂O. Dissolved Fe(II) species inhibited the oxidizing dissolution by consuming H₂O₂ and precipitating magnetite at the extreme surface of the pellet. On the contrary, the increase of temperature significantly affected the water chemistry and the amount of iron corrosion products (chukanovite and siderite).

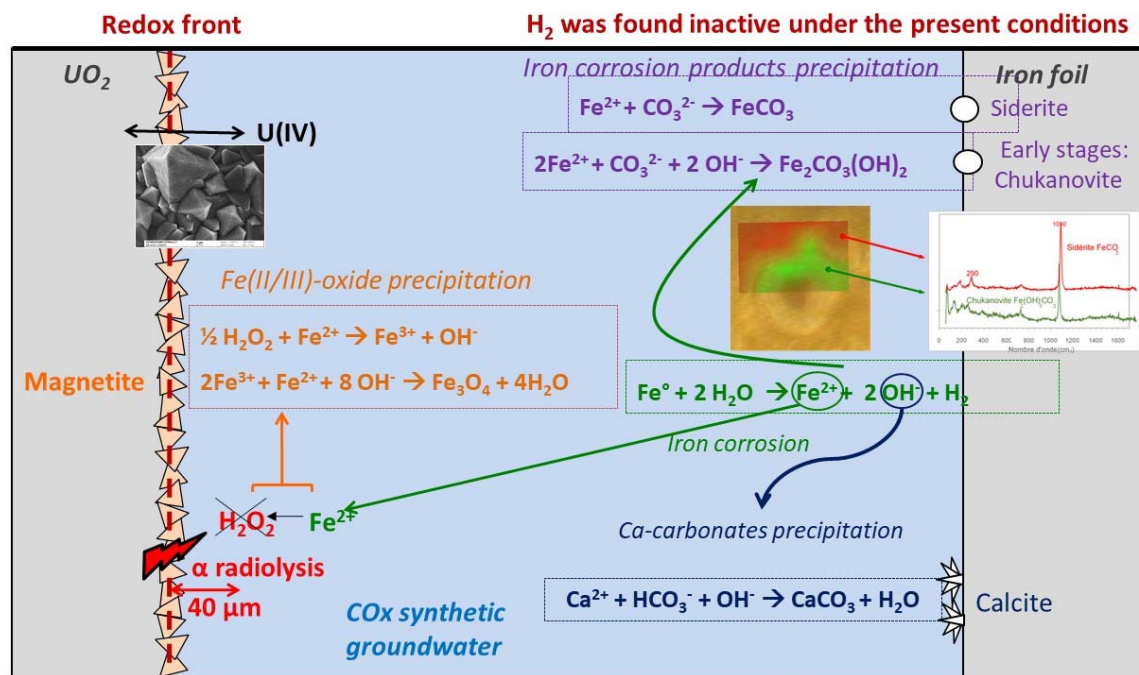


Figure 1: Sequence of chemical reactions supported by the reactive transport modeling at 70°C.

References

- [1] Odorowski, M., Jégou, C., De Windt, L., Broudic, V., Jouan, G., Peugot, S., Martin, C. (2017). Effect of metallic iron on the oxidative dissolution of UO₂ doped with a radioactive alpha emitter in synthetic Callovian-Oxfordian groundwater, *Geochimica et Cosmochimica Acta* 219, 1-21.
- [2] Van der Lee, J., De Windt, L., Lagneau, V., Goblet, P. (2003). Module-oriented modeling of reactive transport with HYTEC. *Comput Geosci* 29, 265–275.
- [3] Giffaut, E., et al. (2014). Andra thermodynamic database for performance assessment: ThermoChimie. *Applied Geochemistry* 49, 225–236.

A1-4 SOLUBILITY AND STRUCTURAL CHARACTERIZATION OF ZR(IV) HYDROUS OXIDES

Christian Kiefer (1,2), Tomo Suzuki-Muresan (1), Xavier Gaona (2), Dieter Schild (2), Oliver Dieste Blanco (2), Taishi Kobayashi (3), Denys Grekov (4), Monica Calatayud (5), Bernd Grambow (1), Horst Geckeis (2)

(1) SUBATECH – IMT Atlantique, Université de Nantes, CNRS/IN2P3, Nantes, France

(2) Karlsruhe Institute of Technology, Institute for Nuclear Waste Disposal, Karlsruhe, Germany

(3) Department of Nuclear Engineering, Kyoto University, Kyoto, Japan

(4) IMT Atlantique, GEPEA, UMR CNRS 6144, Nantes, France

(5) Laboratoire de Chimie Théorique, Sorbonne Université, Paris, France

Tetravalent metal ions (M(IV), e.g. actinides, Zr, Tc, Sn) are characterized by a strong hydrolysis and the formation of sparingly soluble amorphous hydrous oxides, $\text{MO}_2(\text{am, hyd})$, controlling M(IV) solubility over a broad range of pH. Ageing or exposure to elevated temperatures expectedly results in a transformation into thermodynamically more stable crystalline phases and thus in a decreased solubility in aqueous systems [1,2]. Zirconium alloys (Zircaloy) are used as cladding material for nuclear fuel, especially in water reactors. Zr-93 ($t_{1/2} = 1.53 \cdot 10^6$ a) is produced by nuclear fission of U-235 as well as by neutron activation of the cladding. $\text{ZrO}_2(\text{s})$ has been identified as possible solid phase controlling the solubility of Zr under repository conditions. The present study systematically investigates the impact of temperature on the crystallinity and water content of $\text{ZrO}_2(\text{s, hyd})$ solid phases, and further their solubility and thermodynamic properties in hyperalkaline conditions. For this purpose, freshly precipitated amorphous solids, solids aged at elevated temperatures and a commercial crystalline ZrO_2 solid are investigated with a combination of solubility batch experiments and comprehensive solid phase characterization methods. Density functional theory (DFT) calculations are performed to gain additional insights on the surface processes governing solubility phenomena. As overarching objective, this work intends to shed light on the mechanisms for the potential transformation of amorphous hydrous oxides into thermodynamically more stable crystalline phases of Zr(IV) relevant in the context of nuclear waste disposal.

The starting solid phase used in this study, $\text{ZrO}_2(\text{am, hyd, fresh})$, was prepared by slow titration of a ≈ 0.02 M ZrOCl_2 solution with 0.1 M NaOH. Independent aliquots of the starting solid phase were equilibrated at $T = 80$ and 22°C in 0.02 M $\text{CaCl}_2\text{-Ca(OH)}_2$, 0.2 M $\text{CaCl}_2\text{-Ca(OH)}_2$ or 0.001 M NaOH solutions at $\text{pH}_m \approx 11.0$ for 4, 10 and 18 months. After cooling the sample solutions down, the solid phases were separated from the supernatant solution and washed 2–3 times with water. These samples, and for comparison also a commercial crystalline ZrO_2 solid phase, were characterized with various methods including XRD, TG-DTA, SEM-EDX, XPS, EXAFS, IR-ATR, BET, TEM, SAXS and zeta potential measurements. Experiments approaching solubility equilibrium from undersaturation conditions were performed with 5–20 mg of the fresh and aged $\text{ZrO}_2(\text{s, hyd})$ solid phases, equilibrated at $T = 22^\circ\text{C}$ with 0.02 M $\text{CaCl}_2\text{-Ca(OH)}_2$, 0.2 M $\text{CaCl}_2\text{-Ca(OH)}_2$ or 0.5 M NaCl-NaOH solutions at $10 \leq \text{pH}_m \leq 13.4$. The concentration of Zr in the aqueous phase was quantified by ICP-MS after ultrafiltration with 3 kD filters.

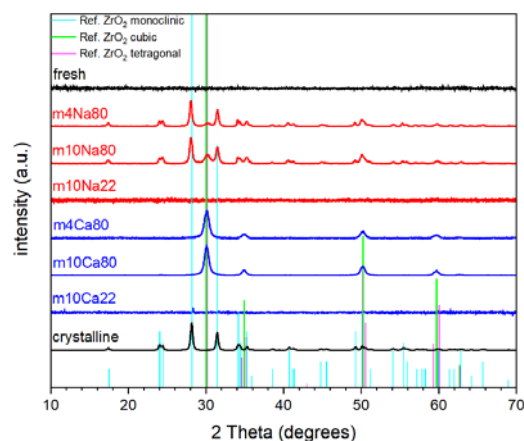


Fig. 1: XRD patterns collected for fresh $\text{ZrO}_2(\text{s})$ (black) and solids aged in NaOH (red) and CaCl_2 (blue) at $T = 80^\circ\text{C}$ for 4 months ($m4\text{Na}80$ and $m4\text{Ca}80$) and 10 months ($m10\text{Na}80$ and $m10\text{Ca}80$) and at $T = 22^\circ\text{C}$ for 10 months ($m10\text{Na}22$ and $m10\text{Ca}22$), compared to a commercial crystalline solid (black) and reference patterns available for $\text{ZrO}_2(\text{cr})$ in the JCPDS database.

XRD (Figure 1), SEM-EDX and TEM show the amorphous character of the fresh $ZrO_2(am, hyd, fresh)$. Solid phases aged at $T = 80^\circ C$ in 0.001 M NaOH solutions resulted in monoclinic ZrO_2 (size of crystal domains: 23-27 nm, Scherrer analysis) with a small fraction of cubic/tetragonal ZrO_2 , in agreement with XRD data reported by Kobayashi et. al. [3]. In contrast, ageing solids at $T = 80^\circ C$ in presence of 0.2 M or 0.02 M $CaCl_2-Ca(OH)_2$ results in the formation of nanocrystals with cubic/tetragonal structure and a size of 11-14 nm. The weight loss determined by TG-DTA (Figure 2) was correlated with the higher water content of the amorphous solids, qualitatively confirmed by IR spectroscopy. Rehydration experiments with amorphous solid phases after removing H_2O and OH^- by heating to $T = 200$ and $400^\circ C$ for 2 hours show that the dehydration process is not completely reversible.

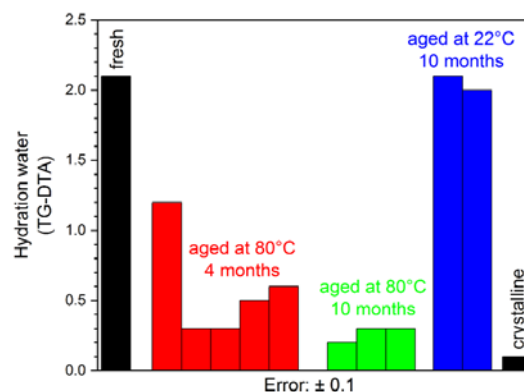


Fig. 2: Amount of water of the $ZrO_2(s)$ solid phases, determined by TG-DTA assuming a stoichiometry of $ZrO_2 \cdot nH_2O(s)$.

All these observations underpin the key role of OH^- and H_2O in the ageing/ crystallization process of $ZrO_2(s)$, which is described more accurately as $ZrO_x(OH)_{4-2x} \cdot nH_2O(s)$. These results highlight also the stabilization of the cubic/tetragonal structure induced by Ca at a concentration level expected in specific repository concepts.

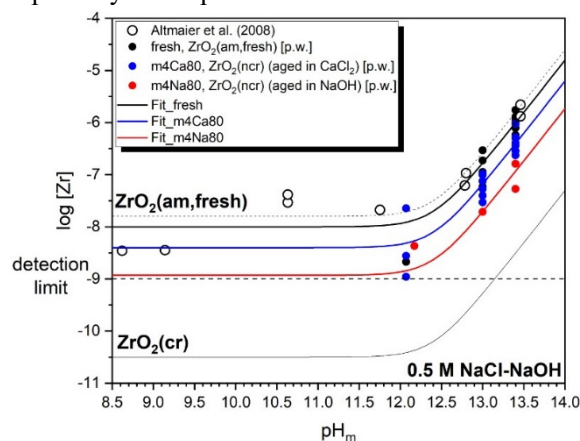


Fig. 3: Solubility data determined for fresh and aged phases ($T = 80^\circ C$, NaOH and $CaCl_2-Ca(OH)_2$) equilibrated at $T = 22^\circ C$ in 0.5 M NaCl-NaOH. Solid lines show solubility calculations for $ZrO_2(am, fresh)$ and $ZrO_2(cr)$ [4,5], as well as model calculations to determine the solubility product for the systems investigated in this work.

Figure 3 exemplarily shows solubility data of Zr(IV) collected in 0.5 M NaCl-NaOH for a fresh solid (amorphous) as well as for solid phases aged in 0.2 M $CaCl_2-Ca(OH)_2$ (cubic/tetragonal) and 0.001 M NaOH (monoclinic) solutions at $T = 80^\circ C$. An evaluation of the $\log^*K^{\circ}_{s,0}$ of these solid phases was conducted for the most alkaline samples, considering the predominance of the $Zr(OH)^{2-}$ (in NaCl) and $Ca_xZr(OH)^{2x-2}$ (in $CaCl_2$) aqueous complexes as reported in the NEA- TDB [4] and Altmaier et al. [5]. $\log^*K^{\circ}_{s,0}$ values of $-(4.5 \pm 0.4)$, $-(4.9 \pm 0.5)$ and $-(5.5 \pm 0.4)$ for the amorphous sample, the sample aged in $CaCl_2$ and the sample aged in NaOH, were determined. Further results from on-going experiments and theoretical calculations will be discussed in this contribution, also with regard to the nature of the solid/liquid interface determining solid phase solubility.

Reference

- [1] Rai et al. (2000). Radiochim. Acta, 88, 297-306.
- [2] Kobayashi et al. (2013). Radiochim Acta, 101, 645-651.
- [3] Kobayashi et al. (2019). Langmuir, 35, 7995-8006.
- [4] Brown et al. (2005). Chemical Thermodynamics of Zirconium, Elsevier
- [5] Altmaier et al. (2008). Radiochim Acta, 96, 541-550.

A1-5 GEOLOGICAL DISPOSAL OF CARBON-14: FROM SOURCE TO SINK

William Bower⁽¹⁾, Antonia Yorkshire⁽¹⁾, David Lever⁽²⁾, Andrew Hoch⁽²⁾, Steve Swanton⁽²⁾, Ben Swift⁽²⁾, Liam Payne⁽¹⁾, Andrew Cooke⁽¹⁾, Sarah Vines⁽¹⁾, Simon Norris⁽¹⁾

(1) Nuclear Waste Services, Harwell, UK

(2) Jacobs, Harwell, UK

Carbon-14 (half-life, 5730 years) is a significant component of the radioactive waste inventories of many national waste management programs, present particularly in activated metals (steel, zircaloy), ion-exchange resins, irradiated graphite and spent fuel, which can release carbon-14 to both the gas and solution phase as they corrode, leach, or degrade. Gaseous carbon-14 species, such as $^{14}\text{CH}_4$ and ^{14}CO , can migrate with bulk gas, but may also dissolve and be transported as part of the groundwater pathway from a future Geological Disposal Facility (GDF) for radioactive wastes. Carbon-14 bearing methane ($^{14}\text{CH}_4$) is likely to be the dominant carbon-14 species transported in the gas phase, potentially reaching the biosphere at low activity concentrations.

The radiological consequences of gaseous and dissolved carbon-14-bearing species is a potential issue and has been recognized as such in the UK's generic Disposal System Safety Case for a GDF [1]. In the UK case, the calculated consequences of carbon-14 are dominated by the corrosion of irradiated reactive metals (in the operational and early post-closure period), and the corrosion of irradiated stainless steel and leaching of irradiated graphite (in the longer post-closure period).

Knowledge regarding the chemical form and the release mechanism of carbon-14 from these types of wastes under disposal conditions of interest is crucial for building a robust future safety case. Over the last decade, Nuclear Waste Services has launched and partnered with a range of projects aimed at advancing the understanding of carbon-14 release and migration through the near and far-field of a Geological Disposal Facility, in order to improve the understanding of the expected evolution of the disposal system and the consequences for the calculated annual risk. Much of this work is summarized in NWS's *Gas Status Report* [2], its *Radionuclide Behaviour Status Report* [3], as well as the outputs from the *Carbon-14 Integrated Project, Phases 1 & 2* [4, 5, 6].

To advance understanding of the source term, a range of experimental studies have been undertaken to assess the release of carbon-14 from irradiated graphite and stainless steel. Early work on graphite concluded that under conditions that are typical of groundwaters in a facility for the disposal of Low-Heat-Generating Waste, the predominant carbon-14 release was to the solution phase. About 1% of the released carbon-14 was present in the gas phase, with the majority of that in methane, along with small quantities of carbon monoxide. NWS is currently considering the option of disposing of reactor core graphite in separate vaults or via alternative (near-surface) routes, subject to appropriate segregation and/or packaging arrangements. Recent work on steel has shown an initial fast release of carbon-14 during early leaching followed by a decreasing release rate over time.

Dissolved carbon-14 was present in the leachate predominantly as ^{14}C -carbonate but also as organic species. Gaseous or volatile species made up less than 10% of the released carbon-14 and were predominantly hydrocarbons.

An improved understanding of carbon-14 behaviour from wastes has implications for the migration of carbon-14 in the near and far-field of a GDF. In the future, account may have to be taken of (i) the specific nature of the carbon-14 inventory and release fraction timing, since not all of the carbon-14 will be released promptly from different wastefroms (ii) the speciation of carbon-14, since a significant fraction of the carbon-14 may be released as aqueous-phase small organic molecules (APSOMs), and not necessarily as carbonate / bicarbonate ions and (iii) the retardation mechanisms of carbon-14 in the geosphere, since the processes controlling the transport of these APSOMs may be different to those controlling the transport of carbonate / bicarbonate ions.

Here, a synthesis of past and ongoing work on carbon-14 source term and migration analysis will be presented.

Reference

- [1] Nuclear Waste Services Corporate Report, Overview of the generic Disposal System Safety Case, 2016, ISBN 978-1-84029-539-9
- [2] Nuclear Waste Services Corporate Report, Geological Disposal: Gas Status Report, 2016, NDA Report no. DSSC/455/01
- [3] Nuclear Waste Services Corporate Report, Geological Disposal: Behaviour of Radionuclides and Non-Radiological Species in Groundwater Status Report, 2016, NDA Report no. DSSC/456/01
- [4] NDA, Geological Disposal, Carbon-14 Project Phase 1 Report, 2012, NDA Report no. NDA/RWMD/092
- [5] Radioactive Waste Management, Geological disposal: Carbon-14 project phase 2: Overview report, RWM Report NDA/RWM/137, Issue 1, Mar. 2016
- [6] Amec Report, Carbon-14 Project Phase 2: Formation of a Gas Phase and its Migration, 2016, AMEC/200047/007, Issue 1.

D-1 RADIOCAESIUM MIGRATION WITHIN A FUKUSHIMA FOREST ECOSYSTEM AND THE ROLE OF BIOMONITORING

T. Dohi, T. Niizato, Y. Sasaki, and K. Iijima

Sector of Fukushima Research and Development, Japan Atomic Energy Agency, Japan

Among the radionuclides emitted during the the Fukushima Dai-ichi Nuclear Power Station (FDNPS) accident that took place on March 2011, ^{137}Cs is the dominant one for exposure assessment due to both its large discharge amount [1] and its relatively long half-life (half-life: 30.2 y). Forests in the Fukushima prefecture account for around 70% of the land area [2] and have been remained without decontamination, making radiocaesium migration in these ecosystems a particular concern. The Japan Atomic Energy Agency (JAEA) has carried out research since the accident in order to clarify the transport behaviour of radiocaesium, particularly that from forests to the ocean via Fukushima river systems. Biomonitoring studies using lichens have also been conducted to investigate the characteristics of deposited radiocaesium. In this paper, the following themes are reviewed:

- (1) Radiocaesium behaviour in forests.
- (2) Modelling the behaviour of radiocaesium from forest to river and in their ecosystem
- (3) Radiocaesium concentrations in wild mushrooms and plants, and mechanisms of radiocaesium accumulation in lichens.

The accumulation of ^{137}Cs (Bq m^{-2}) in coniferous forest approximately 30 km from the FDNPS four years after the accident, has been estimated to be ca. 90% for forest soils, with ca. 10% distributed in cedar trees. Furthermore, the same study found that ^{137}Cs in forest soils was distributed, ca. 60% in the top 5 cm of the mineral soil layer and ca. 40% in the litter and humus layers [3]. Within the mineral soil layer ^{137}Cs was found to be strongly bound to clay particles and therefore difficult to remove [4]. A similar trend was revealed by monitoring results conducted in five forests (coniferous and broad leaved), also within the Fukushima prefecture. In a study carried out by the Japanese Forest Agency over a 10-year period (2011-2021), ^{137}Cs accumulation reached over 85% in the mineral soil layers by 2021[5]; this is in good agreement with the results of the aforementioned study [3]. Both these findings suggest that since the time of the accident, radiocaesium has not been significantly translocated from forest soils to trees.

Such migration of ^{137}Cs to the forest floor with the lapse of time may cause eventually lead to the outflow of ^{137}Cs from the forest to river systems during rainy/storm events, and the migration to river fish. Calculations were performed using compartment models based on our environmental monitoring data accumulated after the accident. These models calculated the movement of ^{137}Cs from forests, migration to rivers and uptake into river fish. As a result it was revealed that three transport pathways were combined; litter fall directly from trees to rivers, elution or runoff from litter layers to rivers and elution into rivers from the organic soil layers via surface and groundwater run-off. This findings are important for the prediction and status of ^{137}Cs in both organic soil layers of forests and concentration in river and river fish [6].

Although forestry has already recovered in less-contaminated areas, wild plants (ferns and angiosperms) and mushrooms in some Fukushima forests have shown relatively high transfer factors (e.g. 0.08 – 12 in wild mushrooms) [3]. Analysis of monitoring data for wild mushrooms (107 species) throughout the entire eastern Japan area revealed certain ^{137}Cs concentration trends among species and genera (and also inter-species differences). Since fungi like mushrooms play important role also in radiocaesium behaviour in organic soil layers of forests, further investigation is expected to elucidate the relationship between mushroom habitat and the mechanisms of radiocaesium absorption. [7].

The authors of this paper focused on lichens: fungi symbiotic with algae, used as biomonitors to investigate the characteristics of radiocaesium deposition. Lichen thalli are composed of hypha, much

like mushrooms, and are similarly likely to accumulate radiocaesium. The mechanism of radiocaesium accumulation in parmelioid lichens was investigated and showed that radiocaesium containing particles derived from the accident were found to be retained stably in/on the surface of lichen thalli and both around and inside medullary layer tissues, six years after the accident [8-10]. In addition, it was suggested that Cs⁺ ions may be stably retained by forming complexes in the melanin-like substances distributed in the lower cortex layer of the tissues [10]. These findings are expected to be useful in elucidating the Cs accumulation mechanism in mushrooms, and, in estimating whether particulate or soluble forms of radiocaesium in fallout were dominant in the study area.

Reference

- [1] Nuclear Emergency Response Headquarters Government of Japan. (2011). "Report of the Japanese Government to the IAEA Ministerial Conference on Nuclear Safety - the Accident at TEPCO's Fukushima Nuclear Power Stations".
- [2] Kitamura, A., Yamaguchi, M., Kurikami, H., Yui, M., and Onishi, Y. (2014). "Predicting sediment and cesium-137 discharge from catchments in eastern Fukushima." *Anthropocene*. 5: 22–31.
- [3] Nagao, F., Niizato, T., Sasaki, Y., Ito, S., Watanabe, T., Dohi, et al. (2020). "Status of study of long-term assessment of transport of radioactive contaminants in the environment of Fukushima (FY2018)". *JAEA-Research 2020-007*: 249.
- [4] Sasaki, T., Matoba, D., Dohi, T., Fujiwara, K., Kobayashi, T., and Iijima, K. (2020). "Vertical distribution of 90Sr and 137Cs in soils near the Fukushima Daiichi nuclear power station." *J. Radioanal. Nucl.* 326: 303–314.
- [5] Ministry of Agriculture, Forestry and Fisheries. Japanese Forest Agency. "The results of the survey on the distribution of radiocaesium in forests in FY2021." https://www.rinya.maff.go.jp/j/kaihatsu/jyosen/attach/pdf/r3_surveys_on_radioactive_cesium-8.pdf
- [6] Kurikami, H., Sakuma, K., Malins, A., Sasaki, Y., and Niizato, T. (2019). "Numerical study of transport pathways of ¹³⁷Cs from forests to freshwater fish living in mountain streams in Fukushima, Japan." *J. Environ. Radioact.* 208-209: 106005.
- [7] Komatsu, M., Nishina, K., and Hashimoto, S. (2019). "Extensive analysis of radiocesium concentrations in wild mushrooms in eastern Japan affected by the Fukushima nuclear accident: Use of open accessible monitoring data." *Environ. Pollut.* 255: 113236.
- [8] Dohi, T., Tagomori, H., Ohmura, Y., Fujiwara, K., Kanaizuka, S., and Iijima, K. (2019). "Electron microscopic analysis of radiocaesium-bearing microparticles in lichens collected within 3 km of the Fukushima Dai-ichi Nuclear Power Plant." *Environmental Radiochemical Analysis*. 4: 58–70.
- [9] Dohi, T., Ohmura, Y., Yoshimura, K., Sasaki, T., Fujiwara, K., Kanaizuka, et al. (2021). "Radiocaesium accumulation capacity of epiphytic lichens and adjacent barks collected at the perimeter boundary site of the Fukushima Dai-ichi Nuclear Power Station." *PLoS ONE* 16(5): e0251828.
- [10] Dohi, T., Iijima, K., Machida, M., Suno, H., Ohmura, Y., Fujiwara, et al. (2022). "Accumulation mechanisms of radiocaesium within lichen thallus tissues determined by means of *in situ* microscale localization observation." *PLoS ONE* 17 (7): e 0271035.

D-2 APPLICATION OF ACCELERATOR MASS SPECTROMETRY TO MEASURE RATIOS OF PLUTONIUM ISOTOPES AND EVALUATE AMERICIUM DISTRIBUTIONS AT THE LITTLE FOREST LEGACY SITE, AUSTRALIA

Timothy E. Payne, David P. Child, Trent Cunynghame, Jennifer J. Harrison, Michael A.C. Hotchkis, Mathew P. Johansen, Lida Mokhber Shahin, Adella Silitonga and Sangeeth Thiruvoth

Australian Nuclear Science and Technology Organisation, Locked Bag 2001, Kirrawee DC NSW 2232, Australia

Low-level radioactive wastes were disposed at the Little Forest Legacy Site (LFLS) near Sydney, Australia between 1960 and 1968 [1]. Various radionuclides were buried in trenches at the site (including ^3H , ^{60}Co , ^{90}Sr , ^{137}Cs , together with uranium and plutonium isotopes). The amounts and isotopic ratios of plutonium in soils and groundwaters from the vicinity of the LFLS have been measured using accelerator mass spectrometry (AMS). The AMS results provide information on both the disposal inventory and the subsequent environmental behavior of the radionuclides. The AMS-measured ratio of $^{240}\text{Pu}/^{239}\text{Pu}$ enables the isotope signature of the Pu derived from the disposed wastes to be differentiated from global fallout. With increasing distance from the trenches, plutonium concentrations decrease from the highly elevated values found near the trenches and the $^{240}\text{Pu}/^{239}\text{Pu}$ ratio tends towards the local background ratio.

The presence of ^{241}Am (half-life of 432.2 years) in the wastes was not specifically noted at the time of disposals. However, ^{241}Am was later detected during environmental monitoring at the site [1]. Its presence in the environmental samples around the LFLS is due to the production of its parent ^{241}Pu (half-life of 14.4 years) during irradiation of fertile sources in a reactor. Although high-activity items, such as fuel rods, were not disposed at LFLS, the wastes, which were derived from research into reactor designs, contained ^{241}Pu with some associated ^{241}Am at the time of burial. The ^{241}Pu forms an ongoing source of ^{241}Am in disposed wastes, and the amount of ^{241}Am increases for the first few decades after removal of Pu from the reactor [2]. The AMS measurements of ^{241}Pu in environmental samples from LFLS show that ^{241}Pu was a major contributor to the radioactive inventory in the decades immediately following disposal. The activities of ^{241}Am and ^{241}Pu at the LFLS will continue to evolve in the future. The AMS results also provide evidence for more than one isotopic signature of plutonium in the disposed wastes. When plotted as ^{241}Pu vs ^{239}Pu , various water and soil samples plot on separate distinct lines. The samples on the two lines originate from different parts of the disposal area. This provides evidence for disposal of wastes with different Pu isotopic compositions, possibly indicating a mixture of wastes of different origins or irradiation histories. Our results confirm that the use of AMS in conjunction with more standard radiochemical measurements of Pu isotopes and ^{241}Am (i.e. alpha and gamma spectrometry) provides unique insights into the disposal practices and subsequent evolution of the site.

References

- [1] Payne, T.E., Harrison, J.J., Hughes, C.E., Johansen, M.P., Thiruvoth, S., Wilsher, K.L., Cendón, D.I., Hankin, S.I., Rowling, B., and Zawadzki, A (2013). Trench ‘Bathtubbing’ and Surface Plutonium Contamination at a Legacy Radioactive Waste Site. *Environmental Science & Technology*, 47, 13284-13293.
- [2] Runde, W (2010) Americium and Curium. In: *Radionuclides in the Environment* (Editor: D.A. Atwood). John Wiley and Sons, United Kingdom.

D-3 RENEWED LEAKAGE FROM SELLAFIELD'S MAGNOX SWARF STORAGE SILOS: OBSERVATIONS & OPPORTUNITIES FOR IMPROVED UNDERSTANDING OF RADIONUCLIDE MIGRATION

James Graham ⁽¹⁾, John Heneghan ⁽²⁾

(1) National Nuclear Laboratory, United Kingdom

(2) Sellafield Ltd, United Kingdom

The Magnox Swarf Storage Silos (MSSS) at the Sellafield site comprise a series of 22 concrete waste silos, for the underwater storage of predominantly irradiated Magnox swarf and miscellaneous beta-gamma waste. The silos are approximately 15 metres high with around 10 metres above ground level and the remaining 5 metres extending below ground. The building was constructed in four phases starting with the Original Building (OB) in 1964 which comprises six compartments and with the final 3rd Extension being completed in 1983. The design of the extensions was modified over time, with the OB comprising a single walled structure with no cooling capability and with later extensions incorporating increasing containment and inventory management functionality.

During the 1970's the MSSS OB was a source of significant leakage of radioactivity to ground. This leakage is considered to relate to the exothermic corrosion of Magnox (a magnesium alloy) swarf which was sufficient to increase the silo temperature beyond its structural design limits, inducing cracking in the building structure. The leakage ceased around 1980, without any intervention.

Subsurface monitoring following historical leakage was undertaken via a series of steel 'blind-tubes' installed in close proximity to the silo for dose rate measurements using Geiger Muller (GM) detectors, as well as a limited groundwater monitoring programme. This monitoring along with associated assessment was used to propose that ¹³⁷Cs, which comprised around 95% of the silo liquor fingerprint was held up close to the silo, while ⁹⁰Sr, which comprised the majority (4.75%) of the remaining inventory was entering into groundwater in limited quantity. Both the identification of the pathway taken by the leak and the assessment of its likely migration rate were hampered by the limited monitoring infrastructure at the time, the presence of contamination from other facility leaks and a lack of understanding of radionuclide attenuation in the heterogeneous quaternary fluvio-glacial deposits underlying the Sellafield site.

Since the historical leak, the retrieval of the waste from the facility has been the key objective for Sellafield. As plans for retrievals have progressed, assessment of the management and consequences of potential future leaks from the building have been undertaken. These assessments have included the established contaminants of concern e.g. ¹³⁷Cs, ⁹⁰Sr & ³H, but also additional radionuclides predicted to be present in the silo waste e.g. ¹⁴C, ⁹⁹Tc, ³⁶Cl, U and Pu, which had not been monitored for during the historical leak. These assessments have also been informed by a number of relevant desk and laboratory-based research studies on contaminant behaviour in quaternary fluvio-glacial deposits, including work on ¹³⁷Cs [1], [2]; ⁹⁰Sr [3], ¹⁴C [4], ⁹⁹Tc, U and Pu [5]. While these studies have been valuable, it has been difficult to ascertain the relevance of its findings to MSSS leakage due to the difficulty of acquiring soil and groundwater samples in close proximity to the silo (to investigate less mobile radionuclides) and as mobile radionuclides from the historical leak are likely to have dispersed.

In July 2019, renewed below ground leakage from MSSS OB was detected by routine liquor balance calculations. This leak continues in 2023 at a rate of *circa* 2.5 m³/day. A leak response plan was initiated including an enhanced groundwater monitoring programme that incorporated a wide suite of contaminants of interest. Directly adjacent to the building only blind-tube monitoring is available, with the routine groundwater monitoring network commencing ~ 15 metres from the building. Monitoring of these boreholes has allowed the breakthrough of all key radionuclides from a leak on the Sellafield Site to be monitored for the first time.

At the time of the 2019 leak, ⁹⁰Sr activities in many local boreholes around and downgradient from MSSS were already elevated and rising, reflecting ongoing migration from historical leakage from

MSSS and other facilities, with only low levels, or a complete absence of other radionuclides. Against this baseline the new leak was first detected in some local boreholes around 16 months after the leak commenced by contemporaneous breakthrough of ^3H and ^{36}Cl , reflecting the non-retarded nature of both these radionuclides. In comparison ^{14}C arrival was delayed, occurring up to 1 year later. This delay is proposed to relate to isotopic exchange with carbonate minerals [4] which have been identified in Sellafield sediments in low concentrations but are likely to be present at much higher levels in the Made Ground directly adjacent to the facility. Dose rate monitoring in the blind-tubes adjacent to the building has detected a progression of dose rate rises, and subsequent plateauing in locations around the facility, but no breakthrough of ^{137}Cs , the principal gamma emitter in the silo liquor, has occurred in the local groundwater monitoring boreholes. The patterns observed in the data are consistent with the limited migration potential of ^{137}Cs in the illite bearing glacial sediments typical at Sellafield [3]; however, suggest ^{137}Cs may be able to migrate more readily within the Made Ground surrounding the facility. Gross alpha measurements in local groundwaters return results around the limit of detection, supporting the understanding that redox sensitive U and Pu species are currently retained in the silo [5]. Only minor low-level perturbations in ^{99}Tc have been detected in the boreholes most responsive to the new leak, consistent with only limited release into the environment due to redox controls in the silo waste.

The results of the monitoring programme are still being assessed; however, at the most fundamental level, the location of mobile radionuclide breakthrough has enabled the migration pathways of the leak to be identified for the first time amongst the wider Sr-90 background. The patterns in the dose rate data close to the silo and the delayed breakthrough of C-14 suggest that the physical and chemical properties of the MSSS Made Ground may be important factors in controlling radionuclide migration away from the building. The results will be used to inform updates to the MSSS conceptual site model, enabling more accurate calculations of leak consequence and informing ongoing leak management activities.

Reference

- [1] Fuller A.J., Shaw S., Ward M.B., Haigh S.J., Mosselmans J.F.W., Peacock C.L., Stackhouse S., Dent A.J., Trivedi D., Burke I.T. (2015). Caesium incorporation and retention in illite interlayers. *Applied Clay Science*, 108, pp. 128 – 134.
- [2] Abrahamsen, L & Graham, J. (2013). PHREEQC transport modelling of Cs-137 to assess the impact of a new leak to ground interacting with existing contamination. *Migration 2013*, 8 - 13 September 2013, Brighton, United Kingdom.
- [3] Wallace S.H., Shaw S., Morris K., Small J.S., Fuller A.J., Burke I.T (2012). Effect of groundwater pH and ionic strength on strontium sorption in aquifer sediments: Implications for ^{90}Sr mobility at contaminated nuclear sites. *Applied Geochemistry*, 27 (8), pp. 1482 – 1491.
- [4] Boylan A.A., Stewart D.I., Graham J.T., Trivedi D., Burke I.T (2017). Mechanisms of inorganic carbon-14 attenuation in contaminated groundwater: Effect of solution pH on isotopic exchange and carbonate precipitation reactions. *Applied Geochemistry*, 85, pp. 137 – 147.
- [5] National Nuclear Laboratory (2021) Chemical Modelling of the Effects of Draining and Re-flooding in MSSS Original Building. NNL Report 15547, ISSUE 1.

D-4 APPROACH OF HANDLING THE SORPTION AND DIFFUSION HETEROGENEITY ACROSS THE OPALINUS CLAY AND ADJACENT CONFINING UNITS IN THE SAFETY CASE FOR THE SWISS DEEP GEOLOGICAL REPOSITORY

Raphael A.J. Wüst ⁽¹⁾, Luc R. Van Loon ⁽²⁾, Martin A. Glaus ⁽²⁾, Dmitrii A. Kulik ⁽²⁾, Maria do Sameiro Marques Fernandes ⁽²⁾, Xiaoshuo Li ⁽¹⁾

(1) National Cooperative for the Disposal of Radioactive Waste (Nagra), CH-5430 Wettingen, Switzerland

(2) Laboratory for Waste Management, Paul Scherrer Institut, CH-5232 Villigen PSI, Switzerland

Nagra is currently working towards a General License Application of a deep geological nuclear waste repository in the Jurassic-age Opalinus Clay at Nördlich Lägern, Switzerland. For the Safety Case, transport parameters, such as effective diffusion coefficients, are critical inputs for the predictions of radionuclide transport in tight clay rich rock formations. In the course of this study, diffusion and sorption data for selected radiotracers were obtained for >130 core samples, together with complementary rock properties, such as porosity, pore size, mineralogical composition and clay speciation, etc. (see [1-3]).

By studying the specific diffusion behaviour of representative radionuclides in model systems [4], a comprehensive picture of the variability of diffusion parameters within the individual geological formations and between those, could be obtained. This was achieved through the complex parameter evaluation workflow which is facilitated by dedicated computer tools such as our JupyterLab pyGEMS implementation of the ClaySorDif model (Kulik et al., Glaus et al., this conf.). This helped to streamline the operation and foster the interaction with other models. The data are then incorporated into an abstracted geomodel purposely built for conducting safety assessment for migration of radionuclides. The large scaled conceptual transport modelling of radionuclides in porous argillaceous media builds on schematic blocks or units that are parametrized and represent units with homogenous diffusion and sorption properties. When multiple parameters exist, geostatistical and advanced numerical modeling techniques are applied to determine the variability and range of the predicted transport behavior. The results of the diffusion and sorption measurements form a sound basis for constraining the variability of the parameters to the maximum necessary range.

In this study, we are detailing the datasets and discussing the rock heterogeneity in comparison to both sorption and diffusion behavior. Within the Opalinus Clay, the homogenization results in relatively small uncertainties with limited variability in transport parameters, while in carbonate, quartz and anhydrite-rich samples, the variability and thus the uncertainties increase. The differences are due to a range of rock parameters, that compound within the diffusion measurements and are hence difficult to discern. Here we are providing insights into several rock types, pore size distribution, CEC variabilities, etc. in order to better characterize the dependency of such transport characteristics to rock fabric, matrix and pore water composition.

The objective of this study is to enhance our understanding of methodological approaches and develop effective methods for upscaling datasets, which can provide meaningful input data for large-scale modelling studies in the safety case for deep geological repositories. Through this presentation, we will discuss the challenges faced and illustrate the parameter sensitivities, which are critical for long-term safety assessments of deep geological repositories for radioactive waste in argillaceous rocks. The findings of this study will enable us to improve our knowledge of upscaling datasets, leading to more accurate modelling of deep geological repositories for the disposal of radioactive waste.

References

- [1] Mazurek, M., T. Gimmi, C. Zwahlen, L. Aschwanden, E. Gaucher, M. Kiczka, D. Rufer, P. Wersin, M. Marques Fernandes, M. Glaus, L. Van Loon, D. Traber, M. Schnellmann, T. Vietor (2023): Swiss deep drilling campaign 2019–2022: Geological overview and rock properties with focus on porosity and pore geometry. *Appl. Geochem.*: to be submitted.
- [2] Van Loon, L.R. and M.A. Glaus, R. Wüst (2023) Diffusion of HTO, ^{36}Cl and ^{22}Na in the Mesozoic cover of Northern Switzerland: I: Measurement of diffusion coefficients and capacity factors. *Appl. Geochem.*: to be submitted.
- [3] Glaus, M.A. and L.R. Van Loon, R. Wüst (2023) Diffusion of HTO, $^{36}\text{Cl}^-$ and $^{22}\text{Na}^+$ in the Mesozoic cover of Northern Switzerland. II: Interpretation in terms of an electrical double layer model. *Appl. Geochem.*: to be submitted.
- [4] Glaus, M.A., and S. Frick, L.R. Van Loon (2020). A coherent approach for cation surface diffusion in clay minerals and cation sorption models. *Geochim. Cosmochim. Acta* 274, 79–96.

PA1-6 TECHNETIUM DIOXIDE SOLUBILITY AT ELEVATED TEMPERATURES

Matthew Riss⁽¹⁾, Shanna L. Estes⁽¹⁾, Brian A. Powell^(1,2)

(1) Department of Environmental Engineering and Earth Sciences, Clemson University, Anderson, SC, 29625, USA.

(2) Department of Chemistry, Clemson University, Clemson, SC 29630, USA.

Technetium-99 (Tc-99), with its long half life, high fission yield, and potential to quickly move through the subsurface,^{1,2} has been identified as a significant risk driver for deep geologic storage of spent nuclear fuel. Under the reducing conditions expected in some geologic repositories, Tc will exist predominantly in the +IV oxidation state, for which technetium dioxide ($\text{Tc}^{\text{IV}}\text{O}_2 \cdot x\text{H}_2\text{O}$) is the solubility controlling phase across environmentally relevant pH values.^{3,4} Understanding the fate and transport of Tc^{IV} in repositories necessitates knowledge of the thermodynamic constants describing the equilibrium behavior of $\text{Tc}^{\text{IV}}\text{O}_2 \cdot x\text{H}_2\text{O}$. Although such constants are available for Tc at room temperature,⁵ data for elevated temperatures are lacking. This represents a significant knowledge gap, as temperatures up to ~ 80 °C are expected to persist within repositories for hundreds of years.⁶ To advance a predictive understanding of Tc^{IV} hydrolysis at elevated temperatures (up to 80 °C), this work uses batch reactions to quantify $\text{Tc}^{\text{IV}}\text{O}_2 \cdot x\text{H}_2\text{O}$ solubility at temperatures 25–80 °C over the pH range 1–11.5.

$\text{Tc}^{\text{IV}}\text{O}_2 \cdot x\text{H}_2\text{O}$ was prepared following the procedure in Hess *et al.*⁷ This synthesis yielded amorphous, aggregated solids with particle diameters of ~ 50 nm (as determined from powder X-ray diffraction and electron microscopy), similar to results reported previously.⁷ Batch reactions contained approximately 4 μg of $\text{Tc}^{\text{IV}}\text{O}_2 \cdot x\text{H}_2\text{O}$ suspended in 0.1 M or 0.5 M NaCl at pH 1–11.5. All reactions were equilibrated in an anaerobic glove bag ($\sim 98\%$ $\text{N}_2/2\%$ H_2), using a dry bath to maintain the desired temperature. Given the propensity of Tc^{IV} to oxidize to Tc^{VII} , extreme care was taken to limit any oxygen intrusion into the glove bag. The batch reactions were sampled approximately biweekly by passing 150- μL aliquots from each suspension through 3 kDa centrifugal filters to remove suspended solids. At each sampling event, pH and E_{H} were measured. Technetium concentrations in the filtrate were measured using inductively coupled plasma mass spectrometry (ICP-MS). To verify that Tc oxidation did not occur during equilibration, additional filtered aliquots from randomly selected reactions were diluted with 0.1 M HCl, then mixed with an equal volume of tetraphenylphosphonium chloride (TPPC) in chloroform, which effectively extracts Tc^{VII} (as TcO_4^-) into the chloroform phase.⁷ Batch reactions were initially equilibrated at 25 °C. Once equilibrium was obtained (defined as no further changes in Tc solubility, pH, or E_{H} over a period of weeks), the temperature was increased and the sampling procedure was repeated to give data at 25, 35, 50, and 80 °C. Expected Tc^{IV} solubility at 25 °C was simulated using the geochemical code PHREEQC v.3.7 and the NEA-TDB database.⁵

The variable temperature solubility data show that dissolved Tc^{IV} concentrations increase with increasing temperature at pH values > 5 , whereas no significant difference in solubility as a function of temperature was observed at pH values < 5 (Figure 1). These data suggest alteration of the $\text{Tc}^{\text{IV}}\text{O}_2 \cdot x\text{H}_2\text{O}$ solid to a more soluble phase and suggest that enthalpies for Tc^{IV} hydrolysis are close to zero. Disagreement

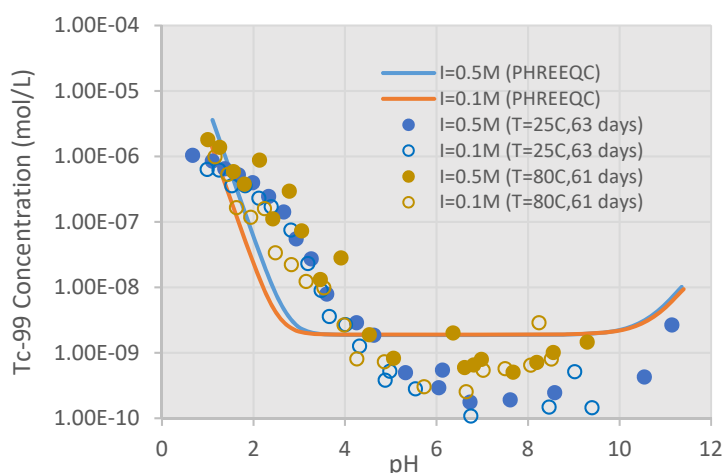


Figure 1. Dissolved Tc^{IV} as a function of pH at 25 °C and 80 °C. Closed and open circles are experimental data; solid lines represent Tc^{IV} solubility as simulated using current NEA-TDB constants⁵ and PHREEQC.

between simulated and measured Tc^{IV} data at both temperatures suggest that selected NEA-TDB constants do not accurately predict Tc^{IV} solubility. Future work will include additional modelling to quantify the Tc^{IV} hydrolysis constants, the associated reaction enthalpies, and to approximate relevant ion interaction parameters for use in activity corrections with the specific ion interaction theory (SIT) or Pitzer models. Additionally, XRD and electron microscopy analyses of the initial and reacted Tc^{IV} solids will be compared to identify possible phase alteration during the experiments.

References

- [1] Bruno, J. and Ewing, R. C (2006). Spent Nuclear Fuel. Element. 2: 343–349. <https://doi.org/10.2113/gselements.2.6.343>.
- [2] Meena, A. H. and Arai, Y (2017). Environmental Geochemistry of Technetium. Environmental Chemistry Letters. 15: 241–263. <https://doi.org/10.1007/s10311-017-0605-7>.
- [3] Cantrell, K. J. and Williams, B. D (2013). Solubility Control of Technetium Release from Saltstone by $\text{TcO}_2 \cdot \text{H}_2\text{O}$. Journal of Nuclear Materials. 437 (1–3): 424–431. <https://doi.org/10.1016/j.jnucmat.2013.02.049>.
- [4] Liu, Y.; Terry, J.; Jurisson, S (2008). Pertechnetate Immobilization with Amorphous Iron Sulfide. Radiochimica Acta. 96 (12): 823–833. <https://doi.org/10.1524/ract.2008.1528>.
- [5] OECD/NEA (2021). Second Update on the Chemical Thermodynamics of Uranium, Neptunium, Plutonium, Americium And Technetium, Volume 14. Chemical Thermodynamics, OECD Publishing. <https://doi.org/10.1787/bf86a907-en>.
- [6] Johnson, L. H.; Niemeyer, M.; Klubertanz, G.; Siegel, P.; Gribi, P (2002). Calculations of the Temperature Evolution of a Repository for Spent Fuel, Vitrified High-Level Waste and Intermediate Level Waste in Opalinus Clay. Wettingen.
- [7] Hess, N. J.; Qafoku, O.; Xia, Y.; Moore, D. A.; Felmy, A. R (2008). Thermodynamic Model for the Solubility of $\text{TcO}_2 \cdot x\text{H}_2\text{O}$ in Aqueous Oxalate Systems. Journal of Solution Chemistry. 37 (11): 1471–1487. <https://doi.org/10.1007/S10953-008-9328-5>.

PA1-7 EVALUATING THE CHEMICAL DURABILITY OF IODINE BEARING GLASS SYNTHESIZED AT HIGH PRESSURE: VAPOR HYDRATION AND AQUEOUS ALTERATION STUDY

Kalyan Roy⁽¹⁾, Esra Onat⁽¹⁾, Tomo Suzuki-Muresan⁽¹⁾, Valerie Bosse⁽¹⁾, Lionel Campayo⁽²⁾, Yann Morizet⁽³⁾, Abdesselam Abdelouas⁽¹⁾

(1) SUBATECH, IMT Atlantique, CNRS/IN2P3, University of Nantes, France

(2) CEA, DES, ISEC, DE2D, University of Montpellier, Marcoule, France

(3) Université de Nantes, Nantes Atlantique Universités, LPG, France

Iodine 129 is a long-lived fission product (15.7 million years) formed in nuclear fuel. In repository site, I-129 constitutes a major contributor to the total dose release at the outlet of the geologic disposal site due to its high mobility in the environment. To minimize the harmful effects it may cause to the living system and the environment, radio-iodine needs to be managed safely and responsibly. Nuclear glass form has demonstrated high qualification for the immobilization of radioactive waste to isolate the release of radionuclides until the end of their radioactive decay[1]. They ought to be disposed-off for long-term in deep geological sites. Glasses are used as the means to incorporate these radioactive wastes mainly because of their: a. Chemical durability over thousands of years, b. Ease of manufacturing, c. Ease of incorporation of wide variety of radionuclides, d. Relatively low waste volume upon waste incorporation. However, incorporation of iodine seems inadequate in the current glass process due to its high volatility and low solubility in glasses. In literature, previous works of I incorporation in glass matrices[2] show that for Ag-phosphate glasses, the presence of phosphate increases the high I incorporation but with a weak glass durability. The durability can be increased with the addition of Nb₂O₅ but with a decrease of I incorporation[3]. The addition of Al₂O₃ enhances the glass durability and I retention. Recent work on borosilicate surrogate glass studies show that 92% retention of I remain entrapped in the hydrated layer showing good promise for this glass[4]. To increase the iodine content in glass, high-pressure process gives promising results[5], but needs to be evaluated in terms of chemical durability. Our work will focus on the chemical durability of iodine bearing glass synthesized at high pressure conditions that has shown enhanced I solubility, as well as understanding the effect of I speciation and the evolution of glass elements during alteration experiments.

It is expected that during long-term disposal, the engineered barriers over-packing the nuclear glasses in geological sites will eventually be in contact with groundwater leading to glass dissolution and release of radionuclides into the environment. However, prior to the total saturation of the disposal cells in an aqueous medium, the metallic containers of the waste-glass package will start getting corroded releasing hydrogen gas, which will slow-down the groundwater penetration due to the generated pressure exposing to an unsaturated vapor environment for tens of thousands of years before being completely immersed in groundwater. Therefore, to evaluate the chemical durability of the iodine bearing glass matrices, the current work will focus on its vapor hydration and aqueous alteration studies. The vapor hydration studies will be conducted under controlled temperature and relative humidity in autoclaves. The aqueous alteration experiments will be performed under unsaturated and saturated conditions with respect to Si-concentration at pH 9 and 90°C. The glass hydration and alteration rates can be estimated determined physically and chemically[4].

First experiments have started with an ISG glass doped with I (0.25 mol%), synthesized at 0.6 GPa and 1300 °C. The composition of the glass used is as follows:

	B ₂ O ₃	Na ₂ O	Al ₂ O ₃	SiO ₂	CaO	ZrO ₂	I
Avg ISG	15.97	12.44	4.25	61.08	5.51	1.76	0.25
SD ISG	0.00	0.07	0.06	0.67	0.08	0.03	0.06

Preliminary results on leaching experiment under unsaturated conditions with respect to Si-concentration show that the behavior of B and Si are released congruently, unlike Al and I. The maximum initial alteration rates are found in the first hours (based on B and Si concentrations) followed

by a rate drop after few days similar to a residual rate. Experiments will continue with the solid characterizations of the altered layer of the glass and future experiments with the effect of I speciation in the glass matrix on the dissolution rate and mechanism.

References

- [1] Grambow, B. (2006) Nuclear Waste Glasses - How Durable? *Elements* **2**, 357–364.
- [2] Riley, B. J., Vienna, J. D., Strachan, D. M., McCloy, J. S. and Jerden, J. L. (2016) Materials and processes for the effective capture and immobilization of radioiodine: A review. *J. Nucl. Mater.* **470**, 307–326.
- [3] Chabauty, A.-L., Méar, F. O., Montagne, L. and Campayo, L. (2021) Chemical durability evaluation of silver phosphate-based glasses designed for the conditioning of radioactive iodine. *J. Nucl. Mater.* **550**, 152919.
- [4] Zhang, H., Suzuki-Muresan, T., Morizet, Y., Gin, S. and Abdelouas, A. (2021) Investigation on boron and iodine behavior during nuclear glass vapor hydration. *Npj Mater. Degrad.* **5**, 10.
- [5] Jolivet, V., Morizet, Y., Paris, M. and Suzuki-Muresan, T. (2020) High pressure experimental study on iodine solution mechanisms in nuclear waste glasses. *J. Nucl. Mater.* **533**, 152112.

PA1-8 SOLUTION AND SOLID-LIQUID-EQUILIBRIUM PROPERTIES OF RADIONUCLIDE-NITRATE AQUEOUS SYSTEMS: EXPERIMENTS AND SIT PARAMETERIZATION

Lassin Arnault⁽¹⁾, dos Santos Pedro F.⁽²⁾, Gaona Xavier⁽²⁾, Altmaier Marcus⁽²⁾, Madé Benoît⁽³⁾

(1) BRGM, France

(2) KIT-INE, Germany

(3) Andra, France

In several concepts of radioactive waste management, including the French case, the recovery of intermediate activity – long life radionuclides from spent fuel involves concentrated nitric acid or nitrate salts. The waste is embedded in a succession of metallic containers, concrete cells, clayey material, and concrete walls in contact with the host-rock formation.

For safety analysis purposes, the long-term behavior of such systems must be anticipated over several tens of thousands of years. According to hydrodynamic simulations, host rock pore waters are expected to re-saturate the porosity of the materials around the waste. In pessimistic scenarios, such waters could come in contact with the waste. Because these waters will infiltrate materials of different nature before reaching the nitrated waste, they will be characterized by a complex chemistry with, in particular, significant dissolved sulfate contents and variable pH. As part of the safety analysis, anticipation of the chemical behavior of the nuclear waste in such conditions must rely on reliable thermodynamic databases.

In this context, the present work aimed at studying the chemical behavior of binary and ternary radionuclide-nitrate aqueous systems. The study includes the collection of published experimental osmotic coefficient and solubility data, the measurement of aqueous speciation by Time-Resolved Laser-induced Fluorescence Spectrometry (TRLFS), solubility measurements, and the development of thermodynamic and activity models based on the Specific Ion Theory (SIT).

For binary nitrate aqueous systems, the collection of published osmotic coefficient and solubility data could cover the complete lanthanide series and two actinides (Th and UO₂). TRLFS and/or solubility measurements were performed in Eu(NO₃)₃-NaNO₃-H₂O and Eu(NO₃)₃-Mg(NO₃)₂-H₂O ternary systems.

Both bibliographic and measured experimental data were used for developing chemical models, using an optimization procedure [1] based on the combination of the geochemical calculation code PhreeqC [2] and the parameter optimization software PEST [3]. In addition, the ThermoChimie thermodynamic database [4] was used as basic support for geochemical calculations. The chemical models considered the formation of aqueous complexes $RN(NO_3)_x^{z-x}$, where RN represents a radionuclide ($z = 2$ to 4 is the electric charge of the radionuclide, and $x = 1$ to 3). The parameters to optimize were the formation constants of the aqueous complexes and the SIT specific binary interaction parameters between oppositely charged species. Depending on the number of aqueous complexes included in the model, the number of involved parameters varied between 1 (full dissociation) and 5 (formation of two aqueous complexes).

Depending on the mass of the radionuclide, two domains could be distinguished based on the ability of the model to reproduce the experimental data. For heavy lanthanides, namely from Dy to Lu, 3-parameter models (involving one aqueous complex) were found very efficient for describing the osmotic coefficient data up to very high concentrations, even beyond the solubility limit of the salts. 5-parameter models were found unnecessary. For light lanthanides, namely from La to Tb, osmotic coefficient data

could be described up to variable maximum concentrations, with no specific trend according to the molar mass of the radionuclides. In addition, considering partial dissociation did not help improving the description of osmotic coefficient data in most cases, except for Ce, Nd and Pm. For the latter elements, the formation of one aqueous complex: $RN(NO_3)^{2+}$ was sufficient to cover a range of concentration up to 3 molal and beyond.

Regarding $Eu(NO_3)_3$ aqueous systems, the additional information provided by TRLFS measurements and solubility data help include additional constraints. Indeed, the deconvolution of the spectra measured on aqueous solutions of constant Eu concentration, but with increasing $NaNO_3$ or $Mg(NO_3)_2$ contents, can provide information about the aqueous speciation of Eu. Such data are being processed and the results will be discussed.

References

- [1] Lach, A., André, L., Guignot, S., Christov, C., Henocq, P., Lassin, A. (2018) A Pitzer Parametrization to Predict Solution Properties and Salt Solubility in the H-Na-K-Ca-Mg- NO_3 - H_2O System at 298.15 K. *J. Chem. Eng. Data*, 63: 787-800
- [2] Parkhurst D.L., Appelo, C.A.J. (2013) Description of input and examples for PHREEQC version 3: a computer program for speciation, batch-reaction, one-dimensional transport, and inverse geochemical calculations. U.S. Geological Survey, Techniques and Methods, 519 p.
- [3] Doherty, J. (2021) PEST. Model-independent parameter estimation. User manual: 7th Edition. Watermark Numerical computing, 7th ed., 369 p.
- [4] Giffaut, E., Grivé, M., Blanc, P., Vieillard, P., Colàs, E., Gailhanou, H., Gaboreau, S., Marty, N.C.M., Madé, B. and Duro, L. (2014) Andra thermodynamic database for performance assessment: *ThermoChimie. Appl. Geochem.* 49: 225–236

PA1-9 DISSOLUTION AND AGING OF METAL MONOURANATES: SIMULATED DEBRIS OF FUKUSHIMA DAIICHI NUCLEAR POWER STATION

T. Sasaki⁽¹⁾, Y. Kato⁽¹⁾, R. Tonna⁽¹⁾, T. Kobayashi⁽¹⁾, Y. Okamoto⁽²⁾

(1) Department of Nuclear Engineering, Kyoto University, Nishikyo-ku, Kyoto 615-8540, Japan

(2) Japan Atomic Energy Agency, 1-1-1, Kouto, Sayo-cho, Sayo-gun, Hyogo 679-5148, Japan

During the severe accident at the Fukushima Daiichi Nuclear Power Station (1F), the fuel in the molten core reacted with zircaloy cladding, reactor structure materials such as stainless steel (SUS), and concrete at the bottom of the primary containment vessel, and formed fuel debris. The properties of fuel debris depend on the atmosphere and temperature at the time of generation. In particular, if the atmosphere entered the reactor vessel, the UO_2 in spent fuel might have been partially oxidized and reacted with a reactor material, resulting in metal monouranates such as CaUO_4 and FeUO_4 . The dissolution reactions from fuel debris would depend on the chemical properties of the water phase as coolant water and deep underground water, such as pH, redox potential, saline concentration, and carbonate concentration. These factors must be considered in the effects of aging and the safety assessments in its safe retrieval, storage, treatment, and final disposal of 1F debris.

Therefore, predictive evaluation of the various chemical properties of the 1F debris prior to sampling is essential. Static leaching tests have investigated the dissolution behavior of nuclides from different simulated debris samples [1,2]. However, in many cases, these samples were a mixture of uranate complexes. An understanding of the dissolution reactions of the constituents, such as a stable $\text{UO}_2\text{-ZrO}_2$ solid solution and metal monouranates, is essential for the interpretation of the apparent dissolution behavior of the mixture. This study focused on CaUO_4 and FeUO_4 .

Experimental

1) Materials; CaUO_4 was synthesized by UO_2 and CaCO_3 and placed on an alumina boat in the atmosphere in the electric furnace at 1473K. The powder sample was suspended in a small amount of dilute HCl and ground in a mortar for purification. Finally, the purified sample CaUO_4 was dried in a desiccator. On the other hand, FeUO_4 was synthesized by U_3O_8 and Fe_3O_4 and placed in a vacuum-sealed quartz tube in the electric furnace at 1473K. The powder sample was suspended in a small amount of hot 1 M HNO_3 to dissolve the unreacted U_3O_8 , washed with water, and then air-dried. This FeUO_4 sample contained a small amount of Fe_2O_3 , which oxidized from the unreacted Fe_3O_4 . Additionally, references U_3O_8 and UO_2 were also prepared.

2) Static leaching test; The aqueous solutions used in the static immersion experiments at 298 K were in various chemical conditions. Shortly, 0.1 M CaCl_2 or NaCl were used in the reducing and oxidizing conditions and the presence and absence of carbonate for the CaUO_4 system. For the FeUO_4 system, 0.5 M NaClO_4 was used. The wide pH condition was adjusted using the corresponding acid/alkali solutions for each system. $\text{Na}_2\text{S}_2\text{O}_4$ was used to keep a reducing condition. After a given immersion period, the pH and Eh values were recorded, and the supernatant was filtered by an ultrafiltration filter. The metal concentrations of U, Ca, and Fe in the filtrate were determined by ICP-MS (2030, Shimadzu), and the DIC was measured by a portable analyzer (CGP-31, DKK-TOA).

3) Spectrometry; XRD measurement of powder samples before and after immersion was performed using SmartLabSE (Rigaku). The microstructure and elemental composition of the sample were evaluated using SEM (JCM-6000, JEOL) instrument equipped with EDX (EX-37001). The U L_3 -edge and Fe K-edge XAFS measurements were performed on the sample at Photon Factory in KEK, Japan.

Result and Discussions

1) CaUO_4 system. The pH-Eh values indicated that uranium was mainly a hexavalent uranium hydroxide in the oxidizing condition. The Ca concentration was about 10^{-5} M, higher than U due to the

dissolution and reprecipitation. Assuming that $\text{Na}_2\text{U}_2\text{O}_7 \cdot \text{H}_2\text{O}(\text{cr})$ was the solubility-limiting solid phase, the measured U concentration agreed with the U concentration calculated thermodynamically. Therefore, it implied that the formation reaction of a secondary mineral $\text{Na}_2\text{U}_2\text{O}_7 \cdot \text{H}_2\text{O}(\text{cr})$ formed on the surface of the powder sample after U dissolution from CaUO_4 . On the other hand, tetravalent uranium species could be predominant in the reducing condition. A shift from the XRD peak pattern of the solid phase (CaUO_4 to CaUO_{4-x}) to a lower angle was observed after the immersion test. XAFS also assigned the reduction reaction of uranium. In the thermodynamic analysis of the U concentration, the solubility-limiting solid phase, $\text{UO}_2(\text{am})$, formed at the sample surface and controlled the lower U concentration than in the oxidizing condition.

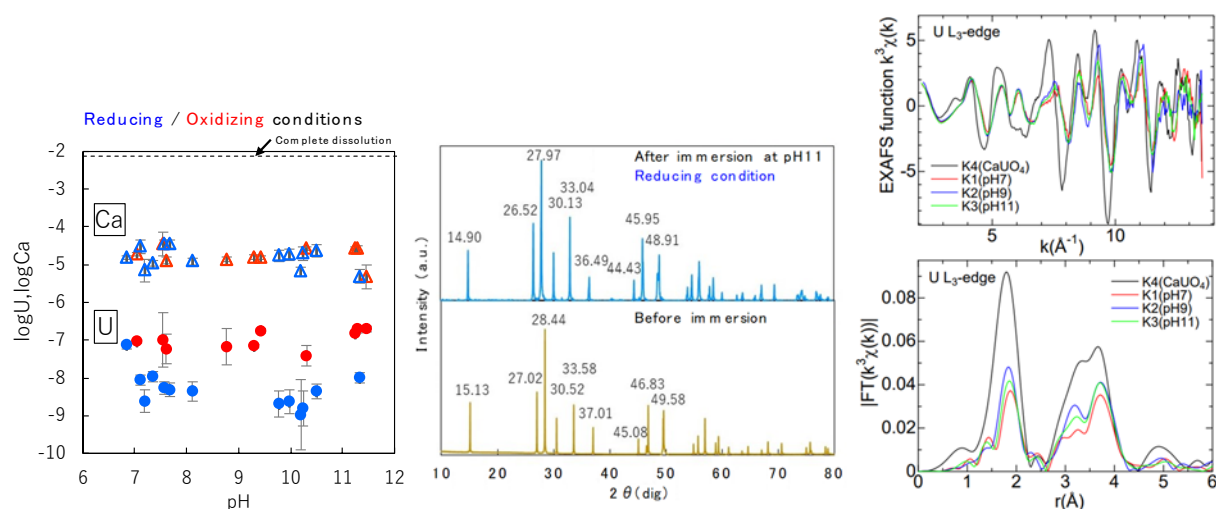


Figure 1 left; pH dependence of U and Ca concentrations under reducing and oxidizing conditions in the absence of carbonate, center; XRD patterns of CaUO_4 before and after immersion, right; U L_3 -edge EXAFS and FT magnitude function at pH 7, 9, and 11.

Under high carbonic acid conditions, calcium ions dissolved from CaUO_4 would be solubility-limited by CaCO_3 . The dissolution of U might be suppressed as Ca dissolution from CaUO_4 , indicating that the formation of CaCO_3 affected the dissolution behavior of CaUO_4 .

2) FeUO_4 system. The dissolution behavior of FeUO_4 in atmospheric conditions changed with aging time, and the reaction was suggested to be accompanied by both redox reactions of +3/+2 for Fe and +5/+6 for U. The oxidation number of both elements in solution was evaluated by XANES. After 3 months of aging, the U concentration could be explained by assuming metaschoepite as a solubility-limiting solid phase. The solid-state before and after immersion was assigned by XRD and EXAFS studies.

References:

- [1] Tonna, R., Sasaki, T. et al. (2023). Phase analysis of simulated nuclear fuel debris synthesized using UO_2 , Zr, and stainless steel and leaching behavior of the fission products and matrix elements. Nucl. Eng. Technol. *in press*. doi.org/10.1016/j.net.2022.12.017.
- [2] Sasaki, T. et al. (2019) Leaching behavior of gamma-emitting fission products, calcium, and uranium from simulated MCCI debris in water. J. Nucl. Sci. Technol. 56, 1092-1102.

PA1-10 STABILITY & PHYSICO-CHEMICAL CHARACTERISATION OF A RECONDITIONED WASTE FORM RELEANT TO RADIOACTIVE WASTES

Gianni F. Vettese⁽¹⁾, Taavi Vierinen⁽¹⁾, Tandre Oey⁽²⁾, Suvi Lanninmaki⁽²⁾, Tapio Vehmas⁽²⁾, Matti Nieminen⁽²⁾, Jaana Laatikainen-Luntama⁽²⁾, Markku Leivo⁽²⁾, Emmi Myllykylä⁽²⁾ & Gareth T. W. Law⁽¹⁾

(1) *The University of Helsinki, Radiochemistry Unit, Finland*

(2) *VTT Technical Research Centre of Finland, Finland*

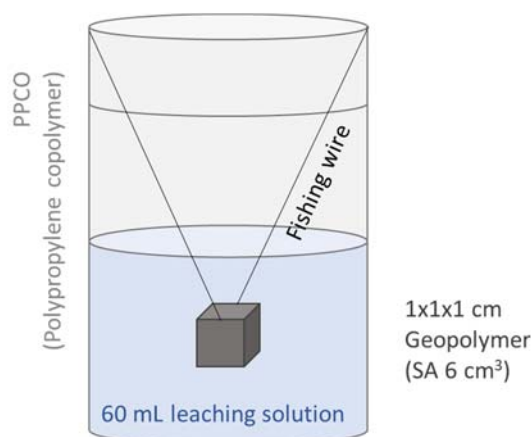
Nuclear power plants use ion exchange resins to remove radioactive contaminants present in the process waters. At certain intervals, spent ion exchange resins are replaced with fresh resin and the now active, spent resins are typically immobilized and disposed of. VTT, Finland, has developed a process to treat spent resins that significantly reduces the volume of resin to be disposed of and enables more efficient immobilization prior to disposal. Here, a tailored gasification process ashes the used resin and the residue is geopolymerized and prepared for disposal. The geopolymerized resin residue could be stored in a Low and Intermediate Level Waste (LILW) geological disposal facility. During storage, the space surrounding the solidified waste packages will be backfilled with cement; and any passing waters will therefore be in equilibrium with this, resulting in a high pH (~12), Ca rich solution which could act as a leachate, potentially mobilizing radionuclides from the geopolymer.

In order to better understand radionuclide stability in the geopolymer and potential for migration, we have conducted laboratory-scale leaching experiments relevant to Finnish LILW disposal in short-term (< 6 months) leaching experiments. Here, we follow the geochemical behaviour of key geopolymer components (e.g., Ca, Al, and Si) and assessed the potential for radionuclide mobilization using stable isotopes (Cs, Ce and Eu) as analogues for several radionuclides of interest (¹³⁷Cs, An³⁺ and An⁴⁺) in 4 varying geopolymer matrices compared to ordinary Portland cement as a standard. At regular intervals we sacrifice geopolymer samples to characterize the mineralogical evolution of the geopolymer and waste element chemistry across leaching zones in the waste form.

As a result of these experiments, we expect to have a comprehensive understanding of this wasteform performance and ability to retain radioelements. These data will demonstrate the reliability of the novel geopolymer and may be used to inform the safety case for the long-term storage of LILW.

This work is part of the EURAD PREDIS project.

Acknowledgments: *This project has received funding from the Euratom research and training programme 2019-2020 under Grant Agreement No 945098.*



PA2-4 SOLUBILITY EVALUATION OF THE COPRECIPITATE URANIUM AND PLUTONIUM OXIDE UNDER HYPERALKALINE AND REDUCING CONDITIONS IN THE CONTEXT OF DEEP DISPOSAL OF ILW RADIOACTIVE WASTES

Mathieu Le Meur⁽¹⁾, Tomo Suzuki-Muresan⁽¹⁾, Solange Ribet⁽¹⁾, Catherine Landesman⁽¹⁾
Thomas Verron⁽¹⁾ Anne Piscitelli⁽¹⁾ Bernd Grambow⁽¹⁾

(1) SUBATECH (IMT Atlantique, CNRS/IN2P3, Nantes Université), France

Actinides, such as uranium and plutonium, lead to long-term radiotoxicity in deep nuclear waste disposal [1]. They may be found entrapped in the subsurface of the internal side of the claddings in contact with spent fuel. After treatment and reprocessing, a fraction of U and Pu may constitute a source term in the repository site for intermediate level wastes for example stemming from compacted nuclear fuel claddings from fuel reprocessing, disposed in metallic container within concrete filled disposal cell in a repository in clay rock. In conditions representative of a deep geological repository in clay rock, after the interaction of clay pore water with cement, hyperalkaline solution are expected to form and may contact the waste products. Reducing conditions are imposed by the production of H₂(g) during the corrosion of the metallic container. In these conditions, various processes can occur like corrosion, adsorption, precipitation and transport. Coprecipitation phenomena can also occur and have been studied concerning their effect on the solubility of several chemical components [2, 3]. According to the recommendation of IUPAC, we define coprecipitation as “simultaneous precipitation of a normally soluble component with a host component from the same solution” [4].

The goals and objectives of this study consist in the investigation of the precipitation of UO₂ and the coprecipitation of thorium (Th) and plutonium (Pu) with UO₂(s) as host phase under hyper-alkaline and reducing conditions that mimic conditions of deep geological repository systems. Our working hypothesis, using both liquid and solid characterization is to evaluate the solubility of the U/Pu coprecipitate in hyperalkaline conditions and show that coprecipitation can play a critical role in the retention of long life radionuclides and leads to a high decrease of their concentration in the clay pore water, a potential pathway for transport of soluble radioactive elements.

All the aqueous solutions were prepared with degassed Milli-Q water. The HCl and NaOH stock solutions were prepared in a glove box under an argon atmosphere (O₂ < 0,5 ppm). The experimental procedure consists (1) in the formation of U(IV) from (U(VI)) nitrate solution by precipitating schoepite by adding 0.5 M NaOH, then dissolving the precipitate in 1 M HCl solution. The dissolved U(IV) stock solution was obtained by coulometric reduction (-1 mA, 10h) in the glove box. The pH of this solution was kept lower than 1 (pH: 0.7) to ensure the stability of dissolved U(IV). The precipitation of UO₂ from the U(IV) solution was achieved in the glove box by adding NaOH to reach a pH of 13. The reduction process and the precipitation were followed by UV-visible spectrophotometric measurements performed on a Shimadzu UV-mini 1240 spectrophotometer installed outside the glove box and connected by optical glass fibers directly to the glove box ($\lambda = 350 - 900$ nm). The U(IV) absorption spectrum was measured periodically in order to check the stability of U(IV) solution (Fig. 1). After precipitation, the concentration of U(IV) in the filtrate was measured by ICP-MS.

The next step will consist in the coprecipitation of U(IV) (0.04 M, pH<1) mixed with Th or Pu (4×10⁻⁴ M). We expect to obtain the coprecipitation of about 1% of Th and/or Pu with UO₂ (Th(Th+U) and Pu(Pu+U) at a molar ratio of 0.01). The alkaline solution composition mimics the artificial cement pore water of a fresh cement paste (CEM V/A Rombas, Calcia) including NaOH, KOH, CaO, Na₂SO₄, NaCl.

Colloidal solid phases of UO₂ and the coprecipitates will be characterized by LIBD, TEM, and EXAFS. LIBD is used in order to check the absence of colloids formation during the acidic U (VI) reduction and the presence of colloids after the addition of NaOH / cement solution. The literature shows that the

breakdown probability under constant experimental conditions depends on number density, size and material of colloids [5, 6]. The colloids detection sizes are expected to be as low as 10 nm.

The Extended X-ray Absorption Fine Structure (EXAFS) and X-Ray Absorption Near-Edge Structure (XANES) spectroscopy measurements are scheduled to be performed on the MARS beamline at the SOLEIL synchrotron facility (Saint-Aubin, France). The different spectra will be collected in the fluorescence mode with 13 element Ge detector at ambient temperature at the plutonium LIII edge (18057 eV) and at the uranium LIII edge (17166 eV).

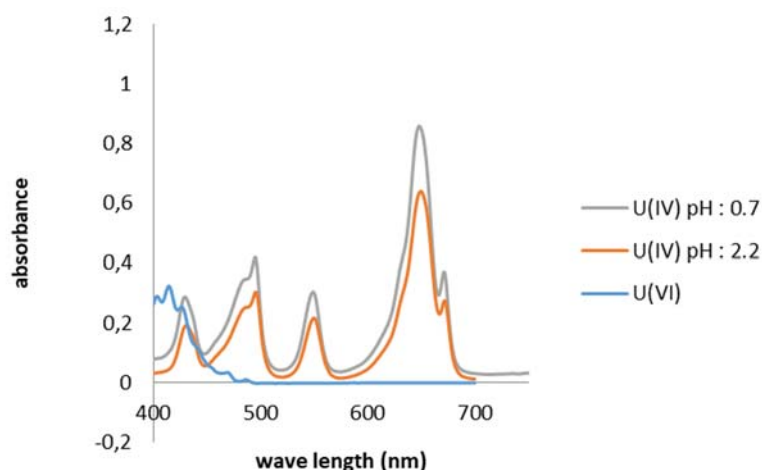


Fig. 1 UV-Vis spectra of U(IV) (blue line); U(VI) at pH 0.7 (grey line) and U(VI) at pH 2.2 (orange line)

Acknowledgements: The authors would like to thank Céline Bailly and Guillaume Blain for their constructive expertise in the realization of this experiment.

References

- [1] Gonzales, E., Na, B.C., Salvatores, M., Zimmerman, C.H., Varaine, F., D'Angelo, A., Schikorr, M., Kuijper, J.C., Coddington, P. and Kim, Y.H. (2006) Physics and safety of transmutation systems - A status report, Nuclear Energy Agency
- [2] van't Hoff, J.H.Z. (1890) *Z. Phys. Chem.* 5, 322
- [3] Roozeboom, H.W.B. (1891) *Z. Phys. Chem.* 8, 504
- [4] International Union of Pure Applied Chemistry: Recommendations on Nomenclature for Contamination Phenomena in Precipitation from Aqueous Solutions. Butterworths (1973) p. 465.
- [5] Kitamori, T., Yokose, K., Sakagami, M. and Sawada, T. (1989). Detection and counting of ultrafine particles in ultrapure water using laser breakdown acoustic method. *JJAP*, 28, 1195.
- [6] Knopp, R., Scherbaum, F. J., and Kim, J. I. (1996). Laser induced breakdown spectroscopy (LIBS) as an analytical tool for the detection of metal ions in aqueous solutions. *Fresenius' j anal. Chem.*, 355,

PA2-5 SOLUBILITY AND SOLID PHASE FORMATION IN THE Nd_2O_3 - EuCl_3 - NdCl_3 - NaCl - $\text{H}_2\text{O}(\text{L})$ SYSTEM

Rama Mohana Rao Dumpala⁽¹⁾, Frank Heberling⁽¹⁾, Xavier Gaona⁽¹⁾, Krassimir Garbev⁽²⁾, Dieter Schild⁽¹⁾, Marcus Altmaier⁽¹⁾, and Horst Geckeis⁽¹⁾

(1) Institute for Nuclear Waste Disposal, Karlsruhe Institute of Technology, Karlsruhe, Germany

(2) Institute for Technical Chemistry, Karlsruhe Institute of Technology, Karlsruhe, Germany

Lanthanides may form mixed oxide phases with other lanthanides, as well as with trivalent actinides. Oxide- and hydroxide phases are primarily expected to control solubility phenomena of actinides and lanthanides under repository conditions [1], thus defining the source term of these elements in safety assessments of nuclear waste repositories. Solubility data and thermodynamic models of individual, binary and mixed lanthanide oxides and hydroxides have been previously reported in the literature [2-3]. However, quantitative descriptions of actinide/lanthanide-hydroxide solid-solution systems are still lacking. As starting point for our planned studies on potential An(III)/Ln(III) solid solutions, we study the characteristics of solubility determining solid phases and related equilibrium concentrations in the Nd/Eu system.

As synthetic pathway, neodymium was taken as solid phase in its oxide form, $\text{Nd}_2\text{O}_3(\text{cr})$, whereas europium was introduced in the system as soluble chloride salt (EuCl_3). In contact with water, $\text{Nd}_2\text{O}_3(\text{cr})$ is known to readily hydrate leading to $\text{Nd}(\text{OH})_3(\text{s})$ within 2-3 weeks [4]. Thus, this combination was expected to provide a dynamic system facilitating the incorporation of Eu(III) into the structure of $\text{Nd}(\text{OH})_3(\text{s})$. All the solubility experiments were carried out at $T = (22 \pm 2)^\circ\text{C}$, $I = 0.1 \text{ M NaCl}$ and $\text{pH}_c = (7.2 \pm 0.2)$. Kinetics of equilibration were studied within 1–70 days at a fixed composition of 1 mM solid $\text{Nd}_2\text{O}_3(\text{cr})$ equilibrated with $\text{EuCl}_3 + \text{NdCl}_3$ (1 mM and 2 mM, respectively) in aqueous solution. In a second set of experiments, three different amounts of $\text{Nd}_2\text{O}_3(\text{cr})$ (0.5–5 mM) were equilibrated with aqueous solutions of constant composition (1 mM $\text{EuCl}_3 + 2 \text{ mM NdCl}_3$), resulting in the systematic variation of the ratio Nd : Eu in the system. All samples were continuously agitated throughout the study. Phase separation was carried out by 10 kD ultrafiltration or centrifugation (6000 rpm for 18 minutes). Total Eu and Nd present in the supernatant as well as in the precipitate (after dilution in HNO_3) were determined by ICP-OES, while the solid phases were characterized by SEM-EDX, XRD and Raman spectroscopy.

After two weeks of equilibration, the pH stabilized and no further adjustments were needed to attain $\text{pH}_c = (7.2 \pm 0.2)$. The concentration of Eu in the aqueous phase decreased with increasing initial $\text{Nd}_2\text{O}_3(\text{cr})$ (Figure 1), which provided indirect evidence on the incorporation of Eu(III) into the structure of the Nd(III) solid.

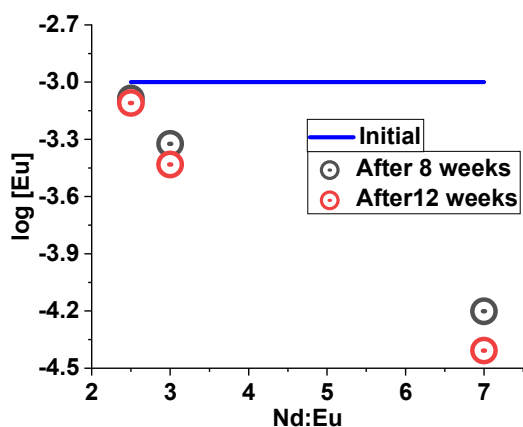


Figure 1: Variation of the aqueous europium concentration as a function of the Nd : Eu ratio in the complete system. Initial concentrations of Nd and Eu in the aqueous phase were kept constant at 0.002 M NdCl_3 and 0.001 M EuCl_3 . All experiments conducted in 0.1 M NaCl solutions at $\text{pH}_c = (7.2 \pm 0.2)$. Solubility samples equilibrated for eight to twelve weeks.

However, SEM-EDX and XRD revealed the formation of two different solid-phases, identified as $\text{Nd}(\text{OH})_3(\text{cr})$ and $(\text{Nd,Eu})(\text{OH})_{2.5}\text{Cl}_{0.5}(\text{H}_2\text{O})_{0.8}(\text{cr})$ (Figure 2), which hinders a direct interpretation of the results assuming the formation of an ideal solid-solution. Diakonov et al. reported that $\text{Nd}_2\text{O}_3(\text{cr})$ transforms to a stable $\text{Nd}(\text{OH})_3(\text{s})$ phase in aqueous solutions [5], and Neck et al. showed that the hydroxide phase remains stable in alkaline conditions in dilute to concentrated chloride media up to 5.0 M NaCl [4]. Aksel'rud and Ermolenko's studies on precipitation of Eu^{3+} at elevated pH in 0.1–2.5 M NaCl media resulted in the formation of Eu(III) hydroxychloride, which eventually transformed to a hydroxide phase over long equilibration periods (> 150 days) [6]. In the present study, the equilibration period considered was 8–12 weeks, so that the hydroxychloride phase could represent a metastable phase. It is interesting to note that Eu(III) is predominantly taken up by the mixed Nd/Eu hydroxychloride phase. Lanthanides form isostructural layered hydroxychlorides. Cell parameters determined in the present work and compared to individual $\text{Nd}(\text{OH})_{2.5}\text{Cl}_{0.5}(\text{H}_2\text{O})_{0.8}(\text{cr})$ and $\text{Eu}(\text{OH})_{2.5}\text{Cl}_{0.5}(\text{H}_2\text{O})_{0.8}(\text{cr})$ phases [7-8] further support the formation of the mixed $(\text{Nd,Eu})(\text{OH})_{2.5}\text{Cl}_{0.5}(\text{H}_2\text{O})_{0.8}(\text{cr})$ phase under present experimental conditions. On-going long-term solubility experiments in combination with advanced spectroscopic techniques (TRLFS) are currently running in order to study possible solid phase transformations and will be discussed in this contribution.

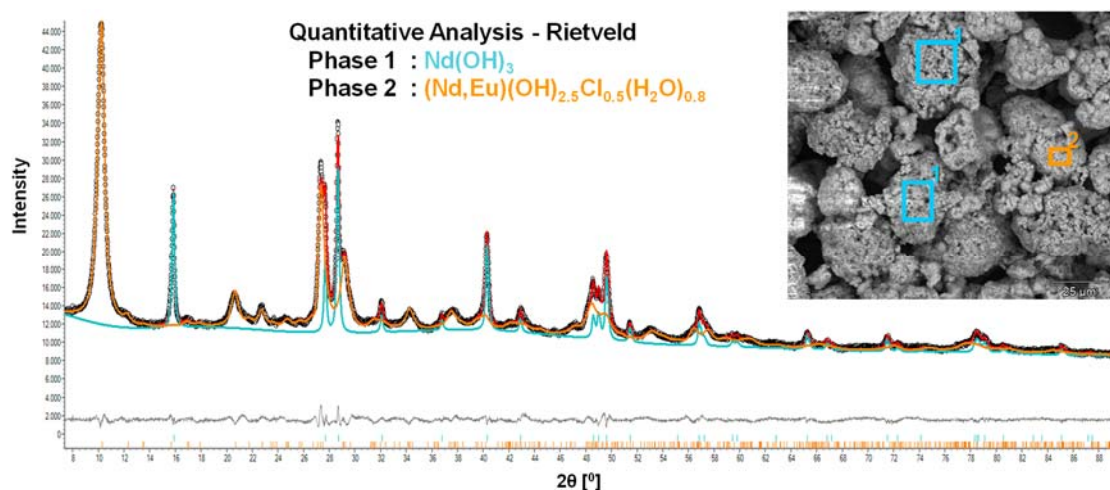


Figure 2: Measured and calculated x-ray diffractogram with quantitative phase analysis of the solid phase obtained in our experiments (0.005 M $\text{Nd}_2\text{O}_3(\text{s})$ equilibrated with 0.002 M NdCl_3 and 0.001 M EuCl_3 in 0.1 M NaCl aqueous solution for six weeks). Insert: SEM-EDX image of the precipitate (Blue colored spot is (Nd, O) enriched, while orange-colored spots are (Nd, Eu, O, Cl) enriched only).

References

- [1] Brown, P. L., Ekberg, C. (2016) Hydrolysis of Metal Ions, Volume 1, Wiley-VCH, Weinheim.
- [2] Fanghänel, Th. and Neck, V. (2002), Pure Appl. Chem., 74: 1895-1907.
- [3] Kobayashi, T. and Sasaki, T. (2020). J. Nucl. Radiochem. Sci. 20: 32-42
- [4] Neck, V., Altmaier, M., Rabung, Th., Lützenkirchen, J., Fanghänel, Th. (2009), Pure Appl. Chem., 81:1555-1568.
- [5] Diakonov, I. I., Tagirov, B. R. and Ragnarsdottir, K. V. (1998), Radiochimica Acta, 81:107-116.
- [6] Aksel'rud, N. V. Ermolenko, V. I. (1961). Russ. J. Inorg. Chem. (Engl. Transl.) 6:397
- [7] Geng, F., Matsushita, Y., Ma, R., Xin, H., Tanaka, M., Izumi, F., Iyi, N., Sasaki, T. (2008) *J. Am. Chem. Soc.* 130 (48): 16344-16350
- [8] Geng, F., Xin, H., Matsushita, Y., Ma, R., Tanaka, M., Izumi, F., Iyi, N. and Sasaki, T. (2008), Chemistry – A European Journal, 14: 9255-9260

PA2-6 STRUCTURE AND PROPERTIES OF CRYSTALLINE CERAMIC PHASES CONTAINING ACTINIDES – FROM BULK TO THE MOLECULAR LEVEL

Nina Huittinen⁽¹⁾, Luiza Braga Ferreira dos Santos⁽¹⁾, Sara E. Gilson⁽¹⁾, Gabriel L. Murphy⁽²⁾, Selina Richter⁽¹⁾, Karin Popa⁽³⁾, Octavian Valu⁽³⁾, Volodymyr Svitlyk⁽¹⁾, Christoph Hennig⁽¹⁾

(1) Helmholtz-Zentrum Dresden-Rossendorf, Institute of Resource Ecology, Bautzner Landstraße 400, 01328 Dresden, Germany

(2) Institute of Energy and Climate Research: Nuclear Waste Management and Reactor Safety, Forschungszentrum Jülich, Wilhelm-Johnen-Straße, 52425 Jülich, Germany

(3) European Commission, Joint Research Centre, P.O. Box 2340, 76125 Karlsruhe, Germany

Spent nuclear fuel (SNF) from nuclear reactors operating worldwide will be disposed of directly or after reprocessing. In the latter case, generation of specific waste streams, *e.g.* minor actinide-containing waste, may require immobilization in durable, crystalline waste forms. Such candidate phases for the immobilization of (minor) actinides are various Zr(IV)-bearing solid phases like pyrochlore and zirconia [1, 2]. In addition to their use as potential ceramic waste matrices or inert matrix fuels for *e.g.* the incineration of waste plutonium, Zr-bearing phases, especially ZrO₂, may be of importance as corrosion products in the dissolution of Zircaloy cladding material of SNF rods [3]. ZrO₂ is monoclinic phase ($P2_1/c$) at ambient conditions, and transforms into tetragonal ($P4_2/nmc$) and cubic phases ($Fm\bar{3}m$) at high temperatures of around 1200 °C and 2370 °C, respectively. However, particle size effects, the incorporation of foreign ions such as the actinides, as well as high radiation fields are also known to influence the stability fields of the polymorphs.

This contribution provides an overview of recent studies addressing the structure, properties and the radiation tolerance of Zr(IV)-based solid phases containing actinides and their surrogates from the lanthanide series. Synthesis strategies and structural transformations taking place as a result of *An*(IV) or *Ln*(IV) incorporation in ZrO₂ will be presented. Combining bulk structural characterization using powder X-ray diffraction (PXRD) with spectroscopic investigations, differences between the host- and dopant environments can be explored. In addition, radiation damage studies combining external heavy-ion irradiation of inactive *Ln*-doped materials and *in situ* self-irradiation of recently synthesized ²⁴¹Am-doped Zr(IV)-phases with monoclinic (see Figure 1), cubic defect fluorite and pyrochlore structures, will be addressed.

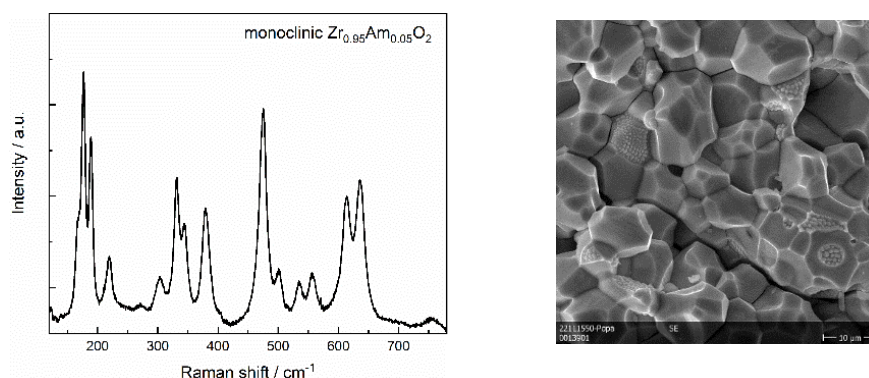


Figure 1: Raman spectrum (left) and SEM image (right) of monoclinic ZrO₂ containing 5 mol% ²⁴¹Am, collected immediately after synthesis.

The aim of these studies is to advance the understanding of how radioactive dopants affect the structure and properties of Zr(IV)-bearing crystalline solid phases, especially in high radiation fields.

References

- [1] Lumpkin, G. R. (2006) Ceramic waste forms for actinides. *Elements*, 2: 365-372
- [2] Ewing, R. C., Weber, W. J., Lian, J. (2004) Nuclear waste disposal—pyrochlore ($A_2B_2O_7$): Nuclear waste form for the immobilization of plutonium and “minor” actinides. *J. Appl. Phys.* 95: 5949-5971
- [3] Cox, B. (2005) Some thoughts on the mechanisms of in-reactor corrosion of zirconium alloys. *J. Nucl. Mater.* 336: 331-368.

PA3-6 INVESTIGATION OF ACTINIDE SPECIATION AND COMPLEXATION WITH SMALL ORGANIC LIGANDS USING CE-ICP-MS

Tobias Reich, Tamara Kutyma, Janik Lohmann, Janina Stietz

Johannes Gutenberg-Universität Mainz, Department of Chemistry, Nuclear Chemistry, 55099 Mainz, Germany

The coupling of capillary electrophoresis (CE) with inductively coupled plasma mass spectrometry (ICP-MS) is a powerful experimental tool for studying the speciation of actinides at environmentally relevant concentrations. CE-ICP-MS benefits from the high separation capability of CE in combination with the possibility of multielement analysis at trace concentrations using ICP-MS. This presentation will highlight the application of CE-ICP-MS for studying the speciation of actinides and their complexation with acetate and gluconate.

The electrophoretic mobilities (μ_e) of ^{232}Th , ^{238}U , ^{237}Np , ^{239}Pu , and ^{241}Am in different oxidation states have been determined by CE-ICP-MS at concentrations of 1×10^{-7} M in 1 M HClO_4 [1]. For the actinides U–Pu, the μ_e follow the order $\text{An(III)} > \text{An(VI)} > \text{An(V)} > \text{An(IV)}$. The observed systematic trends in the μ_e values have been rationalized by speciation calculations and corresponding averaged effective charges of the actinides in the background electrolyte.

CE-ICP-MS was used to determine the stability constants of the acetate complexation of $^{241}\text{Am(III)}$, $^{232}\text{Th(IV)}$, $^{237}\text{Np(V)}$, and $^{238}\text{U(VI)}$ [2]. It was possible to investigate these actinides simultaneously at concentrations in the range of 5×10^{-8} M to 1×10^{-6} M. The stability constants that were extrapolated to zero ionic strength agree with the available literature data obtained at higher actinide concentrations. For U(VI) and Am(III) three successive acetate complexes were observed and for Th(IV) up to five. In contrast to literature data, only the formation of a 1:1 complex of Np(V) with acetate could be confirmed. The formation of a negatively charged Np(V) complex with more than one acetate ligand could be ruled out.

The complexation of $^{232}\text{Th(IV)}$ with gluconate (GLU) at pH 10 and 0.1 M ionic strength (NaClO_4) in the absence and presence of Ca^{2+} was studied by CE-ICP-MS [3]. The concentrations were 4×10^{-7} M Th(IV) and 1×10^{-2} M GLU. The electrophoretic mobility of Th(IV) in solutions without Ca^{2+} and GLU was almost zero, indicating the predominance of the $[\text{Th}(\text{OH})_4]_{\text{aq}}$ species. Upon addition of GLU, the formation of negatively charged ternary Th-OH complexes with GLU was indicated by the measured negative mobility of $\mu_e = -(2.72 \pm 0.09) \times 10^{-4}$ $\text{cm}^2/(\text{Vs})$. In the presence of 1×10^{-2} M Ca^{2+} , the electrophoretic mobility of the Th-OH-GLU species changed to $\mu_e = -(0.65 \pm 0.04) \times 10^{-4}$ $\text{cm}^2/(\text{Vs})$. This indicates the association of Ca^{2+} to the Th(IV)-OH-GLU complex species. The calculated complexation constant for this Th(IV) species and results of similar CE-ICP-MS measurements with $^{239}\text{Pu(IV)}$ will be reported as well.

A short outlook on future CE-ICP-MS studies of actinides related to the long-term safety analysis for future nuclear waste repositories will be given at the end of this presentation.

Acknowledgements: *This work was funded in part by the European Union's Horizon 2020 Research and Innovation Programme (CORI project, no. 847593) and by the German Federal Ministry for Economic Affairs and Energy (BMWi) within the GRaZ II project 02E11860A.*

References

- [1] Willberger, C., Amayri, S., Häußler, V., Scholze, R. and Reich, T. (2019). Investigation of the electrophoretic mobility of the actinides Th, U, Np, Pu, and Am in different oxidation states. *Anal. Chem.* 91: 11537-11543
- [2] Willberger, C., Leichtfuß, D., Amayri, S. and Reich, T. (2019). Determination of the stability constants of the acetate complexes of the actinides Am(III), Th(IV), Np(V), and U(VI) using capillary electrophoresis-inductively coupled plasma mass spectrometry. *Inorg. Chem.* 58: 4851-4858
- [3] Dettmann, S., Huittinen, N.M., Jahn, N., Kretschmar, J., Kumke, M.U., Kutyma, T., Lohmann, J., Reich, T., Schmeide, K., Shams Aldin Azzam, S., Spittler, L. and Stietz, J. (2023). Influence of gluconate on the retention of Eu(III), Am(III), Th(IV), Pu(IV), and U(VI) by C-S-H (C/S = 0.8). *Frontiers Nucl. Engineering.* in press

PA3-7 INVESTIGATION OF THE CARBONATE COMPLEXATION OF ACTINIDES AND THE INFLUENCE OF ALKALI CATIONS USING CE-ICP-MS

Janik Lohmann, T. Reich

Johannes Gutenberg-Universität Mainz, Department of Chemistry, Nuclear Chemistry, 55099 Mainz, Germany

For the safety analysis of a high-level nuclear waste repository, it is necessary to investigate the behaviour of the actinides under environmentally relevant conditions. Processes like actinide diffusion and sorption are strongly dependent on the actinide species present. Therefore, it is important to have a thorough understanding of the complexation of actinides, including thermodynamic constants and molecular structures.

Carbonate is together with hydroxide one of the most environmentally relevant ligands regarding actinides. The corresponding complex formation constants have been previously studied using various spectroscopic methods or by solubility experiments. Most of these experiments were carried out at significantly higher actinide concentrations than expected in the case of actinide leakage into the environment.

To investigate the complexation behaviour of actinides at trace-level, some previous studies [1][2] have successfully used the coupling of capillary electrophoreses with inductively coupled plasma mass spectrometry (CE-ICP-MS). In the presented work, the complexation behaviour of $^{241}\text{Am(III)}$, $^{232}\text{Th(IV)}$, $^{237}\text{Np(V)}$ and $^{238}\text{U(VI)}$ with carbonate was investigated by CE-ICP-MS. These four actinides were chosen based on their stable oxidation state.

All experiments were conducted in 0.1 M alkali carbonate solution (Li^+ , Na^+ and K^+). The concentration of the free carbonate ligand was varied by adjusting the pH value with HCl and the corresponding alkali hydroxide. The ionic strength was adjusted to 0.37 M with the corresponding alkali chloride. All actinides were measured simultaneously, and the actinide concentrations varied between 2×10^{-8} M and 1×10^{-6} M.

The CE-ICP-MS measurements were carried out with a 50 cm long fused silica capillary at 10 kV. 2-Bromopropane was used as EOF marker. The determination of the effective electrophoretic mobilities, μ_{eff} , as well as the evaluation of the complex formation constants were performed as described by Willberger et al.[1].

Clear progressions of μ_{eff} as a function of pH and carbonate concentration were observed for all actinides. Since μ_{eff} is proportional to the average ionic charge of the actinide, the progressions of μ_{eff} shown in Figure 1 are compared to the calculated average charge of the corresponding actinide using known thermodynamic data.

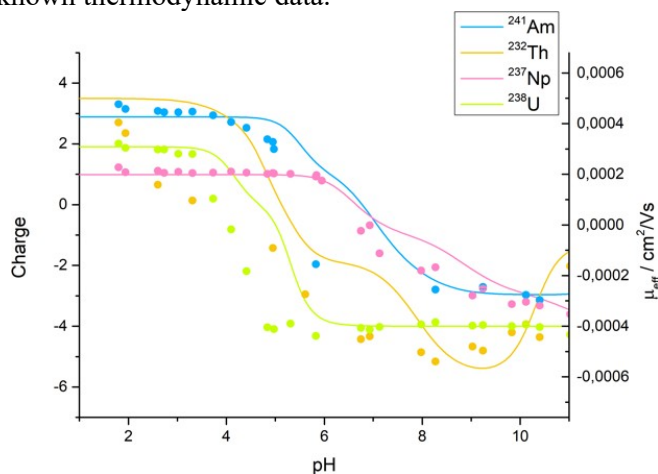


Figure 1 Plot of charge distribution and measured mobilities μ_{eff} of Am(III), Th(IV), Np(V), and U(VI) in Na^+ containing solutions versus pH.

By modelling the measured μ_{eff} values over the entire pH range from 2 to 11, carbonate complex formation constants could be determined for all actinides studied. For the Na^+ containing electrolyte, these values are summarized in Table 1.

Table 1 Experimentally determined complex formation constants of the actinide-carbonate complexes at 25°C and $I = 0 \text{ M}$ for Na^+ containing solutions (without considering the $\text{Na}[\text{An}(\text{CO}_3)_3]^{z-5}$ complex).

	Am(III)	Th(IV)	Np(V)	U(VI)
$\log\beta^1_0$	8.7 ± 0.2	16.1 ± 0.3	4.99 ± 0.06	10.9 ± 0.1
$\log\beta^2_0$	15.2 ± 0.2	28.9 ± 0.3	6.9 ± 0.2	18.8 ± 0.2
$\log\beta^3_0$	16.2 ± 0.4	35.6 ± 0.4	5.9 ± 0.2	25.7 ± 0.1
$\log\beta^4_0$		39.4 ± 0.7		
$\log\beta^5_0$		37.5 ± 1.5		

Complex formation constants for the 1:1 to 1:4 complexes of Th(IV) could be determined experimentally for the first time. A comparison to the semi-empirically predicted values by Neck et al. [3] deems complex formation constants plausible. The experimentally determined complex formation constants for Am(III), Np(V) and U(VI) are within the range of literature values. However, it was observed that with increasing charge of the complex, the experimentally determined constant is larger than those in the literature.

This effect is greatest for the $[\text{UO}_2(\text{CO}_3)_3]^{4-}$ complex. Together with the observed low mobility of this complex, a charge balance with an alkali cation is assumed. Such an association has already been discussed in the literature^[4]. Assuming the formation of $\text{Me}[\text{UO}_2(\text{CO}_3)_3]^{3-}$ complexes, the corresponding constants were determined. The strength of the complexation decreases from Li^+ to K^+ . According to the speciation for $\text{pH} < 6$, the $\text{Li}[\text{UO}_2(\text{CO}_3)_3]^{3-}$ complex should be present at 100%, the $\text{Na}[\text{UO}_2(\text{CO}_3)_3]^{3-}$ complex at about 80% and the $\text{K}[\text{UO}_2(\text{CO}_3)_3]^{3-}$ only at about 60%. The decrease in complexation strength from Li^+ to K^+ was also observed in the literature [4].

In summary, the complex formation constants of the actinide carbonate systems were determined by CE-ICP-MS. A significant effect of the alkali cation on the U(VI) carbonate complexation was observed. Further experiments focusing on the effect of counter ions will be presented.

Acknowledgements: Funding from the Federal Ministry for Economic Affairs and Energy (BMWi) under contract number 02E11860A, and from the European Union's Horizon 2020 project EURAD (WP CORI), EC Grant agreement no. 847593, is acknowledged.

References

- [1] Willberger, C. et al. (2019). Determination of the Stability Constants of the Acetate Complexes of the Actinides Am(III), Th(IV), Np(V), and U(VI) Using Capillary Electrophoresis-Inductively Coupled Plasma Mass Spectrometry. *Inorg. Chem.* 58: 4851–4858
- [2] Aupias, J. et al. (2020). The NpV and PuV Carbonate Systems: Thermodynamics and Coordination Chemistry. *Eur. J. Inorg. Chem.* 2: 216-225.
- [3] Neck, V. and Kim, J. I. (2000). An electrostatic approach for the prediction of actinide complex formation constants with inorganic ligands-application to carbonate complexes. *Radiochimica Acta* 88: 815-822.
- [4] Philippini, V. et al. (2008). Evidence of different stoichiometries for the limiting carbonate complexes across the lanthanide(III) series: a capillary electrophoresis-mass spectrometry study. *Electrophoresis* 29: 2041-2050.

PA3-8 COMPLEXATION OF NI(II) WITH CITRATE IN CEMENTITIOUS SYSTEMS: THERMODYNAMIC DESCRIPTION

O. Almendros-Ginestà¹, S. Duckworth², T. Missana¹, M. Altmaier², X. Gaona²

¹CIEMAT, Unit Physical chemistry of actinides and fission products, Madrid (Spain)

²Karlsruhe Institute of Technology, Institute for Nuclear Waste Disposal (Germany)

e-mail: oscar.almendros@ciemat.es; xavier.gaona@kit.edu

Cementitious materials are widely used in repositories for low and intermediate level waste (L/ILW) for the construction of galleries and vaults, but also as a component for the waste stabilization. These materials impose highly alkaline pH conditions to the contacting water. ⁵⁹Ni ($t_{1/2} = 7.5 \cdot 10^4$ a) and ⁶³Ni ($t_{1/2} = 96$ a) are present in certain waste streams of L/ILW and can be important contributors to the radiotoxicity in such repositories. Citrate (cit) is used as decontamination agent, and is also present as additive in some cement formulations. Citrate forms very stable complexes with metal ions due to its three carboxylate functionalities, in addition to an alcohol group that can participate also in chelate formation. In the presence of Ca, citrate forms the sparingly soluble salt $\text{Ca}_3(\text{Cit})_2 \cdot 4\text{H}_2\text{O}(\text{s})$, which decreases the ligand concentration available for complexation. Four aqueous Ni(II)-cit complexes are currently selected in the NEA-TDB, *i.e.* $\text{Ni}(\text{H}_2\text{cit})^+$, $\text{Ni}(\text{Hcit})(\text{aq})$, $\text{Ni}(\text{cit})^-$ and $\text{Ni}(\text{cit})_2^{4-}$ [1]. In the alkaline to hyperalkaline conditions defined by cementitious systems, the formation of ternary complexes $\text{Ni}(\text{OH})_x(\text{cit})_y^{(2-x-3y)}$ (or $\text{Ni}(\text{cit-H})_z^{(2-4z)}$, where cit-H corresponds to a citrate ligand with deprotonated alcohol group) are expected. Although a number of previous studies reported the formation of such ternary complexes [2-3, among others], evidences were considered insufficient by the NEA-TDB, thus resulted in the selection of Ni(II)-cit binary complexes uniquely. Moreover, the formation of complexes with high negative charges in hyperalkaline conditions may result in strong interactions with Ca^{2+} ions and thus in the formation of quaternary complexes Ca-Ni(II)-OH-cit, even if concentrations of cit^{3-} and Ca^{2+} are limited by solubility. In this context, this study aims at investigating the complexes of nickel and citrate forming in alkaline to hyperalkaline conditions, both in the absence and presence of Ca^{2+} , and deriving the corresponding thermodynamic properties.

Undersaturation solubility experiments were conducted using commercial $\beta\text{-Ni}(\text{OH})_2(\text{cr})$. Independent batch samples were prepared in 0.1, 0.5, 1.0 and 3.0 M NaCl–NaOH–Na₃Cit solutions with $1 \cdot 10^{-4} \text{ M} \leq [\text{Na}_3\text{Cit}] \leq 0.1 \text{ M}$ and $9.0 \leq \text{pH}_m \leq 13.5$, with $\text{pH}_m = -\log [\text{H}^+]$ and $[\text{H}^+]$ in molal units. Additional solubility series were prepared in 0.1, 1.0 and 3.0 M NaCl–NaOH–Na₃Cit solutions with $[\text{Na}_3\text{Cit}] = 1 \cdot 10^{-3} \text{ M}$, $[\text{Ca}] = 2 \cdot 10^{-2} \text{ M}$ and $9.0 \leq \text{pH}_m \leq 12.5$. The values of pH_m and $[\text{Ni}]$ (after 10 kD ultrafiltration) were monitored at regular time intervals for up to 180 days. The starting material as well as selected solid phases after attaining equilibrium conditions were characterized by XRD.

Solid phase characterization confirmed that $\beta\text{-Ni}(\text{OH})_2(\text{cr})$ is the only phase controlling the solubility of Ni(II) in the investigated systems, and that $\text{Ca}_3(\text{Cit})_2 \cdot 4\text{H}_2\text{O}(\text{s})$ did not precipitate in the systems containing Ca. In the absence of Ca, a clear increase in the solubility with respect to citrate-free systems is observed in less alkaline conditions ($\text{pH}_m \leq 10.5\text{--}11$, depending upon ionic strength). The slope of the solubility curves in this region predominantly follows a slope of ≈ -2 , although deviations are observed at the highest $[\text{Ni}]$, possibly due to slow equilibration kinetics. This slope is consistent with the solubility reactions $\beta\text{-Ni}(\text{OH})_2(\text{cr}) + 2\text{H}^+ + x\text{cit}^{3-} \leftrightarrow \text{Ni}(\text{cit})_x^{2-3x} + 2\text{H}_2\text{O}(\text{l})$, with $x = 1\text{--}2$. For the same pH_m -region, a significantly lower increase in solubility is observed in the presence of Ca. This effect is predicted by thermodynamic calculations using the NEA-TDB data selection, and results from the significant decrease of $[\text{cit}]_{\text{free}}$ due to complexation with Ca. Above $\text{pH}_m \approx 11\text{--}11.5$, solubility calculations predict the predominance of the aqueous complex $\text{Ni}(\text{OH})_2(\text{aq})$ and a solubility limit of $[\text{Ni}] \approx 10^{-7.6} \text{ M}$, even at high ligand concentrations. Instead, a clear increase of the solubility is observed, both in the absence and presence of Ca. These observations support the formation of ternary and quaternary complexes,

Ni(II)-OH-cit and Ca-Ni(II)-OH-cit, possibly involving the participation of citrate ligands with deprotonated alcohol group, cit_H. The stoichiometry and stability of these complexes will be discussed in this contribution, as well as the implications for the retention of nickel in cementitious systems.

Acknowledgments: *This project has received funding from the European Union's Horizon 2020 research and innovation program under grant agreement No 847593 (WP CORI) and the R+D Spanish national plan ARNO (PID2019-106398GB-I00). O.A.-G. acknowledges funding from the EURAD mobility action for his research stay at KIT-INE.*

References

- [1] Hummel, W., et al. (2005) Chemical thermodynamics of compounds and complexes of U, Np, Pu, Am, Tc, Se, Ni and Zr with selected organic ligands. NEA. OECD Publishing, Paris.
- [2] REF within NEA-TDB
- [3] REF within NEA-TDB

PA3-9 COMPLEXATION OF NEPTUNIUM(V) WITH AQUEOUS PHOSPHATE USING A DUAL EXPERIMENTAL AND QUANTUM CHEMICAL APPROACH

Eya Miladi^{(1),(2)}, Florent Real⁽¹⁾, Valérie Vallet⁽¹⁾, Norbert Jordan⁽²⁾, Nina Huittinen⁽²⁾

(1) *Université de Lille, CNRS, UMR 8523 – PhLAM – Physique des Lasers Atomes et Molécules, F-59000 Lille, France*

(2) *Helmholtz-Zentrum Dresden-Rossendorf, Institute of Resource Ecology, Bautzner Landstraße 400, 01328 Dresden, Germany*

Understanding and quantifying the chemistry of actinides with strong complexing ligands found in the environment is of key importance for predicting their mobility in the subsurface, especially with respect to the safety of high-level nuclear waste disposal. Phosphate ligands are present in the environment as they originate from the natural decomposition or microbially mediated solubilization processes of phosphate containing rocks and minerals. They can also be produced by anthropogenic activities such as fertilizers spread on the fields or phosphate-based detergents. Furthermore, phosphates are constituents of glasses and ceramics that may be used to immobilize high-level wastes.

Current thermodynamic databases contain very little data on actinide-phosphate complexes [1]. For the trivalent actinide curium, a recent study combining luminescence spectroscopy, thermodynamics, and quantum chemical (QC) calculations could unambiguously establish the formation of 1:1 and 1:2 phosphate complexes with the H_2PO_4^- ligand [2]. Complexation constants for both species were derived and extrapolated to standard conditions using the specific ion interaction theory. By combining the data obtained in the luminescence spectroscopic investigations, such as the crystal-field splitting of the emitting excited states and the luminescence lifetimes, with quantum chemical calculations, the coordination number of the complexes could be determined. At room temperature, both the 1:1 and 1:2 complexes are coordinated by 9 ligands. At elevated temperature, only the 1:1 complex retains a coordination number of 9, while one water molecule is released from the 1:2 complex, thereby reducing its coordination number to 8.

In this study, a similar combined experimental and computational approach will be applied to bridge the gaps in the databases for neptunium(V)-phosphate complexes. The complexation reaction will be studied with UV-vis and infrared (IR) spectroscopies at varying ionic strengths and temperatures under acidic pH conditions. Thereby, complexation constants and thermodynamic parameters for Np(V) aqua ion with phosphate can be derived for the formed Np(V)- H_2PO_4^- complex(es) (Figure 1). However, the experimental data alone, do neither hold information on the coordination of phosphate to the NpO_2^+ cation (mono or bidentate binding), nor on the overall coordination number. This calls for relativistic QC calculations that will help characterizing the stoichiometry and geometries of the complexes. Indeed, QC methods can quantify the relative stability of these structures as well as the complexation strengths with aqueous phosphate through potential change of the coordination number with increasing temperature. The calculated vibrational frequency supports the assignment of bands within the measured IR spectra. In addition, the electronic structures at fundamental and excited states will be computed in order to predict the absorption bands of Np(V) – phosphate complexes in acidic solution. Ultimately, by using the quantum theory of atoms in molecules (QTAIM), the topology of the neptunyl-ligand bonds can be scrutinized to i) discuss the evolution of its character as additional phosphate ligands bind neptunyl and ii) to complement the evolution of the complexation constants determined experimentally.

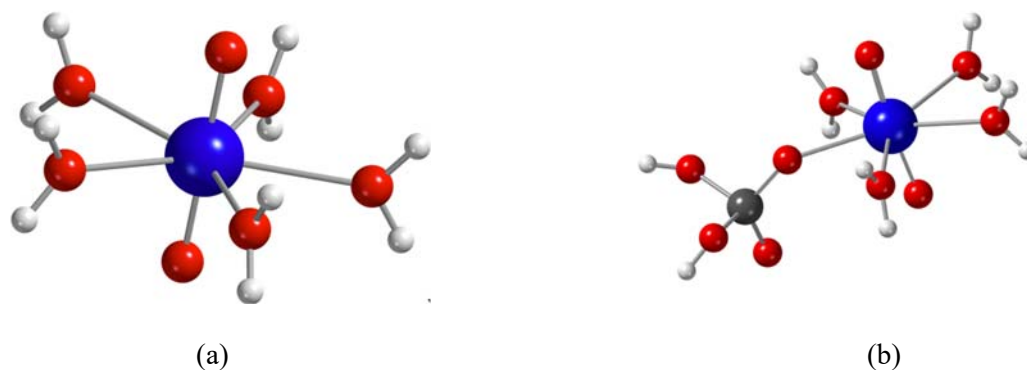


Figure 1. Optimized structures of $[NpO_2(H_2O)_5]^+$ (a) and $[NpO_2(H_2PO_4)(H_2O)_4]$ (b).

References

- [1] Grenthe, I. Gaona, X. Plyasunov, A. Rao, L. Runde, W.H. Grambow, B. Konings, R.J.M. Smith, A.L. Moore, E.E. (2020). Second Update on the Chemical Thermodynamics of Uranium, Neptunium, Plutonium, Americium and Technetium. Chemical Thermodynamics Volume 14, OECD Publications, Paris.
- [2] Huittinen, N., Jessat, I., Réal, F., Vallet, V., Starke, S., Eibl, M., and Jordan, N. (2021). Revisiting the complexation of Cm(III) with aqueous phosphates: new insights from luminescence spectroscopy and ab initio simulations. *Inorg. Chem.* 60:10656–10673.

PA3-10 LUMINESCENCE SPECTROSCOPIC INVESTIGATIONS OF U(VI) COMPLEXATION WITH AQUEOUS SILICATES AT (HYPER)ALKALINE CONDITIONS

Chengming Shang(1), Hanna Oher (2), Sarah Duckworth (1), Robert Polly (1), Andrej Skerencak- Frech (1), Marcus Altmaier (1), Xavier Gaona (1)

(1) Institute for Nuclear Waste Disposal (INE), Karlsruhe Institute of Technology (KIT), Germany

(2) Institut des Sciences Chimiques de Rennes (ISCR), Université de Rennes, France

Uranium is one of the main constituents in spent nuclear fuel (SNF), and thus will be present in large inventories in underground repositories for the disposal of high-level radioactive waste. The ubiquitous presence of silicon in the environment in different forms of monomeric, polymeric or colloidal silicate species has entered into scientific considerations relevant in the context of clay formations as well as for underground repository concepts involving cementitious materials. In vitrified wastes, the dissolution of borosilicate glasses is an additional source of silicon potentially interacting with radionuclides. Orthosilicic acid, H_4SiO_4 , is known to dominate the aqueous speciation of Si over a wide pH range below $\text{pH} \approx 9$. The formation of the complex $\text{UO}_2\text{OSi}(\text{OH})_3^+$ has been reported in acidic pH conditions using different experimental methods.¹⁻⁹ In alkaline to hyperalkaline systems, the interaction of U(VI) with H_3SiO_4^- and $\text{H}_2\text{SiO}_4^{2-}$ may trigger the formation of stable complexes of the type $\text{UO}_2(\text{OH})_x\text{OSi}(\text{OH})_{3-1-x}$ or $\text{UO}_2(\text{OH})_y\text{O}_2\text{Si}(\text{OH})_{2-y}$, which have been rarely studied in the literature.

In this work, the complexation of U(VI) with silicate was investigated at three pH values, *i.e.* 9.2, 10.5 and 11.5 by laser-induced fluorescence spectroscopy. The TRLFS measurements were collected with a pulsed laser Nd:YAG to excite uranium at 266 nm. Fluorescence spectra were recorded in the 440-610 nm range. The U(VI) concentration was fixed at $1 \cdot 10^{-6}$ M at pH 9.2 and 10.5 and $5 \cdot 10^{-6}$ M at 11.5. The silicon concentration was varied below the solubility limit of amorphous silica and the ionic strength was kept constant at 0.05 M NaNO_3 . Spectroluminescence titration of Si was performed in an Ar glovebox to avoid the formation of uranyl carbonate complexes. Ultracentrifugation was applied to exclude U-Si particles being even smaller than 10 kD, notwithstanding the experiments were designed to minimize the precipitation of any U(VI) solid phase (*e.g.* boltwoodite, weeksite, or $\text{Na}_2\text{U}_2\text{O}_7 \cdot \text{H}_2\text{O}(\text{cr})$). The polymerization effects of silicic acid were minimized by excluding samples with a fraction of monomeric silicate acid $< 90\%$, as determined with molybdate-method and ICP-OES. The luminescence properties of $\text{UO}_2(\text{OH})_2\text{SiO}(\text{OH})_3^-$ and $\text{UO}_2(\text{OH})_2\text{SiO}_2(\text{OH})_2^{2-}$ complexes were additionally investigated by means of relativistic density functional theory (DFT) and its time-dependent (TD-DFT) extension.

The stoichiometry of the complexes $\text{UO}_2(\text{OH})_2\text{SiO}(\text{OH})_3^-$ and $\text{UO}_2(\text{OH})_2\text{SiO}_2(\text{OH})_2^{2-}$ was confirmed by slope analysis of TRLFS data and quantum chemical calculations. Conditional equilibrium constants determined at $I = 0.05$ M NaNO_3 from TRLFS data were corrected to infinite dilution using the Davies equation. The $\log_{10}\beta^\circ(\text{UO}_2(\text{OH})_2\text{SiO}(\text{OH})_3^-) = -(17.53 \pm 0.40)$ determined at pH 9.2 and 10.5 is in good agreement with a previous value obtained from sorption experiments.¹⁰ For the first time, we report $\log_{10}\beta^\circ(\text{UO}_2(\text{OH})_2\text{SiO}_2(\text{OH})_2^{2-}) = -(28.57 \pm 0.20)$, although this species becomes predominant only within a narrow pH-range around ≈ 1 and high silicate concentrations. The characteristic decay times were determined to be (12.2 ± 2.4) μs for $\text{UO}_2(\text{OH})_2\text{SiO}(\text{OH})_3^-$ and (25.4 ± 2.2) μs for $\text{UO}_2(\text{OH})_2\text{SiO}_2(\text{OH})_2^{2-}$. Luminescence spectral profiles and peak positions do not show any change with increasing silicate concentration by peak decomposition.

Thermodynamic data derived in this work from TRLFS data provide important insights on the speciation of U(VI) in cementitious environments of relevance in the context of nuclear waste disposal (see figure). This predominance diagram includes also typical [Si] experimentally measured in cement systems, shown by symbols, including calcium silicate hydrate (C-S-H) phases with different Ca:Si ratios. Thick grey line corresponds to the Si concentration calculated with the CASH+ model¹¹. The hydrolysis species $\text{UO}_2(\text{OH})_4^{2-}$ dominates in the hyperalkaline conditions defined by the degradation stages I and II of cement. In the early phase of the cement degradation stage III, characterized by C-S-H with high

Ca:Si ratios and low [Si], $\text{UO}_2(\text{OH})_3^-$ prevails. On the other hand, the ternary complex $\text{UO}_2(\text{OH})_2\text{SiO}(\text{OH})_3^-$ becomes predominant in the higher [Si] characteristic of C-S-H phases with low Ca:Si ratio. The predominance of the complex $\text{UO}_2(\text{OH})_2\text{SiO}_2(\text{OH})_2^{2-}$ requires higher Si concentrations, which cannot be achieved in the presence of Ca due to the formation of C-S-H phases.

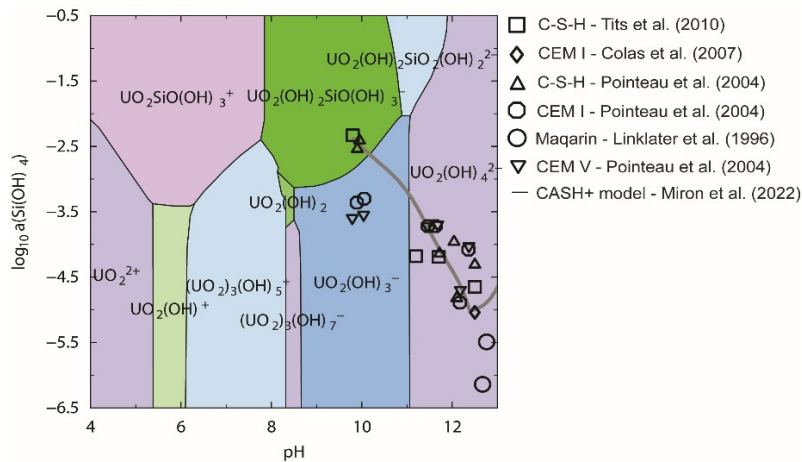


Figure 1: Predominance plots for the U(VI)-Si-H₂O(l) system were constructed with ThermoChimie considering the newly determined $\log 10\beta^\circ(\text{UO}_2(\text{OH})_2\text{SiO}(\text{OH})_3^-)$ and $\log 10\beta^\circ(\text{UO}_2(\text{OH})_2\text{SiO}_2(\text{OH})_2^{2-})$.

Acknowledgements: This work is partly funded by the BMWK within the GraZ II project (contract number 02E11860C).

References

- [1] Lösch, H., Raiwa, M., Jordan, N., Steppert, M., Steudtner, R., Stumpf, T., and Huittinen, N. (2020) Temperature-dependent luminescence spectroscopic and mass spectrometric investigations of U(VI) complexation with aqueous silicates in the acidic pH-range, *Environment international* 136, 105425.
- [2] Moll, H., Geipel, G., Brendler, V., Bernhard, G., and Nitsche, H. (1998) Interaction of uranium(VI) with silicic acid in aqueous solutions studied by time-resolved laser-induced fluorescence spectroscopy (TRLFS), *J Alloy Compd* 271-273, 765-768.
- [3] Satoh, I., and Choppin, G. R. (1992) Interaction of Uranyl(VI) with Silicic Acid, *Radiochimica Acta* 56, 85-88.
- [4] Jensen, M. P., and Choppin, G. R. (1998) Complexation of Uranyl(VI) by Aqueous Orthosilicic Acid, *Radiochimica Acta* 82, 83-88.
- [5] Hrnccek, E., and Irlweck, K. (1999) Formation of Uranium(VI) Complexes with Monomeric and Polymeric Species of Silicic Acid, *Radiochimica Acta* 87, 29-36.
- [6] Pathak, P. N., and Choppin, G. R. (2007) Silicate complexation of NpO_2^+ ion in perchlorate media, *Journal of Radioanalytical and Nuclear Chemistry* 274, 3-7.
- [7] Yusov, A. B., and Fedoseev, A. M. (2005) A Spectrophotometric Study of the Interaction of Uranyl Ions with Orthosilicic Acid and Polymeric Silicic Acids in Aqueous Solutions, *Radiochemistry* 47, 345-351.
- [8] Saito, T., Aoyagi, N., and Kimura, T. (2015) Time-resolved laser-induced fluorescence spectroscopy combined with parallel factor analysis: a robust speciation technique for UO_2^{2+} , *Journal of Radioanalytical and Nuclear Chemistry* 303, 1129-1132.
- [9] Porter, R. A., and Weber, W. J. (1971) The interaction of silicic acid with iron(III) and uranyl ions in dilute aqueous solution, *J. Inorg. Nucl. Chem.* 33, 2443-2449.
- [10] Lösch, H. (2020) Spectroscopic studies on the complexation and incorporation of actinides: Uranium(VI) Complexation with Dissolved Silicates and Stability of Europium(III) Xenotime Solid Solutions, In *Mathematik und Naturwissenschaften*, Technische Universität Dresden, Germany.
- [11] Miron, G. D., Kulik, D. A., Yan, Y., Tits, J., and Lothenbach, B. (2022) Extensions of CASH+ thermodynamic solid solution model for the uptake of alkali metals and alkaline earth metals in C-S-H, *Cement and Concrete Research* 152, 106667.

PA3-11 SOLUBILITY OF Tc(IV) IN THE PRESENCE OF ISOSACCHARINIC ACID: THERMODYNAMIC DESCRIPTION

Kyungwon Kim⁽¹⁾, Sarah Duckworth⁽²⁾, Wooyong Um^(1,3), Marcus Altmaier⁽²⁾, Xavier Gaona⁽²⁾

(1) Division of Advanced Nuclear Engineering (DANE), Pohang University of Science and Technology (POSTECH), South Korea

(2) Institute for Nuclear Waste Disposal (INE), Karlsruhe Institute of Technology (KIT), Germany

(3) Division of Environmental Science & Engineering (DESE), Pohang University of Science and Technology (POSTECH), South Korea

⁹⁹Tc is one of the main fission products of ²³⁵U and ²³⁹Pu in nuclear reactors. Due to its long half-life ($t_{1/2} \sim 2.1 \cdot 10^5$ a), redox sensitive character and large inventory in spent nuclear fuel, ⁹⁹Tc plays an important role in the context of safety assessment of repositories for radioactive waste. Under reducing conditions as those foreseen in underground repositories, Tc is expected to form the sparingly soluble Tc^{IV}O₂(am, hyd) whereas the soluble and mobile pertechnetate anion will form under oxidizing and redox-neutral conditions. Isosaccharinic acid (ISA) is the main degradation product of cellulose in the hyperalkaline conditions defined by cementitious systems foreseen in certain repositories concepts, e.g. for low and intermediate-level wastes (L/ILW) [1]. ISA is known to form strong complexes with transition metals, lanthanides and actinides [2-5]. However, only a few experimental studies have previously investigated the interaction of Tc(IV) with ISA [6], and no thermodynamic data is currently available for this system. Kobayashi and co-workers studied the interaction of Zr(IV) with ISA, and reported equilibrium constants for the formation of the aqueous complexes Zr(OH)₄(ISA)₂²⁻ and Zr(OH)₄(ISA)(ISA-H)³⁻, prevailing within pH_m ~ 8–10 and 10–12, respectively [4]. In this context, the present work aims at obtaining a complete thermodynamic description of the Tc(IV)-ISA system in alkaline to hyperalkaline conditions defined by cementitious systems.

All experiments were performed at $T = (22 \pm 2)$ °C in Ar gloveboxes with < 3 ppm O₂. The impact of ISA on the solubility of Tc was investigated from undersaturation conditions with TcO₂(am, hyd). Solubility samples were prepared in 0.5 M NaCl-NaOH-NaISA solutions with $6 \leq \text{pH}_m \leq 12.5$ and $10^{-6} \text{ M} \leq [\text{ISA}]_{\text{tot}} \leq 0.2 \text{ M}$. Reducing conditions were chemically set for each independent sample with Sn(II). [Tc], pH_m and E_h values were monitored at regular time intervals for up to 128 days. After attaining equilibrium conditions (assumed after repeated measurements with constant [Tc] and pH_m), the redox speciation of Tc in the aqueous phase of selected samples was investigated by solvent extraction. Solid phases of selected solubility experiments were characterized by XRD.

All measured E_h values were below the redox borderline of Tc^{IV}O₂(am, hyd)/Tc^{VII}O₄⁻. Solvent extraction confirmed the predominance of Tc(IV) in the aqueous phase of samples containing 0.2 M ISA (88–104%). XRD indicated the amorphous character of the solid phase, whereas solubility experiments conducted in the absence of ISA were in excellent agreement with the solubility of TcO₂(am, hyd) as calculated with the current NEA-TDB selection [7]. The presence of ISA promoted the enhancement of the solubility in near-neutral to weakly alkaline pH conditions, whereas no significant increase in the solubility was observed in hyperalkaline systems. The latter observation is explained by the strong hydrolysis of Tc(IV) and the predominance of the anionic species TcO(OH)₃⁻ above pH ~ 11. Solubility datasets (log [Tc] vs. pH_m and log [Tc] vs. log [ISA]) were used to derive chemical, thermodynamic and SIT activity models, which successfully explain the solubility of Tc(IV) in the investigated conditions (Figure 1). The chemical model includes the complexes TcO(OH)(ISA)₂⁻ and TcO(OH)₂(ISA)₂²⁻. The latter complex is analogous to the Zr(OH)₄(ISA)₂²⁻ described previously by Kobayashi et al. [4]. Differences in the chemical models for the Tc(IV)-ISA and Zr(IV)-ISA systems are explained on the basis of the stronger hydrolysis of Tc(IV). These results provide key inputs for source term estimations

including the effect of ISA in a variety of geochemical conditions relevant to the context of nuclear waste disposal.

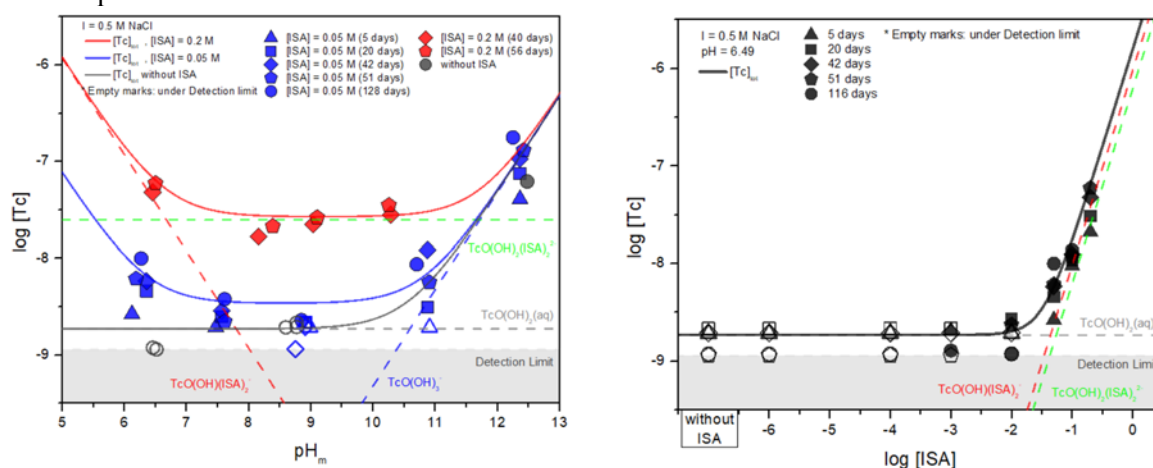


Figure 1. Experimental solubility data of $TcO_2(am, hyd)$ as a function of pH_m (left) and $\log [ISA]$ (right). Solid lines correspond to the chemical, thermodynamic and activity models derived in this work.

Acknowledgments: This work was funded by the 2022 Nuclear Global Internship program Korea Nuclear International Cooperation Foundation (KONICOF) and supported by the Institute for Korea Spent Nuclear Fuel (iKSNF) and National Research Foundation of Korea (NRF) grant funded by the Korea government (Ministry of Science and ICT, MSIT, No.2021M2E1A1085202).

References

- [1] Glaus, M. A., Van Loon, L. R., Achatz, S., Chodura, A., & Fischer, K. (1999) Degradation of cellulosic materials under the alkaline conditions of a cementitious repository for low and intermediate level radioactive waste: Part I: Identification of degradation products. *Analytica Chimica Acta*, 398(1), 111-122.
- [2] Hummel, W., Anderegg, G., Puigdomènech, I., Rao, L., & Tochiyama, O. (2005) The OECD/NEA TDB review of selected organic ligands. *Radiochimica acta*, 93(11), 719-725.
- [3] Vercammen, K., Glaus, M. A., & Van Loon, L. R. (2001) Complexation of Th (IV) and Eu (III) by α -isosaccharinic acid under alkaline conditions. *Radiochimica Acta*, 89(6), 393-402.
- [4] Kobayashi, T., Teshima, T., Sasaki, T., & Kitamura, A. (2017) Thermodynamic model for Zr solubility in the presence of gluconic acid and isosaccharinic acid. *Journal of Nuclear Science and Technology*, 54(2), 233-241.
- [5] Tasi, A., Gaona, X., Fellhauer, D., Böttle, M., Rothe, J., Dardenne, K., ... & Geckeis, H. (2018) Thermodynamic description of the plutonium- α -D-isosaccharinic acid system I: Solubility, complexation and redox behavior. *Applied Geochemistry*, 98, 247-264.
- [6] Maset, E. R., Sidhu, S. H., Fisher, A., Heydon, A., Worsfold, P. J., Cartwright, A. J., & Keith-Roach, M. J. (2006) Effect of organic co-contaminants on technetium and rhenium speciation and solubility under reducing conditions. *Environmental science & technology*, 40(17), 5472-5477.
- [7] Grenthe, I., et al. (2020) Second update on the chemical thermodynamics of uranium, neptunium, plutonium, americium and technetium. *Chemical thermodynamics volume 14* (No. NEA--7500). Organisation for Economic Co-Operation and Development.

PA4-9 DESIGN AND SYNTHESIS OF NOVEL D/A BULK HETEROJUNCTION ORGANIC CONJUGATED FILM MATERIALS AND PHOTOCATALYTIC REDUCTION FOR REMOVAL OF IONS

Li, Zuojia

School of Chemistry, Biology and Materials Science, East China University of Technology, China

In recent years, with the rapid development of the nuclear industry, the demand for uranium ore has increased greatly. The photocatalytic reduction property of semiconductor can effectively eliminate uranyl ion contamination, which is considered as one of the methods with great potential to solve radioactive contamination. However, there are still some key problems that seriously restrict the practical application of photocatalytic technology. For example, the catalyst has poor trapping ability in the visible region, easy electron-hole recombination, and poor interaction between uranyl ions and the catalyst.

In view of these problems, based on the foundation of our research group in the field of organic photoelectric materials and photocatalytic reduction of uranium, through ingenious molecular design, we developed a series of organic conjugated materials with strong absorption in the visible region and good interaction with uranyl ions, as shown in Figure 1. Based on the previous experimental results, the acceptor Y6 with high light absorption efficiency and photocatalytic reduction efficiency was selected for modification study. By introducing hydrophilic functional groups on the X substituent group, the compatibility between the material and water was enhanced, which was conducive to the transmission of electrons to uranyl ions.

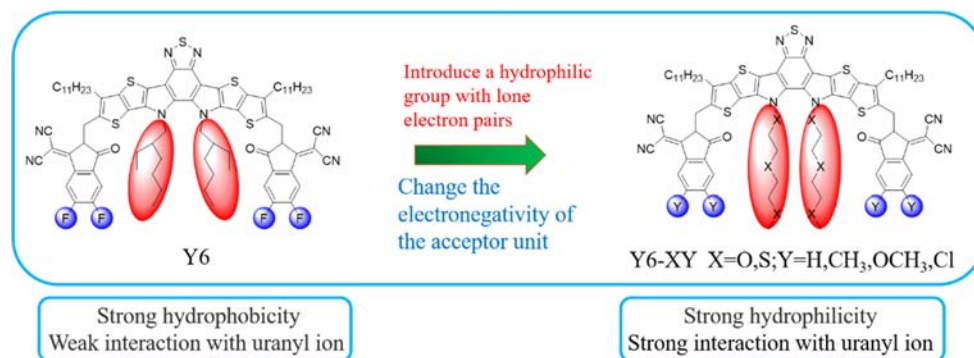


Figure 1 Schematic diagram of molecular design

The energy level of the material can be continuously adjusted by introducing different absorptive functional groups into the Y substituent. By selecting appropriate donor materials, on the one hand, the energy levels of the donor and the acceptor are required to match (as shown in Figure 2a) to achieve efficient charge separation between the donor and the acceptor; on the other hand, complementary absorption between the donor and the acceptor material is required (as shown in Figure 2b) to achieve full spectral absorption in the visible region; By constructing D/A bulk heterojunction structure (as shown in Figure 2c), the electron-hole separation efficiency can be effectively improved. By preparing the film, the recovery of photocatalytic materials and the effective utilization rate of materials can be realized. The prepared film is shown in Figure 2d. Finally, through a series of characterization means to clarify the mechanism of the introduction of specific groups for the removal of uranium with high capacity and high selectivity, and finally clarify the photocatalytic reduction mechanism of photobulk heterojunction structure, and further explore the general principles of such materials and structure design for photocatalytic reduction of uranium.

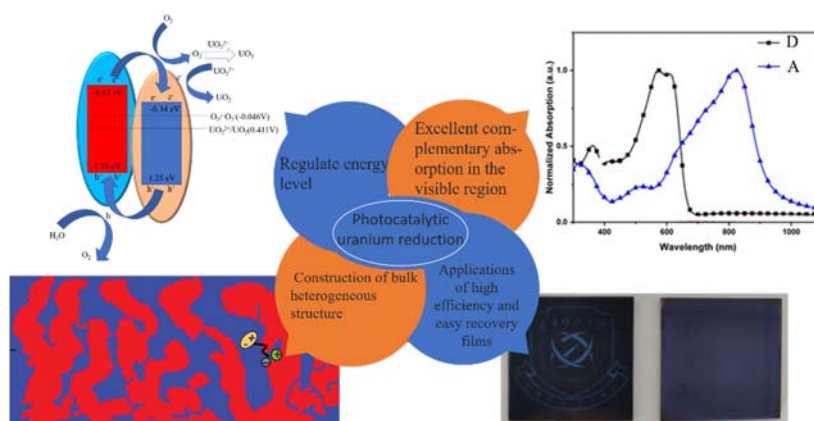


Figure 2 (a) Level of energy level and (b) spectral absorption of donor and acceptor (c) bulk heterojunction and (d) film device of schematic diagram

We prepared the bulk heterojunction film (2.5 cm×2.5 cm) on the glass substrate by spin coating method. The color of the film was close to black, indicating that it had strong absorption in the visible region. The thickness of the film was about 100 nm, and the mass of the film was 0.2 mg. The film was placed in 20 mL uranyl solution at 25 ppm, and the removal rate reached 80% in 300 min (as shown in Figure 3). However, we found that during the first 1 h of light exposure, there is a buffer period during which almost no photocatalysis occurs. We suspect that it may be due to the hydrophobicity of the selected material and the disordered arrangement on the glass substrate. Therefore, the glass substrate was treated with UV-ozone and then spin-coated, and the buffer period disappeared at this time, because the O_3 -ions on the surface of the substrate after UV-ozone treatment can promote the directional arrangement of the film material. Under this condition, the photocatalytic efficiency can be improved by adjusting the D/A ratio and balancing holes and electrons, as shown in Figure 4.

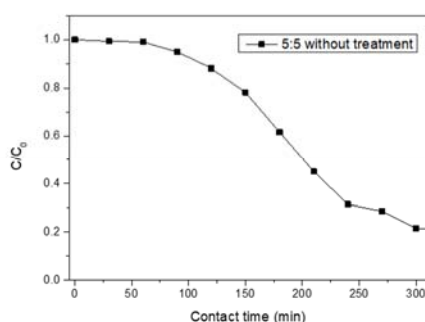


Figure 3 U(VI) curve of photocatalytic reduction of untreated substrate

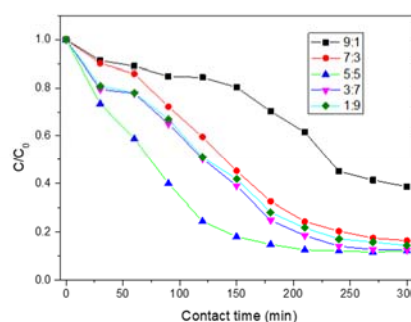


Figure 4 Effect of different D/A ratios on photocatalytic reduction of U(VI)

PA4-10 ROLE OF FE-PHASES ON SELENITE MIGRATION IN BENTONITE: UP-SCALING FROM DISPERSED TO COMPACTED SYSTEM

Ursula Alonso, Miguel García-Gutiérrez, Tiziana Missana

CIEMAT - Physical Chemistry of Actinides and Fission Products Unit Avenida Complutense 40, 28040 Madrid (Spain)

At the canister/bentonite interface of a deep geological repository (DGR) for high-level radioactive waste, steel canister corrosion can be enhanced by waste irradiation, microbial activity or by the chemical effects produced by the presence of bentonite. Corrosion leads to the formation of new Fe-phases that can modify the retention properties of the bentonite barrier, either by providing new sorption sites or by modifying the redox conditions, key issue for redox sensitive radionuclides like selenium.

This study analyses the effects of different iron phases on the retention/migration of selenium in bentonite. For the study, FEBEX bentonite, metal Fe(0) shavings and two iron oxides, goethite and magnetite, were chosen as relevant steel corrosion products. $^{75}\text{Se(IV)}$ was selected as tracer, for being the most stable selenium species in moderate redox potential, whose main aqueous species are neutral (H_2SeO_3) or anionic (HSeO_3^- and SeO_3^{2-}), more mobile in clay barriers.

Experiments were carried out in three steps, which aim to verify the up-scaling and transferability of selenite sorption from the dispersed bentonite and Fe mixtures to the more complex compacted mixtures. First, batch sorption experiments were carried out on purified and Na-homoionised FEBEX bentonite, mixed with different proportions of Fe(0) shavings, magnetite or goethite (2 g/L) at two different pH (4 and 8-9), under N_2 atmosphere with limited CO_2 . Second, selenite batch sorption experiments were carried out on raw FEBEX bentonite, mixed with the same Fe-phases, and under the same conditions. Third, $^{75}\text{Se(IV)}$ in-diffusion experiments were carried out on compacted bentonite samples mixed with known proportions of Fe(0) shavings, powdered goethite or magnetite (10, 15 and 20%) compacted at 1.65g/cm^3 .

Selenium sorption in dispersed Na-homoionised FEBEX bentonite was always improved by the incorporation of any of the selected Fe - phases. The experiments with goethite and magnetite suggested that selenium sorption improvement was due to the increase of sorption sites provided by the Fe-oxide addition, rather than to the redox evolution. However, experiments with metal Fe(0) shavings reached significant negative redox potential capable to reduce selenium. Comparatively, selenite sorption experiments carried out with raw FEBEX bentonite and Fe-phases, under dispersed conditions, showed lower distribution coefficients than in the purified Na-homoionised bentonite.

Selenium sorption experiments on the mixtures were simulated considering surface complexation models, already available on the independent Na-homoionised bentonite [1, 2], goethite and magnetite systems [2], to verify model additivity and transferability. The additive models were capable to simulate selenium sorption in the mixtures with Na-homoionised bentonite and Fe-oxides. To adequately simulate, selenium sorption data on mixtures with raw FEBEX bentonite, the Cl^- , HCO_3^- and SO_4^{2-} salt inventory in the raw clay was accounted for to adequately simulate the sorption data. These anions competed with selenium for sorption sites, decreasing selenium retention.

In-diffusion selenium experiments carried out in FEBEX bentonite mixed with different quantities of Fe-phases showed that selenite diffusion was hindered by the incorporation of Fe-phases. As example, Figure 1 shows selenium concentration profiles measured in compacted bentonite samples with different goethite proportions.

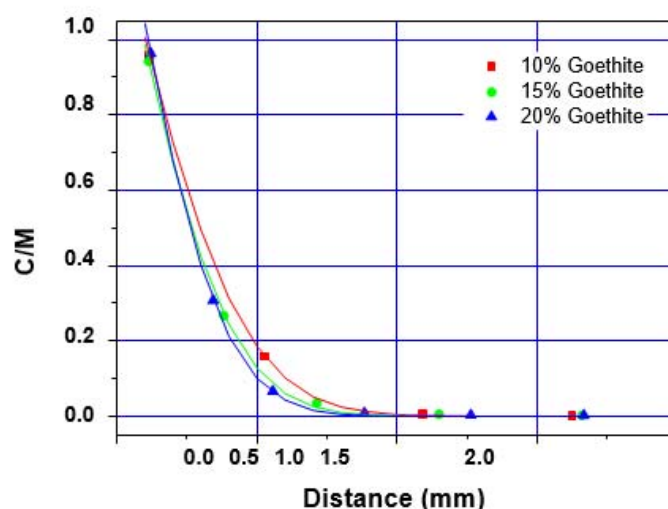


Fig. 1 Comparative diffusion profiles of ^{75}Se in compacted FEBEX bentonite at 1.65 g/cm^3 mixed with goethite particles at different proportions, 10%, 15% and 20%. Diffusion time 154 days.

From the concentration profiles, the apparent diffusion coefficient (D_a) were determined, which include the sorption capacity of selenium in the compacted mixtures. The presence of Fe(0) shavings inhibited selenium diffusion in bentonite, inducing precipitation. The presence of magnetite and goethite reduced selenium apparent diffusion coefficient in compacted bentonite, being goethite more effective, diminishing selenium apparent diffusion coefficients from $D_a = (5.8 \pm 0.5) \cdot 10^{-13} \text{ m}^2/\text{s}$ (no goethite) to $D_a = (2.8 \pm 0.3) \cdot 10^{-15} \text{ m}^2/\text{s}$, with a 20% of goethite.

The surface complexation models obtained for selenium in batch purified materials can be transferred to the compacted system, accounting for the established redox conditions, which were not the same as in batch, and for the dissolved anions coming from salt dissolution from the clay, which are larger in the compacted system and compete with selenium species for sorption sites.

Verification of system additivity facilitates predictive capability and transferability of results to other environments, where higher content of Fe-phases may be present.

Acknowledgment. *This study was partially supported by the European Union's Horizon 2020 Research and Innovation Programme under Grant Agreement no. 847593 (EURAD) and by the Spanish Ministry of Science Innovation (PID2019-106398GB-I00, ARNO Project).*

References

- [1] Missana, T., Alonso, U., García-Gutiérrez, M., (2009) Experimental study and modelling of selenite sorption onto illite and smectite clays. *J. Colloid Interface Sci.* 334, 132–8
- [2] Mayordomo, N., Alonso, U., Missana, T. (2016) Analysis of the improvement of selenite retention in smectite by adding alumina nanoparticles. *Science of the Total Environment* 572, 1025- 1032.
- [3] Missana, T., Alonso, U., Scheinost, A.C., Granizo, N., Garcia-Gutiérrez, M. (2009) Selenite retention by nanocrystalline magnetite: Role of adsorption, reduction and dissolution/co-precipitation processes. *Geochimica et Cosmochimica Acta* 73, 6205–6217.

PA4-11 INFLUENCE OF IRON OXIDE NANOPARTICLE CRYSTALLITE SIZE ON THE SORPTION AND REDUCTION OF PLUTONIUM

Frances Elisa Zengotita⁽¹⁾, Manuel R. Vejar⁽¹⁾ Amy E. Hixon⁽¹⁾

(1)Department of Civil and Environmental Engineering & Earth Sciences, University of Notre Dame USA

Plutonium (Pu) is present in the environment due to nuclear weapons production and testing. The primary factor in determining the mobility of plutonium in the subsurface environment is oxidation state. While Pu(IV) is generally assumed to be the least mobile oxidation state and Pu(V) the most mobile oxidation state, certain caveats exist.^{1,2} One example is nanoparticle-facilitated transport. Due to their small size (1–100 nm), mineral nanoparticles (i.e., inorganic material found in surface and groundwater environments²) can move through pore spaces, which would enhance Pu(IV) mobility.¹⁻⁴ Far-field studies revealed that mineral nanoparticles were associated with plutonium and enhanced its mobility in the subsurface environment.²

Mineral nanoparticles play a large role in the sorption and reduction of heavy metals due to their high reactivity in solution and the undercoordinated sites found at the surface.^{3,4} Studies report that varying particle diameter can impact the chemical behavior of a metal sorbate due to the increase of chemical reactivity and surface area at smaller sizes.⁴ Further, decreasing the diameter of mineral nanoparticles can impact the chemical behavior of metals due to the distorted binding environments at the surface. Nanoscale sizes can influence oxidation and reduction reactions at the nanoparticle surface.^{1,4} Iron oxide nanoparticles are significant because they are abundant in oxidizing environments and are components of the engineered barrier systems of proposed geologic repositories. Iron oxide nanoparticles have been found to reduce Pu(V/VI) and can serve as a vector for plutonium migration at the subsurface.¹ It is imperative that we increase our understanding of the controls that hematite ($\alpha\text{-Fe}^{\text{III}}_2\text{O}_3$) and magnetite ($\text{Fe}^{\text{II}}\text{Fe}^{\text{III}}_2\text{O}_4$) mineral surfaces may exert on plutonium redox behavior, and by extension, its mobility in the subsurface.

Batch sorption experiments (mass- and surface area- normalized) were conducted under ambient laboratory conditions as a function of iron oxide nanoparticle size at average plutonium concentration ($[\text{Pu(V/VI)}]_i = 1.02 \times 10^{-5} \text{ M}$) and ionic strength ($I = 0.1 \text{ M NaCl}$). Preliminary results for mass-normalized experiments revealed that more plutonium sorbed to nano-magnetite (8 nm) than bulk magnetite. In the ten-day period, nano-magnetite reached nearly > 99% sorption of Pu, while bulk magnetite reached ~ 80% sorption of Pu. The hematite system displayed opposite behavior. Bulk hematite had more sorbed plutonium (> 90%) than nano-hematite 40 nm. This may be because nano-hematite is forming strong bonds with plutonium at the surface, whereas bulk hematite has both weakly and strongly bound Pu (Figure 1A-B).

A solvent extraction and co-precipitation procedure was utilized to quantitatively determine the amount of plutonium that is left on the mineral surface as sorbed Pu(IV).¹ In Figure 1 C-D, the hematite system (*left*), shows that nano-hematite (40 nm) has more sorbed Pu(IV) than bulk hematite. In the magnetite system (*right*), the data show that the bulk magnetite has more sorbed Pu(IV). This suggests that although nano-magnetite (8 nm) may adsorb more plutonium onto its surface than bulk magnetite, there is less bound Pu(IV) at the surface. The Pu(IV) that is sorbed on nano-hematite is potentially more stable than Pu(IV) that is sorbed on bulk hematite. Interestingly, bulk magnetite is more favorable for Pu(IV) complexes than nano-magnetite. The Fe(II) in nano-magnetite may favor more Pu(V/VI) adsorption, but not all is reduced, suggesting a reduction-limited mechanism.

Pu L₃-edge EXAFS (extended X-ray absorption fine structure) spectroscopy was used to examine the minerals from the batch sorption experiments and determine the coordination environment of plutonium. Data analysis and other EXAFS-relevant experiments are ongoing. The overall result of this research will be a mechanistically-accurate conceptual model describing plutonium sorption and reduction in the presence of hematite and magnetite nanoparticles.

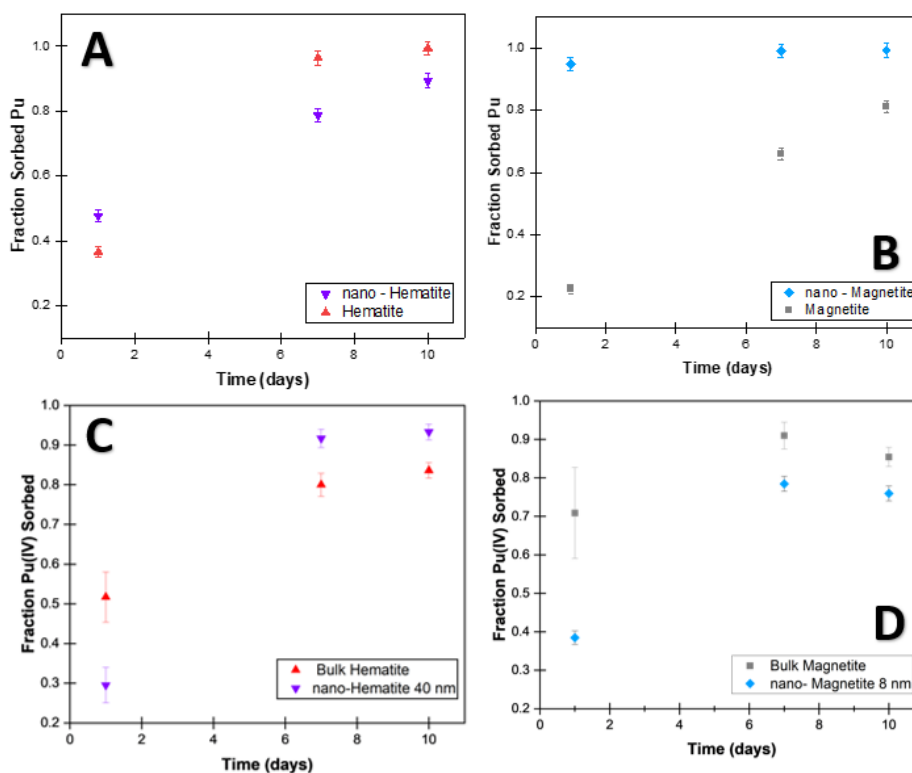


Figure 1A – B). Fraction of sorbed plutonium as a function of time in mass-normalized experiments (targeted mineral concentration of $2 \text{ g}\cdot\text{L}^{-1}$, $(1.26 \pm 0.04) \times 10^{-5} \text{ M Pu(V/VI)}$, and 0.1 M NaCl). **Figure 1C – D)** Fraction Pu(IV) sorbed over time in mass-normalized experiments. The hematite systems are on left. Bulk hematite is represented by red triangles (\blacktriangle) and nano-hematite (40 nm) is represented by upside-down purple triangles (\blacktriangledown). The magnetite systems are on the right. Bulk magnetite is represented by gray squares (\blacksquare) and nano-magnetite (8 nm) is represented by blue diamonds (\blacklozenge).

References

- [1] Hixon, A. E.; Powell, B. A. (2018) Plutonium Environmental Chemistry: Mechanisms for the Surface-Mediated Reduction of Pu(V/VI). *Environ. Sci. Process. Impacts* 20 (10), 1306–1322.
- [2] Kersting, A. B. (2012) Impact of Colloidal Transport on Radionuclide Migration in the Natural Environment. In *Radionuclide Behaviour in the Natural Environment*; Elsevier, 2012; pp 384–410.
- [3] Waychunas, G. A.; Kim, C. S.; Banfield, J. F. (2005) Nanoparticulate Iron Oxide Minerals in Soils and Sediments: Unique Properties and Contaminant Scavenging Mechanisms. *J. Nanoparticle Res.* 7 (4–5), 409–433.
- [4] Madden, A. S.; Hochella, M. F.; Luxton, T. P. (2006) Insights for Size-Dependent Reactivity of Hematite Nanomineral Surfaces through Cu²⁺ Sorption. *Geochim. Cosmochim. Acta* 2006, 70 (16), 4095
- [5] Phan, H. T.; Haes, A. J. What Does Nanoparticle Stability Mean? *J. Phys. Chem. C* 2019, 123 (27)

PA4-12 PLUTONIUM REDOX CHEMISTRY IN THE PRESENCE OF CITRATEMatthew B. Comins⁽¹⁾, Amy E. Hixon⁽¹⁾, J. Beam⁽²⁾, J.-F. Lucchini⁽²⁾*(1) University of Notre Dame, Notre Dame, IN, 46556, USA**(2) Los Alamos National Laboratory-Carlsbad Field Office, Carlsbad, NM, 88220, USA*

Citrate (cit; $C_6H_5O_7^{3-}$) is a tricarboxylic acid that forms strong complexes with plutonium, thereby enhancing its mobility. This organic ligand is present in actinide waste streams (e.g., in the TALSPEAK process), inventory at the Waste Isolation Pilot Plant (WIPP), and is naturally occurring in the environment. However, few studies have focused on the effect of citrate and pH_m on the long-term oxidation state distribution of plutonium.¹ The oxidation state of plutonium strongly dictates its degree of mobility in a repository or environmental setting, with Pu(V) and Pu(VI) generally being more soluble than Pu(III) and Pu(IV). We hypothesized that citrate plays a role in the reduction of Pu(VI) and Pu(V) by way of oxidative decarboxylation (e. g., $PuO_2^{2+} + R-COO^- \rightarrow PuO_2^+ + CO_2(g) + R^-$).

In this work, we demonstrated plutonium redox behavior in the presence of excess citrate ($[cit]:[Pu] = 10$) as a function of pH_m at low ionic strength ($I = 0.1$ M NaCl-HCl-NaOH- $NaC_6H_7O_7$ - $Na_3C_6H_5O_7$), using freshly prepared stocks of Pu(III) and Pu(VI). All experiments were conducted under inert gas atmosphere with < 2 ppm O_2 at 23 ± 2 °C. Plutonium oxidation state distributions were measured by a solvent extraction-based technique²⁻⁴ coupled with LaF_3 coprecipitation;^{5,6} Pu concentrations were measured by liquid scintillation counting (LSC) after 10 kD ultrafiltration; and ultraviolet-visible-near infrared (UV-Vis-NIR) spectroscopy was used to probe speciation changes. Experimental observations were compared to geochemical models using available equilibrium constants.

Speciation changes in the Pu(VI)-citrate system were observed with increasing pH_m and suggest the formation of $PuO_2(cit)^-$ and $PuO_2(cit)_2^{4-}$ in the acidic to circumneutral pH_m region. These results agree with those of Nebel and Anders⁷ and our own geochemical modeling. Higher-order Pu(VI)-citrate complexes are expected to be predominant in the neutral to alkaline region. Because Pu(VI)-citrate complexation is expected to increase with increasing pH_m due to the deprotonation of citric acid, the role of citrate in the reduction of Pu(VI) is substantiated by our observations of faster reduction with increasing pH_m (Figure 1). Preliminary rate constants for citrate-mediated reduction of Pu(VI) increase with pH and can be expressed as a pseudo-first-order reaction, due to the excess of citrate. Unlike the Pu(VI)-citrate system, we expected no pH dependency in the rate of Pu(III) oxidation to Pu(IV) when citrate was present. Speciation determinations for the Pu(III)-citrate system could not be made by spectroscopy, but a speciation change is seen at $pH_m = 7.6$. Spectra point to the same Pu(IV)-citrate complex being formed at each pH_m (2.9, 5.6, and 7.6), except for pH_m 11.4, where no Pu(IV)-citrate peaks are observed with time. Rate constants for Pu(III) oxidation to Pu(IV) exhibit only a minor pH_m dependence, with slightly faster oxidation occurring at $pH_m = 7.6$. A clearer pH_m dependency is seen for Pu(III) oxidation in the absence of citrate, with modestly faster oxidation occurring at higher pH_m . Under alkaline conditions ($pH_m \geq 11$), plutonium precipitation was observed with time as plutonium was oxidized or reduced to Pu(IV) (Figure 1), demonstrating the relative strength of Pu(IV) hydrolysis versus citrate complexation. Additional work is needed to elucidate Pu-citrate speciation for each oxidation state in order to further understand the role of citrate in plutonium redox reactions.

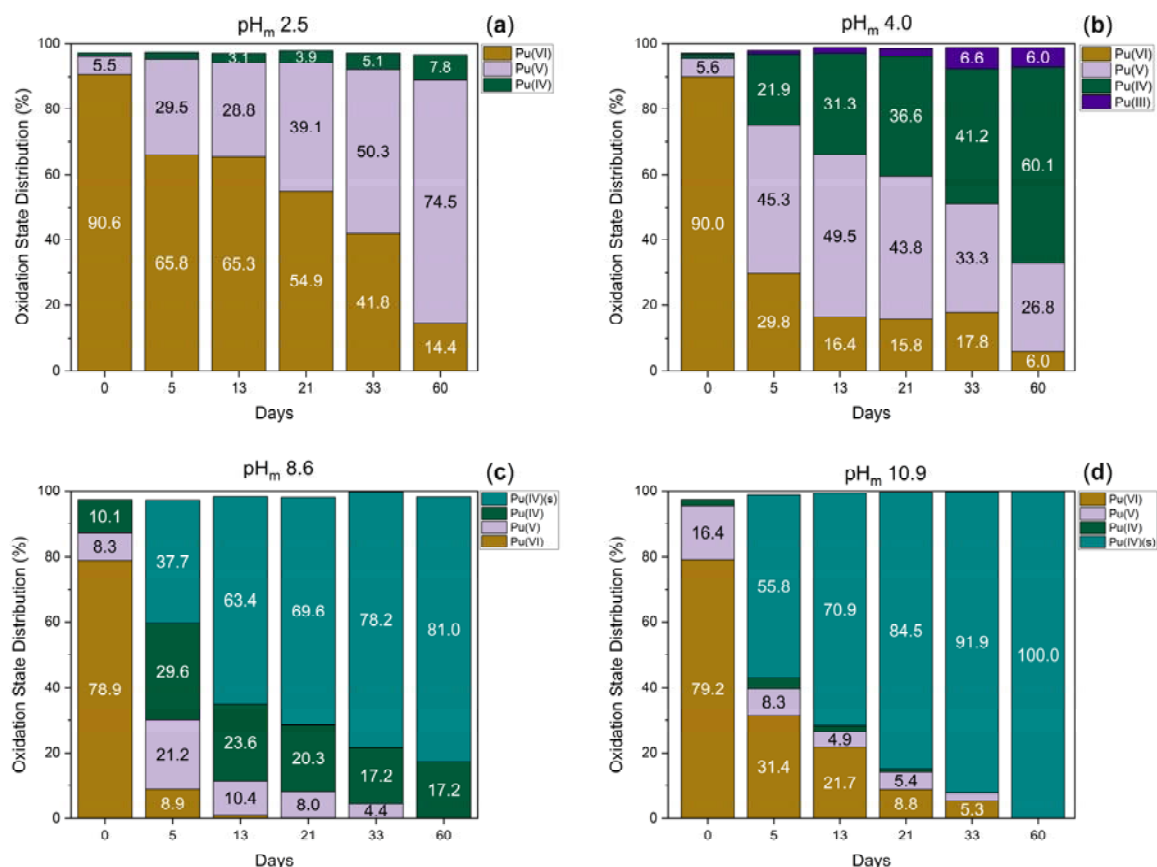


Figure 1. Liquid scintillation counting results from solvent extraction-based oxidation state analysis of the Pu(VI)-citrate system. After the initial sampling, samples were filtered through Amicon 10 kD filters and any plutonium not in the filtrate was presumed to be Pu(IV)(s). $[Pu]_T = 0.12 \pm 0.01$ mM, $[cit]_T = 1$ mM, $I = 0.1$ M NaCl-HCl-NaOH- $Na_3C_6H_5O_7$.

References

- [1] Reed, D. T.; Wygmans, D. G.; Aase, S. B.; Banaszak, J. E. (1998). Reduction of Np(VI) and Pu(VI) by Organic Chelating Agents. *Radiochim. Acta* 82: 109–114.
- [2] Nitsche, H.; Lee, S. C.; Gatti, R. C. (1988). Determination of Plutonium Oxidation States at Trace Levels Pertinent to Nuclear Waste Disposal. *J. Radioanal. Nucl. Chem* 124 (1): 171–185.
- [3] Neu, M. P. and Hoffman, D. C. (1994). Comparison of Chemical Extractions and Laser Photoacoustic Spectroscopy for the Determination of Plutonium Species in Near-Neutral Carbonate Solutions. *Radiochim. Acta* 66–67: 251–258.
- [4] Hixon, A. E.; Arai, Y.; Powell, B. A. (2013). Examination of the Effect of Alpha Radiolysis on Plutonium(V) Sorption to Quartz Using Multiple Plutonium Isotopes. *J. Colloid Interface Sci.* 403: 105–112.
- [5] Nelson, D. M. and Lovett, M. B. (1978). Oxidation State of Plutonium in the Irish Sea. *Nature* 276: 599–601.
- [6] Kobashi, A.; Choppin, G. R.; Morse, J. W. (1988). A Study of Techniques for Separating Plutonium in Different Oxidation States. *Radiochim. Acta* 43 (4): 211–215.
- [7] Nebel, D. and Anders, G. (1975). Zur Komplexbildung und Solvatioii einiger Actinide I. Untersueclungcii zur Komplexbildung mit Acetat und Citrat. *Isotopenpraxis* 11 (4): 152–155.

PA4-13 REDOX BEHAVIOUR AND SPECIATION OF PLUTONIUM IN THE PRESENCE OF ALUMINIUM-DOPED IRON OXIDE MINERAL SURFACES

Manuel R. Vejar,⁽¹⁾ Frances E. Zengotita,^(1,2) Sharon E. Bone,⁽³⁾ Dimosthenis Sokaras,⁽³⁾ Stephan Weiß,⁽⁴⁾ Salim Shams Aldin Azzam,⁽⁴⁾ Nina M. Huittinen,⁽⁴⁾ Elena F. Bazarkina,^(4,5) Kristina O. Kvashnina,^(4,5) and Amy E. Hixon.⁽¹⁾

(1) *Department of Civil and Environmental Engineering and Earth Sciences, University of Notre Dame, Indiana 46556, USA*

(2) *Department of Materials Science and Engineering, University of Notre Dame, Indiana 46556, USA*

(2) *Stanford Synchrotron Radiation Lightsource, SLAC, 2575 Sand Hill Road, Menlo Park, California 94025, USA*

(3) *Helmholtz-Zentrum Dresden-Rossendorf, Institute of Resource Ecology, Bautzner Landstraße 400, 01328 Dresden, Germany*

(4) *The Rossendorf Beamline, The European Synchrotron Radiation Facility, P.O. Box 40220, 38043 Grenoble, France*

Plutonium (Pu) is a radiotoxic element present in used nuclear fuel, in fuel reprocessing products, and at legacy contaminated sites.¹ To facilitate the continued use of commercial nuclear power and address environmental contamination, it is essential to understand Pu fate and transport in subsurface environments, which is tied to its rich redox chemistry (i.e., generally, Pu(IV) is less mobile and Pu(V) is more mobile).¹

Iron oxides (e.g. hematite (α -Fe₂O₃) and goethite (α -FeOOH)) are some of the most abundant and sorption-reactive mineral phases in surface and subsurface environments, and commonly contain up to ~15% aluminium (Al).² The presence of Al in the crystal lattices of iron oxides is expected to impact the semiconducting properties of the mineral and thus facilitate or obstruct surface-mediated reduction of a sorbed contaminant.^{3,4} Iron oxides are also an integral part of determining the performance of a generic geologic repository (e.g., granite, clay, salt) for used nuclear fuel, as they may be found in or as by-products of engineering barriers and in the rocks hosting the repository. Furthermore, iron oxides influence contaminant fate and transport in the environment.⁵

Predictive geochemical models are necessary for long-term performance assessments of potential nuclear waste repositories. However, current geochemical models do not accurately predict actinide behaviour under field conditions, they have failed to predict km-scale transport of Pu,⁶ they do not account for complexity in mineral assemblages (such as chemical impurities), and they do not explicitly consider surface-mediated reduction.⁷

This work tests mineralogically-complex systems where Pu(V/VI) is the sorbate and Al-substituted hematite or Al-substituted goethite are the sorbent. This work focuses on the sorption and ensuing surface-mediated reduction behaviour of Pu in binary systems at circumneutral pH in atmospheric conditions. The overall goal is to relate Pu behaviour to the physicochemical properties of the sorbent minerals, specifically the effects of Al-substitution on surface-mediated reduction of Pu, and on the speciation of Pu with increasing surface loading.

Liquid scintillation counting paired with solvent extractions were used to determine the concentrations and oxidation state of Pu in the aqueous-phase. X-ray absorption spectroscopy was used for in-situ analyses of Pu associated with the solid-phase. Combining solvent extraction techniques with M₄-edge HERFD-XANES^{8,9} and L₃-edge EXAFS,^{5,9,10} we 1) probe the electronic configuration of Pu and quantify the extent of Pu surface-mediated reduction in systems containing Al-substituted hematite and

Al-substituted goethite; and 2) assess how the redox behaviour and speciation of Pu change as a function of surface loading.

Our preliminary results suggest that in short time scales, Pu sorption to Al-hematite and Al-goethite is slower than to Al-free minerals, however, the extent of sorption is comparable as the reactions approach steady state (2-4 weeks). Stability and surface site properties of Al-substituted minerals may play a role in Pu redox behaviour. Pu(V/VI) surface-mediated reduction to Pu(IV) is observed in our systems via M₄-edge HERFD-XANES.^{8,9} L₃-edge EXAFS suggests that Pu(IV) can be found on the mineral surface as sorption complexes, Pu-oxide solids, or a combination of the two species.^{5,10}

Studying the redox behaviour and speciation of Pu associated with the solid phase will improve our understanding of surface-mediated reduction and immobilization of Pu in the environment, and its interactions with geologic materials.

References

- [1] Hixon A. E. and Powell B.A. (2018). Plutonium Environmental Chemistry: Mechanisms for the Surface-Mediated Reduction of Pu(V/VI). *Environ. Sci.: Processes Impacts*. 20 (10), 1306–1322.
- [2] Hsu, L.-C. E. et al., (2020). Preferential Phosphate Sorption and Al Substitution on Goethite. *Environmental Science: Nano*. 7 (11), 3497–3508.
- [3] Cao, S. et al., (2015). Influence of Al Substitution on Magnetism and Adsorption Properties of Hematite. *Journal of Solid State Chemistry*. 228, 82–89.
- [4] Taylor, S. D. et al., (2017). A First Principles Investigation of Electron Transfer between Fe(II) and U(VI) on Insulating Al- vs. Semiconducting Fe-Oxide Surfaces via the Proximity Effect. *Geochimica et Cosmochimica Acta*. 197, 305–322.
- [5] Balboni, E. et al., (2020). Transformation of Ferrihydrite to Goethite and the Fate of Plutonium. *ACS Earth Space Chem*. 4 (11), 1993–2006.
- [6] Kersting, A. B. et al., (1999). Migration of Plutonium in Ground Water at the Nevada Test Site. *Nature*. 397 (6714), 56–59.
- [7] Davis, J. A. et al., (1998). Application of the Surface Complexation Concept to Complex Mineral Assemblages. *Environ. Sci. Technol*. 32 (19), 2820–2828.
- [8] Kvashnina, K. O. et al., (2019). A Novel Metastable Pentavalent Plutonium Solid Phase on the Pathway from Aqueous Plutonium(VI) to PuO₂ Nanoparticles. *Angew. Chem. Int. Ed*. 58 (49), 17558–17562.
- [9] Gerber, E. et al., (2020). The Missing Pieces of the PuO₂ Nanoparticle Puzzle. *Nanoscale*.
- [10] Balboni, E. et al., (2021). Plutonium Co-Precipitation with Calcite. *ACS Earth Space Chem*. 2021, 5, 12, 3362–3374

PA4-14 THE REDOX BEHAVIOR OF URANIUM AND SELENIUM UNDER RADWASTE REPOSITORY CONDITION

Mingliang Kang⁽¹⁾, Yixiao Kang⁽¹⁾, Wujian Jin⁽¹⁾, Jingye She⁽¹⁾, Qiaoya Lin⁽¹⁾, Ju Wang⁽²⁾

(1) *Sino-French Institute of Nuclear Engineering and Technology, Sun Yat-sen University, China*

(2) *Beijing Research Institute of Uranium Geology, China*

Uranium dioxide is the matrix material of nuclear fuel and oxidative damage of spent nuclear fuel may cause leaching of fission products and transuranium actinides. ⁷⁹Se is one of the key fission products concerned in the geological disposal of high-level radioactive waste (HLRW). Understanding the speciation of U and Se under the HLRW repository condition is essential for the safety assessment of the potential repository.

The Beishan area in Gansu province and Tamusu area in Inner Mongolia are considered for the granite-based and clay-based sites of China's HLRW repository, respectively. The redox behavior of U and Se on Beishan granite and Tamusu claystone was studied. Results showed that U(VI) could be partially reduced by Beishan granite, due to the presence of Fe²⁺-containing fluorannite. Meanwhile, partial oxidation of UO₂ was observed when UO₂ contacted Beishan granite directly. Consequently, aliovalent oxides (e.g., U₃O₈, U₃O₇, U₄O₉, etc.) should be the thermodynamically stable form in Beishan granite^[1]. Aqueous Se(IV) can be reduced to insoluble Se(0) by the Beishan granite from borehole 16 and the removal efficiency is favorable at acidic condition. We proposed that release of the structure Fe²⁺ in granite, followed by surface adsorption and reaction could be responsible for the Se(IV) reduction. Interestingly, in addition to Se(0) product, FeSe₂ was also observed for the reaction of aqueous Se(IV) with the granite from borehole 28. This is the first time observed the formation of FeSe₂ for Se(IV) reduction by natural mineral, which is mainly ascribed to the simultaneous occurrence of aqueous sulfide dissolved from the ground granite powder. The reactive sulfide might be generated from the breakage of Fe(S)–S bonds of iron sulfides (e.g., pyrite) contained in the granite during the anoxic grinding process. Reductive precipitation of aqueous U(VI) and Se(IV) was also observed on Tamusu claystone, because of the occurrence of Fe²⁺-containing fluorannite and pyrite. Nevertheless, the Fe²⁺ contained in Tamusu claystone is less reactive in comparison with that in Beishan granite, probably due to the concomitant organic matters^[2].

Magnetite is a corrosion product of iron being used in nuclear waste canisters. Thermodynamically, UO₂ is the most stable form in the stability area of magnetite. Prevalently, incomplete reduction of aqueous U(VI) to U(V)/U(IV)-containing species have been observed on chemosynthetic magnetite. Our study revealed that nitrate ion associated with uranyl or present in groundwater as well as the ferric ion contained in magnetite structure or generated from U(VI) reduction have a non-negligible oxidative effect on the final products^[3].

Pyrite (FeS₂), the Earth's most abundant sulfide mineral, is one of the important minerals buffering the reducing conditions in nuclear waste repositories where it is present in host claystone or granite as well as in near-field bentonite materials. Thermodynamically, aqueous U(VI) can be reduced to UO₂ by pyrite in a wide pH range. In contrast, our previous study showed that U(VI) reduction by synthetic and natural pyrite samples with acid-washed surfaces was largely inhibited under most pH conditions^[4]. Our later work revealed that surface Fe²⁺/Fe³⁺ and S²⁻ sites generated from breakage of Fe(S)–S bonds during ball milling or weathering as well as surface Pb- and As-impurities play a significant role on the reactivity of pyrite toward U(VI)^[5].

References

- [1] Chen, P., Ma, Y., Kang, M. L., Shang, C. M., Song, Y., Xu, F. Q., Wang, J., Song, G., Yang, Y. Q (2020). The redox behavior of uranium on Beishan granite: effect of Fe²⁺ and Fe³⁺ content. *J. Environ. Radioact.* 217, 106208.
- [2] Wu, J. C., Guo, B. L., Kang M. L., Kang, Y. X., Jin, W. J., Wu, H. Y., Wu S. J (2022). Comparative study on the reductive immobilization of Se(IV) by Beishan granite and Tamusu claystone. *Appl. Geochem.* 146, 105447.
- [3] Ma, Y., Cheng, X., Kang, M. L., Yang, G. Z., Yin, M. L., Wang, J., Song, G (2020). Factors influencing the reduction of U(VI) by magnetite. *Chemosphere.* 254, 126855.
- [4] Yang, Z. W., Kang, M. L., Ma, B., Xie, J. L., Chen, F. R., Charlet, L., Liu C. L (2014). Inhibition of U(VI) reduction by synthetic and natural pyrite. *Environ. Sci. Technol.* 48: 10716–10724.
- [5] Ma, B., Fernandez-Martinez, A., Kang, M. L., Wang, K. F., Lewis, A. R., Maffei, T. G. G., Findling, N., Salas-Colera, E., Tisserand, D., Bureau, S., Charlet, L (2020). Influence of Surface Compositions on the Reactivity of Pyrite toward Aqueous U(VI). *Environ. Sci. Technol.* 54(13): 8104–8114.

PA4-15 SELENITE SORPTION STUDIES ONTO FE(II) - AND FE(III) - NONTRONITES

Francisco Javier León Vicente ⁽¹⁾, Ana María Fernández ⁽¹⁾, Tiziana Missana ⁽¹⁾

(1) CIEMAT. Avda. Complutense 40, Madrid, Spain

Bentonites with high smectite content are selected as engineered barriers in radioactive waste repositories for their suitable confinement properties and for their high radionuclide retention capability. One of the most important risks that can occur in the clay barrier system is the corrosion of the canister, which could be coupled with reduction of iron (Fe) in the clay structure. These processes could greatly decrease the long-term stability of the clay and, consequently, of the barriers themselves. The oxidation state of iron (Fe) in the crystal structures of smectite clay minerals has been found to be a critically important factor underlying the behavior of the clay. However, the reduction of Fe³⁺ within the structure of nontronites and ferruginous smectites is a subject of interest due to the role of Fe-bearing clays in geochemical redox cycles and in particular the reductive degradation of contaminants so, the synthesis and characterization of synthetic and natural nontronites and other Fe-rich smectites with different Fe(II)/Fe(III) ratio are important for the analysis of both the possible alterations of the clay mineral structure, affecting the properties of the bentonite barrier, and redox effects affecting radionuclide retention in clays.

In this context, 79-Selenium, present in spent nuclear fuel high-level radioactive waste deep geological repository, is a critical element because of its long half-life (550.000 y), and because its negative charge limits adsorption onto geological material [1]. Selenium chemistry is quite complicated because it depends not only on the redox state of the system but on many factors influencing its speciation. Besides, selenium mobility is affected by the chemistry of the system [2].

Within this framework, this study provides a large set of experimental selenite sorption data for two Fe-rich nontronite (NAu-2), one fully oxidized (Fe(III)-nontronite) and other partially reduced (Fe(II)-nontronite) with the aim of improving the knowledge of the mechanisms involved in Se sorption on clay minerals with different Fe(II)/Fe(III) contents.

NAu-2 nontronite was purchased from Uley Mine, Australia [3]. A batch of purified NAu-2 has been fully oxidized to Fe (III) at octahedral sites following the methodology described by Jackson et al. (1985) [4]. Also, a batch of purified NAu-2 has been partially reduced to Fe(II) nontronite with the citrate bicarbonate method following the methodology described in Stucki et al. (1984) [5]. The structure and properties of both NAu-2 nontronite clay minerals was characterized by XRD, Far-, Mid- and Near-infrared spectroscopy, TEM, BET and Mössbauer techniques, as well as for their BET and CEC.

At second stage, sorption experiments were performed with both nontronites and compared with the data of the raw clay. Sorption kinetics tests were carried out at pH5 and pH8 to investigate the time required for the attainment of the sorption equilibrium, and samples were maintained under continuous stirring during the selected contact time (from 1 to 90 days). Sorption edges were executed by varying the pH of the suspensions from pH3 to pH9. Finally, sorption isotherms were carried out by varying the radionuclide concentration ($\sim 1 \cdot 10^{-8}$ to $1 \cdot 10^{-3}$ M). The radionuclide used in this study was a carrier-free ⁷⁵Se, which half-life is 119.8 days and the solid and liquid phases were separated by centrifuging (25 000g, 30 min) with a JOUAN MR23i centrifuge. After the solid separation, three aliquots of the supernatant were extracted from each tube for the analysis of the final Se. The rest of the solution was used to check the final pH.

Selenite sorption studies onto NAu-2 Fe(III) nontronite and NAu-2 Fe(II) nontronite showed important aspects. Sorption onto both clays is linear within a very wide range of selenite concentrations. Furthermore, the distribution coefficient (K_d) for NAu-2 Fe(II) nontronite reaches a nearly constant value after 30 days of contact time at pH5 and pH8, while the distribution coefficient for NAu-2 Fe(III) nontronite doesn't reach a nearly constant value until 90 days at pH 5. At pH8, Se sorption increases with time after this period. This is long-term reactions are an indication that adsorption is not the only retention process (redox effects and precipitation might be involved).

Finally, sorption edges shows that K_d values decrease as pH increases from 3.0 to 8.5 observing a certain ordering in the K_d values between the different nontronites, being higher in the NAu-2 Fe(II) nontronite, followed by NAu-2 Fe(III), lowest being found in natural NAu-2, as shown in Fig. 1. Even the effect is not very large, the presence of Fe(II) seems enhancing selenite retention under acidic conditions.

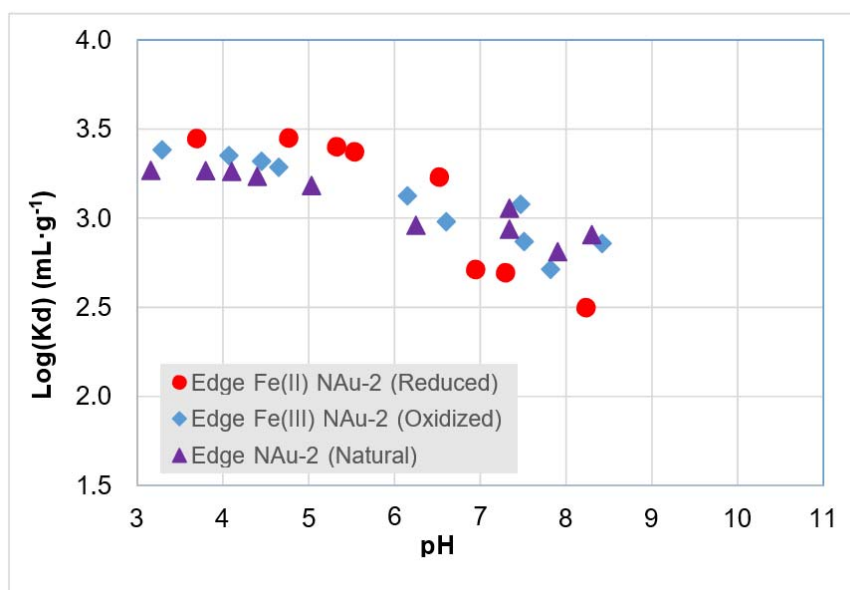


Figure 1. Sorption Edges of Selenite onto NAu-2 (Natural), NAu-2 Fe(III) Nontronite and NAu-2 Fe(II) Nontronite. Conditions: Anoxic.

References

- [1] Duc, M., Lefebvre, G., Federoff, M., Jeanjean, J., Rocuchaud, J.C., Monteil-Rivera, F., Dumonceau, J and Milonjic, S. (2003). Sorption of selenium anionic species on apatites and iron oxides from aqueous solutions. *J. Environ. Radioactiv.* 70: 61
- [2] Séby, F., Potin-Gautier, M., Giffaut, E. and Donard, O.F.X. (1998). Assessing the speciation and the biogeochemical processes affecting the mobility of selenium from a geological repository of radioactive wastes to the biosphere. *Analisis.* 26: 193-198
- [3] Keeling, J.L., Raven, M.D. and Gates, W.P. (2000). Geology and characterization of two hydrothermal nontronites from weathered metamorphic rocks at the Uley Graphite Mine, South Australia. *Clays and Clay Miner.* 48 (5): 537-548
- [4] Jackson, M.L. (1985). *Soil chemical analysis-advanced course*, revised 2nd edition. 11th printing. [5] Stucki, J.W., Golden, D.C. Roth, C.B. (1984). Preparation and Handling of Dithionite-Reduced Smectite Suspensions. *Clays Clay Miner.* 32: 191-197

PA4-16 IS THERE A ROLE FOR PU(III) IN PREDICTING THE SUBSURFACE MIGRATION OF PLUTONIUM?

Donald T. Reed

Los Alamos National Laboratory, USA

Understanding and accounting for the subsurface migration of plutonium is critically important in the assessment of contaminated sites and nuclear repositories when plutonium is present. Its environmental chemistry is understood through oxidation-state-specific chemistry making redox control a key contributor to predicting its potential mobility [1, 2]. Under a broad range of subsurface conditions the most important oxidation state is Pu(IV) with its sparingly soluble oxide and oxy-hydroxide phases (Figure 1). Through 2010, it was argued that Pu(III) phases were thermodynamically unstable at the higher pHs typically predicted for deep geologic nuclear repositories. The predicted predominance of Pu(IV) also explains the relatively low mobility observed under a wide range of near-surface conditions. This thesis is evaluated in light of recent data [3-8] that show long-term stabilization of Pu(III) under some relevant environmental conditions. Additionally, new data from long-term studies will be presented. In this context, a discussion is needed within the field of actinide environmental chemistry to account for and explain these data in the context of current environmental assessments and repository evaluations.

There are many key and critical data that support the long-held belief and understanding that the environmental chemistry should be dominated by the Pu(IV) oxidation state. Plutonium oxide is a highly insoluble and stable form of plutonium that is readily formed under most environmental conditions and is often the predominant form of plutonium disposed in a permanent geologic repository. The most important evidence of its predominance in many near-surface contaminant sites is its relatively low mobility (in many cases its immobility) when compared with other redox-sensitive actinides that are present as co-contaminants. There are many site-specific data, particularly in the US, where this type of disparity was observed.

There is now also a growing amount of data that point to the possible importance of Pu(III) [3-8]. This argues for its further consideration in long-term performance assessments and comes from two general areas of research. The first is from microbial studies of metal-reducing and sulfate reducing bacteria where the bio-reduction of PuO₂ has been shown to be possible under anaerobic conditions. These results, for plutonium, were recently summarized [9]. The mechanism and prevalence of these microbial effects are however not well understood and, although co-metabolic processes are likely, it is not clear that enzymatic reduction of Pu(IV) to Pu(III) occurs. Overall, even if this microbiology can occur under certain subsurface conditions, there remains a question of long-lasting effects that contribute to enhanced mobility.

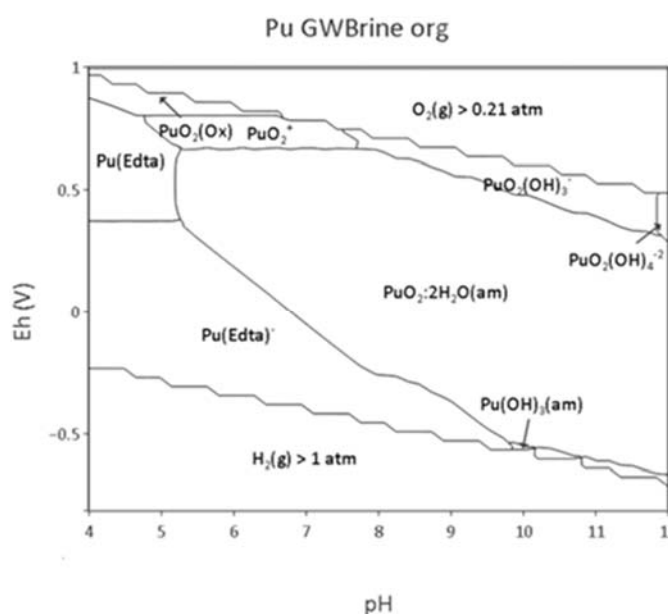


Figure 1. Pourbaix diagram for plutonium solids in simulated GWB high ionic strength brine in the presence of EDTA. This shows a very large stability field for Pu(IV) solids with a small area of stability for Pu(III) at the lower (most reducing) boundary [7].

The second source of data that raise questions about the possible role for Pu(III) in the environmental fate and transport of plutonium is from the long-term Fe (0, II) dominated repository studies that show a sustainable presence of Pu(III) species [3-8]. Pu(III) hydroxide, as an amorphous phase, can be readily precipitated in $\text{pH} > 8$ systems. A Pu(III) crystalline phase has been observed in some experiments but is not commonly observed. Regardless, the long-term stability of Pu(III) phases appears to be quite small and at/near the water line (See Fig. 1) making it difficult to envision as a sustainable phase in the E_h range typically seen in most environments. Where high concentrations of plutonium exist (e.g., the source term of a repository), radiolysis will likely cause increases in E_h that may destabilize or prevent Pu(III) formation. Additionally the measured solubilities under these conditions is often more consistent with a Pu(IV) phase even when the solid phase is predominantly Pu(III). The idea that higher Pu(III) solubilities will exist is based on data from short term solubility studies of Pu(III) hydroxide amorphous phases and may not represent phases formed in sustained highly reducing conditions. This chemistry is not yet fully understood and continues to be the focus of ongoing studies.

Pu(III) data that relate to both biologically-induced reduction and iron reduction in high pH reducing conditions will be summarized and assessed. Additionally, long-term (10-year) plutonium results in iron dominated high ionic strength systems, along with Pu-dominated systems where radiolytic effects play a greater role will be presented. These data show that Pu(III) can be formed and stabilized but under most realistic conditions a significant impact on overall mobility may not be observed. Altogether, the research focus should be on the role of Pu(III) in environments where highly reducing conditions can persist, rather than arguments against its thermodynamic stability.

References

- [1] Runde, W.; Neu, M. P. Actinides in the Geosphere. In *The Chemistry of the Actinide and Transactinide Elements*, 4th ed.; Morss, L. R., Edelstein, N. M., Fuger, J. Katz, J. J., Eds.; Springer: Netherlands, 2011; Vol. 1–6, pp 3475–3593.
- [2] Geckeis, H., M. Zavarin, B. Salbu, O. Lind, and L. Skipperud. “Environmental Chemistry of Plutonium.” Chapter 25 in *Plutonium Handbook*, D. Clark, D. Geeson and R. Hanranhan, eds., American Nuclear Society, pp. 1979, 2019.
- [3] Reed, D.T., M. Borkowski, J. Swanson, M. Richmann, H. Khaing, J.f. Lucchini and D. Ams. 2011. Redox-controlling processes for multivalent metals and actinides in the WIPP. 3rd Annual Workshop Proceedings, 7th EC FP - ReCosy CP, pp. 1-12.
- [4] D.T. Reed. 2018. *Plutonium Oxidation State Distribution in the WIPP: Conceptual Model, Project-Specific Data, and Current/Ongoing Issues*. LA-UR-18-25748. Los Alamos National Laboratory; Carlsbad, NM.
- [5] Cho, H.-R., Youn, Y.-S., Chang Jung, E., Cha, W., 2016. Hydrolysis of trivalent plutonium and solubility of Pu(OH)₃ (am) under electrolytic reducing conditions. Dalton Transactions 45, 19449–19457. <https://doi.org/10.1039/C6DT03992H>
- [6] Tasi, A., Gaona, X., Fellhauer, D., Böttle, M., Rothe, J., Dardenne, K., Schild, D., Grivé, M., Colàs, E., Bruno, J., Källström, K., Altmaier, M., Geckeis, H. 2018. “Redox Behavior and Solubility of Plutonium under Alkaline, Reducing Conditions”. *Radiochimica Acta* 106: 259-279.
- [7] Colas, E., D. Garcia and L. Duro. 2020. “Systematic Calculation of Pu Pourbaix Diagrams: Modelling Support for the LANL ACRSP Team.” Los Alamos report LA-UR-20-26859.
- [8] J.A. Schramke, E.F.U. Santillan, R.T. Peake. “Plutonium oxidation states in the Waste Isolation Pilot Plant repository.” *Applied Geochem*, (116) 104561.
- [9] Reed, D.T., R. Kinder, J. Lloyd, and J.S. Swanson, “Plutonium Microbial Interactions in the Environment”, Chapter 26 in *Plutonium Handbook*, D. Clark, D. Geeson and R. Hanranhan, eds., American Nuclear Society, pp. 2119, 2019.

PA5-17 DETERMINATION OF URANIUM(VI) SPECIATION DURING SORPTION TO GIBBSITE USING PARALLEL FACTOR ANALYSIS ON EXCITATION EMISSION MATRICES

Laura Lopez-Odrizola (1), Samuel Shaw (1), Liam Abrahamsen-Mills (2) and Louise Natrajan (1)

(1) School of Natural Sciences, The University of Manchester, Oxford Road, M13 9PL, United Kingdom

(2) National Nuclear Laboratory, Chadwick House, Warrington Road, Birchwood Park, WA3 6AE, United Kingdom

Fundamental understanding of radionuclide speciation during the interaction with minerals and materials relevant to radioactive waste storage and disposal is essential in supporting the generation of accurate and robust safety cases. The characteristic and highly informative luminescence properties of the uranyl(VI) moiety have been utilised in a number of areas, due to its effectiveness as a tool for determining differences in the bonding environment of the radionuclide and ability to provide information on its chemical speciation. [1] Despite the extensive research carried out into systems representative of environmental scenarios, there is a knowledge gap related to the effect change environmental conditions e.g. pH and carbonate concentration, on adsorption processes, which are relevant to near-surface environmental systems (e.g. soils). The mineral gibbsite ($\gamma\text{-Al}(\text{OH})_3$) is not only ubiquitous in the environment, but also representative of the alumina layer in clays (e.g. kaolinite $\text{Al}_2\text{Si}_2\text{O}_5(\text{OH})_4$), and uranyl(VI) has been demonstrated to interact with the mineral surface in a number of studies. In carbonate-free systems, U(VI) sorption onto gibbsite to forms outer sphere complexes and both monodentate and polynuclear inner sphere surface complexes between pH 4 and 9. [2] In the presence of carbonate at pH 6, mononuclear inner sphere complexes continue to form alongside carbonate containing polynuclear complexes. [3] Solid schoepite-like precipitation on the gibbsite surface has also been proposed above pH 6. [4] Despite these studies, bulk techniques often result in overlapping signals from uranyl centres and challenges arise in deconvolution of spectra. Consequently, there is difficulty in the quantification and assignment of uranyl species, particularly in the presence of carbonate, when there are a number of different species present in the systems. This has resulted in a knowledge gap with regard to the impact of carbonate and pH on the sorption of U(VI) to gibbsite. The effect this has on radionuclide behaviour and migration in environmental scenarios highlights the need to investigate these systems using a combination of techniques in order to bridge this gap.

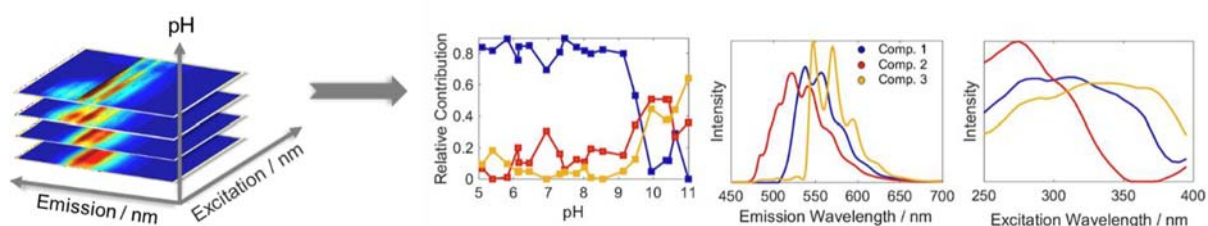


Figure 1. Schematic showing the decomposition of a three-dimensional dataset of excitation- emission matrices (EEMs) to three individual components and their contributions to the luminescence signal in each of the three modes of the dataset (pH, emission and excitation).

In this work, the speciation of U(VI) in a gibbsite containing system under ambient conditions was determined as a function of pH by deconvolution and analysis of luminescence data. The results show full removal of uranyl(VI) from solution between pH 6 and 11 in the presence of gibbsite, suggesting that sorption and/or precipitation on the gibbsite surface are key processes involved in the removal of U(VI) from solution. Excitation emission maps (EEMs) for the sorption set were collected at cryogenic temperatures (20 K). Parallel factor (PARAFAC) analysis was carried out on a dataset of EEMs for

sorption samples of uranyl(VI) on gibbsite across a pH range of 5.4 to 11. A validated model comprised of three components was obtained and the components assigned to U(VI) species, improving our understanding of U(VI) behaviour in this system.

The PARAFAC model is comprised of an individual emission spectrum and excitation spectrum for each of the three derived components, as well as their contribution to the luminescence intensity across the pH range 5.4 – 11. The validation of this PARAFAC model by split half analysis demonstrates the uniqueness of the solution. Evaluation of the spectral outputs from the models with existing knowledge of the characteristic, vibrationally resolved, uranyl(VI) emission patterns that are often observed in U(VI) solids at cryogenic temperatures,^[5] suggests that in this model each component is representative of one to two emissive uranyl(VI) centres. With the assistance of geochemical modelling (PHREEQC), thermodynamically derived models have been used to inform the assignment of the components. The predicted precipitation of schoepite and sodium-compreignacite phases from PHREEQC modelling, and by comparison to 331 synthesized standards, leads to the assignment of the three components as a schoepite- like uranyl(VI) oxyhydroxide mineral, a sodium containing uranyl(VI) oxyhydroxide and finally a component comprised of two emissive uranyl(VI) carbonate centres, likely sorbed on the gibbsite surface. Our combined experimental and statistical approach shows that assignment of uranyl(VI) species within a sorption system over a large pH range can be achieved using PARAFAC to deconvolute a three way dataset, elucidating the speciation of luminescent U(VI) In this system.

References

- [1] Lopez-Odriozola, L., Walker L. and Natrajan L. S. (2022) Luminescence properties of the actinides and actinyls in Reference Module in Chemistry, Molecular Sciences and Chemical Engineering. Elsevier, Amsterdam, Netherlands.
- [2] Baumann, N., Brendler, V., Arnold, T., Geipel, G., and Bernhard, G. (2004) Uranyl sorption onto gibbsite by time-resolved laser induced fluorescence spectroscopy (TRLFS). *J. Colloid Interface Sci.* 290: 318-324.
- [3] Gückel, K., Rossberg, A., Brendler, V., and Foerstendorf, H. (2012) Binary and ternary surface complexes of U(VI) on the gibbsite/water interface studied by vibrational and EXAFS spectroscopy. *Chem. Geol.* 326-327: 27-35.
- [4] Chang, H.-S, Korshin, G. V., Wang, Z. and Zachara, J. M. (2006) Adsorption of Uranyl on Gibbsite: A Time-Resolved Laser-Induced Fluorescence Spectroscopy Study. *Environ. Sci. Technol.* 50: 1244-1249.
- [5] Wang, Z., Zachara, J. M., Liu, C., Gassman, P. L., Felmy, A. R., and Clark, S. B. (2008) A cryogenic fluorescence spectroscopic study of uranyl carbonate, phosphate and oxyhydroxide minerals. *Radiochim. Acta* 96: 591-598.

PA5-18 THE COMBINED EFFECT OF ISA- AND CA-CONCENTRATION ON PU-SORPTION TO A CEM III/C-BASED MORTAR FOR IMMOBILIZATION OF NUCLEAR WASTE

Wouters Katinka ⁽¹⁾, Coppens Erik ⁽²⁾, de Blochouse Benny ⁽²⁾, Durce Delphine ⁽¹⁾

(1) Belgian Nuclear Research Centre (SCK CEN), Belgium

(2) Belgian Agency for Radioactive Waste and Enriched Fissile Materials (ONDRAF/NIRAS), Belgium

In the frame of the safe disposal of nuclear waste, ONDRAF/NIRAS (Belgium) has submitted a license application for the exploitation of a near surface facility for the disposal of short-lived low and intermediate level waste in Dessel (Belgium). When processing different types of waste, including radioactive waste, cementitious materials have been widely used as solidification/stabilization agents [1, 2]. A significant part of waste intended to be disposed of in the surface repository is Pu-contaminated and has been conditioned by means of CEM III/C based mortar. Sorption data for Pu to cementitious matrices are available, mostly for Ordinary Portland Cement (OPC) [3], and are used in the safety case for near surface disposal. However, uncertainties persist, especially concerning non-OPC binders like this particular mortar, leading to an experimental program aiming at obtaining adequate sorption values.

At the start of the research program, an experimental matrix was designed in order to screen which factors would affect sorption of Pu to the mortar. By using factorial design, the effects of multiple variables were addressed in one experimental set-up, thereby significantly reducing the number of tests needed, compared to the more traditional and intuitive “one-factor-at-a-time-approach”. A Plackett-Burman (P.-B.) design was selected for this screening.

The different factors of the design were variables related to the (synthetic) pore water composition of the mortar on one hand (concentrations of Ca^{2+} , Cl^- , SO_4^{2-} , S^{2-} , K^+ and OH^- (pH)), and variables characteristic for batch sorption experiments on the other hand (concentration of Pu, solid-to-liquid ratio and equilibration time). From this screening, it was concluded that only $[\text{Ca}^{2+}]$ in the synthetic pore water affected Pu sorption to the CEM III/C mortar to a significant extent. Additionally, from literature it is expected that the concentration of isosaccharinic acid (ISA), a cellulose degradation product, would affect Pu sorption [4].

The nature and extent of the impact of both $[\text{Ca}^{2+}]$ and [ISA] (including their combined effect) on sorption of Pu to the mortar, was addressed in a second step. A new experimental set-up was designed, to allow for Surface Response Measurement (SRM). A Central Composite Design in two factors was selected for the SRM, with a four point repetition of the center point and test points.

The execution of this experimental set-up and the resulting responses, allowed for the development of a model to predict the average response of Pu sorption as a function of [ISA] and $[\text{Ca}^{2+}]$. In addition, the $[\text{Ca}^{2+}]$ in equilibrium with the mortar could be assessed from the established dataset, which allowed to predict Pu-sorption as a function of [ISA] at the intrinsic $[\text{Ca}^{2+}]$ in the mortar's pore water, as presented in Figure 1.

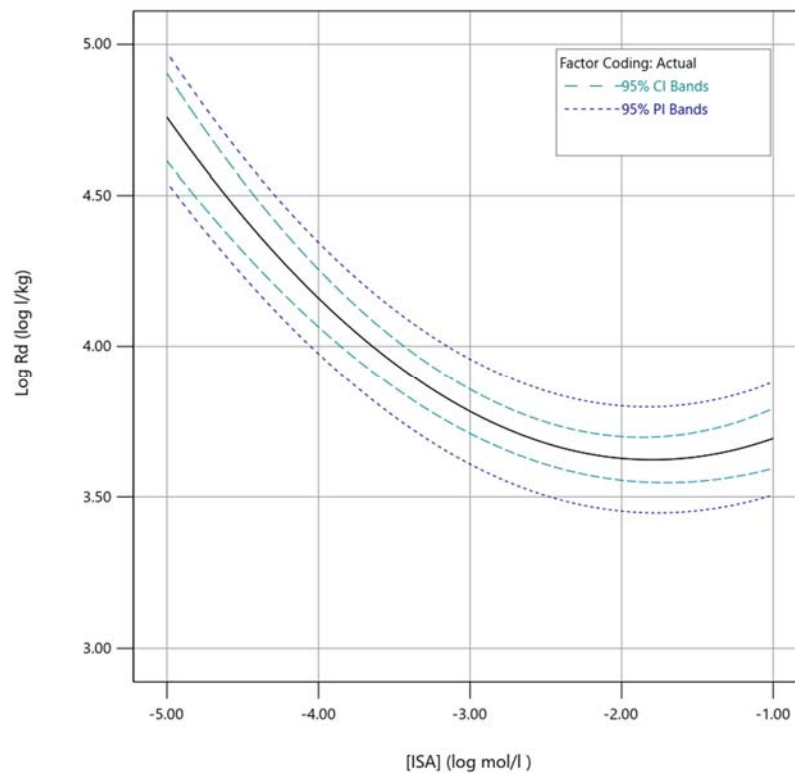


Figure 1: Model predictions for R_d as a function of the ISA concentration, for a fixed $[Ca^{2+}]$ of 3.09 mM. Both the best estimate and a 95% prediction interval (PI) and 95% confidence interval (CI) are visualized.

The prediction shows a clear decreasing trend of the distribution coefficient R_d with approximately 2 decades when [ISA] increases from 10^{-5} M to 10^{-2} M, and a stabilisation of R_d at [ISA] above approximately 10^{-2} M. At the lower estimate of the 95% prediction interval for the R_d , predictions fall slightly below a log R_d value of 3.5, while the lower estimate of the 95% confidence interval is just above a log R_d value of 3.5.

In a next step, sorption of Pu to CEM III/C hardened cement paste are being investigated, in order to explore whether the obtained sorption values and predictions could be extended to other CEM III/C based matrices. The results of this ongoing experimental design will be presented as well.

References

- [1] Chen, Q.Y., Tyrer, M., Hills, C.D., Yang, X.M., Carey, P (2009) Immobilisation of heavy metal in cement-based solidification/stabilisation: a review. *Waste Manage.* 29(1): 390-403.
- [2] Atkins, M., Glasser, F.P. (1992) Application of portland cement-based materials to radioactive waste immobilization. *Waste Manage.* 12(2-3): 105-131.
- [3] Wang, L., Martens, E., Jacques, D., De Cannière, P., Berry, J.A. and Mallants, D. (2009) Review of sorption values for the cementitious near field of a near surface radioactive waste disposal facility. ONDRAF/NIRAS, Brussels.
- [4] Wang, L. (2020) Recent literature on sorption values of Pu and other actinides on cementitious materials – Support to the experimental program determining sorption value of Pu on CILVA mortar. SCK CEN, Mol.

PA5-19 THE EFFECT OF CELLULOSE DEGRADATION PRODUCTS ON THE SORPTION AND DIFFUSION OF NICKEL IN DEGRADED HARDENED CEMENT PASTE

Durce Delphine ⁽¹⁾, Bleyen Nele ⁽¹⁾, Wouters Katinka ⁽¹⁾, Maes Norbert ⁽¹⁾

(1) Belgian Nuclear Research Centre (SCK CEN), Belgium

Cellulosic materials are widely used in the nuclear industry, and therefore make up a large quantity of waste streams. Both during interim storage and final disposal, cellulose will undergo radiolytic and/or hydrolytic degradation in cement water at highly alkaline pH. The generated degradation products and especially the α -isomer of isosaccharinic acid (α -ISA) could complex waste-relevant radionuclides (RNs), thereby affecting their retention and transport within the various barriers of the storage concept. Cement-based materials are omnipresent in nuclear waste repository designs acting as immobilization matrix of the waste or as structural reinforcement of the facility during the operational phase. Because cement-based materials can actively contribute to the retardation of RNs, it is essential to assess to which extent the presence of cellulose degradation products (CDP) might enhance the mobility of the relevant RNs and this along the full degradation process undergone by cement over time.

^{63}Ni is a waste-relevant RN and the effect of α -ISA on its sorption was investigated on degraded ordinary hardened cement paste (HCP) within the framework of the EURAD/CORI WP. The HCP was prepared from CEM I at a water/cement ratio of 0.5, powdered, grinded and degraded to state III by leaching in ultrapure water under inert atmosphere. The sorption of ^{63}Ni was investigated in batch experiments in presence and absence of α -ISA. For comparison purposes, the same experiments were performed on the fresh HCP and on the CORI reference HCP degraded to state II.

α -ISA is expected to be the main RN complexant in the mix of CDP. However, to investigate whether other CDP could also play a role, ^{63}Ni sorption experiments in presence and absence of a mixture of CDP were also initiated, with the same substrates as for α -ISA. The CDP mixture was obtained by gamma irradiation followed by long-term hydrolytic degradation of cellulosic tissues at pH 13.

The results obtained so far (Figure 1) show that both the degradation degree of the HCP and the presence of α -ISA affect the extent of Ni sorption. Sorption of Ni is favored with degradation, which can be related to the change of zeta potential along decalcification. The presence of α -ISA shows a significant effect on Ni sorption from a concentration of $\sim 10^{-3}$ mol/L for both the CORI reference and degraded HCP while its effect can be observed from $\sim 10^{-4}$ mol/L on fresh cement when α -ISA is added in the CDP mixture. This suggests a possible effect of some of the other cellulose degradation compounds. This observation remains however to be confirmed by the results on degraded HCP and CORI reference cement in presence of CDP, which are expected in the near future.

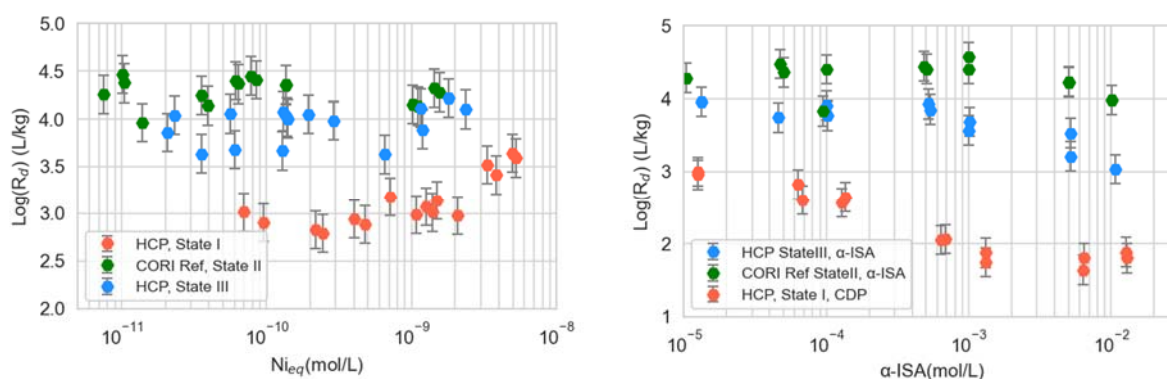


Figure 1. Sorption of Ni in absence (left) and presence (right) of cellulose degradation products and/or α -ISA.

Diffusion experiments were also launched to investigate the effect of α -ISA on the transport of Ni in degraded HCP discs. HCP discs of dimensions 2-4 mm \times 45.7 mm (thickness \times diameter) were degraded in UP water for approximately 9 months. The degradation was followed in time by a range of solid and liquid characterization techniques (XRD, SEM-EDX, ICP-MS, IC) allowing to assess the progression of the degradation front. The discs were then embedded in resin and loaded in custom-made diffusion cells. A synthetic cement solution representative of the cement degradation state was prepared and spiked with only Ni for the first experiment and with both Ni and α -ISA for the second experiment. The evolution of the Ni concentration in the inlet is currently being monitored in time and the diffusion profile will be measured at the end of the experiment by LA-ICP-MS in SUBATECH (Nantes, France).

Both the sorption and diffusion experiments will be modelled and the obtained experimental and modelling results will be presented.

Acknowledgments: *This study was partially supported by the European Union's Horizon 2020 Research and 399 Innovation Programme under Grant Agreement no. 847593 (EURAD, CORI)*

PA5-20 RETENTION OF RADIONUCLIDES (CAESIUM, NICKEL) IN FRACTURE INFILLS UNDER DIFFERENT GEOCHEMICAL CONSTRAINS

Filip Jankovský⁽¹⁾, Karol Kočan⁽¹⁾, Václava Havlová⁽¹⁾, Milan Zuna⁽¹⁾, Lucie Mareda⁽²⁾

(1) ÚJV Řež, a.s., Disposal Processes and Safety Department, Hlavní 130, 25068 Husinec, Czech Republic

(2) SÚRAO, Radioactive waste repository authority, Dlážděná 6, 11000 Praha, Czech Republic

Crystalline host rock represents the last barrier in the system of deep geological repository (DGR). Fracture infills can intensively increase retention rate of radionuclides during their transport from DGR to the environment. The retention rate is quantified by sorption coefficients (K_d), which serve as an input parameter in reactive transport modelling. Those are determined by batch sorption experiments (BSE) [1]. Two radionuclides with different chemistry (^{134}Cs and ^{63}Ni) were selected to prove retention function of the fissure infill. Caesium represents a medium sorbing cation with stable chemistry in wide pH range and also refers to one of the radionuclides presented in spent nuclear fuel (SNF) as a fission product of ^{235}U . Nickel on the other hand represents a group of radionuclides with high sorption properties and relatively complex chemistry influenced by pH. The radionuclide is produced during neutron activation as a fission product [2].

Two types of fracture filling in crystalline rock formation were extracted at the Bukov Underground Research Facility (Bukov URF) on the 12th level (550 m below the surface), where rock samples have been previously collected for evaluation of migration processes of radionuclides in the environment of crystalline rocks [3]. One of the fracture infill represents rather homogeneous material consisting mainly of calcite. The other one represents a complex clay material with high content of secondary clay minerals, chlorite and mica as determined by XRD. All samples were processed to required grain size fractions (0,125 – 0,63 mm). Batch sorption experiments were performed under constant concentration of non-active carrier Cs, Ni (spiked with active tracers ^{134}Cs and ^{63}Ni) with different m/V ratio during the time period of 14 days. Linear isotherm was used to determine K_d . In order to simulate the real in-situ conditions within the laboratory experiments, the synthetic granitic water (SGW2) was used as a solution. Sorption experiments were performed in both aerobic and anaerobic conditions mainly to distinguish the role of the carbonates in the system on the pH and therefore indirectly on the Ni speciation with complex chemistry. The mineralogical composition and specific surface area (SSA) of fracture infills were determined. Sorption experiments with Cs were complemented by radiocaesium interception potential (RIP) [4].

Specific surface area of the fracture infill with clay significantly differs in comparison with the calcite infill. Clay fracture infill is characterized by much higher SSA and thus higher number of sorption sites than calcite filling. These findings were also supplemented by radiocaesium interception potential (RIP). Results are also showing that Cs as an element with higher ionic radius than calcium ion could very poorly be exchanged or sorbed to the surface of calcite [5]. Results from the sorption experiments with Cs on clay revealed non-linear isotherm in the range of investigated m/V ratios. The behaviour of Ni during sorption experiments showed that both calcite and clay fracture infills can significantly decrease its concentration in the surrounding aqueous phase to much more extend than in the case of Cs. The results of Ni retention under different $p\text{CO}_2$ showed that CO_2 presence influence sorption through its pH and thus Ni speciation.

Acknowledgment: *This work has been funded from the European Union's Horizon 2020 research and innovation programme under grant agreement n° 847593, WP Future.*

References

- [1] Hakanen M., Ervanne H., Puukko E. (2014). Safety Case for the Disposal of Spent Nuclear Fuel at Olkiluoto: Radionuclide Migration Parameters for the Geosphere. *Technical Report 2012-41*. Posiva, Eurajoki, Finland.
- [2] Fišera O., Šebesta F. (2010). Determination of ^{59}Ni in radioactive waste. *J. of Radioanal. Nucl. Chem.* 286(3): 713–717.
- [3] Havlová V., Zuna M., Brázda L., Kolomá K., Galeková E., Rosendorf T., Jankovský F. (2019). Migration processes of radionuclide in the environment of crystalline rocks and migration parameters of the rocks of the Czech massif. *Final Report 333/2018*, SÚRAO, Prague, Czech Republic.
- [4] Wauters J., Sweeck L., Valcke E., Elsen A., Cremers A. (1994). Availability of radiocaesium in soils: a new methodology. *Sci. Total Environ.* 157: 239-248.
- [5] Torstenfelt B., Anderson K., Allard B. (1982). Sorption of strontium and caesium on rocks and minerals. *Chemical Geology.* 36: 123-138.

PA5-21 INFLUENCE OF THE COMPETITION OF AL ON THE RETENTION OF TRIVALENT ACTINIDES AND THEIR HOMOLOGUES IN FELDSPAR

Jessica Lessing ⁽¹⁾, Julia Neumann ⁽²⁾, Frank Bok ⁽¹⁾, Johannes Lützenkirchen ⁽³⁾, Vinzenz Brendler ⁽¹⁾, Moritz Schmidt ⁽¹⁾, Thorsten Stumpf ⁽¹⁾

(1) Helmholtz-Zentrum Dresden-Rossendorf, Institute of Resource Ecology, Germany

(2) Argonne National Laboratory, Chemical Sciences and Engineering Division, USA

(3) Karlsruher Institut für Technologie, Institute for Nuclear Waste Disposal, Germany

The safest concept for disposal of nuclear waste is considered to be in a deep geological formation, e.g., crystalline rock. There, main components are (alumino-)silicates, such as feldspars, mica and quartz. The minor actinides (Np, Am, and Cm) as well as plutonium dominate the radiotoxicity of spent nuclear fuel over geological time scales. Understanding the mechanisms of their prevalent retention processes is of utmost importance for a realistic safety assessment of such a repository. The stable lanthanide Eu^{3+} (with excellent luminescence properties) is often used as a homologue for the trivalent actinides. The retention of trivalent actinides by K-feldspars was recently investigated by our group [1]. However, no sorption data of minor actinides is available for the series of Ca-feldspars (plagioclases), which possess a different Al:Si ratio in the crystal lattice, possibly causing differences in surface charge, dissolution, and sorption behavior. Here, we study the sorption of trivalent actinides and their rare earth element homologues on Ca-feldspars quantitatively and mechanistically [2].

Our new experimental data show that the sorption of trivalent actinides (Am^{3+} , Cm^{3+}) on feldspars depends on its main cation component (K^+ , Na^+ , or Ca^{2+}). Orthoclase, a K^+ -bearing feldspar, shows a slightly lower sorption affinity in comparison to the Ca^{2+} -bearing feldspar anorthite. However, the same sorption complexes are formed on both minerals, thus it can be concluded that the structure of the formed inner sphere complex is independent on the feldspar type. Furthermore, a surface complexation model was derived from these data. A possible explanation for the differing sorption edges may be found in the fact that anorthite dissolves more strongly, which leads to a higher concentration of Al^{3+} in the surrounding aqueous phase. This in turn directly affects surface charge and sorption processes. In addition to competition for sorption sites, Al^{3+} may also re-precipitate on a primary mineral's surface and form a secondary phase [3,4,5], which will impact the interaction of radionuclides with these minerals.

To understand the impact of Al^{3+} on the sorption behavior of trivalent actinides and lanthanides on feldspars in more detail, different methods to characterize the surface of feldspar in presence of Al^{3+} were used. Firstly, zeta potential investigations reveal a strong impact of Al^{3+} onto the surface charge of feldspar (see figure 1 right). The zeta potential increases for pH 4.5 – 7.5, with a stronger increase with higher added Al^{3+} concentration, even reaching charge reversal to up to 20 mV. Batch sorption experiments of Eu onto K-feldspar (see figure 1 left) show a steeper sorption edge upon adding Al^{3+} to them, which can be interpreted as a slightly stronger sorption affinity, indicating that the higher Eu retention by Ca-feldspar may be indeed connected to the role of Al^{3+} .

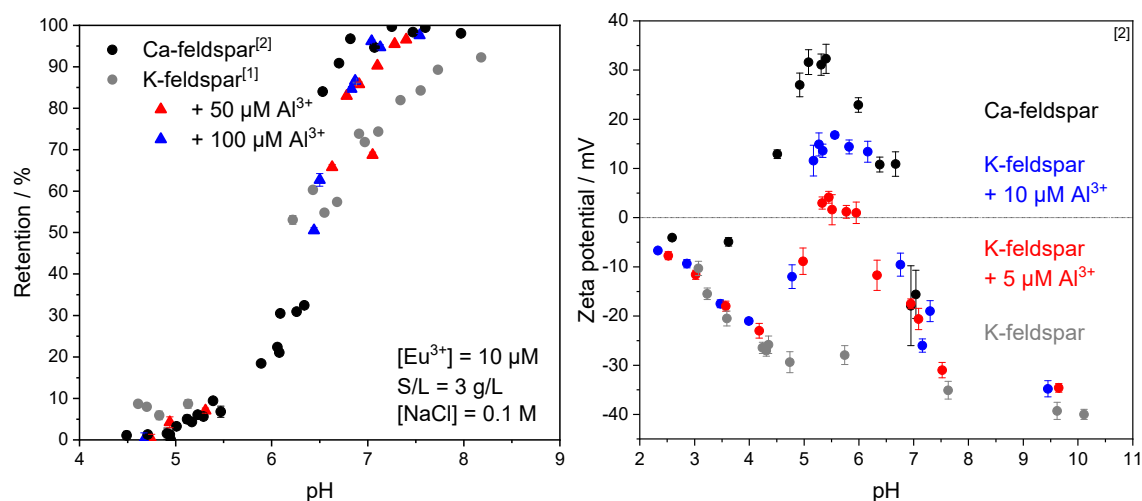


Figure 1 Left: sorption experiments of Eu^{3+} onto feldspar without and in the presence of added Al^{3+} . Right: Zeta potential measurements ($\text{S/L} = 0.2 \text{ g/L}$; $[\text{NaCl}] = 0.1 \text{ M}$) of feldspar without and in the presence of added Al^{3+} .

For further analysis of the responsible mechanisms of the increased retention we will apply time resolved laser-induced fluorescence spectroscopy, from which information about the formed surfaces complexes can be gained. Potential secondary phases are searched for by a combination of scanning electron microscopy, transmission electron microscopy, Raman analysis, atomic force microscopy, and surface X-ray diffraction. In summary, our work will achieve a better understanding of the fundamental mechanisms of sorption process of the minor actinides on naturally occurring aluminosilicate phases under close to nature conditions.

References

- [1] Neumann, J. et al. (2021) A comprehensive study of the sorption mechanism and thermodynamics of f-element sorption onto K-feldspar. *J. Colloid Interface Sci.* 591, 490-499.
- [2] Lessing, J. et al. (2023) Natural and synthetic plagioclases: Surface charge characterization and sorption of trivalent lanthanides (Eu) and actinides (Am, Cm). *J. Colloid Int. Sci.* In preparation.
- [3] Fendorf, S. et al. (1994) Mechanism of Aluminum Sorption on Birnessite: Influences on Chromium (II) Oxidation. *World Congr. Soil Sci.*, No. VI.
- [4] Legg, B. A. et al. (2022). Hydroxide films on mica form charge-stabilized microphases that circumvent nucleation barriers. *Sci. Adv.* 8: 1-11.
- [5] Lee, S. S. et al. (2016). Structural Characterization of Aluminum (Oxy)hydroxide Films at the Muscovite (001)–Water Interface. *Langmuir* 32: 477-486.

PA5-22 CHEMICAL TOMOGRAPHY OF PYRITE COMPOSITES EXTRACTED FROM OPALINUS CLAY AND REACTED WITH NEPTUNIUM AND PLUTONIUM

Markus Breckheimer⁽¹⁾, Samer Amayri⁽¹⁾, Dario Ferreira Sanchez⁽²⁾, Daniel Grolimund⁽²⁾, Tobias Reich⁽¹⁾

(1) *Johannes Gutenberg-Universität Mainz, Department of Chemistry, Nuclear Chemistry, 55099 Mainz, Germany*

(2) *Paul Scherrer Institute, Swiss Light Source, microXAS Beamline Project, 5232 Villigen PSI, Switzerland*

The final disposal of high-level radioactive waste (HLW) in a deep geological repository requires a thorough understanding of the geochemical processes governing the fate of potentially mobilized radionuclide species. Argillaceous rock is being considered as a potential host rock, with Opalinus Clay (OPA) from the Mont Terri rock laboratory (St-Ursanne, Switzerland) serving as a reference for natural clay rock, featuring characteristic properties of a sedimentary rock such as structural and compositional heterogeneities on different length scales [1]. In batch sorption experiments with dispersed [2] and diffusion studies in bulk OPA, gaining diffusion profiles through abrasive peeling [3], the influence of the heterogeneous microstructure of the host rock is not accounted for, yielding spatially and compositionally averaged retention and transport parameters.

To further elucidate the role of the heterogeneous OPA microstructure and its potentially reactive mineral phases, previous synchrotron-based, multimodal chemical imaging studies were performed at the microXAS beamline (Swiss Light Source, Paul Scherrer Institute, Villigen, Switzerland), utilizing the different modalities of micro-X-ray absorption (μ XAS), micro-X-ray fluorescence (μ XRF) and micro-X-ray diffraction (μ XRD). These sorption and diffusion studies of Np(V) and Pu(V,VI) with bulk OPA samples revealed an enhanced retention and redox transformation to reduced tetravalent, less mobile radionuclide species in spatial correlation to domains of pyrite (FeS_2) [4-6], contained as a microstructural, Fe(II)-bearing component in OPA to about 1 wt. %. Varying degrees of correlation across the studies and sample systems suggest a potentially decoupled redox and sorption mechanism.

To gain a better understanding of this relevant reactive transport mechanism, preferably pristine pyrite composites were extracted from OPA as sub-mm-sized particles. SEM/EDX analyses allowed a general classification of the retrieved particles into two representative composite morphologies based on crystallite sizes and ordering: micro-crystalline and (poly)framboidal aggregates of pyrite crystallites, predominantly cemented by calcite. A selection of sub-100 μm sized particles of both morphologies was exposed to radionuclide species in sorption experiments with solutions of 7.4 μM $^{237}\text{Np(V)}$ and, respectively, 13-14 μM $^{242}\text{Pu(VI)}$ in OPA pore water (pH 7.7-7.9, I=0.4 M). All processes involving wet chemistry, in particular the composite extraction and sorption experiments, were conducted under anaerobic conditions and calcite saturation to prevent a composite altering pyrite oxidation and dissolution of the cementing phase.

A selection of reacted particles was prepared into capillaries and measured by multimodal chemical tomography, gaining volume information with voxel sizes of 1-1.5 μm^3 of the inner structure, chemical and mineralogical compositions and distributions by tomographic reconstruction of the respective modalities of X-ray absorption contrast (μ CT), μ XRF-CT and μ XRD-CT. Spatial distributions of the studied radionuclides were gained by LIII absorption edge contrast and deconvolution of simultaneously recorded full XRF spectra.

Despite the necessary selection of a limited sample size in this study, the results so far provide two relevant observations concerning the geochemical interaction of radionuclide species and the pyrite

composites: an enhanced retention reactivity of the framboidal morphology and a spatial correlation of the immobilized radionuclides with the interspace of the pyrite aggregates, predominantly cemented by calcite.

In conclusion, the results of this study contribute to an enhanced understanding of reactive transport in Opalinus Clay as a reference for a natural heterogeneous host rock, relevant for the safety case of a deep geological HLW repository.

Acknowledgements: *Funding from the German Federal Ministry of Education and Research (BMBF) under contract number 02NUK044B, from the Federal Ministry for Economic Affairs and Energy (BMWi) under contract numbers 02E11415A and 02E11860A, and from the European Union's Horizon 2020 project EURAD (WP FUTuRE), EC Grant agreement no. 847593, is acknowledged.*

References

- Nagra (2002). Tech. Ber. 02-03. Projekt Opalinuston. Wettingen, Switzerland.
- Amayri, S., Fröhlich, D.R., Kaplan, U., Trautmann, N. and Reich, T. (2016). Distribution coefficients for the sorption of Th, U, Np, Pu, and Am on Opalinus Clay. *Radiochim. Acta* 104(1): 33- 40.
- Wu, T., Amayri, S., Drebert, J., Van Loon, L.R. and Reich, T. (2009). Neptunium(V) sorption and diffusion in Opalinus Clay. *Environ. Sci. Technol.* 43: 6567-6571.
- Fröhlich, D.R., Amayri, S., Drebert, J., Grolimund, D., Huth, J., Kaplan, U., Krause, J. and Reich, T. (2012). Speciation of Np(V) uptake by Opalinus Clay using synchrotron microbeam techniques. *Anal. Bioanal. Chem.* 404: 2151-2162.
- Kaplan, U., Amayri, S., Drebert, J., Rossberg, A., Grolimund, D. and Reich, T. (2017). Geochemical interactions of Plutonium with Opalinus Clay studied by spatially resolved synchrotron radiation techniques. *Environ. Sci. Technol.* 51: 7892-7902.
- Börner, P.J.B. (2017). Sorption and diffusion of Neptunium in Opalinus Clay. PhD thesis. Johannes Gutenberg-Universität Mainz, Mainz, Germany.

PA5-23 INTERACTIONS BETWEEN RADIONUCLIDES AND CALCITE SURFACE

Xiaodong Li (1), Michaela Matulova (2), Alexandra Sticker (3), Eini Puhakka (1), Shangyao Guo (4), Mireille Delnero (4), Filip Jankovsky (5), Lucie Mareda (2), Marja Siitari-Kauppi (1)

(1) *Department of Chemistry-Radiochemistry, University of Helsinki, Helsinki, Finland*

(2) *Radioactive Waste Repository Authority (SÚRAO), Dlážděná 6, 11000 Prague 1, Czech Republic*

(3) *Faculty of Chemistry and Mineralogy, University of Leipzig, Leipzig, Germany (graduated)*

(4) *Institut pluridisciplinaire Hubert Curien (IPHC), Strasbourg, France*

(5) *ÚJV Rez, a.s., Hlavní 130, Rez, Husinec, Czech Republic*

Calcite is a common mineral in the environment, comprising approximately 4% of the earth's crust. The surface reactions of calcite play an important role in many geological and environmental systems, including the production of oil and gas, the geological storage of nuclear waste and CO₂ etc. For example, the sorption of a radionuclide from nuclear waste on calcite surfaces affects significantly its mobility and removal from aqueous phases. Ba-133 and Ni-63 are radionuclides of interest due to their prevalence in nuclear waste and their potential impact on human health and the environment. Understanding the interactions between these radionuclides and calcite surfaces is important for enhancing the confidence in safety assessments.

Calcite surface studies

Despite numerous studies that have been performed, the fundamental parameters of calcite surface charge in aqueous solutions, especially at conditions relevant to natural systems, remain poorly understood. The calcite surface composition and charge are linked to its reactivity and sorption properties, and thus, they are the primary data source to understand the sorption properties of radionuclides on calcite surfaces. A clear illustration of the potential determining ions for calcite surface and expressions of zeta potentials at the molecular level can give a fundamental understanding of the surface complexation reactions that happen on calcite surfaces and provide basic data for later surface studies with modelling approaches. In this work, the surface properties of Bukov calcite are studied by a combination of experimental and different modelling methods. To ensure precision of the experiments, an investigation into the equilibrium of the calcite surface should be conducted. The surface properties and cross-sections of crushed calcite samples are characterized experimentally by cation exchange capacity (CEC), B.E.T. (Kr) for specific surface area (SSA), scanning electron microscope (SEM) and zeta potential measurements (ZP, Figure 1a). DFT molecular modelling shows that the calcite (104) surface is the most active surface for reacting with radionuclides. On calcite (104) surface, the carbonate groups are diagonal oriented, and the calcium ions are parallel to the carbonate groups (Figure 1b) [1].

Reactions of Ni-63 and Ba-133 on calcite surface

A batch sorption experiment was conducted to investigate the sorption behavior of Ni-63 and Ba-133 on calcite under varying pH and concentration conditions. The study utilized batch sorption techniques, and the results showed that both Ni-63 and Ba-133 exhibited strong sorption on calcite. The K_d values measured varied as a function of both pH and concentration, as demonstrated in Figure 2a. Furthermore, the results indicated that precipitation and coprecipitation were significant mechanisms for immobilizing Ni-63 and Ba-133 in the solution, particularly with high concentrations of free-carbonates in the aqueous phase, as illustrated in Figure 2b. The pH effect revealed that calcite can remove Ni-63 and Ba-133 more effectively in alkaline solutions. The effect of precipitation on calcite immobilization of radionuclides will be determined by in situ ATR-FTIR spectroscopy to investigate the interacted surface functional groups and structural changes occurring during the sorption process [2].

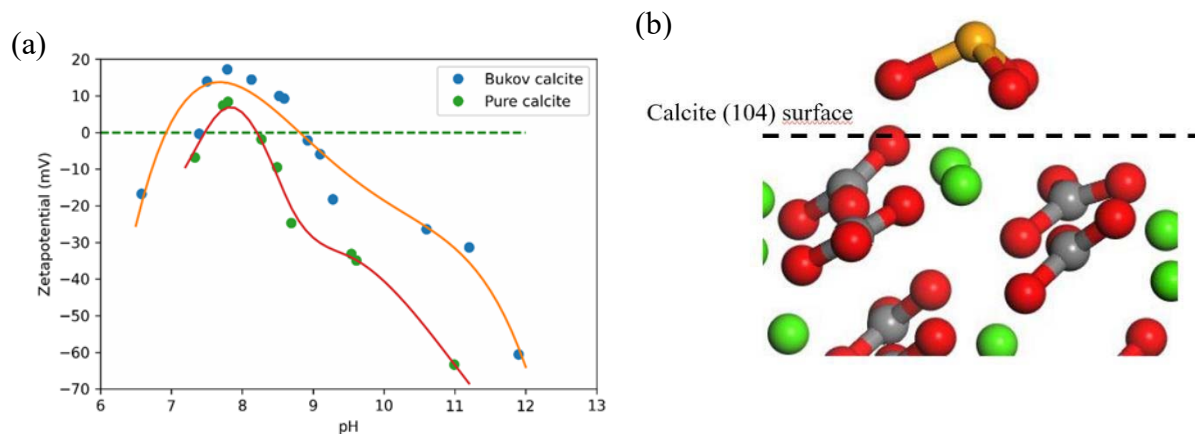


Figure 1. (a): Zeta potential measurements of Bukov calcite and pure calcite in equilibrium with 0.002 M NaCl background solution as a function of pH from 7 to 12 in N_2 -atmosphere glovebox. (b): Molecular modelling for calcite (104) surface.

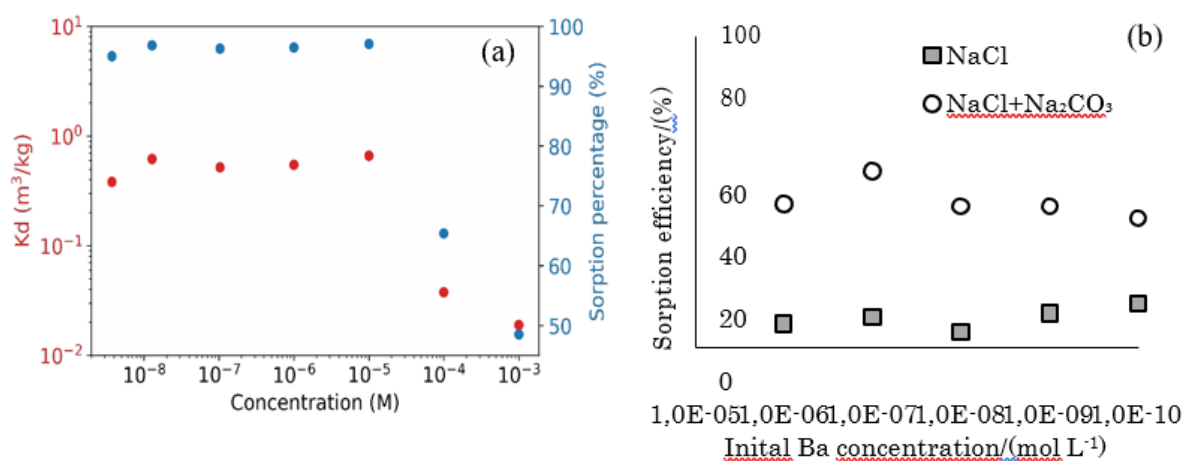


Figure 2. (a): Sorption isotherm (K_d and sorption percentage) of Ni-63 sorption on pure calcite. (b): Sorption isotherm of Ba-133 sorption on pure calcite in $0.1 mol L^{-1}$ NaCl and mixture of $0.1 M$ NaCl and $0.1 mol L^{-1}$ Na₂CO₃ background solution.

References

- [1] Puhakka, E., Li, X., Ikonen, J., Siitari-Kauppi, M. (2019). Sorption of selenium species onto phlogopite and calcite surfaces: DFT studies. *Journal of Contaminant Hydrology* 227, 103553.
- [2] Del Nero, M., Galindo, C., Barillon, R., Halter, E., Madé, B. (2010). Surface reactivity of α -Al₂O₃ and mechanisms of phosphate sorption: In situ ATR-FTIR spectroscopy and ζ potential studies. *Journal of Colloid and Interface Science* 342, 437–444.

PA5-24 THE STUDY OF MARINE SOLUTIONS INFLUENCES ON THE SORPTION OF ^{226}Ra TO MINERALS

Jiusi Wang, Brian A. Powell

Environmental Engineering and Earth Sciences Department, Clemson University, 342 Computer Court, Anderson, South Carolina 29625, United States

Currently, the knowledge of discrete radioactive material (RAM) within marine systems is limited. More specifically, the effects of RAM on marine biota have not been well defined. Radium-226 (^{226}Ra) from ^{226}Ra painted dials and paint chips is a typical example of a discrete. Thus, the ^{226}Ra potential for adverse effects of small-scale ^{226}Ra behavior needs to be evaluated to understand the possible damage from radioactive isotopes to its surrounding marine systems. However, few studies have investigated the ^{226}Ra sorption process under marine system similar conditions. Therefore, we examined ^{226}Ra sorption process under different concentrations of seawater conditions to several types of minerals through batch sorption test. After the system reaches equilibrium, the solid/liquid partition coefficients (K_d) for each solid were then determined using the liquid phase ^{226}Ra concentration data.

Batch sorption experiments were conducted for 7 days on end-over-end shaker to fully mix the samples. In the first part of the experiment, ^{226}Ra adsorption in 10mM NaCl solution and Seawater are studied. Quartz, Crushed Shell (mainly Calcite), Montmorillonite as clay, and Goethite as Ferrihydrite are used as adsorbents. Three different initial ^{226}Ra concentrations (5, 25, 50 ng/L) were used in duplicate batch reaction systems. The results prove that ^{226}Ra adsorption is different in 10mM NaCl solution and Seawater. To further study how seawater influences ^{226}Ra adsorption behavior, 5 different solutions (DI water, 1% seawater, 10% seawater, 60% seawater, 100% seawater) were used in the second part of the experiment. Pure calcite, Crushed Shell (mainly Calcite), Montmorillonite as clay, and Goethite as Ferrihydrite are used as adsorbents.

In general, different solution tends to influence the ^{226}Ra adsorption to the minerals. In the first part of the experiment, the solid/liquid partition coefficients (K_d) for crushed shell (mainly calcite) and clay (Montmorillonite) changed significantly due to the change of base solution (seawater/ NaCl solution). The increase in NaCl concentration (from 10mM to 600mM) significantly drops K_d value of crushed shell (mainly calcite) and clay (Montmorillonite). The K_d value of Crushed Shell (mainly calcite) and clay (Montmorillonite) in 10mM NaCl was around 50 times and 9 times larger than in seawater respectively. For the quartz, the change in K_d values is not significant (within same magnitude). The K_d value of quartz in seawater is only 2 times larger compared to the 10mM NaCl solution. For Goethite (Ferrihydrite), the K_d value remains the same for seawater and 10mM NaCl solution.

In the second part of the experiment, the K_d values decrease while the seawater concentration is increasing for crushed shell, which is consistent with the result from first part of the experiment. However, the K_d values of calcite remain in the same magnitude (no significant change). The difference between crushed shell and calcite may be due to their different surface situation or the more complex composition of crushed shell. For Clay, the KD value increases at first but then drops after the SW concentration exceeds 10%. For Goethite (Ferrihydrite), the change in K_d values is not significant, which is consistent with the result from the first part of the experiment.

As a conclusion, our result suggests that the ^{226}Ra sorption process to the minerals should be different in the marine system compared to other nature aqueous system. Further studies about Radium leaching experiment under different conditions and batch sorption experiments were also produced to provide supply information to help us understand the ^{226}Ra behavior in marine system.

PA5-25 MOLECULAR SCALE UNDERSTANDING OF Ni^{2+} ADSORPTION ON SWELLING CLAY MINERALS

Vasyl Stotskyi^(1,2), Fulvio Di Lorenzo^(1,2), Maria Marques Fernandes⁽¹⁾, Matthias Krack⁽¹⁾, Andreas Scheinost^(3,4), Martine Lanson⁽⁵⁾, Bruno Lanson⁽⁵⁾ and Sergey V. Churakov^(1,2)

(1) Paul Scherrer Institut (PSI), Laboratory for Waste Management, Switzerland

(2) University of Bern, Institute of Geology, Switzerland

(3) Helmholtz-Centre Dresden-Rossendorf, Institute of Resource Ecology, Germany

(4) The Rossendorf Beamline at ESRF, France

(5) Univ. Grenoble Alpes, Univ. Savoie Mont Blanc, CNRS, IRD, Univ. Gustave Eiffel, ISTERre, France

Adsorption on clay minerals is a key process for the immobilization of hazardous metals in natural environments and engineered systems, such as deep geological radioactive waste repositories. A detailed understanding of the retention mechanisms, including knowledge of the exact binding sites, is essential for reliable and robust predictive transport modeling and safety analyses [1-3].

Bradbury and Baeyens [1] developed the 2SPNE SC/CE model, which postulates two different types of surface complexation sites for divalent [4] and trivalent [5] metals on 2:1 clay minerals such as illite and montmorillonite. So-called “strong” sites have a high affinity, but low capacity, while “weak” sites have a high capacity, but low affinity. The molecular structure of both sites on edge surfaces of montmorillonite has been explained only for a few elements, namely for Zn [2][3] and Fe[4], and Am [5] by employing extended X-ray absorption fine structure (EXAFS) spectroscopy, partly also coupled to ab initio MD simulations to derive theoretical reference spectra for linear combination fitting.

Our project aims to extend this work on the common di- and trivalent elements (Zn^{2+} , Ni^{2+} , Lu^{3+}) on clay mineral surfaces and, at the same time, to improve thermodynamic sorption models by using advanced atomistic simulations and EXAFS for quantitative description of sorption processes. We use the synthetic trioctahedral swelling clay, saponite, since it allows us to obtain a material with almost zero impurities and to adjust its composition.

Similar to the adsorption of Ni^{2+} on montmorillonite [1], Ni^{2+} on saponite shows a non-linear adsorption behavior however with much higher sorption (see Fig.1). Based on the sorption isotherms obtained on saponite, self-oriented clay films were prepared, with Ni loadings assumed to correspond to adsorption to strong and weak sites, and then polarized Ni K-edge EXAFS spectra were recorded. Applying P-EXAFS to layered clay minerals allows depending on the orientation of the beam to probe preferentially the contributions of cations from the tetrahedral (Si in saponite) or the octahedral (Mg in saponite) sheets.

For samples with low Ni^{2+} loadings (below 4 mmol/kg), EXAFS results confirmed the existence of strong sorption sites. An increase of Ni loading (up to 40 mmol/kg) leads to decreasing in Ni-Mg bond length and an increase in Ni-Si coordination number, indicating the formation of a secondary phase. The exact structure of the new phase is still under evaluation, but this solid phase will certainly mask Ni sorbed to weak sites.

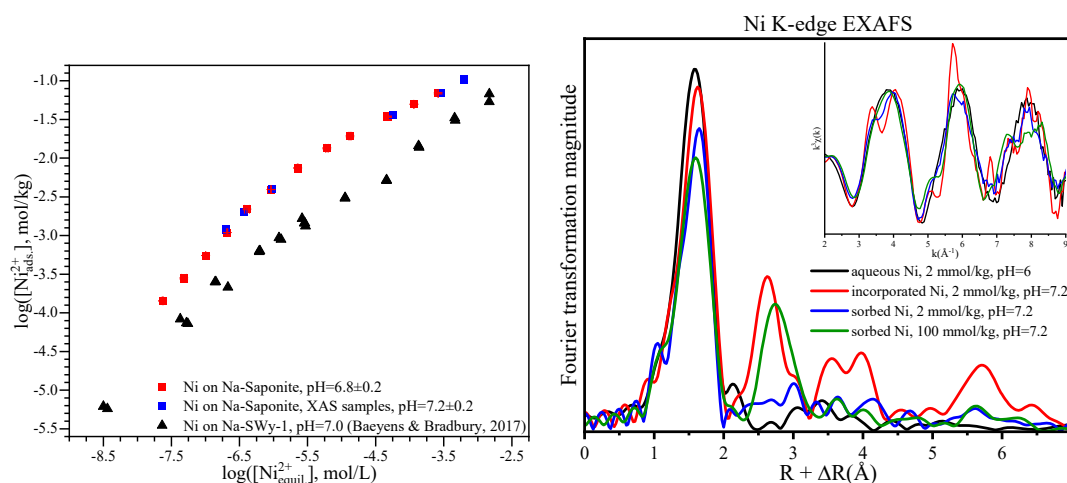


Figure 1. Sorption isotherm for Ni^{2+} on saponite and montmorillonite (left), and experimental Ni-K EXAFS spectra (right). Only polarized EXAFS spectra at the 35° angle are shown here.

The most stable surfaces, their structure, and speciation were determined using geometry optimization and the Wulff construction method. The molecular structure of cations adsorbed on the water-edge interfaces for the most stable surfaces was modeled using ab initio MD. These simulations enable us to provide a theoretical estimation of the free energies of Zn-Ni cation exchange reactions between weak and strong sites on (100) and (130) edges of saponite. Since experimental values are being currently investigated, we used results obtained for montmorillonite as a trustworthy proxy. Theoretical values obtained for Zn-Ni exchange on saponite are equal to 13.516 ± 0.418 and 5.460 ± 0.025 kJ/mol for (100) and (130) surfaces, respectively. The experimental value obtained for the same reaction on montmorillonite is 9.129 kJ/mol. Considering good agreement between the two systems, this suggests a stronger affinity of Zn to strong sites than Ni.

The simulated structures are used to generate theoretical EXAFS spectra with FEFF software, which, using the linear combination fit method, could help to reveal the exact structure of Zn^{2+} and Ni^{2+} sorption complexes on saponite edge surfaces.

References

- [1] Bradbury, M.H. and B. Baeyens (1997). A mechanistic description of Ni and Zn sorption on Na-montmorillonite Part II: modelling. *J. Contam. Hydrology* 27: 223-248.
- [2] Dähn, R., Baeyens, B., and M.H. Bradbury (2011). Investigation of the different binding edge sites for Zn on montmorillonite using P-EXAFS – The strong/weak site concept in the 2SPNE SC/CE sorption model. *Geochimica et Cosmochimica Acta* 75: 5154-5168.
- [3] Churakov, S.V. and R. Dähn (2012). Zinc adsorption on clays inferred from atomistic simulations and EXAFS spectroscopy. *Environmental Science & Technology* 46: 5713-5719.
- [4] Keri, A. et al. (2020). Iron adsorption on clays inferred from atomistic simulations and X-ray absorption spectroscopy. *Environmental Science & Technology* 54: 11886-11893.
- [5] Marques Fernandes, M., Scheinost, A.C., and Baeyens, B. (2016). Sorption of trivalent lanthanides and actinides onto montmorillonite: Macroscopic, thermodynamic and structural evidence for ternary hydroxo and carbonato surface complexes on multiple sorption sites. *Water Research* 99: 74-82.

PA5-26 SORPTION PROPERTIES OF EU ONTO GRANITE AND MX-80 BENTONITE IN CA-NA-CL SOLUTIONS

Jianan Liu ⁽¹⁾, Shinya Nagasaki ⁽¹⁾, Tammy Yang ⁽²⁾

(1) Department of Engineering Physics, McMaster University, 1280 Main St. West, Hamilton, Ontario, Canada, L8S4L7

(2) Nuclear Waste Management Organization, 22 St. Clair Ave. East, 4th Floor, Toronto, Ontario, Canada, M4T 2S3

Plutonium (Pu) is one of the key elements in high-level radioactive waste due to its long half-life. Pu is identified as a radionuclide of interest in the safety assessment of the Deep Geological Repository (DGR) for the used nuclear fuel in Canada. The sorption behavior of key radionuclides such as Pu and U will impact the safety assessment calculation results. Europium (Eu), a chemical analogue of Pu, has been proved to share similar sorption behaviors with Pu. The aim of this study is to investigate the sorption properties of europium onto MX-80 bentonite and crystalline rock (granite), a potential hosting rock for a DGR being considered in Canada, as a function of pH and ionic strength of solutions using batch experiment technique and surface complexation modeling. The sorption experiments are conducted in Ca-Na-Cl solutions that would be expected at the repository depth. For granite, the sorption coefficient (K_d) value showed proportionate dependence on the pH of the solution. The sorption of Eu is dependent on ionic strength at low $\text{pH} \leq 6$ while not dependent on ionic strength at higher pH. For MX-80 bentonite, the sorption of Eu has little dependence on the ionic strength. A surface complexation modeling is being carried out to examine the experimental results.

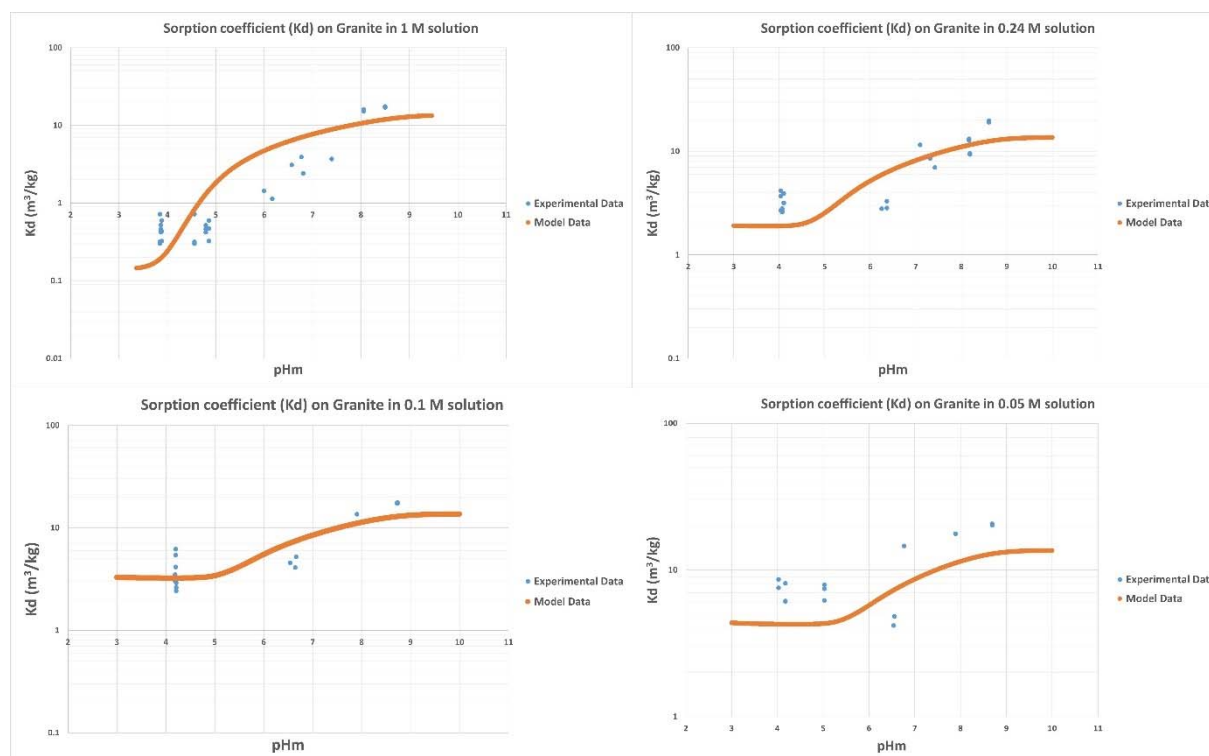


Figure 1: Sorption modeling results of Eu on granite for 1 M, 0.24 M, 0.1 M, and 0.05 M Ca-Na-Cl solutions (solid lines). Dots are experiment data.

It is shown (Figure 1) that at $\text{pH} \leq 6$, the sorption K_d value decreases as ionic strength increases. However, at $\text{pH} > 6$, the sorption K_d value shows no dependence on the ionic strength. It is also shown that at $\text{pH} \leq 8$, sorption increases with pH, with a dramatic rise from pH 5 to 8, and then reaches plateau over pH 8 and 9. This is consistent with studies conducted in low ionic strength solutions [1-2].

The sorption modeling fits with most of the experimental data, except for the experimental data at pH of 5 in 0.1 M and 0.24 M solutions, which requires further investigation. The speciation modeling shows that at low pH, the ionic exchange reaction plays a main role which produces $(\text{Biotite} - x)_3\text{Eu}$. However, as the pH increases to around 4.5 to 5, the surface complexation reactions dominate as $\text{Biotite} - \text{soEu}^{+2}$ and $\text{Biotite} - \text{soEu}(\text{OH})_2$ being the main species. This indicates that the main affinity to Eu sorption might be biotite, which is consistent with the findings of other studies [1-3].

References

- [1] Qiang, J., G. Wang, M. Ge, Z. Chen, W. Wu and Z. Guo. (2014). The Adsorption of Eu(III) and Am(III) on Beishan Granite: XPS, EPMA, Batch and Modeling Study. *Applied Geochemistry* 47:17-24.
- [2] Hong, L., B. He, P. Li, Q. Fan, H. Wu, J. Liang, C. Liu and T. Yu. (2019). Adsorption Behaviors of Eu(III) on Granite: Batch, Electron Probe Micro-Analysis and Modeling Studies. *Environmental Earth Sciences* 78 (8): 249.
- [3] Keisuke, F., Y. Hasegawa, K. Maeda, Y. Aoi, A. Tamura, S. Arai, Y. Yamamoto, D. Aosai and T. Mizuno. (2013). Sorption of Eu(III) on Granite: EPMA, LA-ICP-MS, Batch and Modeling Studies. *Environmental Science & Technology* 47 (22): 12811-18.

PA5-27 SORPTION OF SELECTED RADIONUCLIDES ON CANADIAN SEDIMENTARY AND CRYSTALLINE ROCKS UNDER SALINE CONDITIONS

Tammy Yang⁽¹⁾, Shinya Nagasaki²

(1) Nuclear Waste Management Organization, Toronto, Canada

(2) McMaster University, Hamilton, Canada

The Nuclear Waste Management Organization (NWMO) is responsible for designing and implementing Canada's plan for the safe, long-term management of used nuclear fuel and is currently evaluating potential sites for a deep geological repository (DGR) for used nuclear fuel in either sedimentary or crystalline rock. Deep groundwaters within the sedimentary rock in Canada at the repository depth contain Na-Ca-Cl brine solutions. Groundwaters within crystalline rock in Canadian Shield at the repository depth contain Ca-Na-Cl saline solutions.

Sorption is a potential mechanism for retarding sub-surface radionuclide migration from a DGR to the environment. The NWMO has developed a sorption distribution coefficient (K_d) database for sedimentary rocks for elements of importance to the safety assessment of a DGR, including C, Cl, Ca, Ni, Cu, As, Se, Zr, Nb, Mo, Tc, Pd, Ag, Cd, Sn, I, Cs, Eu, Hg, Pb, Bi, Ra, Th, Pa, U, Np, Pu and Am [1]. The database development included sorption measurements for Canadian sedimentary rocks (shale and limestone) and bentonite in saline solutions (with ionic strength (I)=0.23-7.2 M) including a reference porewater SR-270-PW brine solution (Na-Ca-Cl type with total dissolved solid (TDS)=270 g/L or I =6.0 M) [2-5]. The NWMO has also been conducting sorption measurements for elements of importance to the safety assessment for Canadian crystalline rocks collected from the Ignace area (e.g., biotite gradiorite tonalite, amphibolite, diabase dyke, feldspar-phyric tonalite) in reference groundwaters CR-10 (Ca-Na-Cl type with TDS=11.3 g/L) which simulates the groundwater geochemical conditions at the repository depth in crystalline environments and CR-0 (Na-Ca-HCO₃ type with TDS=0.5 g/L) which simulates the shallow groundwater geochemical conditions in crystalline environments. The elements of interest include Ag, Cd, Cr, Cs, Eu, Mo, Np, Pb, Pd, Rh, Sb, Se, Sr, I, Sn, Tc, U and Zr. The sorption of redox sensitive elements are measured under both oxidizing and reducing conditions. The effects of ionic strength and pH on sorption are investigated. The measured K_d values will be used to develop the NWMO's database of sorption values for Canadian crystalline rock.

References

- [1] Vilks, P. and Yang, T. (2018) Sorption of Selected Radionuclides on Sedimentary Rocks in Saline Conditions – Updated Sorption Values. NWMO Report NWMO-TR-2018-03. Toronto, Canada.
- [2] Vilks, P. and Miller, N.H. (2014) Sorption Studies with Sedimentary Rock under Saline Conditions. NWMO technical report NWMO TR-2013-22. Toronto, Canada.
- [3] Bertetti, F.P. (2016) Determination of Sorption Properties for Sedimentary Rocks Under Saline, Reducing Conditions – Key Radionuclides. NWMO Report NWMO-TR-2016-08. Toronto, Canada.
- [4] Vilks, P. and Miller, N.H. (2018) Sorption Experiments with Sedimentary Rocks for Sn, Zr, Cs, Th and Pd under Saline Conditions. NWMO Report NWMO-TR-2018-16. Toronto, Canada.
- [5] Nagasaki, S. (2018) Sorption Properties of Np on Shale, Illite and Bentonite Under Saline, Oxidizing and Reducing Conditions. NWMO Report NWMO-TR-2018-02. Toronto, Canada.

PA5-28 UPTAKE OF NIOBIUM BY CEMENT AND C-S-H PHASES IN THE ABSENCE AND PRESENCE OF ISA AND CHLORIDE: QUANTITATIVE DESCRIPTION AND MECHANISTIC UNDERSTANDING

Yongheum Jo^{(1),(2)}, Nese Cevirim-Papaioannou⁽¹⁾, Markus Fuss⁽¹⁾, Karsten Franke⁽³⁾, Benny de Blohouse⁽⁴⁾, Marcus Altmaier⁽¹⁾, Xavier Gaona⁽¹⁾

(1) *Institute for Nuclear Waste Disposal, Karlsruhe Institute of Technology, Karlsruhe (Germany)*

(2) *Department of Nuclear Engineering, Hanyang University (Republic of Korea)*

(3) *Institute of Resource Ecology / Institute of Radiopharmaceutical Cancer Research, Helmholtz-Zentrum Dresden-Rossendorf, Research Site Leipzig (Germany)*

(4) *ONDRAF/NIRAS, Sint-Joost-ten-Node (Belgium)*

Niobium is present in structural components in nuclear reactors, mostly in reactor vessels constructed using Inconel alloy. The isotope ^{94}Nb ($t_{1/2} = 2 \cdot 10^4$ a) is produced by neutron activation of natural ^{93}Nb during the operation of a nuclear reactor. In the waste, ^{94}Nb is mostly present in streams resulting from the dismantling of nuclear power plants, as well as from the treatment of the primary cooling circuit [1]. Niobium is predominantly found in the +V oxidation state within the stability field of water. Isosaccharinic acid (ISA) is a polyhydroxycarboxylic acid forming upon degradation of cellulose in hyperalkaline conditions. It is known to form strong complexes with hard Lewis acids (e.g. An, Zr, among others), thus potentially affecting radionuclide retention in cementitious systems. High concentrations of stable chloride (up to $\approx 4\text{--}5$ M) have been described for specific waste streams containing evaporator concentrates, which may also impact the sorption properties of Nb(V). This study focuses on the sorption of Nb(V) onto hardened cement pastes (HCP) CEM I, CEM III, CEM III + CaCO_3 and C-S-H phases in the absence and presence of ISA and chloride.

Sorption experiments were performed using a combination of ^{93}Nb (stable) and ^{95}Nb ($t_{1/2} = 34.97$ d) isotopes. The nuclear reaction $^{nat}\text{Zr}(d,x)$ was used to produce ^{95}Nb (n.c.a.) at a cyclotron Cyclone 18/9® (IBA RadioPharma Solutions, Belgium). The separation of ^{95}Nb from the Zr matrix was achieved using a modified version of the protocol described in [2]. Sample preparation and handling were performed in an Ar-glove box at $T = (22 \pm 2)$ °C. The content of stable ^{93}Nb in pristine HCP was quantified by alkaline fusion and ICP-MS. Batch sorption samples were prepared in synthetic cement pore waters with solid-to-liquid ratios (S/L) of 0.1–50 g/L and $3.6 \cdot 10^{-13} \text{ M} \leq [\text{Nb(V)}]_0 \leq 1.0 \cdot 10^{-9} \text{ M}$ (as ^{95}Nb or $^{93}\text{Nb} + ^{95}\text{Nb}$ mixtures) in the absence and presence of ISA ($1.0 \cdot 10^{-5} \text{ M} \leq [\text{ISA}] \leq 0.1 \text{ M}$) and chloride ($1.0 \cdot 10^{-5} \text{ M} \leq [\text{Cl}^-] \leq 1.0 \text{ M}$). Total concentration of Nb(V) in the aqueous phase was quantified by Gamma spectrometry after ultrafiltration with 10 kD filters. Upper solubility limits (solubility) of niobium were quantified with ^{93}Nb in the same pore water solution used in the sorption experiments.

Nb(V) solubility in the degradation stage I was determined to be $7 \cdot 10^{-8} - 2 \cdot 10^{-6}$ M. Inactive Nb content in CEM I was quantified to be (3.1 ± 0.3) ppm, equivalent to $(3.3 \pm 0.3) \cdot 10^{-8}$ mol/kg. Nb(V) sorption kinetic was fast and equilibrium conditions were attained after 2 days. Sorption experiments revealed a strong uptake of Nb(V) by cement ($5 \leq \log R_d \leq 7$, R_d in $\text{L} \cdot \text{kg}^{-1}$). Isotopic exchange with ^{93}Nb pre-present in HCP is considered as plausible retention mechanism for ^{95}Nb , although the uptake by calcium silicate hydrate (C-S-H) phases is tentatively proposed as main retention process on the basis of the high affinity of these phases for the uptake of Nb(V) and their large inventory in HCP. ISA significantly decreases the uptake of Nb(V) at $[\text{ISA}]_{\text{aq}} \geq 10^{-3}$ M, reflecting the formation of stable (Ca-)Nb(V)-ISA complexes in the aqueous phase. Sorption of Nb(V) is not significantly affected by chloride within the investigated concentration range. This work represents the first experimental evidence on the uptake of niobium by young cement in the absence and presence of ISA and Cl^- , thus providing key inputs for the assessment of ^{94}Nb retention in the context of the Safety Case for repositories for nuclear waste.

Acknowledgements: *This work was partly funded by the Belgian National Agency for Radioactive Waste and enriched Fissile Material (ONDRAF/NIRAS).*

References

- [1] Wang, L., Martens, E., Jacques, D., De Cannière, P., Berry, J., Mallants, D. (2009). NIROND TR 2008–23 E.
- [2] Busse, S., Brockmann, J., Rösch, F. (2002). Radiochim. Acta 90, 411–415.

PA5-29 INFLUENCE OF NA-CA-CL AND CA-NA-CL PHYSICOCHEMICAL SOLUTION PROPERTIES ON THE ADSORPTION OF ⁷⁹SE(-II) AND ⁹⁹TC(IV) ONTO SEDIMENTARY AND CRYSTALLINE ROCKS

Joshua Racette⁽¹⁾, Shinya Nagasaki⁽¹⁾, and Tianxiao Tammy Yang⁽²⁾

(1) Department of Engineering Physics, McMaster University, 1280 Main St. W., Hamilton, Ontario, Canada, L8S 4L7

(2) Nuclear Waste Management Organization, 22 St. Clair Ave. E., Fourth Floor, Toronto, Ontario, Canada, M4T 2S3

The Nuclear Waste Management Organization (NWMO) is responsible for designing and implementing Canada's plan for the safe, long-term management of used nuclear fuel and is currently evaluating potential sites for a Deep Geologic Repository (DGR) in either sedimentary or crystalline rock. Deep groundwaters within the sedimentary rock in Canada at the repository depth contain Na-Ca-Cl brine solutions. Groundwaters within crystalline rock in the Canadian Shield at the repository depth contain Ca-Na-Cl saline solutions. ⁷⁹Se and ⁹⁹Tc are long-lived radionuclides that have been identified as radionuclides of interest to the post-closure safety assessment or a DGR for used nuclear fuel waste in Canada. This study utilizes kinetic adsorption and batch adsorption experiments to determine the effect that the Na-Ca-Cl brine and Ca-Na-Cl saline physicochemical solution properties (pH and ionic strength) have on adsorption. Surface complexation modelling was then applied to the experimental data to deduce the possible surface complexes. Presently, adsorption of ⁷⁹Se is described with both $\equiv\text{S_HSe}^-$ and $\equiv\text{SOH}_2^+\text{HSe}^-$, whereas adsorption of ⁹⁹Tc is described with $\equiv\text{SO_TcO(OH)}$ and $\equiv(\text{SO})_2\text{TcO(OH)}^-$.

PA5-30 INFLUENCE OF TEMPERATURE ON CATION ION EXCHANGE AND SORPTION TO MONTMORILLONITE CLAY

Brian A. Powell,^{1,2,3} Reid Williams,¹ Xuechun Tang,¹ Salome Kwong-Moses,¹ Matthew Riss,¹ Shanna L. Estes^{2,3}

(1) Department of Environmental Engineering and Earth Sciences, Clemson University, Anderson, SC 29625, USA

(2) Department of Chemistry, Clemson University, Clemson, SC 29630, USA

(3) The Center for Nuclear Environmental Engineering Sciences and Radioactive Waste Management, Clemson University, Clemson, SC 29630, USAManagement,

Gaining a mechanistic understanding of interfacial processes governing the sorption/sequestration of actinides at mineral-water interfaces is fundamental for the accurate prediction of actinide behavior in waste repositories. This proposed work seeks to characterize actinide sorption to mineral surfaces and examine possible mechanisms of sorption at high temperature/ionic strength through examination of the effects of hydration and hydrolysis on actinide sorption. Batch sorption tests examining sorption of actinides to engineered barrier materials at waste repositories (iron oxides and smectite clays) were performed as a function of temperature and ionic strength. These conditions are meant to simulate those expected in the repository but for which we have very few data.[1]

The overarching hypothesis of this research is that strong actinide interactions with metal (oxyhydr)oxide surfaces are manifested by large stability constants for the actinide surface complexes. These large stability constants are due to positive entropies which are mechanistically driven by displacement of solvating water molecules from the actinide ion and the mineral surface during sorption. Such entropies are accessible through measurement of sorption enthalpies and stability constants using surface complexation modeling and calorimetric titration techniques.

Sorption of Eu(III), Nd(III), Th(IV), Np(V), and U(VI) to montmorillonite has been examined from temperatures of 25 °C to 80 °C and at ionic strengths of 0.01 M NaCl, 0.10 M NaCl, and 1.0 M NaCl. Generally, the sorption behavior of each ion follows the expected trend where sorption affinity increases with the general increase in effective charge of the ion [2, 3]. There are notable differences for each ion regarding the influences of temperature and ionic strength on sorption. Increasing ionic strength generally had little influence on the sorption of Th(IV), Np(V), and U(VI) but rather profoundly influenced Nd(III) sorption (Figure 1). Sorption of Nd(III) at low pH values decreased significantly as the ionic strength increased, consistent with an ion exchange mechanism. However, there was relatively little influence of temperature compared with the changes induced by increasing ionic strength.

Increasing temperature had greater impacts on the sorption on Th(IV), Np(V), and U(VI). Under low pH conditions, sorption generally increased for all ions with increasing temperature. The increase in sorption of Np(V) was relatively small compared to Th(IV) and U(VI). Sorption of U(VI) also increases with increasing temperature and an increase in U(VI) sorption is observed at higher ionic strengths above pH ~ 5 but not below. Therefore, it is hypothesized that the decreased dissolved carbonate concentration due to higher temperatures and influences of higher ionic strengths on uranyl-carbonate activities both result in an increase in sorption.

These observed influences of temperature appear to be related to the enthalpic and entropic contributions of 1) the structure and stability of water in hydration spheres and on the mineral surface, 2) ion exchange reactions, 3) surface complexation and protolysis reactions on aluminol and silanol clay edge sites, and 4) changes in aqueous speciation facilitated by changes in temperature. The magnitude by which each

of these processes' influences partitioning is discussed in terms of the enthalpy of ion exchange and surface mediated reactions.

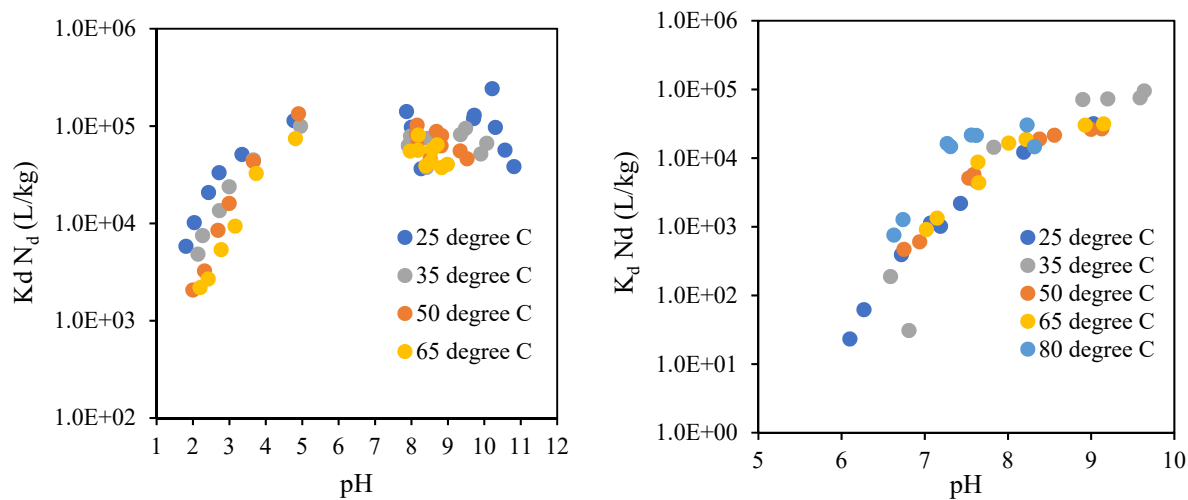


Figure 1: Sorption of Nd(III) to montmorillonite as a function of temperature in 0.01 M NaCl (left) and 1.0 M NaCl (right).

References

- [1] U.S. Department of Energy, O.o.C.R.W.M., *Yucca Mountain Science and Engineering Report Rev. 1, Technical Information Supporting Site Recommendation Consideration*. 2002, US Department of Energy: North Las Vegas, NV.
- [2] Silva, R.J. and H. Nitsche, *Actinide environmental chemistry*. Radiochimica Acta, 1995. **70-1**: p. 377-396.
- [3] Kim, J.I., *Chemical Behavior of Transuraniuc Elements in Natural Aquatic Systems*, in *Handbook on the Physics and Chemistry of the Actinides*, A.J. Freeman and C. Keller, Editors. 1986, Elsevier Science Publishers B. V.

PA5-31 PLUTONIUM ADSORPTION TO HEMATITE AT VARIABLE pH, TEMPERATURE, AND CONCENTRATION

Salomé Kwong-Moses⁽¹⁾, Shanna L. Estes⁽¹⁾, and Brian A. Powell⁽¹⁾

(1) Department of Environmental Engineering and Earth Sciences, Clemson University, USA

Improving the accuracy of risk-assessments for deep geologic nuclear waste repositories necessitates a complete understanding of radionuclide behavior under geochemically relevant conditions. This includes understanding radionuclide adsorption to mineral surfaces, which contribute significantly to radionuclide fate and transport in the environment.^[3, 8] This work studies the adsorption of plutonium(V/VI) to hematite at variable pH and temperature. Plutonium (Pu) is expected to comprise 91% of the radionuclide inventory (by activity) from pressurized water reactor spent fuel after 10,000 years of emplacement^[5] and is a significant component of defense-generated waste.^[4, 9] Hematite is an abundant corrosion product of steel waste canisters and a common natural mineral phase expected in the near-field subsurface.^[3, 8] Thus, to advance a cohesive, accurate model of Pu geochemistry relevant to existing and future waste repositories, thermodynamic data describing Pu adsorption to hematite at variable pH and temperature are needed.

In this study, ²⁴²Pu adsorption to synthetic hematite was studied at variable pH, concentration, and temperature using batch reactions. Solutions of 2.0×10^{-7} mol/L, or 7.3×10^{-8} mol/L ²⁴²Pu(V/VI) were reacted with 1 g/L hematite in 0.01 M NaCl at a pH range of 3–9 for approximately eight months. The temperature of the reactions was increased over time to give data at 25, 35, 50, 65, and 80 °C. These temperatures are within the range expected for planned geologic repositories, in which thermal output from radioactive decay of waste packages will yield elevated local temperatures over time.^[10] Aqueous Pu concentrations, solution pH, and solution E_H were measured during sampling after ~50 days of equilibration.

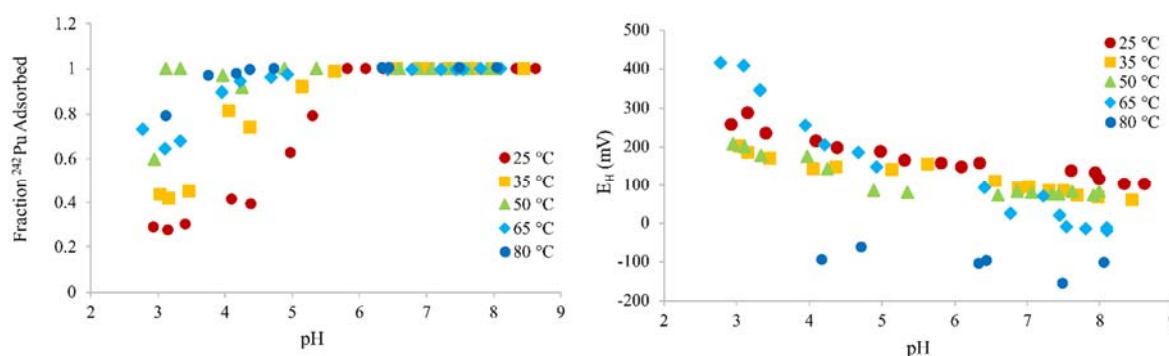


Figure 1. Fraction of ²⁴²Pu adsorbed to hematite as a function of pH (left) and measured E_H as a function of pH (right) at 25, 35, 50, 65 and 80 °C for solutions of 2.0×10^{-7} mol/L ²⁴²Pu.

As reaction temperatures increased, ²⁴²Pu adsorption to hematite increased and the adsorption edge shifted to lower pH values (Figure 1, left). In general, the fraction of adsorbed Pu increased with increasing pH, with ~100% adsorption observed at pH > 6 for all temperatures. Changes in E_H for each of the suspensions were also observed with increasing temperature (Figure 1, right). The data collected at 25 °C are consistent with reported room-temperature Pu-hematite adsorption studies.^[6, 7] As expected,

at the same pH and temperature, less fractional Pu adsorption was observed for reactions with higher total Pu concentrations (Figure 2).

Previous work has shown that Eu(III) and U(VI) sorption on hematite increases with temperature as the result of the formation of entropically favorable inner-sphere surface complexes. [1, 2] A similar mechanism is expected for Pu adsorption to hematite. Future work will utilize surface complexation modelling to determine the enthalpy for the formation of Pu-hematite surface complexes using the van't Hoff equation. Measured E_H values will help to define appropriate Pu redox couples for inclusion in the surface complexation modelling and may also help to elucidate the role of surface-mediated reduction on Pu adsorption processes. The results from this work will be combined with existing Pu-hematite and goethite data sets to construct a self-consistent thermodynamic surface complexation model, ultimately contributing to a cohesive understanding of Pu fate and transport in the environment.

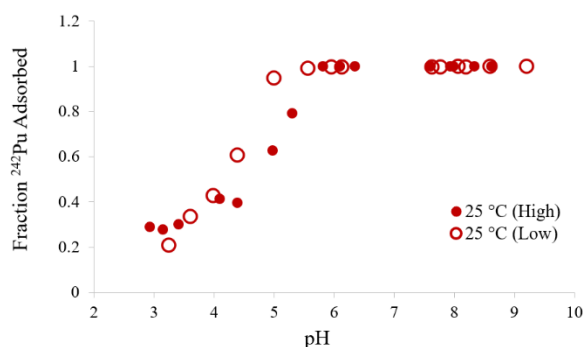


Figure 2. Fraction of ^{242}Pu adsorbed to hematite as a function of pH for solutions of “high” ^{242}Pu concentration (2.0×10^{-3} mol/L, closed circles) and “low” ^{242}Pu concentration (2.0×10^{-2} mol/L, open circles).

References

- [1] Estes, S. L.; Arai, Y.; Becker, U.; Fernando, S.; Yuan, K.; Ewing, R. C.; Zhang, J.; Shibata, T.; Powell, B. A. A Self-Consistent Model Describing the Thermodynamics of Eu(III) Adsorption onto Hematite. *Geochimica et Cosmochimica Acta* **2013**, *122*, 430–447. <https://doi.org/10.1016/j.gca.2013.08.023>.
- [2] Estes, S. L.; Powell, B. A. Enthalpy of Uranium Adsorption onto Hematite. *Environ. Sci. Technol.* **2020**, *54* (23), 15004–15012. <https://doi.org/10.1021/acs.est.0c04429>.
- [3] Geckeis, H.; Lützenkirchen, J.; Polly, R.; Rabung, T.; Schmidt, M. (2013) Mineral–Water Interface Reactions of Actinides. *Chem. Rev.* *113*: 1016–1062.
- [4] Hu, Q.; Weng, J.; Wang, J. Sources of Anthropogenic Radionuclides in the Environment: A Review. (2010) *J. Environ. Radioact.* *101*:426–437.
- [5] Oversby, V. M. (1986) Important Radionuclides in High Level Nuclear Waste Disposal: Determination Using a Comparison of the EPA and NRC Regulations.
- [6] Powell, B. A.; Fjeld, R. A.; Kaplan, D. I.; Coates, J. T.; Serkiz, S. M. (2005) Pu(V)O₂⁺ Adsorption and Reduction by Synthetic Hematite and Goethite. *Environ. Sci. Technol.* *39*:2107–2114.
- [7] Romanchuk, A.; Kalmykov, S.; Aliev, R. (2011) Plutonium Sorption onto Hematite Colloids at Femto- and Nanomolar Concentrations. *Radiochim. Acta* *99*:137–144.
- [8] Silva, R. J.; Nitsche, H. (1995) Actinide Environmental Chemistry. *Radiochim. Acta* *70–71*:377–396.
- [9] Smith, D.; Finnegan, D.; Bowen, S. (2003) An Inventory of Long-Lived Radionuclides Residual from Underground Nuclear Testing at the Nevada Test Site, 1951–1992. *J. Environ. Radioact.* *67*:35–51.
- [10] United States Department of Energy (2002). Yucca Mountain Science and Engineering Report, Rev. 1. DOE/RW-0539–1, Office of Civilian Radioactive Waste Management: North Las Vegas, NV.

PA5-32 METAL IONS ADSORPTION AND MODELING ON A PRE-NEOGENE SEDIMENTARY ROCK

Linyi HOU, Kanako TODA and Takumi SAITO

School of Engineering, University of Tokyo, Japan

1. Introduction

Pre-Neogene sedimentary rock is widely distributed in Japan, estimated to occupy almost half of the area at around 1,000 m depth [1]. It exhibits a block-in-matrix appearance with complex internal structures, which most likely affects the process of immobilization and transport of radionuclides. As a candidate host rock for deep geological disposal of high-level radioactive wastes (HLWs), there are no relevant studies, and an understanding of radionuclides migration behavior in this type of rock is needed. In this work, pre-Neogene sedimentary rock was characterized by various methods, and the adsorption behaviors of Cs(I), I(-I), and Eu(III) were studied. The connection of the adsorption of these ions with underlying mineralogy was established, and mechanistic sorption models were applied, taking into account possible adsorption processes such as surface complexation and ion exchange.

2. Materials and methods

The core samples (\varnothing 92mm, 25 m length, 2 cores) were drilled from the Chichibu belt in the northern Kanto region of Japan, which is a part of Jurassic and Cretaceous accretionary complex [2], and named 1-3, 1-12, and 2-3. Disk samples (\varnothing 20 mm, 5 mm thick) of the cores were observed with an optical microscope. Fourier-transformed infrared (FT-IR) spectroscopy, X-ray fluorescence (XRF), X-ray diffraction (XRD), and Raman spectroscopy were used for elemental determination and lithological composition analyses.

Adsorption experiments of ions such as Cs(I), I(-I), and Eu(III) to the powdered rock samples were carried out at 25°C under a simulated groundwater composition with a $\text{HCO}_3^-/\text{CO}_3^{2-}$ buffer and a solid-liquid ratio of 1 g/L. The contact time and pH effects on the sorption were studied, and the adsorption isotherms were obtained. The concentrations of the adsorbate ions in supernatants after centrifugation and filtration were measured by an inductively-coupled plasma mass spectrometry (ICP-MS) for Cs^+ and Eu^{3+} or ion chromatography (IC) for I. The powder samples loaded with the adsorbed ions were characterized by scanning electron microscopy (SEM) and energy dispersive X-ray spectrometry (EDS) after washing and drying.

3. Result and discussion

Fig. 1 shows the optical microscopic images of the rock samples. The dominant parts of the 1-3 and 1-12 were mudstone, and heterogeneous appearances with characteristic block-in-matrix structures were apparent. The dominant part of 2-3 was sandstone, which was relatively homogeneous. By FT-IR, the stretching vibration peaks of the Si-O and Si-Al-O bonds were identified, and three rock cores contained similar functional groups. The XRD patterns showed that the main mineralogical phases were quartz, chlorite, albite, illite, and calcite, which were consistent with the results of the XRF analyses showing that Si, Al, Fe, and Ca were major elements of the rock samples. Both the higher Na content in XRF and the intensities of the corresponding peaks in XRD evidenced more albite content in 2-3. The presence of the illite phase in all of the rock samples was confirmed by characteristic peaks at 10.05, 5.01, and 3.35 Å, which did not change for the oriented samples after K^+ saturation and heat treatment.

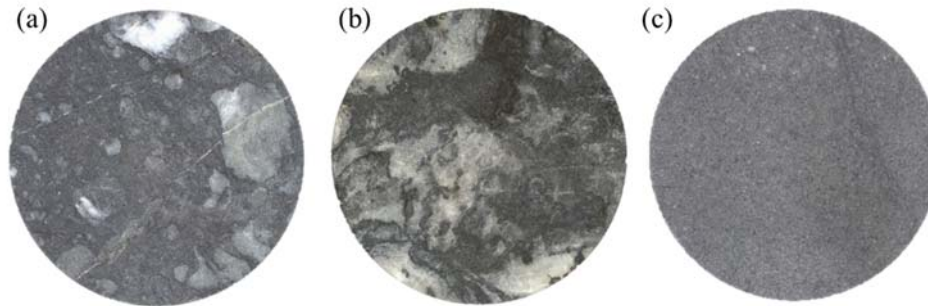


Figure 1. Microscope images of 1-3 (a), 1-12 (b) and 2-3 (c)

Cs(I) adsorption increased with the contact time and reached equilibrium after 48 h. The adsorption capacity of 2-3 was the largest. The Cs(I) adsorption isotherms resembled those reported for illite, suggesting this mineral was responsible for the adsorption of Cs(I) in the present pre-Neogene sedimentary rocks [3]. By obtaining adsorption isotherms for I(-I) and Eu(III) and performing SEM-EDS observations, we will discuss minerals responsible for the adsorption of these ions and report the results of the application of mechanistic sorption models to reveal possible sorption processes and relevant parameters such as site densities and formation constants at the conference.

4. Conclusion

The characterization of the pre-Neogene sedimentary rock samples revealed that the samples 1-3 and 1-12 have the block-in-matrix features found in an accretionary complex. The sample 2-3, on the other hand, largely consisted of sandstone. Illite was found in all the samples and suggested to be responsible for the adsorption of Cs(I). The adsorption experiments showed that the pre-Neogene sedimentary rock samples adsorbed some ions analogous for important radionuclides for the safety assessment of HLWs geological disposal, indicating that this type of the rocks has a certain retardation effect on the migration of the radionuclides to the biosphere. Further research on the diffusion behaviors of these ions through the pre-Neogene sedimentary rocks will be performed in the future, from which migration models will be established.

References

- [1] Yokota, H., Oshiro, Y., and Goto, J. *et al.* (2022) Accumulation of the data of geological environment characteristics in Pre-Neogene accretionary sedimentary rocks, NUMO-TR-22-01. Nuclear Waste Management Organization of Japan.
- [2] Matsuoka, A. (1992) Jurassic-Early Cretaceous tectonic evolution of the Southern Chichibu terrane, southwest Japan. *Palaeogeogr., Palaeoclimatol., Palaeoecol.* 96: 71-88.
- [3] Bradbury, M. H. and Baeyens, B. (2000). A generalised sorption model for the concentration dependent uptake of caesium by argillaceous rocks. *J. Contam. Hydrol.* 42: 141-163.

PA6-4 STRENGTHENED EROSION RESISTANCE OF COMPACTED BENTONITE BY OPPOSITELY-CHARGED MATERIALS: FROM COLLOIDAL PARTICLES INTERACTION TO EROSION EXPERIMENTS

Zongyuan CHEN^(1,2), Ganlin ZU⁽²⁾, Huijuan HOU⁽²⁾, Zhen ZHANG⁽²⁾, Pengyuan GAO⁽²⁾, Qiang Jin^(1,2), Wangsuo Wu^(1,2), Zhijun GUO^(1,2)

(1) *Frontiers Science Center for Rare Isotopes, Lanzhou University, P. R. China*

(2) *Radiochemistry Laboratory, School of Nuclear Science and Technology, Lanzhou University, P. R. China*

Deep geological disposal is the most suitable solution for the long-term safe disposal of high-level radioactive waste (HLW). China adopted a multiple barriers principle-based deep geological disposal for HLW, and granitic formations in Beishan region (northwestern China) was considered as potential host rock for China's HLW repository. Due to its low permeability, high sorption capacity, and self-sealing characteristics, bentonite is usually used as buffer backfill material to restrict the inflow of groundwater and block the migration of released radionuclides. Therefore, inhibiting the damage and maintaining the integrity of the bentonite barrier are critical to the safe geological disposal of HLW.

In the HLW repository built in granitic host rock, due to inevitable fractures in granite, the long-term contact of bentonite with groundwater will generate freely movable colloidal particles. When contacting groundwater with low ionic strength (I), montmorillonite, the main component of bentonite, swells and then results in its dispersion in the form of small particles in aqueous phase. These particles and aggregates of bentonite will be lost under drag stress of water flow, the magnitude of which depends on the flow speed and fracture characteristics. The loss of particulate material from the surface of compacted bentonite caused by water is also called "bentonite erosion". The erosion weakened the integrity and effectiveness of the engineering barrier of compacted bentonite.

Inhibiting the formation and migration of bentonite colloids is therefore a key issue for ensuring the long-term integrity of the compacted bentonite barrier. Although bentonite erosion can be obviously weaker when bentonite was in high I aqueous solution and/or bentonite was in Ca-form, these two conditions are not easy to realize. Since the thermal conductivity of compacted bentonite can be increased by addition of quartz sand, crushed rock and so on, adding additives may be a good way to inhibit the erosion and loss of compacted bentonite, which is also practical in applications.

Our study [1] found that a proper amount of gibbsite colloids into bentonite colloids can significantly inhibit the transport of bentonite colloids. This is because bentonite and gibbsite colloids are oppositely charged in the range of pH 3.0-8.9 and electrostatic attraction can cause these two colloids to combine together and form aggregates that are difficult to migrate. Similar results were obtained with layered double hydroxides (Mg-Al LDH). Addition of appropriate amount of LDH colloid could inhibit the transport of bentonite colloid because of the aggregation with each other. Such aggregation can occur even under weak ionic strength. Thus, oppositely charged materials could be used as additives, and this is a "new" method of choice to enhance bentonite erosion resistance.

In order to fully present their interaction process and understand the corresponding results, the interaction between bentonite and LDH was studied by dropwise addition of colloidal LDH into colloidal bentonite suspension, during which the variation in electrical conductivity, zeta potential and particle size was measured [2]. The "titration" data indicate a strong interaction between bentonite and LDH. Release of the two counter-ions would suggest that in the aggregates, a portion of the structural charges of montmorillonite and LDH is compensated by one another. In other words, montmorillonite layers may be superimposed with LDH layers. Interestingly, in addition to their aggregation, intercalated structures of LDH and montmorillonite were found in their composite (BEN@LDH) by a combined

characterization of X-ray diffraction (XRD) and high-resolution transmission electron microscopy (HR-TEM), and were confirmed by density functional theory (DFT) calculation.

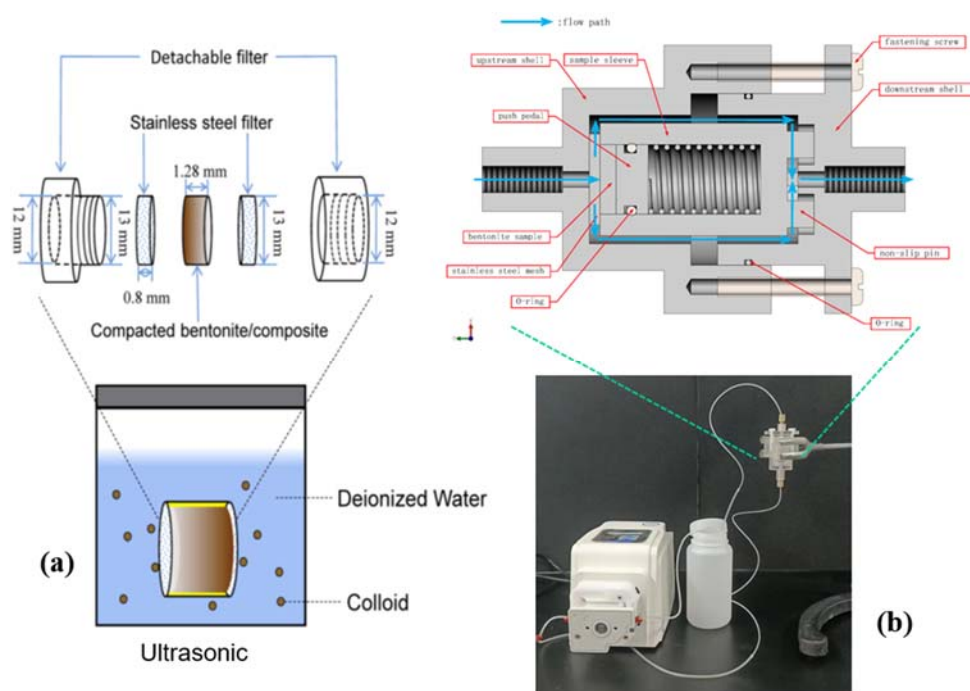


Figure 1. Experimental set-up for erosion experiments under (a) static and (b) dynamic conditions

We have then tested whether or not the strong interaction between LDH and bentonite, as laid out above, will improve the erosion resistance of compacted bentonite. Erosion experiments on compacted bentonite, two BEN@LDHs (BEN:LDH = 1:1 and 9:1) and a BEN+LDH (simple powder mixture, BEN:LDH = 99:1) were carried out under both static and dynamic conditions (Fig.1). Ultrasound (40 kHz, 15/25 W) was applied to accelerate the erosion process under static conditions. Colloid generation of compacted BEN@LDH under ultrasonic conditions is negligible comparing with that of compacted bentonite, indicating a significantly higher erosion resistance. Besides, a small amount of LDH by mechanically mixing with bentonite (mass ratio 1:99) can also effectively improve the erosion resistance of compacted bentonite.

High erosion resistance is also requested for other geotechnical structures, such foundations, embankments, high slopes and so on in order to achieve long-term functional stability. Besides bentonite, clays and soils are also negatively charged in common pH range, and application our idea to enhance the erosion resistance by electrostatic attraction using positively charged “glue” may be of great significance and have wide applicability.

References

- [1] Zhang, Z., Gao, C., *et al.*, (2021). Co-transport of U(VI) and bentonite colloids: influence of colloidal gibbsite. *Appl. Clay Sci.* 205:106033.
- [2] Zhang, Z., Gao, P., *et al.*, (2022). Strengthened erosion resistance of compacted bentonite by layered double hydroxide: A new electrostatic interaction-based approach *Chemosphere* 292: 133402.

PA6-5 PROBING THE NUCLEATION AND GROWTH OF PuO_2 NANOPARTICLES IN AQUEOUS SOLUTION

Simon Bayle (1), Matthieu Viroto (1)*, Thomas Dumas (2), Xavier Le Goff (1), Denis Menut (3), Sandrine Dourdain (1), Sergey I. Nikitenko (1)

(1) ICSM, CEA, Univ Montpellier, CNRS, ENSCM, Bagnols sur Cèze, France

(2) CEA, DES, ISEC, DMRC, Univ Montpellier, Marcoule, France

(3) Synchrotron SOLEIL, L'Orme des Merisiers Saint Aubin, Gif-sur-Yvette, France

*matthieu.viroto@cea.fr

A better knowledge about the structural and physico-chemical properties of plutonium oxide nanoparticles (PuO_2) is of potential interest for the clarification of the environmental fate of this long-lived radioactive element. Recent studies have provided relevant information about the size, morphology and local structure of intrinsic Pu(IV) colloids that can be described as crystalline PuO_2 nanoparticles of about 2 nm in diameter and exhibiting a structural disorder related to a surface effect [1]. The formation of these species is related to complex hydrolysis properties of Pu(IV) that can lead to the formation of oligomers and their condensation into extremely stable colloidal suspensions. However, the related formation mechanism is not clearly identified and recent publications suggest the contribution of oxohydroxo polynuclear structures of Pu (i.e. clusters). Particularly, the synthesis of Pu nanoclusters composed of 16, 22, and 38 Pu atoms decorated with inorganic molecules to limit their growth has been described. [2] The examination of their resolved structures highlighted Pu at the tetravalent state and also revealed their common basic core structure agreeing with a deformed PuO_2 core. While Pu_{38} cluster is only composed of oxo bridges favouring a condensation mechanism based on oxidation, the observation of hydroxo groups in smaller Pu(IV) nanoclusters suggests that Pu(IV) colloids and precipitates may be formed by a succession of oxidation and hydroxylation mechanisms [3].

Deciphering the mechanism for PuO_2 nanoparticle formation and identifying the involved species represent a difficult task with direct environmental implications including, for instance, storage and corrosion of spent nuclear fuel, decommissioning or decontamination of polluted sites. Recently, the development of an analytical bench on MARS beamline of the synchrotron SOLEIL - a beamline dedicated to measurements on radioactive samples - allowed to characterize Pu(IV) intrinsic colloids by small-angle X-ray scattering (SAXS) in quasi-instantaneous combination with X-ray absorption spectroscopy (XAS). [2] The results allowed probing intrinsic colloids of different sizes (ca. 2 nm and $5.7 \times 30 \text{ nm}^2$) and particularly demonstrated that the structural properties of the colloids are strongly influenced by the preparation method. More recently, this analytical bench allowed to characterize with quite a good resolution, a polynuclear oxo-hydroxo structure composed of 6 Pu(IV) atoms and measuring about 1 nm in diameter.[4] Therefore, the combination of synchrotron SAXS with XAS appears particularly relevant for the multi-scale characterization of colloidal Pu nanostructures in the nm range, with measurements acquired on large sample volumes, directly in the synthesis medium and without specific preparation.

In situ observation of aqueous Pu(IV) intrinsic colloids formation using a synchrotron beam would be very informative about the mechanism responsible for intrinsic colloid accumulation. This presentation will focus the development of a measurement cell that will allow probing the nucleation and growth stages of PuO_2 nanoparticles in aqueous solution. The sample holder will be used for the gentle heating of a Pu aqueous solution to provoke and control Pu(IV) hydrolysis kinetics. The size, morphology and local structure of the involved intermediates will be measured in the meantime. The Figure 1 provided below gathers preliminary results obtained with UV-Vis absorption spectroscopy during the thermal conversion of a Pu(IV) precursor into Pu(IV) intrinsic colloids. The development of the cell will allow to couple these observations with synchrotron SAXS/XAS approach.

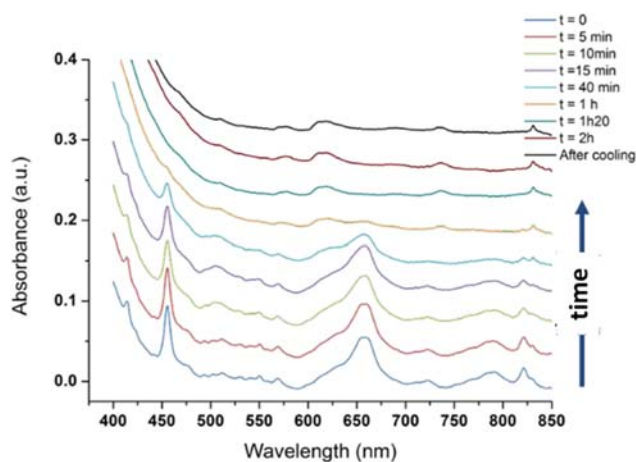


Figure 1: UV-Vis absorption spectra accumulated during the thermal conversion (ca. 80 °C) of a Pu(IV) precursor into Pu(IV) intrinsic colloids.

References

- Micheau et al. Relevance of formation conditions to the size, morphology and local structure of intrinsic plutonium colloids, *Environ. Science: Nano* 2 (2020) 214.
- Sigmon et al. Extension of the Plutonium Oxide Nanocluster Family to Include {Pu16} and {Pu22}, *Chem. Eur. J.* 25 (2019) 2463.
- Cot-Auriol et al. First observation of $[\text{Pu}_6(\text{OH})_4\text{O}_4]^{12+}$ cluster during the hydrolytic formation of PuO_2 nanoparticles using H/D kinetic isotope effect. *Chemical Communications* 58.94 (2022) 13147-13150.
- Dumas et al. Size and structure of hexanuclear plutonium oxo-hydroxo clusters in aqueous solution from synchrotron analysis, *J. Synchr. Rad.* 29 (2022) 30.

PA7-5 GEOCHEMICAL INFLUENCE ON THE RADIONUCLIDE MOBILITY IN GEOLOGICAL FORMATIONS ANALYSED BY ICP-MS AND ICP-QQ COUPLING METHODS

Ralf Kautenburger⁽¹⁾, Kristina Brix⁽¹⁾, Aaron Haben⁽¹⁾

(1) WASTe group, Inorganic Solid State Chemistry, Saarland University, Germany

The development of a repository for high level nuclear waste (HLW) in deep geological formations is a very important task for the future. The long-term safety assessment for more than hundred thousand years needs a full knowledge of all processes of interaction between the radioactive waste and the surrounding host rock formations as natural barrier but also the interaction with the engineered barriers. A wide set of geochemical parameters can influence the retention of radionuclides originated from a leakage in a waste disposal. For example, competing ions released from clay minerals or from C-S-H (calcium silicate hydrate) phases as major part of hardened cement by infiltration of percolating water, natural organic matter (NOM) as complex forming ligands, changes in temperature or pH-milieu of the aquifer [1, 2].

As speciation method, capillary electrophoresis hyphenated with inductively coupled plasma mass spectrometry (CE ICP-MS) was used to study the complexation behaviour of Eu(III) and U(VI) with NOM from different sources [3]. The influence of metal concentration, the presence of competing cations from clay or concrete dissolution as well as cations from clay porewater on the complexation behaviour was analysed. Using the CE-ICP-MS method, the determination of complex stability constants $\log \beta$ through the simultaneous determination of all species, and the analysis of relevant influencing factors (e.g. source of NOM) is possible (Fig. 1).

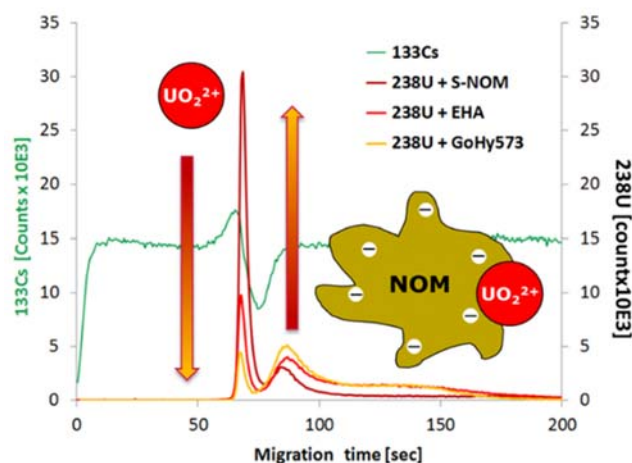


Figure 1. Electropherograms of U(VI) complexation by NOM from different sources (SNOM: Suwannee River NOM, EHA: Elliott soil HA, GoHy573: HA from Gorleben site borehole 573).

For the sorption/desorption studies common batch experiments with the analytes and clay mineral suspensions as well as are performed. To study the mobility of the analytes at high saline (>1 M ionic strength) and hyperalkaline conditions at pH values about 12-13 (caused by the dissolution of clay and cement concrete in the presence of water), a new analytical tool was developed to get more insight into the possible interactions between metals and geochemical matrix [4].

By the application of the developed transient ICP-MS measurement method a quantification of all elements in samples with high salinity (up to 5 M NaCl) without any complex sample preparation is

realized. This transient method enables the determination of the classical static distribution coefficients (K_D or R_D values) even in highly saline and hyperalkaline background electrolytes.

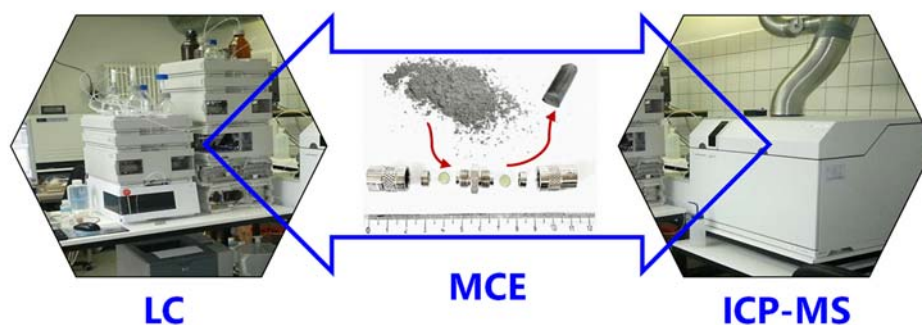


Figure 2. Mini-column experiment (MCE) setup by coupling LC with a quadrupole ICP-MS [5].

In addition, newly developed mini-column experiments (MCE) enable the visualization of dynamic sorption and desorption processes of the waste cocktail elements used (such as U(VI), Mo(VI), Eu(III), Pd(II), Cs(I)) on clay or C-S-H phases by online coupling of LC with a single quadrupole ICP-MS (Fig. 2) or a triple quadrupole ICP-QQQ to prevent isotopic interferences more effectively [5]. The MCE using LC -ICP-QQQ leads to quantitative information about the elemental composition of the eluent from the mini-column directly after the determination of the UV/Vis-active compounds in the diode array detector of the LC. By using the MCE, maximum loading capacities can be determined, from which dynamic distribution coefficients can then be derived which can be used for geochemical modelling. This can provide a more realistic prediction for the retention of the metals on clay or other repository-relevant materials. Soon, a coupling of laser-ablation (LA) to a triple quadrupole ICP-QQQ will be developed to analyse the spatial distribution of metals in the mini-columns consisting of clay or cement alteration phases.

Acknowledgements: We would like to thank the Federal Ministry for Economic Affairs and Climate Action (BMWK), represented by the Project Management Agency Karlsruhe (PTKA-WTE) for funding (projects 02E10991, 02E11415D and 02E11860D) and our project partners for the kind collaboration.

References

- [1] Baur, S., Brix, K., Feuerstein, A., Janka, O. and R. Kautenburger (2022). Retention of waste cocktail elements onto characterised calcium silicate hydrate (C–S–H) phases: A kinetic study under highly saline and hyperalkaline conditions, *Appl. Geochem.* 143: 105319
- [2] Brix, K., Baur, S., Haben, A. and R. Kautenburger (2021). Building the bridge between U(VI) and Ca-bentonite - Influence of concentration, ionic strength, pH, clay composition and competing ions. *Chemosphere* 285: 131445.
- [3] Kautenburger, R., Sander, J.M. and C. Hein (2017). Europium(III) and Uranium(VI) complexation by natural organic matter (NOM): effect of source. *Electrophoresis* 38: 930-937.
- [4] Hein, C., Sander, J.M. and R. Kautenburger (2017). New Approach of a transient ICP-MS measurement method for samples with high salinity. *Talanta* 164: 477-482.
- [5] Kautenburger, R., Brix, K., Baur, S. and J. M. Sander (2022). Development of mini column experiments (MCE) by coupling microliter flow HPLC with ICP-MS for the analysis of metal retention under conditions close to nature. *Talanta Open* 5: 100111.

PA7-6 SIMULTANEOUS DETERMINATION OF TRANSURANIUM RADIONUCLIDES BY COMPACT ACCELERATOR MASS SPECTROMETRY

Shan Xing^(1,2), Chenyang Peng^(1,2), Marcus Christl⁽³⁾, Kelian Shi^(1,2), Hans-Arno Synal⁽³⁾, Xiaolin Hou^(1,2), Kuzmenkova, Natalia⁽⁴⁾

(1) *Frontiers Science Center for Rare Isotopes, Lanzhou University, Lanzhou 730000, P. R. China*

(2) *School of Nuclear Science and Technology, Lanzhou University, Lanzhou 730000, P. R. China*

(3) *Laboratory of Ion Beam Physics, ETH Zurich, Zurich 8093, Switzerland*

(4) *Department of Chemistry, Division of Radiochemistry, Lomonosov Moscow State University, Moscow 119991, Russia*

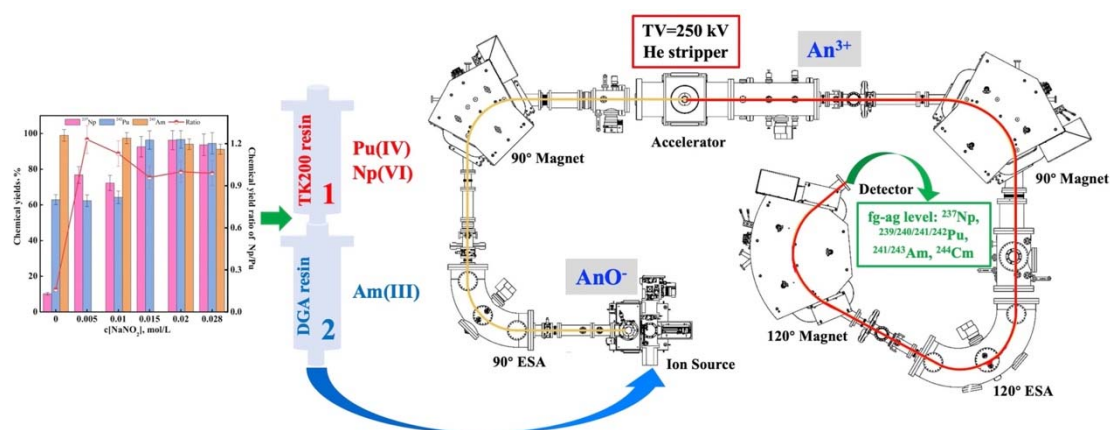
Most of transuranium isotopes (TRUs), including those of neptunium (Np), plutonium (Pu), americium (Am) and curium (Cm) are anthropogenic radionuclides, and usually considered as highly radiotoxic radionuclides. In groundwater specimens, the concentrations of TRUs are in the order of 10^6 to 10^9 atoms/kg, while the concentration of the naturally occurring ^{238}U is 10^{16} atoms/kg. The major challenge for such work is that the sample size is often very small, and a highly sensitive method to measure attogram-femtogram level radionuclides is therefore needed. In order to achieve detection at such levels, this usually requires a complete separation of TRUs from matrix and potential interferences in combination with the measurement techniques with high sensitivity.

Although a large number of analytical methods for determination of TRU radionuclides have been developed, many of them are very time-consuming/tedious to operate and cover only few radionuclides of interest. Sequential separation procedures using stacked column chromatographic techniques could elevate analysis efficiency. It is noteworthy that the purity of chemical agents especially the isotopic dilution standards or chemical yields tracers is often a critical obstacle for the analysis of TRUs at ultralow levels. However, the content of impurities (especially the radionuclides of interest) in most of commercial standards of TRU radionuclides is to a level that seriously influences the analytical quality of ultra-low-level samples.

For the measurement of long-lived radionuclides of TRUs, mass spectrometry is often used because of their better detection limits compared to the classic radiometric techniques (e.g., α spectrometry, liquid scintillation counting). Mass spectrometric techniques as thermal ionization mass spectrometry (TIMS), traditional ICP-MS, sector field ICP-MS (SF-ICP-MS) and multicollector ICP-MS (MC-ICP-MS) have been successfully employed for TRUs measurement. Although TIMS is often applied for measurement of ultra-low-level radionuclides, especially isotope ratios due to its low detection limits down to fg to ng, the tedious sample preparation on filament has largely limited the sample analysis throughput by this technique. Traditional ICP-MS has the ability to perform faster analysis, but its detection limits is still higher and cannot measure ultra-low-level radionuclides especially for nuclear forensic samples. The upgraded SF-ICP-MS and MC-ICP-MS have improved the capability to detect ultra-trace quantity of plutonium at femtogram level, but some interferences (e.g., isobaric, polyatomic and molecular interferences) could not be effectively eliminated due to the worse abundance sensitivity. AMS is one of the most sensitive techniques to analyze the isotopic signature of intermediate- and long-lived radionuclides. Recently developed compact low energy AMS, which combines with high sensitivity, robustness, and comparably high sample throughput, is considered as a powerful analytical tool that is able to reliably detect ultra-trace amounts of heavier actinides.

In this work, an analytical method for simultaneously determination of transuranium radionuclides was developed by sequential separation using extraction chromatography and sensitive measurement with AMS. ^{242}Pu and ^{243}Am were used as tracers to monitor the chemical yields of Np/Pu isotopes and

Am/Cm isotopes during chemical separation, respectively. The chemical behaviors of Np and Pu were similar during chromatographic separation using TK200 resin when the sample was prepared in 8-9 mol/L of HNO_3 with 0.015-0.03 mol/L of NaNO_2 media, which offers an easy-operated condition to reach the same chemical yield for both Np and Pu during the radiochemical separation. Meanwhile, high chemical yields of Am were also obtained for their separation using stacked TK200-DGA cartridges under this condition. The 300 kV AMS system was demonstrated to be an extremely sensitive and reliable technique for measurement of radionuclides of TRUs at ultralow levels at a terminal voltage of about 250 kV. Np/Pu and Am/Cm isotopes can be simultaneously measured using ^{242}Pu and ^{243}Am tracers after the normalization by a correction factor obtained from home-made standards. The detection limits of ^{239}Pu , ^{240}Pu , ^{241}Am and ^{244}Cm were estimated to be 7.0 ag, 5.3 ag, 44.3 ag and 8.1 ag, respectively. Isotopes of Np, Pu, Am and Cm in samples spiked with single TRUs standard solutions were successfully determined by AMS.



PA7-7 IMPROVED SOLID PHASE EXTRACTION MATERIALS FOR SR-90 AND CS-137Jiangang He^{1,2,3}

(1) *Frontiers Science Center for Rare Isotopes, Lanzhou University, 730000, Lanzhou, P. R. China*

(2) *Radiochemistry Lab, School of Nuclear Science and Technology, Lanzhou University, 730000, Lanzhou, P. R. China*

(3) *Key Laboratory of Special Function Materials and Structure Design, Ministry of Education, Lanzhou University, 730000, Lanzhou, P. R. China*

Strontium (⁹⁰Sr) and cesium (¹³⁷Cs) in spent fuel have high calorific value and strong radioactivity, which have an important impact on the solidification treatment and geological disposal of high-level radioactive waste liquid. Separating and recovering them can not only greatly reduce the disposal cost of high-level radioactive waste, but also ⁹⁰Sr and ¹³⁷Cs have very important application values in radioactive or heat sources. In recent years, solid-phase extraction technology has been widely concerned in the separation of ⁹⁰Sr and ¹³⁷Cs due to its advantages of high efficiency and easy operation. The silicon-based resin used in this technology is currently the most representative material, but it has disadvantages such as low loading rate of extractant, high loss rate and poor stability. In response to this situation, we start from the carrier modification technology and develop the high-performance resins that can separate and recover ⁹⁰Sr and ¹³⁷Cs in a complex system of high acid, high salt and strong radiation, laying a good research foundation for engineering applications.

The main research direction of our group: (1) Silicon-based resin; (2) Polymer-based resin.

For more information, see the personal website:

<http://snst.lzu.edu.cn/shiziduiwu/fujiaoshou/2023/0104/207814.html>.

PA7-8 MIXED FROM A WASTE COCKTAIL: CONSIDERATIONS ON BACKGROUND ELECTROLYTE'S COMPOSITION AND SALINITY, PBTC AND IRON INFLUENCING THE RETENTION OF REPOSITORY-RELEVANT ELEMENTS ON POTENTIAL BARRIER MATERIALS

Kristina Brix⁽¹⁾, Aaron Haben⁽¹⁾, Ralf Kautenburger⁽¹⁾

(1) WASTE group, Inorganic Solid-State Chemistry, Saarland University, Germany

Nowadays the world's demand for energy is growing and is a more pressing problem than ever before. For this reason, some countries are increasingly turning to nuclear power. One of the biggest problems with this technique is that after almost 70 years of using nuclear power, no repository for high-level radioactive waste (HLW) operates worldwide. The main reason for this may be the challenging task of ensuring humanity's and the environment's safety from this radio- and chemo-toxic substances for millions of years.

In a repository for high-level radioactive waste (HLW), the hazardous substances will not be stored separately. On the long-term, after the failure of the HLW containers, the geological and technical barriers must deal with many different elements simultaneously. These elements can influence each other in their retention behaviour.

A cocktail of Zr(IV), Mo(VI), Ru(III), Pd(II), Cs(I), Sm(III), Eu(III) and U(VI) is studied separately and as mixture via batch experiments concerning their retention behaviour on potential barrier materials. Depending on the prevailing conditions, a variety of different retention mechanisms must be considered. Since the usage of cementitious materials in a HLW disposal is very likely, the pH of intruding water increases above 10 due to the leaching of the cement or concrete. Besides precipitation, only few thermodynamic data is already achieved for binding mechanisms at pH 10-13.

For U(VI) e.g., no thermodynamic model could describe its almost quantitative retention in presence of Ca(II) on bentonite or cement alteration phases such as calcium silicate hydrate (C-S-H) phases in the hyperalkaline pH range so far [1,2]. For Cs(I), adsorption on Ca-bentonite and C-S-H phases strongly depends on the salinity of the background electrolyte. It decreases with increasing ionic strength and especially with the potassium content. Nevertheless, a noticeable amount of Cs(I) can be retained on Ca-bentonite even in 5 M NaCl and in around 2.6 M diluted Gipshut solution on C-S-H phases. A slightly decrease in the Cs(I) adsorption could be seen in presence of high concentrations of the other waste cocktail elements [3].

For Mo(IV) no retention on C-S-H phases could be observed in single element experiments. In the waste cocktail, a slight immobilisation was visible. An enhancement in the retention in the presence of the waste cocktail elements could also be observed for Pd(II). Zr(IV), Ru(III), Sm(III) and Eu(III) are retained almost quantitatively and irreversible on C-S-H phases. Mechanistic observations for an equilibrium time of 7 d reveal wall adsorption on the reaction vessels as major mechanism in absence of adsorbent material. In presence of the C-S-H phases, an interaction, e.g. adsorption or surface precipitation, between the waste cocktail elements and the adsorbent material predominates the wall adsorption.

There are also other influential parameters such as the presence of complexing agents, e.g. 2-phosphonobutane-1,2,4,-tricarboxylic acid (PBTC) as a commonly used cement additive or Fe(II/III) as competing ion released from concrete or steel. For PBTC, the type of addition: directly in the background electrolyte or during the synthesis of the C-S-H phases plays a major role. The direct addition decreases the retention on C-S-H phases for every waste cocktail element except Cs(I), U(VI)

and Mo(VI) dramatically. The immobilisation of Cs(I) and U(VI) on the C-S-H phases decreases comparatively slightly. For Mo(VI) there is no more retention noticeable in the presence of the waste cocktail after the addition of PBTC. The reason for this is the formation of complexes between PBTC and the elements which hinder adsorption on the C-S-H phases and even precipitation.

If the PBTC is already present in self synthesised C-S-H phases, a substance containing ^{31}P gets leached out to some extent but the retention of Zr(IV), Mo(VI), Ru(III), Pd(II), Cs(I), Sm(III), Eu(III) and U(VI) decreases only a little bit compared to the behaviour in the absence of PBTC.

The presence of a 100-fold excess of Fe(II), which can oxidise in solution to Fe(III), has no relevant influence on the retention behaviour of every investigated element except Mo(VI) and Pd(II). In case of Mo(VI) the retention increases. For Pd(II) competing effects are possible.

In presence of PBTC and Fe(II), mainly Fe(II) forms complexes with PBTC. Consequently, the retention of Ru(III), Cs(I), Sm(III), Eu(III) and U(VI) increases again. For Ru(III), Sm(III) and Eu(III) an immobilised amount of around 50% could be reached. Nevertheless, without complexing agent, the retention was almost quantitative.

This study demonstrates the importance of taking different critical elements and parameters into account, especially in the same experiment. In this way, new phenomena and possibly binding mechanisms can be revealed.

Acknowledgements: *We would like to thank the Federal Ministry for Economic Affairs and Climate Action (BMWK), represented by the Project Management Agency Karlsruhe (PTKA-WTE) for funding (projects 02E10991, 02E11415D and 02E11860D) and our project partners for the kind collaboration.*

References

- [1] Brix, K., Baur, S., Haben, A. and R. Kautenburger (2021). Building the bridge between U(VI) and Ca-bentonite – Influence of concentration, ionic strength, pH, clay composition and competing ions. *Chemosphere* 285: 131445
- [2] Philipp, T., Huittinen, N., Shams Aldin Azzam, S., Stohr, R., Stietz, J., Reich, T. and K. Schmeide (2022). Effect of Ca(II) on U(VI) and Np(VI) retention on Ca-bentonite and clay minerals at hyperalkaline conditions - New insights from batch sorption experiments and luminescence spectroscopy. *Sci. Tot. Environ.* 842: 156837
- [3] Brix, K., Hein, C., Haben, A. and R. Kautenburger (2019). Adsorption of caesium on raw Ca-bentonite in high saline solutions: Influence of concentration, mineral composition, other radionuclides and modelling. *Appl. Clay Sci.* 182: 105275

PA7-9 X-RAY ANALYSES ON RADIOACTIVE MATTER AT THE MARS BEAMLINE OF SYNCHROTRON SOLEIL

Pier Lorenzo Solari⁽¹⁾, Denis Menut⁽¹⁾, Myrtille Hunault⁽¹⁾, William Breton⁽¹⁾

(1) Synchrotron SOLEIL, L'Orme des Merisiers, Départementale 128, 91190, Saint-Aubin, France

The MARS (Multi-Analyses on Radioactive Samples) beamline at the SOLEIL synchrotron (France) is opened to the international community since 2010 and is dedicated to the study of radioactive samples [1] with a specific radioprotection safety design that fulfills the French ASN (Autorité de Sureté Nucléaire) requirements. The MARS beamline is fully devoted to advanced structural and chemical characterizations of radioactive matter (solid or liquid) using hard X-rays in the 3-35keV energy range and has been built thanks to a close partnership with the CEA. Today, the maximum total equivalent activity present at the same time, including the storage on the beamline, is 185 GBq with a maximum of 18.5 GBq (0.5 Ci) per sample. Currently, different types of experiments are available: standard and high-resolution X-ray absorption spectroscopy (XAS) [2,3], transmission X-ray diffraction (TXRD), high-resolution X-ray diffraction (HR-XRD) [4], and associated X-ray microbeam techniques (μ XRF/ μ XRD/ μ XAS). Small angle and wide-angle X-ray scattering (SAXS/WAXS) are also available.[5]

This contribution presents the latest status of the beamline and a brief overview of the most recent achievements on a selection of topics related in particular to the environmental field.

References

- [1] Sitaud, B. et al., (2012). Characterization of radioactive materials using the MARS beamline at the synchrotron SOLEIL. *Journal of Nuclear Materials* 425: 238-243
- [2] Llorens, I. et al., (2014). X-ray absorption spectroscopy investigations on radioactive matter using MARS beamline at SOLEIL synchrotron. *Radiochimica Acta* 102: 957-972
- [3] Hunault, M.O.J.Y. et al., (2019). Speciation Change of Uranyl in Lithium Borate Glasses. *Inorganic Chemistry* 58: 6858-6865
- [4] Jizzini, M., et al., (2022) Cationic local composition fluctuations in rapidly cooled nuclear fuel melts. *Nuclear Materials and Energy* 31: art.n° 101183
- [5] Dumas, T., et al. (2022). Size and structure of hexanuclear plutonium oxo-hydroxo clusters in aqueous solution from synchrotron analysis. *Journal of Synchrotron Radiation* 29: 30-36

PA8-5 MOLECULAR UNDERSTANDING OF HYDROGEN ADSORPTION AND TRANSPORT IN HYDRATED NA- AND CA-MONTMORILLONITES IN THE CONTEXT OF GEOLOGICAL DISPOSAL OF RADIOACTIVE WASTE

Pinar Citli (1)*, Andrey Kalinichev (1)

(1) Laboratoire SUBATECH - UMR6457, IMT (Institut Mines-Télécom) Atlantique, Campus de Nantes, 4 rue Alfred Kastler, 44307 Nantes Cedex 3, France

*e-mail : pinar.citli@subatech.in2p3.fr

Clay-rich geological formations are currently considered to be optimal candidates as the host rocks for geological repository facilities of high-level radioactive waste due to their certain features such as low permeability of the host rocks, reducing environment, high thermal conductivity, and self-sealing properties. Callovo-Oxfordian (COx) clay formation that contains 25-60% of clay minerals (illite, smectite, interstratified illite/smectite, chlorite, and kaolinite) and also quartz, carbonates, and a trace amount of other phases [1] was chosen as the host rock for a radioactive waste disposal facility in France. Gas generation may occur in such environments as a result of mechanisms, such as anaerobic corrosion of metals, degradation of organic matter, and radiolysis of water due to the residual radioactivity of wastes. The anoxic corrosion of stainless-steel waste containers and water radiolysis reactions caused by alpha decay leads formation of H₂ which is expected to be the most abundant gas in the repository. Generation and accumulation of gases in the repository may cause the gas pressure build-up, resulting in a risk of overpressure and fracture of the surrounding clay rock unless it diffuses, reacts, or gets absorbed by constituent clay rocks which have high sorption capacities due to their high surface areas. Therefore, molecular scale understanding of H₂ adsorption and transport processes is crucial for ensuring safe geological disposal and storage of radioactive waste.

In this project, montmorillonite which is common smectite was selected as a clay model. Atomistic simulations of H₂ adsorption and transport in hydrated Na- and Ca-montmorillonites interlayers are performed at 25, 50 and 90°C up to 120 bar by means of classical molecular dynamics and Monte Carlo methods of computer simulation in order to improve fundamental understanding of the physical and chemical processes controlling the interactions between H₂, aqueous solutions, and clay minerals.

References

- [1] ANDRA (2005) Dossier 2005 Argile - Phenomenological evolution of a geological repository. Report Series.

PA8-6 MOLECULAR LEVEL INSIGHTS ON THE PHYSISORPTION MECHANISMS OF HYDROGEN GAS ON MONTMORILLONITE CLAY SURFACES

Sylvia M. Mutisya and Andrey G. Kalinichev

SUBATECH (IMT-Atlantique, Université de Nantes, CNRS-IN2P3) Nantes, France

Effective and safe measures for the management of radioactive nuclear waste are crucial for the continued adoption of nuclear technology. In this regard, a multi-barrier deep geological storage system consisting of both natural geological formations and engineered barriers has been proposed by several countries as a viable approach to store radioactive waste [1-3]. Gas generation and migration is an important issue in the quantitative risk analysis of a radioactive waste disposal repository. Hydrogen (H_2) gas, resulting from the anaerobic metal corrosion and water radiolysis processes is the most significant gas expected after the closure of the facility. In this environment, the gas migration is controlled mainly by sorption and diffusion processes. However, if the rate of gas generation exceeds the diffusion rate within the engineered and host rock formations, the gas pressure increases and the solubility limit will eventually be surpassed. The elevated gas pressure may affect the host rock mass transport properties, perturb the groundwater flux, lead to over-pressurization of waste containers and the release of gases and contaminated ground water to the environment. The uncertainties associated to gas generation and transfer processes therefore necessitate a detailed understanding of the interaction mechanisms of gases with the engineered barriers and host rock formations.

A universal component of the identified geological sites is the presence of clay minerals, notably, the Callovo-Oxfordian (COx), Opalinus (OPA), and Boom clay formations in France, Switzerland and Belgium, respectively [1-3]. Clays exhibit unique properties such as low hydraulic conductivity, high sorption and retention capability of radionuclides and swelling/self-sealing properties which make them excellent candidates as host rocks for radioactive waste disposal repositories. This work is focused on understanding the interaction mechanisms of H_2 gas with clay minerals. We employ molecular dynamics (MD) simulations to study the site-specific sorption, structure and energetics of hydrogen gas adsorption on the interlayer, basal and edge surfaces of a montmorillonite clay model. A special attention is given to the effects of local compositional and structural heterogeneity of montmorillonite's basal and edge surfaces as well as to the effects of different cations on the sorption mechanisms. The simulations reveal preferential adsorption of H_2 molecules on the hexagonal cavities of the basal siloxane clay surface with the Al/Si isomorphic substitutions on the tetrahedral sheet of clay limiting the occupation of those sites. A detailed quantitative analysis of the adsorption at the edge surfaces of clay particles reveals that the local structure of water governs the adsorption energetics of H_2 on the edges and controls its intercalation within the interlayer pores.

References

- [1] Andra Dossier (2005). Synthesis: Evaluation of the feasibility of a geological repository in an argillaceous formation.
- [2] Société coopérative nationale pour l'entreposage de déchets radioactifs (Suisse), and Johnson, L. (2002). Project Opalinus Clay: safety report: demonstration of disposal feasibility for spent fuel, vitrified high-level waste and long-lived intermediate-level waste (Entsorgungsnachweis). Nagra.
- [3] Neerdael, B., and Boyazis, J. P. (1997). The Belgium underground research facility: Status on the demonstration issues for radioactive waste disposal in clay. Nuclear Engineering and Design 176(1-2): 89-96.

PA8-7 MOLECULAR DYNAMICS COMPUTER SIMULATIONS OF THE EFFECTS OF ORGANIC MOLECULES ON THE CLAY-RADIONUCLIDE INTERACTIONS IN THE CONTEXT OF GEOLOGICAL DISPOSAL OF RADIOACTIVE WASTE

Jakub Licko ⁽¹⁾, Andrey G. Kalinichev ⁽¹⁾

(1) SUBATECH (UMR 6457 – IMT-Atlantique, Nantes Université, CNRS-IN2P3) Nantes, France

Storage and disposal in deep geological formations underground is the preferred long-term solution for high-level radioactive waste (HLW). In France, this is due to be done at the Cigeo facility within the Callovo-Oxfordian (COx) clay host rock formations at a depth of about 500m [1]. The clay minerals in COx – montmorillonite (smectite), illite, and interstratified illite-smectite (I/S) – are layered aluminosilicates possessing negative structural charge that can adsorb and intercalate positively charged cations, including radionuclides (e.g., Cs⁺, Sr²⁺, UO₂²⁺). Such adsorption can occur on the clay's basal surfaces, as well as at the edges of clay nanoparticles. A detailed molecular scale understanding and prediction of the adsorption mechanisms of radionuclides by COx is therefore a subject of great importance for the assessment of long-term safety and stability of the storage.

Small organic molecules (OM) (particularly carboxylates) are expected to be present as part of the waste composition. Their presence in the system may therefore affect the effectiveness of clay as a barrier for radionuclide adsorption and transport, and the effect of OM on radionuclide retention may also depend on their polarity [2-3].

To quantitatively investigate the structural, energetic, and dynamic aspects of the effects of OM on the radionuclides-clay interactions, we are using classical molecular dynamics (MD) computer simulations. ClayFF [4] and CGenFF [5-6] force-fields are used to describe interatomic interactions in the simulated systems which are known to accurately describe the clay and organic parts of our models, respectively. By computing properties such as the diffusion coefficients (D) and potentials of mean force (PMF), we can quantify whether the presence of organic molecules inhibits or enhances the radionuclides' mobilities and adsorption free energies, respectively. Similarly, we can investigate any changes in interatomic interactions by computing radial distribution functions (RDF). RDFs can also provide atomistic insight on adsorption mechanisms on the clay surface, by identifying whether adsorption is more favoured on certain clay regions over others. Lastly, by producing adsorption isotherms, we can investigate the concentration dependence of adsorption and compare it with existing experimental data.

Hydrated Cs⁺ and Sr²⁺ cations are selected as representative waste radionuclides for our simulations as having substantial amount of diverse experimental data on their interactions with clay surfaces, thus allowing for thorough comparison with experiments. Uranium is another major component of HLW. Most of the previous research has been focused on U(VI), in the form of uranyl (UO₂²⁺) cation. However, despite the focus on U(VI) as an adsorbing species, recent data suggest that adsorption of uranium on COx may instead be dominated by U(IV) [7] due to the reducing conditions of COx (Eh ~ -190 mV). The adsorption mechanism of U(VI) may therefore involve reduction to U(IV) on the clay surface, while U(VI) dominates in the aqueous phase. All these variables fundamentally affect the adsorption processes, and warrant further mechanistic investigation.

In addition, to account for the effect of OM polarity, we selected to model three OMs that represent three polarity extremes (e.g. dicarboxylate, monocarboxylate, apolar), with the possibility of also investigating OM flexibility (e.g., malonate vs oxalate). This will allow for both comparison with existing experimental data, as well as prediction of real-world conditions to assess the impact of small organic molecules on the effectiveness of the COx barrier.

References

- [1] ANDRA Dossier (2005). Argile : Évaluation de La Faisabilité Du Stockage Géologique En Formation Argileuse.
- [2] Rasamimanana, S., Lefèvre, G., and Dagnelie, R. V. H. (2017). Adsorption of polar organic molecules on sediments: Case-study on Callovian-Oxfordian claystone. *Chemosphere* 181: 296-303.
- [3] Fralova, L., Lefèvre, G., Madé, B., Marsac, R., Thory, E. and Dagnelie, R. V. H. (2021). Effect of organic compounds on the retention of radionuclides in clay rocks: Mechanisms and specificities of Eu(III), Th(IV), and U(VI). *Applied Geochemistry* 127: 104859.
- [4] Cygan, R. T., Greathouse, J. A., and Kalinichev, A. G. (2021). Advances in Clayff molecular simulation of layered and nanoporous materials and their aqueous interfaces. *J. Phys. Chem. C* 125, 17573-17589.
- [5] Vanommeslaeghe, K. and MacKerell, A. D. (2012). Automation of the CHARMM general force field (CGenFF) I: Bond perception and atom typing. *J. Chem. Inf. Model.* 52, 3144-3154.
- [6] Vanommeslaeghe, K., Raman, E. P., MacKerell, A. D. (2012). Automation of the CHARMM general force field (CGenFF) II: Assignment of bonded parameters and partial atomic charges. *J. Chem. Inf. Model.* 52, 3155-3168.
- [7] Montavon, G., Ribet, S., Loni, Y. H., Maia, F., Bailly, C., David, K., Lerouge, C., Madé, B., Robinet, J. C., and Grambow, B. (2022). Uranium retention in a Callovo-Oxfordian clay rock formation: From laboratory-based models to in natura conditions. *Chemosphere* 299, 134307.

PA8-8 SITE-SPECIFIC STRUCTURE AND ENERGETICS OF URANYL ADSORPTION AT HYDRATED MUSCOVITE (001) SURFACE PROBED BY CLASSICAL MOLECULAR DYNAMICS SIMULATIONSNarasimhan Loganathan ⁽¹⁾, Andrey G. Kalinichev ⁽²⁾*(1) Department of Chemistry, Michigan State University, East Lansing, Michigan, United States**(2) SUBATECH (UMR 6457 – IMT-Atlantique, Nantes Université, CNRS-IN2P3) Nantes, France*

Increased mining activities, weathering and other natural and technological processes related to the production of nuclear power contribute to mobilizing uranium from its ore deposits [1]. However, uranium also finds its way to the ecosystem due to the extensive use of phosphate fertilizers containing noticeable amounts of natural uranium [2]. Under oxic conditions, uranium exists in its U(VI) oxidation state as the uranyl ion, UO_2^{2+} [3].

Clay minerals are among most common products of rock weathering and the primary mineral component of soil. Due to their strong ion adsorption and exchange capacities, clays are often considered as potential adsorbent of toxic and radioactive waste, including uranium, around contaminated mining sites and in nuclear waste repositories [4]. Therefore, a detailed quantitative understanding of the adsorption and retention mechanisms of uranyl ions at the mineral-water interface on the fundamental molecular-scale level is highly necessary.

The adsorption and transport of aqueous species at mineral interfaces and in their nanoporous space has been a topic of intensive research in the context of multiple geochemical, environmental, and materials science applications. Atomistic-scale details have been obtained by various surface-specific experimental methods as well as by computational molecular modeling approaches.

Illite are one of the most common groups of 2:1 layered clay minerals used extensively in the studies of environmental containment of nuclear waste because of their high surface area and high layer charge. Meanwhile, muscovite mica represents a good simplified model for illitic type clay minerals by having similar layered crystal structure, similar layer charge, and serves as an ideal substrate because of its cleavage properties. Various experimental techniques have been used to characterize the uranyl adsorption at the muscovite surface, but their results are not always consistent with each other. For instance, EXAFS investigation [5] indicated that uranyl sorption is possible at the muscovite basal surface through surface precipitation. However, another experimental study [6] suggested that the uranyl ions were adsorbed at the edge surfaces of muscovite through aluminol groups and ruled out adsorption at the basal surfaces. Second harmonic generation spectroscopy provided quantitative information of the adsorption strength and uranyl speciation at different pH values for uranyl at the muscovite basal surface [7]. These results clearly indicated that UO_2^{2+} ions are one of the most predominant positively charged speciation forms in aqueous solutions, but they did not provide details on the specific surface adsorption sites because of experimental limitations.

At the same time, a series of atomistic computer simulations have been performed to examine uranyl ion adsorption at muscovite surfaces [8]. Several sites for uranyl adsorption as inner-sphere and outer-sphere surface complexes were identified in this work, but the energetics of adsorption was not qualitatively studied.

Here we report the results of classical molecular dynamics computer simulations of the adsorption of uranyl ions at hydrated muscovite (001) surface, focusing specifically on the structure of the near-surface hydration layer, the topology of its hydrogen bonding, and surface atomic distributions around

various adsorption sites. Finally, we are quantitatively probing the site-specific adsorption energetics of uranyl adsorption at the muscovite basal surfaces using the free energy calculations approach [9] that was successfully used recently to quantify site-specific uranyl speciation and adsorption at the hydrated surfaces of C-S-H phases of cement [10, 11].

References

- [1] Abdelouas, A. (2006). Uranium mill tailings: Geochemistry, mineralogy, and environmental impact. *Elements* 2, 335-341.
- [2] Yamazaki, I. M. and Geraldo, L. P. (2003). Uranium content in phosphate fertilizers commercially produced in Brazil. *Applied Radiation and Isotopes* 59, 133-136.
- [3] Grenthe I., Fuger J., Konings R. J. M., Melire R. J., Muller A. B., Nguyen-Trung C. and Wanner H. (1992). *Chemical Thermodynamics of Uranium*. Elsevier, New York.
- [4] Grambow, B. (2016). Geological disposal of radioactive waste in clay. *Elements* 12, 239-245.
- [5] Moyes L. N., Parkman R. H., Charnock J. M., Vaughan D. J., Livens F. R., Hughes C. R., Braithwaite A. (2000). Uranium uptake from aqueous solution by interaction with goethite, lepidocrocite, muscovite and mackinawite: An X-ray adsorption spectroscopy study. *Env. Sci. Technol.* 34, 1062-1068.
- [6] Arnold T., Utsunomiya S., Geipel G., Ewing R. C., Baumann N. and Brendler V. (2006). Adsorbed U(VI) surface species on muscovite identified by laser fluorescence spectroscopy and transmission electron microscopy. *Env. Sci. Technol.* 40, 4646-4652.
- [7] Gomez S. A. S., Jordan D. S., Troiano J. M. and Geiger F. M. (2012). Uranyl adsorption at the muscovite (mica)/water interface studied by second harmonic generation. *Env. Sci. Technol.* 46, 11154-11161.
- [8] Teich-McGoldrick S. L., Greathouse J. A. and Cygan R. T. (2014). Molecular dynamics simulations of uranyl adsorption and structure on the basal surface of muscovite. *Mol. Sim.* 40, 610-617.
- [9] Loganathan N. and Kalinichev A. G. (2017). Quantifying the mechanisms of site-specific ion exchange at an inhomogeneously charged surface: Case of Cs^+/K^+ on hydrated muscovite mica. *J. Phys. Chem. C* 121, 7829–7836.
- [10] Androniuk, I., Landesman, C., Henocq, P., and Kalinichev, A. G. (2017). Adsorption of gluconate and uranyl on C-S-H phases: Combination of wet chemistry experiments and molecular dynamics simulations for the binary systems. *Phys. Chem. Earth, Parts A/B/C* 99, 194-203.
- [11] Androniuk, I. and Kalinichev, A. G. (2020). Molecular dynamics simulation of the interaction of uranium (VI) with the C-S-H phase of cement in the presence of gluconate. *Appl. Geochem.* 113, 104496.

PB2-10 IN SITU INVESTIGATIONS: RADIONUCLIDE MOBILITY AT CONCRETE-ROCK-INTERFACE

Juuso Sammaljärvi⁽¹⁾, Xiaodong Li⁽¹⁾, Andrew Martin⁽²⁾, Urs Mäder⁽³⁾, Marja Siitari-Kauppi⁽¹⁾

(1) *University of Helsinki, Finland*

(2) *Nagra, Switzerland*

(3) *University of Bern, Switzerland*

In nuclear waste repositories that will contain concrete structures in contact with the bedrock (e.g., claystone or granitic host rock), the largest uncertainties in the repository safety assessments are related to the behaviour of radionuclides with small or poorly known retention, such as C-14, Cl-36 and I-129. In addition, the long-term performance of a cement-based barrier may be affected by interactions with its surroundings, driven by chemical gradients in the pore water composition at the interfaces.

We set out therefore to characterise the retention and diffusion behaviour of such radionuclides and investigate possible structural and mineralogical changes caused by long contact time between rock and concrete. The study involved the characterization of changes in structure and mineralogy on samples from in situ-diffusion experiment in Grimsel Test Site (Switzerland) as part of a Carbon and Iodine Migration (CIM) project (<https://grimsel.com>). Parallel to the structural studies laboratory experiments were conducted as part of Radionuclide mobility in concrete-rock interface (RASK) project.

Laboratory experiments were performed to investigate the retention behavior of several radionuclides (HTO, organic C-14, Cl-36 and I-125) in different cementitious materials. The distribution and effective diffusion coefficients were determined by through-diffusion experiments. Methods were developed to measure diffusion profiles of the retarded part of RN via autoradiography. Quantification and distribution of porosity were studied in a mortar and mylonitic granodiorite interface sample by C-14-PMMA autoradiography to identify any changes/zoning towards the mortar-granite interface at the sub-mm scale. In addition, mineral-chemical information was provided by element mapping by SEM/EDS.

The results from diffusion experiments are summarized in Figure 1. It can be seen from these results that the diffusion coefficients were mostly smaller in the CEM2-based concrete. Cl-36 and organic C-14 had larger diffusion coefficients than I-125. In terms of distribution coefficients, the Cl-36 and I-125 had quite similar values, while organic C-14 was one decade smaller. There was no significant difference in the distribution coefficients between different cementitious materials.

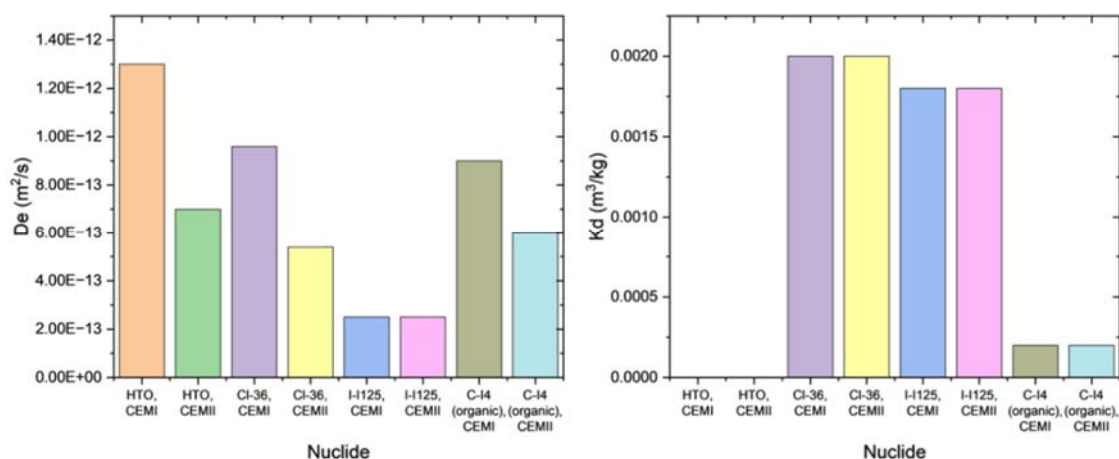


Figure 1 Summary of the diffusion coefficients and distribution coefficients.

The characterisation of an in-situ rock-concrete interface showed that crystalline rock had not experienced any notable amount of alteration, while concrete is slightly degraded during 15 years of contact. This was seen as increased porosity near the interface area with autoradiography as highlighted by results in Figure 2. Electron microscopy analysis showed that degradation had produced an interface region with width of 200-400 μm that was partially filled with porous material and partially empty. Elemental and morphological analysis indicated that the porous material originated from the cement phase and its origin probably involved leaching and dissolution of the cement matrix.

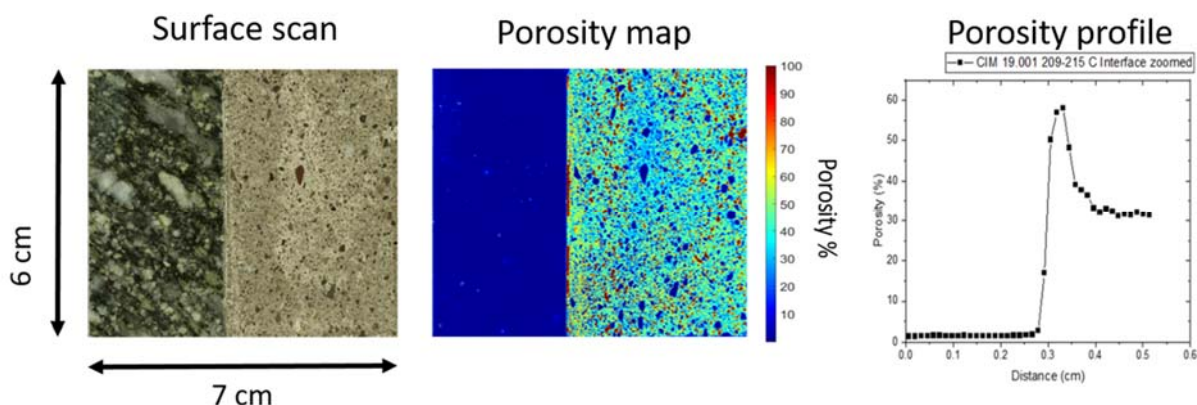


Figure 2 Surface scan (left), corresponding porosity map (centre) and porosity profile (right) of an in situ concrete-rock-interface from Grimsel Test Site.

During the course of this work, we determined the effective diffusion coefficients and distribution coefficients of several radionuclides with small or poorly known retention. The analysis on in situ-interface samples showed the rock appears to be stable against the alkaline conditions but the concrete phase is slightly degraded. We also developed methods and optimized methods to image pore space and to image the retention of radionuclides. The in-situ diffusion experiment is planned to be overcored in 2024, and the methods developed here will help to analyse samples from the upcoming overcoring campaign.

Acknowledgements: This work received funding from the Finnish National Nuclear Waste Research Fund (VYR) and from Nagra, which is gratefully acknowledged.

PB2-11 HOW STRONG DOES NICKEL AFFECT THE SORPTION AND DIFFUSION OF ZINC IN COMPACTED ILLITE?

Van Laer Liesbeth⁽¹⁾, Verhaegen Dorien⁽¹⁾, Aertsens Marc⁽¹⁾, Maes Norbert⁽¹⁾

(1) SCK CEN, Belgium

In the framework of geologic disposal research, the sorption/retardation and transport of radionuclides have already been extensively studied on pure mineral systems (illite, montmorillonite), but in general this is done in single element studies. In real systems, different radionuclides will be present together and in addition the pore water will contain stable elements from different sources (amongst others canister corrosion, dissolution of the waste, backfill material) or originating from the host rock itself as well. Hence, it is key to assess the influence of competitive adsorption of the different elements on the transport of radionuclides in the host rocks.

In this study we focus on the competition effect of Ni on the sorption and diffusion of Zn on clay. Nickel and zinc are both divalent and are assumed to compete for the same sorption sites on the clay. Former studies showed already the influence of the Zn concentration on Ni sorption on illite [1]. The main goal in this research was to assess the competition effect of Ni on the diffusion behavior of Zn-65 through compacted illite. For completeness, the sorption was studied at the same experimental conditions as well.

Diffusion and sorption of Zn-65 were studied in a 0.1 M NaClO₄ background solution, buffered at pH 7 with 5 mM MOPS at four different Ni concentrations between 1.5x10⁻⁸ M (background concentration Ni²⁺ in illite suspension) and 1x10⁻⁴ M. The studied clay was the purified and Na-conditioned Illite du Puy. For the batch sorption experiments, the distribution coefficient (K_d, L/kg) was determined after a 7-day equilibration of the clay suspensions (1 g/L) spiked with Zn-65 (Zn²⁺ concentration of 5x10⁻⁷ M). For the in-diffusion, a membrane-confined diffusion cell (similar design as in [2]) was used with illite clay plugs of 10 mm length and 5.1 mm diameter, compacted at a bulk density ~1.8 g/cm³. The evolution of the Zn-65 concentration was monitored with frequent samplings during a period of ±100 days. In addition, the clay profile was analysed at the end after slicing the clay (resolution of 100 to 200 nm). Experiments are evaluated using a diffusion model implemented in the Comsol Multiphysics code. Simultaneous fitting of the concentration in solution with the clay profile provides the diffusion parameters D_a (apparent diffusion coefficient) and ηR (capacity factor with n accessible porosity and R retardation factor) of Zn.

The batch sorption experiments (Figure 1) revealed that the competition effect starts at Ni concentrations above the background concentration of Zn. At the highest Ni concentration (1x10⁻⁴ M) a decrease in sorption of a factor 2.5-3.5 (±0.5 log unit) was observed. The in-diffusion experiments are currently ongoing and results will be presented at the conference.

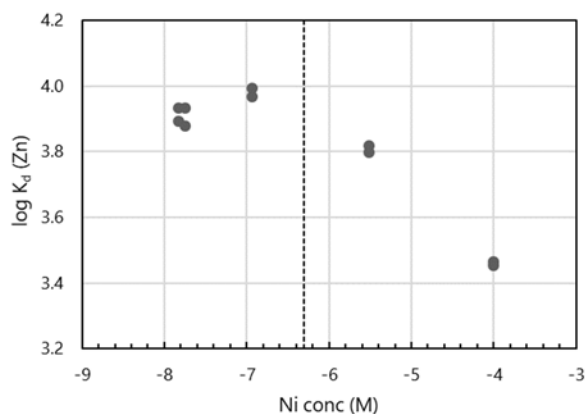


Figure 1 Sorption of Zn^{2+} (expressed as $\text{Log } K_d$, distribution coefficient, L/kg) on purified Na-Illite (du Puy) as function of the Ni concentration (M). Zn^{2+} concentration (5×10^{-7} M) is indicated with the dotted line.

Acknowledgements: This study has received funding from the European Union's Horizon 2020 research and innovation programme under grant agreement n° 847593 and has been performed in the framework of the WP FUTURe.

References

- [1] Marques Fernandes, M. and Baeyens, B. (2020). Competitive adsorption on illite and montmorillonite: Experimental and modelling investigations. Technical Report 19-05, NAGRA, Wettingen, Switzerland.
- [2] Glaus, M.A., Aertsens, M., Appelo, C.A.J., Kupcik, T., Maes, N., Van Laer, L., Van Loon, L.R. (2015). Cation diffusion in the electrical double layer enhances the mass transfer rates for Sr^{2+} , Co^{2+} and Zn^{2+} in compacted illite. *Geochimica et Cosmochimica Acta* 165, 376-388.

PB2-12 INTERACTION OF RADIONUCLIDES WITH FRACTURE FILLINGS AND MIGRATION THROUGH A MATRIX OF CRYSTALLINE HOST ROCK

Milan Zuna⁽¹⁾, Filip Jankovský⁽¹⁾, Karol Kočan⁽¹⁾, Václav Znamínko⁽¹⁾, Eva Bedrníková⁽¹⁾,

(1) UJV Řež, a.s., Disposal Processes and Safety Department, Hlavní 130, 25068 Husinec, Czech Republic

In safety assessments of geological repositories for radionuclide wastes, advection through fractures in the rock matrix and matrix diffusion are considered to be potentially the main transport path for radionuclides in naturally occurring rock barriers [1]. Therefore, determining the transport characteristics of the chosen radionuclides under laboratory-scale conditions is essential to understand the transport under *in situ* conditions and is an important input variable for geochemical and reactive transport modelling. Fracture fillings are usually characterised by a complex mineral composition with high retention capacities (e.g., phyllosilicates, oxides, calcite) of radionuclides [2]. The most important variables include the retention characteristics of the fracture filling and matrix expressed by means of a distribution coefficient (e.g., R_d) and diffusion through the rock matrix characterised by an effective diffusion coefficient (e.g., D_e). Caesium and its radioactive isotope (^{134}Cs) were chosen for sorption experiments, due to their presence as a fission product, their chemical stability under various chemical conditions, and their specific intermediate retention properties (e.g., specific sorption on non-expandable phyllosilicates – illite, biotite, etc.) [3]. The radioactive isotope of hydrogen (^3H) was used in the form of tritiated water (HTO) as a neutral tracer for the diffusion experiments through the rock matrix via the connected pores [4].

Both fracture filling samples and the matrix of crystalline rock formation were extracted at the Bukov Underground Research Facility (Bukov URF) from a depth of 550 m [5]. After the preparation of the material (crushing, sieving, washing), kinetic batch sorption experiments were performed under the constant concentration of the non-active carrier Cs (spiked with active tracers of ^{134}Cs) and a constant m/V ratio in various time periods. To simulate *in situ* conditions, groundwater (S1) with a defined composition was used as a background aqueous phase. All the samples were characterised by X-ray diffraction analysis (XRD) for mineral composition, BET-specific surface area analysis (SSA), and cation exchange capacity (CEC) analysis. The effective diffusion coefficient of HTO in the rock matrix samples was determined by a specially designed through diffusion method through diffusion cells.

All the samples were characterised by increasing R_d values with the increasing interaction time, meaning that sorption equilibrium was not reached. It was more pronounced for the fracture filling samples with high chlorite or kaolinite content (higher SSA and CEC values) than for the rock matrix. One of the reasons may be the introduction of new sites during sorption, which was higher for the fracture fillings with a higher content of minerals with higher sorption capacities and relatively more accessible sorption sites than in the rock matrix sample. It is also apparent that the relatively different SSA and CEC values of the fracture filling samples with high kaolinite and chlorite content had practically the same R_d . [6]. The effective diffusion coefficients for the selected matrix samples were proportional in their order of magnitudes (around 10^{-13} m²/s), which is comparable with the data presented in the literature [7]. Electromigration experiments with negatively charged iodine I⁻ were performed on selected rock matrix samples, which showed that in the case of the anionic tracer, the values were one order of magnitude lower than for HTO, most likely as a consequence of the characteristics of the rock matrix, such as the size of pores (linked with anion exclusion), mineral composition, and the presence of a fissure having a much higher influence on anionic tracer diffusion [8].

Acknowledgment: *This work was funded from the SÚRAO project (SO 2019 – 03) “Research of fracture connectivity at the Bukov URF” and from the European Union’s Horizon 2020 research and innovation programme under grant agreement No. 847593, WP Future.*

References

- [1] Maes N., Glaus M., Baeyens B., et al. (2021). State-of-the-Art report on the understanding of radionuclide retention and transport in clay and crystalline rocks. Final version as of 30.04.2021 of deliverable D5.1 of the HORIZON 2020 project EURAD.
- [2] Poteri A. (2009). Retention properties of flow paths in fractured rock. *Hydrogeology J.*, 17(5), 1081-1092.
- [3] Muuri, Eveliina & Ikonen, Jussi & Matara-aho, Minja & Lindberg, Antero & Holgersson, Stellan & Voutilainen, Mikko & Siitari-Kauppi, Marja & J., Martin. (2016). Behavior of Cs in Grimsel granodiorite: sorption on main minerals and crushed rock, *Radiochimica Acta*.
- [4] Tachi Y, Ebina T, Takeda C, et al.(2015). Matrix diffusion and sorption of Cs⁺, Na⁺, I⁻ and HTO in granodiorite: Laboratory-scale results and their extrapolation to the in situ condition. *J. Contam. Hydrol*, 179, 10-24.
- [5] Havlová V., Zuna M., Brázda L., Kolomá K., Galeková E., Rosendorf T., Jankovský F.(2019).Migration processes of radionuclide in the environment of crystalline rocks and migration parameters of the rocks of the Czech massif. *Final Report 333/2018*, SÚRAO, Prague, Czech Republic.
- [6] Okumura M., Kerisit S., Bourg I.C., Lammers L.N., Ikeda T., Sassi M., Rosso K.M., Machida M. (2019). Radiocesium interaction with clay minerals: Theory and simulation advances Post-Fukushima. *J. Environ. Radioact.*, 210, 105809.
- [7] Voutilainen M., Ikonen J., Sammaljärvi J., Siitari-Kauppi M., Lindberg A., Timonen J. Kuva J., Löfgren M. (2018). Investigation of Rock Matrix Retention Properties – Supporting Laboratory Studies II: Diffusion coefficient and Permeability. Working Report 2017-39, Posiva Oy, Finland.
- [8] Voutilainen M., Ikonen J., Sammaljärvi J., Juka K., Lindberg A., Siitari-Kauppi M., Koskinen L. (2016). Through diffusion on Olkiluoto veined gneiss and pegmatitic granite from structural perspective. *MRS Advances*, 1(61), 4041-4046.

PB2-13 STUDY OF THE INFLUENCE OF FRACTURE FILLINGS ON RADIONUCLIDE TRANSPORT IN CRYSTALLINE ROCK SYSTEMS

Milan Zuna⁽¹⁾, Filip Jankovský⁽¹⁾, Karol Kočan⁽¹⁾, Jan Smutek⁽²⁾, Johannes Kulenkampff⁽³⁾

(1) ÚJV Řež, a.s., Disposal Processes and Safety Department, Hlavní 130, 25068 Husinec, Czech Republic

(2) SÚRAO, Radioactive waste repository authority, Dlážděná 6, 11000 Prague, Czech Republic

(3) Helmholtz-Zentrum Dresden-Rossendorf e.V. (HZDR), Department of Reactive Transport, Permoserstr. 15, 04318 Leipzig, Germany

The rock environment is the final barrier against the potential entry of radionuclides into the biosphere. The migration of radionuclides in crystalline rock environments is mainly related to the flow in fractures (advective transport); however, the transfer of radionuclides from the fracture also occurs through the fracture filling minerals by diffusion in the direction of the lower concentration gradient. Fracture filling minerals (clay minerals, chlorites, calcites, etc.) may represent important sorbents that may contribute to the further retention of radionuclides in the rock. However, advection/diffusion processes in the fissure have not been sufficiently described in transport models so far, including the description of the wetted fissure surface or the so-called channeling associated with it [1] [2].

For the sorption experiments, the altered parts of the rock cores of the rock matrix and the main fracture infill (calcite, chlorite, and secondary clay minerals) were taken from the Bukov Underground Research Facility (Bukov URF) from a depth of 550 m. The effective diffusion coefficient (D_e) of HTO in rock matrix samples was determined by the through diffusion method in through diffusion cells.

In the first phase, experiments were conducted to optimise the methodology and to study the influence of the individual parameters (e.g., pre-treatment method, contact time, fraction size, washing and equilibration method, phase ratio, influence of CO₂, etc.) [3]. Sorption experiments were conducted using batch experiments and the values of (K_d) were evaluated. The sorption experiments were conducted on selected rock samples with radionuclides (¹³⁷Cs, ⁸⁵Sr, ³⁶Cl, ¹²⁵I) to compare different fracture infill types and different rock types simultaneously [2].

For the transport experiments, the suitable sections of drill cores with parallel fractures were prepared. These samples were collected from the Bukov URF (SURA) [3,4], while a sample from the GAM fault zone was extracted at the Grimsel Test Site (GTS) (NAGRA) [5]. The main criteria were as follows: stability of the core for subsequent modifications, the fracture aperture for potential transport, and healing of the fracture with a mineralogical filling.

The rock samples including the fracture infill were characterised in detail (mineralogy, CEC, XRD analysis, SSA, SEM, etc.) and the fissure segmentation was performed based on the μ CT results. Tracer tests were first performed using conservative tracers (KI, Fluorescein) for transport characterisation of the samples and based on the results, tests with selected radionuclides (HTO, ²²Na, ¹³⁴Cs) were performed. The experiments will be predictively simulated and then the results will be validated. After the experiments (¹³⁴Cs), autoradiographic analysis of the fracture surface will be performed to study the sorption positions. When short-lived radionuclides are used, it is possible to use 3D visualisation of RN propagation using a system combining 2-12 gamma cameras such as Timepix3 or GeOPET (HZDR).

The study of transport parameters under in-situ conditions is currently being conducted as part of the project “Research of fracture connectivity at the Bukov URF” [4].

Acknowledgment: *This work was funded from the European Union's Horizon 2020 research and innovation programme under grant agreement No. 847593, and WP Future, SÚRAO Projects "Research support for the safety assessment of the deep geological repository", and "Research of fracture connectivity at the Bukov URF (SO 2019 -31), Long term diffusion (LDT IV) (NAGRA, SÚRAO)".*

References

- [1] Poteri A. (2009). Retention properties of flow paths in fractured rock. *Hydrogeology J.*, 17(5), 1081-1092.
- [2] Havlová V., Zuna M., Brázda L., Kolomá K., Galeková E., Rosendorf T., Jankovský F. (2019). Migration processes of radionuclide in the environment of crystalline rocks and migration parameters of the rocks of the Czech massif. Final Report 333/2018EN, SÚRAO, Prague, Czech Republic.
- [3] Havlová V., Kočan K., Hofmanová E., Jankovský F., Zuna M., Macková D. (2021): WP 5 FUTURE: Summary of the results of the Czech side of the EURAD project – MS SURAO TR 560/2021. SURAO, Praha.
- [4] Zuna M., Havlová V., Jankovský F., Švagera O., Sosna K., Gvoždík L., Holeček J., Řihošek J., Hofmanová E., Kočan K., Kryl J., Zelinková T., Kořalka S., (2021): Research of fracture connectivity at the Bukov URF – Report no.3. SÚRAO 551/2021
- [5] Havlová V., Zuna M., Jankovský F., Hokr M. (2022): Progress Report No. 1 of the Long-Term Diffusion Project - Phase 4. MS SURAO, TZ 622/2022, SURAO, Praha.

PB2-14 HOW DO ALTERATION AND STRUCTURAL HETEROGENEITIES INFLUENCE DIFFUSIVITY WITHIN GRANODIORITES?

Annemie Kusturica⁽¹⁾, Thorsten Schäfer⁽¹⁾

(1) Institute of Geosciences, Applied Geology, Friedrich-Schiller-University Jena, Germany

The safe long-term storage of nuclear waste in deep geological formations is a key aspect of current research. In the German site selection procedure, the comparison of three different host rock types, namely rock salt, clay stone and crystalline rock is an additional challenge.

Within the dual porosity system of crystalline rocks, diffusion into the rock matrix is of great importance, as the volume and reactive surface reached by diffusive transport processes has a high potential in retention of radio- and chemotoxic elements depending on their speciation. When estimating transport processes in crystalline rocks a layered rock model (Crawford & Löfgren, 2019) is currently state-of-the-art with a parametrization of fracture classes and layers.

Parameters as transport porosity ε_p , layer thickness L , effective diffusivity D_e , sorption partitioning coefficient K_d and finally the surface coverage fraction has to be determined.

In this work, the influence of natural heterogeneities and alteration processes on diffusive transport processes in granodiorites is investigated. Samples from an exemplary region within the Lusatian Granodiorite Massif (Saxony, Germany) are presented. The pluton investigated contains areas with varying degrees of hydrothermal alteration along open and (partially) healed fracture systems.

We sampled and cored the pluton in a manner to cover a large variety of domains. Using drill cores vertically and in parallel to the natural fracture surfaces allowed for the analysis of depth profiles of the respective fracture. We combined high-resolution 3D x-ray microscopy scans with gas porosity and permeability measurements. In parallel, geochemical and mineralogical analyses such as powder x-ray diffractometry (XRD), powder and spatially resolved micro x-ray fluorescence (μ XRF) as well as laser-ablation supported inductive coupled plasma-mass spectroscopy (LA-ICP-MS) were performed. On selected altered feldspars, the elemental distribution within the mineral was mapped using LA-ICP-MS^[2]. The mappings are used in correlation with spatially resolved sorption data of rare-earth elements, Th and U.

By intersecting 3D pore space geometry and mineral distribution with the 2D element content and mineral maps, the parameters controlling diffusion intensity of the individual areas within the site were elaborated. We found enhancement of the micro-porosity mainly by feldspar alteration as well as by tectonic forces within an alteration front of approximately 1.5–10 cm thickness. Porosity increase from $3.38 \pm 0.10\%$ to $5.90 \pm 0.54\%$ between the less altered matrix and the stronger hydrothermally alteration front could be determined by He-pycnometry. Furthermore, clogging effects in response to infiltrating clay minerals could be observed. This results in a decrease of the porosity to $2.86 \pm 0.07\%$ at the directly adjacent to the fracture surface, where the infiltrated clay minerals were observed by microscopic observation.

References

- [1] Crawford, J., and Löfgren, M. (2019). "Modelling of radionuclide retention by matrix diffusion in a layered rock model. SKB report R-17-22". Svensk Kärnbränslehantering AB).

- [2] Kusturica, A., Van Laaten, N., Drake, H., and Schäfer, T. (2022). LA-ICP-MS analysis of trace and rare-earth element distribution in calcite fracture fillings from Forsmark, Simpevarp and Laxemar (Sweden). *Environmental Earth Sciences* 81, 371.

PB2-15 ASSESSMENT OF CESIUM MIGRATION IN THE SHALLOW GROUNDWATER-SOIL SYSTEM OF A PROPOSED NNP SITE

Lewen Sun ⁽¹⁾, Qiaoya Lin ⁽¹⁾, Dongyang Chen ⁽²⁾, Wenjie Chen ⁽³⁾, Yuan Chen ⁽⁴⁾, ⁽⁵⁾, Jie Yang ⁽⁴⁾, ⁽⁵⁾, Yong Li ⁽⁴⁾, ⁽⁵⁾, Hanyu Wu ⁽¹⁾, ⁽⁴⁾, ^{*}, Mingliang Kang ⁽¹⁾, ⁽⁴⁾, ^{*}

(1) Sino-French Institute of Nuclear Engineering and Technology, Sun Yat-sen University, Zhuhai, Guangdong, 519082, P. R. China

(2) School of Nuclear Science and Engineering, East China University of Technology, Nanchang, Jiangxi, 330013, P. R. China

(3) School of Resources and Geosciences, China University of Mining and Technology, Xuzhou, Jiangsu, 221116, P. R. China

(4) State Key Laboratory of Nuclear Power Safety Monitoring Technology and Equipment, China Nuclear Power Engineering Co., Ltd, Shenzhen, Guangdong, 518172, P. R. China

(5) China Nuclear Power Engineering Co., Ltd., Shenzhen 518124, Guangdong, P. R. China

Nuclear power plants (NPPs) are becoming increasingly attractive worldwide due to the increasing demand for nuclear energy [1,2]. The long-distance transport of liquid effluents from nuclear power plants where raises concerns about the potential deposition of radionuclide in the shallow groundwater-soil system in the event of abnormal operating conditions. ¹³⁷Cs is the most significant radionuclide released into the ecological environment by human activities [3]. The migration behavior of ¹³⁷Cs in the shallow groundwater-soil systems is largely influenced by factors such as the interaction with the environmental media, as well as groundwater flow velocity [4]. Study the ¹³⁷Cs migration in the shallow groundwater- soil system will provide important data for the safety evaluation of the long-distance transport of the radioactive liquid effluent from the NPPs.

In this study, the migration behavior of Cs(I) in a proposed NPP site in China is investigated using a method combining in-situ investigation, adsorption/diffusion experiments, and Visual MOFFLOW modeling. We divided the study area into four regions (A, B, C and D) according to the hydrogeological framework and collected soil and groundwater samples for adsorption/diffusion experiments at five sites (SK02, SK05, SK12, SK18 and SK20) in these four regions (Fig. 1). Sites I and II were selected for simulation based on the experimental results and hydrological parameters (Fig. 1).

The physicochemical analysis shows that the soil samples in the D region contain clay minerals (montmorillonite) that promote Cs(I) adsorption, and there are very few ions (K^+ , Na^+ , Ca^{2+} , and Mg^{2+}) in the groundwater at SK18 to compete with Cs(I) for adsorption. The results of Cs(I) adsorption experiments show that the adsorption capacity achieved equilibrium in 48 hours, with the maximum Cs(I) adsorption capacity by SK18 at the D region. The apparent diffusion coefficients (D_a) of Cs(I) are determined by penetration diffusion experiments in the research regions of A, B and D. The result shows the lowest apparent diffusion coefficient ($D_a = 5.04 \times 10^{-11}$ m²/s) at the D region, which is consistent with the data of adsorption experiments. Furthermore, Visual MODFLOW software is used to predict the potential contamination area, in combination of the experimental data and hydrogeological framework. The result shows that the Cs(I) contamination area is less than 30 m² in a period of 30 years.

In summary, this study provides valuable insights into the migration behavior of cesium at a proposed NPP site in China, highlighting the importance of considering the site-specific hydrogeological and physicochemical characteristics when predicting Cs(I) migration in the groundwater. These results can be used for elevating the feasibility of long-distance transport of liquid effluent from the NPPs. Additionally, the findings of this study might be used as a reference for future research on radionuclide migration in the shallow groundwater-soil systems.

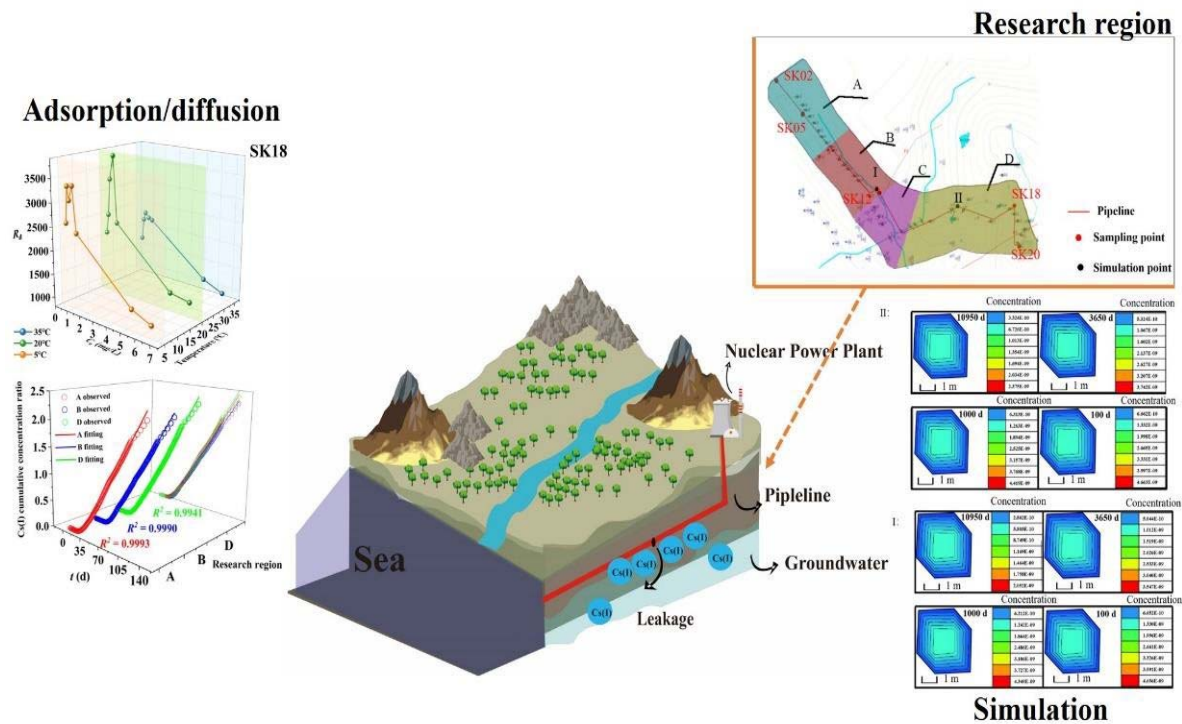


Figure 1: Graphical Abstract

References

- [1]. Yu S, Yarlagadda B, Siegel JE, Zhou S, Kim S (2020) The role of nuclear in China's energy future: Insights from integrated assessment. *Energy Policy* 139:111344.
- [2]. Wang J, Zhang L, Qu J (2022) Distribution laws for radioisotopes in receiving freshwater of Inland Nuclear Power Plant. *Annals of Nuclear Energy* 166:108656.
- [3] Steinhauser G, Merz S, Hainz D, Sterba JH (2013) Artificial radioactivity in environmental media (air, rainwater, soil, vegetation) in Austria after the Fukushima nuclear accident. *Environmental Science and Pollution Research* 20:2527-2534.
- [4]. Testoni R, Levizzari R, De Salve M (2020) Transport dynamic of strontium in groundwater: Safety Assessment study. *Progress in Nuclear Energy* 119:103179.
- [5]. Janipella R, Pujari PR (2022) Review on Groundwater Flow and Solute Transport Modelling in India: Recent Advances and Future Directions. *Journal of the Geological Society of India* 98:278-284.

PB2-16 OUT-LEACHING EXPERIMENTS OF ROCK CORES AFTER IRRADIATION BY NEUTRONS; STUDY OF PORE WATER SALINITY IN CRYSTALLINE ROCK

M. Nyman(1), N. Pakkanen(1), X. Li(1), K. Helariutta(1), M. Siitari-Kauppi(1), L. Aioanei(2), T. Morales(3), A-M. Jakobsson (3) and J. Byegård(4)

(1) *Department of Chemistry, University of Helsinki, Helsinki, Finland*

(2) *Department Institute for Nuclear Research, Pitesti, Romania*

(3) *Swedish nuclear fuel and waste management co SKB, Solna, Sweden*

(4) *Rejlers, Göteborg, Sweden*

The spent nuclear fuel from Swedish and Finnish power plants is planned to be permanently placed in deep geological facilities at the depth of 400-500 m. As a part of the KBS-3 disposal system, the spent nuclear fuel will be deposited in specially engineered canisters with carefully considered containment procedures. In a containment failure, the most important barrier against the spread of harmful nuclear waste-borne compounds into the biosphere is the stable crystalline bedrock surrounding the facilities. In the post-closure safety assessment, salinity estimation is included for the next tens of thousands of years for assessing the fundamental palaeohydrogeological flow modeling in fractured crystalline rock. In addition, the groundwater elements' processes in the bedrock are essential for assessing the radionuclide transport modelling tools for safety calculations. For example, a discrepancy between the chemical composition of matrix pore water and bedrock fracture water in the brittle deformation zones was observed in Olkiluoto conditions [1] where the pore water was measured as less saline than the corresponding fracture water. Such conditions could cause uncertainties in the assessment over geological timescales. Additionally, the importance of the pore water composition for the site description, verification, and temporal evaluation of the groundwater chemistry has to be considered one of the most important issues to be assessed and understood.

The elemental composition of the pore water in low porous crystalline rocks is very difficult to analyse. To obtain information on the pore water composition, out-leaching of chloride originating from the rock core to distilled water combined with measurements of the diffusivities and the total connective porosities of the samples is commonly used [2]. As this method involves out-leaching a very low amount of chlorine from the rock (due to low pore volume), there are suspicions that the method is very sensitive to contamination from drilling waters. In this work, we therefore tested another method to study the salinity of the low-porous crystalline rocks by neutron activation of the intact rock cores. The method is accompanied by out-leaching the activated mobile elements from the pores to a natural groundwater simulant. The effective diffusion coefficients of mobile elements were determined from the out-leaching experimental data to determine the total amount of activated mobile nuclides in the studied rocks' pore space. The number of produced radioisotopes during the irradiation was compared with calculations using the FISPACT-II software [3], which is a code system that can be used for modelling neutron activation and time-dependent inventory by nuclear reactions and decays. The software uses evaluated cross-sections and radioactive decay data to calculate the production and decay of the activation products, provided that the neutron flux and the chemical composition of the target material are known.

Two crystalline rock cores – KFR121 159.48-159.58 m and KFM08C 751.48-751.53 m from the Forsmark area, Sweden – were activated by neutron irradiation at the Annular-Core Pulsing Reactor (ACPR) operated by the Institute for Nuclear Research (INR) Pitești, Romania. The total neutron flux was $1.63 \times 10^{12} \text{ cm}^2\text{s}^{-1}$ in KFR121 and $1.48 \times 10^{12} \text{ cm}^2\text{s}^{-1}$ in KFM08C during the four-hour irradiation. Cl-35 is activated to S-35 and Cl-36 in (n,p) and (n, γ) reactions, respectively.

These nuclides are likely to exist in the non-sorbing chemical forms of SO_4^{2-} and Cl⁻ in the matrix pore volume. In this test, irradiated pore water's volume is estimated to be 0.6 ml (KFR121) and 0.5 ml (KFM08C) based on the rock volume and a porosity of 0.5%. Based on FISPACT-II calculation and

applying an assumption that the pore volume is filled up with water with the reference groundwater composition [3], the activity of S-35 was estimated to be 4.4 kBq (KFR121) and 4.0 kBq (KFM08C) in the pore volume.

After the irradiation, out-leaching experiments on the rock cores were carried out, and Cl-36 and S-35 were measured from the synthetic groundwater. The method for analyzing S-35 from the water samples by precipitation and liquid scintillation counting was tested; the out-leaching curves are shown in Fig.1. Results show that the method can be used for analyzing pore water chloride concentration in in-situ conditions.

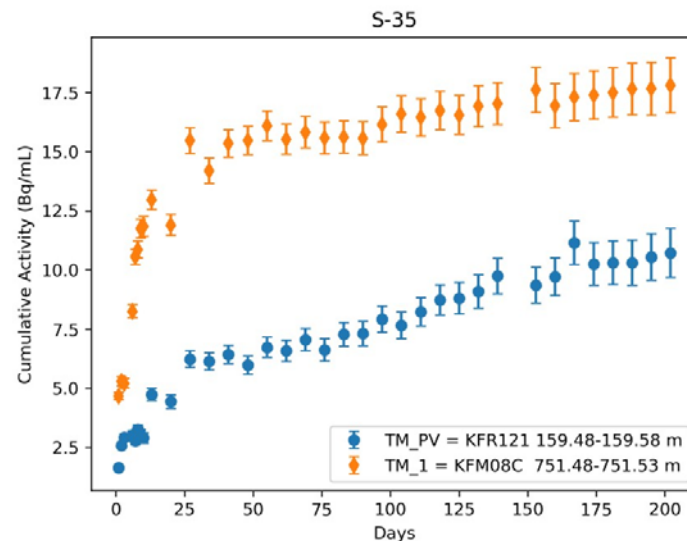


Figure 1. The out-leached amount of S-35 (the cumulative activity concentrations in the leaching solutions) from the irradiated rock core samples as a function of time.

This prestudy's objective was to test if the production and out-leaching of the S-35 and Cl-36 can be done. In addition, the FISPACT-II scoping calculations provided data for chloride concentration in the pore water. The irradiation, out-leaching, and tracer separation/measurement were successfully tested and indications of the applicability of this method used for analysing pore water chloride concentration in crystalline rock were obtained.

Acknowledgement: This work received funding from Svensk Kärnbränslehantering SKB, which is gratefully acknowledged.

References

- [1] Smellie, J., Pitkänen, P., Koskinen, L., Aaltonen, I., Eichinger, F., Waber, N., Sahlstedt, E., Siitari-Kauppi, M., Karhu, J., Löfman, J., and Poteri, A., (2014) Evolution of the Olkiluoto site: Palaeohydrogeochemical Considerations, Posiva Working Report 2014-17
- [2] Waber, H. N., Gimmi, T., deHaller, A. and Smellie, J. (2009). Porewater in the rock matrix; Site descriptive modelling SDM-Site Laxemar, SKB Report R-09-112
- [3] <https://fispact.ukaea.uk/>
- [4] Byegård, J., Selnert, E. and Tullborg, E-L. (2008). Bedrock transport properties; Data evaluation and retardation model, SKB Report R-08-98, Svensk Kärnbränslehantering AB

PB2-17 THE MIGRATION BEHAVIOR OF RADIOACTIVE COBALT AT THE REGION FOR A PROPOSED NUCLEAR POWER PLANT: EXPERIMENTS AND SIMULATION STUDIES

Qiaoya Lin (1), Lewen Sun (1), Jiayu Zhou (1), Dongyang Chen (2), Wenjie Chen (3), Yuan Chen (4), (5), Jie Yang (4), (5), Yong Li (4), (5), Hanyu Wu (1), (4), *, Mingliang Kang (1), (4), *

(1) Sino-French Institute of Nuclear Engineering and Technology, Sun Yat-sen University, Zhuhai, Guangdong, 519082, P. R. China

(2) School of Nuclear Science and Engineering, East China University of Technology, Nanchang, Jiangxi, 330013, P. R. China

(3) School of Resources and Geosciences, China University of Mining and Technology, Xuzhou, Jiangsu, 221116, P. R. China

(4) State Key Laboratory of Nuclear Power Safety Monitoring Technology and Equipment, China Nuclear Power Engineering Co., Ltd., Shenzhen, Guangdong, 518172, P. R. China

(5) China Nuclear Power Engineering Co., Ltd., Shenzhen 518124, Guangdong, P. R. China

Some nuclear power plants (NPPs) sites closing to coastal are under consideration due to the regional demand of energy in China. The liquid effluent in the long-distance pipelines should be pondered in non-coastal NPP constructions. In case of leakage caused by the pipeline corrosion, accident or damage, the radionuclides contained in the effluent will be released to the surroundings. The radioactive cobalt (Co) isotopes are highly concerned in the effluent [1,2]. The object of this study was to investigate the migration behavior of radioactive Co isotopes in the groundwater-soil system surrounding the pipelines, to establish the effective risk management strategies for the liquid effluent of a proposed NPP site in China.

The boreholes were drill along the pipelines of a proposed NPP in China to collect the natural groundwater and soil samples. The surroundings was categorized into three districts according to the topography: (1) coastal-loose rock pore water, which near the liquid effluent outlets; (2) inland-loose rock pore water; and (3) inland-bedrock fissure water respectively. Stable $^{59}\text{Co}(\text{II})$ was used for experiments, instead of radioactive ^{58}Co and ^{60}Co [3]. The batch adsorption experiments were performed at 5 and 35°C. The results indicated that Co(II) adsorption on soil surface were entropy-driven, spontaneous, endothermic and chemical processes in the groundwater-soil systems from the above three districts. The adsorption of Co(II) was found to be reversible, because the dimensionless separation factors (RL) was calculated to be between 0 and 1 [4]. The Visual MINTEQ calculation results showed that $\text{CoSO}_4(\text{aq})$ is the predominant specie in the studied groundwater. Partial Co(II) was found to diffuse in the groundwater due to the equilibrium of the adsorption and the occurrence of desorption on soil surface. The soil and groundwater samples from the two inland boreholes were used to investigate the diffusion and solute transport of Co(II). Diffusion column experiments revealed that about 24 days were needed for the penetration of the 0.30 cm soil column using 190 mg/L Co(II). The corresponding experimental data fitted well with the simulation models using the least square method and one-dimensional diffusion theory, with the root mean square error (RMSE) $< 1.40\text{E}-2$ and the determination coefficient (R -Square) > 0.99 . The apparent diffusion coefficients (D_a) were $7.18\text{E}-13$ (loose rock pore water) and $7.29\text{E}-13 \text{ m}^2\cdot\text{s}^{-1}$ (bedrock fissure water) in inland districts surrounding the pipelines. Therefore, Similar diffusion level in two inland districts was demonstrated by the diffusion parameters (RMSE, R -Square and D_a). The effect of groundwater flow on Co transport was verified by Visual MODFLOW simulation [5]. The simulation results revealed that the impact of Co(II) contaminant plume was limited within 3 m from the leak site in 30 years.

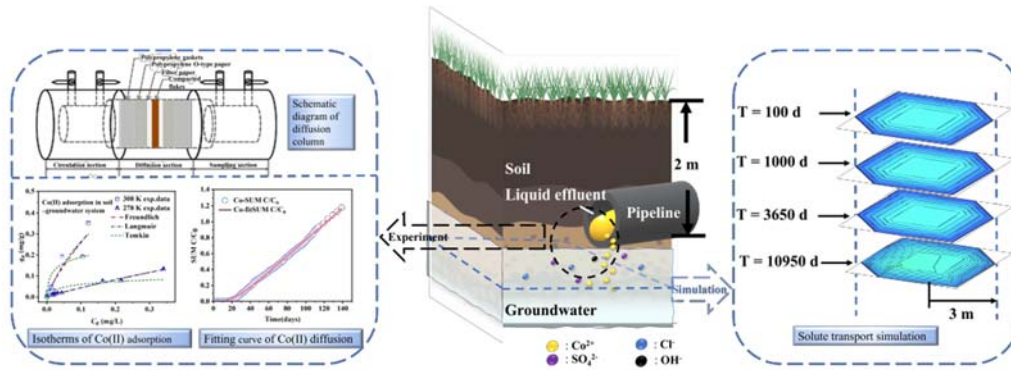


Figure 1: Graphic abstract for cobalt migration

References

- [1] Wendling LA, Ma Y, Kirby JK, McLaughlin MJ (2009) A Predictive Model of the Effects of Aging on Cobalt Fate and Behavior in Soil. *Environ. Sci. Technol.* 43:135-141
- [2] Lim Y, Kim B, Jang J, Lee DS (2022) Buckwheat hull-derived biochar immobilized in alginate beads for the adsorptive removal of cobalt from aqueous solutions. *J. Hazard. Mater.* 436:129245
- [3] Liu X, Wu J, Liu C, Wang J (2017) Removal of cobalt ions from aqueous solution by forward osmosis. *Sep. Purif. Technol.* 177:8-20
- [4] Hamed MG, El-Dessouky SI, Borai EH (2022) Utilization of modified polymeric composite supported crown ether for selective sorption and separation of various beta emitting radionuclides in simulated waste. *J. Mol. Liq.* 353:118799
- [5] Vilensky MY, Berkowitz B, Warshawsky A (2002) In Situ Remediation of Groundwater Contaminated by Heavy- and Transition-Metal Ions by Selective Ion-Exchange Methods. *Environ. Sci. Technol.* 36:1851-1855

PB3-3 INSIGHT INTO IMPACT OF PHOSPHATE ON THE COTRANSPORT AND CORELEASE OF EU(III) WITH BENTONITE COLLOIDS IN SATURATED QUARTZ COLUMNS

Qingfeng Tang, Zhen Xu, Duoqiang Pan, Wangsuo Wu*

(1) School of Nuclear Science and Technology, Lanzhou University, China

(2) Frontiers Science Center for Rare Isotopes, Lanzhou University, China

E-mail: wuws@lzu.edu.cn

Colloid-borne radionuclides (RNs) migration has been a major concern for decades and plays a significant role in security assessment of high-level radioactive waste (HLW) repositories. Particulate solids with a size of 1 nm to 1 μm in natural waters can significantly alter RNs migration behavior by forming not only the pseudo colloids with carrier particles such as inorganic minerals, organic matters and microorganisms, but also the intrinsic colloids originating from the hydrolysis or mineralization of RNs. As the widely accepted buffer barrier for HLW repository, the compacted bentonite is eroded over time resulting in gel formation and release of free bentonite particles, which acts as an effective carrier for RNs migration in the subsurface media. However, the transport of radioactive pollutants with colloids particles in natural environment is not a simple binary system but a complicated system. Phosphate (P) is widely distributed in natural geological media (> 3000 ppm in alkali basalts), steel canisters (450 ppm) and waste streams (9.5 ppm in TBP-containing wastes). Phosphate and clay minerals are widely distributed in natural geological media, and they will inevitably alter RNs migration behavior by forming not only the pseudo-colloids by attaching to environmental particulates, but also the intrinsic colloids originating from the hydrolysis or mineralization of RNs. The mechanism of phosphate intrinsic colloids transport is not clear, and the detailed interactions in such ternary system are still unveiled, the predominant occurrence and mechanism in regulating the colloids-driven mobility of Ln/An(III) remain unclear. Therefore, the assessment of RNs behavior in environment under phosphate rich conditions should take such colloids phases into consideration, since the formation of phosphate containing Ln(III)/An(III) colloids in the surroundings of a nuclear waste repository cannot be ruled out.

In current work, the effect of phosphate on the transport and release of Eu(III) in different colloids systems (P-Eu(III), P-BC, P-BC-Eu(III)) was investigated by taking the fundamental colloid chemistry approach and a complementary suite of characterization techniques. Eu(III) is taken as the chemical analogue for Am(III) due to the similar electronic configuration, the saturated compacted quartz column is represented as the saturated porous subsurface media in investigating the transport patterns of RNs at the laboratory scale. Results showed that intrinsic europium colloids with size of 685 nm were formed by precipitating with phosphate, which affected the mobility of Eu(III) due to the colloids stability and physical straining. Phosphate showed significant promotion on both BC and BC-Eu(III) transport, high phosphate concentration promoted BC transport by eliminating physical straining and enhancing electrostatic repulsion. The crystal structure of EuPO_4 was not destroyed by the subsequent introduction of BC, which carried EuPO_4 for further migration. However, when phosphate, bentonite and Eu(III) coexisted in colloids suspension, and phosphate promoted Eu(III) transport by preferentially interacting with BC to form ternary BC-P-Eu(III) pseudo-colloids rather than forming the intrinsic EuPO_4 colloids. The synergetic role of P and BC on Eu(III) transport was a relatively complex process, which was not a simply additive effect. Findings in this work highlight the significance of phosphate in controlling the fate and transport of Ln(III)/An(III) radionuclides in P-rich colloids bearing environments.

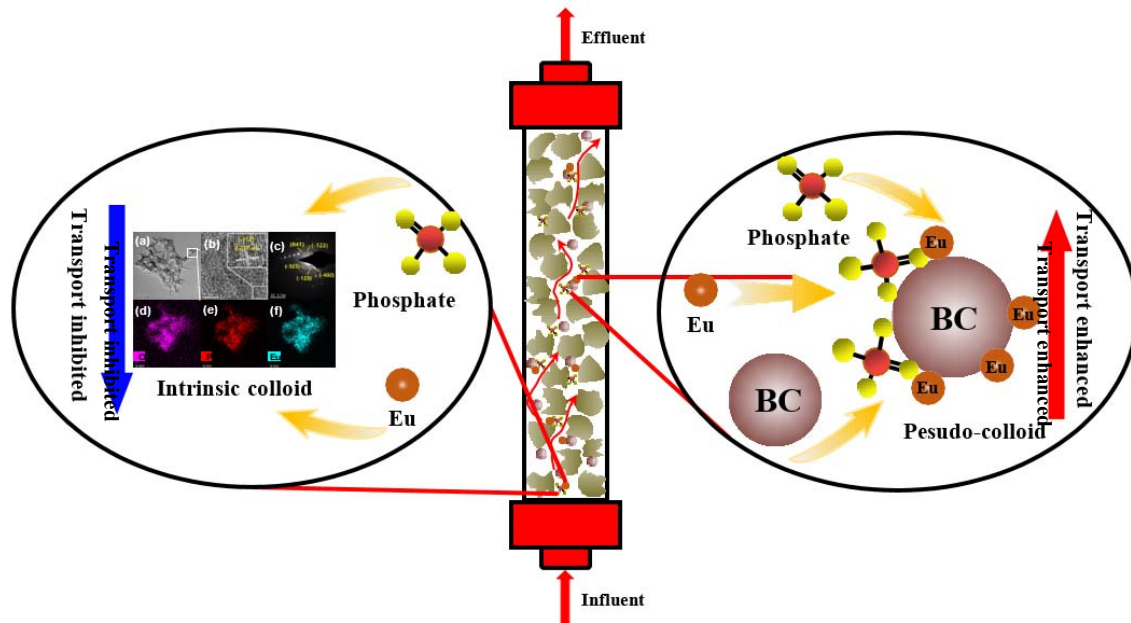


Fig. 1 Hypothetic diagram of the mechanism on co-transport of BC-P Eu(III).

References

- [1] Xu. Z, Tang. Q, Pan. D, Wei. X, Chen. X, and W. Wu (2023) Co transport of bentonite colloids and Eu(III) transport in saturated heterogeneous porous media. *J. Radioanal Nucl. Chem.* <https://doi.org/10.1007/s10967-022-08718-y>
- [2] Xu. Z, Pan. D, Tang. Q, Wei. X, Liu. C, Li. X, Chen. X, and W. Wu (2022) Co-transport and co-release of Eu(III) with bentonite colloids in saturated porous sand columns: controlling factors and governing mechanisms. *Environ. Pollut.* 298:118842.
- [3] Xu. Z, Niu. Z, Tang. Q, Wei. X, Chen. X, Pan. D, and W. Wu (2021) Adsorption characteristics of Eu(III) on colloidal bentonite particles in aqueous solution: impact of colloid concentration, pH, foreign ions, and temperature. *J. Radioanal Nucl. Chem.* 330:765-773.
- [4] Xu. Z, Niu. Z, Pan. D, Zhao. X, Wei. X, Li. X, Tan. Z, Chen. X, Liu. C, and W. Wu (2021) Mechanisms of bentonite colloid aggregation, retention, and release in saturated porous media: role of counter ions and humic acid. *Sci. Total Environ.* 793:148545.

PB3-4 CO-TRANSPORT OF U(VI) AND COLLOIDAL BIOCHAR IN QUARTZ SAND HETEROGENEOUS MEDIA

Qiang Jin^(1, 2), Yufeng Sun⁽²⁾, Zongyuan Chen^(1, 2), Zhijun Guo^(1, 2)

(1) *Frontiers Science Center for Rare Isotopes, Lanzhou University, 730000 Lanzhou, China*

(2) *Radiochemistry Laboratory, School of Nuclear Science and Technology, Lanzhou University, 730000 Lanzhou, China*

Biochar has promising potential in remediation and recovery of contaminated soils because of the adsorption of organic pollutants and heavy metals^[1]. In the case of uranium, biochar has high performance for U(VI) adsorption and forms inner sphere complexes with U(VI) which are stable across a wide range of geological conditions^[2]. Accordingly, biochar can effectively remove U(VI) even at U(VI)-contaminated sites with generally low pH^[3]. However, when biochar is applied to uranium remediation, very little is known about the potential risks resulting from the transport of biochar particles in the environment. In contaminated sites, biochar amendment can decrease the mobility of U(VI) due to its high adsorption affinity. However, once being released into the aquifer, suspended biochar colloids also compete for loading U(VI) with stationary matrix in the environment and thus the transport of biochar colloids (BC) may potentially involve BC-associated U(VI) movement. Although there are some studies refer to the transport behavior of BC alone^[4, 5], co-transport behavior of BC and U(VI) in saturated porous media has not been thoroughly investigated. Whether the BC-facilitated U(VI) transport occurs or not and how the environmental factors impact the process are needed to reveal.

The objectives of this study are to explore how colloidal biochar affects U(VI) transport in a water-saturated heterogeneous media of quartz sand and to understand the involved mechanisms. Individual and co-transport experiments of U(VI) and BC were performed at environmental relevant pH and ionic strength. The effects of pyrolysis temperature and aging degree on co-transport of BC and U(VI) were also focused. In addition to the application of the extended Derjaguin-Landau-Verwey-Overbeek (XDLVO) theory, zeta potential and size distribution of the colloids in the influent and representative effluents were analyzed to better understand the mechanism controlling the transport process. Finally, a two-site kinetic attachment/detachment model was applied to simulate the transport of BC in the absence/presence of U(VI).

Results showed that the transport of U(VI) in the individual transport system was pH-dependent and insensitive to ionic strength, whereas the individual BC transport was more sensitive to the changes in ionic strength compared to those in pH, indicating that electrostatic interaction plays a major role during BC transport but chemical interaction dominates U(VI) transport. In the presence of BC, the transport of U(VI) was significantly facilitated because of U(VI) adsorption on BC. The existence of low concentration of U(VI) (2.5×10^{-6} M), however, did not affect the breakthrough curves (BTCs) of BC, except for the co-transport at relatively high ionic strength (100 mM) where BC transport was impeded due to the decrease of colloid suspension stability. The functional groups on biochar surface gradually decomposed as the pyrolysis temperature increased, resulting in a decrease in adsorption capacity for U(VI). The corresponding colloid-facilitated effect on U(VI) transport in quartz sand heterogeneous media was also decreased. Although aging treatment has no obvious effect on the transport of BC itself, the transport-facilitating effect of BC on U(VI) transport was enhanced with the increase of aging degree. The transport of BC in both individual and co-transport systems could be well described by a two-site kinetic attachment/detachment model. XDLVO calculations demonstrated that electrostatic force played a major role in BC transport. Colloid size exclusion effect existed in both individual and co-transport systems according to the evolution of effluent zeta-potential and particle size.

This study revealed that the potential negative impacts of BC-facilitated uranium transport must be considered before application of biochar in the uranium contamination remediation. The obtained

transport parameters of BC in quartz sand heterogeneous media may will provide an important reference for the quantitative description of fate and mobility of biochar particle alone in natural soil, as well as the facilitated effect of BC on transport of other pollutants, such as heavy metal, organic contaminant, fertilizer residues and microplastics.

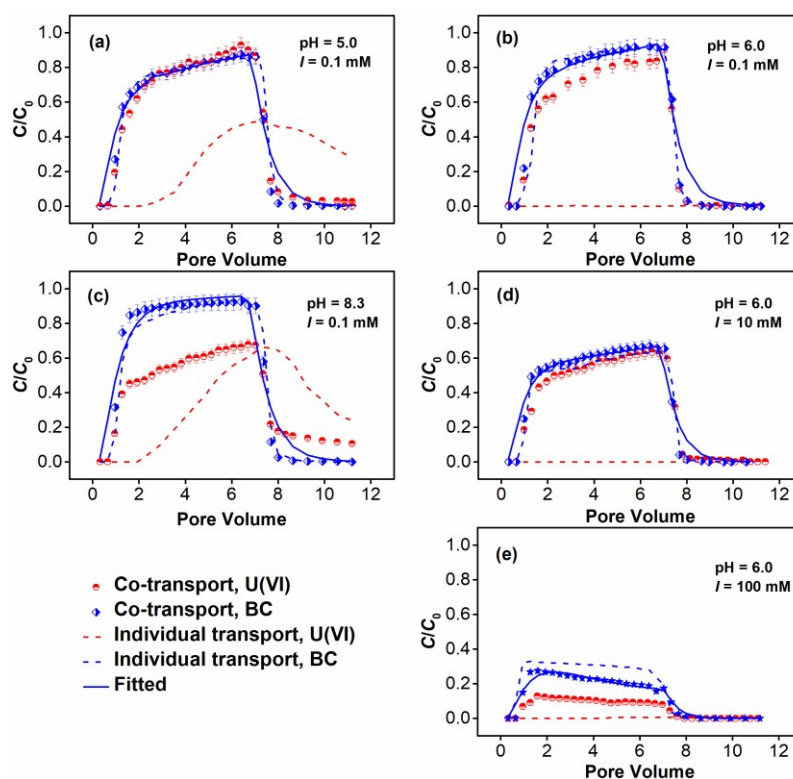


Figure 1. BTCs of U(VI) (red points) and BC (blue points) in the co-transport system at various pH values and ionic strengths, $C_{U(VI)} = 2.5 \times 10^{-6} M$, $C_{BC} = 34.0 \text{ mg/L}$. For comparison, BTCs of individual U(VI) (red dashed lines) and BC (blue dashed lines) under the same conditions are also presented, respectively. The solid lines represented the model-fitted data for BC BTCs in the co-transport system

References

- [1] Inyang, M.I., Gao, B., Yao, Y., Xue, Y.W., Zimmerman, A., Mosa, A., Pullammanappallil, P., OK, Y.S., Cao, X.D., 2016. A review of biochar as a low-cost adsorbent for aqueous heavy metal removal. *Crit. Rev. Environ. Sci. Technol.* 46: 406-433.
- [2] Li, X., Pan, H., Yu, M., Wakeel, M., Luo, J., Alharbi, N.S., Liao, Q., Liu, J., 2018. Macroscopic and molecular investigations of immobilization mechanism of uranium on biochar: EXAFS spectroscopy and static batch. *J. Mol. Liq.* 269: 64-71.
- [3] Kumar, S., Loganathan, V., Gupta, R.B., Barnett, M.O., 2011. An assessment of U(VI) removal from groundwater using biochar produced from hydrothermal carbonization. *J. Environ. Manag. Tour.* 92: 2504-2512.
- [4] Wang, D.J., Zhang, W., Hao, X., Zhou, D.M., 2013. Transport of biochar particles in saturated granular media: effects of pyrolysis temperature and particle size. *Environ. Sci. Technol.* 47: 821-828.
- [5] Yang, W., Braford, S.A., Wang, Y., Sharma, P., Shang, J.Y., Li, B.G., 2019. Transport of biochar colloids in saturated porous media in the presence of humic substances or proteins. *Environ. Pollut.* 246:855-863.

PB3-5 COLLOID-MEDIATED TRANSPORT AND MECHANISM OF U(VI/IV) IN REDUCTION CONDITIONS

Duoqiang Pan⁽¹⁾, Xiaoyan Wei^(1,2), Xinyi Shi⁽¹⁾, Wangsuo Wu⁽¹⁾

(1) Radiochemistry Laboratory, School of Nuclear Science and Technology, Lanzhou University, Lanzhou 730000, China

(2) Laboratory for Waste Management, Paul Scherrer Institut (PSI), CH-5232 Villigen PSI, Switzerland

Uranium resources were mass mining as the principal power generation in most of nuclear facility, the resulting uranium-containing wastewater was inevitably introduced to the aquifer and induced the ecological threat. In order to efficiently mitigate the mobility of uranium via groundwater and confine the exacerbation of uranium contamination, multidisciplinary *in-situ* and *ex-site* remediation strategies have been proposed, such as adsorption and enrichment with inorganic or organic recyclable sorbents, *in-situ* mineralization, or reduction to insoluble UO_2 with reductive agents or microorganisms. As a rule, the mobility of uranium is strongly dependent on its oxidation state, the redox transformations from soluble hexavalent uranium species (UO_2^{2+}) to insoluble tetravalent species (UO_2) largely constrain uranium geochemical behavior. Therefore, redox-mediated immobilization of uranium in the subsurface is considered to be a plausible strategy for the remediation of uranium-contaminated sites [1]. However, substances with sparingly solubility can not only be immobilized in the form of bulk precipitates, but also dispersed and migrated as the form of stable colloidal phase (usually refers to particles with a particle size between 1 nm - 1 μm) [2]. Field experimental studies have revealed that the colloid-facilitated transport of radionuclides in groundwater played a significant role in radionuclides migration, as the formation of intrinsic colloids deriving hydrolysis or precipitation of radionuclides, or as the form of pseudo-colloids by attaching radionuclides onto the environmental colloidal particulates [3]. Therefore, overlooking the colloidal phase may dilute the effectiveness of the reduction or mineralization remediation strategy, the understanding on the colloids-mediated transport of uranium is important for the effective remediation of contaminated sites, as well as the environmental safety assessment system for the redox-sensitive radionuclides. In this work, the co-transport of illite colloids (IC) and U(VI/IV) under reduction conditions was systematically investigated, the detailed interaction between IC and U(VI/IV) was explored by combining column experiment and spectroscopic evidences.

Colloidal UO_2 particles showed considerable mobility in the saturate porous media. The transport of UO_2 was sensitive to the ionic strength, the mobility of UO_2 was facilitated in the presence of illite colloids (IC). The retention of UO_2 was mainly distributed at inlet of column, which indicated that the UO_2 transport in colloidal state was primarily controlled by the size exclusion between particles and media pores. Individual transport of UO_2 was blocked due to the exacerbated aggregation of UO_2 colloids with the increasing ionic strength. However, the presence of IC resulted in the facilitated co-transport of UO_2 colloids even at high ionic strength, and the retention profiles was evenly distributed in the column, implying that the IC prevented the aggregation of colloidal UO_2 particles, and the IC may act as the carrier for UO_2 during the co-transport system. Therefore, U(IV) displayed potential transport risk as the colloidal phase, the presence of other environmental colloids would enhance such risk.

The co-transport of U(VI) and IC in Fe(0)-rich reduction media was investigated as well. The individual transport of U(VI) was retained due to the reductive immobilization effect; however, the presence of IC promoted the transport of U(VI). During the transport process, the hexavalent uranium was reduced to tetravalent state, and then co-transported with IC in the reductive porous media. The co-transport of such yielded U(IV) with IC was facilitated with the decrease of influent velocity and the increase of ionic strength (Figure 1). TEM-mapping of IC-uranium effluent showed that the distribution of IC and uranium was highly related, implying that the IC as vectors facilitated the transport of U(IV), which was consistent with the co-transport of UO_2 colloids and IC. Therefore, the potential transport risk of uranium,

including the intrinsic UO_2 colloids as well as the pseudo-colloids deriving from environmental colloids, is essential and critical in designing reduction-fixation remediation strategies for uranium-contaminated sites, as well as blocking strategies against colloidal phase migration.

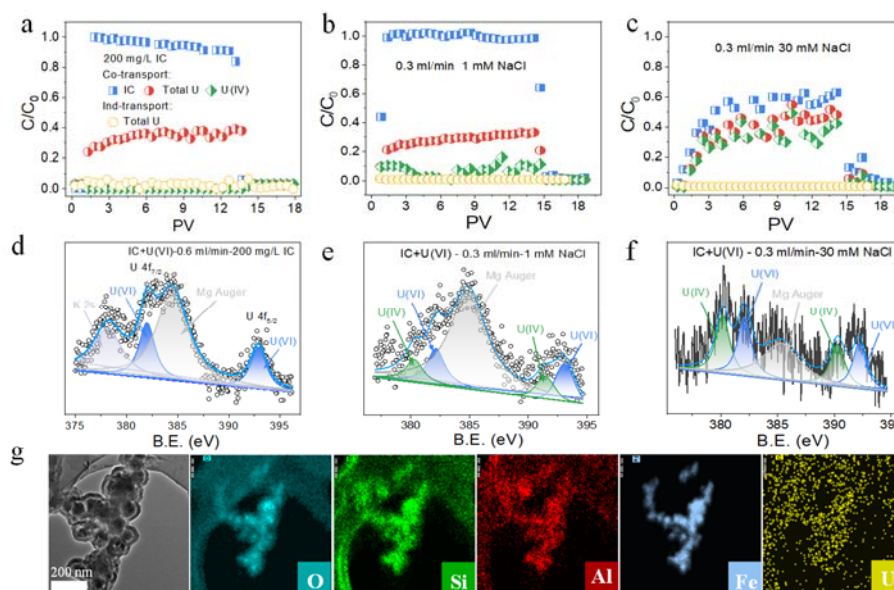


Figure 1. (a)-(c) The transport behaviors of IC and U(VI) under the reduction condition; (d)-(f) XPS spectrum of co-transport effluent; (g) TEM-mapping of co-transport effluent.

References

- [1] Jung, H.B., Boyanov, M.I., Konishi, H., Sun, Y., Mishra, B., Kemner, K.M., Roden, E.E., Xu, H. (2012). Redox behavior of uranium at the nanoporous aluminum oxide-water interface: implications for uranium remediation. *Environ. Sci. Technol.* 46: 7301-7309
- [2] Kind, M. (2002). Colloidal aspects of precipitation processes. *Chem. Eng. Sci.* 57: 4287-4293.
- [3] Kersting, A., Efurud, D., Finnegan, D. et al. (1999). Migration of plutonium in ground water at the Nevada test site. *Nature* 397: 56-59.

PB4-8 EXPLORATION OF THE BIO-REDUCTION BEHAVIOR AND MECHANISM OF ⁹⁹Tc(VII) BY *KLEBSIELLA VARIICOLA* STRAIN X-21

Junyuan Gong⁽¹⁾, Shunzhang Chen⁽¹⁾, Yuqi Guo⁽¹⁾, Feize Li⁽¹⁾, Tu Lan⁽¹⁾, Yuanyou Yang⁽¹⁾, Jiali Liao^{(1)*}, Ning Liu⁽¹⁾

(1) Key Laboratory of Radiation Physics and Technology of the Ministry of Education, Institute of Nuclear Science and Technology, Sichuan University, Chengdu 610064, P. R. China

It is well known that a stock of radioactive waste has been generated in the development and utilization of nuclear energy. Technetium-99 (⁹⁹Tc, fission yield 6.06%), as a vital fission product with a long half-life ($T_{1/2}=2.13\times 10^5$ years), may be released into the environment in the nuclear fuel cycle^[1]. It can pose a long-term risk to the health of human and ecosystems since it is typically present as the soluble Tc(VII)O₄⁻ with highly migratory and bioavailable in the environment^[2]. The reduction of Tc(VII) is a precursor of its weakened migration, which could occur in a directly or indirectly biotic manner via some bacteria, and the behaviours and mechanisms have attracted extensive attention^[3].

Therefore, this study systematically investigated the Tc(VII) reduction behavior of a novel facultative anaerobic bacterium (*Klebsiella variicola* strain X-21, which was isolated from radioactivity contamination soil in southwest China), involving the effects of environmental conditions, electron donors, and electron mediators. Moreover, the mechanism of Tc(VII) bioreduction induced by X-21 and the electron transmission were delineated through the characterization and experimental results.

The results showed that the reduction of Tc(VII) by strain X-21 occurred in an anaerobic condition, and about 40%~70% of Tc(VII) could be reduced by resting cells in 8 days (pH=6.0~9.0, 25~45°C). The presence of Fe³⁺ promoted the Tc(VII) reduction, while Cu²⁺ and NO₃⁻ inhibited the effects. Moreover, strain X-21 could utilize various electron donors and electron mediators to accelerate the Tc(VII) reduction, especially sodium pyruvate and AQS. This indicated that the Tc(VII) reduction of X-21 might be restrained by the transport system in the cell membrane, and it was demonstrated by subsequent permeable cell experiments again. The characterization results indicated that the reduction products were mainly inside the cells as Tc(IV) precipitates. Further experiments were carried out to explore the mechanism of Tc(VII) reduction by X-21, and it was found that the Tc(VII) reduction by X-21 was an enzymatic reaction, the relevant enzymes were mainly stored in the cytoplasm. Furthermore, there was evidence that the complexes (II, III, and IV) of the electron transport chain were involved in the bio-reduction of Tc(VII).

In spite of its limitations, this study is of referential significance for the biochemical and geochemical studies of Tc. Furthermore, it provides theoretical support for the risk assessment of nuclear accidents and new ideas for radioactive contamination treatment.

* E-mail: liaojiali@scu.edu.cn

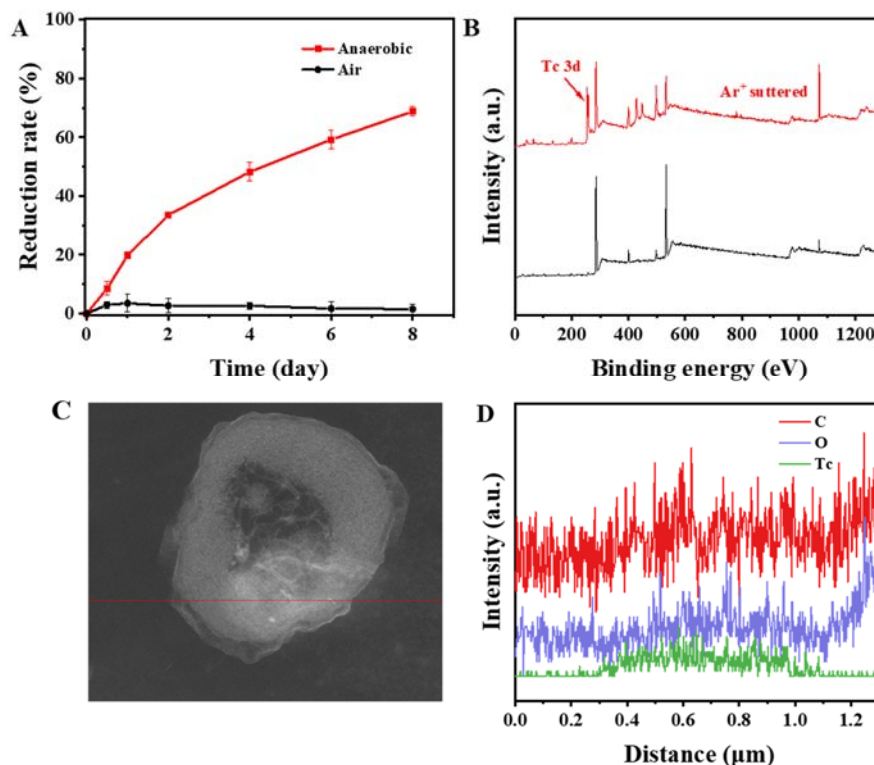


Fig.1 Tc reduction by X-21 under anaerobic and aerobic conditions (A); XPS (B), TEM (C) and line scan of TEM-EDS (D) results for samples after reaction.

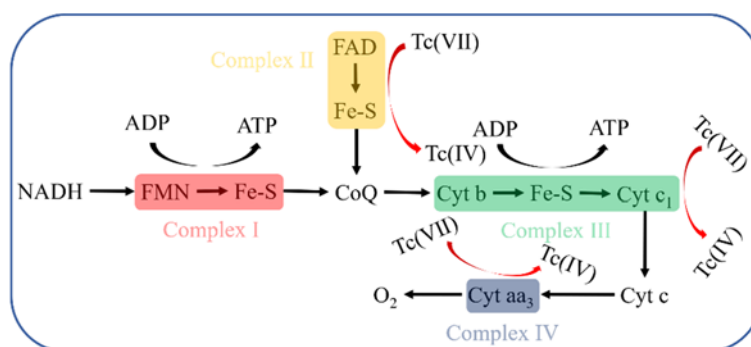


Fig.2 Localization of Tc(VII) reduction in the electron transport chain.

Acknowledgment: This work was financially supported by National Natural Science Foundation of China (Grant No. 21876123) and the National Fund of China for Fostering Talents in Basic Science (J1210004).

References

- [1] Alberto, R. (2003). Technetium. In Comprehensive Coordination Chemistry II. Pergamon, Oxford.
- [2] Schulte, E. H. and Scoppa, P. (1987). Sources and behavior of technetium in the environment. *Sci. Total Environ.* 64 (1): 163-179.
- [3] Brookshaw, D. R. and Patrick, R. A. D. (2015). Redox interactions of Tc(VII), U(VI), and Np(V) with microbially reduced biotite and chlorite. *Environ. Sci. Technol.* 49 (22), 13139-13148.

PB4-9 OVERVIEW ON THE EURAD WORKPACKAGE CORI (CEMENT-ORGANIC-RADIONUCLIDE-INTERACTIONS)

M. Altmaier¹, D. Garcia², P. Henocq³, N. Mace⁴, T. Missana⁵, D. Ricard³, J. Vandendorre⁶

1) Institute for Nuclear Waste Disposal, Karlsruhe Institute of Technology, Karlsruhe (Germany)

2) Amphos21 Consulting S.L., c/ Veneçuela, 103. 2nd floor. 08019 Barcelona (Spain)

3) ANDRA, 1-7, rue Jean-Monnet - 92298 Châtenay-Malabry CEDEX (France)

4) Université Paris-Saclay, CEA, Service d'Etude du Comportement des Radionucléides, 91191, Gif-sur-Yvette (France)

5) CIEMAT, Avda. Complutense 40 - 28040 Madrid (Spain)

6) SUBATECH, UMR 6457, Institut Mines-Télécom Atlantique, CNRS/IN2P3, Université de Nantes; 4, Rue Alfred Kastler, La chantrerie BP 20722, 44307 Nantes cedex (France)

The CORI (Cement-Organic-Radionuclide-Interactions) Workpackage integrated into EURAD (EURAD – European Joint Programme on Radioactive Waste Management, <https://www.ejp-eurad.eu>) performs research to improve the knowledge on the organic release issues which can accelerate the radionuclide migration in the context of the post closure phase of geological repositories for ILW and LLW/VLLW including surface/shallow disposal. The R&D in CORI extends the current state-of-the-art and will contribute to optimize disposal solutions and consider questions of regulatory concern. CORI results will help member states to further develop their national R&D programs and support programs at an early implementation stage.

CORI research addresses topics in the context of cement-organics-radionuclides-interactions. Organic materials are present in some nuclear waste and as admixtures in cement-based materials and can potentially influence the performance of a geological disposal system, especially in the context of low and intermediate level waste disposal. The potential effect of organic molecules is related to the formation of complexes in solution with some radionuclides of interest (actinides + lanthanides) which can (i) increase radionuclide solubility and (ii) decrease radionuclide sorption. Organic substances require special attention since a significant quantity exists in the waste and in the cementitious materials, with a large degree of chemical diversity. Cement-based materials will be degraded with time, leading to specific alkaline pH conditions under which the organics can degrade, thus increasing their impact on repository performance. CORI has prepared a State-of-the-Art document which gives an introduction to the main research topics targeted in CORI (available at: <https://www.ejp-eurad.eu/publications/eurad-deliverable-31-cori-sota-cement-organic-radionuclide-interactions-content-lilw>).

The three R&D Tasks in CORI shortly summarized in this contribution are:

Organic Degradation. Focus is on the characterization of soluble organic species generated by radiolytic and hydrolytic degradation of selected organics (PVC, cellulose, resins, superplasticizers). Studies also include the analysis of degradation and stability of small organic molecules such as carboxylic acids and the determination of degradation rates.

Organic-Cement-Interactions. Studies focus on investigating the mobility of selected organic molecules in cement-based materials. Mobility of organic molecules includes sorption and transport properties. Organics will also include small ¹⁴C bearing molecules as identified in the EC EURATOM project CAST. Both retention on individual cement phases and cementitious systems are investigated.

Radionuclide-Organic-Cement-Interactions. Radionuclide migration processes are studied in the ternary system. The role of organic molecules on the transfer properties of radionuclides are investigated through sorption and transport experiments. Selected radionuclides cover a range of chemical characteristics and redox states relevant for conditions in L/ILW disposal.

This contribution will provide information on how and where to get more detailed technical information on the work performed in EURAD-CORI as well as integrated summary information on main results, and announce forthcoming dissemination activities organized in EURAD-CORI.

Acknowledgments: *The EURAD-CORI project leading to this application has received funding from the European Union's Horizon 2020 research and innovation program under grant agreement No 847593.*

PB4-10 IMPACT OF THE DEGRADATION PRODUCTS OF UP2W FILTER AID MATERIAL ON THE UPTAKE OF RADIONUCLIDES BY CEMENT

P. Szabó¹, A. Tasi¹, X. Gaona¹, A. C. Maier², S. Hedström², M. Altmaier¹, H. Geckeis¹

(1) *Institute for Nuclear Waste Disposal, Karlsruhe Institute of Technology, Karlsruhe (Germany)*

(2) *Svensk Kärnbränslehantering AB (SKB), Solna (Sweden)*

UP2W is a filter aid based on polyacrylonitrile (PAN), which is widely used in nuclear and fossil-based power plants for particle removal and as support material for ion exchange resins. Significant amounts of used UP2W fiber mass are therefore disposed of in underground repositories for low and intermediate level nuclear waste (LILW), e.g. in SFR, Sweden. The hydrolytic degradation of PAN may result in organic degradation products affecting the mobility of radionuclides in cementitious environments, and thus are of particular interest in the context of nuclear waste disposal. This work aims at investigating the impact of the degradation products of UP2W on the solubility and sorption of selected radionuclides in cementitious systems under alkaline, reducing conditions as those expected at SFR after repository closure.

All experiments were performed under Ar atmosphere with $O_2 < 2$ ppm. Long-term degradation studies (up to 3 a) involving the original UP2W material with solid to liquid ratio (S:L) of $\sim 50 \text{ g}\cdot\text{dm}^{-3}$ were conducted in various NaOH media as well as in $\text{Ca}(\text{OH})_2$ -buffered solutions with $\text{pH} = 12.5$ at $T = 25$ and 80°C in the absence and presence of $\text{Fe}(0)$. Supernatant solutions were systematically characterized by organic carbon content measurements (NPOC), various spectroscopic analyses ($^1\text{H} / ^{13}\text{C}$ NMR, IR, UV-vis), and chromatographic analyses (LC-OCD-OND and HPLC-MS). Solubility experiments with $\text{Ca}(\text{OH})_2(\text{s})$, $\beta\text{-Ni}(\text{OH})_2(\text{cr})$, $\text{Nd}(\text{OH})_3(\text{s})$ and $\text{PuO}_2(\text{ncr, hyd})$ (with ncr and hyd standing for nanocrystalline and hydrated, respectively), as well as sorption experiments with ^{63}Ni , ^{152}Eu and ^{242}Pu were carried out in the absence and presence of selected proxy ligands in porewater solutions corresponding to cement CEM I in the degradation stage II ($\text{pH} \approx 12.5$, $[\text{Ca}] \approx 0.02 \text{ M}$). In experiments involving Pu, reducing conditions were maintained by hydroquinone or Sn(II). Parameters such as total ligand, radionuclide concentrations and S:L were varied on a wide range. Retrieved solid phases from the degradation studies, solubility and sorption experiments were extensively characterized.

Based on ^1H NMR and in accordance with other experimental observations, three proxy ligands are proposed to simulate the chemical characteristics of the UP2W degradation products. Glutaric acid (GTA) represents the bulk chain of the generated polymer fragments, whilst α -hydroxyisobutyric acid (HIBA) and 3-hydroxybutyric acid (HBA) simulate the effect of the end groups. These proxy ligands show no significant impact on the solubility of $\text{Ca}(\text{II})$, $\text{Nd}(\text{III})$ or $\text{Pu}(\text{IV})$, whereas a slight increase in the solubility of $\text{Ni}(\text{II})$ was observed at $[\text{L}]_{\text{tot}} > 10^{-2} \text{ M}$. This suggests the possible formation of stable ternary Ni-OH-L (or Ni-L-H , with L-H corresponding to a ligand with deprotonated alcohol group) complexes in hyperalkaline systems. The uptake of $\text{Ni}(\text{II})$ and $\text{Pu}(\text{IV})$ by cement is weakly affected by HIBA, HBA and GTA at $[\text{L}]_{\text{tot}} > 0.1 \text{ M}$ 10^{-2} M , whereas no effect was observed in the case of $\text{Eu}(\text{III})$. Degradation leachates obtained from the degradation experiments induced an evident but modest decrease in the retention of the investigated radionuclides, so R_d values remained high in all cases. These results highlight the relevance of conducting sorption experiments with real degradation leachates in order to properly capture the impact of complex organic materials disposed in L/ILW. This work provides an improved quantitative and mechanistic understanding of the retention properties of radionuclides in cement systems in the presence of UP2W degradation products.

Acknowledgments: *The project leading to this application has received funding from the European Union's Horizon 2020 research and innovation program under grant agreement No 847593. SKB is likewise acknowledged for financially supporting this work.*

PB4-11 INFLUENCE OF MICROORGANISMS ON THE MOBILITY OF +3 ACTINIDES FROM THE WASTE ISOLATION PILOT PLANT

Juliet Swanson (1), Adrienne Navarrette (1), Floyd Stanley (2), Hannah Kim (1), Jandi Knox (1)

(1) Los Alamos National Laboratory, USA

(2) Savannah River Nuclear Solutions, USA

Microorganisms can affect the mobility of actinides through various means, including but not limited to, biosorption, biomineralization, and biologically induced precipitation. These processes are included in measurements of the biocolloid parameters used in Performance Assessment calculations for the Waste Isolation Pilot Plant (WIPP). In order to update these parameters for the +3-actinide oxidation state, several WIPP microbial isolates were tested for their influence on neodymium concentrations in simple sodium chloride solutions and concentrated WIPP brines. The tested organisms (*Halobacterium*, *Chromohalobacter*, *Salinicoccus*, *Nesterenkonia*, *Thalassobacillus* spores, and an unidentified haloarchaeon) comprise bacterial and archaeal isolates from different phyla, with varying degrees of halophilicity or halotolerance, and with different cell surface characteristics. Batch sorption experiments were carried out over a period of 4-5 weeks in simple NaCl solutions at each organism's optimum concentration. The three most halophilic of these organisms (*Halobacterium*, *Chromohalobacter*, and the unidentified haloarchaeal isolate) were further tested in WIPP brines. Select final samples were analyzed by SEM/EDS.

In many cases, the loss of neodymium from solution in the presence of microorganisms was immediate and extensive, and in most cases, the extent of biological influence reached 100% by the end of the experiments. There was a weak correlation between the salt concentration of the test matrix and Nd removal from solution at time zero, but this disappeared with time. There was no correlation between Nd loss and organism type, except for a possible correlation with cell surface availability in the case of cell clumping, but this too disappeared over time. However, the extent of biological influence on Nd in solution differed between test matrices (simple NaCl versus high-magnesium brine versus high NaCl brine). The smallest effect of organisms on Nd in solution was observed in high-magnesium brines, such as Generic Weep Brine (GWB). Neodymium removal from solution was moderate, but significant, in high NaCl WIPP brine, and loss was extensive in simplified NaCl solutions, regardless of sodium concentration (Figure 1). Two possible reasons for this (cation competition for available cell surface binding sites, changes in cell surface structure or morphology) are currently under investigation.

It is hypothesized that the immediate loss of Nd from solution is due to biosorption but that biological influence over longer periods of time is from induced precipitation or biomineralization. The disposition of Nd in SEM images could not be determined, given the low concentrations of Nd in the experiments. However, some images revealed possible encapsulation of biomass within precipitated salt crystals and cellular exudate or debris entangled in the precipitates, suggesting immobilization of associated Nd (Figure 2). XRD analyses are pending.

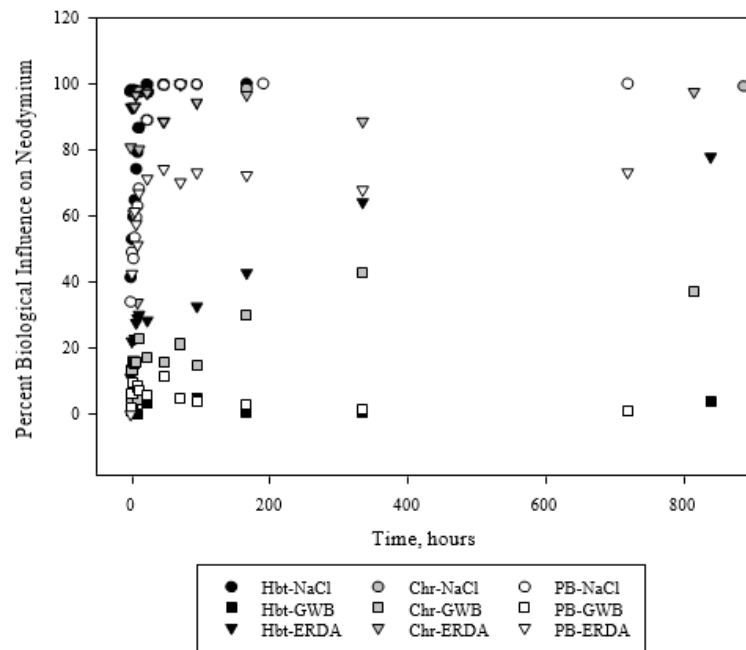


Figure 1. Percentage influence of three halophilic WIPP isolates (*Halobacterium* sp., Hbt; *Chromohalobacter* sp., Chr; and archaeal isolate, PB)—on Nd in solution in three different matrices (Generic Weep Brine, GWB; Energy Research and Development Administration Well 6 brine, ERDA; and simplified NaCl solution). Higher percentages indicate less Nd in solution.

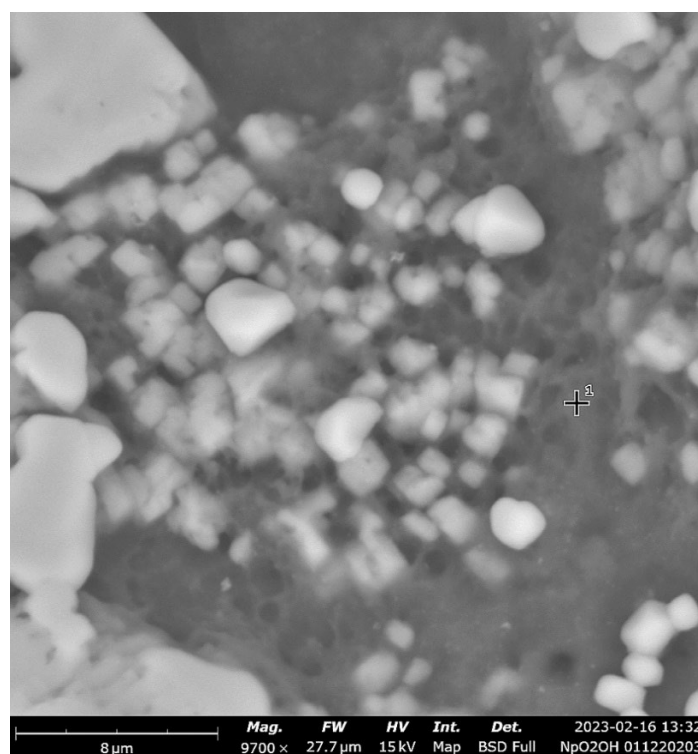


Figure 2. SEM image of *Chromohalobacter* sp. debris/exudate (light gray webbing in background) and NaCl precipitate.

PB4-12 IMPACT OF THE EXTRACTION OF SOLUBLE ORGANIC MATTER (SOM) FROM SOILS ON THE QUALITY OF INSOLUBLE ORGANIC MATTER (IOM) IN VIEW OF PROTON BINDING SITES AND RADIONUCLIDE BINDING

Marawit Tesfa⁽¹⁾, Jésus Raya⁽²⁾, Régis Gougeons⁽³⁾, Philippe Schmitt-Kopplin⁽⁴⁻⁵⁾, Gilles Montavon⁽¹⁾

(1) *SUBATECH, UMR 6457, IMT Atlantique/IN2P3-CNRS/Nantes Université, 4, Rue Alfred Kastler, BP 20722, Nantes Cedex 3, 44307, France*

(2) *UMR PAM Université de Bourgogne/AgroSup Dijon, Institut Universitaire de la Vigne et du Vin, Jules Guyot, Dijon, France*

(3) *Université de Strasbourg, CNRS, Membrane Biophysics and NMR, Institute of Chemistry, 1 Rue Blaise Pascal, 67000 Strasbourg, France*

(4) *Helmholtz Munich, Analytical BioGeoChemistry; Ingolstaedter Landstraße 1, 85764 Neuherberg, Germany.*

(5) *Technische Universität München, Maximus-von-Forum 2, 85354 Freising, Germany*

Natural organic matter (NOM) is a ubiquitous entity present in soil, sediments and water. In all of these compartments, NOM interacts with natural, anthropic, organic or inorganic particles. Indeed, it was found to influence: (1) elements bio-geochemical cycles by hindering biological physical and chemical degradation, (2) ions speciation by changing oxidation state, (3) both element and particle transport by adsorption. Thus, because NOM hosts transports and influences the solubility, bioavailability and biotoxicity of metallic contaminants, it has a paramount role in environmental issues like water and soil pollution. For this reason, NOM behavior towards contaminants was extensively studied, but predicting its role still remains difficult.

Efficient reactive models predicting contaminants adsorption and transport by solid phases like minerals exist. However, they are rarely suitable for NOM because it is extremely heterogenous (with both soluble and insoluble active phases which have a high chemical diversity), and even more so with everchanging biological, physical and chemical parameters i.e. the case of environmental conditions. To overcome this difficulty, researchers conducted laboratory experiments on standardized extracted organic matter, i.e. humic substances, made internationally available by the International Humic Substance Society (IHSS). This trend allowed comparative studies and establishment of models describing NOM proton and by extension cation binding sites such as NICA-Donnan [1], WHAM [2], SPBT [3].

Some research groups prefer using fresh natural samples to infer NOM behavior to stay as close as possible to environmental conditions. Though greatly practical and widely accepted in the community, using standardized acid/base extracted organic matter samples has been questioned in the literature [4]. This debate is rooted in the fact that extraction and isolation protocols, could generate changes in the physico-chemical properties. For instance, it has been shown that extreme alkaline conditions, necessary to solubilize NOM, increase radical species; parallelly, extreme acid conditions, necessary to separate fulvic acids (FA) from humic acids (HA) may generate hydrogen and cation bonds. Olk et al. [5] however emphasized the needs of chemical fractionations into soluble FA, HA, and insoluble organic matter (IOM) fraction for the study of organic pool dynamics and interactions to pollutants. To bridge the gap between natural and standardized samples, it is thus critical to understand the effect of the extraction protocol on the NOM physical and chemical properties. In this context, a comprehensive approach is proposed to characterize the organic fractions involved in radionuclides interaction and transport in soils (interactions with both SOM and IOM), along the classical IHSS organic matter soil extraction.

Studies comparing various soil samples with different extraction phases were previously conducted [6]. However, the variability between samples makes it difficult to relate the found conclusions regarding the physico-chemical characteristics to either the sample nature itself or to the reactions undergoing the different extraction phases. To properly assess the effect of NOM extraction protocol on both SOM and on IOM, we propose to apply IHSS isolation and extraction protocol parallelly to two environmental samples, while characterizing at each extraction step NOM physico-chemical properties. One used sample is the “bulk” Leonardite reference sample (IHSS - 1BS104L) and the second (further referred to as “Rophin” sample) a sample extracted from a site close to a uranium mine (in January 2023) in the context of the European RadoNorm project (task 2.7).

The IHSS extraction protocol yields at each step, a solid and a liquid phase which will be analyzed individually focusing on the acid-base properties of the NOM which drive NOM reactivity towards metallic ions. The liquid phase was characterized by UV-vis spectrophotometry acid-base titration as described in Janot et al. [7], by fluorescence 3D. The solid phase was studied by DRX by solid state ^{13}C NMR and ^1H NMR in line with Thorn et al. [8] work. These spectroscopic characterizations will allow to evaluate qualitatively (UV-vis spectrophotometry) and quantitatively (^{13}C NMR & ^1H NMR) the proton-binding site density, the nature of the sample (fluorescence 3D), and ultimately the purity of the NOM sample (XRD).

Each extraction phase effect on the sample was deduced by comparison of the evaluated characteristics to the previous extraction phase. This allowed to infer the “initial” reactivity of NOM prior to the extraction operation. The extraction method was validated by comparing the characteristics of purified Leonardite-1S104H humic acid (directly made available by the IHSS) with the final fraction of the extraction protocol of the same bulk Leonardite -1BS104L.

This work made it possible to evaluate the “true” reactivity of NOM; the obtained parameters will be used to evaluate the interaction of SOM and IOM with Ra and U for the case of the Rophin sample.

References

- [1] Benedetti, M. F.; et al. (1995). Metal Ion Binding to Humic Substances: Application of the Non-Ideal Competitive Adsorption Model. *Environ. Sci. Technol.*, 29 (2), 446–457.
- [2] Tipping, E. (1994). WHAMC—A Chemical Equilibrium Model and Computer Code for Waters, Sediments, and Soils Incorporating a Discrete Site/Electrostatic Model of Ion-Binding by Humic Substances. *Comput. Geosci.*, 20 (6), 973–1023.
- [3] Tesfa, M.; et al. (2022). Absolute and Relative Positioning of Natural Organic Matter Acid–Base Potentiometric Titration Curves: Implications for the Evaluation of the Density of Charged Reactive Sites. *Environ. Sci. Technol.*, 56 (14), 10494–10503.
- [4] Lehmann, J. and Kleber (2015). M. The Contentious Nature of Soil Organic Matter. *Nature*, 528 (7580), 60–68.
- [5] Olk, D. C.; et al. (2019). M. Environmental and Agricultural Relevance of Humic Fractions Extracted by Alkali from Soils and Natural Waters. *J. Environ. Qual.*, 48 (2), 217–232.
- [6] Mao, J.; et al. (2017). Advanced Solid-State NMR Spectroscopy of Natural Organic Matter. *Prog. Nucl. Magn. Reson. Spectrosc.*, 100, 17–51.
- [7] Janot, N.; et al. (2010). Using Spectrophotometric Titrations To Characterize Humic Acid Reactivity at Environmental Concentrations. *Environ. Sci. Technol.*, 44 (17), 6782–6788.
- [8] Thorn, K. A.; et al. (1989) Characterization of the International Humic Substances Society Standard and Reference Fulvic and Humic Acids by Solution State Carbon-13 (^{13}C) and Hydrogen-1 (^1H) Nuclear Magnetic Resonance Spectrometry; Geological Survey; Vol. 89–4196.

PB4-13 CHARACTERIZATION OF BOOM CLAY (BC) DISSOLVED ORGANIC MATTER (DOM) AND ITS INTERACTION WITH RADIONUCLIDES

Bouby Muriel⁽¹⁾, Thumm Aline⁽¹⁾, Lunz Alexander⁽¹⁾, Geyer Frank⁽¹⁾, Beiser Cornelia⁽¹⁾, Altmaier Marcus⁽¹⁾, Geckeis Horst⁽¹⁾, Brassines Stephane⁽²⁾

(1) *Institute for Nuclear Waste Disposal (INE), Karlsruhe Institute of Technology, P.O. Box 3640, 76021 Karlsruhe, Germany*

(2) *ONDRAF/NIRAS, Belgian Agency for Radioactive Waste and Enriched Fissile materials, Geological Disposal, R&D, Avenue des Arts 14, 1210 Brussels, Belgium*

Poorly indurated clay formations like the oligocene Boom Clay (BC) are discussed in Belgium as a potential host rock for an underground nuclear waste repository. BC contains 1 to 5% wt organic matter (OM) [1] distributed in the solid phase as well as in pore water. Radionuclides (RN) are known to interact with OM, which in turn has an impact on RN speciation and mobility [2].

The LC-OCD-UVD-OND method [3] is applied within the current study to characterize dissolved organic matter (DOM) present in BC pore water (BCPW) samples representative of different horizons of the BC formation in Mol (Belgium). Pore water samples were collected from three piezometers (i.e. SPRING, MORPHEUS (Filter -F4, -F8, -F12, -F20), and EG/BS) at the HADES underground laboratory (Mol, Belgium), transported and stored in Swagelok containers and transferred into an Ar glove box at INE laboratories. pH and Eh values of the porewater samples were at 8.5-9.5 and -154 to -240 mV, respectively, showing characteristics close those known for the in-situ conditions [4].

BC-DOM present in all BCPW samples shows similar size distributions. Acc. to LC-OCD analysis all samples contain small sized entities in a molecular weight (MW) range of < 0.1-4 kDa while the dominating size fraction is centered at 0.9 - 1 kDa (or 1.5 – 1.6 nm). Durce et al., (2015) found a cutoff for colloid mobility in BC of 20 kDa or 5-6 nm hydrodynamic diameter perpendicular to the BC bedding [5], which fits to the size ranges found for BCPW samples. Porewater from EG/BS and Morpheus F8 shows a shoulder in UV-chromatograms towards somewhat larger sizes, which might be due to the somewhat larger pores size of the silty layer of the so called “double band” structure where those samples come from. The humic/fulvic-acid like fraction represents 40 to 50 % of the total dissolved organic carbon. Relatively high specific ultraviolet absorbance (SUVA) values confirm their aromatic nature. Nitrogen is found within the entire size distribution of the BC-DOM, confirming the presence of nitrogen containing functional groups independent of size. Handling the samples under oxidizing conditions does not affect the BC-DOM size distribution [6].

Coupling LC-OCD-UVD-OND with ICP-MS provides some information on the chemical state of naturally abundant trace metal ions in BC-DOM. Metal ions in BCPW can be assigned to 1) ionic species like aquo or carbonate complexes, 2) species associated with small sized humic/fulvic acid type OM or 3) embedded in larger sized colloidal fractions. Interestingly, we could clearly identify the presence of iron oxy/hydroxide nanoparticles (NPs). They contain part of the naturally abundant lanthanides and actinides (U, Th) and some transition metals, emphasizing the importance of such colloids for the speciation of polyvalent metal ions. At present it is unclear, whether those NPs are generated during sample transport and handling in the lab due to Fe(II) oxidation (despite working under Ar atmosphere conditions) or whether they exist already in the samples collected from the piezometers. Further study will focus on the role of Fe in the BCPW.

Recently, the BC-DOM interaction with the elements Nb and Pa has been examined by SEC/LC-UVD-ICPMS for the BCPW SPRING and EG/BS. Both, Nb and Pa, appear to be associated to DOM in the BCPW only to a minor extent.

Nb exists in BCPW mainly as hydroxo/carbonato complex and partly bound to iron oxy/hydroxide NPs.

Pa added to BCPW could not be detected in the outflow of the SEC column suggesting that Pa-species strongly sorb to the column matrix despite the presence of DOM. Increasing the Pa concentration above assumed solubility limit results in the elution of larger sized species (> 30 kDa), possibly consisting of Pa-oxyhydroxide nanoparticles or polymeric species.

Acknowledgement: *We are grateful to ONDRAF/NIRAS for funding these studies under contract n° CCHO 2015-0707/01/00.*

References

- [1] Bruggeman, C. and M. De Craen (2012). Boom clay natural organic matter. Status report 2011, SCK.CEN-ER206, External report.
- [2] Maes, N., Bruggeman, C., Govaerts, J., Martens, E., Salah, S. and Van Gompel, M. (2011). A consistent phenomenological model for natural organic matter linked migration of Tc(IV), Cm(III), Np(IV), Pu(III/IV) and Pa(V) in the Boom Clay. *Phys. Chem. Earth* **36**(17-18): 1590-1599.
- [3] Huber, S. A., Balz, A., Abert, M., and Pronk, W. (2011). Characterisation of aquatic humic and non-humic matter with size-exclusion chromatography - organic carbon detection - organic nitrogen detection (LC-OCD-OND). *Wat. Res.* **45**(2): 879-885.
- [4] De Craen, M., L. Wang, L., van Geet, M. and Moors, H. (2004). Geochemistry of Boom Clay pore water at the Mol site. Scientific report, SCK-CEN. SCK.CEN-BLG-990.
- [5] Durce, D., Bruggeman, C., Maes, N., Van Ravestyn, L. and Brabants, G. (2015). Partitioning of organic matter in Boom Clay: Leachable vs mobile organic matter. *App. Geochem.* **63**: 169-181.
- [6] Thumm, A. (2020). Characterization of nanovectors for radionuclides and trace elements in surface and clay porewater samples. Master thesis report, KIT Faculty of Chemistry and Biosciences.

PB5-6 PLUTONIUM TRANSPORT IN VADOSE ZONE SEDIMENTS UNDER ACIDIC SOLUTION CONDITIONS AT THE HANFORD SITE, USA

Teresa Baumer⁽¹⁾, Mavrik Zavarin⁽¹⁾, Carolyn Pearce⁽²⁾, Hilary P. Emerson⁽²⁾, Annie B. Kersting⁽¹⁾

(1) *Glenn T. Seaborg Institute, Physical & Life Sciences Directorate, Lawrence Livermore National Laboratory, Livermore, CA 94550, USA*

(2) *Energy and Environment Directorate, Pacific Northwest National Laboratory, Richland, WA 99352, USA*

Between 1955 and 1962 over 4 million liters of acidic processing waste, containing an estimated 40-150 kg of plutonium (Pu), were released into the sediments of the 216-Z-9 (Z-9) trench at the Hanford Site, USA. The waste was characterized as having a high ionic strength (~ 5 M nitrate), low pH (~pH 2.5), and contained organic processing solvents including tributyl phosphate (TBP). The majority of the Pu precipitated in the first several centimeters beneath the unlined Z-9 trench, but a small fraction was detected in the vadose zone at depths up to 37 m.¹ Previous research has shown that the Pu and TBP are detected concurrently in the subsurface in the sediments with the lowest pHs¹; however, the mechanisms controlling past and future Pu mobility beneath the trench are unknown.

In an effort to better understand Pu migration below the Z-9 trench, we undertook a series of bench-scale saturated column experiments using uncontaminated Hanford sediments. We injected Pu into the sediments in a range of high nitrate, acidic solution compositions with and without TBP in dodecane. We designed two types of experiments to investigate, 1) Pu mobility in low pH aqueous fluids, and 2) Pu mobility with mixed aqueous organic fluids. The effluent was analyzed for Pu, changes in pH, and solution chemistry, and the data compared and modeled. Our results show that Pu does not become mobile until the pH of the sediments is reduced below pH 4. In low pH aqueous fluids, significant Pu mobility (14% total Pu breakthrough) is not observed until pH < 2. Pu in organic TBP-containing solvents is highly mobile in sediments that have been treated with high nitrate low pH acidic fluids (pH below 4). Pu can travel with these organic solvents virtually uninhibited with 94.8% and 86.8% total Pu breakthrough observed at pH 1 and pH 3 respectively. The results of this study show that Pu migration is likely driven by weak sorption of aqueous Pu under low pH conditions as well as the formation of Pu-TBP-nitrate complexes in the organic phase at pH < 4. Pu migration in the subsurface will be limited by the natural buffering capacity of the sediments as well as the dispersal of the nitrate plume.

Acknowledgement: *This work performed under the auspices of the U.S. Department of Energy by Lawrence Livermore National Laboratory under Contract DE-AC52-07NA27344. LLNL-ABS-845560*

Reference

[1] Cantrell, K. J.; Riley, R. G. (2008) A review of subsurface behavior of plutonium and americium at the 200-PW-1/3/6 operable units.

PB5-7 STUDY OF THE MIGRATION BEHAVIOUR OF ANTHROPOGENIC ACTINIDES IN LAKE SEDIMENTS AND PEAT BOG CORES

Janis Wolf^(1,2), Stephan Glatzel⁽³⁾, Robin Golser⁽¹⁾, Andreas Maier⁽³⁾, Maria Meszar⁽⁴⁾, Peter Steier⁽¹⁾, Michael Strasser⁽⁵⁾, Michael Wagreich⁽⁴⁾, Andreas Wiederin⁽¹⁾ and Karin Hain⁽¹⁾

(1) University of Vienna, Faculty of Physics, Austria

(2) Helmholtz-Zentrum Dresden-Rossendorf, Germany

(3) University of Vienna, Department of Geography and Regional Research, Austria

(4) University of Vienna, Department of Geology, Austria

(5) University of Innsbruck, Department of Geology, Austria

Accelerator Mass Spectrometry (AMS) enables the measurement of ultra-low abundances of long-lived radionuclides with very high sensitivity. Especially anthropogenically produced actinides, e.g. ^{233}U , ^{236}U , ^{237}Np , ^{239}Pu , ^{240}Pu and ^{241}Am , can be detected in a variety of environmental reservoirs.

Atmospheric nuclear weapons testing in the mid-20th century is the most important source of anthropogenic radionuclides in the environment on a global scale [1]. In that way, minor actinides, especially U, Pu and Np, which are naturally rare, were released into the atmosphere. The subsequent global fallout distributed these actinides globally, and deposited them on the earth's surface. This synchronous input of actinides is used to study the distribution and migration of actinides in a multitude of different environmental reservoirs under real environmental conditions [2].

In this presentation, the distribution of multiple actinides in three different environmental archives and the inferred post-depositional migration will be discussed. These include urban sediments (Vienna, Austria), lake sediments (Lake Hallstatt, Austria) and a peat bog (Pürgschachen Bog, Austria). The urban and lake sediments have been event-dated, which allows to directly compare the age of the layer in which the maximum actinide concentration can be found to the year of maximum deposition from the global fallout, 1963.

In the lake sediment core, we detected the maximum concentration of ^{239}Pu and ^{240}Pu in layers older than the year of maximum deposition, which indicates a post-depositional downward-migration of Pu. While the highest ratio of $^{236}\text{U}/^{238}\text{U}$ was found in the year of the maximum deposition, the ratio $^{233}\text{U}/^{238}\text{U}$ reaches its maximum in the earliest years of the weapons test. This shift has been previously observed by Hain et al. (2020) [3] in a peat core from the Black Forest, Germany and Lin et al. (2021) [4] in sediment cores of the Baltic sea. A ^{137}Cs profile, measured in a Lake Hallstatt sediment core, shows two peaks, corresponding to the Chernobyl accident in 1986 and the global nuclear weapons fallout [5]. No increase of the actinide concentration due to the Chernobyl accident could be observed in the lake sediment core.

The Pürgschachen Bog is an ombrotrophic peat bog, which characteristically provides an anoxic and strongly reducing environment in deeper layers. These unique conditions may have lead to a different speciation of the actinides than in other reservoirs. The age of the layers of the analyzed peat bog core have been estimated using ^{210}Pb data. The obtained depth profiles of the different actinides are compared with each other. Two peaks of ^{239}Pu and ^{240}Pu are observed. This differs from the Pu profile observed in the sediments and other peat cores, for example a peat core from the Wildseemoor, which shows a single Pu peak [6]. The $^{233}\text{U}/^{236}\text{U}$ ratio consistently shows the same behavior as in the other reservoirs, with the highest values in the samples corresponding to the time of the earliest testing phase and a decrease towards younger layers.

In the last century, Karlsplatz, a public square in the center of the city of Vienna, has been remodeled multiple times. This produced several layers of anthropogenic sediment, corresponding to distinct times

in the history of the city. The layers include rubble from the Second World War, the foundation of buildings, artificial park ground, and backfilled soil material [7]. This first-time detection of actinides in such heterogeneous, anthropogenic materials underlines the unprecedented sensitivity of AMS and offers insight into the distribution of actinides in urban environments. While the concentration of all measured actinides, was the highest in the uppermost part of the rubble, which had been exposed during the height of the global-fallout, the isotopic uranium ratio $^{233}\text{U}/^{236}\text{U}$ has its maximum in the rubble from the Second World War, which was exposed to the nuclear weapons fallout only during the earliest testing phase.

In general, little migration of the U isotopes ^{233}U and ^{236}U has been observed in the different environmental reservoirs, but all reservoirs show an increase of the $^{233}\text{U}/^{236}\text{U}$ ratio in the samples towards older ages, which indicates unidentified sources that released considerable amounts of ^{233}U in the earliest years of the global fallout. Provided this distribution can be confirmed in future measurements, this characteristic would make the $^{233}\text{U}/^{236}\text{U}$ ratio a unique fingerprint for the onset of atmospheric weapons testing. The Pu isotopes show downward migration in the lake sediment core, and two separate peaks in the peat core. The source of the Pu can be determined using the $^{241}\text{Pu}/^{239}\text{Pu}$ ratio, which is source sensitive.

References

- [1] UNSCEAR (2000). Sources and effects of ionizing radiation. United Nations Publications, vol. I (annex C).
- [2] Hain, K., et al. (2023) Radionuclide Distributions in (time-resolved) Natural Archives Determined by AMS, this conference.
- [3] Hain, K., Steier, P., Froehlich, M. B., et al. (2020). $^{233}\text{U}/^{236}\text{U}$ Signature Allows to Distinguish Environmental Emissions of Civil Nuclear Industry From Weapons Fallout. *Nat. Commun.* 11:1275.
- [4] Lin, M., Qiao, J., Hou, X., et al. (2021). 70-Year Anthropogenic Uranium Imprints of Nuclear Activities in Baltic Sea Sediments. *Environ. Sci. Technol.* 55(13):8918-8927.
- [5] Strasser, M., Berberich, T., Fabbri, S., et al. (2019). Geomorphology and Event-Stratigraphy of Recent Mass-Movement Processes in Lake Hallstatt (UNESCO World Heritage Cultural Landscape, Austria). *Geol. Soc. Spec. Publ.*, 500.
- [6] Quinto, F., Hrnccek, E., Krachler, M., et al. (2013). Measurements of ^{236}U in Ancient and Modern Peat Samples and Implications for Postdepositional Migration of Fallout Radionuclides. *Environ. Sci. Technol.*, 47(10):5243-5250.
- [7] Wagreich, M., Meszar, M., Lappé, K., et al. (2022). The Urban Sediments of Karlsplatz, Vienna (Austria) as a Candidate Auxiliary Boundary Stratotype Section and Point for the Anthropocene Series. *Anthr. Rev.*, 0(0).

PB5-8 FULL-SCALE PROTOTYPE, A LONG-TERM EXPERIMENT AT ÄSPÖ LABORATORY, SWEDEN.

T. Morales Aguilera⁽¹⁾, J. Dahlström⁽¹⁾, S. Pontér⁽¹⁾, L. Alakangas⁽¹⁾, M. Kronberg⁽¹⁾

(1) Swedish Nuclear Fuel and Waste management Company, Sweden.

The spent nuclear waste in Sweden is planned to be disposed a repository system consisting of several technical barriers in deep crystalline bedrock at about 400-500 meters depth. The prototype experiment at Äspö (at about 450 meters depth) is a full-scale experiment simulating a repository of KBS-3 type. The experiment originally consisted of six deposition holes with copper canisters, bentonite buffer, backfill and plug (Figure 1). The canisters were equipped with heaters to simulate the decay-heat of spent nuclear fuel.

After ~10 years of operation the outer section was dismantled (Section 2). The outer section of the prototype repository has provided experience in all from constructing a full-scale repository system, in continuously monitoring the repository environment under relevant conditions and analysing samples from the different materials. Now the dismantling of the inner section (Section 1) is on-going, this work was preceded by a pre-modelling which provided input to the dismantling, sampling and analysis.

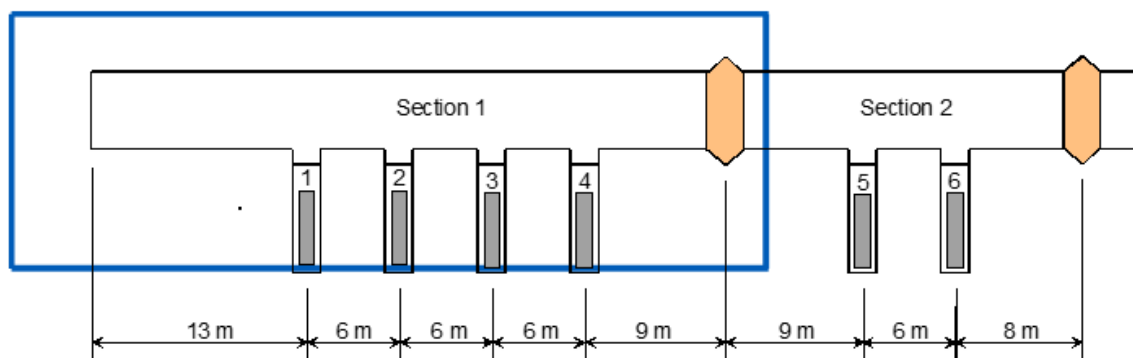


Figure 1. Sketch of the Prototype repository with canisters (gray) in vertical deposition holes surrounded by bentonite buffer. The horizontal deposition TBM-tunnel is backfilled with a mixture (30/70) of bentonite and TBM muck. Concrete plugs (orange) are placed at the end of each section.

Hydro-geochemical-mechanical interaction during elevated thermal conditions has been studied through continuous monitoring and sampling the surrounding conditions. The groundwater sampling campaign before dismantling (autumn 2022), was initially planned for sampling 41 borehole sections and resulted in the sampling of 20 sections (i.e. 14 bore holes) giving enough groundwater for the analysis of complete set of chemical analysis (SKB standard program) and additional gases (H_2 , CO_2 , CO , CH_4 , C_2H_4 , C_2H_6 , O_2 , He , N_2). The groundwater sampling yielded > 8000 L (including turn-over volumes). Observation of the rock surrounding the deposition holes due to hydraulic flow, pressure changes and thermal effects will be performed after excavating each deposition hole.

Porewaters are sensitive to the state of gas-hydraulic pressures which may affect solubility and redox conditions. In these clay-rich systems, porewater are not easily extracted. This will be further studied using installed titanium sampling cups containing in-diffused small volumes of water. In total nineteen of these titanium porewater collecting cups has been installed, fourteen in the bentonite buffer and five in the back-fill. Figure 2 shows the two different types of porewater titanium cups. Moreover, two of the cups in the buffer and five in the back-fill are connected with PEEK tubing connected and lead to an adjacent tunnel where in-situ samples of pore water have been collected using high-vacuum, stainless steel, pressure vessels.

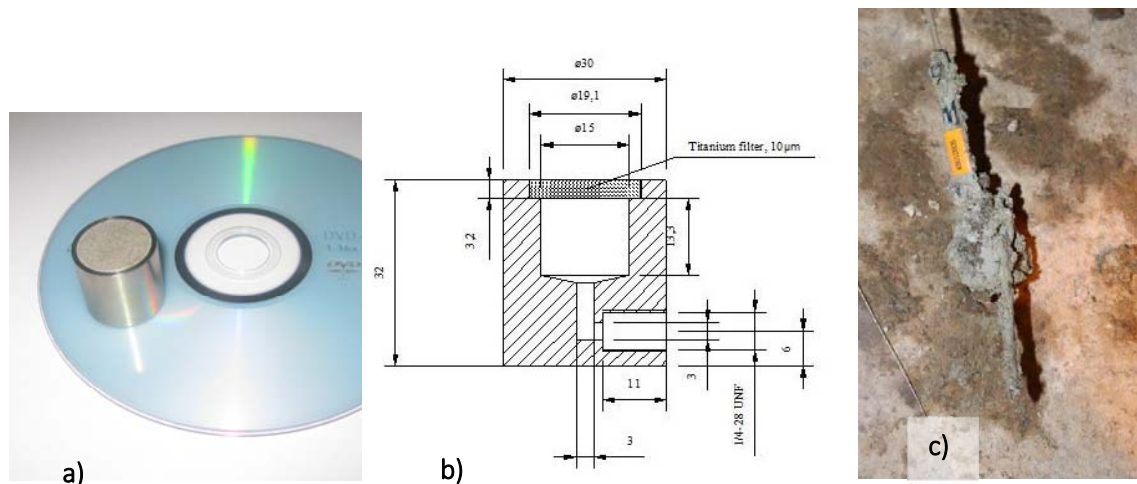


Figure 2. Prototype Titanium cups of a) “passive” type; b) “sampling” type; c) one retrieved titanium cup.

One challenge is to sample enough volumes of porewater to perform redox-sensitive analysis including anions, and gases. Retrieved material need to be sampled and stored under anaerobic and low-temperature conditions. Modelling the chemical evolution of buffer-influenced porewater may give valuable information in mineral interaction acquired through porewater analysis.

Sampling of gases, dissolved organic compounds, mineralogy, iron-sulphur and carbon components have been performed during several sampling campaigns [1]. Iron-reducing bacteria (IRB), Sulphate-reducing bacteria (SRB) and thermophilic anaerobic bacteria have previously been found through cultivation, even if bacteria are shown to be undetectable in most of the samples. Other biomolecular methods are searched for and might be applied.

Preliminary results of the gas analysis indicate similar conditions through time (unpublished results) whiles the extracted porewater chemistry indicates increased or elevated concentration with time and needs to be further elaborated upon to give any conclusive remarks. In addition, data needs to be compared with information from the leaching of the surrounding materials of the titanium cups, along with surrounding groundwater gas- and elemental composition.

All activities within the rock domain is connected through the water phase hence both groundwater and porewater in buffer and backfill is sampled and will be analysed, especially the interface between the engineering barriers, the rock and the plug. When initiating the dismantling, hydro monitoring has been used to follow-up surrounding groundwater pressures whiles sampling. The dismantling of the inner section will give large amounts of material, alongside all the installed technical monitoring equipment, that will be needed to be cautiously retrieved and analysed. Further analysis of gases, through on-line equipment may be applied if possible and sampling for future analysis of biomolecular compounds will be performed.

Reference

- [1] Lydmark, S. (2011). Analysis of microorganisms, gases and water chemistry in buffer and backfill, 2010. Prototype repository, Äspö Hard Rock Laboratory, SKB P-11-16, Swedish Nuclear Fuel and waste management company, Sweden.

PB5-9 URANIUM SPECIATION IN SOILS AND SEDIMENTS IMPACTED BY ACIDIC RUNOFF ORIGINATING FROM ALUM SHALE WASTE ROCKMila K. Pelkonen ⁽¹⁾, Estela Reinoso-Maset ⁽¹⁾*(1) Faculty of Environmental Sciences and Natural Resource Management (MINA), Norwegian University of Life Sciences (NMBU), Norway*

Construction and mining often lead to the accumulation of large volumes of crushed rock waste that may release hazardous elements into the environment, especially if the rock contains acid generating minerals. For example, in Norway, alum shale debris has been used as grading material in farming, leading to acid rock drainage. Alum shale is a type of black shale (sedimentary mudrock) formed under reducing conditions that contains silicates, carbonates, sulfide phases, and organic matter, and is often enriched in elements of environmental concern. When exposed to air and water, sulfide oxidation generates sulfuric acid, which dissolves other minerals and leads to a release of contaminant rich acidic drainage from the rock masses, usually including U. In this work, we have studied the biogeochemical interactions of U at a non-remediated, legacy site 25 km southeast of Oslo (Norway), where ca. 50,000 m³ of crushed acid producing alum shale rocks were disposed of in the 1980s. Since then, this rock waste has released acid runoff containing potentially harmful elements. As a mitigating strategy, a precipitation pond was constructed in the 2000s to contain and reduce migration of contaminants to the near stream that feeds a drinking water reservoir.

Our 2022 field measurements showed rather acidic pond waters and sediments and slightly buffered soils between the pond and stream. Laboratory analyses showed high concentrations of mobile U species in surface waters and, yet, U is strongly retained in soils and sediments adjacent to the source materials with total concentrations breaching legal limits for radioactive waste (1 Bq/g). The total U, Fe and Mn concentrations vary with depth and so does the phase association of U. Preliminary solid phase speciation analysis by X-ray absorption spectroscopy on core samples (collected preserving the native redox conditions) showed that U(VI) predominates in soils and upper sediment layers, where it probably occurs as sorbed species to clay minerals, Fe/Mn hydrated oxides and organic matter, whereas U(IV) dominates at the deeper sediment layers, where anoxic conditions may promote bioreduction of the mobile U(VI) species into U(IV) phases. Nevertheless, infiltration of oxic waters can induce desorption, oxidation, and solid phase dissolution, potentially leading to U remobilisation.

The aim of this work was hence to determine the solid phase speciation of U in order to understand the mechanisms governing retention at the site and the potential effect on release upon contact with surface waters under different environmental and remediation scenarios. The presented results will be of interest for predictions on long-term fate of U, remediation strategies, and biosphere safety assessments for sites impacted by shale runoffs as well as those by acidic waste discharges from nuclear fuel cycle operations, i.e., sites where the migration of U into water bodies can represent an environmental risk.

PB5-10 PLUTONIUM AND CS-137 MOBILITY IN AN EPHEMERAL STREAM BED AT NEVADA NATIONAL SECURITY SITE (NNSS), USA

Naomi L. Wasserman⁽¹⁾, Jordan Stanberry⁽²⁾, Annie B. Kersting⁽¹⁾, Mavrik Zavarin⁽¹⁾

(1) Seaborg Institute, Lawrence Livermore National Laboratory, USA

(2) University of Central Florida, USA

While many studies have examined radionuclide mobility on short spatial and temporal scales, few address the long-term fate of radioactive isotopes in watersheds. Here, we examine plutonium and cesium-137 (Cs-137) distribution in sediments within a network of ponds associated with the U12e tunnel (Figure 1) at the Nevada National Security Site (NNSS). The E-Tunnel ponds comprise an ephemeral stream bed that receives groundwater discharge from the U12e tunnel complex, where several underground nuclear tests were conducted from 1958 through 1977. The pond sediments, which are only a few feet thick at most, provide a barrier for radionuclide transport to the underlying highly transmissive fractured dolomite which contains the regional aquifer. U12e groundwater was directed into the most upstream ponds beginning in the 1960's and has been redirected into additional downstream ponds every several years.

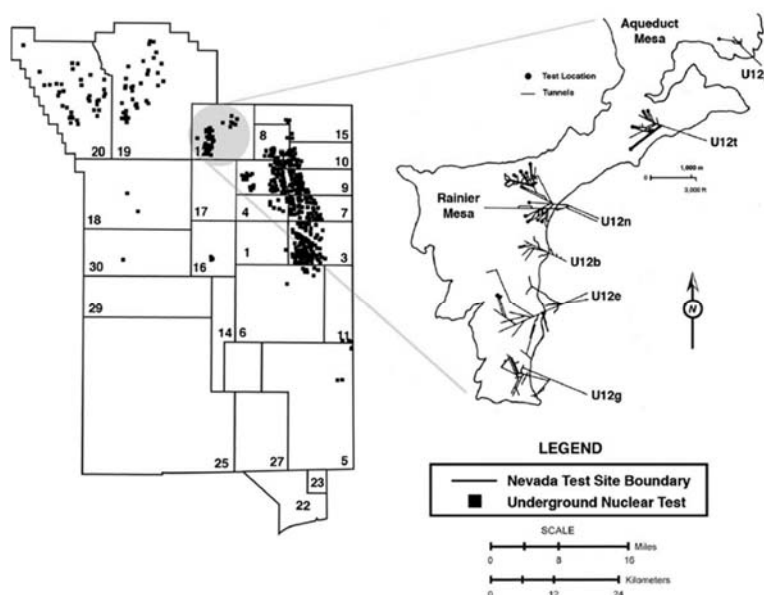


Figure 1. Location of U12e tunnel at the Nevada National Security Site (formerly the Nevada Test Site).

Little is known about the contaminant distribution or what biogeochemical and mineralogical processes impact their mobility in the E-Tunnel ponds. For example, plutonium may be complexed with organic matter derived from plant growth where water is entering the pond, as has been noted extensively in previous studies [e.g. 1]. Cs-137, meanwhile, has a lower affinity to organic complexants and may be concentrated instead on clay minerals and zeolites [2]. Effects of aging on pond sediments may also result in increasing recalcitrance of radionuclides [3]. Several sediment cores sampled in April 2022 (Figure 2) were sectioned and analyzed for Cs-137 activity, plutonium concentrations and isotope abundances, mineralogy, and organic carbon characterization. Our results indicate that both Cs-137 and plutonium accumulate in shallow sediments, but colloid-facilitated transport may facilitate the transport of radionuclides further down core in older ponds. In addition, higher abundance of vegetation and total organic carbon in the sediments seems to correlate with greater plutonium accumulation. The differences in contamination history, vegetation abundance, and mineralogical abundances allow us to examine the influences of these factors on plutonium and Cs-137 mobility on the decadal scale.



Figure 2. Example of cores collected from the E-tunnel ponds at the Nevada National Security Site.

References

- [1] Santschi, P., Xu, C., Zhang, S., Schwehr, K.A., Grandbois, R., Kaplan, D.I., Yeager, C.M. 2017. Iodine and plutonium association with natural organic matter: A review of recent advances, *Applied Geochemistry*, 85: 121-127.
- [2] Durrant, C., Begg, J.D., Kersting, A.B., Zavarin, M. 2018. Cesium sorption reversibility and kinetics on illite, montmorillonite, and kaolinite, *Science of The Total Environment*, 610–611: 511-520.
- [3] Lin, P., Xu, C., Kaplan, D., Chen, H., Yeager, C., Xing, W., Sun, L., Schwehr, K.A., Yamazaki, H., Saito-Kokubu, Y., Hatcher, P., Santschi, P. 2019. Nagasaki sediments reveal that long-term fate of plutonium is controlled by select organic matter moieties, *Science of The Total Environment*, 678: 409-418.

PB6-3 HYDRO-GEOPHYSICAL APPROACH TO UNDERSTAND THE DEPOSITIONAL AND GEOCHEMICAL CHARACTERISTICS OF THE URANIUM DEPOSITS IN THE OKCHEON METAMORPHIC BELT, KOREA

Seong-Sun Lee⁽¹⁾, Dongbok Shin⁽²⁾, Sung-Wook Jeon⁽³⁾, Min Sub Sim⁽¹⁾, Min-Hoon Baik⁽⁴⁾, Ji-Hun Ryu⁽⁴⁾, Youngchul Yu⁽⁵⁾, Kang-Kun Lee⁽¹⁾

(1) School of Earth and Environmental Sciences, Seoul National University, Republic of Korea

(2) Department of Geoenvironmental Sciences, Kongju National University, Republic of Korea

(3) Department of Earth and Environmental Sciences & The Earth Environmental System Research Center, Jeonbuk National University, Republic of Korea

(4) Korea Atomic Energy Research Institute, Republic of Korea

(5) KOTAM, Republic of Korea

The issue of the long-term safety of deep underground disposal related to the treatment of high-level radioactive wastes has been continuously raised. For the stable management and operation of a deep underground disposal facility, it is an important task to understand and evaluate the behavior of uranium. This study was proposed as part of the natural analogue study dealing with the long-term behaviors of radioactive elements in natural conditions. This study carried out hydro-geophysical analysis to obtain the depositional and hydro-geochemical characteristic data from the study site (Hoenam uranium deposit, Boeun) located in the Ogcheon Metamorphic Belt with high uranium contents in Korea. Especially, because the study area exists in the vicinity of Daecheongho Lake, the interactions between groundwater and surface water induced by the behavior of groundwater in the uranium-containing aquifer can be considered. Firstly, various hydraulic tests such as pumping test, slug test, and step-drawdown tests were carried out to collect the hydrogeological information about the study site. From the results of hydraulic test, it is identified that the study site has preferential connectivity through fractured zone between monitoring boreholes. Electrical Resistivity (ER) survey designed to obtain the data of geological formation and uranium ores and performed on land and lake. The results of ER survey show the anomaly with low resistivity which indicates fractured zone in the coal seam. In the case of geophysical logging conducted for identifying the character, relation, and orientation of lithologic and structural planar features for fractured-rock aquifers, Acoustic televiewer (ATV) survey was applied to characterize fractures and lithology penetrated by boreholes. Also, multi-item water quality, fluid resistivity, and flowmeter logs along the vertical borehole depth were performed to define which fractures identified on the ATV images are transmissive. Natural gamma and resistivity logs are also applied to interpret the image logs to assist characterize lithology and water quality of the study site. From results of total natural gamma ray and resistivity logs, four fractured uranium ore zone with low resistivity value in the coal seam were identified. Through the results of geophysical logging, existence and location of uranium ore and fractured zone were identified. These results were investigated to be in good agreement with the results of the ER survey and spectral gamma ray (SGR) log.

Generally, the presence of natural isotopes such as potassium (^{40}K), uranium (^{238}U , ^{234}U , ^{235}U) and thorium (^{232}Th) and the products of their decay induce the natural radioactivity of rocks. Natural radioactivity can be measured by geophysical surveys. Among various surveys, SGR has the ability to distinguish gamma emissions from K, U and Th. Especially, SGR logging can interpret determination of radiogenic heat value secreted during the decay of radioactive elements and the characteristics of sedimentary conditions, identification of fissure zones. In this study, SGR logging in the BH-1 borehole was performed. Information on the K, U and Th concentrations obtained from SGR survey is used to analyze the sedimentary conditions and to identify the mineral composition of studied deposits. The ratio between Th/U obtained from the SGR survey indicates sedimentary conditions related to marine sediments, reducing conditions, marine black shales, and shale. Also, the ratio of U/K shows high values at specific depths (20 m and 55m from the surface). This result indicates the condition containing high organic matter content. From the results of the SGR survey, the rock formations around the BH-1 borehole appear to have been deposited in an anaerobic sedimentation environment. In particular, it is

estimated that there was less oxygen inflow and abundant organic matter at depths of 20 m and 55 m (especially around 55m) where uranium is intensively distributed. There is a possibility that this environment was accompanied by submarine volcanic activity, not just sedimentation. These hydro-geophysical outcomes were well matched with the results for the physicochemical occurrence and evolution environments of uranium deposits analyzed in the study site.

The results of this study can be provided as a momentous data necessary for developing an occurrence model and investigating the evolution environments of uranium deposits in the Ogcheon Metamorphic Belt, Korea. Also, it will be helpful to construct safety cases of deep geological disposal for high-level radioactive waste including spent nuclear fuel.

Acknowledgments: *This work was supported by the National Research Foundation of Korea (NRF) grant funded by the Korea government (MSIP) (NRF-2021M2E1A1099413).*

PC1-6 THE PSI CHEMICAL THERMODYNAMIC DATABASE TDB 2020 TO SUPPORT NAGRA SAFETY ASSESSMENTS FOR DEEP GEOLOGICAL REPOSITORY

G. Dan Miron⁽¹⁾, Dmitrii A. Kulik⁽¹⁾, Raphael Wüst⁽²⁾

(1) Paul Scherrer Institute, Laboratory for Waste Management, 5232 Villigen PSI, Switzerland

(2) National Cooperative for the Disposal of Radioactive Waste (Nagra), 5430 Wettingen, Switzerland

A high-quality, internally consistent, up-to-date Thermodynamic Data Base (TDB) is an essential prerequisite for assessing the transport and retention of dose-relevant radionuclides and modeling the geochemical evolution of engineered and natural barriers of deep geological repositories. Hence, the chemical thermodynamic database TDB 2020 has been developed by the Paul Scherrer Institute (PSI) for the National Cooperative for the Disposal of Radioactive Waste (Nagra) in Switzerland as the successor of four previous versions [1-5].

TDB 2020 contains thermodynamic data for a wide range of chemical elements and compounds for all dose-relevant radionuclides to be considered for RGB, for some important chemotoxic elements, as well as a complete dataset for the related pore water models (Figure 1). The selected thermodynamic data for chemical species (mainly equilibrium constants of the formation reactions from “master” species) refer to unimolar/molal standard states and reference conditions, i.e. infinite dilution (zero ionic strength $I = 0$) for aqueous species. Experimental data have been extrapolated to $I = 0$ using the Brønsted-Guggenheim-Scatchard activity model [6], also called Specific Ion Interaction Theory (SIT) model. The present version of the database contains mainly the data at 25 °C, and is currently used for calculations at ambient temperature (25 °C) and pressure (1 bar). For elements Li, Na, K, Mg, Ca, Sr, Ba, Ra, Mn, Al, a complete set of reaction enthalpy values (and sometimes also reaction heat capacities) is available for compounds and complexes involving OH^- , F^- , HCO_3^- , CO_3^{2-} , SO_4^{2-} .

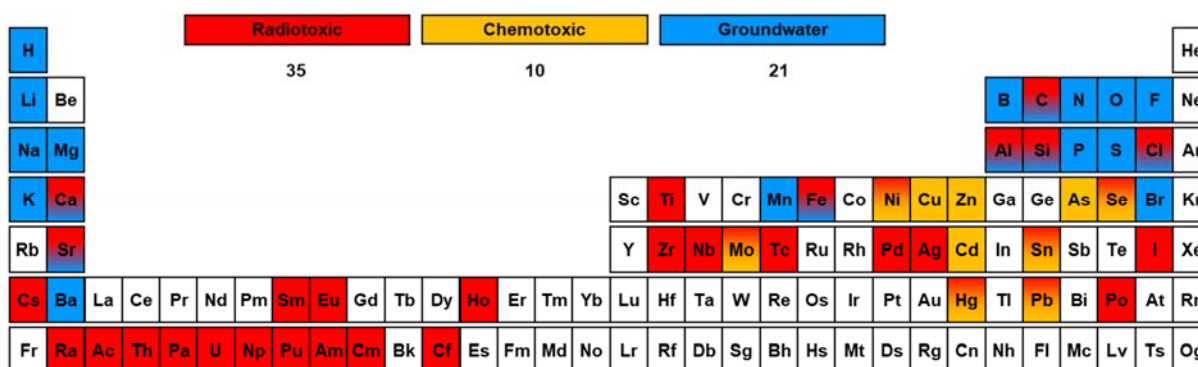


Figure 1. Chemical elements considered in the PSI Chemical Thermodynamic database 2020. TDB 2020 includes thermodynamic data for: 53 elements, 1034 aqueous species (and SIT ion interaction coefficients for all species), 358 solids, and 8 gases.

TDB 2020 has been regularly updated with data and extensions to ensure its accuracy and reliability. A recent review work was carried out in 2017 – 2020 by Wolfgang Hummel and Tres Thoenen [5]. This included review data for the elements Ac, Ag, Cd, Cf, Cu, Hg, Ho, Pa, Pb, Po, Sm, Ti and Zn, and updates for Al, alkali (Li, Na, K) and alkaline earth elements (Mg, Ca, Sr, Ba), Eu, Fe, Mn, Mo, Nb, organic ligands, Pd, Ra, S, Se, silicates and Sn, as well as updates from NEA TDB for U, Np, Po, Am and Tc [7].

Using the innovative ThermoHub database and the ThermoMatch code tool with its import/export scripts (<https://thermohub.org/thermomatch>), the TDB 2020 database has been made provisionally available for the popular GEM-Selektor [8] and Phreeqc [9] geochemical modeling tools.

TDB 2020 has been used for defining pore water models, for calculating solubility limits of radionuclides in the normative clayrock, bentonite and concrete pore water, and for updating the sorption and diffusion databases for ambient conditions (25 °C and 1 bar). Future work is foreseen to extend the database with more thermochemical data and methods to account for temperature effects and with molar volumes for solids and major aqueous species needed to account for porosity changes in reactive transport simulations. This will result in a GEMS TDB 2020 variant to be used and distributed with Gibbs Energy Minimization Software (GEMS, <https://gems.web.psi.ch>), and help PSI-Nagra TDB to retain its position and competitiveness with respect to other TDBs maintained by several European organizations.

References

- [1] Pearson, F.J. and U. Berner (1991). Nagra Thermochemical Data Base I. Core Data. Nagra Technical Report NTB 91-17, Nagra, Wettingen, Switzerland, 70 pp.
- [2] Pearson, F.J., and U. Berner, W. Hummel, W. (1992). Nagra Thermochemical Data Base II. Supplemental Data 05/92. Nagra Technical Report NTB 91-18, Nagra, Wettingen, Switzerland, 284 pp.
- [3] Hummel, W., and U. Berner, E. Curti, F.J. Pearson, T. Thoenen (2002): Nagra/PSI Chemical Thermodynamic Data Base 01/01. Nagra Technical Report NTB 02-16, Nagra, Wettingen, Switzerland, and Universal Publishers, Parkland, Florida, 565 pp.
- [4] Thoenen, T., and W. Hummel, U. Berner, E. Curti (2014). The PSI/Nagra Chemical Thermodynamic Database 12/07. Technical Report, PSI Bericht Nr. 14-04, Paul Scherrer Institut, Villigen, Switzerland, 416 pp.
- [5] Hummel, W., and T. Thoenen (2022). The PSI Chemical Thermodynamic Database 2020. Nagra NTB 21-03.
- [6] Grenthe I., and I. Puigdomenech (eds) (1997) Modelling in aquatic chemistry, Chapter IX, NEA OECD, Paris.
- [7] Grenthe, I., and X. Gaona, A.V. Plyasunov, L. Rao, W.H. Runde, B. Grambow, R.J.M. Konings, A.L. Smith, E.E. Moore (2020). Second Update on the Chemical Thermodynamics of Uranium, Neptunium, Plutonium, Americium and Technetium. Chemical Thermodynamics, Vol. 14. OECD Publications, Paris, France, 1503 p.
- [8] Kulik, D. A., and T. Wagner, S.V. Dmytrieva, G. Kosakowski, F.F. Hingerl, K.V. Chudnenko, U.R. Berner (2013). GEM-Selektor geochemical modeling package: Revised algorithm and GEMS3K numerical kernel for coupled simulation codes. *Computat. Geosci.*, 17(1): 1-24.
- [9] Parkhurst, D. L., and C.A.J. Appelo (2013). Description of Input and Examples for PHREEQC Version 3. U.S. Geological Survey Techniques and Methods, book 6, chapter A43, 497 p.

PC1-7 SOLUBILITY ASSESSMENT IN CRYSTALLINE AND SEDIMENTARY ROCKS

Eli Colàs (1), Olga Riba (1), Jordi Rodríguez-Mestres (1), Alba Valls (1), David García (1), Tammy Yang (2), Lara Duro (1).

(1) *Amphos 21, c/ Venezuela, 103, 2, 08019 Barcelona, Spain*

(2) *NWMO, 22 St. Clair Ave. East, Toronto, Ontario M4T 2S3, Canada*

The assessment of the solubility limits and aqueous speciation of an extensive list of radionuclides and chemical elements (Am, Ag, Bi, C, Ca, Cd, Cs, Cu, Fe, Hg, Mo, Nb, Np, Pa, Pb, Pd, Pu, Ra, Rn, Ru, S, Sb, Se, Sn, Sr, Tc, Th, U and Zr) [1,2] is required to support the preparation of the safety case for a deep geological repository (DGR) in Canada. Both crystalline and sedimentary rocks are currently being considered as hosting rock for a DGR for used nuclear fuel waste. The groundwaters in Canadian crystalline rock have low ionic strength ($I < 0.5$ m) at the repository depth, whilst high ionic strength groundwaters (~ 7 m) have been characterized in Canadian sedimentary rocks at the proposed repository depth. The solubility and speciation assessment is done for both crystalline and sedimentary reference groundwaters, considering the effect of temperature as well as the interaction with the bentonite buffer and with the metallic carbon-steel container.

The different groundwater compositions of crystalline and sedimentary rocks require different approaches for ionic strength corrections. The Specific Ion Interaction Theory (SIT) can be used for the less concentrated solutions. For those systems (i.e., crystalline rock reference groundwater), most of the calculations have been performed using the reference thermodynamic database ThermoChimie version 10a (www.thermochimie-tdb.com) [3,4]. ThermoChimie version 10a has been complemented with thermodynamic data for Bi, Cu, Hg, Rn and Ru, selected after reviewing the available information in the scientific literature.

The Pitzer approach is preferred (when possible) for mixtures of electrolytes over 3-4 m ionic strengths as the sedimentary reference groundwater. Several high-quality and traceable thermodynamic databases based on the Pitzer approach [5-7] are available. However, none of them is complete enough to fulfil the requirements of the extensive, multi-element solubility study proposed here. Thus, the thermodynamic database DGR-Pitzer-TDB has been developed for the solubility assessment carried out in this work. The thermodynamic database builds on the Yucca Mountain Pitzer (YMP) database data0.ypf.R2 [6]. The initial YMP dataset was significantly modified, updated and expanded in order to cover all the elements and conditions of interest. The main limitation of the database is the lack of experimental data in concentrated systems for some radionuclides and the difficulty to guarantee the consistency of the whole thermodynamic data set. The approach followed to overcome these difficulties has been: i) selection of thermodynamic data for element of interest, ii) speciation and solubility calculations for different systems of interest, and iii) comparison of the calculated results with those calculated by other thermodynamic databases and with experimental data (when available). This work also includes an analysis of the uncertainties and remaining data gaps.

The selection of the solid phase most likely controlling the solubility of a given element is mainly based on the expert judgement, considering that the less crystalline phases are kinetically favored (Ostwald's rule). The maximum aqueous concentration of the element studied is then given by equilibrium with the selected solid phase and the porewater composition, and the corresponding aqueous

PC1-8 ENCHMARKING THE THERMOCHIMIE DATABASE FOR ITS APPLICATION TO CEMENTITIOUS AND ARGILLACEOUS ENVIRONMENTS

D. Jacques¹, S. Liu¹, V. Montoya¹, B. Madé², W. Bower³, S. Brassinnes⁴

(1) *Belgium Nuclear Research Centre SCK CEN, Belgium*

(2) *Agence nationale pour la gestion des déchets radioactifs (Andra), France*

(3) *Nuclear Waste Services (NWS), UK*

(4) *Belgian Agency for Radioactive Waste and Enriched Fissile Materials (ONDRAF/NIRAS), Belgium*

Engineered barrier systems in a geological disposal system contain many cementitious components. A strong geochemical interaction is expected between these repository components and the surrounding host rock, since cement is not at equilibrium under relevant disposal conditions and thus will evolve with time. Thermodynamic modelling is a useful approach to assess the geochemical evolution of these components in the long term. The information within the selected thermodynamic database and its quality (e.g., consistency, applicability) may strongly affect the simulated evolution and/or specific details of the calculations. The objective of this benchmarking study is to perform rigorous geochemical calculations of the expected evolution of a cementitious engineered barrier emplaced in an argillaceous environment and evaluate the mineralogical evolution and possible neoformation of zeolites using two different state-of-the-art thermodynamic databases: ThermoChimie V11A (<https://www.thermochimie-tdb.com/>) and CEMDATA 18.1 (Lothenbach et al. [1]). Calculations have been performed for different types of cement (i.e., CEMI, CEM II and CEM III) containing different supplementary materials (e.g., granulated blast furnace slag, silica fume). We followed a systematic approach to compare the two thermodynamic database. First the solid phase and pore water composition for the reference compositions of the different cement types were compared. Next, thermodynamic modelling of the chemical evolution of the cements in contact with single reactants (e.g., CO₂, SO₃, MgO) or argillaceous pore waters were evaluated. The analysis was done for two tiers: (i) reaction path modelling to focus on the geochemical evolution, and (ii) reactive transport models (diffusive transport conditions in cement with a constant pore water concentration boundary condition at one side) to focus on the effect of a thermodynamic databases on the assessment of degradation fronts in porous media. The main similarities and differences between the two thermodynamic models are discussed and recommendations regarding possible ways of improvement of the ThermoChimie database are formulated.

Reference

- [1] Lothenbach, B., D.A. Kulik, T. Matschei, M. Balonis, L. Baquerizo, B. Dilnesa, G.D. Miron, and R.J. Myers (2019)., Cemdata18: A chemical thermodynamic database for hydrated Portland cements and alkali-activated materials. *Cement and Concrete Research*, 15: 72-506

PC1-9 THEREDA - THERMODYNAMIC REFERENCE DATABASE

Xavier Gaona¹, Vinzenz Brendler², Daniela Freyer³, Helge Moog⁴, Laurin Wissmeier⁵

(1) Institute for Nuclear Waste Disposal, Karlsruhe Institute of Technology, Karlsruhe, Germany

(2) Helmholtz-Zentrum Dresden-Rossendorf, Institute of Resource Ecology, Dresden, Germany

(3) Institute for Inorganic Chemistry, TU Bergakademie Freiberg, Freiberg, Germany

(4) Gesellschaft für Anlagen- und Reaktorsicherheit (GRS) mbH, Braunschweig, Germany

(5) CSD Engineers AG, Aarau, Switzerland

email: xavier.gaona@kit.edu

Part of the process to ensure the safety of radioactive waste disposal is the predictive modelling of the solubility of all relevant toxic components in a complex geochemical matrix. To ensure the reliability of thermodynamic equilibrium modelling as well as to facilitate the comparison of such calculations done by different institutions it is necessary to create a mutually accepted thermodynamic reference database. To meet this demand several institutions in Germany joined efforts and created THEREDA [1].

THEREDA is a suite of programs at the base of which resides a relational databank. Special emphasis is put on thermodynamic data along with suitable Pitzer coefficients, which allow for the calculation of solubilities in highly-saline solutions. Registered users may either view single thermodynamic data and Pitzer interaction parameters or download ready-to-use parameter files for the geochemical speciation codes PHREEQC, Geochemist's Workbench, CHEMAPP, or TOUGHREACT. The dataset can also be downloaded in a generic JSON-format to allow for the import into other codes. The database can be accessed via the World Wide Web: www.thereda.de.

Prior to release, the released part of the database is subjected to many tests. Results are compared to results from earlier releases and among the different codes. This is to ensure that by additions of new and modification of existing data no adverse side effects on calculations are caused. Furthermore, the THEREDA website offers an increasing number of examples for applications, including graphical representation, which can be filtered by components of the calculated system.

Acknowledgements: *THEREDA is funded by BGE – the federal company for radioactive waste disposal.*

Reference

- [1] Moog, H. C., Bok, F., Marquardt, C. M., and Brendler, V., Disposal of Nuclear Waste in Host Rock formations featuring high-saline solutions - Implementation of a Thermodynamic Reference Database (THEREDA). *Appl. Geochem.*, 55, 72-84, 2015.

PC1-10 DIGITIZATION OF LITERATURE DATA AND SURFACE COMPLEXATION MODEL PARAMETER ESTIMATION FOR TRIVALENT AMERICIUM, CURIUM, AND EUROPIUM SORPTION

Ethan Fix¹, Fanny M. Coutelot¹, Mavrik Zavarin², Brian A. Powell^{1,3}

(1) *Department of Environmental Engineering and Earth Sciences, Clemson University, Anderson, SC 29625, USA*

(2) *The Glenn T. Seaborg Institute, Lawrence Livermore National Laboratory, Livermore, CA 94550, USA*

(3) *Department of Chemistry, Clemson University, Clemson, SC 29630, USA*

Thermodynamics are integral to understanding adsorption reactions at the solid-water interface. System conditions such as temperature, electrolyte concentration, atmospheric composition, mineral specifications, pH, and Eh, ultimately define adsorption of a species onto a solid material. Gaining a thermodynamic understanding of the conditions that affect adsorption is essential to model systems for nuclear waste repository performance assessments.¹ Surface complexation models (SCM), ion exchange models, and reactive transport models (RTM) provide the numerical framework for representing physically measured data within a laboratory setting.

These models can be used to predict and interpret adsorption processes under defined conditions which ultimately aid in the development of environmental remediation plans and the design of waste repositories.

Most contaminant transport models represent contaminant migration using empirical distribution coefficients that do not account for changing geochemical conditions. Surface Complexation Models can account for changing geochemical conditions. However, Multiple SCMs exist in the literature and each model is based on different conceptualizations of the mineral-water interface, reaction stoichiometries, and electrostatics. Such models include the CD- MUSIC model that explicitly addresses formal charges on specific surface coordination environments on surfaces, double or triple layer models (DLM and TLM respectively) that implement electrostatic interactions of different numerical forms, or non-electrostatic (NE) models that do not include any electrostatic interactions. The scope of this work is to create a database of sorption data to globally fit all data sets simultaneously and test the ability for each model to approximate the data. A community driven database that is findable, accessible, interoperable, and reusable (FAIR) would implement multiple SCM constructs for optimal prediction outputs¹.

Twelve references from literature were digitized into a dataset for the trivalent americium, curium, and europium species. Each reference contains the minerals used as the sorbent, with a total of six total mineral types which include goethite, hematite, illite, montmorillonite, quartz, and ferrihydrite. The source for each mineral of a reference was recorded, whether synthesized in lab, purchased, or collected from a specific location. System parameters were also digitized into the dataset, including reaction temperature, electrolyte concentrations and non-unified concentration units, sorbate and sorbate concentration (in mol/L), mineral parameters (concentration, surface area, site density), cation exchange capacity, and atmospheric conditions. The raw data from figures reported in a reference was digitized using GetData Graph Digitizer. Raw values for pH and adsorption, recorded in either sorbed %, logRd, Rd, Kd or percent aqueous concentration and a pH range approximately between 2 and 10, were collected and stored as x-axis and y-axis data with the corresponding reference and figure ID, with specifications for figures that contain multiple sets of data. After a reference was digitized, adsorption values from data subsets can then be optimized using PHREEQC coupled with Model- Independent Parameter Estimation and Uncertainty Analysis (PEST). SCM constants are then taken from the open-source RES³T database and are used as initial values prior to optimization.² The PEST-PHREEQC coupled modeling allows for fitting of the reported data from each reference by varying the initial values to simulate the data. The system parameters used to best fit the data using each SCM will be compared to each other to determine which model can efficiently and accurately approximate the data.

This FAIR and community driven database allow for the inclusion of multiple types of SCM constructs, and a larger consideration for the assumptions made in each model can be included within data analysis. Parameter estimation with the coupled use of PHREEQC and PEST allow for the evaluation of experimental or simulated conditions used to fit the data reported in literature, allowing for the determination of optimized adsorption constants and associated uncertainties.

References

- [1] Zavarin, M.; Chang, E.; Wainwright, H.; Parham, N.; Kaukuntla, R.; Zouabe, J.; Deinhart, A.; Genetti, V.; Shipman, S.; Bok, F.; Brendler, V. Community Data Mining Approach for Surface Complexation Database Development. *Environ. Sci. Technol.* 2022, 56, 2827–2838.
- [2] Helmholtz-Zentrum Dresden-Rossendorf. RES³T-Rossendorf Expert System for Surface and Sorption Thermodynamics; HelmholtzZentrum Dresden-Rossendorf, 2022. <https://www.hzdr.de/db/res3t.login>

PC1-11 STATE OF THE ART REPORT IN REDOX AND KINETICS APPLIED TO NUCLEAR WASTE DISPOSAL FACILITIES

Olga Riba⁽¹⁾, Xavier Gaona⁽²⁾, Pascal E. Reiller⁽³⁾, Elisenda Colàs⁽¹⁾, Gabriela Román-Ross⁽¹⁾, James Begg⁽¹⁾, David García⁽¹⁾, Lara Duro⁽¹⁾, Stéphane Brassinnes⁽⁴⁾, Benoît Madé⁽⁵⁾, Will Bower⁽⁶⁾

(1) *Amphos 21 Consulting S.L., Spain*

(2) *KIT-INE, Germany*

(3) *Université Paris-Saclay, CEA, Service de Physico-Chimie, France*

(4) *ONDRAF/NIRAS, Belgium*

(5) *ANDRA, France*

(6) *Nuclear Waste Services, UK*

Geological nuclear waste repositories are based on the 'multiple barrier principle', in which long-term safety is assured by a series of engineered (EBS) and natural barrier systems (1). In the multi-barrier system of a repository there will be a number of redox-active components and aqueous species that will influence redox conditions. Characterization of redox potential in the disposal facilities both in the near- and far-field is essential to assess the speciation and the migration of redox sensitive radionuclides and chemical pollutants in the context of deep geological and surface disposal systems. It is known that the redox potential of a geochemical system is controlled by both the thermodynamics and kinetics of redox reactions including abiotic and biotic processes, such as microbial catalysis. Despite the accurate determination of redox potential in geochemical systems has been the focus of study in the two last decades, some uncertainties are still remaining.

The uncertainties concerning redox potential measurements and their interpretation are well recognized. Despite field measurements are often limited to semiquantitative information, they still are useful to identify a change in conditions, such as the onset of reducing conditions caused by the depletion of O₂ and NO₃ or the intrusion of dissolved oxygen into a system (2, 3). On the other hand, laboratory measurements of carefully controlled systems can provide near-quantitative predictions of important redox processes for modelling purposes (4).

The challenge of dealing with redox systems is not limited to the experimental redox measurements and extends to the numerical simulation of relevant redox processes. For instance, it is normally assumed in conceptual models that reducing conditions will prevail over the lifetime of the multi-barrier system (5). However, different redox conditions should be expected when including the disturbance of the site during the construction of the repository (6, 7). In particular, the corrosion of the adjacent canister and microbial activity will be able to consume the ingress of oxygen restoring the reducing condition (8, 9). Despite restoring the reducing conditions in the repository is desired to promote the retention of important redox-sensitive radionuclides (10), some redox processes can have a negative effect promoting the degradation of the barrier components and diminishing their retention properties. The production of corrosive species, such as sulphide, may challenge the EBS of the facility. Therefore, an accurate predictive modelling of these processes is required for safety assessment (11).

To tailor the EBS materials and their designs, the different occurring redox processes, and their beneficial or detrimental consequences, must be carefully investigated and understood. This would ensure the longevity of EBS and their capability to retain radionuclides and chemical pollutants. With this motivation, a State-of-the-Art report on redox and kinetics applied to surface and geological disposal facilities is developed in the framework of ThermoChimie consortium.

This work brings together a range of fields of expertise and summarizes the fruitful technical discussions to compile and update more than five decades of investigation and research on redox and kinetics. The report is structured around the following main blocks of knowledge: 1) theoretical aspects of the redox potential, including kinetic considerations and the influence of microbes and organic matter in the measurement of redox; 2) experimental determination of the key redox processes in natural environments and geological disposal facilities; and 3) geochemical modelling aspects of the redox potential. In particular, this report aims at providing the reader with:

- concise description of the current knowledge on the relevant governing processes applied to (geological and surface) disposal of radioactive waste;
- discussion of the considerations that need to be taken into account when designing the need for an experimental programme, if any, ensuring its consistency with the operational objectives;
- guidelines on how to implement relevant and essential processes in geochemical modelling (including, redox disequilibrium, biotic processes, ...);
- recommendations for future activities on redox processes within repositories in relation to the needs of radioactive waste management agencies.

Therefore, the report goes beyond analyzing the uncertainties, challenges, and difficulties in redox measurements and conceptual models. It provides recommendations for future experimental programmes and practical examples for modelling the most relevant redox systems in disposal facilities. These recommendations are gathered with the support of a set of benchmarking exercises between different modeling approaches that cover the effect of nitrate and sulphate, organics, oxygen flux, effect of gas (H_2 , CH_4), microbes, and reactive metals.

References

- [1] AEA. (2020). Design Principles and Approaches for Radioactive Waste Repositories (IAEA Nuclear Energy Series, Issue. IAEA, NW-T-1.27.
- [2] Grenthe, I., Stumm, W., Laaksoharju, M., Nilsson, A. C., & Wikberg, P. (1992). Redox potentials and redox reactions in deep groundwater systems. *Chemical Geology*, 98(1-2), 131-150.
- [3] Patrick, W.H. and Wyatt, R. (1964) Soil nitrogen loss as a result of alternate submergence and drying. *Soil Science Society of America Journal*, 28, 647-653.
- [4] Patrick, W.H., Gambrell, R.P. and Faulkner, S.P. (1996). Redox Measurements of Soils. In *Methods of Soil Analysis* (eds D. Sparks, A. Page, P. Helmke, R. Loeppert, P.N. Soltanpour, M.A. Tabatabai, C.T. Johnston and M.E. Sumner). <https://doi.org/10.2136/sssabookser5.3.c42> (standard soil chemistry analysis handbook)
- [5] Salas, J., Molinero, J., Juarez, I., Gimeno, M. J., Auque, L., & Gomez, J. (2010). SR-Site-hydrogeochemical evolution of the Forsmark site. SKB TR-10-58.
- [6] Jenni, A., Wersin, P., Mäder, U. K., Gimmi, T., Thoenen, T., Baeyens, B., ... & Leupin, O. (2019). Bentonite backfill performance in a high-level waste repository: a geochemical perspective (No. NTB--19-03). University of Berne.
- [7] Behrends, T., & Bruggeman, C. (2016). Determining redox properties of clay-rich sedimentary deposits in the context of performance assessment of radioactive waste repositories: conceptual and practical aspects. OPERA-PU-UTR611-1.
- [8] Wersin, P., Johnson, L., Schwyn, B., Berner, U., & Curti, E. (2003). Redox Conditions in the Near Field of a Repository for SF/HLW and ILW in Opalinus Clay (Nagra TR 02-13).
- [9] Bradbury, M., Berner, U., Curti, E., Hummel, W., Kosakowski, G., & Thoenen, T. (2014). The long term geochemical evolution of the nearfield of the HLW repository. NAGRA TR-12-01
- [10] Ma, B., Charlet, L., Fernandez-Martinez, A., Kang, M., & Madé, B. (2019). A review of the retention mechanisms of redox-sensitive radionuclides in multi-barrier systems. *Applied Geochemistry*, 100, 414-431.
- [11] Bengtsson, A., & Pedersen, K. (2017). Microbial sulphide-producing activity in water saturated Wyoming MX-80, Asha and Calcigel bentonites at wet densities from 1500 to 2000 kg m⁻³. *Applied Clay Science*, 137, 203-212.

PC2-4 REACTIVE TRANSPORT MODEL OF THE LONG-TERM GEOCHEMICAL EVOLUTION AT THE DISPOSAL CELL SCALE IN A HLW REPOSITORY IN GRANITE

Javier Samper⁽¹⁾, Luis Montenegro⁽¹⁾, Alba Mon⁽¹⁾, Laurent De Windt⁽²⁾, Aurora-Core Samper⁽¹⁾, & Enrique García⁽³⁾

(1) *Centro de Investigaciones Científicas Avanzadas (CICA). E.T.S.I. Caminos, Canales y Puertos. Universidad de A Coruña. Campus de Elviña, 15071 A Coruña, Spain.*

(2) *MINES Paris, PSL University, Centre for Geosciences and Geoengineering, Fontainebleau, France*

(3) *ENRESA Empresa Nacional de Residuos Radiactivos, S.A. C/ Emilio Vargas 7, 28043 Madrid, Spain*

The assessment of the long-term performance of the engineered barrier systems (EBS) of high-level radioactive waste (HLW) in a deep geological repository requires the use of reactive transport models. The EBS in a HLW repository in granite includes the vitrified waste, the canister and the compacted bentonite buffer. A conceptual, mathematical and numerical reactive transport model was proposed for a generic HLW disposal cell in granite within the context of the ACED Task 4.1 [1]. The model of the reference case considers 3 successive periods. Period I covers the oxic transient stage. Period II starts when the bentonite barrier is fully saturated and the anoxic conditions are prevailing. Canister corrosion, the interactions of corrosion products and the bentonite and the interactions of bentonite and granite are considered in this period. Period III starts after canister failure and considers the vitrified glass alteration and the interactions of the glass with corrosion products and bentonite. Here we present a 1D non-isothermal reactive transport model of the long-term geochemical evolution of a HLW disposal cell in a granitic host rock. The model was computed with the CORE code [2]. The model includes the vitrified waste (40 cm in diameter), the carbon-steel canister (5 cm thick), the saturated FEBEX bentonite buffer (75 cm thick) and the reference granitic rock. Model predictions have been performed for Period II (canister corrosion) which last 25.000 years and Period III (vitrified waste dissolution) from 25.000 to 50.000 years. The model accounts for the thermal transient stage and assumes generalized steel corrosion under anaerobic conditions with a corrosion rate equal to 1.41 m/y. Canister failure is assumed to occur in the model when the remaining canister thickness is equal to 3.5 cm at the end of Period II at 25.000 years. Canister corrosion causes an increase in pH. The computed pH in the canister just before canister failure ($t = 25,000$ years) is equal to 9.24 and ranges from 7.82 to 9.24 in the bentonite. Magnetite is the main corrosion product which precipitates in the bentonite and especially in the canister. The thickness of magnetite precipitation band in the bentonite is 1 cm (Figure 1). Siderite precipitates at both sides of the canister/bentonite interface (Figure 1). The precipitation front penetrates more than 1 cm into the bentonite. The glass waste dissolution starts at Period III after canister failure ($t > 25.000$ years). The concentration of the computed dissolved silica increases in the inner part of the glass until 30.000 years and decreases in the outer part of the glass due to the out diffusion of dissolved silica into the canister and the bentonite. This diffusive flux causes the precipitation of greenalite at the glass/canister and canister/bentonite interfaces. The pH at the end of the simulation (50,000 years) ranges from 7.93 to 7.98 in the glass, from 7.89 to 8.66 in the canister and from 7.86 to 8.57 in the bentonite. Magnetite precipitates in the canister (Figure 1) while there is carbon steel to corrode. Once the canister is fully corroded, magnetite redissolves near the glass/canister interface. Greenalite precipitates in the canister and the bentonite, especially at the glass/canister interface and siderite precipitates at the canister/bentonite interface (Figure 1). Model results are sensitive to [3]: 1) A decrease of the threshold silica concentration of the kinetic glass dissolution rate; 2) An increase in the groundwater water flux in the granite; 3) A porosity feedback effect; 4) A variable corrosion rate depending on temperature and Fe(0) saturation index; and 5) A reduction of the time for canister failure from 25.000 years to 10.000 years. On the other hand, model results are less sensitive to smectite dissolution.

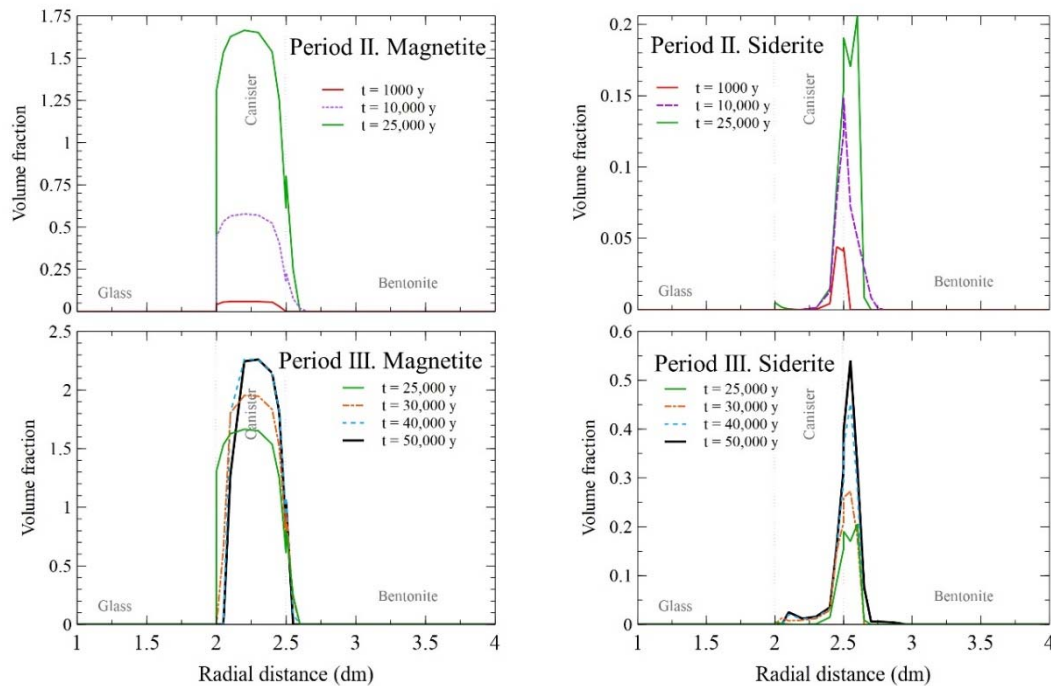


Figure 1. Spatial distribution of the computed volume fraction of magnetite (left) and siderite (right) at selected times of Period II (top) and Period III (bottom).

Acknowledgments: The research leading to these results was funded by ENRESA through a Research Contract within the Work Package ACED of EURAD (European Joint Programme on Radioactive Waste Management of the European Union). The work was partly funded also by the Spanish Ministry of Science and Innovation (Project PID2019-109544RB100) and the Galician Regional Government (Grant number ED431C2021/54 from “Consolidación e estruturación de unidades de investigación competitivas”).

References

- [1] Samper, J., L. Montenegro, L. De Windt, V. Montoya, J. Garibay-Rodríguez, D. Grigaliuniene, A. Narkuniene, Poskas, P. (2022): Conceptual model formulation for a mechanistic based model implementing the initial SOTA knowledge (models and parameters) in existing numerical tools. Deliverable D2.16. EURAD Joint Project. EC Grant Agreement no: 847593.
- [2] Samper, J., Xu, T., Yang, C. (2009). A sequential partly iterative approach for multicomponent reactive transport with CORE2D. *Comput. Geosci.* 67, 42-51.
- [3] Montenegro, L, J Samper, A Mon, L De Windt, AC Samper & E García (2023) Reactive transport models of the geochemical evolution in a disposal cell at a HLW repository in granite, *Applied Clay Science*

PC2-5 DEVELOPMENT AND IMPROVEMENT OF NUMERICAL METHODS AND TOOLS FOR MODELLING COUPLED PROCESSES

Claret Francis ⁽¹⁾, Pepin Guillaume ⁽²⁾, Cances Clément ⁽³⁾, Kolditz Olaf ⁽⁴⁾, Prasianakis Nikolaos ⁽⁵⁾, Baksay Attila ⁽⁶⁾, Lukin Dmitry ⁽⁷⁾

(1) BRGM, France

(2) Andra, France

(3) Inria, France,

(4) UFZ, Germany

(5) PSI, Switzerland

(6) Ts Enercon, Hungary

(7) SURAO, Czech republic

Understanding of multi-physical Thermo-Hydro-Mechanical-Chemical coupled processes (THMC) occurring in radioactive waste disposal is a major and permanent issue to support optimization of design and safety case abstraction. Numerical simulations are necessary to make predictive multi-physical analyses for time periods and space scales larger than experiments can cover [1, 2]. These numerical simulations require integrating, in a consistent framework, an increasing scientific knowledge acquired for each of the individual components of a system for radioactive waste disposal. This implies to consider couplings of different and non-linear processes from a wide range of materials with different properties as a function of time and space in ever-larger systems. The development of cutting-edge and efficient numerical methods is thus necessary, in the scope of having useful, powerful and relevant numerical tools for assessments. It is also necessary to manage the uncertainties associated to the input data feeding the models and the representation of the processes, to assess the range of variability of the results and to identify the main parameters and processes driving the behavior of the systems of interest. Managing uncertainties in these complex systems require the improvement and the development of innovative, appropriate and efficient numerical methods. To tackle the above-mentioned challenges a R&D work package entitled “DONUT : Development and improvement of numerical methods and tools for modelling coupled processes” has been launched about 4 years ago within the EURAD joint programming initiative. Organized around four technical tasks the objectives of DONUT are the: (i) development of relevant, performant & cutting-edge numerical methods that can easily be implemented in existing or new tools, in order to carry out high-performance computing for the study of highly coupled processes in large systems (reactive transport, 2-phase flow & THM modelling in porous and fractured media), (ii) development of numerical scale transition schemes for coupled processes (meso to macro scale, or pore to Darcy scale) supporting the study of specific multi-scale couplings e.g. chemo-mechanics, (iii) development of innovating numerical methods to carry out uncertainty and sensitivity analyses, (iv) the realization of benchmark exercises, on representative test cases, to test the efficiency of developed methods (robustness, accuracy, time computational) on relevant tools. The achievement of DONUT will be illustrated and discussed through relevant examples (e.g.[3-6]).

References

- [1] O. Bildstein, F. Claret, P. Frugier. *Reviews in Mineralogy and Geochemistry* **85**, 419-457 (2019).
- [2] F. Claret, A. Dauzeres, D. Jacques, P. Sellin, B. Cochepin, L. De Windt, J. Garibay-Rodriguez, J. Govaerts, O. Leupin, A. Mon Lopez, L. Montenegro, V. Montoya, N. I. Prasianakis, J. Samper, J. Talandier. *EPJ Nuclear Sci. Technol.* **8**, 41 (2022).
- [3] O. Kolditz, D. Jacques, F. Claret, J. Bertrand, S. V. Churakov, C. Debayle, D. Diaconu, K. Fuzik, D. Garcia, N. Graebing, B. Grambow, E. Holt, A. Idiart, P. Leira, V. Montoya, E. Niederleithinger, M. Olin, W. Pfingsten, N. I. Prasianakis, K. Rink, J. Samper, I. Szöke, R. Szöke, L. Theodon, J. Wendling. *Environmental Earth Sciences* **82**, 42 (2023).
- [4] P. Sochala, C. Chiaberge, F. Claret, C. Tournassat. *Scientific reports* **12**, 15077 (2022).
- [5] C. Soulaine, S. Pavuluri, F. Claret, C. Tournassat. *Environmental Modelling & Software* **145**, 105199 (2021).
- [6] N. I. Prasianakis, R. Haller, M. Mahrous, J. Poonoosamy, W. Pfingsten, S. V. Churakov. *Geochimica et Cosmochimica Acta* **291**, 126-143 (2020)

PC2-6 VARS GLOBAL SENSITIVITIES FOR REACTIVE TRANSPORT SIMULATIONS IN A HLW REPOSITORY IN GRANITE

Samper⁽¹⁾, Carlos López⁽²⁾, Alba Mon⁽¹⁾, Bruno Pisani⁽¹⁾, Aurora-Core Samper⁽¹⁾, Javier Samper II⁽¹⁾, Fernando Lentijo⁽³⁾

(1) Centro de Investigaciones Científicas Avanzadas (CICA). E.T.S.I. Caminos, Canales y Puertos. Universidad de A Coruña. Campus de Elviña, University of A Coruña, 15071 A Coruña.

(2) Universidad Ort - Montevideo (Uruguay)

(3) Empresa Nacional de Residuos Radiactivos (ENRESA) - Madrid (Spain)

Reactive transport models are used intensively for the long-term safety assessment of high-level radioactive waste repositories. Sophisticated methods of sensitivity analysis of numerical models have been developed in recent years such as the Morris, Sobol and VARS (Variogram Analysis of Response Surfaces) methods [1]. These methods require performing Monte Carlo simulations of the model output, Y , for a large number of parameter combinations. VARS is a method which provides a comprehensive and efficient tool to analyze the structure of a response function Y [2]. The Morris and the Sobol methods are particular cases of the VARS method. Here we report the application of VARS to evaluate the global sensitivities of the long-term geochemical model predictions for a HLW disposal cell. Sensitivities are calculated for a 1-D axisymmetric non-isothermal multicomponent reactive transport model of the long-term (50.000 years) interactions of a carbon-steel canister and the FEBEX bentonite in a HLW disposal cell in granite is presented (Figure 1). A constant corrosion rate of $2 \mu\text{m}/\text{year}$ is assumed [3]. Simulations were performed with CORE^{2D} V5 in the Galician Supercomputing Center. The model outputs, Y , considered are the computed pH at the canister/bentonite interface at $t = 10 \text{ k}$, 25 k and 50 k years. Global sensitivities were analyzed for the following parameters: corrosion rate, effective bentonite solute diffusion, groundwater flow through the granite, Fe cation exchange selectivity and magnetite stability constant. Log-uniform probability density functions were assumed for the parameters, except for the corrosion rate, which was assumed to be uniform.

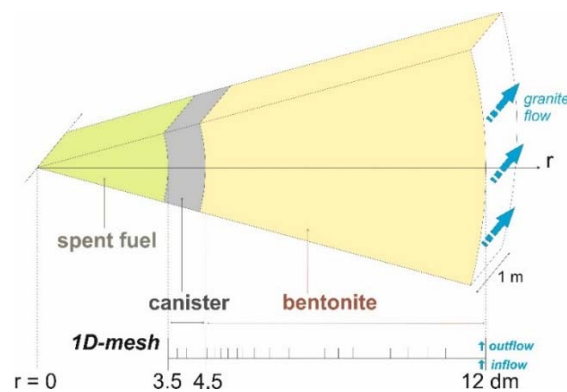


Figure 1: 1D axisymmetric section of a HLW repository in granite.

Figures 2a and 3a show the sample directional variograms of the pH at $t = 10\text{k}$ and 50 k years for the five parameters. One can see that the corrosion rate, the flow in the granite and the selectivity of Fe are the main parameters which exhibit larger variograms. Figures 2b and 3b show the values of the IVARS-0 or IVARS-ABE (equivalent to the Morris elementary effects), IVARS-50 and IVARS-100 (equivalent to the total Sobol index) indexes. One can see that all these three indexes give similar results. There are some small differences for some parameters. The Morris indexes (IVARS-ABE) tend to reach larger values than those of the IVARS-50 and Sobol indexes for the less influential parameters. The results of the global sensitivity analysis lead to the conclusion that the most influential parameters are the corrosion rate, the granite flux and the Fe cation selectivity, with more than 90% confidence. Work is progress to extend our analysis to: 1) Other model outputs such as Eh, the concentrations of dissolved

Fe, sorbed and exchanged Fe and the volume of precipitated corrosion products and 2) A larger list of uncertain parameters.

VARS analysis of the geochemical model results is part of JOSA (Joint Sensitivity Analysis Group), an initiative to develop and test sensitivity and uncertainty methods for radioactive waste disposal. Several tests cases have been prepared by some groups. Different partners apply different methods and model results are compared. Available results are compiled in Volume 1 which was published by SNL (USA) (see <https://www.osti.gov/servlets/purl/1822591>). Volume 2 is in progress.

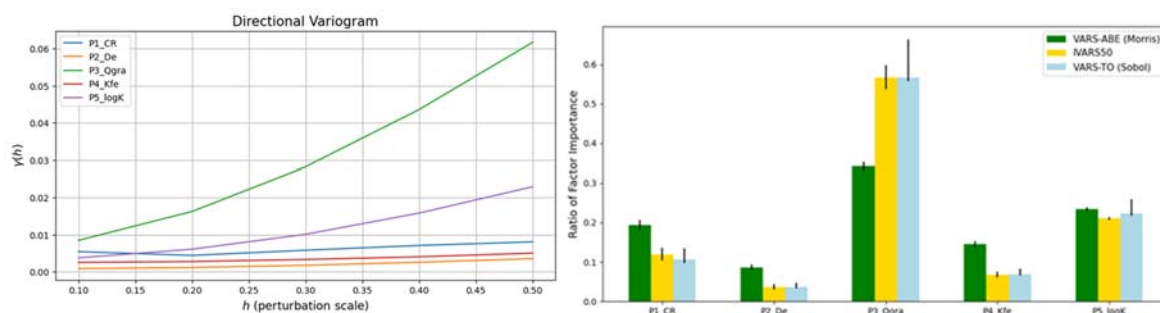


Figure 2: a) Sample variograms of the output (pH at 10000 years) for the five parameters (left) and b) values of the IVARS-0, IVARS-50 and IVARS-100 indexes (right)

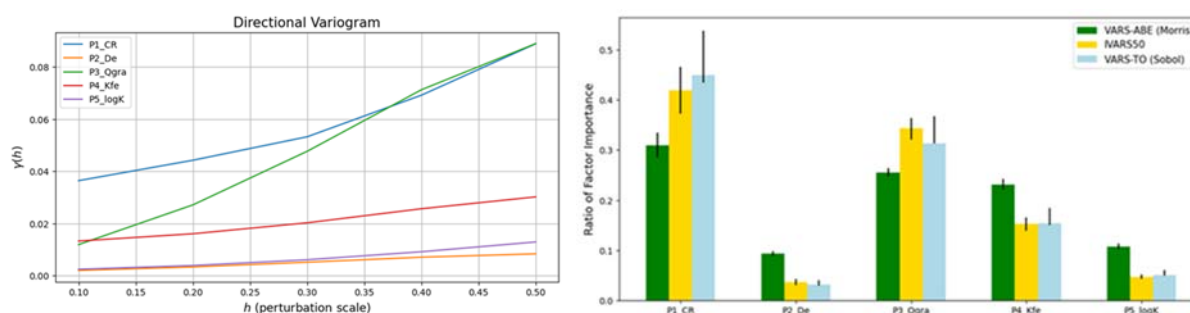


Figure 3: a) Sample variograms of the output (pH at 50000 years) for the five parameters (left) and b) values of the IVARS-0, IVARS-50 and IVARS-100 indexes (right)

Acknowledgements: The research leading to these results was funded by ENRESA through a Research Contract within the Work Package DONUT of EURAD (European Joint Programme on Radioactive Waste Management of the European Union, grant agreement n° 847593). The work was partly funded also by the Spanish Ministry of Science and Innovation (Project PID2019-109544RBI00) and the Galician Regional Government (Grant number ED431C2021/54 from “Consolidación e estruturación de unidades de investigación competitivas”).

References

- [1] Razavi et al. (2021) The future of sensitivity analysis: An essential discipline for systems modeling and policy support. *Env Modelling and Software* 137 (2021) 104954.
- [2] Razavi & Gupta, 2016 Razavi, S., and Gupta, H. V. (2016), A new framework for comprehensive, robust, and efficient global sensitivity analysis: 2. Application, *Water Resour. Res.*, 52, 440– 455.
- [3] Samper, J., L. Montenegro, L. De Windt, V. Montoya, J. Garibay-Rodríguez, D. Grigaliuniene, A. Narkuniene, & P. Poskas, (2021): Conceptual model formulation for a mechanistic based model implementing the initial SOTA knowledge (models and parameters) in existing numerical tools. Deliverable D2.16 of the EURAD Joint Project. EC Grant Agreement no: 847593.

PC3-3 SUPPORTING TOOLS IN THE DEVELOPMENT OF THE THERMOCHIMIE DATABASE: THE XCHECK TOOL

Darío Pérez (1), Jordi Rodríguez-Mestres (1), Eli Colàs (1), David García (1), Lara Duro (1), Liz Harvey (2), Will Bower (3), Stéphane Brassinnes (4), Benoît Madé (5)

(1) *Amphos 21 Consulting SL, Spain*

(2) *Galson Sciences Ltd., UK*

(3) *Nuclear Waste Services, UK.*

(4) *Belgian Agency for Radioactive Waste and Enriched Fissile materials (ONDRAF/NIRAS), Belgium*

(5) *Andra, French National Radioactive Waste Management Agency, Research & Development Division, France*

ThermoChimie (<http://www.thermochimie-tdb.com/>) [1,2] is a thermodynamic database developed by Andra (France), Nuclear Waste Services (UK) and Ondraf/Niras (Belgium). It is intended to be used for geochemical calculations supporting radioactive waste management activities.

The main application for management of the ThermoChimie database is the XCheck Tool. This tool is a software developed by Amphos 21 to automate tasks related to the consistency and traceability of the ThermoChimie database. The full version of the XCheck Tool can be used to modify and delete the species and their associated thermodynamic data and to include new species in the database.

The XCheck Tool can automatically perform internal calculations to guarantee consistency with the fundamental laws of thermodynamics among the Gibbs energy, enthalpy, and entropy parameters. It can re-calculate the whole database when thermodynamic data for a master species or a reference state is changed. The tool can also keep an automatic record of the changes and modifications, which are afterwards reported in the corresponding documents, increasing the traceability and reducing human-made errors.

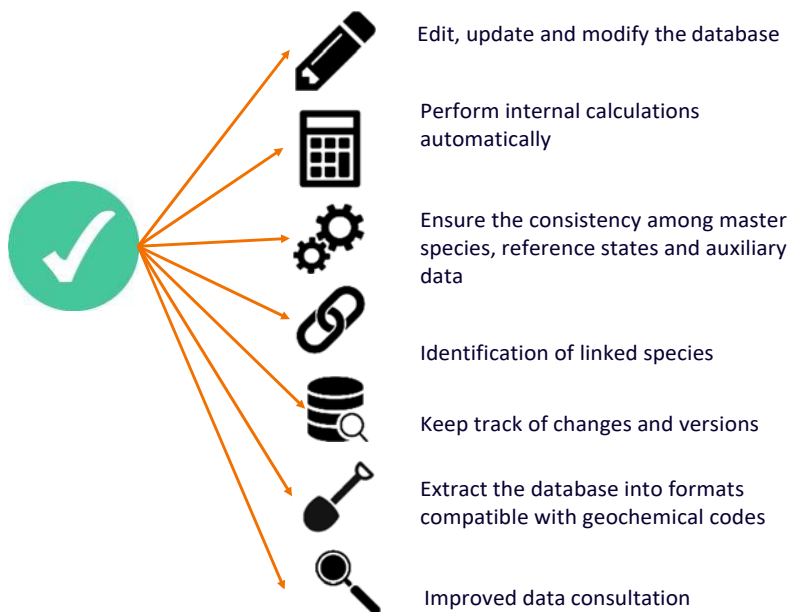
Besides the relationships among Gibbs energy, enthalpy and entropy values of a compound, chemical dependencies established among the species are also taken into account. Once the necessary information is provided, the XCheck Tool will allow the administrator to identify species that belong to a consistent chemical group. Species related by estimations, correlations and analogies will also be labelled and identified.

Another important feature of the tool is the possibility of extracting the thermodynamic data into different formats compatible with geochemical codes, such as PhreeqC, Crunch, ToughReact, CHESS, Geochemist Workbench, Spana and PFLOTTRAN, ensuring that the information is not lost or altered during the process.

Consultation of the information in the database has been improved with powerful query features which allow filtering and extraction by using the XCheck Tool. For that reason, a tailor-made software with only this data-consultation capability has been released and made public through the ThermoChimie database website. Users interested in this XCheck Tool User Version can access it by logging to <https://register.thermochimie-ctool.com>. Once registered, the user can access it through a virtual Windows desktop. Data filtering and data extraction in CSV (comma separated values) format is also allowed. The user version of the tool will allow the modelers to query the different parameters included in the database using different filtering capabilities and to export this information to better analyze the results obtained in the modelling applications.

Feedback from users is highly welcomed: consortium-tc3-tech@thermochimie-tdb.com.

XCheck Tool



XCheck Tool capabilities

References

- [1] Giffaut, E., M. Grivé, P. Blanc, P. Vieillard, E. Colàs, H. Gailhanou, S. Gaboreau, N. Marty, B. Madé and L. Duro. (2014). Andra thermodynamic database for performance assessment: ThermoChimie. *Applied Geochemistry* 49: 225-236.
- [2] Grivé, M., L. Duro, E. Colàs and E. Giffaut. (2015). Thermodynamic data selection applied to radionuclides and chemotoxic elements: An overview of the ThermoChimie-TDB. *Applied Geochemistry* 55: 85-94.

PC5-1 APPROACH OF CONSEQUENCE ANALYSES SUPPORTING THE SAFETY-BASED COMPARISON OF THE CANDIDATE SITING REGIONS FOR THE SWISS DEEP GEOLOGICAL REPOSITORY

Xiaoshuo Li⁽¹⁾, Olivier X. Leupin⁽¹⁾, Nikitas Diomidis⁽¹⁾, Raphael Wüst⁽¹⁾

(1) Nagra, Switzerland

The Swiss Radioactive Waste Management Programme foresees two types of deep geological repository: a high-level waste repository (HLW repository) for spent fuel (SF) and vitrified high-level waste (HLW) and a repository for low- and intermediate-level waste (L/ILW repository). A combined repository for all of these waste types, with separate disposal areas for SF/HLW and for L/ILW, is also considered. For the selection of the preferred site for the repository, three candidate siting regions (Jura Ost, Nördlich Lägern and Zürich Nordost) were examined in detail. In September 2022, Nagra formally proposed Nördlich Lägern as the site for a combined repository for all of waste types and currently is working towards a general licence application for the site. This presentation provides an overview of the workflow and methodology of the consequence analyses supporting the safety-based comparison of the siting regions.

The consequence analyses are performed based on a reference scenario, which represents the expected evolution of the repository system. The radionuclide (RN) transport in both the aqueous and the gas phase is modelled based on two types of numerical models: a) a 1-D model for the RN transport in aqueous phase (see the example in Fig.1 left), and b) a so-called 3-D macro element modelling approach (see the example in Fig.1 right) is used to simulate the gaseous C-14 migration by considering two-phase flow processes. Both modelling approaches are processed in the same workflow.

As the first step of the analyses, a conceptual model of each site is developed based on site specific geological information and data, such as the thicknesses and transport-relevant properties of the various geological layers. This provides a common foundation for the development of site-specific models of radionuclide retention and transport in the geosphere both in the aqueous phase and in the gas phase. The two models are then applied separately in carrying out the following steps:

1. Radionuclide inventory screening to identify safety-relevant radionuclides for each model. For the gaseous radionuclide migration, C-14 is the only radionuclide considered. Other gaseous radionuclides are either highly soluble (e.g., I-129) or are short-lived and/or present in only minor amounts (e.g., Rn-222).
2. Setup of the reference calculation using reference parameters (most likely or conservative assumptions). The objective of this calculation is to obtain the reference dose rate and to develop an understanding of the general behaviour of the investigated site.
3. Define probability density functions (PDFs) for uncertain model parameters using all available data.
4. Perform a Monte-Carlo simulation, sampling each uncertain parameter randomly from its respective PDF, and analyse the resulting uncertainty in the calculated maximum dose rate. Finally, the results from all the simulation realisations are aggregated and analysed.
5. Based on the results of the Monte-Carlo simulation, a global sensitivity analysis is performed to identify the sensitive parameters of the RN transport modelling. The maximum dose rate from the Monte-Carlo simulations within the period under consideration is taken as the quantity of interest for parameter sensitivity analysis, e.g., the maximum total dose rate from the geosphere within one million years for the HLW repository (SF and HLW) and within 100'000 years for the L/ILW repository. In order to ensure that all sensitive parameters are taken into account in the sensitivity analysis, several sensitivity measures are used in a systematic manner to determine the parameter importance.

6. Based on the parameter sensitivities, a set of deterministic calculation cases is defined and analysed. The values of the most sensitive parameters are assigned by taking a bounding value on the pessimistic side of their respective distributions individually in each deterministic case (according to the parameter sensitivities obtained in the sensitivity analysis). There is also an additional deterministic case for each site-specific model, combining the pessimistic bounding values of the sensitive parameters.
7. The results of the probabilistic uncertainty analysis and the deterministic calculation cases are combined and compared to assess the safety margins available for each siting region.

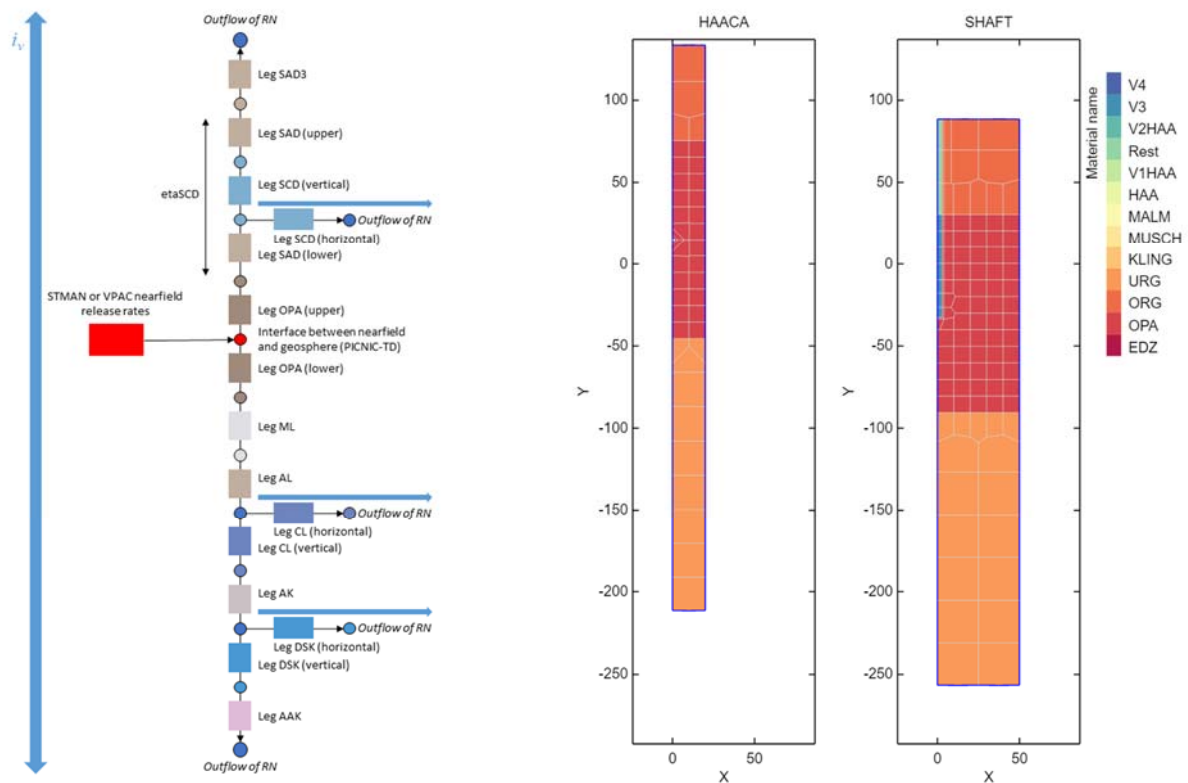


Fig. 1: *Left:* an example of the 1-D model set for simulating the RN transport in aqueous phase; *Right:* an example of the 3-D macro element model set for simulating the gaseous C-14 migration under two phase flow condition

PD-5 THE UK'S RADIOACTIVE WASTE MANAGEMENT AND ENVIRONMENTAL REMEDIATION (RADER) NATIONAL NUCLEAR USER FACILITY

Katherine Morris⁽¹⁾, Francis Livens⁽¹⁾, Jon Lloyd⁽¹⁾, Sam Shaw⁽¹⁾, Anthony Stockdale⁽¹⁾

(1) Department of Earth & Environmental Sciences, The University of Manchester, Oxford Road, Manchester, M13 9PL, United Kingdom

The Radioactive Waste Management and Environmental Remediation National Nuclear User Facility was funded by EPSRC in 2019 and opened in 2022. The new facility supports research into characterizing and understanding the behavior of radioactive species in natural and engineered environments. This science base is crucial for underpinning large parts of the UK's >100 year, >£130 billion nuclear decommissioning, clean-up and waste management programs. The newly refurbished laboratories support radiological counting facilities, specialist experimental equipment, aqueous and colloid analysis instruments and instruments for solids characterization including specialist labs for:

- Radiometrics
- Instrumental analysis
- Column studies
- Wet chemistry
- Sample preparation, including cutting and polishing

We briefly discuss the laboratory capabilities and highlight recent work that has used these facilities to demonstrate the range of work undertaken. This includes underpinning work on environmental alteration of U(VI) incorporated goethite (Stagg et al., 2022), on adsorption / precipitation processes controlling U-solubility in the presence of hydrotalcite colloids, a layered double hydroxide phase (Foster et al., 2022). We also discuss recent contaminated land studies exploring Se- and U- mobility in contaminated land environments (Ho et al., 2022; Fallon et al., 2023).

We welcome discussions on research collaborations with external academic and industry users and details of the facility are available at <https://www.nnuf.ac.uk/rader>.

References

- [1] Stagg, O., Morris, K., Townsend, L.T., Kvashnina, K.O., Baker, M.L., Dempsey, R.L., Abrahamsen-Mills, L., Shaw, S. (2022) Sulfidation and Reoxidation of U(VI)-Incorporated Goethite: Implications for U Retention during Sub-Surface Redox Cycling. *Environmental Science and Technology*, DOI: 10.1021/acs.est.2c05314
- [2] Fallon, C.M., Bower, W.R., Powell, B.A., Livens, F.R., Lyon, I.C., McNulty, A.E., Peruski, K., Mosselmans, J.F.W., Kaplan, D.I., Grolimund, D., Warnicke, P., Ferreira-Sanchez, D., Kauppi, M.S., Vettese, G.F., Shaw, S., Morris, K., Law, G.T.W. (2023) Vadose-zone alteration of metaschoepite and ceramic UO₂ in Savannah River Site field lysimeters. *Science of the Total Environment*, DOI: 10.1016/j.scitotenv.2022.160862.
- [3] Foster, C., Shaw, S., Neill, T.S., Bryan, N., Sherriff, N., Natrajan, L.S., Wilson, H., Lopez-Odriozola, L., Rigby, B., Haigh, S.J., Zou, Y.-C., Harrison, R., Morris, K. (2022). Hydrotalcite Colloidal Stability and Interactions with Uranium(VI) at Neutral to Alkaline pH. *Langmuir*, DOI: 10.1021/acs.langmuir.1c03179
- [4] Ho, M.S., Vettese, G.F., Morris, K., Lloyd, J.R., Boothman, C., Bower, W.R., Shaw, S., Law, G.T.W. (2022) Retention of immobile Se(0) in flow-through aquifer column systems during bioreduction and oxic-remobilization. *Science of the Total Environment*, DOI: 10.1016/j.scitotenv.2022.155332

PD-6 EFFECT OF SEASONAL ANOXIA ON TRACE ELEMENTS AND PLUTONIUM CYCLING IN A WARM MONOMICTIC LAKE

Fanny Coutelot⁽¹⁾, Jessica Wheeler⁽¹⁾, Reid Williams⁽¹⁾, Nimisha Edayilam⁽¹⁾, Nancy Merino⁽²⁾, Naomi Wasserman⁽²⁾, Daniel I. Kaplan³, Annie B. Kersting⁽²⁾, Brian A. Powell⁽¹⁾, Mavrik Zavarin⁽²⁾

(1) Clemson University, Clemson, SC, USA

(2) Lawrence Livermore National Laboratory, Livermore, CA, USA

(3) Savannah River Ecology Laboratory, Aiken, SC, USA

This study investigated the influence of seasonal anoxia in a warm monomictic pond on the composition the cycling of natural and anthropogenic elements in sediment and lake water. Pond B at the Savannah River Site (Aiken, SC) received cooling water from the R-reactor which resulted in contamination of anthropogenic radionuclides ²³⁹Pu and ¹³⁷Cs, which can be used as tracers to monitor natural hydrobiogeochemical processes¹. Seasonal stratification leads to seasonally anaerobic hypolimnion and profound changes in geochemical conditions which can impact the cycling of trace elements and organic matter through the system. Two consecutive years of monitoring demonstrated the occurrence of highly correlated concentration profiles of arsenic, iron, aluminum, plutonium, and dissolved organic matter, all of which increased in concentration by 1–2 orders of magnitude within the anaerobic hypolimnion (Figure 2).

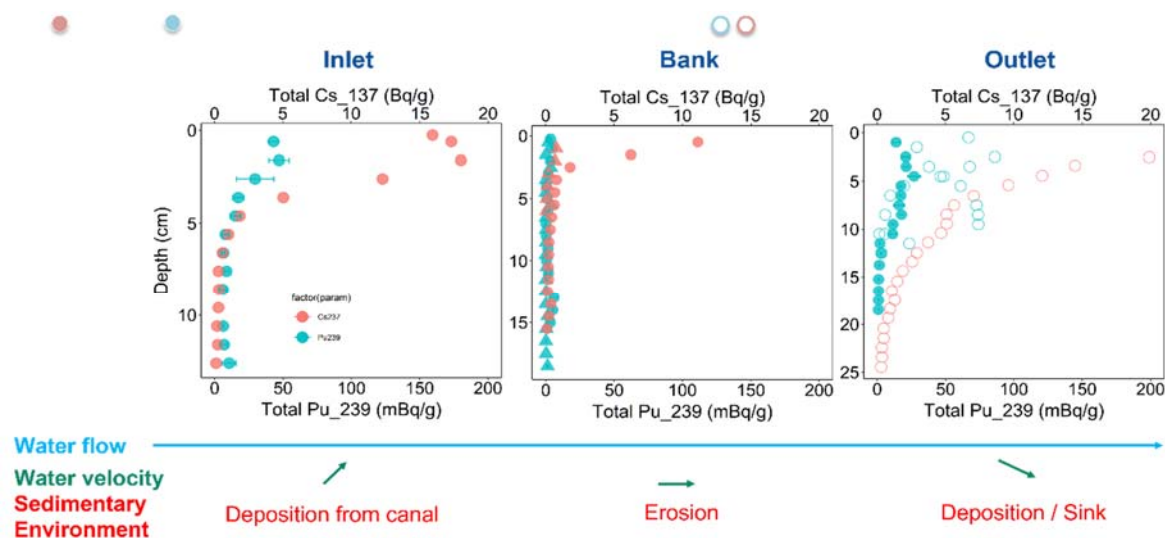


Figure 2: ²³⁹Pu (blue) and ¹³⁷Cs (pink) total concentrations versus depth in sediment cores (solid shapes) collected from the inlet (source), the bank and outlet of pond B the compared the decay corrected cores collected by Whicker et al¹ at random location.

Sediment cores were collected to determine concentrations of Pu-239, Cs-137, and major and minor elements in solid phase, pore water and an electrochemical method was used on wet cores to determine dissolved elemental concentrations. More than 50 years after deposition, Pu-239 and Cs-137 in sediments are primarily located in the upper 5 cm in area where deposition of particulate-bound contaminants was prevalent and located between 5 and 10 cm in areas of high sedimentation, showing a limited migration of Pu-239 and Cs-137². A Factor analysis demonstrated different sediment facies across the pond resulting in a range of geochemical processes controlling accumulation of Pu and Cs. Highest concentrations appear to be controlled by particulate input from the influent canal, dominated by clay, silt, and sand minerals bearing Fe (Figure 3). Elevated Pu-239 in the sediments were observed

in areas with high organic matter and high deposition rates near the outlet indicating strong association of Pu with OM and particulates. Therefore, organic matter cycling likely plays a role in Pu redistribution between sediment and overlying pond water, and deposition in organic rich sediments accumulating near the outlet. Though Pu appears to have been distributed throughout the pond, Cs-137 concentrations remained the highest near the influent canal.

References

1. Whicker, F. W., Pinder, J. E., Bowling, J. W., Alberts, J. J. & Brisbin, I. L. Distribution of Long-Lived Radionuclides in an Abandoned Reactor Cooling Reservoir. *Ecological Monographs* **60**, 471–496 (1990).
2. Coutelot, F. *et al.* Temporal evolution of Pu and Cs sediment contamination in a seasonally stratified pond. *Science of The Total Environment* **857**, 159320 (2023).

PD-7 PRELIMINARY APPROACH FOR SAFETY DISPOSAL OF RADIOACTIVE WASTES FROM FDNPS FOR OPTIMIZATION OF WASTE MANAGEMENT STREAM

Kazuki Iijima

Collaborative Laboratories for Advanced Decommissioning Science (CLADS), Sector of Fukushima Research and Development, Japan Atomic Energy Agency (JAEA), Japan

On the way of decommissioning of Fukushima Dai-ichi Nuclear Power Station (FDNPS), it is estimated that huge amount of various radioactive solid wastes will be generated. The purpose of the waste management is to reduce risks in every stage of management, such as handling, storage, treatment and disposal. In case of the FDNPS, due to their high radioactivity, generated wastes have been managed focusing on safe handling and storage so far. However, to ensure the safety during storage, solidification into the stable form are expected for some wastes.

Solidification methods should be selected in considering that the solidified wastes are safe enough to store for specific duration and have adequate long-term performance expected in the disposal system without significant disturbance. In addition, the disposal system for the wastes has to be constructed and its performance should be evaluated. However, there is less information on the wastes generated in the FDNPS compared with usual nuclear facilities from the following point of views:

- Only limited chemical and radioactive data have been obtained even for already generated wastes.
- It is difficult to obtain further data of the generated waste with quite strong radioactivity.
- Estimation of radioactivity data of the waste generated in the future as decommissioning progresses is difficult at this time due to limited access to the place of generation.

Therefore, different approach is required for selection of the solidification method.

Nuclear Damage Compensation and Decommissioning Facilitation Corporation (NDF), which conducts research and development, as well as provides advice and guidance, required for decommissioning, established "Technical Strategic Plan for Decommissioning of TEPCO's Fukushima Daiichi Nuclear Power Station" every year. In the Plan 2022, as a waste management strategy for the next 10 years, it is mentioned that "Creation of options for processing/disposal measures and their comparison and evaluation should be conducted with promoting characterization to establish a waste stream that are suitable for features of solid waste. Proceed study on specific management of the solid waste to present appropriate measures as a whole." [1]. In other words, considering the characteristics of the solid wastes, we will compare and evaluate various treatment and disposal options to optimize the overall solid waste management stream. Therefore, in this study, in the presence of great uncertainties not only in the disposal environment conditions but also in the characteristics both of the solidified and original wastes, a methodology for using the safety assessment of disposal as one of the optimization tools for the overall management system of the solid waste generated at the FDNPS.

Preliminary performance evaluations have been conducted by International Research Institute for Nuclear Decommissioning (IRID), in which JAEA also participated. In the 2020 project, the following sensitivity analysis was conducted [2].

- The inventory was estimated assuming the transfer pathways and transfer rates of radionuclides to waste based on the characteristics of radionuclides and limited analytical data.

- The performance evaluation was conducted assuming shallow land disposal. The concepts of the disposal follows the concept of trench disposal and pit disposal, which have already been implemented in Japan, and the concept of subsurface disposal, which is currently under consideration. In addition, a model, hydraulic parameters, radionuclide migration parameters, leaching rate, etc. were set assuming the similar disposal environment.
- For these values, sensitivity analysis was performed for a basic case using central values and conservative cases assuming performance degradation of one to two orders of magnitude.

As a result, C-14 and I-129 became the dominant nuclides in the groundwater scenario. Since these nuclides are mobile, results of calculated dose were greatly affected by inventory, infiltration water velocity, and leaching rate. The dose assessment results showed a 5- to 8-order variance, with some wastes exceeding the reference dose of 10 μ Sv/y. Under such a condition, conservative consideration of all great uncertainties may result in requiring excessive performance of the solidified waste. Therefore, following approach was considered to be needed.

- At first, the performance required for solidified waste is clarified under the reference case in which the most plausible disposal concept, scenarios, models, with mean values for waste properties, parameters, and so on.
- Some conservative cases are clearly set, considering the prospects of reduction of uncertainties due to data acquisition in future, probability distribution of uncertainties, with scientific proves.
- Furthermore, after selecting a solidified body in future, it is effective to prepare engineering barriers that can complement the performance of the solidified wastes in preparation for uncertainties different from assumptions emerge.

Acknowledgement: *This study was performed under the subsidy program “Project of Decommissioning and Contaminated Water Management” conducted by the Ministry of Economy, Trade and Industry of Japan.*

References

- [1] Nuclear Damage Compensation and Decommissioning Facilitation Corporation (2022). Technical Strategic Plan 2022 for Decommissioning of the Fukushima Daiichi Nuclear Power Station of Tokyo Electric Power Company Holdings, Inc. https://dd-ndf.s2.kuroco-edge.jp/files/user/pdf/en/strategic-plan/book/20230112_SP2022eFT.pdf
- [2] International Research Institute for Nuclear Decommissioning (2021). R&D for Treatment and Disposal of Solid Radioactive Wastes FY2020 Final Report. https://irid.or.jp/wp-content/uploads/2022/04/IR_for_FY2020_06_RandD_for_Treatment_and_Disposal_of_Solid.pdf

PD-8 OVERVIEW OF THE JAPANESE RADIOACTIVE WASTE DISPOSAL PROJECT

Ayaka Koike⁽¹⁾, Keisuke Ishida⁽¹⁾, Kenichi Kaku⁽¹⁾

(1) Nuclear Waste Management Organization of Japan (NUMO), Japan

In Japan, high-level radioactive waste (HLW) and specific low-level radioactive waste which includes long-lived radionuclides are planned to be disposed of in the geological formations at depths greater than 300 m. The disposal site will be selected through a phased site investigation process that consists of a Literature Survey (LS), Preliminary Investigation (PI) and Detailed Investigation (DI).

The Nuclear Waste Management Organization of Japan (NUMO), the implementer of the geological disposal program, has been soliciting candidate disposal sites from all over Japan since 2002. Considering heavy burden on local government leaders, a new process was added in 2007 to allow the national government to propose municipalities to accept LS. Even adding the process of the Government's proposal, no municipalities had been applied for a LS. In March 2011, the accident at the Fukushima Daiichi NPP occurred as a result of the Great Tohoku Earthquake, causing loss of public trust in both the nuclear technologies and industries. Taking such situation into account, the Government revised the "Basic Policy on Final Disposal of Designated Radioactive Wastes" (hereafter the "Basic Policy on Final Disposal") in 2015, emphasizing that it is necessary to foster both nationwide and regional understanding of the HLW management and the Government is to take the lead in key areas, such as identifying regions that are considered to be scientifically more suitable, providing information to relevant local governments to support their understanding and cooperation etc. In order to contribute to the selection of suitable sites and to provide an opportunity for the general public to recognize and understand the need for final disposal, Ministry of Economy, Trade and Industry (METI) published "the nationwide map of "scientific features" relevant for geological disposal" (hereafter the "Nationwide Map") in 2017. In October 2020, two municipalities in Hokkaido prefecture accepted the LS that is the first phase of the site investigation process and the LS is currently underway.

Continuous evaluation regarding the technical confidence of geological disposal based on the state-of-the-art scientific and technical knowledge is an essential role of an implementer. Although the H12 Report published in 1999 by Japan Nuclear Cycle Development Institute (, now Japan Atomic Energy Agency (JAEA)) had demonstrated the feasibility of geological disposal in Japan, NUMO also needs to show the technical confidence to implement safe geological disposal by integrating required technologies including the latest R&D results since H12 Report. Developing a safety case, that is defined as "a collection of arguments and evidence in support of the safety of a facility or activity (IAEA, 2018)", would be an appropriate way for demonstrating technical confidence of geological disposal implementation, even at a generic stage that candidate sites and a type of host rock have not been determined yet. In addition, while NUMO is conducting LSs at two municipalities, the Government and NUMO continue to promote dialogue throughout Japan to enhance public understanding of geological disposal and to encourage more municipalities to accept an LS. It is thus important for NUMO to explain the methods for assuring safe geological disposal for relevant geological environments and to demonstrate the NUMO's capability to implement the program to a broad range of stakeholders. Therefore, NUMO has developed the "Pre-siting SDM-based Safety Case" (NUMO, 2021) (hereafter the "NUMO Safety Case"), which the site descriptive models (SDMs) provide more advanced site-specific basis than the generic safety case in H12 Report and the "Second progress report on research and development for TRU waste disposal in Japan" (JAEA and The Federation of Electric Power Companies of Japan (FEPC), 2007) (hereafter the "TRU-2 Report").

This was developed in a manner that will allow to provide the basic structure of future safety cases that would be applicable to any site that might arise from the site selection process. The safety case has presented R&D challenges to enhance technical confidence of the project, including R&D topics related

to rock mechanics. It is also expected that the safety case enhances stakeholder confidence in the safe implementation of geological disposal. This report presents the current status of the geological disposal program in Japan, together with the status of the literature survey and an overview of the safety case.

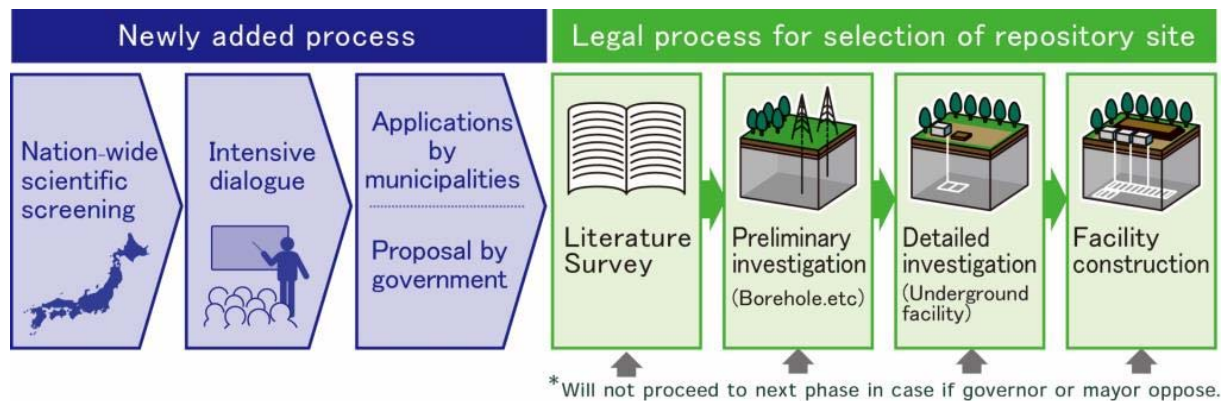


Figure 1: Site selection process in Japan

References

- [1] IAEA (2018). IAEA Safety Glossary, Terminology used in nuclear safety and radiation protection, 2018 Edition.
- [2] JAEA (Japan Atomic Energy Agency) and FEPC (The Federation of Electric Power Companies of Japan) (2007). Second progress report on research and development for TRU waste disposal in Japan, JAEA-Review 2007-010, FEPC TRU-TR2-2007-01.
- [3] NUMO (Nuclear Waste Management Organization of Japan) (2010). The NUMO Pre-siting SDM-based Safety Case, NUMO-TR-21-01.

https://www.numo.or.jp/technology/technical_report/pdf/NUMO-TR21-01_rev220222.pdf

PE-3 MODELING OF HYDROGEOCHEMICAL PROCESSES INFLUENCING URANIUM MIGRATION IN ANTHROPIZED SUB-SAHARAN ENVIRONMENTS

De Windt L.⁽¹⁾, Grizard P.⁽²⁾, Besançon C.⁽²⁾, Seigneur N.⁽¹⁾, Reiller P. E.⁽³⁾, Descostes M.^(1,2)

(1) Mines Paris, PSL University, Geosciences Dpt., France

(2) ORANO Mining, Environmental R&D Dpt., France

(3) Université Paris-Saclay, CEA, Service de Physico-Chimie, France

Sandstone-hosted uranium deposits are economically exploited in the Sahel region. As most sub-Saharan aquifers, the local groundwaters present a strong oxidizing signature shown by relatively high concentrations of redox-sensitive metals such as U, and long lifetimes of O₂ and NO₃. Indeed, low organic matter content and very low water recharge prevent any significant reducing microbiological activity. Determining the baseline of any anthropogenic activity for U, which is usually considered as immobile, is a key issue in such aquifers. In this context, the present study is aiming at modeling the migration of the minor element U in these oxidizing aquifers by underlining the importance of the groundwater chemistry (major elements) and the minerals participating in the regulation of the groundwater chemistry (clays).

The Teloua aquifer, located beneath ore processing facilities of the Cominak mining site (Niger), consists of medium to coarse sandstones, mainly composed of quartz grains whose inter-grain porosity is partially filled by tosudite, an interstratified chlorite/smectite clay with sorption capacities. The modeling is based on data acquired on the Teloua aquifer. The natural water is moderately mineralized, oxidizing, with a pH value close to neutrality, and low carbonate content. The background U concentration is about 20 µg/L. Industrial activities have led to an increase of the U and SO₄ aqueous concentrations located and limited to the perimeter of the mining license through the use of a hydraulic barrier. The acidic pH indirectly induced by sulfuric acid treatment has been neutralized by carbonate minerals from the environment, leading to an additional enrichment in Ca and HCO₃ of the disturbed groundwaters. Therefore, the disturbed groundwater chemistry shows significant variations in dissolved species concentrations (Ca²⁺, HCO₃⁻, SO₄²⁻) that influence U migration.

The evolution of the groundwater chemistry and U migration was modeled with the reactive transport code HYTEC in 1D and 2D simplified geometries. The modeling showed that the clay fraction had a key role in the regulation of water chemistry, including pH buffering. The mitigating factor for SO₄ was gypsum precipitation close to the source term and then dispersion within the aquifer. The main factor of U attenuation seemed to be sorption by tosudite, and not precipitation of a solid phase such as soddyite. U sorption was strongly dependent on the perturbation of the groundwater chemistry. The modeled amount of sorbed U could drop by two or three orders of magnitude under the disturbed water conditions, due to the formation of Ca_nUO₂(CO₃)₃⁽⁴⁻²ⁿ⁾⁻ complexes evidenced with TRLFS acquisition on the sampled waters. This large variability of sorption efficiency was addressed via a sensitivity analysis to uranyl complex speciation and translated in terms of retardation coefficients. Eventually, modeling of the progressive attenuation of the source term suggested the immobilization of anthropogenic U while going back to the natural hydrogeochemistry.

PE-4 HIGHLY SENSITIVE QUANTIFICATION OF AQUATIC NANOPARTICLES BY LIBD

Piscitelli Anne ⁽¹⁾, B chet B atrice ⁽²⁾, Bouby Muriel ⁽³⁾, Courtier-Murias Denis⁽²⁾, Dia Malak ⁽²⁾, Landesman Catherine ⁽¹⁾, Mafaldi Salma ⁽¹⁾, Mallet Clarisse ⁽⁴⁾, Montavon Gilles ⁽¹⁾

(1) SUBATECH, France

(3) LEE, France

(3) KIT, Germany

(4) LMGE, France

All natural aquatic systems contain nanoparticles: they can be inorganic, organic and even include microorganisms. The quantification of these aquatic nano-colloids presents considerable difficulties as they are often present at very low concentrations and with a predominance of the size distribution over small diameters ($d < 100$ nm) [1] [2]. The methods traditionally used for their characterization are based on separation and/or fractionation (ultrafiltration, ultracentrifugation, size exclusion chromatography, Flow Field Fractionation...) but also on static and dynamic light scattering methods. However, these techniques have important limitations: separation and fractionation interfere with the colloidal system and easily lead to changes in the colloidal population (coagulation, sorption and precipitation) while light scattering (LS) has relatively high detection limits for particles with an average diameter of less than about 100 nm.

LIBD (Laser Induced Breakdown Detection) was developed in parallel to the previous analytical techniques [3] [4]. It was invented in the late 1980s for monitoring ultrapure water in the semiconductor industry [5] and was rapidly used and improved for the characterization of synthetic or natural aquatic nano-colloids [6]. This detection method uses a high-energy pulsed laser beam that is focused in the measuring cell to selectively generate a plasma when the solid matter (the colloid) interacts with the high-intensity light (the laser beam). The absorption of photons by the nanoparticles during the laser pulse leads to the heating and expansion of the plasma, which can then be detected acoustically or optically via, respectively, the propagation of the shock wave in the medium or the emitted light.

LIBD allows very sensitive detection at small diameters (from about 5 nm to 1000 nm) and at very low concentrations (from about 1 ng/L to mg/L). This very high sensitivity to small sizes and low concentrations can be seen in Figure 1 where the detection limits of two particle analysis techniques are compared: LIBD versus LS.

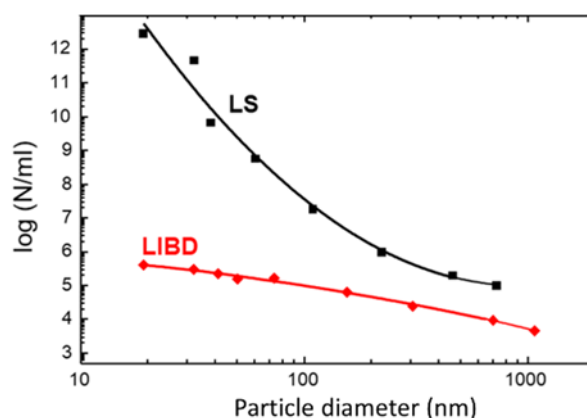


Figure 1: LIBD versus LS, detection limit in particle density [1].

Practically, the L.I.B.D. is not invasive, the analysis is direct (no or little sample preparation) and the measurement can be done in-situ.

The current focus of this technique at Subatech is therefore based on a wide range of colloid characterization studies: nanoparticles in run-off water, platinum nanoparticles from car exhausts in road environments, iron oxide colloids in mining environments. This is directly related to the environmental risk assessment of the transfer of nanoparticles in water and porous media, as these inorganic or organic particles are highly reactive with metals or are themselves metallic particles.

To carry out these studies, the calibration of the technique is performed with different standard dispersions of synthetic nano-colloids, ranging from 20 nm to 1000 nm in diameter, and for concentrations up to ng/L. Then, natural matrices from very different environmental contexts will be studied.

Firstly, samples from a research study within the framework of the ZATU ("Zone Atelier Territoires Uranifères") will be analyzed. The samples of interest come from a contaminated wetland located near a former uranium mine and from different mineral sources. They are of various natures: humic substances, clay colloids and iron oxy-hydroxide in particular and will be also characterized by other analytical techniques: chromatography and thus detection by UV-VIS, Multiple Angle Light Scattering, Refractometer and ICP-MS. The objective is to validate the transition from the use of synthetic standards to the study of natural samples, through the LIBD characterization of these "known" natural samples, and therefore to optimize the results provided by LIBD.

Finally, this work will continue with the analysis of roadway run-off samples containing colloids of natural and anthropogenic origin. These stormwater samples are taken from the Cheviré basin, a retention-infiltration basin that overflows into the Loire: site referenced in the ONEVU- SNO Observil ("Observatoire Nantais des Environnements Urbains - Service National d'Observation Observil"). The sample of interest are characterized using the "Single Particle" mode of an SP-ICP-MS but this technique only allows the characterization of some of the metallic nanoparticles and LIBD will provide access to a range of sizes and concentrations not explored until now. These LIBD results will also complement the chemical data obtained in fractions up to 5 kDa [7] [8]. The objective is thus to characterize these "unknown" samples and to obtain more global information on the occurrence of nanoparticles in run-off water.

The LIBD analytical technique as well as the results obtained in the above-mentioned studies will hence be presented.

References

- [1] Plaschke, M. and al. (2001). Size characterization of bentonite colloids by different methods. *Anal. Chem.* 73: 4338-4347
- [2] Kim, J. I. (1994). Actinide Colloids in Natural Aquifer Systems. *MRS Bulletin* 19: 47
- [3] Bundschuh, T. and al. (2005). Laser-induced Breakdown Detection (LIBD) for the highly sensitive quantification of aquatic colloids. Part I: Principle of LIBD and mathematical model. *Part. Part. Syst. Charact.* 22: 172-180
- [4] Wagner, T. and al. (2005). Laser-induced Breakdown Detection (LIBD) for the highly sensitive quantification of aquatic colloids. Part II: Experimental setup of LIBD and applications. *Part. Part. Syst. Charact.* 22: 181-191
- [5] Kitamori, T. and al. (1989). Detection and counting of ultrafine particles in ultrapure water using laser breakdown acoustic method. *Japanese Journal of Applied Physics* 28 (7): 1195-1198
- [6] Hauser, W. and al. (2002). A mobile laser-induced breakdown detection system and its application for the in situ-monitoring of colloid migration. *Colloids and Surfaces A: Physicochemical and Engineering Aspects* 203: 37-45
- [7] Lange, K. and al. (2020). Metal speciation in stormwater bioretention: Removal of particulate, colloidal and truly dissolved metals. *Science of The Total Environment* 724: 138121.
- [8] Béchet, B. and al. (2009). *Size Fractionation of Heavy Metals in Highway Runoff Waters*. Highway and Urban Environment, Springer Netherlands, Dordrecht

PE-5 BACTERIAL DIVERSITY DOWNSTREAM FROM A FORMER URANIUM MINE AND IN WATERS FROM NATURALLY RADIOACTIVE MINERAL SOURCES: POTENTIAL ROLE ON URANIUM MIGRATION IN THE ENVIRONMENT

Sergeant Claire¹, Holub Guillaume¹, Mallet Clarisse², Vesvres Marie-Hélène¹, Beauger Aude³, Chardon Patrick⁴, del Nero Mireille⁵, Courson Olivier⁵, Montavon Gilles⁶, Breton Vincent⁴

(1) *Laboratoire de Physique des 2 Infinis Bordeaux (LP2IB), Gradignan, France*

(2) *LMGE, Aubière, France*

(3) *GEOLAB, Clermont-Ferrand, France*

(4) *LPC Aubière, France*

(5) *IPHC, Strasbourg, France*

(6) *Subatech, Nantes, France*

all members of LTSER “Zone Atelier Territoires Uranifères”

Microorganisms are the first living beings to have appeared on Earth, and populate many habitats, including the most extreme. Among these environments, some are characterized by naturally high levels of radiation where microorganisms have developed over thousands of years by adopting various strategies to respond to the stresses induced by ionizing radiation [1].

The Massif Central is a region made up of uranium-rich geological formations (granite massif), well known for its naturally radioactive mineral sources but also for these former uranium mining sites. Microbial inhabitants of natural uranium enriched environment exhibit various adaptive features to support their growth and survival, giving rise to uranium tolerant populations in such sites [2].

In TIRAMISU and INSPECT projects from the “Zone Atelier Territoires Uranifères (ZATU)”, we try to understand the effects of radioelements (radiation / chemical toxicity) on microbial communities from a diverse range of naturally radioactive mineral springs in the French Massif Central, and in sites near a former uranium mine (Rophin).

In this study, we focused on the study of samples from six naturally radioactive mineral springs of varying radioelement concentration gradient (<3.71 ppb U) in the Massif Central sampled in autumn, and of soil core samples from a wetland downstream of the old Rophin mine, characterised by a uranium-rich layer (>1200 ppm U).

The bacterial biodiversity of these samples was characterized by next generation sequencing (Illumina Miseq), targeting the 16S rRNA gene. In addition, the influence of the different physico-chemical parameters on these bacterial communities was studied. The results highlight the presence of bacterial populations specific to the environments most charged with uranium.

To understand how these bacteria have adapted to these particular conditions, a culture on non-selective medium was performed for samples from these six mineral springs and a seventh with a higher concentration of uranium (15.91 ppb U); and from samples of the soil core of the wetland downstream of the former mine site. A collection of several hundred bacterial strains has been formed and identified, many of which are close to species known to be radioresistant.

Some of these bacteria have been studied for their potential resistance and interaction with uranium. Indeed, the diversity of mechanisms used to resist high concentrations of uranium and other metals

(biosorption, bioaccumulation, bioreduction, biomineralization) suggests that bacteria from these environments may have an impact on the migration and the toxicity of these elements into the environment.

All the results of these two studies will be presented and discussed.

References

- [1] Shuryak, I. (2019). Review of Microbial Resistance to Chronic Ionizing Radiation Exposure under Environmental Conditions. *J. Env. Rad.* 196: 50-63
- [2] Chandwadkar, P., Hari Sharan M., and Acharya C. (2018). Uranium Biomineralization Induced by a Metal Tolerant *Serratia* Strain under Acid, Alkaline and Irradiated Conditions. *Metallomics* 10 (8): 1078-88

A5-5 ELECTROSTATIC INTERACTIONS AT CLAY MINERAL SURFACES: AT THE CROSSROADS BETWEEN MINERALOGY, GEOCHEMISTRY, AND GEOPHYSICS

Christophe Tournassat

ISTO, University of Orléans, France;

EESA, Lawrence Berkeley National Laboratory, USA

Clayey materials show a remarkable array of desirable macro-scale properties such as very low permeability, strong adsorption, semi-permeable membrane properties, and high swelling pressure, which lead to slow advective transport rates, contaminant retardation, limited diffusion for anions, and self-sealing of fractures. These properties arise from the interactions of charged mineral surfaces with water and solutes present in the nanopores of these materials, among which electrostatic interactions often play a dominant role.

The study of interactions between water molecules, ions, and individual clay mineral surfaces remains an intense field of research, providing a basic understanding to build predictive models for the simulation of clayey material behavior as a function of physical and chemical forcing. However, the behavior of nanoporous clay environments is complicated by the fact that the pore structure of clay materials, but also the surfaces and compositions of clay minerals, are heterogeneous, and that water and ions can be present in bulk water, incorporated within interlayer spaces, adsorbed to external surfaces, whether at basal or edge surfaces, or located within the electrical double layer. Mutual interactions between these system components lead to highly coupled processes and these couplings manifest themselves in macroscopic observations up to geological formation scale. To understand and predict the coupling phenomena, a preferred approach is usually built on the following sequence:

- i) to examine the physical processes at the molecular and pore scale
- ii) to up-scale the physical laws toward the continuum scale, and
- iii) to compare continuum scale model predictions to geophysical and geochemical observables.

My talk will address some of the challenges related to this type of upscaling strategy focusing on the role of electrostatic interactions on clay minerals properties related to adsorption processes and diffusion.

A5-6 U(VI) SORPTION ON ILLITE IN THE PRESENCE OF CARBONATE STUDIED BY CRYOGENIC TIME-RESOLVED LASER FLUORESCENCE SPECTROSCOPY AND PARALLEL FACTOR ANALYSIS: COMPARISON WITH TRIVALENT LANTHANIDES*

Huiyang Mei⁽¹⁾, Noboru Aoyagi⁽¹⁾, Takumi Saito⁽²⁾, Yuki Sugiura⁽³⁾, Takamitsu Ishidera⁽³⁾, Kazuya Tanaka⁽¹⁾, Yukio Tachi⁽³⁾

(1) *Advanced Science Research Center, Japan Atomic Energy Agency, Japan*

(2) *Nuclear Professional School, School of Engineering, The University of Tokyo, Japan*

(3) *Nuclear Fuel Cycle Engineering Laboratories, Japan Atomic Energy Agency, Japan*

Deep geological disposal has been accepted worldwide as a potential and promising choice for disposing of high-level nuclear wastes. The knowledge of the immobilization mechanism of radionuclides along the migration pathways is one of the bases on which the quantification of the transport of radionuclides relies. Particularly, the presence of dissolved inorganic carbon (DIC) in sedimentary groundwater (> 2,000 mg/L as HCO_3^- in some cases) may inhibit the sorption of radionuclides on minerals obviously. However, even in the presence relatively high concentration of DIC, metal ions could sorb to rock surface by the formation of ternary surface complexes, which is only justified by analytical technique sensitive to surface speciation [1]. However, further development and more credibility of the sorption reaction models rely on identifying the sorption species on rock surfaces. Herein, the sorption of U(VI) on illite at different pH (7.4 - 10.9) and DIC levels (0.90 – 18.75 mM) was investigated by using the batch sorption technique, surface complexation modeling, and the cryogenic time-resolved laser fluorescence spectroscopy (cryo-TRLFS) with Parallel Factor Analysis (PARAFAC) [2]. The results of U(VI) were also compared with those of two trivalent lanthanides (Eu(III) and Sm(III)), which are common chemical analogs of trivalent actinides.

Sorption experiments of U(VI) on illite in the presence of DIC were conducted under ambient conditions. Aliquots of NaCl, carbonate, and NaOH stock solutions were added into the centrifuge tubes first, followed by adding aliquots of an acidified U(VI) stock solution little by little, and then the residual desired carbonate stock solutions. Afterward, the weighed pretreated illite was added into the tube, followed by adjusting the pH value. The tubes were then shaken for seven days, followed by pH measurement, centrifugation and filtration. The U(VI) concentrations were analyzed by using an inductively coupled plasma - mass spectrometry instrument. The residual solids were freeze-dried and subsequently analyzed by using the Nd:YAG laser with an excitation wavelength of 360 nm at near liquid Helium temperature. The fluorescent decay spectra with different delay times were recorded. The shape and decay lifetime of the normalized spectra after background subtraction were analyzed and compared. Those spectra were also combined and analyzed by using the PARAFAC method embedded in the *N*-way Toolbox for MATLAB [3].

The obvious inhibition effect of DIC on U(VI) sorption was revealed from the macroscopic batch experimental results, which was also observed for Eu(III)/Sm(III) sorption. The updated 2-site protolysis non-electrostatic surface complexation and cation exchange model considering the formation of two uranyl-carbonate sorption complexes was able to reproduce the experimental results well. The variation of the sorption species as a function of the DIC level was also provided by the modeling process. Based on the PARAFAC analysis on the cryo-TRLFS spectra, three components were differentiated (Figure 1). In addition, there is clear correspondence in the variation of the sorption species between the modeling and spectroscopic analysis results. The formation of ternary uranyl-carbonate sorption complexes was successfully identified. As for the modeling of Eu(III) sorption, it was also necessary to consider the formation of Eu-carbonate sorption complexes, which was confirmed by the PARAFAC analysis on the TRLFS spectra at room temperature. Identification of the sorption species adds more credibility to the predictive sorption model, which provides more confidence in the safety assessment of deep geological disposal. In addition, these results help better understand the fate and transport of radionuclides in natural environments.

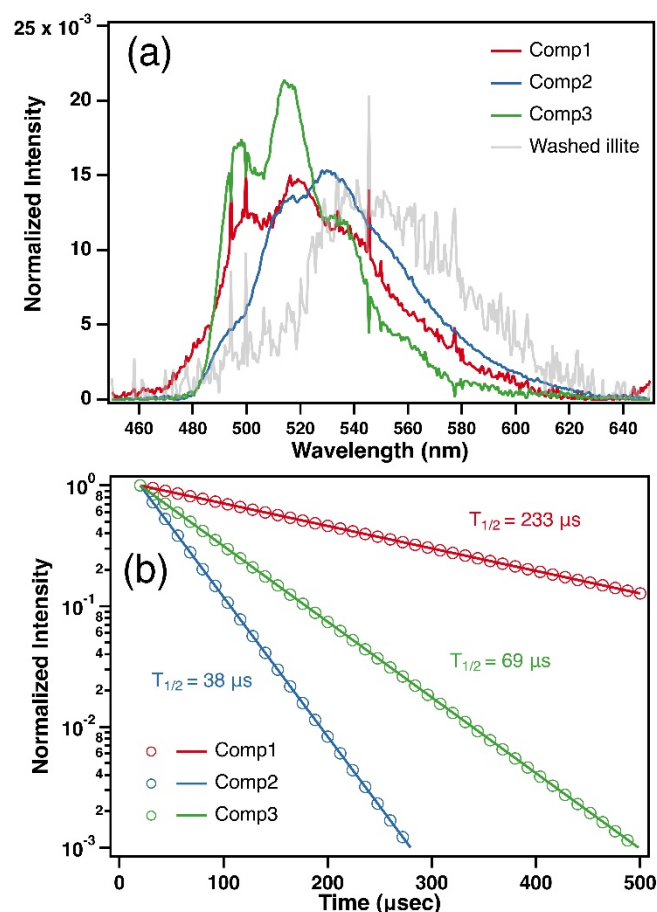


Figure 1. The PARAFAC-decomposed fluorescence spectra (a) and decay curves (b) of the sorption samples of U(VI) on illite in the presence of DIC.

Acknowledgement: This work was part of “The project for validating near-field system assessment methodology in geological disposal (FY2020-2022, JPJ007597)” supported by the Ministry of Economy, Trade and Industry of Japan.

References

- [1] Mei, H., Aoyagi, N., Saito, T., Kozai, N., Sugiura, Y. and Tachi, Y. (2022). Uranium (VI) sorption on illite under varying carbonate concentrations: Batch experiments, modeling, and cryogenic time-resolved laser fluorescence spectroscopy study. *Appl. Geochem.* 136: 105178.
- [2] Ishida, K., Saito, T., Aoyagi, N., Kimura, T., Nagaishi, R., Nagasaki, S. and Tanaka, S. (2012). Surface speciation of Eu^{3+} adsorbed on kaolinite by time-resolved laser fluorescence spectroscopy (TRLFS) and parallel factor analysis (PARAFAC). *J. Colloid Interface Sci.* 374(1): 258-266.
- [3] Andersson, C. A. and Bro, R. (2000). The N-way Toolbox for MATLAB. *Chem. Intell. Lab. Syst.* 52: 1-4.

A5-7 RETENTION OF SILVER IN CEMENTITIOUS MATERIALS

Macé Nathalie, Page Jacques

(1) Université Paris-Saclay, CEA, Service de Physico-Chimie, 91191 Gif-sur-Yvette, France

Evaluation of the capability of retention of toxic or radionuclide species are a major concern for radioactive waste management. As the radioactive isotope ^{108m}Ag ($T_{1/2} = (438 \pm 9)$ years) is present in some specific waste packages, in which cement-based matrices are considered for stabilization. Solubility of silver in alkaline conditions is well known. In particular, the concentration of Ag is limited in presence of hydroxide, chloride and carbonate ion by the precipitation of AgOH , AgCl and Ag_2CO_3 , respectively. However, there is a lack of knowledge concerning its retention in cementitious media.

Experimental work consisted in determining the distribution ratio (R_d) of silver in batch-suspensions prepared from a large panel of physico-chemical conditions *i.e.* various cement-based materials and a pH value of the equilibrium solution ranging from 9 to 13.5. The effect of the presence of chloride and carbonate ions was also investigated. These conditions have been selected to simulate different alteration states of cementitious matrices from fresh state (pH 13.5) to carbonated state (pH 9). Silver behavior has been reached by using a radio-labelled tracer: ^{110m}Ag ($\gamma : 657,8$ keV). In these conditions, it has been possible to reach $3 \cdot 10^{-11}$ mol/L as quantification limit of Ag by γ counting (Wizard², PerkinElmer), which is sufficient for retention experiments.

The Figure 1 corresponds to the evolution of the R_d values as a function of the concentration of silver in solution after equilibrium for suspensions prepared with concrete at pH 13.5; hydrated cement paste (HCP) at pH 13.5 and pH 11; tobermorite-11Å at pH 11, calcareous aggregate at pH 9 and calcite at pH 9.

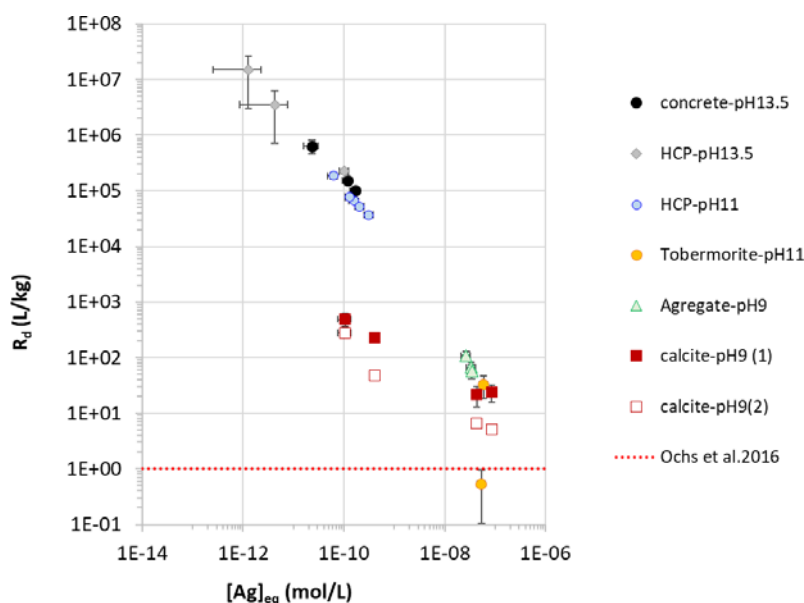


Figure 1: Distribution ratio values obtained for silver in contact with different cementitious matrices compared to literature data [1]

These results suggest a significant retention of silver in the investigated cementitious matrices regardless of the chloride ion concentration investigated, the pH value or the presence of carbonate ions in the cement system. With alteration of the cement-matrices, the R_d values are decreasing but still enough high to significantly delay the migration of silver out of the waste-package. This study confirms that the initial evaluation of the R_d , based from a literature review [1] - where a range of 0 to 1 L/kg is considered

as best R_d value for silver as a function of alteration state of the cement-based matrix– is largely underestimated. Those newly results will be considered by Andra for performance assessment calculations.

Acknowledgement: *This work received financial support from the French National Agency for Radioactive Waste Management (Andra).*

References

- [1] Ochs, M., Mallants, D., Wang, L., (2016) Radionuclide and metal sorption on cement and concrete. Topics in safety, Risk, reliability and Quality, Springer. Ed. Springer International Publishing, Switzerland.

A5-8 ANALYSIS OF COBALT RETENTION BY NA- AND CA- SMECTITE AND THE EFFECT OF EDTA PRESENCE

Tiziana Missana, Ursula Alonso, Miguel García-Gutiérrez

CIEMAT - Physical Chemistry of Actinides and Fission Products Unit, Avenida Complutense 22, 28040 Madrid (Spain)

Radiocobalt is widely used as gamma-ray source for nuclear medicine or sterilization, furthermore, ^{60}Co can be formed by neutron activation of the stable ^{59}Co existing in structural materials (stainless steel and other important alloys) of nuclear reactors, and it may be present in nuclear facilities and their liquid effluent discharges. Even the mean life of ^{60}Co is not very large (5.27 years), the emission of high energy gamma rays cause problems in decommissioning or decontamination activities.

The remediation of soils or materials from nuclear facilities is often carried out with organics, and ethylenediaminetetraacetic acid, EDTA, amongst others, because their strong capability of complexing metals [1, 2]. However, metals coordinated with organics form very stable aqueous complexes, reducing their adsorption, enhancing their mobility, causing a significant environmental hazard. Co-EDTA complexes have been of concern because they are toxic, produced radiocobalt mobilization from waste sites and because they are very difficult to degrade or be removed from solutions [3].

The objectives of this study are: 1) to analyze the adsorption of ^{60}Co in Na- and Ca- smectite under a wide range of experimental conditions (pH, ionic strength, Co concentration, presence of carbonates) to develop an integral sorption model; 2) to evaluate the presence of EDTA on Co adsorption considering the possible role of the main smectite exchanging cations; 3) to model Co adsorption in the presence of EDTA and 4) to appraise methodologies to improve Co-EDTA retention in clayey materials.

The first part of the study was carried out with the homoionised (in Na and in Ca) FEBEX bentonite, which has been widely characterized in the past. Figure 1 shows an example of adsorption tests obtained with the Na-clay at the ionic strength of 0.1 M (in NaClO_4) under anoxic conditions (N_2 atmosphere).

Figure 1a shows an example of the adsorption edges and Figure 1b shows an example of sorption isotherm. The continuous lines correspond to the modelling calculations considering a similar approach as that previously adopted for another transition metal (Cd), which considers cationic exchange and the metal complexation on the weak and strong sites of the clay [4].

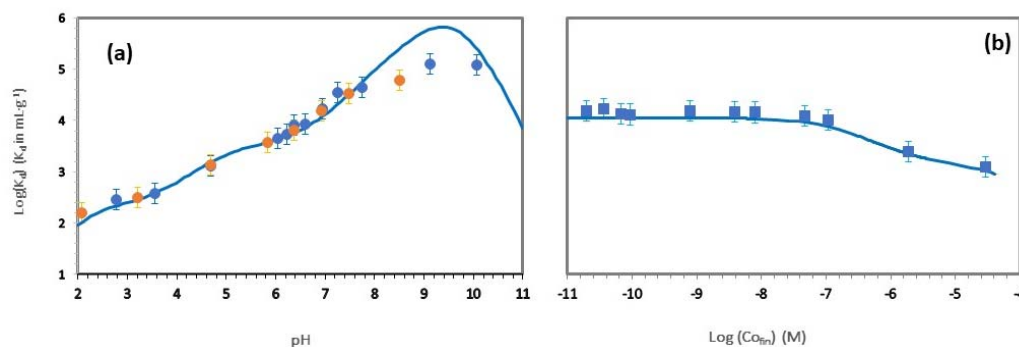


Figure 1: Sorption tests in the Na-clay at 0.1 M NaClO_4 under anoxic conditions. **a)** adsorption edges. Blue dots: $[\text{Co}] = 8.6 \cdot 10^{-10}$ M, $1.35 \text{ g}\cdot\text{L}^{-1}$; orange dots $[\text{Co}] = 7.6 \cdot 10^{-10}$ M, $2.7 \text{ g}\cdot\text{L}^{-1}$; **b)** adsorption isotherm at pH 6.9, $1.35 \text{ g}\cdot\text{L}^{-1}$. The line corresponds to modelling calculations.

The second part of the study was carried out with homoionised and raw clays under oxic conditions. As raw clays, additionally to the FEBEX bentonite, MX-80 (natural Na-clay) and SAZ-1 (natural Ca-clay) were selected. Both adsorption edges and isotherms were carried out on the natural clays using NaClO_4 or $\text{Ca}(\text{ClO}_4)_2$ as suspending electrolyte, depending on the main natural exchanging ion. The model developed for the homoionised FEBEX was used to interpret sorption data in the raw clays, accounting for the respective surface properties, and to calculate the K_d without and with EDTA ($1 \cdot 10^{-4}$ M). Figure 2 shows an example of the sorption isotherms obtained in the MX-80 (Fig.2a) and the SAZ-1 (Fig.2b).

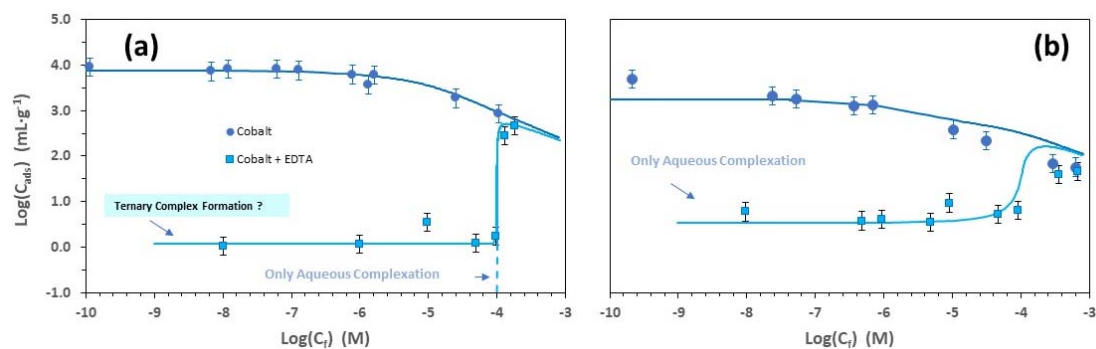


Figure 2: Sorption isotherms without and with the presence of EDTA ($1 \cdot 10^{-4}$ M) under oxic conditions: **a)** MX-80 in NaClO_4 0.1, pH 8; **b)** SAZ-1 in $\text{Ca}(\text{ClO}_4)_2$ 0.033 M pH 6.5-7.

The decreasing of Co retention in the presence of EDTA is notable (3-4 orders of magnitude) in both cases, but the presence of Ca slightly reduces the effect of the chelate and improves metal retention in the presence of EDTA. Modelling indicates a very good agreement with the experimental data in the SAZ-1 clay, only considering the Co-EDTA aqueous complexation. In the case of MX-80, the predicted sorption value in presence of EDTA would be null (representing a large difference with the data expressed in a logarithmic scale, even not quantitative); the small (but not null) adsorption of EDTA in the clays could explain the experimentally observed behavior.

Acknowledgements: This research has received funding from the European Union's Horizon 2020 research and innovation programme under grant agreement number 847593 (**EURAD**) and from the Spanish Ministry of Innovation and Science (PID2019-106398GB-I00, **ARNO Project**).

References

- [1] Mahmoud, M.R., Soliman, M.A., Rashad, G.M., (2017). Performance appraisal of foam separation technology for removal of Co(II)-EDTA complexes intercalated into in-situ formed Mg-Al layered double hydroxide from radioactive liquid waste. Chem. Eng. J. 326, 781–793.
- [2] Borggaard, O.K., Holm, P.E., Strobel, B.W., (2019). Potential of dissolved organic matter (DOM) to extract As, Cd, Co, Cr, Cu, Ni, Pb and Zn from polluted soils: A review. Geoderma 343, 235–246.
- [3] Malinen, L., Repo, E., Harjula, R., Huittinen, N., (2022). The effect of UV-C irradiation and EDTA on the uptake of Co^{2+} by antimony oxide in the presence and absence of competing cations Ca^{2+} and Ni^{2+} . Nucl. Eng. Technol. 54, 627–636.
- [4] Missana, T.; Alonso, U., Mayordomo, N.; García-Gutiérrez, M., Analysis of Cadmium Retention Mechanisms by a Smectite Clay in the Presence of Carbonates. (2023) Toxics, 2023, 11, 130.

A5-9 ACTINIDE ADSORPTION TO HEMATITE AT ELEVATED TEMPERATURES

Shanna L. Estes,^(1,2,3) Salomé Kwong-Moses,^(2,3) Fanny M. Coutelot,^(2,3) Brian A. Powell^(1,2,3)*(1) Department of Chemistry, Clemson University, USA**(2) Department of Environmental Engineering and Earth Sciences, Clemson University, USA**(3) The Center for Nuclear Environmental Engineering Sciences and Radioactive Waste Management, Clemson University, USA*

Understanding the influence of temperature on actinide adsorption reactions is an important component of modeling and predicting the long-term fate of actinides in the environment. This is particularly true (1) for assessing the performance of proposed geologic repositories, as many concepts predict an increase in local repository temperature (up to ~ 100 °C),¹ and (2) for predicting behavior of actinides (and other metal ions) in natural environments, where temperatures vary widely, depending on, e.g., geography and geologic depth. Including temperature effects in models of metal ion adsorption is a difficult task, however, as there are myriad temperature-dependent physicochemical processes that occur simultaneously in aqueous heterogeneous systems, making it difficult to tease out the specific effects of increased temperatures on actinide reactions at the solid-water interface. Further complicating this issue is the general lack of thermodynamic data describing surface reactions at elevated temperatures. In this work, we address these needs by combining data from numerous batch adsorption and calorimetry studies to systematically probe and model actinide adsorption on hematite. Specifically, surface complexation modeling is used to describe Eu(III) (as an analog of trivalent actinide ions), Th(IV), U(VI), Np(V), and Pu(V/VI) adsorption on hematite as a function of pH, ionic strength, and temperature. In addition, a detailed examination of hematite surface chemistry across a range of ionic strengths and temperatures provides the necessary foundation for isolating the influence of temperature on actinide specific surface reactions.

In general, increasing temperature causes an increase in actinide adsorption to hematite. For Eu(III)² and for U(VI),³ increased adsorption results from the entropically favorable displacement of water molecules from the metal ion primary hydration sphere and the hematite surface upon adsorption. For Th(IV), a similar increase in adsorption at elevated temperatures is observed (Figure 1, top), but surface complexation modeling indicates that the enthalpy of the best-fitting surface reaction is close to zero, suggesting that the increase in adsorption is driven by factors other than endothermic Th(IV) surface complexation. For Pu(V/VI), preliminary data indicate that adsorption onto hematite increases from 25 to 50 °C, then remains unchanged or decreases at 65 and 80 °C. This complicated behavior may result from Pu redox chemistry, including surface mediated Pu reduction. Continued data collection and surface complexation modeling are necessary to further understand the influence of temperature on Pu(V/VI) adsorption. For Np(V), the adsorption behavior also exhibits a curious reversal, with adsorption increasing from 15 to 50 °C (Figure 1, bottom), but then decreasing at 80 °C (data not shown). Increasing the ionic strength in the Np(V) system from 0.01 to 1 M NaCl gives Np data in which adsorption decreases with increasing temperature. For the weakly adsorbing Np(V) cation, these data suggest the possible formation of a NpO_2Cl aqueous species or an increased

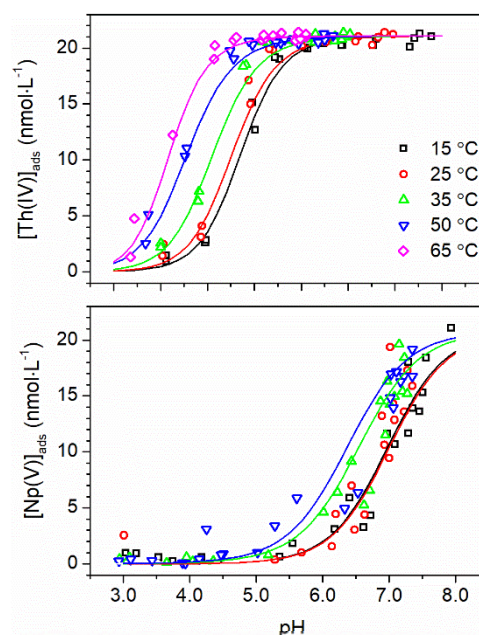


Figure 1. Th(IV) (top) and Np(V) (bottom) adsorption on hematite as a function of pH and temperature ($[\text{Th(IV)}]_{\text{TOT}} = 2.11 \times 10^{-8}$ M, $[\text{Np(V)}]_{\text{TOT}} = 2.09 \times 10^{-8}$ M, $I = 0.01$ M NaCl). Solid lines are the corresponding best-fit surface complexation models (single-site DLM), which represent the surface complexes: $\equiv\text{FeOHTh}^{4+}$; $\equiv\text{FeONpO}_2^0$ at 15 and 25 °C; and $\equiv\text{FeOHNpO}_2^+$ at 35 and 50 °C.

competition of electrolyte cations (Na^+) for hematite surface sites. The specific adsorption of sodium cations on the hematite surface is confirmed from an in-depth study of hematite surface charging at various temperatures and ionic strengths. In the absence of actinide ions, the surface complexation model that best fits the extensive hematite potentiometric and calorimetric titration data requires inclusion of an inner-sphere sodium surface complex. The modeling results indicate that although the formation of this sodium surface complex is weak ($\log K \approx -14$), it is also strongly endothermic ($\Delta H \approx >90 \text{ kJ mol}^{-1}$), suggesting that formation of this sodium surface complex is only relevant at high sodium concentrations or high temperatures.

Combining the adsorption data above indicates that actinide adsorption processes cannot be well-described with empirical models that fail to account for changes in surface speciation at varied temperatures and ionic strengths. Future work will further use these modeling results to examine discrepancies and variations in published actinide adsorption data and trends in actinide adsorption behavior. It is expected that the holistic and self-consistent model of actinide adsorption to hematite developed through this work will provide a means to more deeply understand the relative role that specific surface chemistry, aqueous conditions, temperature, and specific metal ion chemistry play in driving surface complexation reactions.

References

- [1] *Yucca Mountain Science and Engineering Report, Rev. 1* (2002). DOE/RW-0539-1; U.S. Department of Energy, Office of Civilian Radioactive Waste Management: North Las Vegas, NV,.
- [2] Estes, S. L.; Arai, Y.; Becker, U.; Fernando, S.; Yuan, K.; Ewing, R. C.; Zhang, J.; Shibata, T.; Powell, B. A. (2013). A Self-Consistent Model Describing the Thermodynamics of Eu(III) Adsorption onto Hematite. *Geochim. Cosmochim. Acta* 122:430–447.
- [3] Estes, S. L.; Powell, B. A. (2020) Enthalpy of Uranium Adsorption onto Hematite. *Environ. Sci. Technol.* 54:15004–15012.

A4-1 EFFICIENT PHOTOREDUCTION STRATEGY FOR URANIUM IMMOBILIZATION BASED ON GRAPHITE CARBON NITRIDE HETEROJUNCTION NANOCOMPOSITESShuyang Li ⁽¹⁾⁽²⁾, Duoqiang Pan ⁽¹⁾, Wangsuo Wu ⁽¹⁾*(1) School of Nuclear Science and Technology (Lanzhou University), No. 222 South Tianshui Road, Lanzhou 730000, Gansu Province, P. R. China**(2) School of Environment and Resource, Southwest University of Science*

The effective treatment of uranium-containing wastewater and recovery of aqueous uranium resources is essential for the sustainable development of nuclear energy. Uranium mainly exists in a soluble hexavalent state in aerobic aqueous solution; however, insoluble tetravalent species are dominant under reducing conditions[1]. Therefore, a reduction strategy has been proposed for the efficient immobilization of uranium by constructing a reducing adsorbent and reducing the permeable reactive barrier. Recent work revealed that uranium could be reduced to an insoluble state by photogenerated electrons[2, 3]; therefore, designing and constructing photocatalysts for efficient uranium recovery has drawn the attention of researchers. A g-C₃N₄ semiconductor with an energy gap of 2.7 eV has a terrific response to visible light, enabling the utilization of sunlight for feasibly reducing U(VI). The conduction band (CB) position of g-C₃N₄ is -1.23 V (vs. SHE at pH 7.0), which is more negative than the reduction potential of UO₂²⁺/U⁴⁺ (0.267 V) and UO₂²⁺/UO₂ (0.411 V). Accordingly, the photocatalytic U(VI) reduction is thermodynamically feasible[4]. However, the photocatalytic activity of g-C₃N₄ is limited due to the slow mobility of surface carriers and the fast recombination of photogenerated electron-hole pairs. This defect is effectively improved by constructing heterojunction structures because their binding structure can accelerate the transfer of surface charges, suppress the rapid recombination of electrons and holes, and prolong the lifetime of the carriers.

Here, we successfully developed a novel type of graphite carbon nitride/perovskite-type oxide heterojunction for the effective photoreduction of U(VI)[5]. The DFT calculation results revealed that the interaction between g-C₃N₄ and LaFeO₃ in the g-C₃N₄/LaFeO₃ heterojunction system was caused by the hybridization of Fe 3d, O 2p, C 2p and N 2p from -7.5 eV to -2.5 eV. The PL spectra and time-resolved PL spectra showed that the recombination of photogenerated carriers was effectively suppressed and their lifetimes were significantly prolonged, and the resulting strong reduction ability improved the U(VI) removal efficiency (extraction capacity: 0.4 mM, 460 mg/g). The photocatalysis experiments under real seawater conditions provided further possibilities for practical application. XPS and XANES analyses were used to identify the species of extracted uranium, which proved the reduction of U(VI). Moreover, the electron spin resonance (ESR) analysis and quenching experiments implied that both e⁻ and ·O₂⁻ were beneficial to the photoreduction of U(VI). More importantly, this work not only provides new strategies and insights for the photoreduction of U(VI) but also broadens the horizon for the use of perovskite materials as catalysts.

Although the g-C₃N₄/LaFeO₃ heterostructure effectively alleviates the problem of rapid recombination of photogenerated electron-hole pairs, the visible light response is still not ideal. Furthermore, the complex composition in seawater or the organic matter in uranium-containing wastewater severely restricts the separation of U(VI). Therefore, to enhance the visible light response of the catalyst, we developed a carbon nitride/ceria (CN-CeO_{2-x}) heterojunction with a type II band structure rich in oxygen vacancies based on the heterojunction-defect synergistic modification strategy, used for photoreduction of U(VI) in organic radioactive wastewater under visible light[6]. Kinetic characterization and density functional theory (DFT) imply that the photoelectrons were transferred from g-C₃N₄ to CeO_{2-x} through the built-in electric field generated by the heterostructure and were trapped by shallow traps generated by surface vacancies to achieve spatial separation. The tremendously enhanced separation rates and lifetime (~125 %) of photoinduced carriers grant the exceptionally improved photocatalytic activity for

U(VI) reduction (up to a 39-fold increase over the bulk $g\text{-C}_3\text{N}_4$). The as-prepared $\text{C}_3\text{N}_4\text{-CeO}_{2-x}$ exhibits good resilience to a variety of competing ions and over a wide range of pH values, thus it maintains excellent performance in uranium-spiked seawater and the organics (RhB) contained water. X-ray absorption fine structure (XAFS) analysis reveals that the reduction and inner-sphere surface complexation contributed to uranium immobilization. The catalytic efficiency of the two catalysts remained relatively high after being used repeatedly 5 times, indicating that the two photocatalysts have good cost-effectiveness and applicability. In short, the proposed carbon nitride-based heterojunction composites provide a promising strategy for using inexhaustible solar energy to recover uranium resources.

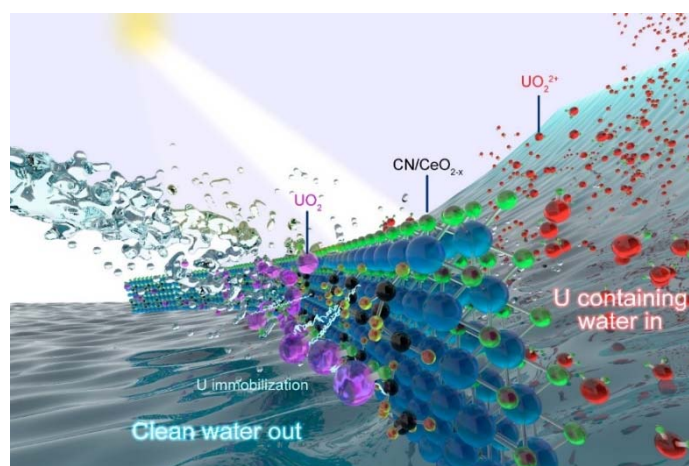


Figure 1. Schematic of the photoreduction separation of U(VI) by CN-CeO_{2-x} heterojunction.

References

- [1] H. Zhang, W. Liu, A. Li, D. Zhang, X. Li, F. Zhai, L. Chen, L. Chen, Y. Wang, S. Wang (2019). Three mechanisms in one material: uranium capture by a polyoxometalate-organic framework through combined complexation, chemical reduction, and photocatalytic reduction. *Angew. Chem., Int. Ed.* 58: 16110-16114.
- [2] Y. Song, A. Li, P. Li, L. He, D. Xu, F. Wu, F. Zhai, Y. Wu, K. Hu, S. Wang, M.V (2022). Sheridan, Unassisted uranyl photoreduction and separation in a donor-acceptor covalent organic framework. *Chem. Mater.* 34: 2771-2778.
- [3] S. Li, Z. Niu, D. Pan, Z. Cui, H. Shang, J. Lian, W. Wu (2022). Efficient photoreduction strategy for uranium immobilization based on graphite carbon nitride/activated carbon nanocomposites. *Chinese Chem. Lett.* 33: 3581-3584.
- [4] J. Wang, Y. Wang, W. Wang, Z. Ding, R. Geng, P. Li, D. Pan, J. Liang, H. Qin, Q. Fan (2020). Tunable mesoporous $g\text{-C}_3\text{N}_4$ nanosheets as a metal-free catalyst for enhanced visible-light-driven photocatalytic reduction of U(VI). *Chem. Eng. J.* 383: 123193.
- [5] S. Li, X. Yang, Z. Cui, Y. Xu, Z. Niu, P. Li, D. Pan, W. Wu (2021). Efficient photoreduction strategy for uranium immobilization based on graphite carbon nitride/perovskite oxide heterojunction nanocomposites. *Appl. Catal., B.* 298: 120625.
- [6] S. Li, D. Pan, Z. Cui, Y. Xu, H. Shang, W. Hua, F. Wu, W. Wu (2022). Synergistic effects of oxygen vacancies and heterostructures for visible-light-driven photoreduction of uranium. *Sep. Purif. Technol.* 301: 121966.

A4-2 URANIUM(VI) REDUCTION BY A *DESULFITOBACTERIUM* SPECIES IN PURE CULTURE AND IN ARTIFICIAL MULTISPECIES BIO-AGGREGATES

Stephan Hilpmann⁽¹⁾, Isabelle Jeschke⁽¹⁾, Dmitrii Deev^(2,3), Maja Zupan^(2,3), Aleš Lapanje⁽²⁾, Tomaž Rijavec⁽²⁾, René Hübner⁽⁴⁾, Frank Bok⁽¹⁾, Stefan Schymura⁽⁵⁾, Andrea Cherkouk⁽¹⁾

(1) Helmholtz-Zentrum Dresden-Rossendorf, Institute of Resource Ecology, Dresden, Germany

(2) Jožef Stefan Institute, Department of Environmental Sciences, Ljubljana, Slovenia

(3) Jožef Stefan International Postgraduate School, Ljubljana, Slovenia

(4) Helmholtz-Zentrum Dresden-Rossendorf, Institute of Ion Beam Physics and Materials Research, Dresden, Germany

(5) Helmholtz-Zentrum Dresden-Rossendorf, Institute of Resource Ecology, Research Site Leipzig, Leipzig, Germany

The reduction of highly mobile and water-soluble U(VI) to less mobile U(IV) represents a key process influencing the migration of this radionuclide in the environment. Microorganisms such as for example iron and sulfate-reducers are capable of reducing U(VI) under various conditions. This interaction mechanism between microbes and U could play an important role in a final disposal site for high-level radioactive waste deposited in deep geological layers. Different host rocks are suitable for the long-term storage of nuclear waste, e.g. clay formations, crystalline rock and rock salt. Besides the geochemical, geophysical and geological properties of such a repository, little is known about the influence of naturally occurring microorganism on the safety of such a site. In a worst-case scenario, if water enters the repository, radionuclides can get distributed in the surrounding host rock and thus interact with the native microorganisms, potentially leading to an immobilization of radionuclides via bioreduction. Furthermore, a reduction of U(VI) could also play an important role in the development of different bioremediation approaches for radionuclide-contaminated environments. As a potential component of new remediation strategies, we introduce the use of artificial bio-aggregates of different bacterial genera. By the use of these artificial biofilms' insights into the complex interactions in a multi-species environment can be obtained. In this study, we used derivatized polyelectrolytes to form aggregates of two different microorganisms to connect advantageous properties of the microorganisms in a complementary way and to investigate the reduction of U(VI) under different conditions.

Desulfitobacterium sp. G1-2 was chosen as an important representative of iron-reducing bacteria in anaerobic environments. This bacterial strain was isolated from bentonite samples of the Full-scale Engineered Barrier Experiment – Dismantling Project (FEBEX-DP) at the Helmholtz Center Dresden-Rossendorf. Bentonites are supposed to serve as a possible backfill material, not only for a final disposal site in clay formations but also in crystalline rock. Furthermore, *Desulfitobacterium* species were detected in other clay formations as well, for example in Opalinus Clay.^[1] These were used to form artificial bio-aggregates with different bacterial strains (among others *Desulfitobacterium* sp. G1-2 and aerobic marine inhabitant *Cobetia marina* DSM 50416) using electrostatic modifications of surface charge of bacterial cells.

Time-dependent experiments of *Desulfitobacterium* sp. G1-2 alone in 30 mM bicarbonate buffer (100 µM U(VI), 10 mM lactate) showed a decrease in U concentrations in the supernatants. Moreover, artificial Opalinus Clay pore water^[2] (100 µM U(VI), 10 mM lactate, pH 5.5) was used as background electrolyte, as well, to create more environment-related conditions. In both cases, approximately 80% of the uranium was removed from the supernatants after one week. In order to be able to exclude abiotic influences on the uranium(VI) reduction, experiments using heat-killed cells were carried out, as well. Thermodynamic calculations of the U(VI) speciation in both solutions revealed the predominance of different U(VI) complexes in the used media. UV/Vis studies of the dissolved cell pellets verified the formation of U(IV) by an almost complete reduction of U(VI) in bicarbonate buffer and artificial

Opalinus Clay pore water. In contrast, experiments with heat-killed cells did not show any reduction of U(VI) in the samples. STEM investigations coupled with EDX analysis of U-incubated cells showed the presence of two different U-containing aggregates inside the cells of *Desulfitobacterium* sp. G1-2. On the one hand, spherical nanoparticles are present, which are probably containing organic uranium phosphate compounds, as shown by EDX mapping of the samples. On the other hand, rod-shaped particles consisting of inorganic uranium phosphate compounds occur inside the cells as well.

First experiments with artificial bio-aggregates that were formed from different bacterial strains (e.g. *Desulfitobacterium* sp. G1-2 and *Cobetia marina* DSM 50416) using electrostatic modification of surface charge of bacterial cells by different polyelectrolytes showed a promising U reduction capacity in bicarbonate buffer (30 mM, 100 μ M U(VI), 10 mM lactate). Future investigation will focus on the elucidation of the complex interaction mechanisms in multi-species environments.

This study helps to close existing gaps in a comprehensive safeguard concept for a repository for high-level radioactive waste in clay rock. Moreover, the results of these investigations provide new insights into the U(VI) reduction by iron-reducing microorganisms and thus, contribute to new knowledge on the migration of uranium in the environment. In addition, it may help to establish new bioremediation approaches of contaminated environments, because beneficial microbes can be used for the artificial bio-aggregates, even if they do not form biofilms themselves.

References

- [1] A. Bagnoud et al. (2016). Reconstructing a hydrogen-driven microbial metabolic network in Opalinus Clay rock. *Nat. Commun.* 2016, 7, 1–10
- [2] P. Wersin et al. (2011). Biogeochemical processes in a clay formation in situ experiment: Part A - Overview, experimental design and water data of an experiment in the Opalinus Clay at the Mont Terri Underground Research Laboratory, Switzerland. *Appl. Geochemistry* 2011, 26, 931–953

A4-3 THE IMPACT OF SULFIDATION ON MAGNETITE-BOUND ⁹⁹Tc

Thomas Neill⁽¹⁾, Olwen Stagg⁽²⁾, Sam Shaw⁽¹⁾, Kath Morris⁽¹⁾

(1) *The University of Manchester, UK*

(2) *Washington University in St Louis, USA*

⁹⁹Tc is a long-lived, high-yield fission product and ⁹⁹Tc mobility is of interest in nuclear decommissioning, radioactively contaminated land and geodisposal scenarios. Here, we investigate the impact of sulfide exposure on the fate of ⁹⁹Tc that has been reacted with the Fe(II)/Fe(III) mineral magnetite (Fe₃O₄). Fe-(oxyhydr)oxide minerals are a key controller of radionuclide mobility, including ⁹⁹Tc, in the environment and the capacity of Fe(II)-bearing phases for radionuclide immobilization is an area of intense research. Fe(II) is capable of reducing many radionuclides, including ⁹⁹Tc and U, resulting in reductive immobilization mechanisms and suppressed radionuclide migration. Reaction of Tc(VII) with magnetite has previously resulted in the formation of reduced Tc(IV) either as a surface precipitate,[1] inner-sphere sorption complex[2] or Tc-incorporated into magnetite[3]. This leads to a net immobilization of Tc, via reduction of the highly soluble Tc(VII) to reduced Tc(IV) which readily sorbs to, or precipitates on minerals in the environment. However, a question remains regarding the reversibility of this immobilization, in particular with respect to reoxidation of the reduced radionuclide-bearing phases. In this context, Tc-sulfides (nominally TcS₂ and Tc₂S₇) present a potentially more stable reduced form of ⁹⁹Tc given that Tc-sulfides may be more recalcitrant to reoxidation than sorbed Tc(IV) or nano-TcO₂, suggesting that these phases may be long-term sinks for ⁹⁹Tc. Tc-sulfides have been identified as the dominant form of Tc in soils and sediments too,[4] making these phases key controllers on Tc mobility when sulfur is present. However, the exact mechanisms for Tc-sulfide formation, and the conditions under which sulfidation may occur, are not fully understood.

Sulfidation of Fe-(oxyhydr)oxide mineral has been previously investigated in the context of exposure of Fe-minerals to sulfide conditions generated by sulfur reducing bacteria. Under these conditions, the sulfide generated reacts with Fe-(oxyhydr)oxide minerals, resulting in the breakdown of the Fe-(oxyhydr)oxide mineral structure and the formation of Fe-sulfide minerals (e.g. mackinawite, FeS).[5] Recent studies have investigated the fate of U during these sulfidation reactions, including U bound to ferrihydrite,[5] magnetite[6] and goethite.[7] In these studies, the breakdown of Fe-(oxyhydr)oxides led to the formation of Fe-sulfide and lepidocrocite phases forming and the formation of nano-UO₂ was the dominant form of U in all experiments.

Here, we use a ‘chemostat’ bioreactor system to induce a controlled sulfidation of magnetite-bound ⁹⁹Tc via Na₂S introduction under an inert, N₂ atmosphere, with a constant pH (9) and temperature, while monitoring Eh of the reaction. Solution and solid-state samples were taken at regular intervals for investigation via ultrafiltration-ICP-MS and dynamic light scattering, and the speciation of Tc was investigated via X-ray absorption spectroscopy. Solution analysis showed a complete reaction of sulfide with magnetite and Tc via consumption of all sulfide in the system over 48 hours, consistent with previous investigations. Fe was observed wholly in the solid/colloidal size fraction (>1.5 nm), with evidence of small (1.5 – 220 nm), potentially colloidal Fe nanoparticles generated during the sulfidation reaction. These nanoparticles had a bimodal size distribution of ~10 nm and >50 nm particles, which is consistent with the disaggregation of nano-magnetite or the formation of nanoparticulate Fe-sulfide. Tc K-edge XAS showed a Tc-incorporated into magnetite starting material which rapidly changed over time. After 4 hours a mixed-phase Tc system with magnetite-incorporated Tc and Tc-sulfide species both present in the solid phase. After 24h, no O shell could be fit to the EXAFS data, consistent with complete reaction to a sulfide species, which persisted over time with further measurements at t=1 week, 1 month and 9 months. EXAFS fits for the Tc-sulfide phase formed did not change over time, meaning the Tc-sulfide formed within the first 24h of the reaction did not alter significantly with aging. On comparison with previous studies, EXAFS fits were similar to previously fit products of Tc

sulfidation,[8, 9] but it was not possible to fit Tc-Tc backscatterers, suggesting a disordered Tc coordination environment was present in the current study, with Tc possibly associated with Fe-sulfides present in the system. Overall, this investigation demonstrated the long-term stability of Tc-sulfides during and after the exposure of magnetite bound Tc to sulfidic conditions.

These results corroborate with other investigations highlighting the importance of Tc-sulfide phases in the long-term mobility of ⁹⁹Tc in sulfide-containing environments.

References

- [1] D. Cui, T.E. Eriksen, Reduction of Pertechnetate in Solution by Heterogeneous Electron Transfer from Fe(II)-Containing Geological Material, *Environmental Science & Technology* 30(7) (1996) 2263-2269.
- [2] T.A. Marshall, K. Morris, G.T. Law, J.F. Mosselmans, P. Bots, S.A. Parry, S. Shaw, Incorporation and retention of 99-Tc(IV) in magnetite under high pH conditions, *Environ Sci Technol* 48(20) (2014) 11853-62.
- [3] T. Kobayashi, A.C. Scheinost, D. Fellhauer, X. Gaona, M. Altmaier, Redox behavior of Tc(VII)/Tc(IV) under various reducing conditions in 0.1 M NaCl solutions, *Radiochimica Acta* 101(5) (2013) 323-332.
- [4] M.J. Wharton, B. Atkins, J.M. Charnockab, F.R. Livens, R.A.D. Patrick, D. Collison, An X-ray absorption spectroscopy study of the coprecipitation of Tc and Re with mackinawite (FeS), *Applied Geochemistry* 15(3) (2000) 347-354.
- [5] L.T. Townsend, S. Shaw, N.E.R. Ofili, N. Kaltsoyannis, A.S. Walton, J.F.W. Mosselmans, T.S. Neill, J.R. Lloyd, S. Heath, R. Hibberd, K. Morris, Formation of a U(VI)-Persulfide Complex during Environmentally Relevant Sulfidation of Iron (Oxyhydr)oxides, *Environ Sci Technol* 54(1) (2020) 129-136.
- [6] L.T. Townsend, K. Morris, R. Harrison, B. Schacherl, T. Vitova, L. Kovarik, C.I. Pearce, J.F.W. Mosselmans, S. Shaw, Sulfidation of magnetite with incorporated uranium, *Chemosphere* 276 (2021) 130117.
- [7] O. Stagg, K. Morris, L.T. Townsend, K.O. Kvashnina, M.L. Baker, R.L. Dempsey, L. Abrahamsen-Mills, S. Shaw, Sulfidation and Reoxidation of U(VI)-Incorporated Goethite: Implications for U Retention during Sub-Surface Redox Cycling, *Environ Sci Technol* 56(24) (2022) 17643-17652.
- [8] D. Fan, R.P. Anitori, B.M. Tebo, P.G. Tratnyek, J.S. Lezama Pacheco, R.K. Kukkadapu, M.H. Engelhard, M.E. Bowden, L. Kovarik, B.W. Arey, Reductive sequestration of pertechnetate ((9)(9)TcO(4)(-)) by nano zerovalent iron (nZVI) transformed by abiotic sulfide, *Environ Sci Technol* 47(10) (2013) 5302-10.
- [9] W.W. Lukens, J.I. Bucher, D.K. Shuh, N.M. Edelstein, Evolution of technetium speciation in reducing grout, *Environ Sci Technol* 39(20) (2005) 8064-70.

A4-4 RECENT EXPERIMENTAL DEVELOPMENTS ON PLUTONIUM OXIDATION STATE DISTRIBUTION UNDER WIPP RELEVANT CONDITIONS

Jean-Francois Lucchini, Ugras Kaplan, Adrienne E. Navarrette, Jandi L. Knox, Ceren Kutahyalı Aslani, Jeremiah Beam

Actinide Chemistry and Repository Science Program (ACRSP) / Los Alamos National Laboratory (LANL) / NM-USA

A joint group of Waste Isolation Pilot Plant (WIPP) project participants, including the Department of Energy's Carlsbad Field Office (DOE-CBFO), the Los Alamos National Laboratory (LANL) Actinide Chemistry and Repository Science Program (ACRSP), and Sandia National Laboratories (SNL), recently decided on a new path forward for the oxidation state model in the WIPP Performance Assessment (PA). Historically, since the initial Compliance Certification Application (CCA) in 1996, a binary approach has been taken in which half of the PA realizations assume solubility to be dominated by the low oxidation states [U(IV), Np(IV), Pu(III)] and the other half assume solubility to be dominated by the higher oxidation states [U(VI), Np(V), Pu(IV)]. The new oxidation state model will decouple the redox active actinides and will instead consider their redox as a function of Eh. To support this effort, LANL ACRSP started a series of experiments to determine the oxidation state of plutonium under a range of expected WIPP conditions. Herein, we present the first results of the experiments that target the upper Eh boundary expected in the WIPP.

Pu solubility experiments were prepared and performed in 90% strength Generic Weep Brines (GWB) at pC_{H^+} 9 and 10, in the presence of WIPP-relevant organic complexants (EDTA, oxalate, citrate, acetate), using Pu-239 isotope (for radiolytic effects) in the Pu(OH)₃ and Pu(OH)₄ forms, and magnetite Fe₃O₄ (estimated to be the most stable oxidized iron phase under WIPP conditions) and Fe(0), from an under saturation approach at $T = 23 \pm 2$ °C, and in a nitrogen-controlled atmosphere (<10 ppm oxygen partial pressure) [1].

After 205 days in the experiments, X-ray absorption spectroscopy (XANES) samples were prepared by removing solid from each experiment, filtering it through a 100K Amicon filter, and diluting the solid in boron nitride. The Pu L_{III}-edge XANES spectra were collected at the 10-BM beamline at the Advanced Photon Source (APS), in order to identify oxidation state distribution in the samples. As shown in Figure 1, the presence of a peak near the absorption edge for Pu(V) and Pu(VI) species enables determination of the speciation between Pu(III/IV) and Pu(V/VI). Additionally, due to the difference in the onset energy and white line position of Pu(III) and Pu(IV) species, a linear combination fit (LCF) using one spectrum of each of these oxidation states can be used to fit the oxidation state of an unknown solid.

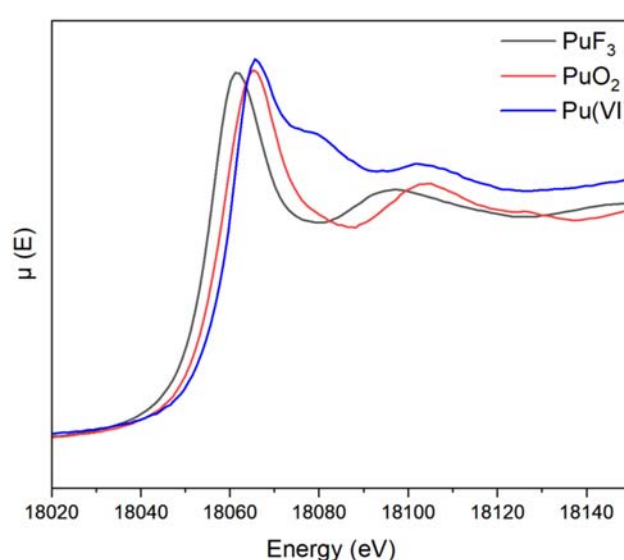


Figure 1: Typical XANES spectra of Pu(III), Pu(IV), and Pu(VI) solids showing the difference in onset energy, white line position, and post-edge features [1].

Linear combination fitting uses the formula:

$$1 - x(A) + x(B) = C,$$

Where A and B are the two component spectra, C is the composite spectra and x is a fitting variable. As changes in the coordination environment can impact both the white line position and onset energy, the component spectra should be similar in composition to the unknown. The species chosen for the linear combination fits for the plutonium spectra were Pu(OH)₃ and PuO₂·xH₂O, as these are the expected solubility controlling phases for each oxidation state under WIPP conditions (Figure 2).

An example LCF result is presented in Figure 3, along with the component spectra and the residual of the fit. The fit range was chosen to encompass both the onset energy as well as the entire absorption feature.

The results of the fits determined that the samples were primarily Pu(IV) with small amounts of Pu(III) character, even in the presence Fe(0).

The measurement of corrected Eh values confirmed that all the experiments were firmly in the stability field of PuO₂ (Figure 2). The experiments containing magnetite resulted in oxidizing conditions (<430 mV). The experiments containing metallic iron maintained reducing conditions over the course of the experiments. However, these reducing conditions were not sufficient to maintain Pu in the +III oxidation state.

The data obtained in this experimental work confirm that Pu(IV) is the dominant oxidation state under the investigated WIPP-relevant conditions.

References:

- [1] Beam, J. (2023). Plutonium Oxidation State Distribution under WIPP Relevant Conditions. Los Alamos Report LCO-ACP-31, Rev.1. Los Alamos National Laboratory, Carlsbad NM, 88220.
- [2] AMPHOS²¹ (2023). Pourbaix Diagrams – Fe, Pu, U, Np. February 2023 – version 3.

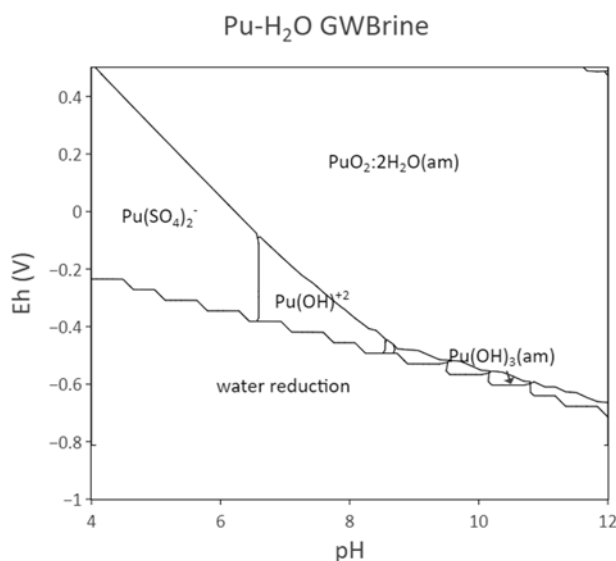


Figure 2: Pourbaix diagram showing Pu speciation including solids in GWB brine under 1 atm H₂(g). This diagram was calculated using the ThermoChimie SIT database, and [Pu]_{tot} = 1.2 × 10⁻⁷ M. [2].

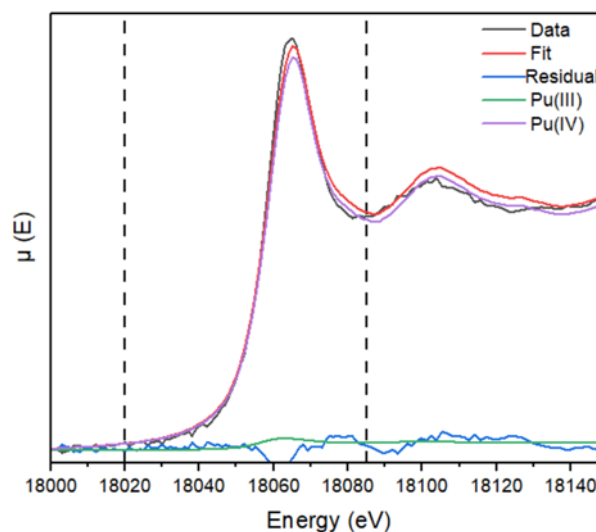


Figure 3: LCF example result showing character of Pu(III) and Pu(IV) spectra. The black dashed lines indicate the range used for the fit [1].

A4-5 REDUCTION OF PERTECHNETATE BY MAGNETITE – INFLUENCE OF PH AND TIME

Thomas Zimmermann⁽¹⁾, Augusto F. Oliveira⁽¹⁾, Natalia Mayordomo⁽¹⁾, Andreas C. Scheinost^(1,2)

(1) Institute of Resource Ecology, Helmholtz-Zentrum Dresden-Rossendorf, 01328 Dresden, Germany

(2) Rossendorf Beamline at ESRF (ROBL), 38000 Grenoble, France

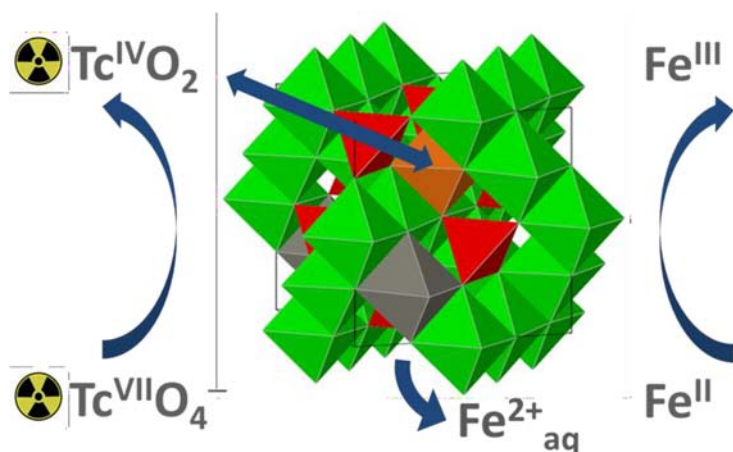


Fig. 1: Schematic process of the interaction of pertechnetate ($Tc^{VII}O_4^-$) with magnetite

Magnetite is arguably the most relevant corrosion product when steel canisters corrode anaerobically in future deep geological radioactive waste repositories. ^{99}Tc is of great concern for the safety assessment of these repositories, due to its long half-life ($t_{1/2} = 2.1 \cdot 10^5$ years). Under oxidative conditions Tc forms an anionic species, pertechnetate ($Tc^{VII}O_4^-$), which is highly mobile due to its high solubility and weak sorption on most minerals. Under anaerobic conditions, Tc^{VII} can be reduced to Tc^{IV} , which strongly interacts with minerals by sorption, structural incorporation and formation

of insoluble oxides like TcO_2 . Fe^{II} -minerals, and among them magnetite, have shown to effectively reduce pertechnetate and play thereby a critical role.^[1]

Previous studies by Yalcintas et al.^[2] suggested that Tc^{VII} reduction by magnetite resulted in the precipitation and surface adsorption of TcO_2 -like oligomers at pH 9, i.e. close to the pH of magnetite solubility minimum. In contrast at pH 6-7, the reduction resulted in a partial incorporation of Tc^{IV} in octahedral Fe-sites of magnetite.^[3] Our initial working hypothesis was that the incorporation is linked to magnetite solubility. To test this, we investigated Tc reaction with magnetite nanoparticles in a wide range of pH (3 - 13), reaction time (1 - 210 days) and varied initial Tc concentration (μM - mM).

To characterize the oxidation state of Tc and its molecular structure, we employed a range of methods including Tc K-edge (21 044 eV) X-ray absorption spectroscopy (XAS) at the Rossendorf Beamline at the ESRF in Grenoble. XANES analysis revealed the predominance of Tc^{IV} at all evaluated pH values, supporting that reductive Tc immobilization is the main retention mechanism. EXAFS analysis suggests that two species are formed. At pH 5 and short equilibration times, Tc is retained by forming $TcO_2 \cdot xH_2O$ polymers, showing the recently reported “zig-zag-chain” structure^[4]. In contrast, Tc^{IV} substituted magnetite forms within a few hours at pH 7 and 10. At pH 5, it forms only after a few days with the proportion of the Tc-magnetite phase growing at the expense of the $TcO_2 \cdot xH_2O$ polymers. Therefore, across the pH range 5 to 10, Tc-magnetite seems to be the thermodynamically preferred phase. The initial formation of $TcO_2 \cdot xH_2O$ polymers at low pH seems to be linked to the release of Fe^{2+} from magnetite (reductive maghemitization)^[5], which leads to substantial Fe^{2+} concentrations in solution due to the lacking re-adsorption at this pH. The mechanism behind the fast incorporation of Tc^{IV} in magnetite, now observed for the first time within days across a wide pH range, remains unsolved. The structural stability of cubic spinel magnetite and the absence of strong evidence for structural uptake of other elements with similar coordination number and ionic radius like Co, Ni and other 3d metals, point to a complex coupled sorption/redox/incorporation mechanism.

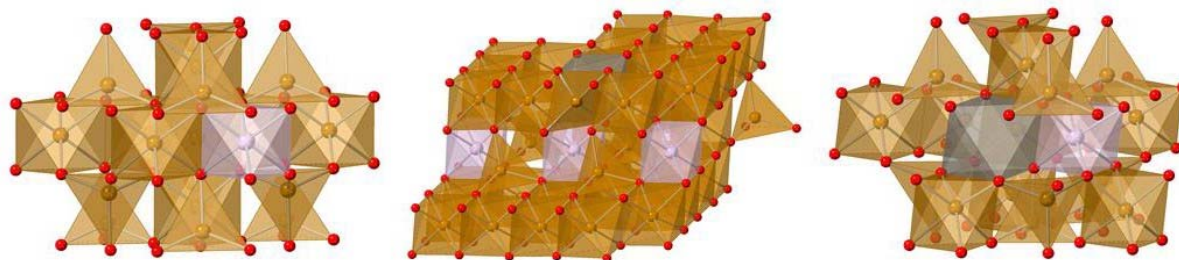


Fig. 2: Possible charge compensation mechanisms identified via density functional theory (DFT), left Tc^{IV} and Fe^{II} substitute 2 Fe^{III} , middle 3 Tc^{IV} substitute 4 Fe^{III} creating a vacancy, right Tc^{IV} substitutes 2 Fe^{II} creating a vacancy

In order to better understand the Tc incorporation into by magnetite, we also conducted density functional theory (DFT) calculations using the PBE^[6] functional implemented in AMS/BAND 2022^[7], with full optimization of atomic coordinates and lattice parameters. For the finite structures, solvent effects were included with the COSMO^[8]. Three charge compensation mechanisms were considered. The calculated incorporation energies and comparison of the Tc coordination structure with experimental EXAFS data indicate that Tc incorporation is most likely to occur either by substitution of two octahedral Fe^{III} sites with a Tc^{IV}/Fe^{II} pair (Fig. 2, left), or by substitution of two Fe^{II} sites with a single Tc^{IV} , thus forming a vacancy (Fig. 2, right). The last mechanism, where three Tc^{IV} replace four octahedral Fe^{III} (Fig. 2, center), could be excluded.

Acknowledgements: We thank the German Federal Ministry of Economic Affairs and Energy (BMWi) for funding the KRIMI project (02NUK056C) as well as the European Commission (EC) through the EURAD FUTURE T3 project (H2020-847593).

References

- [1] Meena, A.H. and Arai, Y. (2017). Environmental geochemistry of technetium. *Environ. Chem. Lett.* 15: 241-263.
- [2] Yalcintas, E. et al. (2016). Systematic XAS study on the reduction and uptake of Tc by magnetite and mackinawite. *Dalton Trans.* 45: 17874-17885.
- [3] Kobayashi, T. et al. (2013). Redox behavior of Tc(VII)/Tc(IV) under various reducing conditions in 0.1 M NaCl solutions. *Radiochim. Acta* 101: 323-332.
- [4] Oliveira, A.F. et al. (2022). Shedding Light on the Enigmatic $TcO_2 \cdot xH_2O$ Structure with Density Functional Theory and EXAFS Spectroscopy. *Chem. Eur. J.*: e202202235.
- [5] Li, Z. et al. (2019). Mechanism and kinetics of magnetite oxidation under hydrothermal conditions. *RSC Advances* 9: 33633-33642.
- [6] Perdew, J.P. et al. (1996). Generalized Gradient Approximation Made Simple. *Phys. Rev. Lett.* 77: 3865-3868.
- [7] BAND 2022.1, SCM, Theoretical Chemistry, Vrije Universiteit, Amsterdam, The Netherlands, <http://www.scm.com>
- [8] Klamt, A. and Schüürmann, G. (1993). COSMO: A new approach to dielectric screening in solvents with explicit expressions for the screening energy and its gradient. *J. Chem. Soc., Perkin Trans. 2*: 799-805.

B2-1 MIGRATION OF REDOX-SENSITIVE PLUTONIUM AND NEPTUNIUM IN OPALINUS CLAY ROCK: DEEPER INSIGHTS FROM IN-SITU REACTIVE TRANSPORT PATTERNS

Daniel Grolimund ⁽¹⁾, Samer Amayri ⁽²⁾, Ugras Kaplan ⁽²⁾, Markus Breckheimer ⁽²⁾, Prashanta J. B. Börner ⁽²⁾, Tobias Reich ⁽²⁾

(1) Paul Scherrer Institute, Swiss Light Source, Chemical Imaging Group & microXAS Beamline, 5232 Villigen PSI, Switzerland

(2) Johannes Gutenberg-Universität Mainz, Department of Chemistry, Nuclear Chemistry, 55099 Mainz, Germany

The long-term safe disposal of radioactive waste corresponds to a challenging responsibility of present societies. Concepts based on a multi-barrier repository in deep geological formations represent a promising class of disposal strategies. Within these concepts, the host rock corresponds to the ultimate safety barrier towards the environment. To assess the performance of such final barriers, detailed information on the interaction between the radiotoxic, long-lived radionuclides such as ²³⁹Pu or ²³⁷Np and the host rock are essential. It is fundamental to identify and understand the physico-chemical reactive (solute) transport mechanisms along the transport paths through the barriers.

Based on their very low hydraulic conductivity and their high retention capabilities, argillaceous rocks such as Opalinus Clay are currently examined by several European countries as potential host rocks for high-level radioactive waste repositories. From a geochemical perspective, argillaceous rocks represent a complex and heterogeneous porous media. The mobility of reactive solutes in such media is the result of a complex interplay of multiple reactions involving a broad variety of mobile and immobile reactive species. The level of complexity is furthermore considerably increased for redox sensitive nuclides.

The geochemical reactivity of barrier material is commonly studied by disruptive batch studies yielding as observable the superimposed outcome of all occurring geochemical processes. Similar, considering solute transport studies, the geochemical processes occurring within the porous medium are commonly 'derived' indirectly based on the observation of flux outside or at the boundary of the rock material. Consequently, both approaches yield empirical, nonmechanistic knowledge concerning the geochemical reactivity of the porous media. By complementing such studies by the investigation of undisturbed reactive transport pattern expressed within the porous medium, two main benefits arise. First, microscopic, multimodal chemical images of reactive transport patterns allow to deconvolute the chemical complexity. Obtaining spatially resolved chemical information and its particular spatial context opens up the possibility to correlate the local chemical nature and state of the porous medium with the expressed reactive transport pattern. As a potential result, new phenomena, relevant mechanism and reactive components can be identified. Second, (ideally subsequent) reactive transport patterns correspond to invaluable data to validate reactive (solute) transport models.

The present study visualizes the *in-situ* micro-scale reactive transport of Pu and Np within pristine Opalinus Clay samples. Long-term diffusion experiments were conducted with these two redox-sensitive elements [1-4]. To characterize the transport and reactivity within the micro-heterogeneous clay rock matrix, we used a combination of synchrotron-based micro-imaging techniques including micro-X-ray fluorescence, micro-X-ray diffraction, and micro-X-ray absorption spectroscopy. Two-dimensional reactive transport patterns and mappings of the geochemical heterogeneity have been recorded and the local chemical speciation of Pu and Np was determined. The microscopic chemical imaging and spatially resolved molecular-level investigations were performed at the microXAS Beamline of the Swiss Light Source (SLS, Paul Scherrer Institute, Villigen, Switzerland). Finally, the obtained chemical distribution patterns were subject of reactive solute transport modelling considering diffusion and interfacial reactivity (sorption as well as electron-transfer reactions).

For both nuclides, we succeeded to record full two-dimensional representations of diffusion profiles in a relevant geological medium (an example is given in Figure 1). Moreover, in addition to the elemental distribution of Pu and Np, respectively, transport relevant chemical information was obtained by micro-XANES. For Pu as well as Np, these spatially resolved speciation measurements showed that both elements were reduced progressively along their diffusion path. The modelling of the diffusion profiles considering the different redox species points to a decisive role of the electron donor pools present in the Opalinus Clay.

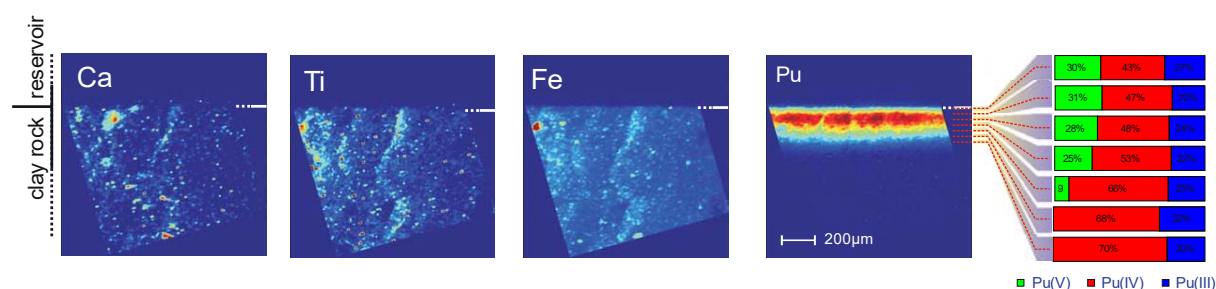


Figure 1. Geochemical heterogeneity (micro-XRF), two-dimensional Pu diffusion profile (edge-contrast micro-XRF) and fractions of different redox species of Pu (micro-XANES). The clay rock sample was cleaved perpendicular to the sample surface along the bedding planes.

The combination of spatially resolved X-ray microprobe methods is a powerful toolset to elucidate relevant transport mechanisms of radionuclides in heterogeneous porous media. Chemical images representing reactive transport patterns correspond to invaluable information to validate reactive transport models. The resulting scientific information is an essential contribution to the evaluation of the long-term safety of a repository and performance of its engineered and geological barrier systems.

Acknowledgements: This work was financially supported by the German Federal Ministry for Economic Affairs and Energy (BMWi, contract no. 02E10981), German Federal Ministry of Education and Research (BMBF, contract no. 02NUK044B), Actinet-I3 (contract no. 232631) and Talisman (contract no. 323300).

References

- [1] Fröhlich, D.R., Amayri, S., Drebert, J., Grolimund, D., Huth, J., Kaplan, U., Krause, J. and Reich, T. (2012). Speciation of Np(V) uptake by Opalinus Clay using synchrotron microbeam techniques. *Anal. Bioanal. Chem.* 404: 2151-2162.
- [2] Kaplan, U., Amayri, S., Drebert, J., Rossberg, A., Grolimund, D. and Reich, T. (2017), Geochemical interactions of Plutonium with Opalinus Clay studied by spatially resolved synchrotron radiation techniques. *Environ. Sci. Technol.* 51: 7892-7902.
- [3] Börner, P.J.B. (2017). Sorption and diffusion of Neptunium in Opalinus Clay. PhD thesis. Johannes Gutenberg-Universität Mainz, Mainz, Germany.
- [4] Kaplan, U. (2013). Speciation of Plutonium during sorption and diffusion in Opalinus Clay. PhD thesis. Johannes Gutenberg-Universität Mainz, Mainz, Germany.

B2-2 DIFFUSIVE TRANSPORT OF U(VI) AND AM(III) THROUGH OPALINUS CLAY STUDIED DOWN TO ULTRA-TRACE LEVELS

Daniel Glückman⁽¹⁾, Francesca Quinto⁽¹⁾, Claudia Joseph⁽¹⁾, Volker Metz⁽¹⁾, Karin Hain⁽²⁾, Peter Steier⁽²⁾, Horst Geckeis⁽¹⁾

(1) Institute for Nuclear Waste Disposal (INE), KIT, Karlsruhe, Germany

(2) Isotope Physics, Faculty of Physics, University of Vienna, Vienna, Austria

Clay rocks are considered as potential host rocks and geo-engineered barriers for the final disposal of high-level nuclear waste (HLW) in deep geological formations. Although the host rock and the geo-engineered barrier (e.g., bentonite) delay groundwater intrusion into the emplacement chambers, groundwater ingress has to be taken into account in the long-term safety assessment of a HLW repository. In this context, the corrosion of canisters and the consecutive release of radionuclides have to be considered. Potentially released actinides, such as uranium (U) and americium (Am), could be transported in a clay rock formation by molecular diffusion. Actinides are known to exhibit low solubility and to sorb strongly onto clay mineral surfaces under the reducing conditions of deep geological repositories. Diffusion experiments at the expected very low actinide concentrations are therefore challenging to perform due to analytical constraints. To our knowledge, the diffusion of U in clay rocks has not been investigated below concentrations of $\approx 10^{-4}$ mol/m³ clay [1]. For Am, up to now, laboratory diffusion experiments have not been performed with clay rock, considered suitable as host rock, such as Opalinus Clay (OPA).

This study aimed at the investigation of the diffusion behavior of U(VI) and Am(III) down to ultra-trace concentrations ($\ll 10^{-4}$ mol/m³) in OPA. In particular, potential differences in the diffusion properties of the two investigated actinide elements at ultra-trace concentrations compared to higher concentrations were explored. Laboratory-scale diffusion experiments were conducted with samples of OPA, obtained from the Mont Terri underground rock laboratory, Switzerland for up to 240 d. Cylindrical OPA samples (length: 10 mm, diameter: 6 mm) were contacted with synthetic OPA pore water (ionic strength: 0.22 ± 0.02 mol/L, pH: 7.2 ± 0.1 [2]), which was spiked with 2×10^{-11} to 3×10^{-9} mol/L of ²³³U and 1×10^{-12} to 3×10^{-9} mol/L of ²⁴³Am. After termination of the experiments, the OPA cylinders were segmented into thin layers of 20–400 μ m. The obtained clay segments were analyzed for their ²³³U and ²⁴³Am content with accelerator mass spectrometry (AMS) at the Vienna Environmental Research Accelerator (VERA) [3].

Diffusion profiles of U(VI) were determined down to $\approx 10^{-9}$ mol/m³ (see Figure 1 *Figure 3*), which represents an improvement in detection sensitivity by five orders of magnitude compared to a previous study of the U(VI)–OPA system [1]. U(VI) showed typical diffusion profiles in OPA, which were interpreted by applying Fick's laws using COMSOL Multiphysics 5.6. Changes in the diffusion behavior of U(VI) through OPA were not observed in a concentration range from 10^{-3} mol/m³ to 10^{-9} mol/m³. The Am profiles were featured by two different sections. The first section exhibited a strong decrease in ²⁴³Am concentration, while in the second section, the concentration decrease was less distinct (see purple and brown lines named “short profile” and “long profile”, respectively, shown in *Figure 3*, right plot). Such two-part profiles were also observed in diffusion experiments with Eu(III) as an analogue to Am(III) through OPA [4].

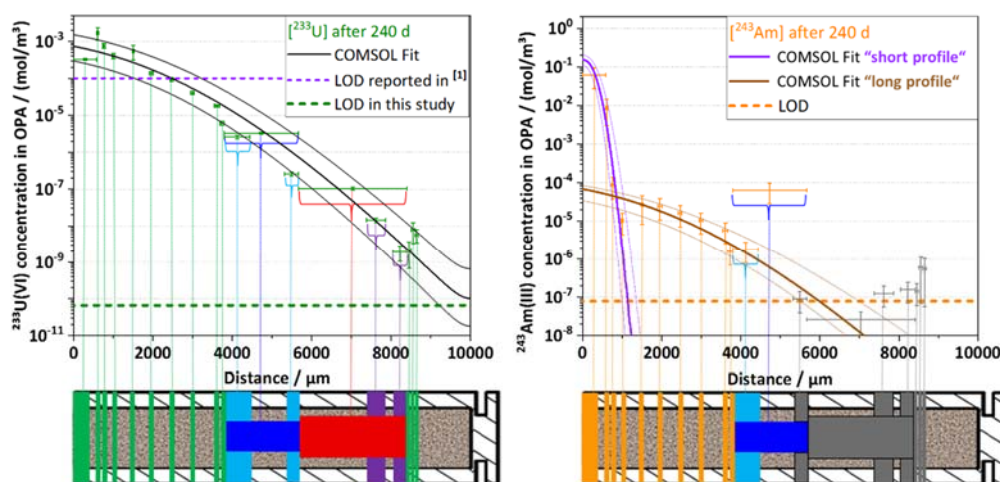


Figure 3: Diffusion profiles of $^{233}\text{U(VI)}$ (left plot) and $^{243}\text{Am(III)}$ (right plot) in OPA after 240 d of diffusion. Limits of detection (LOD) are indicated as dashed horizontal lines.

X-ray microtomography investigations of OPA cylinders revealed the presence of 40–80 μm wide micro-cracks, most likely being responsible for the observation of an Am fraction with a longer diffusion distance. Modelling of the two parts of the Am profile with a 1D pore diffusion model was possible hypothesizing the presence of two migrating Am species dominating the mobile phase. One is assumed to be the aqueous species $[\text{Am}(\text{CO}_3)]^+$. This cationic species undergoes strong retardation by negatively charged clay mineral surfaces, resulting in slow migration, causing the observed short diffusion profile of Am. The other species is believed to be colloidal, featured by poor retention and faster migration through the micro-cracks in the OPA cylinder. While presence and nature of the hypothesized colloids needs still to be verified and investigated, the results of the present study provide relevant insight into the migration behavior of U(VI) and Am(III) in OPA over a wide range of concentrations down to ultra-trace levels.

Acknowledgment: This work was partially funded by the German Federal Ministry for Education and Research under grant agreement 02NUK 053 C and from the Helmholtz association under grant agreement SO-093 through the iCross collaborative project. Furthermore, funding of AMS beam time was received under RADIATE by the European Union's Horizon 2020 research and innovation program under grant agreement No. 824096.

References

- [1] Joseph, C., Van Loon, L. R., Jakob, A., Steudtner, R., Schmeide, K., Sachs, S. and Bernhard, G. (2013). Diffusion of U(VI) in Opalinus Clay: Influence of temperature and humic acid. *Geochim. Cosmochim. Acta* 109: 74–89.
- [2] Gimmi, T., Leupin, O. X., Eikenberg, J., Glaus, M. A., Van Loon, L. R., Waber, H. N., Wersin, P., Wang, H. A. O., Grolimund, D., Borca, C. N., Dewonck, S. and Wittebroodt, C. (2014). Anisotropic diffusion at the field scale in a 4-year multi-tracer diffusion and retention experiment – I: Insights from the experimental data. *Geochim. Cosmochim. Acta* 125: 373–393.
- [3] Quinto, F., Blehshmidt, I., Garcia Perez, C., Geckeis, H., Geyer, F., Golser, R., Huber, F., Lagos, M., Lanyon, B., Plaschke, M., Steier, P. and Schäfer, T. (2017). Multiactinide analysis with accelerator mass spectrometry for ultratrace determination in small samples: Application to an in situ radionuclide tracer test within the colloid formation and migration experiment at the Grimsel Test Site (Switzerland). *Anal. Chem.* 89: 7182–7189.
- [4] Paul-Scherrer-Institut (2020). Annual Report 2019. <https://www.psi.ch/de/luc/annual-reports>.

B2-3 EFFECT OF THE WATER SATURATION ON THE DIFFUSION OF WATER AND SOLUTES IN REFERENCE CLAY-RICH POROUS MEDIA

Desert Lucas^(1,2,3), Savoye Sébastien⁽³⁾, Ferrage Eric⁽¹⁾, Pierre Hénocq⁽²⁾, Tournassat Christophe⁽⁴⁾, Tertre Emmanuel⁽¹⁾

(1) IC2MP, Equipe HydrASA, UMR 7285 CNRS/Université de Poitiers, France

(2) Andra, France

(3) Université Paris-Saclay, CEA, Service de Physico-Chimie, France

(4) ISTO, Université d'Orléans, France

Due to their high sorption properties and very low permeability, clay-rich porous media are envisaged as barriers against contaminants spreading in radioactive waste disposal facilities. In this situation, the transfer of radionuclides is thus limited to the very slow process of diffusion that is strongly dependent on the types of clay media. In the French Cigéo project of deep geological disposal in the Callovian-Oxfordian argillaceous formation, recent calculations indicate that the generation of hydrogen due to the corrosion of canisters may partially dehydrate clayey host rocks and engineered barriers (including clay-based materials) for more than 100 000 years [1], and thus may change the confinement properties of these materials.

Clay minerals are lamellar aluminosilicates. Depending on their type, porous media made with these minerals can present various porosity organizations. For instance, kaolinite clay mineral is a non-swelling and non-charged clay mineral and diffusion performed in a porous medium made with these types of particles only takes place in the interparticle porosity. Illite is a non-swelling clay mineral with charged surfaces, which influence aqueous species mobility in the interparticle porosity. Finally, swelling clay minerals like vermiculite and smectite have surface charges and porous media made with these particles present a double porosity: (i) an interparticle porosity and (ii) an interlayer porosity where water and solutes mobility is mainly controlled by surface effect.

This work aims to experimentally investigate the effect of water saturation on the diffusion of water and solutes through porous media made with these different clay minerals considering an increasing complexity, i.e., kaolinite, illite, vermiculite, and smectite. For that purpose, through-diffusion experiments were performed with water tracers (HTO and HDO), anionic tracers ($^{36}\text{Cl}^-$ and $^{125}\text{I}^-$), and cationic tracer ($^{22}\text{Na}^+$) into compacted clay materials to have similar interparticle porosity of 25-29%. The osmosis method was used to impose suction at 1.9 MPa and 9 MPa and to create partially water-saturated conditions throughout the duration of the diffusion tests. Note that the current study focused on the data acquisition on porous media made with illite and vermiculite particles since diffusive data were already obtained by using kaolinite particles [2] and bentonite, a material containing more than 90% of smectite [3].

For water-saturated conditions, results confirm the influence of surface charge on ion diffusivity (i.e., effective diffusion coefficient over diffusion coefficient in bulk, D_e/D_0 ; Figure 1). In porous media made with no-charged kaolinite, water and ions behave in the same manner, while with media made with the three charged clay materials an enhanced diffusion for $^{22}\text{Na}^+$ and a reduction of diffusive rates for anionic species compared to those of water tracers have been measured. When the clayey materials are partially water-saturated, each type of tracer shows distinct evolution of their diffusivity. We observe a relatively low decrease in the extent of the diffusivity values for water tracers compared to solutes, suggesting that the contribution of water diffusing in the gaseous phase has to be considered in addition to that in the liquid phase. For cationic tracer, i.e., $^{22}\text{Na}^+$, diffusivity values show a significant decrease in porous media made with charged clayey materials when dehydrating, associated with a drop of the distribution ratio, K_D , suggesting a more limited access to charged surfaces. Lastly, partial dehydration would magnify the effect of anionic exclusion with a strong drop in iodide diffusivity.

A conceptual model is then proposed to describe the evolution of the values of the effective diffusion coefficient for water and solutes as a function of water saturation.

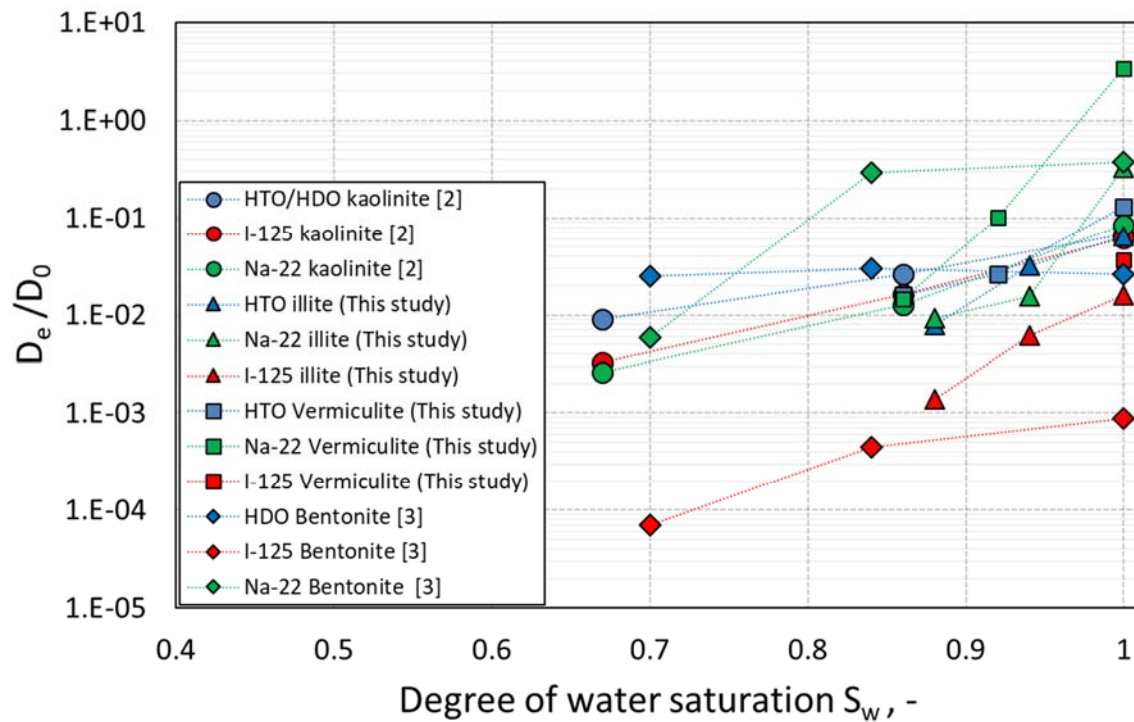


Figure 1- Evolution of diffusivity for water tracers (HTO and HDO), anionic tracer ($^{125}\text{I}^-$) and cationic tracer ($^{22}\text{Na}^+$) as a function of degree of water saturation of four reference clay-rich porous media

References:

- [1] Andra, 2016. Dossier d'options de sûreté, partie après fermeture (DOS-AF) https://www.andra.fr/sites/default/files/2018-04/dossier-options-surete-apres-fermeture_0.pdf
- [2] Wang, J. Savoye, S. Ferrage, E. Hubert, F. Lefevre, S. Radwan, J. Robinet, J.C. Tertre, E. Gouze, P., 2022. Water and ion diffusion in partially-water saturated compacted kaolinite: Role played by vapor-phase diffusion in water mobility, *Journal of Contaminant Hydrology*, 248.
- [3] Wang, J., 2022. Effet de la désaturation sur les propriétés de confinement des matériaux gonflants soumis à des fluides agressifs. Thèse de doctorat de l'Université de Montpellier.

B2-4 IMPACT OF CRACKING ON THE TRANSFER OF RADIONUCLIDES IN CEMENTITIOUS MATERIALS

J. Marliot^(1,2,3), P. Sardini⁽²⁾, C. Landesman⁽³⁾, P. Henocq⁽¹⁾, M. Siitari-Kauppi⁽⁴⁾, S. Hedan⁽²⁾, J. Bodin⁽²⁾

(1) Andra – French National Agency for radioactive waste management, France

(2) IC2MP Laboratory, UMR CNRS 7285, University of Poitiers, France

(3) Subatech Laboratory, CNRS/IN2P3, IMT Atlantique, Nantes University, France

(4) Radiochemistry, Department of Chemistry, Helsinki University, Finland

In the context of surface, sub-surface or underground repositories, Andra considers the use of cementitious materials as conditioning materials, concrete structures, and waste packages. However, physical and chemical alterations can damage the cementitious materials and lead to preferential paths for radionuclides, mainly fractures, which would presumably influence the transport of radioactive elements into the biosphere. Understanding of the consequences of these damages on the radionuclide migration is crucial for verifying the expected radionuclide behaviour. In this work, constrained mechanical damages have been induced on mortar samples and two types of transport experiments have been carried out:

- i) through diffusion (TD) experiments driven by the concentration gradient and
- ii) percolation (advection + diffusion) experiments driven by a pressure gradient.

By combining the results obtained on sound and damaged materials, it has been possible to characterize the effect of fracture aperture and density on the transport of different tracers through the mortar samples.

Mortars (Water/Cement = 0.5 and Sand/Cement = 3.20) were cast as cylinders (65 mm in height and 35 mm in diameter) with two cement types, CEM I (Val d'Azergues, Lafarge) and CEM V (Calcia, Heidelberg). Samples were fractured but not broken, using a triaxial fracturation method coupling a confining pressure of 0.8 MPa and a deviator stress. Reproducibility of the final damage geometry is not possible to achieve, and only 45% of the damaged samples were suitable for tracer tests, even if the deviator stress at failure was nearly the same for all experiments (≈ 30 MPa for CEM I). From these damaged samples, sub-cylinders were prepared for both diffusion and advection cell. The crack network was characterised by X-ray computed tomography (XRCT), ^{14}C -PMMA [1] and Digital Volume Correlation methods. This last method is very recent and consists in comparing the voxels (3D pixels) of XRCT images recorded before and after the fracturing of a sample, in order to estimate the displacement of each voxel in the three directions of space (X Y Z) [2]. The application of this method to our samples offers an innovative way for determining the aperture of fractures. Based on the XRCT images, an original imaging routine was developed to calculate the fracture density and 3D mapping of the aperture distribution. This routine was based first on skeletonization of fractures. Second, from each pixel of the skeleton, a porosity profile was computed perpendicularly to the fracture surface. The fracture aperture was determined at each point of the fracture by analysing each profile (Figure 1). The ^{14}C -PMMA method was used to verify the apertures obtained by XRCT [3].

TD experiments were performed both at the Helsinki University Radiochemistry (HYRL, Finland) with HTO, ^{36}Cl and ^{75}Se tracers and at the Subatech laboratory (Nantes, France) with HTO, ^{137}Cs and the stable isotope of Se (IV) tracers. Percolation experiments were performed at the Subatech laboratory with HTO and ^{137}Cs . Post-mortem autoradiographs were performed after the completion of these experiments. Preliminary interpretations of TD results were made with the 1D analytical solution of Crank [4]. Alternatively, 2D and 3D modelling with MODFLOW-USG [5], integrating fracture and matrix geometry, has been performed to interpret the results. As shown in Figure 2, modelling with the 1D analytical model allows reproducing the diffusion results of the sound sample (A). Values of the effective diffusion coefficient (D_e) was obtained, for the CEM I sound samples, $D_e(\text{HTO}) = (4.2 \pm 0.4) \cdot 10^{-12} \text{ m}^2/\text{s}$. For the CEM V sound samples, $D_e(\text{HTO}) = (5.0 \pm 0.9) \cdot 10^{-13} \text{ m}^2/\text{s}$ was measured. These results fit well with the existing data [6] and previous Andra's work on the same mixes. For fractured samples, fracture openings and densities are different between each sample. Crack networks are visible with XRCT only if the grey levels between fractures and the solid mortar is sufficiently contrasted (B). In contrast, for ^{14}C -PMMA autoradiography, the fractures are well observed among the cementitious matrix, the bubbles, and the sand grains (C). For

a given sample, (ref 5I), the average fracture aperture is comparable, processed either by XRCT (133 ± 26 μm) and by ¹⁴C-PMMA autoradiography (135 ± 20 μm).

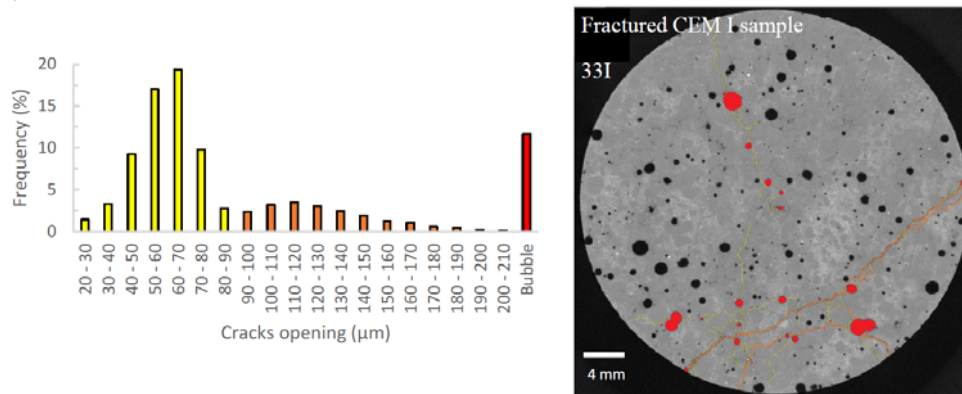


Figure 1: Distribution of crack openings (yellow and orange) and bubbles (red) (left) related to the fractures crosscutting sample 33I (right)

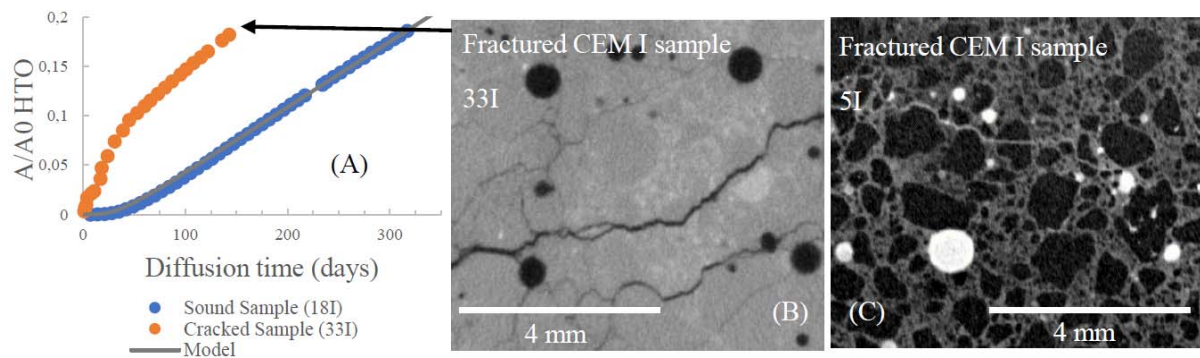


Figure 2: Comparison between TD experiments results of sound and fractured samples for CEM I mortar, performed at HYRL (A). Images of fractured CEM I mortars obtained from XRCT method on 33I sample (B) and by autoradiography using ¹⁴C-PMMA method on 5I sample (C)

The TD results on fractured materials were not adjustable using 1D homogeneous modelling. The shape of the curves obtained for damaged material differs strongly from the results of the sound material (blue curve in Figure 2 (A)), showing an initial concavity of the tracer concentration evolution (red curve in Figure 2 (A)). The 2D/3D modelling approach, a basic parameterization from the results of the sound material modelling and the fracture aperture distribution was successfully used to interpret these curves.

References

- [1] K.H. Hellmuth, M. Siitari-Kauppi, A. Lindberg (1993). Study of porosity and migration pathways in crystalline rock by impregnation with ¹⁴C-polymethylmethacrylate. *Journal of Contaminant Hydrology*. 13, 403-418
- [2] V. Valle, P. Bokam, A. Germaneau, S. Hedan (2019). New Development of Digital Volume Correlation for the Study of Fractured Materials. *Experimental Mechanics*. 59, 1-15
- [3] M. Bonnet, P. Sardini, S. Billon, M. Siitari-Kauppi, J. Kuva, L. Fonteneau, L. Caner (2019). Determining Crack Aperture Distribution in Rocks Using the ¹⁴C-PMMA Autoradiographic method: Experiments and Simulations. *JGR Solid Earth*. Volume 125, Issue 1
- [4] J. Crank (1975). *The Mathematics of Diffusion*. 2nd edition, Oxford (UK), Clarendon Press.
- [5] Panday, Sorab, Langevin, C.D., Niswonger, R.G., Ibaraki, Motomu, and Hughes, J.D., 2017, MODFLOW-USG version 1.4.00: An unstructured grid version of MODFLOW for simulating groundwater flow and tightly coupled processes using a control volume finite-difference formulation: U.S. Geological Survey Software Release, 27 October 2017, <https://dx.doi.org/10.5066/F7R20ZFJ>
- [6] Y. Akagi, H. Kato, Y. Tachi and H. Sakamoto (2018). Diffusion and sorption behavior of HTO, Cs, I and U in mortar. *Nuclear Science and Technology*. Volume 5, pp: 233-236

E-1 DEVELOPMENT OF R&D ON RADIONUCLIDE MIGRATION FOR CIGÉO

Jean-Charles Robinet, Christelle Martin

Andra, Châtenay-Malabry (France)

For more than 25 years, Andra has been studying the feasibility and operation of a deep geological repository for long-lived high- and intermediate-level radioactive waste in France. The long-term safety of the repository depends largely on its ability to limit the flux of radionuclides released from the waste canisters to the biosphere. During this period, a great deal of research has been developed to characterise and understand the migration of radionuclides for the various components of the repository, with particular attention being paid to the Callovo-Oxfordian Formation, the clay-rich host rock formation.

The strategy adopted by Andra was first to acquire a robust dataset characterising the migration of a large variety of radionuclides through the Callovo-Oxfordian Formation in order to support the parameterisation of the safety assessment. The main processes governing the migration of radionuclides (diffusion, sorption and solubility) were targeted and investigated through a multi-scale approach combining (i) fundamental microscale modelling, (ii) laboratory studies on mm/cm clay rock and mock-up experiments on cm/dm samples, (iii) in-situ tracer injection tests in the Meuse/Haute Marne underground research laboratory and (iv) characterisation and interpretation of natural tracer profiles for extrapolation to geological space-time scales. A large part of the research has also been developed in the framework of European programmes (FunMig, CatClay, Recosy...), allowing to decipher the fundamental processes governing radionuclide migration in clays (anion exclusion, cation enhanced diffusion...).

Since the beginning of the studies, special attention has also been given to the evaluation of aqueous radionuclide speciation with the development of Thermochimie, a thermodynamic database to support geochemical modelling. The assessment of radionuclide speciation is now an important aspect of the safety assessment, linking the overall behaviour of the radionuclide and the governing parameters.

Since 2007, studies have focused mainly on the impact of potential perturbations generated by wastes (organic matter, temperature, saline plume...) or materials (cements, unsaturated conditions related to H₂ production...). The systems studied were selected based on an assessment of the extent of the perturbations and the expected impact on radionuclides. Thanks to this series of studies, the migration of radionuclides under different perturbations has been carried out to support the safety assessment and repository design.

Ongoing studies focus on specific issues aimed at increasing safety margins (Se mobility from waste, including behaviour in waste cells, unsaturated conditions...) and waste acceptance (U mobility and reconcentration for further acceptance of spent fuel, combined saline and organic perturbations...).

E-2 IN SITU DIFFUSION OF ORGANIC COMPOUNDS IN ANDRA'S UNDERGROUND LABORATORY: A 4-YEAR INSIGHT FROM THE "DRO" EXPERIMENT

Dagnelie Romain V.H.(1), Wechner Stefan(2), Labat Marc(3), Daumas Sylvie(4), Le Milbeau Claude(5) Lettry Yanick(6) Lundy Mélanie(7)

(1) *Université Paris-Saclay, CEA, Service de Physico-Chimie, 91191, Gif-sur-Yvette, France*

(2) *Hydroisotop GmbH, Schweintenkirchen, Germany*

(3) *Aix-Marseille Université, CNRS/INSU, IRD, MIO, Marseille, France*

(4) *CFG, Marseille, France*

(5) *ISTO, Orléans, France*

(6) *Solexperts AG, Mönchaltorf, Switzerland*

(7) *Andra, Centre de Meuse Haute-Marne, Bure, France*

The development of deep geological disposals has led to many studies on radionuclides migration in natural and engineered barriers. In addition to laboratory experiments and modelling exercises, in situ experiments provide relevant and complementary tools. They help confirming driving phenomena and migration data on long-term / large-scale. They also provide additional information on specific mechanisms, e.g. local specificities, excavated damaged zones, biotic conditions, etc. In this context, several in situ diffusion experiments were performed in Bure underground research laboratory [1]. More recently, diffusion experiments were settled for the study of radionuclides diffusion in absence or presence of organic compounds [2,3]. This study will detail recent results on the modelling and interpretation of the "DRO" experiment (Diffusion / Radionuclides / Organic compounds).

The DRO in situ experiment aims at assessing the effect of anthropogenic organic compounds on radionuclides diffusion in the Callovian-Oxfordian clay-rich rock. To this aim, α -Isosaccharinate (α -Isa) and o-phthalate (o-phthal.) were selected as compounds potentially released from cellulose containing waste and cementitious plasticizers respectively. Two preliminary injections of α -Isa and then o-phthal., with conservative reference tracers, were performed in a pre-existing borehole (PAC1001 [4]). These injections were designed to assess: i) the diffusive retardation of organic compounds; ii) their possible in situ bio(geo)degradation; and iii) their potential effects on the geochemical media.

A first modelling is performed on some of the monitored compounds: HDO, Br^- , SO_4^{2-} , α -Isa, o-phthal., Na^+ , Th(IV). The interpretation of data is discussed regarding: diffusion processes (anion exclusion, effect of excavated damaged zone, etc.), and (bio)chemical processes (adsorption, biotic degradation). Concerning α -Isa, the current results tend to confirm two antagonist effects (Fig. 1, left): anion/size exclusion slightly decreasing the diffusive flux compared to neutral reference (HDO), and chemical retention, which increases the flux at solid/solution interface and limits the penetration depth of the compounds inside the host rock. Concerning o-phthalate, the higher injection concentration, $[\text{o-phthal.}] \sim 10^{-2} \text{ mol.L}^{-1}$, may have induced a slight shift of surface and carbonates chemical equilibria. The concomitant out-diffusion of Ca^{2+} and Mg^{2+} modified aqueous speciation during the experiment, in agreement with ESI-MS measurements (Fig. 1, right).

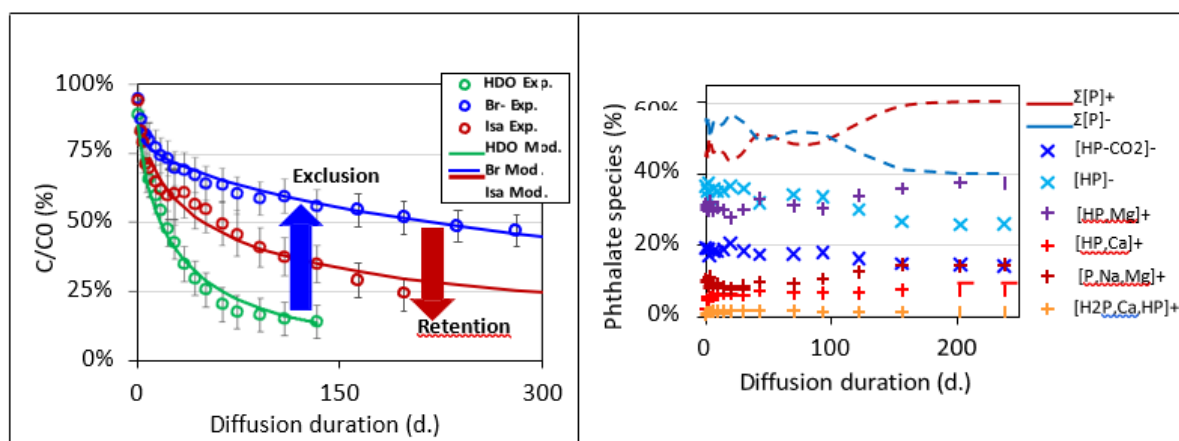


Figure 1: in-diffusion of organic compounds during DRO experiment.
 (Left) Monitoring of HDO, Br and α -Isa concentrations in circulating solution.
 Signs: experimental data. Lines: adjusted diffusion modelling.
 (Right) Evolution of o-phthalate speciation monitored by ESI-MS.

After α -Isa injection, a progressive increase of the biodiversity was also observed, followed by a stabilization, at a level that remained above the initial biodiversity. This could indicate a possible α -ISA metabolization, despite a degradation mechanism lower than retention. Such evolution was not observed 120 days after o-phthalate injection, where global biodiversity seems to be declining. All these data allowed an accurate quantification of in situ migration properties of compounds in biotic conditions. The available measurements of various compounds and major ions encourage for further multi-elements or multi-species reactive-transport modelling. A third injection is also discussed with a focus on in situ biodegradation of α -Isa, physico-chemical conditions favoring biotic activity and the corresponding degradation pathways.

References

- [1] Delay, J. et al. (2014). Three decades of underground research laboratories: what have we learned? Geological Society, London, Special Publications 400, 7-32.
- [2] Vinsot et al., (2022). Evaluating Uranium Mobility in situ in the Callovo-Oxfordian Argillaceous Rock. 8th international Clay Conference, June, 13-16th, Nancy, France.
- [3] Lundy et al., (2022). Diffusion of α -Isosaccharinic acid in a clay-rich rock: an in situ experiment. 8th international Clay Conference, June, 13-16th, Nancy, France.
- [4] Appelo C.A.J. et al. (2008). Obtaining the porewater composition of a clay rock by modeling the in- and out-diffusion of anions and cations from an in-situ experiment. J. Contam. Hydrol., 101, 67-76

E-3 EVALUATING RADIONUCLIDES MOBILITY *IN SITU* IN THE CALLOVIAN- OXFORDIAN ARGILLACEOUS ROCK

Agnel Myriam I.⁽¹⁾, Dagnelie Romain V.H.⁽²⁾, Thory Emilie⁽²⁾, Hautefeuille Benoît⁽³⁾, Lettry Yanick⁽⁴⁾, Parisi Melvin⁽⁴⁾, Vinsot Agnès⁽¹⁾

(1) Andra, CMHM, Bure (France),

(2) Université Paris-Saclay, CEA, Service de Physico-Chimie, 91191, Gif-sur-Yvette, France

(3) AXINT SAS -Lucenay (France),

(4) Solexperts AG - Mönchaltorf (Switzerland)

Argillaceous rocks are studied internationally for the disposal of high-level and/or long-life radioactive waste. Andra, the French radioactive waste management agency, has built an Underground Research Laboratory (URL) to characterize of Callovian-Oxfordian argillaceous rock in the east of Paris basin (Meuse Haute-Marne, France) [1]. An experiment named DRN is being currently performed in this URL to investigate radionuclides mobility in the Callovian-Oxfordian argillaceous rock under *in situ* conditions.

Two tests are ongoing and each will last 8 to 10 years:

- Migration of ^{22}Na and tritiated water (HTO). Tracers were injected in November 2021 through a horizontal borehole (Figure 1). The migration occurring in both horizontal and vertical directions will allow to quantify migration anisotropy. The injected activity is approximately 131 kBq for HTO and 3.14 MBq for ^{22}Na ($\approx 2019 \pm 17$ Bq/mL).
- Migration of $\text{U(IV)O}_2(\text{s})$ mixed with Callovian-Oxfordian argillaceous rock and compacted into pellets. Pellets were inserted in 2019 into in a 25-cm diameter and 33-cm length Callovian-Oxfordian rock core (Figure 2). This correspond to two sources of ~ 1 g of Uranium ($\sim 2 \times \{5.10^4\}$ Bq(U)). The core is installed at 9 m depth in the packed-off interval of a vertical downward borehole into the Callovian-Oxfordian argillaceous rock.

The novelty of these tests is the presence of gamma (γ) probes to follow the distribution of the γ emitters related to the spatial evolution of radionuclides concentrations in the rock in real time. These sensors have been specifically developed to withstand the *in situ* conditions (pressure, chemical composition of water, signal emissions of the rock, etc.). For the test with ^{22}Na , gamma probes are positioned around the injection borehole to follow the migrations in both the horizontal and vertical plan (

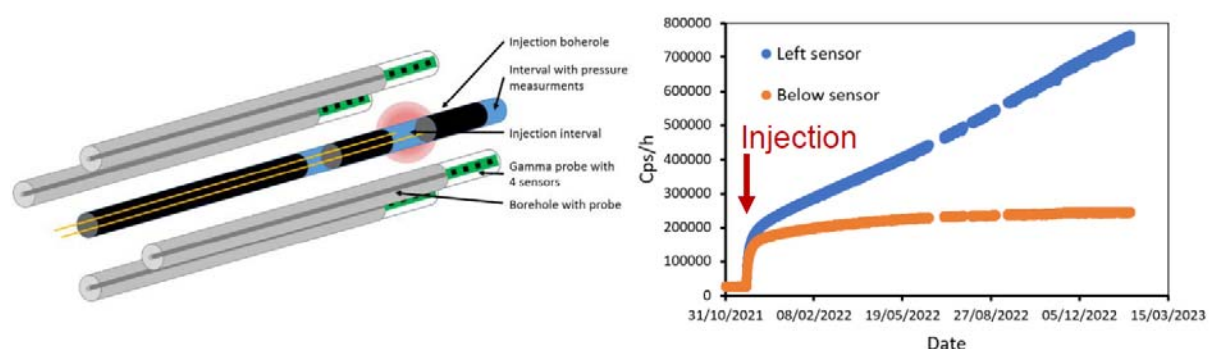


Figure 1). For the test with U, which displays a lower lability, a movable probe is placed in the center of the core. The motion of the probe, remotely controlled and programmed (Figure 2), allows to map the spatial distribution of the sources as a function of time. These results are complemented with water sampling to follow the in-diffusion of ^{22}Na and HTO.

Preliminary results and models gave an average effective diffusion coefficient $D_e(^{22}\text{Na}) \sim 8 \cdot 10^{-11} \text{ m}^2 \cdot \text{s}^{-1}$ if the damaged zone around the borehole is not taken into account, or $\sim 1.6 \cdot 10^{-11} \text{ m}^2 \cdot \text{s}^{-1}$ if it is taken into account (1.6 cm of damaged zone around the borehole). These coefficients are consistent with previous studies in Callovian-Oxfordian argillaceous rock (on core samples and in another in situ diffusion experiments). Modelling of gamma maps are ongoing to determine the effective diffusion coefficient parallel or perpendicular to bedding planes of the rock and the corresponding anisotropy coefficient. A third experiment should start in 2023 with the injection of ^{36}Cl and HTO into a similar horizontal borehole. Beta probes will be placed all around the interval of injection with the goal to quantify ^{36}Cl migration after a few years.

With these three *in situ* tests, the DRN experiment will provide migration data of a reference tracer (HTO), a cation (^{22}Na), an anion (^{36}Cl), and an actinide (U(IV)). This data and other the potential observations, such as redox reactions, should improve the understanding of migration and the various underlying models.

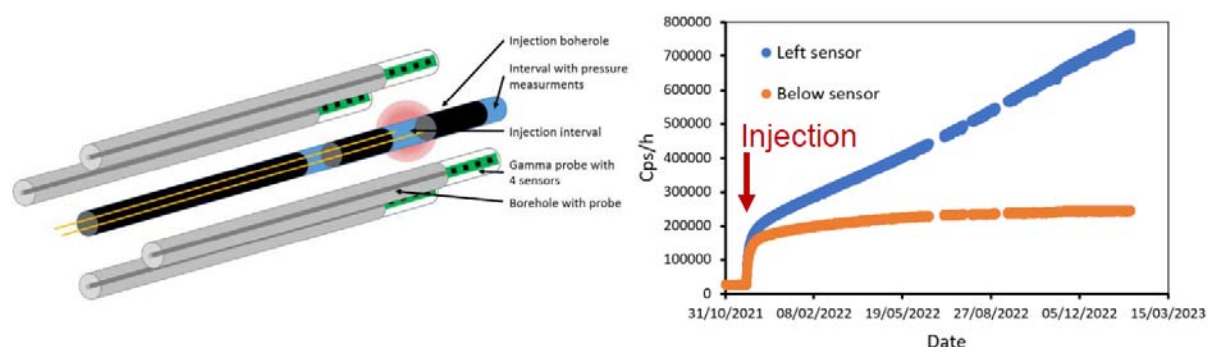


Figure 1. (Left) Scheme of HTO/ ^{22}Na experiment.

(Right) Gamma radiations measured by sensors around the injection borehole.

Data from the sensors placed on the left (blue dots) / or below (orange dots) the injection borehole.

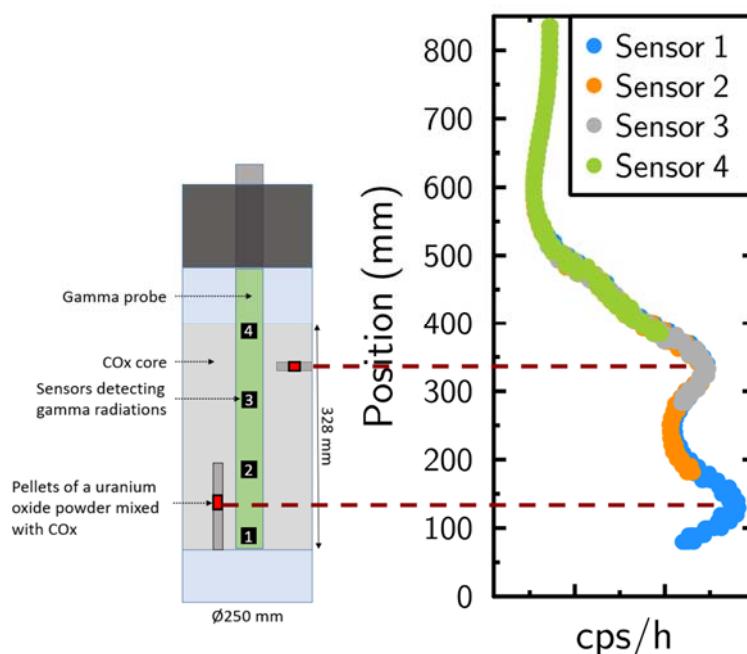


Figure 2. (Left) Scheme of the U(IV) experiment. A movable gamma probe is placed in the center of the rock core. This core contains two pellets with $\text{U(IV)}\text{O}_{2(s)}$. The gamma probe displays four sensors measuring gamma emissions along the vertical axis of the core.

(Right) Gamma radiations measured by sensors on the gamma probe.

Reference

- [1] Delay, J. et al. (2014). Three decades of underground research laboratories: what have we learned? Geological Society, London, Special Publications 400, 7-32.

E-4 QUANTITATIVE ANALYSIS OF RADIONUCLIDE CONTAINMENT AS PART OF THE SAFETY ASSESSMENTS IN THE GERMAN SITE SELECTION PROCEDURE

Behrens, Christoph⁽¹⁾, Gelleszun, Marlene⁽¹⁾, Miro, Shorash⁽¹⁾, Renz, Alexander⁽¹⁾, Kreye, Phillip⁽¹⁾, Rühaak, Wolfram⁽¹⁾

(1) *Bundesgesellschaft für Endlagerung (BGE) mbH, Germany*

The German search for a high-level nuclear waste repository in the subsurface as codified by the Site Selection Act [1] is a challenging and complex assignment. Three different types of host rock – halite, clay rock and crystalline rock – are under consideration all over Germany, starting from a blank map. In 2020, a first milestone was reached with the publication of the Sub-areas Interim Report [2], marking the end of step 1 of the first phase of the site selection procedure. The report details the sub-areas that are still under consideration after extensive application of exclusion criteria, minimum requirements, and geoscientific weighing criteria; see [3] for details.

In the second step of phase 1 of the site selection procedure, preliminary safety assessments have to be conducted for the sub-areas (see [4] for the legal basis). The challenges in this step are manifold. First, the sub-areas cover a vast area – about 54% of Germany. Second, in this stage the assessments solely rely on already existing data, as on-site exploration will only start in the following phase. Third, different host-rock types call for a flexible approach in the assessments, with heterogeneous and scarce data availability posing an additional difficulty.

To achieve a consistent and fair treatment of all sub-areas, a methodology with a set of criteria for the assessments is developed. The status of this development was published in March 2022 [5]. The current phase of the site selection procedure is planned to conclude in 2027, with the publication of a considerable small set of siting regions that display the most favorable conditions for a nuclear waste repository.

One important part of the representative preliminary safety assessments is the analysis of the potential repository system and the prospects of radionuclide containment. Different from other repository site selection programs, the Germany Site Selection Act specifies (besides others) limits on the maximum of material (in mass and amount) that can be released into the geosphere over a total time span of one million years, and a maximum rate of release per year. The estimation of these limits is a challenge, requiring individual methodologies for the different host rocks, as they display vastly different transport processes and properties.

We implemented a quantitative method based on a 1D finite-differences code for modeling the transport of radionuclides in the subsurface. The code “TransPyREnd” includes diffusion, advection, equilibrium sorption, decay of radionuclides, and the build-up of the daughter nuclides. An outline of the method was given in [5, 6]. While this approach is robust, it crucially relies, for instance in clay rocks, on knowledge of parameters like the porosity, the nuclide- and geology-specific diffusion coefficients, sorption properties, and other transport parameters. While in addition to existing research different research programs are funded to close existing gaps in the data, all of the relevant parameters come at a varying degree of uncertainty that needs to be accounted for.

In order to exploit the limited data as efficiently as possible, we use and modify a parameter workflow proposed by Nagra for calculating the diffusion coefficients [7] and the sorption parameters [8] depending on a small number of input parameters, like the temperature and the effective porosity of the relevant layer. We extend this workflow to allow for differing geochemical conditions as expected in the respective German areas.

In post-processing, we define several indicators to consolidate the results of these assessments. All indicators are based on the notion of an effective transport length, and defined as the minimum distance from the repository for which the legal limits on radionuclide migration are fulfilled. This transport length is then compared with the total distance from the repository to the boundary of the host rock, resulting in intuitive and easily understandable measures for the performance of containment. Depending on context, different variants of this measure are calculated.

To account for parameter uncertainties, we make extensive use of non-deterministic ensemble calculations to propagate the uncertainties of the input parameters to the model results, namely, the transport length. Since the total number of relevant parameters is of the order of 1000, we apply methods of sensitivity analysis to allow a reduction of the number of parameters considered in the ensemble calculations. This also helps in building a deeper understanding of the modelled system behavior and its most relevant properties.

References

- [1] Standortauswahlgesetz (Site Selection Act) (2017, last changed 2020). BGBl. I, 1074
- [2] BGE (2020). Summary Sub-areas Interim Report according to Section StandAG.
- [3] Hoyer, E. et al. (2021). Preliminary safety analyses in the high-level radioactive waste site selection procedure in Germany. *ADGEO*, 56: 67–75
- [4] Endlagersicherheitsuntersuchungsverordnung (Disposal Safety Assessment Ordinance) (2020). BGBl I: 2904-2103
- [5] BGE (2022). Methodenbeschreibung zur Durchführung der repräsentativen vorläufigen Sicherheitsuntersuchungen gemäß Endlagersicherheitsuntersuchungsverordnung.
- [6] Behrens, C. et al. (2023). TransPyREnd: a code for modelling the transport of radionuclides on geological timescales. *ADGEO*, 58: 109-119
- [7] Van Loon, L.R. (2014). Effective diffusion coefficients and porosity values for argillaceous rocks and bentonite: measured and estimated values for the provisional safety analyses for SGT-E2. NTB 12-03
- [8] Baeyens. B. et al. (2014). Sorption Data Bases for Argillaceous Rocks and Bentonite for the Provisional Safety Analyses for SGT-E2. NTB 12-04

E-5 WHAT RESEARCH CHALLENGES FOR NORM AND TE-NORM MANAGEMENT WORLDWIDE?

L. Février

IRSN/PSE-ENV/SPDR/LT2S, France

The Council Directive 2013/59/EURATOM laying down basic safety standards for protection against the dangers arising from exposure to ionising radiation has introduced requirements to include protection against natural radiation sources in regulatory framework of EU members states for workers, members of the public and the environment in any planned, existing or emergency exposure situation. Whereas the Directive does not apply to exposure to the natural level of radiation (such as radionuclides contained in the human body and cosmic radiation prevailing at ground level) or aboveground exposure to radionuclides present in the undisturbed earth's crust, It applies in particular to the exposure resulting from the processing of materials with naturally-occurring radionuclides. From an operational point of view, it means that a dosimetric assessment has now to be performed in all situations where naturally occurring radioactive material (NORM) is encountered. Such assessment relies on an identification of all exposure pathways to consider and a quantification of the dose in each of them with predictive models. Since NORM may contain a huge diversity of radionuclides (mainly coming from the disintegration chain of ^{238}U and ^{232}Th), the realization of realistic dose assessment needs a good understanding of the behaviour and distribution of all these radionuclides in the different compartment of the environment. After reminding some elements of context, the presentation will address some research challenges for NORM management through specific examples from the literature.

E-6 MODELLING OF RADIONUCLIDES MOBILITY AFTER LEGACY SITE RESTORATION: THE CASE OF FLUORITE SLUDGE NORM

Marcin Płachciak (1), Fidel Grandia (1)

(1) Amphos 21 Consulting S.L., Spain

The production of dicalcium phosphate (DCP), which is used as an additive for animal feeding, leads to the generation of NORM called fluorite sludge. DCP precipitates after phosphoric acid production via reaction of F-rich phosphorite with HCl. During such a reaction, fluorite (CaF₂) precipitates, reaching up to 40-50% in wt. in the final sludge. The legacy site at El Hondón (Cartagena, South Spain) contains more than 1 Mt of the fluorite sludge and restoration plans are currently being developed. One critical issue in the restoration project is to ensure the geochemical and hydrogeological stability of radionuclides. In this study, geochemical and reactive transport modelling have been performed to predict future radionuclide mobility after restoration.

Fluorite precipitation during DCP production triggers radionuclide separation from the phosphoric acid since it fixes significant activities of ²¹⁰Po, ²²⁶Ra, ²³⁰Th, ²³⁸U and ²¹⁰Pb. The final activity of the fluorite sludge is of few Bq·g⁻¹. The mobility of these radionuclides in the site and their potential impact on the environment depend on many parameters and processes, such as permeability of the residues, chemical stability of host mineral under the given pH-Eh-salinity conditions or sorption of the radionuclides on the minerals occurring in the site, such as iron oxides or hydroxides.

To reduce the environmental impact of the sludges, a number of restoration options of the site have been considered including covering the landfill with layers of technosols and waste such as foundry slag, fly ash from biomass plants, glass remains, clay, bricks, construction waste, organic material, and compost. Some of these materials (mainly construction waste through cement degradation) would induce alkaline reducing conditions within the fluorite sludge residues; also, the use of organic materials could lead to reducing conditions. Considering all these scenarios, it was found necessary to predict how the CaF₂, accessory minerals and radionuclides occurring in the sludge would behave under alkaline and reducing conditions (pH > 10, < 200 mV) and to assess the potential radionuclide release to the aquifers beneath the site.

First, the stability of fluorite host under these conditions was calculated when this mineral is in contact with (1) three alkaline waters, representative of different states of cement degradation, and (2) the neutral pore-water currently existing in the porewaters of the sludge. The calculation estimated that the proportion of fluorite that would be dissolved by infiltration of alkaline water would be very low, less than 0.01%, (Fig. 1).

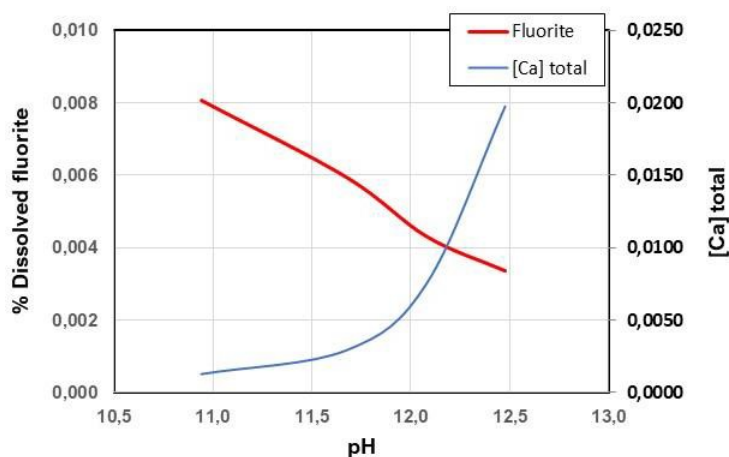


Figure 1. Calculated percentage of fluorite that would dissolve until reaching thermodynamic equilibrium in the case of infiltration of hyperalkaline waters associated with the different degrees of degradation of the Portland cement. The initial concentration of F in the porewater has been 1×10^{-5} M.

To model the stability of the aqueous species of the U, Th, Po, Pb and Ra under the redox conditions below 200 mV, it has been conservatively assumed that the water would dissolve 1% of the fluorite sludge and the relative activity of these radionuclides would be released into the porewater.

The results of the geochemical calculations show that polonium and lead would be the radionuclides with higher increase of mobility due to the formation of anionic complexes with low affinity with sorption sites. The most relevant risk of radionuclide mobility, however, is dissolution of Fe(III) oxyhydroxides existing in the geological formations beneath the fluorite sludge piles due to the infiltration of hyperalkaline ($\text{pH} > 11.5$) and reducing fluids (< 400 mV) (Figure 2). These minerals are the solubility-limiting solids of these radionuclides (except radium) through surface sorption and their dissolution could lead to their release.

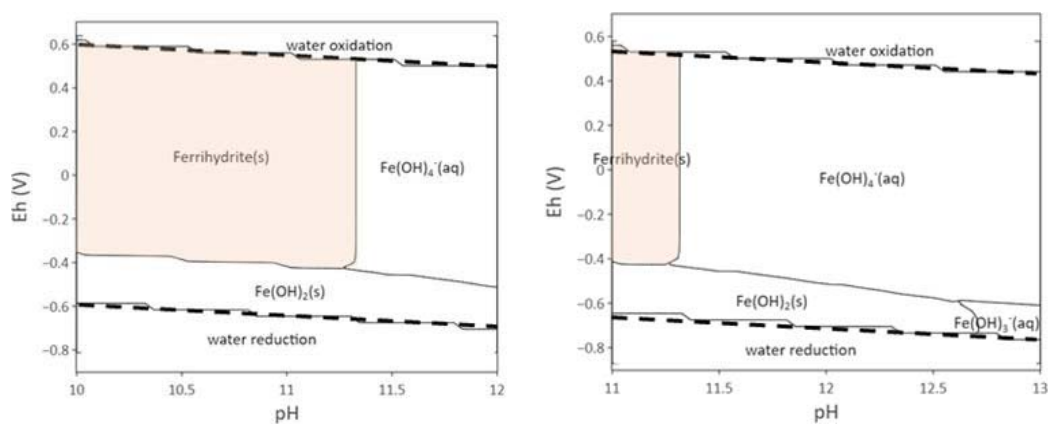


Figure 2. Pourbaix diagram showing the stability of amorphous ferrihydrite. (left) pH 10-12; $[\text{Fe}]_T = 1 \times 10^{-6}$; $[\text{C}]_T = 8 \times 10^{-6}$. (right) pH 11-13; $[\text{Fe}]_T = 1 \times 10^{-6}$; $[\text{C}]_T = 8 \times 10^{-7}$.

On the other hand, reactive transport calculations predicted that the low permeability of fluorite sludge would prevent a significant advective solute transport down to the underlying aquifer. The conclusion of this study is, therefore, that the use of cementitious materials and/or technosols with organic matter will not represent a significant reduction in the stability of the fluorite sludge.

E-7 UNDERSTANDING URANIUM FATE IN WETLAND SOILS: A SPECIATION AND LABILE BEHAVIOR STUDY IN THE FORMER EXTRACTION MINE OF ROPHIN (FRANCE)

Nivesse Anne-Laure ⁽¹⁾, Landesman Catherine ⁽¹⁾, Arnold Thuro ⁽²⁾, Sachs Susanne ⁽²⁾, Stumpf Thorsten ⁽²⁾, Scheinost Andreas ⁽²⁾, Coppin Frédéric ⁽³⁾, Fevrier Laureline ⁽³⁾, Den Auwer Christophe ⁽⁴⁾, Gourgiotis Alkiviadis ⁽⁵⁾, Del Nero Mireille ⁽⁶⁾, Montavon Gilles ⁽¹⁾

(1) SUBATECH, UMR 6457, IMT Atlantique/IN2P3-CNRS/Nantes Université, 4, Rue Alfred Kastler, BP 20722, Nantes Cedex 3, 44307, France

(2) Helmholtz-Zentrum Dresden-Rossendorf (HZDR), Institute of Resource Ecology, Bautzner Landstraße 400, 01328 Dresden, Germany

(3) Institut de Radioprotection et de Sécurité Nucléaire (IRSN), PSE-ENV, SRTE, LR2T, Cadarache, Saint-Paul-lès-Durance, France

(4) Institut de Chimie de Nice, Université Côte d'Azur, 28 Avenue Valrose, 06108, Nice Cedex 2, France

(5) Institut de Radioprotection et de Sécurité Nucléaire (IRSN), PSE/ENV - SEDRE/LELI BP 17, Fontenay-aux-Roses, 92262, France

(6) Institut Pluridisciplinaire Hubert Curien, 23 rue du Loess, BP 28, 67037, Strasbourg Cedex 2, France

Uranium (U) mining and milling activities, as well as mineral processing plants, raise environmental concerns due to the possible release of radioactive and other potentially toxic elements. To understand their fate in the environment and evaluate their potential impact, the main scientific challenge calls for identifying their solubility, mobility and bioavailability in the environment. Around former U mining and processing plants, wetlands prove to be specific zones with significant amounts of U. This is partly explained by the reduction of the mobile U(VI) into U(IV) due to strongly reducing conditions related to the microbial activity and/or by complexation with the organic matter occurring with high concentrations in wetlands.

At the center of the ancient mining district of Lachaux in France (45.994°N, 3.596°E), the site of Rophin (within the ZATU: Uranium Working Zone = Long Term Socio-Ecological Research Tool of CNRS, Fig.1.a) is characterized by a wetland area with large U concentrations up to 16 g.kg⁻¹ of dry mass of soil [1]. Several cross-analyses indicate that U was transported in particulate forms into the wetland during the exploitation of U(VI) phosphate minerals [1]. The Rophin site therefore provides the opportunity to study the stability of these U minerals over almost 70 years in a non-manipulated wetland since the closure of the mine. In this context, the main challenge is to describe the behavior of U (and decay products of interest) in the wetland using a predictive model that combines transport and chemical speciation. The overall adopted scientific approach is to propose a mechanistic description of the mobility of these elements, from the molecular scale (speciation) to *in natura* behavior (lability), by coupling field investigations and laboratory experiments.

A simplified three-layer model describes the soil profile of the Rophin wetland, with variable U concentrations and specific physico-chemical soil properties (Fig.1.b). Analyses carried out by X-absorption spectroscopy on *in natura* soil samples mainly indicate the presence of an adsorbed form of U(IV) in the highly contaminated layer, while both U(IV) and U(VI) are identified in the organically rich part at the surface. Additional SEM-EDX and μ -XRF mapping measurements also indicate that U minerals transported into the wetland were partially dissolved and re-adsorbed in soils.

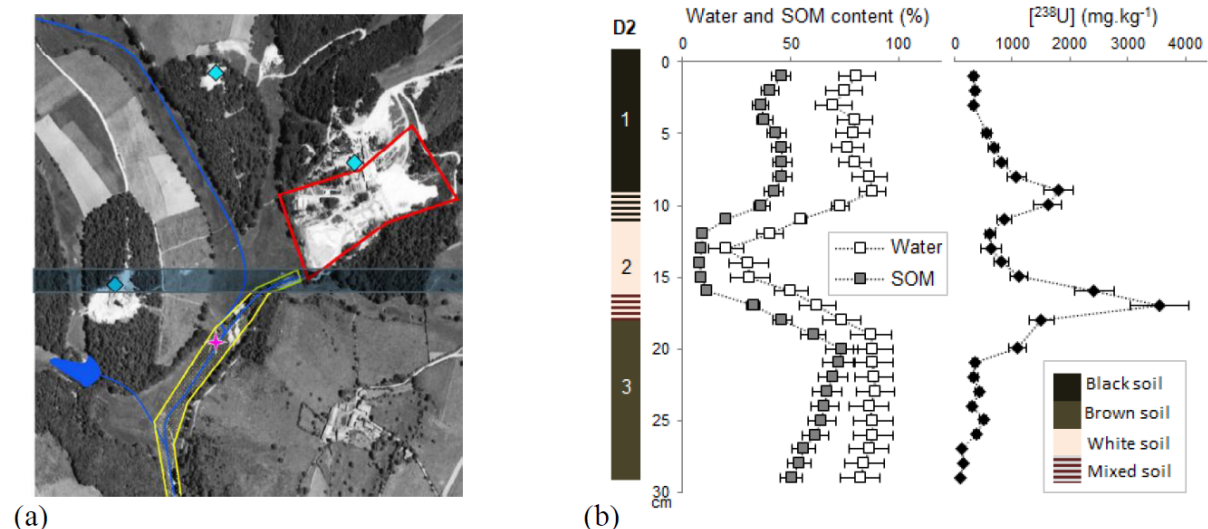


Fig. 1. (a) Aerial photograph of the Rophin site in 1954, and (b) simplified soil-layers profile (left), water and SOM (Soil Organic Matter) contents, and ^{238}U concentrations in dry mass of soil (right) [1].

The objective was to determine which fraction is finally labile, i.e. the fraction that is adsorbed and whose resupply in solution is rapid. This was assessed by desorption experiments under representative site conditions with two complementary approaches [2,3]. Overall, the available fraction is very low (3 to 10 % for the highly contaminated layer and less than 1% for the surface layer) and is characterized by distribution coefficient (K_d) values of the order of 10^2 L.kg^{-1} . These results were then compared with field data using DGT/DET techniques coupling (Diffusive Gradient in Thin-films/ Diffusive Equilibrium in Thin-Films) [4]. We found an available fraction in the whitish zone, which is rapidly eliminated with time, whereas a labile U fraction is almost undetectable in the surface layer. Combined with time-dependent deployment DGT/DET coupling, results highlighted the predominance of a kinetic parameter and thus, the expected key role of the organic matter in the U mobile behavior in the surface soil.

This study provides access to the input data (labile quantity and (K_d) values) for the establishment of a reactive transport model at the scale of the Rophin mining-affected wetland, but also allows to determine significant information on U interactions in soils. As such, this multi-scale and interdisciplinary study contributes to the improvement of the global understanding of U migration and fate in wetland soils.

References

- [1] Martin, A., Hassan-Loni, Y., ... & Montavon, G. (2020). An integrated approach combining soil profile, records and tree ring analysis to identify the origin of environmental contamination in a former uranium mine (Rophin, France). *Science of the Total Environment*, 747, 141295.
- [2] Loni, Y. H., David, K., ... & Montavon, G. (2021). Investigation of europium retention on Callovo-Oxfordian clay rock (France) by laser ablation inductively coupled plasma mass spectrometry (LA-ICP-MS) and percolation experiments in microcells. *Applied Clay Science*, 214, 106280.
- [3] Flouret, A., Henner, P., Coppin, F., Pierrisnard, S., Carasco, L., & Fevrier, L. (2022). Cesium transfer to millet and mustard as a function of Cs availability in soils. *Journal of Environmental Radioactivity*, 243, 106800.
- [4] Martin, A., Montavon, G., & Landesman, C. (2021). A combined DGT-DET approach for an in situ investigation of uranium resupply from large soil profiles in a wetland impacted by former mining activities. *Chemosphere*, 279, 130526.

E-8 MODELLING WATER CIRCULATION AND SOLUTE TRANSPORT AT A FORMER FRENCH URANIUM MINING SITE

Amandine Katz (1), Edouard Veilly (1), Laureline Février (1), Danyl Pérez-Sánchez (2), Thuro Arnold (3), Frank Bok (3), Gilles Montavon (4), Clotilde Bertin (5), Patrick Chardon (6), David Sarramia (6), Pierre Vaudelet (7), Clarisse Mallet (8), Laura Urso (9)

(1) Institut de Radioprotection et de Sûreté Nucléaire (IRSN), France,

(2) Research Centre for Energy, Environment and Technology, Spain,

(3) Helmholtz-Zentrum Dresden-Rossendorf, Germany,

(4) Subatomic Physics and Associated Technologies, France,

(5) French Geological Survey, France,

(6) Laboratoire de Physique de Clermont Ferrand, France,

(7) NAGA Geophysics, France,

(8) Laboratoire Microorganismes Genome Environment, France,

(9) Federal Office for Radiation Protection, Germany.

Within the frame of the RadoNorm project (<https://www.radonorm.eu/>), the goal of the present study is to better understand the importance of hydrogeochemical and chemical processes for the transfer of radionuclides in the environment with a focus on Naturally Occurring Radioactive Material (NORM). In that context, a wetland in a downstream area of a former uranium mine tailing, i.e., the Rophin site, has been selected. The following water flow and solute transport codes, in 1, 2 or 3 D are envisaged: HYTEC [1], HYDRUS [2], CIEMAT model [3], and MELODIE [4]. This application should allow to understand the fate of uranium and radium observed in the wetland area, the link between radionuclide concentration in the wetland and in the crossing stream and also to highlight a possible transfer of radionuclides to the groundwater.

The Rophin site is located in the department of Puy-de-Dôme of the region Auvergne-Rhone-Alpes (France). There, the measured dose rates are 20 to 30 times higher than the background along the Gourgeat stream and in a so-called “wetland area” (Figure 1). A source of contamination is present due to successive discharges from settling ponds during the operational phase of the mine and located in the whitish layer of the wetland, where three different soil horizons are identified (an organic-rich surface layer, a whitish layer, and a paleosol layer).

The watershed has been equipped since 2019 with piezometers and surface sensors to monitor the water (electrical conductivity, temperature and water level). Meteorological data is available to identify patterns for precipitation and temperature regimes for the wet and dry seasons. First results from measurement campaigns of the water table in 2021 and 2022 confirm the presence of a groundwater table in the wetland, which is rather close to the surface and varies depending on meteorological conditions.

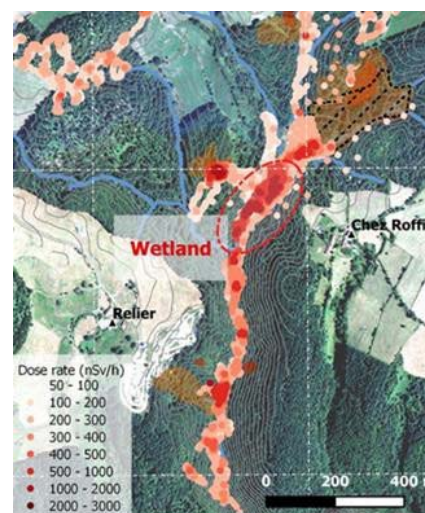


Figure 1: radiological mapping with focus on the wetland (red circle) of Rophin site.

Kindly provided by Zone-Atelier Territoires Uranifères (ZATU).

A geophysical survey was carried out in October 2022 to provide the geometry of the different horizons of the wetland, as well as information on water content, permeability and CEC. In parallel, parameters such as soil permeability, soil porosity, diffusion coefficients and dispersivity will be obtained by laboratory measurements in Spring 2023. Surface mapping data (dose rates and gamma-ray spectroscopy analysis) and Light Detection and Ranging (LiDaR) data are available as well as information about water chemical composition and soil/sediment mineralogy both in the wetland and in the Gourgeat stream. To evaluate radionuclides sorption onto the various soil layers and partition of

radionuclides between solid and liquid phases, distribution coefficients are determined either experimentally (K_d) or modelled with the mechanistic “Smart K_d ” approach [5].

A description of water flows and soil layers to be modelled is presented with Figure 2. In a first approach assuming a saturated zone, modelling of the three layers system will be performed in 1D and 2D. Two types of simulation will be considered, one with a low flux regime when the stream and the wetland seem to be disconnected and the other with a high flux regime when the stream and the wetland should be hydraulically connected. The aim is to evaluate the evolution of uranium and radium concentration within the layers of the wetland and also to quantify the concentrations of those radionuclides released into the environment, i.e., groundwater and Gourgeat stream.

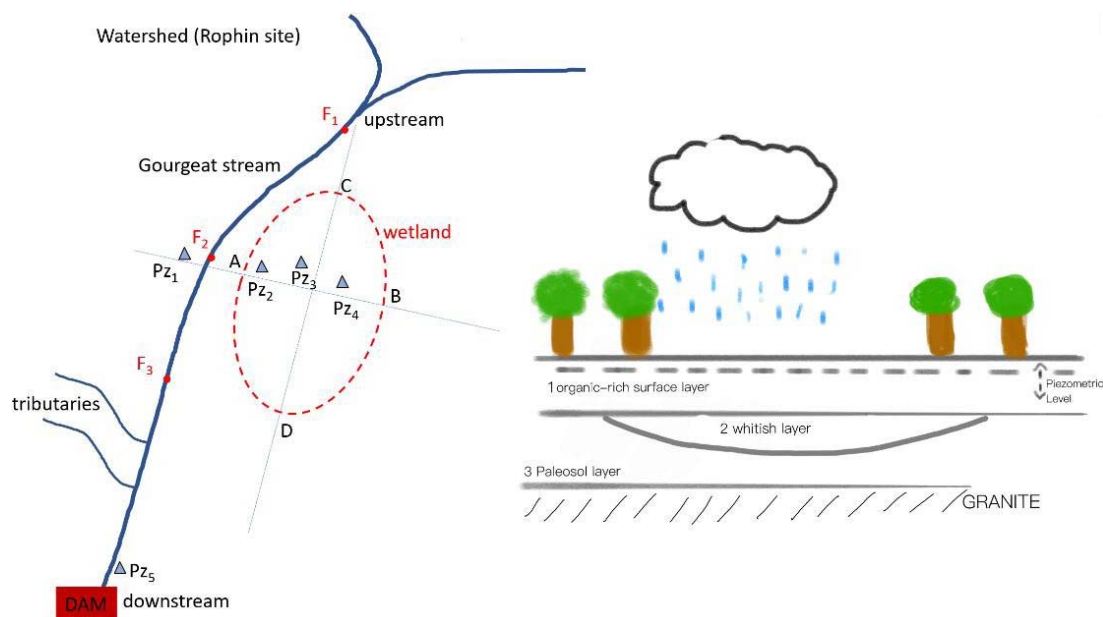


Figure 2. Conceptualisation of Rophin site. On the left the schematisation from above: the oval is the wetland. Piezometer (Pz1-5) locations are indicated as well as measurement locations of the water flows along the Gourgeat stream (F1-3). Points A and B indicate transversal direction to the wetland, points C and D indicate longitudinal direction to it. On the right, the section of the wetland along the longitudinal direction in which the three layers (1, 2, 3) of the wetland are indicated.

Acknowledgments: The RadoNorm project has received funding from the Euratom research and training programme 2019-2020 under grant agreement No 900009.

References

- [1] Van Der Lee, J., De Windt, L., Lagneau, V., & Goblet, P. (2003). Module-oriented modeling of reactive transport with HYTEC. *Computers & Geosciences*, 29(3), 265-275.
- [2] Simunek, J., Jacques, D., van Genuchten, M. T., & Mallants, D. (2006). Multicomponent geochemical transport modeling using HYDRUS-1 D and HP 1. *Journal of the American water resources Association*, 42(6), 1537-1547.
- [3] Pérez-Sánchez, D., & Thorne, M. C. (2014). Modelling the behaviour of uranium-series radionuclides in soils and plants taking into account seasonal variations in soil hydrology. *Journal of environmental radioactivity*, 131, 19-30.
- [4] Mathieu, G., Dymitrowska, M., & Bourgeois, M. (2008). Modeling of radionuclide transport through repository components using finite volume finite element and multidomain methods. *Physics and Chemistry of the Earth, Parts A/B/C*, 33, S216-S224.
- [5] Stockmann, M. & Schikora, J. & Becker, D.-A. & Flüge, J. & Noseck, U. & Brendler, V. (2017). Smart K_d -values, their uncertainties and sensitivities - Applying a new approach for realistic distribution coefficients in geochemical modeling of complex systems. *Chemosphere*. 187. 10.1016/j.chemosphere.2017.08.115.

A3-1 THE AQUATIC CHEMISTRY OF PENTAVALENT ACTINIDES (NP, PU): DETERMINATION OF THE FIRST TWO HYDROLYSIS CONSTANTS

Aupiais Jean⁽¹⁾, Chistin Christopher⁽¹⁾, Levier Martin⁽¹⁾

(1) CEA, DAM, DIF, F-91297 Arpajon Cedex

Up to now, no recommendations have been made by the Organisation for Economic Co-operation and Development Nuclear Energy Agency (OECD-NEA) for the first two hydrolysis constants of pentavalent plutonium.¹ We have determined them, as well as those of Np(V), by means of capillary electrophoresis coupled with inductively coupled plasma mass spectrometry (CE-ICP-MS) in 0.1 M NaCl at 25°C. This technique is so sensitive that it enables the use of very dilute concentrations ($< 10^{-7}$ M) in which disproportionation is sufficiently hampered not to be observed over a period of one week. The first hydrolysis of Pu(V) is expected to be detectable at $\text{pH} > 11$ based on values obtained for Np(V). Unfortunately, this pH is high enough that we must consider the absorption of CO_2 and its concomitant complexation with pentavalent actinides. In particular, for $\text{pH} > 11$ under air, the species $[\text{AnO}_2(\text{CO}_3)_3]^{5-}$ is expected to be dominant. In a conventional laboratory, and especially in an alkaline medium, it is impossible to completely protect a sample against CO_2 . We therefore adopted a strategy based on limiting CO_2 diffusion by covering the sample with a film of mineral oil. This protection is efficient up to $\text{pH} \approx 10$, with no carbonate anions being detected after five days. For higher pH values, carbonate anions were quickly detected after one or two days only. However, the resolution of CE is very high, enabling the separation of both An-carbonate species from the An-hydrolyzed species. Since the information about the speciation is provided by the migration time (due to fast kinetics) and not by the area (the chemical equilibrium is kinetically blocked), the presence of carbonate is not problematic as long as its concentration is not so high that the peak corresponding to hydrolyzed pentavalent actinides can no longer be detected. In practice, for $\text{pH} > 11$, all samples were prepared immediately prior to analysis. The sample was thus stable enough to survive for several hours, which allowed sufficient time to carry out the separation by CE. An example is given in Figure 1 for Np(V), where the presence of two peaks is observed. The peak related to the species $[\text{NpO}_2(\text{OH})_2]^-$ does not interfere with the peak of interest (the hydrolyzed species).

The fitting of experimental data obtained in 0.1 M NaCl (see Figure 2) for Np(V) and Pu(V) allows extracting the corresponding stability constants (see Table 1).

Table 1: Stability constants for the reactions of hydrolysis with An(V) (An = Np, Pu) in 0.1 M NaCl, 25°C.

Element	$\log \beta_1^I$	$\log \beta_2^I$	$\log \beta_1^0$	$\log \beta_2^0$	$\log {}^*\beta_1^0$	$\log {}^*\beta_2^0$	Ref
Np(V)	2.43±0.13	3.39±0.33	2.63±0.13	3.59±0.33	-11.36±0.13	-24.40±0.33	2
Review					-11.3±0.7	-23.6±0.5	1
Pu(V)	2.29±0.12	3.56±0.26	2.50±0.12	3.76±0.26	-11.50±0.12	-24.24±0.26	2

The fitting procedure led to a β_2 value for Np that was different from the one recommended,¹ despite the fact that the β_1 values were in excellent agreement. This strongly suggests the presence of a third species, in fast equilibrium with NpO_2^+ , $[\text{NpO}_2(\text{OH})]$ and $[\text{NpO}_2(\text{OH})_2]^-$, because just a single peak is observed. Based on the observation that the experimental mobility values are more positive than expected, this third species is either positive or neutral. The presence of a cationic neptunium species in an alkaline medium is doubtful, but a neutral species is more likely. Indeed, the separation was performed in NaCl, i.e. in the presence of a large amount of sodium cations. One possible explanation would be to assume that there is an association between Na^+ and $[\text{NpO}_2(\text{OH})_2]^-$. In the case of this hypothesis, an association constant can be estimated which lead to the following value:

$\log K_{\text{Na}}^0[\text{NpO}_2(\text{OH})_2] = (1.6 \pm 0.5)$. This value seems a bit high for an association. A possible explanation is to consider that the neptunyl cation has an effective charge of +2.2. Since the interactions with the ligands take place in the equatorial plane, no steric constraint prevents the sodium cation from being near the 1:2 anionic complex. This result is consistent with recent work where Petrov and coworkers evidenced the incorporation of Na^+ (> 10%) in all solid phases after terminating two-year solubility experiments, suggesting the formation of ternary Na-Np(V)-OH solid phases in Na-rich hyperalkaline solutions.³

In accordance with the discussion above, it must be considered that for the second hydrolysis reaction of An(V) with water, a mixed constant that includes an association between Na^+ has been determined.

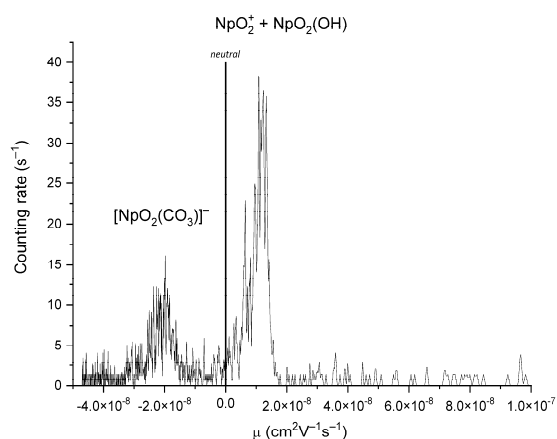


Figure 1: Electrophoregram of an Np(V) sample solution at $\text{pH} = 10.79$. Conditions : $L = 79 \text{ cm}$, $V = 8 \text{ kV}$, 0.8 psi , $T = 25^\circ\text{C}$, $I = 0.1 \text{ M NaCl}$.

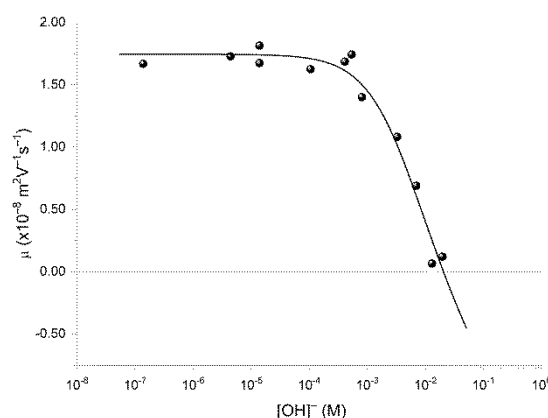


Figure 2: Variation of the electrophoretic mobility of Pu(V) species as a function of the concentration of hydroxide ions. Black line: fitting of experimental data. Experimental electrophoretic mobilities $\mu_{\text{PuO}_2^+} = 1.745 \cdot 10^{-8}$, $\mu_{[\text{PuO}_2\text{OH}]} = 0$ and $\mu_{[\text{PuO}_2(\text{OH})_2]^-} = -1.204 \cdot 10^{-8} \text{ (m}^2 \text{ V}^{-1} \text{ s}^{-1})$ extracted from the black curve.

References

- [1] Grenthe, I.; Gaona, X. Second Update on the Chemical Thermodynamics of Uranium, Neptunium, Plutonium, Americium and Technetium; North-Holland, 2020.
- [2] Aupiais, J.; Christin, C.; Levier, M. The aquatic Chemistry of pentavalent plutonium: determination of the first hydrolysis constant, *Inorg. Chem.*, under revision.
- [3] Petrov, V. G.; Fellhauer, D.; Gaona, X.; Dardenne, K.; Rothe, J.; Kalmykov, S. N.; Altmaier, M. Solubility and hydrolysis of Np(V) in dilute to concentrated alkaline NaCl solutions: formation of Na-Np(V)-OH solid phases at 22 °C. *Radiochim. Acta* 2017, 105 (1), 1-20.

A3-2 SPECTROSCOPIC STUDY ON FORMATION OF AQUEOUS URANIUM(VI)-SILICATE COMPLEXES AT ALKALINE PH

Tae-Hyeong Kim^{1,*}, Euo Chang Jung¹, Yongheum Jo¹, Hee-Kyung Kim¹, Hye-Ryun Cho¹, Wansik Cha¹, Jong-Il Yun²

(1) Korea Atomic Energy Research Institute, Daejeon, Republic of Korea

(2) Korea Advanced Institute of Science and Technology, Daejeon, Republic of Korea

Understanding the migration behavior of actinide elements is essential for long-term safety assessments of deep geological repository for radioactive wastes. The migration behavior is highly dependent on its aqueous chemical speciation, which is affected by various parameters such as pH, temperature, chemical composition and etc. Silicate is one of the most common ligands present in natural ground water by dissolution of silica and other various silicate minerals. The study of the complex formation of actinides in silicate-containing solutions is complicated by the complex chemistry of silicates. To avoid the complexity of silicate chemistry, most of the studies have been conducted in the low pH region. Up to now, only two aqueous actinide monosilicates, $\text{UO}_2\text{SiO}(\text{OH})_3^+$ and $\text{AmSiO}(\text{OH})_3^{2+}$, were selected in the Thermochemical Database Project (NEA-TDB) [1], which provides the reliable thermodynamic data for geochemical modelling of the repository. In alkaline pH ranges, the solubility of amorphous silica increases due to formation of various polynuclear silicates and which the formation of aqueous actinide silicates in this pH range has not been reported. In this study, the formation of uranium(VI) complex in silicate-containing solutions at alkaline pH was investigated using the time-resolved laser-induced luminescence spectroscopy (TRLLS).

The silicate stock solutions were freshly prepared for each experiment by acid hydrolysis of tetramethylorthosilicate. The pH of the solution was maintained at 10.0 using HClO_4 and NaOH , while the ionic strength of the solution was kept at 0.1 mol/L by using NaClO_4 . All solutions were prepared in the glove box under argon atmosphere excluding the complexation with carbonates. For TRLLS measurement, the excitation wavelength was 355 nm with a laser pulse energy of 2.0 mJ. The spectra were recorded with an ICCD at a delay time (t_d) of 1 μs with a gate width of 1000 μs . The luminescence lifetime of uranium(VI)-silicate complex was determined by using an exponential decay function with Levenberg Marquardt iteration algorithm in Origin 2020 program.

Figure 1 shows the solubility diagram of amorphous silica depending on pH and silica concentrations [2]. The solubility line, which gives the maximum soluble silicate, follows the concentration line $\text{Si}(\text{OH})_4$ up to pH of around 9, and then dramatically increases as pH increases. The so-called mononuclear wall represents the lower concentration limit below which polynuclear silicate species are not stable. The area between the mononuclear wall and the solubility line represents a stable multimeric silicate species domain. Above the solubility line is the insolubility domain in which the colloidal amorphous silica is formed.

Figure 2 shows the normalized luminescence spectra and its decay of uranium(VI) complex formed in silicate-containing solution with varying silicate concentrations at pH of 10.0. The luminescence intensity is dramatically increased when the silicate concentration exceeds the mononuclear wall (2 – 3 mmol/L). The luminescence spectra and their lifetimes measured in stable multimeric domain (3 – 7 mmol/L) are significantly different from those of $\text{UO}_2\text{SiO}(\text{OH})_3^+$ [3] and those in insolubility domain (10 mmol/L), which showed the same luminescence characteristics found in the silica adsorption experiment [4]. In the stable multimeric domain, the luminescence intensity remains unchanged before and after ultracentrifugation (146,600 g, 30 min) and ultrafiltration (1 kDa, Microsep, Pall Corp), indicating that the aqueous uranium(VI)-multimeric silicate complex is formed in this condition. Additional studies are on-going to determine the stoichiometry and formation constant of the uranium(VI)- multimeric silicate complex formed in the stable multimeric silicate domain.

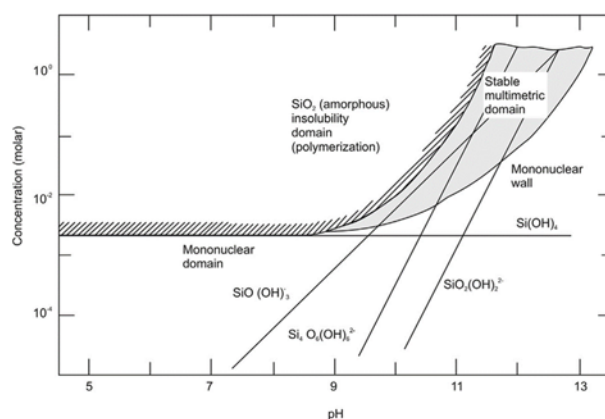


Figure 1. Species in equilibrium with amorphous silicate [2]

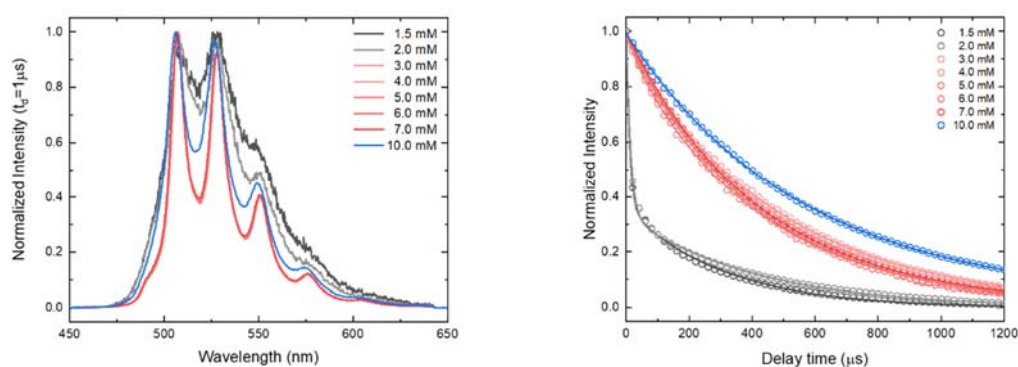


Figure 2. Normalized luminescence spectra ($t_d = 1 \mu\text{s}$) and their decays of uranium(VI)-silicate complexes at pH 10.0 with varying $[\text{Si(IV)}]_{\text{tot}} = 1.5 - 10 \text{ mmol/L}$ and at $[\text{U(VI)}] = 5 \mu\text{mol/L}$

Acknowledgement: This work was supported by the Institute for Korea Spent Nuclear Fuel (iKSNF) and National Research Foundation of Korea (NRF) grant funded by the Korea government (Ministry of Science and ICT, MSIT) (No. 2021M2E1A1085202).

References

- [1] I. Grenthe et al. (2020). Second update on the chemical thermodynamics of uranium, neptunium, plutonium, americium and technetium. Chemical thermodynamics volume 14. Organisation for Economic Co-Operation and Development
- [2] W. Stumm and J.J. Morgan (1995) Aquatic Chemistry: Chemical Equilibria and Rates in Natural Waters, 3rd edition. John Wiley & Sons, New York
- [3] H. Lösch, M. Raiwa, N. Jordan, M. Steppert, R. Steudtner, T. Stumpf, and N. Huittinen (2020). Temperature-dependent luminescence spectroscopic and mass spectrometric investigations of U(VI) complexation with aqueous silicates in the acidic pH-range. Environment International. 136
- [4] E.C. Jung, Y. Jo, T.-H. Kim, H.-K. Kim, H.-R. Cho, W. Cha, M.H. Baik, and J.-I. Yun (2022). Surface Coverage- and Excitation Laser Wavelength- Dependent Luminescence Properties of U(VI) Species Adsorbed on Amorphous SiO₂. Minerals. 12(2)

A3-3 STRUCTURAL IDENTIFICATION OF AQUATIC U(VI)-PBTC COMPLEXES BY SPECTROSCOPIC INVESTIGATIONS

Wollenberg^(1,2), J. Kretzschmar⁽³⁾, S. Tsushima⁽³⁾, R. Kraft⁽⁴⁾, M. Kumke⁽⁴⁾, M. Acker⁽²⁾, S. Taut⁽²⁾, T. Stumpf^(1,3)

(1) Technische Universität Dresden, Professorship for Radioecology and Radiochemistry, 01062 Dresden, Germany

(2) Technische Universität Dresden, Radiation Protection, Central Radionuclide Laboratory, 01062 Dresden, Germany

(3) Helmholtz-Zentrum Dresden-Rossendorf, Institute of Resource Ecology, 01328 Dresden, Germany

(4) Universität Potsdam, Institute of Chemistry, Central Radionuclide Laboratory, 14469 Potsdam, Germany

In a nuclear waste repository, cement-based materials are to be used for waste conditioning and as an engineered barrier. The ingress of water into the nuclear waste repository, described as a worst-case scenario, leads to increased aging and degradation of the concrete. These processes are associated with a leaching of diverse organic substances usually added to the cement to realize the desired physicochemical and mechanical properties of the cement-based materials. The impact of the additives is based on their excellent ability to complex metal ions. Consequently, the complexation behavior of such additives towards radionuclides (RN) and thus their impact on RN mobilization and migration into the environment is essential for a comprehensive risk assessment. One of the additives commonly used for long-term retardation of cement hardening is 2-phosphonobutane-1,2,4-tricarboxylic acid (PBTC).

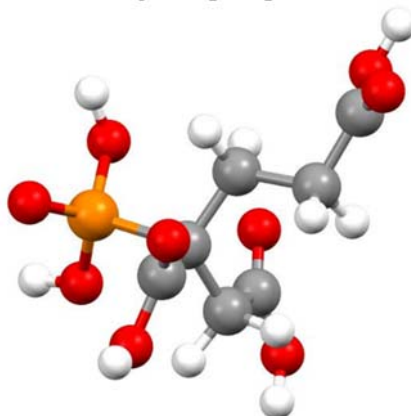


Figure 3: Molecular structure of 2-phosphonobutane-1,2,4-tricarboxylic acid (PBTC).

PBTC is a polyfunctional ligand possessing three carboxyl groups and one phosphonate group, which have been shown to make PBTC a strong complexing agent for various metal ions (e.g. Ca^{2+} , Zn^{2+} , Al^{3+} , Fe^{3+}) [1,2]. However, to date, there are no studies on PBTC interaction with radionuclides. Therefore, the complexation of PBTC with U(VI) was investigated for the first time, using different spectroscopic methods over a wide pH range (2 through 11) to identify and characterize possible complex species.

U(VI)-PBTC species with solubility as high as 100 mM were observed throughout the entire pH range studied, especially when PBTC is in excess. This allowed the convenient application of structure-sensitive methods such as NMR, IR, and Raman spectroscopies. Furthermore, time-resolved laser-induced fluorescence spectroscopy (TRLFS) and UV-Vis titration studies provided insight into U(VI)-PBTC system's speciation.

In particular, ^{31}P NMR spectroscopy proved to be the method of choice, facilitating the selective investigation of compositional and configurational changes in the individual U(VI)-PBTC complex species, irrespective of impurities in the commercially available PBTC product. The results evince U(VI) chelation by the phosphonate group and one of the carboxyl groups. Moreover, with this method it was also possible to determine $\text{p}K_{\text{a}}$ values of free [3] and U(VI)-bound PBTC, which enabled an unambiguous and complete structural elucidation of the U(VI)-PBTC complexes. IR and Raman spectroscopic studies as well as DFT calculations complemented these structural NMR studies.

Only upon the combination of the various experimental and theoretical methods it was possible to detect and characterize for the first time in detail highly soluble and thus potentially mobile U(VI) complexes with the widely-used cement additive PBTC.

Acknowledgement: *The German Federal Ministry for Economic Affairs and Energy (BMWi) is thanked for financial support within the GRaZ II project, no. 02E11860G (TU Dresden), 02E11860B (HZDR), 02E11860F (Uni Potsdam)*

References

- [1] Demadis, K. D. et al. (2006). Phosphonopolycarboxylates as chemical additives for calcite scale dissolution and metallic corrosion inhibition based on a calcium-phosphonotricarboxylate organic–inorganic hybrid. *Cryst. Growth Des.* 6.5: 1064-1067.
- [2] Solvadó, V. et al. (1999). A study of the complex formation between trivalent ions (Al^{3+} , Fe^{3+}) and 2-phosphonobutane-1, 2, 4-tricarboxylic acid and their industrial applications. *Polyhedron.* 18.25: 3275-3280.
- [3] Kretzschmar, J. et al. (2022). 2-Phosphonobutane-1, 2, 4-Tricarboxylic Acid (PBTC): pH-Dependent Behavior Studied by Means of Multinuclear NMR Spectroscopy. *Molecules.* 27.13: 4067.

A3-4 CHEMICAL EQUILIBRIUM OF PLUTONIUM(VI) IN WEAKLY ALKALINE SYSTEMS CONTAINING ALKALINE EARTH METAL IONS AND CARBONATE

Y. Jo^(1,2,3), H.-R. Cho⁽⁴⁾, X. Gaona⁽²⁾, D. Fellhauer⁽²⁾, K. Dardenne⁽²⁾, J. Rothe⁽²⁾, M. Altmaier⁽²⁾, J.-I. Yun⁽¹⁾

(1) Department of Nuclear and Quantum Engineering, Korea Advanced Institute of Science and Technology (KAIST), Republic of Korea

(2) Institute for Nuclear Waste Disposal, Karlsruhe Institute of Technology (KIT)-INE, Germany

(3) Department of Nuclear Engineering, Hanyang University, Republic of Korea

(4) Nuclear Chemistry Research Team, Korea Atomic Energy Research Institute (KAERI), Republic of Korea

Plutonium (Pu) in the Earth's environment has been primarily generated from anthropogenic activities such as nuclear power generation and nuclear weapon programs, with the exception of ultra-trace amounts of Pu-239 occurring naturally in uranium ores as well as primordial Pu-244. The mobilization from legacy wastes in the past caused widespread pollutions with Pu, and environmental clean-up projects of contaminated sites are still in progress with a relatively high costs. Global fallout from nuclear weapon testing and severe accidents at Chernobyl and Fukushima Daiichi have also contributed to the release of Pu into the environment. For the assessments of the fate of Pu in the environment and the design of remediation activities of contaminated sites, a profound understanding of the chemical behaviour of Pu is required. Natural waters such as groundwater, rainwater, and seawater may play an important role in transporting Pu into the environment by leaching Pu-bearing pollutants and carrying Pu via natural fluids. In natural waters contacting atmospheric air, the presence of higher oxidation states of Pu, namely Pu(V) and Pu(VI), was reported [1].

Carbonate (CO_3^{2-}) is one of the most relevant inorganic ligands in natural waters due to its natural abundance and strong affinity for metal ions. Similarly to previous observations reported for U(VI) carbonate complexes in groundwater and seawater, the mobility of Pu(VI) is increased by the formation of anionic carbonate species (e.g. $\text{PuO}_2(\text{CO}_3)_2^{2-}$ and $\text{PuO}_2(\text{CO}_3)_3^{4-}$) [2]. In case of U(VI), the formation of $\text{M}_x\text{UO}_2(\text{CO}_3)_3^{2x-4}$ (M = alkaline earth metal ions with $x = 1$ and 2) has been extensively reported in the literature [3]. These studies support that the behaviour of U(VI) in natural waters containing CO_3^{2-} , Ca^{2+} , and Mg^{2+} is predominantly governed by the formation of these stable ternary complexes. The formation of analogous strongly stabilized complexes of Pu(VI) may affect plutonium chemistry in certain natural systems, and thus deserves dedicated experimental efforts beyond purely scientific interest.

This contribution provides experimental evidence on the formation of ternary complexes of Pu(VI) with CO_3^{2-} in the presence of Ca^{2+} and Mg^{2+} . The results of Vis-NIR absorption spectroscopy confirm the formation and predominance of the complexes $\text{M}_1\text{PuO}_2(\text{CO}_3)_3^{2-}$ (M = Mg^{2+} , and Ca^{2+}) in near-neutral to weakly alkaline pH conditions [4]. Thermodynamic data derived in this work supports that $\text{CaPuO}_2(\text{CO}_3)_3^{2-}$ dominates the aqueous speciation of Pu in oxidizing groundwater and seawater systems. Dedicated efforts are made at KIT-INE to gain insight into the structure of the forming complexes using X-ray absorption methods. Beyond being a topic of fundamental scientific interest, chemical equilibria involving the formation of highly stabilized M^{2+} -Pu(VI)- CO_3^{2-} complexes may affect the geochemical behaviour of Pu in certain natural waters, including solubility and sorption phenomena.

Acknowledgements: We acknowledge KIT Institute for Beam Physics and Technology (IBPT) for the operation of the storage ring, the Karlsruhe Research Accelerator (KARA), and provision of beamtime at the KIT synchrotron light source.

References

- [1] Nelson, D. M. and Lovett M. B. (1978). Oxidation state of plutonium in the Irish Sea. *Nature*. 276: 599-601
- [2] Reilly, S. D., Runde, W., Neu, M. P. (2007). Solubility of plutonium(VI) carbonate in saline solutions. *Geochimica et Cosmochimica Acta*. 71: 2672-2679
- [3] Endrizzi, F. and Rao, L. (2014). Chemical Speciation of uranium(VI) in marine environments: Complexation of calcium and magnesium ions with $[(\text{UO}_2)(\text{CO}_3)_3]^{4-}$ and the effect on the extraction of uranium from seawater. *Chemistry—A European Journal*. 20: 14499-14506
- [4] Jo, Y., Cho, H.-R., Yun, J.-I. (2020). Visible-NIR absorption spectroscopy study of the formation of ternary plutonyl(VI) carbonate complexes. *Dalton Transactions*. 49: 11605-11612

D-5 EURAD, A EUROPEAN PROGRAMME ON RADIOACTIVE WASTE MANAGEMENT, SCIENTIFIC OUTCOMES AND CHALLENGES AS SEEN BY THE EXTERNAL ADVISORY BOARD

Pierre Toulhoat⁽¹⁾, Saida Engstroem Laarouchi⁽²⁾ Philippe Lalieux⁽³⁾, Hans Wanner⁽⁴⁾

(1) *Académie des Technologies, France*

(2) *Vattenfall, Sweden*

(3) *NIROND-ONDRAF, Belgium*

(4) *retired from ENSI, Switzerland*

Since 2019, EURAD, the European joint program on radioactive waste management gathers more than 100 actors from 20 Member States, 3 associated countries and 3 international partners [1]. Thanks to such a unique platform, waste management organizations (WMOs), technical support organizations to nuclear safety authorities (TSOs) and research entities (REs) have developed together 10 RD&D work packages, 2 strategic studies work packages and a dedicated action for Knowledge Management with 3 work packages. Currently, EURAD is mostly focusing on RD&D in support of geological disposal of HLW/ILW/SF. After 2024, EURAD-2 will incorporate predisposal topics that have been - until now - developed in the PREDIS project [2]. An External Advisory Board has been established to ensure that EURAD hears about and acts upon the expectations of 'the outside world', and that EURAD is visible to and heard by 'the outside world'. The EAB focuses for instance on: advise the General Assembly/Bureau/PMO on strategic issues related to the EURAD vision; help guide the overall direction and priorities of EURAD by providing advice on how best to reach short, medium, and long-term objectives; act as ambassadors, raising the profile and visibility of EURAD and building stakeholder awareness and support. The External Advisory Board has no executive powers, nor does it have any formal monitoring role.

Such a common platform, gathering the three main categories of actors, is a real step forward in order to produce a roadmap, a shared strategic agenda and sound and well-focused calls for projects. In addition, EURAD is now a community, where everybody is able to exchange, and designed to be open to young researchers, with a wealth of engagement and motivation. With the increasing links between EURAD and PREDIS, there is a progressive build-up of a common and shared integral perception (from cradle to grave) of main features, events and processes, which is absolutely required. However, there is still much to do to convince the designers of new reactor systems that they need to take into account the back-end (predisposal and disposal issues), in order to lower the economic and social burden of the waste streams to be produced. A key issue is the ability to minimize by design the inventories of some dose determining radionuclides (long-lived, poorly sorbed nuclides such as ¹⁴C and ³⁶Cl), and to minimize the volume of wastes to be disposed of. In addition, due to the present revival of nuclear energy in Europe, and to the hatching of many SMR projects, to be utilized in industrial sites (as decarbonized heat and energy providers), safety during and after operation (including possible accidents, waste treatment, storage and disposal, etc....) of such reactor systems may raise new challenges. As end-users, regulators, and waste generators are more than welcome to be involved in EURAD, especially in the next program - EURAD2. These are especially important in terms of radionuclides to be considered, boundary conditions to be selected, and scenarios to be shared. Some examples will be given concerning the behavior and migration of actinides and fission products in the geosphere.

Another major issue, on which the EAB has insisted since the beginning, is the need for a quick and efficient development of digital twins for deep geological repositories, which is complex due to the coupling of an industrial system (for which digital twins are already operating) and a natural system, for which monitoring, data treatment, kriging and 3D fully coupled THMC are real challenges. EURAD is on the right track [3], but a lot of efforts are still needed.

References

- [1] Garcia M., Beattie T., and Schumacher S. (2020) EURAD the European Joint Programme for research on radioactive waste management between EU members states national programmes. EPJ Nuclear Sci. Technol. 6, 21.
- [2] Holt, E.Oksa, M. Nieminen, M., Abdelouas, A., Banford, A. Fournier, M., Mennecart T., and Niederleithinger, E. (2022) Predisposal conditioning, treatment, and performance assessment of radioactive waste. EPJ Nuclear Sci. Technol. 8, 40 (2022).
- [3] Kolditz O., Diederik J., Claret F., Bertrand J., Churakov S. V., Debayle, C., Diaconu D., Fuzik K, Garcia D., Graebing N., Grambow B., Holt E., Idiart A., Leira P., Montoya V., Niederleithinger E., Olin M., Pfingsten W., Prasianakis N.I., Rink K, Samper J., Szöke I., Szöke R., Theodon L. and Wendling J. Digitalisation for nuclear waste management: predisposal and disposal (2023) Environmental Earth Sciences (2023) 82:42.

A6-1 FORMATION, REACTIVITY AND COLLOIDAL BEHAVIORS OF TETRAVALENT URANIUM NANOPARTICLES UNDER GROUNDWATER CONDITIONS

Wansik Cha^{1,*}, In Hak Yoon^{1,2}, Hyejin Cho¹, Hye-Ryun Cho^{1,2}, Euo Chang Jung¹

(1) Korea Atomic Energy Research Institute and 2University of Science and Technology Daejeon, Republic of Korea

In aqueous solutions the speciation of tetravalent uranium (U(IV)) changes drastically depending on the pH, i.e., from free ion U^{4+} ($pH \sim 1$) to hydrolyzed products and finally to amorphous or crystalline phases as the solution becomes basic. Its low solubility in a wide pH range is well-known to induce the formation of solid precipitates. Unlike other solid phases that limit aqueous solubility, nanoparticles or aqueous colloids occurring via dissolution of spent nuclear fuels or mineral transformation from U(VI) in both biotic and abiotic aqueous systems can actively contribute to subsurface migration of uranium via a colloid-facilitated transport mechanism through groundwater [1,2]. In this perspective, understanding the surface properties and the factors affecting the overall ‘colloidal’ stability is important. Here we report our recent results regarding the nanoparticle formation process from aqueous solutions of UOH^{3+} (1:1 hydrolyzed species), the surface reactivity of U(IV) nanoparticles (U(IV)-NPs), and factors affecting their colloidal stability. For our investigation various analytical techniques were applied; for example, the electrophoretic and dynamic light scattering analysis measured zeta potential values, isoelectric points (IEP) and particle sizes; the controlled potentiometric acid/base titration estimated points of zero charge (PZC) and surface acidity; the UV-Vis spectrophotometry and attenuated total reflection (ATR) FTIR spectroscopy identified surface complex structures and adsorption isotherms of organic ligands. With the dry powder of U(IV)-NPs, the surface site density and the state of U-O chemical bonds were evaluated using BET analysis and X-ray photoelectron spectroscopy (XPS), respectively.

As prepared in acidic solutions ($\sim pH 2$) via the hydrothermal synthesis method that we reported previously [3,4], the colloidal stability of U(IV)-NPs was retained for weeks at room temperature. This stability was primarily owing to the positive charges (i.e., $> +30$ mV zeta potentials) developed on the particle surfaces. The sites that provided (+)-charges on the surface were evidently responsible for bonding to hydroxyl ions and protic organic ligands. The IEP and PZC were measured at approximately $pH 6 - 7$ in 0.1 M perchlorate media. These results correspond to the significant surface property changes at neutral and higher pH regions, which induce instability of the aqueous colloids and particle aggregations. In addition, the acidity (i.e., pK_a) of the surface sites was estimated based on the acid/base titration results. In fact, our spectrophotometric reaction monitoring studies on the U(IV)-NP formation process revealed that further hydrolysis from $U(OH)^{3+}$ leads to the evolution of U(IV)-NPs, which are clusters ($\sim 20-30$ nm in diameter) of primary particles (typically 5-6 nm sizes estimated by TEM analysis) of a crystalline uraninite(UO_2)-like bulk-phase structure. Based on the temperature-dependent kinetic studies of monitoring the consumption rate of $U(OH)^{3+}$, we propose a U(IV)-NPs nucleation mechanism (see Fig. 1) involving the generation of oligomeric oxyhydroxy-U(IV) intermediates and finally resulting in metal oxide crystalline phase formation. The structure of the proposed reaction intermediates is thought to provide insight into that of the charged surface sites of U(IV)-NPs.

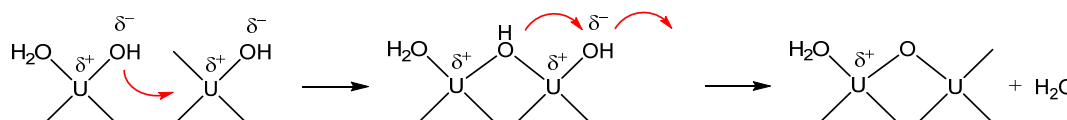


Figure 1. Condensation of hydrolyzed U(IV) ions as an initiating step of U(IV)-NP nucleation via a two-step associative mechanism [4].

The primary factors influencing the colloidal stability of U(IV)-NPs, which we explored in this study, include pH, ionic strength, the nature of electrolytes, the presence of organic and inorganic ligands and their concentrations. Most effects of these factors can be described as the changes in the surface charge density and the double-layer structure of positively charged metal oxide particles following the DLVO theory. Among these factors, we focused our investigation on the effect of two organic ligands, i.e., p-nitrophenylphosphate (nPP) and p-nitrocatechol (nCA), which we selected as model compounds of natural organic materials. For nPP, the surface of the U(IV)-NPs exhibited catalyst-like activities that enhanced the rate of hydrolysis or cleavage of its phosphoester bond. The proposed nPP decomposition mechanism consists of a rapid surface adsorption step through the anionic phosphate group and the subsequent slow hydrolysis of ester linkage (i.e., the rate-determining step) aided by the surface hydroxyl group on U(IV)-NPs. The overall reaction kinetics was found to be highly dependent on the solution pH and temperature. In contrast, nCA formed strong and stable surface complexes on the U(IV)-NPs. Quantitative analysis of its adsorption equilibria was well fitted to the Langmuir isotherm model, which indicated a mono-layer surface adsorption of nCA. The colloidal stability of aqueous solutions containing U(IV)-NPs turned out to be highly dependent on the nCA concentration and the solution pH; the measured IEP shifted to lower pH regions as the nCA concentration increased. One of important results in this study was that at a higher pH ($> \sim 9$) the colloidal stability of U(IV)-NP solutions recovered in the presence of the excess levels of nCA. Such enhanced stability of nanoparticles at a high pH should be noted when considering the colloid-facilitated transport model of radionuclides. Experimental results providing information on the surface complex structures, including those from XPS and ATR-FTIR spectroscopy, are discussed in detail.

Acknowledgment: *This study was supported by the Nuclear Research and Development program of the National Research Foundation of Korea and the Institute for Korea Spent Nuclear Fuel (Grant Nos. 2017M2A8A5014719 and 2021M2E1A1085202).*

References

- [1] Walther, C. and M. A. Denecke (2013). Actinide colloids and particles of environmental Concern. *Chem. Rev.* 113: 995-1015
- [2] Zänker, H. and C. Hennig (2014). Colloid-borne forms of tetravalent actinides: A brief review. *J. Contam. Hydrol.* 157: 87-105
- [3] Cho, H. and W. Cha (2019). Rapid hydrolysis of Organophosphates induced by U(IV) nanoparticles: A kinetic and mechanistic study using spectroscopic analysis. *Colloids and Interfaces.* 3: 63
- [4] Cha, W., H.-K. Kim, H. Cho, H.-R. Cho, E. C. Jung and S. Y. Lee (2020). Studies of aqueous U(IV) equilibrium and nanoparticle formation kinetics using spectrophotometric reaction modelling analysis. *RSC Adv.* 10: 36723-36733

A6-2 EVIDENCES ABOUT THE CONTRIBUTION OF PU(IV) OXO-HYDROXO CLUSTER $[\text{Pu}_6(\text{OH})_4\text{O}_4]^{12+}$ DURING THE FORMATION OF PU(IV) INTRINSIC COLLOIDS

Matthieu Virost^{(1)*}, Manon Cot-Auriol⁽¹⁾, Thomas Dumas⁽²⁾, Denis Menut⁽³⁾, Olivier Diat⁽¹⁾, Sandrine Dourdain⁽¹⁾, Philippe Moisy⁽²⁾, Sergey I. Nikitenko⁽¹⁾

(1) ICSM, CEA, Univ Montpellier, CNRS, ENSCM, Bagnols sur Cèze, France

(2) CEA, DES, ISEC, DMRC, Univ Montpellier, Marcoule, France

(3) Synchrotron SOLEIL, L'Orme des Merisiers Saint Aubin, Gif-sur-Yvette, France

*matthieu.virost@cea.fr

Because of nuclear testing, space exploration or industrial development, anthropogenic activities significantly contributed in the release of radioactive particles in the environment. Both pseudo- and intrinsic colloids of the element plutonium have been considered as potential sources of radioactivity migration in aquifers. [1,2] While the former deals with natural colloids where Pu has been incorporated or adsorbed, the latter rather rely on the exceptional property of Pu to form its own colloid as a result of hydrolysis and condensation reactions, even under strongly acidic conditions. Such a property was already discussed by Kraus during the Manhattan project who reported the formation of an opalescent green solution when ammonia or sodium hydroxide aqueous solutions were contacted with acidic solutions of Pu(IV).[3] Through the years, these suspensions were rather prevented in industrial processing by using strongly acidic conditions thus resulting in a knowledge gap regarding the formation, properties and reactivity of these species. Nevertheless, much insights have been reached during the last decade about the structural properties of Pu(IV) intrinsic colloidal phases which are now described as *ca.* 2 nm spherical particles exhibiting a PuO₂-like local structure and a local disorder attributed to a surface effect mostly resulting from the nanometric size of the particle.[4] It has been reported that the formation conditions of intrinsic Pu colloids may significantly impact their structural properties and intensify their environmental migration relevance.[5,6]

A better knowledge about the formation conditions and stability of PuO₂ nanoparticles in geochemical conditions thus appear of particular interest for the clarification of the environmental fate of this long-lived radioactive element. Nevertheless, tetravalent Pu exhibits a complex chemistry in aqueous solution particularly expressed by hydrolysis, complexation, redox and disproportionation reactions.[7] While hydrolysis leads to the accumulation of PuO₂ nanoparticles, disproportionation reactions may lead to the additional observation of Pu(III), Pu(V) and Pu(VI) species. Furthermore, the additional contribution of polynuclear Pu nanostructures during the formation of the colloids has been interrogated. Indeed, the recent examination of oxo-hydroxo clusters containing 16, 22 and 38 atoms of tetravalent Pu revealed related PuO₂ core structures and suggested that bigger entities could result from the assembly of smaller units.[8,9] The gradual loss of hydroxo-bridges in aid of oxo-ligands in the Pu₃₈ structures, which shows some striking structural properties with Pu(IV) colloids, suggested that the latter might be formed by a succession of olation and oxolation reactions.

In this work, the formation kinetics of intrinsic Pu(IV) colloids was studied in different aqueous solutions including light (H₂O) and heavy water (D₂O) but also electrolyte model systems encountered in natural aquifers rich in alkaline or alkaline-earth elements (LiCl, NaCl, LiNO₃, MgCl₂, etc.). Time-dependent measurements were carried out with UV-Vis absorption spectroscopy and coupled with deconvolution studies. The colloidal particles formed in these systems were characterized with synchrotron radiation using X-ray scattering and absorption techniques. New insights were established about the formation mechanism of Pu(IV) intrinsic colloids with the transient observation of $[\text{Pu}_6(\text{OH})_4\text{O}_4]^{12+}$ oxohydroxo cluster (Fig. 1). Furthermore, the reaction medium was interrogated about their effect on the structural characteristics of the final PuO₂ nanoparticles.

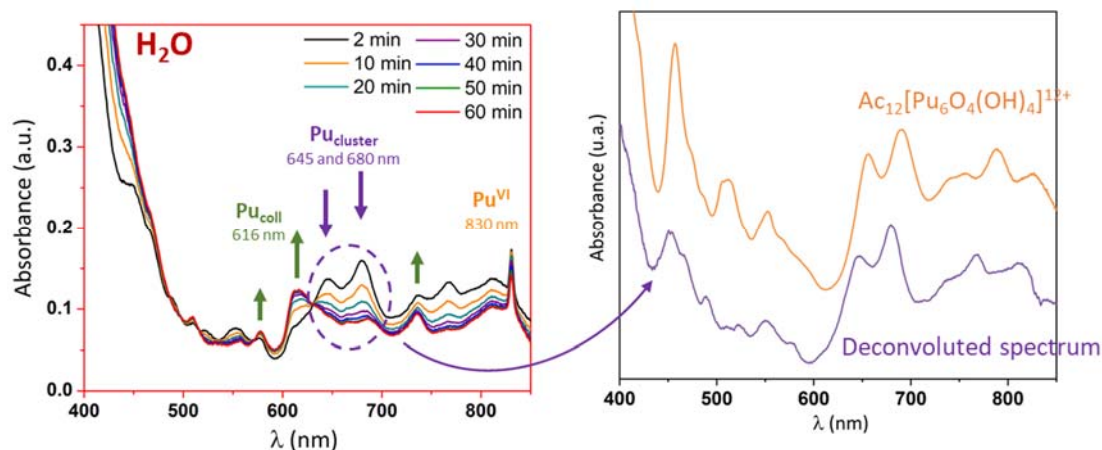


Fig. 1: Formation kinetics of Pu(IV) intrinsic colloids in pure water. UV-vis absorption spectra acquired during synthesis were deconvoluted and revealed the appearance of $[Pu_6(OH)_4O_4]^{12+}$ cluster.

References

- [1] Walther, C. and M. A. Denecke (2013) Chem. Rev. 113: 995–1015.
- [2] Kalmykov, S. N. and Denecke, M. A. (2011) Actinide Nanoparticle Research, Springer, Berlin Heidelberg.
- [3] The transuranium elements: research papers. (1949) 1. Papers 1.1 to 6.39, G. T. Seaborg, J. J. Katz and W. M. Manning, N.Y.: McGraw-Hill, USA.
- [4] Viro, M.; Dumas, T.; Cot-Auriol, M.; Moisy P. and S. I. Nikitenko (2022) Synthesis and multi-scale properties of PuO₂ nanoparticles: recent advances and open questions. Nanoscale Adv. 4: 4938–4971.
- [5] Zhao, P.; Zavarin, M.; Dai, Z. and A. B. Kersting (2020). Stability of plutonium oxide nanoparticles in the presence of montmorillonite and implications for colloid facilitated transport. Appl. Geochem. 122: 1-10
- [6] Micheau, C.; Viro, M.; Dourdain, S.; Dumas, T.; Menut, D.; Solari, P. L.; Venault, L.; Diat, O.; Moisy, P. and S. I. Nikitenko (2020). Relevance of formation conditions to the size, morphology and local structure of intrinsic plutonium colloids. Environ. Sci.: Nano. 7: 2252-2266.
- [7] Clark, D. Hecker, S. Jarvinen G. and Neu, M. (2011) in The Chemistry of the Actinide and Transactinide Elements, ed. L. Morss, N. Edelstein and J. Fuger, Springer Netherlands, ch. 7, pp. 813–1264.
- [8] Sigmon, G. E. and A. E. Hixon (2019). Extension of the Plutonium Oxide Nanocluster Family to Include {Pu16} and {Pu22}. Chem. Eur. J. 25: 2463-2466.
- [9] L. Soderholm, P. M. Almond, S. Skanthakumar, R. E. Wilson and P. C. Burns, Angew. Chem., Int. Ed., 2008, 47, 298–302.

A6-3 ROLE OF NITRATE ON THE FORMATION AND RETENTION OF Th^{IV} NANOPARTICLES AT THE MUSCOVITE (001)-WATER INTERFACE

Julia Neumann⁽¹⁾, Jessica Lessing⁽²⁾, Amanda J. Carr⁽¹⁾, Sang Soo Lee⁽¹⁾, Michael Patzschke⁽²⁾, Corey Taylor⁽²⁾, Peter J. Eng⁽³⁾, Joanne E. Stubbs⁽³⁾, Paul Fenter⁽¹⁾, Moritz Schmidt⁽²⁾

(1) Argonne National Laboratory, Chemical Science and Engineering Division, United States

(2) Helmholtz-Zentrum Dresden-Rossendorf, Institute for Resource Ecology, Germany

(3) Center for Advanced Radiation Sources, The University of Chicago, United States

Actinide nanoparticles have been shown to alter the mobility of tetravalent actinides in the environment and bear great uncertainties in risk assessments of deep geological repositories for radioactive waste [1]. Especially tetravalent actinides (U^{IV}, Th^{IV}, and Pu^{IV}) are known to form polynuclear species, i.e., oligomers and nanoparticles, because of their high charge and strong hydrolysis.

In the past it was shown that muscovite mica, an abundant phyllosilicate mineral, is capable of immobilizing almost twice as much Th^{IV} as expected based on simple surface charge compensation, i.e. 0.4 Th/A_{UC} instead of 0.25 Th/A_{UC} (A_{UC}: unit cell area of the muscovite (001) basal plane) [2]. A later study indicated that the extent of Th uptake and its broad distribution of electron density at the mineral surface might be connected to the formation of polynuclear species, i.e., Th nanoparticles [3], which was then confirmed using *in situ* atomic force microscopy (AFM) [4]. The electrolyte composition had a strong impact on the efficiency of Th removal by muscovite [3,4]. A systematic and gradual decrease in Th immobilization within the alkali series was observed that is consistent with competitive adsorption by the electrolyte cation. While this trend was consistently observed for most of the investigated electrolytes (LiCl, LiClO₄, KCl, KClO₄, NH₄Cl, and CsCl), measurements in Na electrolytes (NaCl and NaClO₄) showed a significantly lower Th uptake than expected.

At the time, it was speculated that nitrate ions stemming from the Th starting material (Th(NO₃)₄ · 4 H₂O) may not behave as spectator ions as commonly assumed. Th forms Th/A⁺/nitrate compounds (A⁺ = Li⁺, Na⁺, K⁺, Rb⁺, Cs⁺), differing in their molecular structures depending on the hydration enthalpy of the alkali cation [5]. It can be hypothesized that such complexes might act as precursors for Th nanoparticles. Indeed, it is striking that the Th-Th distance in the case of the Na[Th(NO₃)₅(H₂O)₂] compound is 8.3 Å and therefore >1 Å larger than those in any other investigated electrolyte (~7.0–7.3 Å for Li⁺, K⁺, Rb⁺, Cs⁺). That larger distance may act to hinder the initial steps of Th oligomerization.

Therefore, the current study aims to address two questions: Are Th-nitrate complexes responsible for the reduced Th immobilization in the case of Na electrolytes? What is the role of the electrolyte anion in the nucleation mechanism of Th nanoparticles? We use X-ray reflectivity (XR) to study Th immobilization in the absence of nitrate by using a ThCl₄ starting material for the two electrolytes that previously showed the largest difference in Th uptake, NaCl (0.4 Th/A_{UC} [2]) and LiCl (8.8 Th/A_{UC} [4]).

Preliminary data analysis of XR data shows that the Th electron density at the muscovite-water interface changes significantly when nitrate is absent (Figure 1A+B). In the case of LiCl, Th is still distributed broadly, extending up to a distance of 40 Å from the surface. However, the overall Th uptake (~0.8 Th/A_{UC}) decreased strongly to about 10% of the previously obtained value (Figure 1C) in the presence of nitrate. The change for the NaCl electrolyte is less pronounced than for LiCl, but also shows a decrease in Th uptake (~0.2 Th/A_{UC}). These results demonstrate the strong impact of trace quantities of nitrate ions on the formation of Th nanoparticles and are consistent with the hypothesis that Th/A⁺/nitrate complexes serve as precursors for nucleation. We will apply *in situ* AFM to confirm the

XR results and computational techniques to extend the molecular understanding of the formation mechanism of Th nanoparticles.

This work highlights how electrolytes abundant in natural groundwaters, like Na^+ and NO_3^- , may significantly decrease the capacity of aluminosilicate surfaces for the immobilized tetravalent actinides, increasing the risks due to contaminant migration. The current study therefore will enable more reliable predictions of the mobility of tetravalent actinides in the environment.

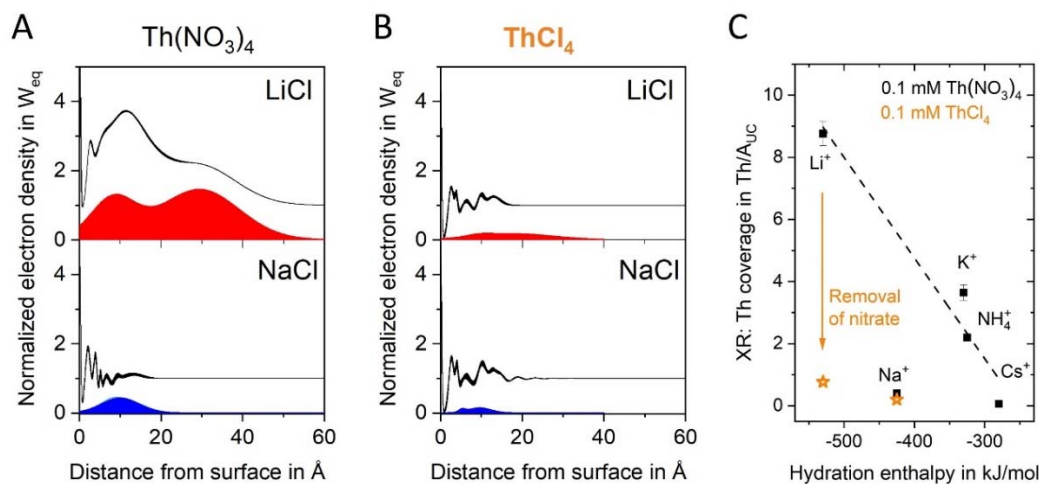


Figure 1. **A + B:** Total electron density profiles (solid lines) and Th contribution (filled areas) in the presence of LiCl or NaCl starting from 0.1 mM Th stock solutions ($\text{pH} = 3.2$). **C:** Comparison of Th uptake in nitrate-containing and nitrate-free samples for the investigated alkali chloride electrolytes. The data for $\text{Th}(\text{NO}_3)_4$ was taken from [2,4] for comparison.

Acknowledgements: This work was partially funded by the U.S. Department of Energy, Office of Science, Office of Basic Energy Sciences, Chemical Sciences, Geosciences, and Biosciences Division under Contracts DE-AC02-06CH11357 to UChicago Argonne, LLC as operator of Argonne National Laboratory. GeoSoilEnviroCARS is supported by the National Science Foundation-Earth Sciences (EAR-1634415) and the Department of Energy-GeoScience (DE-FG02-94ER14466). This research used resources of the Advanced Photon Source, a U.S. Department of Energy (DOE) Office of Science User Facility operated for the DOE Office of Science by Argonne National Laboratory under Contract DE-AC02-06CH11357.

References

- [1] Kersting et al. (2013). Plutonium transport in the environment. *Inorg. Chem.*, 52, 3533–3546.
- [2] Schmidt et al. (2012). Sorption of tetravalent thorium on muscovite. *Geochim. Cosmochim. Acta*, 88, 66–76.
- [3] Schmidt et al., (2015). Effects of the background electrolyte on Th(IV) sorption to muscovite mica. *Geochim. Cosmochim. Acta*, 165, 280–293.
- [4] Neumann et al., (2021). Effect of Background Electrolyte Composition on the Interfacial Formation of Th(IV) Nanoparticles on the Muscovite (001) Basal Plane. *J. Phys. Chem. C*, 125(30), 16524–16535.
- [5] Jin et al., (2017). Influence of Counteranion Hydration Enthalpies on the Formation of Molecular Complexes: A Thorium–Nitrate Example. *J. Am. Chem. Soc.*, 139, 18003–18008.

A6-4 NEW CFM RADIONUCLIDE TRACER TEST DEDICATED TO KINETIC PROCESSES UNDER IN-SITU CONDITIONS AT THE GRIMSEL TEST SITE

Francesca Quinto⁽¹⁾, Ingo Blechschmidt⁽²⁾, Muriel Bouby⁽¹⁾, Zhen Chen⁽¹⁾, Horst Geckeis⁽¹⁾, Bill Lanyon⁽³⁾, Christian Marquardt⁽¹⁾, Ulrich Noseck⁽⁴⁾, Markus Plaschke⁽¹⁾, Raphael Schneeberger⁽²⁾, Thorsten Schäfer⁽⁵⁾

(1) Karlsruhe Institute of Technology, Institute for Nuclear Waste Disposal (KIT-INE), Germany

(2) NAGRA (National Cooperative for the Disposal of Radioactive Waste), Switzerland

(3) Fracture Systems Ltd, Tregurrian, Ayr, TR26 1EQ St. Ives, United Kingdom

(4) Gesellschaft für Anlagen- und Reaktorsicherheit (GRS) GmbH, Germany

(5) Friedrich-Schiller-University (FSU), Institute for Geosciences (IGW), Applied Geology, Germany

Grimsel Test Site (GTS) [1] is NAGRA's generic underground research laboratory located within the crystalline Aar Massif in Switzerland. It provides unique location and infrastructures for the study of physicochemical processes that might influence the performance of bentonite engineered barrier systems and the migration of radionuclides (RNs) in fractured granite host rock. The test site groundwater is a $\text{Na}^+/\text{Ca}^{2+}$ - HCO_3^- - SO_4^{2-} groundwater type with a pH of 9.6, an Eh(SHE) of ca. -220 mV and an ionic strength 1.2 mM, providing conditions for high stability of bentonite colloids [2,3].

In the frame of two international Grimsel projects, namely Colloid and Radionuclide Retardation (CRR, 1997 - 2002) and Colloid Formation and Migration (CFM, 2004 -), several *in-situ* RN tracer tests have been conducted in presence of bentonite colloids to investigate the retention and transport mechanisms of RNs through a water conducting fracture zone under advective mass transport conditions. In particular, three tests, CRR run 1&2 [2,3] (2002 CE) and CFM run 13-05 [4,5] (2013 CE), were performed in the same borehole dipole¹. The residence time for the fluid in the latter test was ca. 31 times higher than in the earlier experiments. Such studies allowed for the *in-situ* observation of colloid mediated transport of the RN tracers ^{242/244}Pu(IV) and ^{241/243}Am(III), and migration of ²³³U(VI) and ²³⁷Np(V) with negligible adsorption onto colloids. It was stated that with higher residence times, the RN tracers recovery strongly decreased. The recovery for Pu(IV) and Am(III) decreased to ca. 33 and 36%, respectively, relative to the CRR tests and was correlated to that for the colloids, pointing to the relevance of colloid retention mechanisms, like adsorption and filtration at the fracture surface and in fracture-filling material pores. The recoveries for U(VI) and Np(V) in CRR run 1&2 was equal to ca. 100 and 80%, respectively, while in CFM run 13-05 only ca. 15 and 4 %, respectively, were recovered. This clearly indicates that sorption/reduction kinetics become evident for those non-colloid bound actinides during the longer residence time.

Under the given hydrogeological conditions, the speciation of U is strongly dependent on the concentration of Ca and carbonates. Thermodynamic modelling indicates $\text{CaUO}_2(\text{CO}_3)_3^{2-}$ as the predominant aqueous species, due to the stabilization of U(VI) in ternary complexes Ca-U(VI)-carbonates (with uranophane $(\text{Ca}(\text{UO}_2)_2(\text{SiO}_3\text{OH})_2 \cdot 5\text{H}_2\text{O})$ as the solubility limiting species) [6]. Decreasing recoveries in this case could be due to isotopic exchange with naturally occurring mineral phases or surface sorption of aquatic ²³³UO₂²⁺ species. Contrarily to U, a reduction of Np(V) to Np(IV) is expected under the given pH and Eh conditions, with the highly insoluble Np(IV)O₂(am) as solubility limiting species [6,7] and Np(OH)₄(aq) as predominant aqueous species [6]. The precipitation of NpO₂(am) predicted by solubility calculations or the surface sorption of Np(IV) species could explain the reduced recovery of Np in CFM 13-05. Such hypothesis is supported by the findings of laboratory studies on cores from the GTS under variation of the residence time demonstrating that sorption/reduction kinetics are significantly controlling the transport of aqueous actinide species [7,8]. Furthermore, there is indication that a fraction of Pu, Am as well as Np tracers from CRR run 1&2

¹ Dipole is understood as the rock volume between two borehole intervals cross-cutting the same fracture zone. The test is carried out by injecting in one interval and extracting from the other.

remained in the fracture zone for more than a decade and was subsequently remobilized by the freshly injected colloids in CFM run 13-05 [5]. Such observations also point towards a partial reduction and adsorption/precipitation of Np(IV) in the fracture zone which also might be (partially) desorbed and transported by bentonite colloids [5].

In order to better investigate the influence of residence time on the *in-situ* reduction of Np(V) to Np(IV), an additional test (named CFM run 22-02) was carried out within the same borehole dipole, but with residence time between the ca. 1.3 h of CRR run 1&2 and ca. 41 h of CFM run 13-05. Together with Np, also other RN tracers are investigated, and in particular the injection cocktail of CFM run 22-02 contained the following RN tracers: $^{232}\text{Th}(\text{IV})$, $^{233}\text{U}(\text{VI})$, $^{237}\text{Np}(\text{V})$, $^{242}\text{Pu}(\text{IV})$, $^{243}\text{Am}(\text{III})$, $^{137}\text{Cs}(\text{I})$, $^{22}\text{Na}(\text{I})$, $^{63}\text{Ni}(\text{II})$ and the conservative fluorescent tracer Amino G (AGA) dissolved in a suspension of bentonite colloids in Grimsel groundwater. Concentrations of RN tracers and colloids were similar to those employed in the previous experiments. On line continuous monitoring of pH, Eh, fluorescence and turbidimetry values at the injection and extraction outflows was performed. At the same time, groundwater samples were periodically collected and transferred to the laboratories of KIT-INE for determination of RN tracers as well as colloids with a variety of analytical techniques. In particular, gamma-spectrometry for ^{137}Cs and ^{22}Na , chromatographic separation and LSC for ^{63}Ni , (SF) ICP-MS for ^{232}Th , ^{233}U , ^{237}Np , ^{242}Pu and ^{243}Am , as well as LIBD and PCS for bentonite colloids.

Preliminary results from the online monitoring show a peak arrival at ca. 23.3 h and a recovery of ca. 94% within 144 hours of the conservative tracer AGA. This confirms that an intermediate residence time between the previous tests was realized. Analysis of RN tracers and notably of Np is ongoing.

In this contribution, we will present the general concept of CFM run 22-02 and the results on the migration behaviours of the several investigated RN tracers.

Acknowledgements: *Part of this work was funded by the Federal Ministry of Economics and Technology of Germany under grant No. FKZ 02E11759A, B&C. The authors acknowledge the support of the international partners of the CFM project and are indebted Karam Kontar (Solexperts) and Andrew Martin (NAGRA) for many fruitful discussions during the CFM field team meetings, as well as to Michael Treuthardt (GTS) for substantial support at the CFM site. Furthermore, the authors would like to acknowledge the invaluable support and expertise of the analytic group of KIT-INE with Cornelia Beiser, Melanie Böttle, Annika Fried, Stephanie Kraft, Markus Fuss and Frank Geyer.*

References

- [1] www.grimsel.com
- [2] Möri, A., W.R. Alexander, H. Geckeis, W. Hauser, T. Schäfer, J. Eikenberg, Th. Fierz, C. Degueldre, T. Missana (2003). The colloid and radionuclide retardation experiment at the Grimsel Test Site: influence of bentonite colloids on radionuclide migration in a fractured rock. *Colloids Surf., A*, 217: 33–47
- [3] Geckeis, H., T. Schäfer, W. Hauser, Th. Rabung, T. Missana, C. Degueldre, A. Möri, J. Eikenberg, Th. Fierz and W. R. Alexander (2004). *Radiochim. Acta.* 92: 675–674
- [4] Project KOLLORADO-e; Final Report, DOI: 10.5445/IR/1000059756
- [5] Quinto, F., I. Blechschmidt, C. Garcia Perez, H. Geckeis, F. Geyer, R. Golser, F. Huber, M. Lagos, B. Lanyon, M. Plaschke, P. Steier and T. Schäfer (2017). Multiactinide Analysis with Accelerator Mass Spectrometry for Ultratrace Determination in Small Samples: Application to an in Situ Radionuclide Tracer Test within the Colloid Formation and Migration Experiment at the Grimsel Test Site (Switzerland). *Anal. Chem.* 89: 7182–7189
- [6] Montoya, V., U. Noseck, F. Mattick, S. Britz, I. Blechschmidt, T. Schäfer (2022) Radionuclide geochemistry evolution in the Long-term In-situ Test (LIT) at Grimsel Test Site (Switzerland) *J. Hazard. Mat.*, 424 127733
- [7] Huber, F.M., S. Heck, L. Truche, M. Bouby, J. Brendle, P. Hoess and T. Schafer (2015). Radionuclide desorption kinetics on synthetic Zn/Ni-labeled montmorillonite nanoparticles. *Geochim. Cosmochim. Acta* 148: 426–441
- [8] Schäfer, T., H. Geckeis, M. Bouby, T. Fanghänel (2004). U, Th, Eu and colloid mobility in a granite fracture under near-natural flow conditions. *Radiochim. Acta* 92: 731–737

A6-5 REVEALING THE ORIGIN AND ION-BINDING PROPERTIES OF DISSOLVED ORGANIC MATTERS IN DEEP SEDIMENTARY GROUNDWATER

Takumi Saito ⁽¹⁾, Shusaku Nishi ⁽²⁾, Hayato Sato ⁽²⁾, Kanako Toda ⁽¹⁾, and Kazuya Miyakawa ⁽³⁾

(1) Nuclear Professional School, School of Engineering, The University of Tokyo, Japan

(2) Department of Nuclear Engineering and Management, School of Engineering, The University of Tokyo, Japan

(3) Horonobe Underground Research Center, Japan Atomic Energy Agency, Japan

Introduction

Dissolved organic matters (DOMs) play an important role for the fate of pollutants in surface and subsurface environments. For migration of radionuclides, the binding to DOMs modulates their aqueous speciation, reduce the adsorption on rock surface, and even enhance their transport, compared with non-sorbing tracers. The origin of DOMs in surface environments have been studied for decades and mechanistic models are proposed, which can describe ion-binding to major fractions of DOMs (i.e. humic and fulvic fractions) over a wide range of environmental conditions. Nevertheless, our understanding on deep groundwater DOMs remains limited, and it is still disputable if model parameters calibrated for surface DOMs can be applied for their counterparts in deep subsurface environments. [1] This study aims to reveal the origin of different DOM components in deep sedimentary groundwater and their ion-binding properties by fluorescence spectroscopy and high-resolution mass spectrometry. The results of both techniques are processed and correlated by multivariate analysis to find different DOM components and pursue their molecular characteristics.

Experimental

Groundwater samples were collected at various depths in the Horonobe underground research center, Japan Atomic Energy agency (JAEA). The sampling depths reside in the Koetoi and Wakkanai formations which are mainly composed of diatomic mudstones and hard shales, respectively. The groundwater contains relatively high concentrations of dissolved ions due to the presence of connate water. Both total organic carbon (TOC) and dissolved inorganic carbon (DIC) concentrations are large (~10 ppm TOC and 2,000 – 3,000 ppm DIC).

Emission Excitation Matrix (EEM) of the DOM samples was measured by a fluorescence spectrometer (JASCO, FP-8300) after decarbonation and dilution. Europium (Eu^{3+}) was added to aliquots of the groundwater samples to investigate the fluorescence quenching, which is known to correlate with the magnitude of ion binding. The collected EEMs are simultaneously processed by parallel factor analysis (PARAFAC) to separate independent fluorescent components.[2] The Stern- Volmer analysis was applied to derive the binding affinity of the components against Eu^{3+} . [3]

High-resolution mass profiles of the DOM samples were acquired by a Fourier-transformed ion cyclotron resonance mass (FT-ICR-MS) spectrometer (Bruker, Solarix-JA) after desalting and concentrating by solid-state extraction (Bond-Elut, C8). Molecular formulae were assigned to the mass peaks.[4] The results of the high-resolution mass spectrometry are correlated with those of EEMs to find molecular characteristics of the different fluorescent components through various matrices.

Results and discussions

Four fluorescent components were separated from a series of the EEMs by PARAFAC; two of them had similar fluorescent characteristics to those of surface DOMs; one had fluorescent characteristics of tryptophan; one had unique characteristics for the Horonobe groundwater. The ratios of these components varied with depth, reflecting mixing of recharged surface water and connate water. It was

also suggested that the fractions of the unique component for the Horonobe groundwater was correlated with activities of methanogenic microorganisms.

Binding of Eu^{3+} to the four components derived by PARAFAC was examined by the Sern-Volmer plot. Two components with the characteristics of surface DOMs exhibited relatively large binding affinity for Eu^{3+} , meanwhile the unique component for the Horonobe groundwater showed the least affinity.

The FT-ICR-MS profiles of the Horonobe groundwater samples contained more than 1,000 peaks, and distinctive molecular formula were assigned within the error of 1 ppm. The intensities of a part of the formula were found to be correlative with the fractions of the four EEM components derived by the PARAFAC decomposition, from which their molecular characteristics were revealed. In the conference, we will present various molecular metrics describing the EEM components with the help of an advanced multivariate technique, which allows us to simultaneously process both the entire data sets of EEM and FT-ICR-MS data, consisting of the different data dimensions.

References

- [1] T. Saito, M. Terashima, N. Aoyagi, S. Nagao, N. Fujitake and T. Ohnuki (2015). Physicochemical and ion-binding properties of highly aliphatic humic substances extracted from deep sedimentary groundwater. *Environ. Sci.: Process. Impacts* 17: 1386-1395.
- [2] K. R. Murphy, C. A. Stedmon, D. Graeber and R. Bro (2013). Fluorescence spectroscopy and multi-way techniques. *PARAFAC. Anal. Methods* 5: 6557-6566.
- [3] T. Saito, S. Nagasaki and S. Tanaka (2002). Molecular fluorescence spectroscopy and mixture analysis for the evaluation of the complexation between humic acid and $\text{UO}_2(2+)$. *Radiochim. Acta* 90: 545-548.
- [4] Q. L. Fu, M. Fujii and T. Riedel (2020). Development and comparison of formula assignment algorithms for ultrahigh-resolution mass spectra of natural organic matter. *Anal. Chim. Acta* 1125: 247-257.

A5-10 RETENTION AND TRANSPORT BEHAVIOUR OF SELENIUM(IV) IN HARDENED CEMENT PASTE: EFFECT OF HIGH SULPHATE CONCENTRATIONS

Catherine Landesman⁽¹⁾, Solange Ribet⁽¹⁾, Karine David⁽¹⁾, Nicolas Bessagnet⁽¹⁾, Pierre Henocq⁽²⁾

(1) *Subatech, CNRS/IN2P3, IMT Atlantique, Nantes Université, France*

(2) *Andra – French National Agency for Radioactive Waste Management, France*

In many concepts developed worldwide for the disposal of radioactive waste, cementitious materials are foreseen to be used for different purposes as waste conditioning matrix, backfill materials for vaults and tunnels or construction materials in surface and underground repositories depending on the classification of waste. The mobility of radionuclides (RN), released from waste packages, in the cementitious near field is then a key-point for safety assessment and a comprehensive understanding of the chemical interaction of radionuclides with the conditioning material is essential. Some waste contain high levels of soluble salts such as sodium sulphate. The diffusion of a saline plume into cementitious materials may induce changes in thermodynamics equilibria (porewater composition, mineralogical changes,...) and thus may impact the migration (retention/transport) properties of radionuclides. Anionic species migration is a crucial problem as they generally present low sorption properties and thus a high mobility under deep geological repository conditions. Thus, Selenium 79, as a long-lived fission product ($T_{1/2} = 3.77 \cdot 10^5$ y), is currently considered as a key-mobile element and one of the main contributors to the dose in the long term (post-closure repository stage). In moderately reducing and alkaline conditions as those encountered in a cement-based material surrounding, selenite (SeO_3^{2-}) is the major selenium species. In this context, the challenge is to comprehensively describe the effect of salt concentration on the migration properties of Se(IV) in order to improve basic knowledge and produce robust dataset for feeding into predictive models.

The effect of sodium sulphate on retention and transport properties of Se(IV) was investigated through sorption (batch) and diffusion experiments. Hardened cement paste (HCP, water/cement = 0.4) was prepared from a sulphate resistant CEM V/A (Rombas, Calcia) cement cured (3 years at least) in an Artificial Cement Water (ACW) representative of a fresh cement (presence of alkaline elements, pH=13.5). Sorption experiments were carried out in ACW on crushed HCP in presence of 0.3 and 1 mol $\text{kg}^{-1}_{\text{sol}}$ Na_2SO_4 for 2 months. Selenite solutions, spiked with ^{75}Se (used as a tracer), ranged from 10^{-7} to 10^{-1} mol L^{-1} . HTO (Through-) and Se(IV) (In-) Diffusion experiments were performed on HCP samples in standard two-compartment diffusion cells with initial and constant upstream compartment conditions ($2 \cdot 10^6$ Bq L^{-1} (HTO) and 10^{-2} mol L^{-1} (Se(IV))). Diffusion experiments lasted up to 995d and 375d for HTO and Se(IV) respectively.

In pure ACW (no Na_2SO_4), batch experiment results (after 59 days) shows that selenite uptake is moderate and depends on Se concentrations. The variation of distribution ratio (R_d) exhibits a classical trend with a “plateau” value ($R_d = 40 \pm 10$ L kg^{-1} for $[\text{Se}]_{\text{sol}} < 10^{-5}$ mol L^{-1}) follows by a decrease (down to $R_d = 7$ L kg^{-1}) for higher Se concentrations (up to $4 \cdot 10^{-2}$ mol L^{-1}). Additional experiments showed also a kinetic effect (R_d “plateau” = 25 L kg^{-1} after 7d of sorption). In presence of Na_2SO_4 , $R_d(\text{Se})$ values strongly decrease ($R_d = 4$ L kg^{-1}) and do not depend on Se concentrations anymore. In literature, selenite sorption on fresh HCP is poorly documented and only for CEM I HCP ($R_d(\text{Se}) = 120$ L kg^{-1} ^[1]). Selenite appears to sorb on all HCP important mineral phases. This suggest the existence of different processes depending on the nature of the phases such as processes for C-S-H and sulphate replacement in sulfoaluminate phases^[2].

Nevertheless, the role of Ca on selenite sorption on C-S-H phases has been recently highlighted by postulating that Ca acts as a bridging element between selenite ions and surface sites where Ca is already adsorbed^[3]. Thus, the same behaviour may be expected for other oxyanions such as sulphate and then

explain the decrease of selenite sorption in presence of Na_2SO_4 by a selenite/sulphate competition for the same sorption sites.

At the end of in-diffusion experiments, selenium distribution profiles were characterized by Laser Ablation HR ICP-MS technique. In order to check the homogeneity of the diffusion, three profiles were acquired for each sample at different positions (Fig. 1a). Spatial resolution of laser ablation spots laid between 50 to 100 μm depending the analyzed zones (Fig. 1b). Selenium profiles acquired in ACW and Na_2SO_4 conditions are reported Fig. 1c.

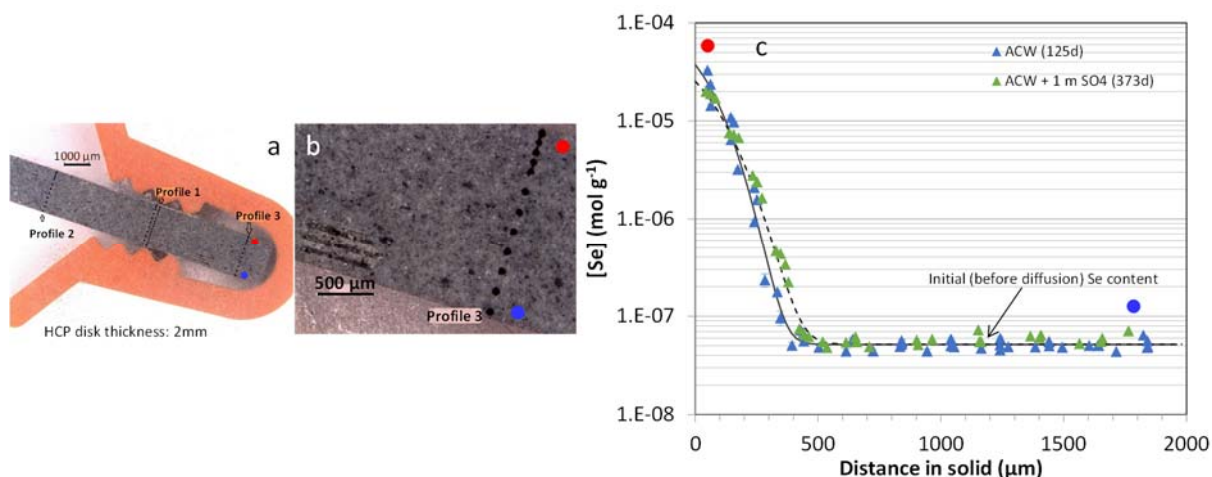


Figure 1: Se distribution profiles: Laser ablation – HR ICP-MS analysis: Global (a) and detailed (b) views of laser spots, (c) Experimental Se profiles and associated modelling in ACW (blue triangles, solid line) and ACW+1m Na_2SO_4 (green triangles, dashed line) conditions (after 125d and 373d of diffusion respectively).

The shape of the profiles shows a progressive decrease of Se concentrations in solid over a depth of around 400 μm where the Se concentration reaches the pristine (before diffusion) Se concentration of 4 mg kg^{-1} . In ACW, $D_e(\text{Se})$ value ($3.6 \cdot 10^{-15} \text{ m}^2 \text{ s}^{-1}$) reflects a diffusion 100 times lower than HTO ($D_e(\text{HTO})_{\text{ACW}} = 4 \cdot 10^{-13} \text{ m}^2 \text{ s}^{-1}$, this work). The presence Na_2SO_4 , by decreasing $D_e(\text{Se})$ values by a factor of almost three, appears to have a significant effect on Se diffusion in HCP. The estimated $R_d(\text{Se})$ values, similar to those obtained from batch experiments, confirm the depletion effect of sulphate salt on Se sorption.

As a conclusion, the presence of sulphate sodium has a small but quantifiable reducing effect on the migration of selenite in HCP which is probably a positive point for the long-term safety assessment.

References

- [1] Pointeau I., Hainos D., Coreau N., Reiller P. Effect of organics on selenite uptake by cementitious materials. *Waste Management* (2006), 26, 733-740
- [2] Ochs M., Mallants D., Wang L. (2016) Radionuclide and metal sorption in cement and concrete. In *Topics in Safety, Risk, Reliability and Quality*, Springer, vol. 29
- [3] Missana, T., Garcia-Gutierrez M., Mingarro M. and Alonso U. Selenite retention and cation coadsorption Effects under alkaline conditions generated by cementitious materials: The case of C-S-H phases. *ACS Omega* (2019), 4, 13418-13425

A5-11 RETENTION OF STRONGLY HYDROLYZING METAL IONS IN CEMENT SYSTEMS: QUANTITATIVE DESCRIPTION AND MECHANISTIC UNDERSTANDING

X. Gaona⁽¹⁾, N. Cevirim-Papaioannou⁽¹⁾, Y. Jo^{(1),(2)}, N. Huber⁽¹⁾, A. Tasi⁽¹⁾, R. E. Guidone⁽¹⁾, I. Androniuk⁽¹⁾, K. Dardenne⁽¹⁾, J. Rothe⁽¹⁾, M. Altmaier⁽¹⁾, H. Geckeis⁽¹⁾

(1) Institute for Nuclear Waste Disposal, Karlsruhe Institute of Technology, Karlsruhe (Germany)

(2) Department of Nuclear Engineering, Hanyang University (Republic of Korea)

Safety concepts regarding nuclear waste disposal in underground repositories generally rely on a combination of engineered and geological barriers, which minimize the potential release of radionuclides out of the containment providing rock zone or even the transport into the biosphere. Cementitious materials are used for conditioning of certain nuclear waste types, as components of waste containers and overpacks as well as constituents of structural materials at the interface between backfilling and host-rock in some repository concepts.

In the event of formation water interacting with cementitious materials, pore water solutions characterized by (highly) alkaline pH conditions will form. These boundary conditions define the chemical behaviour of the radionuclides, but also can influence the neighbouring components of the multi-barrier system, e.g. bentonitic or argillaceous backfilling and host-rock, respectively. Hardened cement paste is considered to be main sorbing materials present in the near field of repositories for low and intermediate level waste (L/ILW). Hence, interactions of radionuclides with cementitious materials represent a very important mechanism retarding their mobility and potential migration from the near field [1-2]. While the quantitative description of the sorption processes (usually in terms of sorption coefficients, i.e. K_d values) is a key input in the Safety Analysis of nuclear waste repositories, the detailed mechanistic analysis and understanding of sorption phenomena provide additional scientific arguments and important process understanding and thus enhance both the quality of safety arguments and the overall confidence in the Safety Assessment process.

This contribution summarizes recent research activities conducted at KIT-INE on the interaction of cementitious materials with key radionuclides, including actinides (Pu), fission and activation products (Zr, Nb, Sn) and chemotoxic elements (Be). These elements have been identified as relevant radionuclides and chemotoxic elements in the context of L/ILW [1-2]. The investigated metal ions extend from very light (⁹Be) to very heavy elements (²⁴²Pu) and a diversity of oxidations states (+II to +V), although all of them are characterized by high charge-to-size ratios (z/d), and thus by strong hydrolysis. Hardened cement paste (HCP) in the degradation stages I and II, as well as calcium silicate hydrate (C-S-H) phases with Ca:Si ratios of 0.6 to 1.5 were considered as representative cementitious materials. Sorption experiments were conducted with stable ⁹Be(II), the long-lived isotope ²⁴²Pu(IV) ($t_{1/2} = 2.41 \times 10^4$ a) and the short-lived isotopes ⁹⁵Zr(IV) ($t_{1/2} = 64.03$ d), ⁹⁵Nb(V) ($t_{1/2} = 34.97$ d) and ¹¹³Sn(IV) ($t_{1/2} = 115.09$ d). Sample preparation and handling were performed in Ar gloveboxes at $T = (22 \pm 2)$ °C. The content of stable ^{nat}Zr, ^{nat}Nb and ^{nat}Sn in pristine HCP was quantified by alkaline fusion and ICP-MS in order to evaluate isotopic exchange as retention mechanism. Batch sorption samples were prepared in synthetic cement pore waters with solid-to-liquid ratios (S/L) of 0.1 – 5 g/L and $1 \cdot 10^{-13}$ M $\leq [M]_0 \leq 1.0 \cdot 10^{-3}$ M (depending upon metal ion and pH). Total concentration of the metal ion in the aqueous phase was quantified after phase separation (ultrafiltration or ultracentrifugation) by ICP-MS (⁹Be, ²⁴²Pu) or gamma spectrometry (⁹⁵Zr, ⁹⁵Nb, ¹¹³Sn). Upper solubility limits of Be(II), Zr(IV), Nb(V), Sn(IV) and Pu(IV) were quantified in the same pore water solution used in the sorption experiments.

A strong uptake ($5 \leq \log R_d \leq 7$, with R_d in $\text{dm}^3 \cdot \text{kg}^{-1}$) is quantified for all investigated metal ions and cementitious systems. Linear sorption isotherms are observed over three to six orders of magnitude in

$[M]_{\text{aq}}$ (depending upon metal ion), confirming that the uptake is controlled by sorption processes and that solubility phenomena are not relevant within the investigated conditions. The analogous behaviour observed for HCP and C-S-H confirm that the latter are the main sink of the investigated metal ions in cementitious systems. MD calculations show that negatively charged hydrolysis species of Be(II) sorb on the surface of the C-S-H phases through Ca-bridges and hydrogen bonds. MD simulations support also Be(II) retention in the C-S-H interlayer. Similar conclusions have been previously reported for An(IV) based on advanced spectroscopic methods [3-4]. In combination with experimental evidences supporting the stabilization of ternary aqueous complexes Ca-M-OH(aq) for Be(II) [5], Zr(IV) [6], Nb(V) [7] and Pu(IV) [6,8], these results highlight as well the key role of surface calcium in the retention of strong hydrolyzing metal ions by cement.

Quantitative chemical analysis after alkaline fusion of HCP confirms the significant presence of stable $^{\text{nat}}\text{Zr}$ (≈ 50 ppm, isotopes 90, 91, 92, 94, 96), $^{\text{nat}}\text{Nb}$ (≈ 7 ppm, isotope 93) and $^{\text{nat}}\text{Sn}$ (≈ 5 ppm, isotopes 112, 114-120, 122, 124). Under repository conditions, isotopic exchange with stable isotopes existing in pristine cement can accordingly influence the uptake of the long-lived radionuclides ^{93}Zr ($t_{1/2} = 1.53 \times 10^6$ a), ^{94}Nb ($t_{1/2} = 2.04 \times 10^4$ a) and ^{113}Sn ($t_{1/2} = 2.3 \times 10^5$ a). Moreover, the role of Th(IV) and Ln(III) present in pristine cement in the retention of key An(IV) and An(III) like plutonium remains unclear and deserves further attention.

This contribution emphasizes the importance of combining comprehensive wet-chemistry studies with advances spectroscopic techniques and theoretical calculations for the full quantitative description and mechanistic understanding of retention processes in cementitious systems.

Acknowledgements: *This work was partly funded by the Swedish Nuclear Fuel and Waste Management Company (SKB) and the Belgian National Agency for Radioactive Waste and enriched Fissile Material (ONDRAF/NIRAS). The research leading to some of these results has received funding from the European Union's European Atomic Energy Community's (Euratom) Horizon 2020 Programme (NFRP-2014/2015) under grant agreement, 662147 – Cebama.*

References

- [1] Ochs, M., Dirk, M., Wang, L. (2016). Radionuclide and metal sorption on cement and concrete, Springer, Switzerland.
- [2] Wieland, E. (2014). Sorption database for the cementitious near field of L/ILW and ILW repositories for provisional safety analyses for SGT-E2. Nagra Technical Report 14-08. Paul Scherrer Institut, Villigen, Switzerland.
- [3] Gaona, X., Dähn, R., Tits, J., Scheinost, A.C., Wieland, E. (2011). Uptake of Np(IV) by C-S-H phases and cement paste: An EXAFS study, *Environmental Science and Technology*, 45, 8765-8771.
- [4] Häußler, V., Amayri, S., Beck, A., Platte, T., Stern, T.A., Vitova, T., Reich, T. (2018). Uptake of actinides by calcium silicate hydrate (C-S-H) phases, *Applied Geochemistry*, 98, 426-434.
- [5] Çevirim-Papaioannou, N., Androniuk, I., Miron, G.D., Altmaier, M., Gaona, X. (2023). Beryllium solubility and hydrolysis in dilute to concentrated CaCl_2 solutions: thermodynamic description in cementitious systems, *Frontiers in Nuclear Engineering* (submitted).
- [6] Altmaier, M., Neck, V., Fanghänel, Th. (2009). Solubility of Zr(IV), Th(IV) and Pu(IV) hydrous oxides in CaCl_2 solutions and the formation of ternary Ca-M(IV)-OH complexes, *Radiochimica Acta*, 96, 541-550.
- [7] Jo, Y., Garbev, K., Çevirim-Papaioannou, N., Blanco, O.D., de Blochouse, B., Altmaier M., Gaona X. (2022). Solubility of niobium(V) in cementitious systems relevant for nuclear waste disposal: Characterization of the solubility-controlling solid phases, *Journal of Hazardous Materials*, 440, 129810.
- [8] Fellhauer, D., Neck, V., Altmaier, M., Lützenkirchen, J., Fanghänel, Th. (2010). Solubility of tetravalent actinides in alkaline CaCl_2 solutions and formation of $\text{Ca}_4[\text{An}(\text{OH})_8]^{4+}$ complexes: A study of Np(IV) and Pu(IV) under reducing conditions and the systematic trend in the An(IV) series, *Radiochimica Acta*, 98, 541-548.

A5-12 THE OPTIMIZED GEMS CLAYSOR MODEL AND DATA BASES TO SUPPORT NAGRA SAFETY ASSESSMENTS FOR DEEP GEOLOGICAL REPOSITORY

G. Dan Miron ⁽¹⁾, Olha Marinich ⁽¹⁾, Maria Marques Fernandes ⁽¹⁾, Dmitrii A. Kulik ⁽¹⁾, Bart Baeyens⁽¹⁾, Raphael Wüst ⁽²⁾

(1) Paul Scherrer Institute, Laboratory for Waste Management, 5232 Villigen PSI, Switzerland

(2) National Cooperative for the Disposal of Radioactive Waste (Nagra), CH-5430 Wettingen, Switzerland

To analyze the safety of deep geological radioactive waste repository in clay rock, it is necessary to obtain solid-liquid distribution coefficients (K_d values) for a large number of radionuclides. The "bottom up" approach, commonly used to derive sorption values for argillaceous rocks across a range of porewater and mineralogical compositions [1-3], assumes that the uptake of radionuclides in complex mineral/porewater systems can be predicted based on mechanistic models that describe the sorption processes on single minerals, such as the 2:1 clay minerals illite, smectite, and illite-smectite mixed layers. The total sorption site capacities are then scaled to the 2:1 clay mineral content in the rock, and the radionuclide speciation in porewater is needed to calculate the sorption isotherms.

Over the last more than two decades, "in-house" mechanistic sorption models have been developed at PSI based on measured experimental datasets, including a generalized Cs adsorption model for deriving K_d values for Cs(I) on argillaceous rocks, and the 2 Site Protolysis Non Electrostatic Surface Complexation and Cation Exchange (2SPNE SC/CE) model [1-3, 5] for key radionuclides comprising Ni(II), Co(II), Pb(II), Eu(III), Am(III), Th(IV), Sn(IV), Np(V), Pa(V) and U(VI). In 2017, the 2SPNE SC/CE model had been reimplemented in GEMS [4] (the Gibbs energy minimization software developed and distributed at PSI, <https://gems.web.psi.ch>) under the name *ClaySor* model [5]. In the *ClaySor* thermodynamic database, surface complexation and cation exchange reactions with standard thermodynamic properties were compiled for montmorillonite and illite using the older thermodynamic data for aqueous species collected from several literature sources, and also did not include the parameter uncertainty estimates. Recently, the standard thermodynamic data of relevant radionuclides has been revised in the PSI-Nagra chemical thermodynamic database TDB 2020 [6].

The update of *ClaySor* model and database consisted of revision of the standard equilibrium constants of sorption species to ensure consistency with the new TDB 2020 data, along with the derivation of parameter confidence intervals. The latter are then used for evaluating the model uncertainty in predicting the uptake of relevant elements in repository safety assessments for a given composition of porewater and clay rock mineralogy. To achieve this goal, the *ClaySor* model was re-parameterized using the GEMSFITS parameter optimization tool [7], which refines the equilibrium constants for surface complexation and ion exchange reactions against experimental data. GEMSFITS also offers a range of statistical methods to evaluate parameter correlation and sensitivity to experimental data, as well as a Monte Carlo method for determining parameter confidence intervals.

Model optimization used the "in house" experimental data sets, which included pH edges and sorption isotherms in different electrolyte solutions (e.g., Figure 1). These data sets were converted into the GEMSFITS experimental data format using preformatted Excel spreadsheets, where each data point was defined in terms of the GEMS chemical system definition. This consist of the amount of aqueous solution, the initial and equilibrium concentration of the investigated chemical element, background electrolyte concentration, pH, and amounts of clay planar sites (CEC) as well as strong and weak edge sites. For each element the measured K_d values of all selected datasets were used to get the refined Gibbs energy values G°_{298} of the sorption and exchange complexes, as well as their 95% confidence intervals.

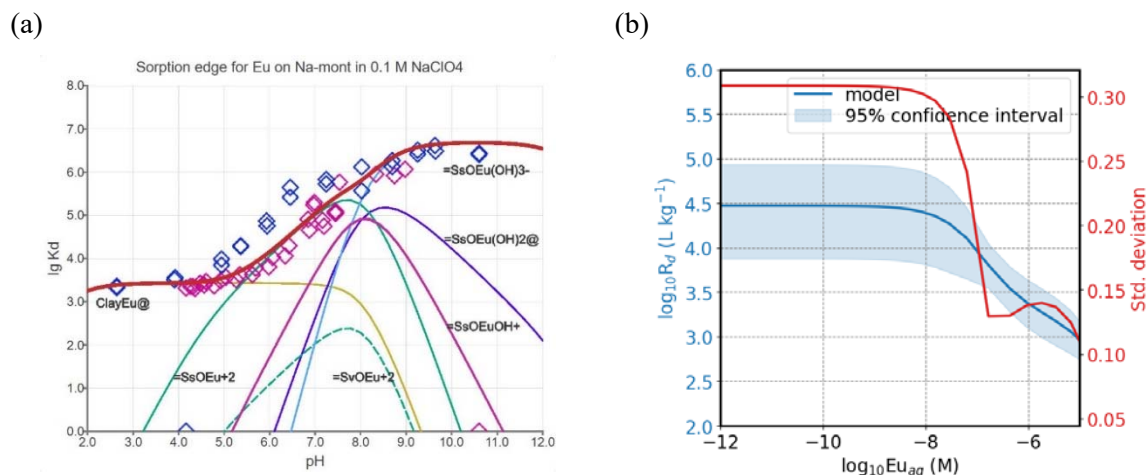


Figure 1. Eu sorption on montmorillonite: (a) experimental K_d (diamonds) and modeling K_d (solid curves strong, dashed weak sorption sites) obtained from the optimized equilibrium constants (25 °C); (b) sorption isotherm with confidence interval at pH 7.5 and 42% illite.

For the Swiss repository performance assessment concept, a state-of-the-art sorption database (SDB) is needed for different siting regions under investigation. Sorption measurements of key radionuclides on samples from the different drilling cores will be available. The GEM-Selektor [4] geochemical code is used to interpret the data and compile the SDB for the safety analysis. The K_d values are calculated directly by GEMS, including aqueous speciation, solubility, and concentration-dependent adsorption of each radionuclide for each argillaceous rock/porewater system defined for the different siting regions. The PSI TBD2020 for Nagra, extended with an internally consistent thermodynamic dataset for surface complexation and ion exchange (the updated "ClaySor" version), is also used in the ClaySorDif model extension for the diffusion coefficients of relevant elements (Glaus et al., this conference).

References

- [1] Marques Fernandes, M. et al. (2015). Predicting the uptake of Cs, Co, Ni, Eu, Th and U on argillaceous rocks using sorption models for illite. *Appl. Geochem.* 59: 189-199.
- [2] Bradbury, M.H. and B. Baeyens (2017). The development of a thermodynamic sorption data base for illite and the application to argillaceous rocks. NTB 17-14, Nagra, Wettingen, Switzerland.
- [3] Bradbury, M.H. and B. Baeyens (2017). The development of a thermodynamic sorption data base for montmorillonite and the application to bentonite. NTB 17-13, Nagra, Wettingen, Switzerland.
- [4] Kulik, D. A. and T. Wagner, S.V. Dmytrieva, G. Kosakowski, F.F. Hingerl, K.V. Chudnenko, U.R. Berner (2013). GEM-Selektor geochemical modeling package: Revised algorithm and GEMS3K numerical kernel for coupled simulation codes. *Computat. Geosci.*, 17(1): 1-24.
- [5] Kulik, D.A. and M. Marques Fernandes, B. Baeyens (2018) The 2SPNE SC/CE sorption model in GEM-Selektor v.3.4 code package (ClaySor): Implementation, tests, and user guide. Nagra Work Report (Nagra Arbeitsbericht) NAB 18-27.
- [6] Hummel, W., and T. Thoenen (2022). The PSI Chemical Thermodynamic Database 2020. Nagra NTB 21-03.
- [7] Miron, G.D., and D.A. Kulik, S.V. Dmytrieva, T. Wagner (2015). GEMSfits: Code package for optimization of geochemical model parameters and inverse modeling. *Appl. Geochem.* 55: 28-45.

A5-13 BENCHMARKING THE THERMOCHIMIE DATABASE: SOLUBILITY AND SPECIATION CALCULATIONS

Eli Colàs⁽¹⁾, Jordi Rodríguez-Mestres⁽¹⁾, Roger Mas⁽¹⁾, David García⁽¹⁾, Lara Duro⁽¹⁾, Will Bower⁽²⁾, Stéphane Brassinnes⁽³⁾, Benoît Madé⁽⁴⁾

(1) *Amphos 21 Consulting SL, Spain*

(2) *Nuclear Waste Services, UK.*

(3) *Belgian Agency for Radioactive Waste and Enriched Fissile materials (ONDRAF/NIRAS), Belgium*

(4) *Andra, French National Radioactive Waste Management Agency, Research & Development Division, France*

ThermoChimie (<http://www.thermochimie-tdb.com/>) [1,2] is a thermodynamic database developed by Andra (France), Nuclear Waste Services (UK) and Ondraf/Niras (Belgium). ThermoChimie provides robust thermodynamic data for a wide range of radionuclides and non-radiological pollutants, as well as major components expected within a geological disposal facility. These thermodynamic data are mainly derived from comprehensive, active literature studies and are supplemented by an experimental program when required.

ThermoChimie is under constant development to broaden the range of conditions to which it can be applied, and further refined for current applications. Validation and verification procedures play an important role in the development of the database, in order to ensure that all the relevant aqueous species and solid phases are included. These procedures also provide information on the consistency and accuracy of the database and whether adequate uncertainty is assigned to less reliable data.

In this frame, ThermoChimie is currently being tested in a large benchmarking exercise. In the benchmarking, calculations for geochemical systems relevant to the disposal of radioactive waste are performed. The results obtained with the ThermoChimie database are compared with those obtained with other high-quality thermodynamic databases and, whenever possible, comparison with independent experimental datasets is also done. The objective of the benchmark is to identify any weaknesses (e.g. gaps, lack of accuracy, etc.) of the ThermoChimie database and/or any significant differences between the thermodynamic databases considered that could provide a path forward to ThermoChimie improvement and development.

The present work will show the results obtained in the benchmarking of ThermoChimie versus other high-quality databases (PRODATA [3], THEREDA [4], JAEA [5] and NAGRA-PSI [6]) in the solubility and associated speciation calculations for a set of safety-relevant radionuclides (RNs) and chemotoxic elements (CTs). Both clay and cementitious conditions are considered. The influence of parameters such as temperature, salinity or the presence of organic agents is also discussed in the calculations.

The methodology includes the selection of the solid phase most likely to precipitate under the studied conditions, calculation of the element concentration and underlying aqueous speciation in equilibrium, and comparison of the solids, concentrations and speciation calculations obtained with different thermodynamic databases or with the results described in the relevant publications.

The comparisons have allowed to identify the need of revising the hydrolysis systems for Eu and Pa. It is also possible to enhance the sulphide system in order to better fit the requirements of the modellers. Furthermore, modelling exercises using recently published experimental data have led to a significant improvement of the data selection for isosaccharinate, gluconate and acetate systems.

Legend:

- X (Green): Included in ThermoChimie vs.11a
- X (Yellow): X

Figure 1: Periodic table showing the elements included in the benchmarking exercise.

References

- [1] Giffaut, E., M. Grivé, P. Blanc, P. Vieillard, E. Colàs, H. Gailhanou, S. Gaboreau, N. Marty, B. Madé and L. Duro. (2014). Andra thermodynamic database for performance assessment: ThermoChimie. *Applied Geochemistry* 49: 225-236.
- [2] Grivé, M., L. Duro, E. Colàs and E. Giffaut. (2015). Thermodynamic data selection applied to radionuclides and chemotoxic elements: An overview of the ThermoChimie-TDB. *Applied Geochemistry* 55: 85-94.
- [3] Reiller, P. E., and M. Descostes. (2020). Development and application of the thermodynamic database PRODATA dedicated to the monitoring of mining activities from exploration to remediation. *Chemosphere* 251: 126301.
- [4] Moog, H.C., F. Bok, C. M. Marquardt, V. Brendler. (2015) Disposal of nuclear waste in host rock formations featuring high-saline solutions – Implementation of a thermodynamic reference database (THEREDA). *Appl. Geochem.* 55: 72–84.
- [5] Kitamura, A. (2021) JAEA-TDB-RN in 2020: Update of JAEA’s Thermodynamic Database for Solubility and Speciation of Radionuclides for Performance Assessment of Geological Disposal of High-level and TRU Wastes. JAEA-Data/Code 2020-020.
- [6] Thoenen, T., W. Hummel, U. Berner, E. Curti. (2014) The PSI/Nagra Chemical Thermodynamic Database 12/07. PSI Bericht Nr. 14-04